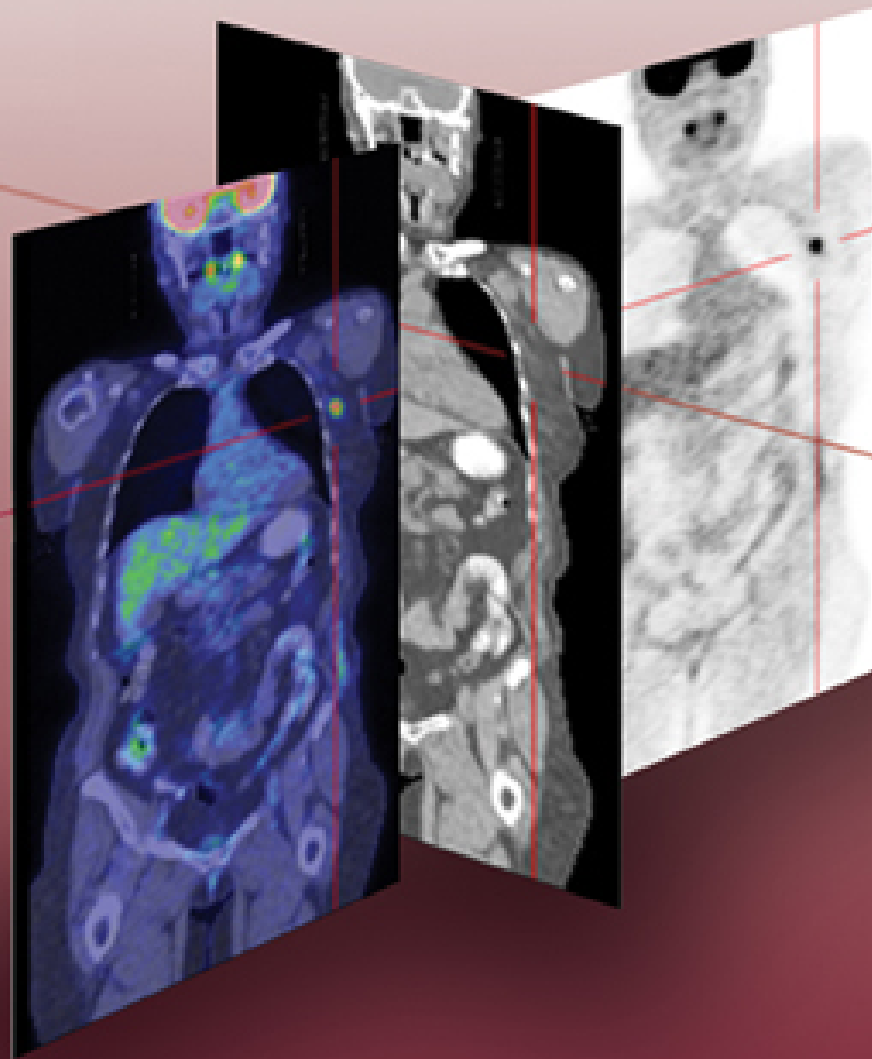


# Introduction to Sectional Anatomy

Second Edition

**Michael E. Madden**



Wolters Kluwer  
Health

Lippincott  
Williams & Wilkins

thePoint 

# Introduction to Sectional Anatomy

Second Edition

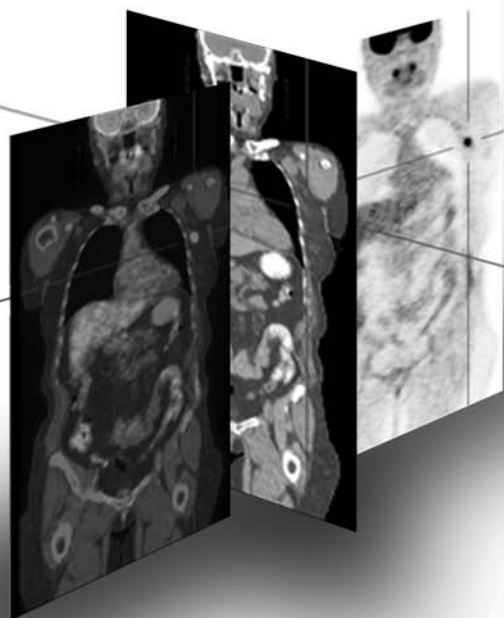


# Introduction to Sectional Anatomy

Second Edition

**Michael E. Madden, Ph D, RT(R) (CT)(MR)**

*Director  
Medical Diagnostic Imaging Programs  
Fort Hays State University  
Hays, Kansas*





*Acquisitions Editor:* Peter Sabatini  
*Managing Editor:* Andrea M. Klingler  
*Marketing Manager:* Allison M. Noplock  
*Project Manager:* Kevin P. Johnson  
*Production Services:* Aptara, Inc.  
*Printer:* Quebecor-Dubuque

Second Edition

Copyright © 2008, 2001, Lippincott Williams & Wilkins, a Wolters Kluwer business.

351 West Camden Street      530 Walnut Street  
Baltimore, MD 21201      Philadelphia, PA 19106

All rights reserved. This book is protected by copyright. No part of this book may be reproduced or transmitted in any form or by any means, including as photocopies or scanned-in or other electronic copies, or utilized by any information storage and retrieval system without written permission from the copyright owner, except for brief quotations embodied in critical articles and reviews. Materials appearing in this book prepared by individuals as part of their official duties as U.S. government employees are not covered by the above-mentioned copyright. To request permission, please contact Lippincott Williams & Wilkins at 530 Walnut Street, Philadelphia, PA 19106, via email at [permissions@lww.com](mailto:permissions@lww.com), or via website at [lww.com](http://lww.com) (products and services).

9 8 7 6 5 4 3 2 1

#### Library of Congress Cataloging-in-Publication Data

Madden, Michael E.

Introduction to sectional anatomy / Michael E. Madden.—2nd ed.

p. ; cm.

Includes bibliographical references and index.

ISBN-13: 978-0-7817-6342-4

ISBN-10: 0-7817-6342-8

1. Human anatomy. 2. Magnetic resonance imaging. 3. Tomography. I. Title. II. Title: Sectional anatomy.

[DNLM: 1. Anatomy, Cross-Sectional. 2. Magnetic Resonance Imaging. 3. Tomography, X-Ray Computed.

QS 4 M179i 2008]

QM23.2.M325 2008

611—dc22

2007007777

#### DISCLAIMER

Care has been taken to confirm the accuracy of the information present and to describe generally accepted practices. However, the authors, editors, and publisher are not responsible for errors or omissions or for any consequences from application of the information in this book and make no warranty, expressed or implied, with respect to the currency, completeness, or accuracy of the contents of the publication. Application of this information in a particular situation remains the professional responsibility of the practitioner; the clinical treatments described and recommended may not be considered absolute and universal recommendations.

The authors, editors, and publisher have exerted every effort to ensure that drug selection and dosage set forth in this text are in accordance with the current recommendations and practice at the time of publication. However, in view of ongoing research, changes in government regulations, and the constant flow of information relating to drug therapy and drug reactions, the reader is urged to check the package insert for each drug for any change in indications and dosage and for added warnings and precautions. This is particularly important when the recommended agent is a new or infrequently employed drug.

Some drugs and medical devices presented in this publication have Food and Drug Administration (FDA) clearance for limited use in restricted research settings. It is the responsibility of the health care provider to ascertain the FDA status of each drug or device planned for use in their clinical practice.

To purchase additional copies of this book, call our customer service department at (800) 638-3030 or fax orders to (301) 223-2320. International customers should call (301) 223-2300.

Visit Lippincott Williams & Wilkins on the Internet: <http://www.lww.com>. Lippincott Williams & Wilkins customer service representatives are available from 8:30 am to 6:00 pm, EST.

*To Theresa, for providing more love and support than I deserve,  
and to Levi and Luke, who are my constant source of inspiration.*





# Preface

Even though everyone has more or less the same anatomy, they are arranged and shaped slightly different in each individual. For example, every person has a mouth, nose, and two eyes arranged together to make their face, but very few people look the same because of variations in shape and arrangement. Similar to the outside, every person has the same parts on the inside and very few people will look alike in sectional images. By using *Introduction to Sectional Anatomy*, the reader will be able to view images from several patients in each region of the body covered allowing them to compare the anatomical appearance. Similarly, the patient images will be shown using a variety of current imaging modalities such as CT, MR, PET/CT, and ultrasound, including 3D imaging of vascular and bony anatomy. Although the book is considered to be at the introductory level for learning sectional anatomy, students are expected to have completed one or two semesters of study in anatomy and physiology before attempting to discern sectional images.

## ORGANIZATION

The book begins with a brief and simple introductory chapter to help the student understand the terminology and plane of sections described in subsequent chapters. To help the students adjust to the higher level of understanding needed for sectional anatomy, it's best to start with the anatomy most familiar to the students. Consequently, the chest is covered in the second chapter, since most students already have a basic knowledge and this chapter is relatively simple as compared to later chapters. Similarly, the chest is followed by the lower parts of the trunk: the abdomen and pelvis. Once the students have become accustomed to learning sectional anatomy in the trunk, the more difficult regions of the body—head, neck, spine, and joints—are covered in the second half of the text.

Before the student will be ready to study the sectional images, they must have a clear understanding of the anatomy within the region with a strong emphasis on the relationship with adjacent structures (e.g., the esophagus lies posterior to the trachea). Each chapter is focused on a

region of the body and begins with an anatomical overview to give the reader a clear understanding of each region essential to understanding the anatomy shown later in sectional images. To demonstrate the clinical application of this anatomy, the overview is followed by a series of patient CT and MR images shown in sequence through multiple planes. After the patient images, clinical cases of selected CT, MR, ultrasound, and PET/CT (including 3D) images have been greatly expanded to motivate students by giving samples of how their knowledge of sectional anatomy can be applied to patient exams.

To provide the reader with the most widely accepted anatomical terminology, the terms used to describe structures are from the *Terminologia Anatomica: International Anatomical Terminology*, developed by the Federative Committee on Anatomical Terminology and adopted by the International Federation on Anatomical Associations and published in 1998 by Thieme Publishing in Stuttgart, Germany. Also, to help the student learn the correct pronunciation of unfamiliar terms, phonetic spelling is found in parenthesis immediately after the name of the anatomical structure. A key for pronunciation is found on page xiii.

## FEATURES AND ITEMS NEW TO THIS EDITION

This second edition of *Introduction to Sectional Anatomy* has been expanded and updated to include the latest imaging technology, including ultrasound, 3D, and PET/CT images. The contemporary layout and added color were designed to facilitate reading and comprehension. Similarly, the patient images have been revised to enable the reader to more quickly compare images between several patients.

To provide a highly regimented learning tool, all of the chapters begin with a series of Chapter Objectives and conclude with a brief series of Clinical Application questions intended to evaluate the reader's understanding of the chapter's material. After the Clinical Application questions are Clinical Cases. Most images include directional

rosettes in the bottom right corner. These are included to help readers orient themselves to the view seen on each cross-section.

## ANCILLARIES

For additional self-examination, an accompanying student workbook is also available and corresponds closely with the textbook. Using most of the sectional images from the textbook, the workbook asks the reader multiple choice questions in the format used on CT and MR registry examinations. Each image is numbered in the workbook to correspond with the appropriate image in the textbook. The workbook also includes more Clinical Application review questions and Clinical Cases for further review. Further student materials are available on the Student Resource Center at <http://thepoint.lww.com/madden2e>, and include two more Clinical Cases per chapter and Resources for further reference.

To help faculty develop their own teaching materials, the Instructors' Resource CD-ROM and Faculty Resource Center at <http://thepoint.lww.com/madden2e> have been designed to provide supplemental teaching materials, including an image bank of the textbook images, as well as an image bank of the workbook images. The image bank of

the workbook images includes three versions of the images: one as seen in the workbook, one with only leader lines for use in class or in assignments, and a blank version. A test generator and PowerPoint slides are also included. Even more Clinical Cases (approximately 20 per chapter) are provided for use as well.

Altogether, these resources provide substantially more patient images as compared to the first edition, and many of those included have been generated with new technology like PET/CT and 3D imaging. Likewise, the on-line resource centers provide more supplemental materials designed to help students learn sectional anatomy.

The art of medical diagnostic imaging requires a strong foundation in anatomy and a dedication to ongoing education and change. Medical diagnostic imaging continues to be in a state of flux because of rapid advances in computer imaging technology. To best prepare students for their clinical practice, dedicated teachers experiment with curricula and course evaluation, always striving to correct deficiencies, to define, to update, and to narrow the gap between what is taught and what is current knowledge. Despite the rapid and ongoing changes, a thorough knowledge of human anatomy is the keystone to the foundation for developing the art and science of medical diagnostic imaging.



# Acknowledgments

This book would not have been possible without the contributions of many individuals and I would like to express my sincere gratitude to the following:

All the staff at Lipincott Williams & Wilkins, especially Peter Sabatini, Andrea Klingler, Jennifer Clements, Mary Martin, and John Goucher, for their expertise and considerable efforts in developing this project for publication.

Janie Meder and Shelly Flax who spent countless hours developing the sectional anatomy drawings.

Jennifer Smith, the illustrator of the anatomy drawings, for contributing her talent.

All the students that critically reviewed the manuscript and gave me their ideas for improvement.

The staff and hospitals that provided the images used throughout the text, including the Central Kansas Medical Center (Great Bend, Kansas); Hays Medical Center (Hays, Kansas); Olathe Medical Center (Olathe, Kansas); Southwest Medical Center (Liberal, Kansas); Sterling Regional Medical Center (Sterling, Colorado); St. Catherine Hospital (Garden City, Kansas); St. Francis Medical Center (Grand Island, Nebraska); University of Kansas Hospital (Kansas City, Kansas); University of Nebraska Medical Center (Omaha, Nebraska); and Western Plains Regional Hospital (Dodge City, Kansas).

This project was partially supported by the NIH Grant Number P20 RR016475 from the INBRE Program of the National Center for Research Resources.





# Reviewers

Robert D. Adams, Ed.D., CMD, RT(R)(T)  
Program Director, Radiation Therapy/Medical Dosimetry  
Programs UNC Hospitals  
Assistant Professor, UNC Department of Radiation Oncology  
University of North Carolina  
Chapel Hill, North Carolina

Barbara Annunziato, BS, RT, RDMS, RVT  
Program Director  
Crozer-Chester Medical Center  
School of Diagnostic Ultrasound  
Upland, Pennsylvania

Kevin D. Evans, PhD, RT(R) (M) (BD), RDMS, RVS,  
FSDMS  
Assistant Professor/Director  
Radiologic Sciences and Therapy Division  
School of Allied Medical Professions  
The Ohio State University  
Columbus, Ohio

Catherine Ford, B.S., R.T.-R  
Chair, Medical Imaging Technologies  
Owens Community College  
Toledo, Ohio

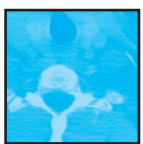
Lisa J. Hight, Ed.D., BS, MS  
Associate Professor of Biology  
Baptist College of Health Sciences  
Memphis, Tennessee

Sonja K. Robb-Belville, BS, RT(R)(MR)  
Assistant Professor  
Palm Beach Community College  
Palm Beach Gardens, Florida

Amy C. VonKadich M.ED, RTT  
Professor  
New Hampshire Technical Institute  
Concord, New Hampshire







# Pronunciation Key

## VOWELS

ā	day, care, gauge
a	mat, damage
ă	about, para
ah	father
aw	fall, cause, raw
ē	be, equal, ear
ě	taken, genesis
e	term, learn
ī	pie
ĩ	pit, sieve, build
ō	note, for, so
o	not, oncology, ought
oo	food
ow	cow, out
oy	troy, void
ū	unit, curable
ů	cut

## CONSONANTS

b	bad
ch	child
d	dog
dh	this, smooth
f	fit
g	got
h	hit
j	jade
k	kept
ks	tax
kw	quit
l	law
m	me
n	no
ng	ring
p	pan
r	rot
s	so, miss
sh	should
t	ten
th	thin, with
v	very
w	we
y	yes
z	zero
zh	azure, measure

Reprinted from *Stedman's Medical Dictionary, 27th Edition/Stedman's Electronic Medical Dictionary, Version 5.0*. Baltimore: Lippincott Williams & Wilkins, 2001 ([www.stedmans.com](http://www.stedmans.com)).

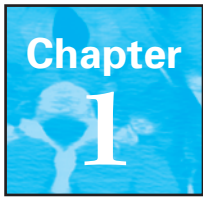




# Contents

Dedication .....	v
Preface .....	vii
Acknowledgments .....	ix
Reviewers .....	xi
Pronunciation Key .....	xiii
<b>Chapter 1</b> Introduction .....	1
<b>Chapter 2</b> Chest .....	9
<b>Chapter 3</b> Abdomen .....	101
<b>Chapter 4</b> Male and Female Pelvis .....	175
<b>Chapter 5</b> Head .....	313
<b>Chapter 6</b> Neck .....	433
<b>Chapter 7</b> Spine .....	493
<b>Chapter 8</b> Joints .....	543
<b>Appendix A</b> Answers to Clinical Application Questions .....	619
<b>Appendix B</b> Glossary .....	626
<b>Appendix C</b> Bibliography .....	629
Index .....	631





# Introduction

## OBJECTIVES

Upon completion of this chapter, the student should be able to:

1. Describe the general concept of sectional imaging.
2. Maintain their perspective when viewing sectional images.
3. Categorize sectional images as sagittal, coronal, or axial.
4. Accurately classify joints within the body.
5. Provide a basic overview of computed tomography (CT).
6. Describe the Hounsfield scale and basic absorption values of common tissues.
7. Provide a basic understanding of magnetic resonance (MR) imaging.
8. Compare T1 and T2 weighted MR images and relative signal generated in structures found within the body.
9. Describe the basic principles and clinical application of Positron Emission Tomography Combined with Computed Tomography (PET/CT).
10. Give a basic overview of the principles and practice of ultrasound imaging.

## ANATOMIC OVERVIEW

Traditional anatomy courses tend to focus primarily on the names and shapes of anatomic structures. By comparison, sectional anatomy places much more emphasis on the physical relationship among structures. To identify anatomic structures on sectional images, a complete understanding of the basic anatomic information is a requisite from which a three-dimensional understanding develops. This textbook follows this organization beginning with an anatomic overview of structures in the region followed by the labeled CT and MR images. To demonstrate the application of this knowledge, selected pathology is included as supplemental information in the following chapters.

Compared to conventional radiographs, computer-generated sectional images are especially useful when evaluating soft tissue structures and those not clearly displayed owing to adjacent structures. For example, although proper positioning will show much of the bony anatomy in the lateral skull, it provides little diagnostic information of soft tissue structures, and demonstrates the right and left sides of the skull superimposed over each other (Fig. 1-1). By comparison, the CT or MR computer-generated sectional images (Fig. 1-2)

eliminate overlapping structures, allowing many structures to be more clearly visualized in a nearly endless variety of planes. Although CT and MR will likely never replace conventional radiography because of affordability and diagnostic value in certain situations, these forms of computerized imaging are found in most clinical facilities.

Similar to conventional radiography, CT and MR images are extremely valuable diagnostic tools. However, for these images to be useful clinically, they must accurately depict the region of the patient's anatomy being studied. Because the image is generated by a computer, technical factors can significantly change or alter the resulting image. If the operator has an introductory knowledge of sectional anatomy, the diagnostic information in the specific region(s) of interest can be altered to best show the patient's condition.

When viewing sectional images, it is important to remember that the image depicts a volume of the body, or what is commonly called a slice of the body (Fig. 1-3). The thickness of the section depends on the technical settings used in generating the sectional images, and usually varies from several millimeters to 1 cm. To visualize all of the structures within a given region of the body, the sections are typically taken in sequence, and the locations are annotated

## 2 Introduction to Sectional Anatomy



**Figure 1-1** Lateral skull radiograph.

on the scanogram or scout image to provide a regional location. Similar to conventional radiographs, your right side should correspond to the patient's left side. For orientation, when viewing axial images you should picture yourself standing at the patient's feet looking up into the body of the



**Figure 1-2** Sagittal MR image of head in median plane.

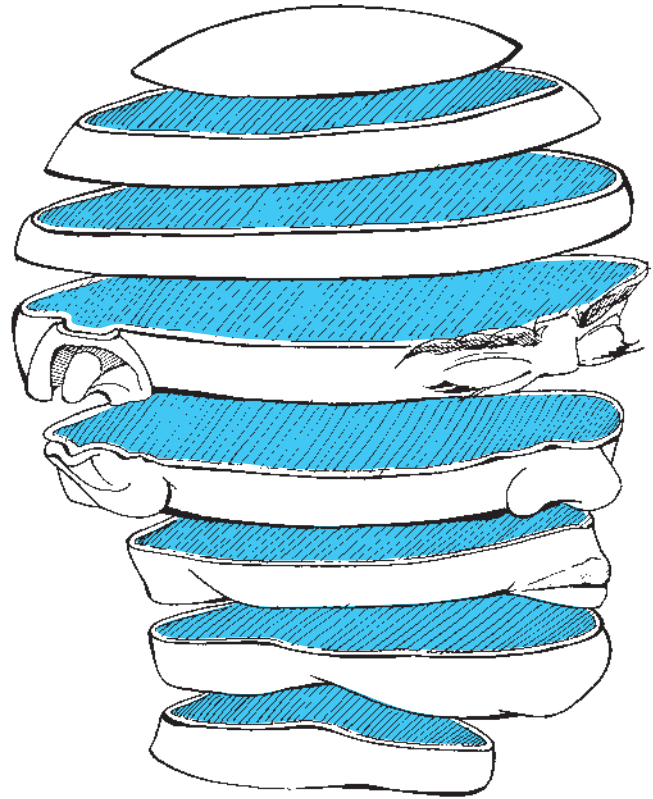


**Figure 1-3** Axial slices through the head.

patient with your right always on the left side of the patient. Although *right* and *left* are simple concepts, keeping the proper orientation on sectional images is critical for correct identification of anatomic structures. Initially, the viewer should emphasize whether the structure is on the left or right side of the body.

When viewing sectional images, the initial impulse is to start in the center of the image and identify eye-catching structures without first discerning the location of the scan within the body. Attempting to identify anatomy without first determining the location of the slice will often result in confusion and errors. Besides the scanogram or scout image that provides general placement, additional information in the image itself can help in more specifically locating the sectioned anatomy. The bones can often provide much of the information necessary to gain a more thoroughly defined perspective. After this perspective is obtained, identification of structures progresses relatively rapidly and accurately, because the appearance of anatomic structures will vary at different levels (Fig. 1-4).

Unlike learning general anatomy, memorization of vertebral levels or sectional images will lead to mistakes, because no two images will ever be the same. Even if the same patient were scanned at the same level, differences in breathing or involuntary movements would result in a slightly different slice of anatomy. If another patient were used and

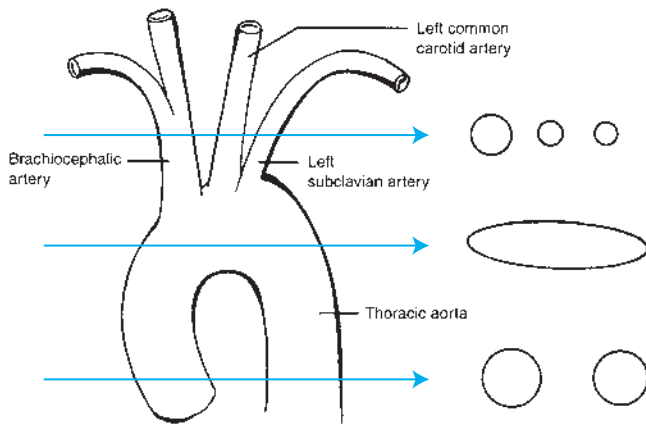


**Figure 1-4** The aortic arch demonstrating differences in axial sections taken at several levels.

scanned at the same level, the differences would be even more evident, because their anatomic arrangement would be somewhat different. For example, when we look at people's faces, we see that everyone has two eyes, one nose, and one mouth; but we don't expect the specific arrangement of these structures to be exactly the same for everyone. Just like on the outside, although most people have two kidneys, one superior vena cava, and one aorta, the specific arrangement of these structures will vary from person to person.

## PLANES OF THE BODY (FIG. 1-5)

**Sagittal** (*SAJ-i-tāl*). A plane extending along the long axis of the body dividing it into right and left sides.

**Median or midsagittal.** A sagittal plane through the body dividing it into equal right and left halves.

**Coronal** (*KÖR-ö-näl*) **or frontal.** A plane extending through the body dividing it into anterior and posterior parts.

**Axial** (*AK-sě-äl*) **or transverse.** A plane extending across or through the axis of the body, extending from side to side, dividing the body into upper and lower portions.

## CLASSIFICATION OF JOINTS

**Synarthrosis** (*SIN-ar-THRÖ-sis*). An immovable joint with no joint cavity. Examples include the sutures of the cranium and the sternocostal joints.

**Amphiarthrosis** (*AM-fi-ar-THRÖ-sis*). Slightly movable joints between two bones.

**Symphysis** (*SIM-fi-sis*). The opposed surfaces of bone are connected through fibrocartilage. Examples include the symphysis pubis and the intervertebral disks.

**Syndesmosis** (*SIN-dez-MÖ-sis*). The fibrocartilage forms an interosseous ligament between the bones. Examples include the inferior tibiofibular articulation and the bones of the infant skull.

**Diarthrosis** (*dī-ar-THRÖ-sis*). A freely movable joint that is lubricated by synovial fluid within the joint space. The joints are surrounded by a fibrous capsule lined with synovial membrane, the articular capsule, which is reinforced by ligaments and muscles extending over the joint.

**Arthrodia** (*ar-THRÖ-dē-ä*). A gliding joint where bones slide face to face and movement is limited by restraining ligaments. Examples include the intercarpal and intertarsal joints.

**Ginglymus** (*JING-gli-mūs*). A hinge joint that allows movement in only one plane. Examples include the elbow and the knee joints.

**Saddle joint.** The opposing bones fit the contour of the other and increase the extent of the hinge movement to include other planes of movement. An example is the first carpometacarpal joint.

**Ellipsoid** (*ē-LIP-soyd*). A modified ball-and-socket joint in which the opposing surfaces are shaped like a spindle or are ellipsoidal instead of being spherical. An example is the wrist joint.

**Trochoid** (*TRÖ-koyd*). A pivot joint that resembles a pulley and allows movement in a partial ring. Examples include the radioulnar joints.

**Enarthrosis** (*en-ar-THRÖ-sis*). A ball-and-socket joint in which the spherical head fits into a cup-like cavity and provides free movement. Examples include the hip and shoulder joints.

## COMPUTED TOMOGRAPHY

In CT, x-rays are used to generate the diagnostic information much like conventional radiography. However, the principle of tomography is used to better visualize overlapping structures. Based on a series of complex mathematical processes, the computer reconstructs the image from a series of digital numbers. The numbers generated are registered on the Hounsfield scale by which bone is +1,000, water is 0, and air is -1,000 (Fig. 1-6). Because CT uses x-rays to generate the image, radiodensity and radiolucency are used to distinguish various tissues within the patient. To enhance the visualization of structures with similar densities, the window level and width can be adjusted to demonstrate only part of the Hounsfield scale.

## MAGNETIC RESONANCE

In MR, the magnetic properties of the hydrogen atoms that constitute 80% of the human body are used to generate data. When the patient is positioned within a strong



#### 4 Introduction to Sectional Anatomy

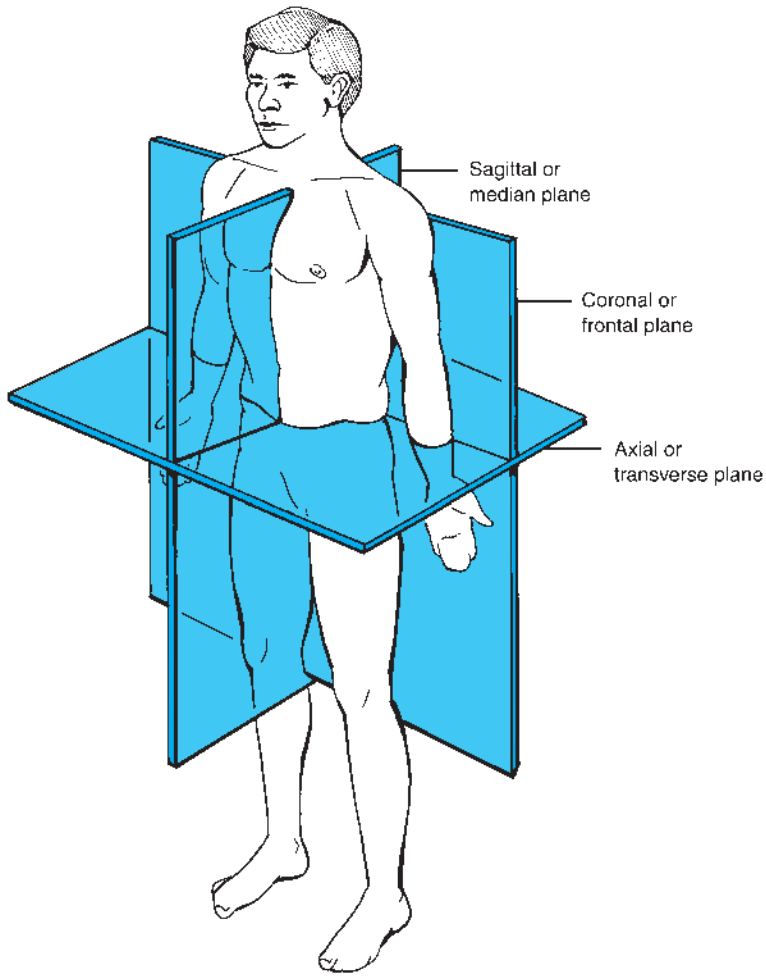


**Figure 1-5** The human body demonstrating planes of section.

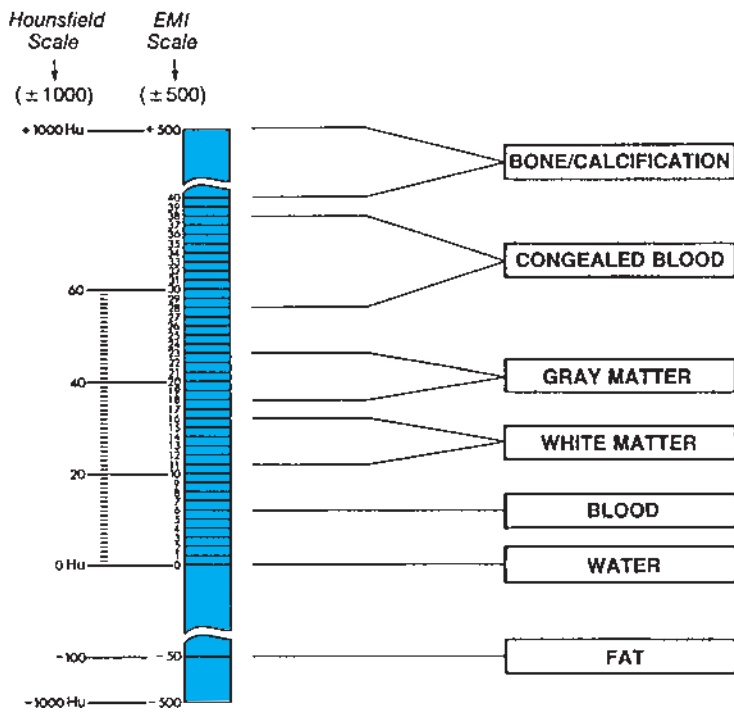


**Figure 1-6** Absorption values common to clinical radiology. The values shown are for the Emergency Medical Information (EMI) and Hounsfield scales.

external magnetic field, the single protons in the hydrogen nuclei align within the field. Radiowaves are then directed at the patient from another angle, causing the nuclei absorbing the energy to flip from their previous positions. Depending on the chemical environment, the hydrogen atoms require different amounts of energy to flip out of the magnetic field. After the termination of the external radio signals, the nuclei within the patient gradually release radio signals as they return to their original state within the magnetic field. Depending on their chemical environment, the hydrogen atoms require different times to return to their original position. The energy released is gathered and used to generate the image; a series of complex mathematical processes produce the digital image. If the technical factors are varied, the signal intensity for a given tissue will change (Fig. 1-7). Similar to CT, adjusting the technical factors can optimize the diagnostic value of the image.

The optimal technical factors depend on the specific MR scanner, and recommended protocols are provided by the manufacturer. To weight an image (Fig. 1-8), the following repetition times ( $T_R$ ) and echo times ( $T_E$ ) are generally used:

T1 weighted images are generated with a short  $T_R$  (250–1,100 ms) and a short  $T_E$  (10–25 ms).

T2 weighted images are generated with a long  $T_R$  (2,000 + ms) and a long  $T_E$  (60 + ms); this setting often better demonstrates pathologies.

## ULTRASOUND

Ultrasound imaging, also called ultrasound scanning or sonography, is a method of obtaining images from inside the human body through the use of high-frequency sound waves. The reflected sound wave echoes are recorded and displayed as a real-time visual image. The ultrasound transducer functions as both a generator of sound (like a speaker) and a detector (like a microphone). When the transducer is pressed against the skin it directs inaudible, high-frequency sound waves into the body. As the sound echoes from the body's fluids and tissues, the transducer records the strength and character of the reflected waves. These echoes are instantly measured and displayed by a computer, which in turn, creates an image of the patient's anatomy (Fig. 1-9).

## POSITRON EMISSION TOMOGRAPHY COMBINED WITH COMPUTED TOMOGRAPHY

The CT scan, using x-ray and measuring signals on the Hounsfield scale, provides a detailed picture of the internal

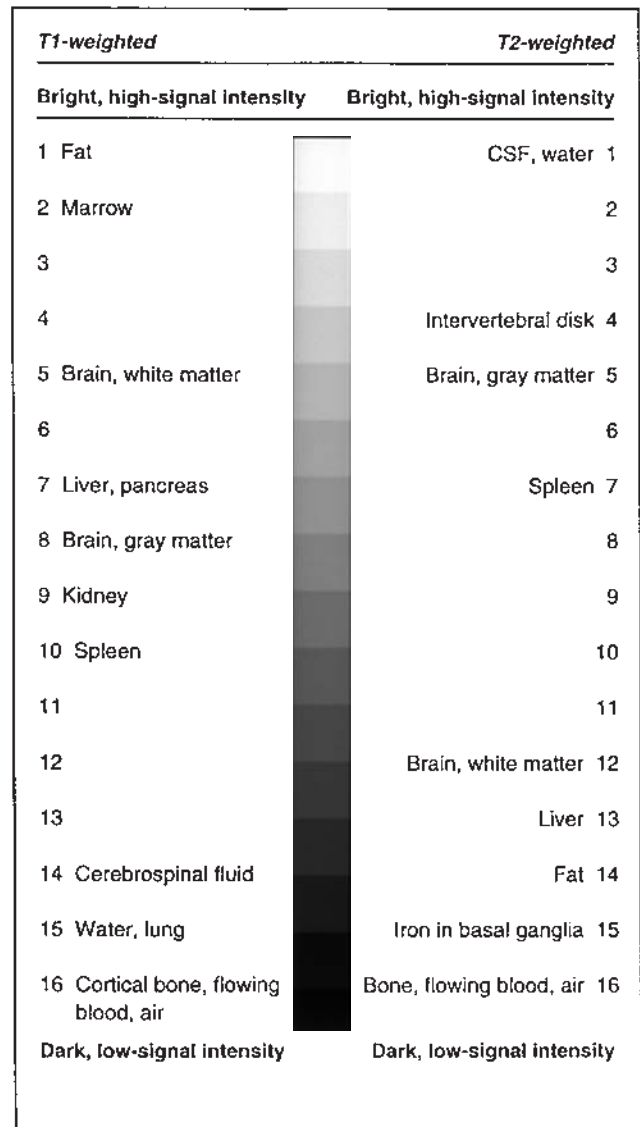
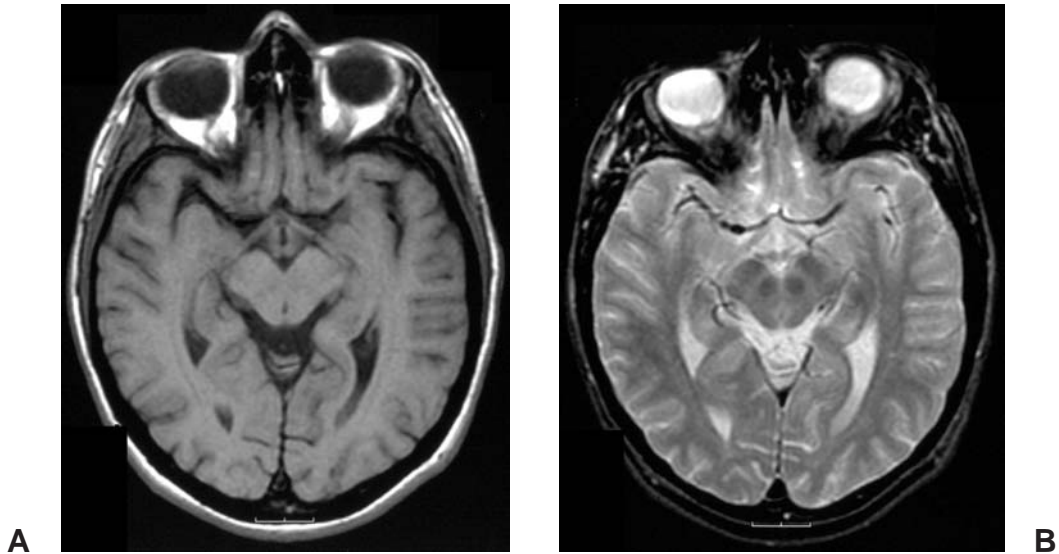


Figure 1-7 Comparison of signal intensities in data generated by T1 versus T2 weighting.

anatomy that reveals the size and shape of abnormal cancerous growths. By comparison, the highly sensitive PET scan picks up the metabolic signal of actively growing cancer cells in the body. This is accomplished by injecting a form of glucose (a crystalline sugar) called FDG into the patient. Rapidly growing cancer cells consume FDG at a very fast rate, and the PET/CT scanner detects the areas of high consumption, mapping them in fine detail to identify both the presence of disease and its precise location. In addition to being a highly sophisticated tool in the early detection of disease, the PET/CT can provide a precise staging and localization of disease progression and accurately monitor the effects of therapy on a patient's body (Fig. 1-10).

6 Introduction to Sectional Anatomy



**Figure 1–8** Even though both MR images are of the same axial section of anatomy, the contrast is substantially different due to changes in technical factors. The image on the left is classified as a T1 weighted image, which is characterized as a bright or high signal from fat (found behind the eyes and under the skin) with weak or low signal from water (dark inside eyes and ventricles). By comparison, the T2 weighted image shown on the right has a weak or low signal from fat and a bright or high signal from water. Typically, T1 images are used to visualize normal anatomy whereas T2 images are used to show pathology, as fluid often accumulates at the site of an injury.

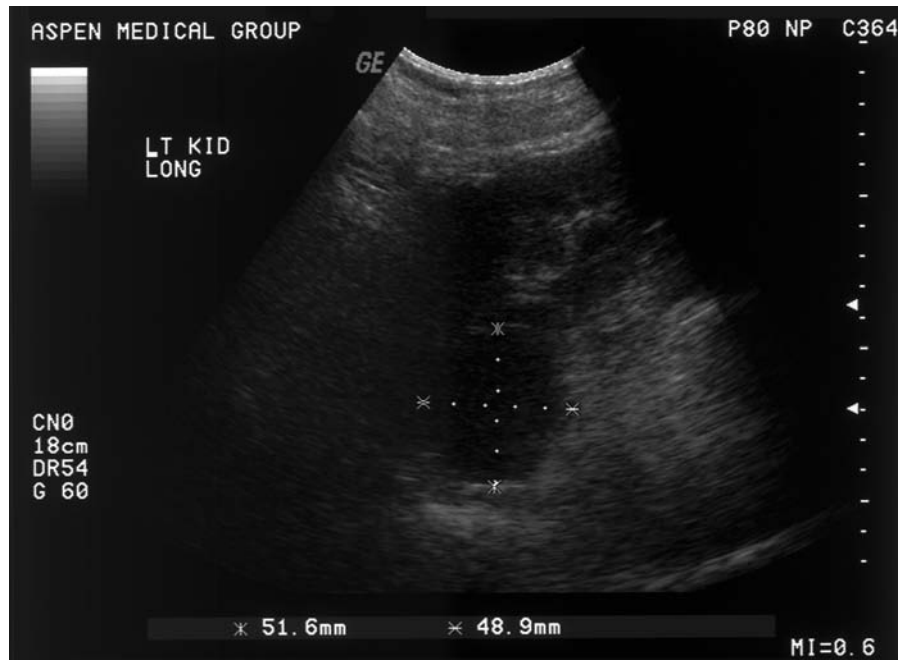


**Figure 1–9** Ultrasound examination of this 76-year-old black female patient generated this image through the longitudinal axis of the left kidney. As shown by the marked measurements, there is a large, fluid-filled, spherical structure originating from the kidney measuring 51.6 mm × 48.9 mm representing a large, simple renal cyst. As shown in this example, ultrasound provides a very effective and noninvasive method for evaluating fluid-filled structures.

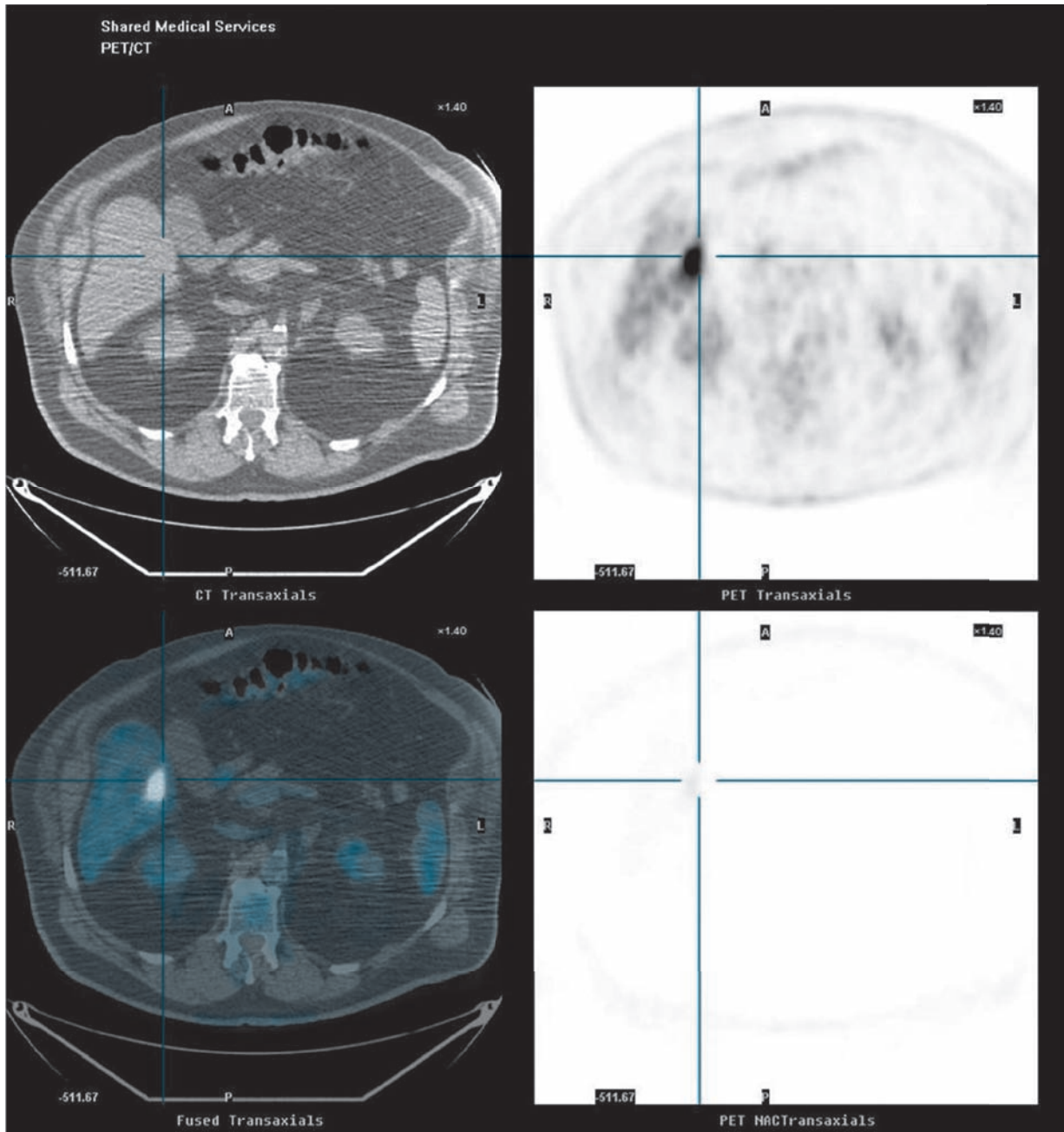
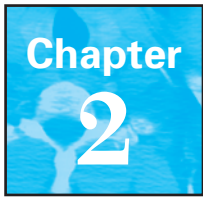


**Figure 1-10** A composite image providing a representative series of axial images generated with Positron Emission Tomography Combined with Computed Tomography (PET/CT). In the upper right quadrant, the PET image is used to evaluate glucose metabolism; areas with a high level of activity, such as those found in actively growing cancer, will appear dark as compared to the surrounding tissues. In the upper left quadrant, the CT image has much better resolution and contrast so the liver, kidneys, spine, etc. can now be seen within this section. In the lower right image, the image represents a PET NAC (non-attenuated corrected) image which is useful primarily in evaluating skin lesions. In the lower left quadrant, the PET is fused with the CT to create an image with the combined information from both, PET/CT, with locator lines correlating a specific region within all four images. In this 65-year-old white male, the high glucose metabolism located within the liver is evidence of metastatic disease that originated from the primary site in the colon.



## CLINICAL APPLICATIONS

1. Describe what part of the patient is shown in a sectional image.
2. When viewing an axial section with the patient in the supine position, the right side of the patient will be on the \_\_\_\_\_ side of the image.
3. A plane or section dividing the body into anterior and posterior parts is classified as \_\_\_\_\_.
4. A gliding joint where bones slide face to face and movement is limited by restraining ligaments is classified as \_\_\_\_\_.
5. \_\_\_\_\_ is the classification of a freely moving joint that is lubricated by synovial fluid within the joint space.
6. A ball-and-socket joint in which the spherical head fits into a cup-like cavity and provides free movement would be classified as \_\_\_\_\_.
7. On the Hounsfield scale, air has a value of \_\_\_\_\_, water of \_\_\_\_\_, and bone of \_\_\_\_\_.
8. In an MR image, a \_\_\_\_\_-weighted image will have a bright or high signal from fat.
9. In a PET scan, the cellular consumption of \_\_\_\_\_ is measured and used to create diagnostic images.
10. Briefly describe how ultrasound is used to make diagnostic images.



# Chest

## OBJECTIVES

Upon completion of this chapter, the student should be able to:

1. Describe the superior and inferior boundaries of the chest.
2. Describe the level of the three parts of the sternum as compared to the viscera or thoracic vertebrae.
3. List the number of floating, false, and true pairs of ribs in the chest.
4. Describe the structures separating the mediastinum and the pleural cavities.
5. Correctly identify the chambers of the heart on sectional images.
6. Identify and describe the airway structures within the chest.
7. Follow the course of blood as it passes through the pulmonary circulation system.
8. Describe the major arteries and veins located within the chest and upper arm.
9. Explain the relationships between structures within the mediastinum.
10. Correctly identify anatomic structures on patient computed tomography (CT) and magnetic resonance (MR) images of the chest.

## ANATOMIC OVERVIEW

The chest or thorax is the region of the bony thoracic cage located between the neck and the abdomen. The upper boundary of the chest, the thoracic inlet, is formed by the first thoracic vertebra, the first ribs, and the upper margin of the manubrium. Inferiorly, the chest extends to the level of the thoracic outlet, marked by the diaphragm, which extends between the inferior margin of the sternum and the upper lumbar vertebrae.

### ■ Skeleton

**Thoracic** (*thō-RAS-ik*) **vertebra**. In the chest, 12 thoracic vertebrae are found in the vertebral column and form the posterior border of the thoracic cage (Fig. 2-1). Compared to other vertebrae, they are average in size and are distinguishable by costal facets for articulation with the ribs. As with other vertebrae, each can be divided into two parts: a body and a vertebral arch.

**Vertebral** (*VER-tě-brāl*) **body**. The largest and heaviest portion of the vertebra, located anterior to the vertebral arch, forming the anterior margin of the vertebral foramen.

When viewed from either the lateral or superior aspect, it is seen anterior to the vertebral foramen. The shape, however, is significantly different in the two views: In the lateral view, the body is wedge shaped, but when viewed from above, it has an oval shape.

**Vertebral arch**. All the vertebral structures except the body are considered part of the vertebral arch. More specifically, it consists of two pedicles, two laminae, and seven processes (two transverse, four articular, and one spinous).

**Pedicles** (*PED-ĭ-klz*). The bony projections forming the lateral walls of the vertebral foramen; they connect the vertebral body to the transverse processes.

**Laminae** (*LAM-i-nē*). The remainder of the vertebral arch is formed by the laminae, which form the posterolateral walls of vertebral foramen, connecting the transverse processes with the spinous process.

**Clavicles** (*KLAV-i-klz*). Commonly called the collar bones. The clavicle forms part of the shoulder girdle, connecting the acromion process of the scapula with the manubrium of the sternum (Figs. 2-2 and 2-3). Owing to the horizontal course of this long bone, axial sections through the upper chest demonstrate the clavicle in longitudinal section.



10 Introduction to Sectional Anatomy

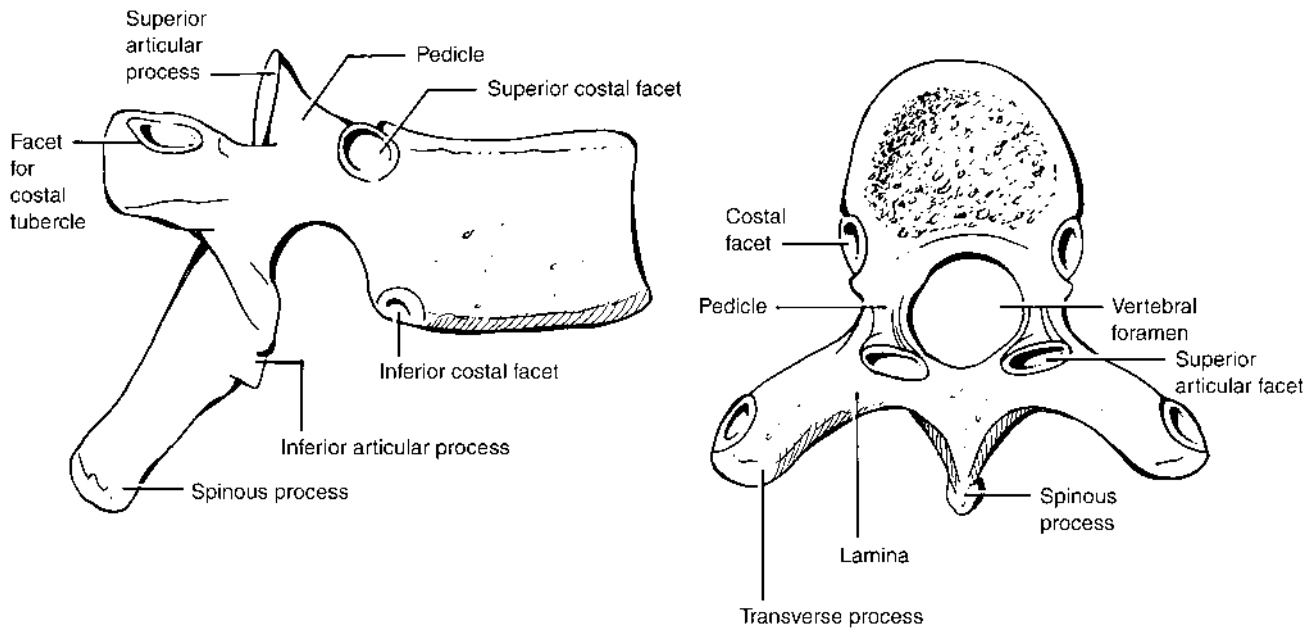


Figure 2-1 Lateral and superior views of a thoracic vertebra.

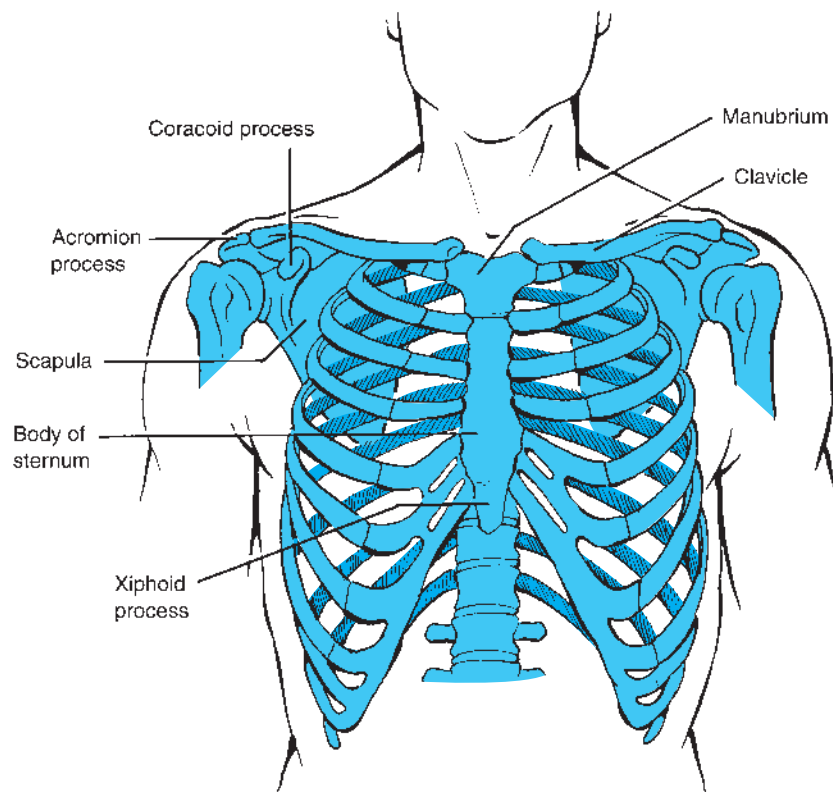
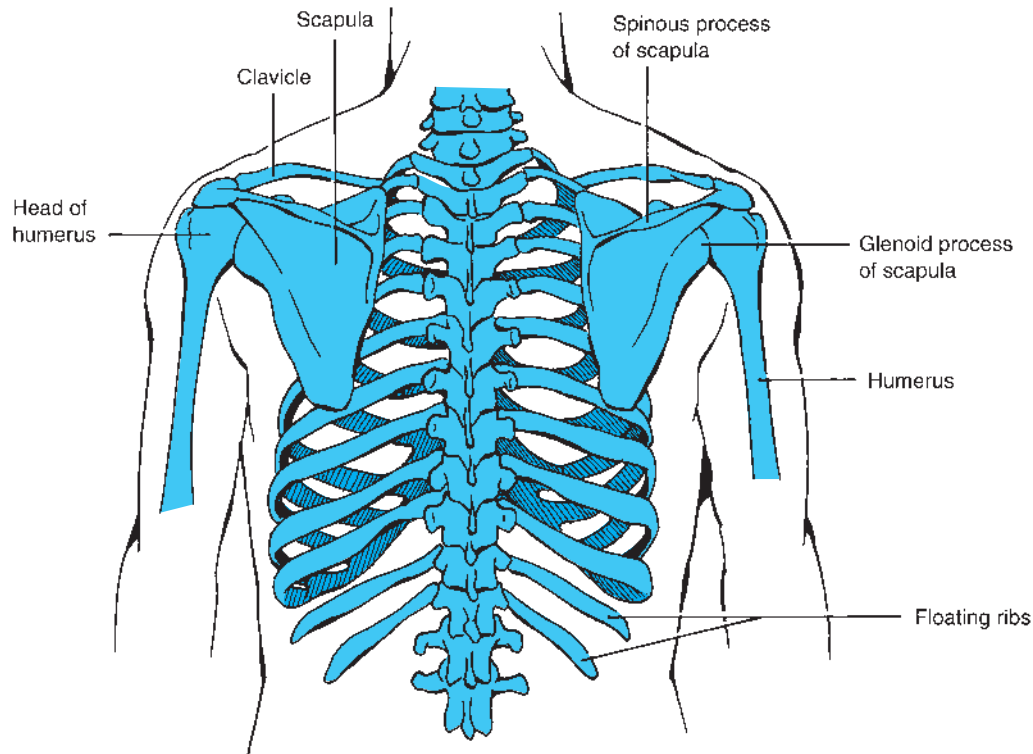


Figure 2-2 Anterior view of the bony chest and shoulder.



**Figure 2-3** Posterior view of the bony chest and shoulder.

**Humeri** (*HYŪ-mer-ī*). The bones within the upper arms; the longest and largest bones of the upper limbs. On the proximal end of the humerus, the shoulder joint is formed by the head of the humerus and the glenoid process of the scapula.

**Scapulae** (*SKAP-yū-lē*). Frequently called the shoulder blades. They are located bilaterally along the posterolateral margin of the thoracic cage. Considered part of the shoulder girdle, the scapula articulates with the humerus to form the shoulder joint. The broad, flat bone is roughly triangular in shape and contains the following features.

**Acromion** (*ā-KRŌ-mē-on*) process. The part of the bone that projects over the top of the shoulder joint and articulates with the lateral end of the clavicle.

**Coracoid** (*KŌR-ā-koyd*) process. The bony projection on the anterior surface of the scapula found just inferior to the lateral clavicle. Its primary function is to provide a site of attachment for the pectoralis minor muscle.

**Glenoid** (*GLĒ-noyd*) process. The bony projection from the lateral margin of the scapula that forms the socket for the head of the humerus.

**Sternum**. The elongated, flat bone forming the anterior wall of the thoracic cage (Fig. 2-2). The sternum is divided into three parts.

**Manubrium** (*mū-NU-brē-ŭm*). The roughly quadrangular-shaped bone forming the superior division of the ster-

num. The superior margin, the jugular notch, can be easily palpated along with the distal ends of the clavicles where they articulate with the superolateral margins of the manubrium. It is generally located at the level of the 3rd and 4th thoracic vertebrae.

**Body**. The middle division of the sternum is long and slender and is generally at a level of the 5th to 9th thoracic vertebrae. The juncture of the body with the inferior margin of the manubrium, called the sternal angle, is often palpable and corresponds to the intervertebral disk between the 4th and 5th thoracic vertebrae.

**Xiphoid** (*ZIF-oyd*) process. The most inferior portion of the sternum is small and often bifid in shape. The process is easily located as the lower margin of the bony thoracic cage in the median plane and corresponds to approximately the 9th thoracic vertebrae.

**Ribs**. There are 12 pairs of ribs in the chest: Seven true and five false, two of which are floating. In general, the long slender bones all articulate with the respective thoracic vertebra and are curvilinear in shape (Figs. 2-2 and 2-3). As the ribs extend from the vertebrae, they slope downward toward their anterior ends. This downward slope of the ribs causes them to be obliquely sectioned in axial images.

**False ribs**. The 8th to 12th pairs of ribs are not considered true ribs because they do not articulate with the



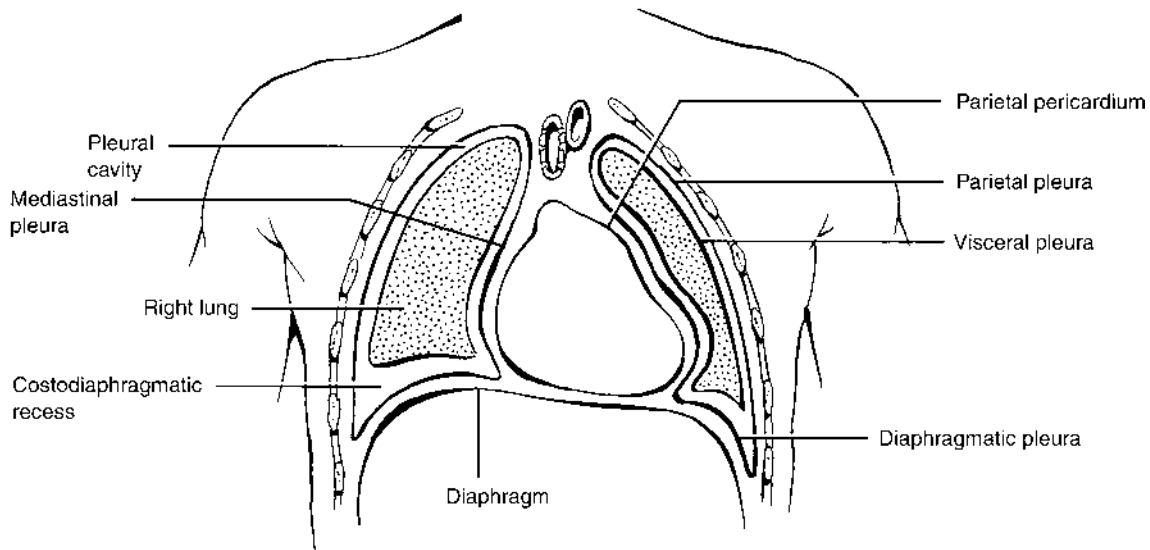


**Figure 2-4** Coronal section through the chest demonstrating the enclosing structures.

sternum. The 8th, 9th, and 10th pairs of ribs articulate with the costal cartilage of the ribs above. The 11th and 12th pairs of ribs also are considered floating because they articulate only posteriorly with the vertebrae. Similar to all the other ribs, the floating ribs generally move downward toward their lateral ends and will be obliquely sectioned in axial images.

### ■ Enclosing Structures

**Mediastinal** (*MĒ-dē-as-TĪ-nāl*) **pleura.** The thick connective tissue membrane that surrounds the region between the lungs, encompassing the heart, the great vessels, and the major divisions of the bronchial tree (Figs. 2-4 and 2-5).

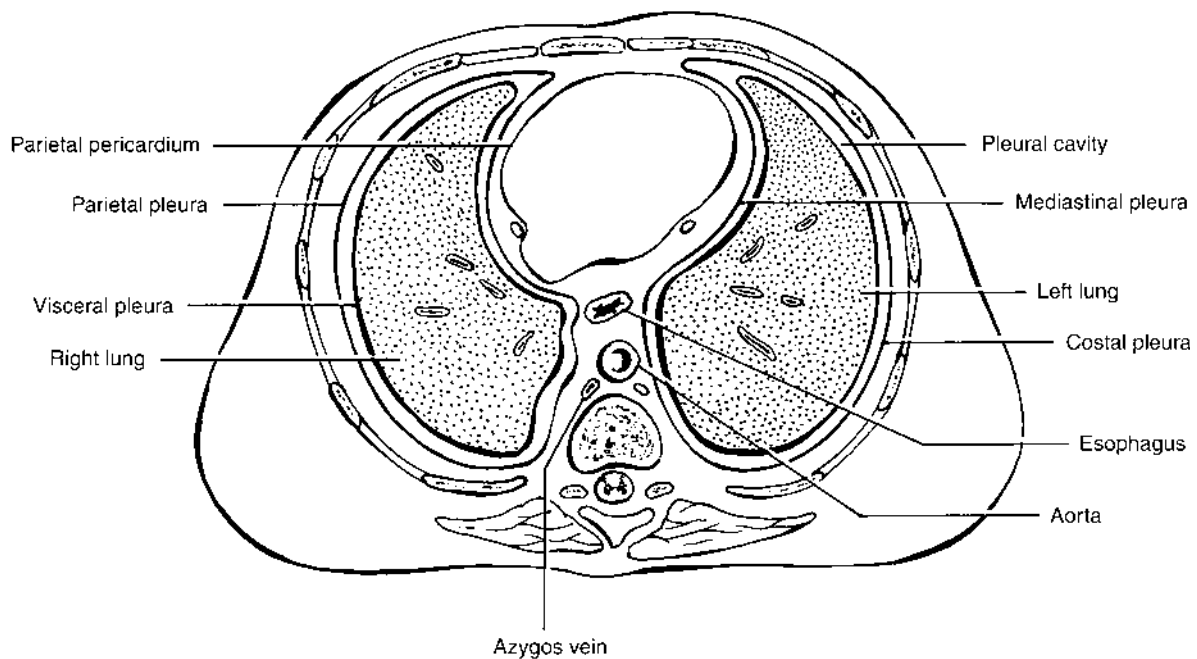


**Figure 2-5** Axial section through the chest demonstrating the enclosing structures.

**Pericardium** (*per-i-KAR-dē-ŭm*). Within the mediastinum, the pericardium is a tough fibrous sac surrounding the heart and separating it from the other mediastinal structures. It has two layers: The parietal pericardium, or the tougher outer layer, and the visceral pericardium, which lines the entire surface of the heart and extends several centimeters along the base of the great vessels until they pass through the parietal pericardium. Regarding function, both the visceral and parietal layers have facing serous membranes that provide a smooth, lubricated surface between the two constantly moving structures.

**Diaphragm** (*DĪ-ă-ſram*). This dome-shaped muscular sheet forms a convex floor for the chest and serves as a septum between the thoracic and abdominal cavities. Its periphery has broad, flat muscle fibers that converge on a central region of dense connective tissue, the central tendon.

**Pleura** (*PLŪR-ă*). There are two separable pleural membranes in the chest: The parietal (*pă-RĪ-ě-tăł*) pleura lines the inside of the thoracic musculoskeletal wall, and the visceral pleura surrounds the surface of the lungs. Together, the pleural membranes reduce friction between the constantly moving lungs and thoracic musculoskeletal structures.

The following spaces are between the pleural membranes.

**Pleural cavity.** The space filled with small amounts of serous fluid situated between the pleural membranes. In some pathologic conditions, fluid or blood outside the lungs accumulates in this space and limits respiration (e.g., pleurisy).

**Costodiaphragmatic** (*kos-tō-DĪ-ă-ſrag-MAT-ik*) **recesses.** The most inferior regions of the pleural cavity at the juncture of the ribs with the posterolateral margins of the diaphragm. In the erect position, fluid within the pleural cavity will be concentrated within the recesses.

## ■ Airway Structures

**Right lung.** The lung on the right side has three lobes: upper, middle, and lower (Fig. 2-6). Although this nomenclature describes the position of the lobes with respect to one another, as shown in a lateral view (Fig. 2-7), it would be incorrect to assume that the middle lobe separates the upper and lower lobes. In an axial section through the upper lung, both the upper and lower lobes are often demonstrated, with the lower lobe being more posterior.

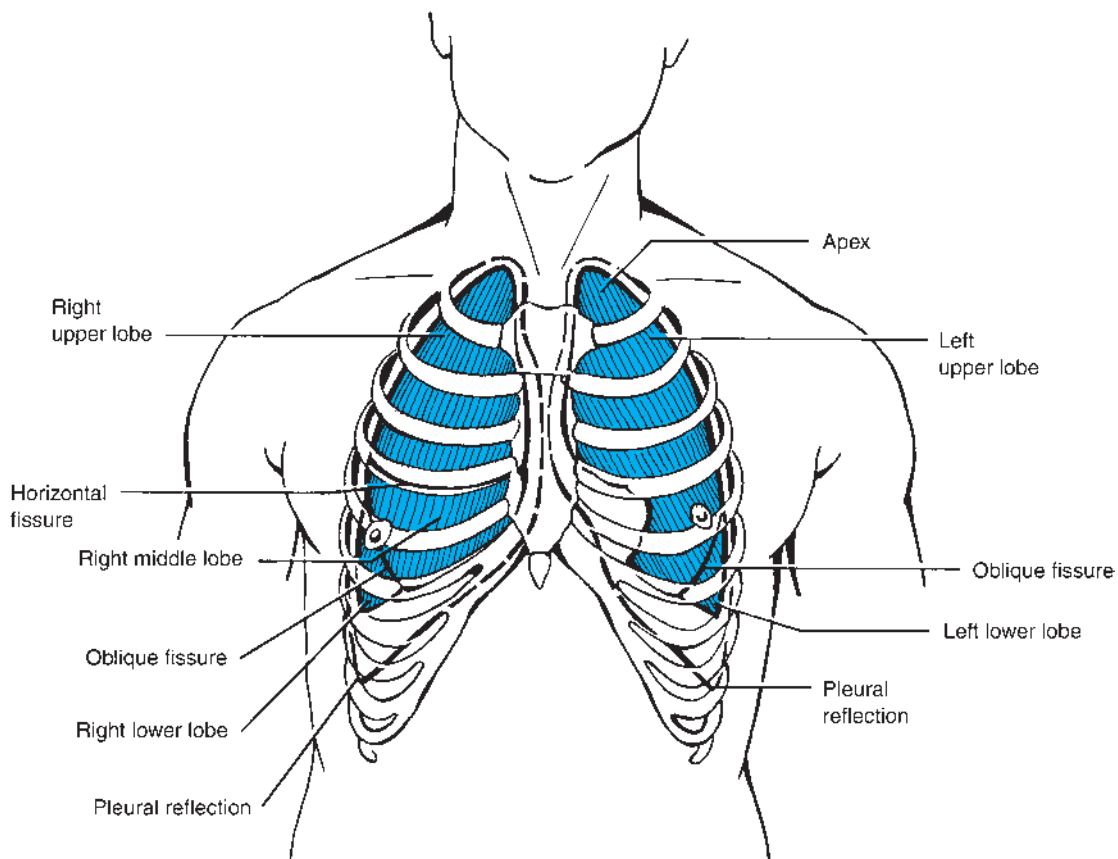


**Figure 2-6** Anterior view of the chest demonstrating the lobes of the lungs.

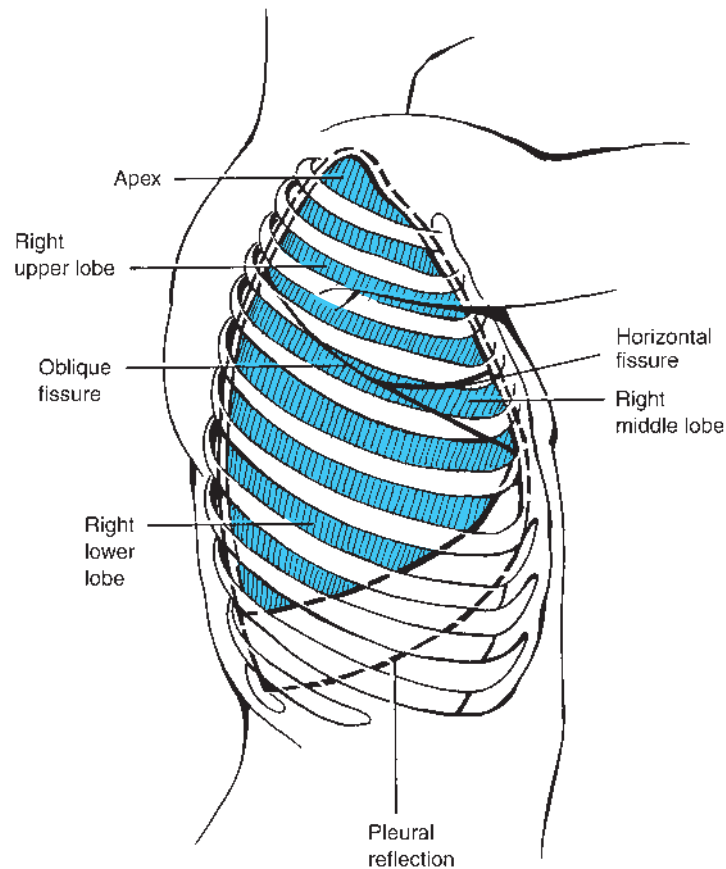


**Figure 2-7** Lateral view of the right lung demonstrating the location of the superior, middle, and inferior lobes.

**Oblique (*ob-LĒK*) fissure.** The space separating the upper and middle lobes from the lower lobe of the right lung.

**Horizontal fissure.** The space separating the upper and middle lobes of the right lung.

**Left lung.** The lung on the left side has two lobes: upper and lower (Figs. 2-6 and 2-8). The nomenclature describes the position of the lobes within the lung. However, in axial sections through the middle of the lung, both lobes will be seen. Because of the course of the oblique fissure, the upper lobe will be more anterior than the lower lobe.

**Hilum (*HĪ-lūm*).** A region near the center on the medial aspect of both the right and left lungs where the bronchi, veins, and arteries enter and exit the lungs next to the heart.

**Trachea (*TRĀ-kē-ă*).** The most superior airway structure in the chest, the trachea extends inferiorly from the larynx, located within the neck, until it bifurcates into the right and left main bronchi (Fig. 2-9). Although the exact level may vary, the trachea terminates at the level of the 5th or 6th thoracic vertebra. Compared to other structures within the region, the trachea is posterior to the great vessels and anterior to the esophagus.

**Carina (*kă-RĪ-nă*).** At the terminal end of the trachea, a ridge extends superiorly, originating the bifurcation of the trachea into the right and left main bronchi. Although the level may vary among individuals, the carina is seen near the level of the pulmonary artery. In an axial section through the terminal trachea, the carina can often be seen within the center of the opening dividing the right and left bronchi.

**Main bronchi (*BRONG-kī*).** The principal divisions of the trachea, dividing the airway into right and left halves. Note that the right main bronchus is the larger and more vertical of the two. Both main bronchi are just posterior to the pulmonary arteries at a level of the 6th or 7th thoracic vertebra.

**Upper lobe bronchi.** The first division of the main bronchi on both the right and left sides, the upper lobe bronchi transport air to and from the superior lobes of the lungs. The right upper lobe bronchus originates more superiorly than does the left.

**Bronchus intermedius.** The other major branch of the right main bronchus that divides to give rise to both the middle and lower bronchi.

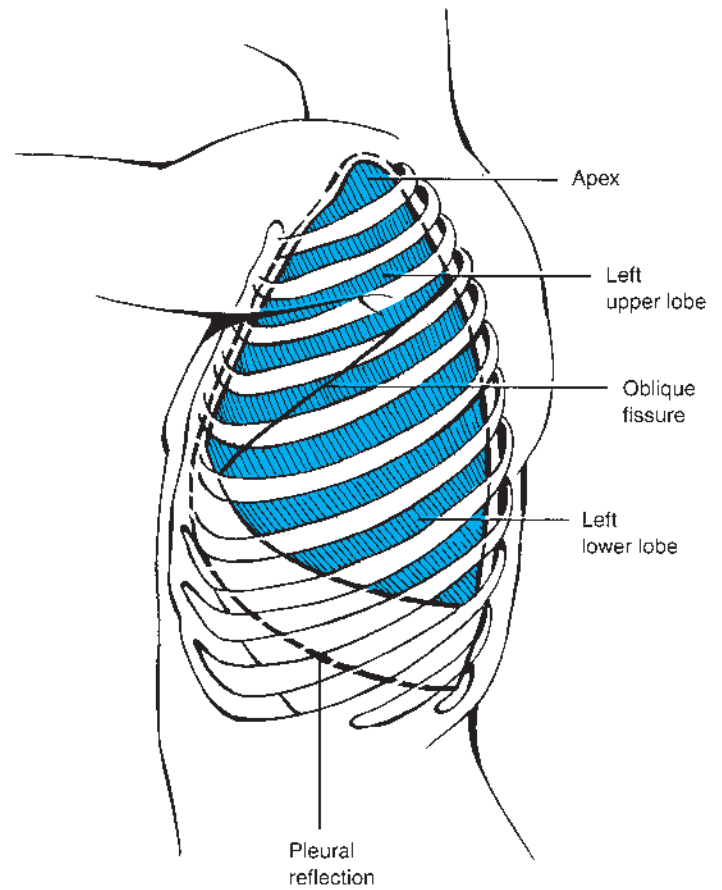


**Figure 2-8** Lateral view of the left lung demonstrating the superior and inferior lobes.

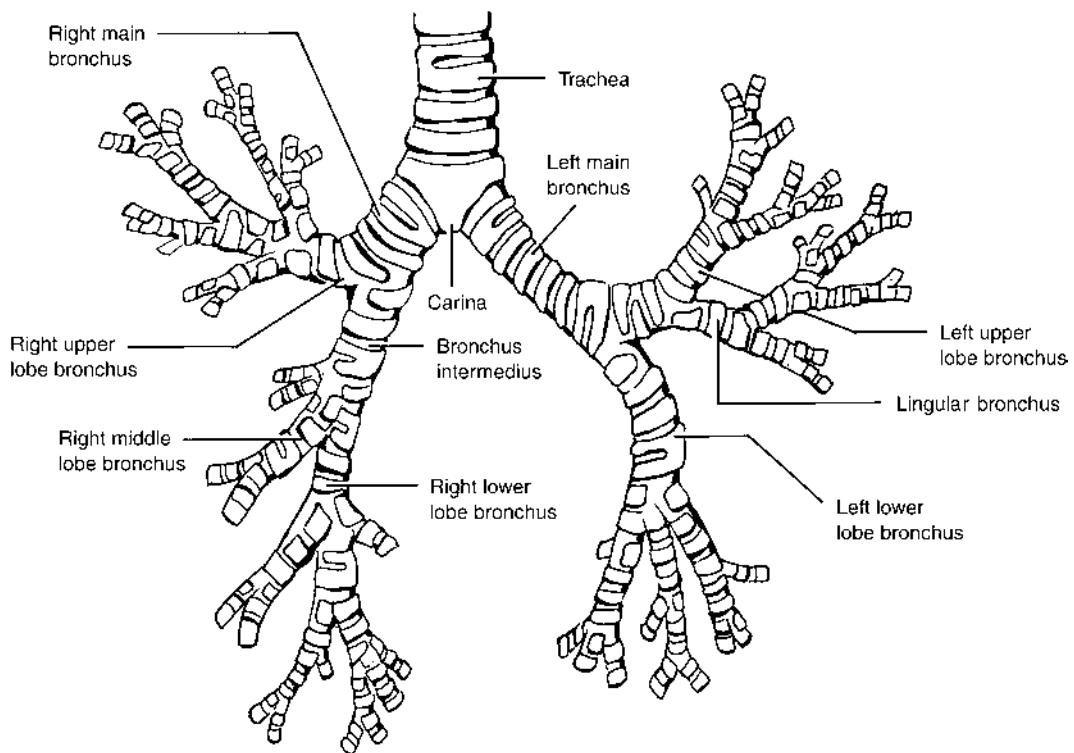


**Figure 2-9** Divisions of trachea and bronchial tree.

**Middle lobe bronchus.** This airway structure is found on the right side as it branches from the bronchus intermedius to transport air to and from the middle lobe of the lung.

**Lower lobe bronchi.** Air is transported to and from the inferior lobes of the lungs via the lower lobe bronchi on both the right and left sides.

### ■ Other Viscera (*VIS-er-a*)

**Heart.** The heart contains four chambers: the right atrium, the right ventricle, the left atrium, and the left ventricle (Fig. 2-10). Although this nomenclature implies that the chambers are located on either the right side or left side, the in vivo chambers of the heart are not truly arranged in this simple fashion (Fig. 2-11). Because the heart rests on the diaphragm, the apex of the heart is shifted toward the left side, placing the right ventricle of the heart in front of the left. In sectional images, the chambers appear skewed off-center, with the right ventricle being the most anterior chamber of the heart and the left atrium being most posterior.

**Right atrium** (*Ā-trē-ŭm*). The drainage point of the superior and inferior vena cavae, it pumps venous blood into

the right ventricle through the tricuspid valve (Fig. 2-10). Within the mediastinum, the right atrium is on the right side of the heart slightly above the ventricles.

**Right ventricle.** This chamber receives venous blood from the right atrium during relaxation. During contraction, the chamber pumps blood into the pulmonary trunk through the pulmonary semilunar valve. In the chest, this chamber of the heart is the most anterior and forms most of the anterior surface of the heart inferior to the right atrium (Fig. 2-11).

**Left atrium.** This chamber receives blood from the four pulmonary veins and pumps it into the left ventricle through the mitral or bicuspid valve. Within the chest, the left atrium is the most posterior chamber at approximately the level of the right atrium.

**Left ventricle.** This chamber receives blood from the left atrium and pumps it into the aorta through the aortic semilunar valve. In the body, this chamber is farthest to the left side of the heart and lies posterior to much of the right ventricle.

**Esophagus** (*ē-SOF-ă-gŭs*). This gastrointestinal tube extends from the pharynx to the stomach. In the upper

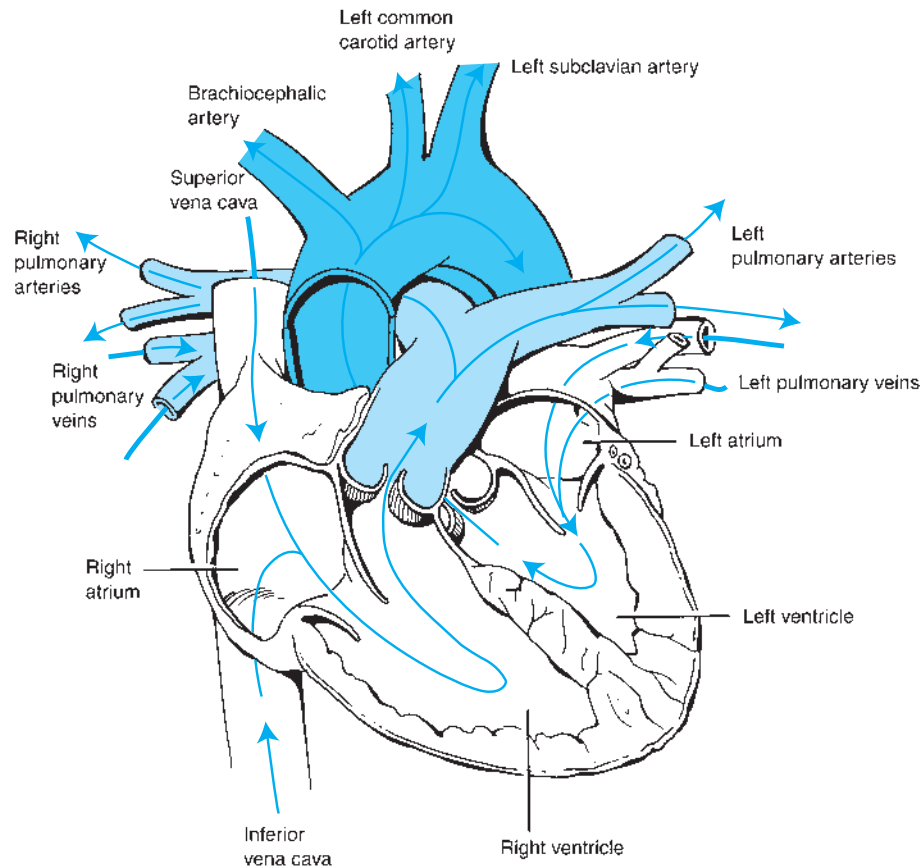


**Figure 2-10** Traditional view of the heart demonstrating the four chambers, valves, openings, and major vessels with arrows indicating the direction of blood flow.

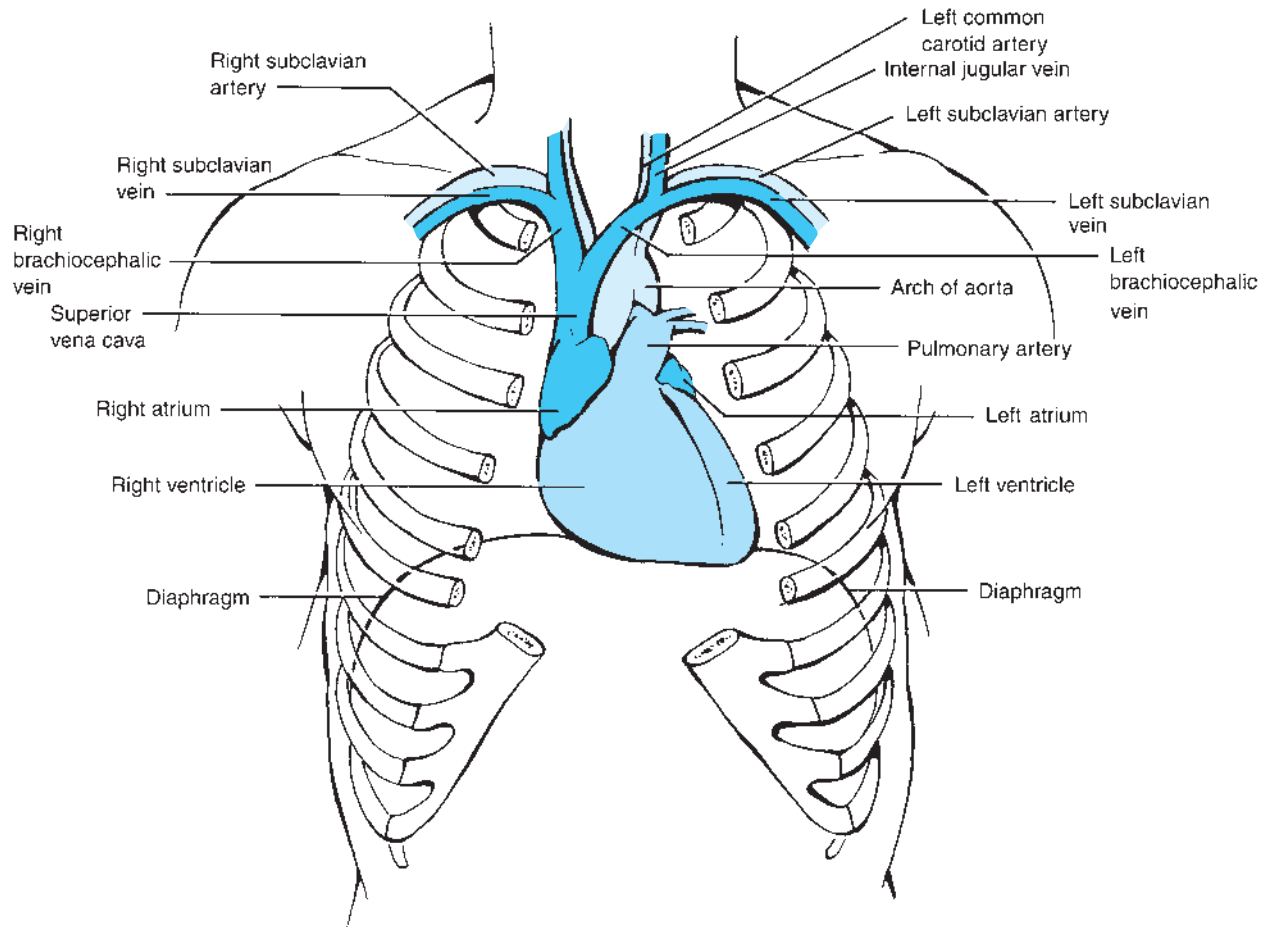


**Figure 2-11** Topography of the heart and great vessels as found in the chest.

mediastinum, the esophagus lies in the midline between the trachea and vertebral column. Below the level of the trachea, the esophagus occupies a position between the heart and vertebral column.

## ■ Arteries

The major arterial structures within the body are within the mediastinum and are adjacent to corresponding venous structures (Fig. 2-12). In the upper mediastinum, the adjacent veins are more superficially located than the corresponding arteries.

**Aorta** (*ā-ŌR-tā*). This major artery is the largest in the body and originates from the left ventricle. The thoracic aorta is divided into three parts.

**Ascending aorta.** The first portion of the artery ascending from the heart. Although originating from the left ventricle, the ascending aorta in an axial image is superior to the right ventricle and next to the superior vena cava.

**Aortic arch.** The second arch-shaped portion of the artery that curves over the pulmonary trunk. This seg-

ment originates from the ascending aorta on the right side of the heart and arches toward the left side to form the descending thoracic aorta. The arch of the aorta passes over both the pulmonary trunk and left main bronchus.

**Descending aorta.** The last segment of the thoracic aorta between the aortic arch and the abdominal aorta. This major artery descends along the left side of the thoracic vertebrae in the posterior mediastinum.

**Brachiocephalic** (*BRĀ-kē-ō-se-FAL-ik*) **artery.** The first major branch off the aortic arch; it extends to the right and divides into the right subclavian and the right common carotid arteries. Note that there is no left brachiocephalic artery, because the aorta arches to the left side of the body and gives rise to the branches that would have been derived from the left brachiocephalic artery.

**Common carotid** (*ka-ROT-id*) **arteries.** The arteries on either side of the trachea that supply arterial blood to much of the head and neck. Although both arteries have the same structure and location, their origins differ, because the right



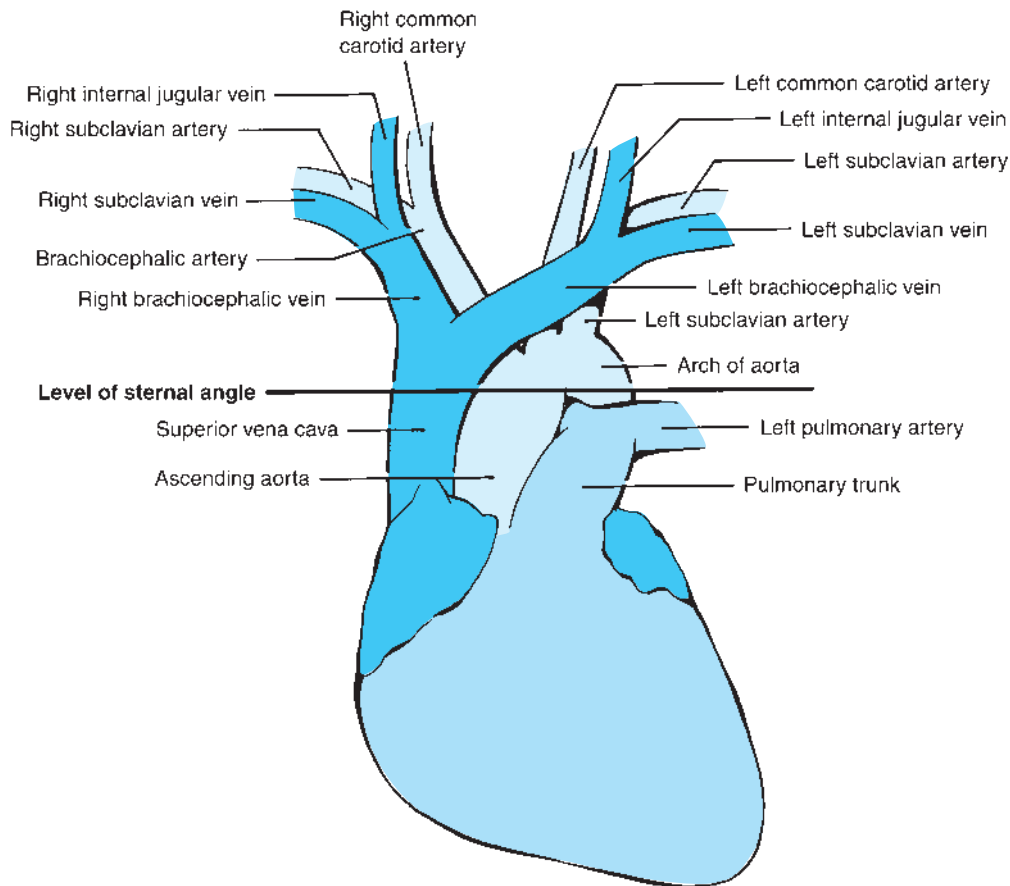


**Figure 2-12** The heart and great vessels seen anteriorly.

artery originates from the brachiocephalic artery and the left artery is the second major branch off the aortic arch.

**Subclavian** (*sŭb-KLĀ-vĕ-an*) **arteries.** Similar to the common carotid arteries, these arteries are bilateral with the same structure and function but have different origins. On the right side, the subclavian artery arises from the brachiocephalic artery. On the left side, the subclavian artery is the third major branch off the aortic arch. Compared to the common carotid arteries, the subclavian arteries are more laterally located and ascend through the upper thorax to exit through the thoracic inlet to form the axillary arteries (Fig. 2-13).

**Axillary** (*AK-sil-ĕ-ĕ*) **arteries.** The bilateral arterial structures that supply blood to the pectoral girdle and arm. As just described, the axillary arteries originate from the subclavian arteries at the level of the first rib. In axial images through the upper chest, the axial vessels are seen longitudinally sectioned outside the ribs, extending toward the region of the shoulder.

**Vertebral arteries.** From the subclavian arteries, the arteries are found bilaterally and run superiorly through the foramen transversarium of the cervical vertebrae. At

the level of the skull, they enter the cranium through the foramen magnum to supply the posterior part of the brain with arterial blood.

**Main pulmonary** (*PŪL-mō-nār-ĕ*) **artery or trunk.** This major artery from the right ventricle moves posteriorly as it ascends to form the right and left pulmonary arteries (Fig. 2-14). Together, the pulmonary trunk and the pulmonary arteries form the characteristic T-shape of the pulmonary arteries. The pulmonary trunk lies below the aortic arch and in front of the esophagus.

**Pulmonary arteries.** Arteries located bilaterally and arising from the pulmonary trunk; they carry deoxygenated blood to the lungs. The pulmonary arteries are the only arteries in the body that carry deoxygenated blood.

## ■ Veins

**Superior vena cava** (*VĒ-nă KĀ-vă*). The major vein located on the superior aspect of the right side of the heart adjacent and slightly posterior to the ascending aorta (Fig. 2-15). It is above the right atrium and lies anterior to

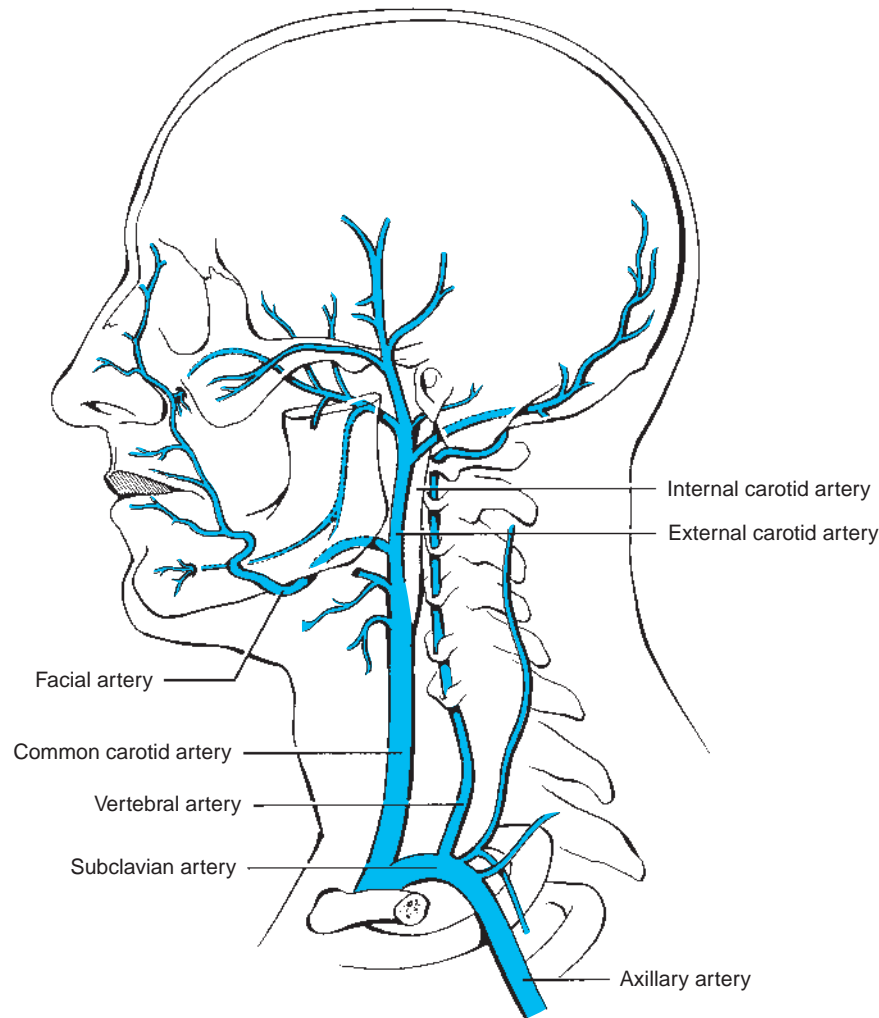


**Figure 2-13** Location of arteries exiting the thoracic cage.

the right pulmonary artery and the right main bronchus. Regarding function, this major vein drains blood from the upper trunk into the right atrium.

**Brachiocephalic veins.** Bilateral veins that originate at the juncture of the internal jugular veins and the subclavian veins; they drain into the superior vena cava. Compared to the adjacent arteries, the veins are more superficial and are found at or above the level of the aortic arch. Although the veins are markedly similar, the course of the right vein is much more vertical than that of the left vein. In an axial section, the oblique course of the left vein will often result in an oblique section, whereas the right vein will be shown as a transverse section.

**Subclavian veins.** Bilateral veins that are continuations of the axillary veins originating from the upper limb and shoulder girdle. The veins begin at the thoracic inlet as they cross over the first rib and drain into the brachiocephalic

veins. Found within the lateral parts of the upper mediastinum, the veins lie just anterior to the adjacent subclavian arteries.

**Axillary veins.** Serve to drain venous blood from the upper extremity and shoulder girdle on both sides of the body. The veins terminate as they cross over the first ribs to join the subclavian veins. Similar to that of the subclavian vessels, the course of the veins is superficial to the adjacent axillary arteries.

**Internal jugular (*JŪG-yū-lar*) veins.** The bilateral veins originate from the sigmoid sinuses inside the skull and drain most of the venous blood from the brain. The veins descend deep in the neck, superficial to the common carotid arteries, and drain into the brachiocephalic veins.

**Azygos (*AZ-ī-gos*).** A vein in the right posterior thoracic cage adjacent to the right side of the vertebral bodies



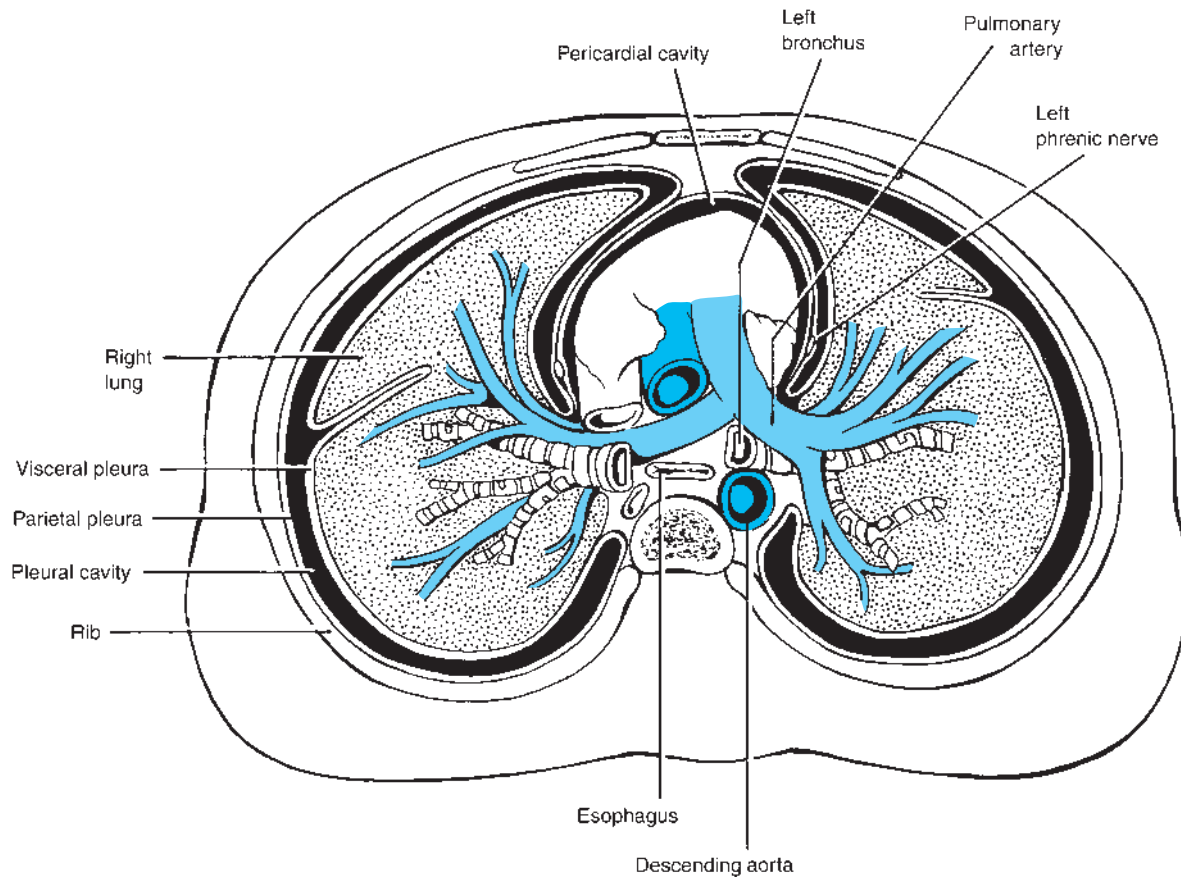


**Figure 2-14** Transverse section through the thorax.

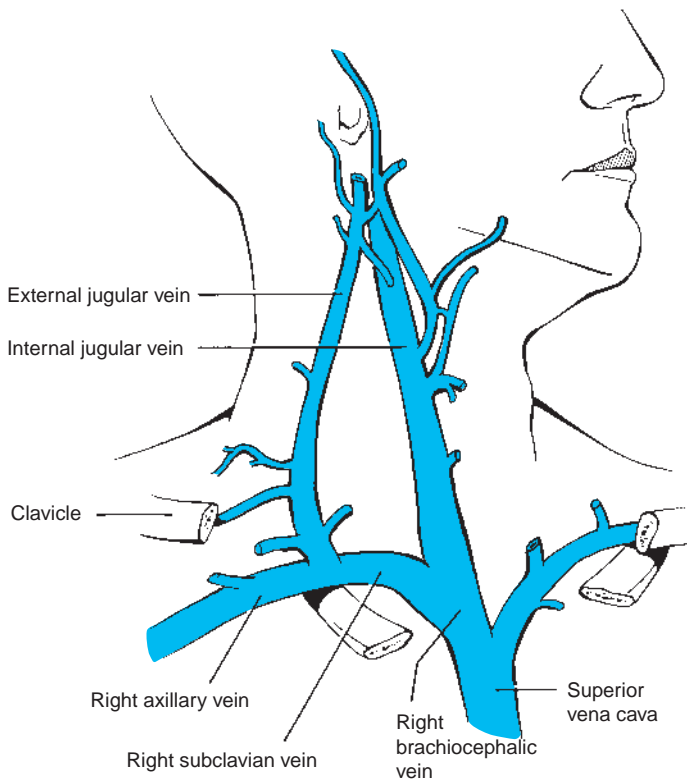


**Figure 2-15** Location of veins exiting the thoracic cage.

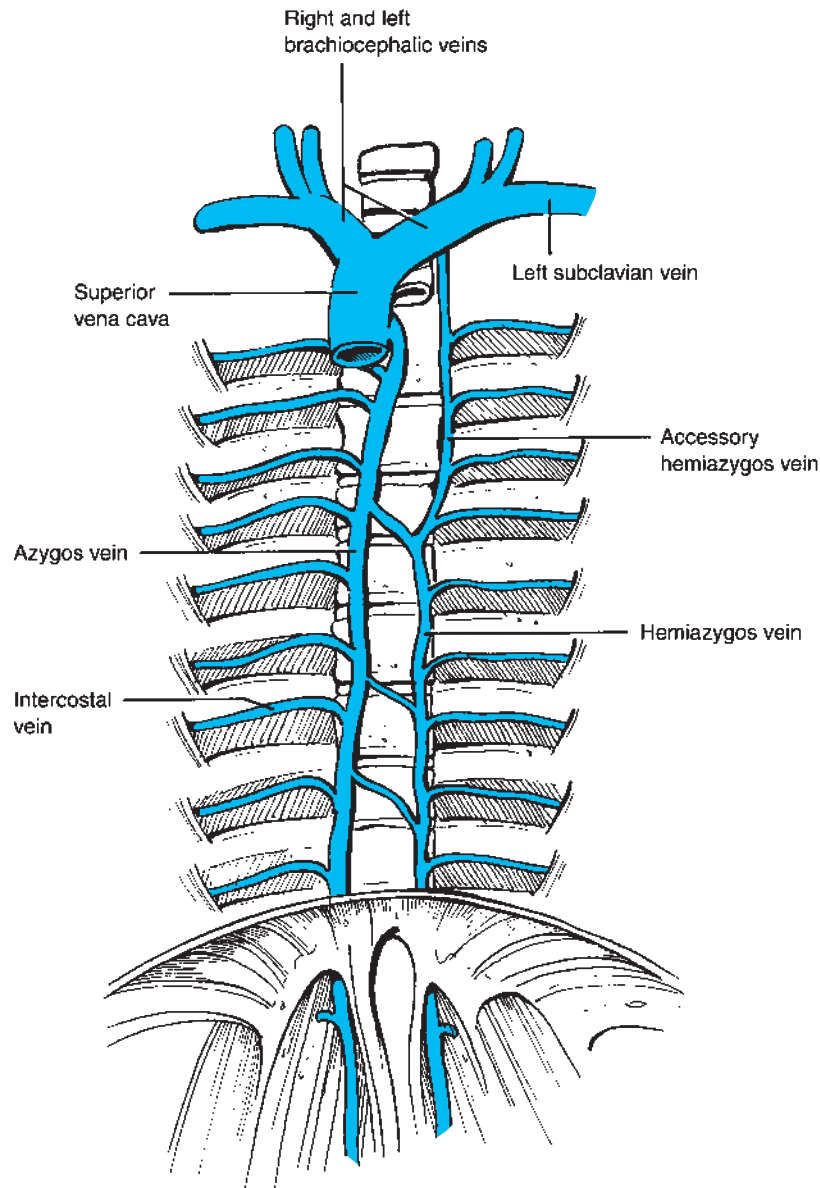


**Figure 2-16** Veins of the posterior thoracic cage.

(Fig. 2-16). The vessel drains much of the venous blood from the posterior thorax and upper abdomen into the superior vena cava.

**Hemiazygos** (*HEM-ē-AZ-ī-gos*). The major vein located on the left side of the vertebral bodies below the accessory hemiazygos or approximately the level of T6. The hemiazygos vein drains the inferior half of the left posterior thoracic cage into the azygos vein.

**Accessory hemiazygos vein.** The vein located inside the posterior thoracic cage next to the vertebral column on the

left side above the level of T6. At the level of T6, the vessel drains blood from the superior half of the left posterior thoracic cage into the hemiazygos vein.

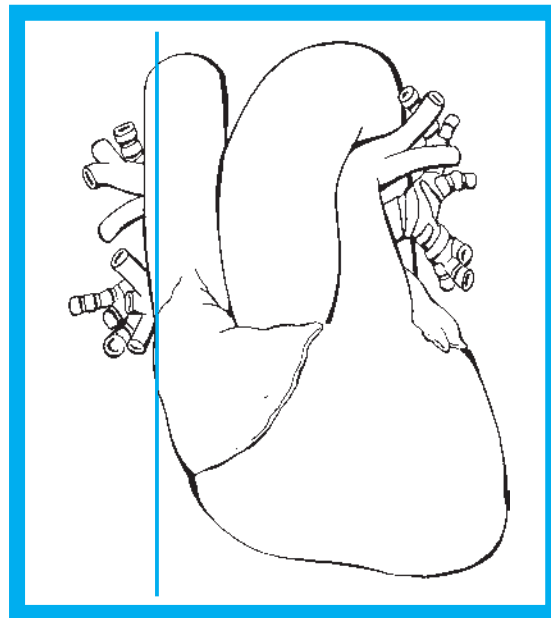
**Inferior vena cava.** A large vein draining most of the lower half of the body into the right atrium (Fig. 2-10). The vessel extends upward through the diaphragm to the right side of the heart and joins to the lower part of the right atrium. At the level of the diaphragm, the inferior vena cava is anterior to the esophagus and the descending aorta.



## Sagittal MR Images

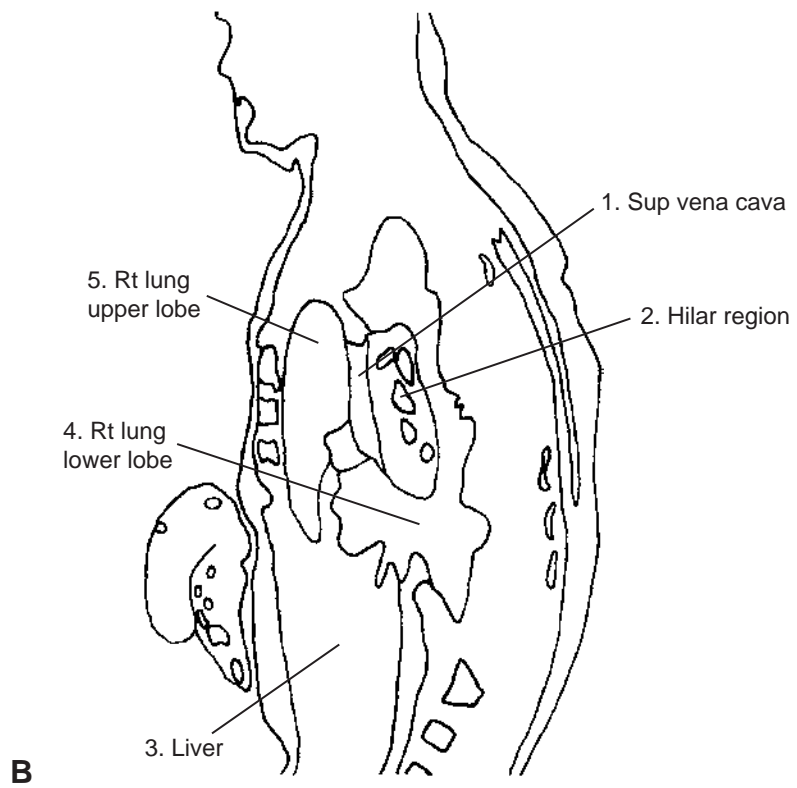
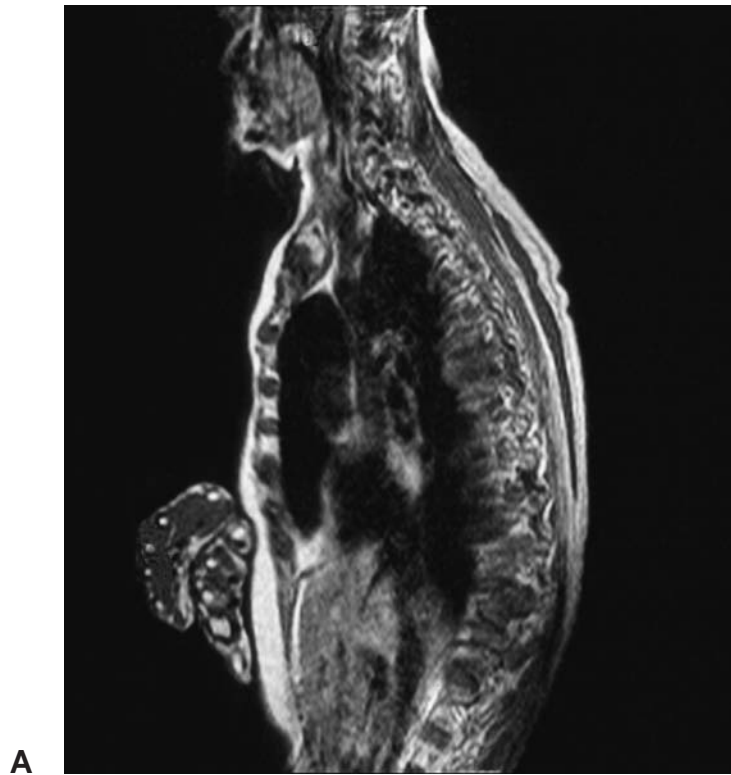
Because of the relatively long acquisition time and the constant movement of the heart and lungs, MR images of the chest provide very limited visualization of moving structures. This section examines eight sequential images taken at 5.0-mm intervals through the middle of the chest from

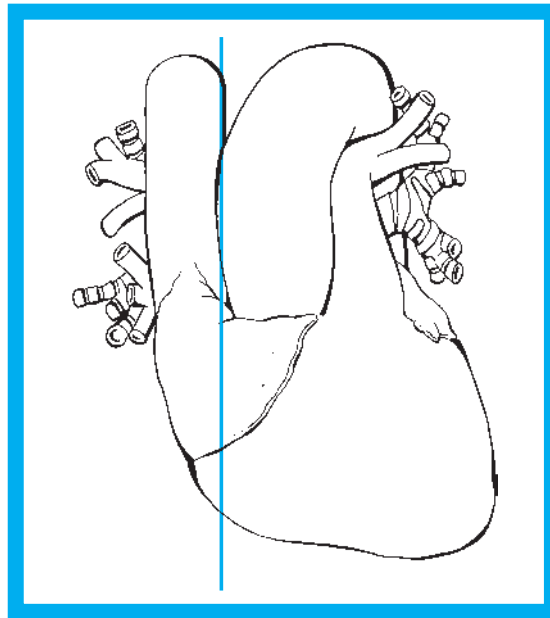
right to left. The images were generated at the following technical factors: repetition time (TR) = 500 ms, echo time (TE) = 20 ms, radiofrequency (RF) = 90°, field of view (FOV) = 45 cm.



**Figure 2–17 (A,B)** Sagittal MR image 1.

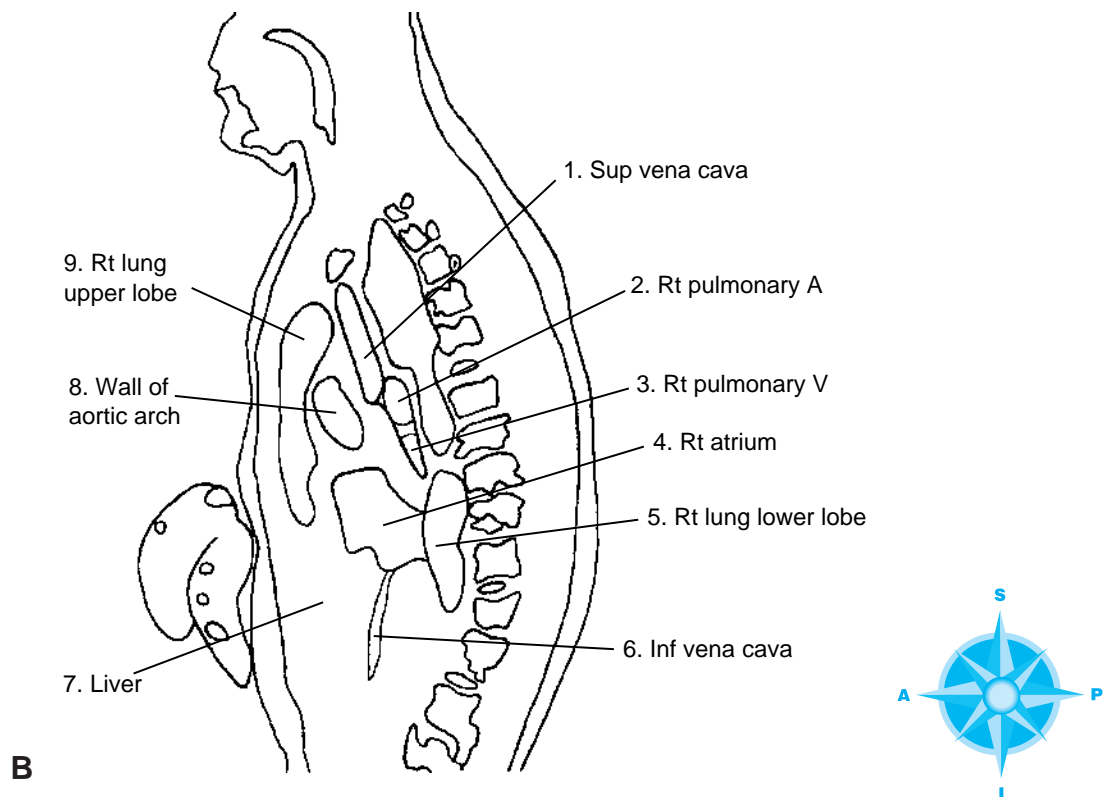
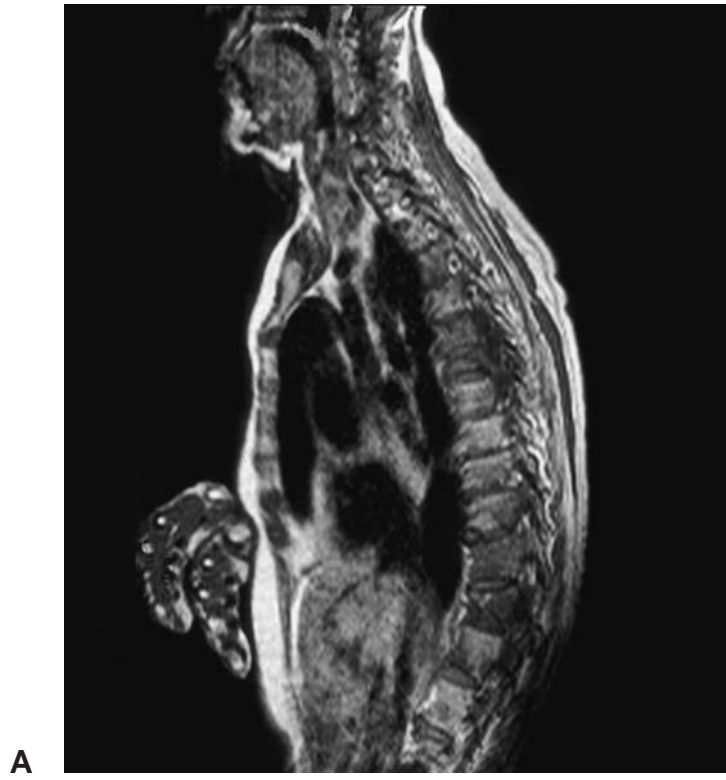
Review of the bony anatomy in the MR image reveals that the vertebral bodies are not yet included within the section, and the anterior musculoskeletal wall demonstrates ribs in cross-section. Regarding soft tissue structures, the right lung forms a background for the mediastinal structures located centrally within the chest. Anteriorly, the upper lobe of the right lung is seen adjacent to the superior vena cava, demonstrated in longitudinal section. Just posterior to the superior vena cava, the hilum is seen, demonstrating vessels and airways in cross-section extending between the right lung and the mediastinum. Posteriorly in the chest cavity, the lower lobe of the right lung can be seen extending inferior to the hilum.

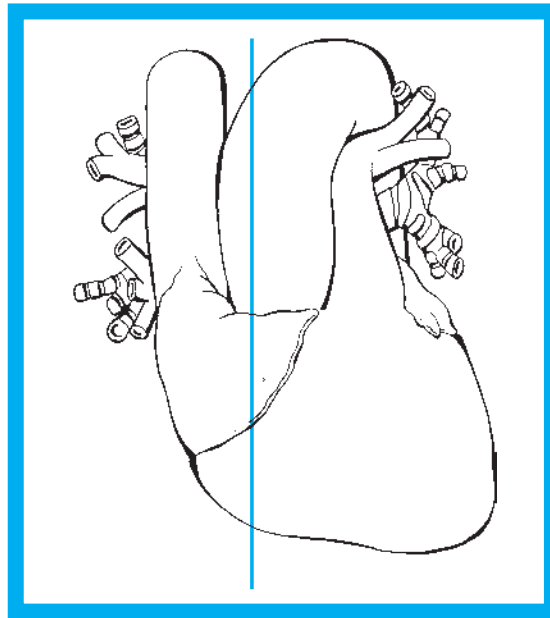




**Figure 2–18 (A,B)** Sagittal MR image 2.

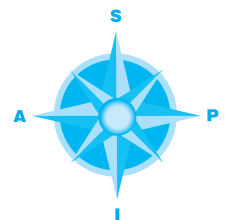
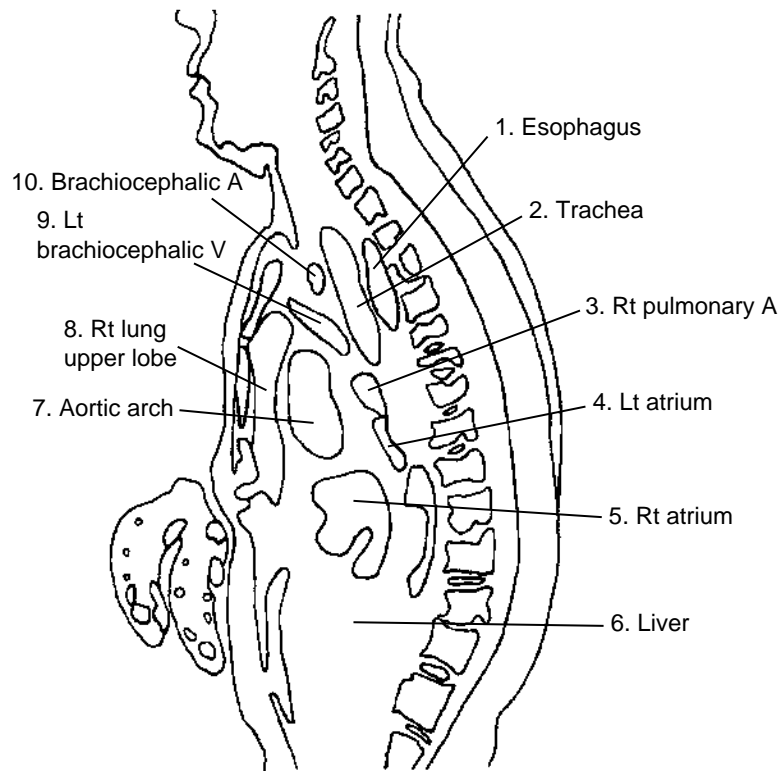
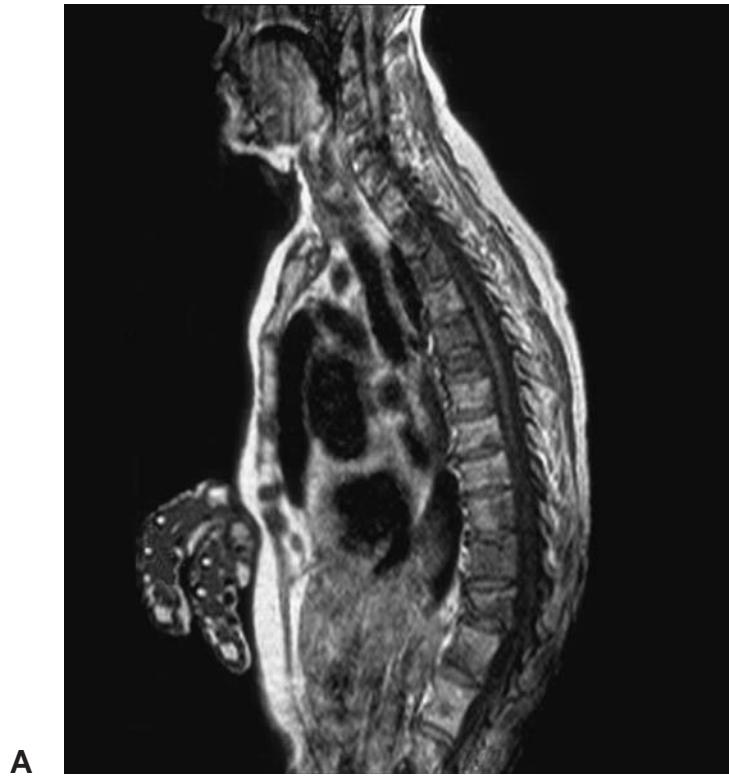
This second MR scan demonstrates structures 5 mm to the left of the first MR image and is slightly closer to the center of the chest. Consequently, less of the right lung is seen and more of the mediastinal structures are visualized. In addition to the superior vena cava just described, the wall of the aortic arch is between the superior vena cava and the upper lobe of the right lung. Posterior to the superior vena cava, the structures within the hilum are more discernible and, based on their positions, can be labeled as the right pulmonary artery and the right pulmonary vein, respectively. Inferior to the pulmonary vessels, the right atrium appears to be resting on the liver, and the inferior vena cava is seen in longitudinal section within the upper abdomen.



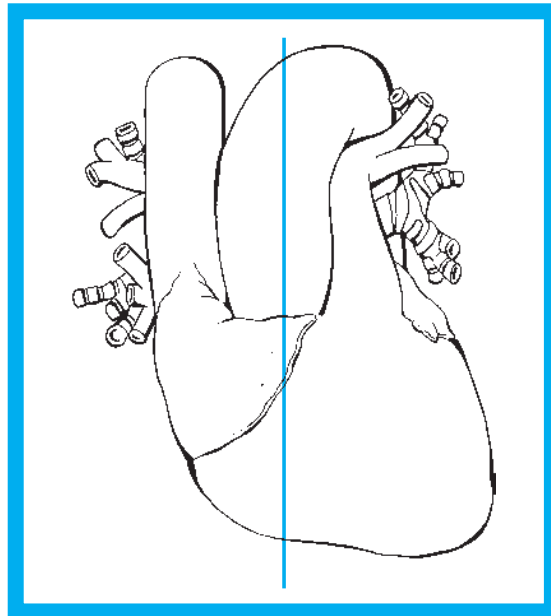


**Figure 2–19 (A,B)** Sagittal MR image 3.

Many of the structures just described are also seen in the section shown in this figure, including the aortic arch, pulmonary artery, right atrium, and liver. However, the superior vena cava is no longer present, and two vessels are demonstrated above the aortic arch. Based on their location, the vessels are labeled as the left brachiocephalic vein and the brachiocephalic artery. As described earlier in this chapter, the veins of the chest are generally located superficial to the corresponding arteries. Immediately posterior to the vessels, two openings are seen extending upward into the region of the neck. Given the large size and its location adjacent to the vessels, the more anterior opening is the trachea; the smaller opening, adjacent to the vertebrae, is within the esophagus. Inferior to the trachea and esophagus, the pulmonary artery is seen above a structure larger than the pulmonary veins. The pulmonary veins empty into the left atrium, and a small section of the left atrium is seen posterior to the right atrium.

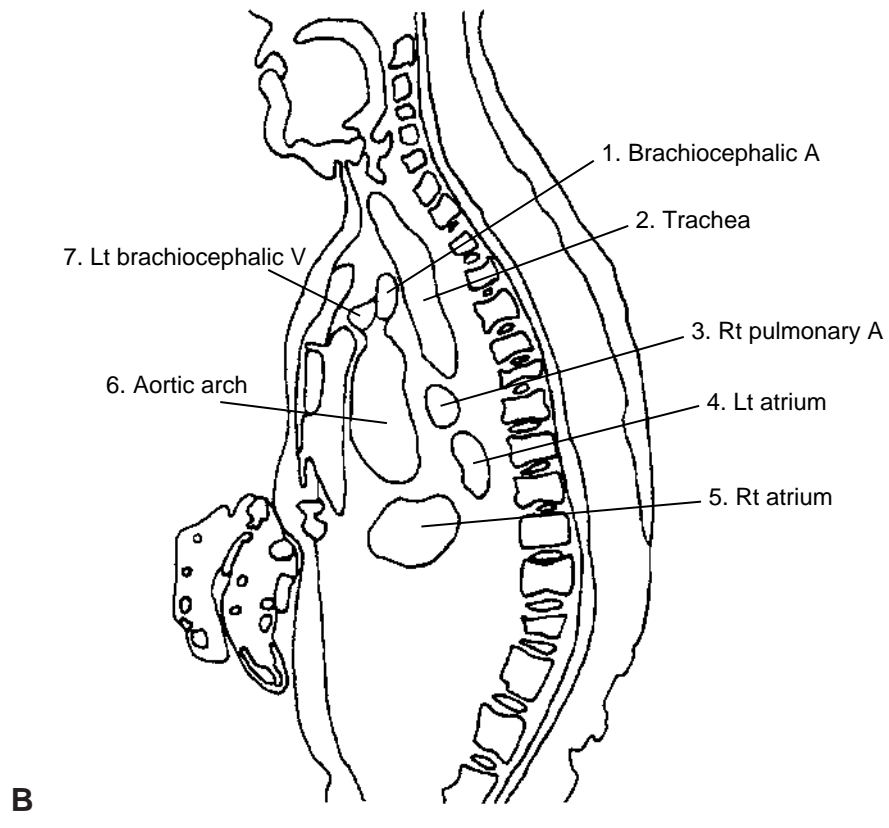
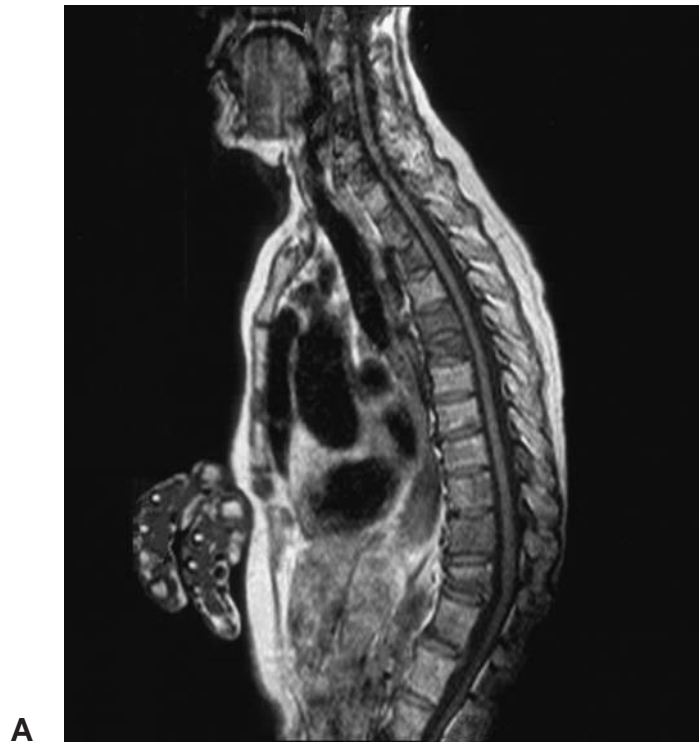


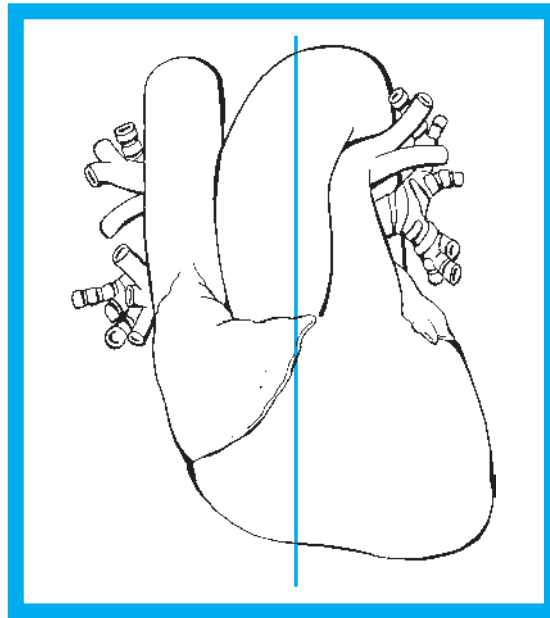




**Figure 2–20 (A,B)** Sagittal MR image 4.

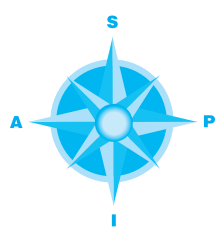
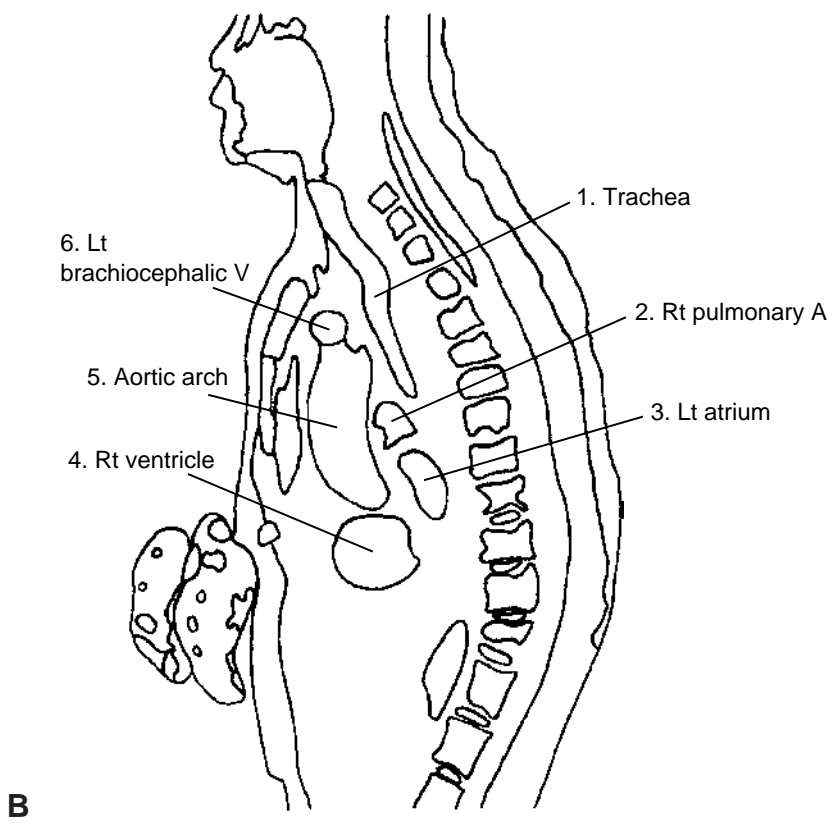
The vertebral bodies are demonstrated in cross-section in front of the spinal cord, indicating that the section is nearing the median plane. The large and most noticeable opening near the center of the chest represents the arch of the aorta. The brachiocephalic artery is originating from the arch, and the left brachiocephalic vein (seen in cross-section) is demonstrated anteriorly. Similar to the previous image, the right pulmonary artery is found just posterior to the aortic arch and superior to the left atrium. Below the great vessels, the right atrium is shown anterior to the left atrium within the heart.

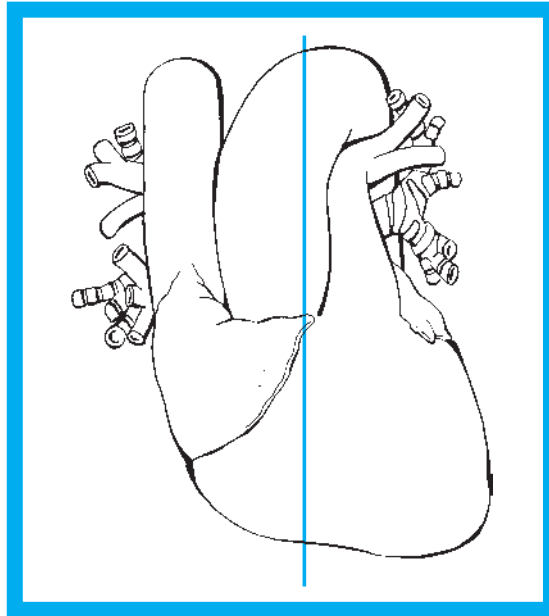




**Figure 2-21 (A,B)** Sagittal MR image 5.

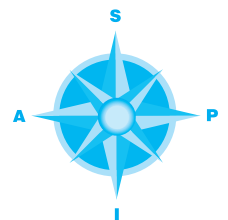
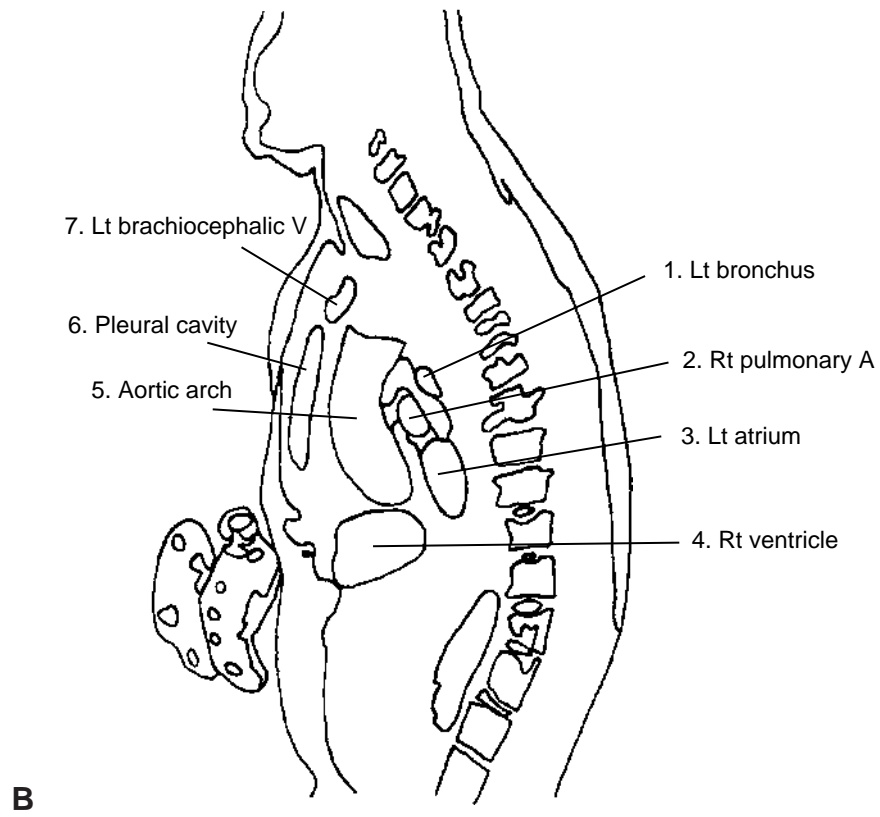
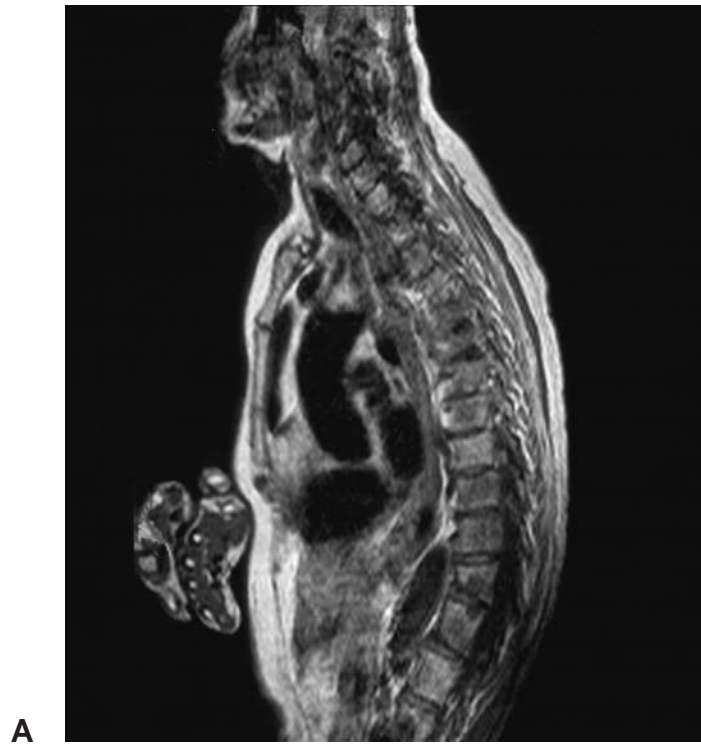
The aortic arch, near the center of the chest, appears larger in this image than in the previous images. The only vessel seen above the aortic arch, the left brachiocephalic vein, is situated anterior to the opening of the trachea, shown extending up through the neck to the head. As described previously, the right pulmonary artery is sectioned just posterior to the aorta and just superior to the left atrium. Although the specific division is not demonstrated, the right atrium has been replaced by the right ventricle within the heart.

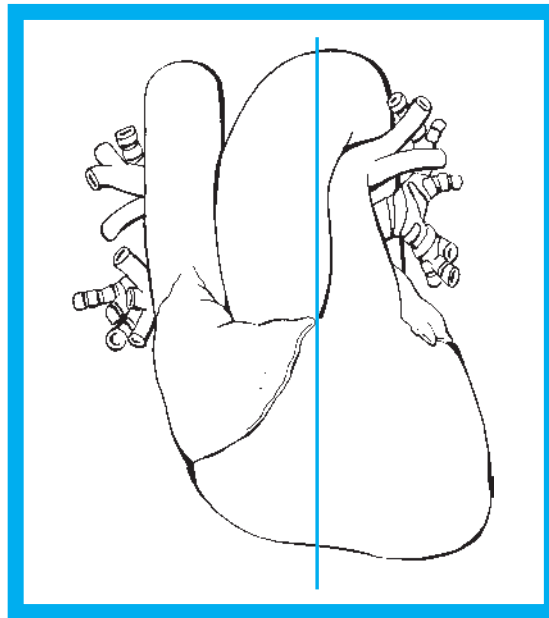




**Figure 2–22 (A,B)** Sagittal MR image 6.

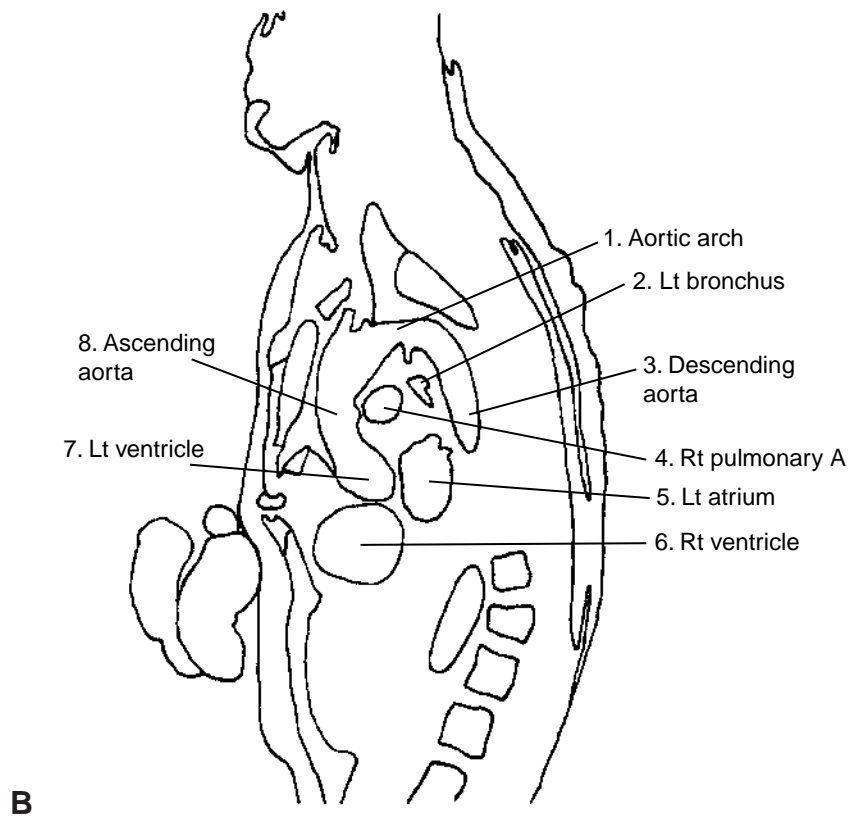
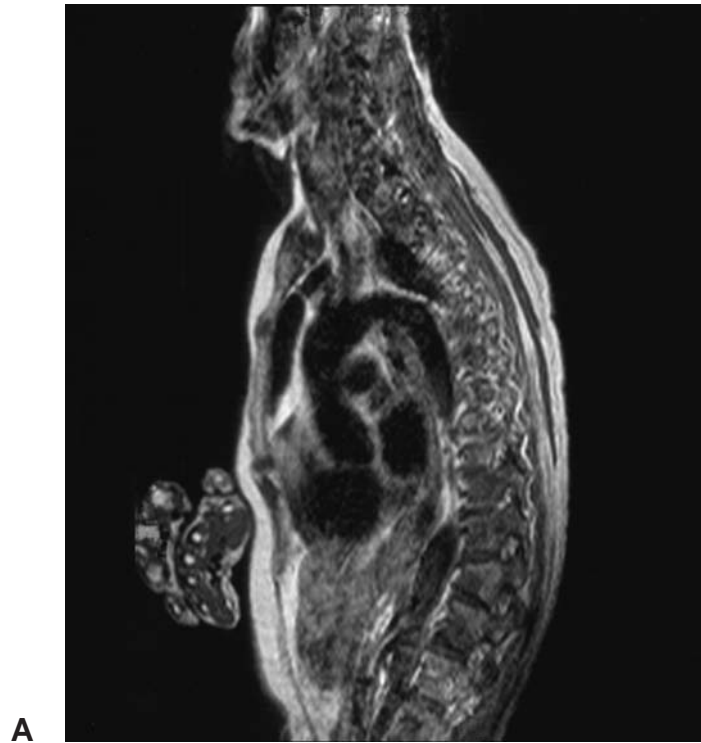
Many of the structures just described are seen in the next section, including the aortic arch, the left brachiocephalic vein, the right pulmonary artery, the left atrium, and the right ventricle. In contrast to the previous image, the trachea is no longer seen and the left bronchus is shown in cross-section extending into the left lung. Also, the pleural cavity is larger than in the previous section, signifying the beginning of the left lung.





**Figure 2-23 (A,B)** Sagittal MR image 7.

Near the center of the chest, all three parts of the thoracic aorta are clearly visualized in this figure: the ascending aorta originating from the left ventricle, the arch moving posteriorly, and the descending aorta on the left side of the posterior thoracic cage. As described earlier, the aorta is arching over the left bronchus and the right pulmonary artery. Below the aorta, three chambers of the heart are included within this section. The right ventricle is the most anterior chamber and lies in front of the left ventricle. Behind the left ventricle, the left atrium is shown to be the most posterior chamber of the heart.





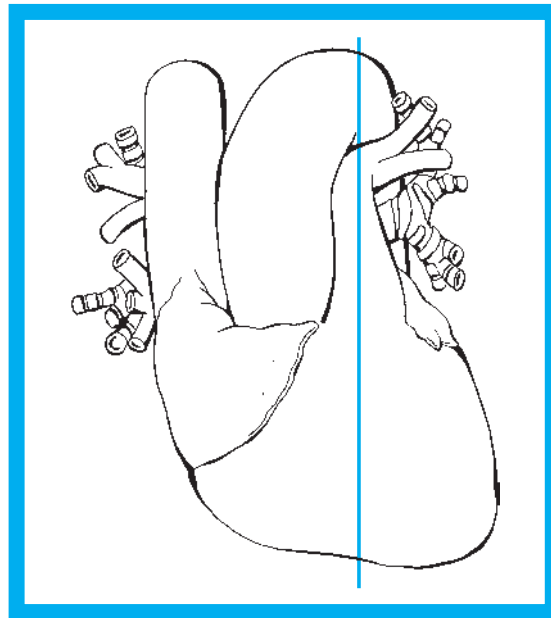
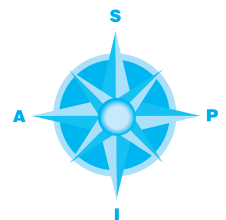
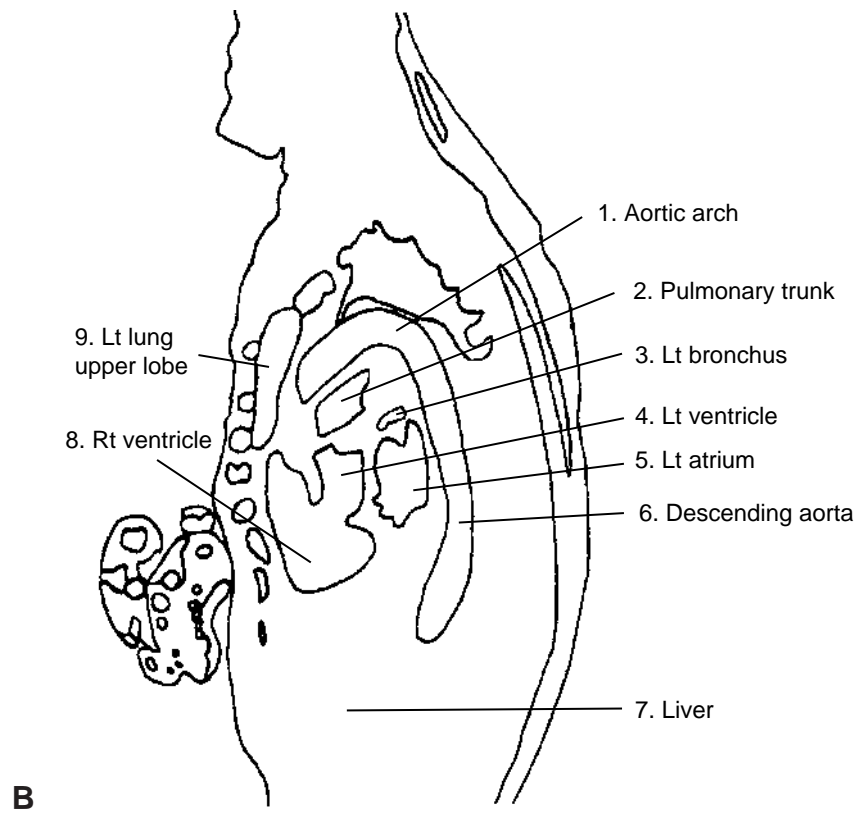
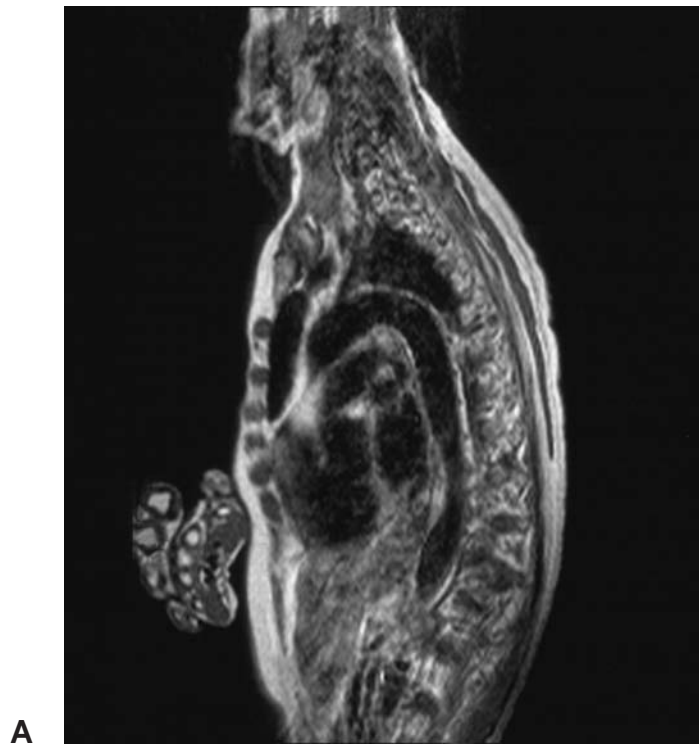


**Figure 2-24 (A,B)** Sagittal MR image 8.

The aortic arch and descending aorta are easily identified adjacent to the heart, but the ascending portion is no longer demonstrated adjoining the left ventricle. Instead, the pulmonary trunk is seen in longitudinal section as a large vessel extending between the upper right ventricle and the arch of the aorta. Adjacent to the arch, the pulmonary trunk divides into the right and left pulmonary arteries, which extend laterally to the right and left lungs along with the bronchi and pulmonary veins. Within the heart, the right ventricle is located most anteriorly and the left atrium is most posterior. If additional sagittal sections were described moving toward the left side of the chest, the left ventricle would enlarge, becoming slightly larger than the right ventricle.

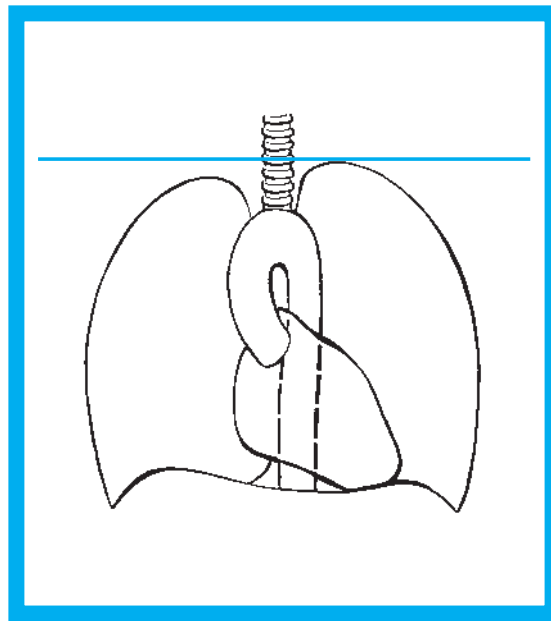




## Axial CT Images

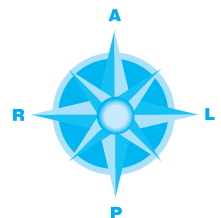
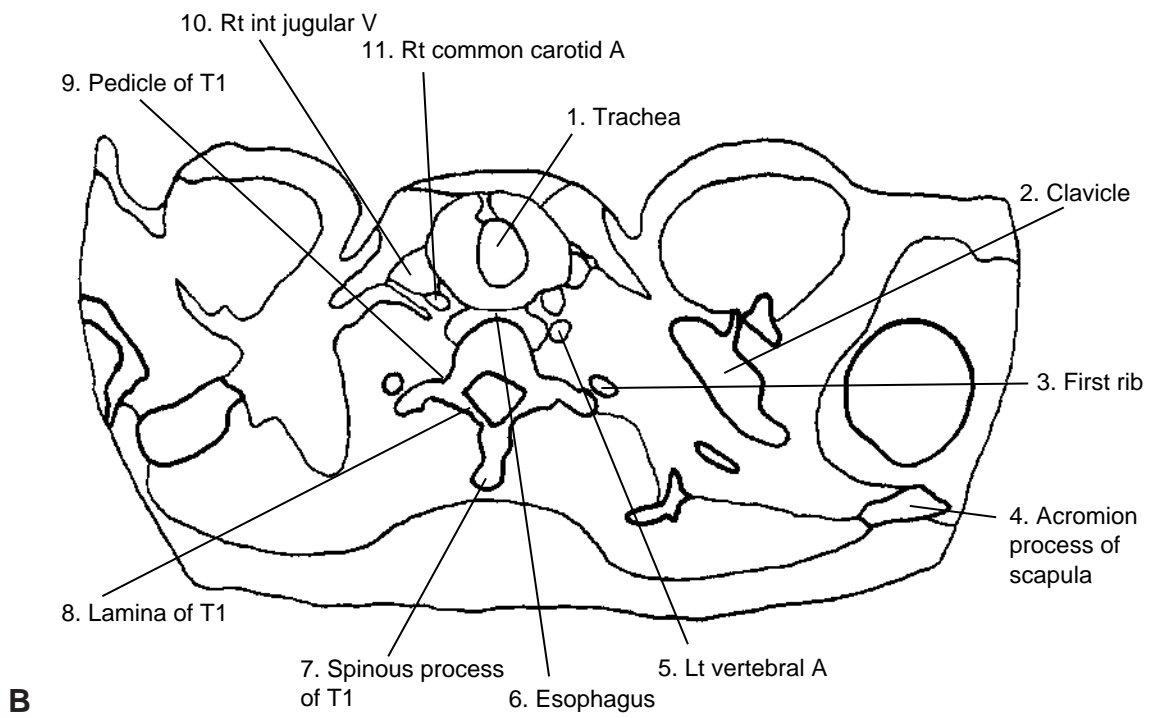
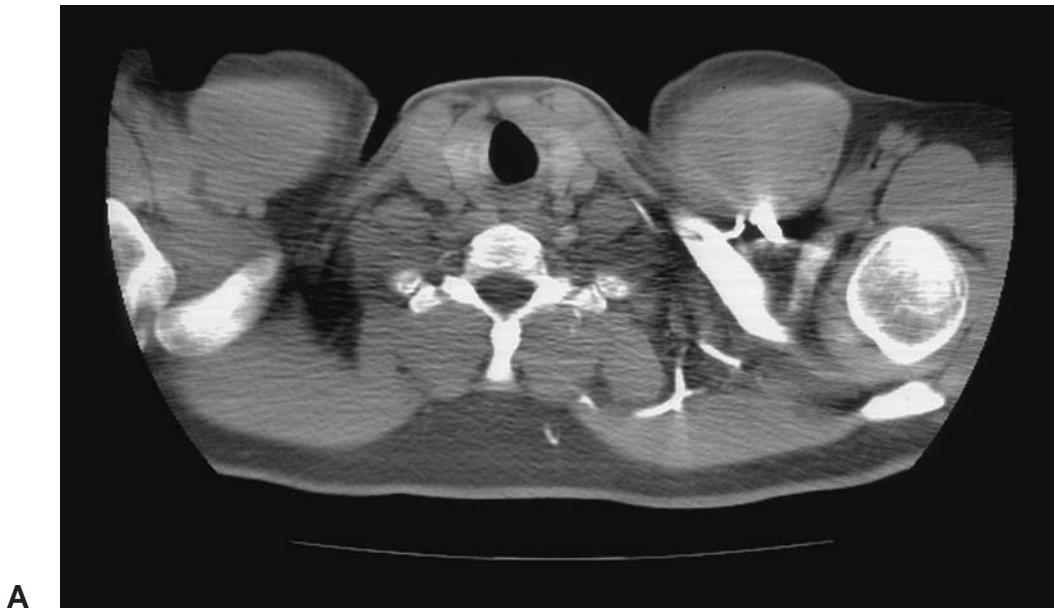
This section examines 26 axial CT images of the chest taken at 10.0-mm intervals through the chest from superior to inferior. In a typical scan of the chest, images are generated throughout the region of the bony thoracic

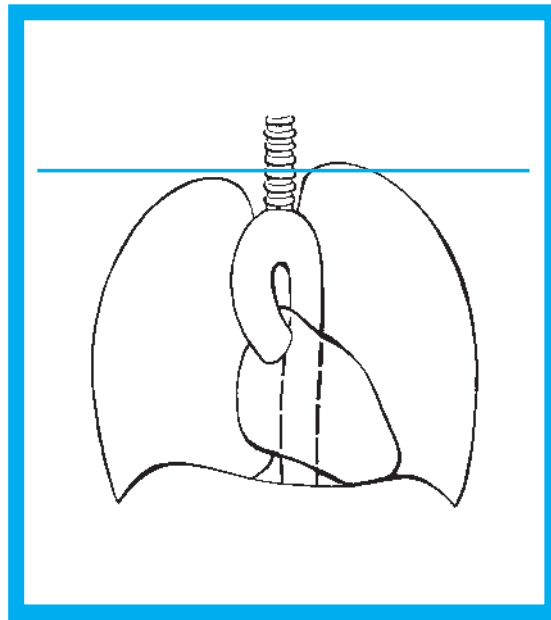
cage. The images were generated immediately after the administration of 100 ml of venous contrast medium at the following technical factors: 120 kilovolt peak (kVp) and 150 millampere-second (mA-s)



**Figure 2-25 (A,B)** Axial CT image 1.

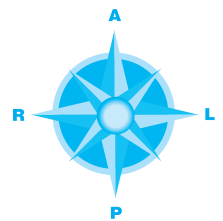
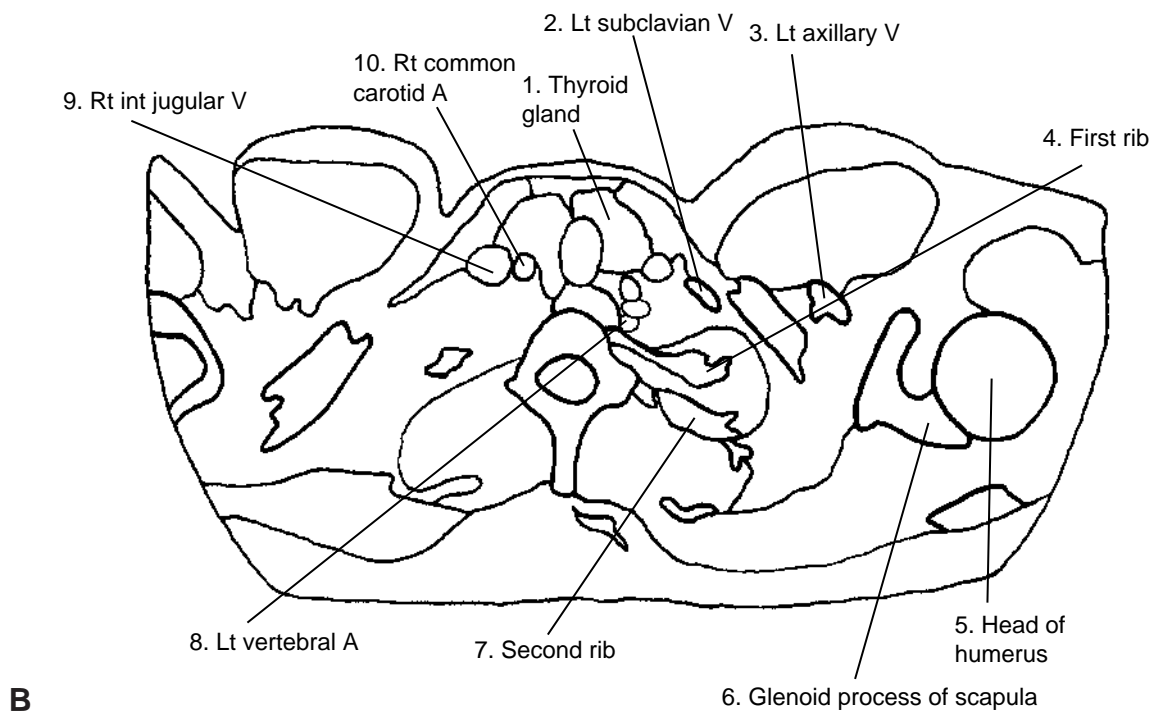
In this first CT image at the top of the chest, the vertebra can clearly be labeled as the first thoracic vertebra by the absence of any ribs except the small sections shown articulating with costal facets on the transverse processes bilaterally. Although one might expect to find the first rib articulating with the vertebral body in this same section, it is demonstrated on the next image, because the transverse processes angle superiorly above the vertebral body. In addition to the other vertebral structures identified, the clavicle is obliquely sectioned on the left side, and the upper head of the humerus is demonstrated anterior to the acromion process of the scapula. Looking at the soft tissues of the upper chest, one can easily identify the trachea: It serves as a landmark for identification of adjacent structures. The esophagus, located directly posterior to the trachea, appears flattened with little or no lumen evident. On the left side, the contrast has enhanced the left vertebral artery lateral to the esophagus and vertebral body. On either side of the trachea, the deep vessels of the neck are shown with the slightly larger internal jugular veins superficial to the common carotid arteries.

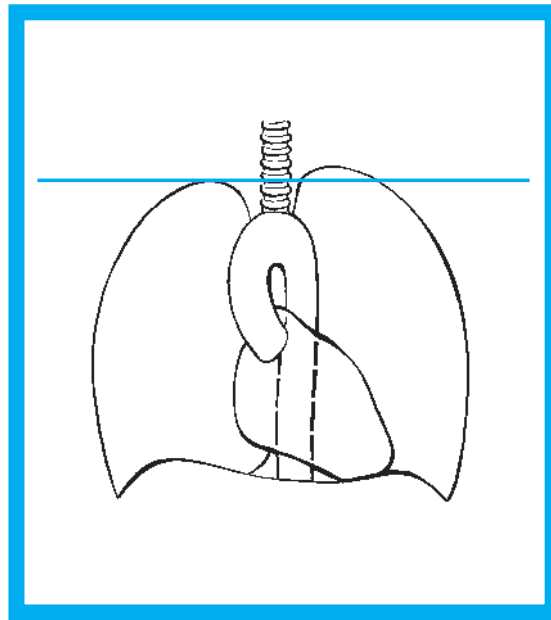




**Figure 2–26 (A,B)** Axial CT image 2.

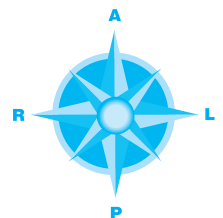
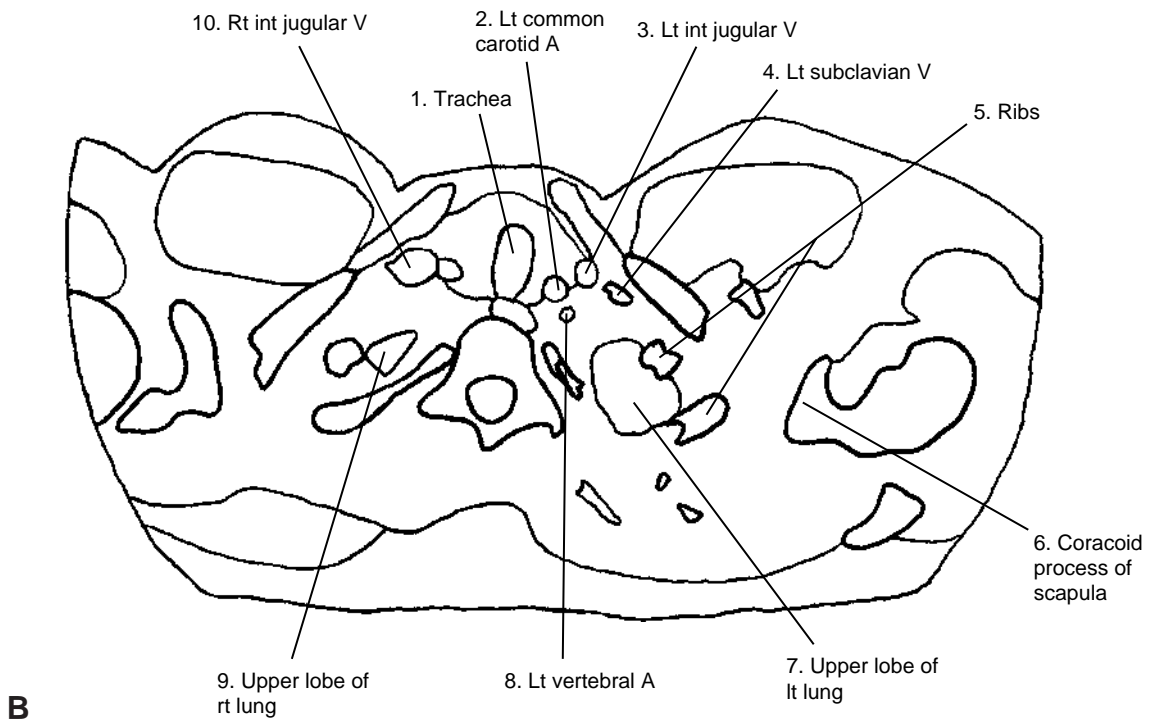
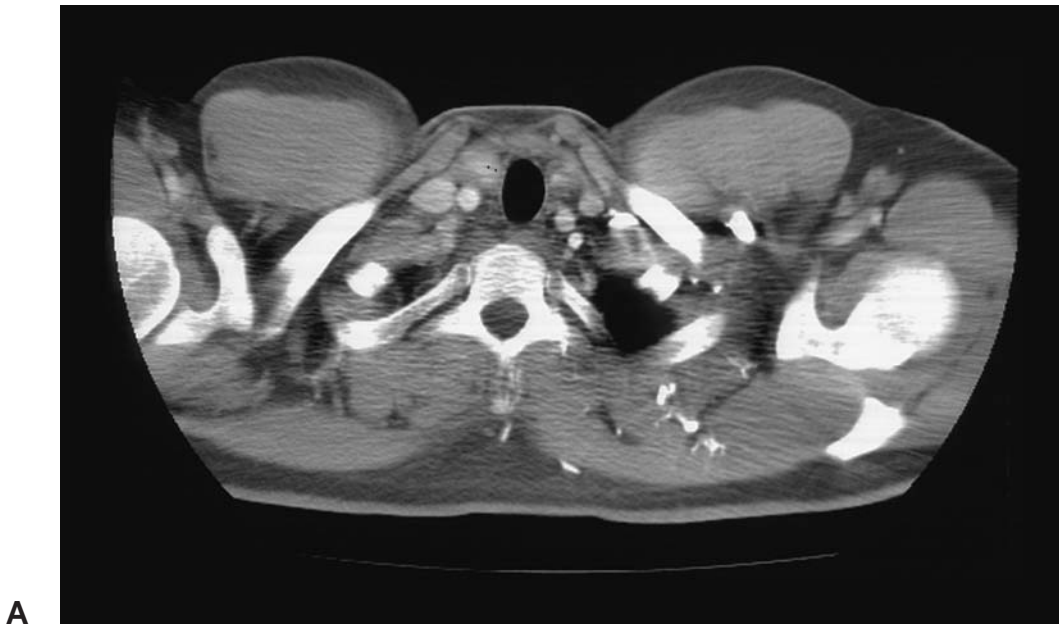
Following the anatomy from the previous image, most of the structures just described are also found within this lower section. However, the first rib is articulating with the costal facet on the vertebral body, and the second rib is sectioned at the costal facet of the transverse process of the second thoracic vertebra. The head of the humerus (shown in full on the left side) is articulating with the glenoid process of the scapula, and the acromion process is no longer seen. When the attention is shifted to soft tissue structures, the center of the thyroid gland is apparent wrapping around the anterior trachea. Lying behind the lobes of the thyroid gland, the internal jugular vein and common carotid artery are on either side. On the left side, the left vertebral artery is shown in cross-section near the first rib, and the vessel highlighted with contrast lateral to the internal jugular vein is the left subclavian vein. Outside of the bony thoracic cage (over the first rib), the left axillary vein is sectioned as it extends from the region of the shoulder.





**Figure 2-27 (A,B)** Axial CT image 3.

The ribs are shown obliquely sectioned encasing the upper lobes of the right and left lungs. The “hook,” or coracoid process of the scapula, is shown bilaterally extending toward the anterior chest wall. Within the mediastinum, the trachea is again shown centrally between the common carotid arteries and internal jugular veins. On the left side, the vertebral artery is cross-sectioned behind the common carotid artery, and the subclavian vein is sectioned lateral to the internal jugular vein.





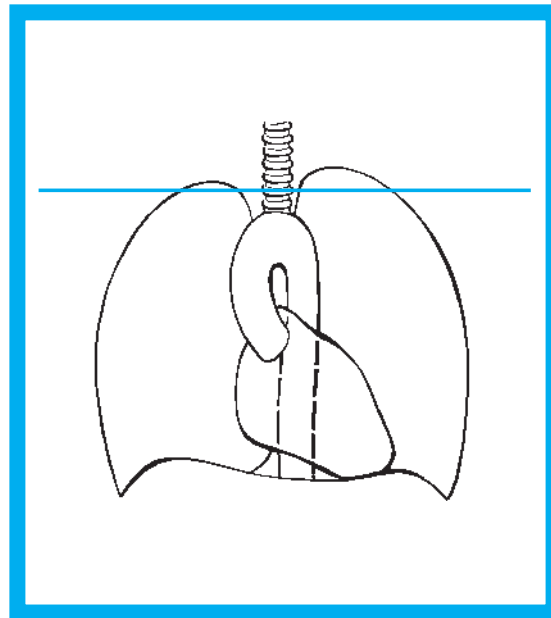
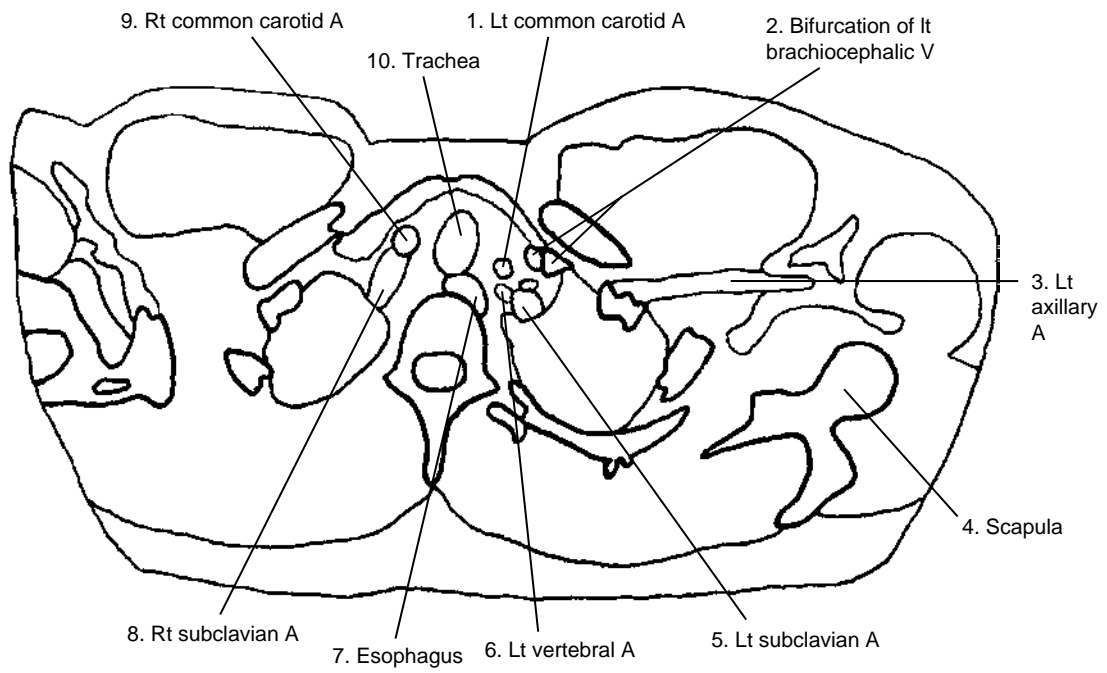


**Figure 2–28 (A,B)** Axial CT image 4.

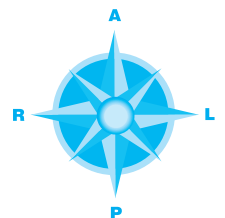
The humerus is no longer seen on the left side, but the head is still demonstrated on the right, indicating that the patient's shoulders are asymmetrical. Within the midline, the trachea is sectioned in front of the esophagus and separates the common carotid arteries. In contrast to the earlier images in the series, the left internal jugular vein and left subclavian vein are not distinctly separable, indicating the level of bifurcation of the left brachiocephalic vein. At this lower level, the left subclavian artery lies adjacent to the vertebral artery. Outside of the thoracic cage, the axillary artery is demonstrated in longitudinal section.



A



B



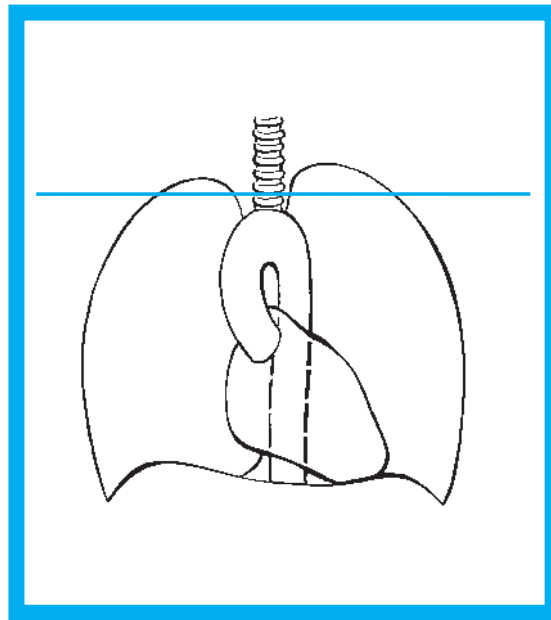
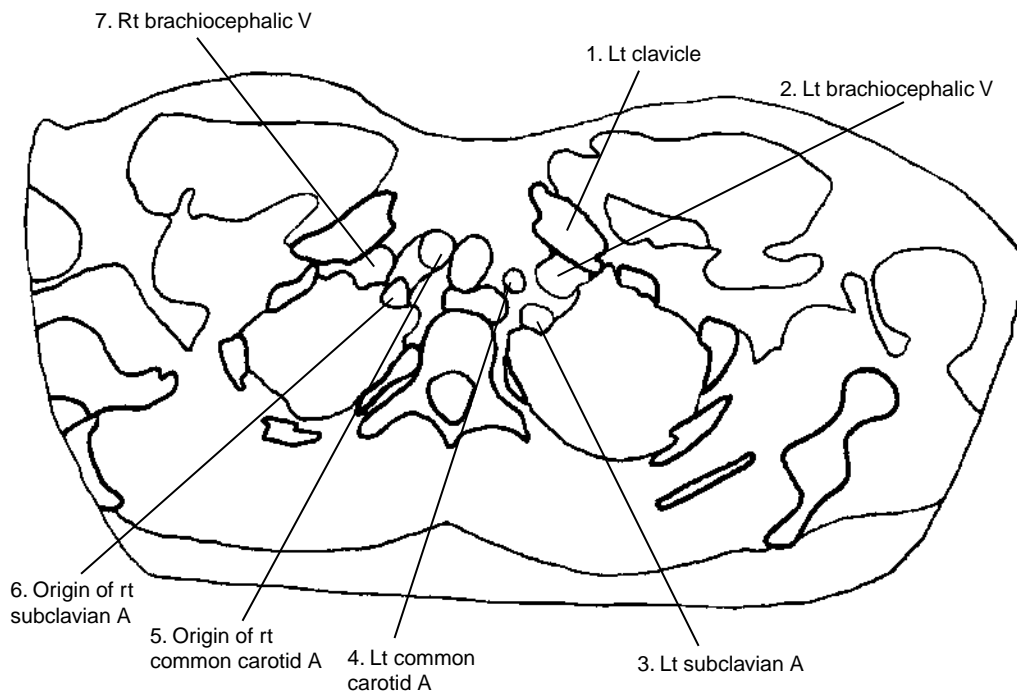


**Figure 2–29 (A,B)** Axial CT image 5.

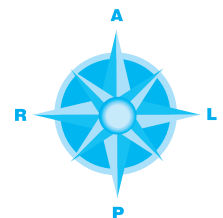
This bony anatomy depicts the inferior parts of the scapulae, and the clavicles are obliquely sectioned in front of the thoracic cage. The right common carotid and subclavian arteries are no longer distinctly separate and are shown at their origin from the brachiocephalic artery. Adjacent to the clavicles, the brachiocephalic veins are superficial to the adjacent arterial structures. On the left side of the patient, the subclavian and common carotid arteries are shown just above their origin, the aortic arch. The left common carotid artery lies near the trachea, and the subclavian artery is found in cross-section near the upper lobe of the left lung.



A



B



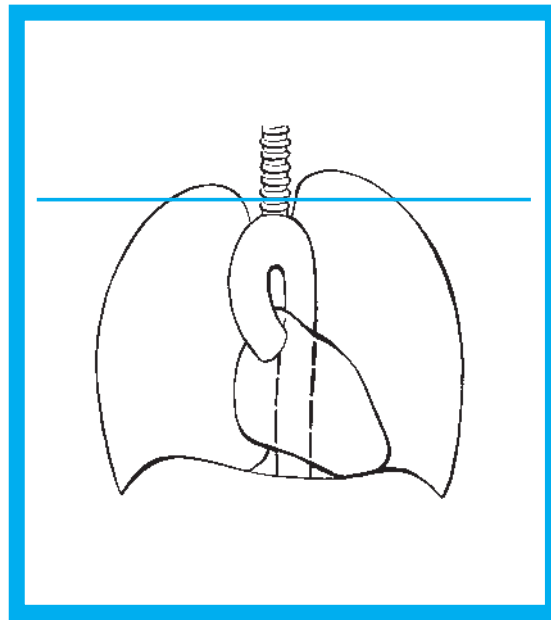
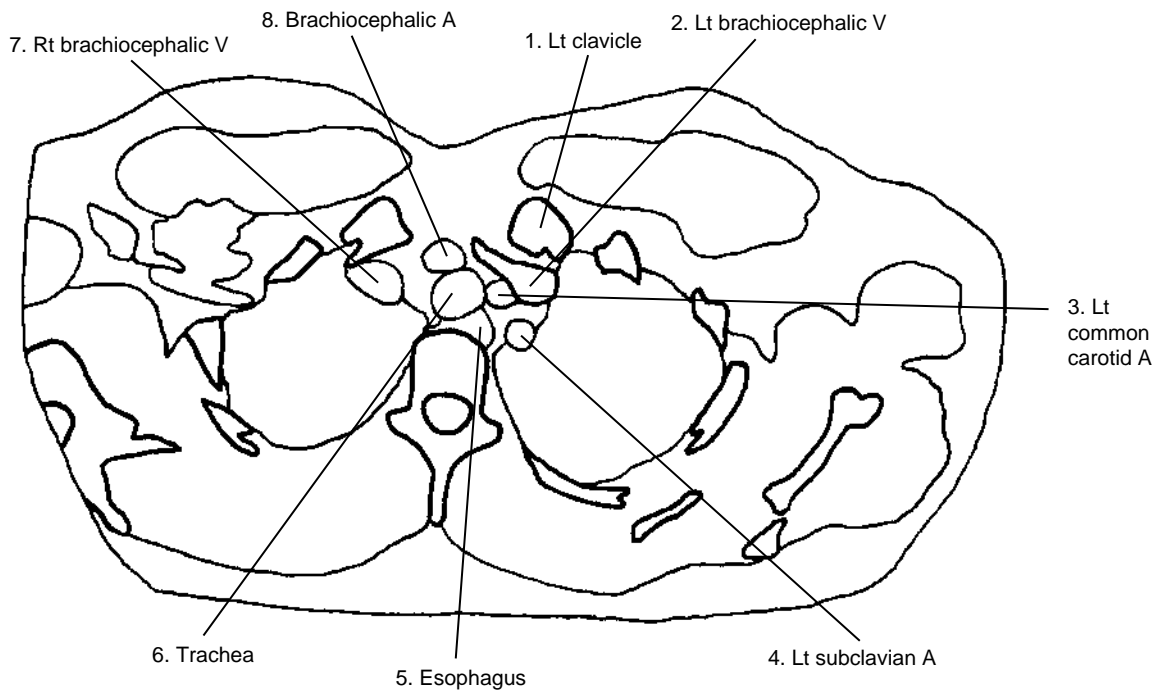


**Figure 2–30 (A,B)** Axial CT image 6.

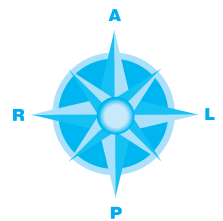
All three of the brachiocephalic vessels can be identified. The right and left brachiocephalic veins are located immediately posterior to the clavicles. Owing to the more horizontal course of the left brachiocephalic vein, an oblique section is highlighted with contrast, whereas the right brachiocephalic vein is in cross-section with little contrast enhancement. Between the veins, the brachiocephalic artery (not labeled right or left because there is only one located on the right side) is just anterior to the trachea. Because the three major arteries within this image all originate from the aortic arch, they can be identified as the brachiocephalic artery, left common carotid artery, and the left subclavian artery. Centrally, the esophagus is found between the opening within the trachea and the vertebral body.

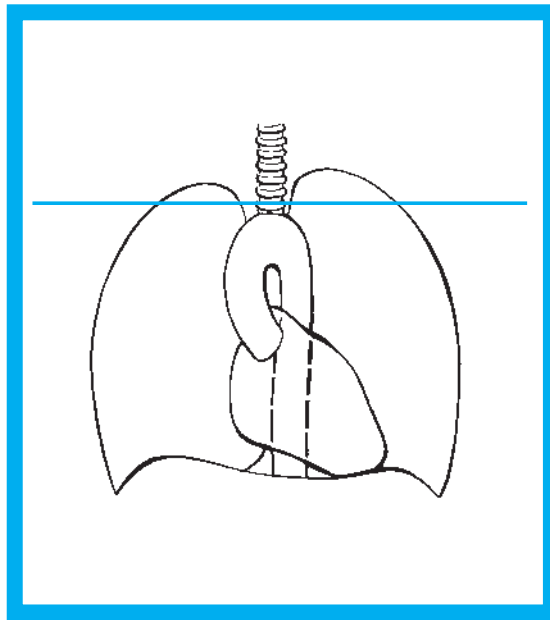


A



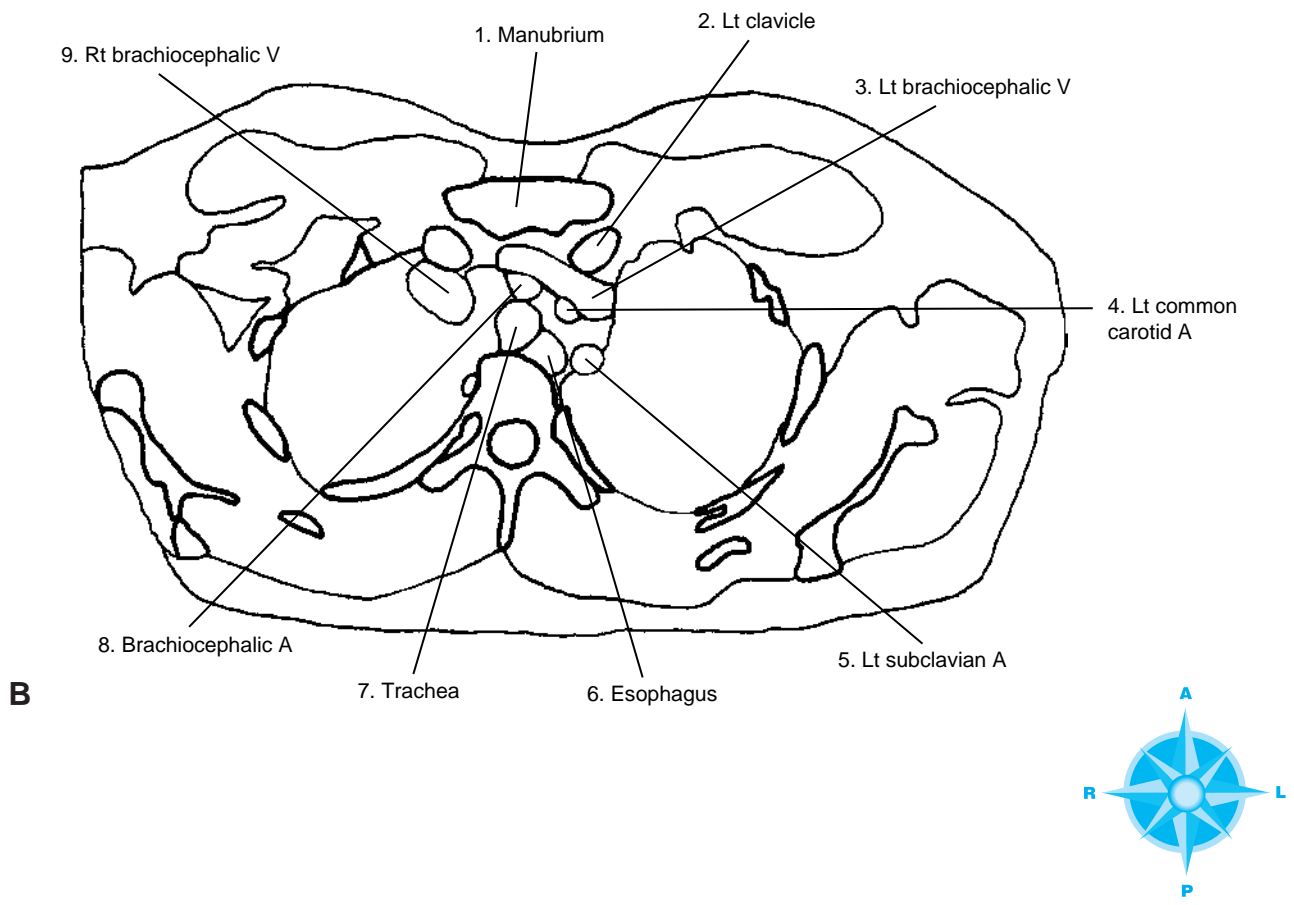
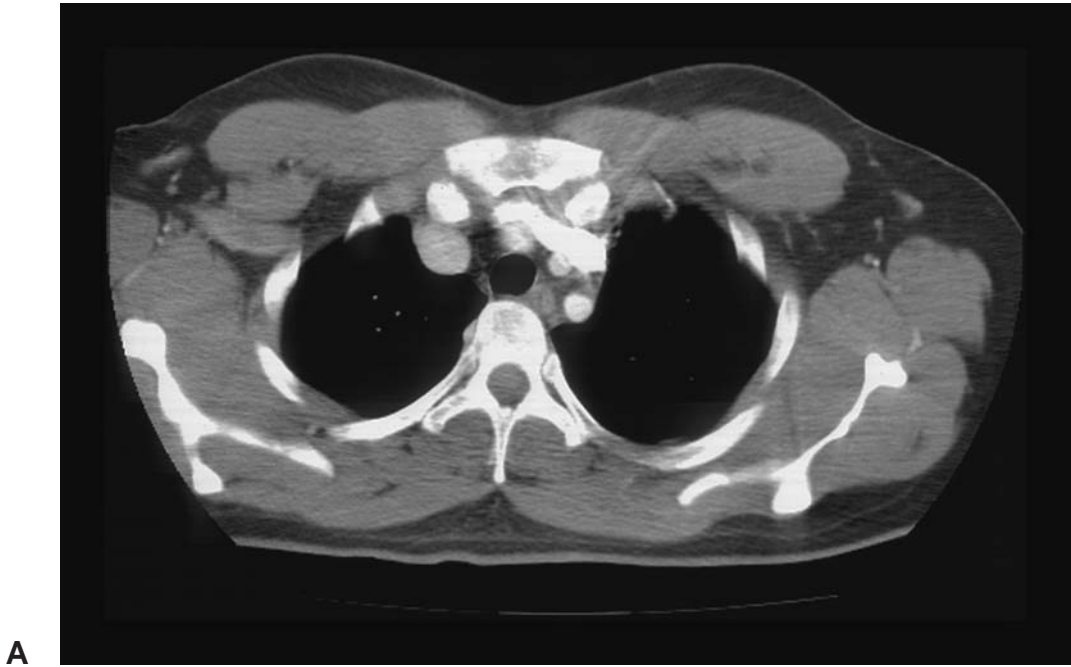
B





**Figure 2-31 (A,B)** Axial CT image 7.

On the anterior aspect of the chest wall, the manubrium of the sternum is shown articulating with the ends of the clavicles. Within the mediastinum, the anatomy is markedly similar to the previous section. The right and left brachiocephalic veins are just behind the clavicles, and the left vein is obliquely sectioned owing to its more horizontal projection within the mediastinum. Behind the veins, the three branches off the aortic arch are shown in order from right to left as the brachiocephalic artery, the left common carotid artery, and the left subclavian artery. The opening within the trachea is shown between the brachiocephalic artery and the vertebral body. Compared to the previous figure, the esophagus has moved to the left of the trachea at this lower level.





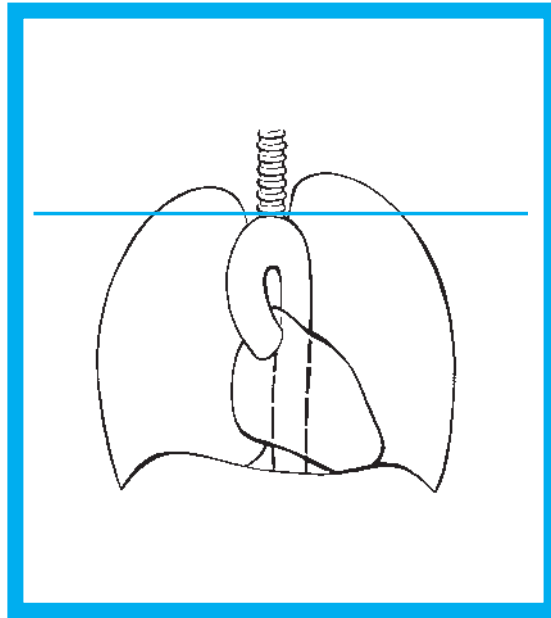
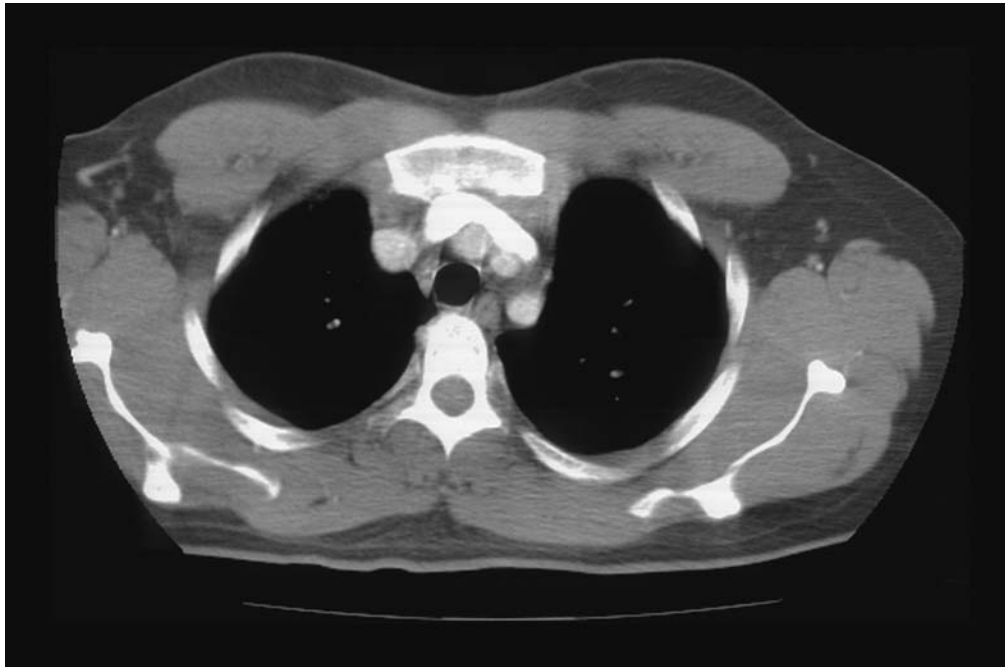
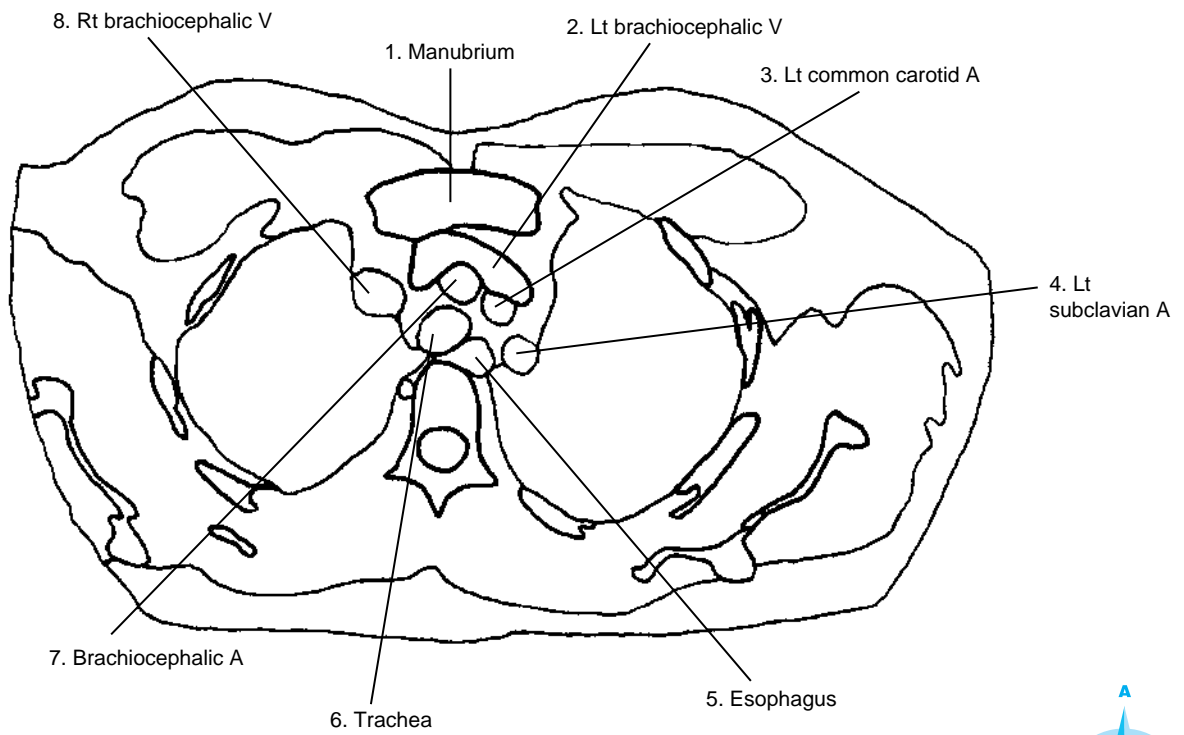


**Figure 2–32 (A,B)** Axial CT image 8.

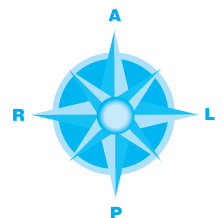
The clavicles are no longer present, and the great vessels are tightly arranged within the mediastinum behind the manubrium. Similar to previous images, the right brachiocephalic vein is found in cross-section, and the left brachiocephalic vein is obliquely sectioned. The left brachiocephalic vein lies just anterior to the three arterial vessels originating from the aortic arch: the brachiocephalic artery, the left common carotid artery, and the left subclavian artery. Within the posterior mediastinum, the esophagus is again shown slightly to the left of the trachea.



A



B



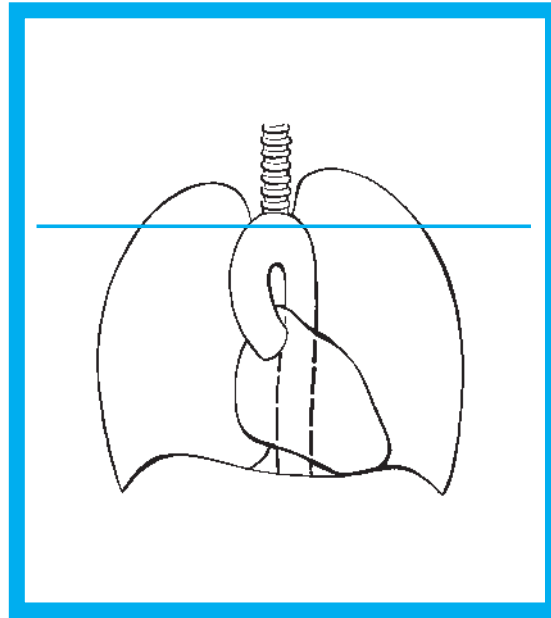
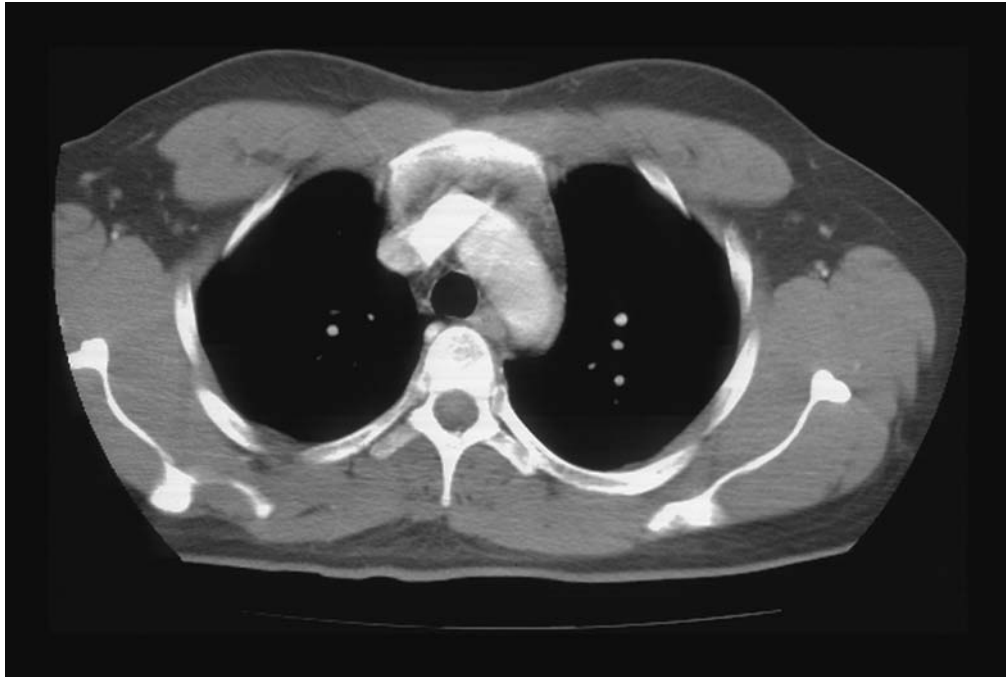
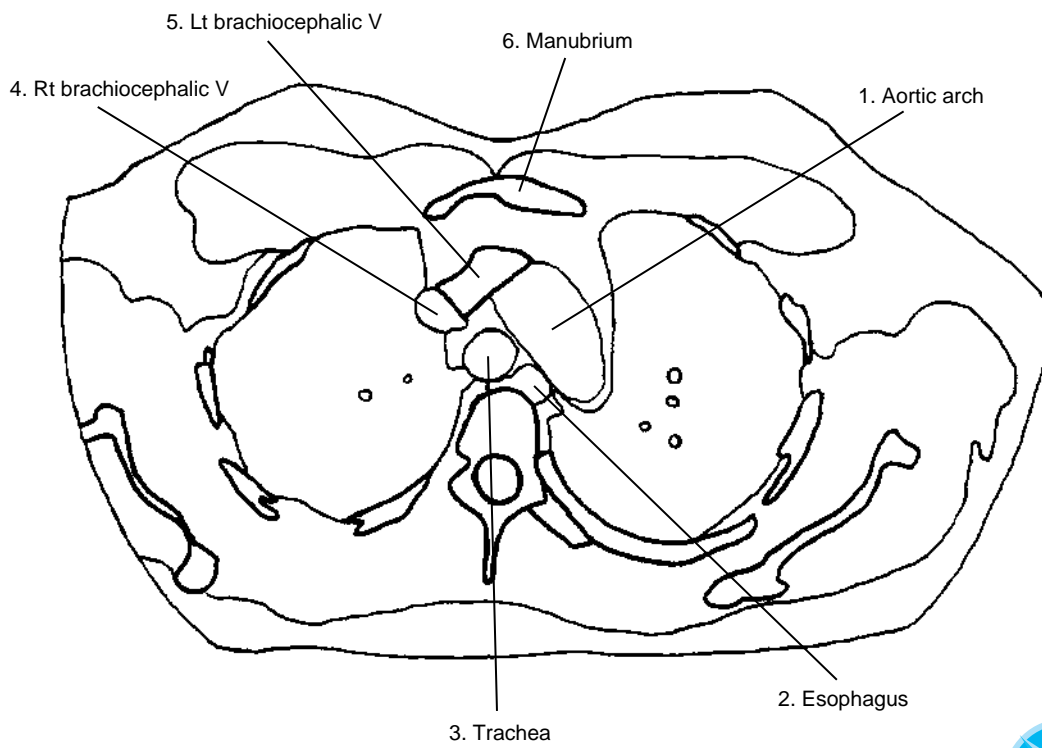


**Figure 2–33 (A,B)** Axial CT image 9.

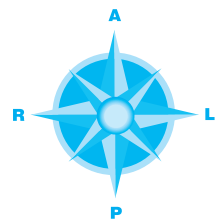
The manubrium—the large, flat bone forming the anterior boundary of the mediastinum. The most distinctive difference between this image and the previous one is the absence of the three arteries, which have merged together to form one large arterial structure, the aortic arch. Also, the brachiocephalic veins are not as distinctly separable as in the previous section and will later be shown to join to form the superior vena cava. Within the posterior mediastinum, the trachea is still centrally located in front of the esophagus.



A



B



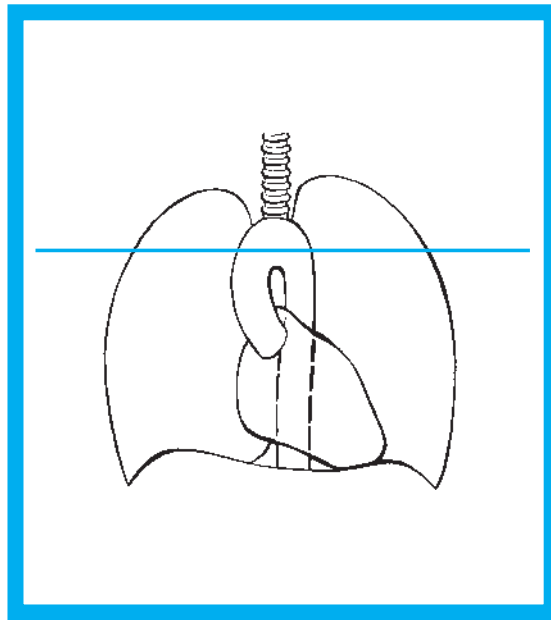
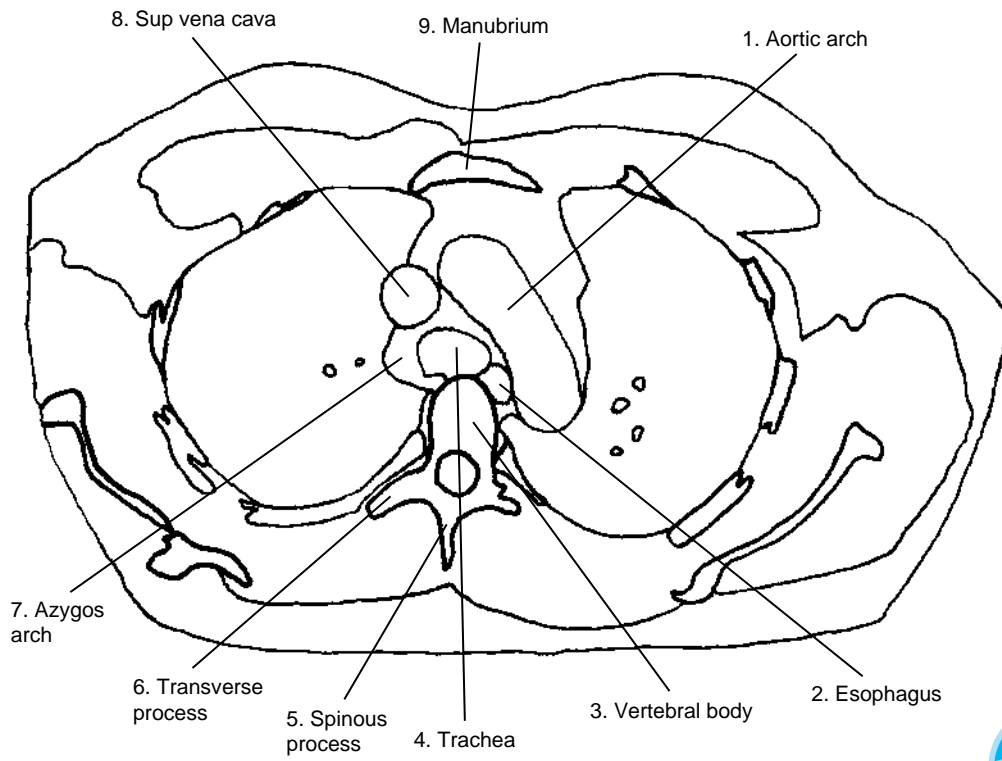


**Figure 2–34 (A,B)** Axial CT image 10.

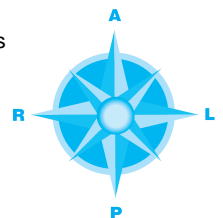
Behind the manubrium, only two large vessels are seen anterior to the trachea. The aortic arch can easily be followed as it extends toward the left side of the posterior thoracic cage. The other major vessel, the superior vena cava, occupies a position adjacent to the right side of the aortic arch. In addition, a portion of a smaller vessel, the azygos arch, is shown on the right side of the trachea, extending from the right posterior thoracic cage toward the superior vena cava.



A



B



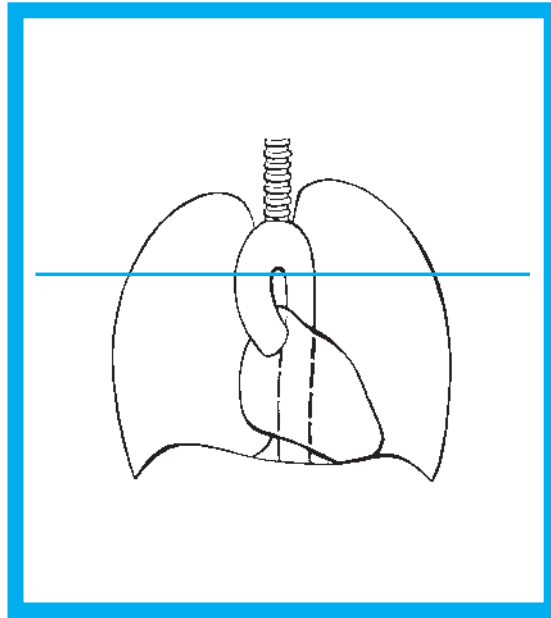
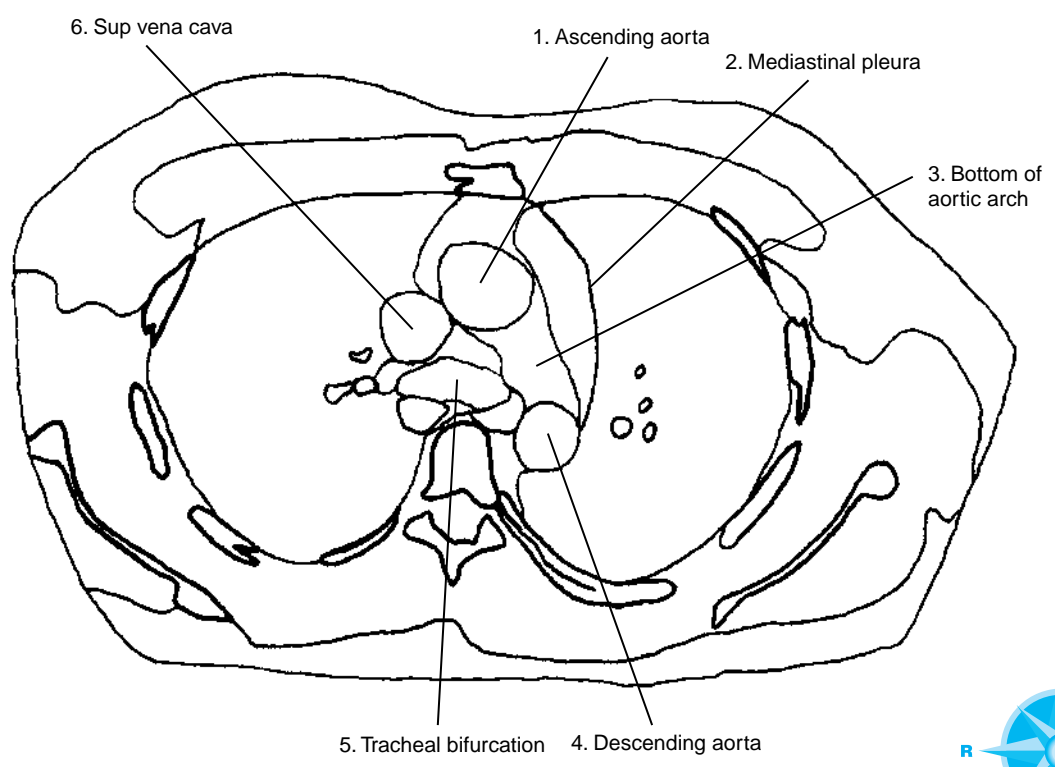


**Figure 2-35 (A,B)** Axial CT image 11.

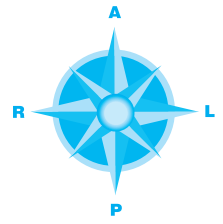
At this level, the aorta can be separated into three parts: ascending (originating from the left ventricle), arch (extending over the pulmonary trunk and left bronchus), and descending (located on the left side of the thoracic vertebral bodies). Near the aorta, the location of the mediastinal pleura marks the boundary between the mediastinum and the pleural space, containing the lungs on either side. Posterior to the superior vena cava, the trachea appears “flattened out,” indicating that the section is nearing the point of bifurcation into the right and left main bronchi.



A



B





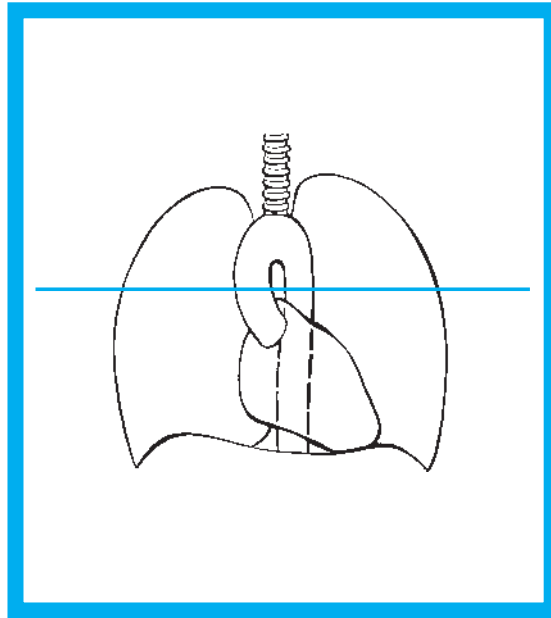
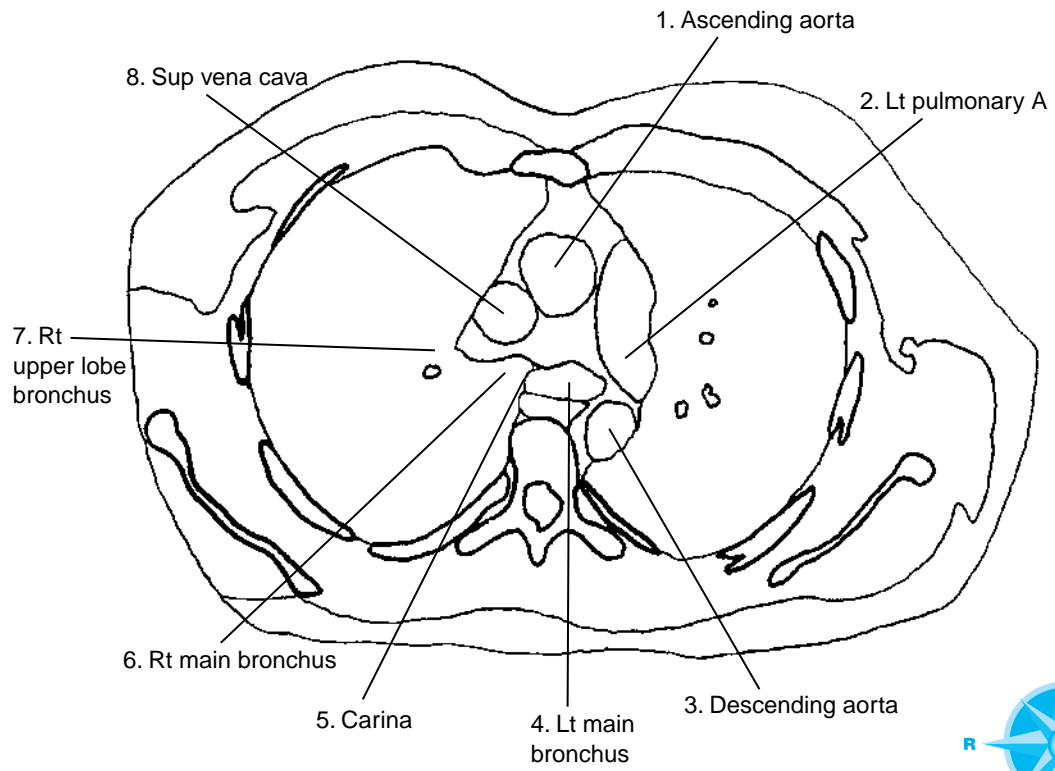


**Figure 2-36 (A,B)** Axial CT image 12.

Compared to the previous images, the most notable distinction in this figure is the absence of the arch between the ascending and descending parts of the aorta. Because this section is below the level of the arch, the left pulmonary artery is demonstrated extending into the left lung. At this level, a thin ridge representing the carina is separating the trachea into the right and left main bronchi. In addition, the right upper lobe bronchus is extending anteriorly from the main bronchus within the hilum of the right lung.



A



B

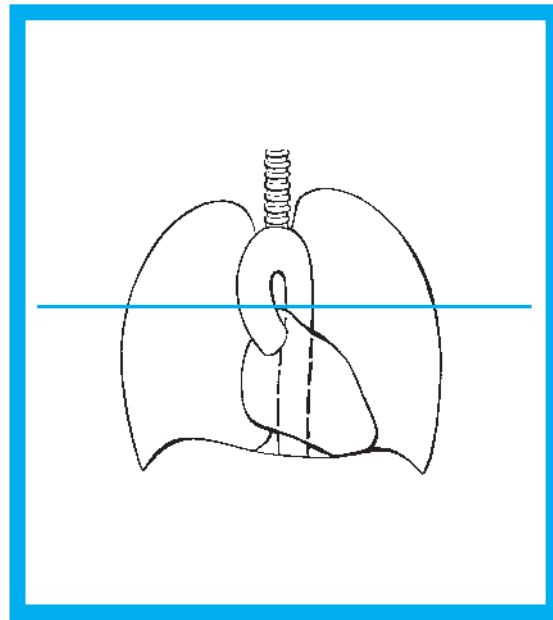
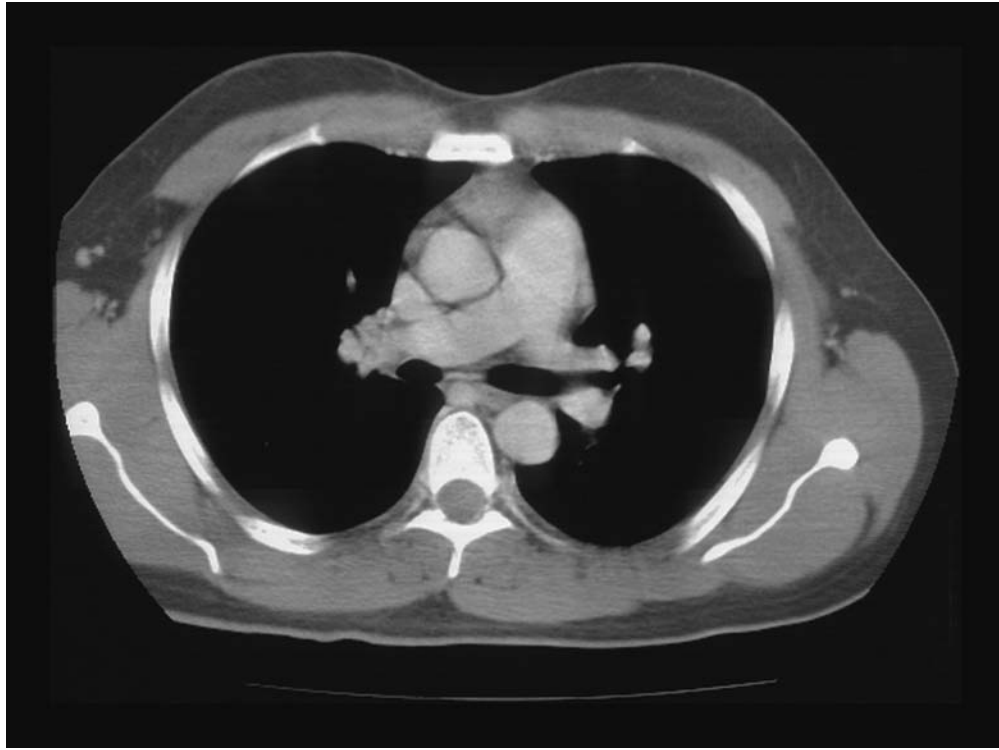
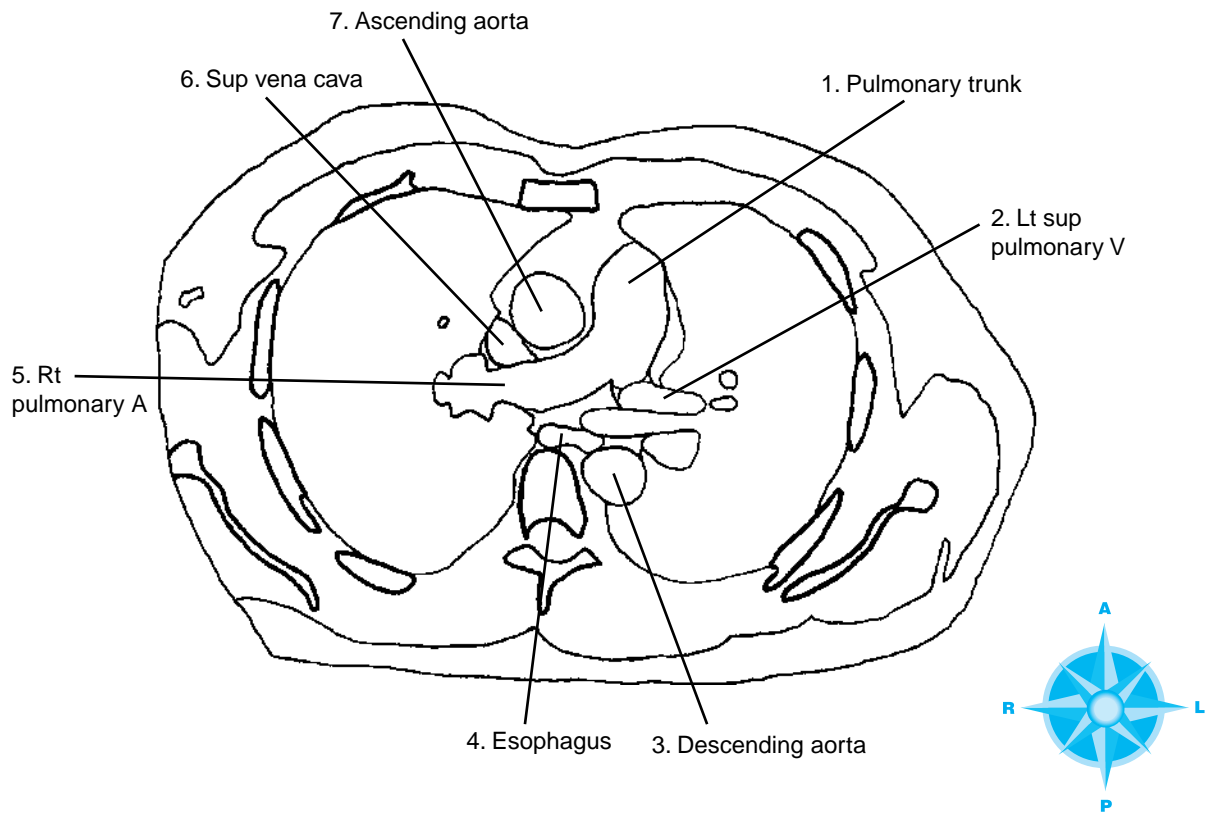


**Figure 2–37 (A,B)** Axial CT image 13.

The T shape of the pulmonary trunk and arteries is demonstrated as obliquely sectioned in this figure, because the left pulmonary artery was demonstrated in the previous section. The pulmonary trunk (originating from the right ventricle) is longitudinally sectioned, originating from the anterior mediastinum and extending posteriorly. At the terminal end, the pulmonary trunk bifurcates forming the right and left pulmonary arteries. Together, these three arterial structures form a T, which can be described as “laying down on the top of the heart” to “go under” the arch of the aorta. Adjacent to the pulmonary trunk, the left superior pulmonary vein is demonstrated inferior to the left pulmonary artery included within the previous section. On the right side of the pulmonary trunk, the ascending aorta and the superior vena cava are shown in cross-section above the heart. Similar to previous images, the descending aorta and esophagus are found within the posterior mediastinum.



A



B

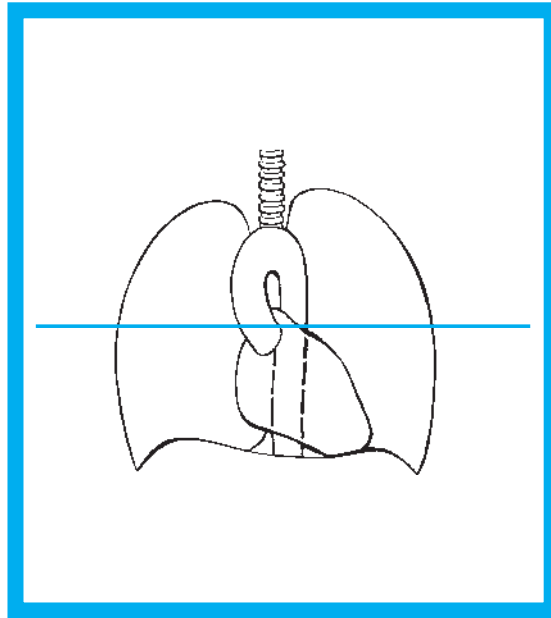
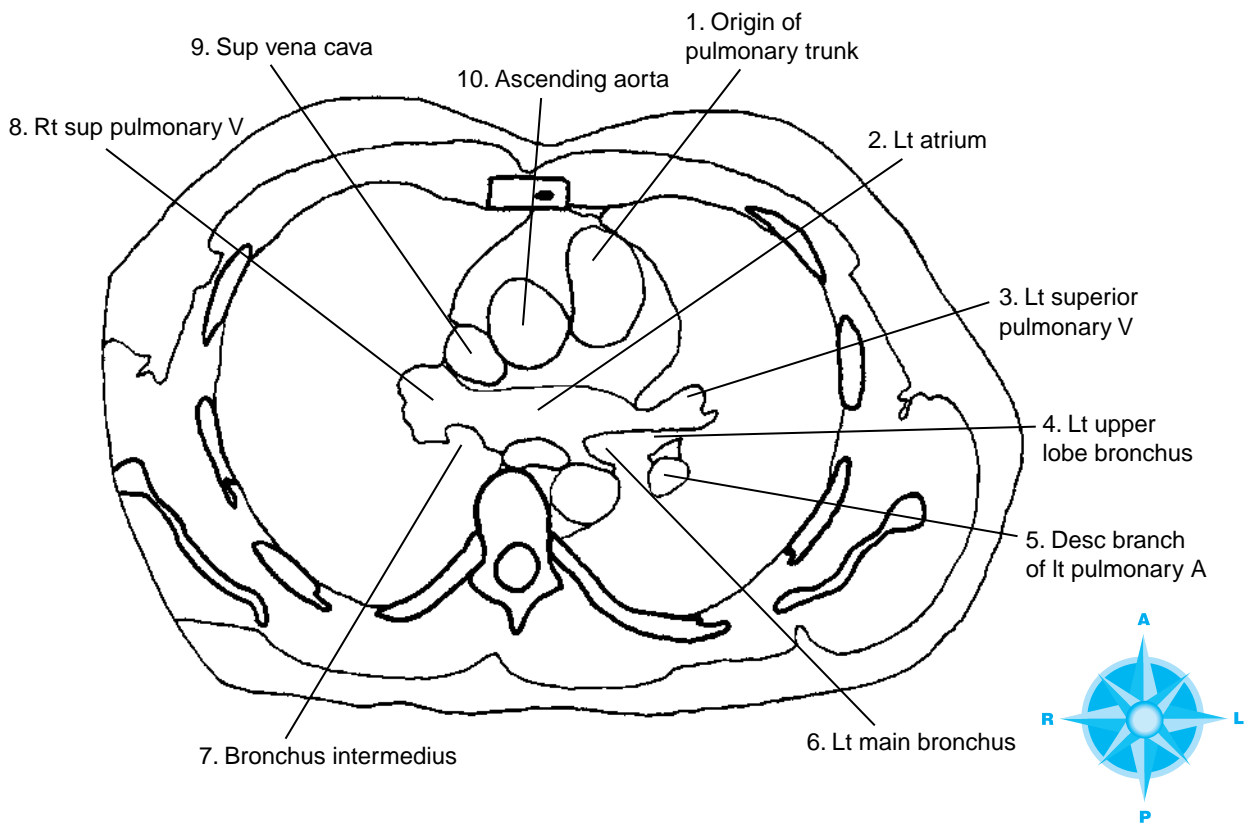


**Figure 2–38 (A,B)** Axial CT image 14.

The major vessels closely associated with the heart are not clearly demonstrated because of the movement caused by the beating of the heart during the scan. However, several major vessels can be identified by location on the anterior aspect of the heart: the superior vena cava, the ascending aorta, and the pulmonary trunk. Posterior to the three major vessels, the superior pulmonary veins from the right and left lungs are shown draining into the left atrium. Posterior to the atrium, the left main bronchus is giving rise to the left upper lobe bronchus, which lies just anterior to the descending branch of the left pulmonary artery. On the right side, the bronchus intermedius (continuation of right main bronchus after the origin of the upper lobe bronchus) is directly behind the superior pulmonary vein.



A



B

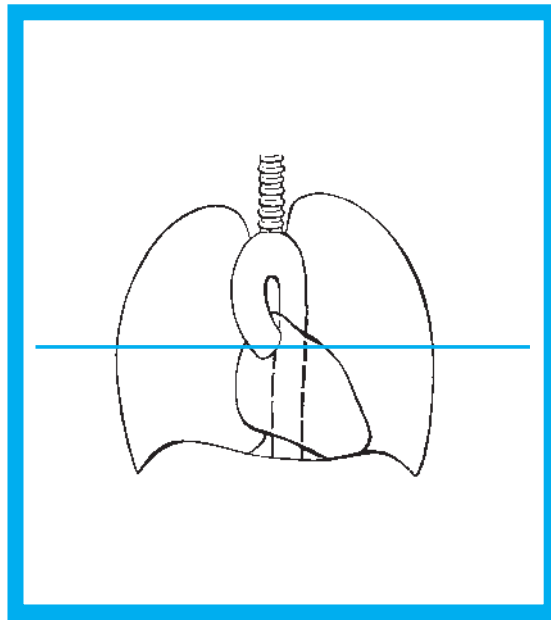
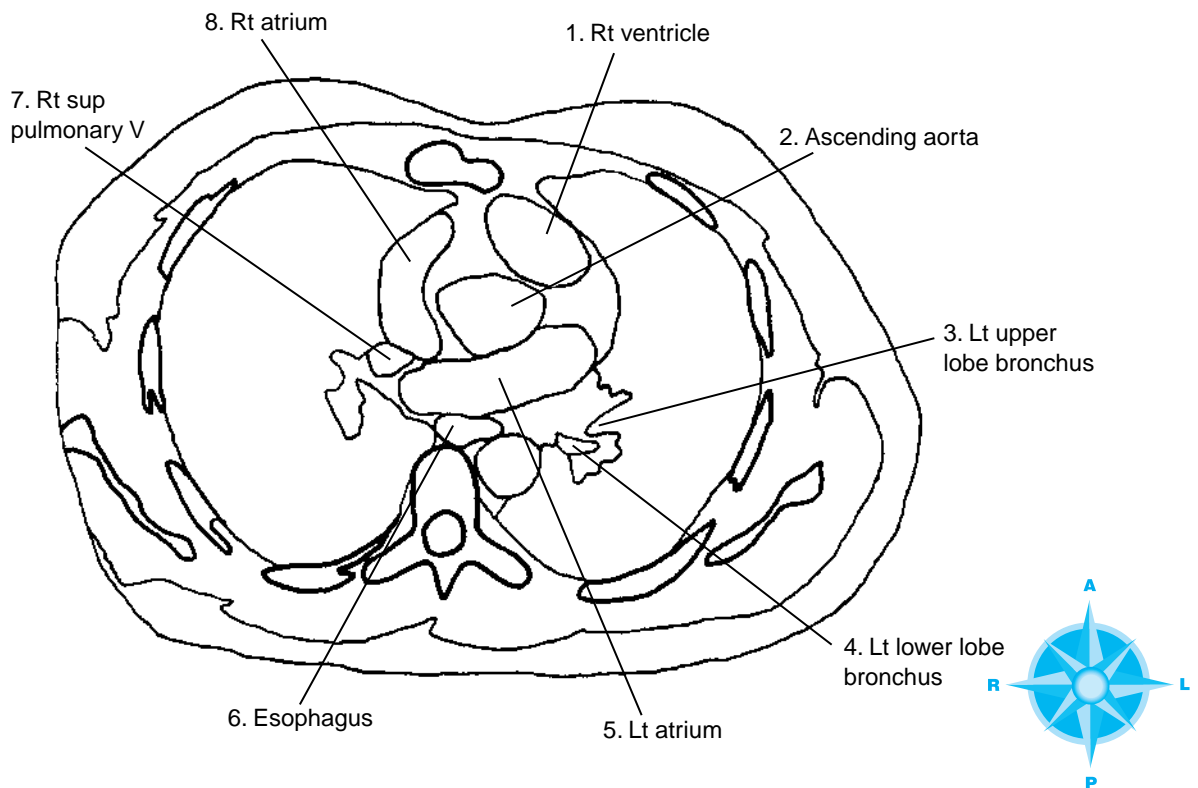


**Figure 2–39 (A,B)** Axial CT image 15.

Within the heart, the chambers are labeled as follows: The left atrium is most posterior, the right atrium is farthest to the right, and the right ventricle is most anterior. Near the center of the heart, the ascending aorta is sectioned as it originates from the left ventricle. Outside of the heart, the upper and lower lobe bronchi are seen on the left side. Because the upper lobe lies more anterior to the lower lobe as a result of the course of the oblique fissure, the upper lobe bronchus is more anterior. On the right side of the mediastinum, the superior pulmonary vein is labeled near its termination at the left atrium. Behind the left atrium, the esophagus continues to be shown in cross-section in front of the vertebral column.



A



B



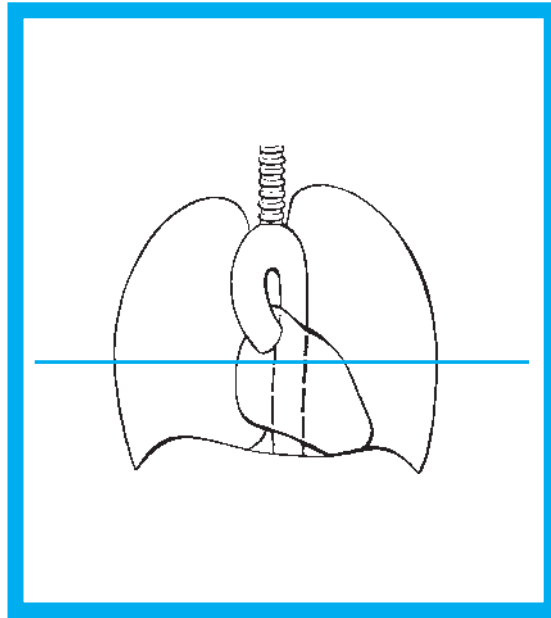
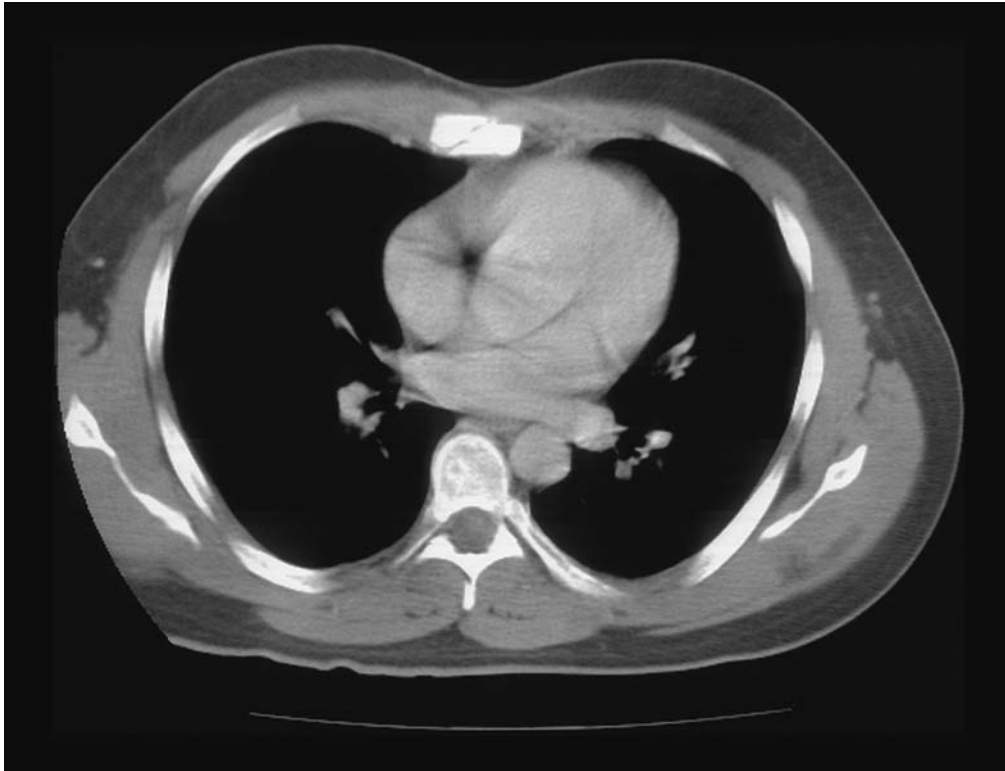
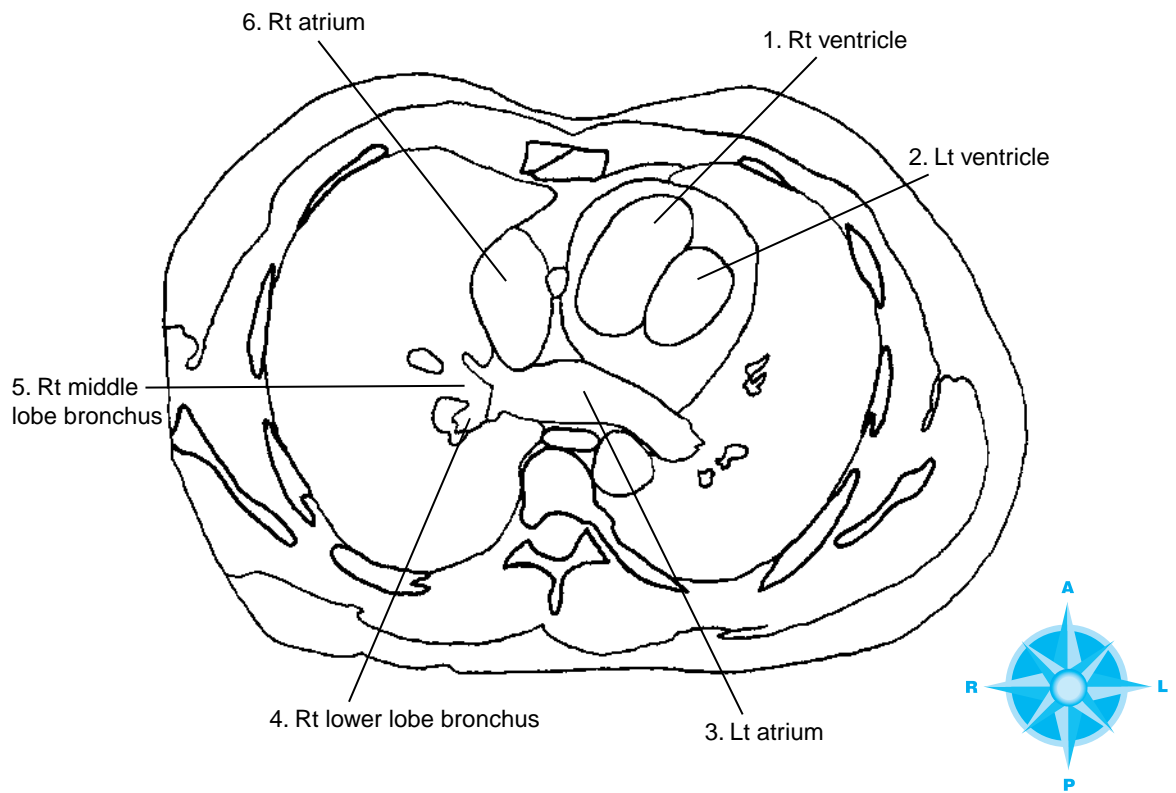


**Figure 2-40 (A,B)** Axial CT image 16.

All four chambers can be identified within the heart. The left atrium is most posterior, and the right atrium is farthest to the right. As described earlier, the right ventricle is most anterior, and the left ventricle is farthest to the left. Outside of the heart, the middle and lower lobe bronchi are seen on the right side near the position previously occupied by the bronchus intermedius.



A



B

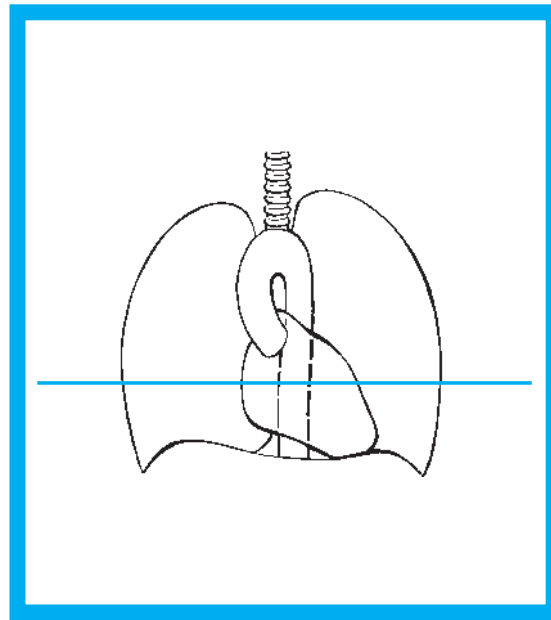
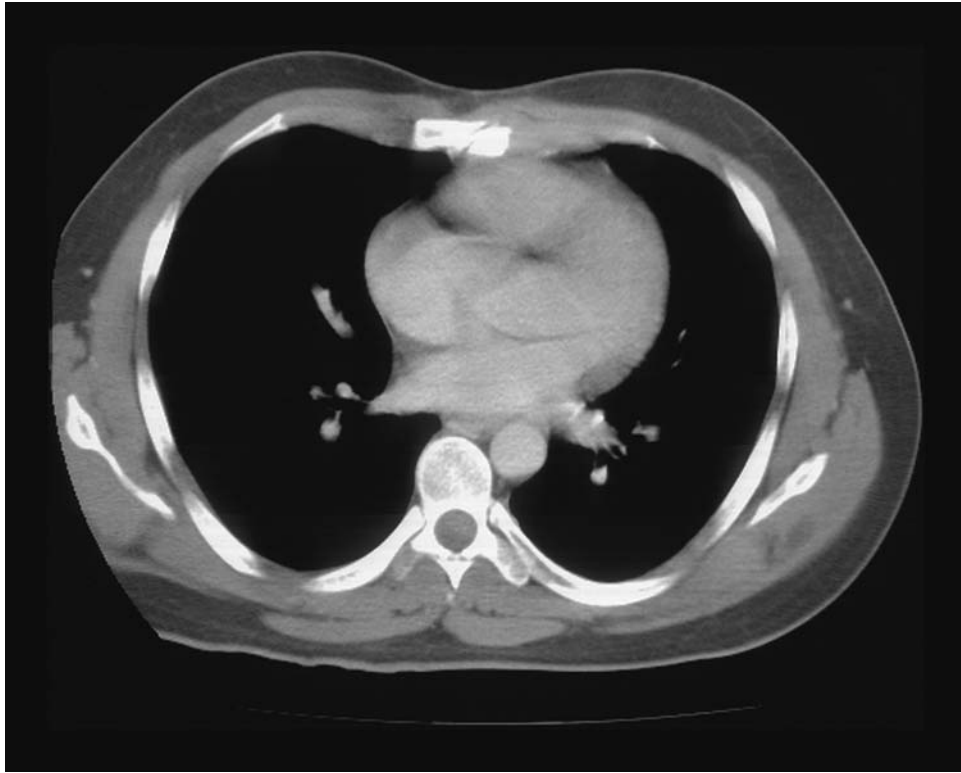
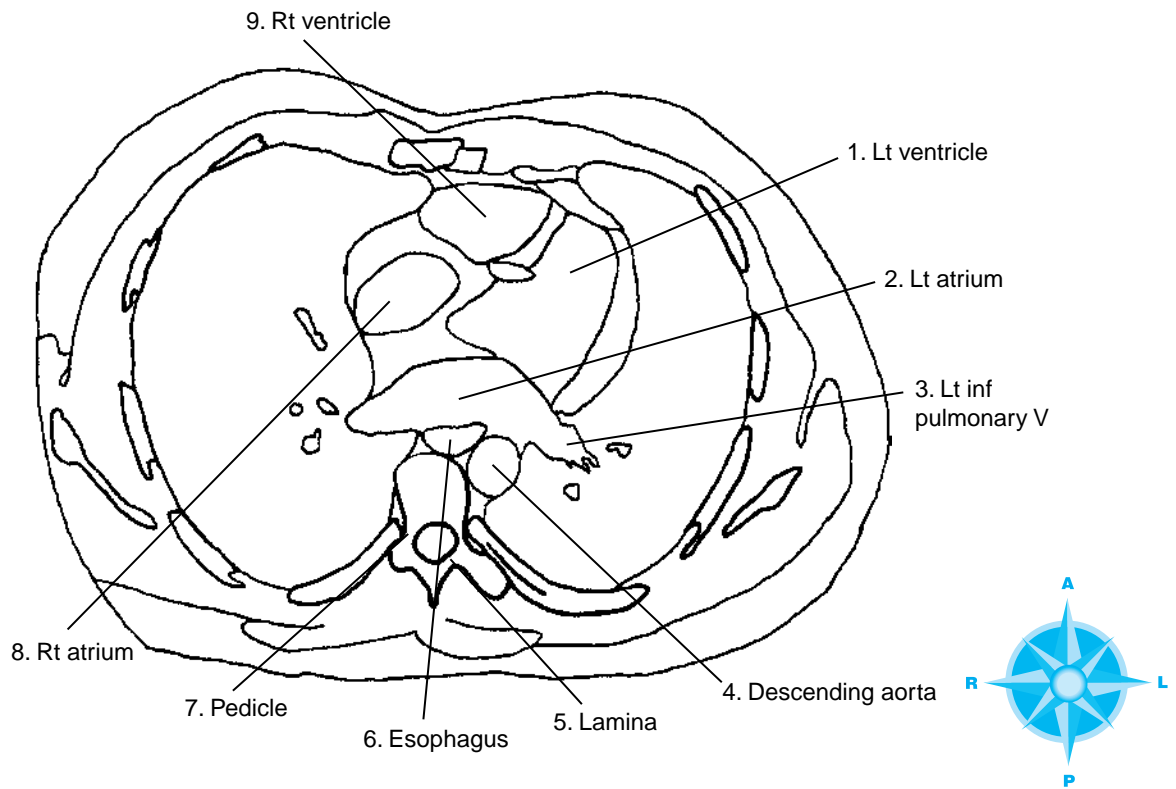


**Figure 2-41 (A,B)** Axial CT image 17.

Although the margin of the heart appears “shadowed” as an artifact of movement, all four chambers are seen. At this level, the left atrium is shown continuous with the left inferior pulmonary vein. As described in the legend to the previous figure, the right atrium is farthest to the right, the right ventricle is most anterior, and the left ventricle is farthest to the left. Posterior to the heart, the esophagus and descending aorta are found beside the thoracic vertebral body. Within the vertebra, a pedicle and lamina, forming the vertebral arch, are labeled.



A



B

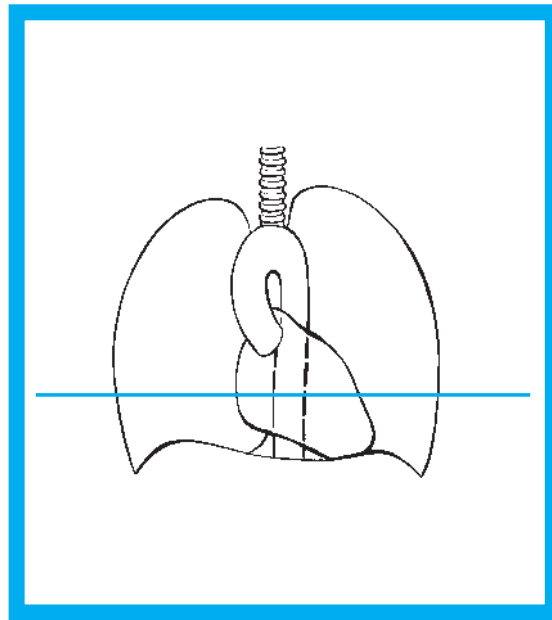
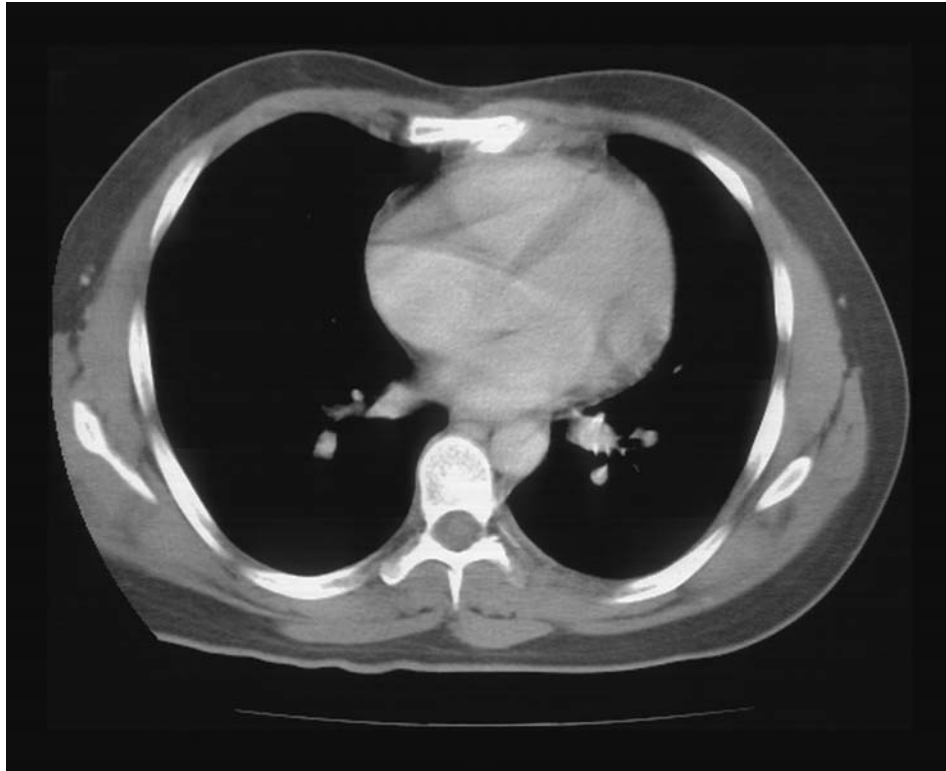
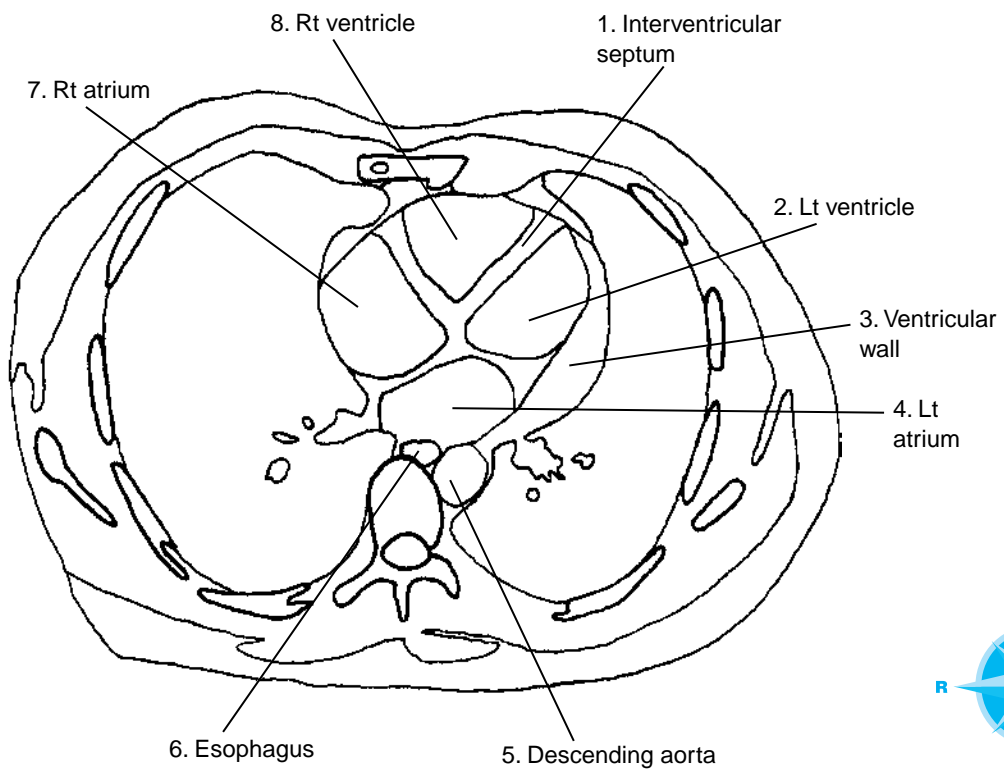


**Figure 2-42 (A,B)** Axial CT image 18.

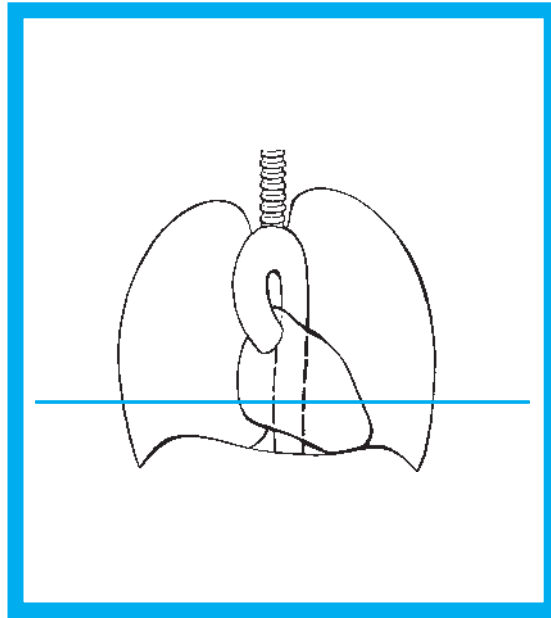
The most remarkable difference in this section compared to the previous two images is the demonstration of the ventricular walls. Despite the shadowing caused by heart movement, the interventricular septum and the outer ventricular wall are shown encasing the ventricular chambers (filled with blood). Because the septum extends toward the left side of the anterior thorax, the right ventricle and atrium are generally found in front of the left ventricle and atrium. Behind the heart, the esophagus and descending aorta are beside the thoracic vertebra.



A

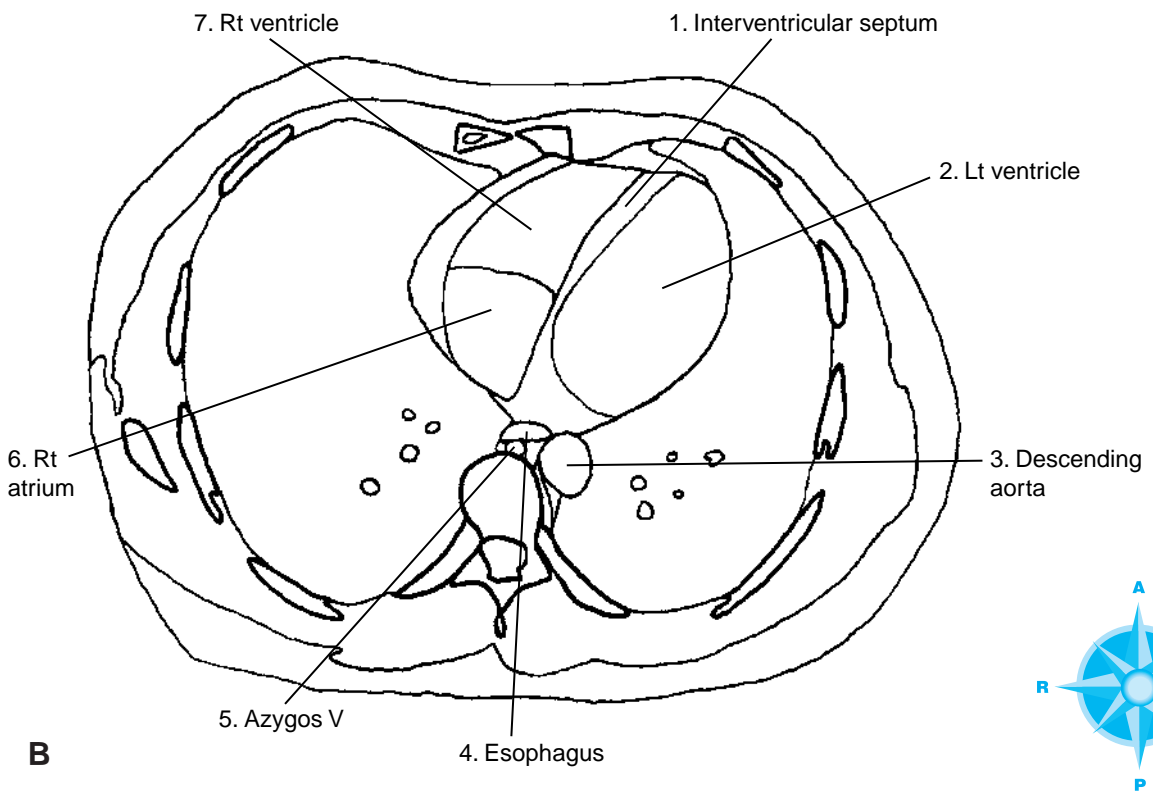
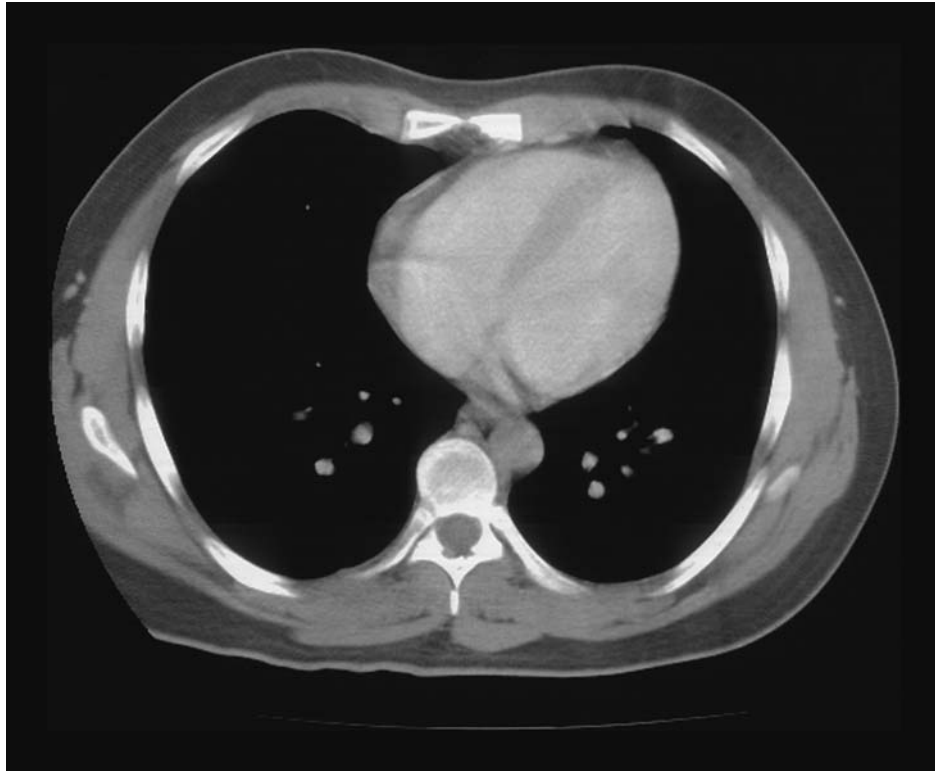


B

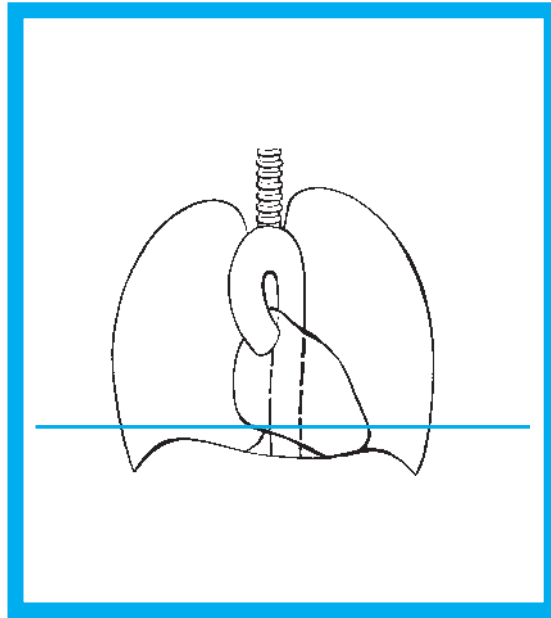


**Figure 2-43 (A,B)** Axial CT image 19.

The left atrium is no longer found on the posterior aspect of the heart, and the chambers of the ventricles are larger at this lower level. Similar to previous views, the right atrium is farthest to the right, the right ventricle is most anterior, and the left ventricle is farthest to the left. Although the esophagus and descending aorta are again shown behind the heart, the azygos vein is clearly discernible between the esophagus and the vertebral body.

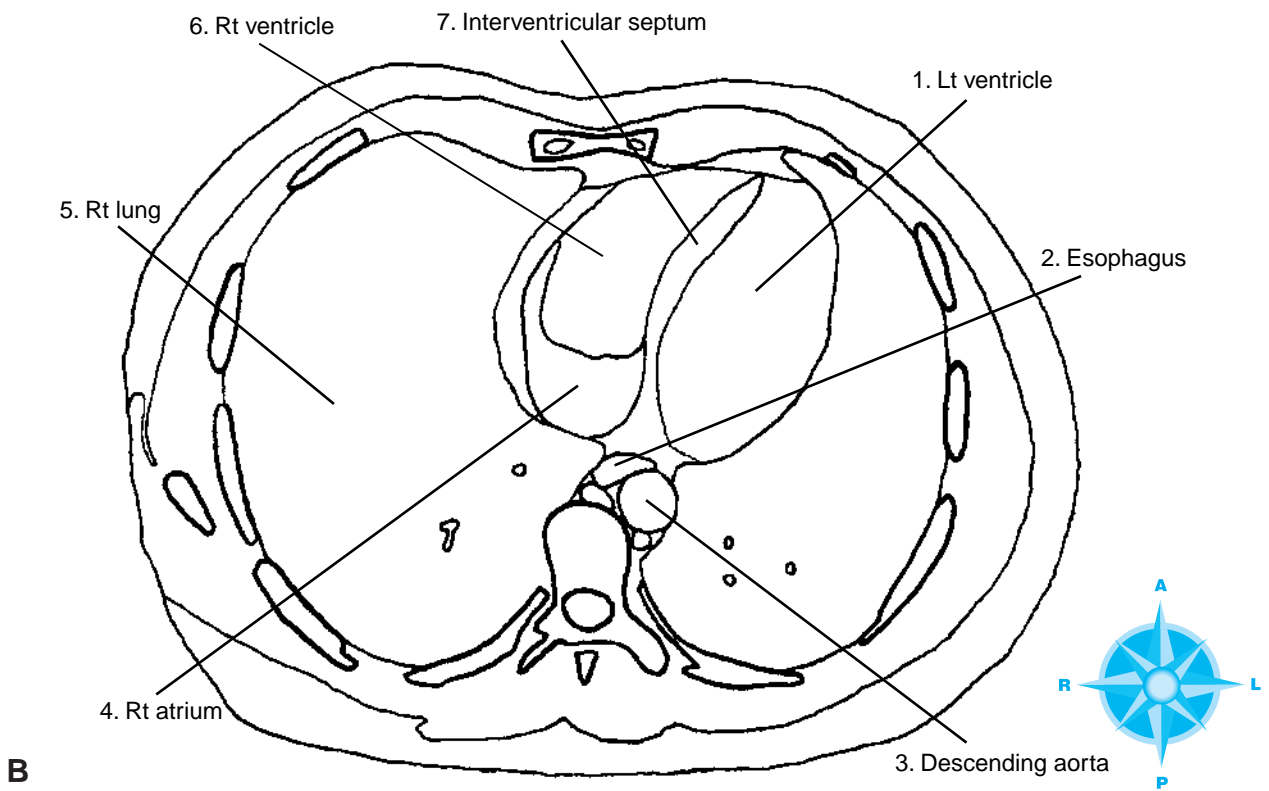
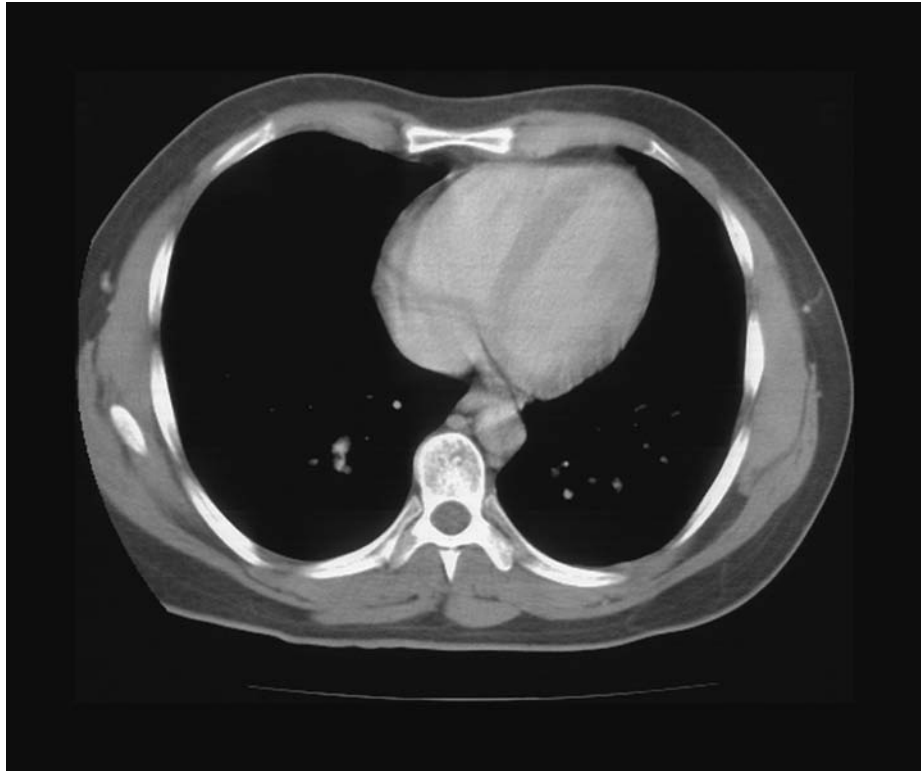






**Figure 2-44 (A,B)** Axial CT image 20.

This image shows a section through the middle region of the heart and includes the bottom of the right atrium. The larger chambers, the right and left ventricles, are separated by the interventricular septum and are larger than in previous views. Behind the heart, the esophagus and descending aorta are labeled within the posterior mediastinum.



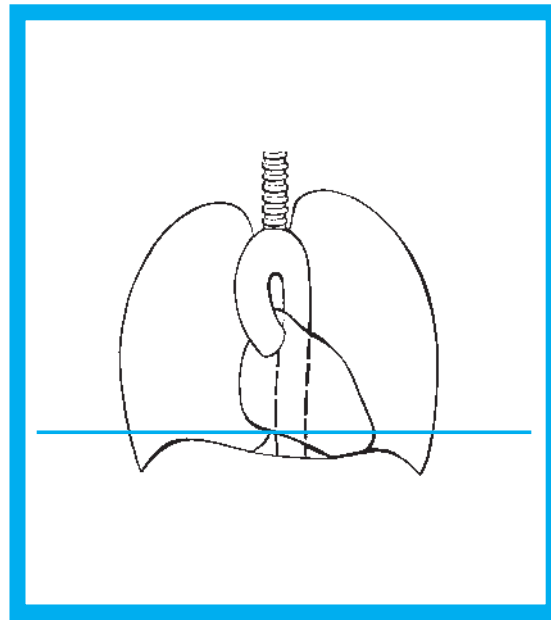
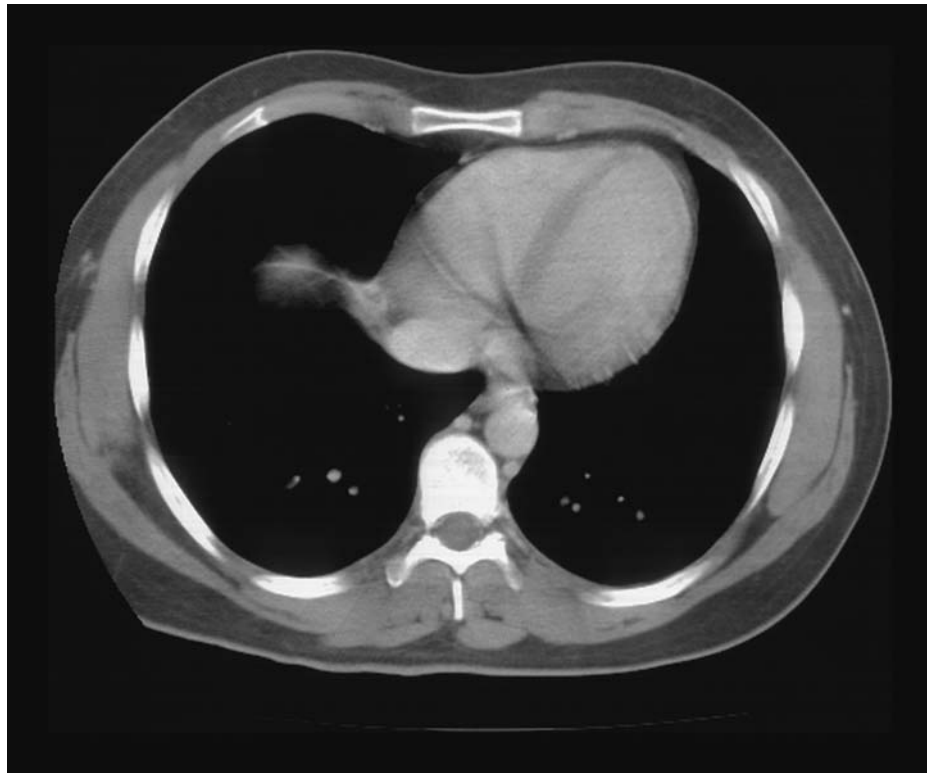
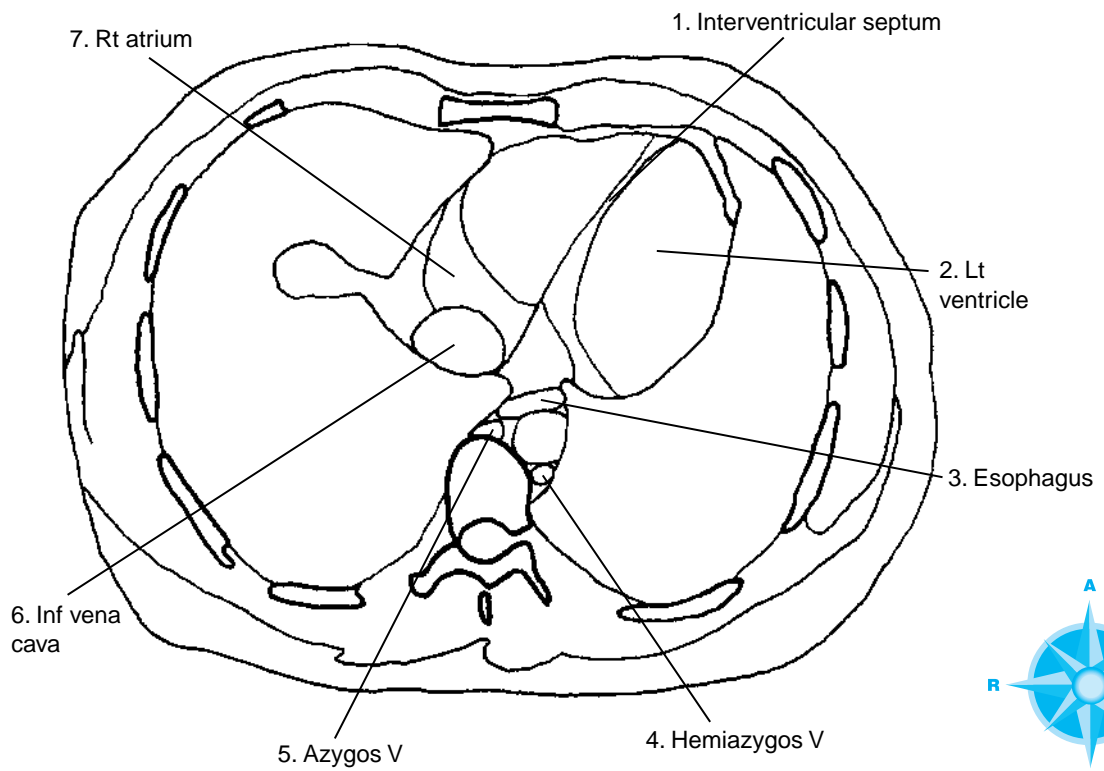


**Figure 2-45 (A,B)** Axial CT image 21.

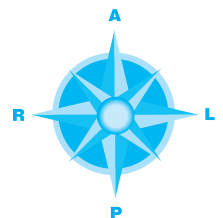
At this level, the right atrium is continuous with the inferior vena cava and can be distinguished by contrast enhancement. As in the previous image, the interventricular septum divides the left and right ventricles. Posterior to the heart, the esophagus and descending aorta are again shown within the posterior mediastinum. On either side of the aorta, the azygos vessels are cross-sectioned adjacent to the vertebral body. Although the azygos vein was previously labeled on the right side of the aorta, this section is the first to clearly show the hemiazygos vein on the left side of the vertebral body. If this section were above the level of T6, a small vein in this position would be the accessory hemiazygos vein.



A



B



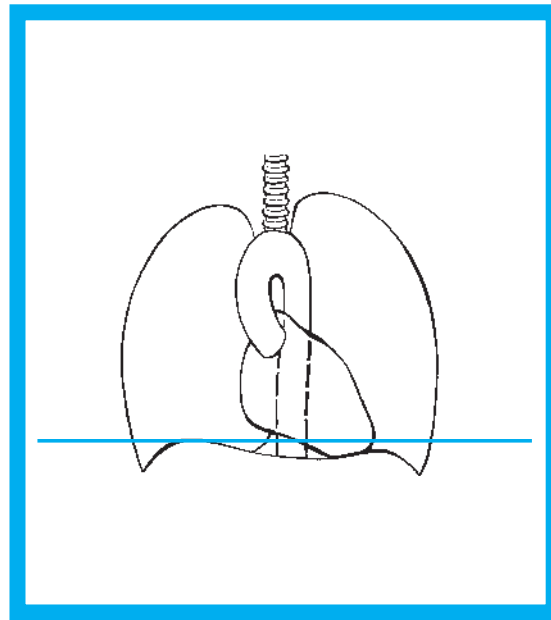
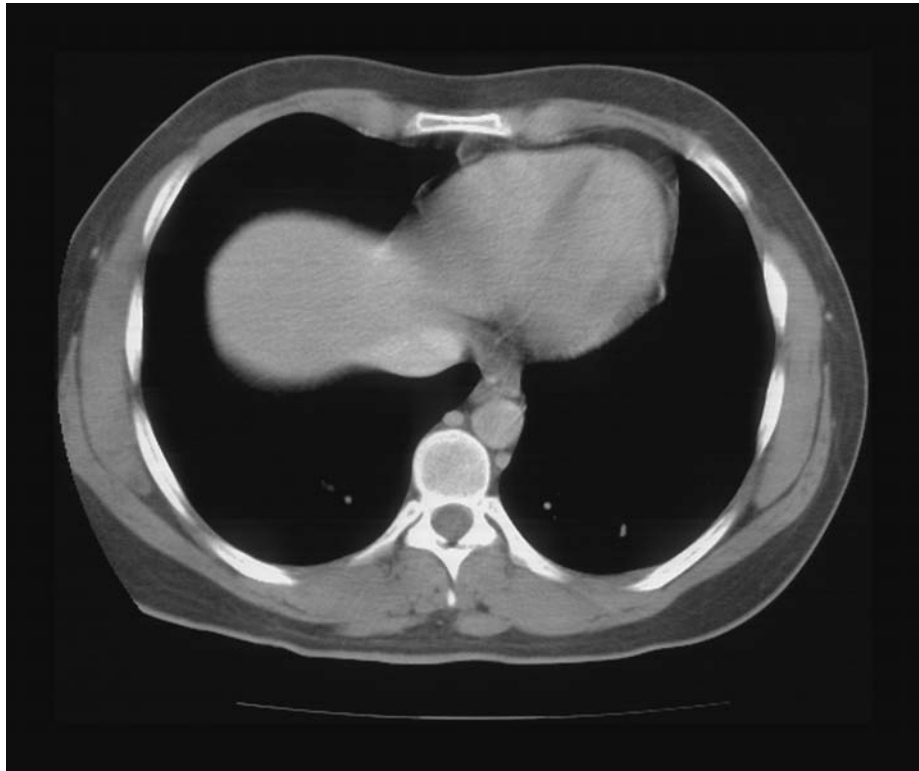
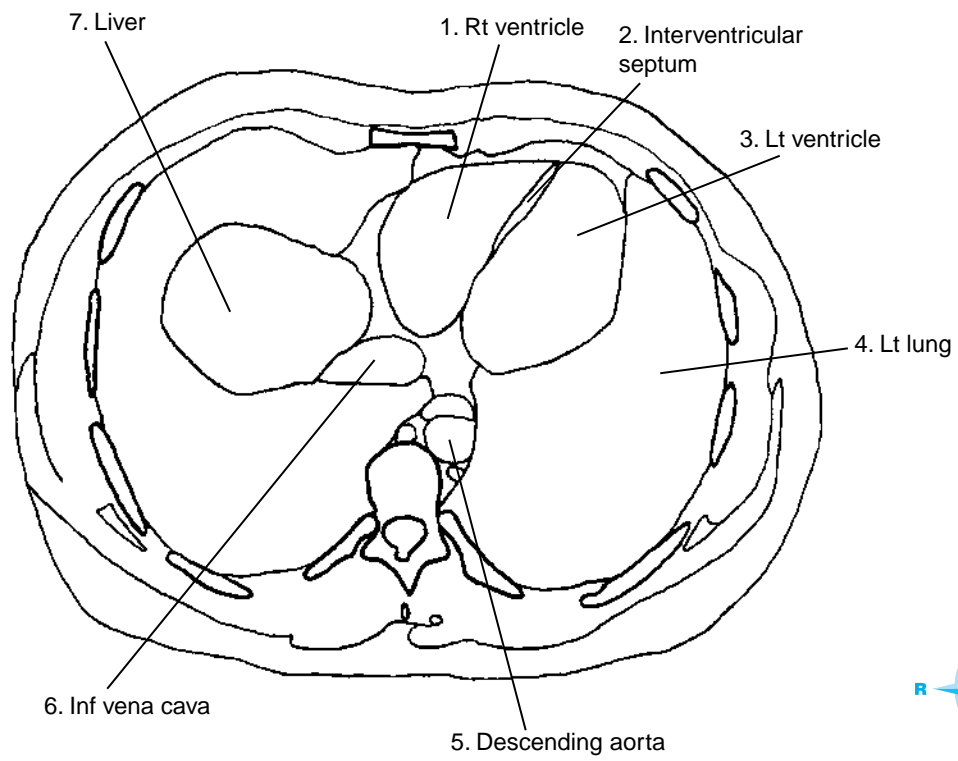


**Figure 2-46 (A,B)** Axial CT image 22.

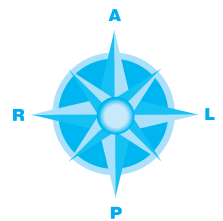
The unique feature of this figure is the appearance of a dense structure, the top of the liver, surrounded by the right lung. The liver appears nearly continuous with the heart, because the central tendon of the diaphragm is obscured by the shadow caused by the beating of the heart during the scan. Between the liver and the heart, the contrast-enhanced inferior vena cava is found in the place previously occupied by the right atrium. Similar to previous views, the interventricular septum separates the right and left ventricles.



A



B



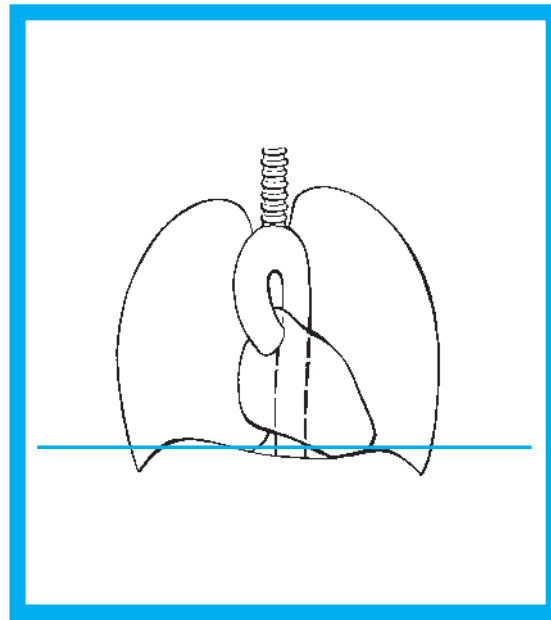
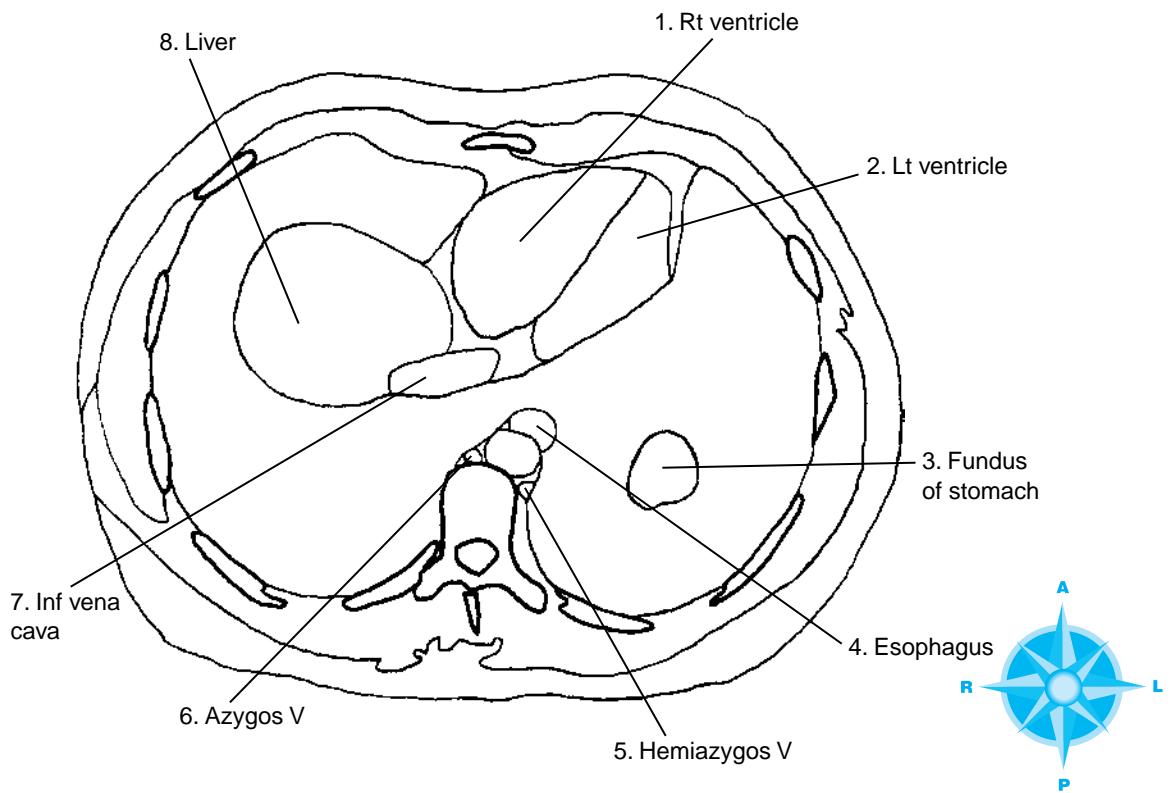


**Figure 2-47 (A,B)** Axial CT image 23.

The liver is readily identified on the right side surrounded by the right lung. Within the mediastinum, the section passes through the lower heart, demonstrating the bottom right and left ventricles. As described previously, the right ventricle is more anterior and lies next to the chest wall. The small part of the left ventricle is more posteriorly situated on the left side. Posterior to the heart, the esophagus is near the midline, and the fundus of the stomach is surrounded by the left lung. Because of the shape of the stomach, the fundus is superior to the gastroesophageal junction. Within the posterior mediastinum, the azygos and hemiazygos veins are shown in cross-section beside the descending aorta.



A



B



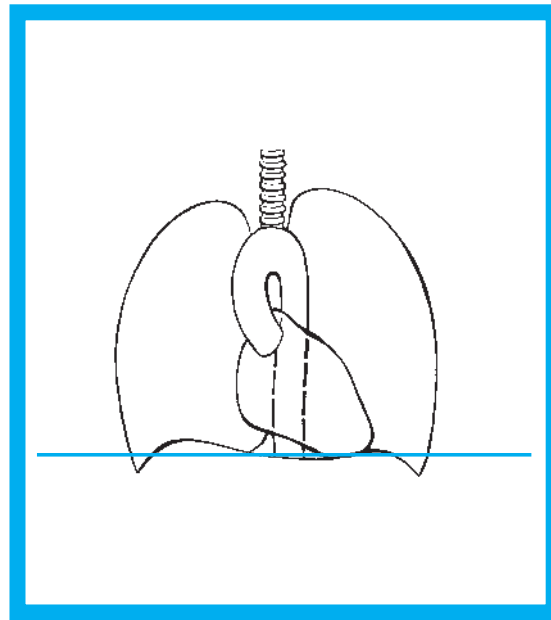
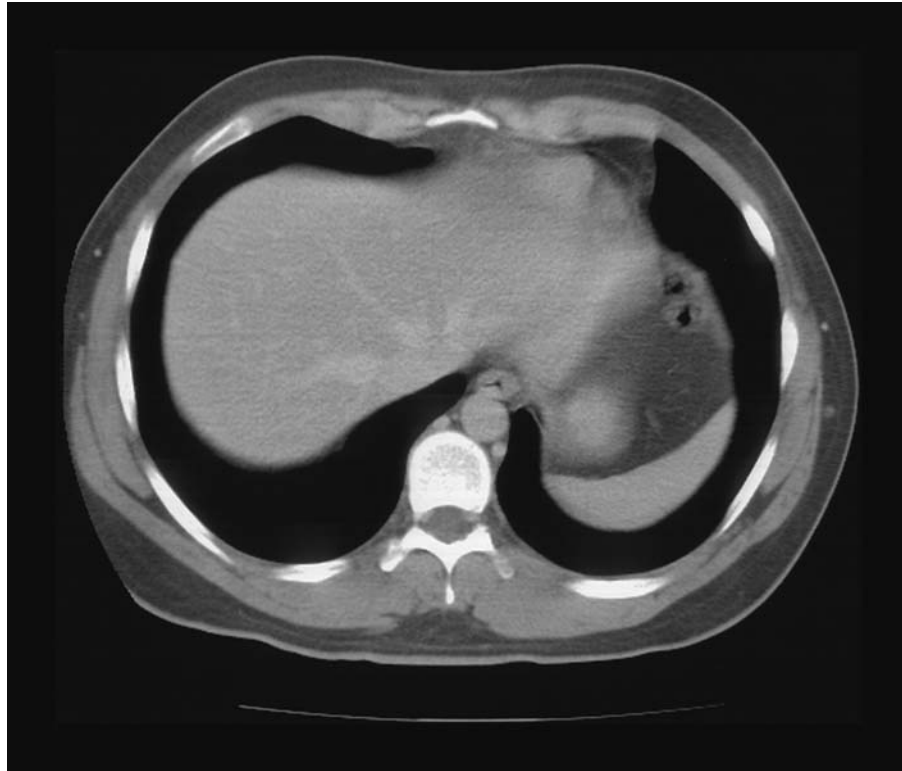
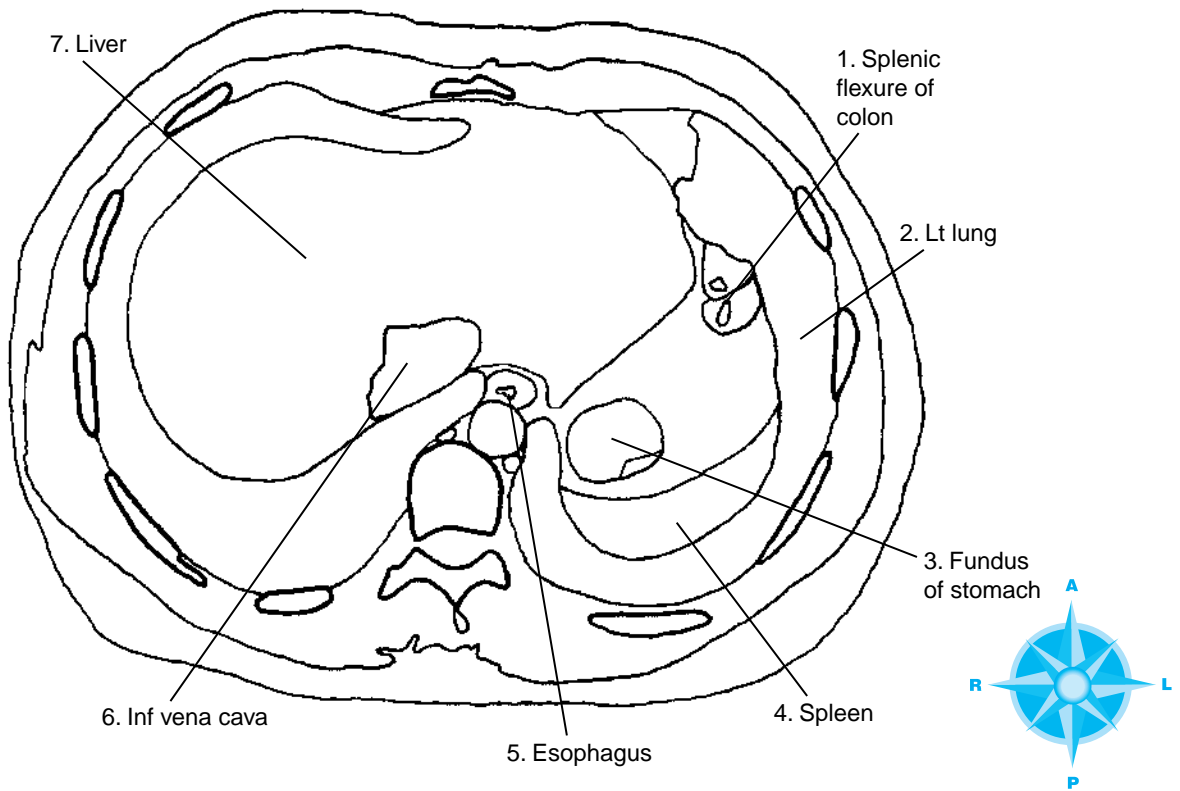


**Figure 2-48 (A,B)** Axial CT image 24.

At this level, the heart is no longer seen, and most of the structures demonstrated are contents of the abdominal cavity. The liver occupies much of the section and extends across the midline to the left side. Within the posterior edge of the liver, the contrast-enhanced inferior vena cava is embedded within the liver. On the left, the fundus of the stomach is slightly closer to the esophagus, and the base of the left lung is seen only adjacent to the chest wall. Posterior to the stomach, the crescent-shaped spleen is demonstrated as a dense structure bordering the base of the left lung. Anterior to the stomach, the splenic flexure of the colon is shown inferior to the left lung as an irregularly shaped structure containing pockets of air.



A



B

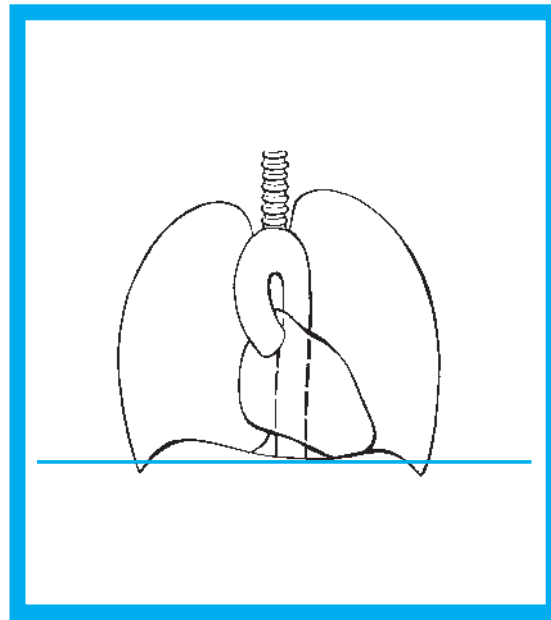
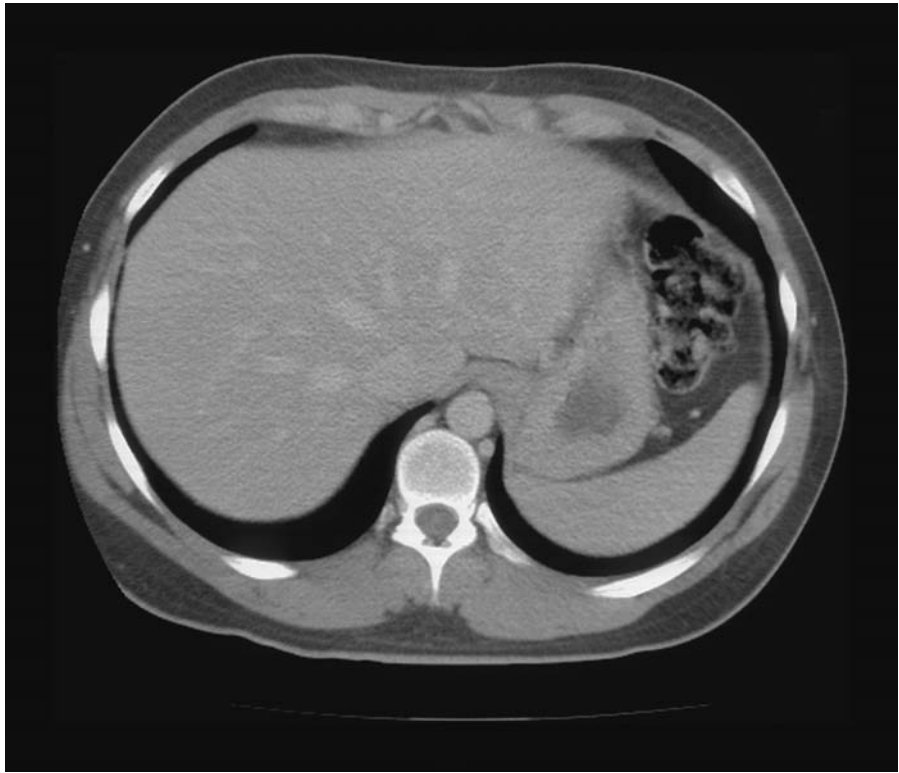
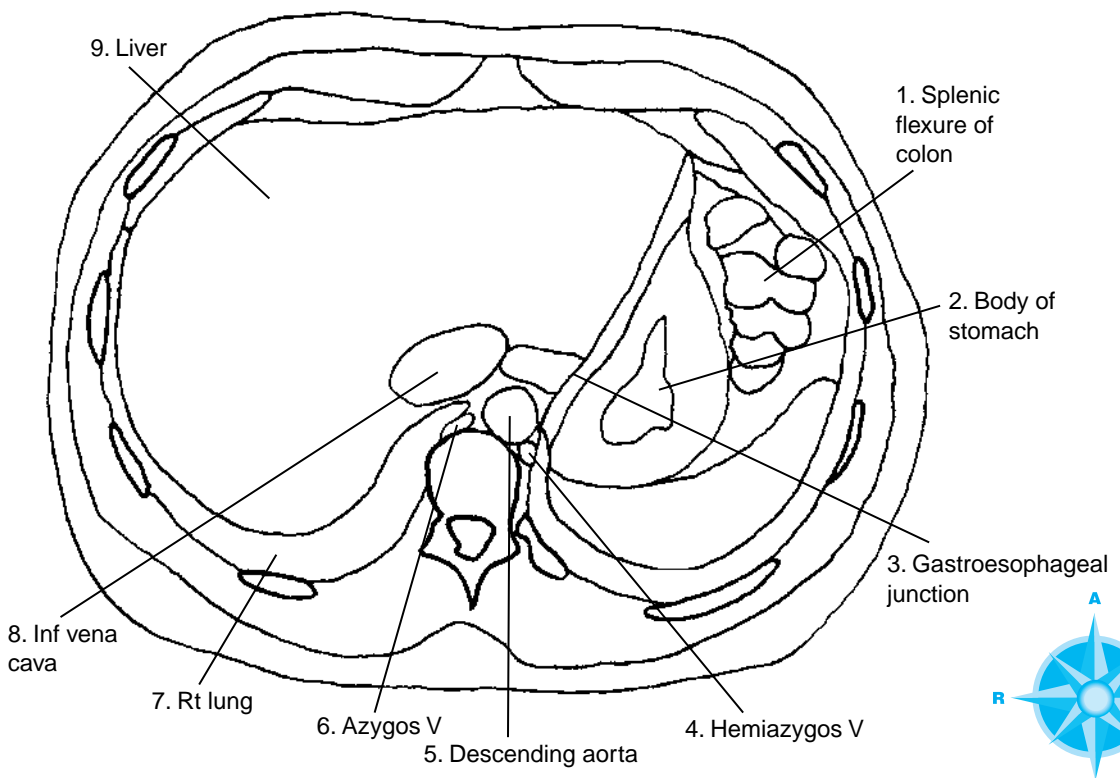


**Figure 2-49 (A,B)** Axial CT image 25.

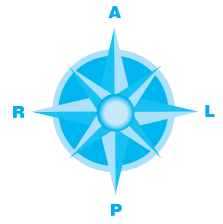
The right lung forms a thin margin around the liver next to the chest wall. Near the midline, the contrast-enhanced inferior vena cava is again found within the posterior margin of the liver. Adjacent to the inferior vena cava, the gastroesophageal junction marks the beginning of the body of the stomach, which is considerably larger than the fundus. On the left side, both the spleen and the splenic flexure of the colon are bordered by the left lung. Although this section is almost below the chest, the descending aorta, azygos vein, and hemiazygos vein are still found within the posterior mediastinum.



A



B



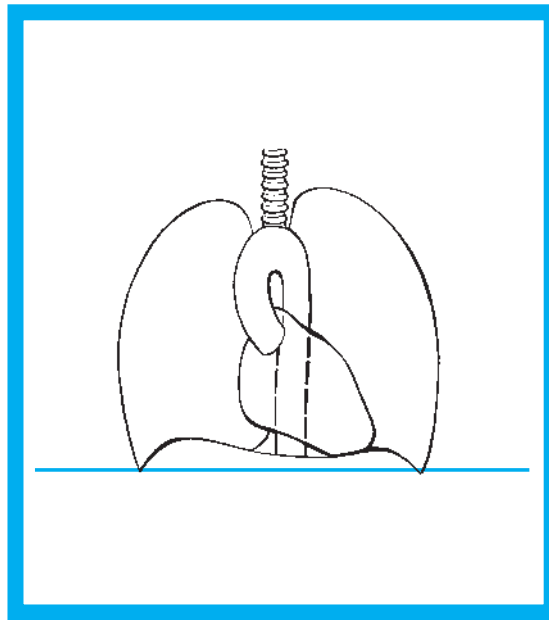
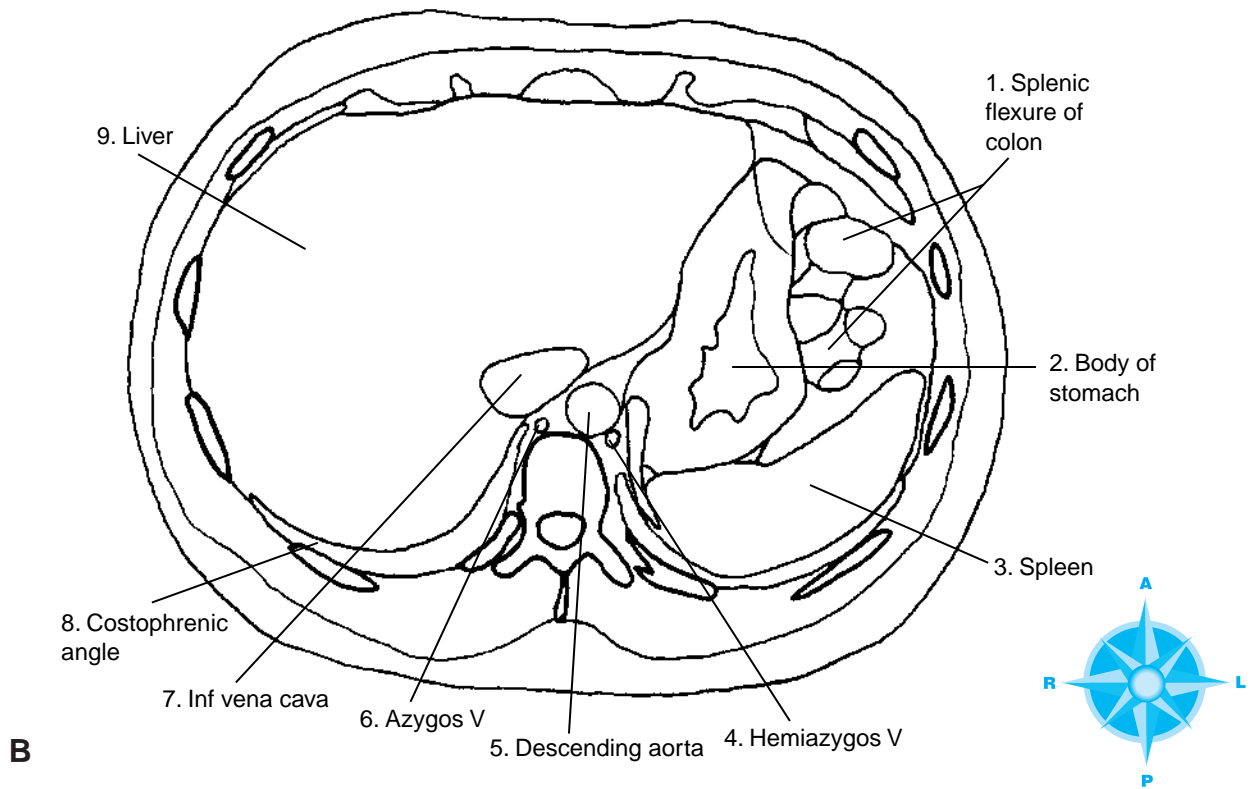
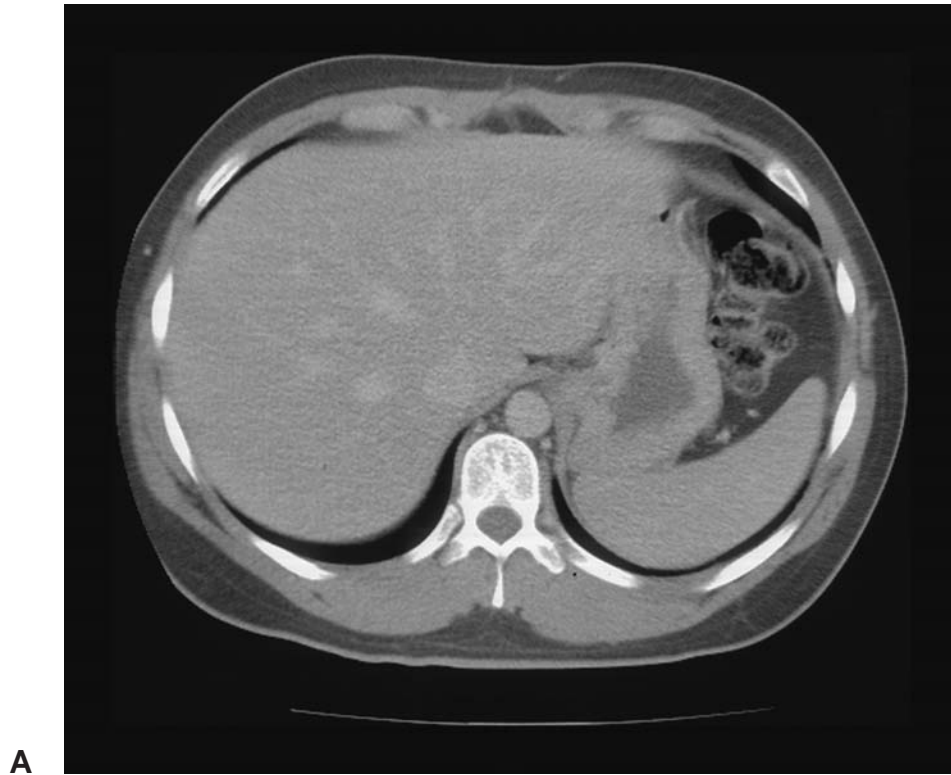


**Figure 2-50 (A,B)** Axial CT image 26.

The costophrenic angles of the right and left lungs are just inside the chest wall, indicating that this is the last image necessary for an examination of the chest. Within the abdomen, the liver occupies most of the right side and appears to wrap around the inferior vena cava. On the left side, the body of the stomach is sectioned by the splenic flexure of the colon and the spleen. Within the lower mediastinum, the descending aorta lies between the azygos vein on the right and the hemiazygos vein on the left.





## Case Study 2-1

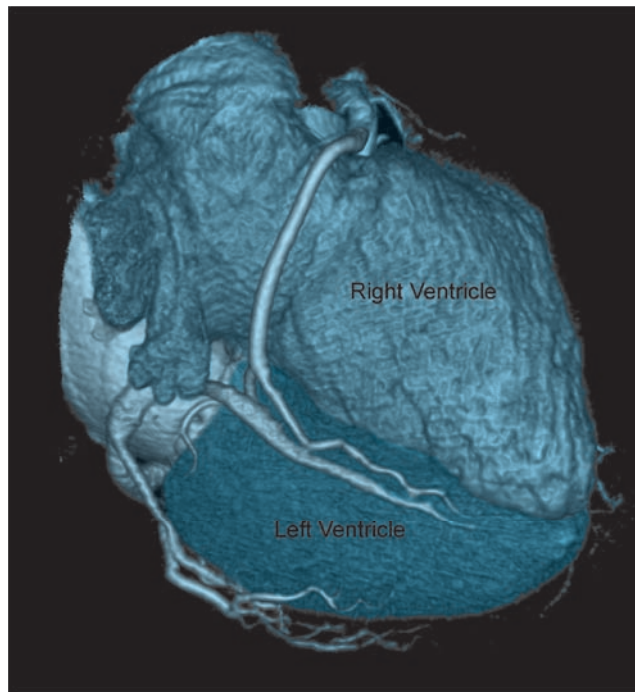


Figure 2-51

### Clinical Correlations

This 68-year-old woman had a CTA (computed tomography angiograph) to evaluate her coronary arteries. During the procedure, the information generated for the cross-sectional images is assembled by computer into a three-dimensional picture of the area being studied. In this volume-rendering image, we are looking at the heart from below and are viewing the surface of the heart that rests on the diaphragm. The right ventricle and left ventricle

are found side-by-side, and coronary vessels are shown wrapping around both sides of the heart extending toward the apex of the posterior heart. From this view, the coronary vessels appear normal, and no strictures are apparent on the right or left coronary arteries. In cases where coronary disease is present, the vessels will have narrowed regions where the blood flow is restricted or will truncate in cases of complete occlusion resulting in a myocardial infarction.

### Questions

1. The arterial blood in the ascending aorta and the coronary arteries flows directly from which chamber of the heart?
2. The pulmonary trunk originates from which chamber of the heart?
3. The venous blood from the body drains into which chamber of the heart?
4. The heart is found more on the right or left side of the chest?
5. Does the right or left side of the heart lie closest to the spine?



## Case Study 2-2

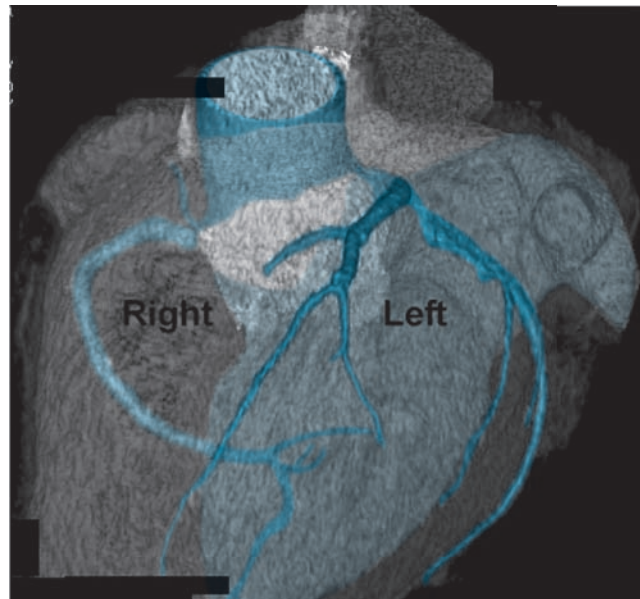


**Figure 2-52**

This 48-year-old man had his heart evaluated with CTA to demonstrate his coronary arteries, and all were reported to have normal blood flow. This selected image provides an anterior view of the heart, and the right and left sides are labeled. Unlike the preceding case study, the heart muscle has been made transparent so that the coronary vessels can be traced around the posterior surface of the heart. As shown in the image, both the right and left coronary arteries originate at the base of the aorta and

travel around the surface of the heart. The right coronary artery wraps around the right side of the heart between the right atrium and right ventricle to reach the posterior side of the heart. Unlike the right coronary artery, the left coronary artery has two major branches: The anterior interventricular found on the anterior surface of the heart between the ventricles, and the circumflex, which wraps around to extend down the posterior side of the heart.

### Questions

1. Does the right or left side of the heart lie closest to the anterior chest wall?
2. Which heart valve is found between the right atrium and right ventricle?
3. Which chamber of the heart is responsible for pumping arterial blood to most of the body?
4. Which heart valve is found between the left atrium and left ventricle?
5. The venous blood returning from the lungs drains into which chamber of the heart?





## Case Study 2-3

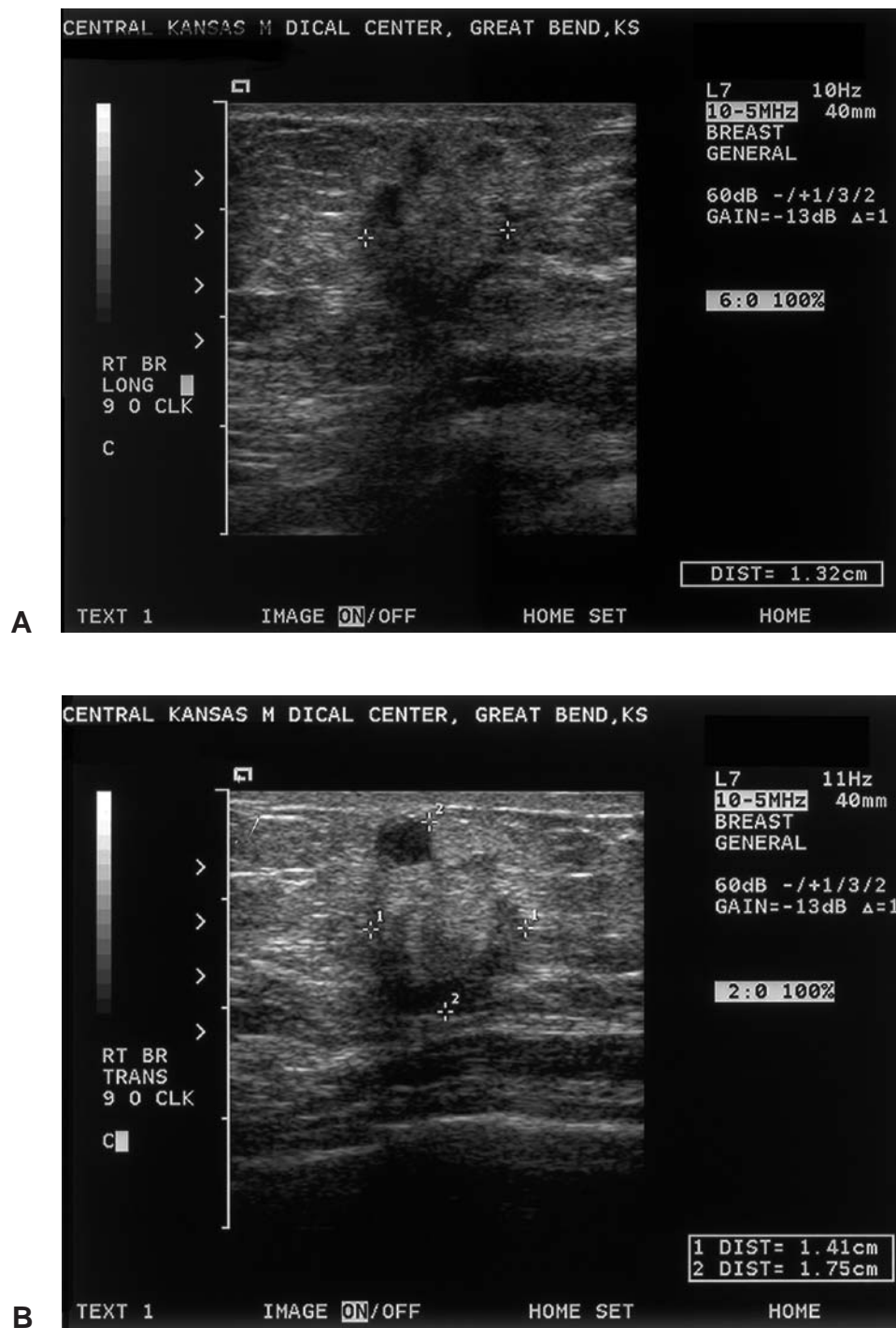


Figure 2-53

This 53-year-old woman had a family history of breast cancer (grandmother was diagnosed with breast cancer) and was initially evaluated with a yearly screening mammogram. On the basis of those findings, she was referred for ultrasound examination. Within the right breast, a lesion was found outside the chest wall; the border is demarcated by measuring marks as shown in both longitudinal and

transverse images. The mass measures about 1.5 cm in diameter and appears solid with some central calcifications that are shadowing. Subsequent to the ultrasound examination, an excisional biopsy of the right breast revealed that the mass was a carcinoma, the most common cancer in women. Current estimates show that one in 14 women will develop breast cancer during her life span.

## Questions

1. Would most of the adipose tissue found within the breast be superficial or deep to the chest musculature?
2. The axillary vein that drains the upper extremity and shoulder crosses the first rib to join with which vessel within the chest?
3. The venous blood within the right intercostal veins will drain into which vessel found within the bony thoracic cage on the right side of the vertebral column?
4. The venous blood within the upper left intercostal veins will drain into which vessel found within the bony thoracic cage on the left side of the vertebral column?
5. All of the venous blood from the chest will be collected and travel through which vessel before draining into the heart?



## Case Study 2-4

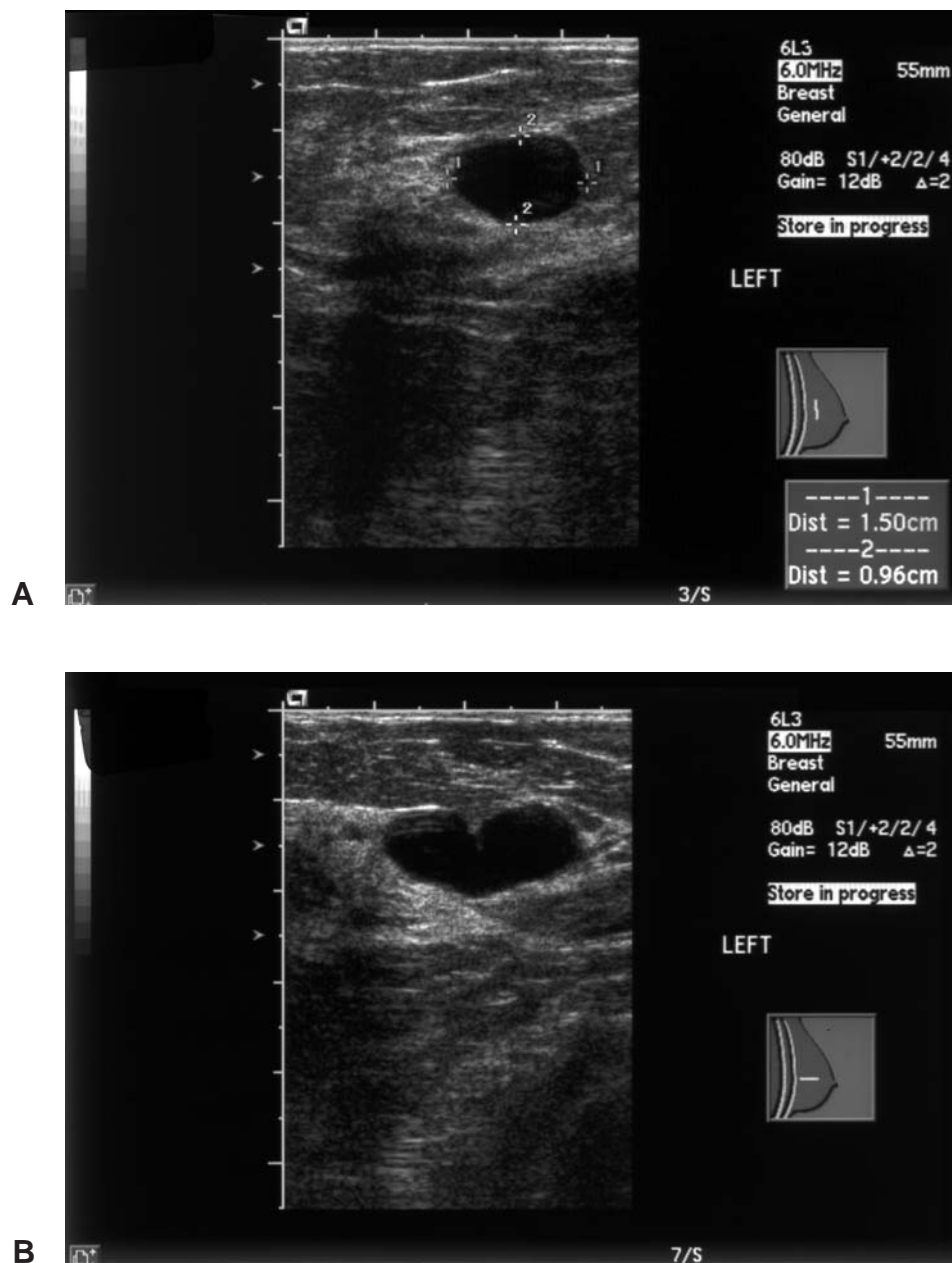


**Figure 2-54**

This 68-year-old woman was referred for an ultrasound examination following her mammogram that had revealed multiple nodules in the left breast. As outlined with measuring marks in the longitudinal image, the masses are large and filled with fluid (sonolucent) providing a well-

defined border with the surrounding tissue. In the transverse image, the fluid appears to be within two cysts located side-by-side. These cysts were determined to be benign in nature, so according to American Cancer Society guidelines only normal follow-up was recommended.

## Questions

1. An infection originating within the chest wall would be separated from the underlying pleural space and lungs by a tough connective tissue membrane lining the inside of the chest wall called?
2. On the right side of the chest, which lobes of the lung would be found in an axial section through the breast just above the horizontal fissure?
3. On the left side of the chest, which lobes of the lung would be found in an axial section through the breast?
4. Considered part of the shoulder girdle, which bone connects the shoulder to the bony rib cage and is frequently fractured in falling accidents?
5. Outside the bony rib cage, which artery gives rise to branches that supply the region of the external chest and breast?



## Case Study 2-5

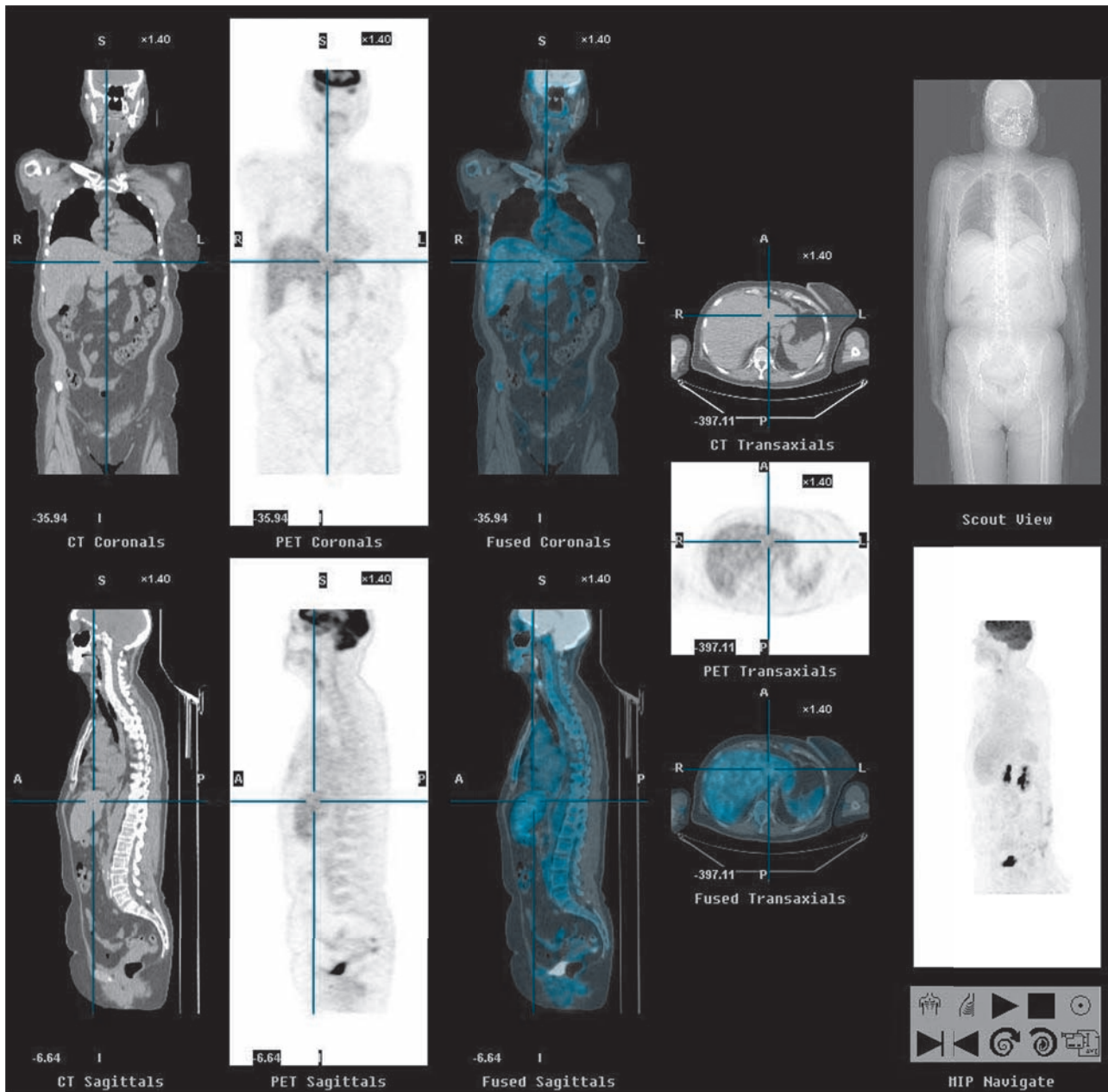


Figure 2-55

The following positron emission tomography (PET)/CT case is a 57-year-old white woman recently diagnosed with carcinoma of the right breast. Before the procedure, the patient received a single IV dose of 15.86 mCi or F-18 FDG, radioactive form of glucose. Cells with a high metabolic rate,

like those found within cancer, will show a high concentration of the FDG and generate a strong signal on the PET scan. At the time of this study, there was no abnormal uptake found, indicating that there was no detectable metastatic disease. The concentration of FDG or high signal in the

brain is considered a normal finding because, even while resting, the brain has a high glucose metabolism and uses about 60% of the glucose within the body. Similarly, the

strong signal within the kidneys and bladder are also considered normal because the waste products from the FDG are primarily removed via the urinary collecting system.

## Questions

1. Describe the location of the descending aorta within the mediastinum.
2. Where is the esophagus found within the mediastinum?
3. In an axial section through the great vessels located just above the heart, which vessel would be found farthest to the right side?
4. What are the two structures found directly under the aortic arch?
5. In an axial section, the ridge found at the point of bifurcation of the trachea into the right and left main bronchi is called?





## Case Study 2-6

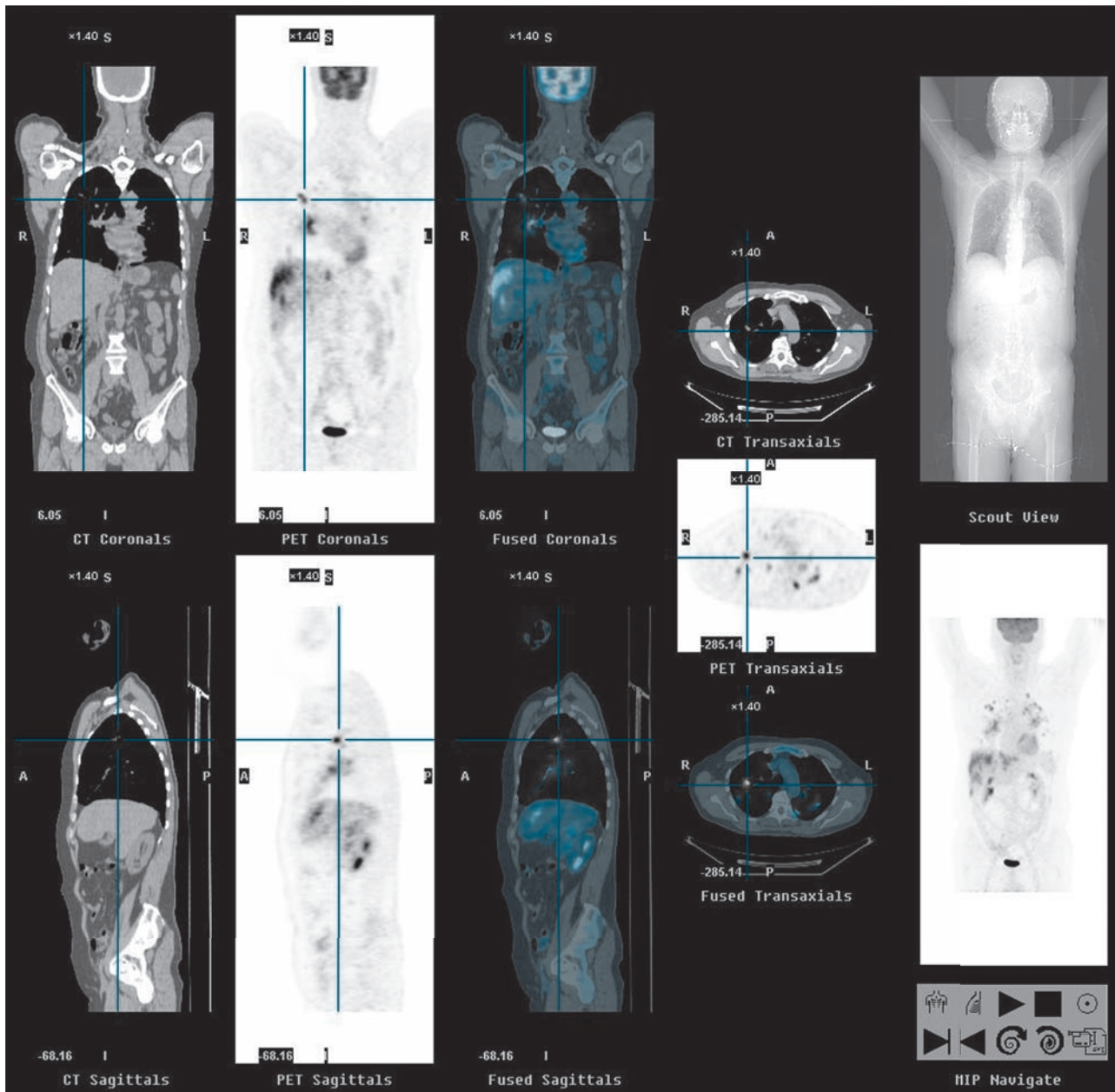


Figure 2-56

The following PET/CT case is a 68-year-old white man being evaluated for recurrent squamous cell carcinoma of the lung. Before the procedure, the patient received a single IV dose of 12.47 mCi of F-18 FDG. The PET/CT study was conducted to more accurately stage the carcinoma.

At the time of this study, abnormal uptake was found at multiple sites within the lung field as well as other sites within the abdomen and pelvis indicating metastatic disease. As marked by the red lines, there is a large signal found within the PET scan in the upper thorax

representing a neoplastic growth; it is shown within the correlating CT images to be located within the upper left lung. Although not marked with locator lines, a strong sig-

nal is also found on the left side of the pelvis, demonstrating that the metastatic disease has moved well below the diaphragm.

## Questions

1. Which artery originating within the mediastinum supplies arterial blood to the left lung?
2. What are the vessels called that drain venous blood from the lungs?
3. List the three main branches originating from the aortic arch that supply arterial blood to the upper half of the body.
4. Does the brachiocephalic artery or vein lie closer to the sternum?
5. What are the two deep vessels that are found beside the trachea? Which of these vessels is larger in diameter and more superficially located?





## CLINICAL APPLICATIONS

1. Describe the azygos vein.
2. The spinous process is connected to the transverse process of the vertebra by the \_\_\_\_\_.
3. Which chamber of the heart lies most posteriorly?
  - A. Left ventricle
  - B. Right ventricle
  - C. Left atrium
  - D. Right atrium
4. Which of the following lobes of the lungs receive air via the bronchus intermedius?
  - A. Right middle and lower
  - B. Right upper and middle
  - C. Left middle and lower
  - D. Left upper and middle
5. When you are viewing an axial image of a patient, your right side should always be the patient's \_\_\_\_\_ side.
6. The hemiazygos vein is located on which side of the body? (right or left)
7. The \_\_\_\_\_ lines the inside of the chest musculoskeletal wall and the \_\_\_\_\_ lines the surface of the lungs to form a smooth lubricated surface for movement resulting from breathing.
8. Which chamber of the heart pumps blood directly into the pulmonary artery?
  - A. Right atrium
  - B. Right ventricle
  - C. Left atrium
  - D. Left ventricle
9. The vertebral arteries originate from the
  - A. Subclavian arteries
  - B. Common carotid arteries
  - C. Aorta
  - D. Axillary arteries
10. The \_\_\_\_\_ is the region on the medial aspect near the center of both the right and the left lungs, and is the site where the bronchi, veins, and arteries enter and exit the lungs next to the heart.

# Chapter 3

# Abdomen

## OBJECTIVES

Upon completion of this chapter, the student should be able to:

1. Describe the superior and inferior boundaries of the abdomen.
2. Describe the general location of the segments of small and large intestine within the abdomen.
3. Identify and describe the location and lobes of the liver.
4. Describe the enclosing structures separating the abdomen.
5. Explain the location and general function of the gallbladder, pancreas, spleen, adrenal glands, and kidneys.
6. Describe the bile duct system.
7. Follow the course of blood as it passes through the portal system.
8. Describe the major arteries and veins located within the lower chest and abdomen.
9. Explain the relationships between structures located within the abdomen.
10. Correctly identify anatomic structures on patient computed tomography (CT) images of the abdomen.

## ANATOMIC OVERVIEW

The abdomen is generally considered as the region of the body between the chest and pelvis. Although this seems quite simple, the boundaries of the abdomen are often defined differently by different texts because the abdominal cavity extends well into each of the adjacent regions. The most superior boundary of the abdominal cavity is the dome-shaped diaphragm, which allows a considerable part of the abdomen to lie within the bony thoracic cage. Inferiorly, the abdominal cavity extends into the pelvis and occupies most of the false or greater pelvis, leading some individuals to consider the pelvis as the lower part of the abdomen. Because the abdomen and pelvis are often imaged separately, the pelvis will be further described in the next chapter.

### ■ Skeleton

**Lumbar** (*LŮM-bar*) **vertebrae**. Typically, the vertebral column contains five lumbar vertebrae, which form the posterior border of the abdominal cavity. Owing to the highly variable division of lumbar vertebrae with adjacent thoracic and sacral vertebrae, four and six lumbar

vertebrae are common anomalies that may confuse the viewer when determining image location. Compared to the other vertebrae, these can be distinguished by their large size and the absence of costal facets and transverse foramina.

### ■ Enclosing Structures

**Diaphragm** (*DĪ-ă-ŕam*). The diaphragm is a broad, flat muscle made up of skeletal muscle along the periphery that converges on a broad flat tendon, the central tendon (Fig. 3-1). It is often described as two hemidiaphragms (the right and left), because the right side is usually more superior because of the underlying liver. Its muscular portion originates from several sources: (a) the sternal process, (b) the costal cartilages and bone of ribs 7 through 12, and (c) the upper lumbar vertebrae. Although the diaphragm forms a septum between the thoracic and abdominal cavities, several structures (inferior vena cava, esophagus, and descending aorta) pass through openings within the diaphragm to pass between the chest and abdomen.

**Crura** (*KRŮ-ră*). The muscular parts of the diaphragm that originate from the lumbar vertebrae and ascend to the

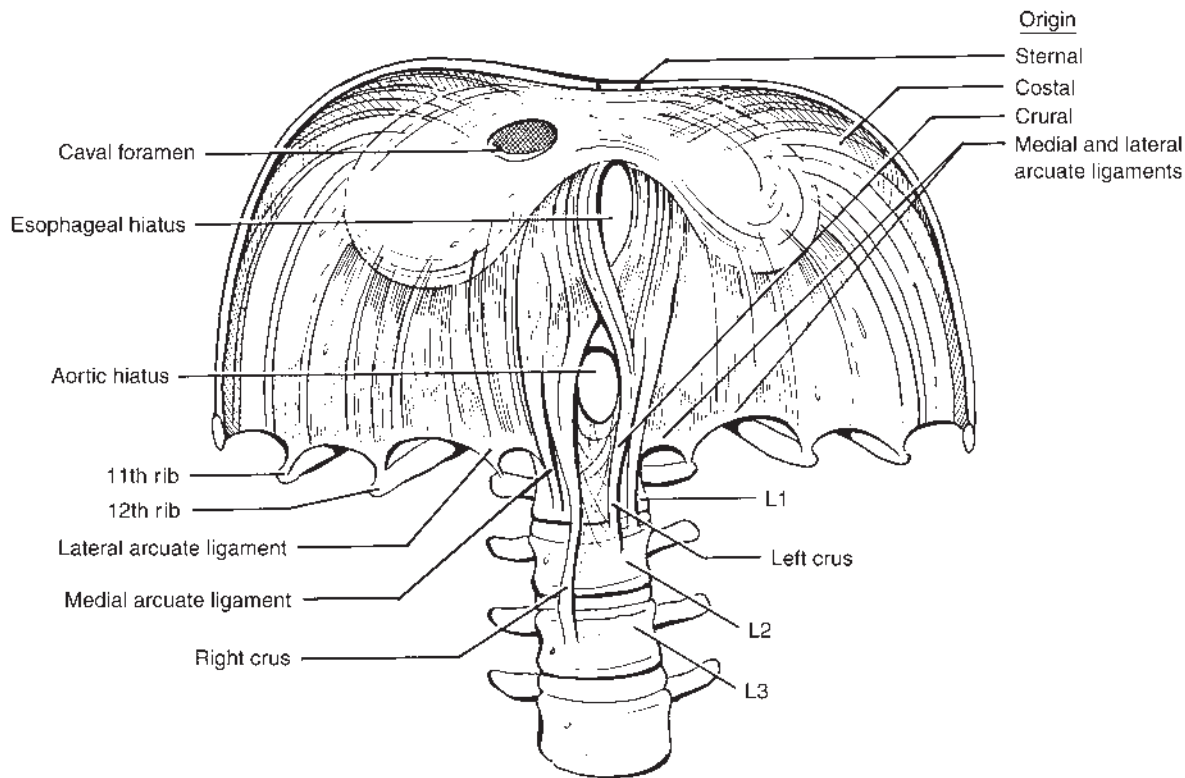


**Figure 3-1** Inferior surface of the diaphragm.

central tendon. The right crus arises from the upper three or four lumbar vertebrae, and the left crus originates from the upper two or three. The crura combine with ligaments to form the openings for the aorta and esophagus.

**Peritoneum** (*PER-i-tō-NĒ-um*). Its structure and function are similar to those of the pleura, described in Chapter 2 (Fig. 3-2). It is a smooth membrane lining the abdominal cavity (parietal peritoneum) and the abdominal viscera (visceral peritoneum), creating the peritoneal cavity. Because the organs within the abdominal cavity are closely arranged, the peritoneal cavity is normally only a small space containing a thin film of serous fluid produced by the membranes. Much like the pleura, the peritoneum minimizes friction and acts as a barrier to the spread of infection within the abdomen.

**Mesentery** (*MES-en-ter-ē*). In addition to the parietal and visceral peritoneum, the mesentery is a double layer of peritoneum that encloses the intestine and attaches it to the abdominal wall. Because of constant movement and changes in shape, much of the intestine is described as having no fixed position, being only loosely organized by the mesentery. The mesentery also contains the arteries and veins of the intestines and is a primary site for fat storage within the body.

**Retroperitoneal** (*RE-trō-PER-i-tō-NĒ-āl*). Behind the peritoneal cavity, this space is adjacent to the posterior abdominal wall and contains the following abdominal organs: Kidneys, pancreas, distal duodenum, and ascending and descending portions of the colon.

## ■ Viscera (*VIS-er-ă*)

**Stomach.** A mobile organ situated in the upper left side of the abdominal cavity just below the left hemidiaphragm. The esophagus descends through the esophageal hiatus in the diaphragm to join the body of the stomach. Above the gastroesophageal junction, the fundus is the part of the stomach found next to the esophagus directly under the diaphragm. Below the body of the stomach, the pyloric part is the narrowing region that is continuous with the duodenum (Fig. 3-3). Although the location and shape of the stomach will vary among individuals and can change over time within a single individual, the relationship of the three segments from superior to inferior will usually remain the same.

**Small intestine.** The site of the major part of digestion. It extends from the termination of the stomach to the large

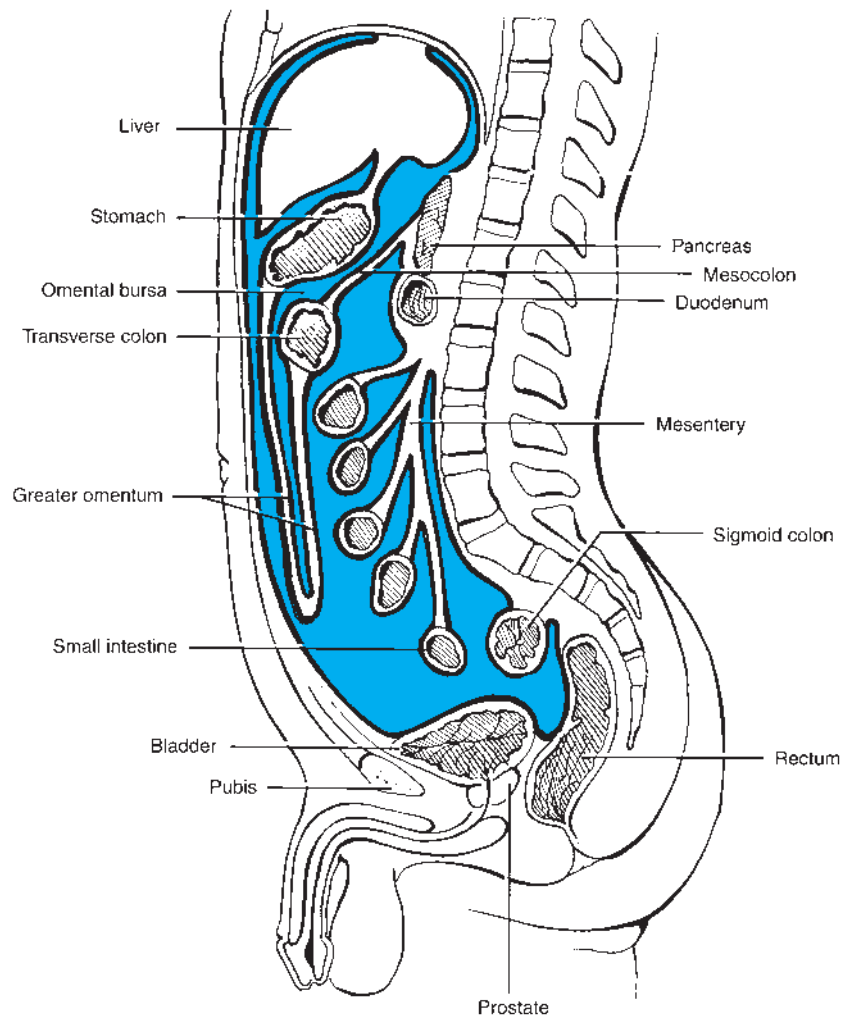


**Figure 3-2** Median sagittal view of abdomen demonstrating the peritoneum and mesentery.

intestine, ranging from 5 to 8 m in length. It includes the duodenum, jejunum, and ileum.

**Duodenum** (*dū-ō-DE-nūm*). The first segment of the small intestine, extending from the pyloric part of the stomach to the jejunum. It is approximately 25 cm long. Its C shape wraps around the head of the pancreas and the superior mesenteric vessels (Fig. 3-4). Only the superior part of the duodenum lies within the peritoneum, the remaining three parts (descending, inferior, and ascending) are all retroperitoneal and are fixed in position.

**Jejunum** (*jě-JŪ-nūm*). The second segment of the small intestine is arranged in numerous coils or loops, is approximately 2.4 m long, and extends from the duodenum to the ileum (Fig. 3-5). It is difficult to distinguish from the ileum, even though it has a thicker wall, greater diameter, and larger vascular supply. In the average patient, location typically provides a general means for distinguishing between the jejunum and ileum; the jejunum usually lies in the

umbilical region, whereas the ileum lies in the lower abdomen and pelvis.

**Ileum** (*IL-ē-ŭm*). The third segment is also arranged in numerous coils or loops and is the longest segment of the small intestine, averaging 3.6 m in length. As noted, the ileum is difficult to distinguish from the jejunum, except for its lower position in the abdominal cavity. It terminates in the lower right quadrant of the abdominal cavity at the ileocecal valve and is continuous with the first part of the large intestine. *Helpful hint:* The spelling of the ileum of the intestine is often confused with the ilium of the bony pelvis. If one notes that the shape of the coiled intestine resembles the letter e, then one should remember the proper spelling for both anatomic structures.

**Large intestine.** The large intestine is approximately 1.5 m in length and extends from the terminal ileum to the anus (Figs. 3-5 and 3-6). The material passing from the terminal ileum to the large intestine is about 90% water, most of which is absorbed by the large intestine. Many individuals

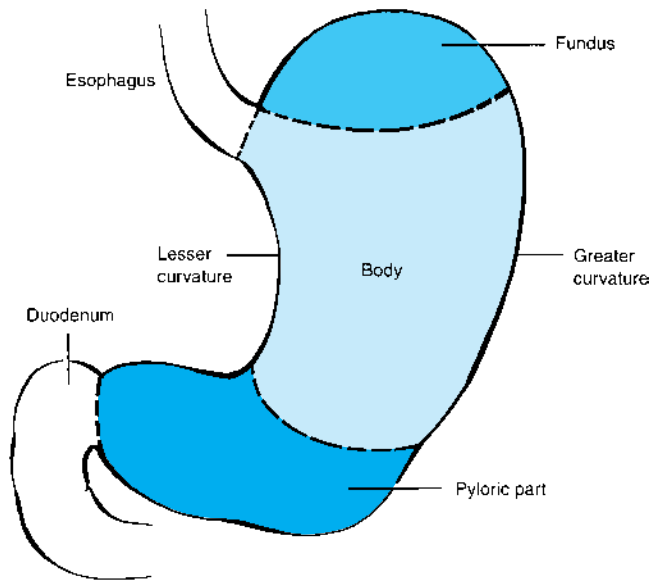


**Figure 3-3** Sketch illustrating the three parts of the stomach.

will use the term *colon* synonymously with *large intestine*; however, this is incorrect. The large intestine is made up of two parts: The cecum and the colon.

*Cecum* (*SE-kūm*). The first segment of the large intestine located in the lower right side of the abdomen posterior to the peritoneum. It is below the ileocecal valve and forms a blind pouch that is continuous with the ascending colon. At 1 to 2 cm below the opening of the ileocecal valve within the cecum, a smaller opening leads into the appendix. The appendix is a long narrow tube averaging about 8 cm in length with a highly variable position that partially depends on the shape and contents of the cecum.

*Ascending colon*. The segment originating above the ileocecal valve that is continuous with the cecum and extends upward to the hepatic flexure next to the liver on the right side of the abdomen. Similar to the cecum, it is retroperitoneal and relatively fixed in position along the posterior wall of the abdomen. In the lower abdomen, it lies adjacent to the musculature forming the posterior abdominal wall; and in the upper abdomen, it lies anterior to the right kidney.

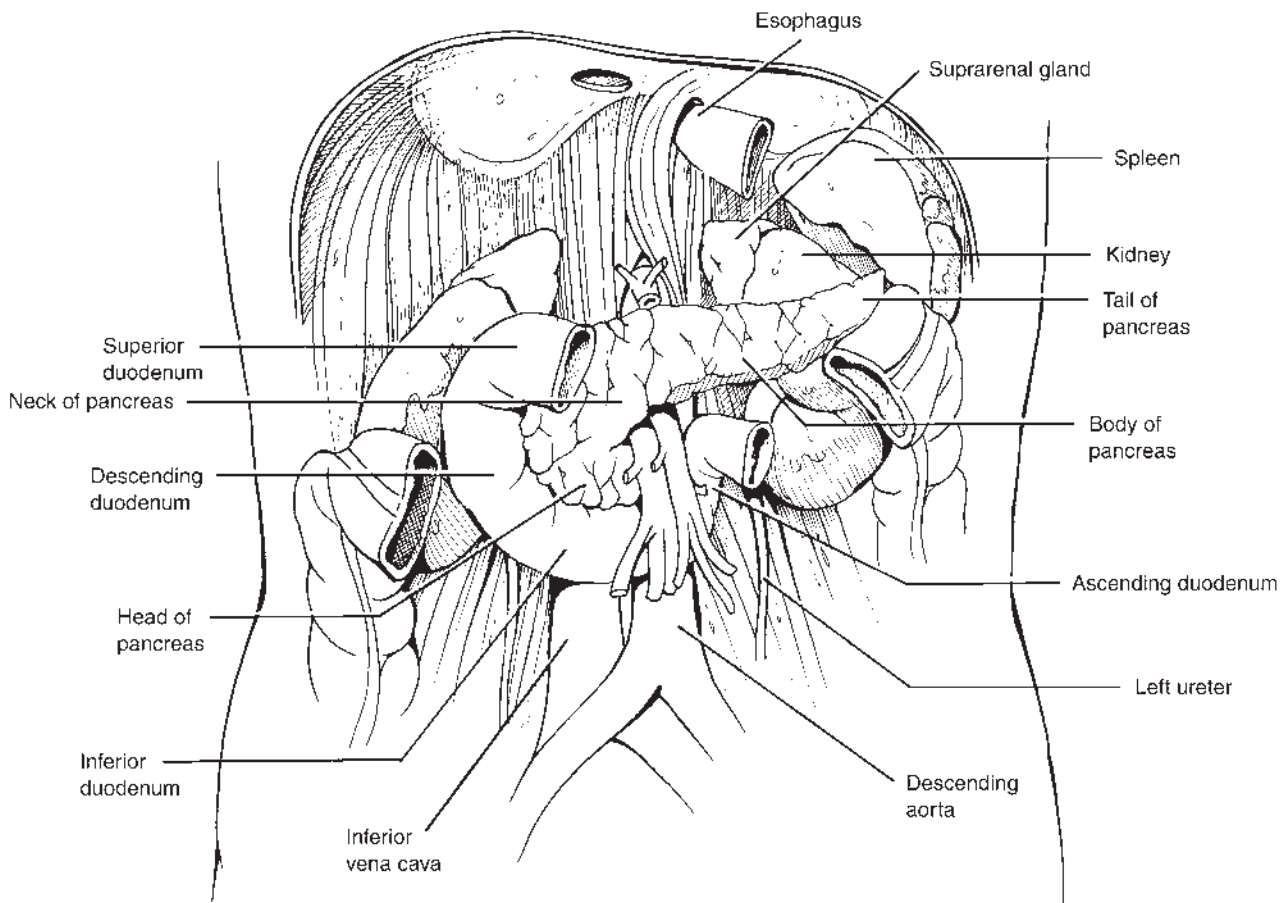


**Figure 3-4** Anterior view of the structures within the upper abdominal cavity after removal of the stomach, jejunum, and transverse colon.

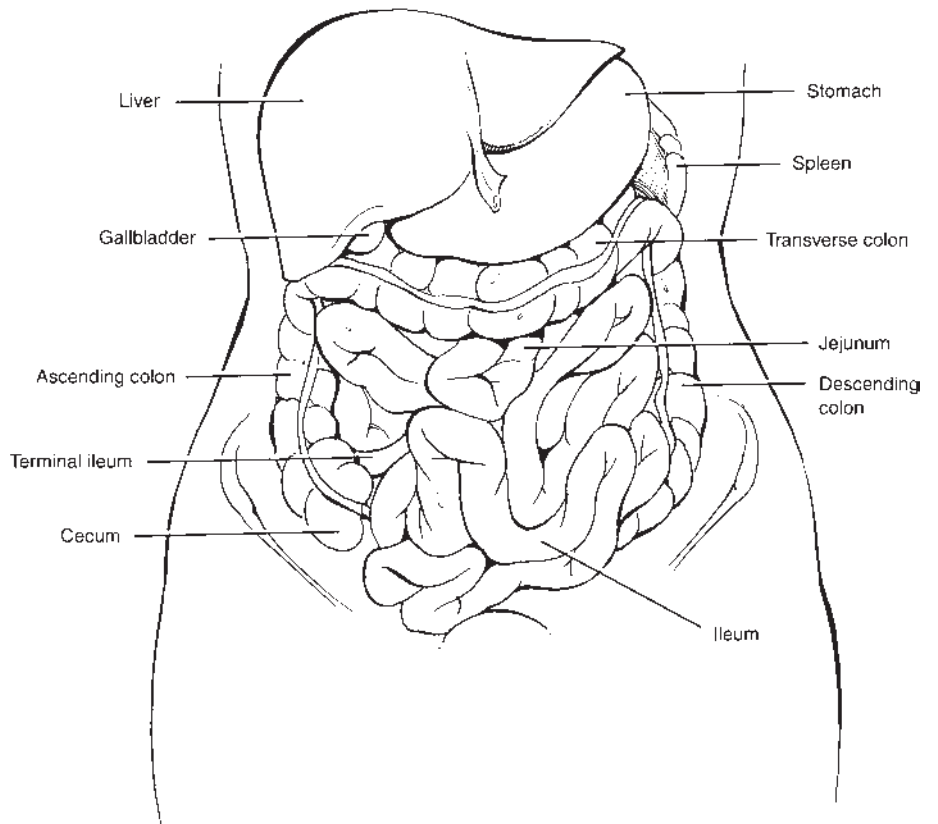


**Figure 3–5** Anterior view of the contents within the abdomen following removal and reflection of the anterior abdominal wall.

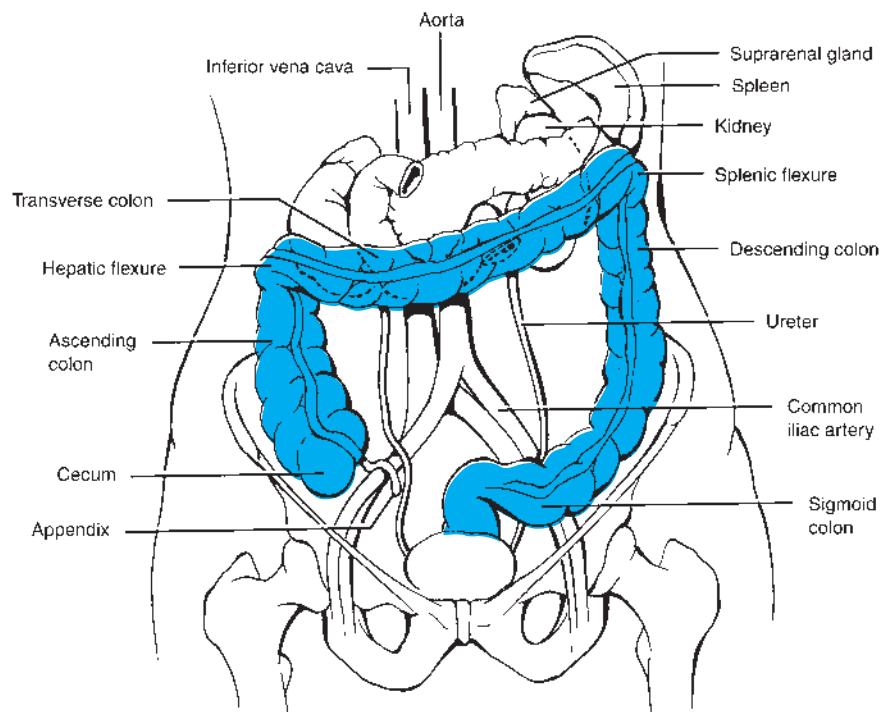


**Figure 3–6** Sketch demonstrating the location of the large intestine as compared to the selected structures adjacent to the posterior abdominal wall.



*Hepatic (he-PAT-ik) flexure of colon.* The bend or right flexure of the colon between the ascending and transverse segments of the colon. As the name implies, the flexure is next to the liver on the upper right side of the abdomen. Owing to the more anterior position of the transverse colon, the hepatic flexure is best demonstrated in an oblique view from the right anterior side.

*Transverse colon.* The segment of the colon traversing across the abdomen between the hepatic and splenic flexures. In contrast to the ascending colon, it is invested with peritoneum and is suspended from the posterior abdominal wall by mesentery (the transverse mesocolon). Although the ends have a fixed position, the location of the middle region is highly variable and may be found from the upper abdomen to the greater pelvis. Despite the level, the middle region usually lies adjacent to the anterior abdominal wall.

*Splenic (SPLEN-ik) flexure of colon.* At the terminal end of the transverse colon, the left flexure of the colon redirects the colon downward to become the descending colon. Unlike the hepatic flexure, this flexure is best

demonstrated in the oblique view from the left anterior side and is usually more superiorly situated, adjacent to the spleen.

*Descending colon.* The part of the large intestine originating at the splenic flexure that extends along the left posterior wall to the level of the pelvic brim or inlet. Within the greater pelvis, it travels downward to join the sigmoid colon. Similar to the ascending colon, it is retroperitoneal and is fixed in position by the musculature of the posterior abdominal wall.

**Liver.** The largest gland in the body, found in the upper abdominal cavity on the right side. For the most part, it lies within the bony thoracic cage, and its superior surface is covered by the diaphragm. The superior liver is dome shaped, following the contour of the diaphragm; and the inferior or visceral surface is somewhat flattened, facing downward toward the other viscera within the abdomen. On the visceral surface, an H-shaped arrangement of fissures and fossae is found dividing the liver into four separate lobes (Fig. 3-7). The transverse part of the H is formed by the porta hepatis, which includes the hepatic ducts, portal

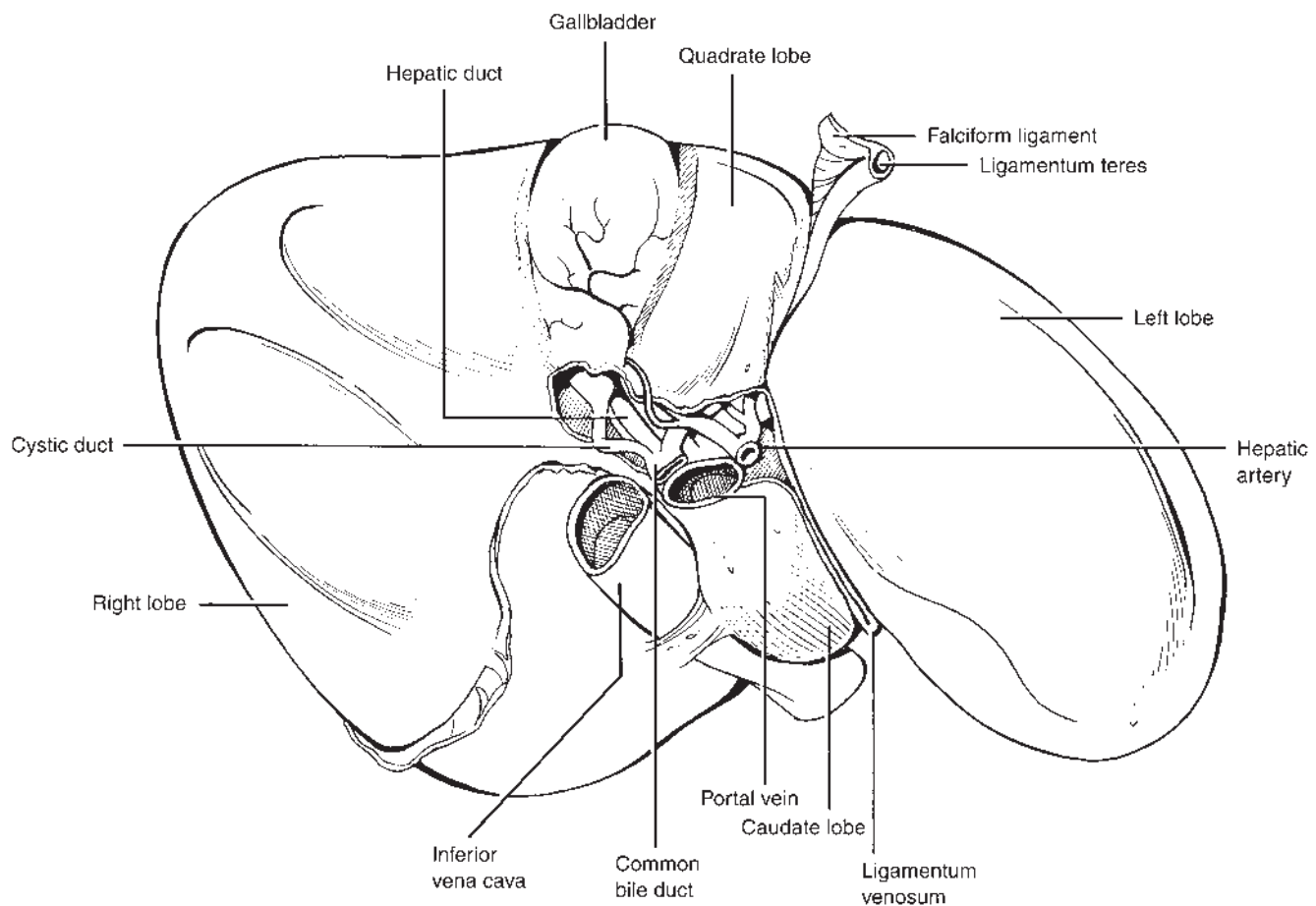


**Figure 3-7** Visceral surface of the liver as seen from below.

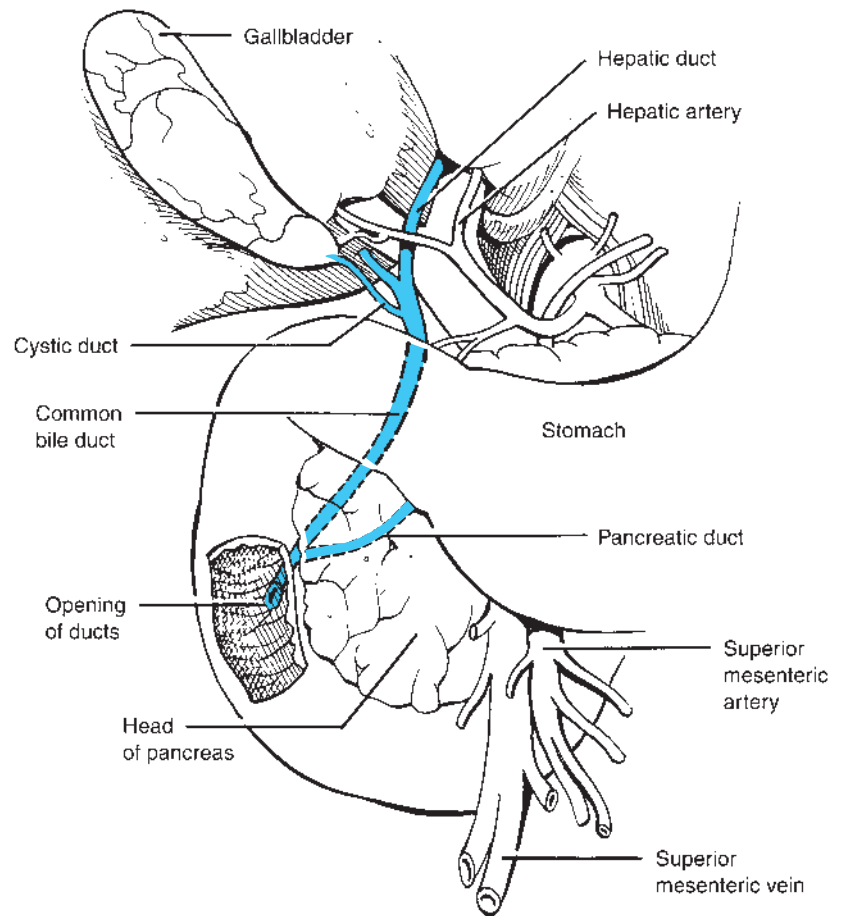


**Figure 3–8** Drawing from an anterior view illustrating the bile duct system and adjacent structures.

vein, and proper hepatic artery. The sides of the H are formed by the gallbladder and the inferior vena cava on the left side and the ligamentum teres (obliterated remains of the left umbilical vein) and ligamentum venosum (the fibrous remains of the embryologic ductus venosus) on the right side.

**Left lobe.** The left part of the liver demarcated on the diaphragmatic surface by the falciform ligament. On the visceral side, the ligamentum teres in front and the ligamentum venosum in back form the boundary for the left lobe. In the abdomen, the left lobe of the liver usually lies anterior to the body of the stomach.

**Right lobe.** The largest part of the liver opposite the left lobe. On the visceral surface, the hepatic flexure of the colon lies by the anterior part of the right lobe and lateral to the gallbladder.

**Caudate (KAW-dāt) lobe.** The small, posterior lobe located between the inferior vena cava and the ligamentum venosum, posterior to the porta hepatis. *Helpful hint:* The “c” in caudate can help you remember that it lies next to the inferior vena cava (also starts with a “c”).

**Quadrate (KWAH-drät) lobe.** The small, anterior lobe located between the gallbladder and the ligamentum teres.

*Helpful hint:* The “q” of quadrate is shaped much like the “g” of gallbladder.

**Gallbladder.** Lies just below the anterior liver within its fossa on the visceral surface and acts as a reservoir for bile produced by the liver.

**Common bile duct.** Transports bile from the gallbladder (via the cystic duct) and the liver (via the hepatic duct) to the duodenum (Fig. 3-8). In its course, it lies posterior to the superior duodenum and beside the head of the pancreas. It is approximately 7.5 cm in length and ends at the duodenal wall, where it joins with the main pancreatic duct.

**Pancreas (PAN-krē-as).** A collection of glandular tissue with little connective tissue, it has both exocrine and endocrine functions (Figs. 3-8 and 3-9).

**Head.** The expanded part of the pancreas lying within the curvature of the duodenum. Because the pancreas is covered only on its anterior surface by peritoneum, it is considered retroperitoneal similar to the adjacent parts of the duodenum. The head of the pancreas is divided by the superior mesenteric artery and vein that partially separate the uncinate process, the part of the pancreas located inferior to the mesenteric vessels.



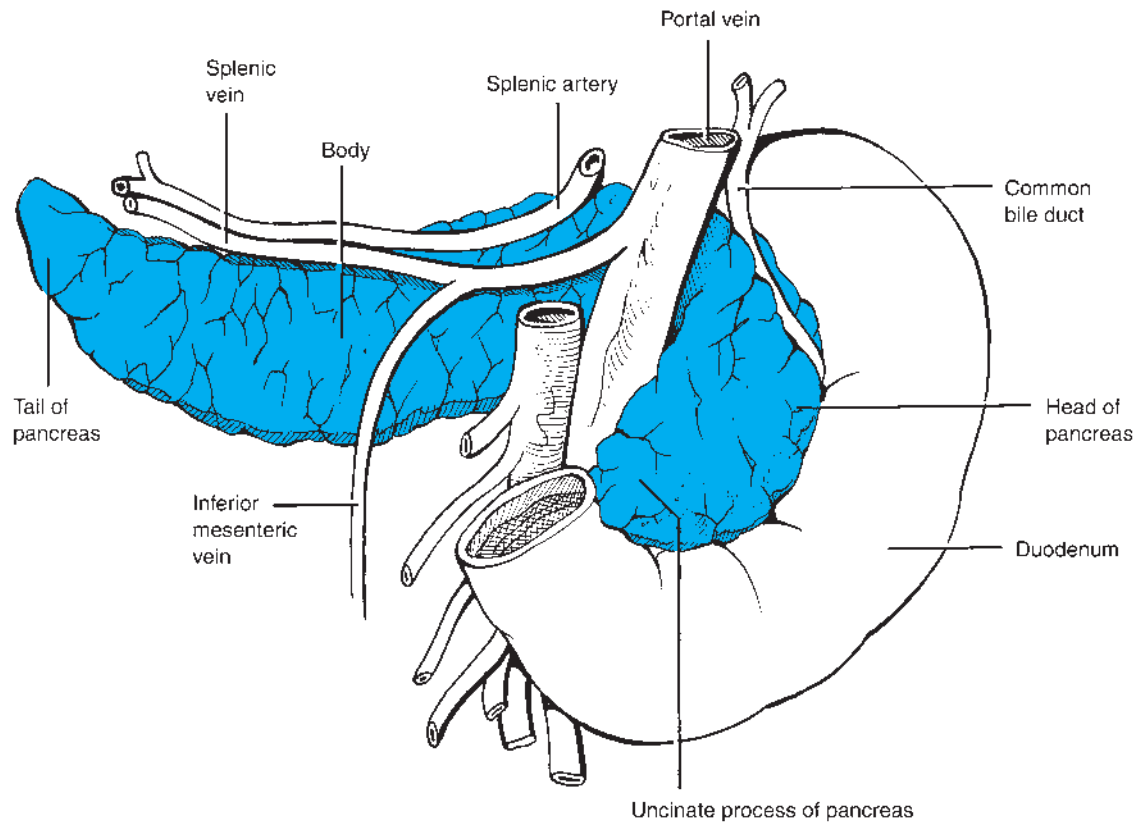


**Figure 3-9** Drawing from a posterior view illustrating the pancreas and adjacent structures.

**Body.** The central region of the pancreas primarily located posterior to the stomach and anterior to the left kidney.

**Tail.** The narrowed left end of the pancreas extending toward the surface of the spleen.

**Spleen (*splēn*).** The soft, lymphatic organ that lies against the diaphragm on the upper left side of the abdomen within the thoracic cage (Fig. 3-4). Its size and shape vary considerably, depending somewhat on the adjacent structures. Its anterior surface is next to the stomach, its posterior surface is next to the left kidney, its superior surface is next to the diaphragm, and its inferior surface is next to the left splenic flexure of the colon.

**Kidneys.** The bean-shaped, retroperitoneal organs on either side of the vertebral column typically centered at the level of the first lumbar vertebra. Anomalies in formation are common during development, resulting in variations in the shape and location of the kidneys. Within the kidney, fluid and waste products are filtered from the blood to form urine, which is collected in the renal pelvis and drains into the ureters (Fig. 3-10).

**Ureters (*yū-RE-terz*).** Retroperitoneal, originating from the renal pelvis and extending downward to drain urine

into the bladder. Although most people have two ureters (one for each kidney), common congenital anomalies include duplication of part or all of the ureter.

**Adrenal (*Ā-DRĒ-nāl*) glands.** Also referred to as the suprarenal glands, these soft, glandular organs are located on the top pole of the kidneys (Fig. 3-11). Roughly triangular in shape, their average dimensions in the adult are approximately 5 cm long, 3 cm wide, and 1 cm thick. Although these endocrine glands are relatively small, they produce hormones with widespread effects, including epinephrine and norepinephrine, which are responsible for the fight-or-flight response. In axial images, the glands are considerably thinner and are less dense than the underlying kidneys (which average 3 cm thick).

## ■ Arteries

**Abdominal or descending aorta (*ā-ŌR-tā*).** The continuation of the thoracic aorta, it originates at the level of the diaphragm and extends to the pelvis (Fig. 3-6). The retroperitoneal artery lies on the left side of the vertebral column and terminates at the origin of the right and left common iliac arteries.

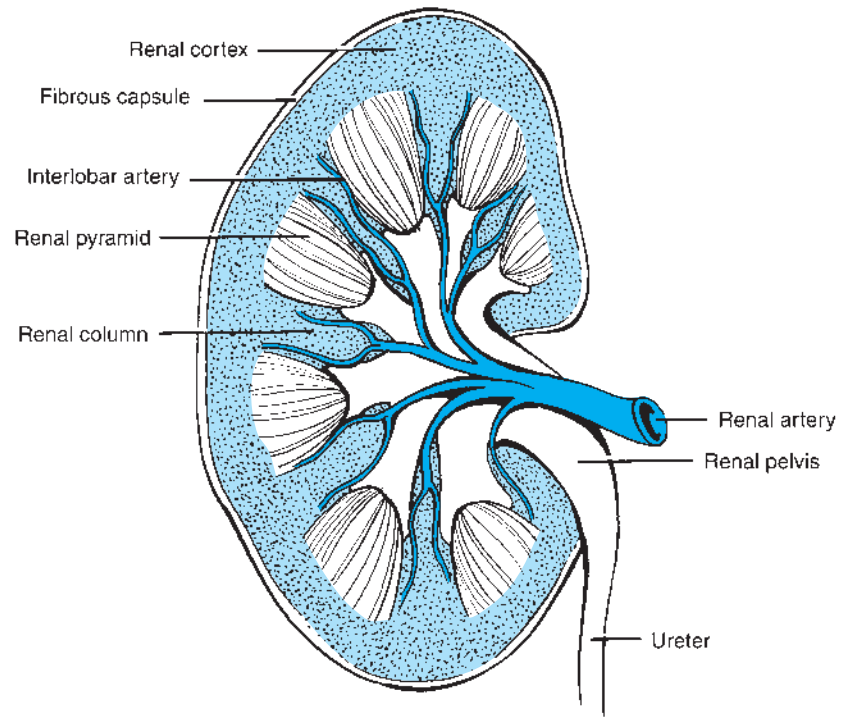


**Figure 3-10** Sketch illustrating the contents of the kidney.

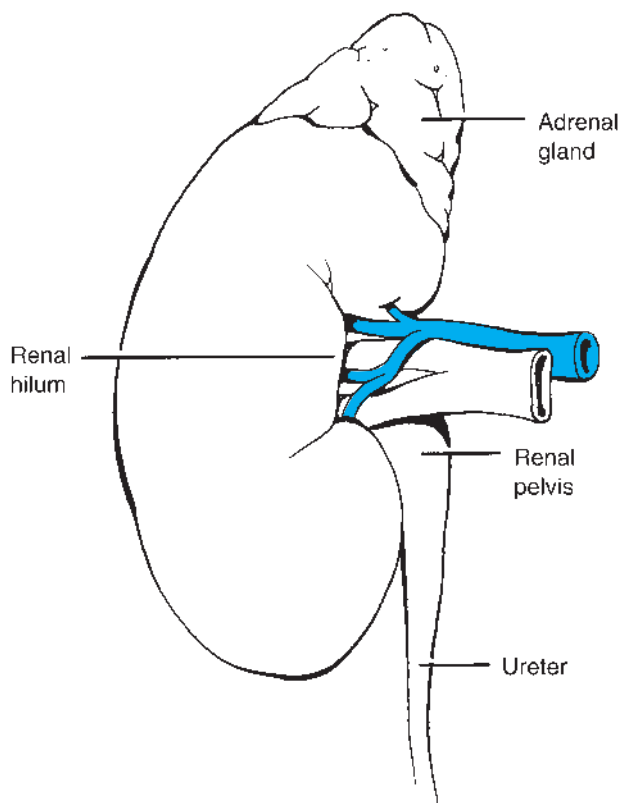


**Figure 3-11** The adrenal gland and kidney with adjoining structures.

**Celiac (*SĒ-lē-ak*) trunk.** The first branch off the abdominal aorta, it originates just below the diaphragm between the lesser curvature of the stomach and the liver (Fig. 3-12). The artery is relatively short (1 to 2 cm long) and originates nearly perpendicular to the aorta. It gives rise to the common hepatic artery, left gastric artery, and splenic artery.

**Common hepatic artery.** The branch of the celiac trunk that gives rise to the proper hepatic artery (supplies the liver and gallbladder) and the gastroduodenal artery (supplies the stomach, duodenum, and pancreas). Anomalies of the artery are quite common. Approximately 41% of patients have aberrant common hepatic arteries, including instances in which the artery originates directly from the aorta or the superior mesenteric artery.

**Splenic artery.** The largest branch of the celiac trunk, it travels behind the stomach to end at the spleen. It usually travels a tortuous path, giving it a distinctive appearance and facilitating its identification in sectional images.

**Superior mesenteric artery.** It originates from the abdominal aorta approximately 1 cm below the celiac trunk. It extends downward to supply blood to the small intestine and the first half of the large intestine, including the cecum, ascending colon, and the right half of the transverse colon (Fig. 3-13). Originating posterior to the pyloric part of the stomach, it extends at an oblique angle from the aorta. Compared to the perpendicular origin of the nearby celiac trunk, its oblique course can be a distinguishing

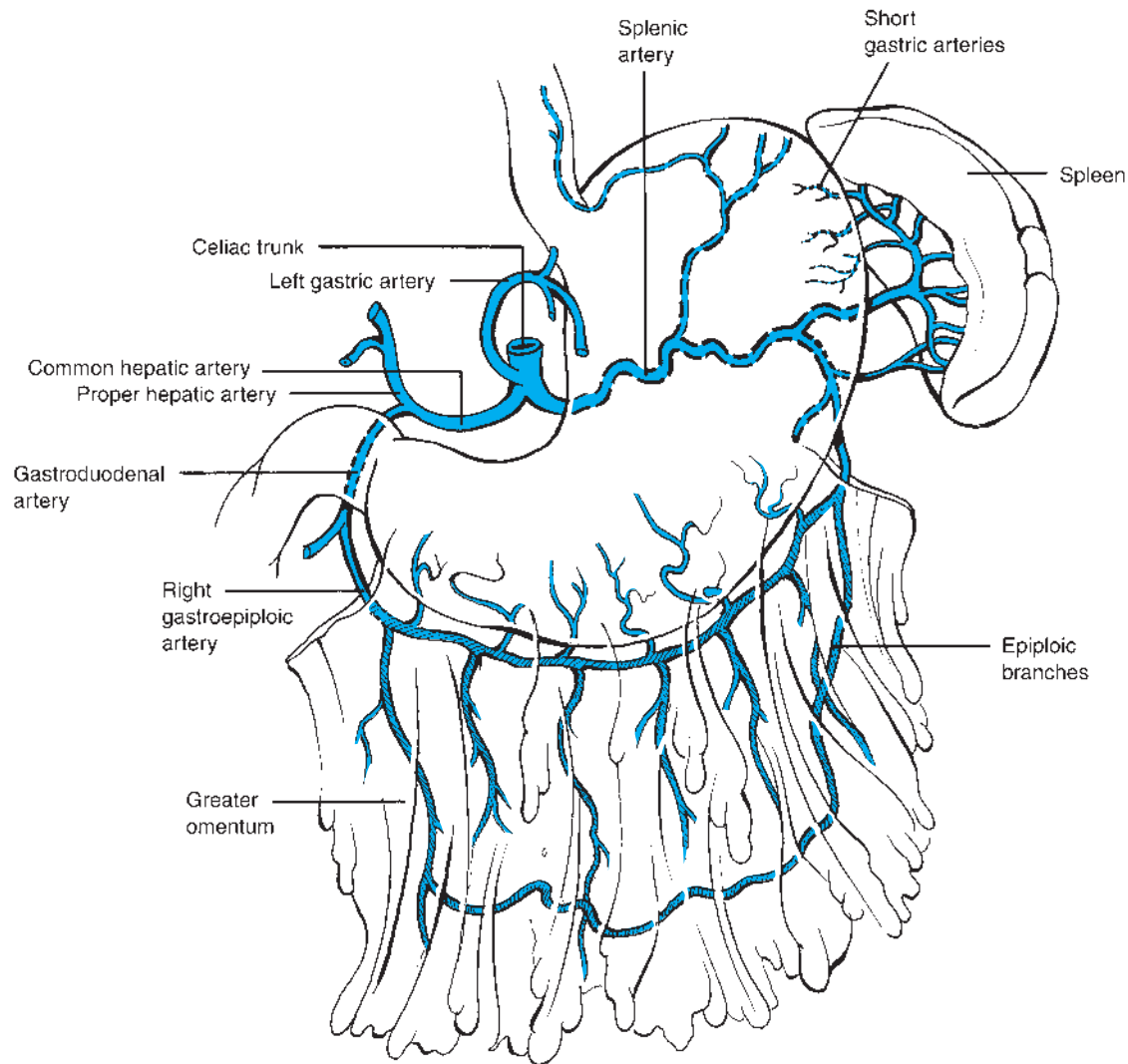


**Figure 3-12** Branches of the celiac trunk as compared to the stomach and spleen.

characteristic in sectional images. As the artery descends into the abdomen, it travels through the head of the pancreas within the C loop of the duodenum to enter the mesentery.

**Renal (*RE-nāl*) arteries.** Two large trunks arising on either side of the aorta just below the superior mesenteric artery. Each artery forms a nearly right angle with the aorta as it extends to the kidneys (Fig. 3-14). Because the right renal artery passes behind the inferior vena cava and the right renal vein, it is usually slightly longer than the left. In approximately one of four cases, additional renal arteries are present and are more frequently found on the left side. Instead of entering the kidney at the hilum, additional renal arteries usually join with either the upper or the lower poles of the kidney.

**Inferior mesenteric artery.** Originating from the aorta in the mid-lumbar region, it enters the mesentery to supply blood to the left half of the transverse colon, descending colon, sigmoid colon, and upper rectum (Fig. 3-15).

**Common iliac arteries.** Bilateral arteries arising from the abdominal aorta at the level of the fourth lumbar vertebra; they diverge laterally as they enter the pelvis. Within the greater pelvis, each artery bifurcates to give rise to the internal and external iliac arteries.

## ■ Veins

**Inferior vena cava (*VE-nā-KĀ-vā*).** The major route for drainage of venous blood from the abdomen, pelvis, and

*(text continues on page 114)*

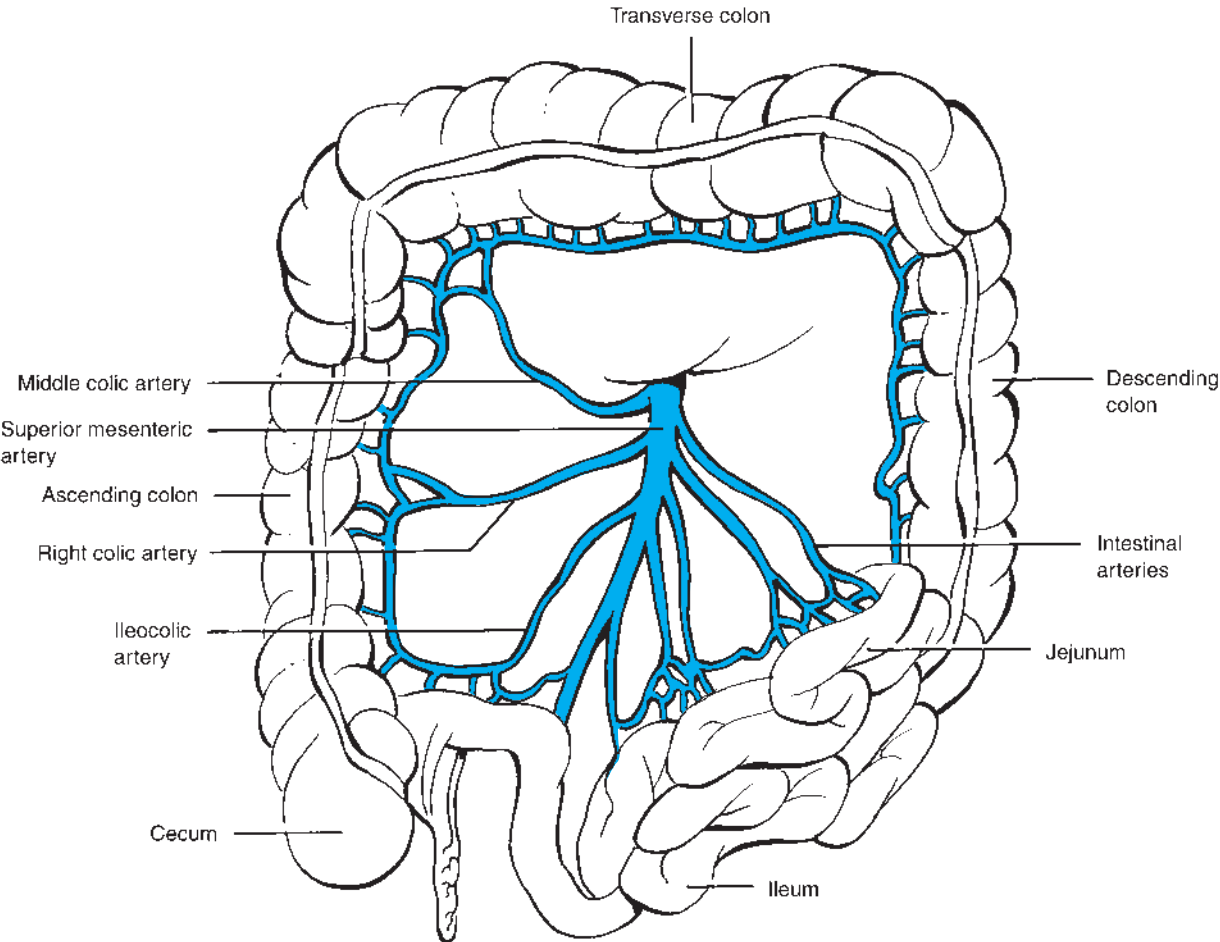


**Figure 3-13** Following superior reflection of the transverse colon, the branches of the superior mesenteric artery.

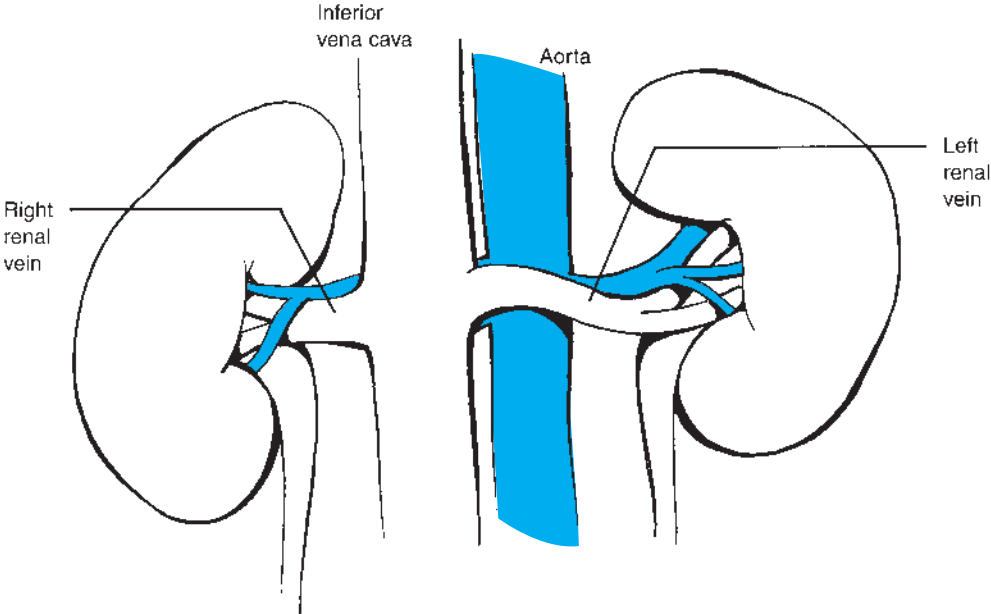


**Figure 3-14** Sketch illustrating the renal arteries and veins.

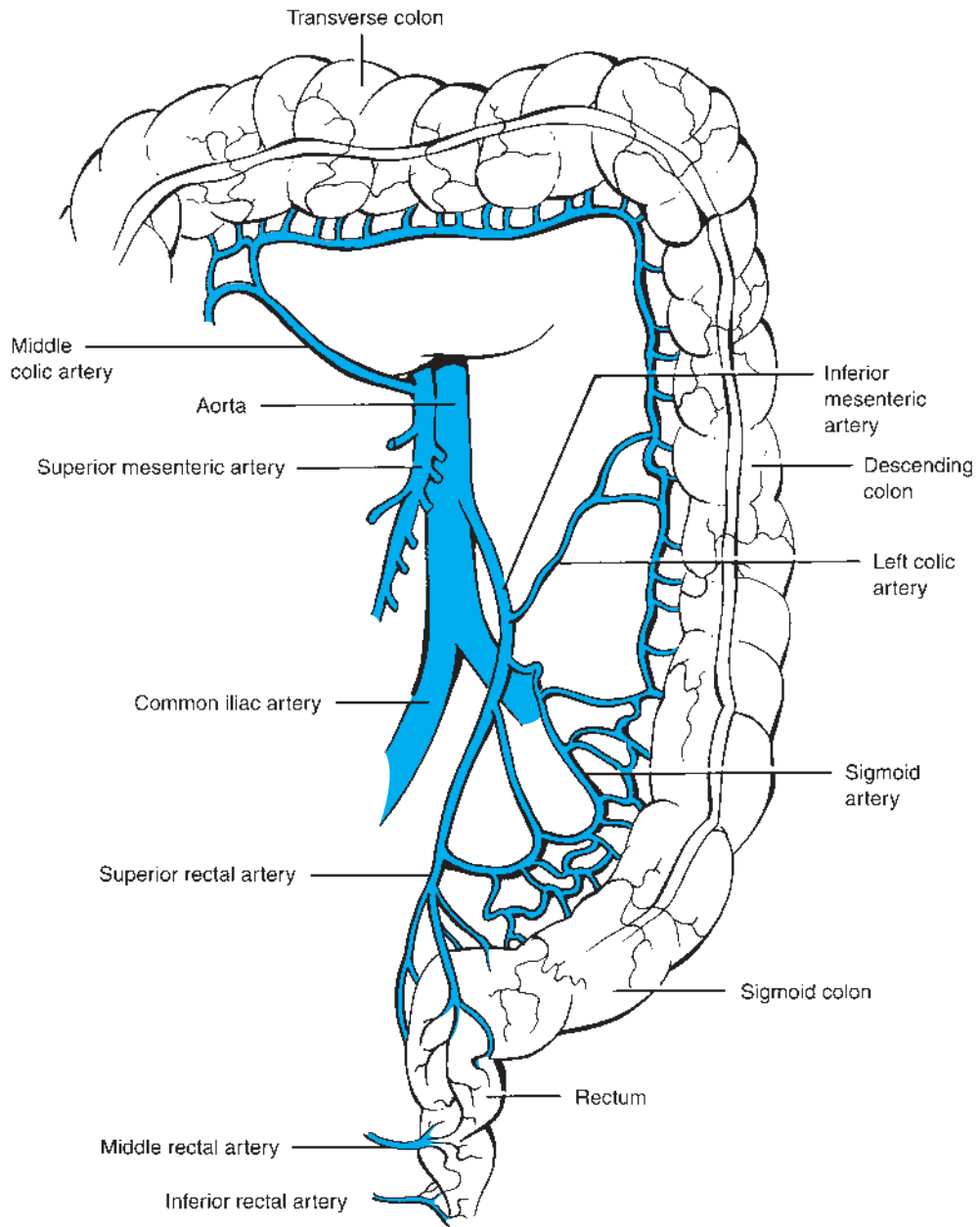


**Figure 3–15** The lower abdominal aorta including the branches of the inferior mesenteric artery and the common iliac arteries.

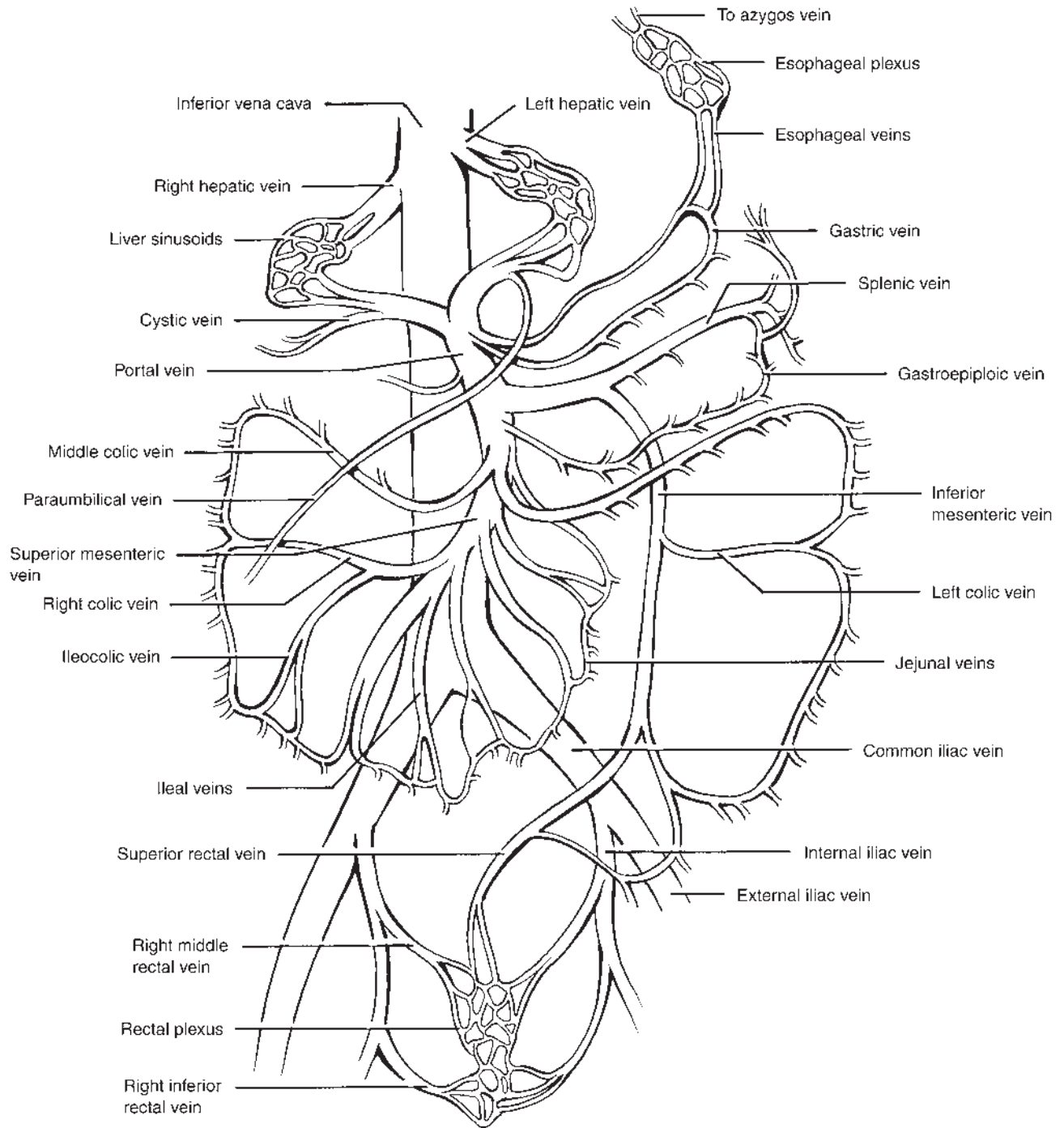


**Figure 3-16** Veins of the abdomen.

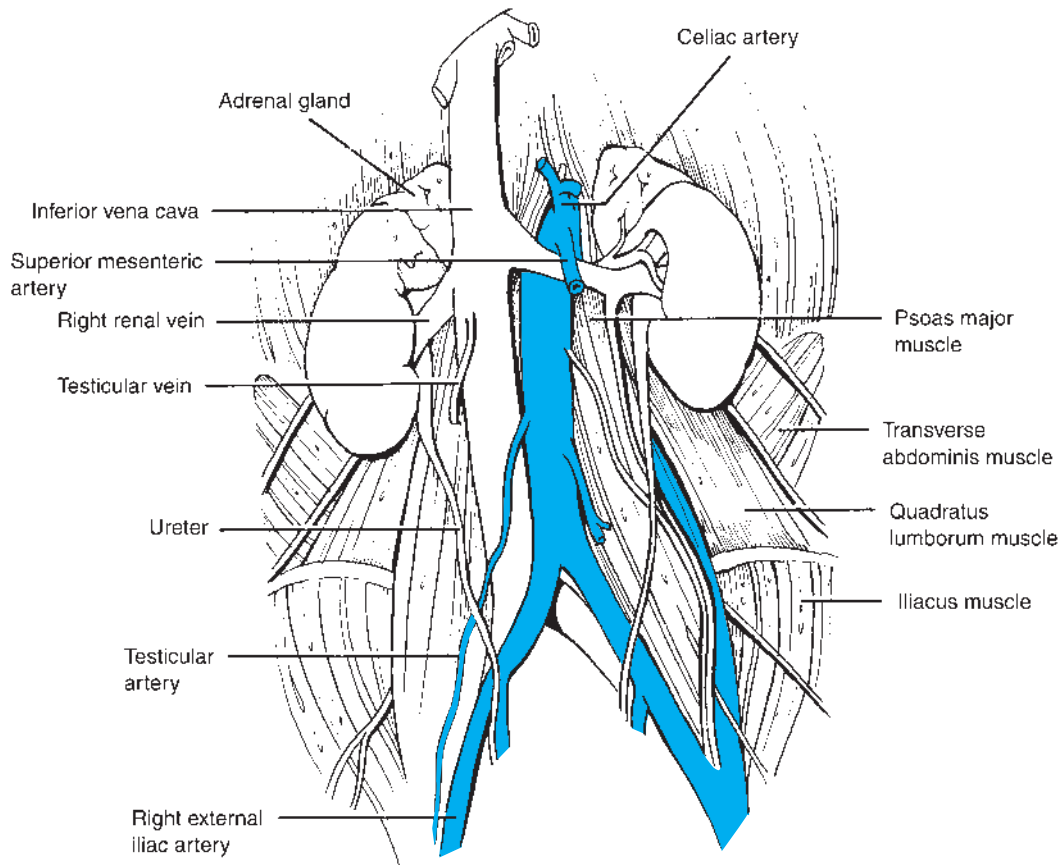


**Figure 3-17** The posterior abdominal wall and adjacent structures.

lower extremities (Fig. 3-16). It lies parallel to the abdominal aorta, on the right side near the lumbar vertebral bodies. Originating from the joining of the common iliac veins within the upper pelvis, it ascends through the abdomen and thoracic cavity to drain into the right atrium of the heart.

**Hepatic veins.** The right and left hepatic veins drain the filtered blood from the liver into the inferior vena cava. The vessels are short and are surrounded by liver tissue molded around the inferior vena cava.

**Portal (PÖR-täl) vein.** Originating from the veins draining most of the gastrointestinal system, it carries nutrient-rich blood to the middle of the visceral surface of the liver. Lying adjacent to the hepatic bile ducts and the hepatic artery proper, it forms part of the porta hepatis, the transverse part of the H on the visceral surface of the liver.

**Splenic vein.** Found traversing the abdomen posterior to the stomach and the pancreas, it drains nutrient-rich blood from the spleen and the inferior mesenteric vein into the portal vein. In contrast to the tortuous path of the splenic

artery, the course of the vein is nearly linear; this difference can be used to distinguish the two neighboring vessels.

**Inferior mesenteric vein.** The vessel draining blood from the rectum, sigmoid colon, and ascending colon, to the splenic vein located posterior to the stomach and pancreas. During its course, the vein lies within the mesentery, attaching the intestine to the posterior abdominal wall.

**Superior mesenteric vein.** Ending at the portal vein immediately posterior to the pancreas, the branches of this vessel drain blood from the stomach, duodenum, jejunum, ileum, cecum, appendix, ascending colon, transverse colon, and pancreas. Like the other mesenteric veins, it lies within the mesentery and carries nutrient-filled venous blood from the intestine to the portal vein.

**Renal veins.** The right and left renal veins drain venous blood from the kidneys to the inferior vena cava (Fig. 3-17). Because the abdominal aorta is on the left side of the inferior vena cava, the longer left renal vein crosses in front of the abdominal aorta.

**Common iliac veins.** These two veins (the right and left) drain venous blood from the lower limbs and pelvis into the inferior vena cava. Arising at the juncture of the internal and external iliac veins, they originate anterior to the L5 to S1 joint space and extend only a short distance to join in front of the L4 vertebral body. Unlike most regions of the body, here the veins are more posteriorly and inferiorly situated than are the adjacent common iliac arteries.

## ■ Muscles

**Psoas** (*SŌ-as*). Originating from the transverse processes of L1 to L5 and inserting on the lesser trochanter of the femur on either side, these muscles form part of the posterior abdominal wall. In axial section, the large muscles are round and readily identified lying on either side of the vertebral column and aid in the identification of the adjacent ureters and vessels.

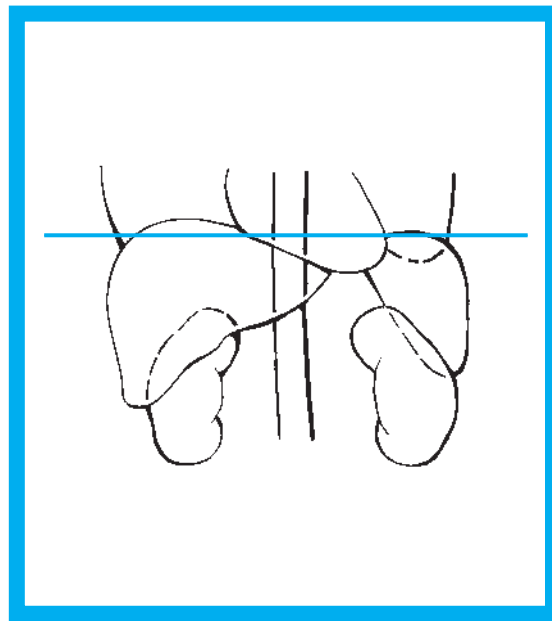




## Axial CT Images

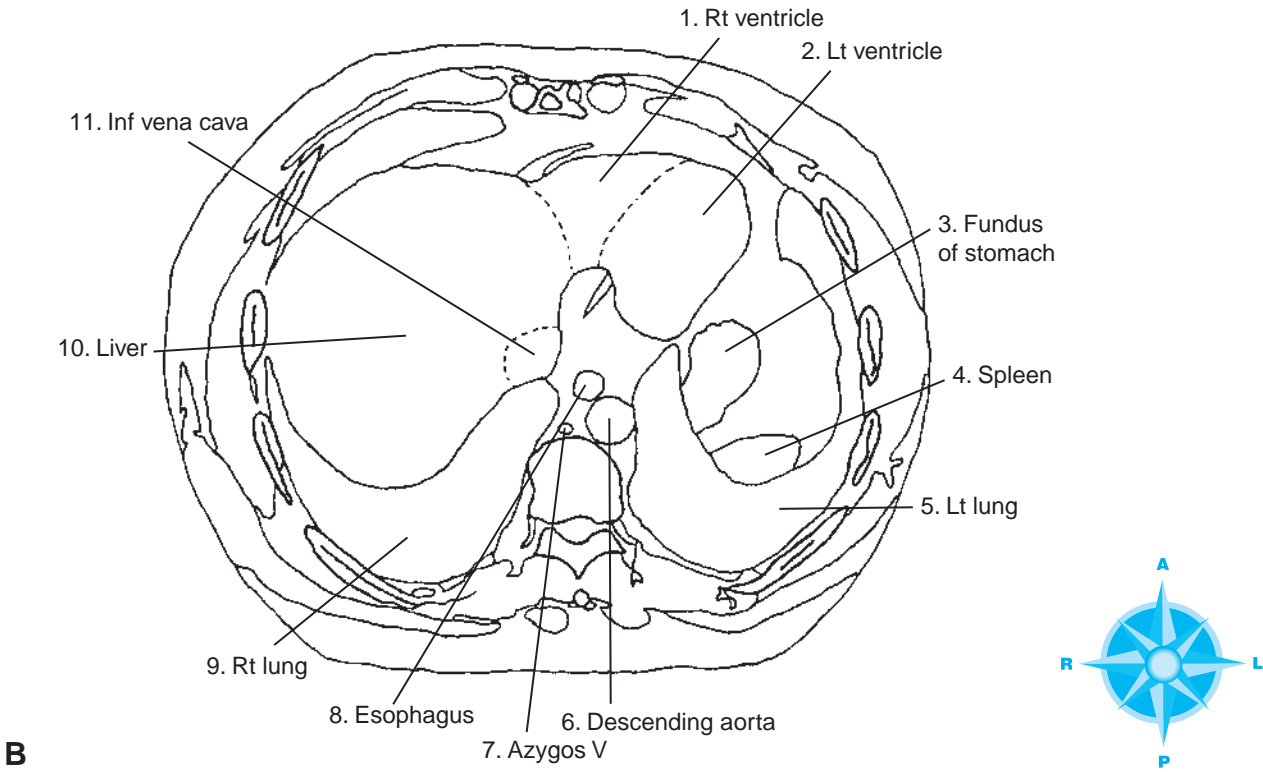
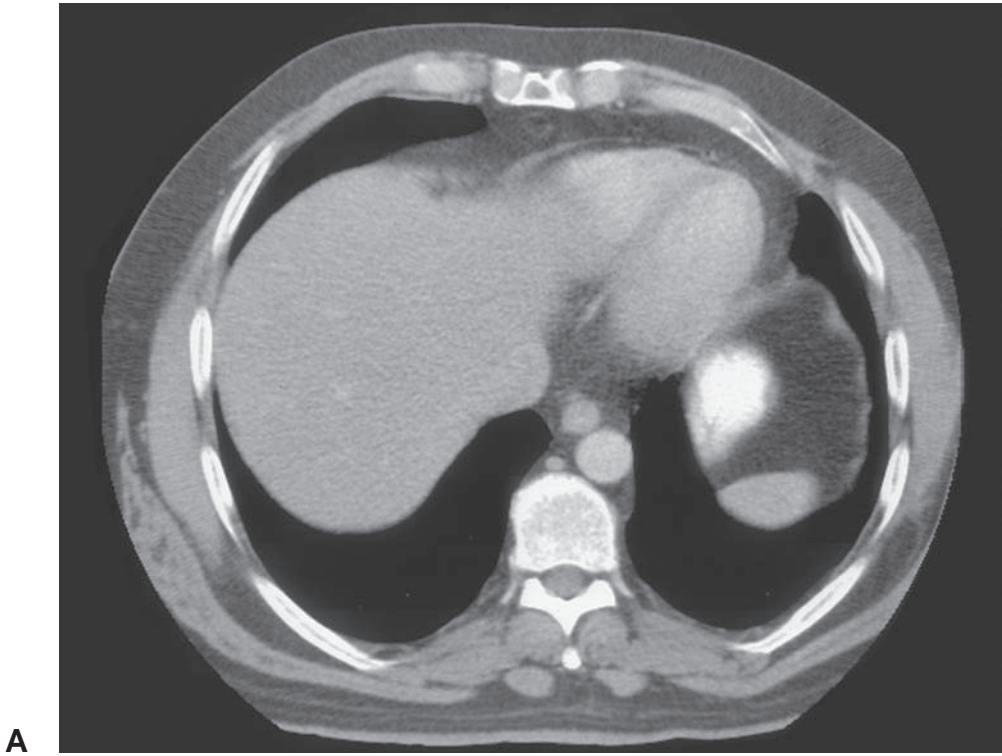
This section describes 24 axial CT images of the abdomen taken at 8.0-mm intervals through the abdomen from superior to inferior. The patient ingested 1,000 mL of oral contrast medium over a 60-minute period, and the images

were generated immediately after the administration of 100 mL of venous contrast medium. The following technical factors were used: 120 kilovolt peak (kVp), 150 milliamperere-second (mA-s).



**Figure 3–18 (A,B)** Axial CT image 1.

At the top of the abdomen, the liver is shown occupying most of the right side surrounded by the lower lobe of the right lung. On the left side, the lower lobe of the lung is forming a margin around the contents of the upper abdomen. Within the window, the upper pole of the dense spleen and the contrast-filled fundus of the stomach are both demonstrated. Within the mediastinum, the bottom of the heart is sectioned, and the right ventricle is more anterior than the left ventricle. Behind the heart, the esophagus is found extending downward to the stomach in front of the descending aorta and the azygos vein. On the right side of the patient, the inferior vena cava is difficult to discern from the surrounding liver tissue.



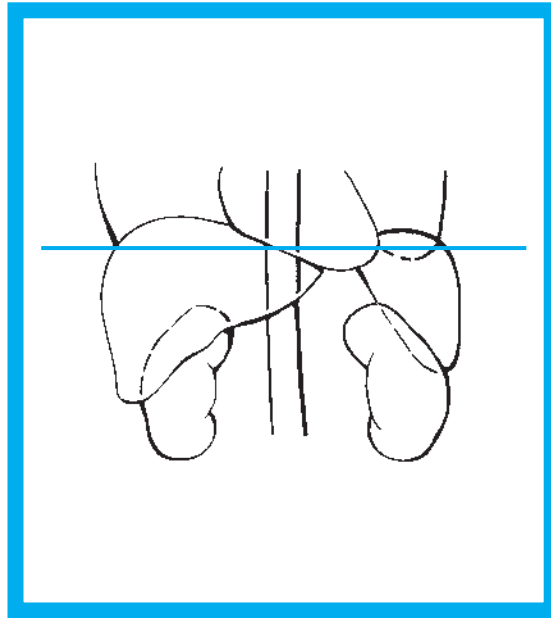
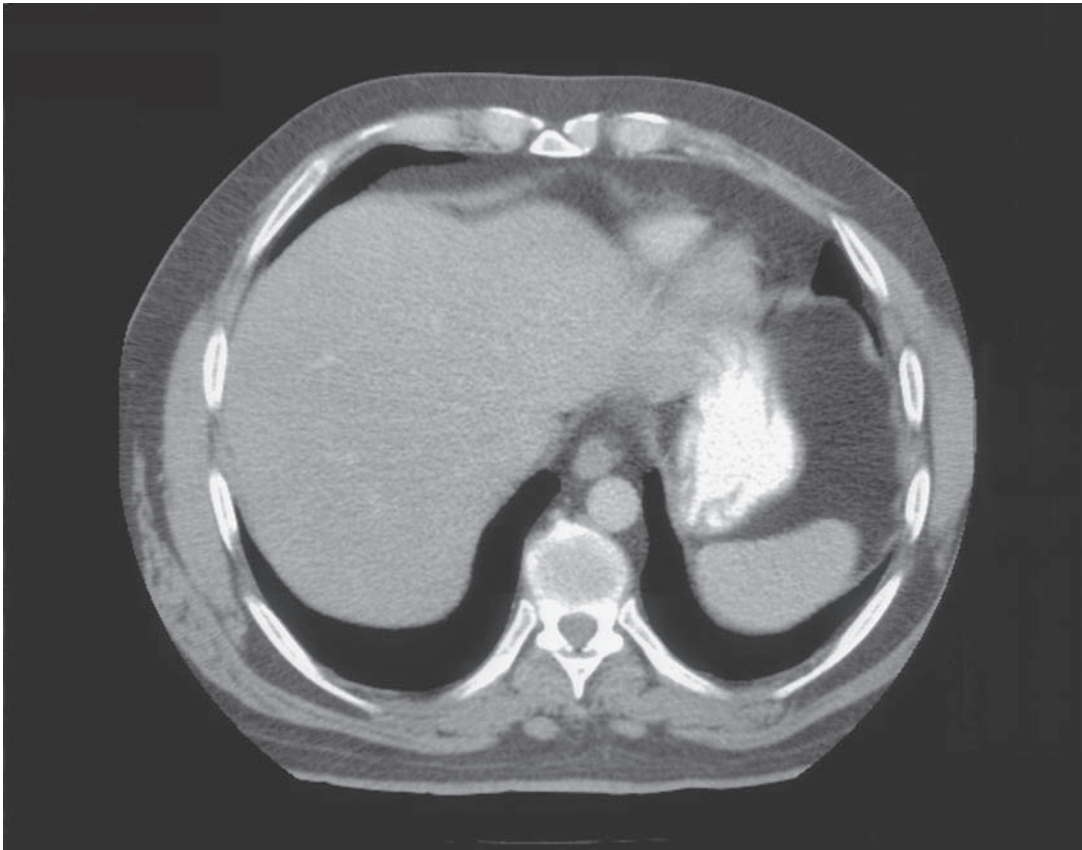
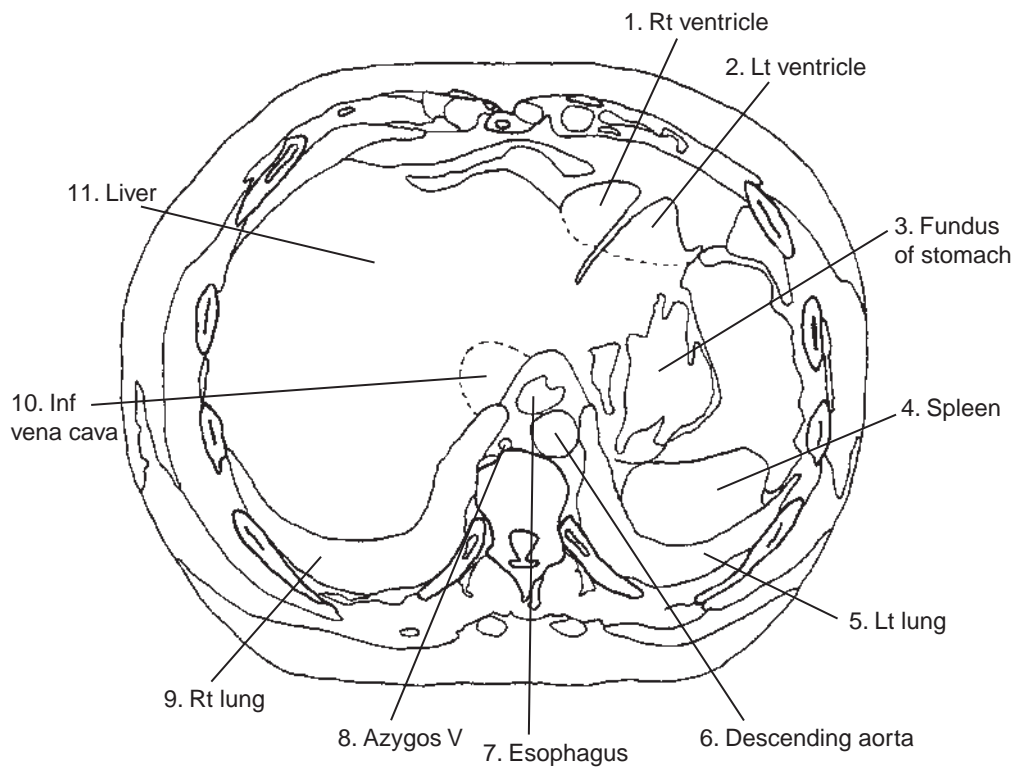


**Figure 3–19 (A,B)** Axial CT image 2.

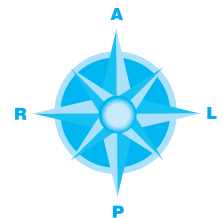
The body of the liver fills most of the right side and is difficult to distinguish from the base of the heart. Even though the diaphragm is not seen between the two organs, the interventricular septum can be seen separating the right and left ventricles of the heart. Next to the heart, the fundus of the stomach, filled with contrast, is shown on the left side. Although the esophagus is still between the descending aorta and inferior vena cava, the fundus of the stomach is also found within this session. Posterior to the stomach, the spleen appears as a dense organ bordered by the lower lobe of the left lung.



**A**



**B**



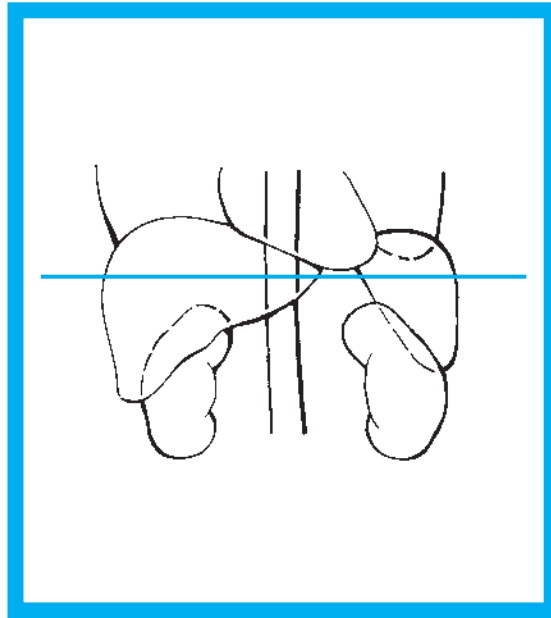
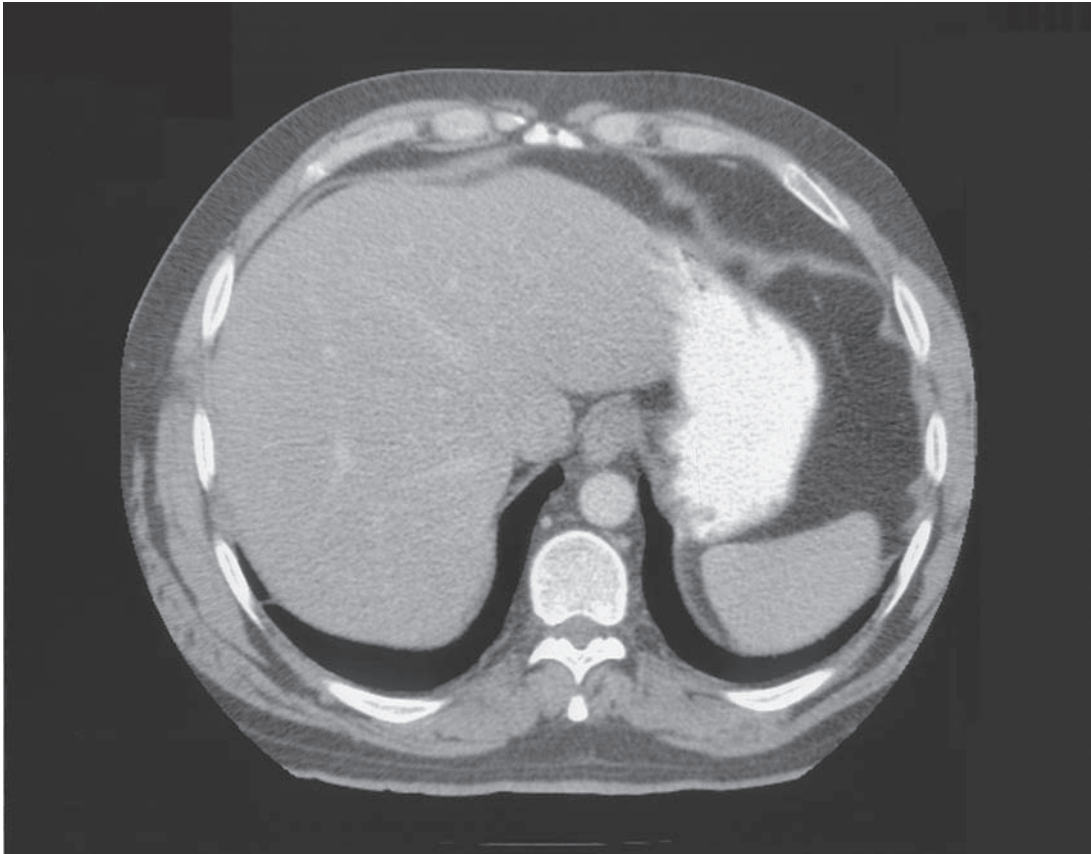
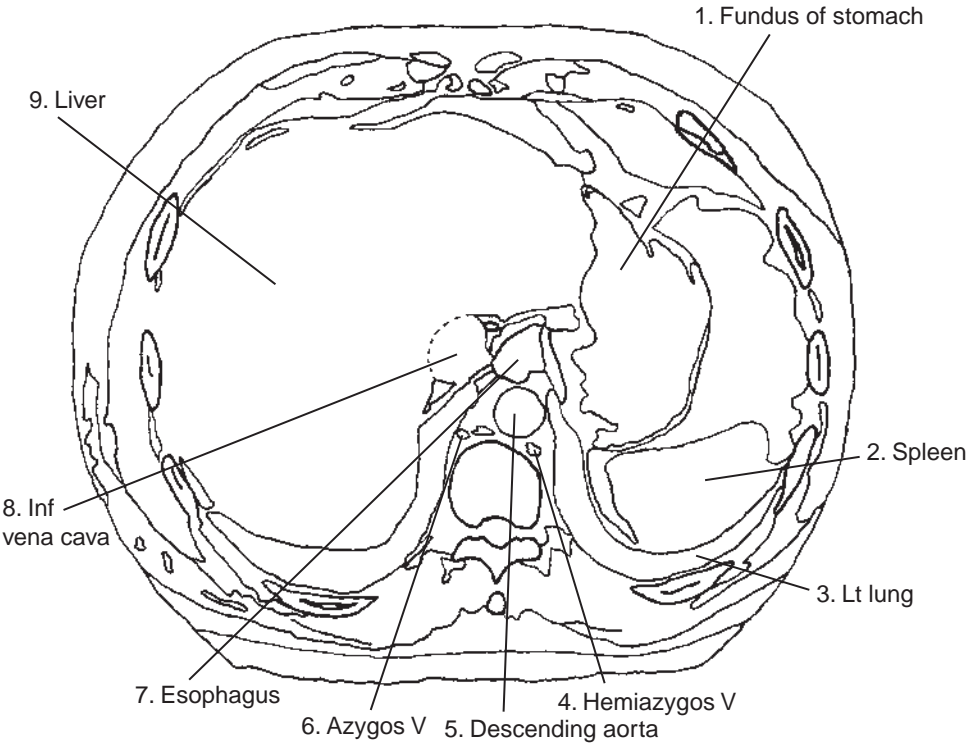


**Figure 3–20 (A,B)** Axial CT image 3.

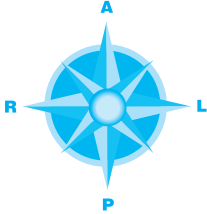
Unlike the previous image, the liver is occupying most of the right side and extending through the midline to lie beside the fundus of the stomach. The esophagus, no longer between the inferior vena cava and descending aorta, is nearing the point where it joins the stomach. On the left side, the costodiaphragmatic recess of the lung is forming a margin around the spleen. Between the lungs, the small azygos and hemiazygos veins are cross-sectioned on either side of the descending aorta.



A



B



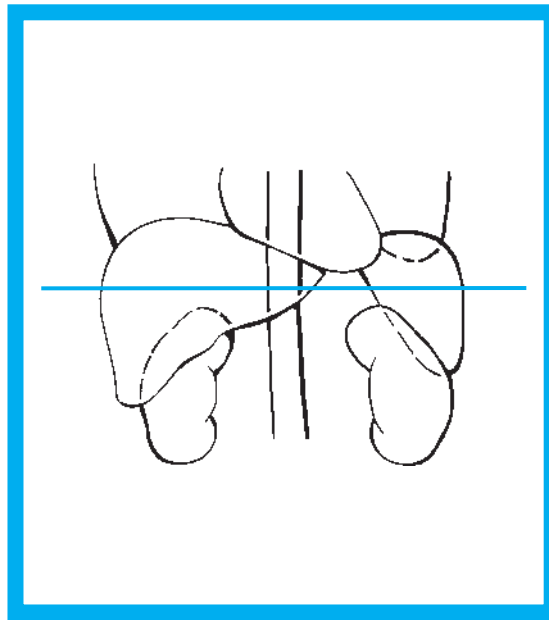
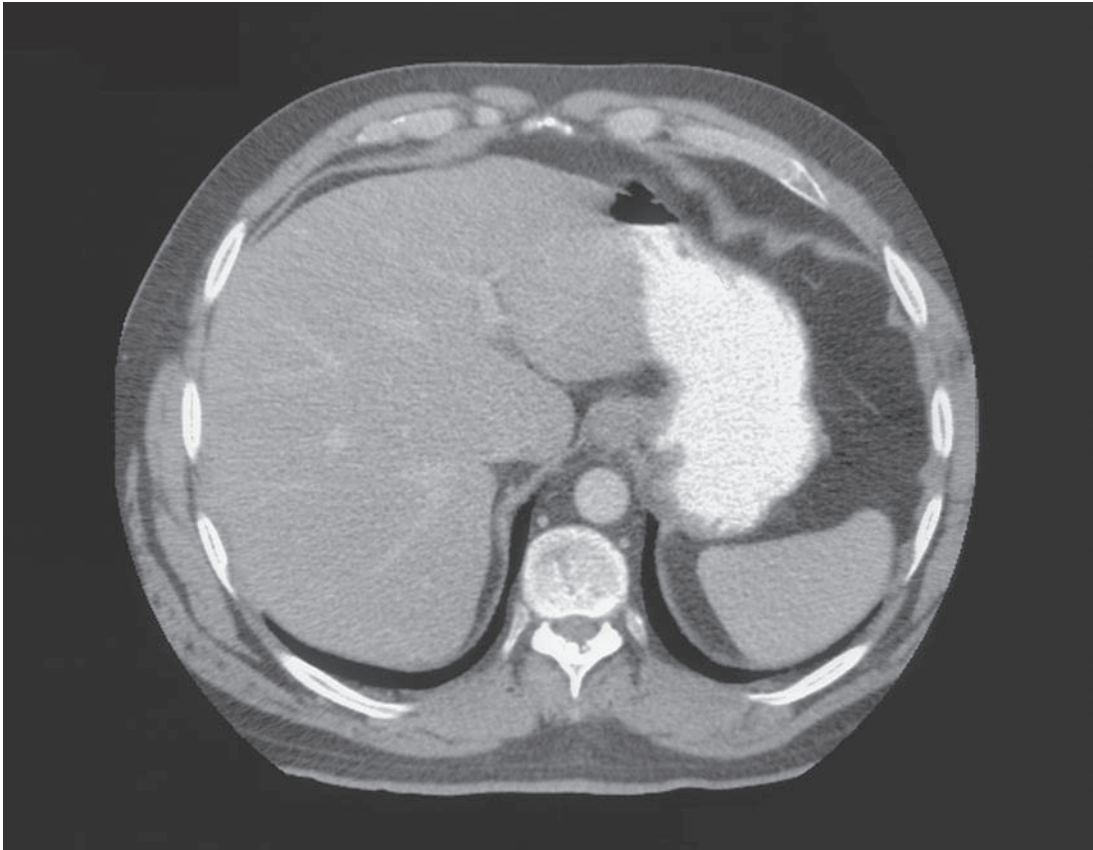


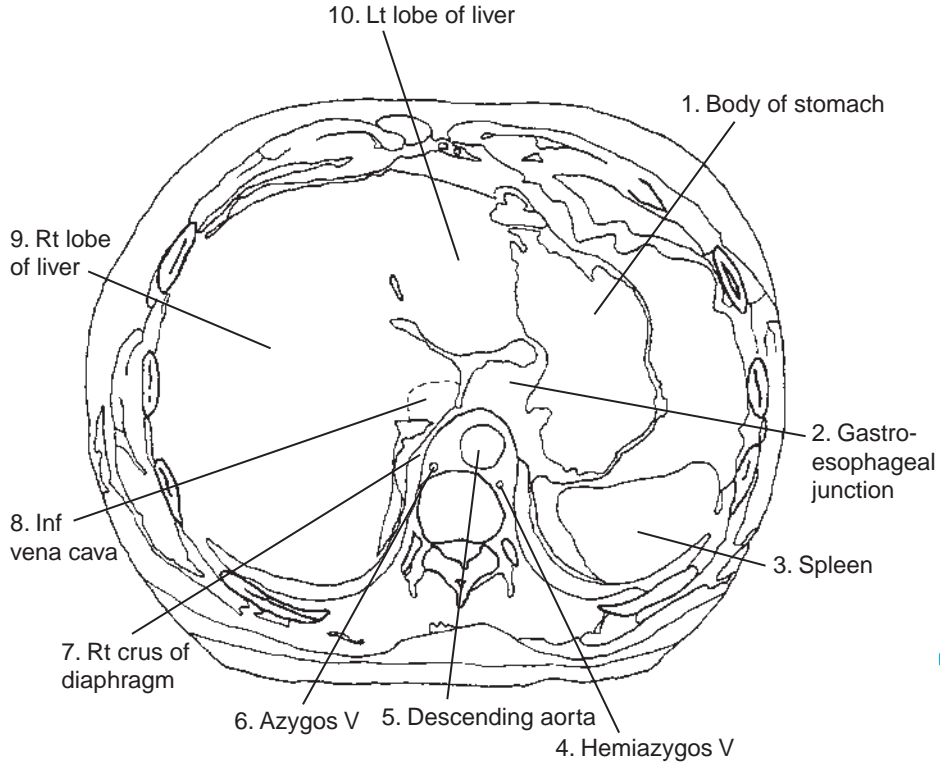
**Figure 3–21 (A,B)** Axial CT image 4.

Similar to the previous image, the liver is occupying the majority of the abdominal cavity. The right and left lobes of the liver can now be identified. In this section, the esophagus is joining the stomach, marking the middle portion of the stomach (the body). The inferior vena cava cannot be clearly distinguished from the liver and is separated from the descending aorta by the right crus of the diaphragm. On either side of the descending aorta, the hemiazygos and azygos veins are clearly seen anterior to the vertebral body. Along the posterior wall of the thoracic cage, the costodiaphragmatic recesses of the lungs form a narrow margin around the liver and spleen.

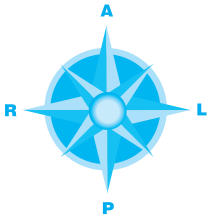




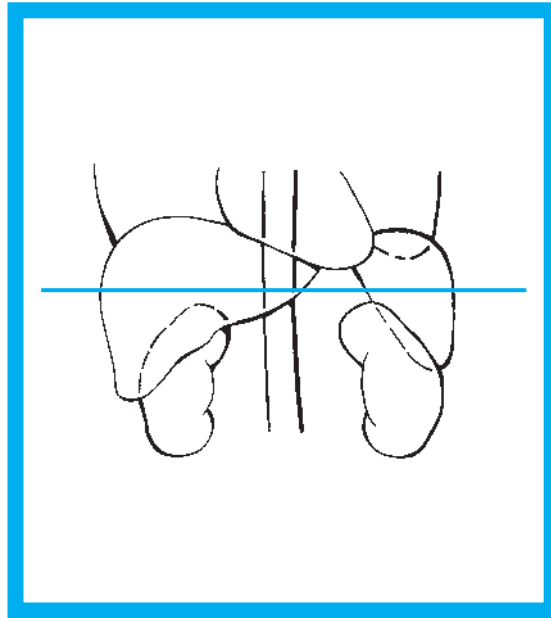
A



B

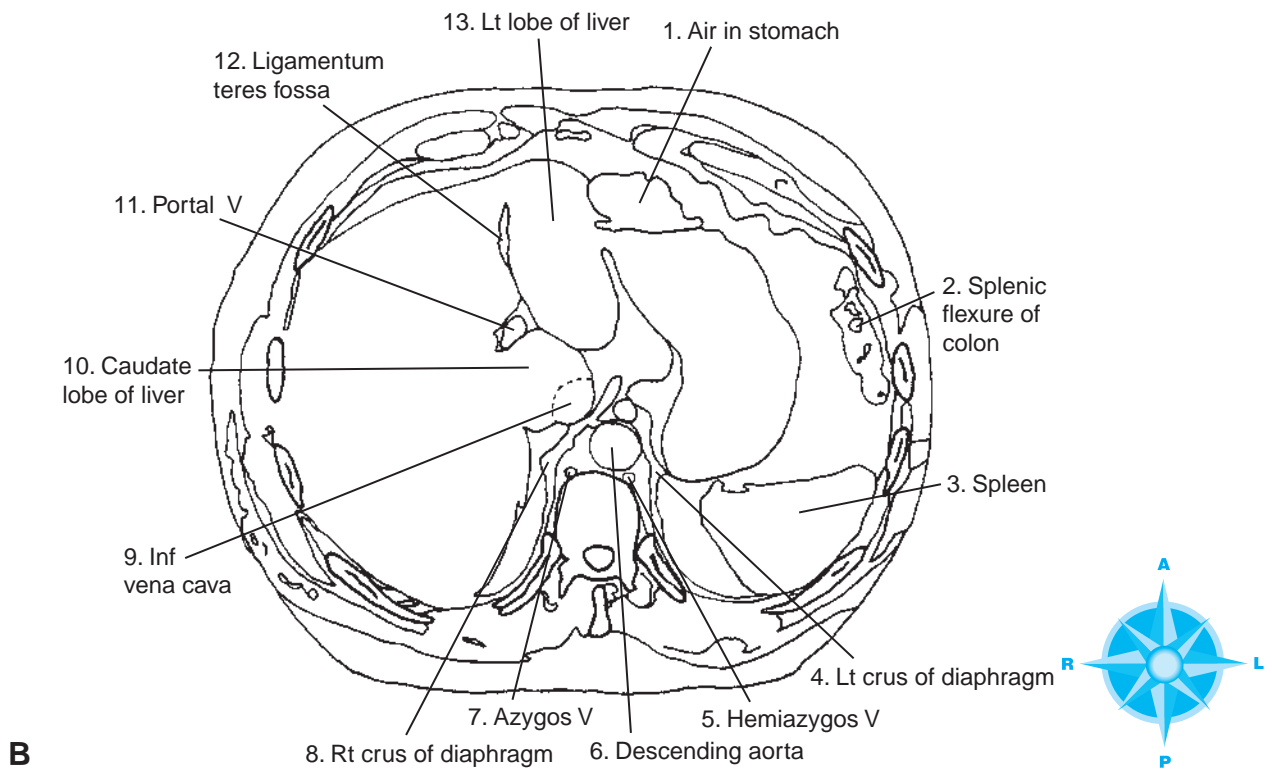
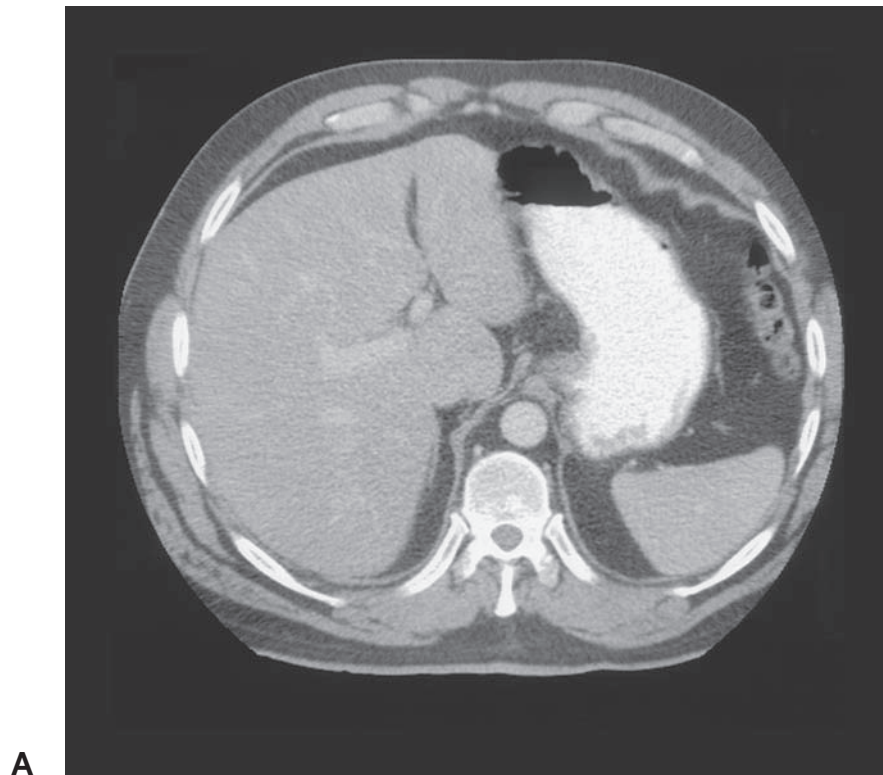






**Figure 3–22 (A,B)** Axial CT image 5.

The liver is limited to the right side of the abdomen and is divided into right and left lobes by the fossa for the ligamentum teres. The portal vein is within the porta hepatis, as described earlier, forming the transverse part of the H on the visceral surface of the liver. The caudate lobe of the liver is between the porta hepatis and the inferior vena cava. As in the previous image, the inferior vena cava is separated from the descending aorta by the right crus of the diaphragm. Behind the descending aorta, the azygos and hemiazygos veins are traversing through the diaphragm and are bordered by crural fibers. On the left side, an air–fluid level is shown in the contrast-filled stomach. Lateral to the stomach, the splenic flexure of the colon is now anterior to the spleen.



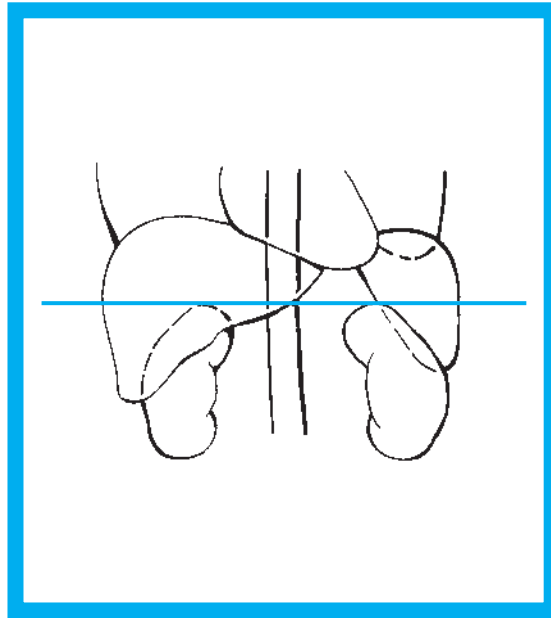
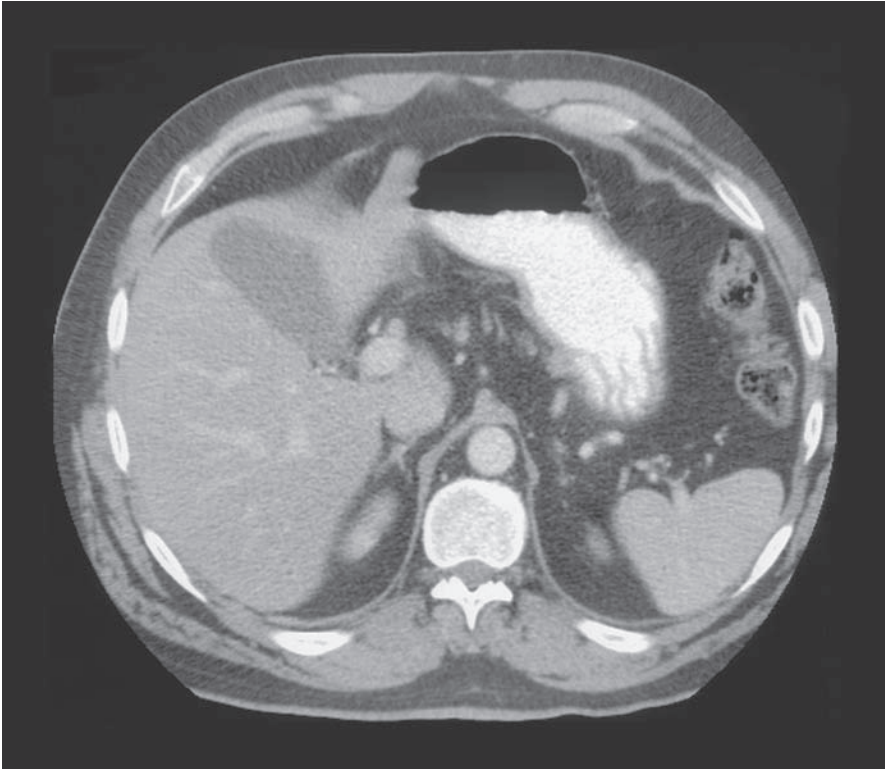
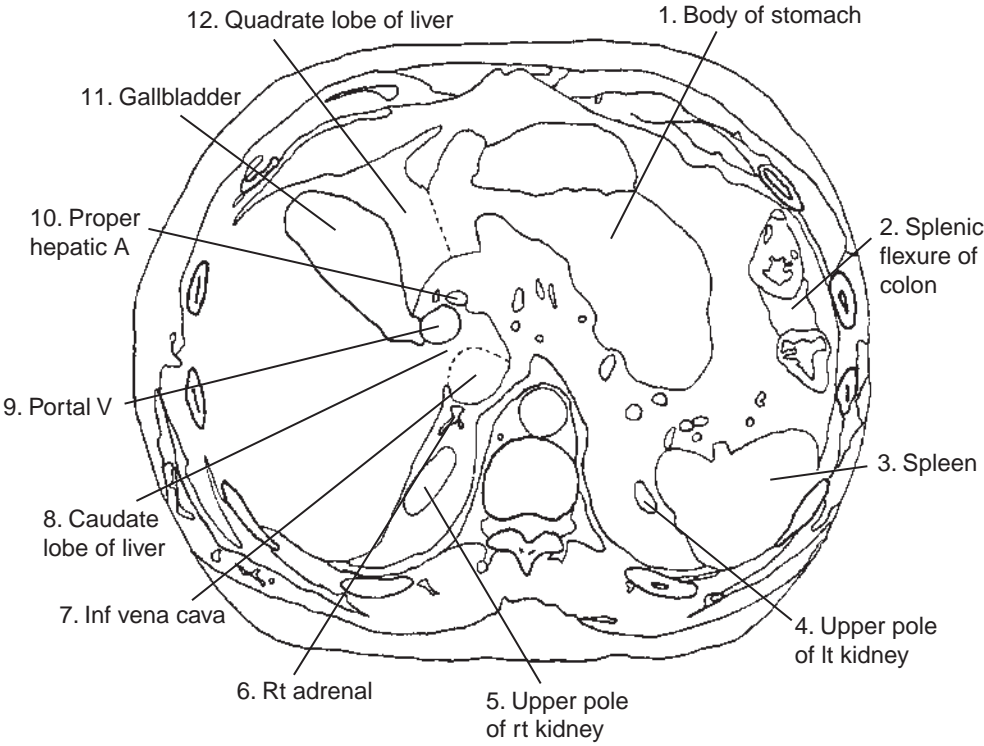


**Figure 3–23 (A,B)** Axial CT image 6.

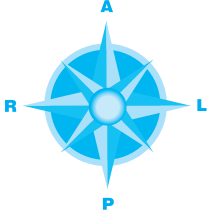
Although the liver fills most of the right side of the abdomen, it has decreased in size compared to the previous image, indicating the section is through the visceral surface. Within the liver, the gallbladder appears as a darkened area, with the tapered end pointing toward the porta hepatis, which contains the portal vein and the proper hepatic artery. On the visceral surface of the liver, the gallbladder marks the borders of the quadrate lobe. Posteriorly, the inferior vena cava marks the separation of the caudate lobe from the remaining right lobe of the liver. Just behind the inferior vena cava, the right adrenal gland is shown extending toward the upper pole of the right kidney and is surrounded by fat. On the left side, the stomach, splenic flexure of the colon, and the spleen appear much the same as described in the previous image.

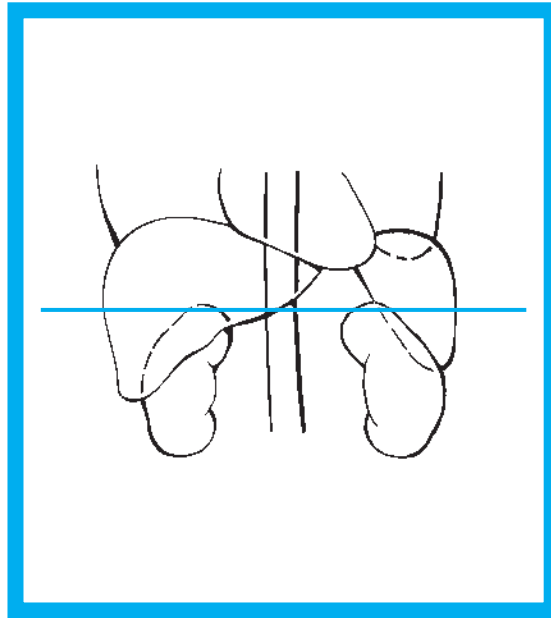


A



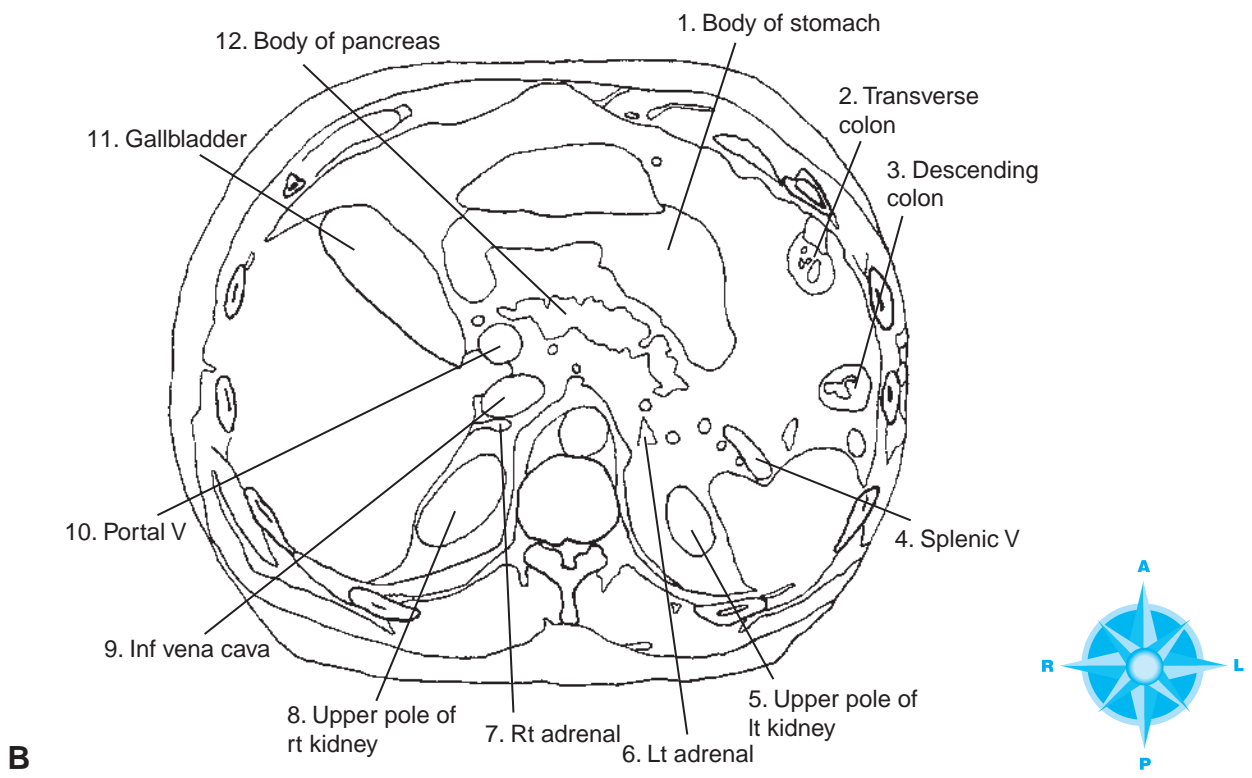
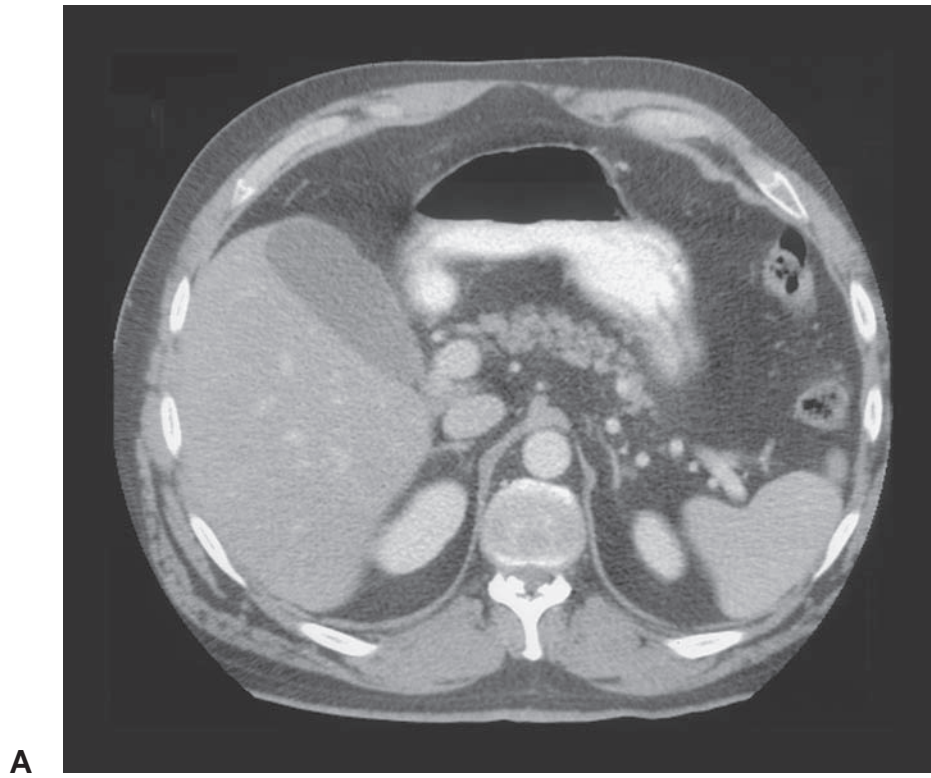
B





**Figure 3–24 (A,B)** Axial CT image 7.

Only the lower right lobe of the liver is shown, and the body of the stomach occupies a more central location. The gallbladder can clearly be discerned and appears as a darkened region within the liver, with the tapered end pointing posteriorly. At this lower level, the inferior vena cava and the portal vein are separated from the liver tissue, and the body of the pancreas is shown posterior to the stomach. To the left of the stomach, the splenic flexure of the colon has divided and given rise to the transverse colon and the descending colon. Adjacent to the posterior wall, the spleen is irregularly shaped, and the splenic vein is shown in longitudinal section as it extends toward the portal vein. On either side, the adrenal glands are found anterior to the upper poles of the kidneys.



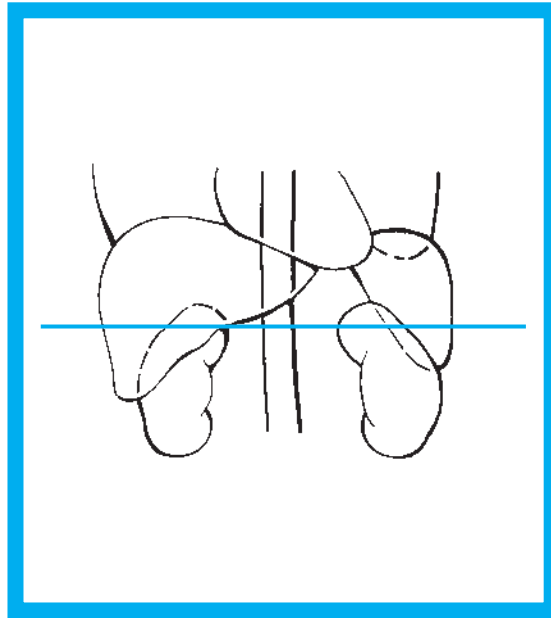
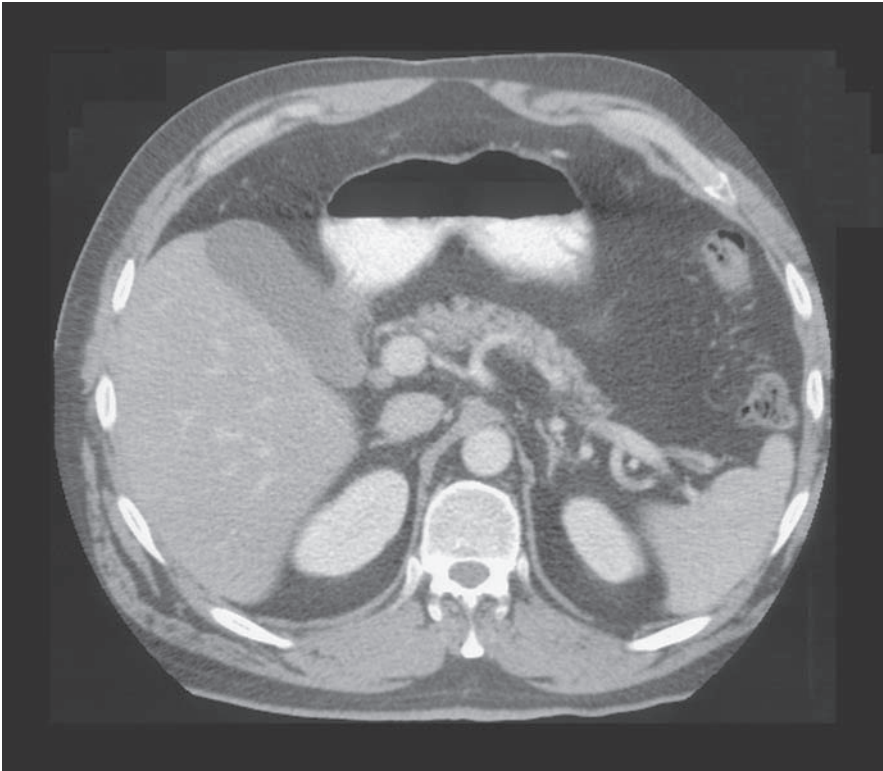
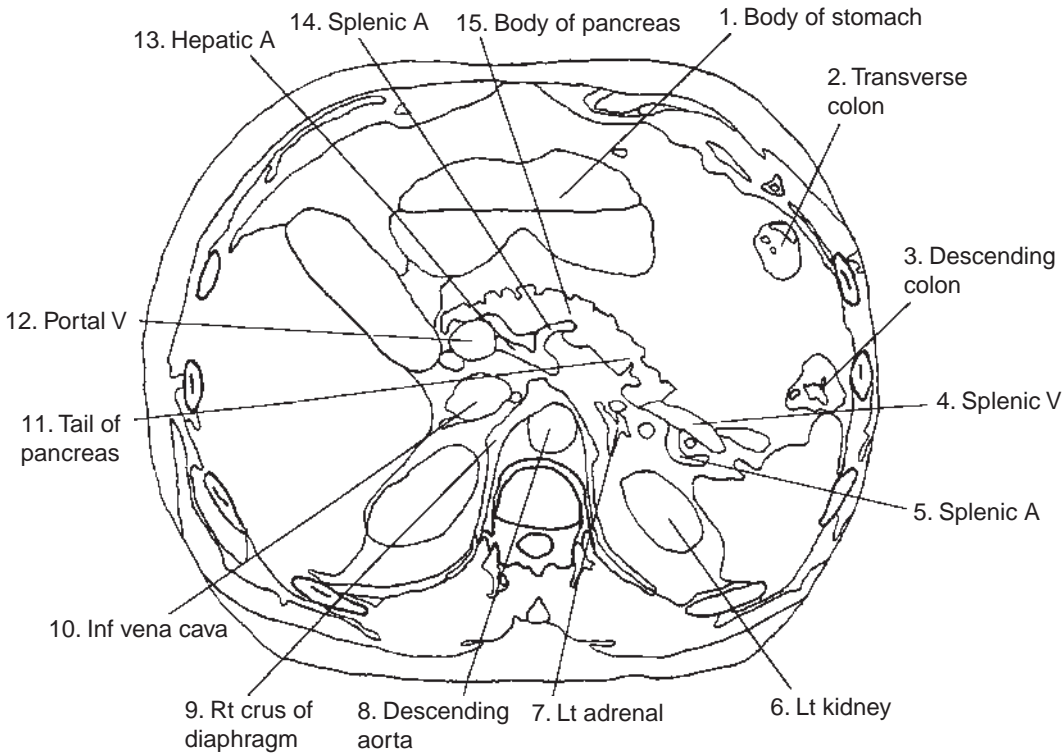


**Figure 3–25 (A,B)** Axial CT image 8.

The air–fluid level within the stomach is found centrally in front of the body of the pancreas in this figure. Within the glandular tissue of the body of the pancreas, the portal vein is next to the hepatic artery. Originating from the celiac trunk, both the hepatic artery and the splenic artery are shown within this section. Although the celiac trunk originates from the aorta, the arterial branches appear separated from the aorta by the crural ligaments of the diaphragm. The tail of the pancreas, extending in front of the left adrenal gland and kidney, points toward the spleen. This image clearly demonstrates the near linear course of the splenic vein beside the tortuous path of the splenic artery. Anterior to the spleen, the descending and transverse parts of the colon are labeled, because this section lies below the splenic flexure.



A



B



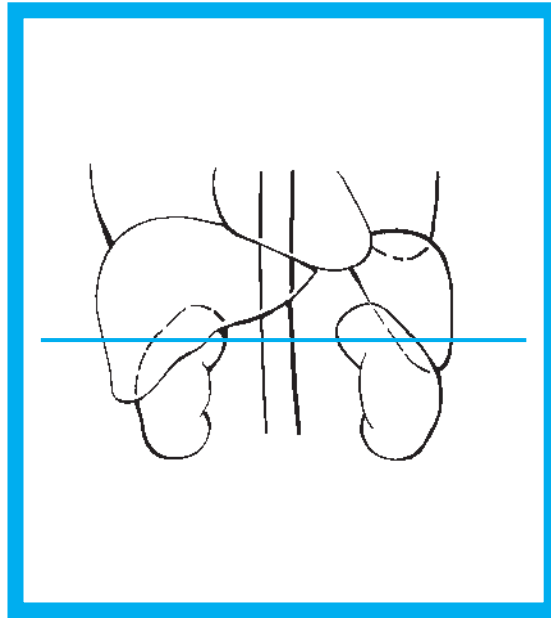
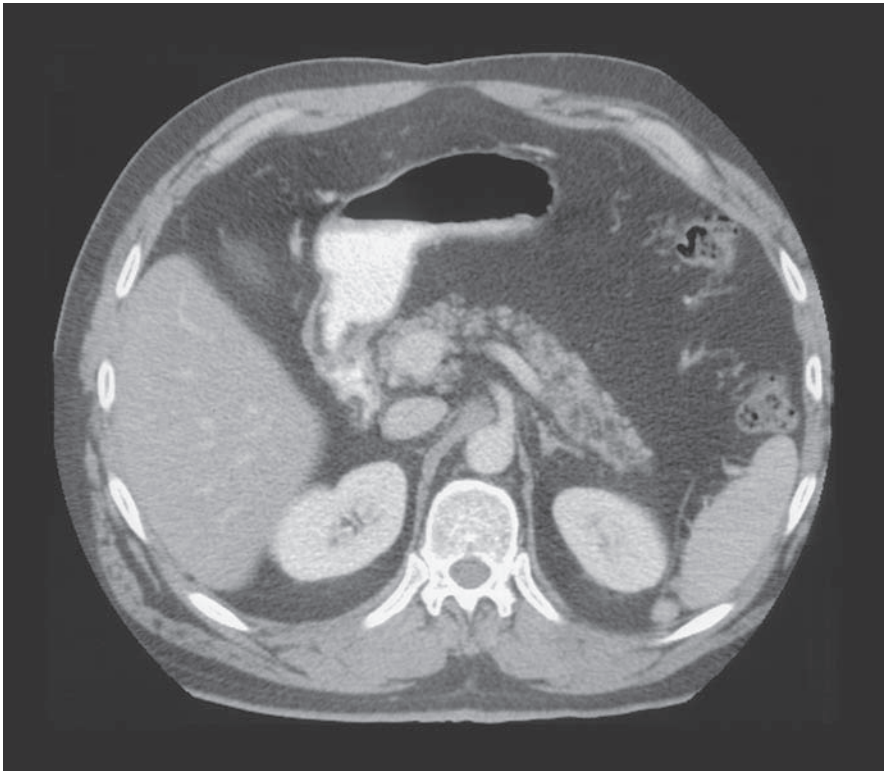
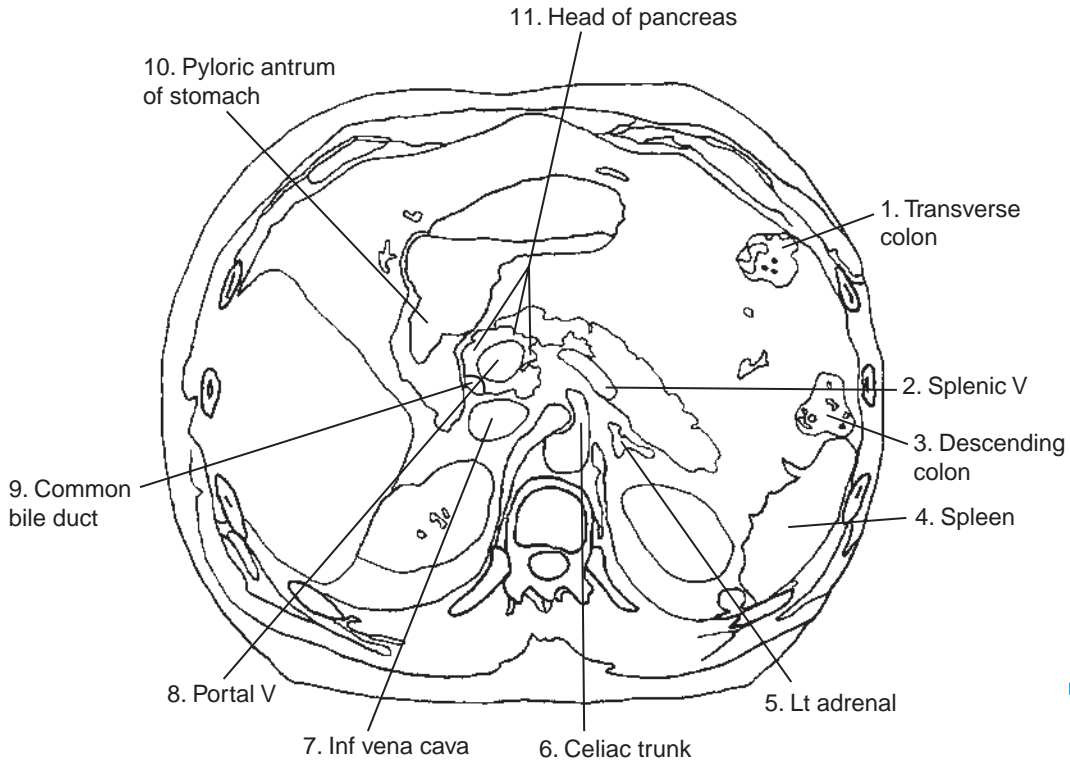


**Figure 3–26 (A,B)** Axial CT image 9.

The tapered end of the stomach, the pyloric antrum, is wrapping around the head of the pancreas that surrounds the common bile duct and the portal vein. Within the body of the pancreas, the near linear splenic vein is found in longitudinal section as it extends toward the portal vein. Posterior to the pancreas, the celiac trunk is shown originating from the abdominal aorta and extending through the crural ligaments. As described earlier, the celiac trunk usually gives rise to the splenic artery and the hepatic artery; however, 41% of individuals have aberrant hepatic arteries (commonly originate from the aorta or superior mesenteric artery). On the left side of the celiac trunk, the left adrenal gland is sectioned in front of the kidney. Much like the previous image, the transverse and descending parts of the colon are sectioned in front of the spleen.



A



B

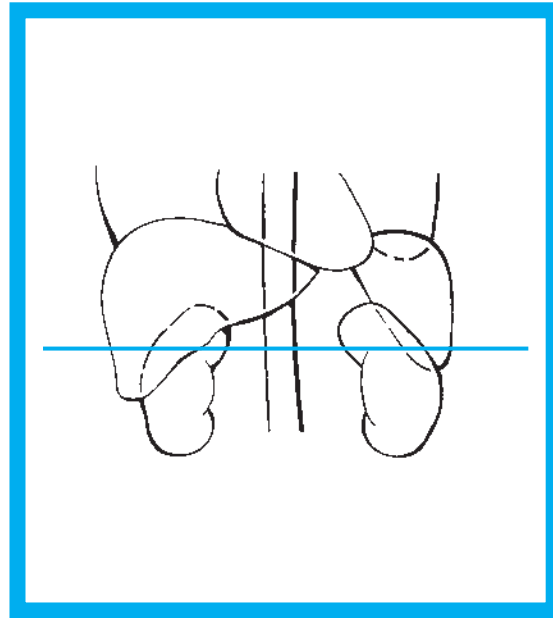
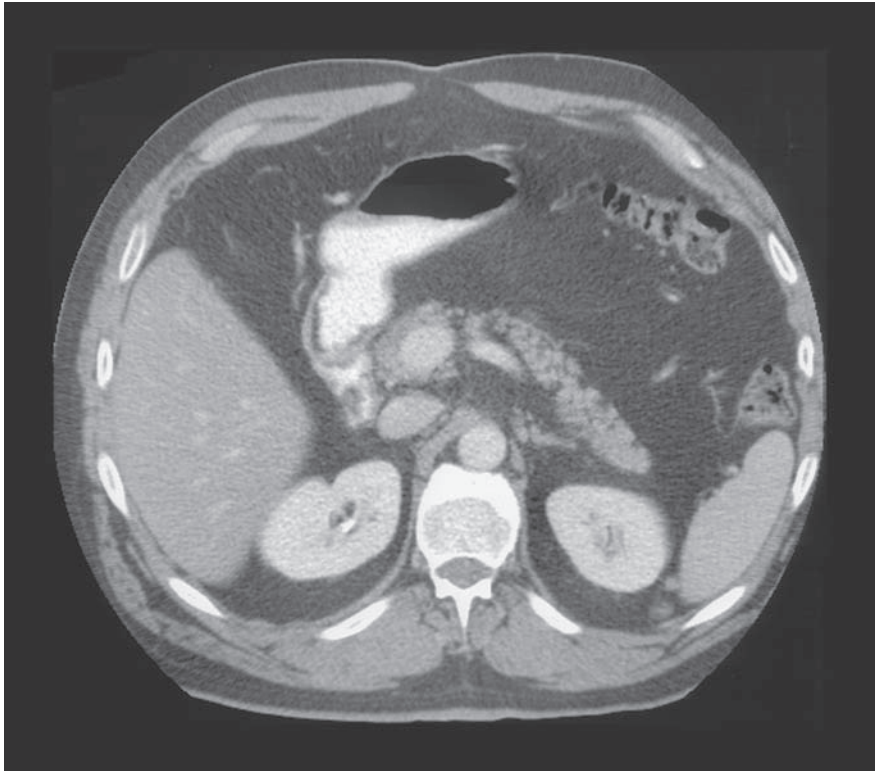
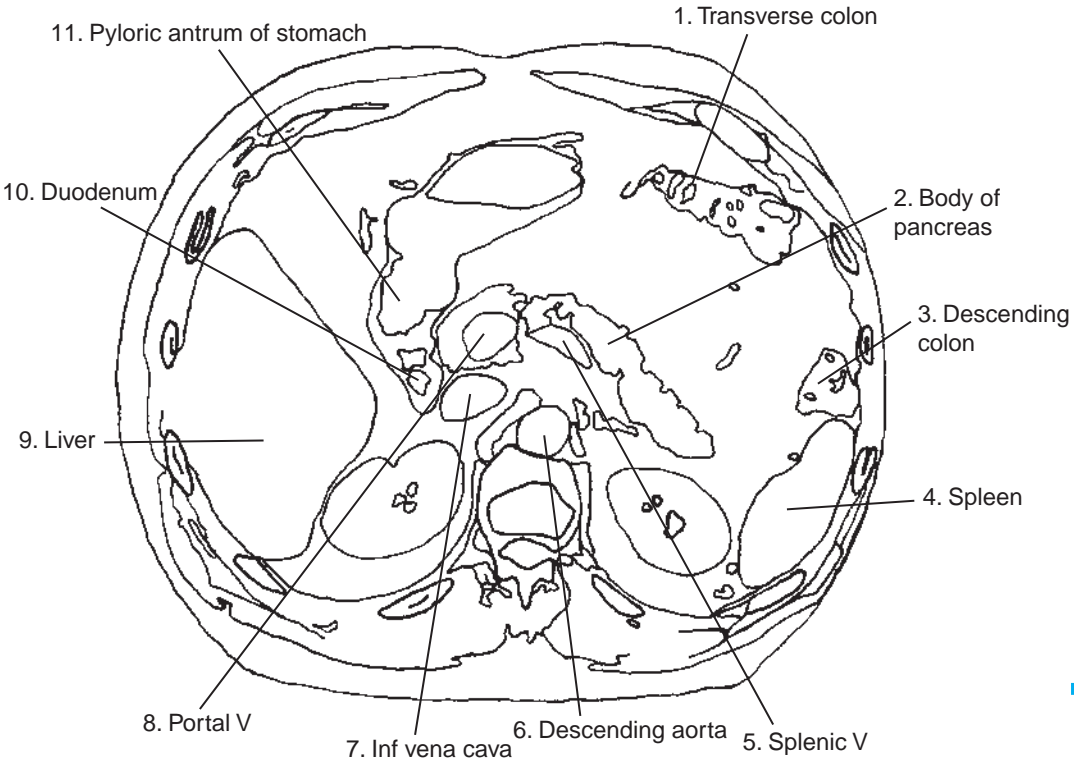


**Figure 3-27 (A,B)** Axial CT image 10.

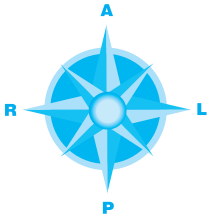
The contrast within the pyloric antrum of the stomach is shown extending into the first part of the duodenum. Together, these structures wrap around the pancreas, which contains the portal and splenic veins. Posterior to the pancreas, the inferior vena cava is on the right side and the descending aorta is slightly to the left. Similar to the previous image, the transverse colon, descending colon, spleen, and liver are shown in the periphery of the abdominal cavity.



A



B



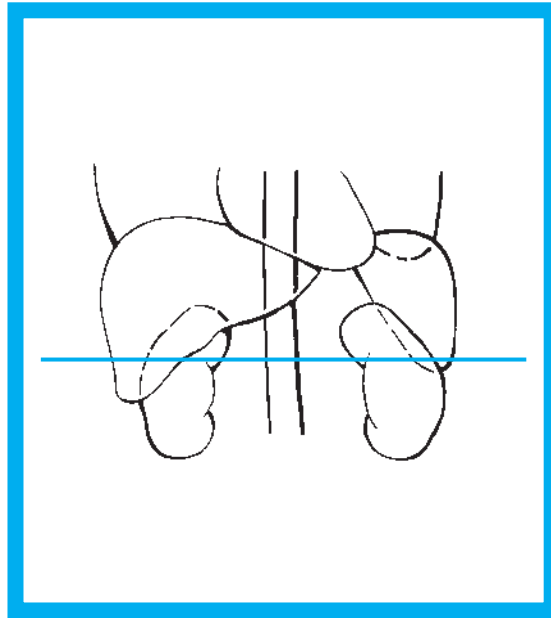
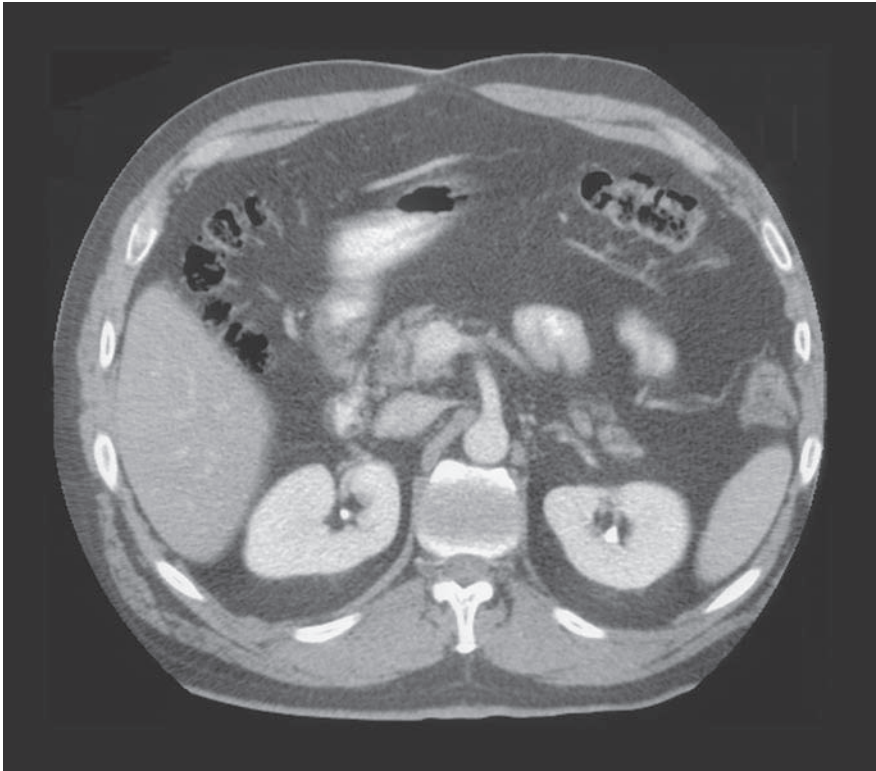
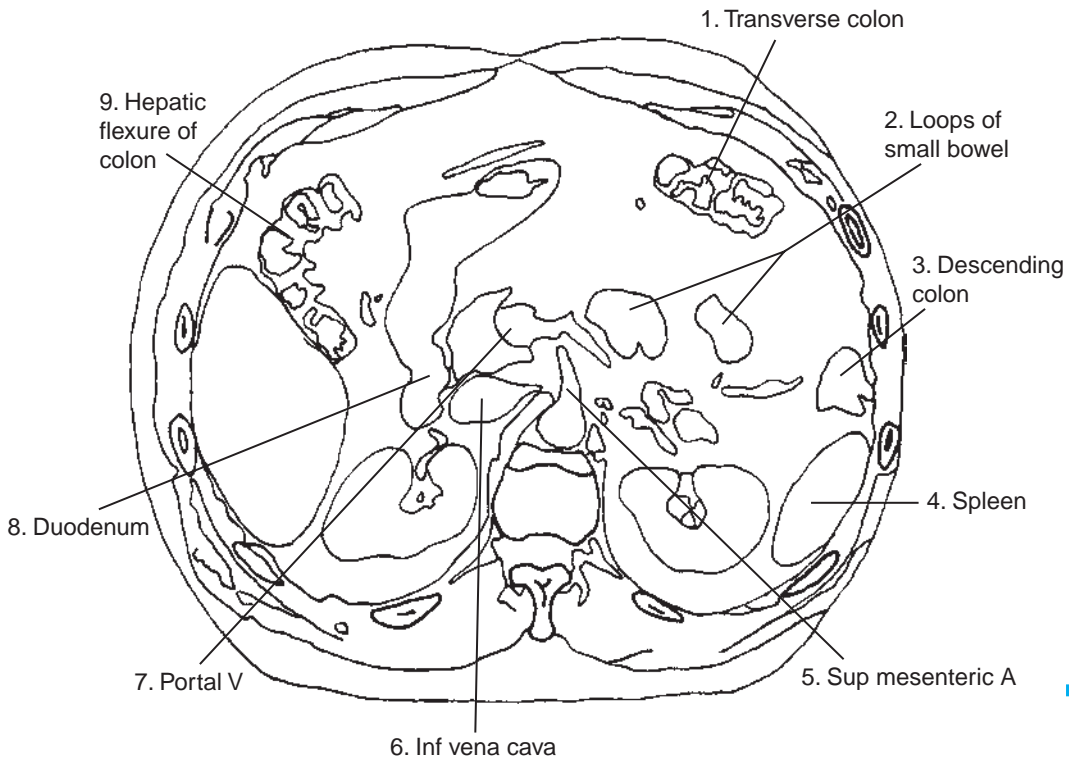


**Figure 3–28 (A,B)** Axial CT image 11.

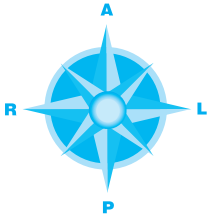
At this level, the lower stomach is seen as continuous with the duodenum and is found adjacent to the head of the pancreas. Although difficult to distinguish, the origin of the portal vein is included in this section. The portal vein originates from the joining of the superior mesenteric vein and the splenic vein. Behind the portal vein, an artery is shown arising from the abdominal aorta. The celiac trunk was described about 1 cm above, and the superior mesenteric artery is shown originating behind the head of the pancreas. The superior mesenteric artery will be shown in lower sections on the left side of the superior mesenteric vein. Like previous views, the descending and transverse parts of the colon are on the left side. At this level, the hepatic flexure of the colon is now found on the right side next to the visceral surface of the liver. Compared to the parts of the colon, the centrally located loops of small bowel are filled with contrast and are slightly smaller in diameter.



A



B



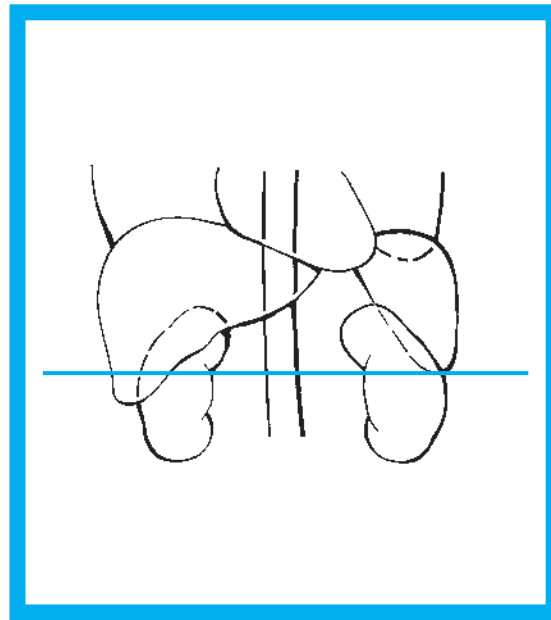
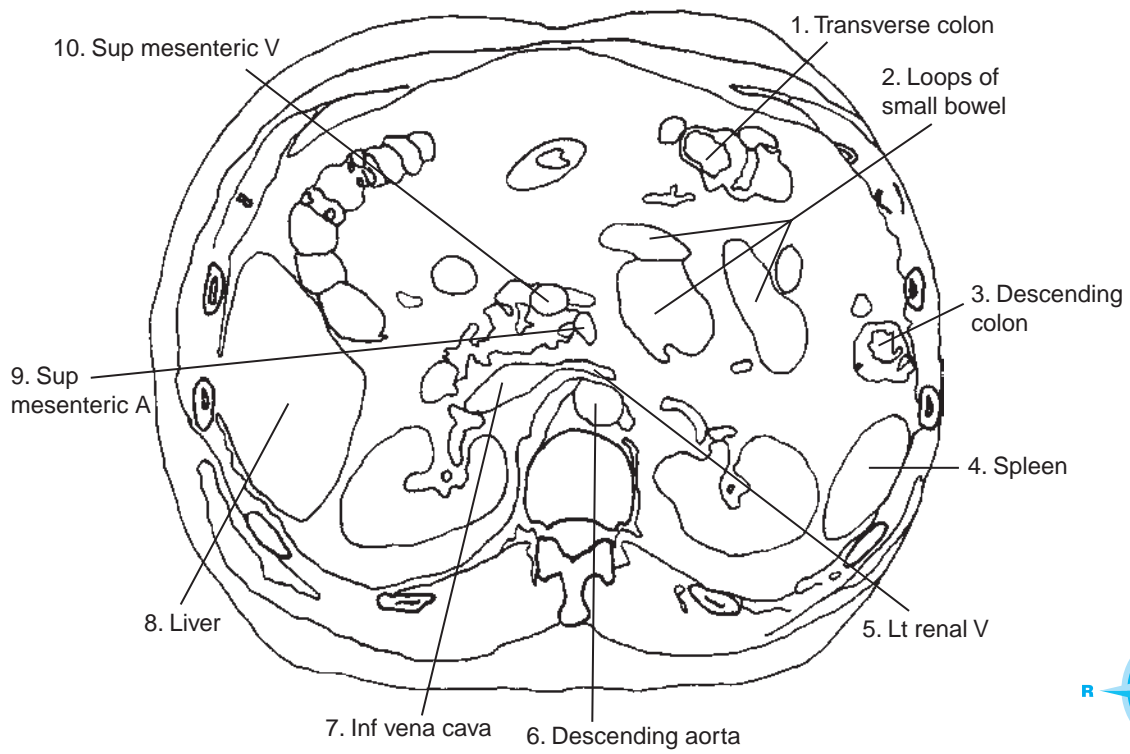


**Figure 3–29 (A,B)** Axial CT image 12.

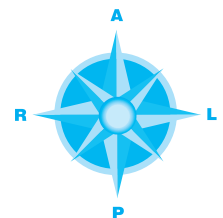
Although the lower portions of the liver and spleen are shown, this section is below the level of the stomach. In the anterior abdominal cavity, the hepatic flexure is found in front of the liver and the descending colon is in front of the spleen. Extending between the two, the transverse colon is next to the anterior abdominal wall in front of the contrast-filled loops of small bowel. Centrally, the superior mesenteric artery and vein are traversing through the head of the pancreas. Posteriorly, the inferior vena cava is joining with the renal veins and the left renal vein is found passing in front of the descending aorta.



A



B





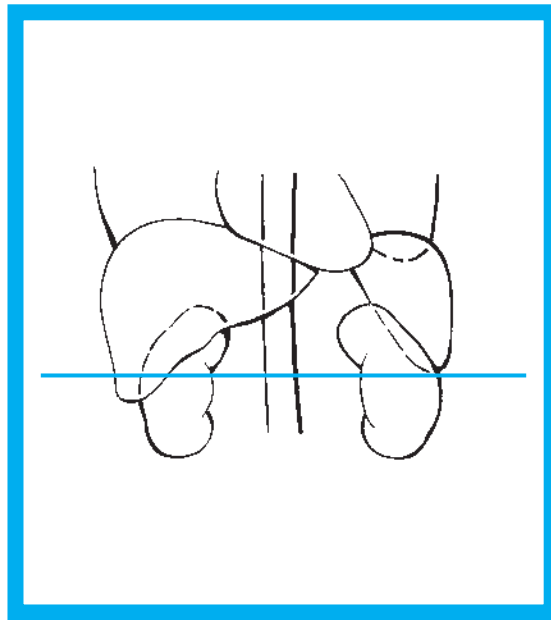
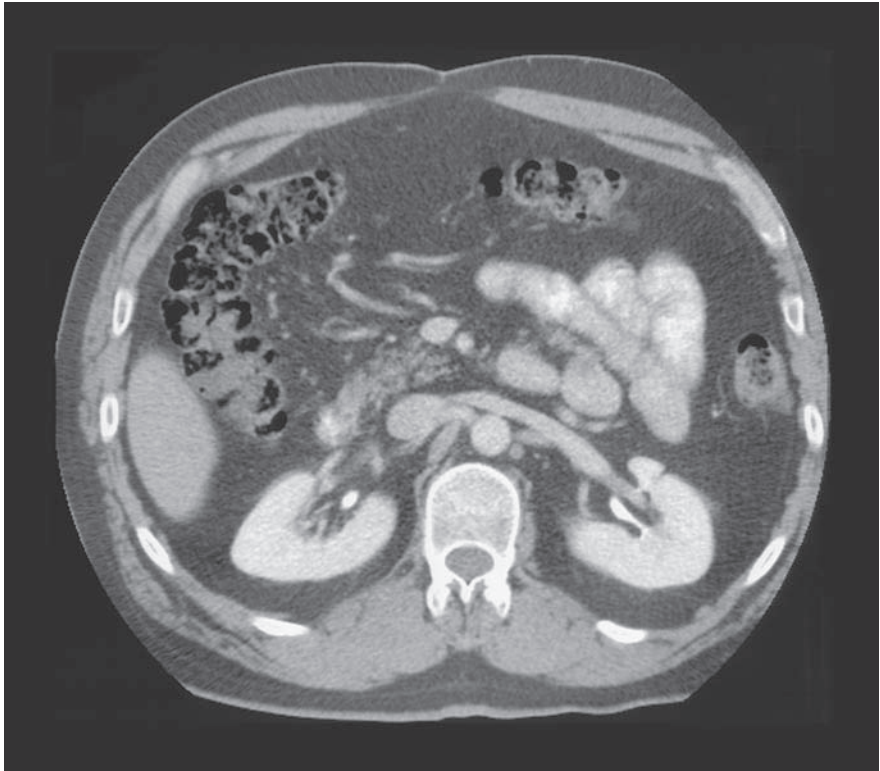
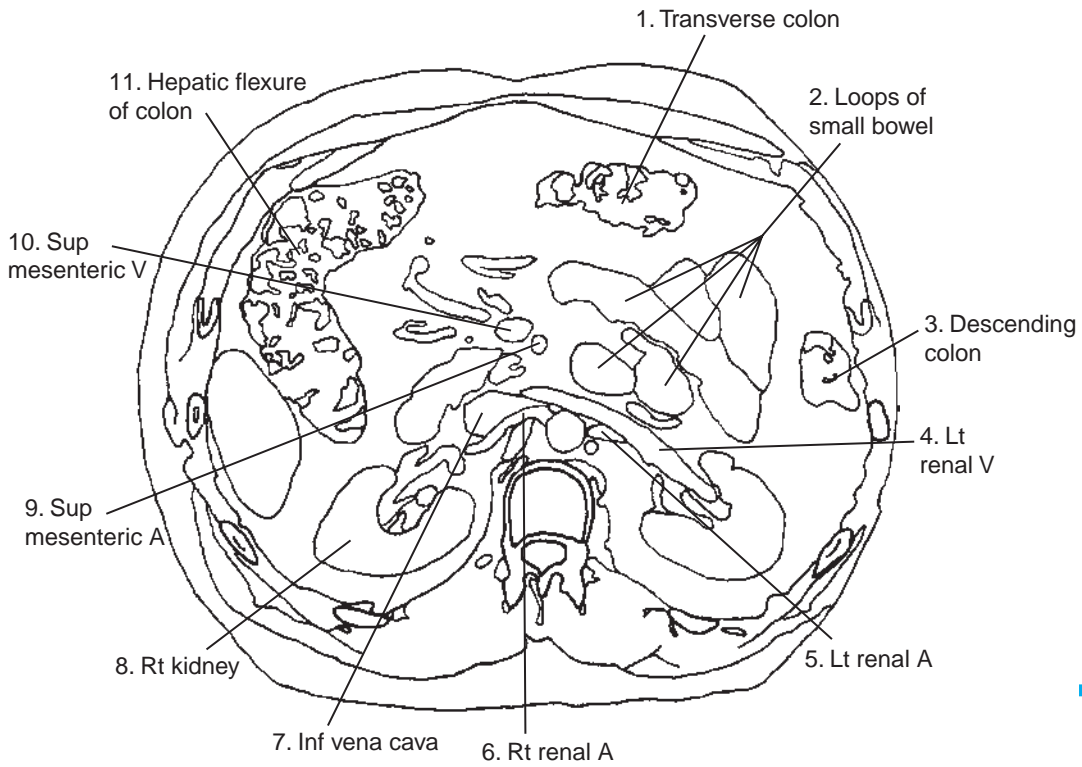


**Figure 3–30 (A,B)** Axial CT image 13.

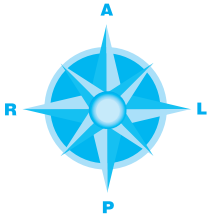
This image clearly demonstrates the hepatic flexure of the colon near the liver, the transverse colon near the anterior abdominal wall, and the descending colon near the left abdominal wall. Between the parts of the colon, loops of contrast-filled small bowel are loosely organized on the left side of the abdomen. Given that the section is in the upper abdomen, the loops of small bowel are most likely the middle part of the small intestine (the jejunum). On the right side, vessels within the mesentery are seen along with the larger superior mesenteric artery and vein. Near the posterior wall, both kidneys are shown sectioned through the region of the hilum, demonstrating renal vessels. The left renal vein is again shown in front of the abdominal aorta, and the renal arteries are sectioned on either side behind the veins.



A



B



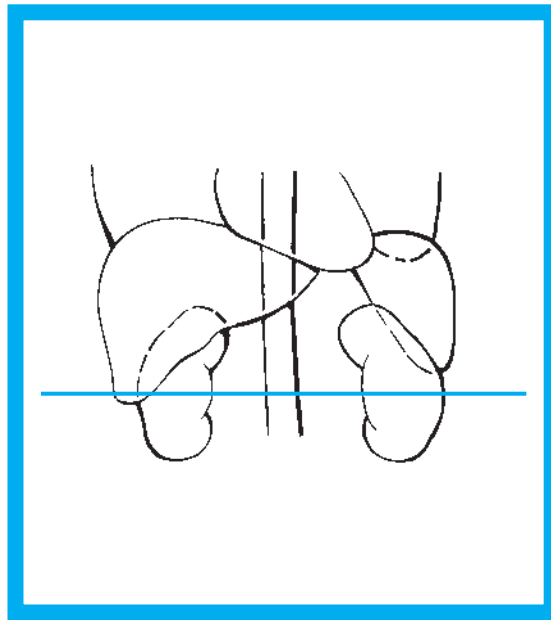
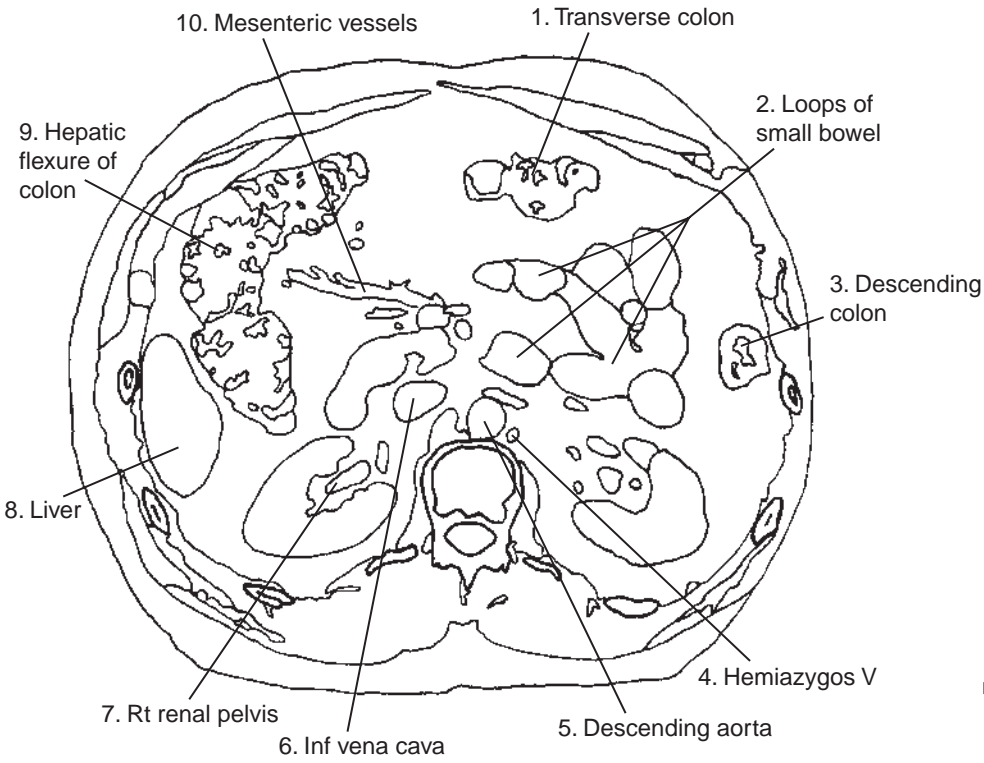


**Figure 3–31 (A,B)** Axial CT image 14.

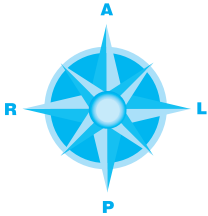
Similar to the previous image, this image shows the hepatic flexure of the colon near the liver, the transverse colon near the anterior abdominal wall, and the descending colon near the left abdominal wall. Loops of small bowel are on the left side, and vessels within the mesentery are again shown on the right side. The kidneys, located behind the peritoneum on either side of the vertebral body, are sectioned through the lower hilar region, demonstrating the contrast-enhanced renal pelvis. Between the kidneys, the descending aorta and inferior vena cava are cross-sectioned in front of the vertebral body. Behind the descending aorta, the hemiazygos vein is found on the left side, even though the azygos vein cannot be clearly delineated on the right.



A



B



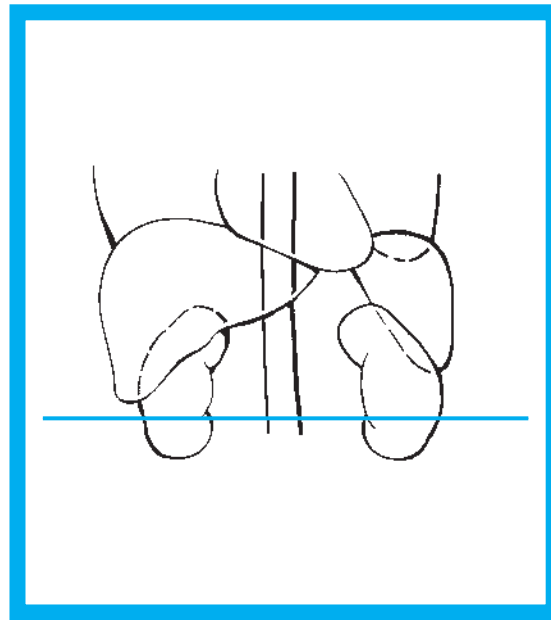
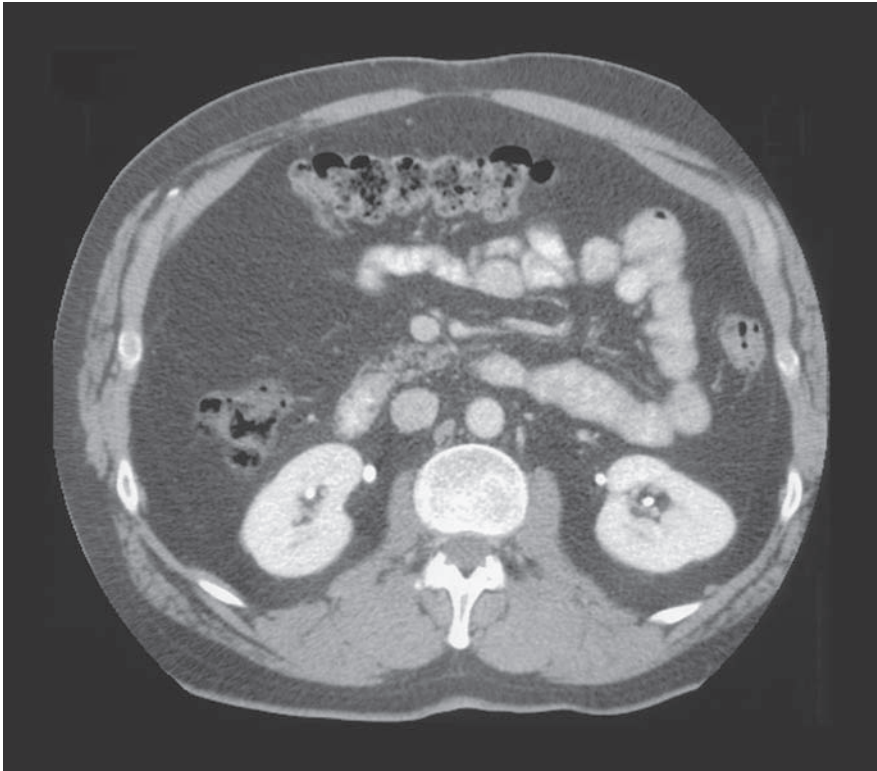
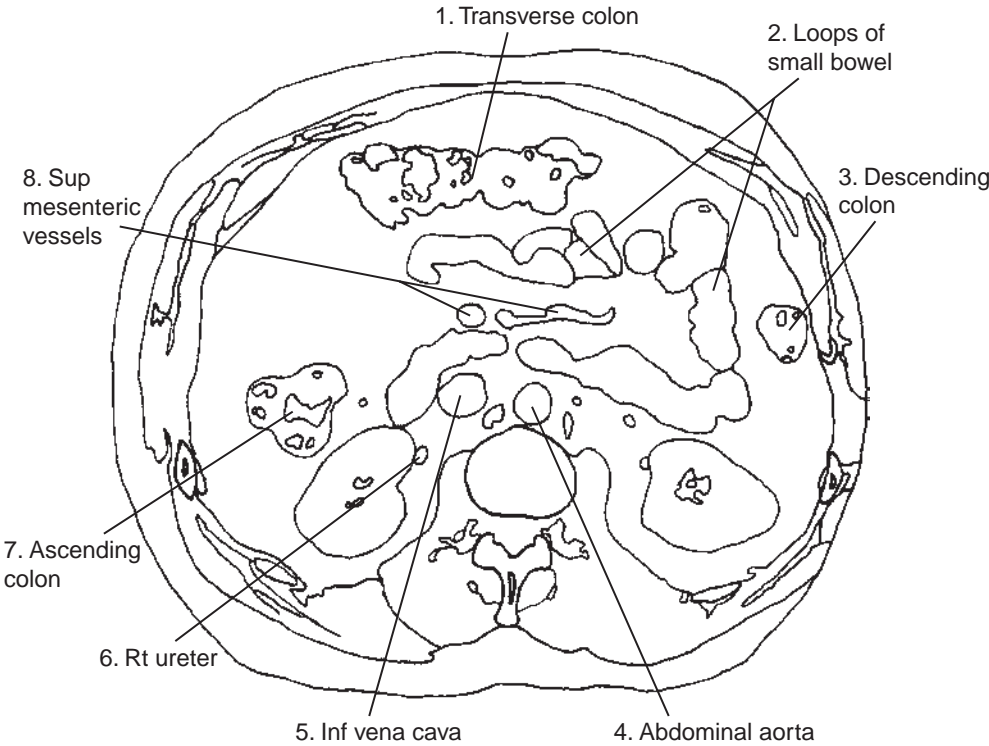


**Figure 3–32 (A,B)** Axial CT image 15.

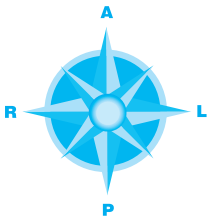
This section, taken below the liver, includes the lower part of the transverse colon next to the anterior abdominal wall. On the right side, the ascending colon is separated from the kidney by the peritoneum and the fat pad surrounding and protecting the kidney. Within the fat, the contrast-enhanced ureter is medial to the kidney. Between the kidneys, the inferior vena cava and abdominal aorta are sectioned behind the loops of small bowel. The loops of small bowel, the jejunum, are wrapped with mesentery, containing branches of the superior mesenteric vessels. As in previous images, the descending colon is near the left abdominal wall.



A



B



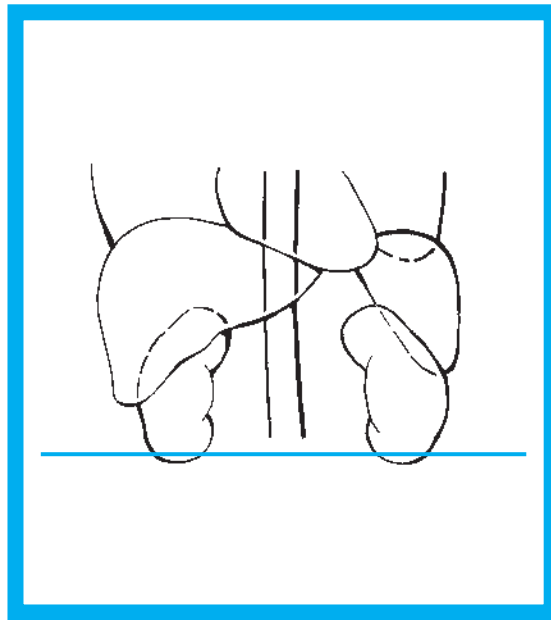
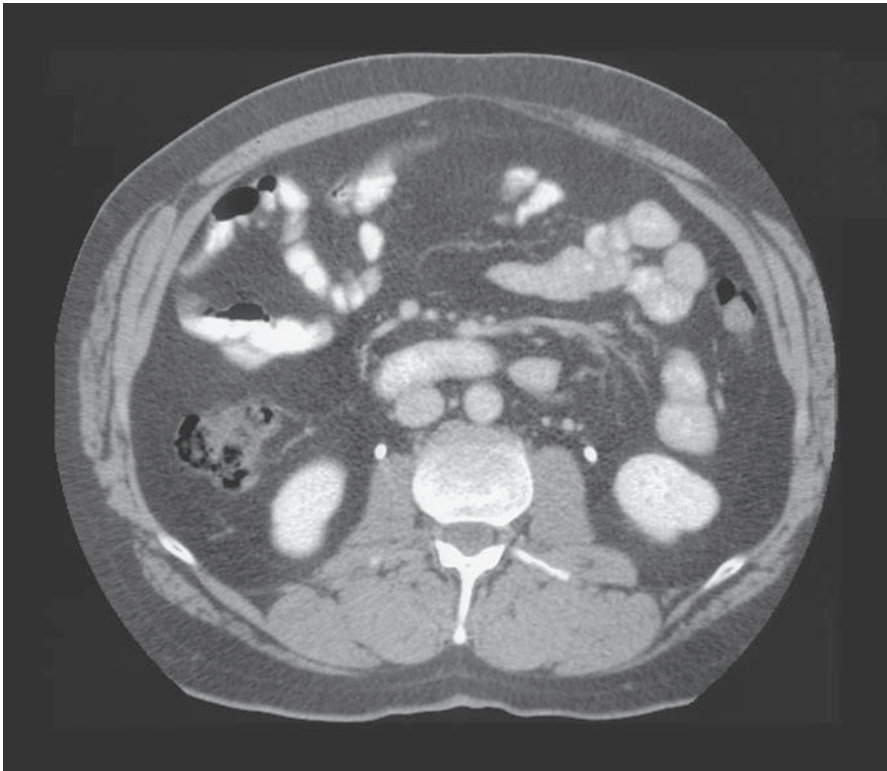
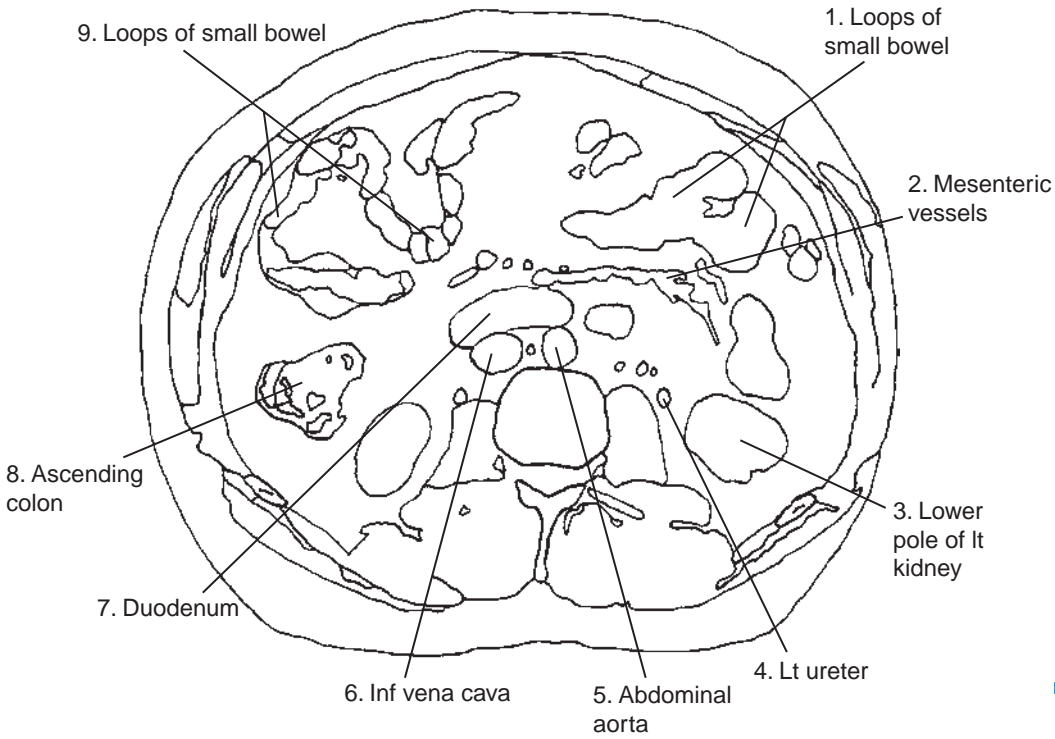


**Figure 3–33 (A,B)** Axial CT image 16.

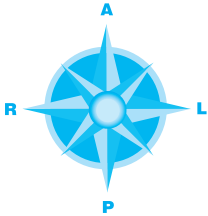
The contrast-filled loops of small bowel and mesenteric vessels are loosely organized in the anterior abdominal cavity, with the exception of the inferior duodenum. The lower part of the duodenum, found below the head of the pancreas, is fixed to the posterior abdominal wall by peritoneum because it lies posterior to the peritoneal cavity. In this retroperitoneal location, the duodenum is next to the inferior vena cava and the abdominal aorta. Similarly, the ascending colon, descending colon, and kidneys are located behind the peritoneum and are attached to the posterior abdominal wall.



A



B





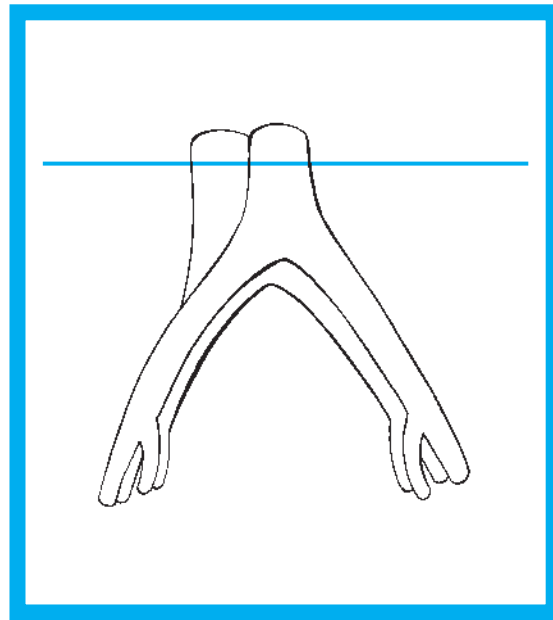
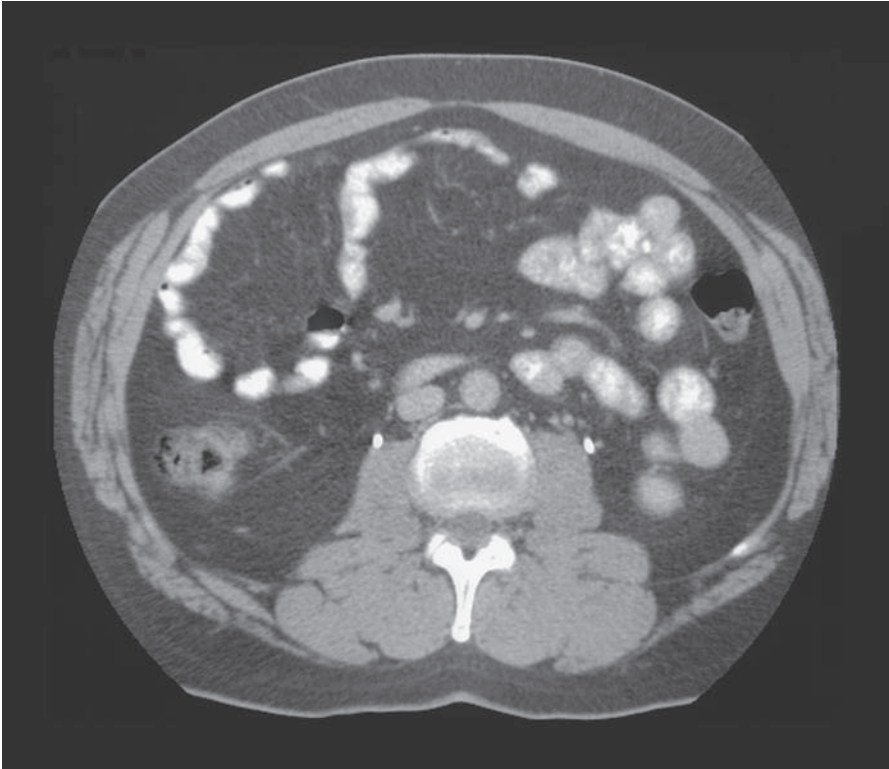
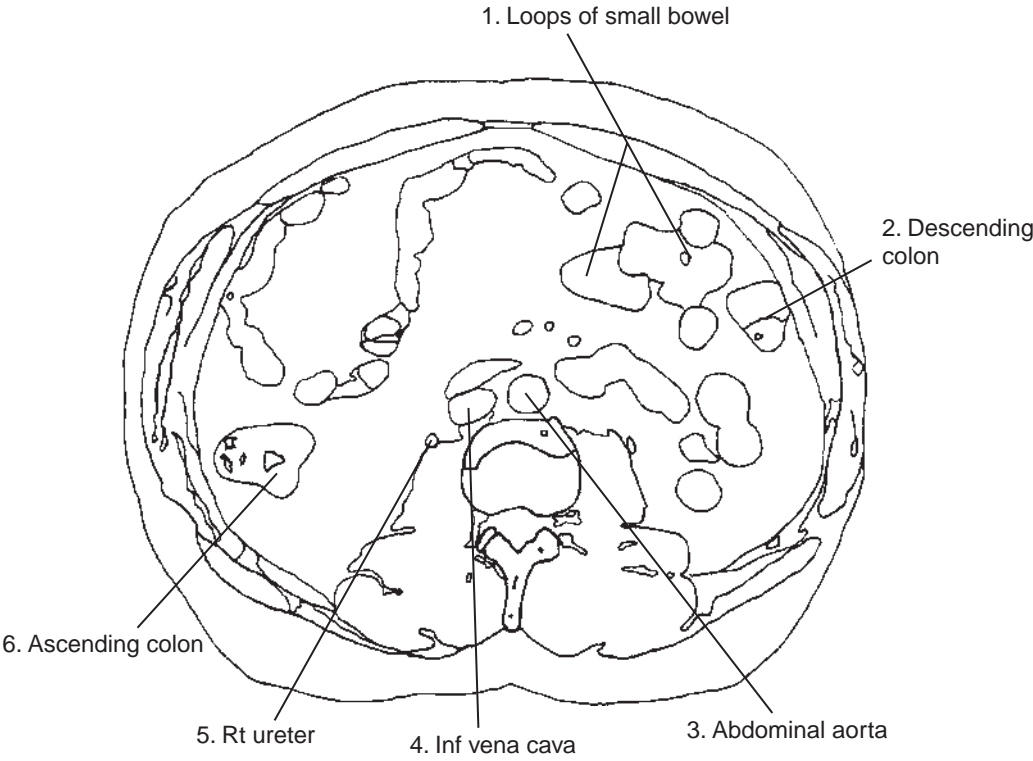


**Figure 3–34 (A,B)** Axial CT image 17.

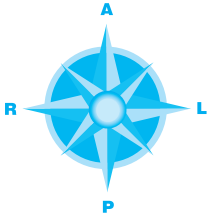
Similar to the previous image, this image shows the contrast-enhanced loops of the small bowel are loosely organized in the anterior abdominal cavity. The location and size can be used to distinguish the segments of small bowel from those of the nearby colon. By comparison, the ascending and descending colon are larger in diameter and are adjacent to the abdominal wall, because both segments are retroperitoneal. In the posterior abdomen, the inferior vena cava, the abdominal aorta, and the ureters are also found retroperitoneal.



A



B



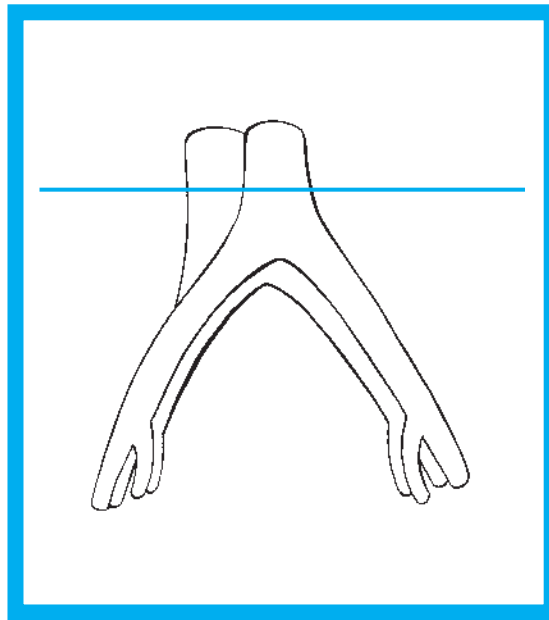
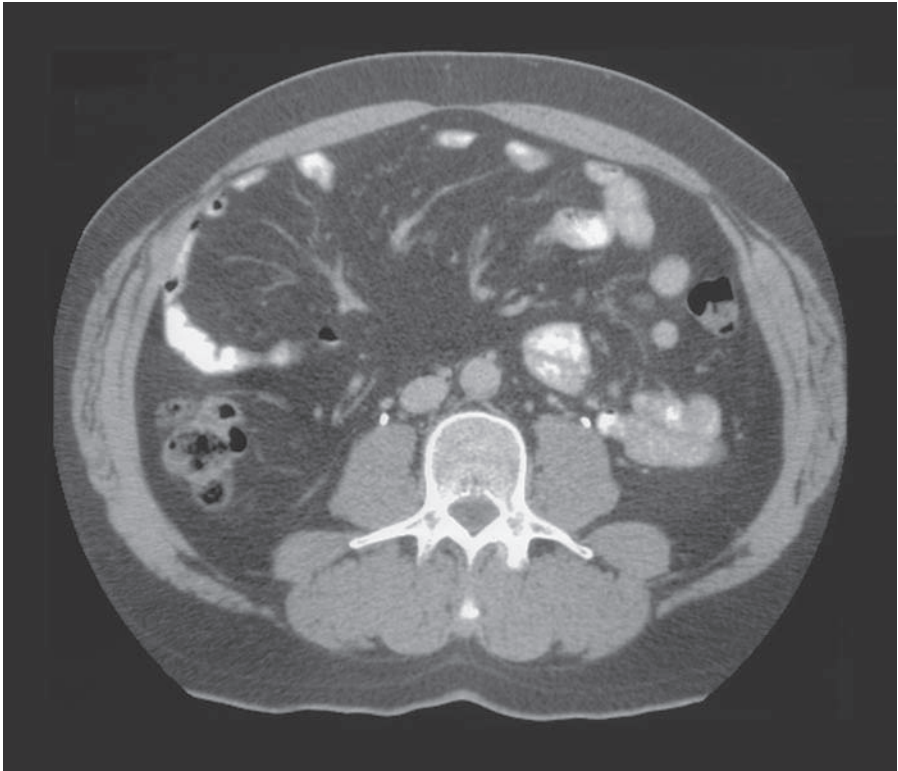
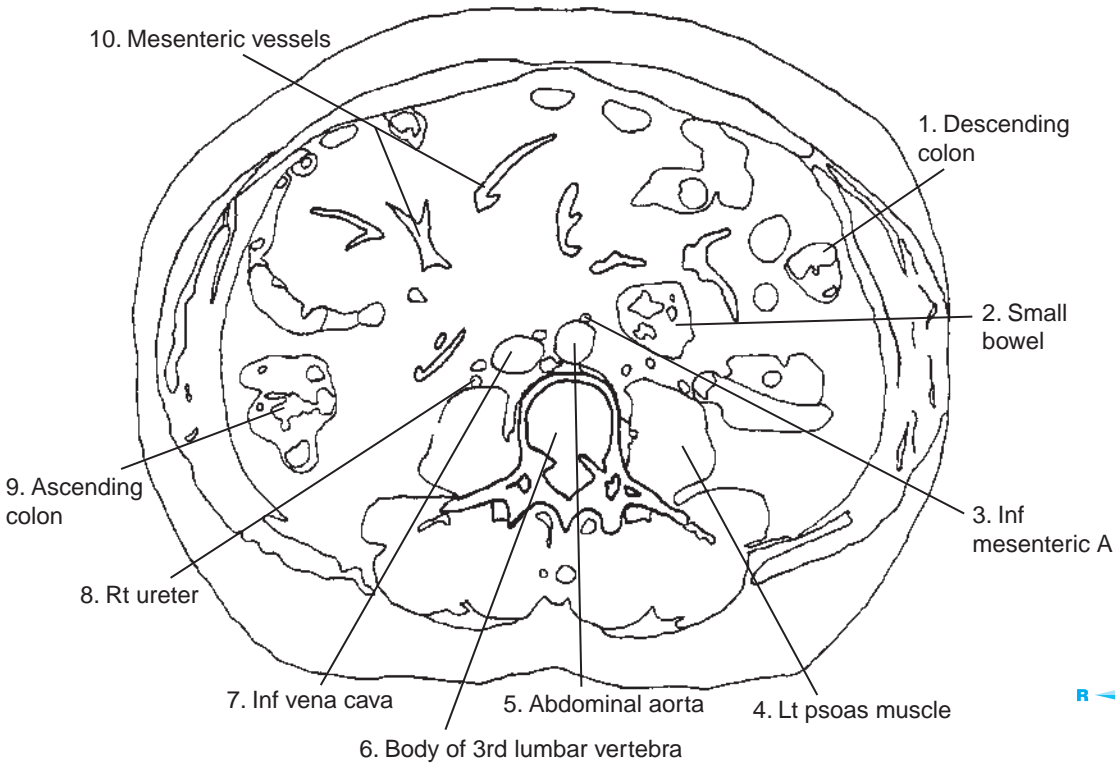


**Figure 3–35 (A,B)** Axial CT image 18.

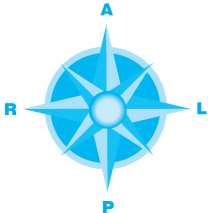
This section, below the level of the ribs, was taken through the level of the third lumbar vertebra. Because lumbar vertebrae are responsible for supporting much of the individual's weight, their bodies are larger than those of other vertebrae. On either side of the vertebral body, the psoas muscles are shown originating from the transverse processes of the lumbar vertebrae. On the anterior surface of the psoas muscles, the ureters appear as "bright spots," owing to contrast enhancement. Between the ureters, the inferior vena cava and the abdominal aorta are next to the vertebral body. Originating on the anterior surface of the abdominal aorta, the inferior mesenteric artery is sectioned as it descends to supply blood to the last half of the large intestine. Similar to the images just described, the ascending and descending parts of the colon are shown behind the peritoneum and mesentery surrounding the loosely organized small bowel.



A



B



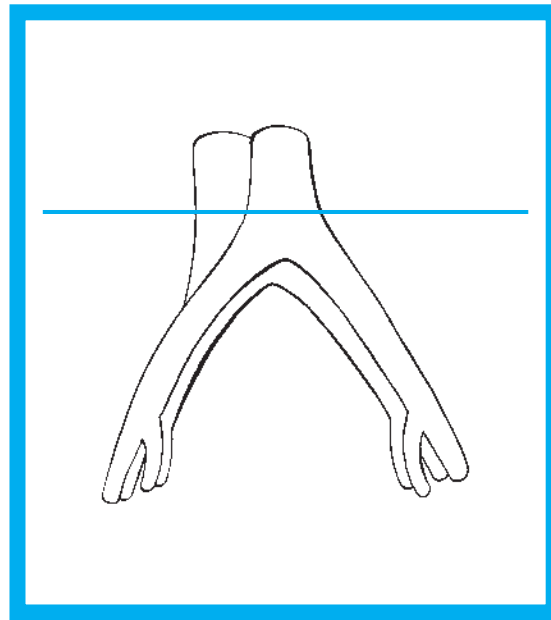
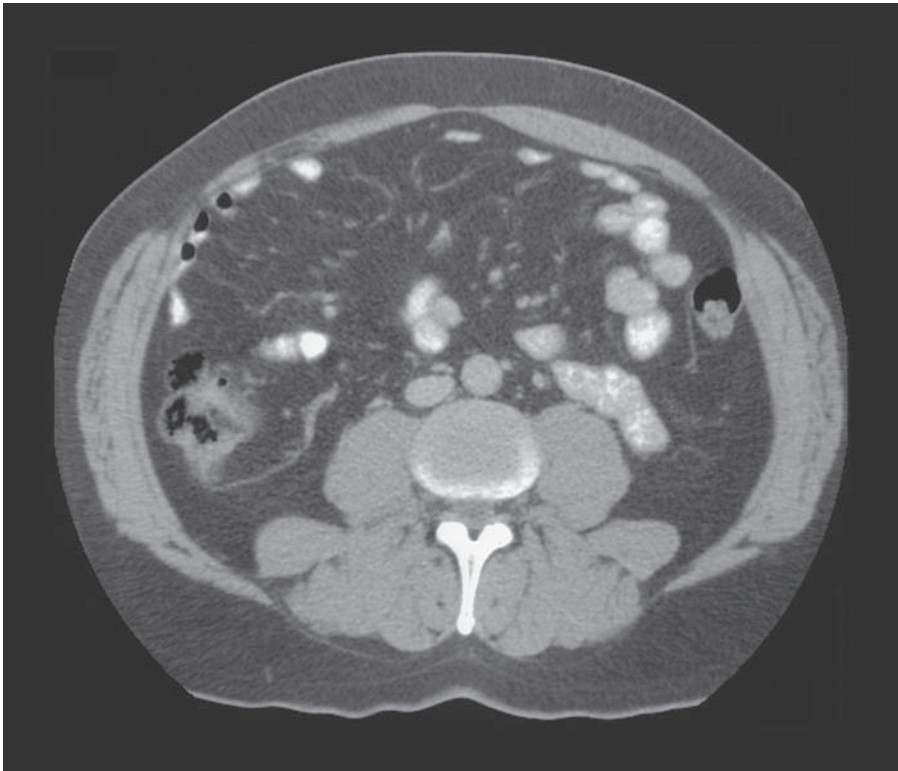
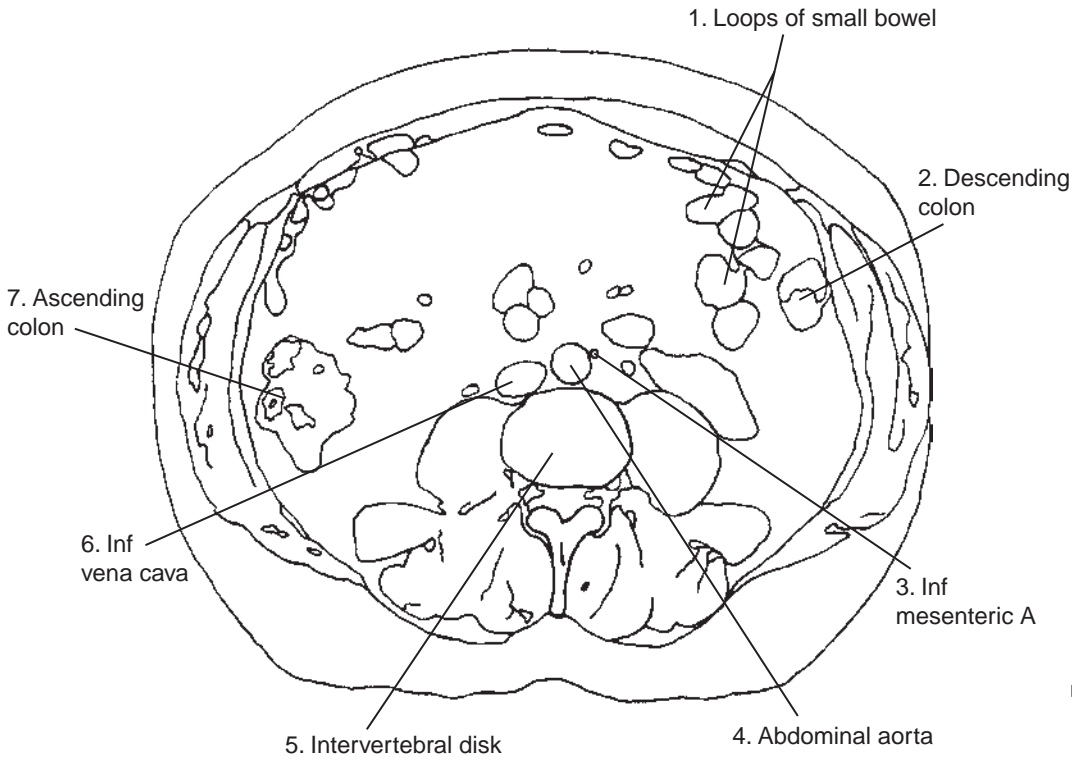


**Figure 3–36 (A,B)** Axial CT image 19.

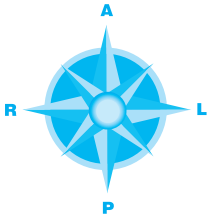
The ascending and descending segments of the colon are on either side of the centrally situated loops of small bowel. Behind the small bowel, the inferior vena cava and the abdominal aorta are sectioned in front of the intervertebral disk between L3 and L4. Unlike the previous image, which showed the inferior mesenteric artery directly anterior to the abdominal aorta, the vessel is now shown on the *left* side of the aorta as it travels toward the left half of the large intestine.



A



B



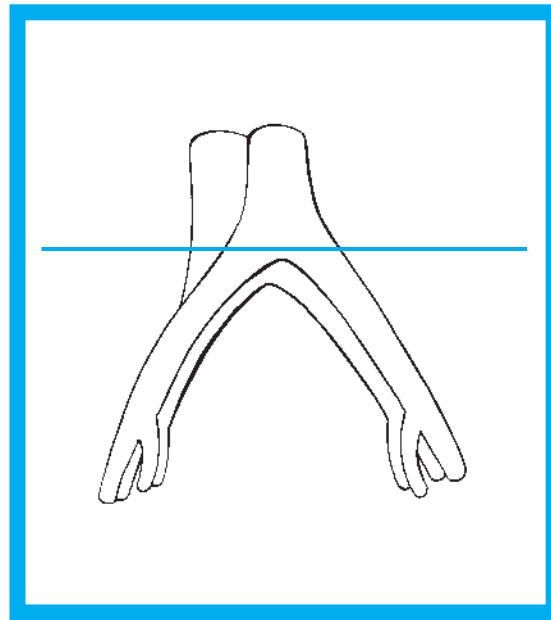
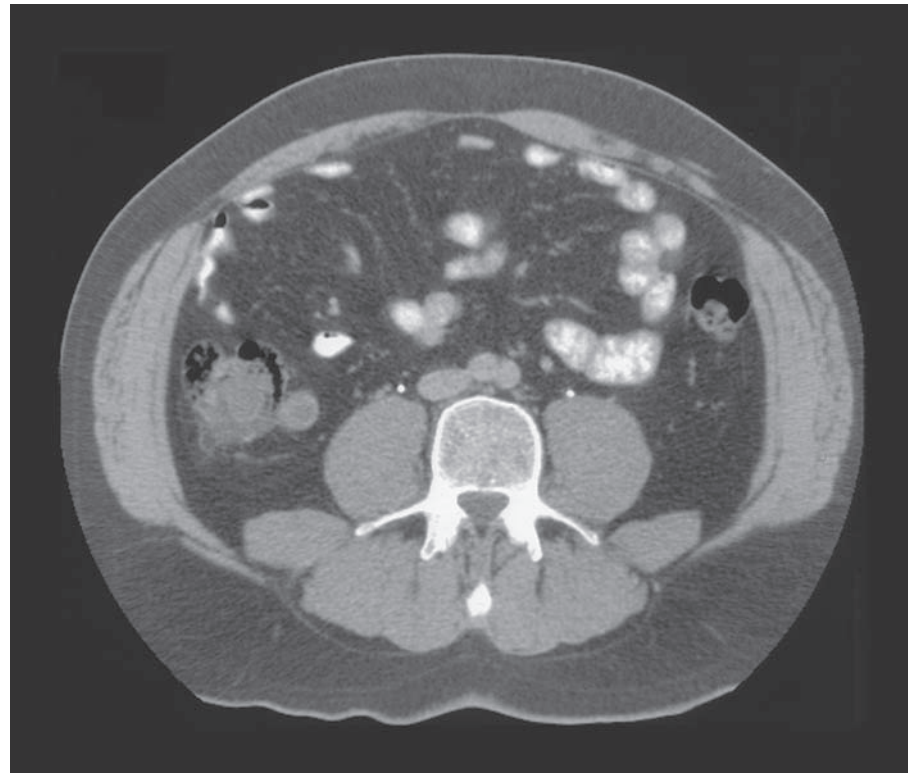
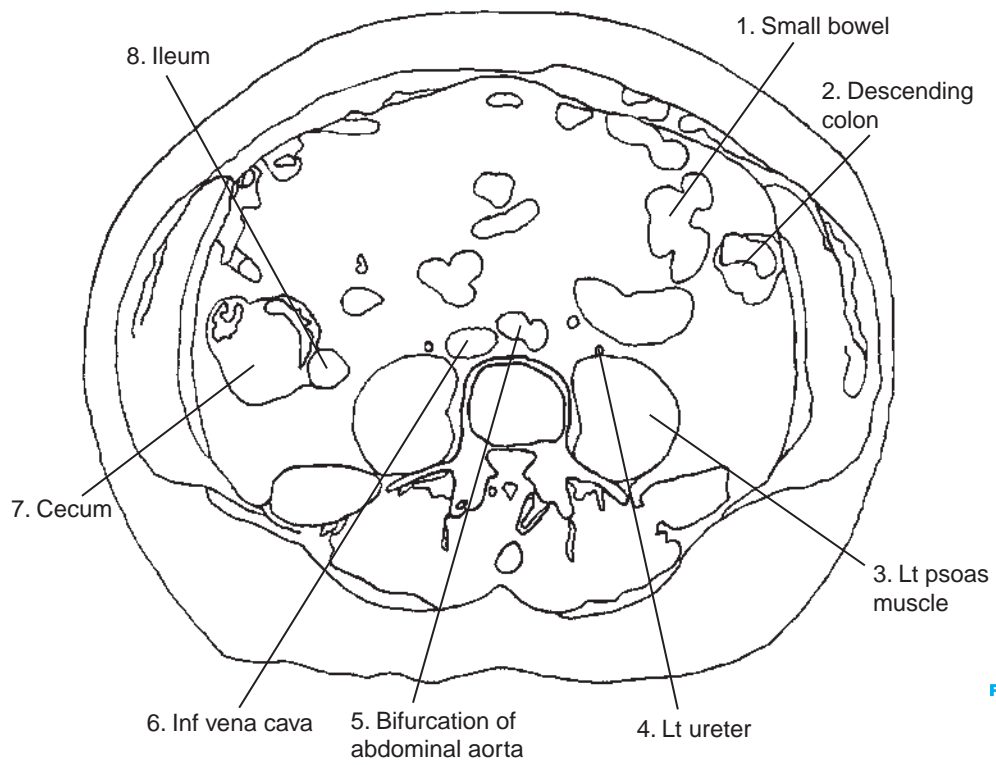


**Figure 3–37 (A,B)** Axial CT image 20.

This image shows the loops of small bowel as loosely organized in most of the anterior abdominal cavity. Even though the descending colon is still on the left side, the cecum is now found in the position previously occupied by the ascending colon. Beside the cecum, the ileum is sectioned near the terminal end of the small bowel. In the posterior abdomen, the inferior vena cava is still found on the right. The abdominal aorta, however, is splitting into two vessels, the right and left common iliac arteries. Lateral to the vessels, the contrast-filled ureters are lying on the anterior surfaces of the psoas muscles.



A



B



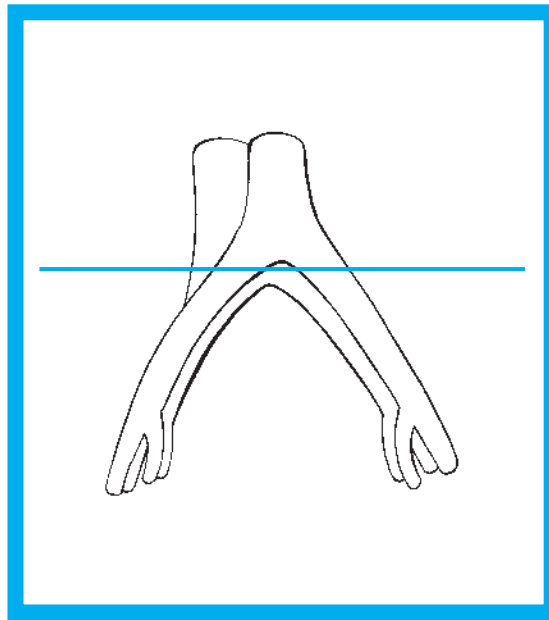
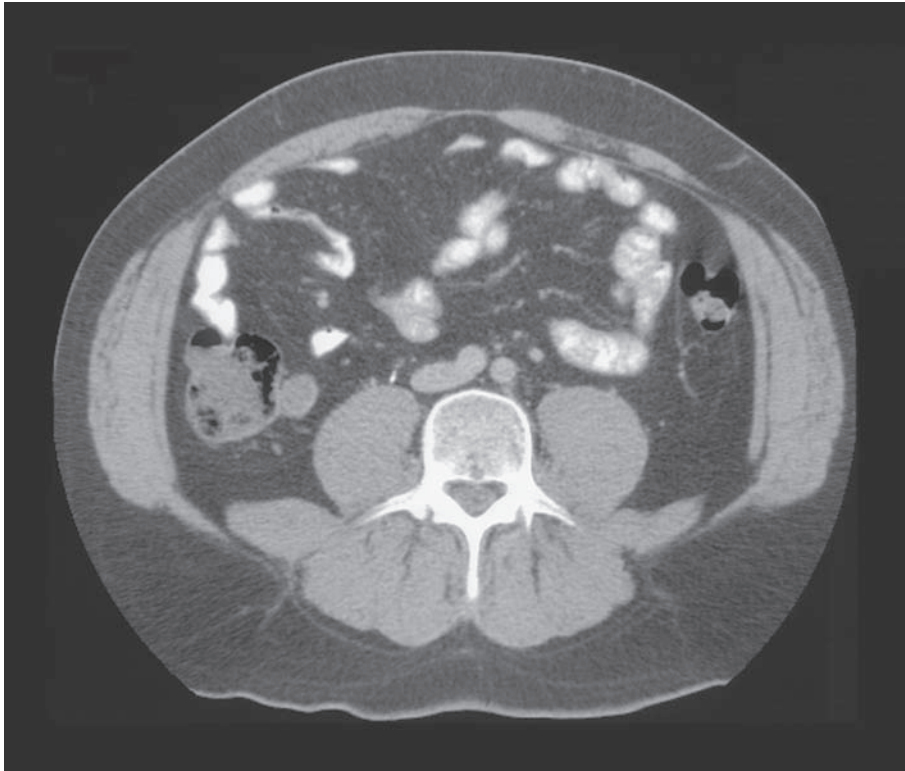
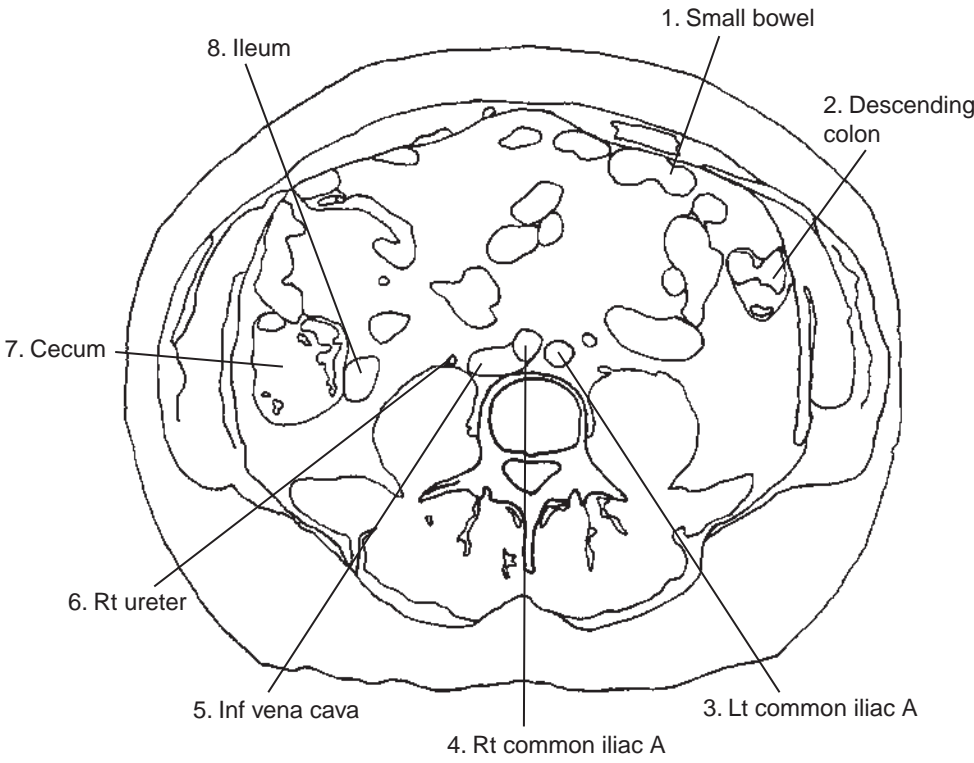


**Figure 3–38 (A,B)** Axial CT image 21.

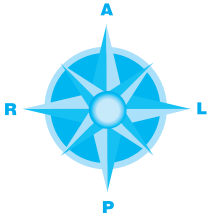
The contrast-filled small bowel occupies most of the anterior abdomen, with large intestine on either side. By comparison, the large intestine can be distinguished from the small bowel by the larger diameter and location beside the abdominal wall. Although most of the small bowel is filled with contrast in this patient, the cross-section through the distal ileum shows it to be filled with fecal material and to be considerably smaller than the adjacent cecum. Behind the peritoneal cavity, three vessels are now distinguishable in front of the vertebral body. The inferior vena cava is on the right, and the right and left common iliac arteries are on the left, because they merge to form the origin of the abdominal aorta.



A



B



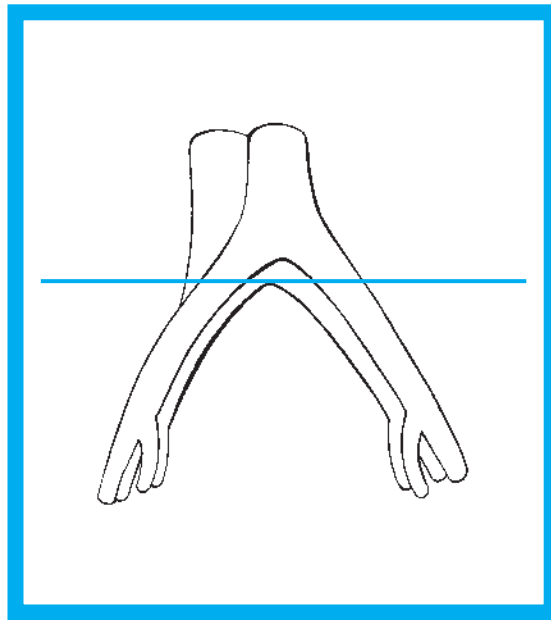
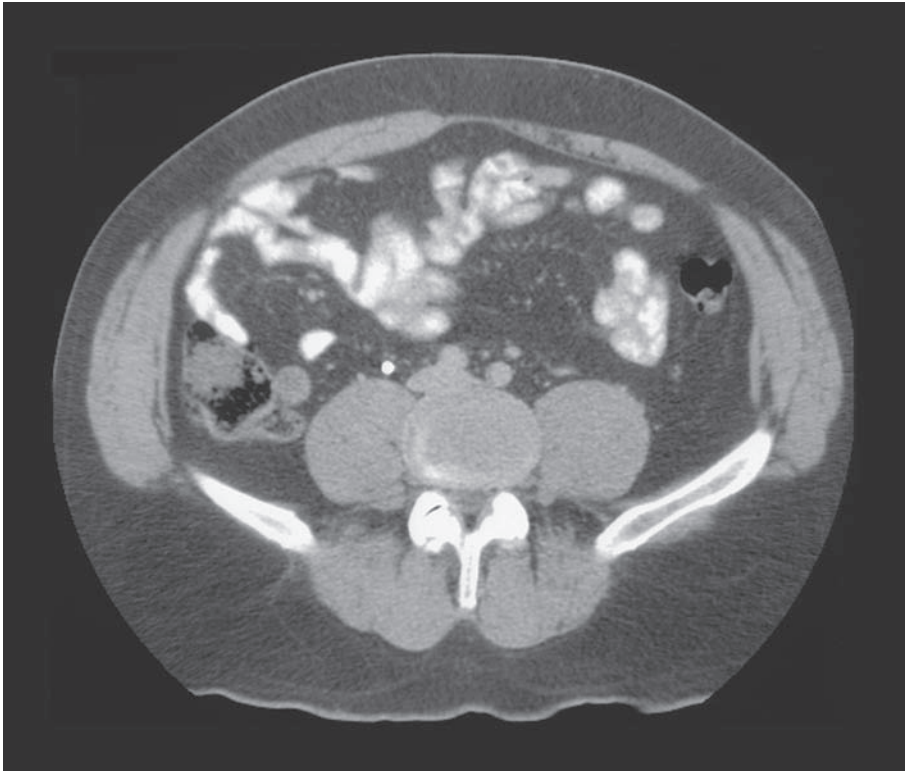
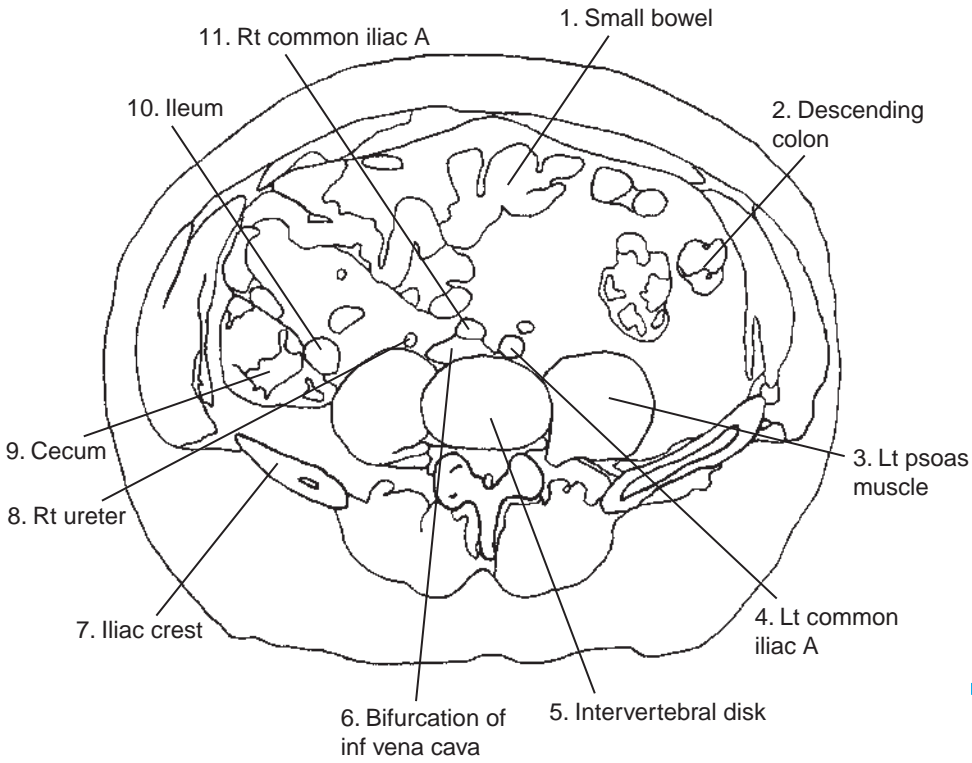


**Figure 3–39 (A,B)** Axial CT image 22.

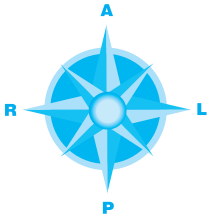
The iliac crest is sectioned on either side of the vertebral column at the level of the intervertebral disk between L4 and L5. On both sides of the intervertebral disk, the large psoas muscles form much of the remaining posterior abdominal wall. Adjacent to the posterior wall, the inferior vena cava appears flattened and is shown bifurcating into the right and left common iliac veins. Compared to the previous image, the right and left common iliac arteries have diverged, and the right common iliac artery lies in front of the inferior vena cava. Similar to previous images, the large intestine is near the abdominal wall on either side of the small bowel, which occupies most of the peritoneal cavity.



A



B



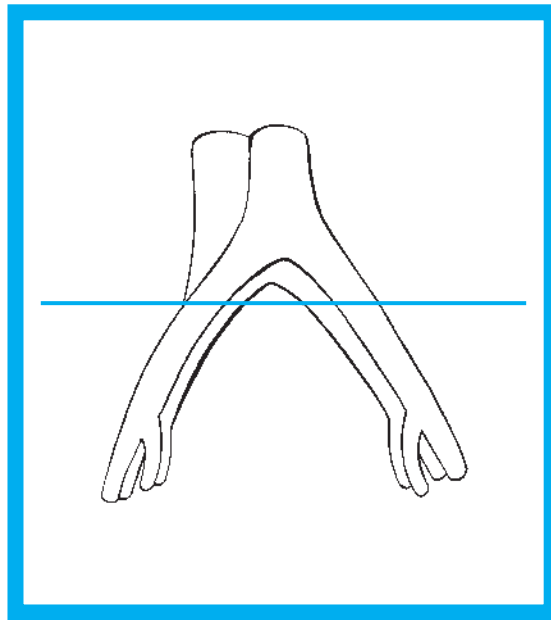
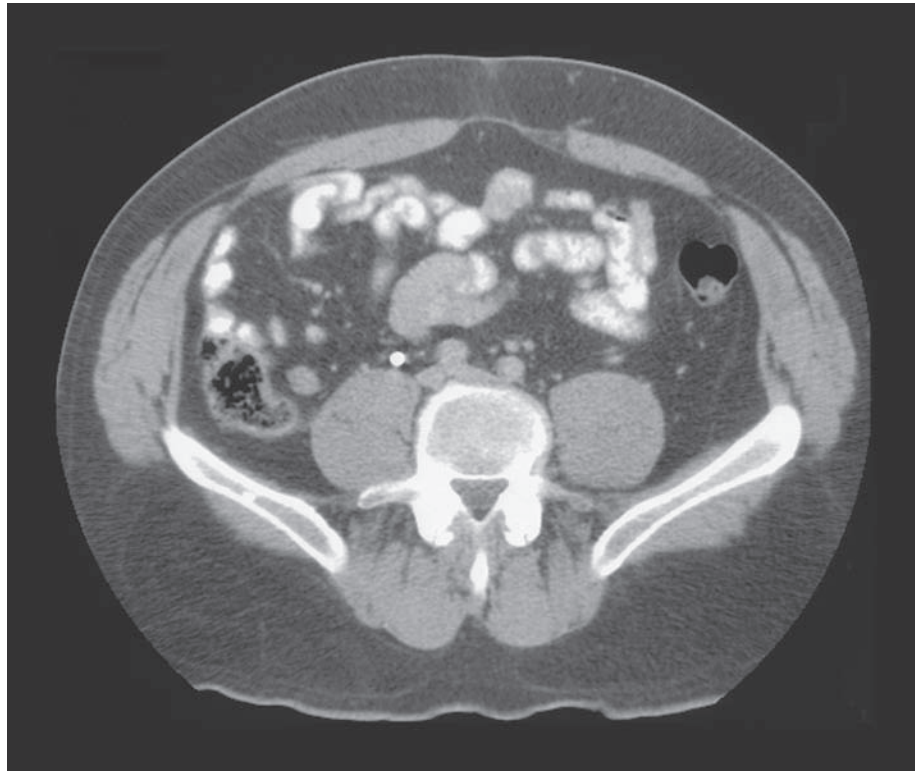
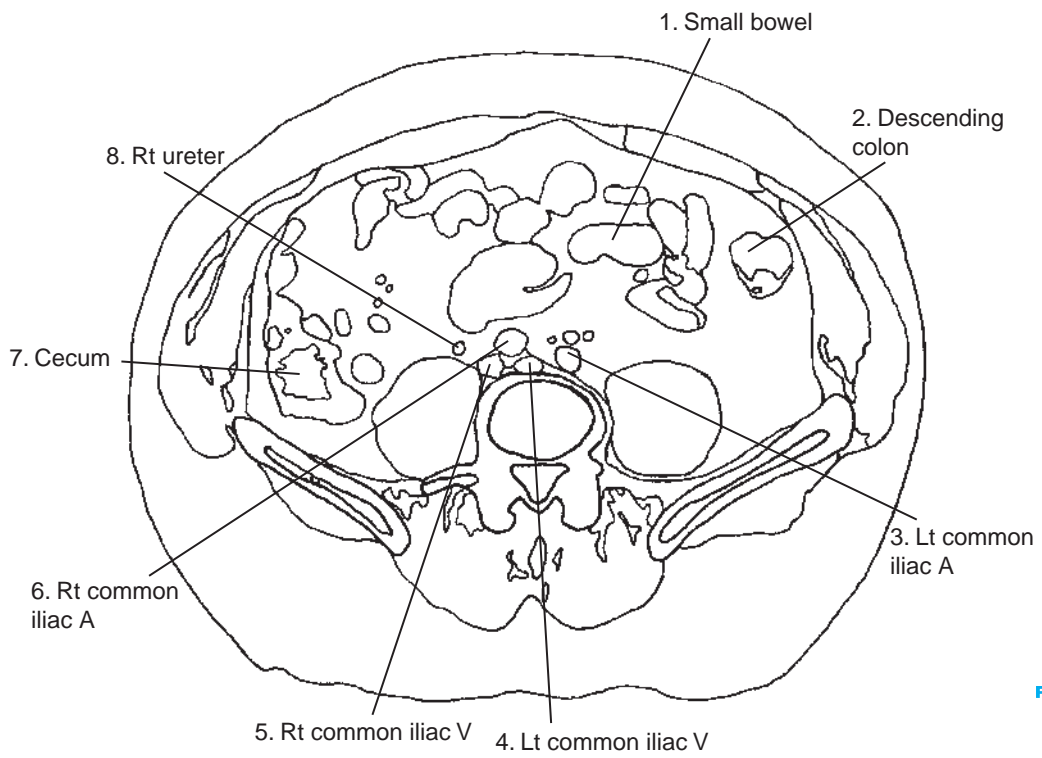


**Figure 3–40 (A,B)** Axial CT image 23.

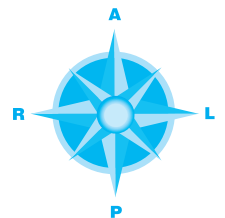
Due to the proximity of the iliac crests to the vertebral body, this section is through the lower abdomen at the level of the L5 vertebra. In this image, four vessels can be distinguished in front of the vertebral body and can be labeled as the right and left common iliac arteries and veins. In the last section, the right common iliac artery was in front of the inferior vena cava. Consequently, the right and left common iliac arteries are more anteriorly situated than the corresponding veins, which are adjacent to the vertebral body of L5. In the anterior abdominal cavity, loops of small bowel are found separating the descending colon and the cecum.



A



B



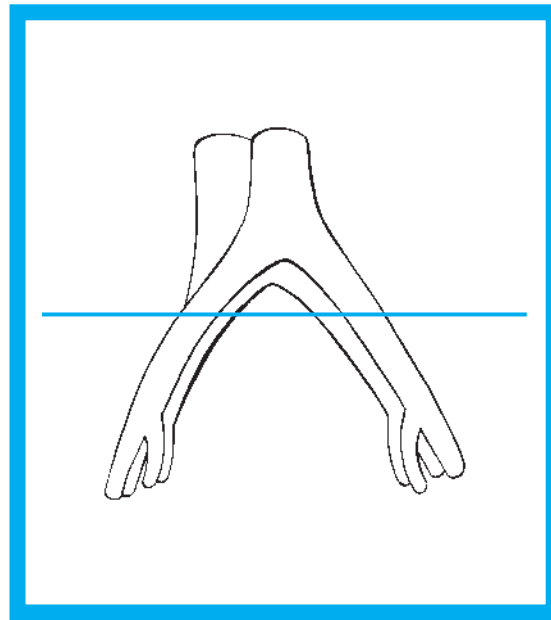
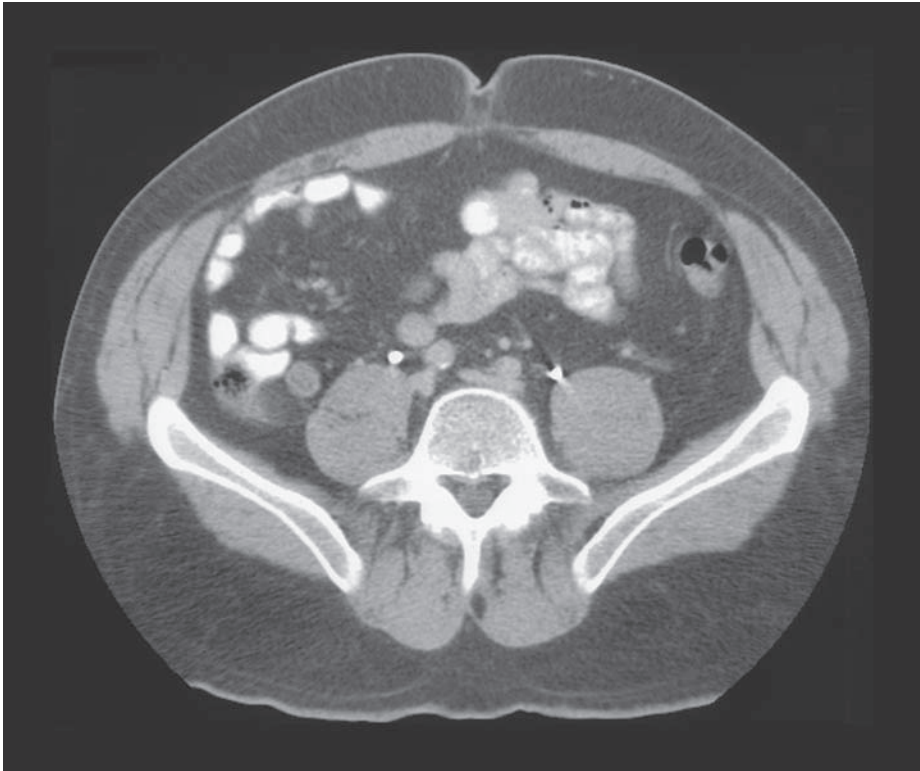
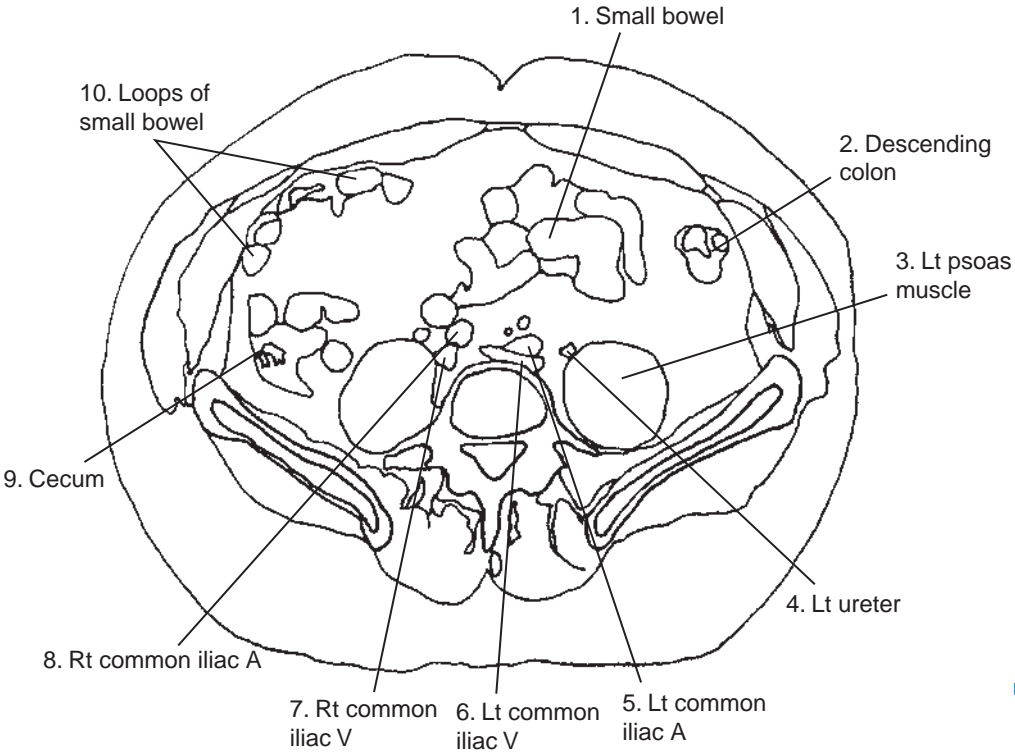


**Figure 3-41 (A,B)** Axial CT image 24.

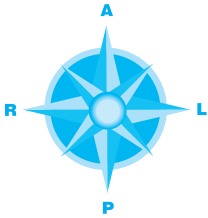
The iliac bones are separate from the vertebral body, indicating the level of the section to be above the sacrum. The round psoas muscles located on either side of the L5 vertebral body are posterior to the contrast-enhanced ureters. Between the ureters, the four vessels have diverged and paired on either side. As seen above, the right and left common iliac arteries are in front of the corresponding veins. Anteriorly, the small bowel fills most of the central abdominal cavity. Because the section is within the greater pelvis, this part of the small bowel would most likely be the ileum. On either side of the small bowel, the retroperitoneal cecum and descending colon are shown next to the abdominal wall.



A



B







## Case Study 3-1

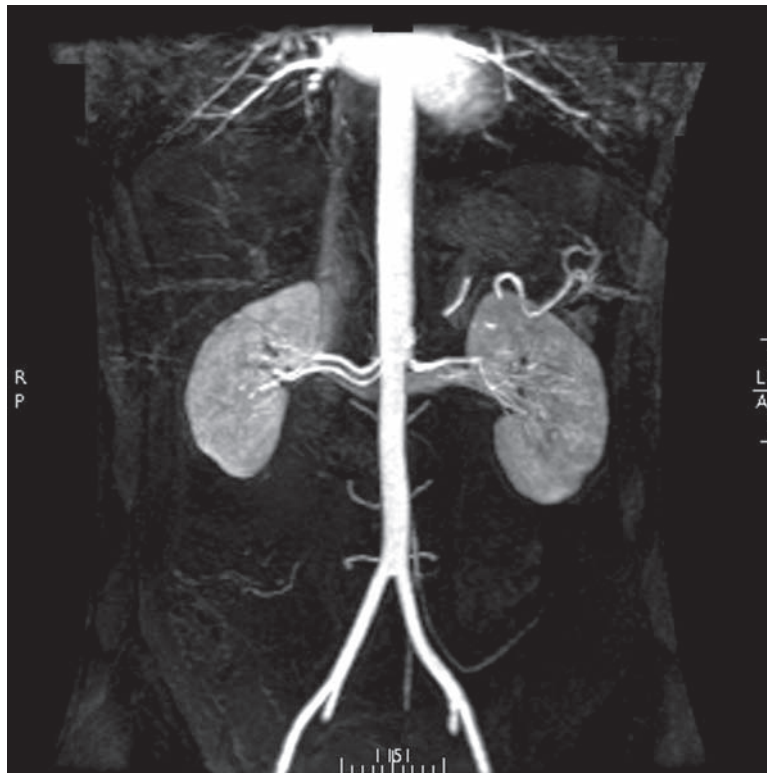


Figure 3–42

### Clinical Correlations

This 42-year-old man had a magnetic resonance angiograph (MRA) examination to evaluate his renal arterial blood flow with a history of high blood pressure. During the procedure, the patient received a bolus injection of contrast (gadolinium); information generated from the axial images is reassembled by computer into a three-dimensional picture of the area being studied. The contrast enhancement or normal blood flow can clearly be seen in the abdominal aorta and extending into the right and left common iliac

arteries. On the right side of the patient, there are two renal arteries feeding the kidney, which is a common anomaly, and is not considered a pathology because there is good blood flow to the right kidney. On the left side, the kidney is supplied with a single renal artery, and the kidney has less contrast enhancement as compared to the right. As the left renal artery appears normal, a high degree of stenosis was reported in several branches of the left renal artery.

### Questions

1. Where are the kidneys found within the abdomen? Are they surrounded by peritoneum?
2. Which of the renal arteries is usually slightly longer?
3. In the image above, the tortuous segment shown extending above the left kidney would be part of what artery?
4. Does the right or left renal artery pass behind the inferior vena cava?
5. What are the small endocrine glands found just superior to each kidney?



## Case Study 3-2



**Figure 3–43**

This 46-year-old man had a magnetic resonance angiograph (MRA) examination to evaluate the arterial flow to his renal transplant in the lower right quadrant of the abdomen. In this three-dimensional reconstructed image, the contrast is easily seen within the abdominal aorta extending into both

the right and left common iliac arteries. On the right common iliac artery, a renal branch is shown extending to the kidney with good flow being apparent in the transplanted organ. Within the kidney, the arterial blood flow appears stronger in the lower pole than in the upper pole.

### Questions

1. In a typical patient, what is the name of the large gland found just below the right diaphragm that has an impression from the upper pole of the right kidney?
2. Describe the location of the abdominal or descending aorta.
3. In a typical patient, would the right renal artery or vein be located more anteriorly?
4. Describe the function of the kidney.
5. In a typical patient, what is the name of the gland found next to the posterior abdominal wall that has an impression from the upper pole of the left kidney?



## Case Study 3-3

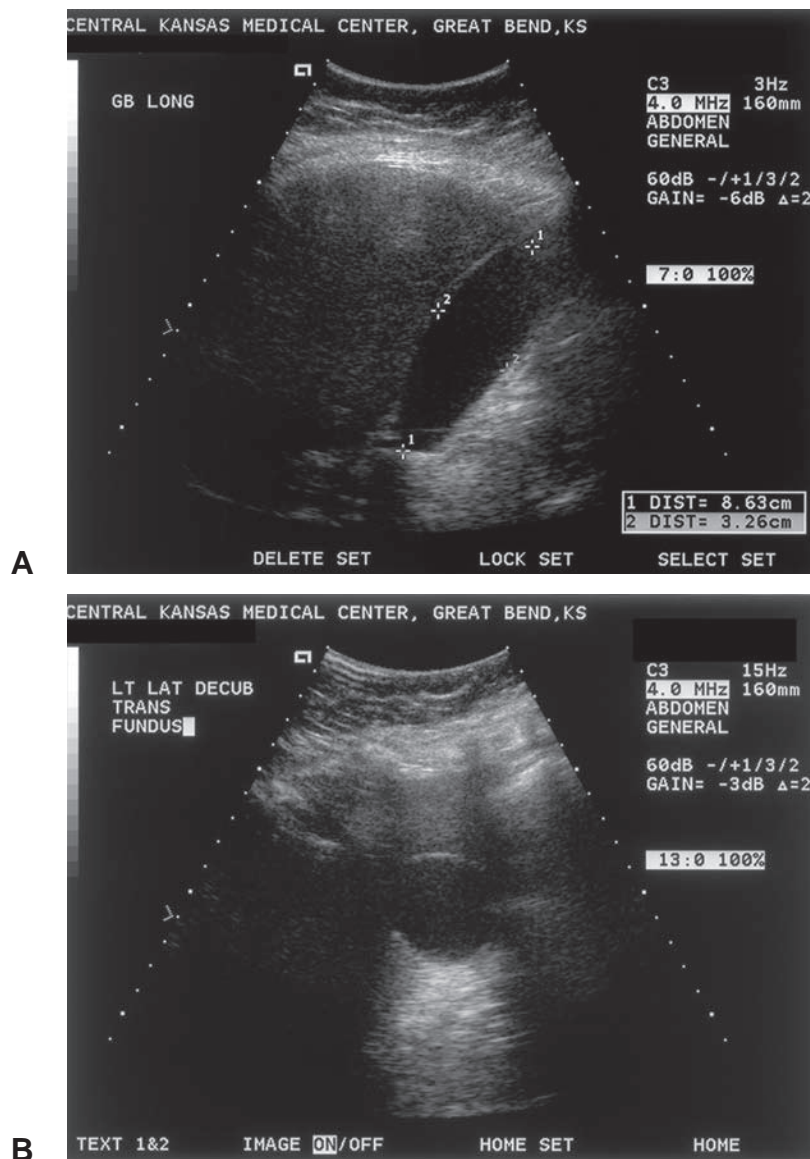


**Figure 3–44**

This 61-year-old woman was referred for an ultrasound examination of the gallbladder due to her history of abdominal pain in the right upper quadrant of the abdomen. Although the patient was being evaluated for cholelithiasis (presence of concretions in the gallbladder or bile ducts), the examination revealed that the gallbladder and biliary system were normal. The wall of the gallbladder can be

readily identified as outlined with measuring marks in the longitudinal image. In the transverse image, the gallbladder is the oval-shaped, fluid-filled structure located near the center of the image. In both planes, the gallbladder appears to be completely filled with fluid (sonolucent) providing a well-defined border with the surrounding tissue.

## Questions

1. Describe the location of the gallbladder.
2. What is the function of the gallbladder?
3. The common bile duct is formed by the joining of which two ducts?
4. Is the common bile duct located anterior or posterior to the duodenum?
5. Which lobe of the liver is found between the gallbladder and the ligamentum teres?



## Case Study 3-4

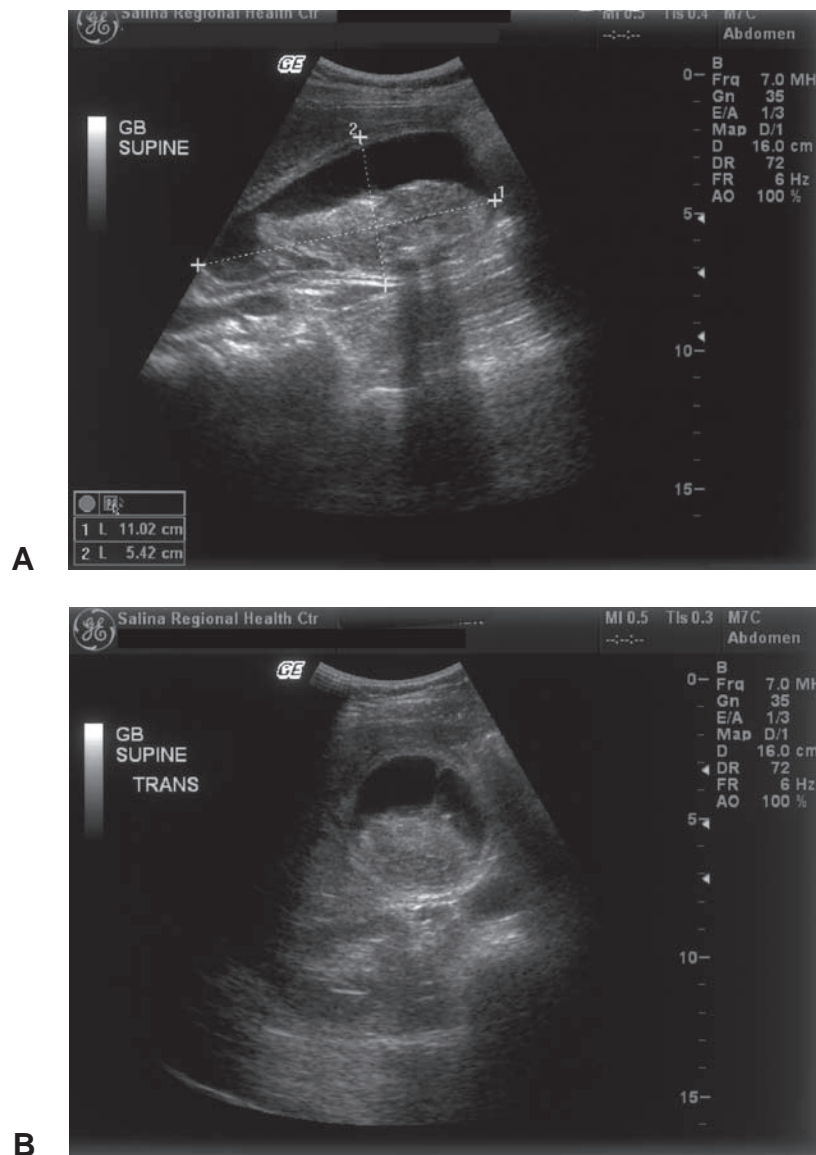


**Figure 3-45**

This 26-year-old woman was referred for an ultrasound examination of the gallbladder due to a history of abdominal pain in the upper abdomen. Much like the previous case, the wall of the gallbladder is outlined by the measuring marks in the longitudinal image. Similarly, the large, oval-shaped structure located near the center of the transverse image is the gallbladder. However, in this patient the gallbladder is only partly filled with fluid because a mass is shown causing a

filling defect within the lumen of the gallbladder. Following this examination, the patient had a cholecystectomy (surgical removal of the gallbladder), and the mass was determined to be a carcinoma. Fortunately, most gallbladder carcinoma found early is limited to the gallbladder and will only grow through the wall of the gallbladder in later stages. The carcinoma originates from the gallbladder wall and is most prevalent in chronic cases of cholelithiasis (gallstones).

## Questions

1. The common bile duct joins with which duct before it empties into the duodenum?
2. Describe the structures found within the porta hepatis.
3. Explain how the structures seen on the visceral surface of the liver may be described as forming an H-shape.
4. Which gland is found just below the stomach and contains the terminal end of the common bile duct ending in the proximal duodenum?
5. Describe the branch of the abdominal aorta that provides blood to the gallbladder, liver, and stomach.



## Case Study 3-5

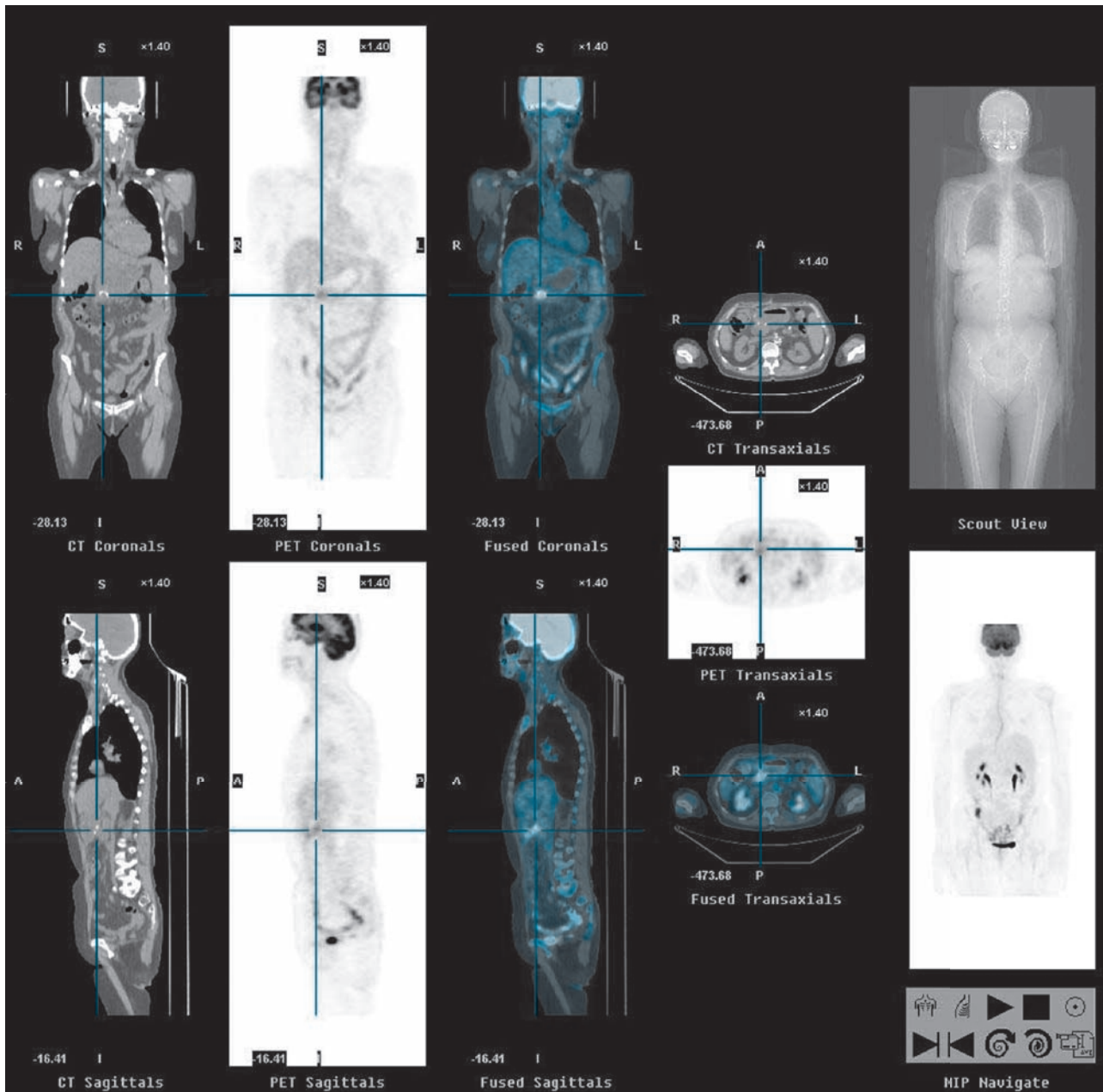


Figure 3-46



This positron emission tomography/computed tomography (PET/CT) case is a 59-year-old white woman previously diagnosed with stomach carcinoma. Before the procedure, the patient received a single IV dose of 15.78 mCi of F-18 FDG for this examination. The PET/CT study was conducted to more accurately stage the stomach carcinoma. At

the time of this study, abnormal uptake was limited to the pyloric part of the stomach, and there was no clear evidence of metastatic disease. The strong signal shown within the brain and urinary collecting system were within normal limits due to the high concentration of glucose or glucose byproducts in these parts of the body.

## Questions

1. Describe the location of the stomach, and include relationships with adjacent organs.
2. What are the parts of the stomach from superior to inferior?
3. In the typical patient, will the lower part of the stomach be directed toward the right or left side?
4. Briefly describe the parts of the small intestine from first to last, and include the general location of each segment.
5. In an axial section through the lower stomach, what part of the intestine would be located closest to the left posterior abdominal wall?





## Case Study 3-6

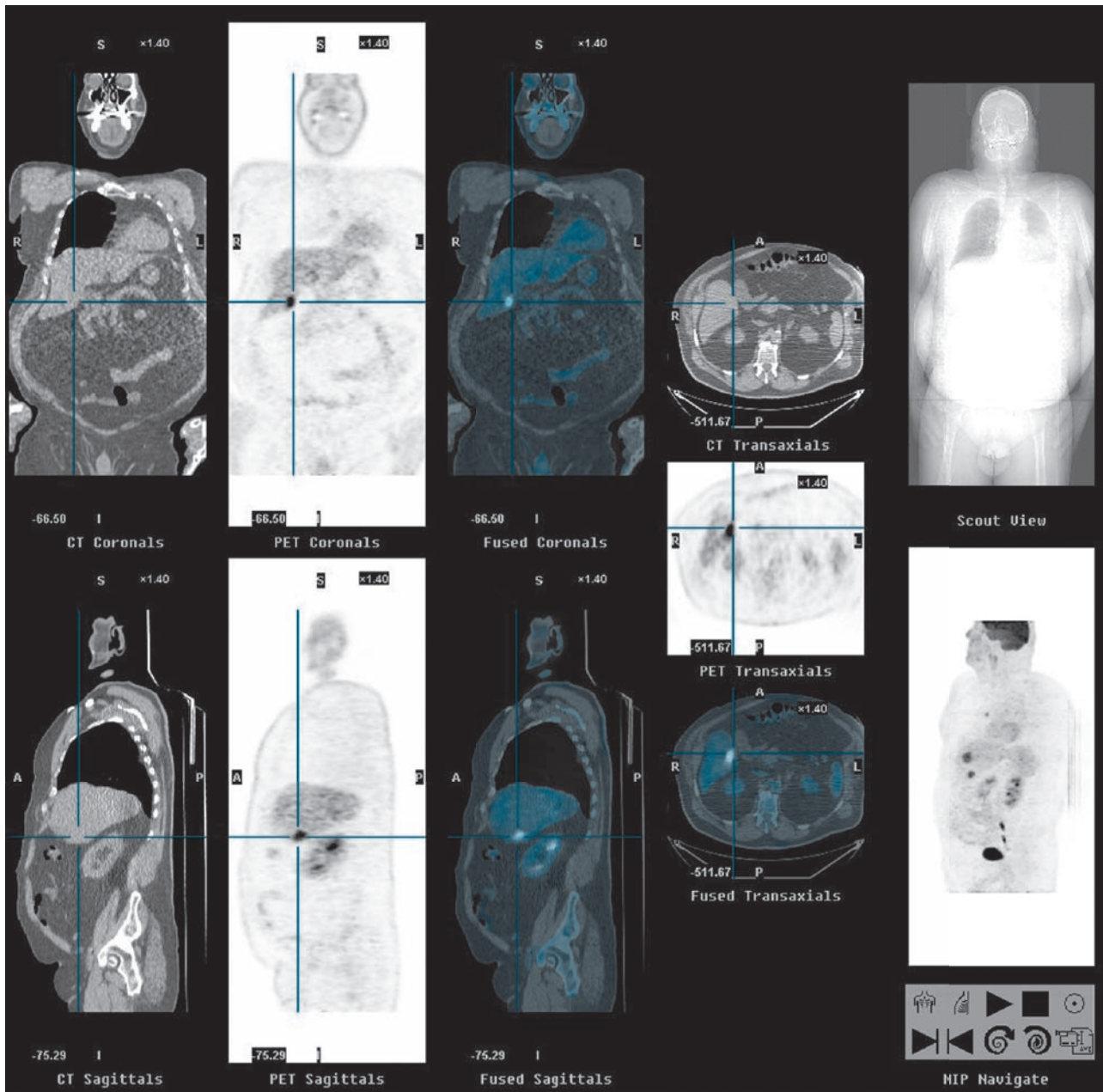


Figure 3-47

This positron emission tomography/computed tomography (PET/CT) case is a 65-year-old white man previously diagnosed with colorectal carcinoma. Before the procedure, the patient received a single IV dose of 12.27 mCi of F-18 FDG for this examination. The PET/CT study was conducted to more accurately stage a previously diagnosed colorectal carcinoma. At the time of this study,

abnormal uptake was clearly shown within the liver consistent with metastatic disease. Metastatic disease frequently is found within the liver because this organ receives all of the portal flow from the alimentary tract. The strong signal from the brain and urinary collecting system (kidneys, ureters, and bladder) were found to be within normal levels.

### Questions

1. Describe the two large veins that join together to form the major branches of the portal vein.
2. Briefly describe the function of the portal venous system.
3. Which part of the pancreas is found anterior to the portal vein?
4. Which part of the pancreas is found closest to the duodenum?
5. Which branch of the abdominal aorta vessel provides arterial blood for the sigmoid colon?



## CLINICAL APPLICATIONS

1. In an axial section through the hilum of the kidneys, which of the following would be most anterior: The right renal artery or the right renal vein?
2. Describe the location of the spleen and its relationship with adjacent structures.
3. List the three major structures found within the porta hepatis.
4. On the visceral surface of the liver, which lobe is located most posteriorly: Caudate or quadrate?
5. List, in order (from superior to inferior), the major branches of the abdominal aorta.
6. Which of the following structures is located most posteriorly as it passes through the diaphragm?
  - A. Esophagus
  - B. Inferior vena cava
  - C. Celiac trunk
  - D. Descending aorta
7. The \_\_\_\_\_ lies just below the anterior surface of the liver and the tapered end points toward the porta hepatis.
8. The smooth connective tissue membrane covering the viscera within the abdomen is called the \_\_\_\_\_, and the \_\_\_\_\_ is found lining the abdominal cavity.
9. Compared to the abdominal aorta, is the inferior vena cava on the right or left side of the abdominal aorta?
10. The \_\_\_\_\_ vein drains nutrient-rich blood from the rectum, sigmoid colon, and ascending colon to the \_\_\_\_\_ vein.

## Chapter 4

# Male and Female Pelvis

## OBJECTIVES

Upon completion of this chapter, the student should be able to:

1. Describe the boundaries of the greater and lesser parts of the pelvis.
2. Describe the three bones making up the pelvic girdle.
3. Identify the contents of the lower abdominal cavity found within the greater pelvic space.
4. Describe the pelvic peritoneum separating the contents of the abdominal cavity from the other structures within the greater pelvic cavity.
5. Correctly identify the major vessels on sectional images.
6. Identify and describe the alimentary structures within the pelvis.
7. Follow the course of urine as it passes through the pelvis.
8. Describe the major genitourinary structures in the male pelvis.
9. Describe the major genitourinary structures in the female pelvis.
10. Correctly identify anatomic structures on patient axial and coronal images of the pelvis.

## ANATOMIC OVERVIEW

The term *pelvis*, meaning “basin,” describes the irregularly shaped opening created by the two hip bones, the sacrum, and the coccyx (Fig. 4-1 A,B). The pelvis is a skeletal feature that differs markedly between men and women. The female pelvis is typically wider because the alae or wings of the ilia are more open.

The opening within the pelvis is often separated into greater and lesser segments, sometimes called the false and true pelves, by an oblique plane at the pelvic inlet. The inlet is a flat plane extending from the sacral promontory to the superior border of the pubic symphysis and the middle of the pelvic brim. Above the pelvic inlet, the greater pelvic space or false pelvis is irregular in shape; and the boundaries are formed posteriorly by the lower lumbar vertebrae, laterally by the alae or wings of the ilia, and anteriorly by the anterior abdominal wall. Below the pelvic inlet, the lesser or true pelvis is the short, curved pelvic space located within the bony pelvis. The size and shape of this space are of great importance in birthing, because the newborn must pass through this space in vaginal deliveries. In general, the functions of the pelvis are to transmit the

weight of the upper body to the lower limbs and to form the lower part of the abdominal cavity.

### ■ Skeleton

**Pelvic girdle.** Also called the innominate (*i-NOM-i-nāt*). A large, irregularly shaped bone with a centrally located socket, the acetabulum (*as-ĕ-TAB-yū-lŭm*), for articulation with the head of the femur (Fig. 4-2). It is divided into three parts—ilium, pubis, and ischium—which are connected by cartilage in the young and are fused in the adult.

**Ilium** (*IL-ĕ-ŭm*). Forms the upper part of the pelvic girdle. The most superior edge, the iliac crest, can easily be palpated along the lateral side. If the iliac crest is followed anteriorly, the termination (the anterior superior iliac spine) can also be felt on the anterior aspect of the hip. Below the superior spine is a second, less prominent, spine (the anterior inferior iliac spine), which also extends from the anterior margin of the ilium. Similarly, on the posterior ilium, the iliac crest ends at the posterior superior iliac spine, and the posterior inferior iliac spine extends more inferiorly. Between the iliac spines, the central wing-shaped

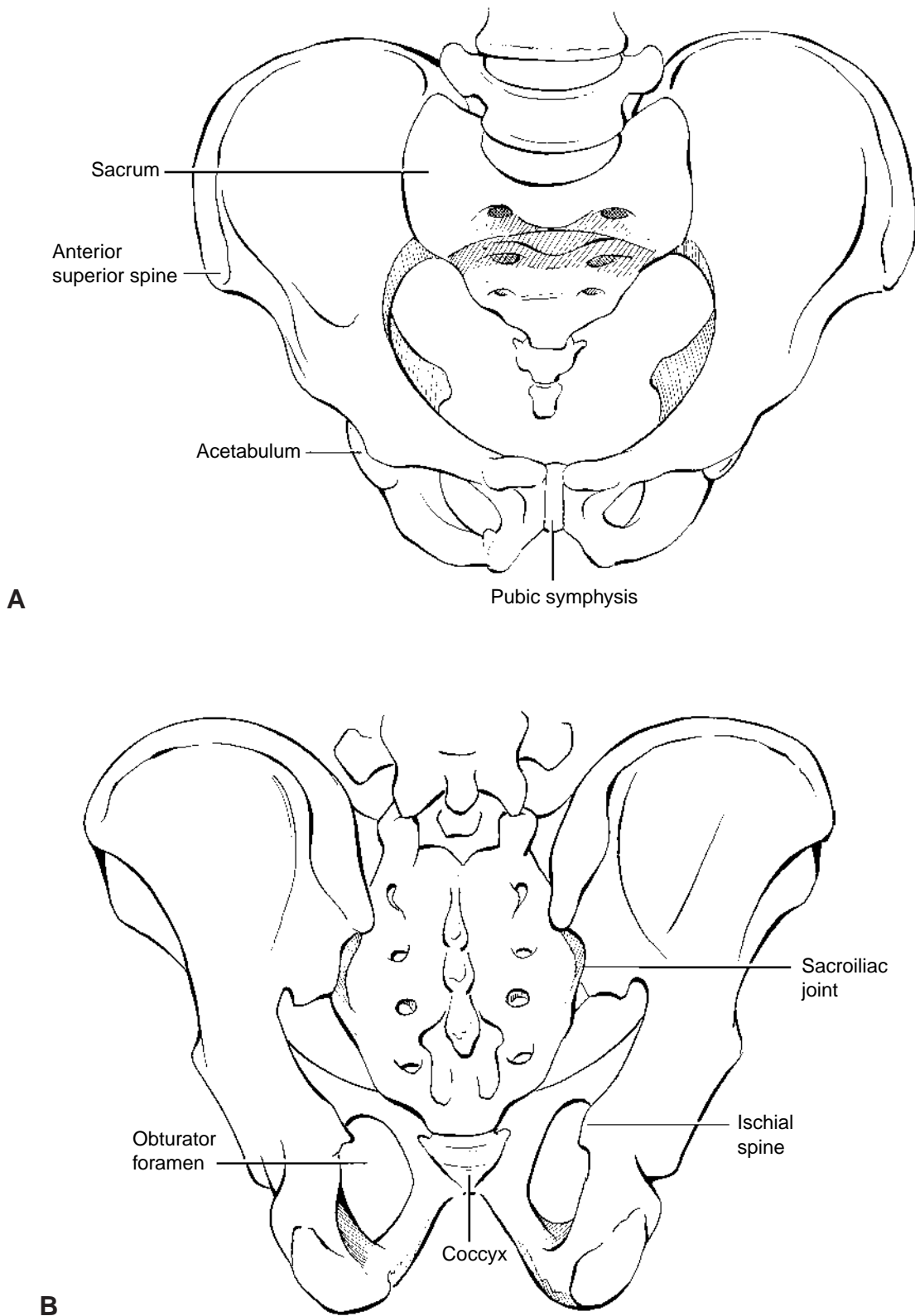


**Figure 4-1** **A:** Anterior view of the bony pelvis. **B:** Posterior view of the bony pelvis.

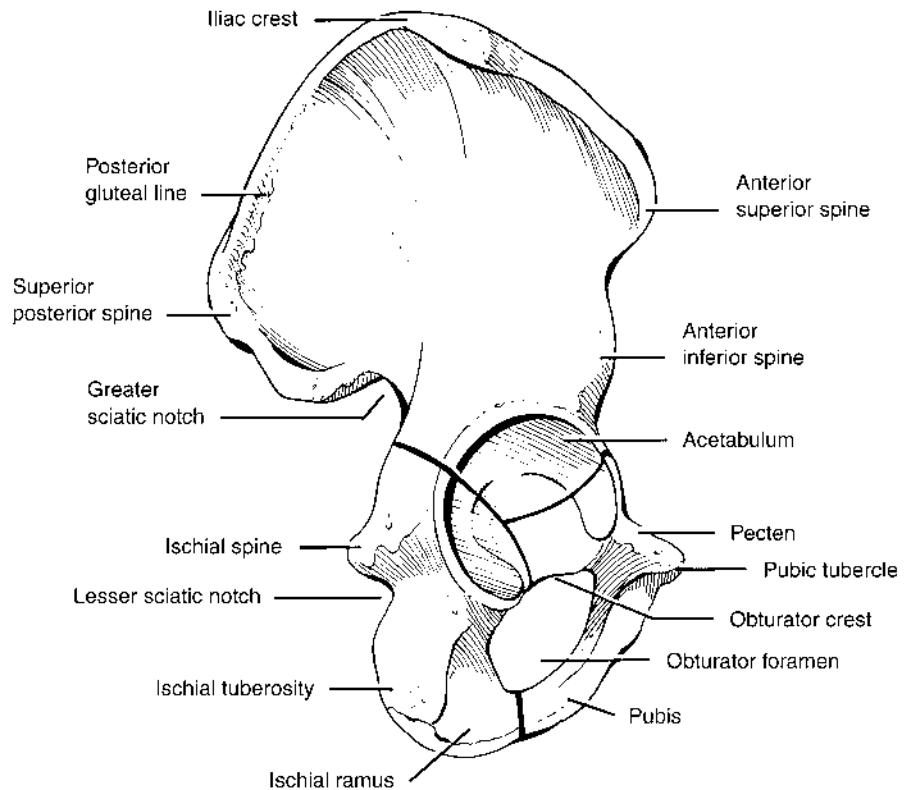


**Figure 4–2** Lateral view of the pelvic girdle.

region of the ilium, the ala (*Ā-lā*), is located above the acetabulum.

**Pubis** (*PŪ-bis*). The lower anterior part of the pelvic girdle, which is divided into three parts: The body, the inferior ramus, and the superior ramus. The body is found most medially near the opposite pubis and forms the symphysis pubis joint. The inferior ramus is the projection of bone that joins with the ischium and forms the lower boundary for the obturator foramen. The superior ramus projects upward to form the upper boundary of the obturator foramen and the anterior part of the acetabulum.

**Symphysis** (*SIM-fi-sis*) *pubis*. The amphiarthrodial joint where the pubic bones meet in the median plane. The thick articular cartilage between the pubic bones is held in place by surrounding ligaments and is generally larger in women than in men. Although this joint is usually capable of only slight movement, separation or rotation may occur during childbirth or pelvic trauma.

**Ischium** (*IS-kē-ūm*). The lower, most inferior, posterior part of the pelvic girdle. It possesses an enlarged roughened area, the ischial tuberosity, which is the bony structure on which the body rests in the seated position. Extending anteriorly from the tuberosity, the ischial rami join the inferior pubic ramus, and together they form the lower boundary of the obturator foramen. Above the

tuberosity, the ischial spine projects posteriorly forming the lower border of the greater sciatic notch.

**Obturator foramen** (*OB-tū-rā-tōr-fō-RĀ-men*). Within the lower aspect of the pelvic girdle, this opening is formed between the pubis and ischium.

**Sacrum** (*SĀ-krŭm*). Composed of five fused vertebral segments. This triangular bone forms the posterior portion of the pelvis (Fig. 4-1). Because it articulates with the fused ilia on either side, the vertebral foramina for the sacral spinal nerves are on both its anterior and its posterior surfaces.

**Sacroiliac** (*SĀ-krō-IL-ē-ak*) **joints**. Between the sacrum and the ilia, the slightly moveable joints (amphiarthrodial) found on either side of the sacrum.

**Coccyx** (*KOK-siks*). Formed by the fusion of three to five vertebral segments, this small, triangular bone is the most inferior portion of the vertebral column.

**Femora** (*FEM-ō-rā*). The longest, strongest, and heaviest bones in the body located within the thighs (Fig. 4-3). The femur (*FĒ-mŭr*) can be subdivided into three parts: Proximal extremity, shaft, and distal extremity. The latter will be described in the region of the knee and is omitted from this chapter.

**Proximal extremity**. The greater trochanter (*trō-KAN-ter*) appears much like an extension of the shaft and is on

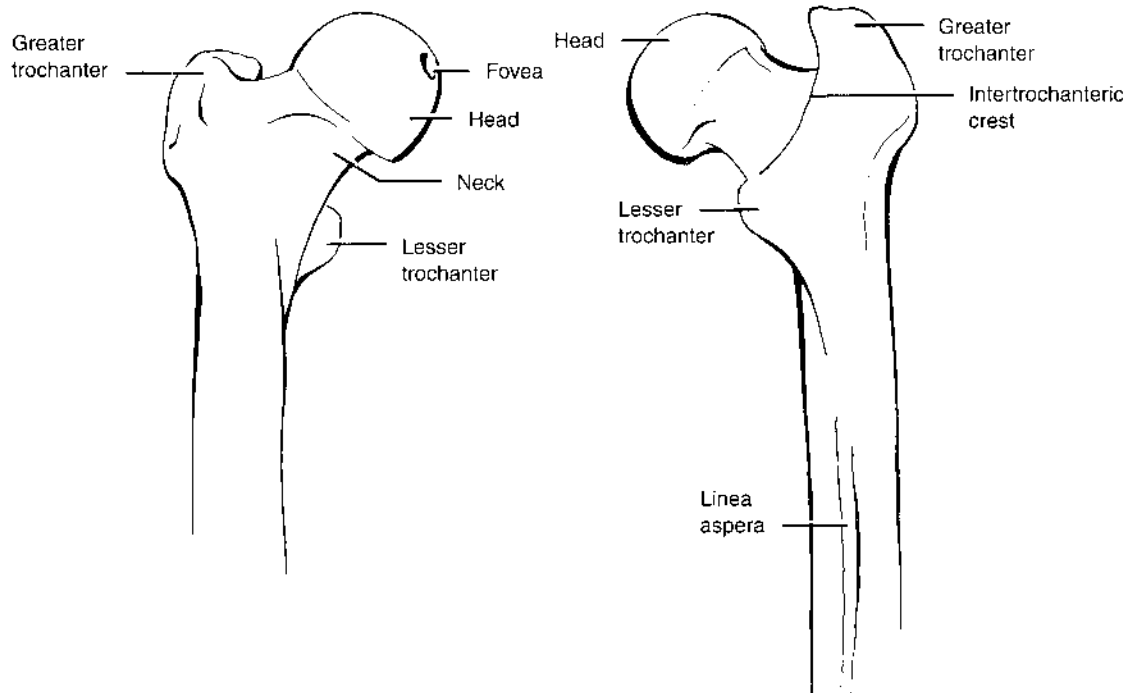


**Figure 4-3** Anterior (**left**) and posterior (**right**) surface of the femur.

the superior, lateral aspect. By comparison, the lesser trochanter is an expansion of bone more inferiorly located on the posterior, medial aspect. On the posterior view, the intertrochanteric crest is a ridge of bone between the greater and lesser trochanters. Next to the trochanters, the narrowed region of the neck extends toward the rounded head with the indentation of the fovea capitis. The angle between the shaft and neck averages 120-125 degrees but is larger in children and smaller in females.

**Shaft.** The long slender portion of the bone, or body, with the posteriorly situated roughened area, the linea aspera, delineated by medial and lateral lips.

### ■ Viscera (*VIS-er-ă*)

**Sigmoid colon.** S-shaped structure at the terminal end of the descending colon on the lower left side of the abdominal cavity; it begins at the pelvic brim (Fig. 4-4). Within the pelvis, this segment of the colon descends and curves toward the midline to cross the sacrum, where it turns downward to end in front of S3 at the rectum.

**Rectum.** Extending from the level of S3 through the lower opening of the pelvis, it lies just in front of the sacrum and coccyx and stops at the anal canal.

**Ischiorectal fossae** (*IS-kē-ō-REK-tăl FOS-ăē*). The wedge-shaped, fat-filled spaces containing rectal vessels

and nerves on either side of the rectum between the ischium and the rectum.

### ■ Arteries

**Internal iliac** (*IL-ē-ak*) **arteries.** Originating in the greater pelvis, the internal branches of the common iliac arteries terminate as they travel through the posterior bony pelvis to give rise to the gluteal arteries in the region of the buttocks. Within the pelvis, the posteriorly situated arteries are the major blood supply for the pelvis.

**Gluteal** (*GLŪ-tē-ăl*) **arteries.** As branches of the internal iliac arteries, the superior and inferior gluteal arteries originate within the true pelvis. The arteries extend out of the posterior pelvis through the greater sciatic foramen to supply the gluteal muscles within the region of the buttocks.

**External iliac arteries.** Originating in the greater pelvis, the external branches of the common iliac arteries travel anteriorly to exit the pelvis above the pubic bones. After the arteries have passed out of the pelvis, they continue as the femoral arteries and are the major source of blood supply for the legs.

**Femoral** (*FEM-ō-răl*) **arteries.** As continuations of the external iliac arteries, they originate as the vessels pass out of the pelvis to enter the region of the anterior thigh.



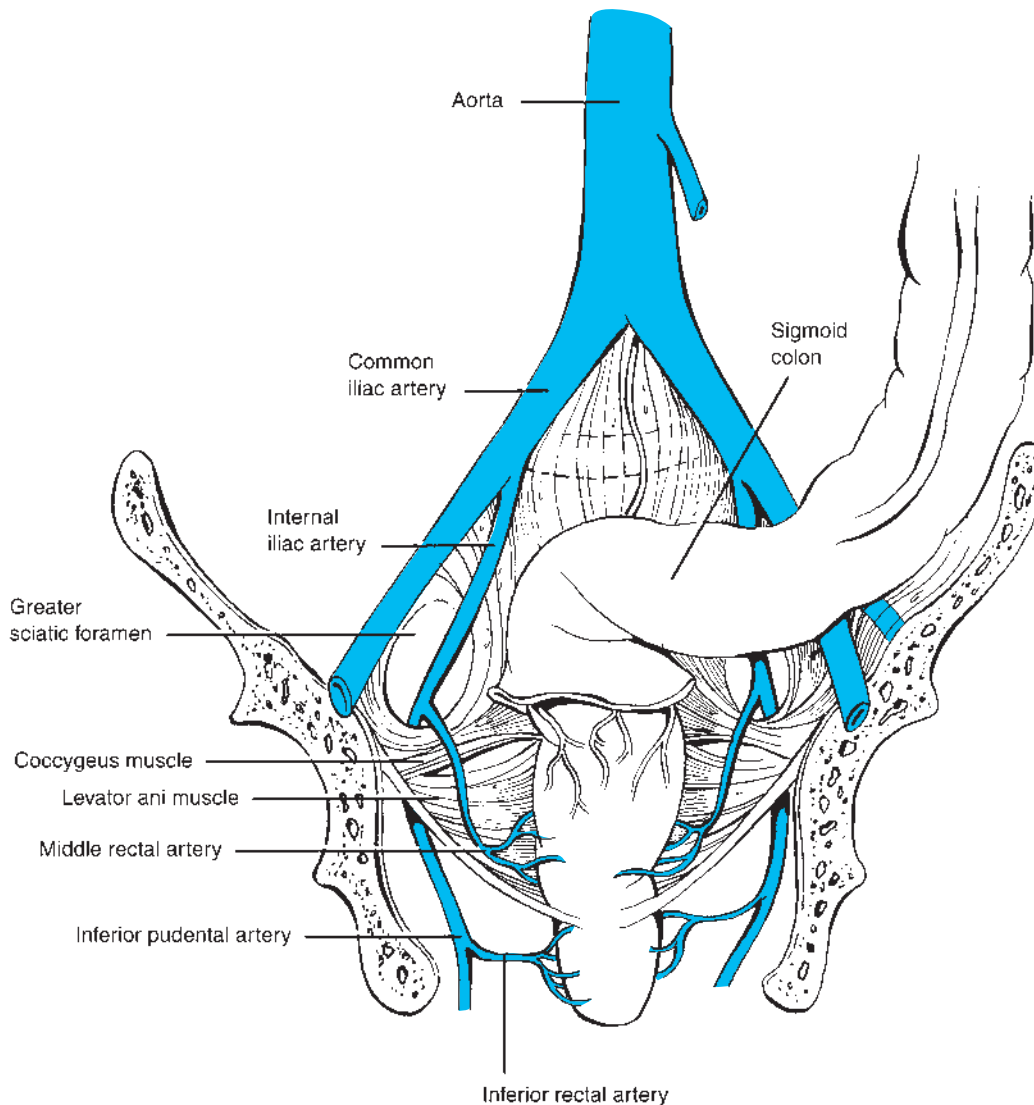


**Figure 4-4** Sketch of the major arteries of the pelvis after removal of the anterior half of the pelvis.

Although the artery lies in close proximity to the femoral vein, the artery can be discerned in sectional images by its position lateral to the femoral vein.

## ■ Veins

**Gluteal veins.** Found by the corresponding arteries, these veins drain venous blood from the gluteal muscles. Originating within the buttocks, the veins extend through the greater sciatic notch to enter the bony pelvis and empty into the internal iliac veins.

**Internal iliac veins.** Originating from the gluteal veins in the region of the buttocks, the vessels travel through the

posterior pelvis to drain into the common iliac veins (Fig. 4-5). During their course through the pelvis, the veins receive many branches draining venous blood from the pelvic viscera.

**Femoral veins.** Similar to the arteries, the veins are located in the anterior thighs. Originating from smaller vessels within the thigh, the femoral vein extends through the thigh to terminate in the external iliac vein as it passes over the pubic bone to enter the pelvis.

**External iliac veins.** Bilateral vessels formed at the termination of the femoral veins. The veins begin at the pubic bone and extend through the pelvis adjacent to the iliacus muscle to end at the common iliac veins.



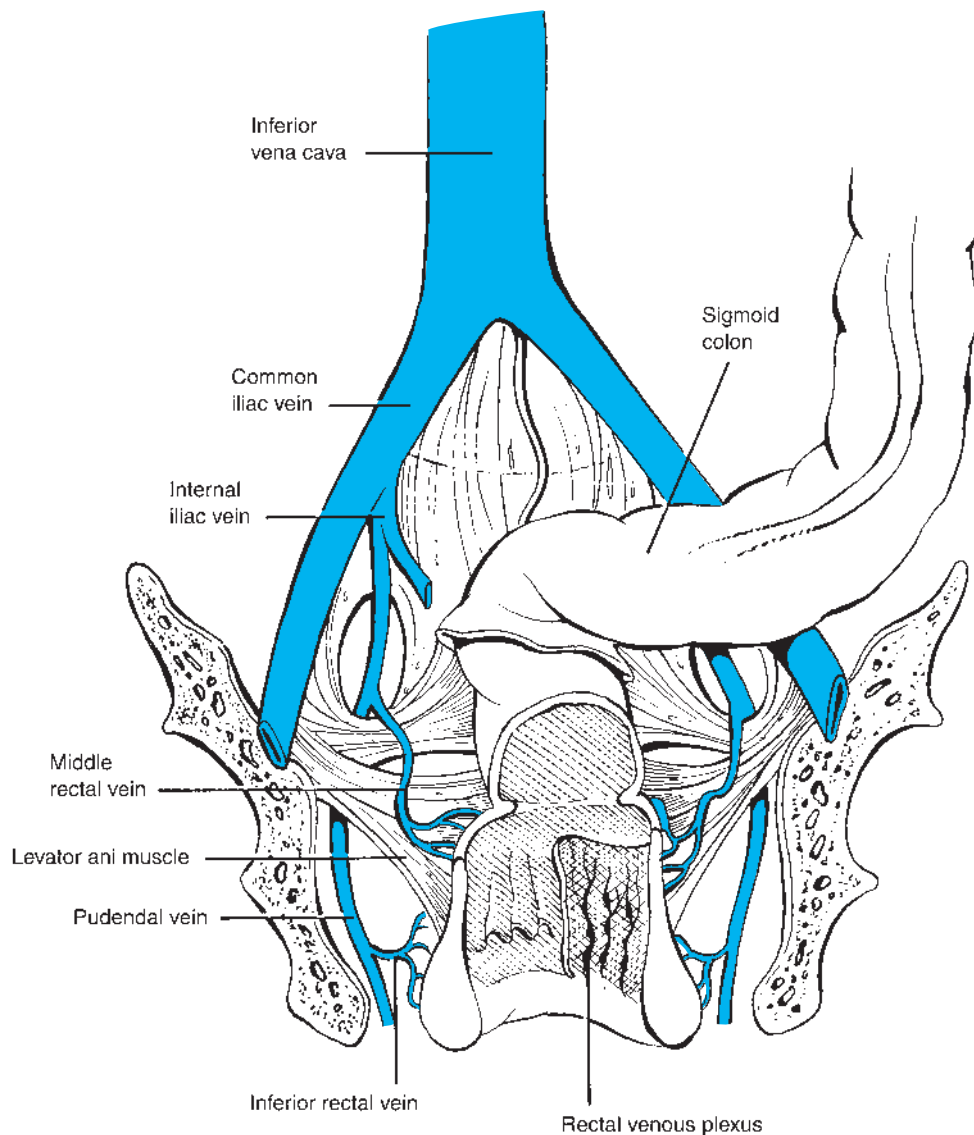


**Figure 4-5** Sketch of the major veins of the pelvis after removal of the anterior half of the pelvis.

## ■ Muscles

**Iliacus** (*il-ĭ-ă-kŭs*). Originating from the inner iliac crest, they join with the psoas (*SŌ-as*) muscles before inserting into the lesser trochanters of the femurs and act to flex the thighs (Fig. 4-6). In sectional images, the muscles are thin and flat on the inner surfaces of the iliac crests.

**Pelvic diaphragm** (*DĪ-ă-fram*). A group of muscles that form a sling across the pelvic cavity (Fig. 4-7). Similar to the diaphragm that forms the floor of the thoracic cavity, the pelvic diaphragm forms a floor that holds and supports the pelvic viscera (e.g., bladder, prostate, uterus).

**Levator ani** (*le-VĀ-ter Ā-nī*). Arising from the ischium, pubis, and coccyx, it attaches with its counterpart behind

the rectum, forming a sling. This group of muscle fibers is primarily responsible for controlling defecation. When they contract or shorten, they pull the rectum forward closing the alimentary opening.

**Coccygeus** (*kok-si-JĒ-ŭs*). Inserting on the sacrum and the coccyx, it arises from the ischial spine and forms the posterolateral portions of the pelvic diaphragm.

## ■ Male Urogenital System

**Bladder**. Roughly pyramidal in shape, its apex points downward between the pubis and the rectum (Fig. 4-8). Its upper surface normally appears flattened; but when the bladder becomes distended with urine, the upper surface

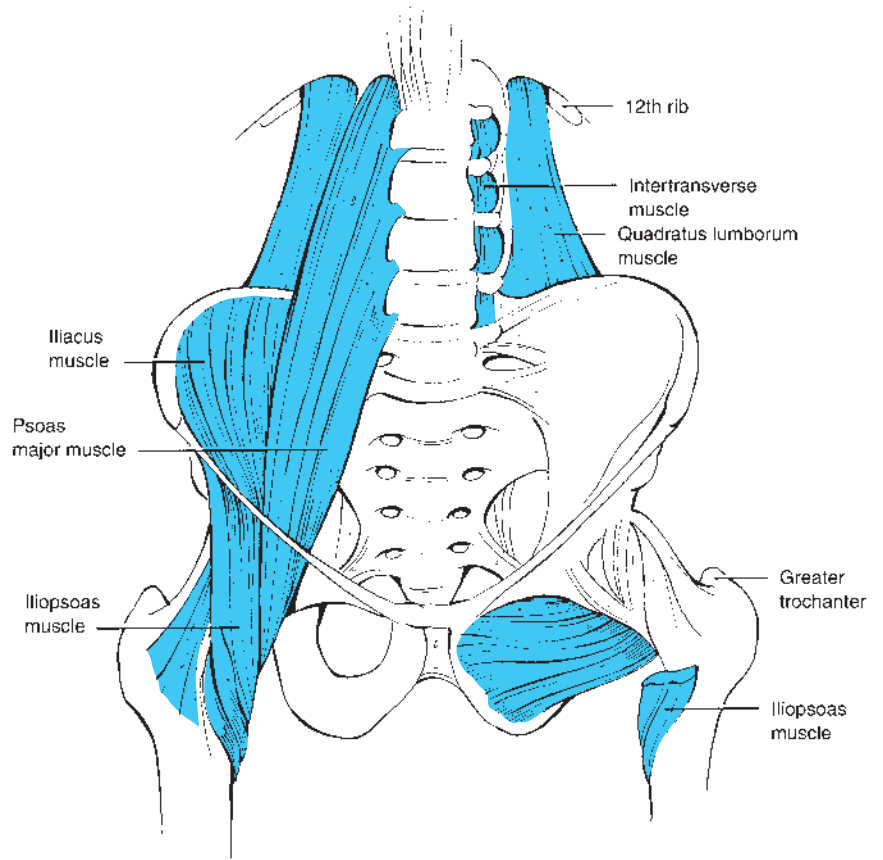


**Figure 4-6** Drawing from an anterior view demonstrating the muscles in the posterior pelvis.

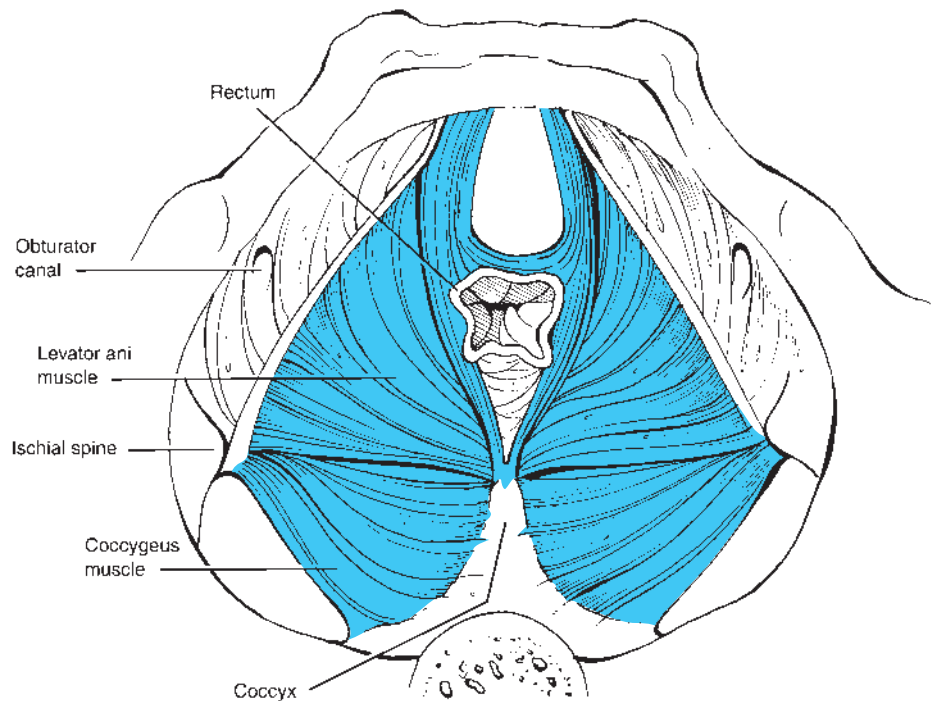


**Figure 4-7** An inferior view of the muscles forming the pelvic diaphragm.

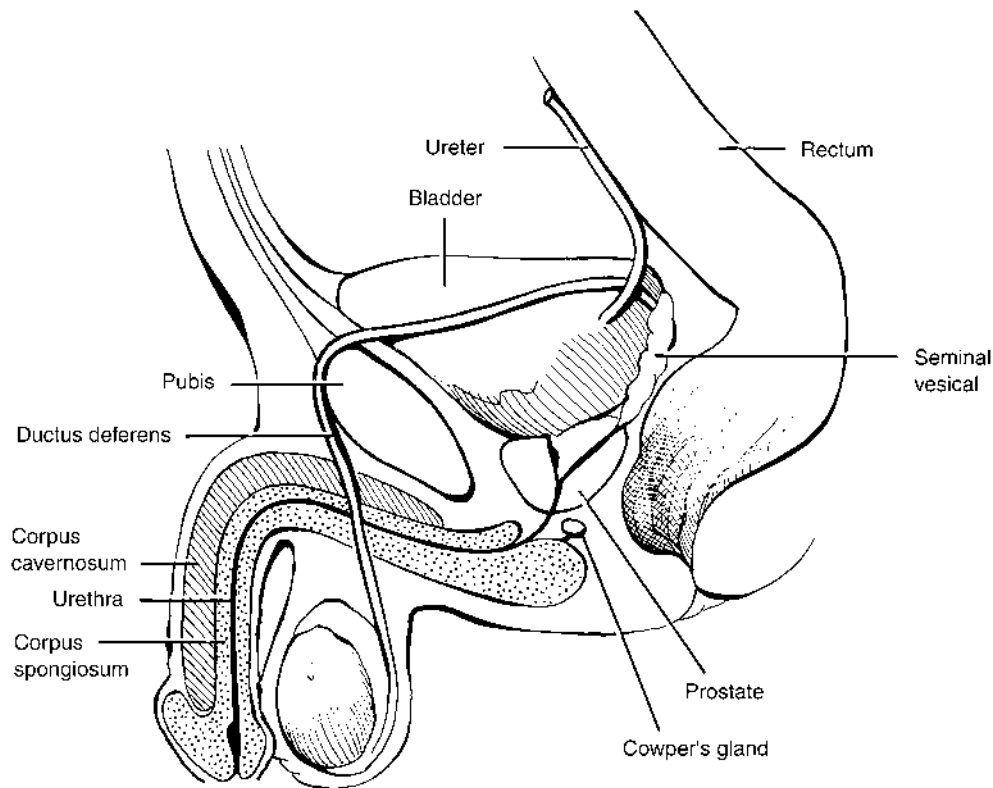


**Figure 4-8** Median sagittal view of the male pelvis.

becomes rounded and extends upward along the anterior abdominal wall. Located below the abdominal cavity, its upper surface is draped with peritoneum; the bladder shifts in position as its volume changes.

**Urethra** (*yū-RE-thrā*). Situated below the bladder, it extends for approximately 20 cm (8 in) through the prostate, pelvic diaphragm, and penis. Besides draining urine from the bladder, it also transmits sperm to the exterior during ejaculation.

**Prostate** (*PROS-tāt*). A chestnut-sized gland that surrounds the upper urethra that is between the bladder and the pelvic diaphragm. It is one of the most dense glands owing to the high concentrations of connective tissue and smooth muscle. During ejaculation, it secretes an alkaline fluid into the prostatic urethra that contributes to sperm motility.

**Seminal vesicles** (*SEM-i-nāl VES-i-klz*). The glands located above the prostate between the bladder and the rectum on either side of the ductus (vas) deferens. Within the prostate, the seminal vesicle ducts join with the ductus (vas) deferens to join the prostatic urethra. During ejaculation, the seminal vesicles secrete an alkaline fluid rich in sugar that contributes to sperm viability.

**Corpus cavernosum** (*KŌR-pūs kav-er-NŌ-sum*). Made up of erectile tissue surrounded by a strong fibrous capsule with tendonlike attachments to the ischiopubic rami. It forms the anterior three-quarters of the penis.

**Corpus spongiosum** (*spūn-jē-Ō-sum*). An irregularly shaped bundle of erectile tissue that contains the penile urethra in the posterior part of the penis.

**Spermatic cords**. Bilateral structures consisting of the ductus (vas) deferens surrounded by thin layers of connective tissue and muscle that connect the testis with the anterior abdominal wall. During embryonic development, the testes, which are formed inside the abdominal cavity, are pulled through the anterior abdominal wall into the scrotum. As a result, the spermatic cords travel over the top of the pubic bones to enter the abdomen.

## Female Urogenital System

**Bladder**. Roughly pyramidal in shape, with the apex pointing downward between the pubis and the vagina (Fig. 4-9). When nearly empty, it rests on the posterior surface of the pubis. Located below the abdominal cavity, the upper surface of the bladder and the uterus are draped with peritoneum.

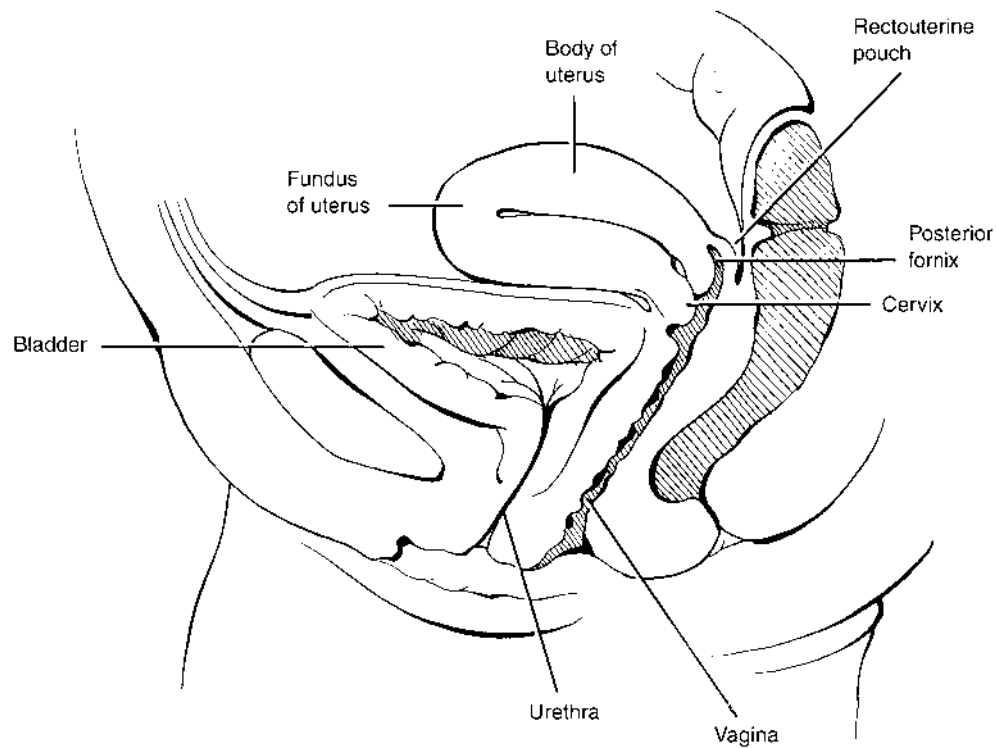


**Figure 4-9** Median sagittal view of the female pelvis.

**Urethra.** Situated below the bladder, it lies directly behind the symphysis pubis and is embedded in the anterior wall of the vagina. As it extends through the pelvic diaphragm, the adult urethra travels obliquely for roughly 4 cm (1.5 in) to open exteriorly.

**Uterus** (*YŪ-ter-ŭs*). Located between the bladder and the rectum, it is shaped like an inverted pear and has three parts: Fundus, body, and cervix.

**Fundus** (*FŪN-dŭs*). The dome-shaped roof of the uterus found above the uterine tubes.

**Body.** The largest part of the uterus, it is centrally located and is tapered in shape.

**Cervix** (*SE-riks*). The most inferior constricted region of the uterus that opens into the vagina.

**Rectouterine** (*rek-tō-YŪ-ter-in*) **pouch.** Also referred to as the pouch of Douglas or the posterior cul-de-sac, it is found within the peritoneum lining the abdominal cavity on the upper surface of the uterus and the rectum. The depressed area between the uterus and the rectum forms the lowest part of the abdominal cavity in the upright and supine positions. As such, the opening is closely evaluated to determine if excessive fluid is present within the peritoneal cavity.

**Vagina** (*vā-JĪ-nā*). Situated below the uterus, this organ can be generally described as a muscular tube, lined with a mucous membrane, that connects the uterine cavity with the exterior. Extending approximately 10 cm (4 in) in length, it is situated between the bladder and the rectum. Although the vagina is described as a hollow organ, a tampon is necessary to clearly delineate the vaginal margin in sectional images.

**Fornix** (*FŌR-niks*). At the juncture of the vagina with the cervix, a recess is formed around the portion of the cervix extending into the vagina. Although the recess is on all sides, the posterior fornix is usually deeper than the other sides.

**Labia majora** (*LĀ-bē-ā mā-JŌR-ā*). Folds of pigmented skin containing pubic hair and covering layers of loose connective tissue and fat found on either side of the labia minora (small, longitudinal folds of skin around the vestibule).

**Vestibule** (*VES-ti-bŭl*). Located between the labia minora, this area has the openings of both the vagina and urethra.

**Broad ligaments.** As the peritoneum extends across the upper surface of the pelvis containing the uterus, oviducts, ligaments, etc., the folds of connective tissue form mesometrium, or the broad ligaments (Fig. 4-10 A,B).

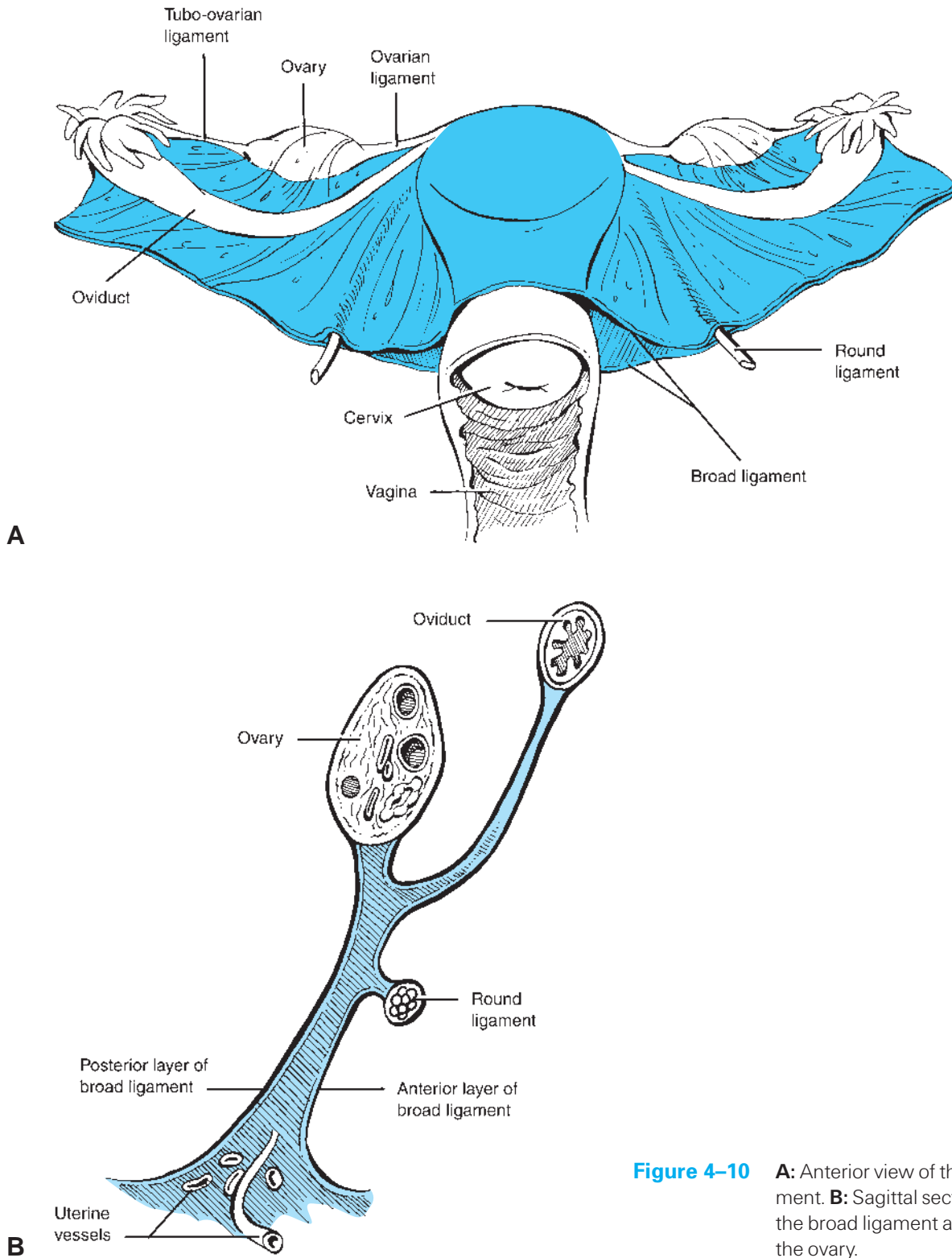


**Figure 4-10** **A:** Anterior view of the broad ligament. **B:** Sagittal section through the broad ligament at the level of the ovary.

Lateral to the uterus, the peritoneum drapes over smaller structures, forming the anterior and posterior layers that attach and support the pelvic organs.

**Adnexal** (*ad-NEK-säl*) **areas**. The uterine appendages including the ovaries, oviducts, ligaments, etc., found within the broad ligaments on either side of the uterus.

**Ovaries** (*Ō-vă-rēz*). The two almond-shaped glands located in the upper pelvis on either side of the uterus

within the adnexal areas. They are on the posterior side of the broad ligament and produce ova as well as hormones partially responsible for regulating the female reproductive cycle.

**Oviducts** (*Ō-vi-dükts*). Also called uterine tubes. Found in the free or upper margin of the broad ligament, extending from the ovaries to the uterus. They transport the ova produced by the ovaries to the uterus.



## Axial Computed Tomography Images: Male

The following 21 axial computed tomography (CT) images of the male pelvis are described at 8.0-mm intervals from superior to inferior. The images were generated immedi-

ately after the administration of 100 mL of venous contrast at the following technical factors: 120 kilovolt peak (kVp) and 150 milliamperes-second (mA-s).

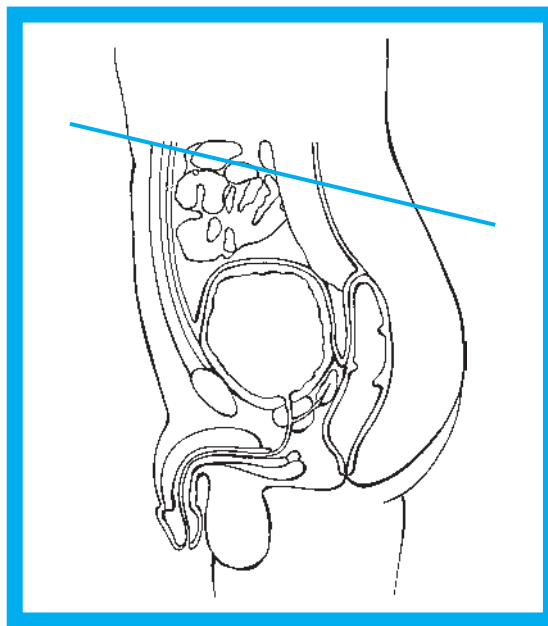
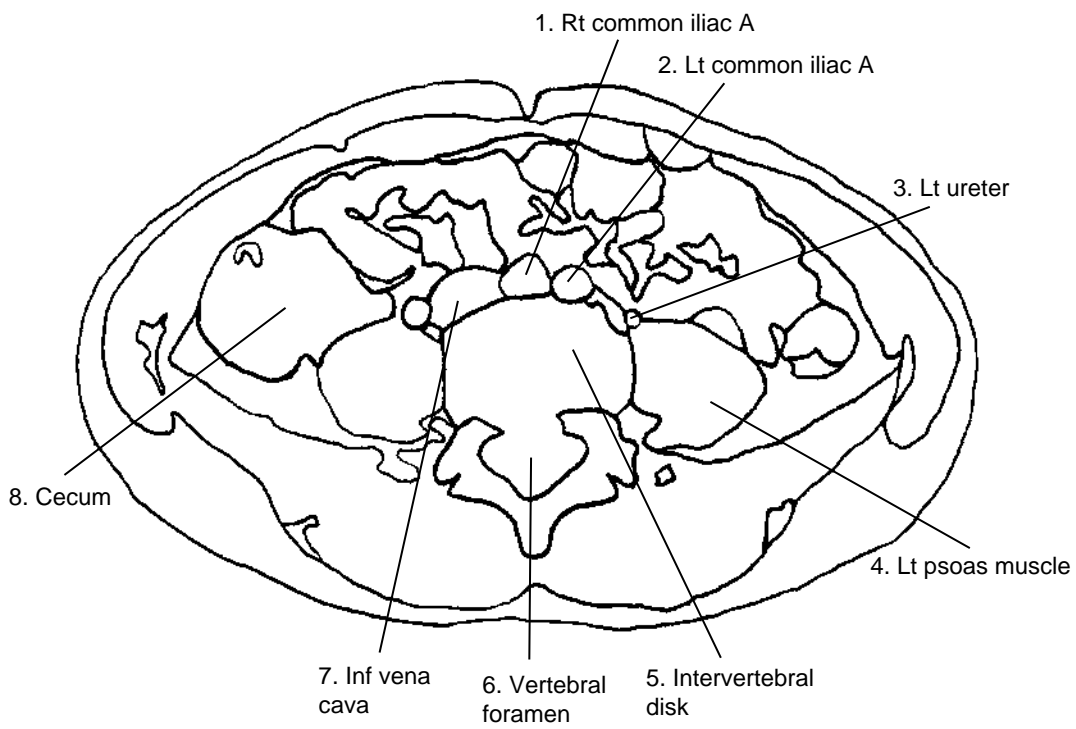


**Figure 4-11 (A,B)** Axial CT image 1: Male.

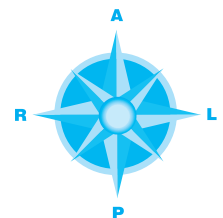
In the first image (A), the intervertebral disk occupies a central location in front of the vertebral foramen. At this level, the iliac crests are not yet seen, indicating that the section is slightly above the pelvis and representing the appropriate location for the first image in an examination of the pelvis. On either side of the intervertebral disk, the psoas muscles appear as large round areas with a density similar to that of the intervertebral disk. Along the anteromedial surface of the psoas muscles, the ureters can be seen because of the contrast enhancement. Medial to the ureters, three major vessels can be discerned within the pelvis. The largest vessel on the right side, the inferior vena cava, has yet to bifurcate; and the two vessels on the left side, the right and left common iliac arteries, have originated from the bifurcation of the abdominal aorta. In the abdominal cavity, the most notable structure is the enlarged area of the intestine on the far right side. Given the large size of this part of the intestine, especially compared to the loops of the small bowel, it can be identified as the cecum.



A



B





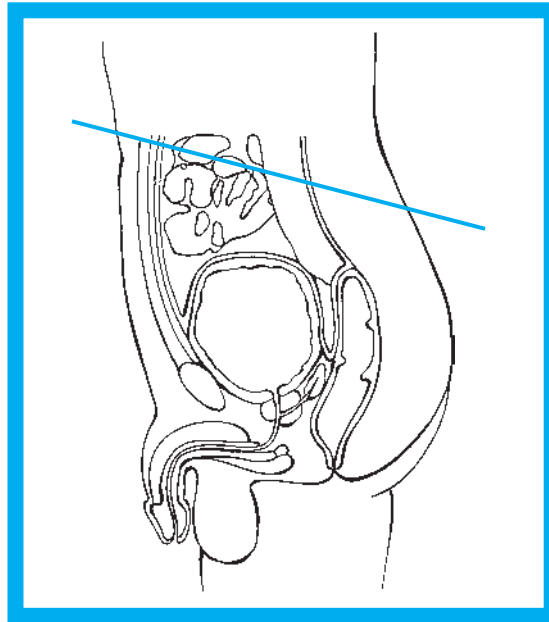
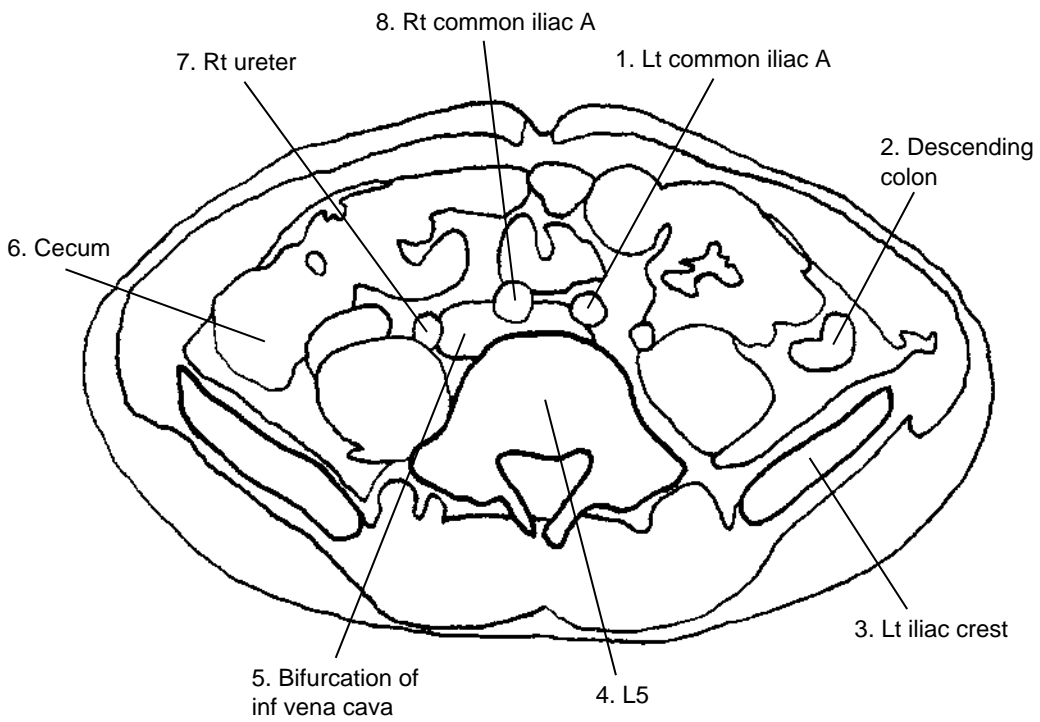


**Figure 4–12 (A,B)** Axial CT image 2: Male.

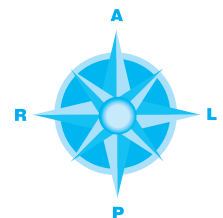
The largest vertebra of the body, L5, is shown in this image between the upper iliac crests. Because the iliac crest is now visible, this section would be the first image showing pelvic structures. Similar to the previous image, the major vessels of the pelvis are shown sectioned just anterior to the body of L5. The three distinct major vessels seen in the previous image have changed at this level; it is now difficult to tell if there are three or four vessels. Because the common iliac arteries were identified on the previous section, they are also present at this level; and the inferior vena cava is shown bifurcating into the right and left common iliac veins. Lateral to the major vessels, the ureters can be seen as bright vessels anteromedially located next to the psoas muscles. Although most intestinal structures are located within the peritoneum, the cecum, identified on the right side, and the descending colon, found on the left side, are retroperitoneal in location.



A



B



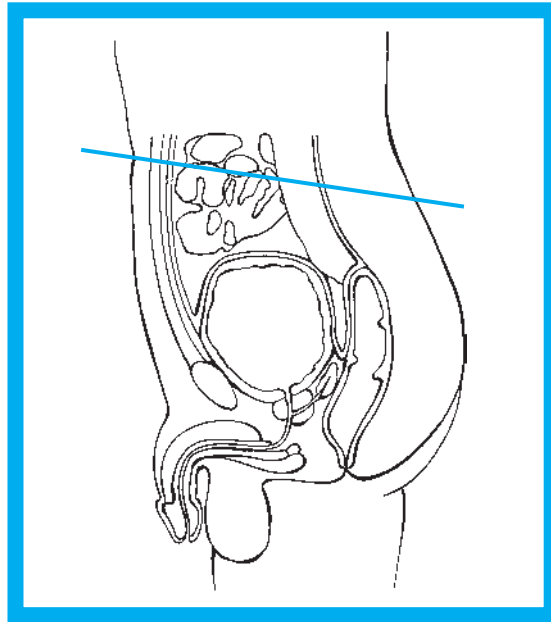
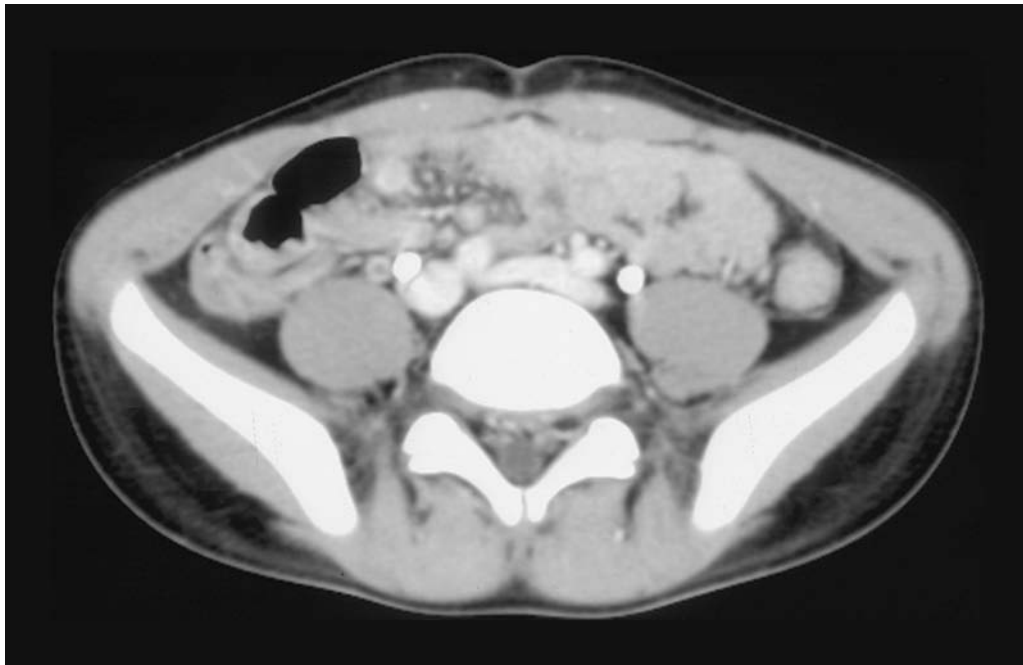
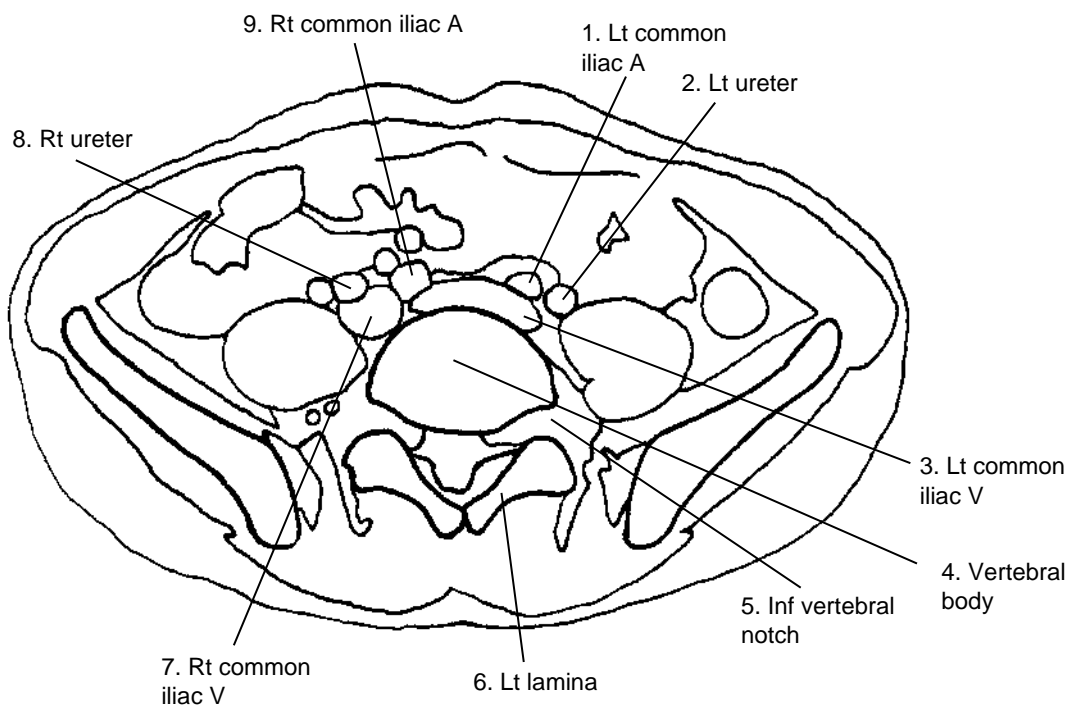


**Figure 4–13 (A,B)** Axial CT image 3: Male.

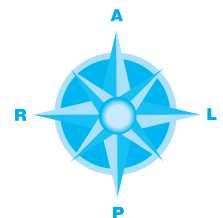
Sectioned through the lower end of the vertebral body of L5, this image demonstrates the inferior vertebral notches between the vertebral body and the lamina. The vertebral notches are the location of the spinal nerves exiting between L5 and S1. Anterior to the vertebra, the major vessels of the abdomen now appear as four distinct vessels. On the right side, the right common iliac artery occupies a more anterior location than the right common iliac vein, which is slightly larger. On the left side, the left common iliac artery is more anterior than the left common iliac vein, which is longitudinally sectioned near the bifurcation of the inferior vena cava. Lateral to the major vessels, the right and left ureters are demonstrated and are clearly visualized owing to their bright contrast enhancement.



A



B



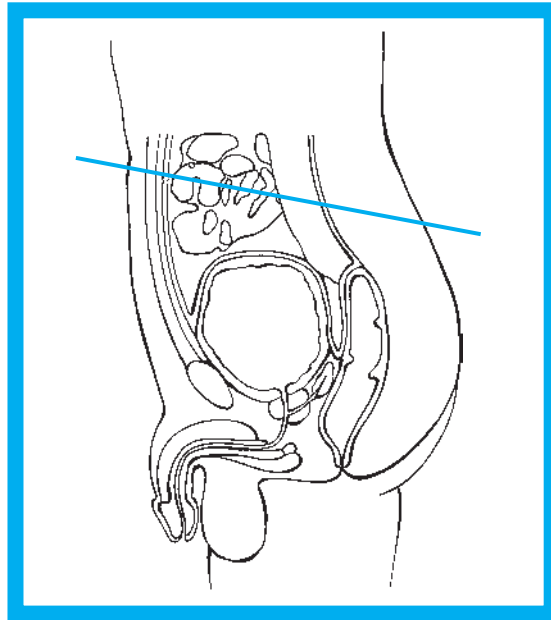
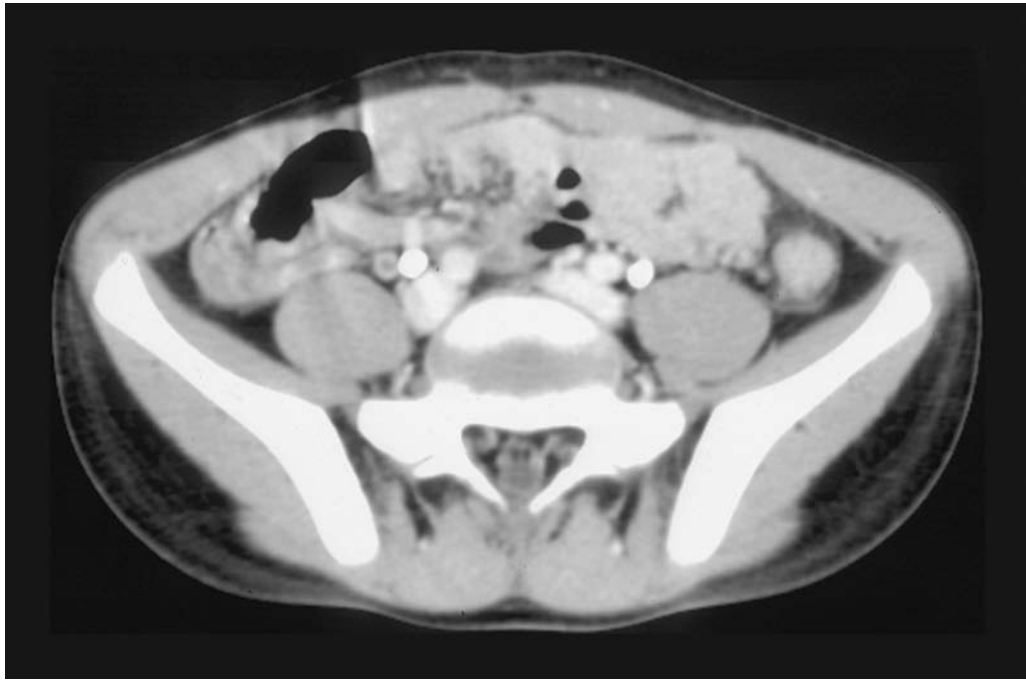
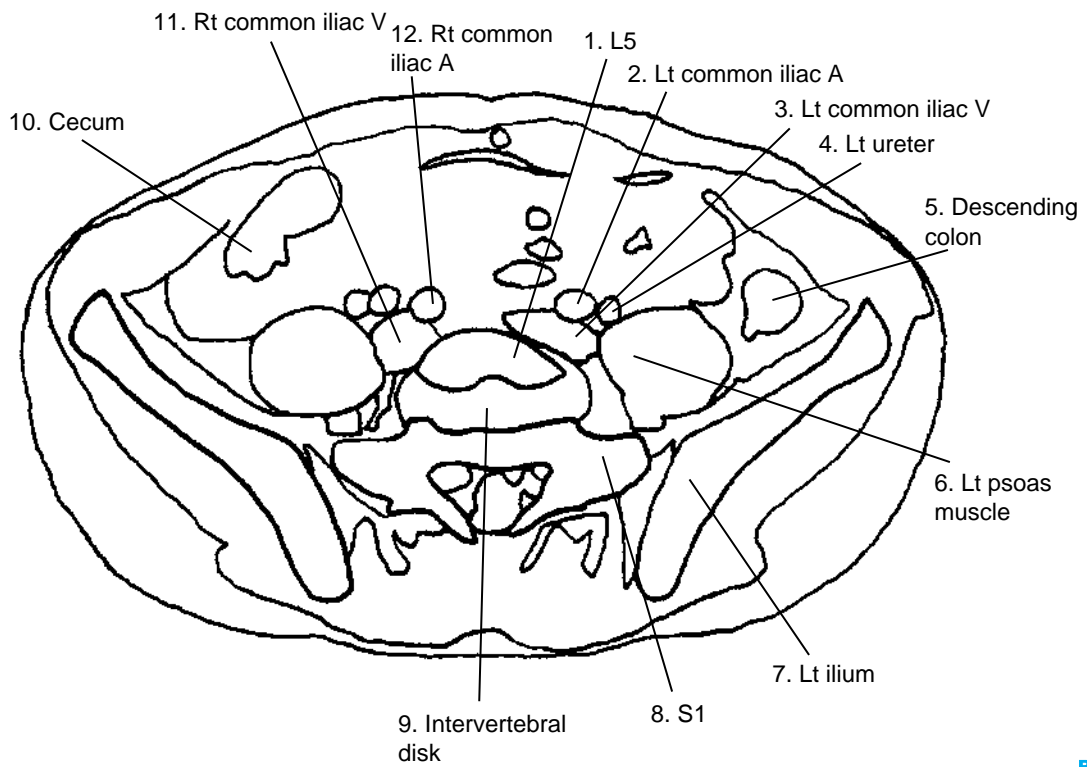


**Figure 4–14 (A,B)** Axial CT image 4: Male.

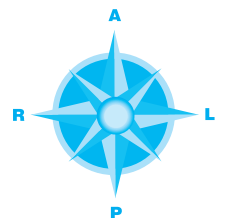
The unique shape of the vertebra indicates that this image is at the level of the sacrum. Compared to previous vertebral bodies, the sacral vertebrae have a distinct “bat” shape, because the transverse processes are fused to form lateral parts that articulate with the iliac bones. In this section, the intervertebral disk can be seen separating the vertebral bodies of L5 and S1. Anterior to the vertebral column, four major vessels are demonstrated in the pelvis. On the right side, the right common iliac artery lies adjacent to the right common iliac vein; on the left side, the left common iliac artery and vein are seen together. As demonstrated previously, the arteries are somewhat smaller than the veins and occupy a more anterior position. On either side of the vertebrae, the psoas muscles are shown in cross-section and serve as landmarks for other structures in the area. Lateral to the psoas muscles, the descending colon and cecum are demonstrated fixed to the posterior abdominal wall.



A



B



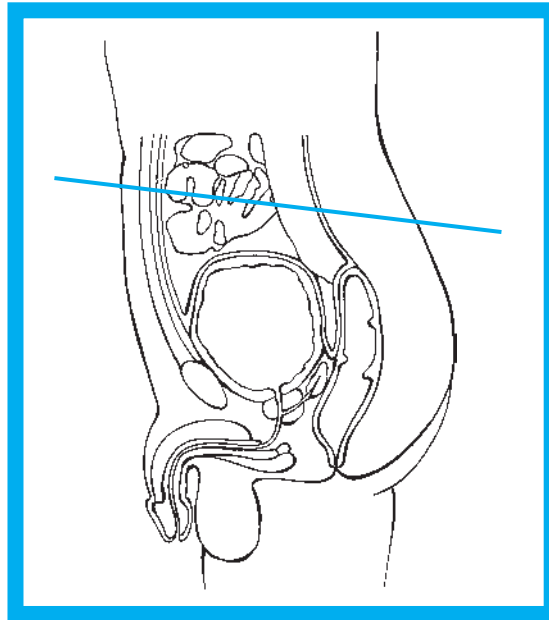
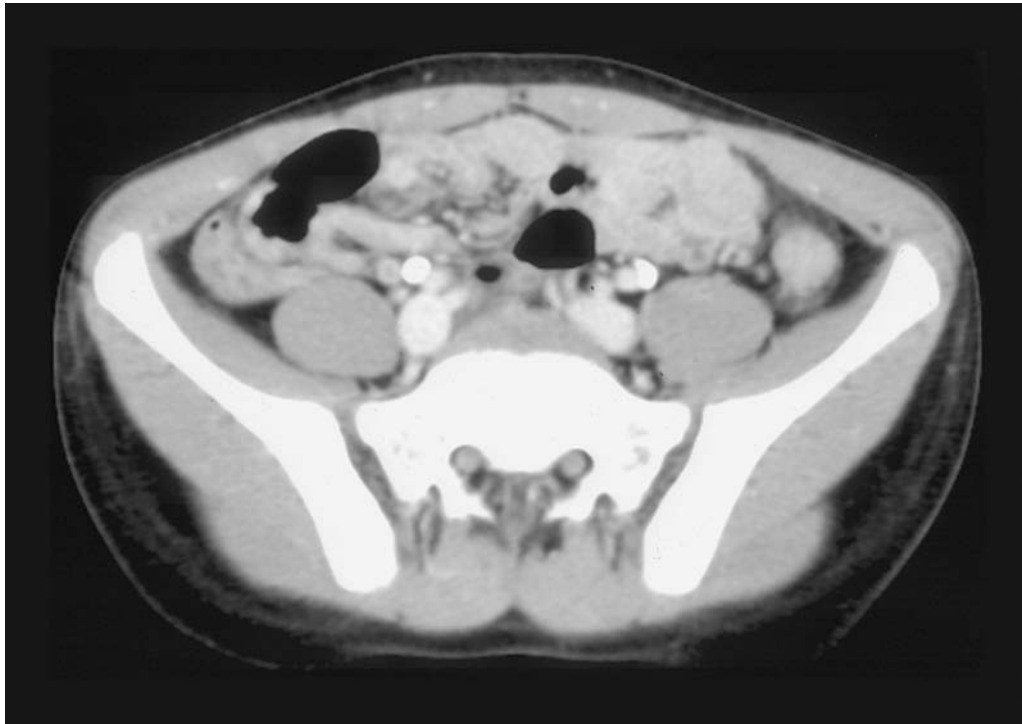
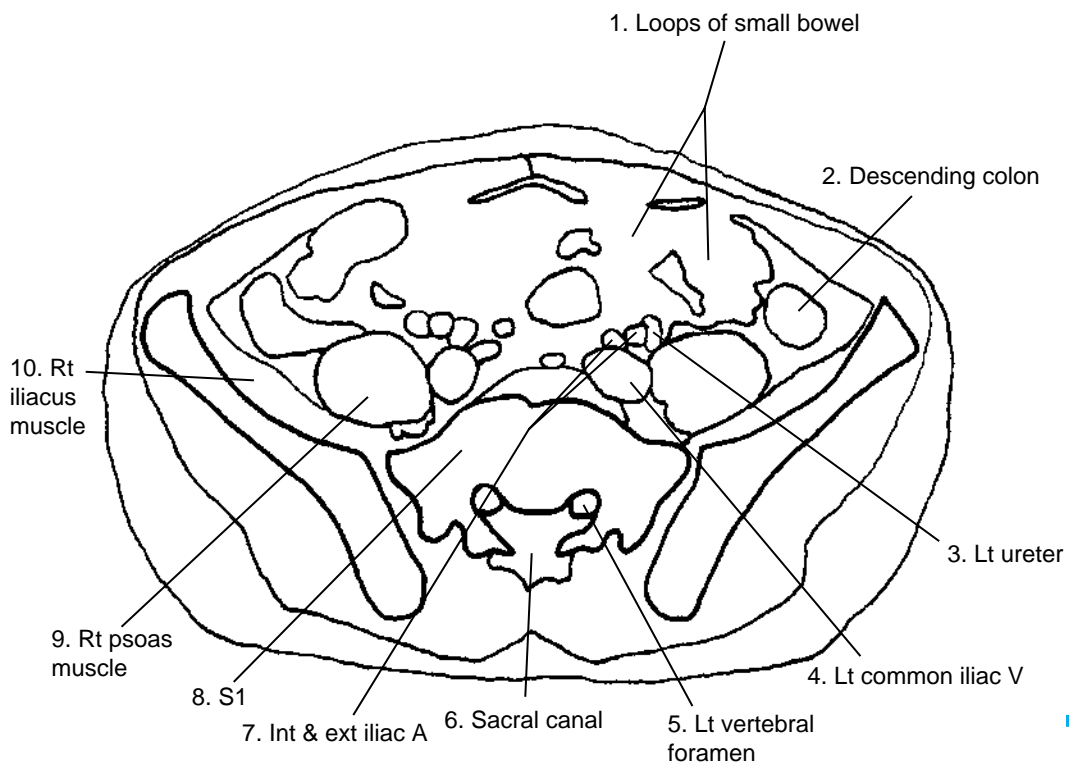


**Figure 4–15 (A,B)** Axial CT image 5: Male.

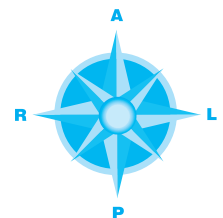
The characteristic appearance of the sacral vertebra is more evident in this section through the body of S1. The lateral parts of S1 are shown articulating with the iliac bones on either side. On the anterior part of S1, a small part of the intervertebral disk can still be seen. On the back side of S1, the first pair of vertebral foramina are emerging from the sacral canal. Within the greater pelvis, the iliacus and psoas muscles are shown lining the posterior wall of the pelvic cavity. Similar to previous images, the ureters appear as bright, contrast-enhanced vessels near the psoas muscles and are in close proximity to the major vessels of the pelvis. As in the previous image, the common iliac veins are continuing in a posterior location adjacent to the vertebral body; however, the common iliac arteries have bifurcated and given rise to the internal and external iliac arteries. In the anterior pelvic cavity, numerous loops of small bowel are loosely organized centrally, and the descending colon is seen on the left side occupying a position near the iliacus muscle.



A



B





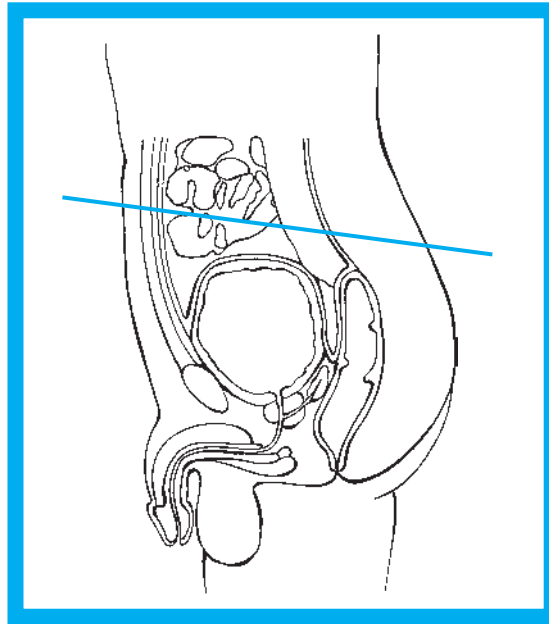
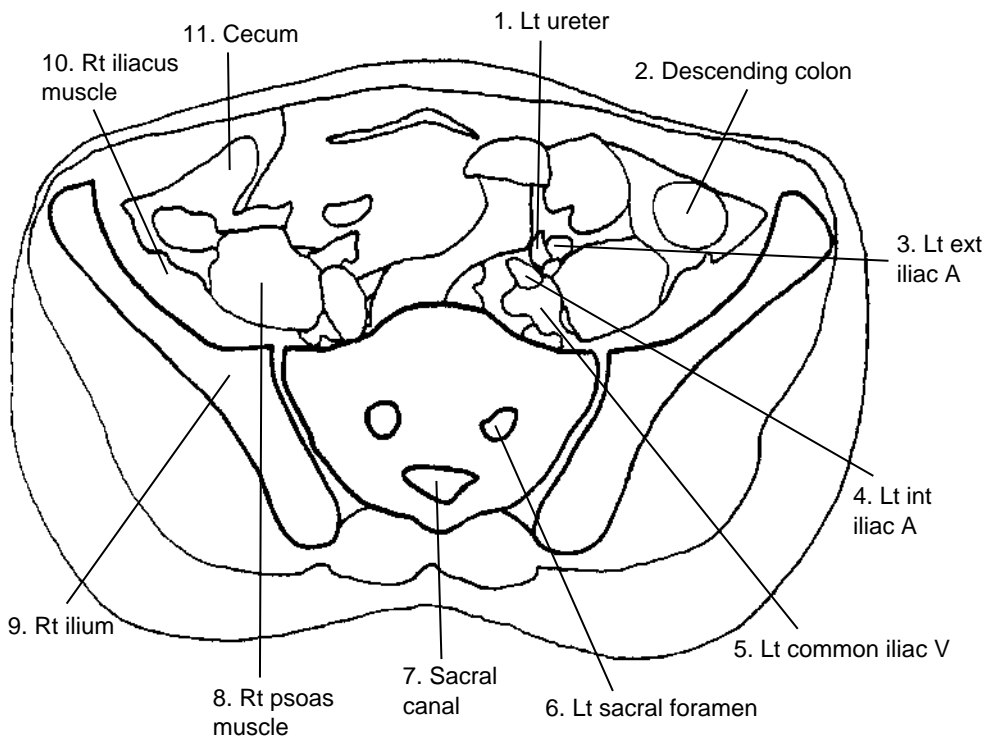


**Figure 4–16 (A,B)** Axial CT image 6: Male.

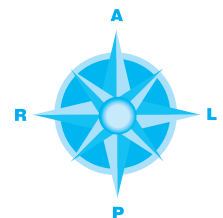
The sacral foramina are separated by bone from the sacral canal at this level. Lining the posterior pelvic wall, the iliacus and psoas muscles are shown in cross-section adjacent to the iliac bones. In this image, the external and internal iliac arteries are shown on either side of the left ureter and in front of the larger common iliac vein. Like previous images, the descending colon and the cecum are on opposite sides of the randomly organized loops of small bowel distributed within the peritoneal cavity.



A



B



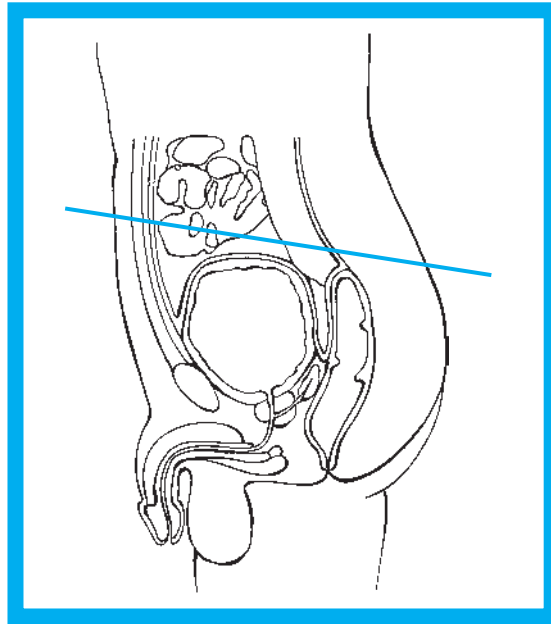
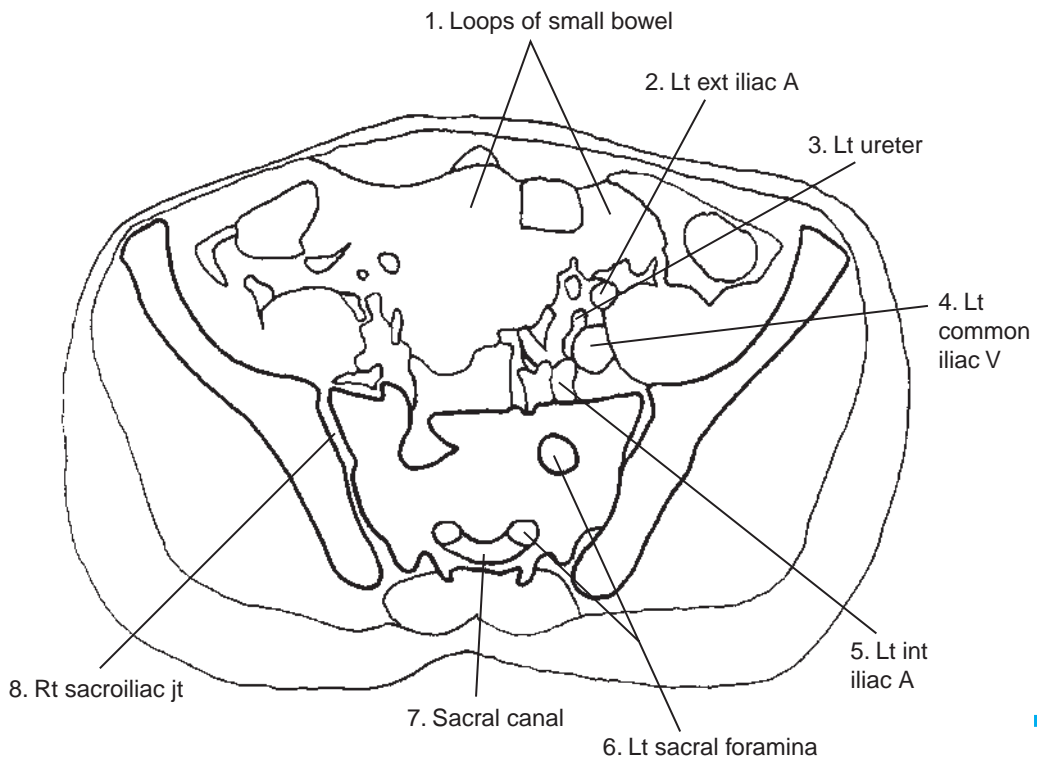


**Figure 4–17 (A,B)** Axial CT image 7: Male.

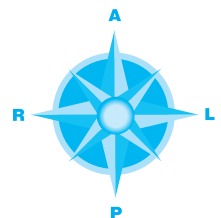
This oblique section through the sacrum shows two pairs of sacral foramina, the first and second. Although the first pair of sacral foramina is near the point of exit from the sacrum, the second pair is just emerging from the sacral canal. On either side of the sacrum, the iliac bones form the sacral iliac joints where they articulate with the lateral parts of the sacrum. Within the greater pelvis, the left ureter is enhanced and lies near the medial border of the psoas muscle. Beside the ureter, the external and internal iliac arteries are diverging; the external iliac artery is moving to a more anterior position, and the internal iliac artery is occupying a more posterior position. Seen between the iliac arteries, the common iliac vein is still larger. Within the peritoneal cavity, the loops of small bowel occupy most of the anterior pelvis. Because this part of the small bowel is within the pelvis, the ileum is probably the part of the small bowel shown.



**A**



**B**



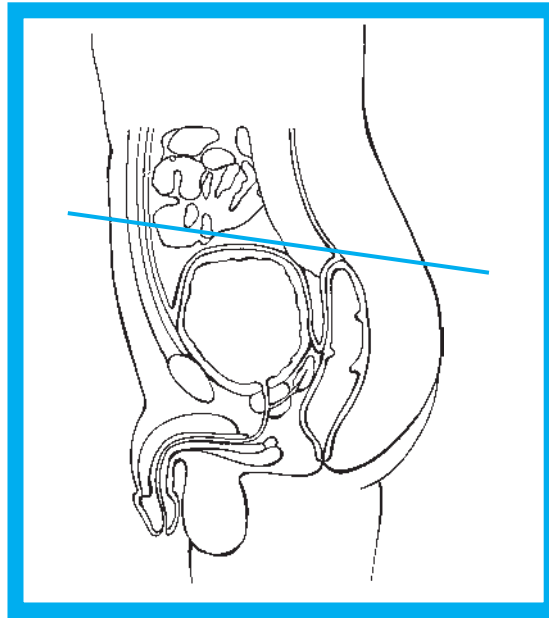
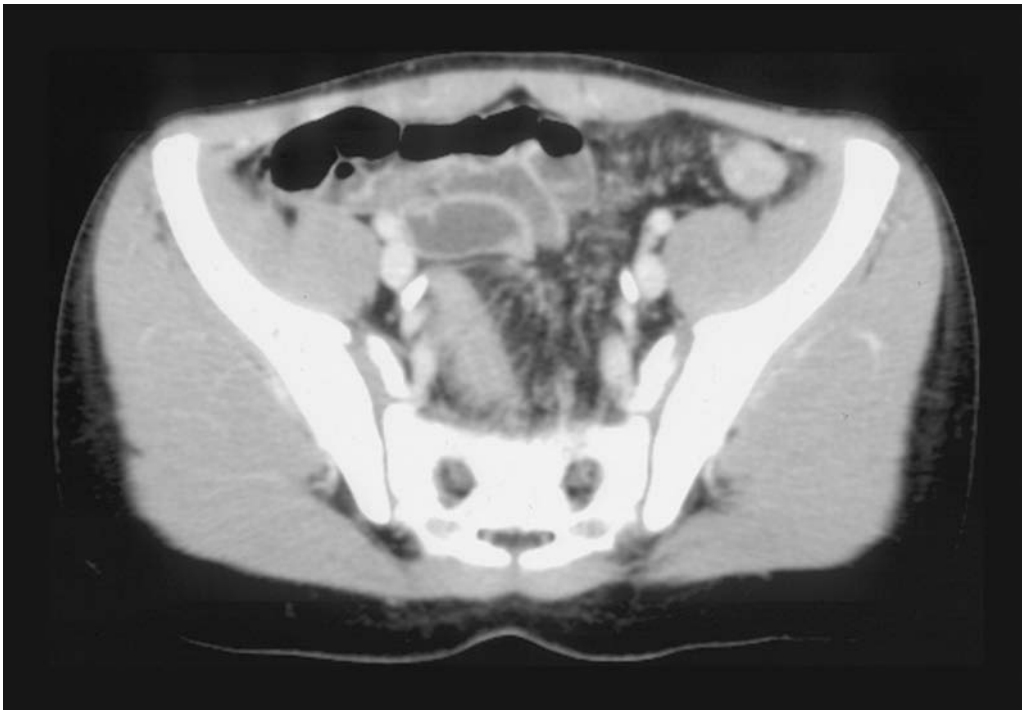
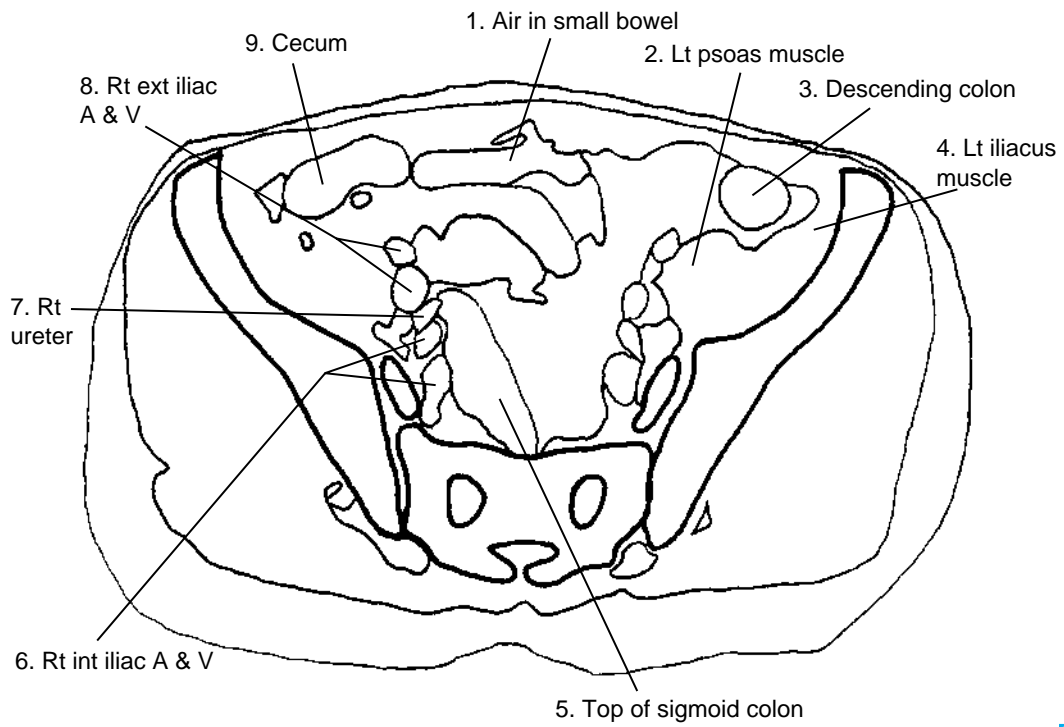


**Figure 4–18 (A,B)** Axial CT image 8: Male.

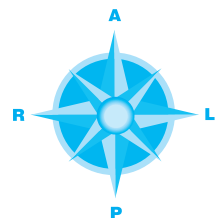
The sacrum, iliac bones, iliacus muscles, and psoas muscles are shown in cross-section forming the posterior wall of the pelvic cavity. Compared to previous images, the psoas and iliacus muscles are not as clearly separable as they join to form the iliopsoas muscles in the lower pelvis. Near the psoas muscles, the ureters are readily visible as contrast-enhanced structures between the external and internal iliac vessels. The intestinal structures are similar to previous views, with the small bowel occupying most of the peritoneal cavity. Posterior to the peritoneum, the lower edge of the cecum is shown on the right and the descending colon is demonstrated on the left. Although the descending colon ends in the sigmoid colon, the irregular shape of the sigmoid colon moves upward so that it is also included within this section.



A



B



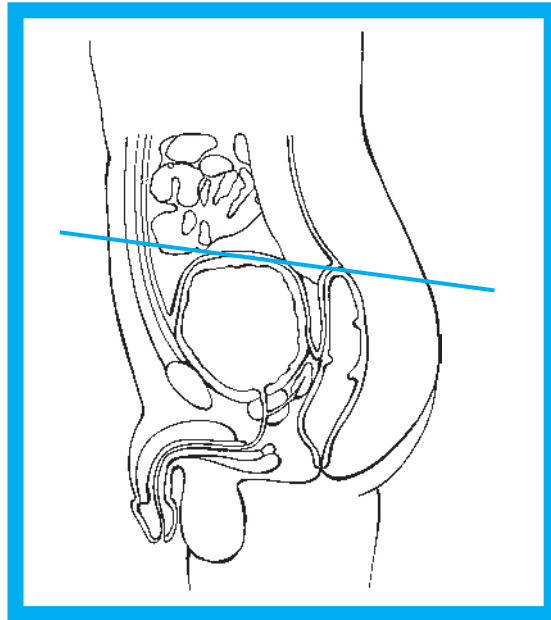
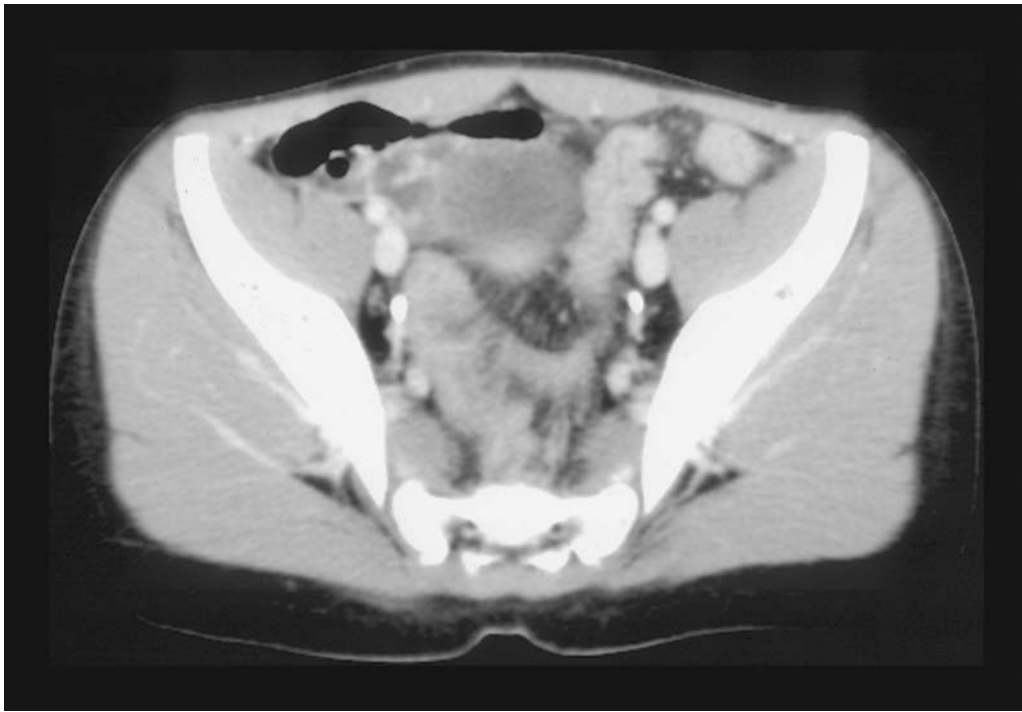
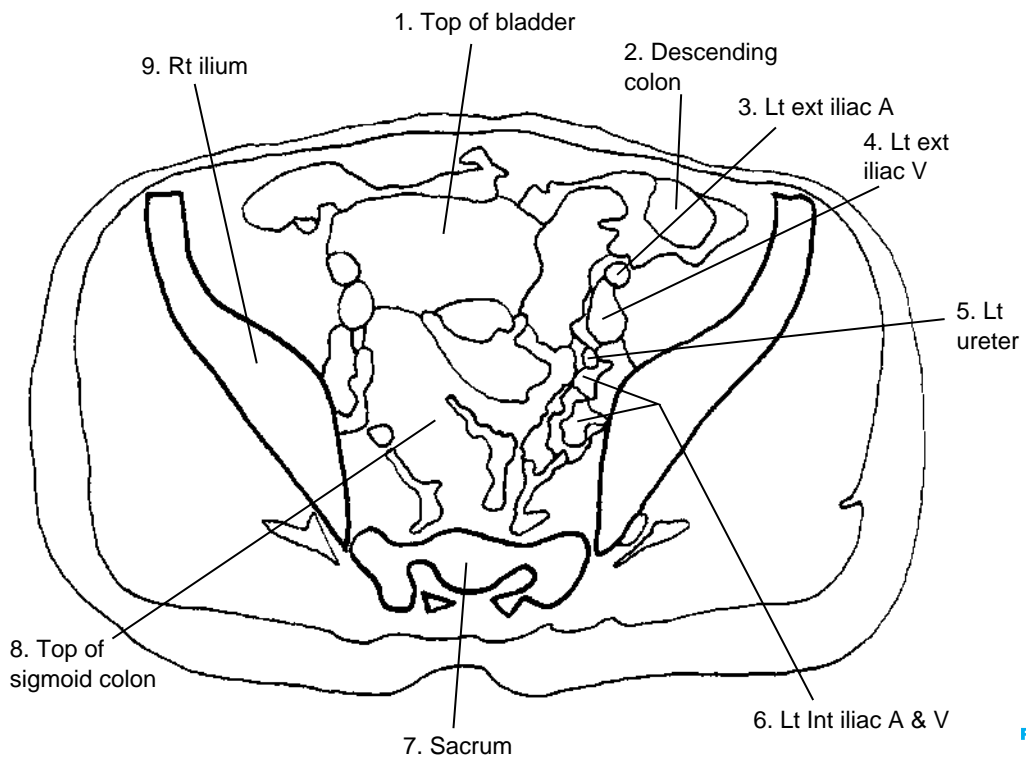


**Figure 4–19 (A,B)** Axial CT image 9: Male.

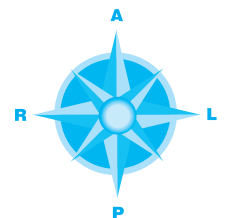
The sacrum is smaller than in the previous images. This image includes the bottom of the sacroiliac joint. Although the ilium is shown in cross-section similar to previous views, the central portion of the ilium is beginning to expand, indicating that the section is nearing the acetabulum. Within the pelvic cavity, the sigmoid colon is more clearly seen in its characteristic S shape as it extends toward the descending colon on the left side. Owing to contrast enhancement, the ureters are easily identified between the iliac vessels. Anterior to the ureter, the external iliac vessels are medial to the psoas muscle, and the artery is more anterior and slightly smaller than the corresponding vein. Posterior to the left ureter, the left internal iliac vessels are between the sigmoid colon and the left ilium. Although some small bowel can be seen in this section, much of the anterior pelvic cavity is occupied by the top of the bladder, which appears as a dense structure between loops of small bowel.



A



B





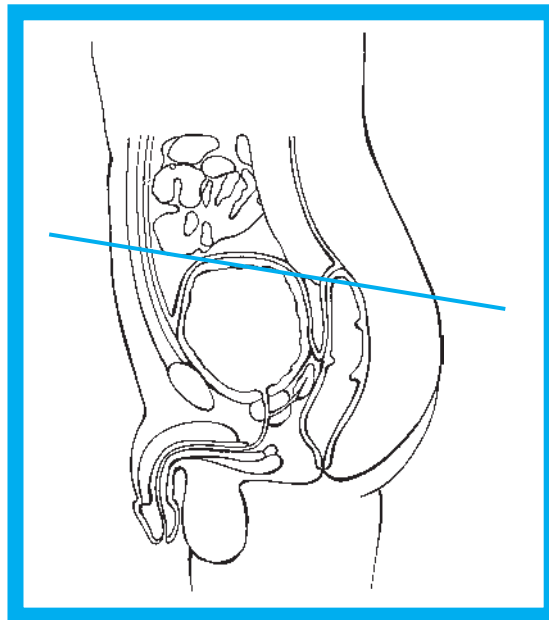
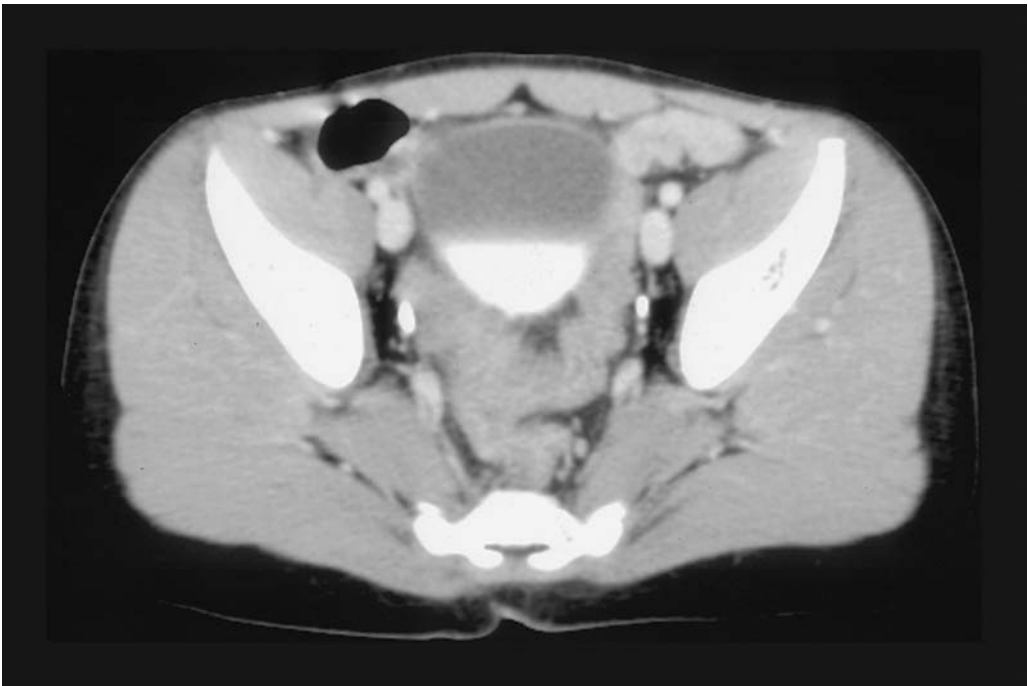
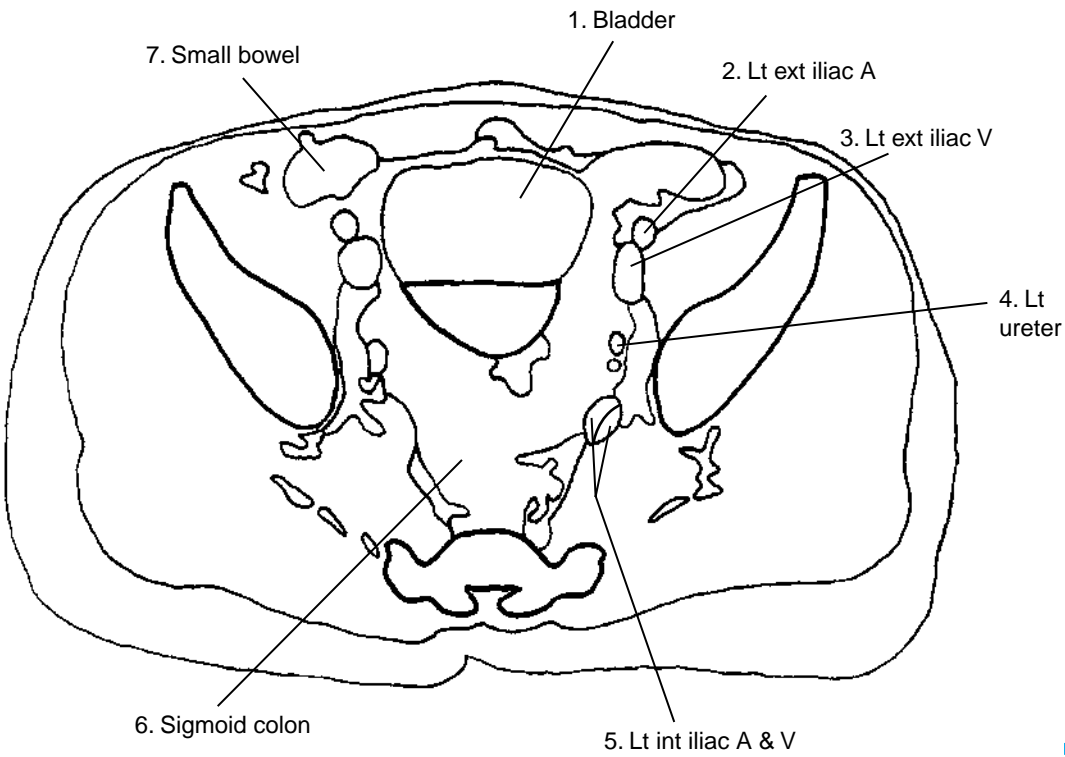


**Figure 4–20 (A,B)** Axial CT image 10: Male.

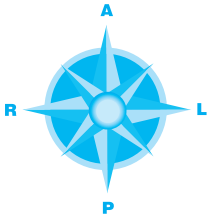
At this level, the sacrum and iliac bones are separated and the bladder is easily recognized occupying most of the anterior pelvic cavity. Within the bladder, a contrast-fluid level is demonstrated, because part of the fluid within the bladder is contrast enhanced. Around the bladder, small bowel can be seen anteriorly, and the characteristic S shape of the sigmoid colon is between the bladder and the sacrum. On either side of these visceral structures, the ureters are seen along with the external and internal iliac vessels.



A



B



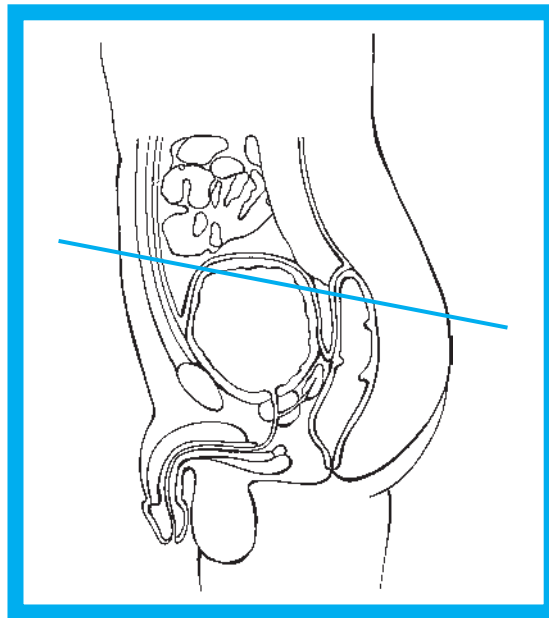
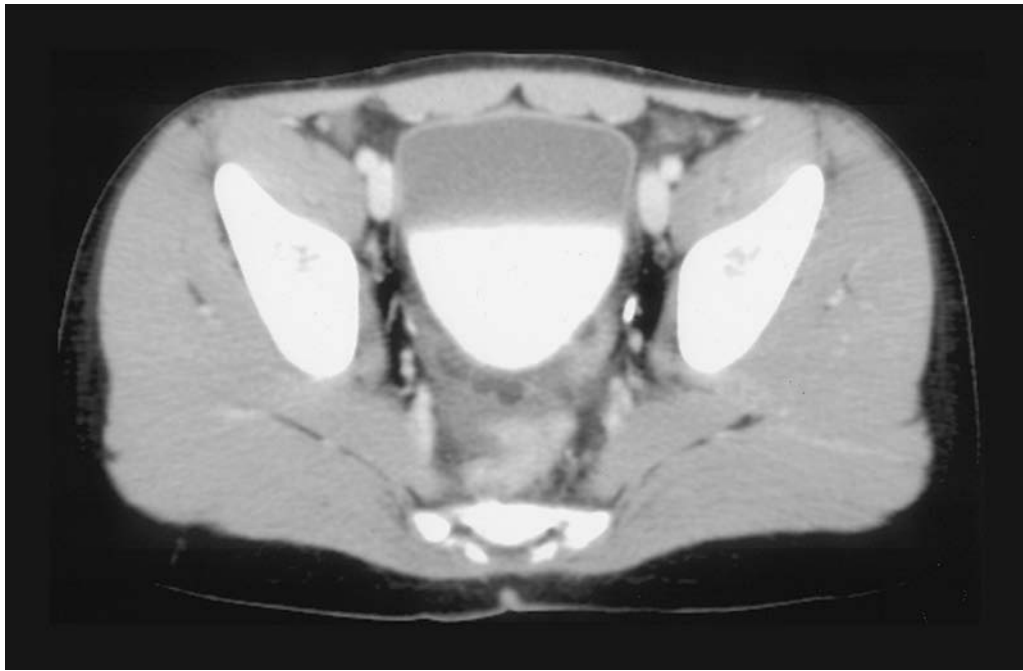
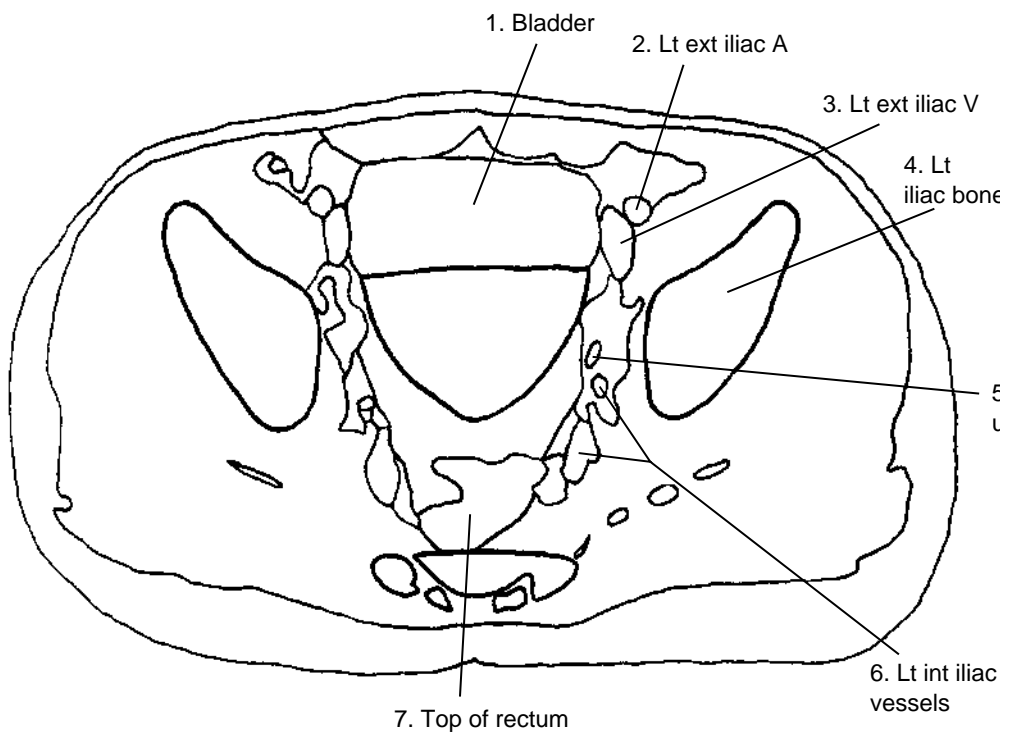


**Figure 4-21(A,B)** Axial CT image 11: Male.

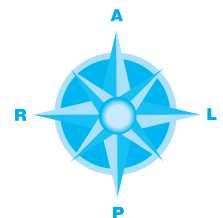
The iliac bones appear shortened and thicker because they are near the level of the acetabula. Although the bladder occupies most of the pelvic cavity, the ureters are demonstrated in cross-section between the iliac bones as they extend toward the lower bladder. On either side of the bladder, the external iliac artery and vein are seen, and the artery is more anterior and slightly smaller in size. Posterior to the bladder, the S-shaped sigmoid colon has been replaced by the top of the rectum, found just in front of the lower sacrum. At this point, the internal iliac vessels have branched and are difficult to discern other than as a group of contrast-enhanced vessels.



A



B



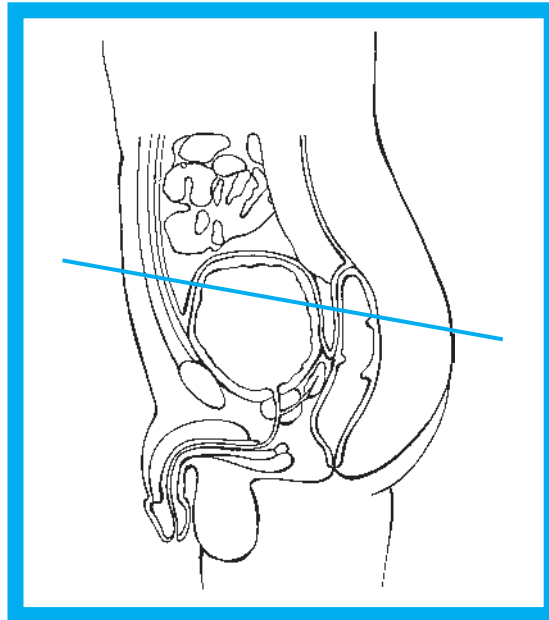
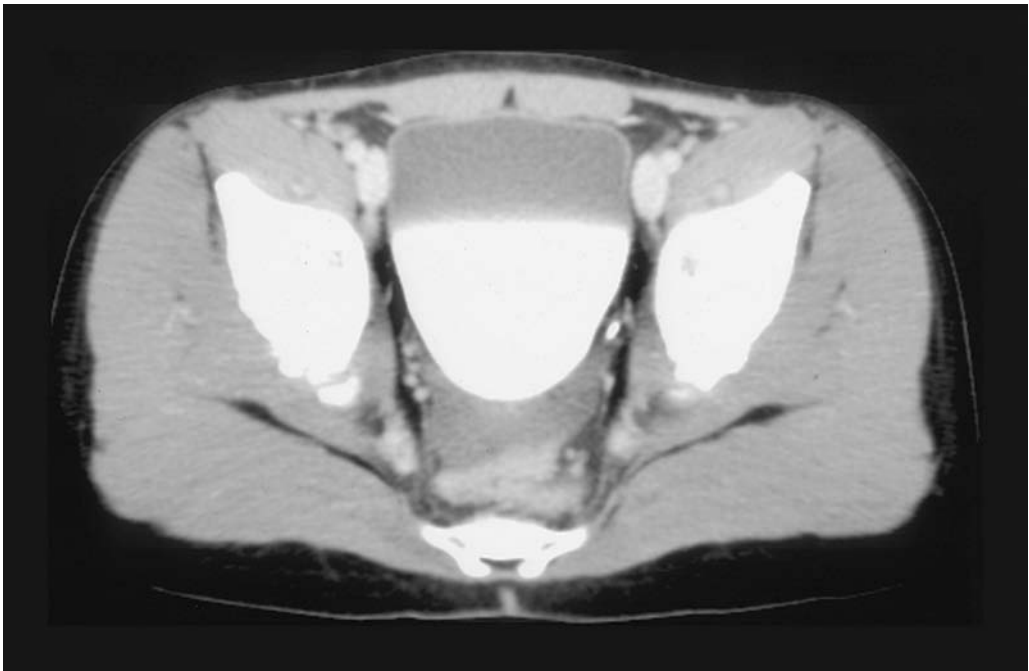
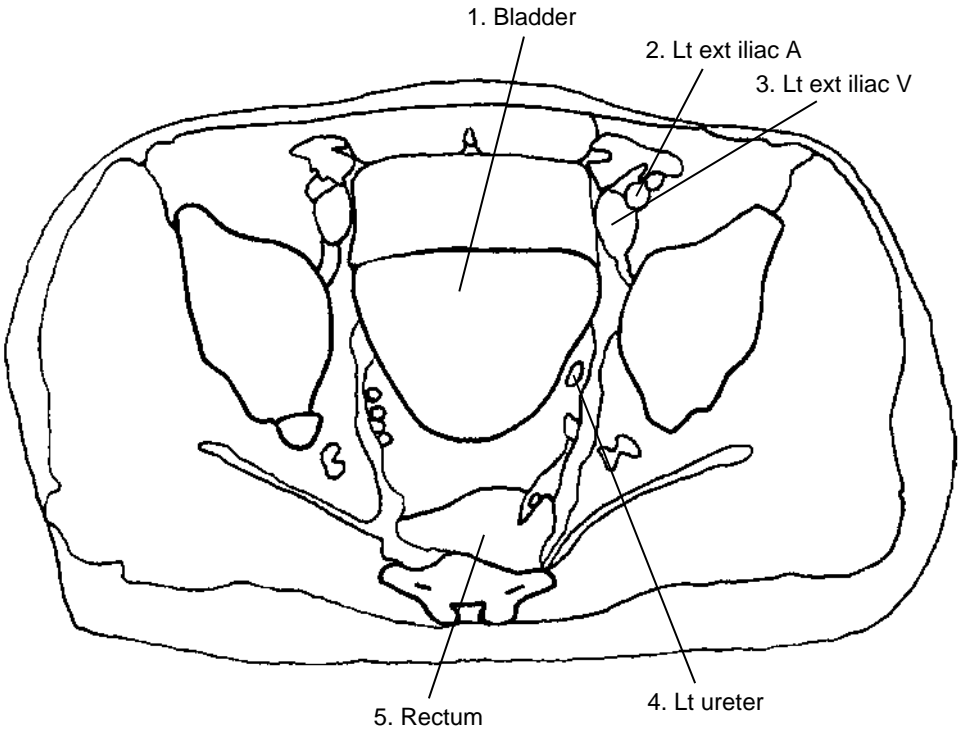


**Figure 4-22 (A,B)** Axial CT image 12: Male.

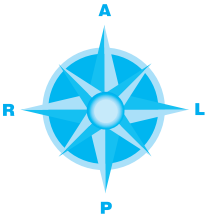
The iliac bones are shortened and thicker, because they are forming the roof of the acetabula. Between the iliac bones, the contrast- and urine-filled bladder occupies most of the pelvic cavity. On either side of the bladder, the external iliac vessels are found; the arteries are more anterior and smaller in size. Between the bladder and the sacrum, the rectum is shown in cross-section along with the internal iliac vessels, which are difficult to distinguish at this low level.

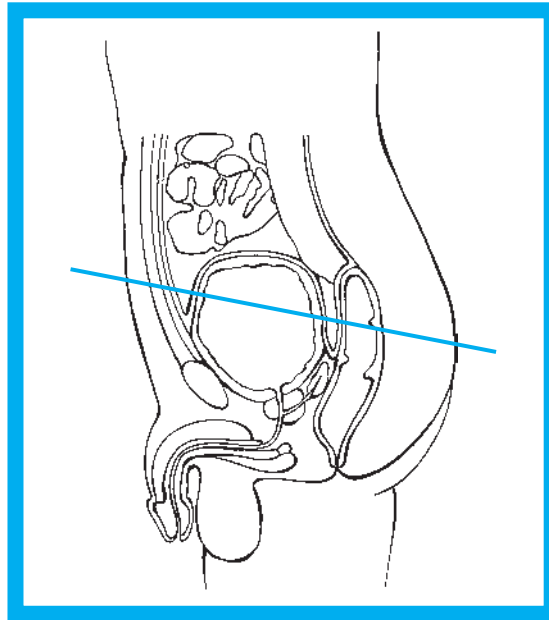


A



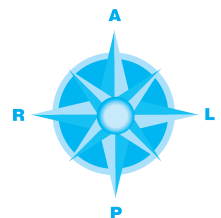
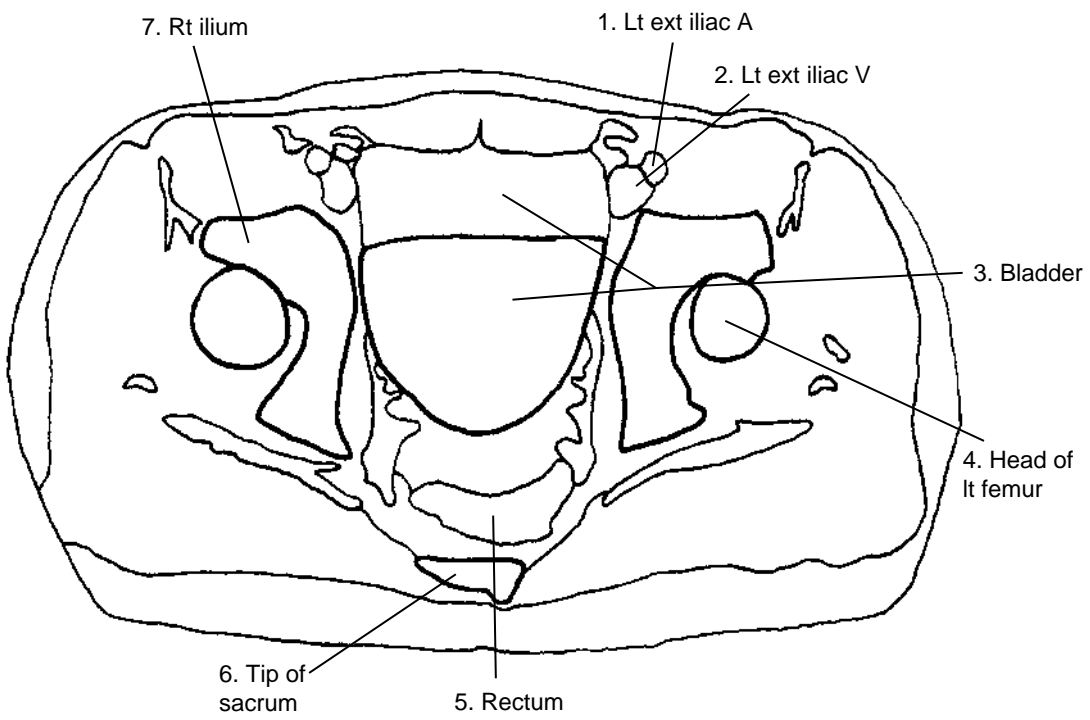
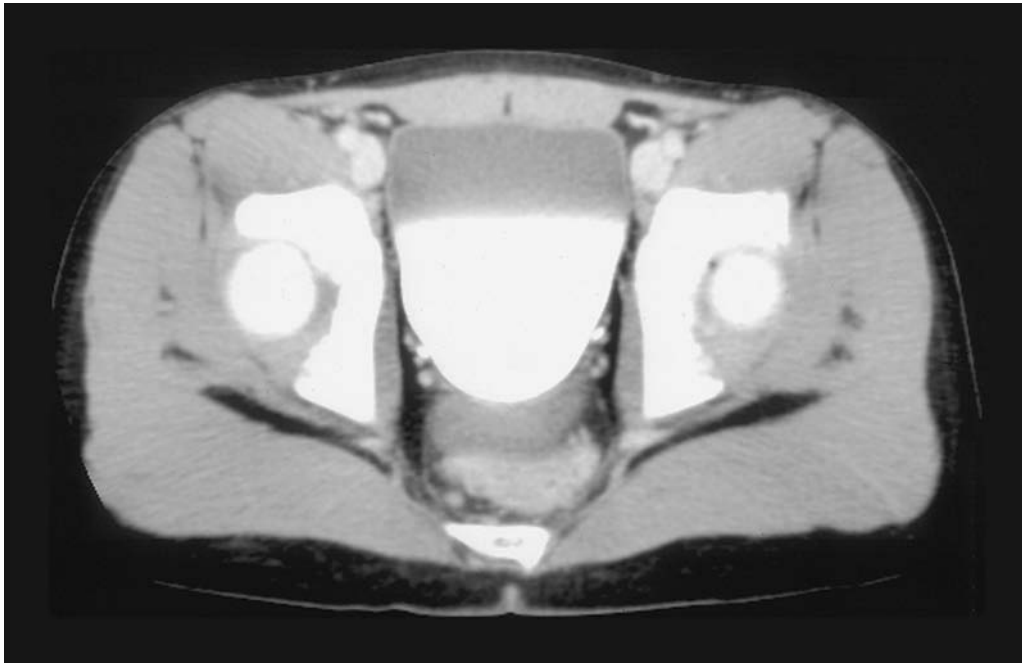
B





**Figure 4–23 (A,B)** Axial CT image 13: Male.

The upper part of the femoral heads are articulating with the iliac part of the acetabula. Similar to previous images, the bladder occupies most of the pelvic cavity and clearly shows a contrast-fluid level. In the anterior pelvic cavity, the left external iliac artery and vein are shown in cross-section lateral to the bladder. Posterior to the bladder, the rectum is found just anterior to the tip of the sacrum.





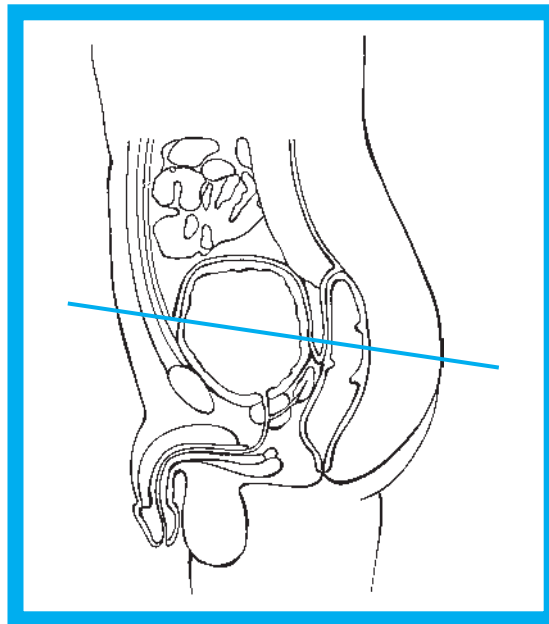
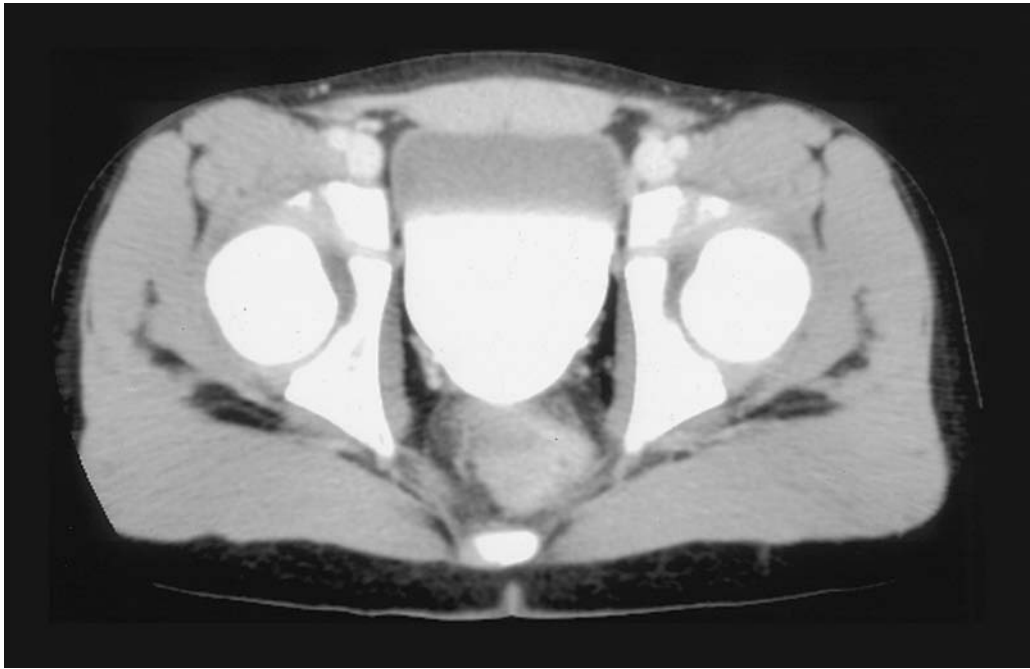
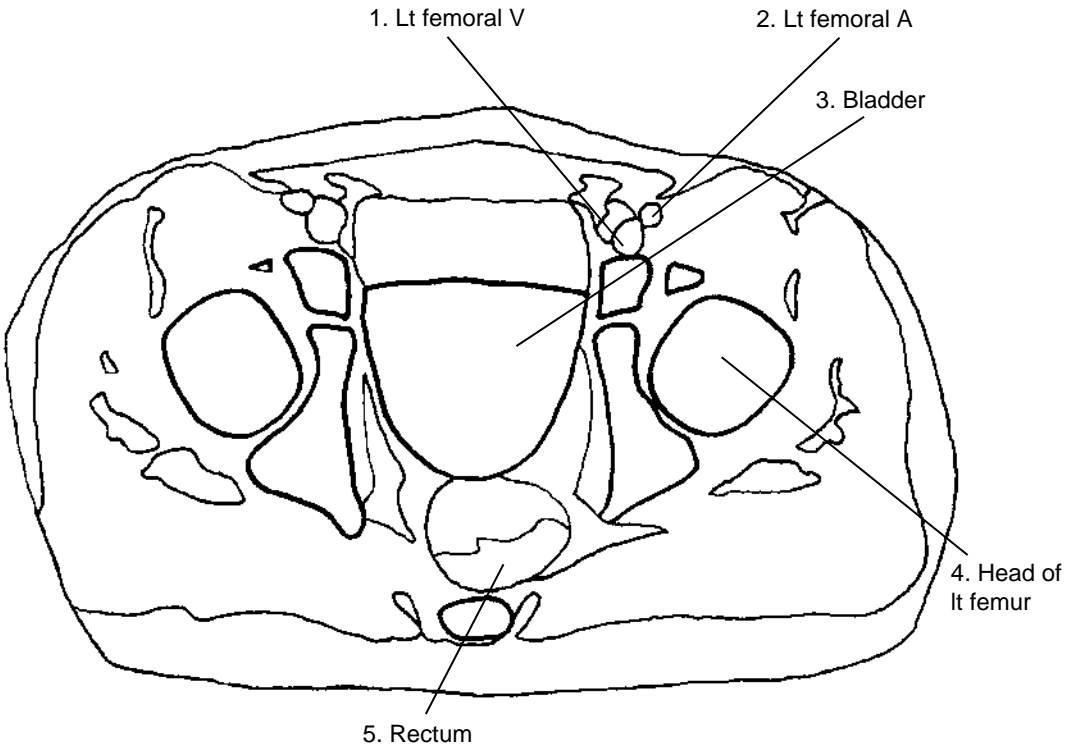


**Figure 4-24 (A,B)** Axial CT image 14: Male.

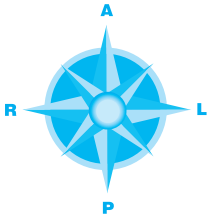
The heads of the femurs are easily identified on either side articulating with the acetabula. Although previous images labeled the bone forming the upper acetabulum as the ilium, the lower half of the acetabulum is formed by the ischial and pubic bones. Similar to previous images, the bladder occupies most of the pelvic cavity, and the rectum is located more posteriorly. In contrast to previous images, the external iliac vessels on either side of the anterior bladder are now labeled as the femoral artery and veins because they are outside of the bony pelvic cavity.

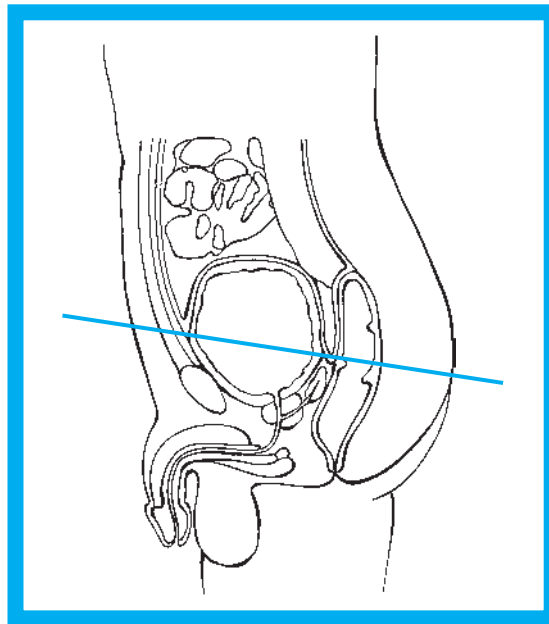


A



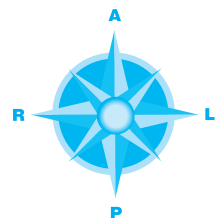
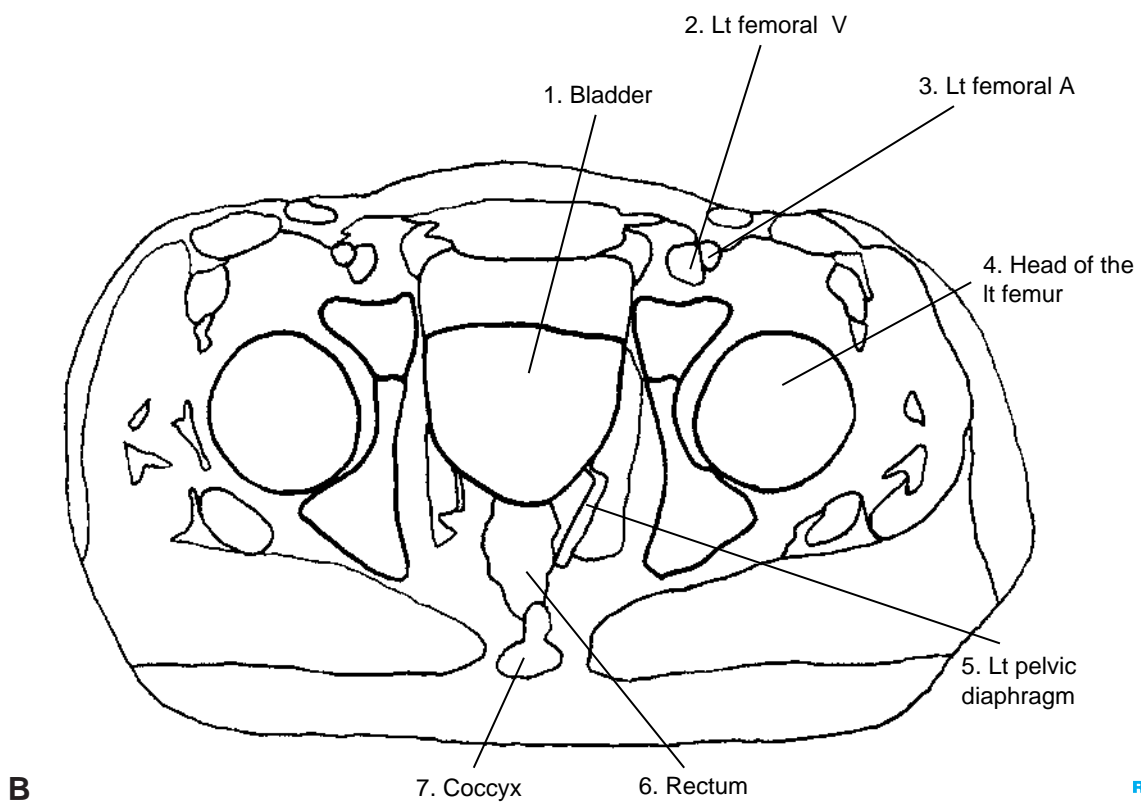
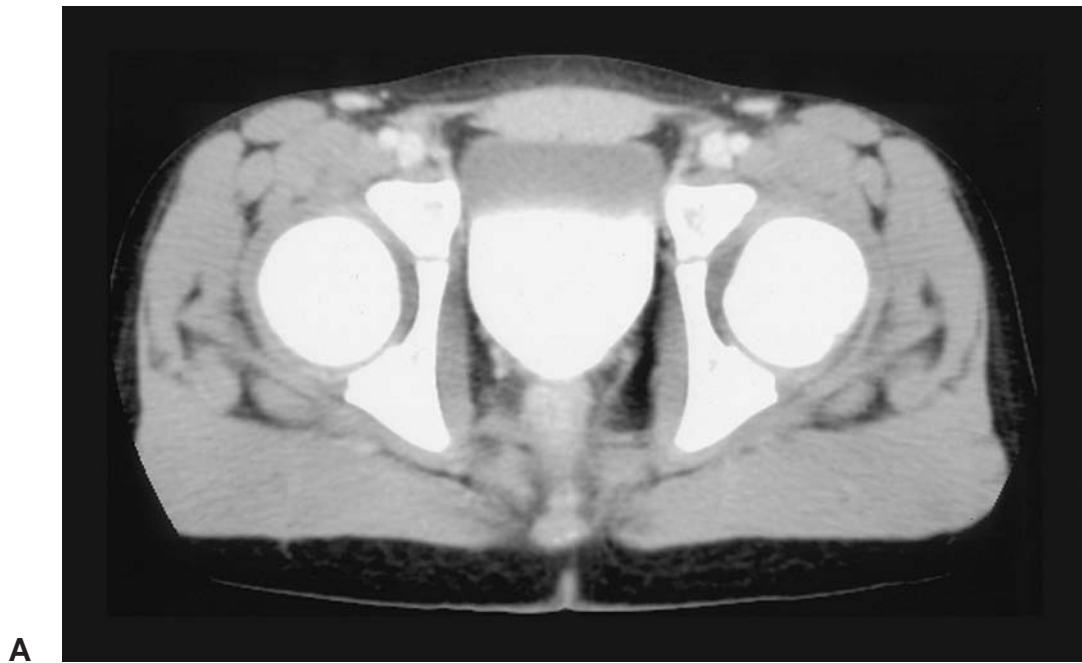
B





**Figure 4–25 (A,B)** Axial CT image 15: Male.

The heads of the femurs are within the acetabula on either side of the lower bony pelvis. Anterior to the pelvic cavity, the femoral arteries and veins are clearly demonstrated outside of the bony pelvis. Within the pelvis, the bladder occupies most of the anterior cavity, and the rectum is the major structure in the posterior pelvic cavity. Lateral to the rectum, the pelvic diaphragm is shown sectioned as it forms a sling across the pelvic cavity. Posterior to the rectum, the sacrum has been replaced by the coccyx, which marks the posterior border of the bony pelvis.



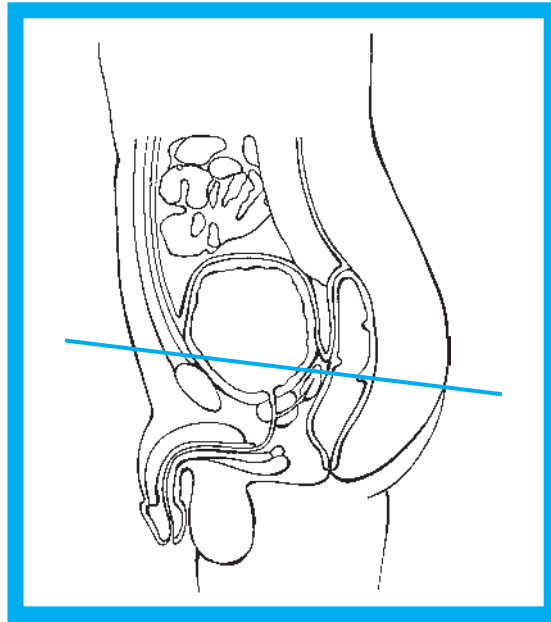
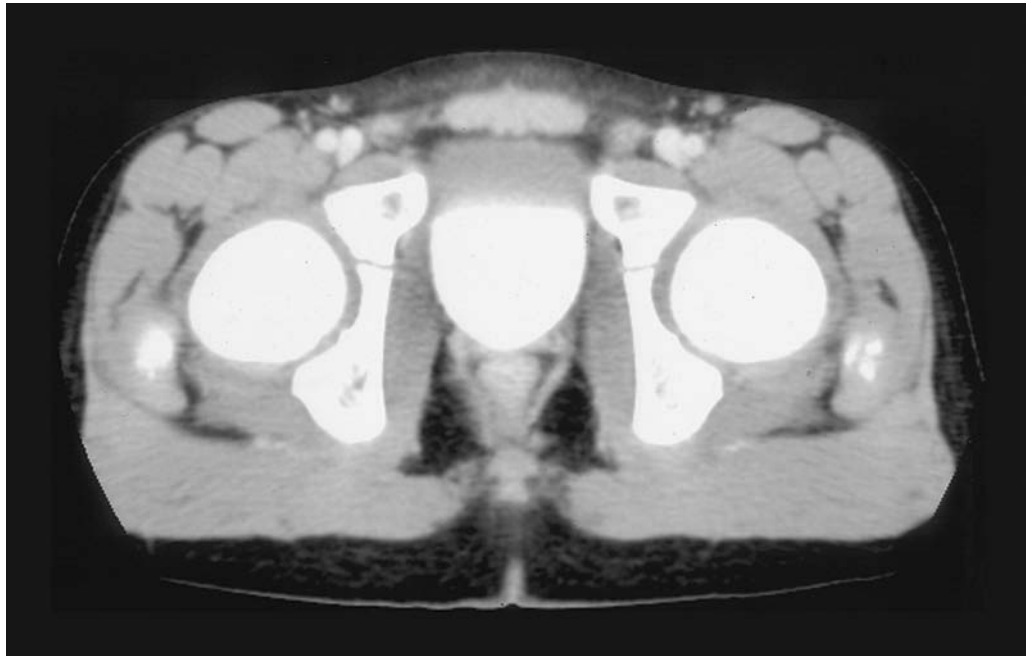
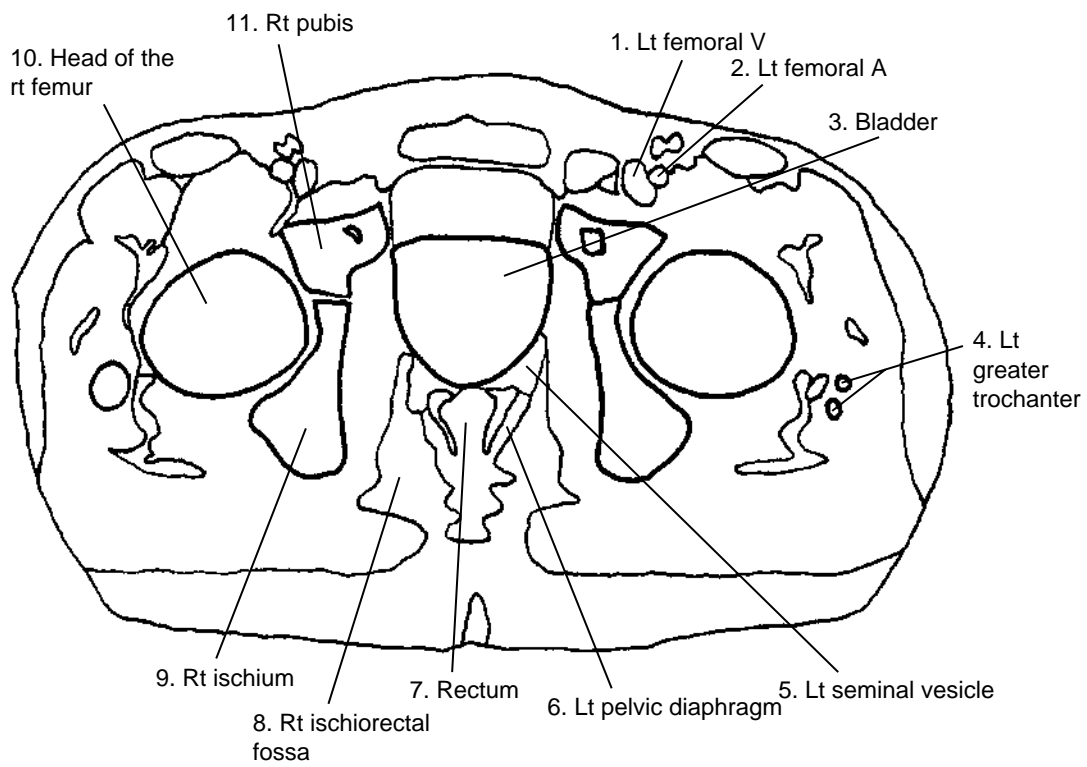


**Figure 4–26 (A,B)** Axial CT image 16: Male.

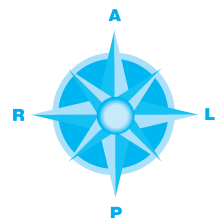
The heads of the femurs can be readily identified as round bony structures on either side of the lower bony pelvis resting in the acetabula. Because this section is through the lower half of the acetabulum, the pubis forms the anterior part and the ischium forms the posterior part. Inside the bony pelvis, the bladder and the rectum are the major structures seen, as in the previous images. Unlike previous images, glandular structures, the seminal vesicles, are now apparent next to the posterior wall of the bladder. As described earlier, the seminal vesicles are located above the prostate gland and are posterior to the bladder. On either side of the rectum, the pelvic diaphragm is shown in cross-section as a thin muscular sheet attached to the bony pelvis forming a sling for the contents of the pelvic cavity. Lateral to the pelvic diaphragm, radiolucent areas representing fat within the ischioanal fossae are demonstrated on either side. Outside the pelvis, the contrast-enhanced femoral artery and vein can be seen in the anterior thigh. As described earlier, the femoral artery is usually smaller and more laterally situated than the femoral vein.



A



B



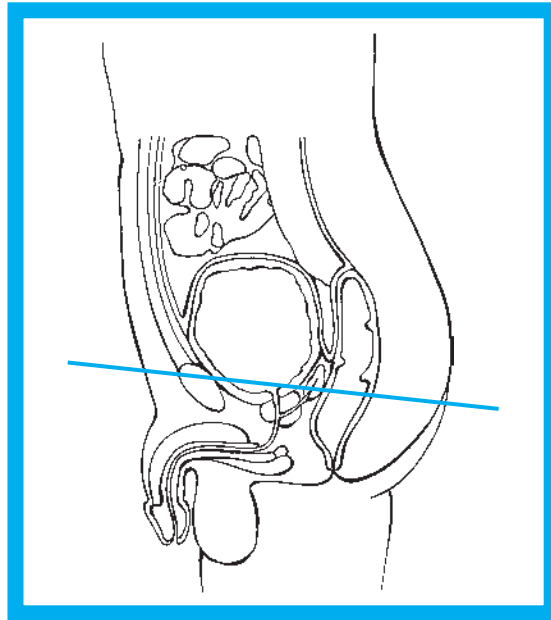
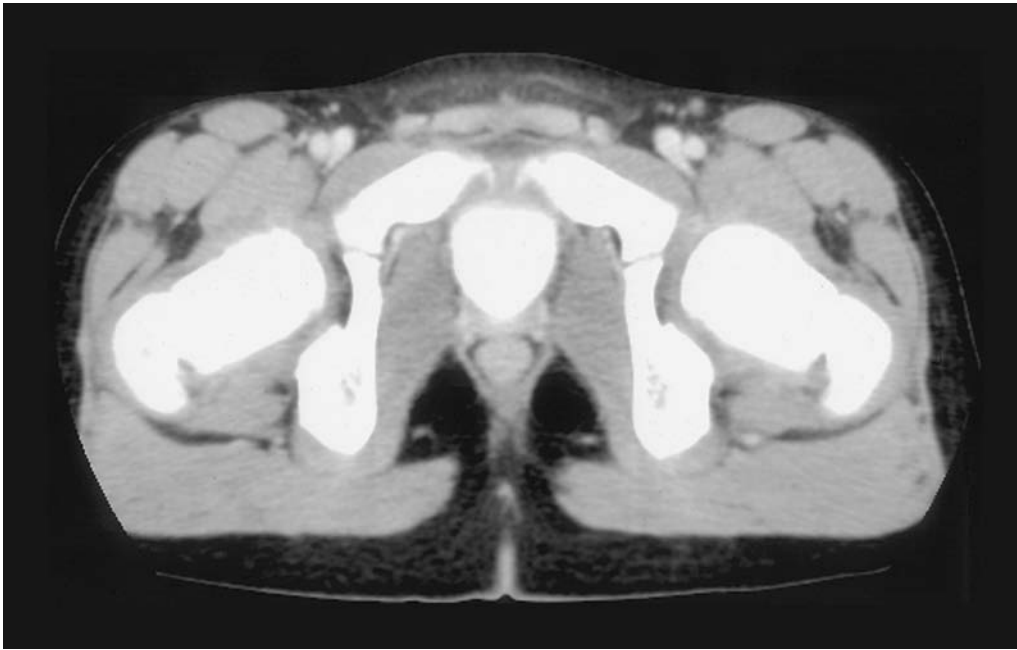
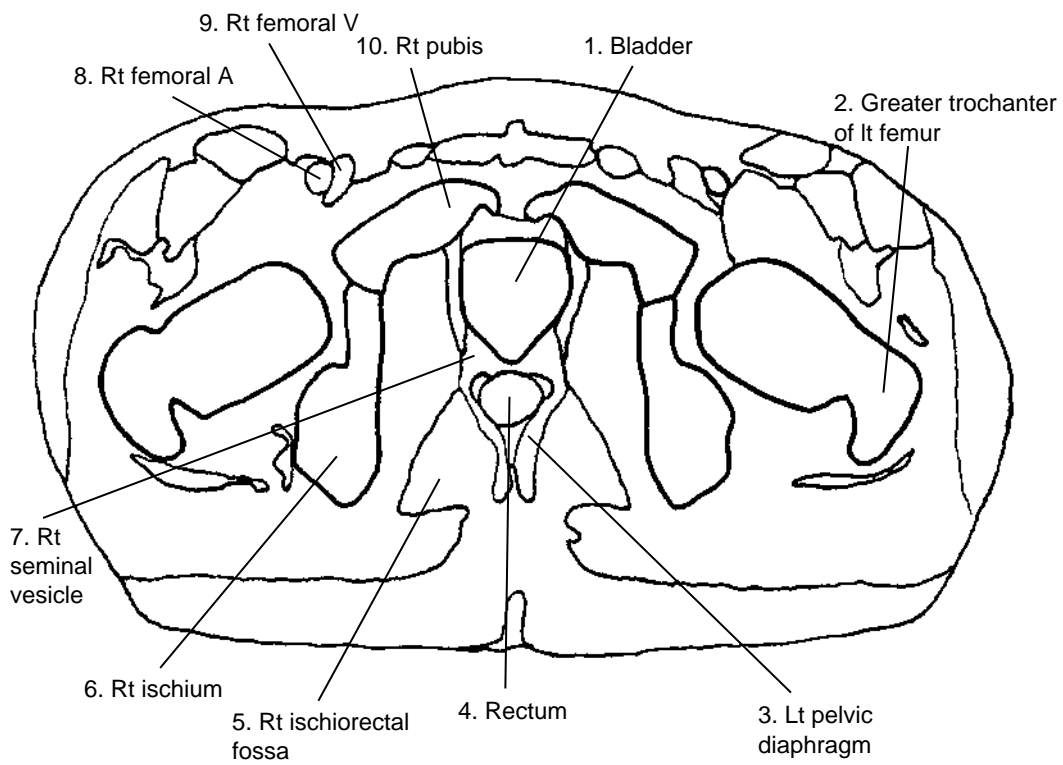


**Figure 4–27 (A,B)** Axial CT image 17: Male.

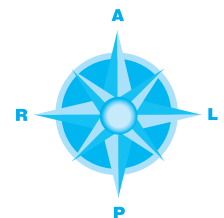
Along with the lower part of the femoral heads, the greater trochanters now appear as large hooklike projections on the posterior femur. The heads of the femurs rest within the lower acetabula formed by the pubic and ischial bones. At this low level, the bladder is much smaller and appears behind the pubic bones. Posterior to the bladder, the seminal vesicles appear larger and are situated between the bladder and the rectum. Similar to the previous image, the pelvic diaphragm is shown in cross-section as a thin sheet of muscle projecting downward, separating the rectum from the fat-filled ischioanal fossae. Much like previous views, the femoral artery and vein are clearly seen anterior to the pubic bones.



A



B





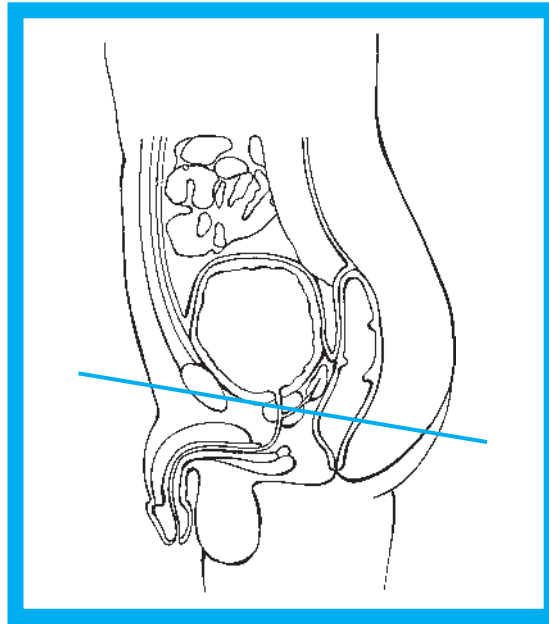
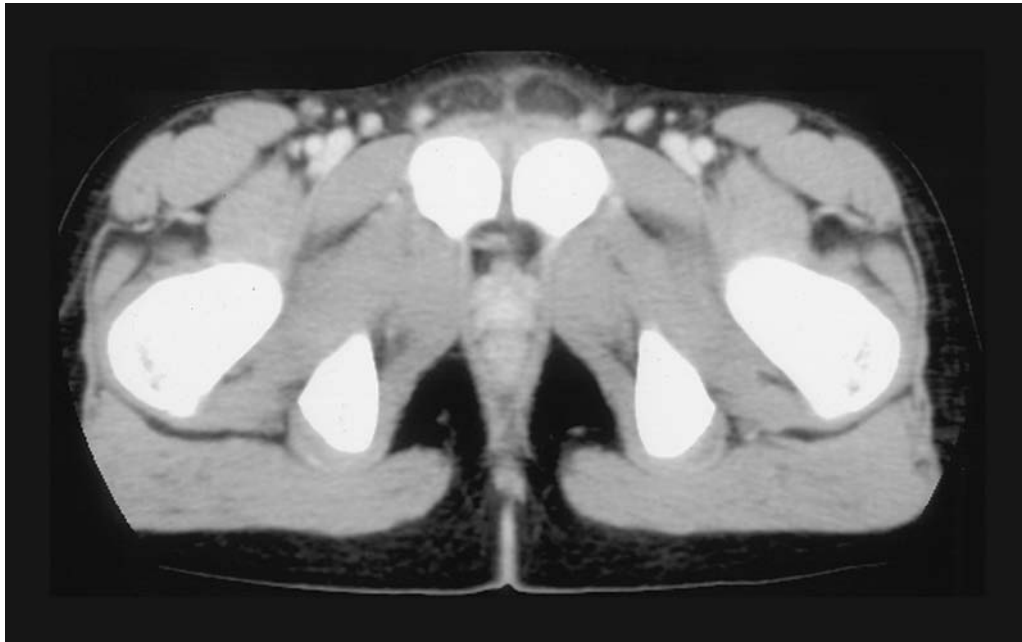
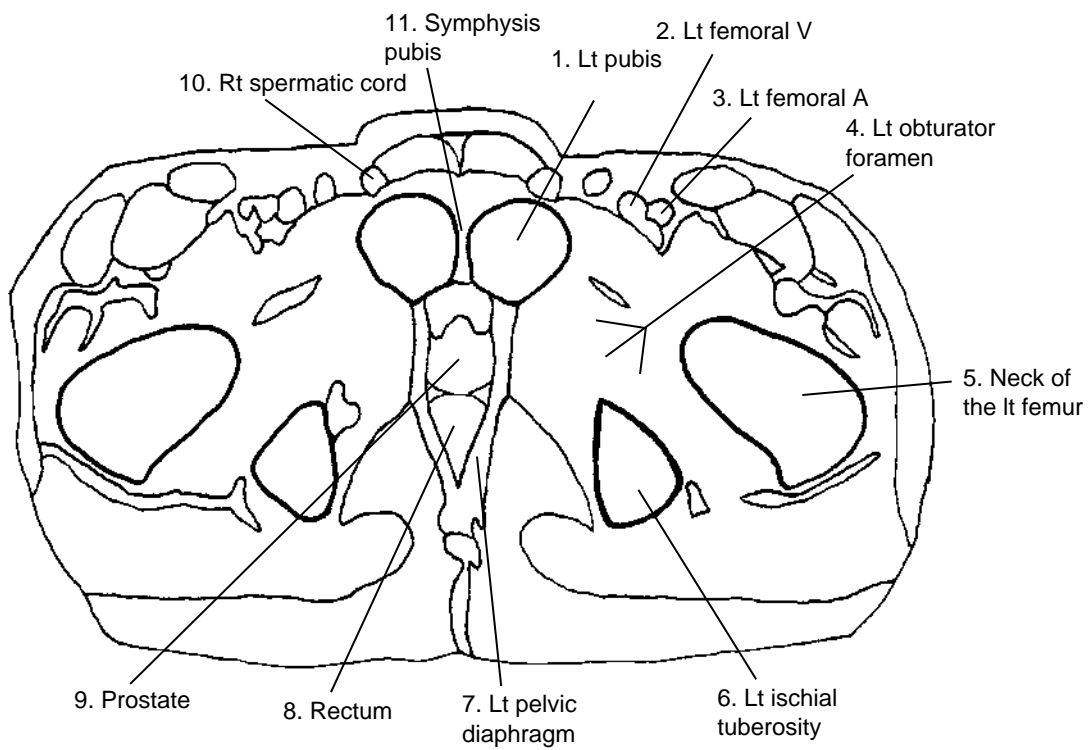


**Figure 4–28 (A,B)** Axial CT image 18: Male.

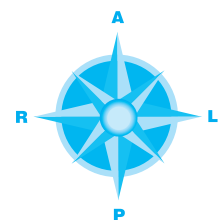
The bony anatomy at the low level through the pelvis has a unique appearance, because none of the bones seems to be attached. The femoral head is no longer present, and the neck is shown obliquely sectioned. In place of the acetabula, the obturator foramina are demonstrated between the pubic and ischial bones. Also, the right and left pubic bones are separated by thick articular cartilage forming the symphysis pubis. Posteriorly, the ischial bones appear expanded compared to previous images, indicating that the level is through the ischial tuberosities. Within the bony pelvis, the bladder is no longer seen and has been replaced by a dense gland, the prostate, which is nearly inseparable from the rectum. Outlining both of these structures, the pelvic diaphragm is shown in cross-section attaching to the pubic bones. Outside of the bony pelvis, the femoral artery and vein are again seen near the anterior surface. Medial to the femoral vessels, the spermatic cords are shown in cross-section as they extend up from the testes to travel over the pubic bones to enter the anterior abdominal wall.



A



B



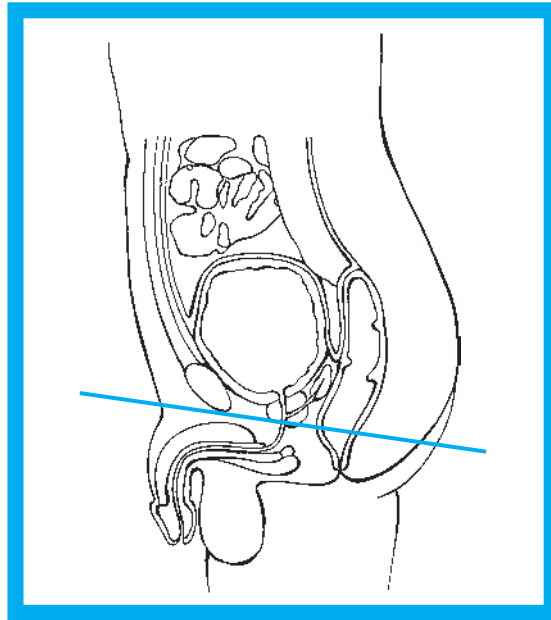
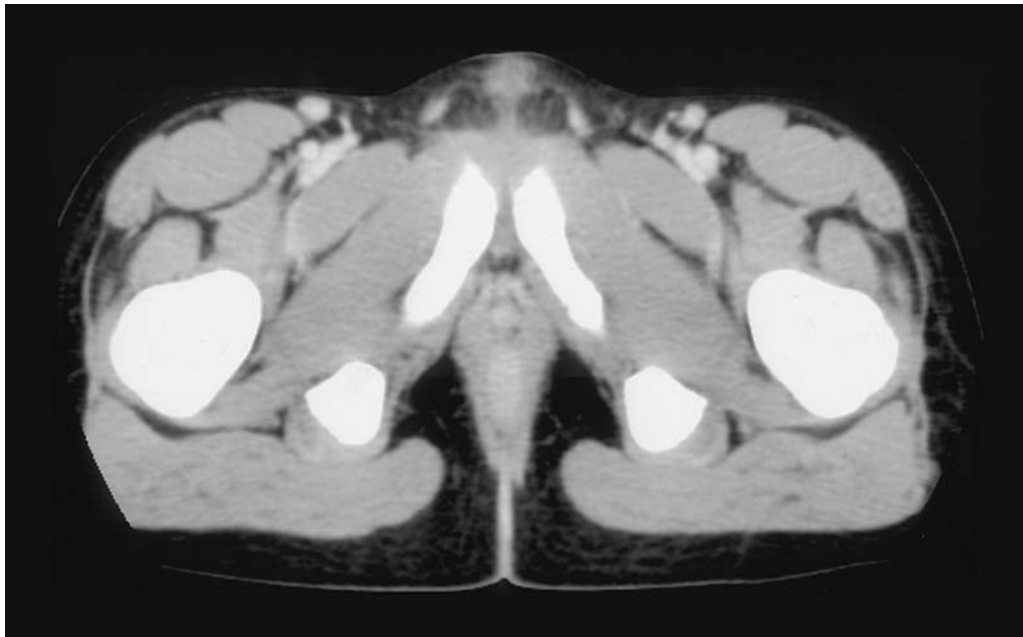
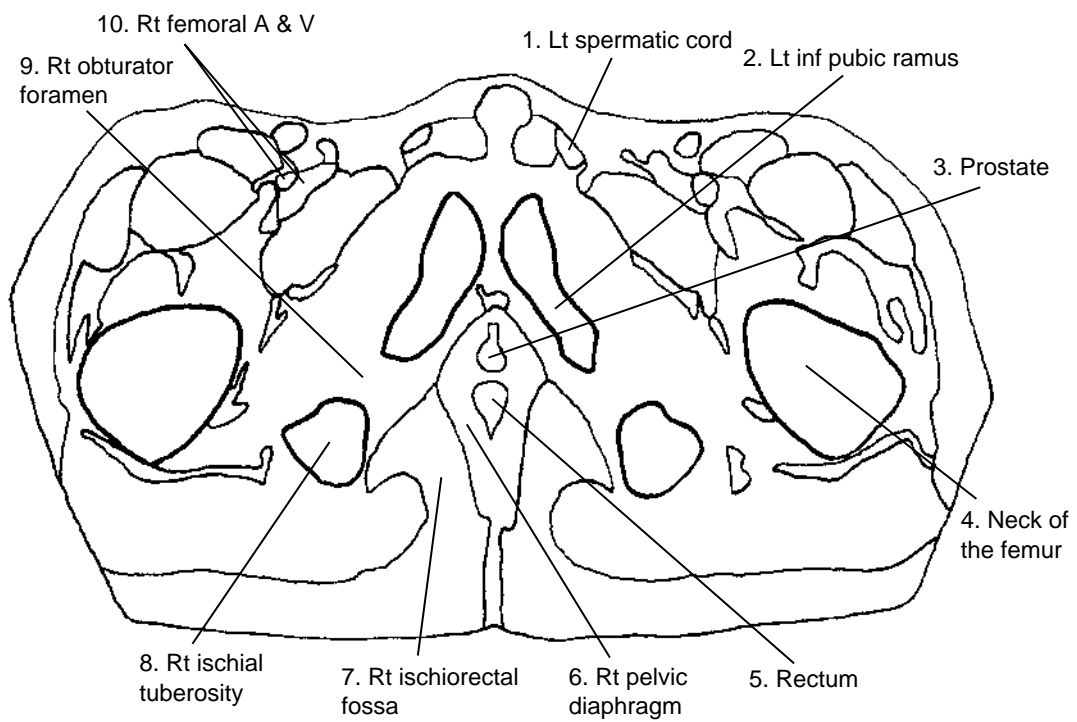


**Figure 4–29 (A,B)** Axial CT image 19: Male.

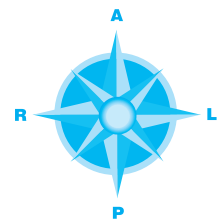
The femurs on either side of the image appear oval-shaped because the section is through the neck. Between the femurs, the enlarged part of the ischial bones, the ischial tuberosities, are separated from the slender inferior pubic rami by the obturator foramina. Within the bony pelvis, the prostate and rectum are surrounded by the pelvic diaphragm. Between the pelvic diaphragm and the ischial tuberosities, the fat-filled areas of the ischioanal fossae are shown on either side and are continuous with the fat in the region of the buttocks. On the anterior aspect of the image, the spermatic cords appear near the surface, whereas the femoral arteries and veins have moved deeper into the musculature of the anterior thighs.

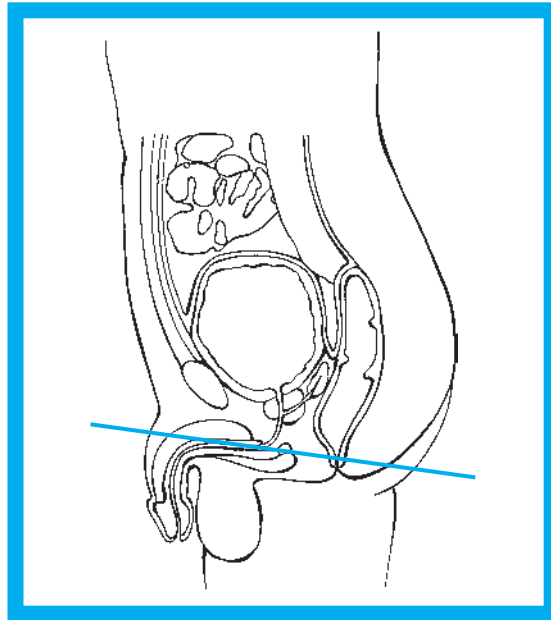


A



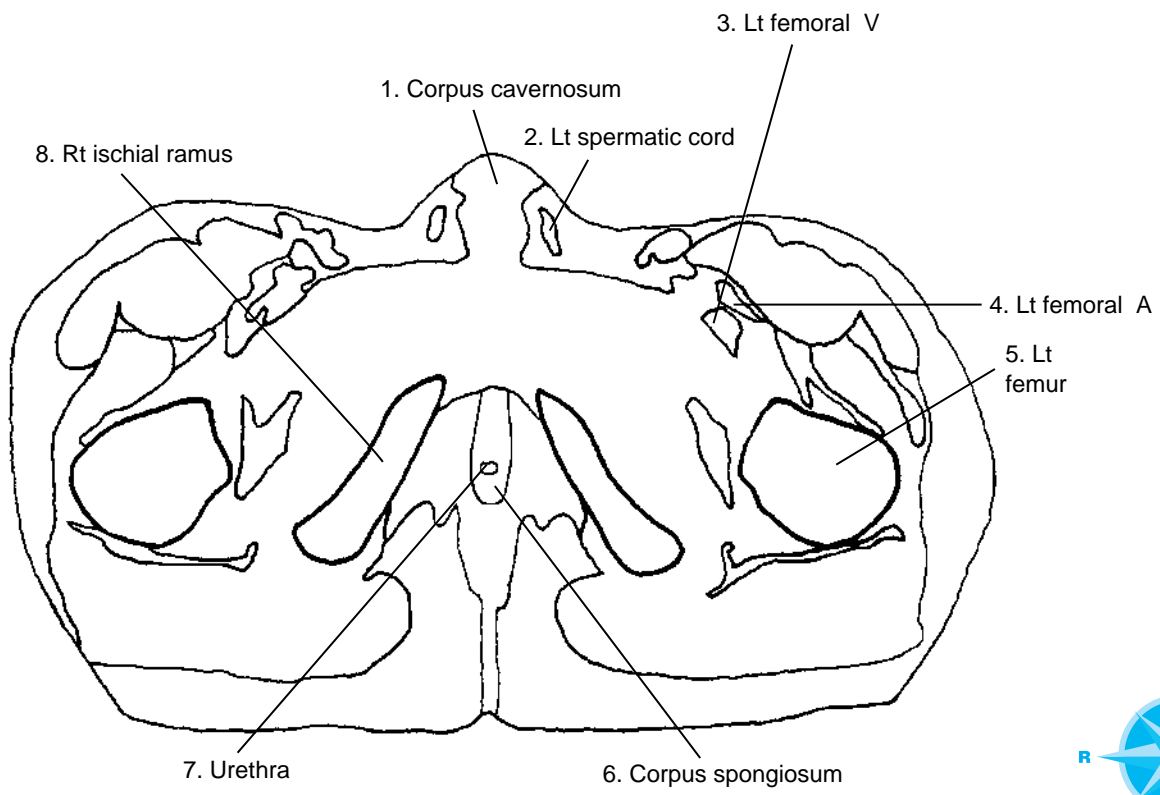
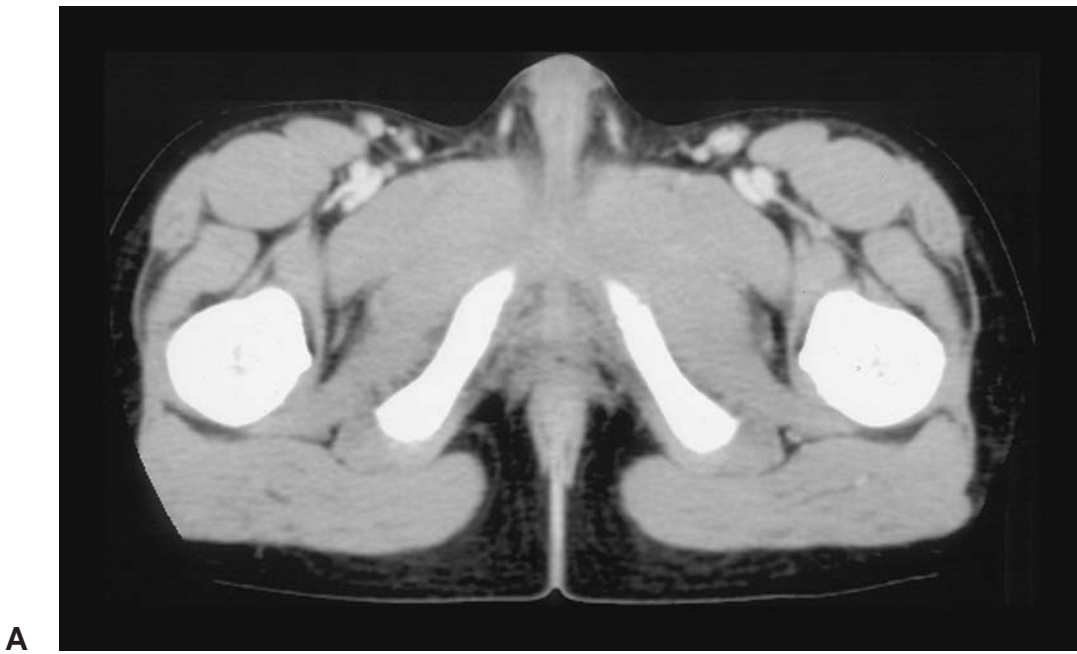
B





**Figure 4–30 (A,B)** Axial CT image 20: Male.

The irregularly shaped femoral bones are shown in cross-section on either side of the image, and the ischial rami appear as long slender bones more centrally located. Between the ischial bones, the prostate and rectum are no longer seen and have been replaced by the corpus spongiosum surrounding the urethra. An erectile tissue of the posterior penis, the corpus spongiosum lies below the pelvic diaphragm and extends out into the penis. By comparison, the corpus cavernosum, forming the anterior erectile tissue of the penis, is sectioned anterior to the bony pelvis. On either side of the corpus cavernosum, the spermatic cords are shown in cross-section as they travel to the testes. The femoral arteries and veins, which previously occupied a superficial position, are found within the musculature of the thighs.



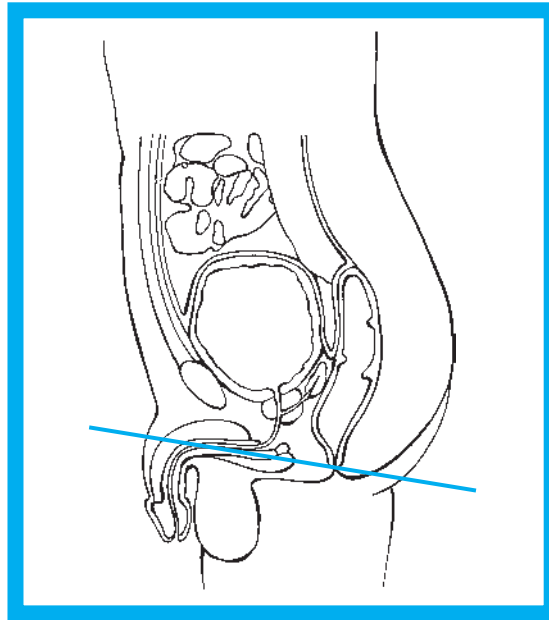
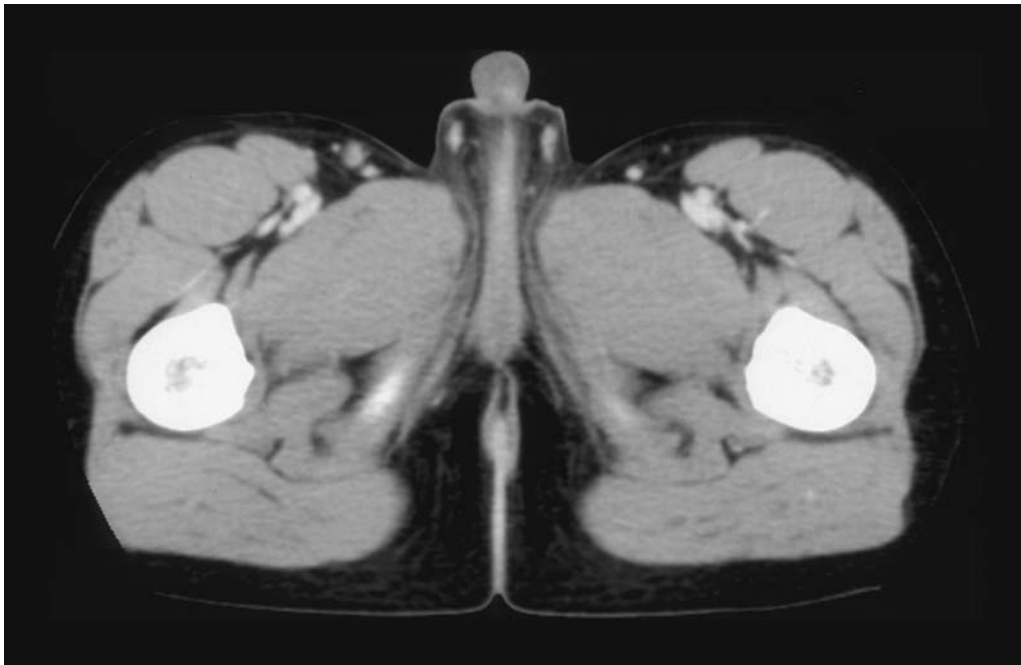
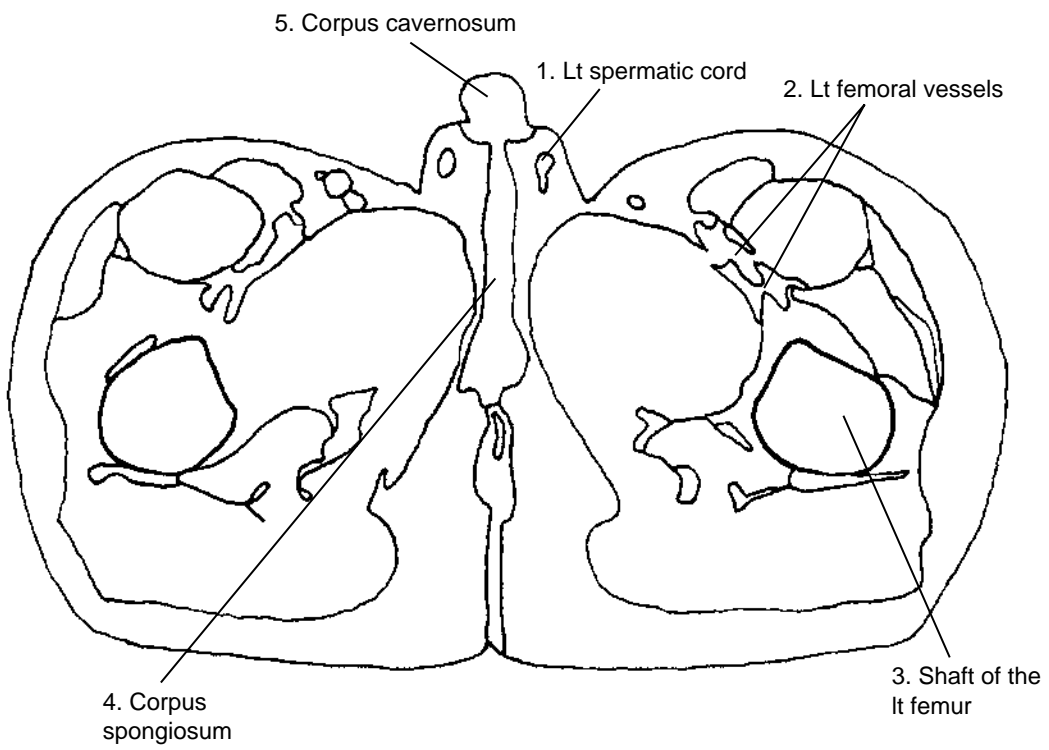


**Figure 4-31 (A,B)** Axial CT image 21:Male.

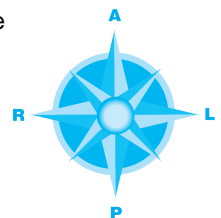
The shafts of the femurs, readily identified on either side, and the absence of pelvic bones indicate that this image is below the level of the pelvis. Typically, this image would indicate the conclusion of an examination of the pelvis. The majority of the structures visualized are muscles in the thighs; however, the corpus spongiosum is demonstrated in longitudinal section extending toward the corpus cavernosum. Together, these two groups of erectile tissue form the penis. On either side, the spermatic cords can be seen superficially, and the femoral vessels are found embedded within the musculature of the anterior thighs.



A



B







## Axial Computed Tomography Images: Female

The following 26 axial computed tomography (CT) images of the female pelvis will be described at 8.0-mm intervals from superior to inferior. The patient was administered 1,000 mL of oral contrast over a 12-hour period; the

images were generated immediately after the administration of 100 mL of venous contrast at the following technical factors: 120 kilovolt peak (kVp) and 150 milliamperesecond (mA-s).

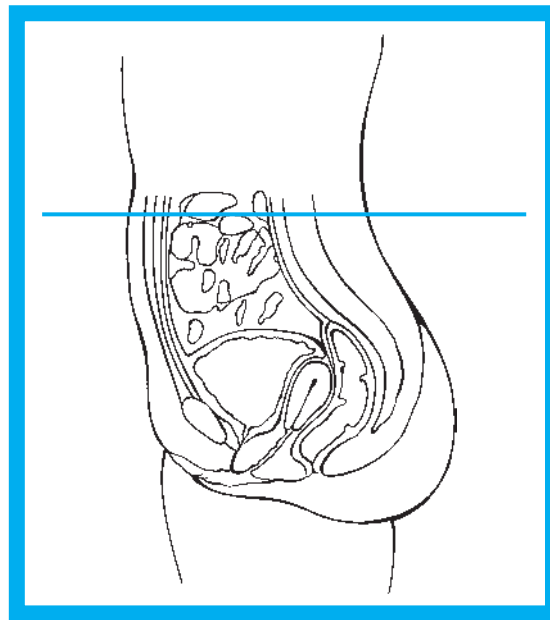
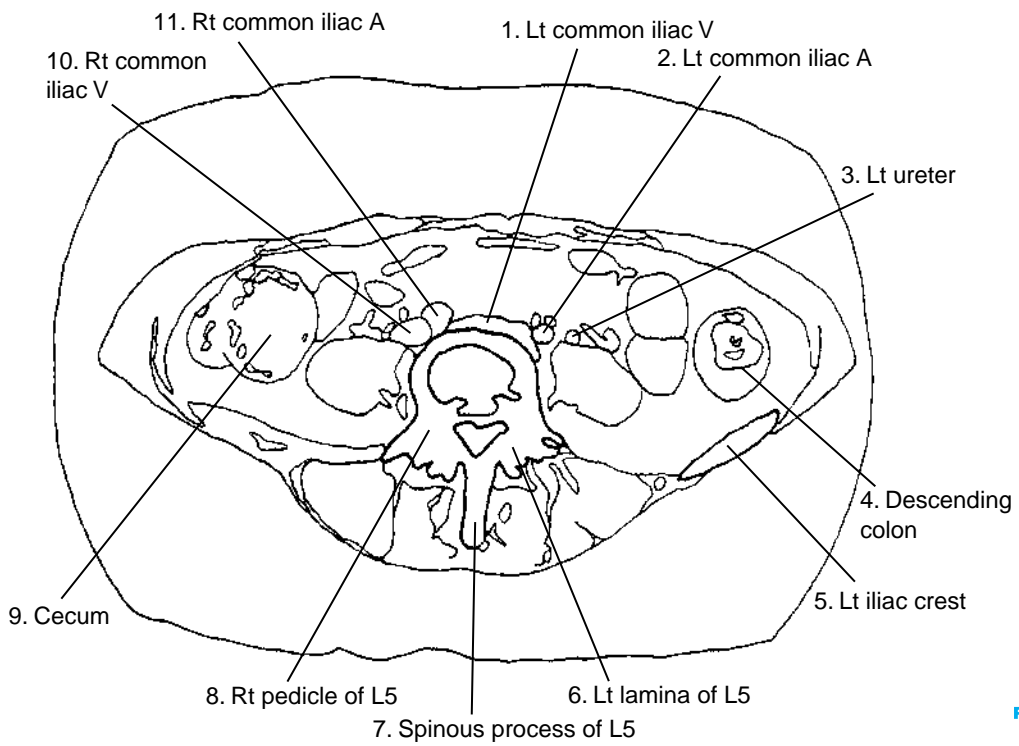


**Figure 4–32 (A,B)** Axial CT image 1: Female.

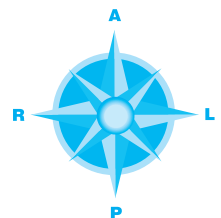
The left iliac crest appears as a thin slice of bone, and the right iliac crest is not yet seen, indicating that this section is located at the upper border of the bony pelvis. Between the iliac crests, the vertebra would be the last of the lumbar, L5. In this image, all of the parts making up the border of the vertebral foramen can be identified, including the pedicles, the laminae, and the spinous process. Anterior to L5, four major vessels are within the upper pelvis. On the right side, the right common iliac vein is slightly larger and more posteriorly situated than the right common iliac artery. On the left side, one round vessel can be distinguished, and the other appears to be in a longitudinal or oblique section. Based on the location, the round vessel can be identified as the left common iliac artery, and the longitudinally sectioned vessel originating from the inferior vena cava can be labeled the left common iliac vein. Lateral to the major vessels, the ureters as well as parts of the large intestine are demonstrated in cross-section. On the far left side, this part of the intestine can be identified as the descending colon by the retroperitoneal location and large size compared to the nearby small bowel. On the right side, the large intestine appears larger than the descending colon and represents the cecum.



A



B



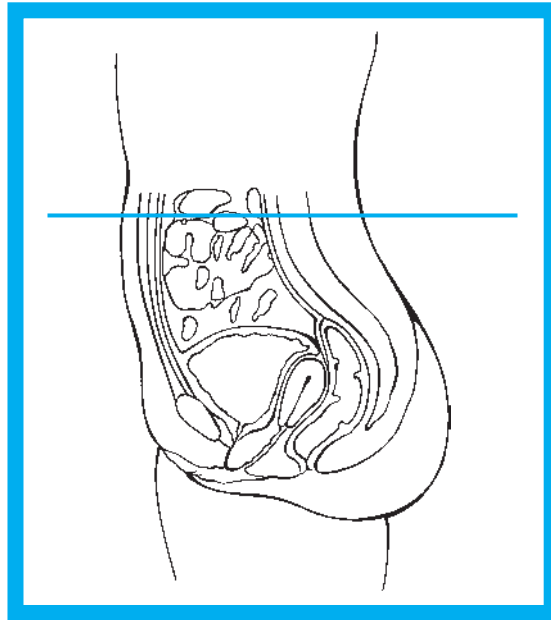
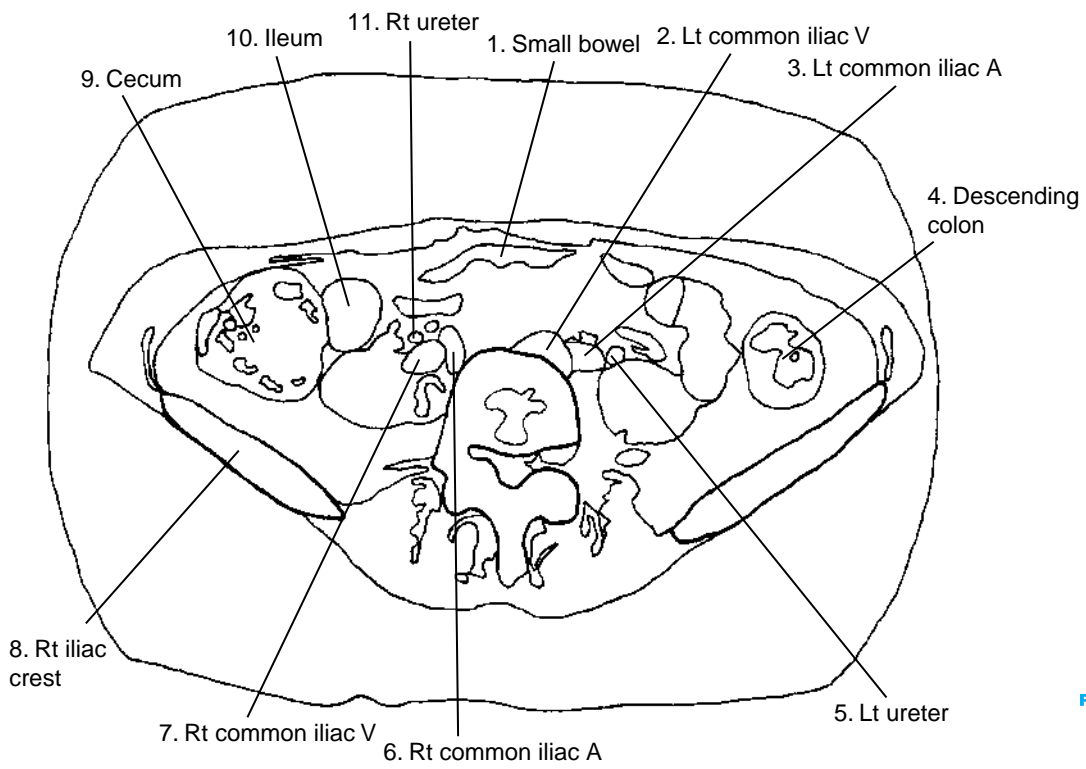


**Figure 4–33 (A,B)** Axial CT image 2: Female.

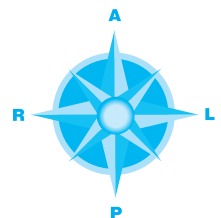
The flat bones sectioned on either side of this image can be readily identified as the iliac crests. Similar to the previous image, the lower part of L5 is demonstrated centrally. Adjacent to the body of L5, four vessels can be distinguished at this level. On the right side, the two rounded vessels represent the right common iliac artery and vein. By comparison, the vein is more posteriorly situated and slightly larger in size. On the left side, the vein is obliquely sectioned as it extends across the vertebral body to the left side to lie adjacent to the common iliac artery. Near the vessels, the ureters can be distinguished owing to contrast enhancement from the other small vessels in the area. With regard to alimentary structures, the descending colon is again shown in a retroperitoneal location on the left side. In this section, the descending colon appears filled with contrast and fecal material. Occupying a similar position on the right side, the cecum appears as an enlarged part of the large intestine containing fecal material and air. Adjoining the cecum, the terminal part of the small bowel, the ileum, is shown in the anterior abdominal cavity.



**A**



**B**



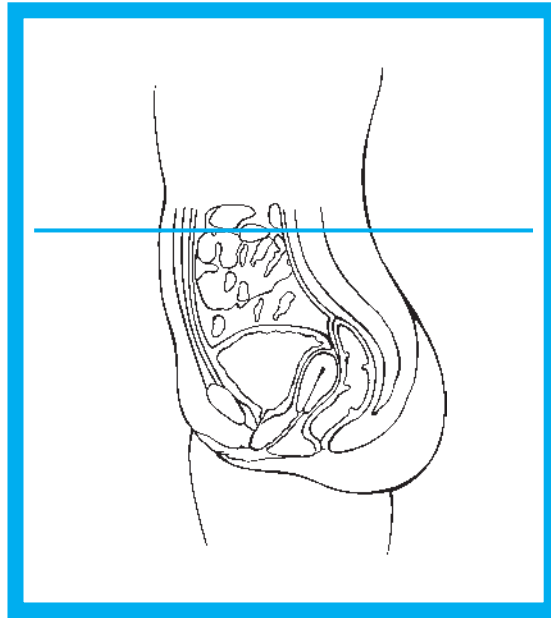
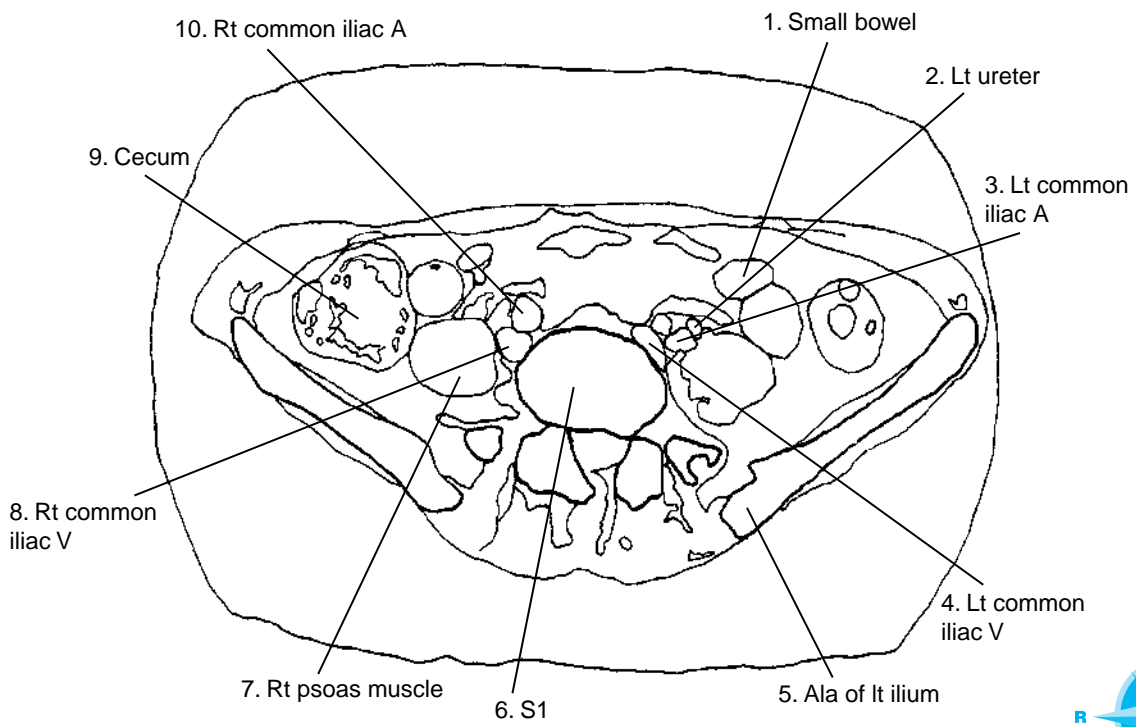


**Figure 4–34 (A,B)** Axial CT image 3: Female.

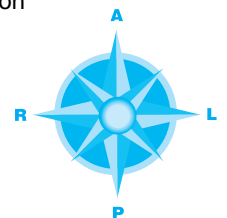
This section demonstrates the right and left alae (wings) of the ilia on either side of upper parts of the sacrum. The sacrum can be distinguished from L5 by the larger size and the lateral parts formed by the fusion of the transverse processes. As described in previous images, the four major vessels can be identified near the body of S1. On the right side, the common iliac artery and vein can again be identified; the vein is more posterior and slightly larger in size. On the left, the vessels are more difficult to distinguish. However, with the aid of adjacent images, the left common iliac artery can be distinguished next to the ureter and the left common iliac vein is obliquely sectioned next to the vertebral body. On either side of the vertebral body, the psoas muscles are shown in cross-section as round muscles that are nearly the same size as the vertebral body. The alimentary structures are much the same as described in the previous section; the enlarged part of the large intestine, the cecum, is shown on the right side, and the contrast-filled small bowel is sectioned in a variety of planes.



**A**



**B**



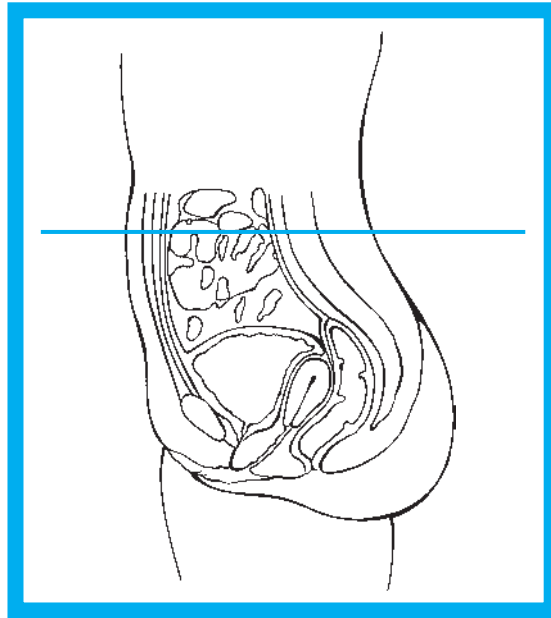
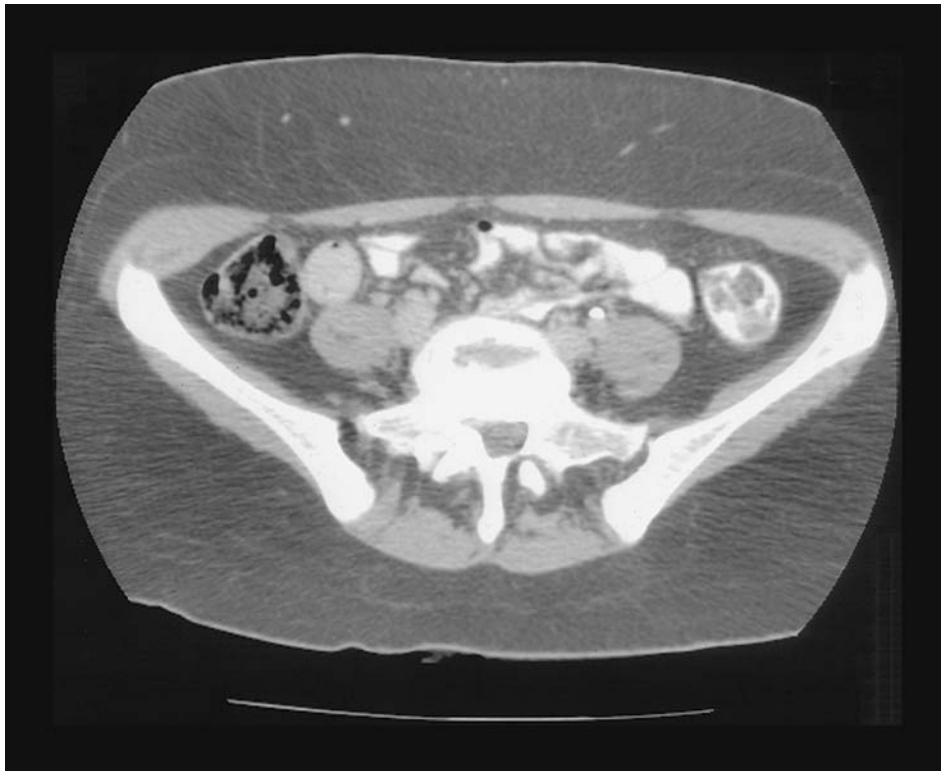
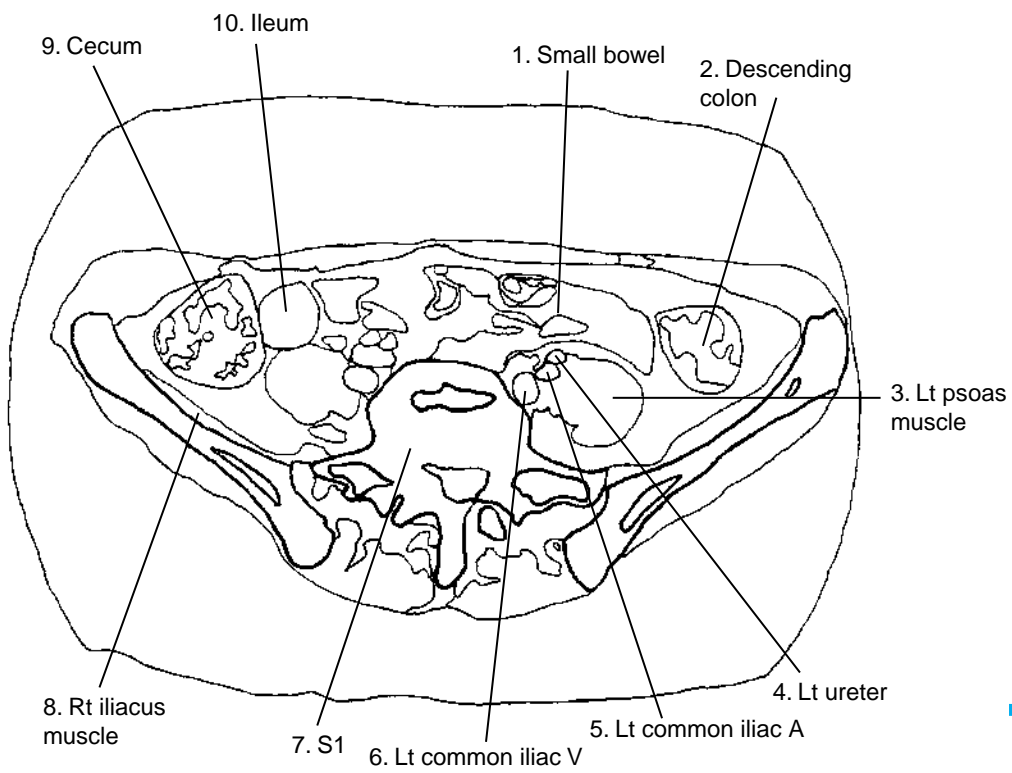


**Figure 4–35 (A,B)** Axial CT image 4: Female.

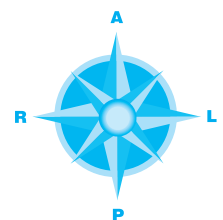
The characteristic “bat” shape of the first sacral vertebra is shown in this image. Adjacent to the alae, the iliacus muscles are shown in cross-section as sheets of muscle covering the anterior surface of the iliac bones. More anteriorly, the psoas muscles are cross-sectioned and nearly equal in size to the vertebral body. Between the psoas muscles, the ureters and major vessels of the pelvis are found adjacent to the vertebral body. Although it is difficult to distinguish the two vessels on the right side previously described, the left common iliac artery and vein are better distinguished at this lower level. The contrast-enhanced ureter lies just anterior to the left common iliac artery and vein. As described previously on the right side, the right common iliac artery is slightly smaller and more anteriorly situated than the common iliac vein. In the anterior pelvis, the descending colon can be labeled on the left side behind the peritoneal cavity owing to its large size and lateral location. The other part of the large intestine shown, the cecum, is seen on the far right side, with the adjoining terminal part of the ileum and various loops of small bowel occupying the anterior pelvis.



A



B





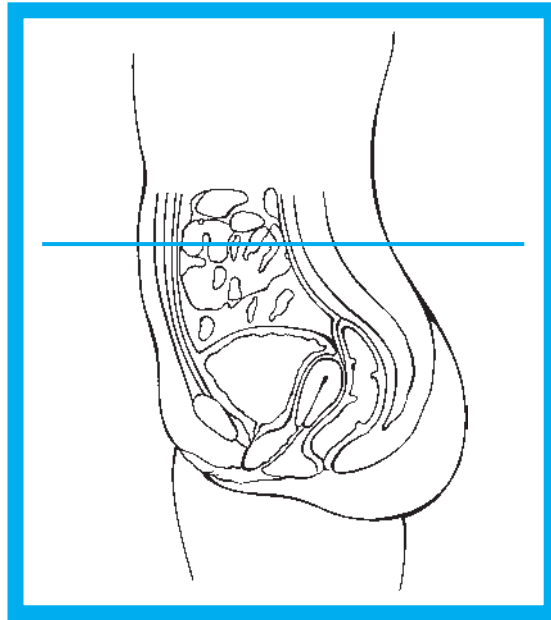
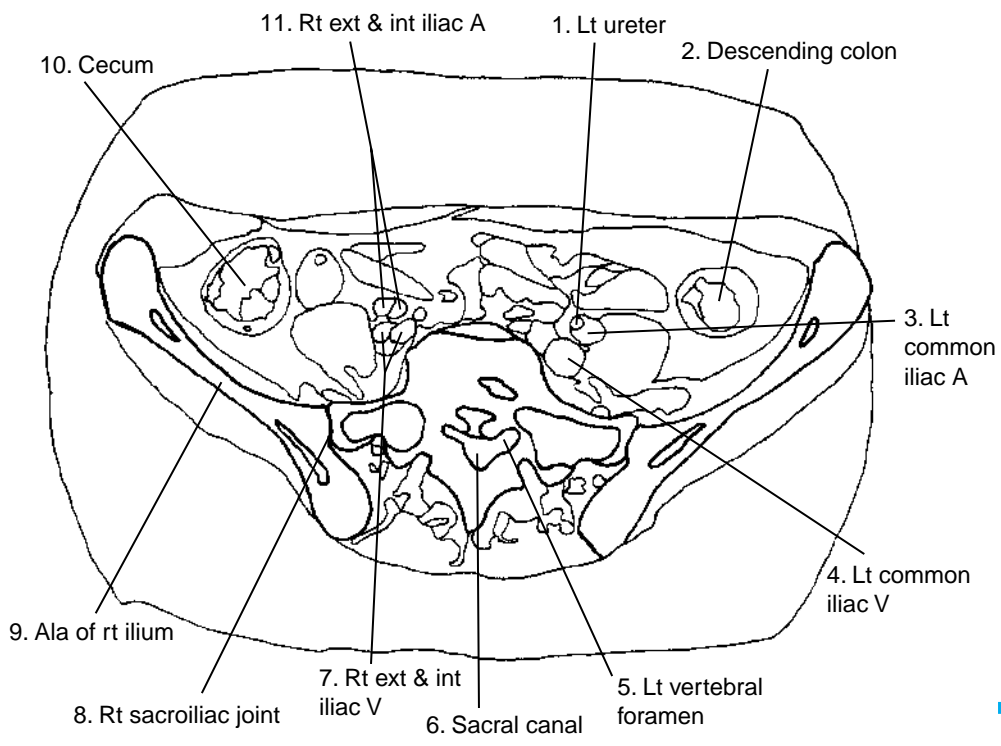


**Figure 4–36 (A,B)** Axial CT image 5: Female.

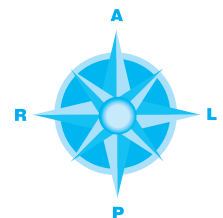
This section passes through more of the sacrum and better demonstrates its unique appearance. Extending from either side of the vertebra, the lateral parts (fused transverse processes) extend to articulate with the iliac bones on either side forming the sacroiliac joints. Between the lateral parts of the sacrum, the sacral canal gives rise to the vertebral foramina that extend through both the anterior and posterior sacrum. Within the bony pelvis, the major vessels are again found adjacent to the vertebral body. However, at this level, four vessels can be identified on the right side. As demonstrated in the previous section, the common iliac artery lies anterior to the common iliac vein. Therefore, the two anterior vessels are labeled the external and internal iliac arteries and the two more posterior vessels are the right external and internal iliac veins. On the left side, two major vessels can be distinguished, the left common iliac artery and the left common iliac vein. Near the vessels, the left ureter can be distinguished because of the contrast enhancement. On the right side, the ureter is not enhanced with contrast in this image and is difficult to distinguish from the other small vessels in the area. Similar to previous images, the anterior part of the pelvis contains the cecum, the descending colon, and loosely organized loops of small bowel.



**A**



**B**



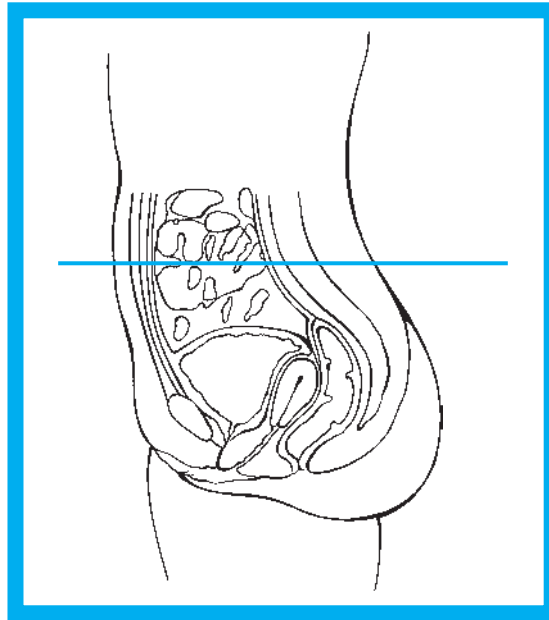
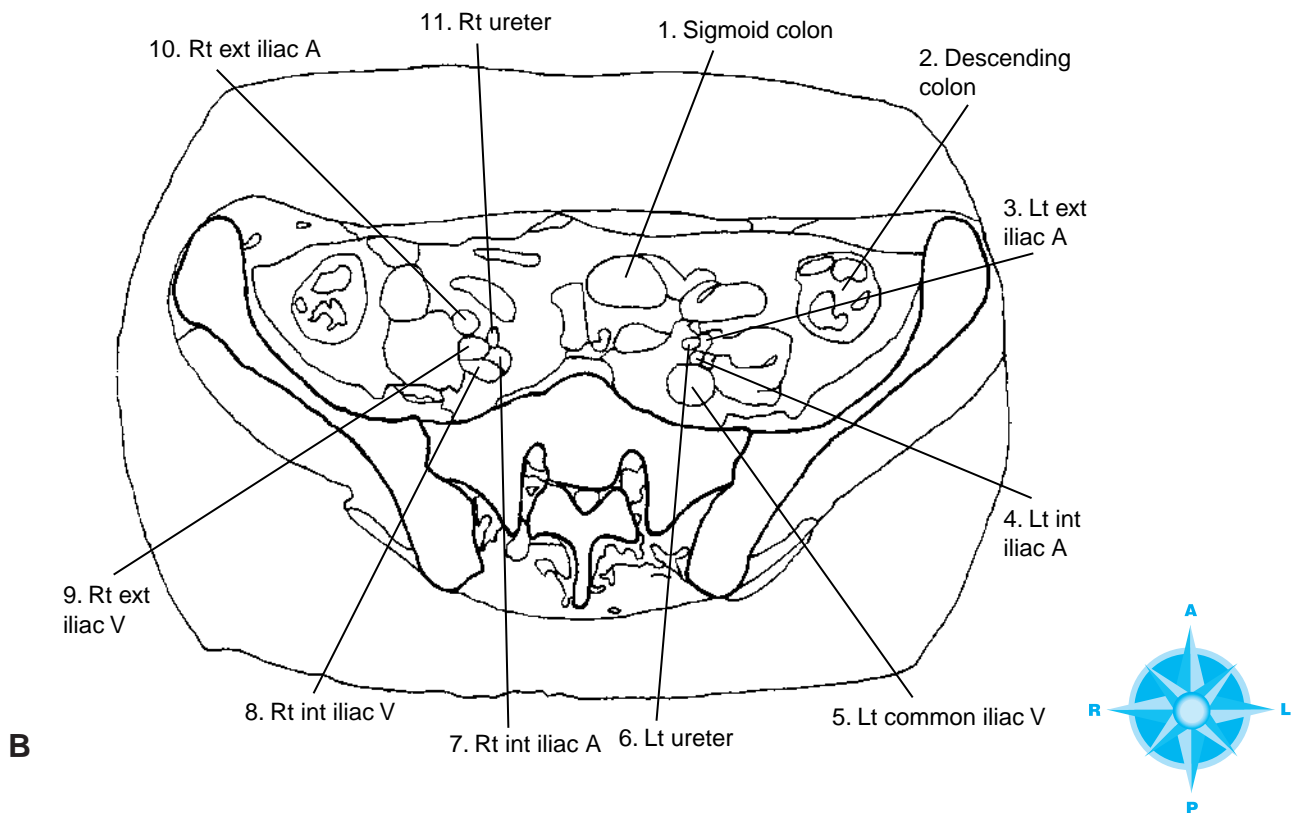


**Figure 4–37 (A,B)** Axial CT image 6: Female.

The upper part of the sacrum is articulating with the iliac bones on either side to form the bony wall of the pelvic cavity. Within the pelvis, a large number of vessels are sectioned on either side of the vertebral body. On the right side, the four vessels previously described have altered in position, and the iliac arteries are now lying near the corresponding veins. Of the four vessels, the external iliac artery is the most anterior and the adjacent vessel represents the external iliac vein. More posteriorly, the internal iliac artery is found directly behind the right ureter, and the adjacent vessel is the right internal iliac vein. On the left side, three vessels can be distinguished; the most posterior vessel is considerably larger than the other two. Based on the previous image, the most posterior vessel would be the left common iliac vein and the other two vessels are the left external iliac artery and the left internal iliac artery. Because the arteries in the pelvis are generally located anterior to the corresponding veins, the iliac vessels on the right side are labeled accordingly. On either side, the contrast-enhanced ureters are adjacent to the iliac vessels. Although the descending colon and the cecum are seen in the upper pelvis, the small bowel previously seen between these structures has been replaced by the sigmoid colon, which is filled with contrast and air.



A



B

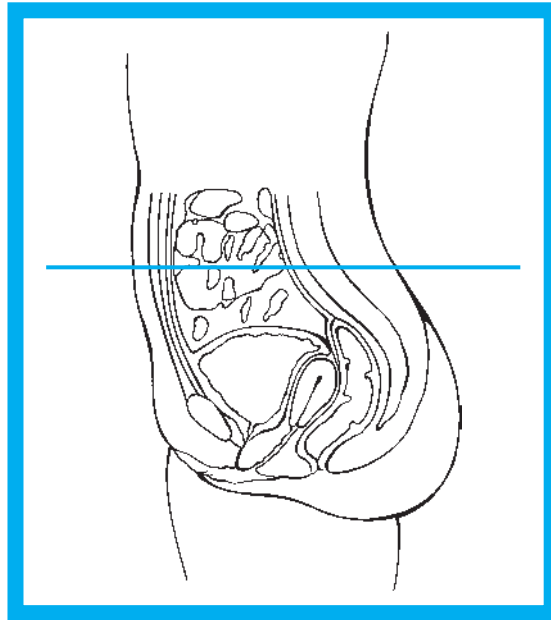
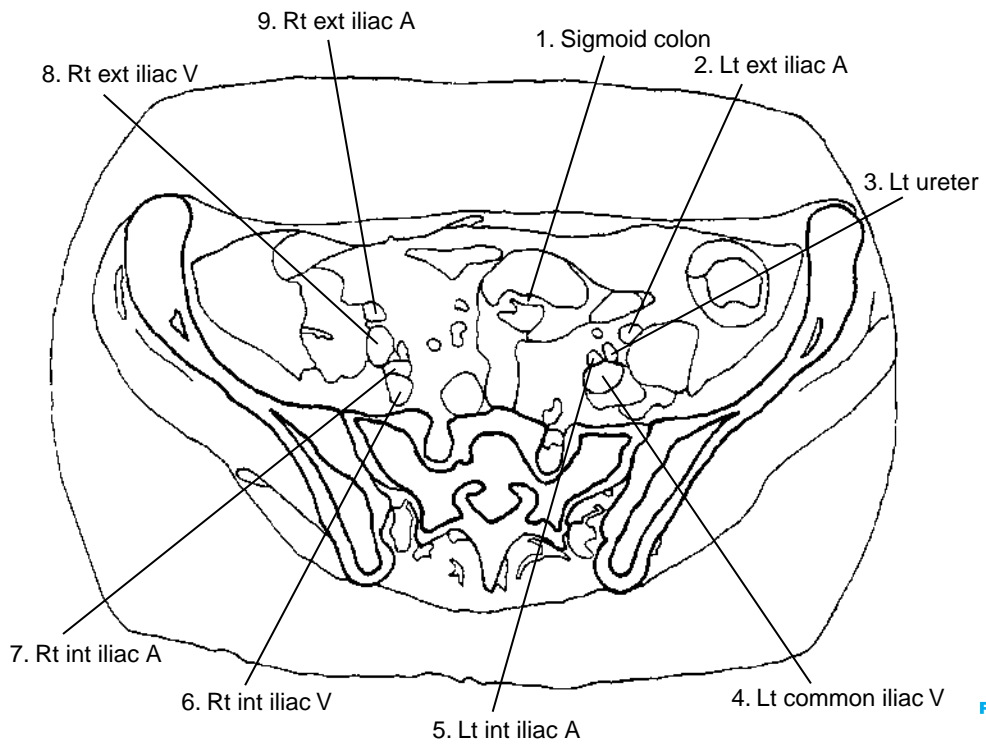


**Figure 4–38 (A,B)** Axial CT image 7: Female.

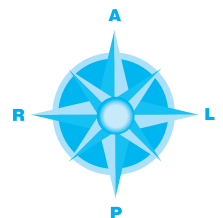
This section is a good example of the batlike appearance of the sacrum; the vertebral body resembles the head of the bat, the spinous process resembles the feet, and the lateral parts extending on either side resemble the wings. Between the lateral parts and the vertebral body, the anterior sacral foramina can be seen, which originate from the sacral canal. The lateral parts of the sacrum articulate with the iliac bones, and together they form the posterior bony wall of the pelvis. Within the pelvis, four major vessels can be distinguished on the right side. Because of the location of the vessels, from anterior to posterior, the vessels can be labeled as the right external iliac artery, right external iliac vein, right internal iliac artery, and right internal iliac vein. On the left side, only three major vessels can be identified: The left external iliac artery, the left internal iliac artery, and the left common iliac vein. In this section, the left common iliac vein has not yet divided into the internal and external iliac veins. Between the major vessels of the pelvis, the sigmoid colon is sectioned, demonstrating the contents to be air and contrast.

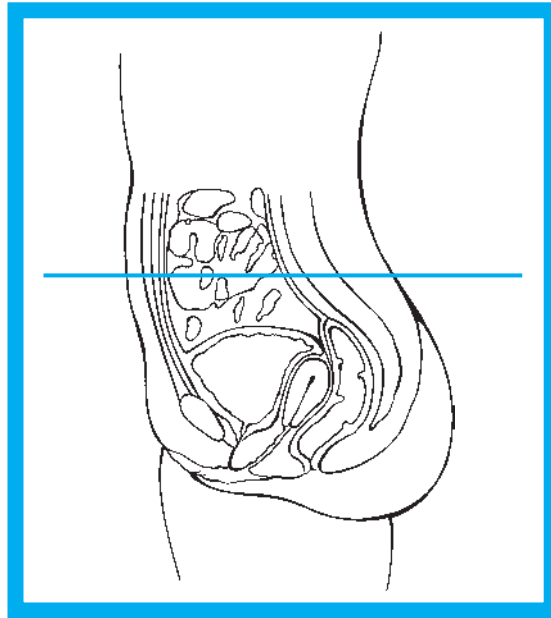


A



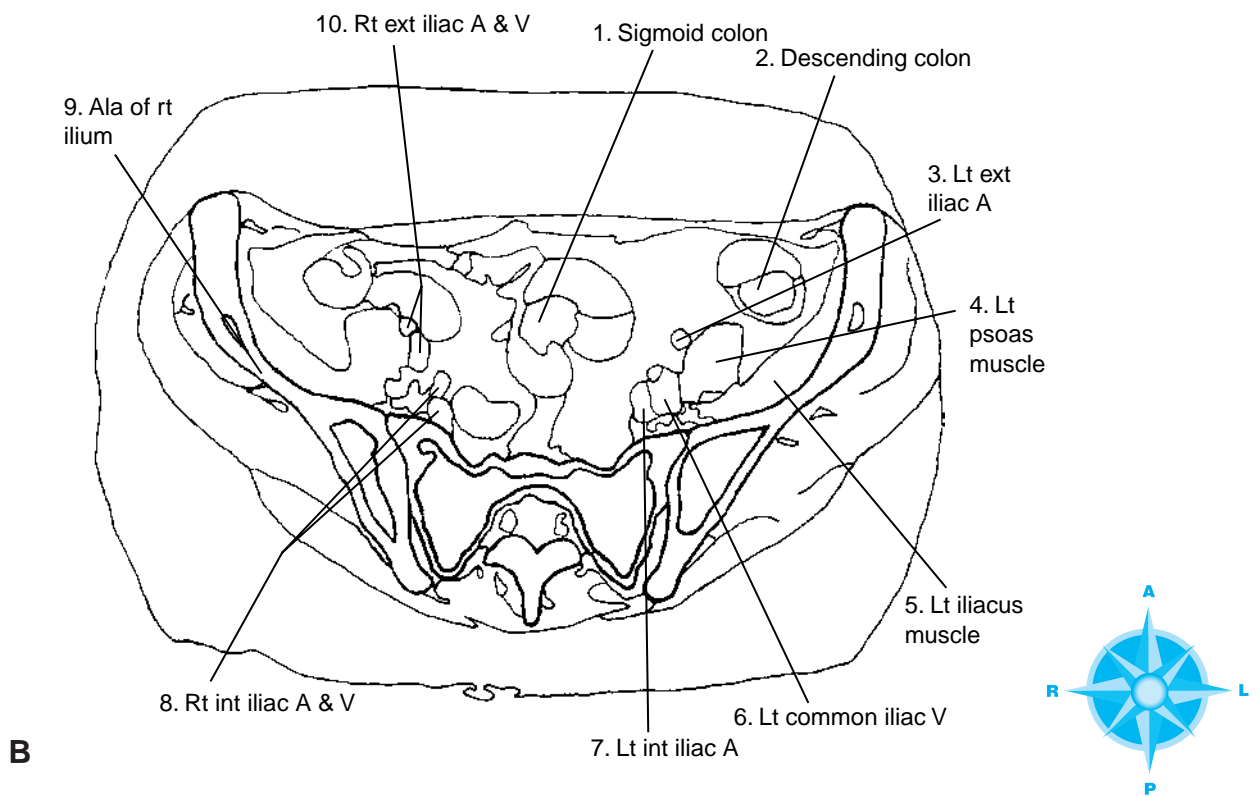
B





**Figure 4–39 (A,B)** Axial CT image 8: Female.

As in the previous image, the sacrum is articulating with the iliac bones on either side, which appear as irregularly shaped flat bones in axial section. Lining the anterior surface of the iliac bones, the iliacus muscles are on either side adjacent to the psoas muscles, originating from the transverse processes of the lumbar vertebrae. Together, the iliopsoas muscles travel downward through the pelvis to insert on the lesser trochanters of the femurs and act to flex the thighs. Medial to the psoas muscles, the major vessels of the pelvis can be seen in cross-section. Although there are four vessels that can be identified on the right side as the external and internal iliac arteries and veins, there are still only three vessels distinguishable on the left side. Based on location, the three vessels can be identified; the most anterior is the left external iliac artery, the most posterior is the left internal iliac artery, and the other is the larger left common iliac vein. Also within the pelvic cavity, the sigmoid colon is shown centrally and is a continuation of the descending colon sectioned on the left side of this image.





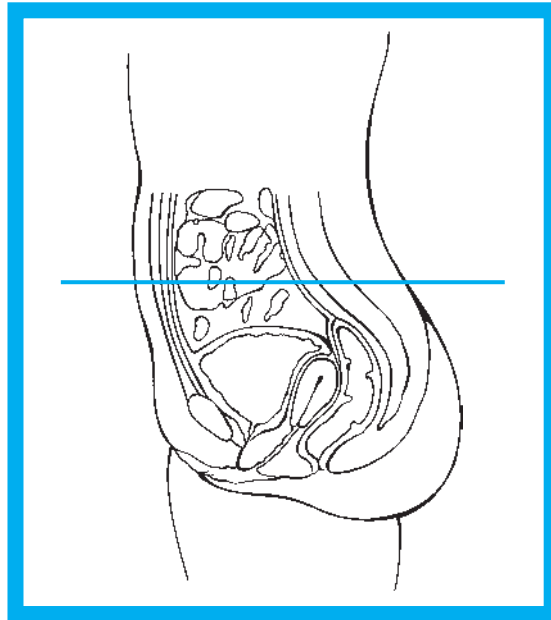
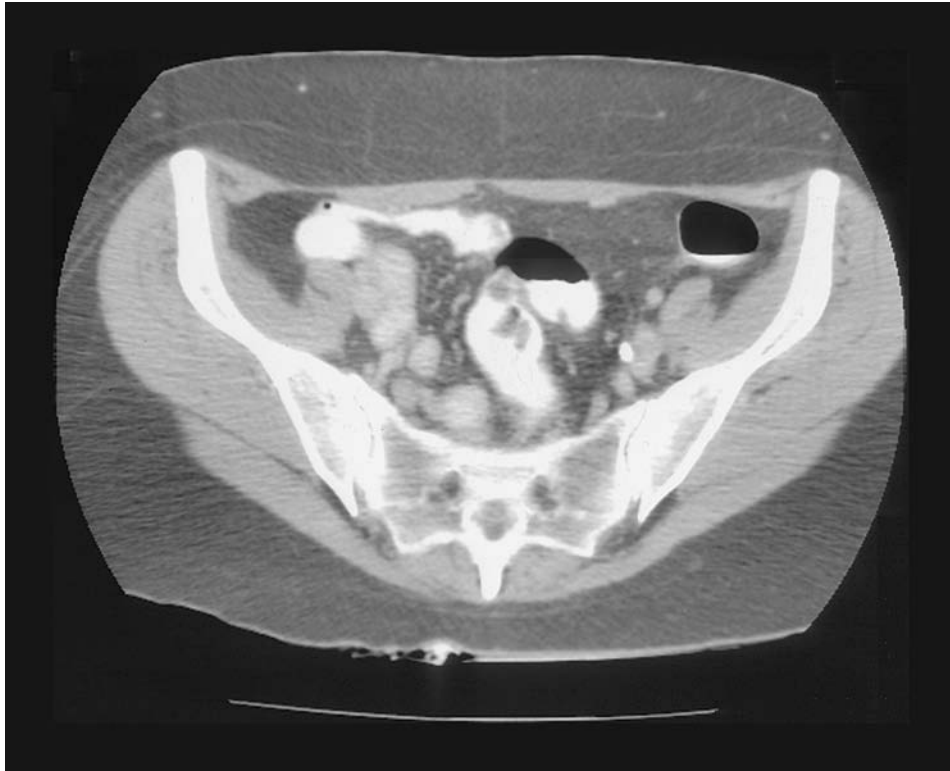
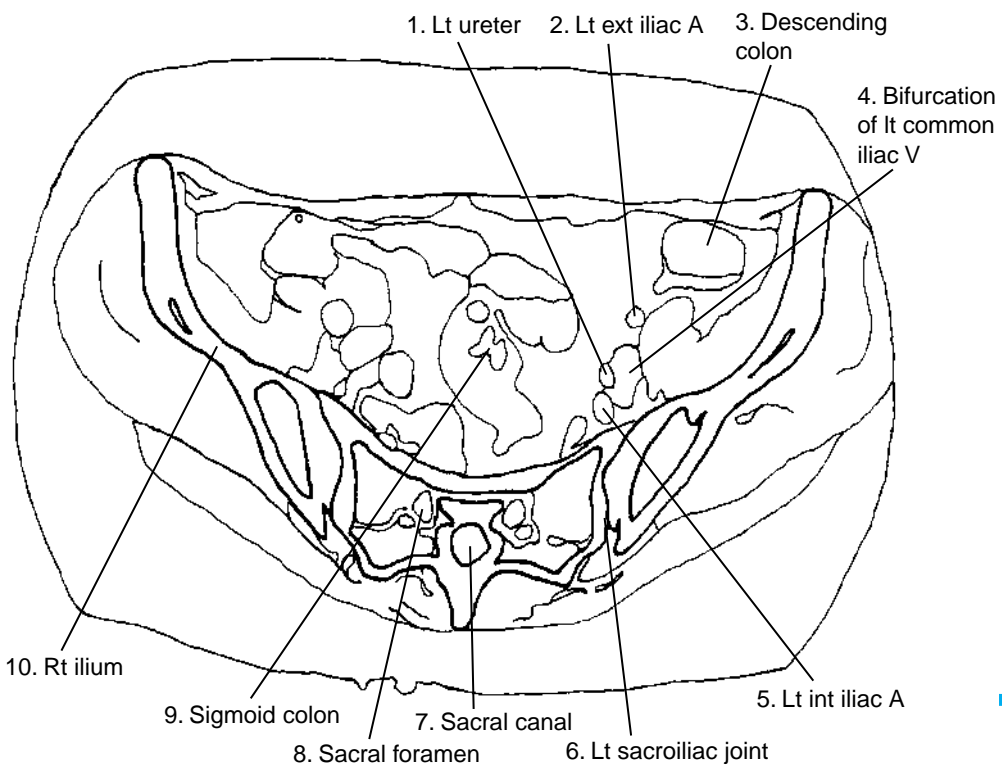


**Figure 4–40 (A,B)** Axial CT image 9: Female.

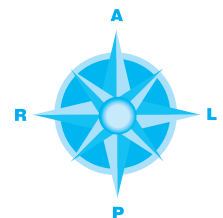
The sacrum is adjoining the iliac bones on either side, forming the right and left sacroiliac joints. Within the sacrum, several foramina can be identified. The largest and centrally located foramen represents the sacral canal containing the cauda equina, which is a collection of spinal roots that descend from the lower part of the spinal cord. On either side of the sacral canal, sacral foramina extend to both the anterior and posterior surfaces of the sacrum and transmit the sacral spinal nerves. Within the bony pelvis, the sigmoid colon occupies a central location. The sigmoid colon can be identified by its large diameter, characteristic S shape, and location near the descending colon. Although the right ureter does not appear contrast enhanced in this section, the contrast-enhanced left ureter is easily identified between the left external and internal iliac arteries. Adjacent to the left ureter, the large vessel represents the point of bifurcation of the left common iliac vein into the internal and external iliac veins.



**A**



**B**



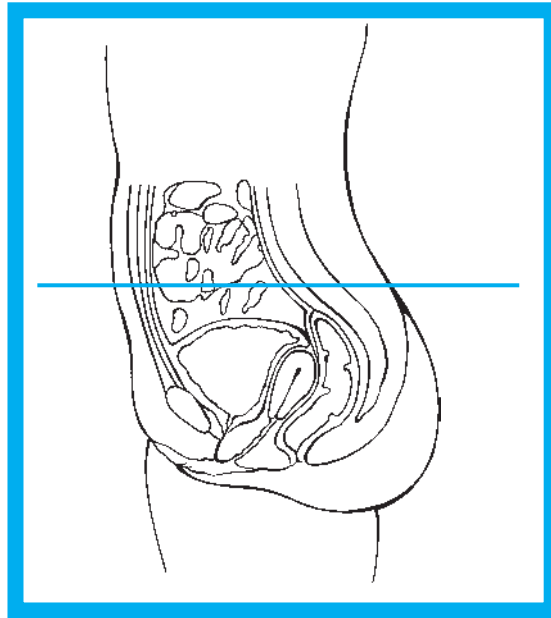
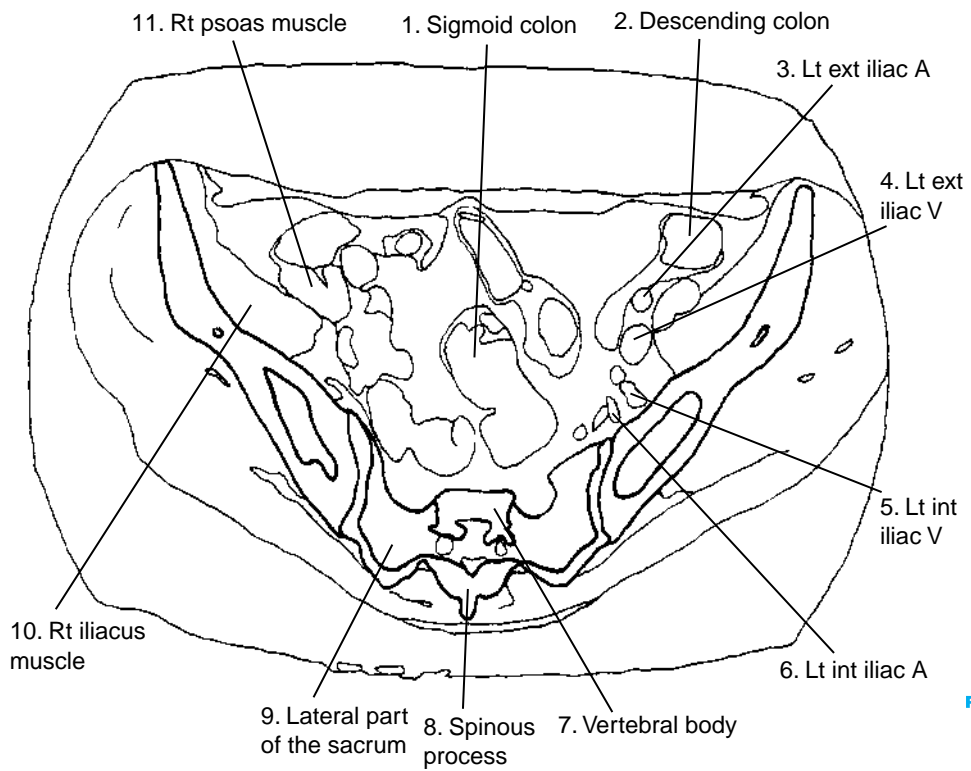


**Figure 4–41 (A,B)** Axial CT image 10: Female.

The sacrum demonstrates its characteristic batlike appearance. On either side of the sacrum, the sacroiliac joints are found between the sacrum with the long, flat iliac bones. Adjacent to the lateral part of the iliac bones, the iliacus and psoas muscles are shown in cross-section. At this level, both the iliacus and psoas muscles appear somewhat smaller than in previous views higher in the pelvis, and occupy a more lateral location. Near the center of the pelvis, the contrast-filled sigmoid colon is shown originating from the terminal part of the descending colon. Based on previous images, four major vessels of the pelvis can be identified on the left side. From anterior to posterior the vessels are the left external iliac artery, left external iliac vein, left internal iliac vein, and left internal iliac artery. Unlike other parts of the body, such as the neck or chest, the arteries in the pelvis tend to occupy a more anterior location than the corresponding veins.



A



B

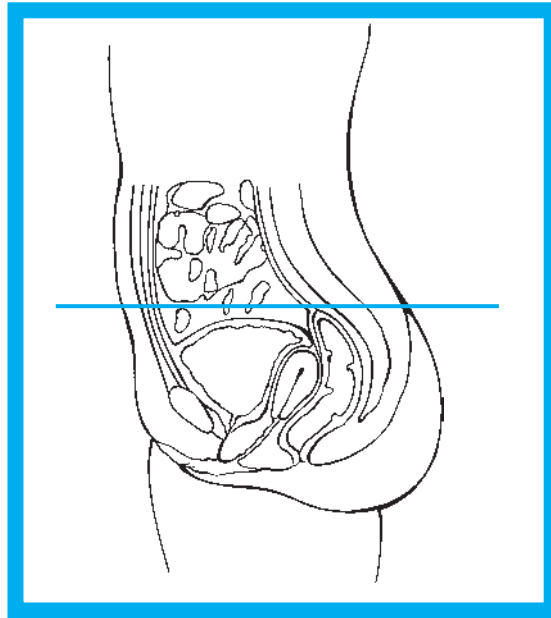
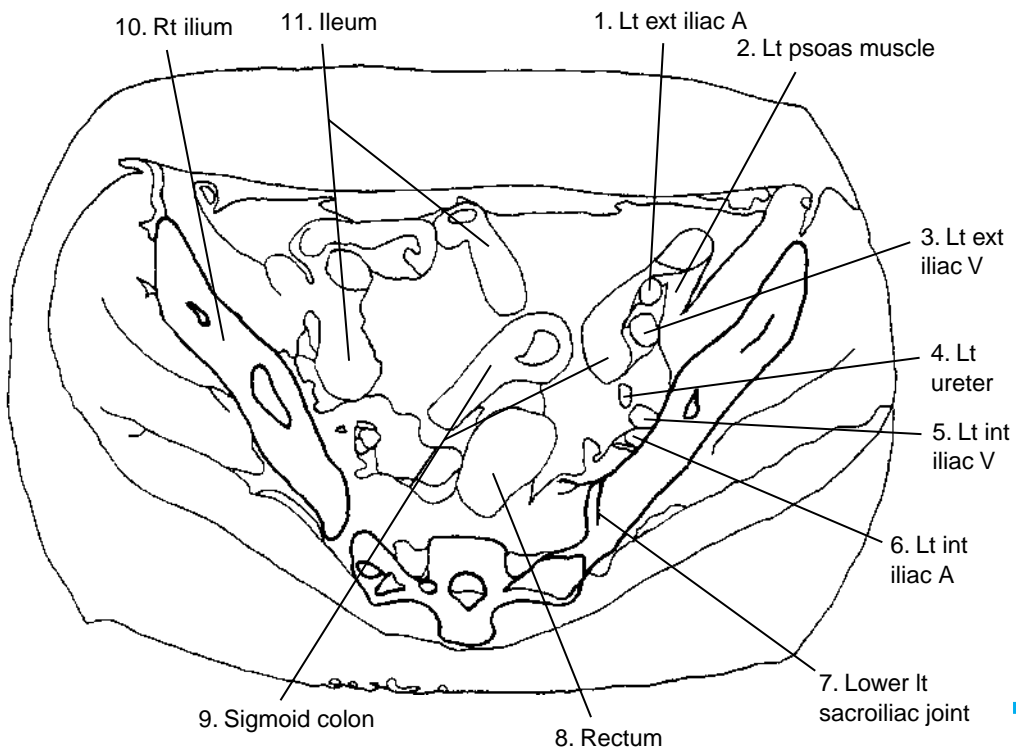


**Figure 4–42 (A,B)** Axial CT image 11: Female.

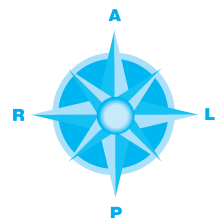
Compared to previous images, the iliac bones appear to be shortened and thicker, and the sacrum is smaller in size. Although the lower sacroiliac joint is shown on the left side, the section lies below the level of the right sacroiliac joint. Within the pelvis, the centrally located sigmoid colon is demonstrated in two parts owing to its irregular S shape. Aside from the sigmoid colon, the rectum is also shown filled with contrast in a more posterior location. Within the right anterior pelvic cavity, loops of small bowel are filled with contrast and air. Because they are within the lower right abdominal cavity, this part of the small bowel can be described as the ileum. (To spell the word ileum correctly, remember the e shape of this part of the small bowel.) The vessels are labeled on the left side along with the contrast-enhanced left ureter. Between the first part of the sigmoid colon and the left psoas muscle, the external iliac vessels can be distinguished; the artery is slightly smaller and more anteriorly situated than the vein. Posterior to the ureter, lying adjacent to the left ilium, the internal iliac vessels can be distinguished; the artery is slightly smaller and more posterior.

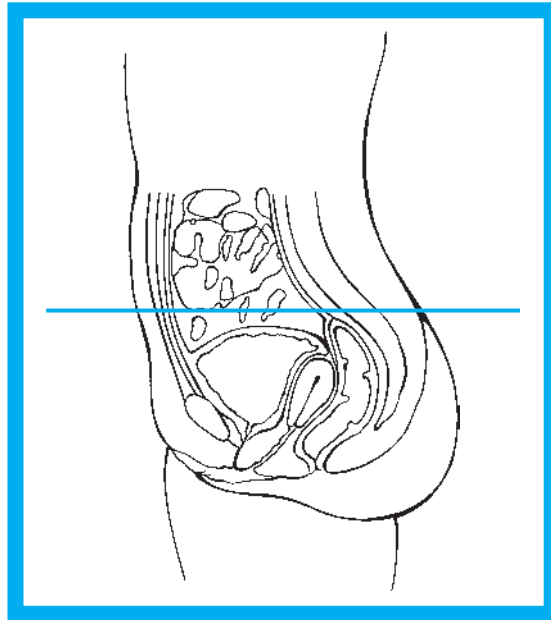


**A**



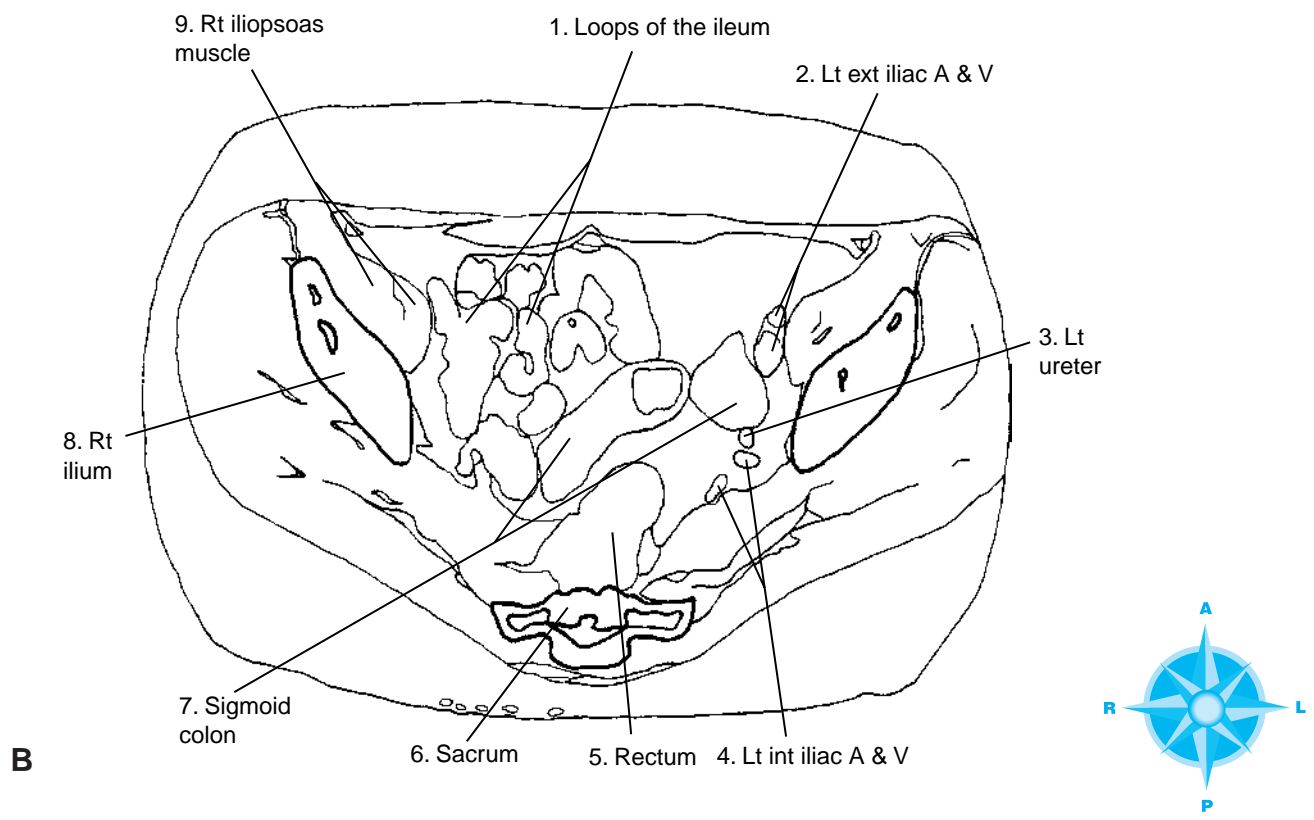
**B**





**Figure 4–43 (A,B)** Axial CT image 12: Female.

This section is through the region of the lower pelvic girdle, because the iliac bones are shortened and thicker and are separate from the sacrum. Within the lower pelvis, the rectum is demonstrated as a large contrast-enhanced structure lying in front of the sacrum. Anterior to the rectum, the S-shaped sigmoid colon is sectioned in two parts and is filled with contrast and fecal material. A concentration of contrast-enhanced small bowel can be seen in the right anterior part of the pelvis. Based on location, this part of the small bowel can be labeled as the ileum. In later images, this concentration of small bowel will be found resting on the roof of the full bladder. Because this section is through the lower pelvis, the previously described psoas and iliacus muscles have now merged to form the right and left iliopsoas muscles. Medial to the left iliopsoas muscle, the external iliac vessels are shown in cross-section in the anterior pelvis, and the internal iliac artery and vein are shown nearing their point of exit through the posterior pelvis. Between the iliac vessels, the left ureter again appears contrast enhanced, although the right ureter is difficult to distinguish in this image.





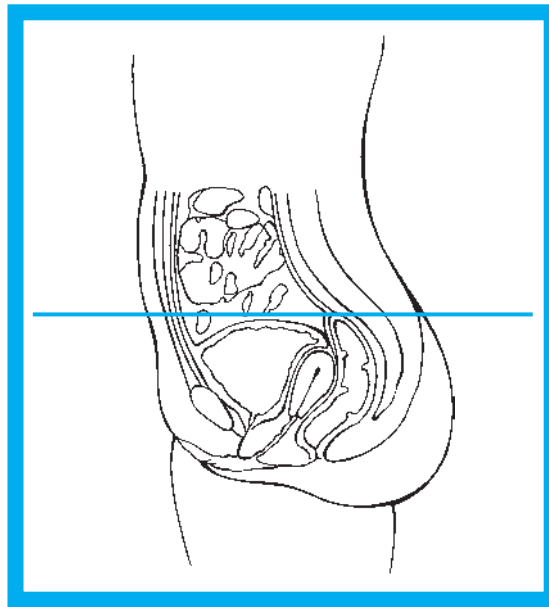
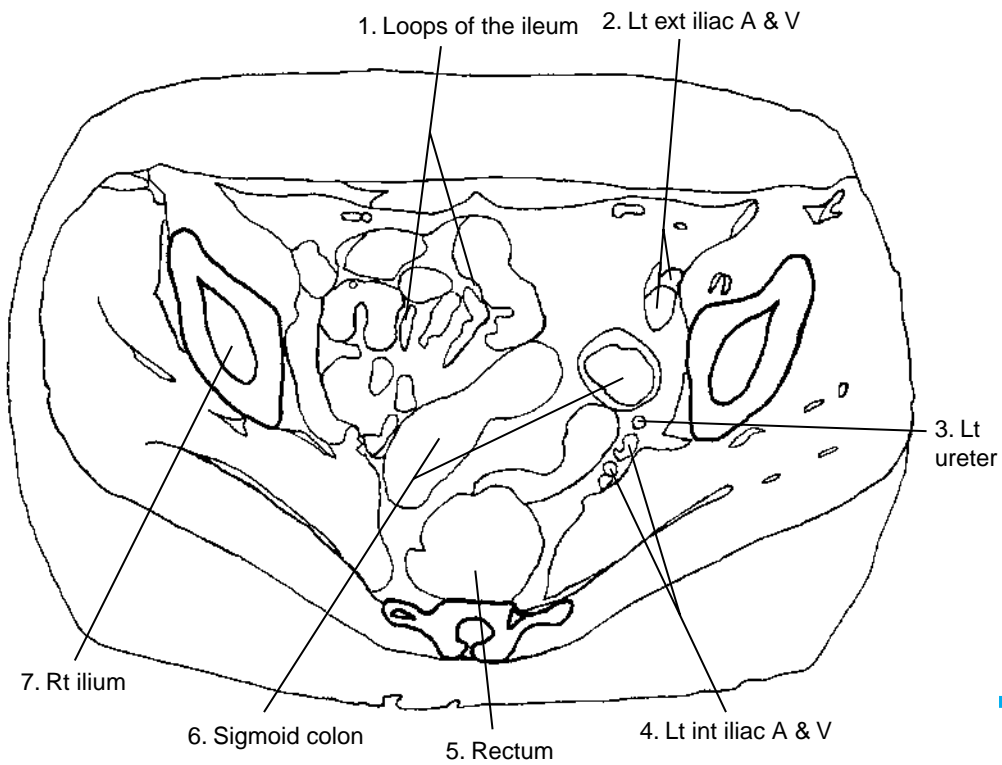


**Figure 4–44 (A,B)** Axial CT image 13: Female.

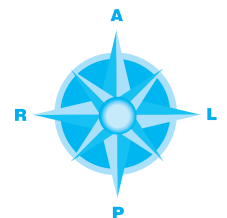
The placement of this section would be slightly above the acetabula, because the iliac bones appear shortened and irregularly shaped. Also, the sacrum is smaller than in previous images. Within the pelvis, the contrast-enhanced rectum is between the sacrum and the sigmoid colon. In the anterior pelvis, numerous loops of the ileum are found on the right side and will be seen in the next image as resting on top of the bladder. With regard to the major vessels, the external iliac artery and vein are in the anterior pelvic cavity nearing the anterior thigh. More posteriorly, the internal iliac artery and vein are beside the posterior pelvic wall and will later be shown to be continuous with the gluteal vessels in the region of the buttocks.

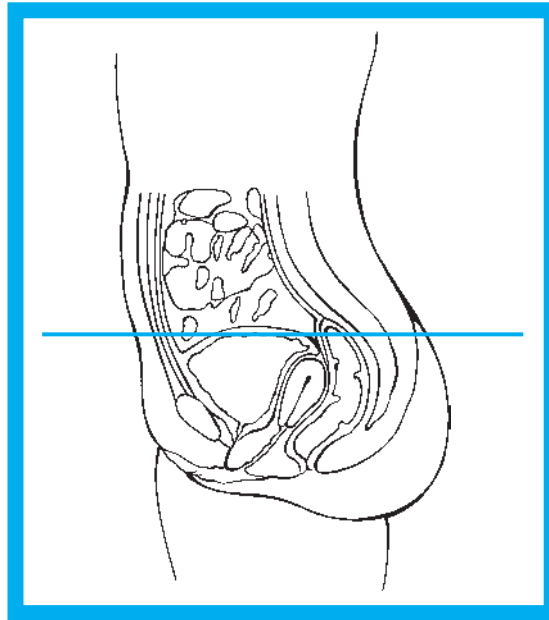


A



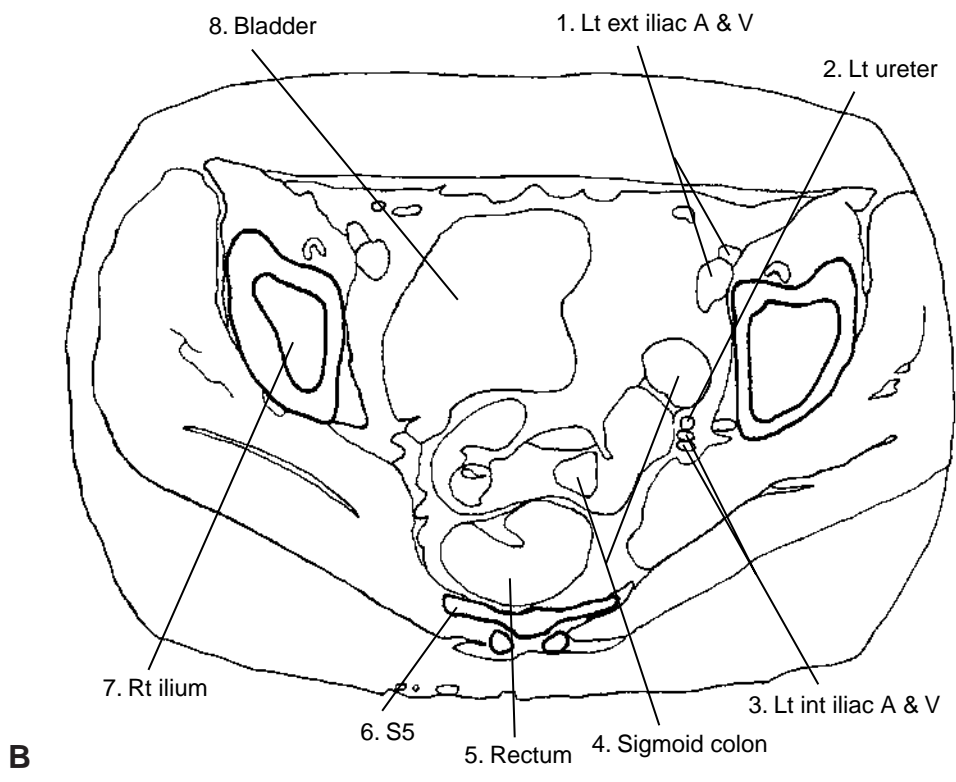
B





**Figure 4–45 (A,B)** Axial CT image 14: Female.

The bony anatomy includes both the right and left iliac bones and the fifth segment of the sacrum. Owing to the short, irregular shape of the iliac bones, this section is located just above the acetabula. Although the sacrum was previously described as bat shaped, the terminal part of the sacrum, lower part of S5, has a unique appearance, because the sacral canal terminates at this level owing to the absence of a posterior border. The most notable feature of this image is the large contrast-enhanced structure occupying most of the pelvis formed by the top of the bladder. Typically, a contrast-fluid level can be distinguished within the bladder. However, in this patient, the bladder is completely filled with contrast-enhanced urine. Behind the bladder, the irregularly shaped sigmoid colon extends from the left anterior part of the pelvis to continue as the rectum. Although the right ureter is not enhanced with contrast in this image, it lies behind the bladder similar to the left ureter. Posterior to the ureters, the internal iliac vessels are found along the posterior wall of the pelvis. Anterior to the ureters, the external iliac vessels are found closer to the anterior abdominal wall than in previous images.



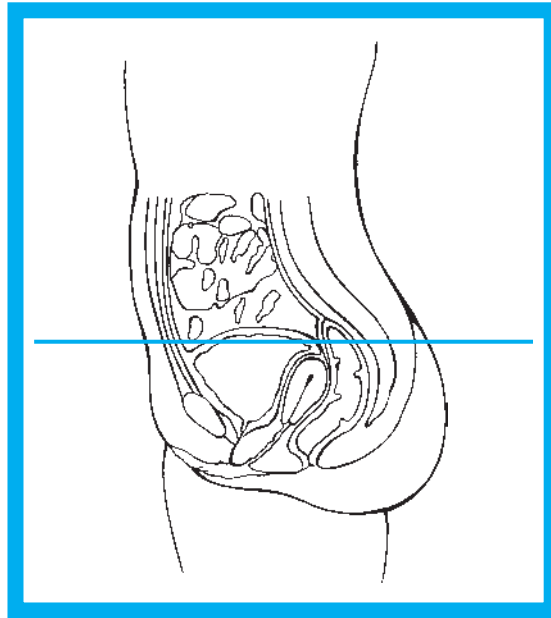
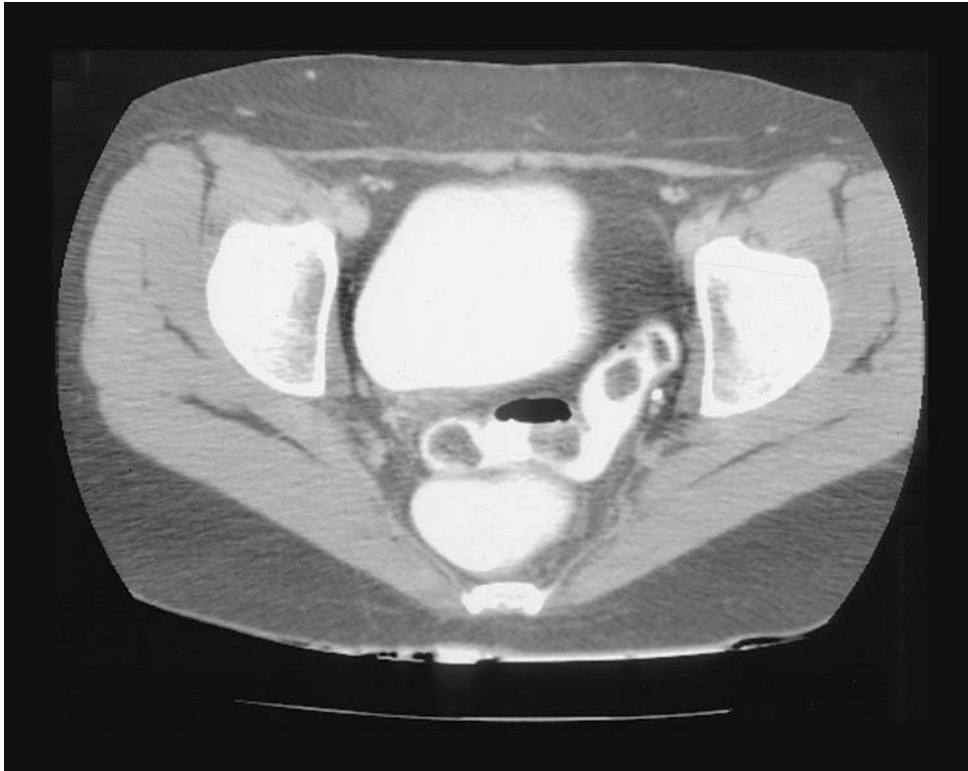
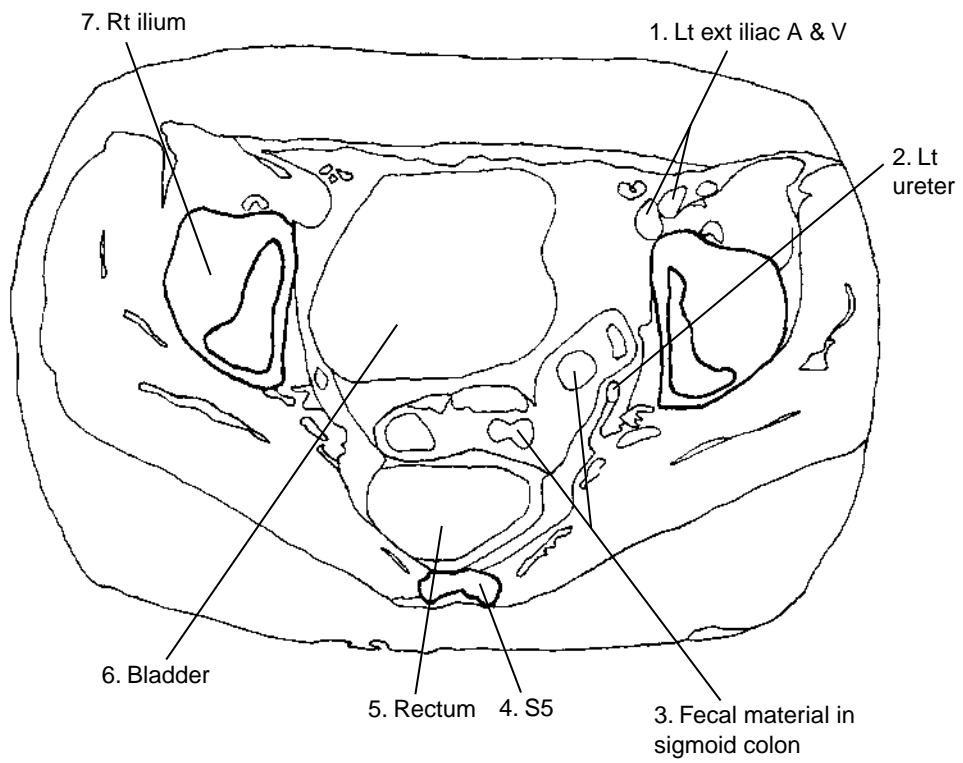


**Figure 4–46 (A,B)** Axial CT image 15: Female.

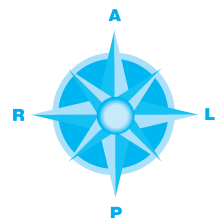
Following the structures described in the previous image, the lower part of S5 and the right and left iliac bones make up the bony anatomy within this image. The most remarkable structure, the bladder, occupies most of the pelvic cavity. Posterior to the bladder, the sigmoid colon is longitudinally sectioned as it extends from the right anterior pelvis to a central location where it joins the rectum. In this patient, the central part of the sigmoid colon ascends to the level described in Figure 4-37. Anterior to approximately S3, the sigmoid colon continues as the rectum, which descends through the lower pelvis. Similar to previous images, the left ureter is enhanced with contrast and the right ureter is difficult to distinguish from other soft tissue vessels behind the right side of the bladder. At this level, it is difficult to distinguish the internal iliac vessels, because they are continuing as the gluteal vessels, which exit the pelvis to enter the region of the buttocks. However, the external iliac vessels can be discerned as they near the anterior abdominal wall and will be shown in lower sections to exit the pelvis to enter the anterior thigh.



A



B



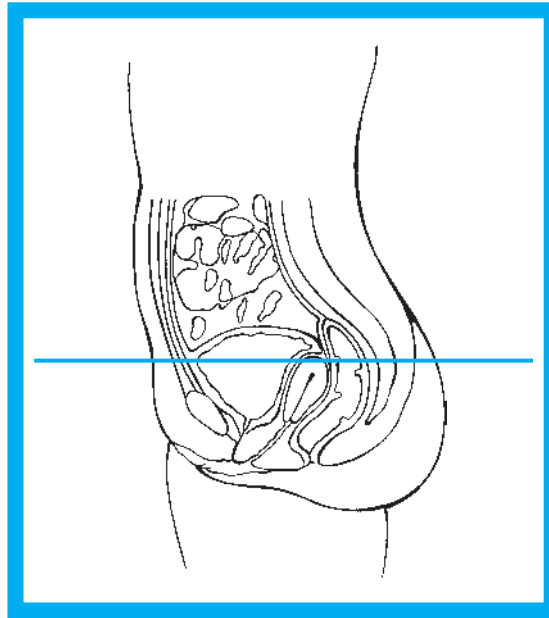
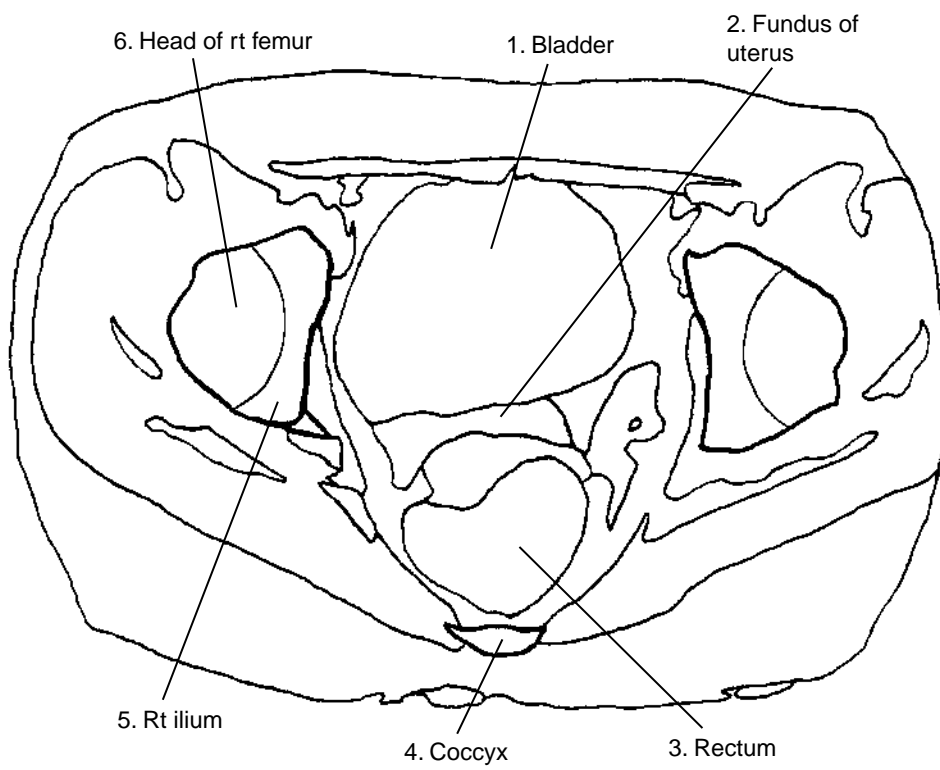


**Figure 4–47 (A,B)** Axial CT image 16: Female.

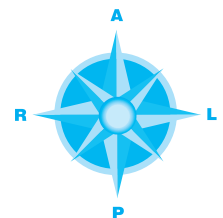
The coccyx is shown at this level because the sacral foramen can no longer be seen. On either side, the heads of the femurs can be seen within the upper part of the acetabula, which are formed by the iliac bones. Within the pelvis, the full bladder occupies most of the anterior cavity and the contrast-enhanced rectum occupies much of the posterior cavity. Between these two structures in what was previously the location of the sigmoid colon, a soft tissue structure is shown, representing the fundus of the uterus. If the bladder were not full, the fundus would be more anteriorly situated within the pelvis.



A



B





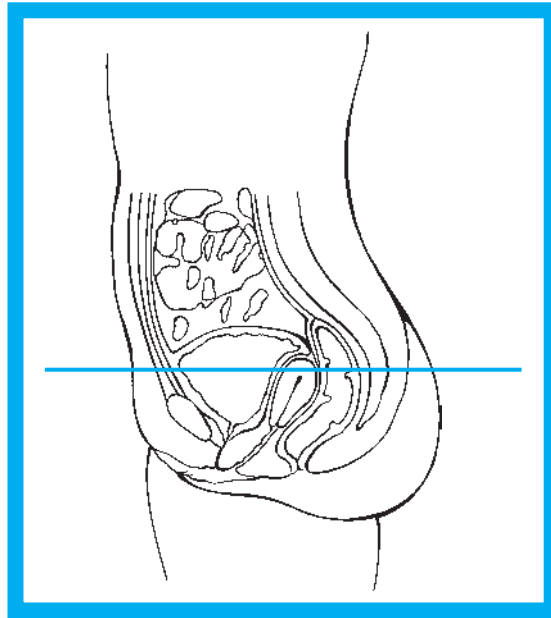
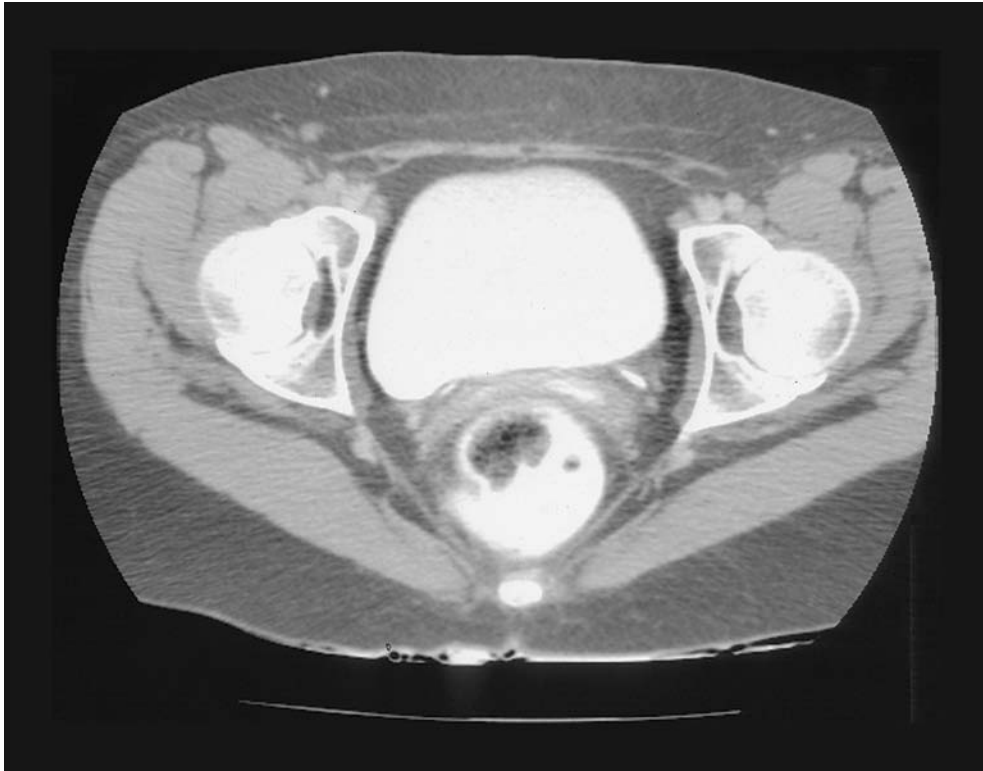
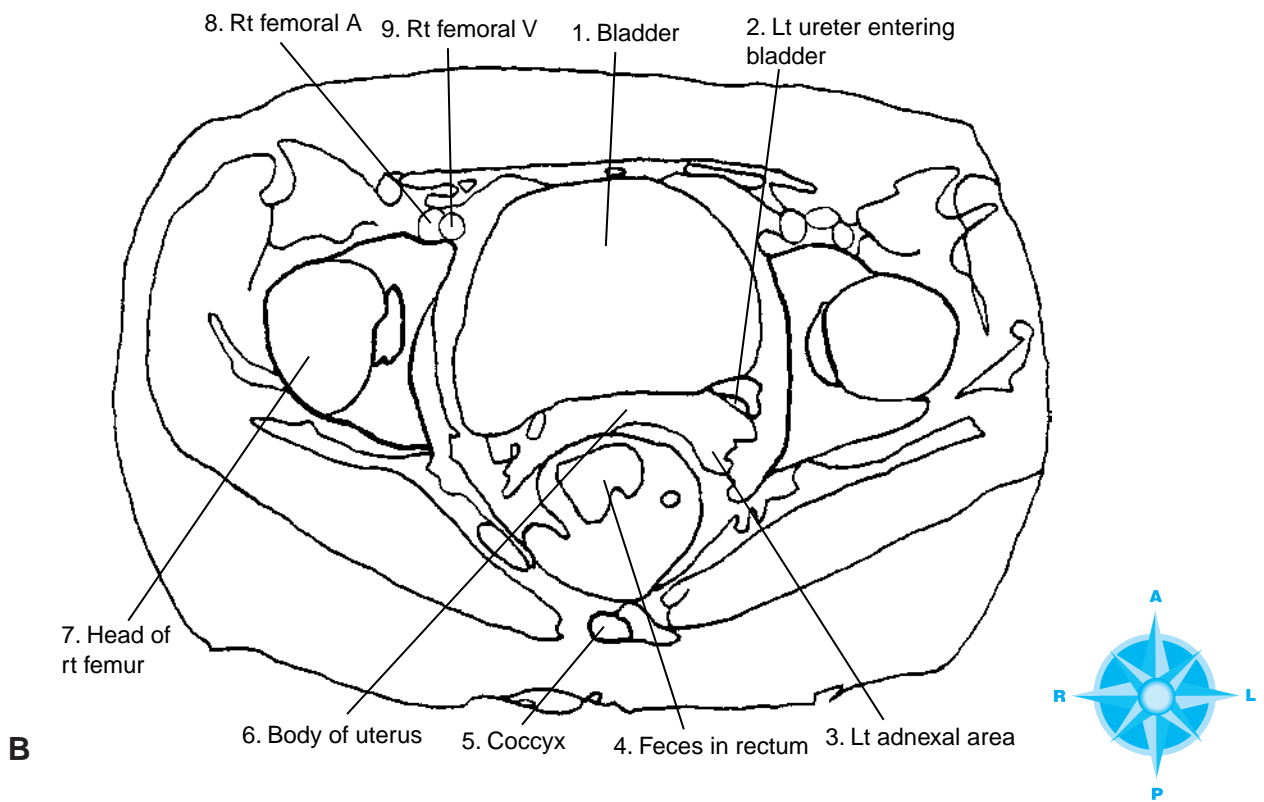


**Figure 4–48 (A,B)** Axial CT image 17: Female.

Owing to the absence of the sacral foramen, the coccyx forms the posterior border of the bony pelvis. On either side, the heads of the femurs can be seen within the middle region of the acetabula where the three bones forming the pelvic girdle (ilium, pubis, and ischium) join. Within the pelvis, the full bladder and contrast-enhanced rectum occupy most of the pelvic cavity. Between the bladder and the rectum, the body of the uterus is sectioned along with appendages extending to either side to form the right and left adnexal areas. As described earlier, the adnexal area is formed by uterine appendages, including the ovaries, oviducts, and other elements of the broad ligament. Because of contrast enhancement, the left ureter is shown obliquely sectioned near its point of entry into the bladder. The major vessels demonstrated in this cross-section are now outside of the bony pelvis, thus they are labeled as the femoral arteries and veins, which are continuations of the external iliac vessels.



A



B

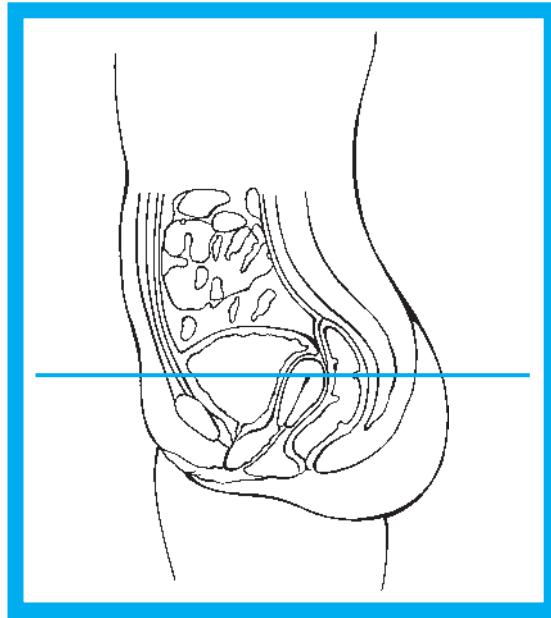
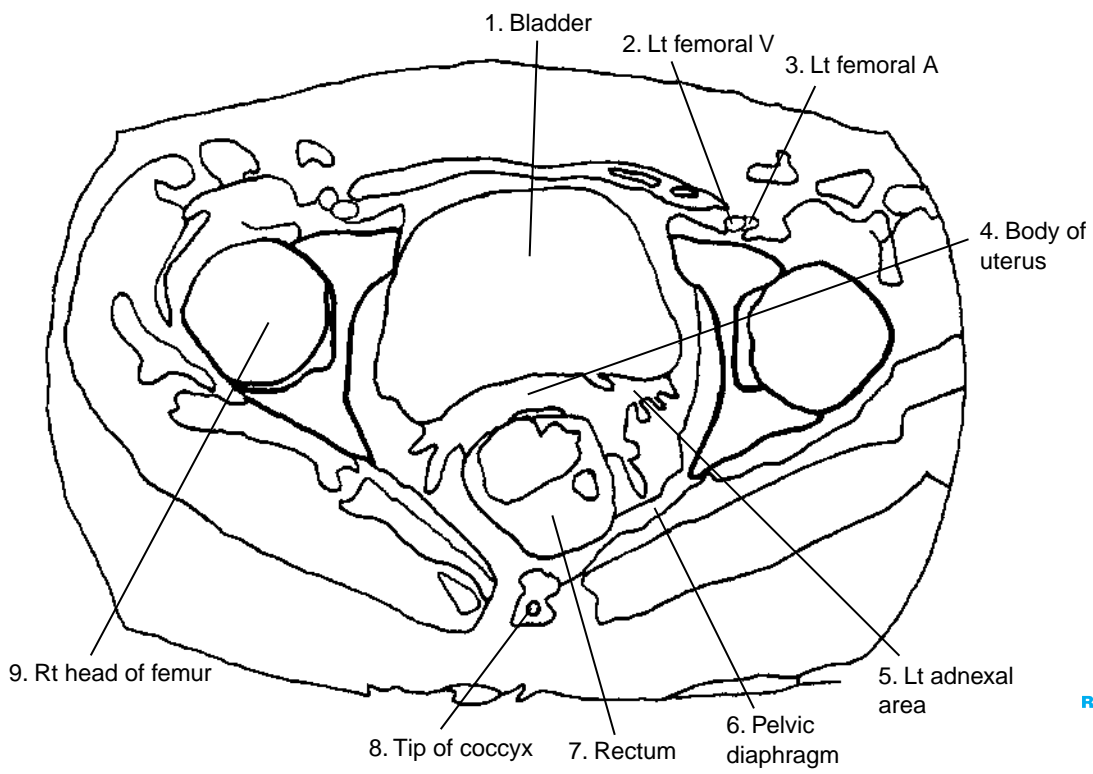


**Figure 4–49 (A,B)** Axial CT image 18: Female.

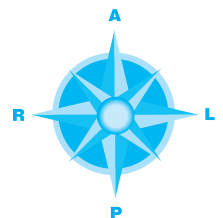
Although very small, the tip of the coccyx is found posterior to the contrast- and feces-filled rectum. On either side, the heads of the femurs are within the midregion of the acetabula. In the anterior pelvis, the urine-filled bladder occupies most of the pelvic cavity and appears to be extending out the anterior pelvic wall above the symphysis pubis. Posterior to the bladder, the body of the uterus is again demonstrated in cross-section, with its appendages, the left and right adnexal areas, on either side. Owing to the filled state of both the bladder and the rectum, the uterus is compressed in this image and appears to wrap around the anterior surface of the rectum. Extending from the pelvic girdle on either side to the coccyx, a thin muscular sheet (the pelvic diaphragm) is demonstrated in cross-section and appears to loop around the posterior rectum. Outside of the pelvic cavity, two vessels are sectioned on either side and can be labeled as the femoral arteries and veins. Because the femoral artery is found in a more lateral location and is slightly smaller than the femoral vein, the four vessels can be individually identified.



A



B



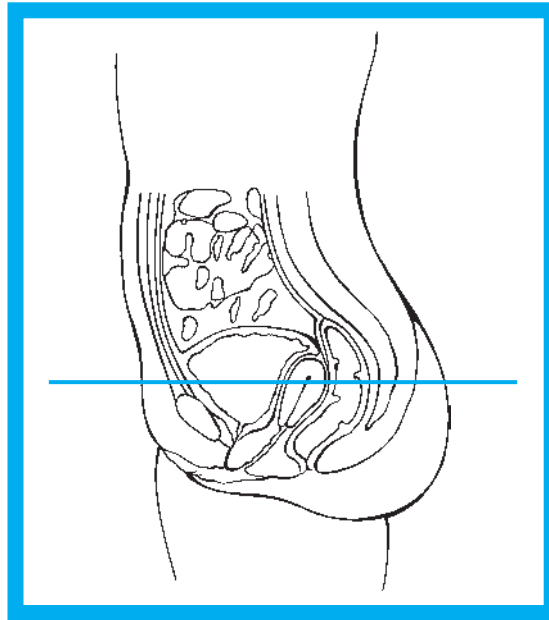
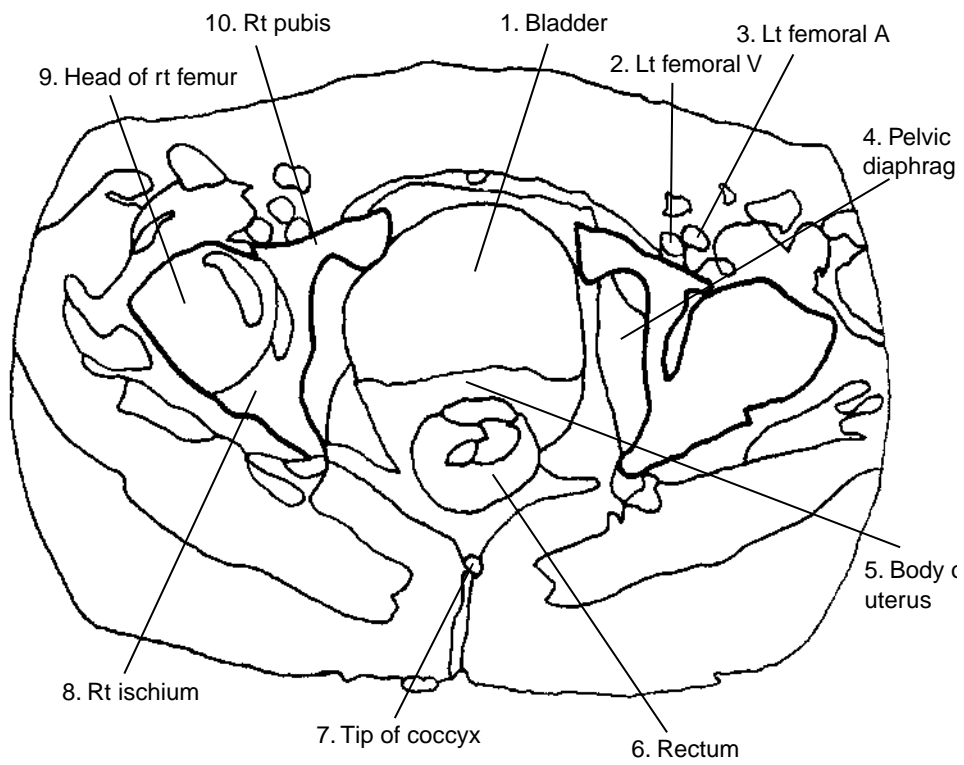


**Figure 4–50 (A,B)** Axial CT image 19: Female.

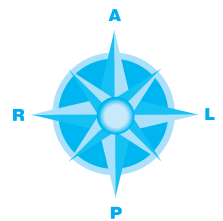
Although small, the tip of the coccyx is cut in cross-section and provides attachment for the posterior pelvic diaphragm. On either side, the heads of the femurs are shown in the lower parts of the acetabula formed by the ischial and pubic bones. Within the bony pelvis, the bladder is somewhat smaller than in previous images but is still completely filled with contrast-enhanced urine. Adjacent to the posterior wall of the bladder, the body of the uterus is sectioned between the bladder and the rectum. Similar to previous images, the femoral arteries and veins are anterior to the bony pelvis as they extend into the region of the anterior thigh.



A



B



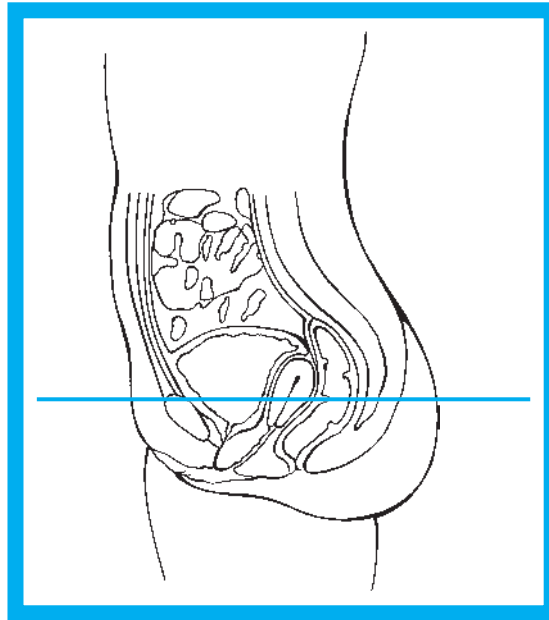
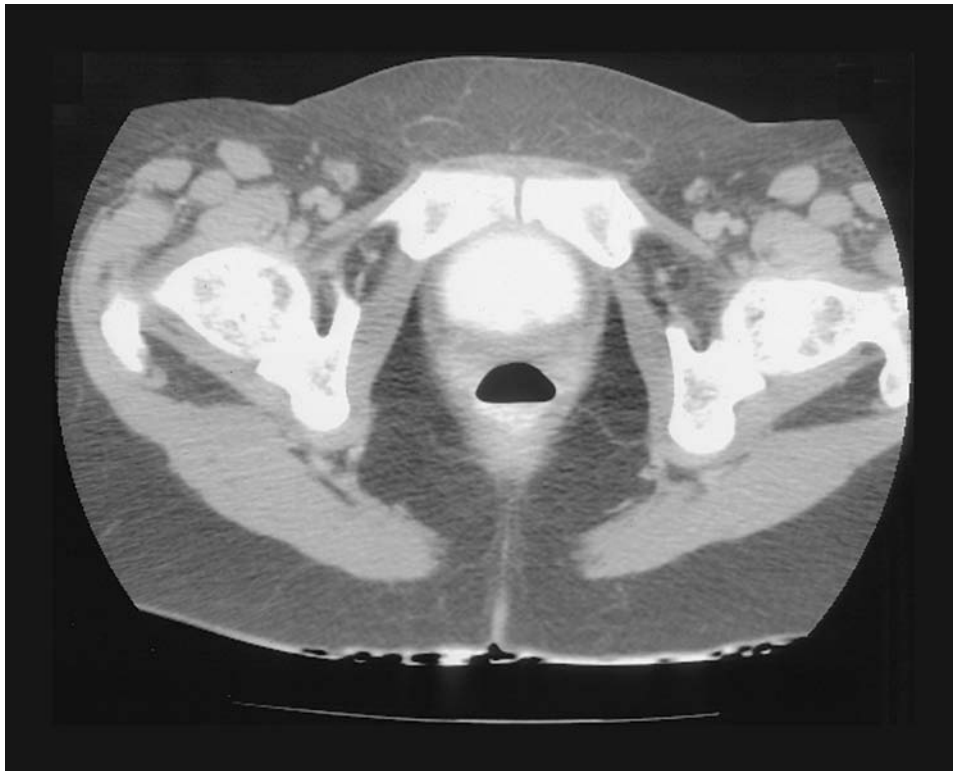
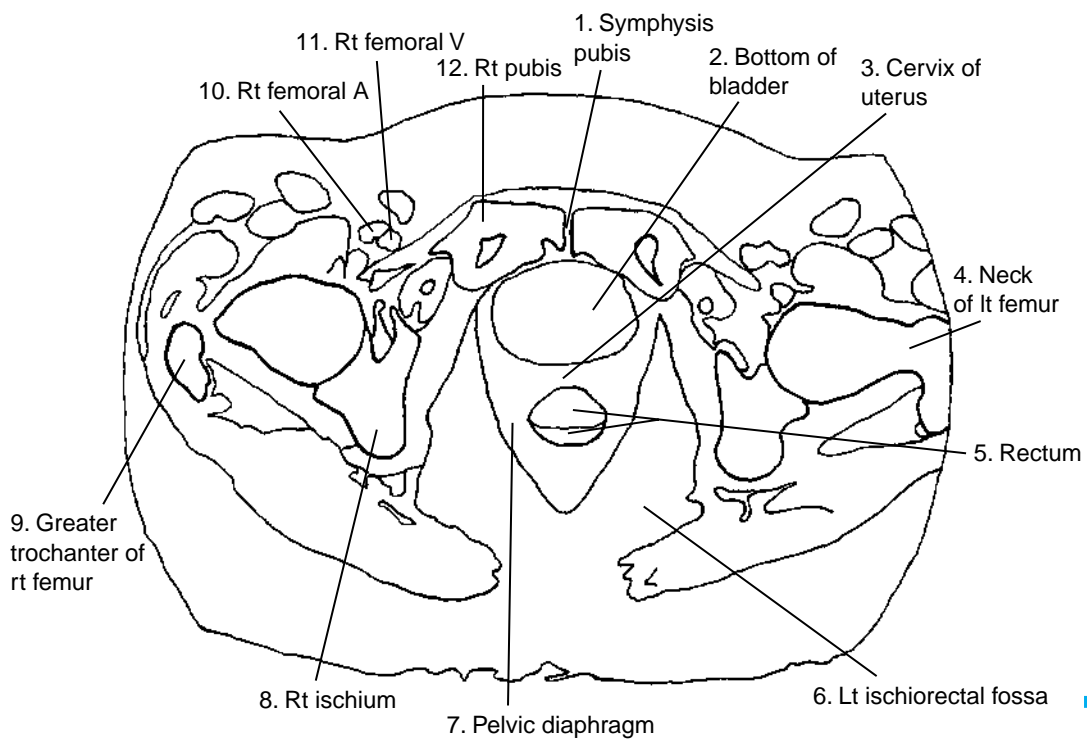


**Figure 4–51 (A,B)** Axial CT image 20: Female.

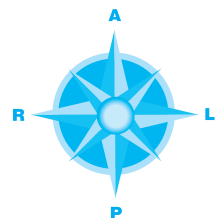
This section below the level of the sacrum and the coccyx demonstrates the symphysis pubis between the right and left pubic bones. On either side, the ischial bones are shown articulating with the proximal part of the femurs. The femurs appear irregularly shaped, demonstrating the heads, the necks, and the greater trochanters. Within the pelvic cavity, the contrast-enhanced bladder is seen anteriorly but is much smaller than in previous images, indicating that we are nearing the bottom of the bladder. Posteriorly, the rectum is sectioned and contains air and a small amount of contrast material, forming an air–fluid level. Between the rectum and the bladder, the cervix of the uterus has a density similar to that of the musculature of the pelvic diaphragm. Previously, this position was occupied by the body of the uterus, which was wider and appeared to wrap around the rectum. At this level, the cross-section through the pelvic diaphragm is V shaped; it appears to be forming a sling around the rectum and is attached anteriorly to the pubic bones. Between the pelvic diaphragm and the ischial bones, deposits of fat can be found in the ischiorectal fossae. On the anterior pelvis, the femoral artery is again found lateral to the femoral vein, as they extend into the anterior thigh.



A



B





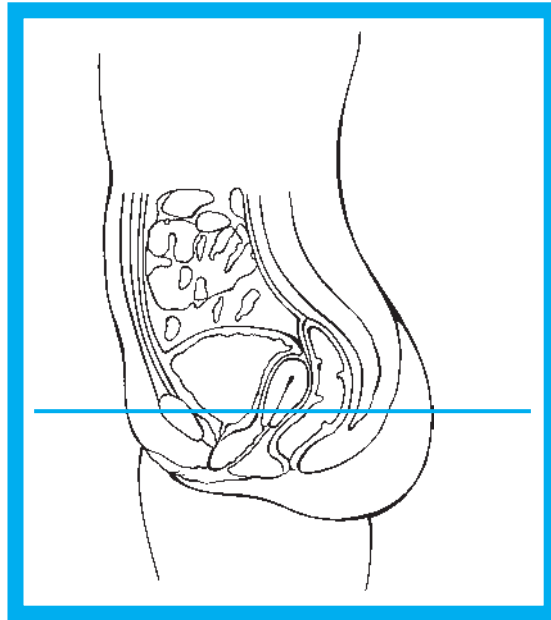
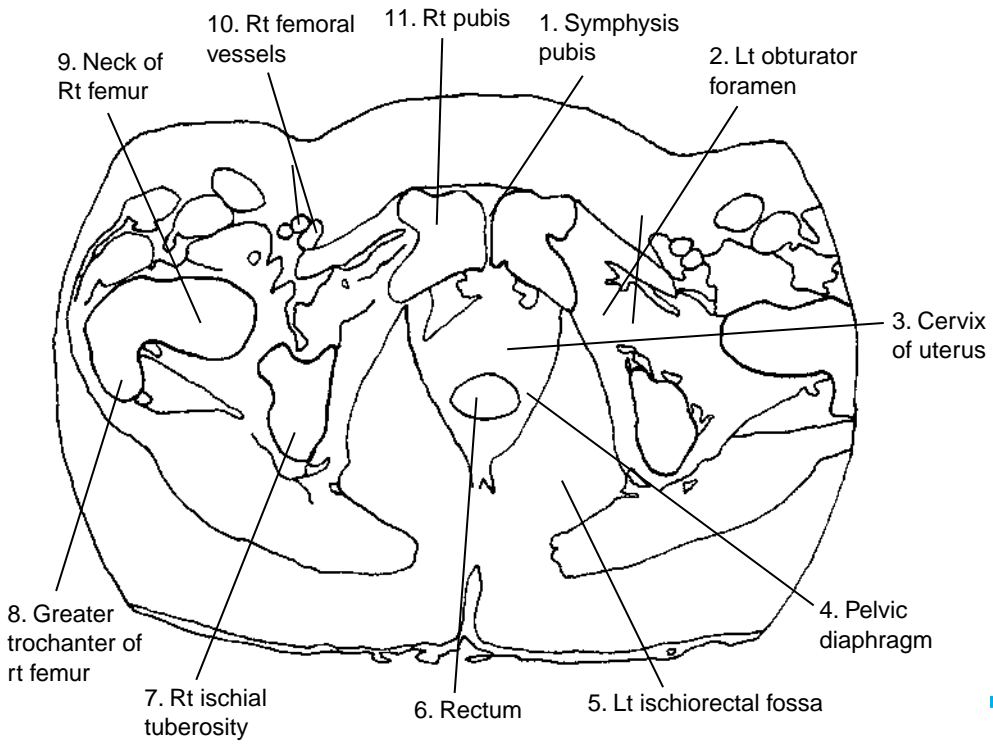


**Figure 4–52 (A,B)** Axial CT image 21: Female.

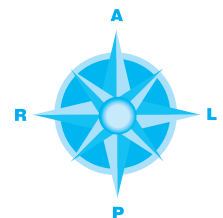
The symphysis pubis is in the middle of this image between the right and left pubic bones, which are separated from the ischial bones by the obturator foramen. In this section, the ischial bones appear to be irregularly shaped thick bones, indicating the level of the ischial tuberosities. Outside the pelvis, the necks and greater trochanters of the femurs are on either side. Within the pelvis, the bladder is no longer seen, because this section is at the level of the urethra, which is difficult to visualize without contrast enhancement. Similar to previous images, the air-filled rectum is readily identified in the central pelvic cavity and is surrounded by the V-shaped muscular sheet of the pelvic diaphragm. Anterior to the rectum, the dense muscular tissue forming the cervix is difficult to distinguish from the surrounding pelvic diaphragm. Between the rectum and the ischial bones, large deposits of fat can be seen in the ischioanal fossae, which are below the pelvic diaphragm. On the anterior surface of the pelvis, several vessels are identified in cross-section and from previous images can be identified as branches of the femoral artery and vein.



**A**



**B**



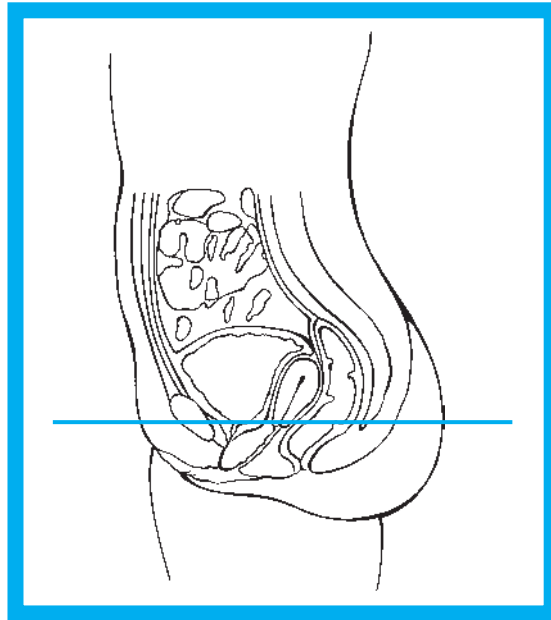
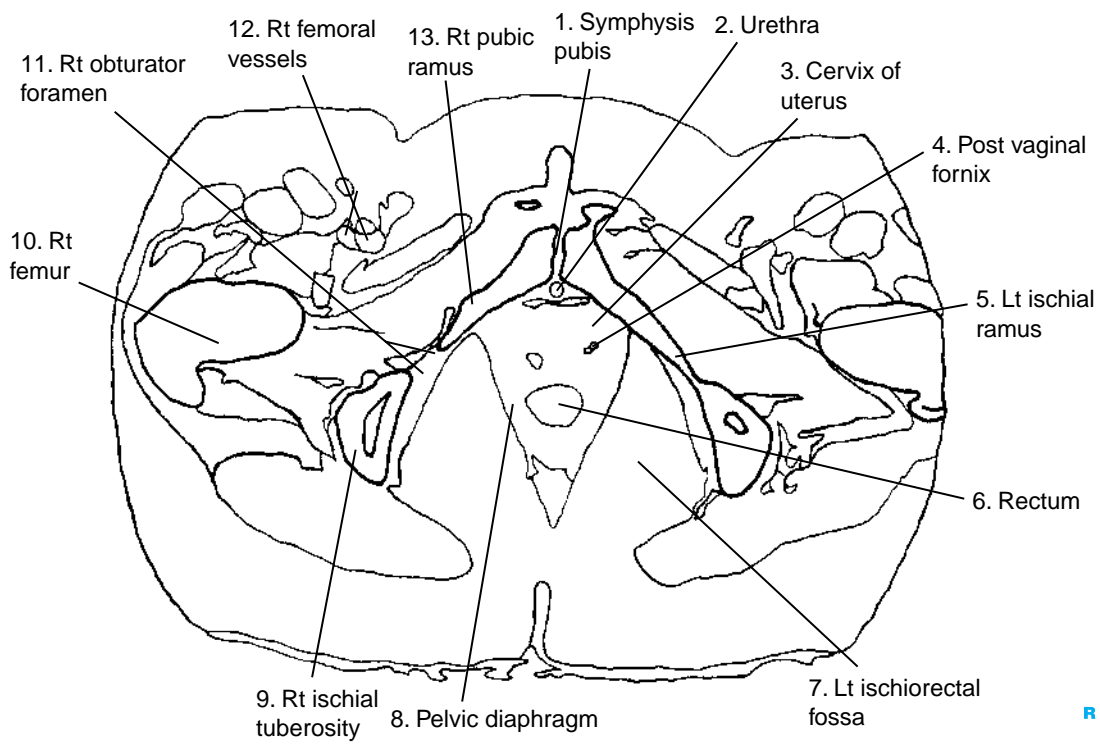


**Figure 4–53 (A,B)** Axial CT image 22: Female.

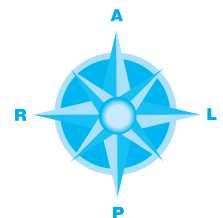
Taken through the lower part of the pelvis, this image demonstrates the lower part of the symphysis pubis between the right and left pubic bones. On the left side, the ischial ramus can be seen to join the pubic ramus, forming continuous bone below the level of the obturator foramen. On the right side, only the ischial tuberosity is demonstrated in this section and is separated from the pubic bone by the obturator foramen. On either side of the bony pelvis, the femurs are demonstrated in cross-section posterior to the femoral vessels in the anterior region of the thigh. Within the pelvis, the air-filled rectum is centrally located and is surrounded by a wedge-shaped muscular structure. Similar to previous images, the pelvic diaphragm is V shaped and forms a sling around the rectum attaching anteriorly to the pubic bones. Although a boundary cannot clearly be distinguished between the pelvic diaphragm and the cervix of the uterus, the air within the posterior vaginal fornix marks the site where the cervix joins the vagina. Between the cervix and the symphysis pubis, the urethra is shown in cross-section as a small, round structure with almost the same density as muscle. Between the pelvic diaphragm and the ischial bones, large triangular shaped areas of fat are found within the ischiorectal fossae and are continuous with the fat on the posterior surface of the buttocks.



A



B



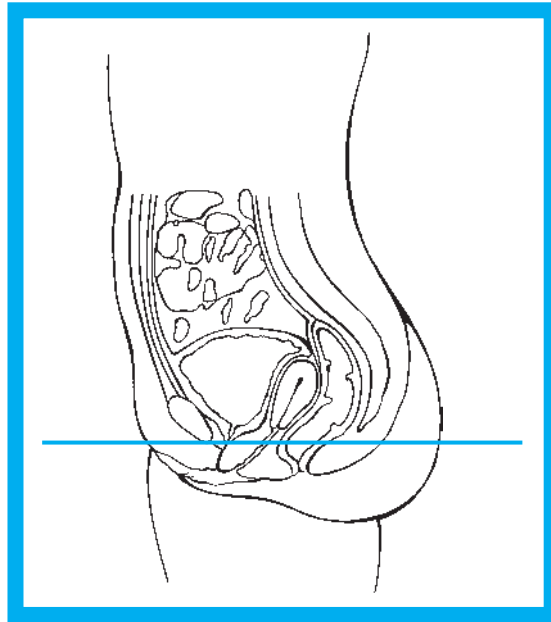
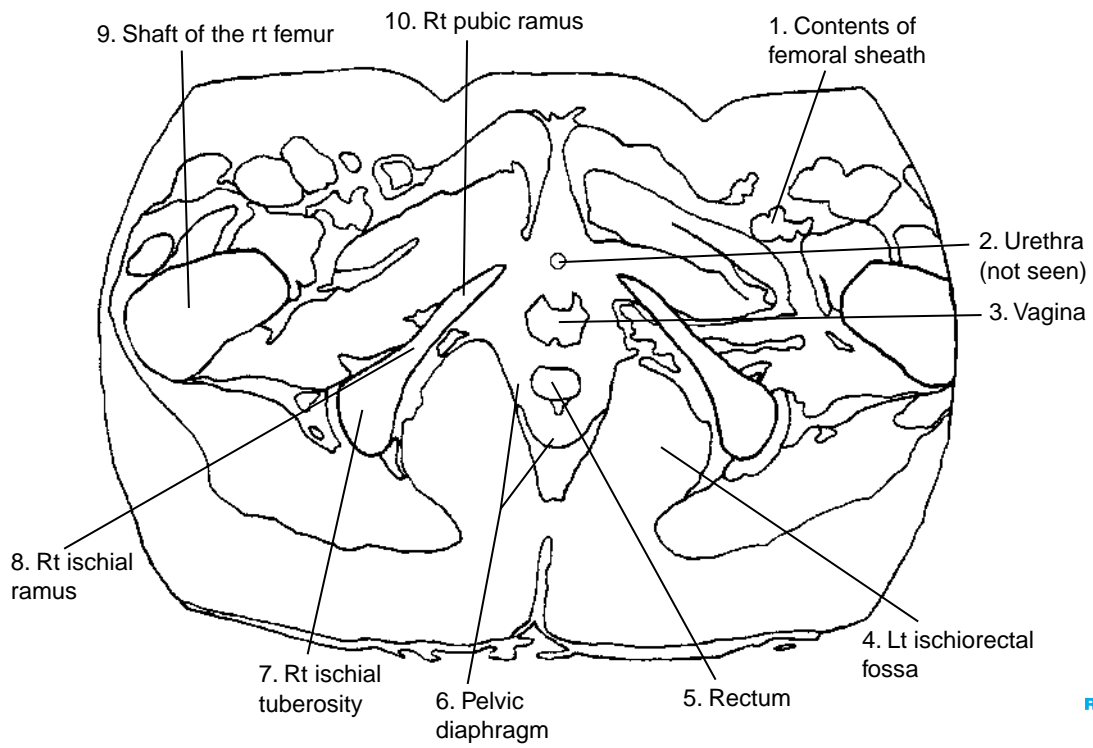


**Figure 4–54 (A,B)** Axial CT image 23: Female.

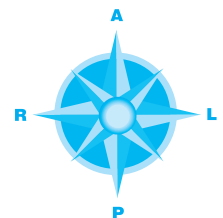
Near the lateral margins of this image, the shafts of the femurs can be identified on either side of the ischial and pubic bones. Because this section is below the level of the symphysis pubis, only the lower part of the pubic bones, the pubic rami, are articulating with the ischial rami. The ischial tuberosities (the enlarged portion of the ischial bones) are still seen at this lower level; however, they are slightly smaller in diameter than in earlier sections. Within the pelvis, the air-filled rectum is seen in the central pelvic cavity surrounded by the V-shaped pelvic diaphragm. In contrast to previous images, the air-filled lumen of the vagina is now seen in the location previously occupied by the cervix. If contrast were introduced to the urethra, it would be found between the ischial rami in the location previously occupied by the bladder. On the posterolateral parts of the pelvic cavity, the fat-filled ischiorectal fossae are found between the pelvic diaphragm and the ischial bones.



A



B



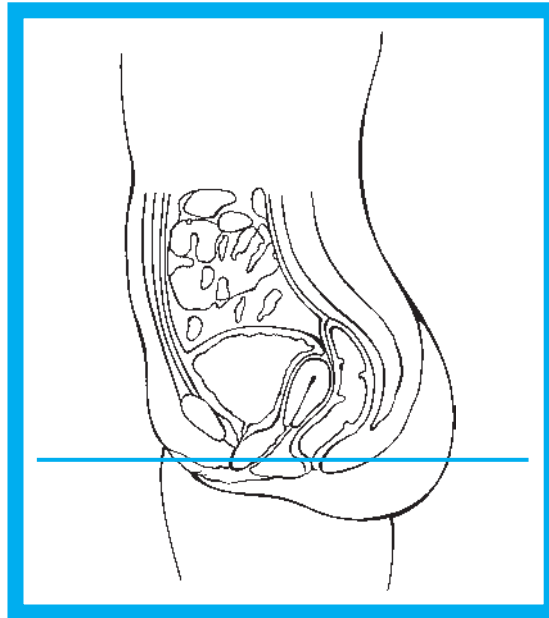
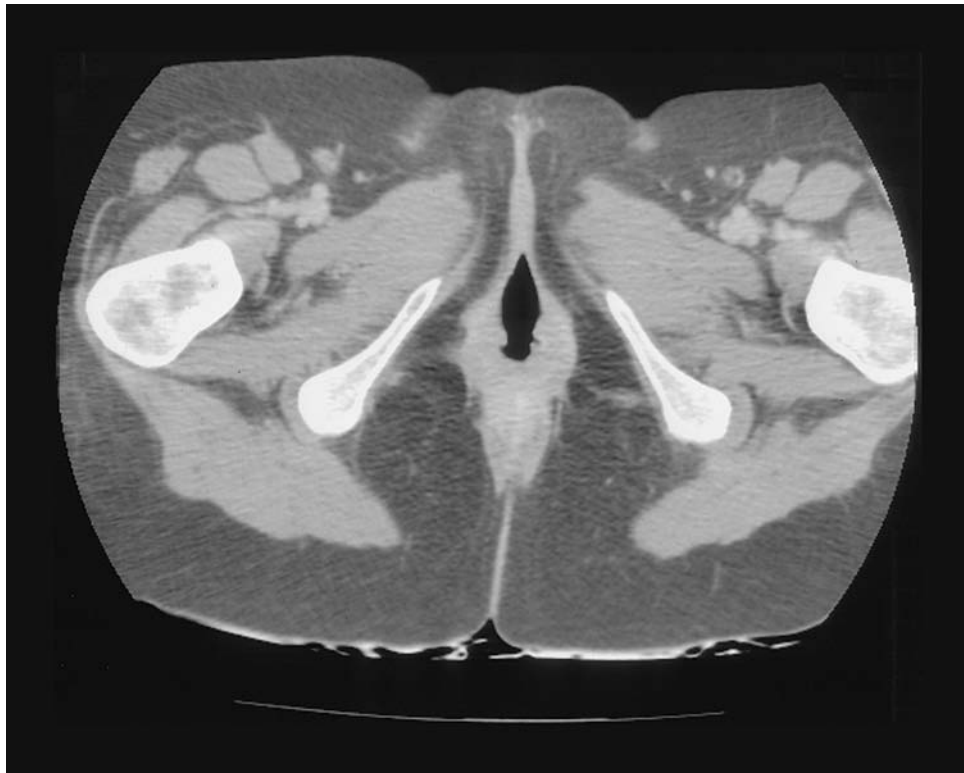
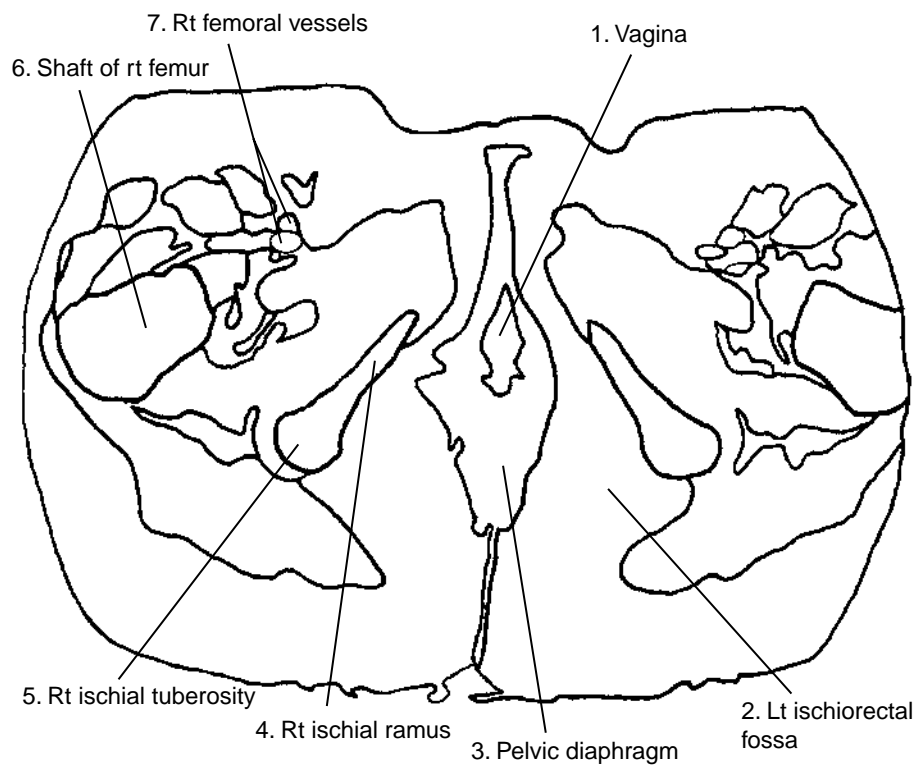


**Figure 4-55 (A,B)** Axial CT image 24: Female.

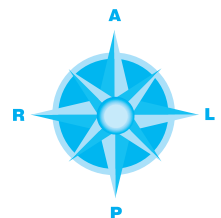
The shafts of the femurs can be seen on either side of the image surrounding the pair of ischial bones centrally located in the lower pelvis. At this low level, the expanded portion of the ischial bone represents the ischial tuberosity, and the thin projection of bone is the ischial ramus. Within the pelvic cavity, air can be seen within the vagina, which appears less oval in shape than in the previous image. The air-filled rectum in the previous image has been replaced by the musculature of the pelvic diaphragm, which includes the external anal sphincter muscle. Between the pelvic diaphragm and the ischial bones, the ischiorectal fossae are again shown filled with fat. Within the musculature of the anterior thigh, a group of femoral vessels can be identified on either side.



A



B





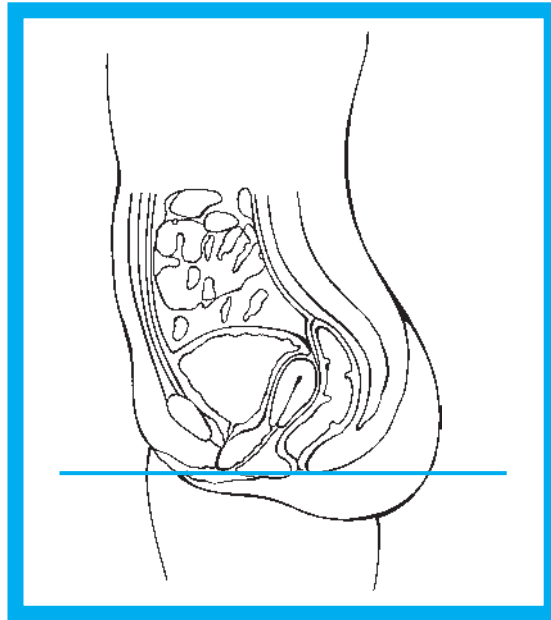
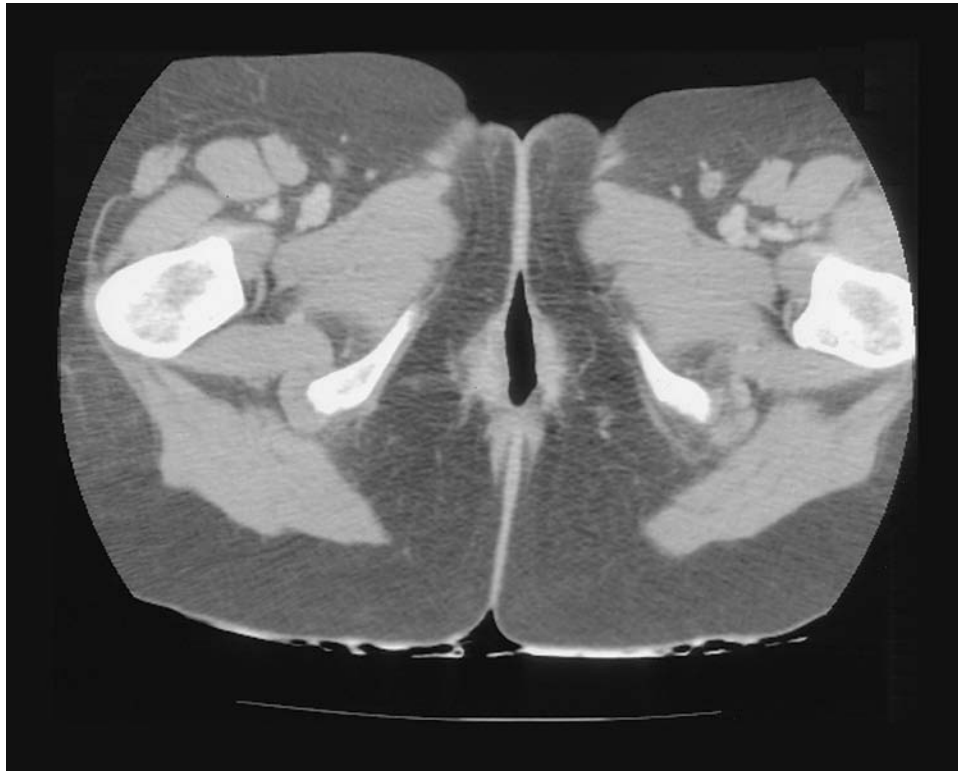
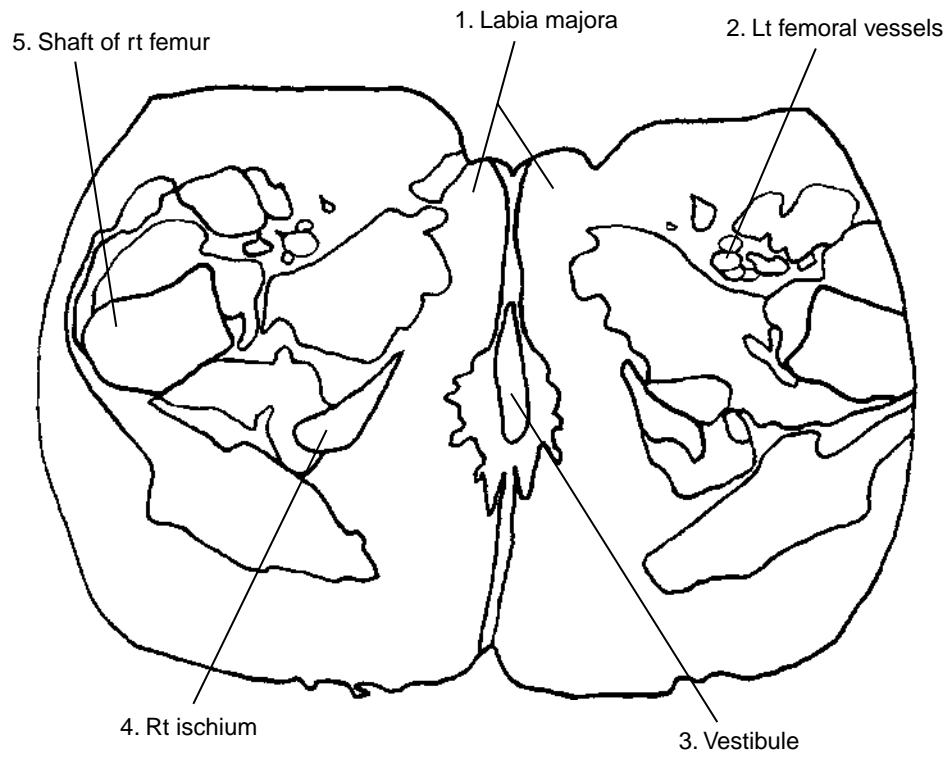


**Figure 4-56 (A,B)** Axial CT image 25: Female.

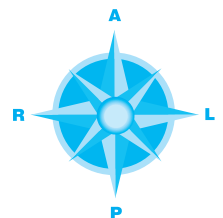
This section, taken through the very lowest part of the pelvis, demonstrates the ischial bones on either side surrounded by the shafts of the femurs, which are thick, irregularly shaped bones. Within the pelvis, an air-filled opening can be seen extending from the region previously occupied by the vagina and the urethra, forming the vestibule posterior to the clitoris between the labia minora. Anterior to the vestibule, the labia majora are found on either side of the midline between the thighs.



A



B



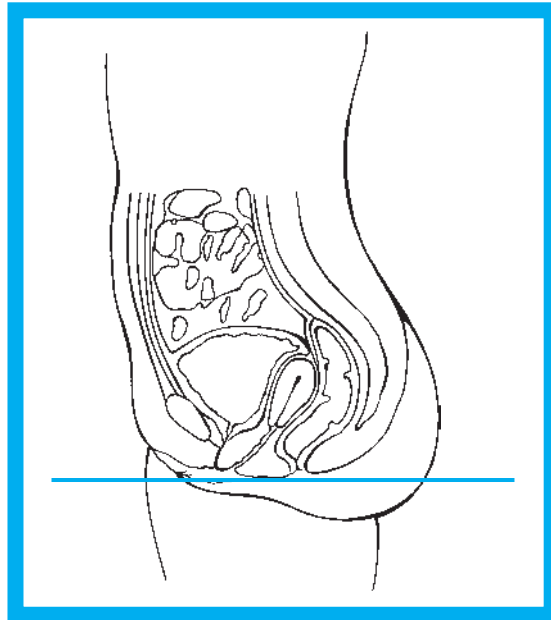
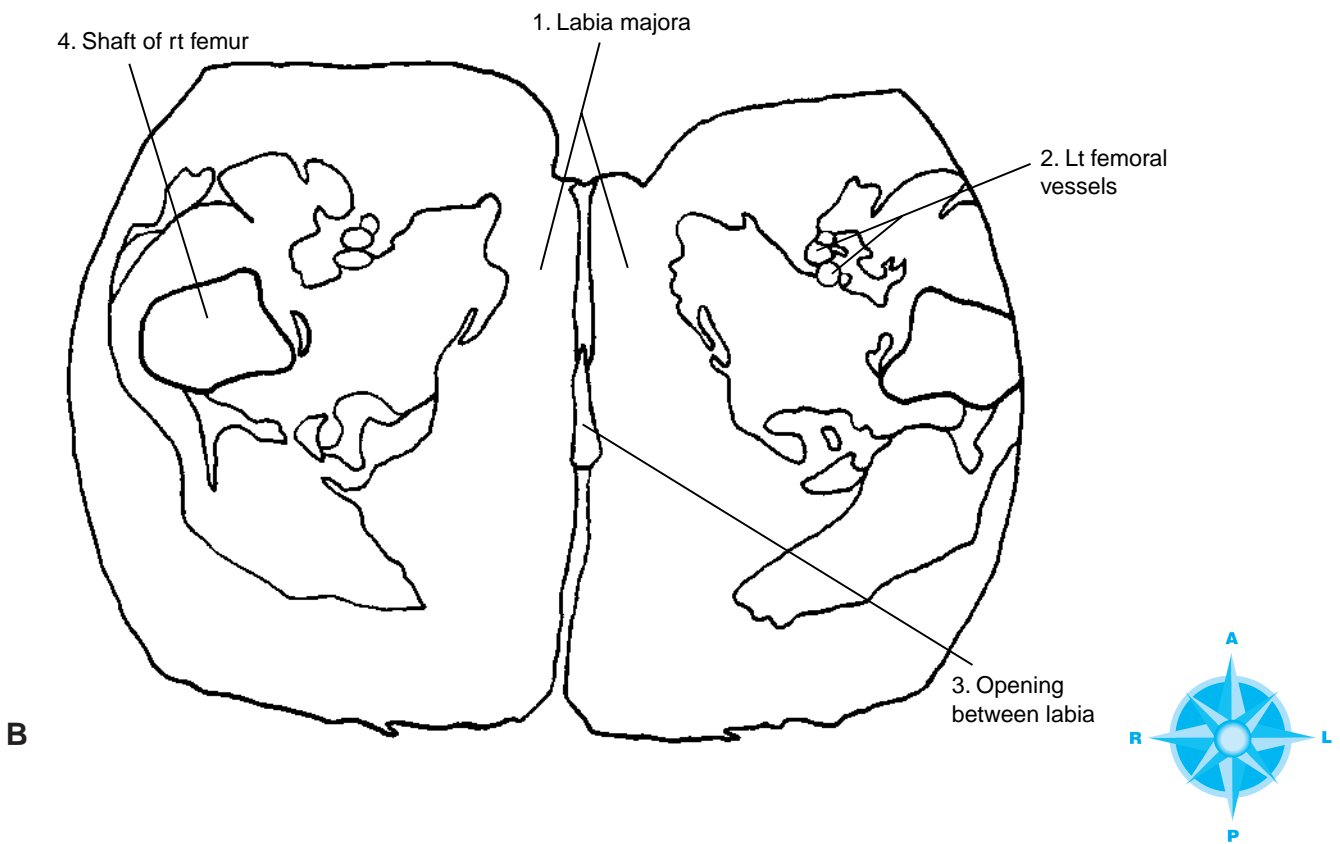
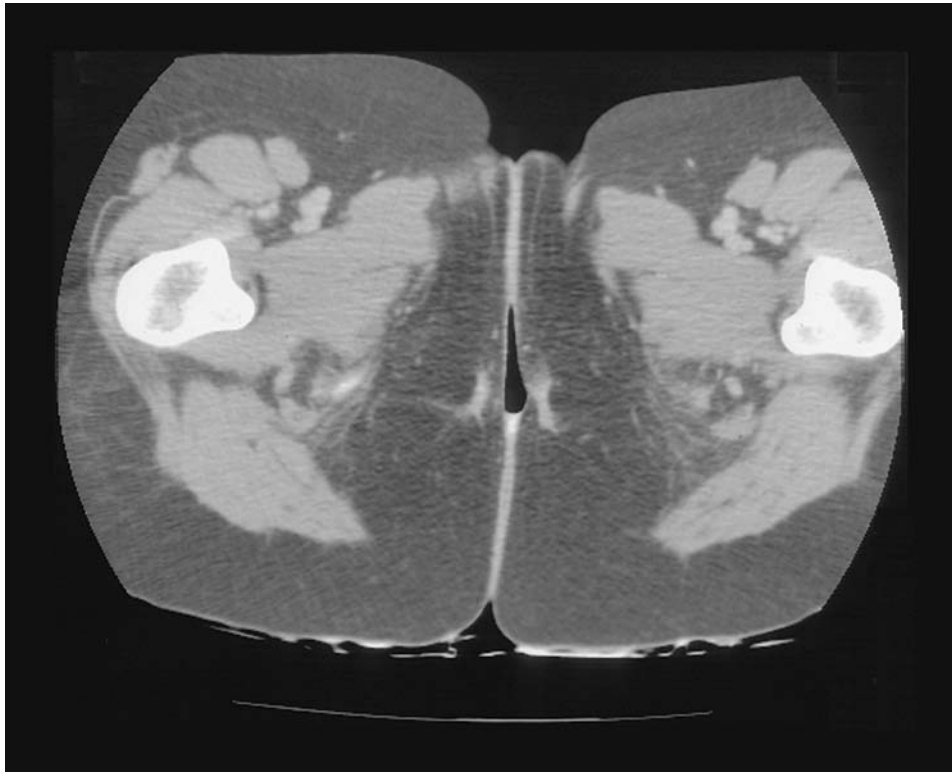


**Figure 4-57 (A,B)** Axial CT image 26: Female.

This section is below the level of the pelvis and indicates completion of an axial examination of the pelvis. Because no pelvic bones can be seen in this image, the only bones are those of the femurs. In cross-section, the shafts of the femurs appear to be large, irregularly shaped bones surrounded by the musculature of the thigh. Within the anterior musculature, a group of femoral vessels can be identified on either side. Between the thighs, the fat-filled labia majora can be identified on either side and are separated by the opening between the thighs.





## Coronal Magnetic Resonance Images: Female

In a typical scan of the pelvis, images are generated throughout the entire bony pelvis. However, the following descriptions will be limited to 11 selected images described at 5-mm intervals from anterior to posterior through the central

region of the female pelvis. The images were generated at the following technical factors: repetition time (TR) = 500 ms; echol time (TE) = 20 ms; field of view (FOV) = 41 cm; slice thickness (TH) = 10 mm (5-mm cuts).

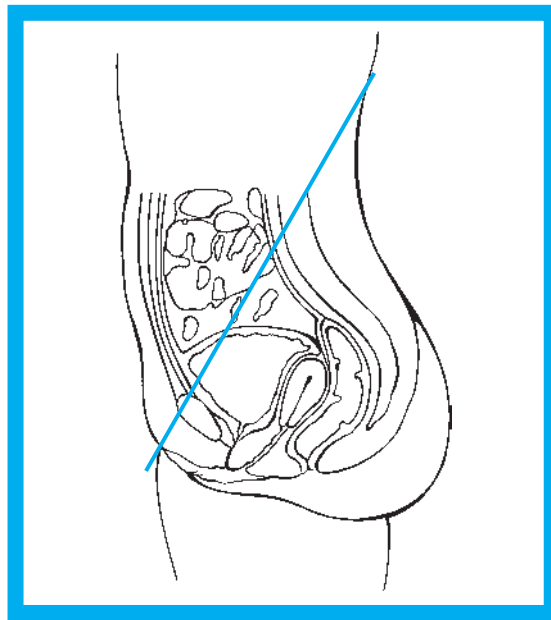
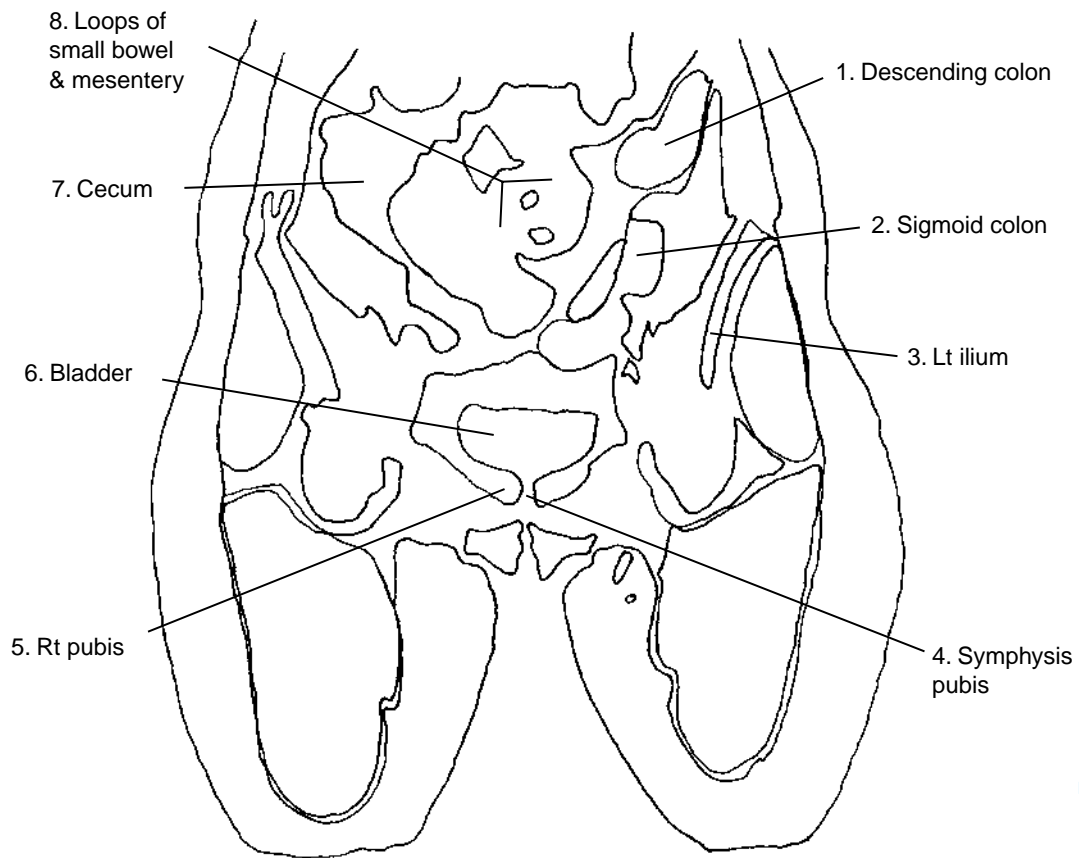


**Figure 4–58 (A,B)** Coronal MR image 1: Female.

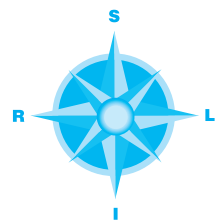
This section is through the anterior pelvis, because the symphysis pubis can be seen between the right and left pubic bones. Outside of the pubic bones, the only other bony structures apparent within this image are the right and left iliac bones forming the lateral borders for the greater or false pelvis. With regard to soft tissue structures, a distinct area of low signal can be seen above the pubic bones representing the anterior part of the urinary bladder. Above the bladder, parts of bowel are sectioned within the greater pelvis or lower abdominal cavity. On the left side, the sigmoid colon is longitudinally sectioned as it extends upward to join with the descending colon. On the opposite side of the lower abdomen, the outline of the cecum can be identified, representing the lowest part of the large intestine found on the right side of the body. Between the segments of large intestine just described, loops of small bowel and mesentery are loosely organized centrally.



A



B



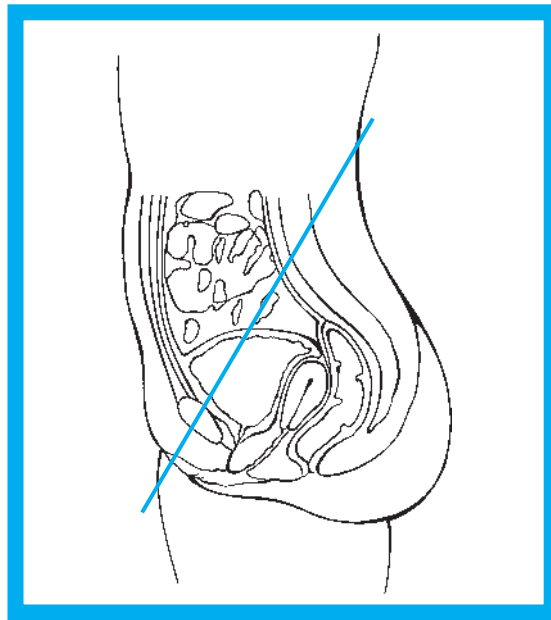
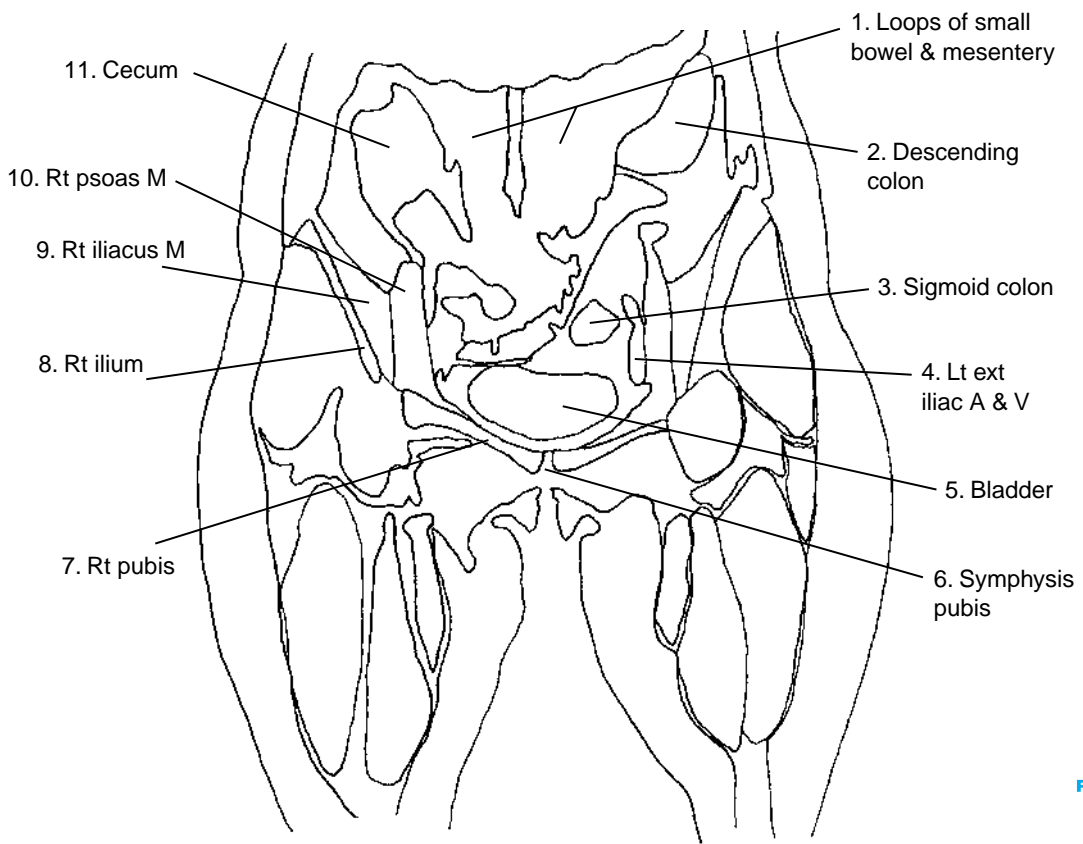


**Figure 4–59 (A,B)** Coronal MR image 2: Female.

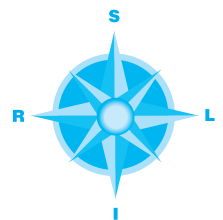
The symphysis pubis can again be seen separating the right and left pubic bones, indicating this plane of section lies within the anterior pelvis. Compared to the previous view, the iliac bones are slightly longer and appear almost continuous with the pubic bones. On the medial aspect of the iliac bones, the flat iliacus muscles are shown near their origin and extend downward through the pelvis to insert on the lesser trochanters of the femurs. Adjoining the iliac muscles, the psoas muscles can be seen on either side extending from their origin on the transverse process of L1 through L5 to join with the iliacus muscles and insert on the lesser trochanters of the femurs. As in the previous image, the urinary bladder is full and appears as a distinct region of low signal intensity directly above the pubic bones. Because this image demonstrates anatomy within the anterior pelvis, the vessels shown on the left side between the urinary bladder and left psoas muscle represent the left external iliac artery and vein. Although the vessels are also seen on the right side in a similar location, they are difficult to discern from surrounding structures. Above the structures just described, various parts of the bowel are sectioned within the greater pelvis. Medial to the left external iliac artery and vein, the sigmoid colon is shown in cross-section as it extends between the rectum in the posterior pelvis to the descending colon in the lower left abdominal cavity. Similar to the previous image, the cecum can be identified on the lower right side of the abdominal cavity and is separated from the descending colon by loops of small bowel and mesentery.



A



B





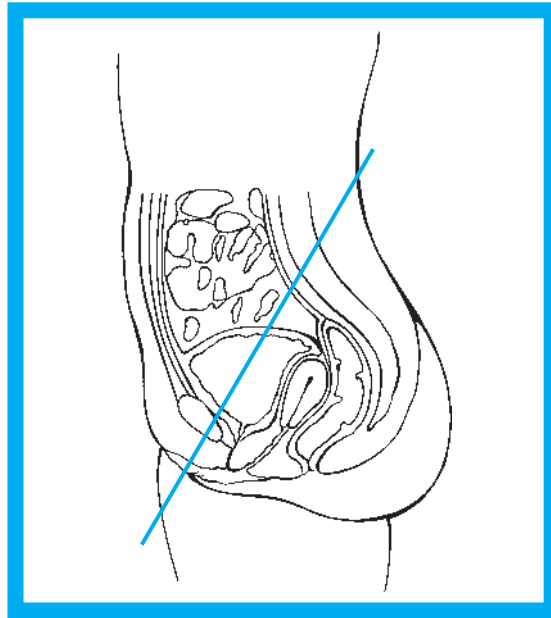
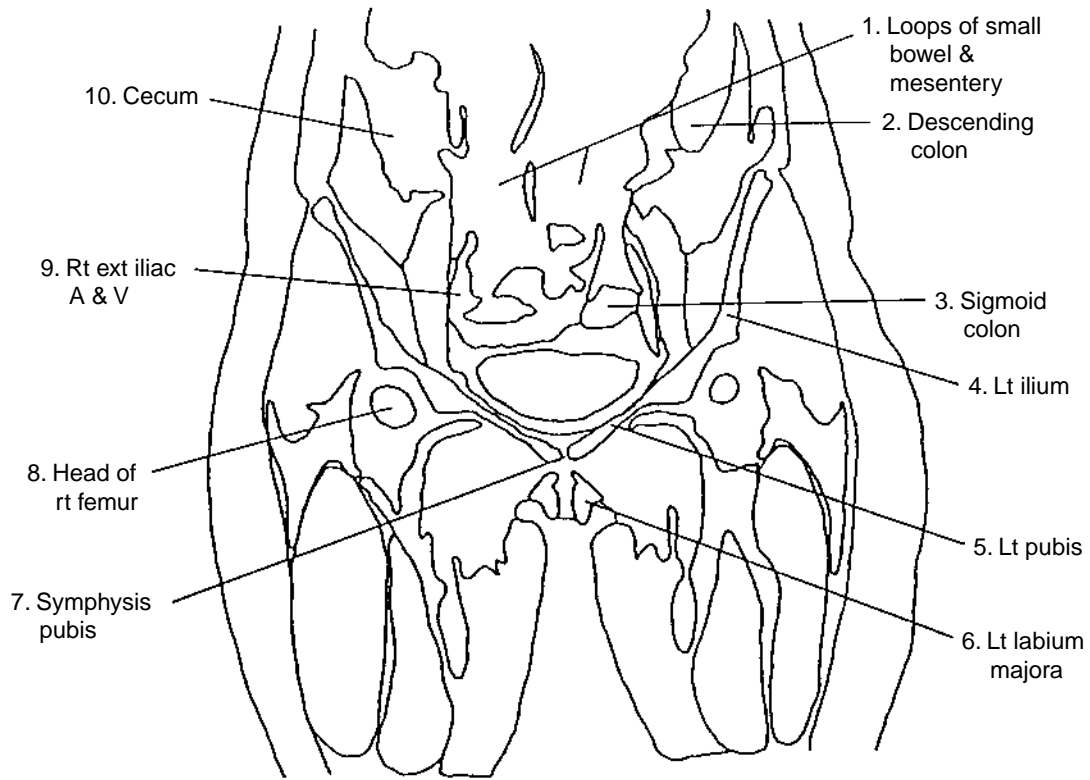


**Figure 4–60 (A,B)** Coronal MR image 3: Female.

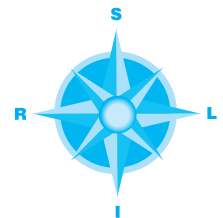
The heads of the femurs are on either side within the acetabula, which separate the iliac and pubic bones. Similar to previous images, the symphysis pubis can be seen between the right and left pubic bones and indicates that this section is within the anterior part of the pelvis. Directly below the symphysis pubis, two irregularly shaped regions of high signal intensity represent the fat-filled labia majora. Within the greater pelvis, the right external iliac artery and vein are more clearly discernible lying near the medial side of the right psoas muscle. Although they are not labeled, the left external iliac artery and vein are also shown medial to the left psoas muscle. Similar to previous images, several bowel structures can be identified within the greater pelvis. The sigmoid colon is again shown in cross-section directly above the bladder as it extends between the rectum and the descending colon. In the lower right abdominal cavity, the cecum is again shown lateral to randomly organized loops of small bowel and mesentery, which appear to lie on the roof of the bladder. Despite the loose organization, all of the bowel structures shown within this image are surrounded by sheets of connective tissue, the peritoneum, that suspend the bowel structures from the posterior abdominal wall and form a variety of mesenteric structures. In addition, the peritoneum forms the lining of the abdominal cavity and separates the structures found within the greater or false pelvis from those in the lesser or true pelvis.

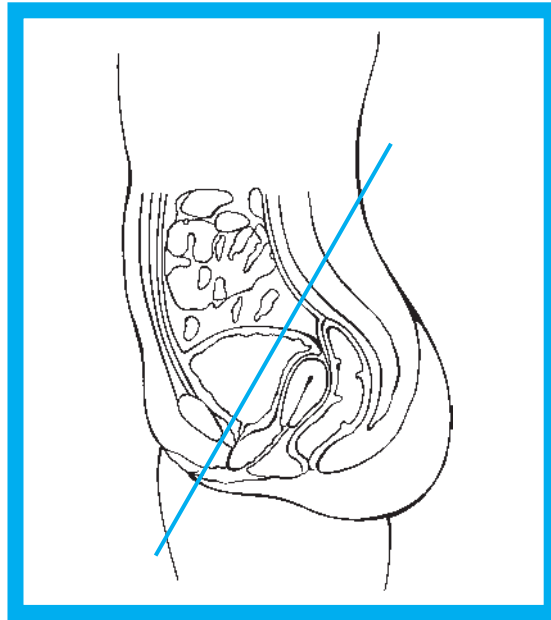


**A**



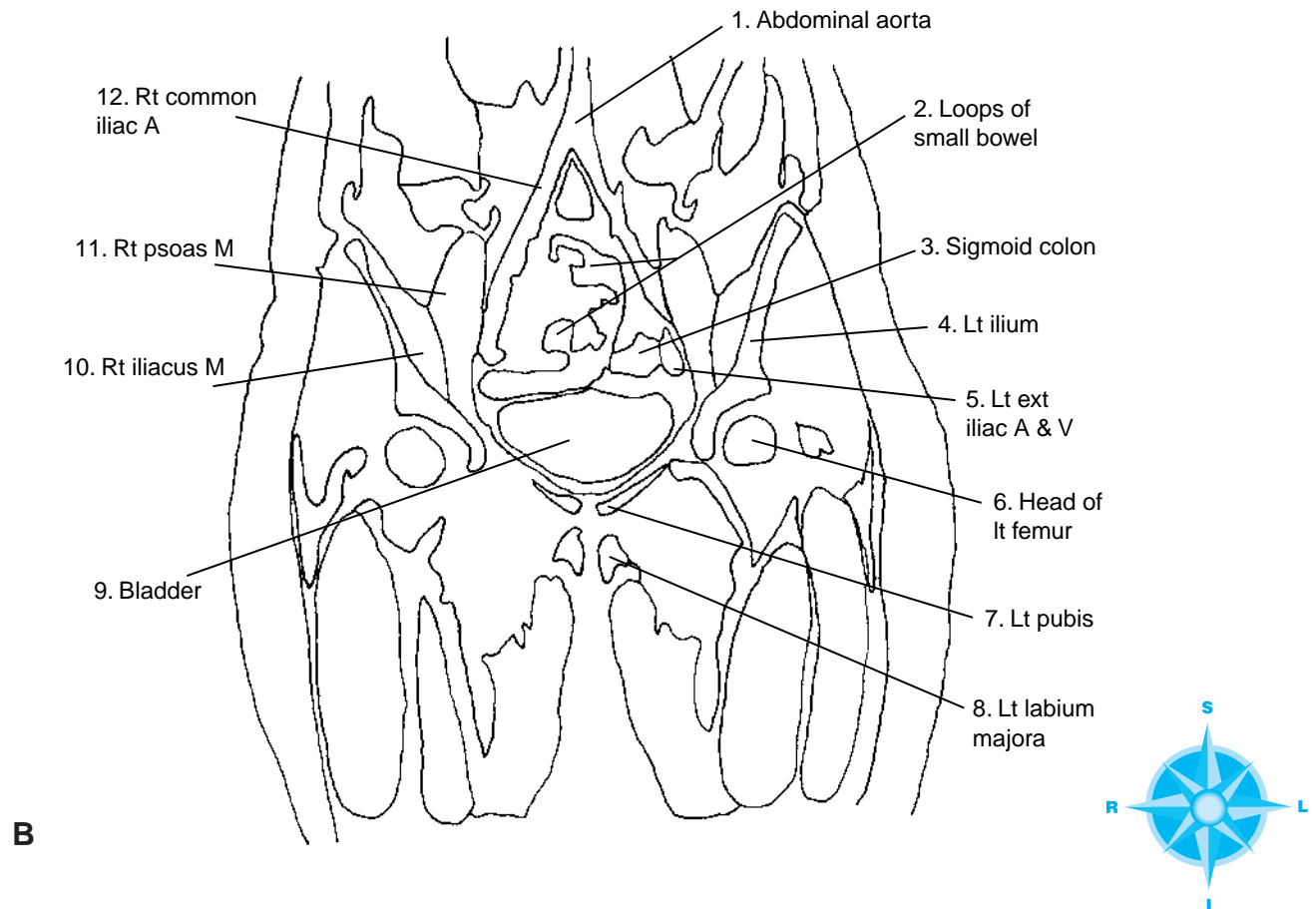
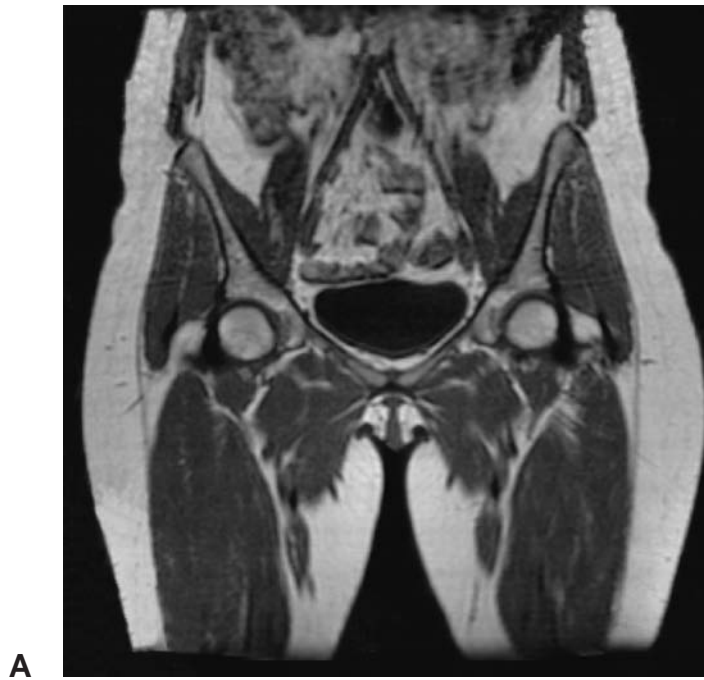
**B**





**Figure 4–61 (A,B)** Coronal MR image 4: Female.

The heads of the femurs appear larger and the iliac bones appear thicker in this image than in the previous image, indicating that we are nearing the midregion of the bony pelvis. Although the pubic bones can again be seen on either side between the urinary bladder and the labia majora, they are thinner than in previous views, indicating that we are nearing the region of the pelvic opening. Within the pelvis, the iliacus and psoas muscles are clearly shown on either side and appear to be joining together as they extend downward inserting into the lesser trochanters of the femurs. Because the psoas muscles originate from the transverse processes of the lumbar vertebrae, they form part of the posterior abdominal wall. Between the psoas muscles the abdominal aorta is shown longitudinally sectioned, giving rise to the right and left common iliac arteries. A shadow slightly to the right of the abdominal aorta represents the inferior vena cava, which also bifurcates near this region to give rise to the right and left common iliac veins. Similar to previous images, the external iliac artery and vein are found on either side just medial to the psoas muscles. Above the urinary bladder, loops of small bowel and sigmoid colon are sectioned within the lower peritoneal cavity.



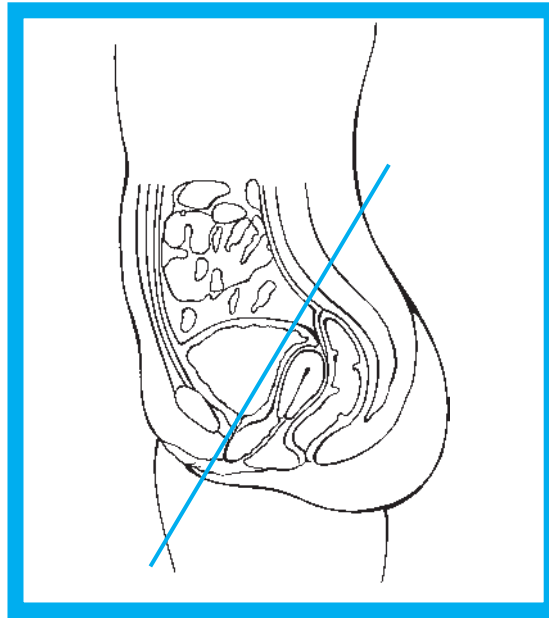
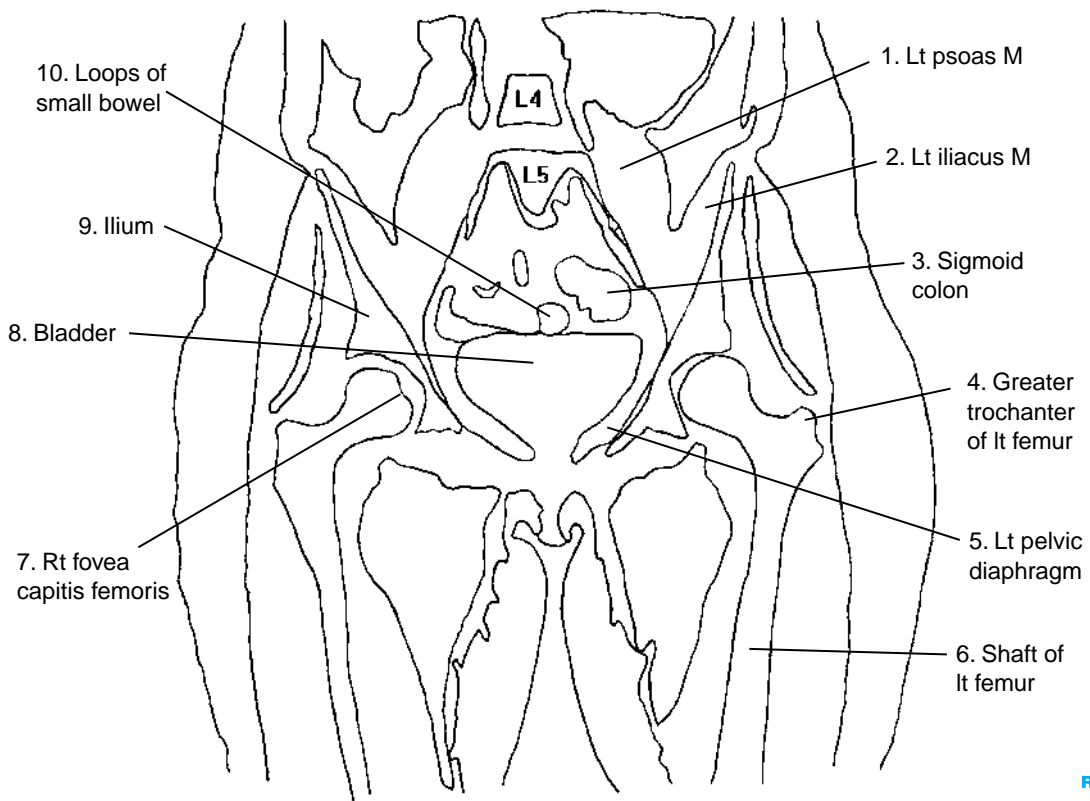


**Figure 4–62 (A,B)** Coronal MR image 5: Female.

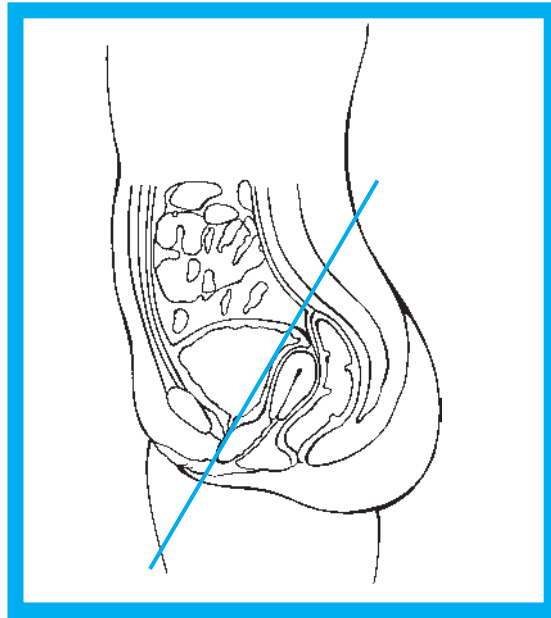
On either side, the proximal end of the femur is readily apparent. On the upper part of the femur, the greater trochanter projects upward and provides a sight of attachment for musculature around the hip joint. The head of the femur is found within the acetabulum, which is formed in this image predominantly by the ilium. On the right side, an indentation within the rounded portion of the head of the femur represents the fovea capitis femoris. The ligamentum teres originating within the acetabular fossa attaches to the head of the humerus at the fovea capitis femoris. Within the pelvis, the urinary bladder appears as a distinct region of low signal intensity. Similar to previous images, loops of small bowel and the sigmoid colon within the lower peritoneal cavity lie just above the bladder. In contrast to previous views, the anterior cortical margins of L4 and L5 are now seen between the proximal ends of the psoas muscles. As mentioned, the psoas muscles originate from the transverse processes of the lumbar vertebrae and extend downward to join with the iliacus muscles to insert on the lesser trochanters of the femurs.



A

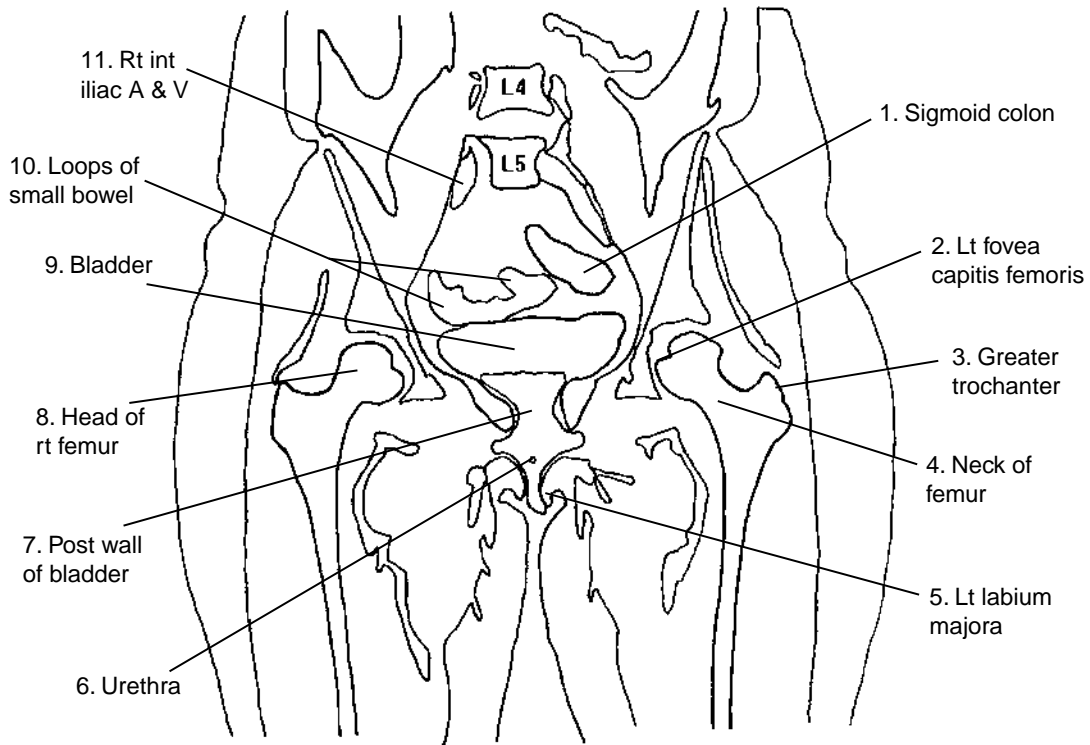
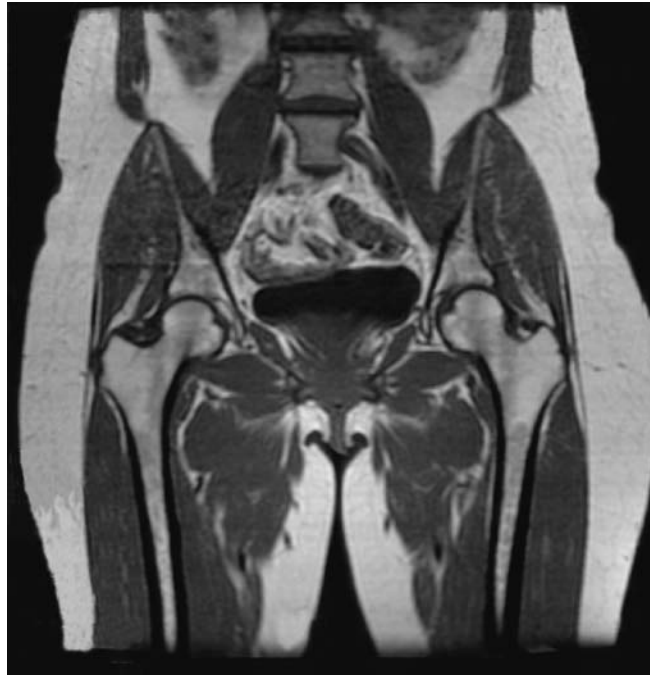


B

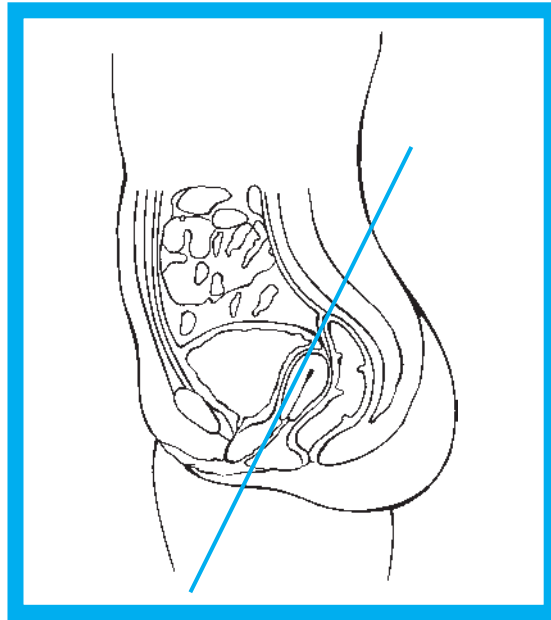


**Figure 4–63 (A,B)** Coronal MR image 6: Female.

The proximal ends of the femurs are readily apparent in this image and demonstrate the following bony features: Shaft, greater trochanter, neck, and head. Within the head of the left femur, the fovea capitis femoris is labeled and represents the site of attachment for the ligamentum teres. Compared to the previous view, the low-signal-intensity region of the bladder is somewhat smaller, indicating that the section is near the posterior wall. Below the bladder, the urethra is cross-sectioned above the labia majora. Similar to previous views, the loops of small bowel and sigmoid colon in the lower peritoneal cavity are shown between the bladder and the vertebral bodies of L4 and L5. On either side of the body of L5, the internal iliac arteries and veins are shown as they project posteriorly to become continuous with vessels in the gluteal region.

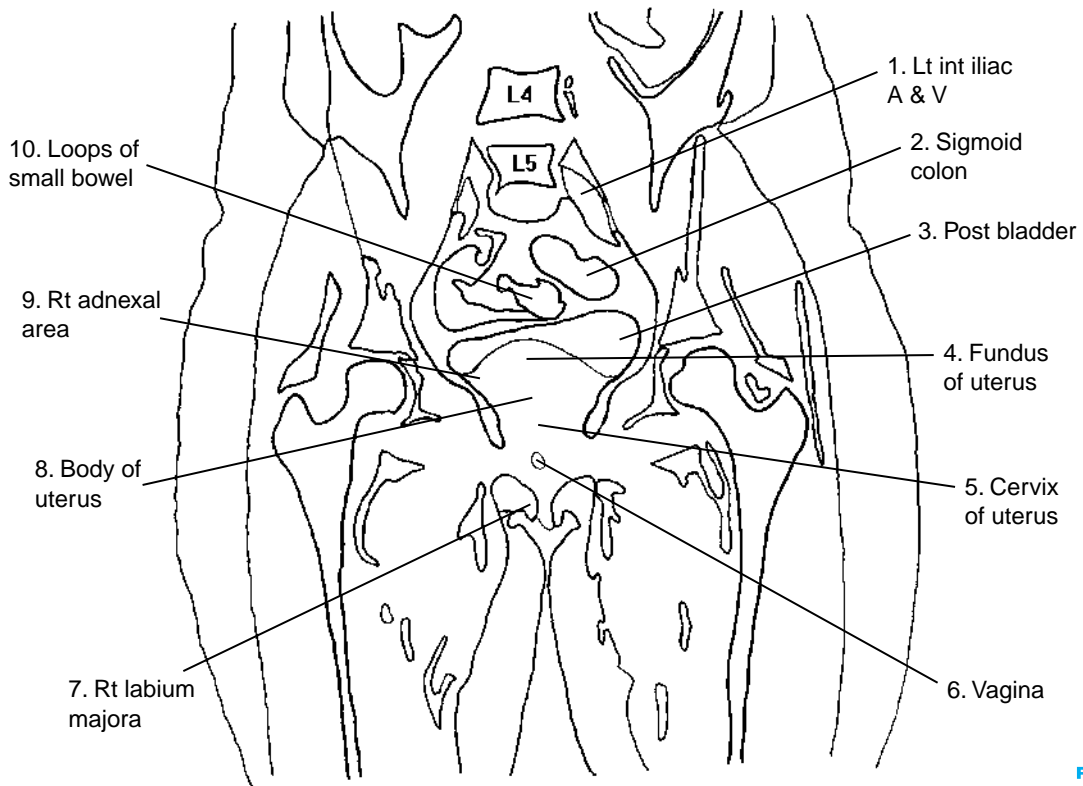
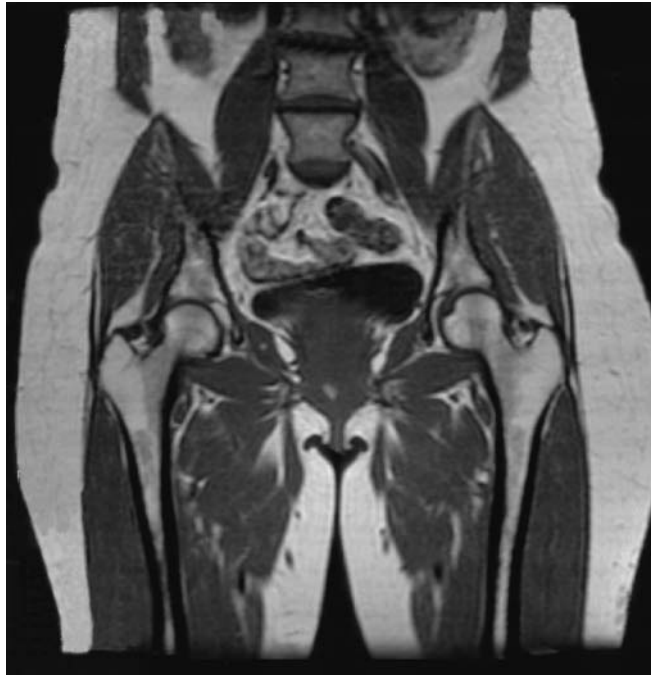






**Figure 4–64 (A,B)** Coronal MR image 7: Female.

The proximal femurs are readily apparent on either side, indicating that this section is through the midpelvic region. Within the pelvis, the posterior part of the bladder appears to lie over the uterus. The upper part of the uterus, the fundus, lies near the midline slightly above the right and left adnexal areas. As described earlier, the adnexal area includes the uterine appendages such as the ovaries, oviducts, and other structures found within the broad ligaments on either side of the uterus. Below the body of the uterus, the cervix or narrowed part is adjacent to the opening of the vagina. Shown in cross-section, the vagina lies between the cervix of the uterus and the labia majora. Above the urinary bladder, loops of small bowel and sigmoid colon are within the lower peritoneal cavity and appear to rest on the roof of the bladder. Above the bowel structures, the posterior branches of the common iliac vessels (the internal iliac artery and vein) are obliquely sectioned on either side of the vertebral body of L5.



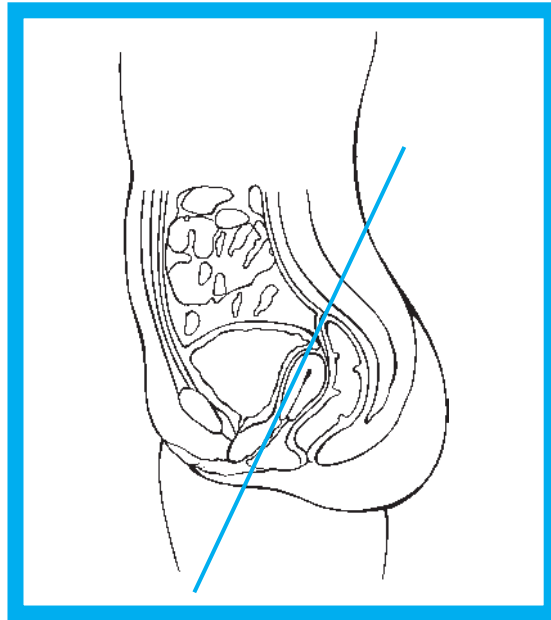
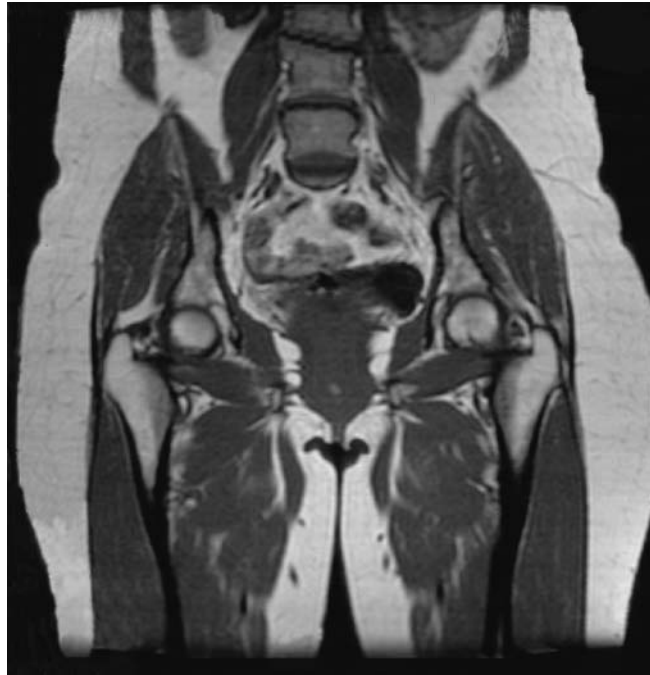
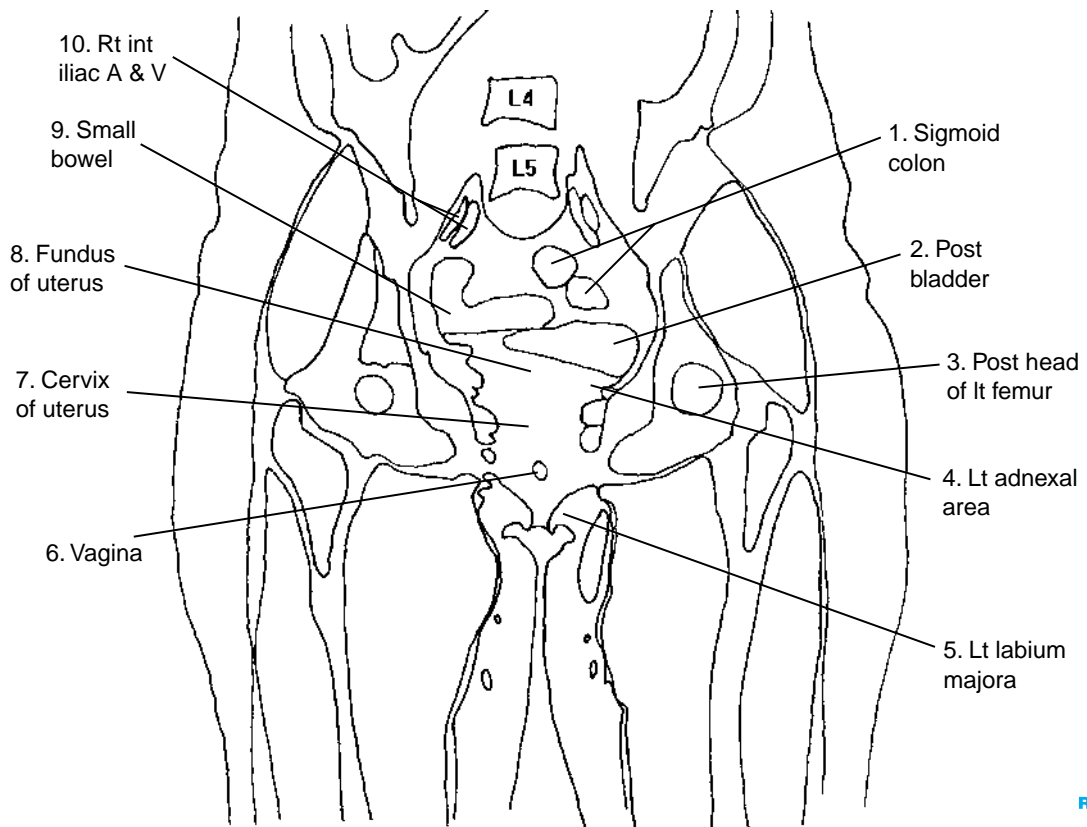


**Figure 4–65 (A,B)** Coronal MR image 8: Female.

In this section, only the posterior parts of the proximal femurs are shown on either side of the pelvis. Similar to the previous view, a small part of the posterior bladder appears to be draping over the fundus of the uterus and its appendages. In this patient, the posterior bladder is predominantly seen on the left side above the left adnexal area. The narrowed region representing the cervix of the uterus lies adjacent to the vagina, which is a muscular tube lined with mucous membrane connecting the uterine cavity to the exterior between the labia majora. Similar to previous images, the small bowel and sigmoid colon are within the lower peritoneal cavity above the posterior bladder. On either side of the vertebral body of L5, the internal iliac vessels are obliquely sectioned as they extend from their origin on the common iliac vessels to extend through the pelvis to become continuous with terminal branches in the gluteal region.



A



B

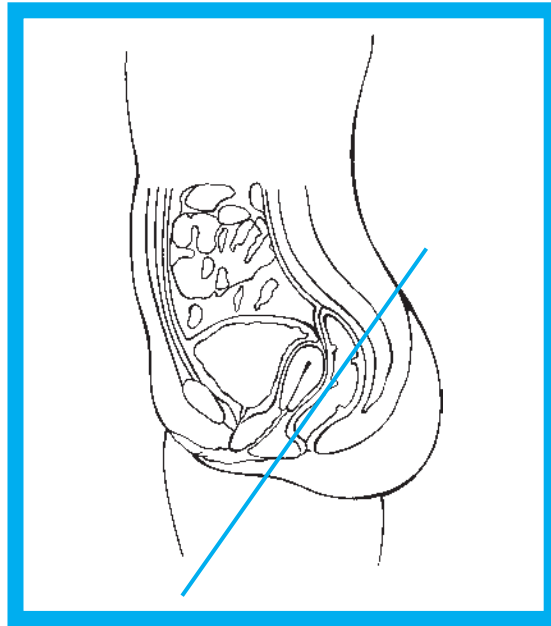
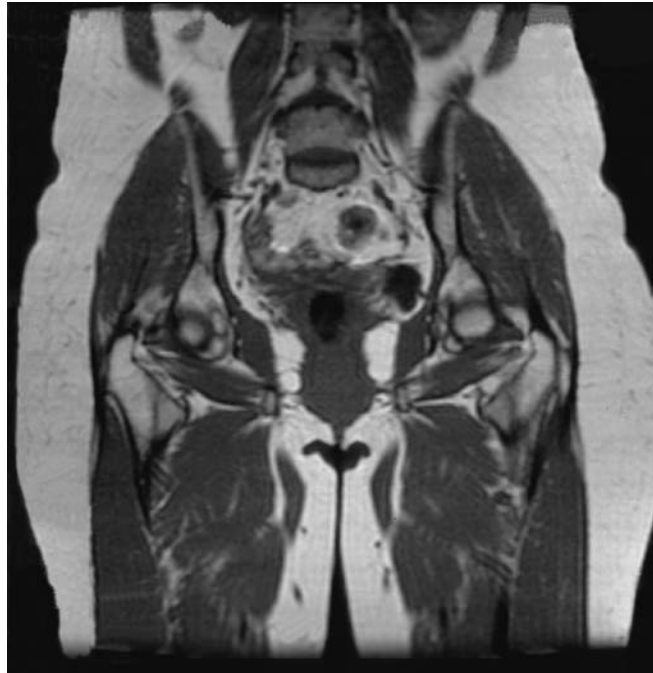
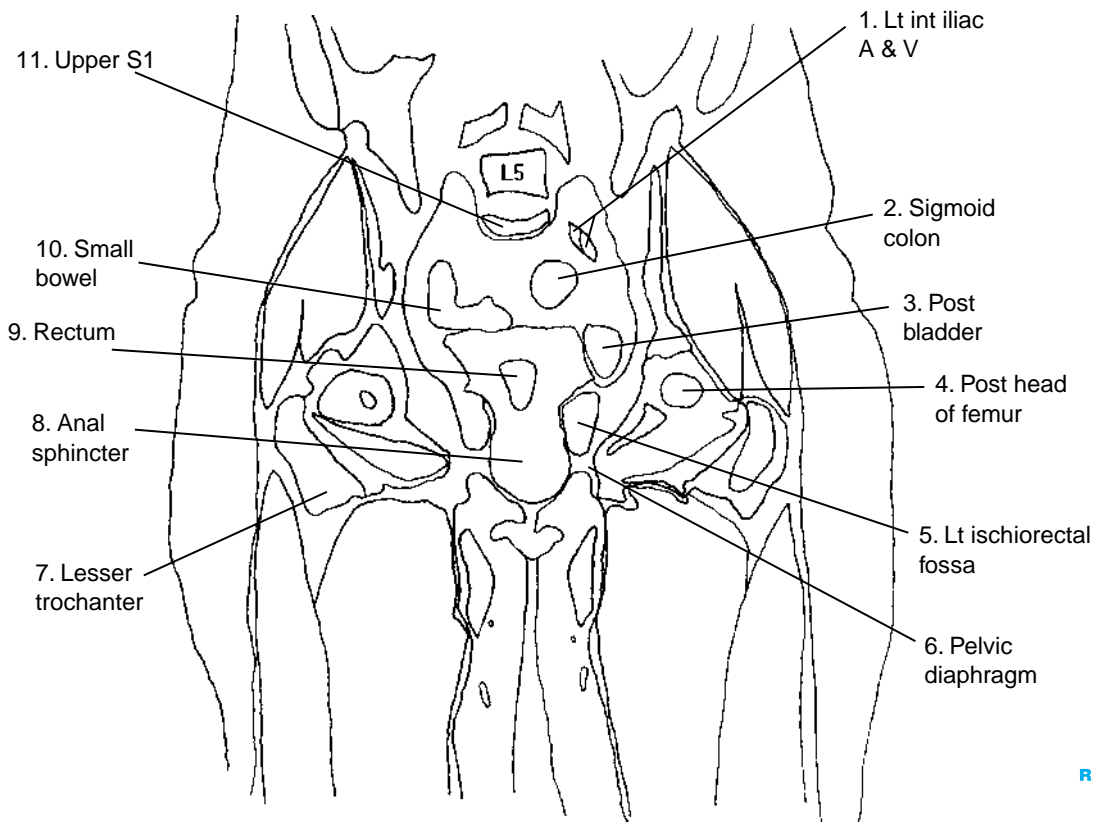


**Figure 4–66 (A,B)** Coronal MR image 9: Female.

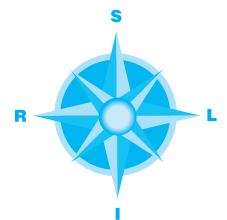
The proximal part of the femur can be seen on either side even though it appears to be in two parts. The rounded region representing the posterior head of the femur is still shown within the acetabulum, whereas the lesser trochanter and the intertrochanteric crest appear within the musculature of the upper thigh. Following the bladder from the previous section, only a small part of the posterior bladder is seen within this section on the left side. In the position previously occupied by the uterus, a region of low signal intensity represents the anterior part of the rectum. Found behind the bladder, the rectum extends between the distal part of the sigmoid colon and the anal canal. Directly below the rectum, the musculature of the anal sphincter is shown between the fat-filled ischioanal fossae and the thin, flat muscular sheet representing the pelvic diaphragm. Similar to previous images, segments of the small bowel and sigmoid colon are sectioned within the lower peritoneal cavity and are found above the bladder and the rectum. On either side of the vertebral column, the internal iliac vessels are sectioned as they extend through the pelvis to enter the gluteal region. In the midline, the vertebral body of L5 is sectioned directly above the upper part of S1.

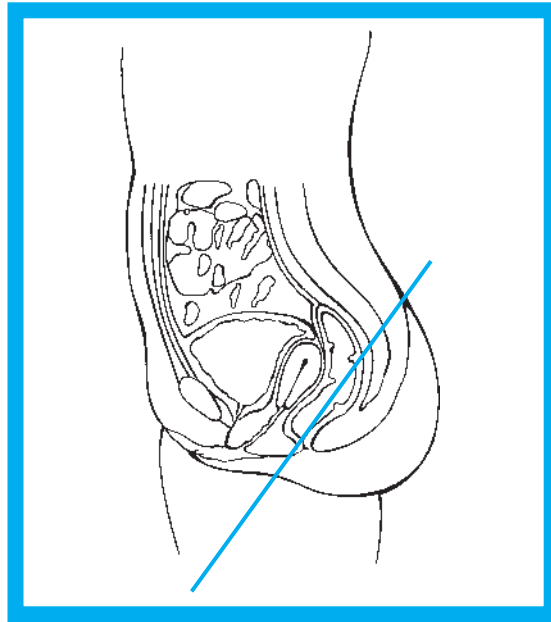


A



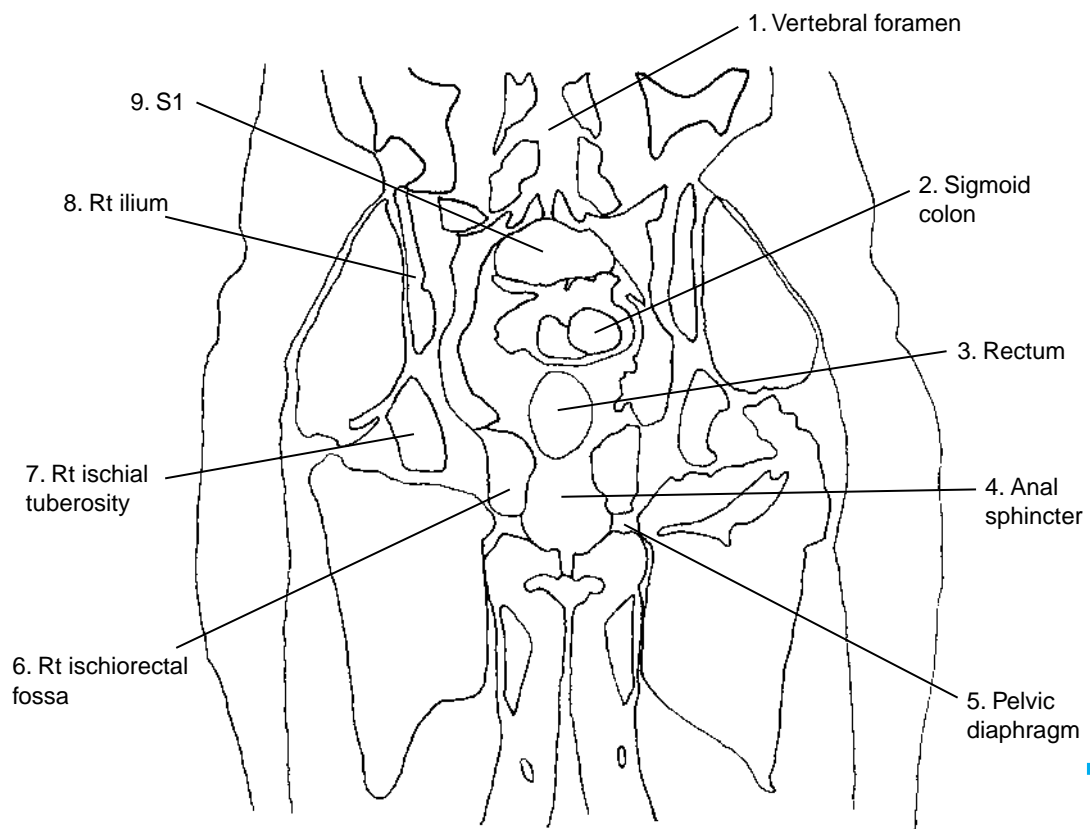
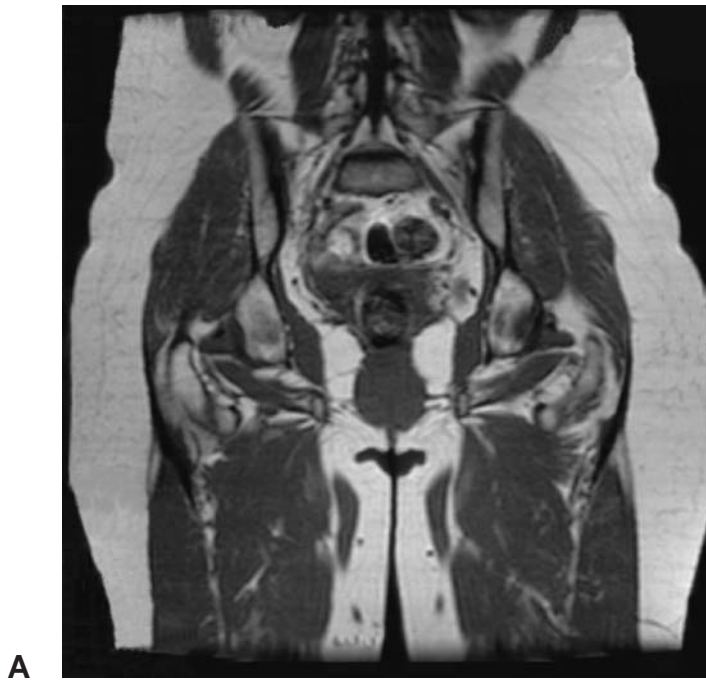
B





**Figure 4–67 (A,B)** Coronal MR image 10: Female.

In the region previously occupied by the vertebral bodies of L4 and L5, the vertebral foramen now appears as a region of low signal intensity containing the dural sac and the cauda equina. In this coronal section, the vertebral body of S1 appears larger and is found between the iliac bones, which appear nearly vertical. On the lower part of the bony pelvis, the ischial tuberosities are found on either side and appear as enlarged or thickened regions of the ischial bones. Within the pelvis, the end of the sigmoid colon is sectioned just above the rectum, which appears larger than it did in the previous image. Below the rectum, the musculature of the anal sphincter is again surrounded by the fat-filled ischioanal fossae and the thin, flat musculature of the pelvic diaphragm, shown in cross-section. As described earlier, the pelvic diaphragm is a group of flat muscles that form a sling across the pelvic cavity and support the pelvic viscera.





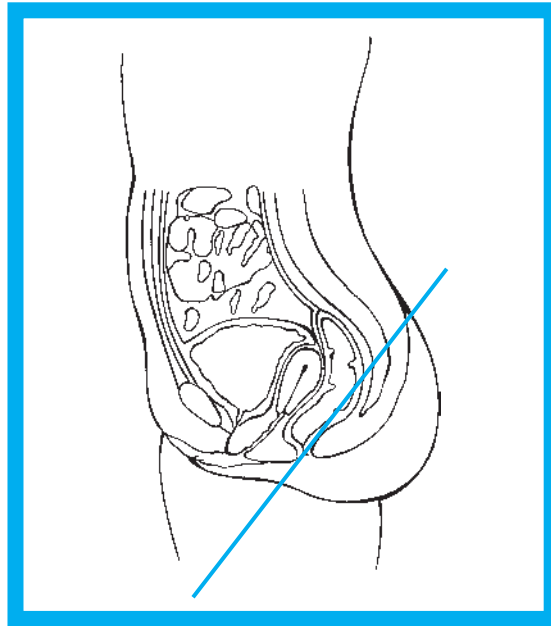
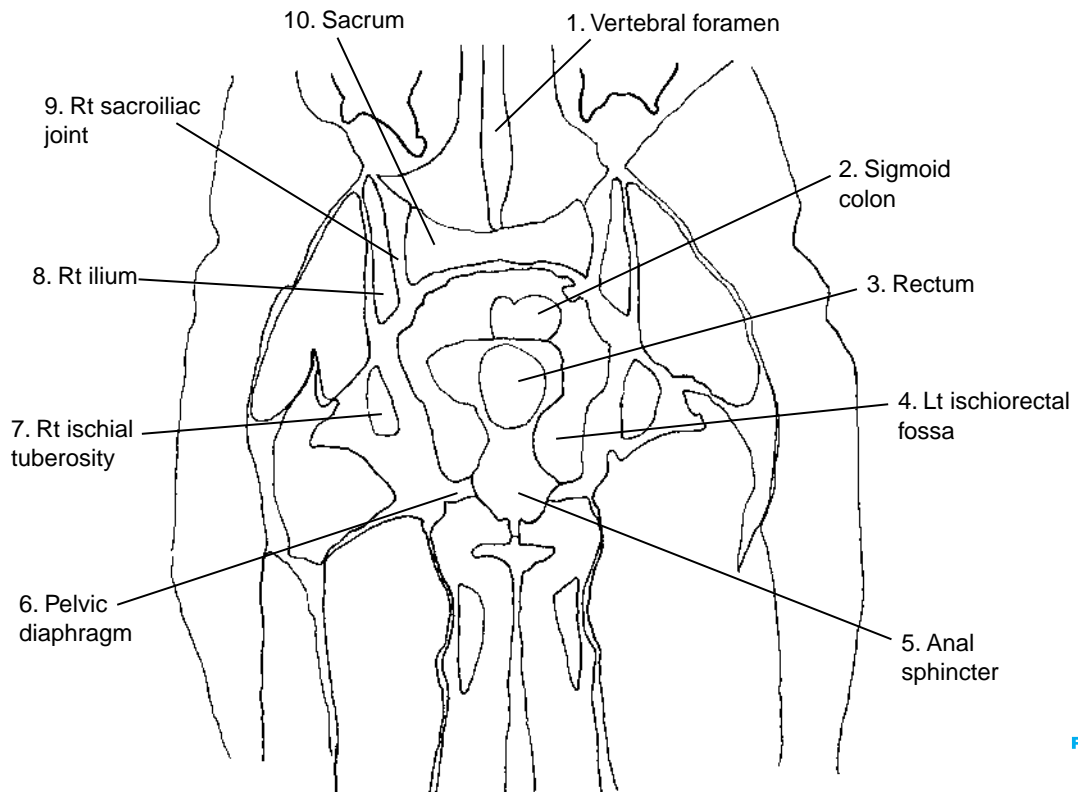


**Figure 4–68 (A,B)** Coronal MR image 11: Female.

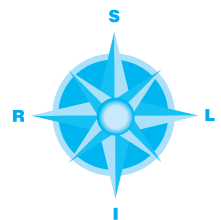
In this plane of section, the lateral parts of the sacrum are shown extending toward either side to articulate with the iliac bones to form the sacroiliac joints. In the position previously occupied by the vertebral bodies of L4 and L5, the vertebral foramen is longitudinally sectioned as it extends downward to the sacrum. Similar to the previous image, the iliac bones appear nearly vertical and are located above the thickened regions of bone found on either side of the pelvis that represent the ischial tuberosities. Within the pelvis, the rectum is centrally located, is larger than in previous views, and is nearing its juncture with the sigmoid colon. Below the rectum, the musculature of the anal sphincter is surrounded by the fat-filled ischiorectal fossae and the cross-section of flat muscles representing the pelvic diaphragm.



A



B





## Case Study 4-1

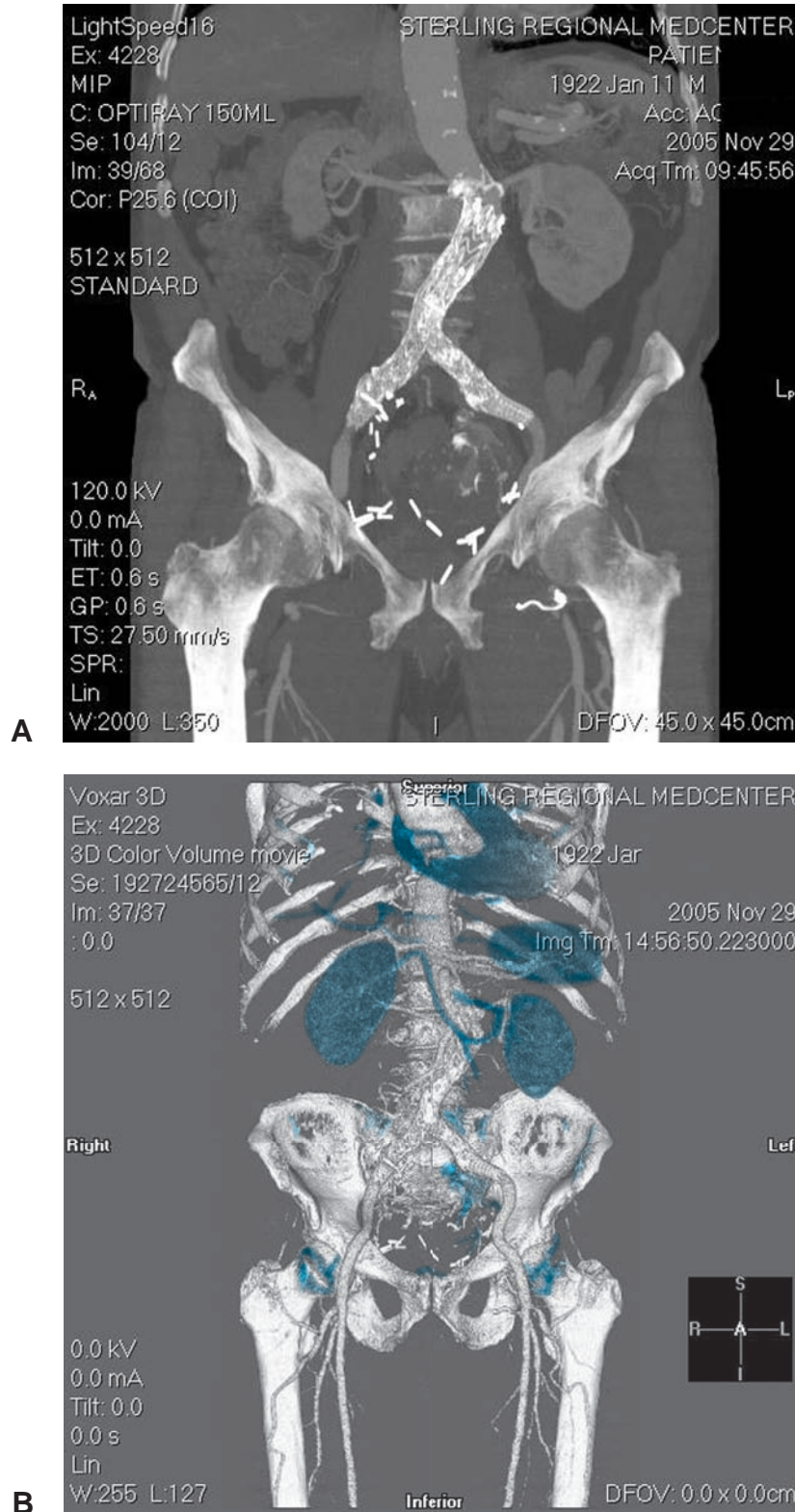


Figure 4-69

## Clinical Correlations

This 84-year-old man underwent a helical dynamic contrast-enhanced arterial phase CT scan for follow-up evaluation of aortobilateral iliac endografting. As shown in the coronal image, the stent graft has been placed below the origins of the renal arteries extending to both external iliac

arteries. For comparison, the three-dimensional reconstructed image shows the stent graft fusing with the external iliac arteries that continue out of the anterior pelvis to become the femoral arteries. As evidenced by the images, the endograft is patent, and there is no evidence for endoleak.

## Questions

1. Define a patent vessel.
2. Describe a vascular stent.
3. Although the inferior vena cava is not shown in the images in Figure 4–69 A and B, would it be found on the right or left side of the abdominal aorta?
4. Do the external or internal iliac vessels provide the major source of blood supply for the legs?
5. When the femoral vessels join the pelvis, is the artery or the vein located closest to the lateral side?



## Case Study 4-2

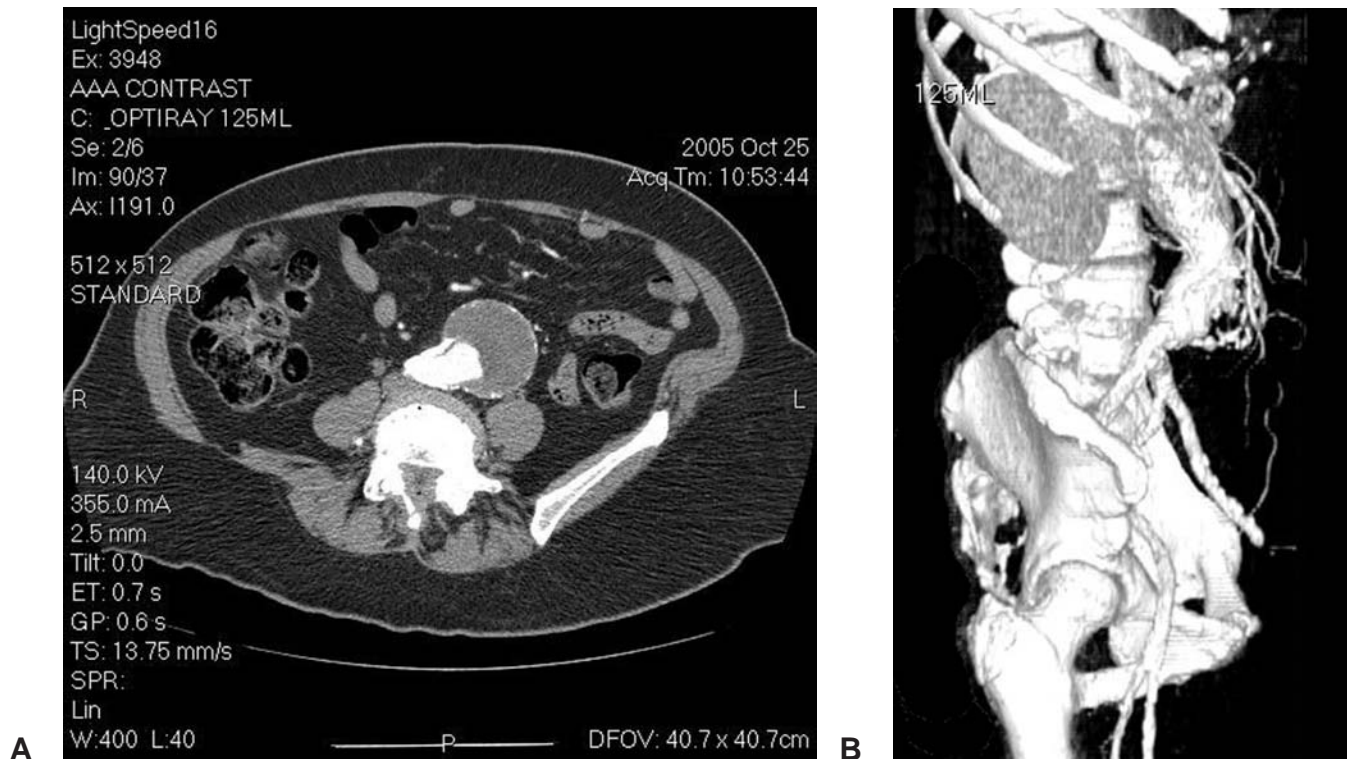


**Figure 4-70**

This 58-year-old man underwent a helical dynamic contrast-enhanced arterial phase CT scan during the injection of 25 mL of Optiray 320 to evaluate an abdominal aortic aneurysm. There is ectasia of the abdominal aorta starting just below the renal arteries. The saccular distal abdominal aortic aneurysm measures 5.7 cm in maximal

transverse diameter with notable atherosclerotic disease. Atherosclerosis disease is noted involving the origins of all the major aortic branch vessels, but these appear to be reasonably well perfused. There is no evidence for retroperitoneal hemorrhage or significant fibrosis.

### Questions

1. How and where does the abdominal aorta terminate?
2. Describe the spatial relationship between the abdominal aorta and the inferior vena cava.
3. The calcium shown within the aorta would best be described as \_\_\_\_\_ disease.
4. Compare the location and appearance of the external iliac artery and vein.
5. Explain how blood from the abdominal aorta is supplied to muscles in the region of the buttocks.



## Case Study 4-3

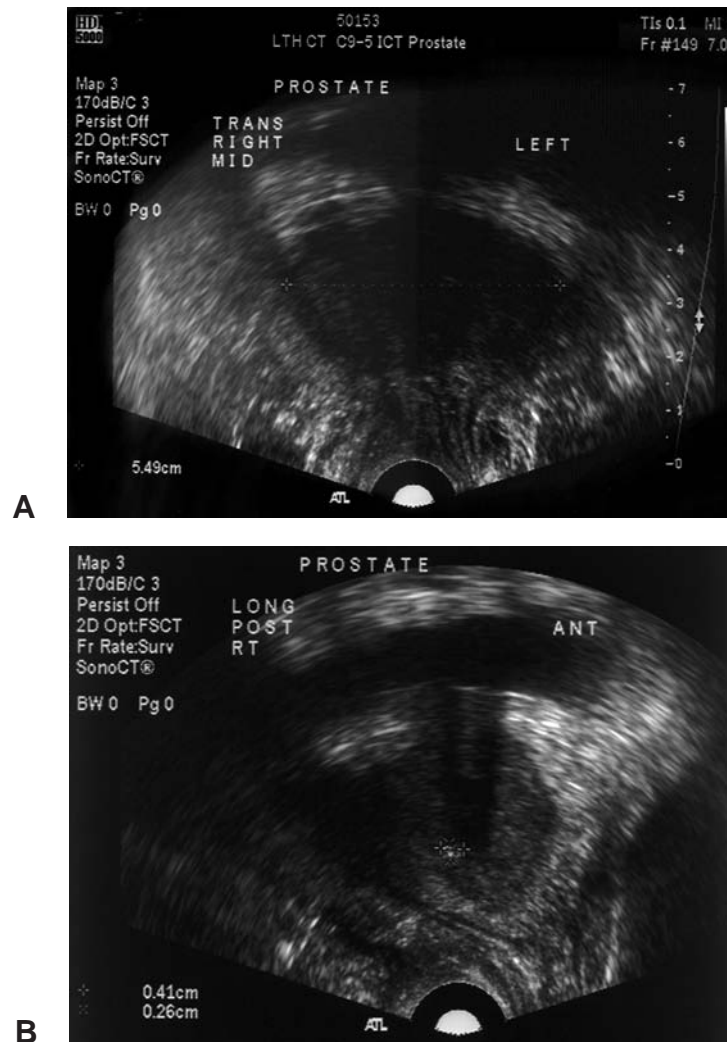


Figure 4-71

This 55-year-old man was referred for an ultrasound examination of the prostate because his prostate specific antigen (PSA) was elevated and his family history included prostate cancer. The prostate surrounds the urethra just below the urinary bladder and should measure 4 cm in the transverse plane. As shown by the marked measurements in the image

above, the prostate gland measured 5.5 cm demonstrating enlargement of the prostate gland. On the longitudinal image, there is a cystic area located centrally that measures  $0.41 \times 0.26$  cm, and there are multiple areas of echogenicity that show shadowing, compatible with prostate gland calcifications. No mass lesion is demonstrated other than the small cyst.

## Questions

1. Where is the prostate gland located including relationships with urinary structures?
2. Describe the tissues in the prostate gland.
3. In a typical patient, where are the seminal vesicles in relation to the prostate gland? Are there any connections?
4. Describe the function of the prostate.
5. What is the name of the erectile tissue surrounding the urethra?





## Case Study 4-4

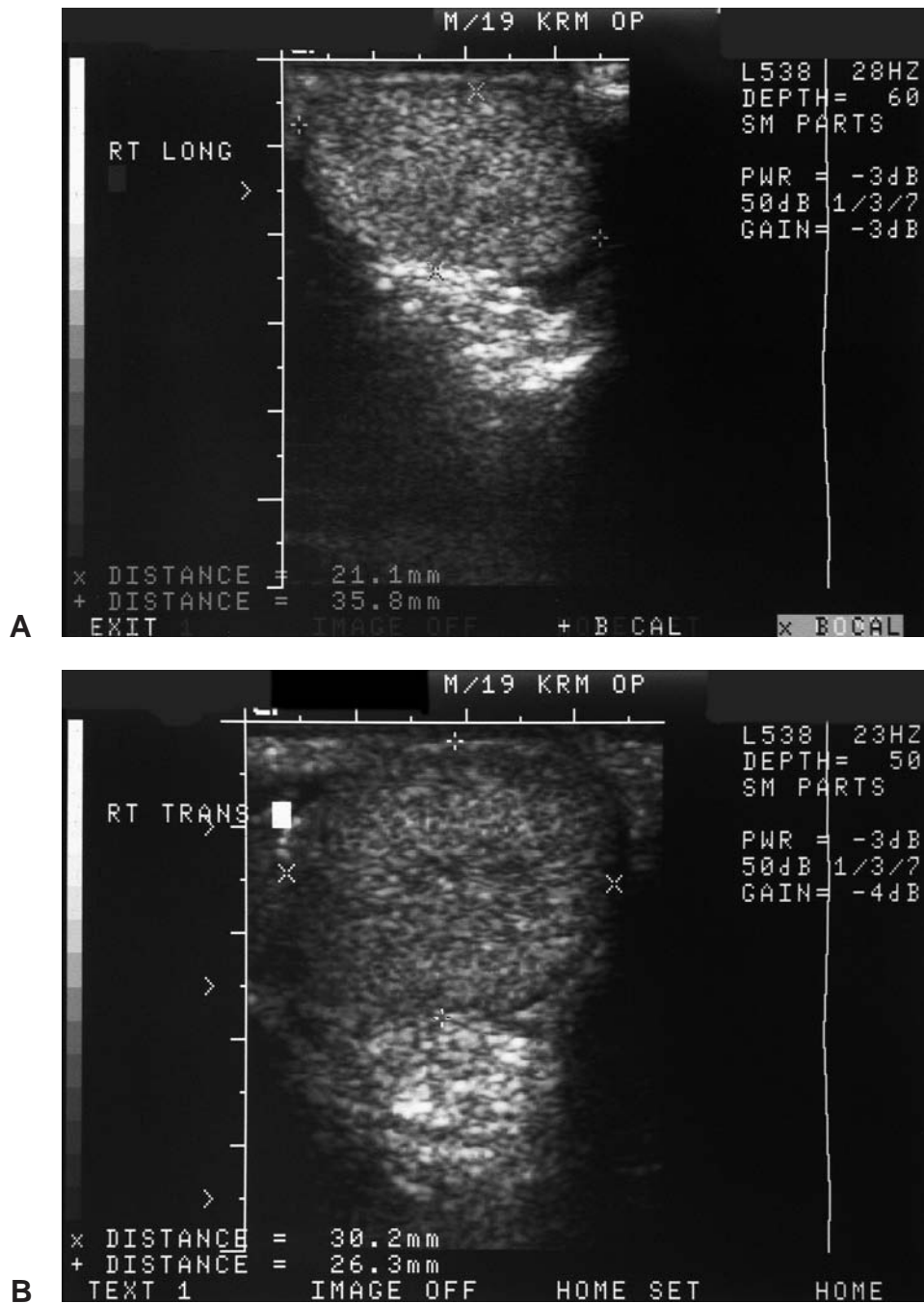


Figure 4-72

This 19-year-old man was referred for an ultrasound examination of the testicles because of an enlarged left testicle discovered during a self-examination. For comparison, the right testicle was evaluated and appears to be homogenous and unremarkable in appearance. The borders of the testicle are marked to measure  $21 \times 36$  mm (longitudinal) and  $30 \times 26$  mm (transverse) in each plane

of section which is well within normal limits. On the left side (not shown), ultrasound imaging demonstrated a heterogenous mass involving a large portion of the testicular parenchyma that was later found after biopsy to consist of germ cell carcinoma. Fortunately, this neoplasm was discovered early and most patients (90%) can be cured if diagnosed in time.

## Questions

1. Describe the location of the testicles as compared to the bony pelvis.
2. Describe the course of the duct connecting between the testicles and urinary structures.
3. How does the spermatic cord enter the pelvis?
4. Describe the course of the male urethra.
5. How does the urethra exit the pelvis?





## Case Study 4-5

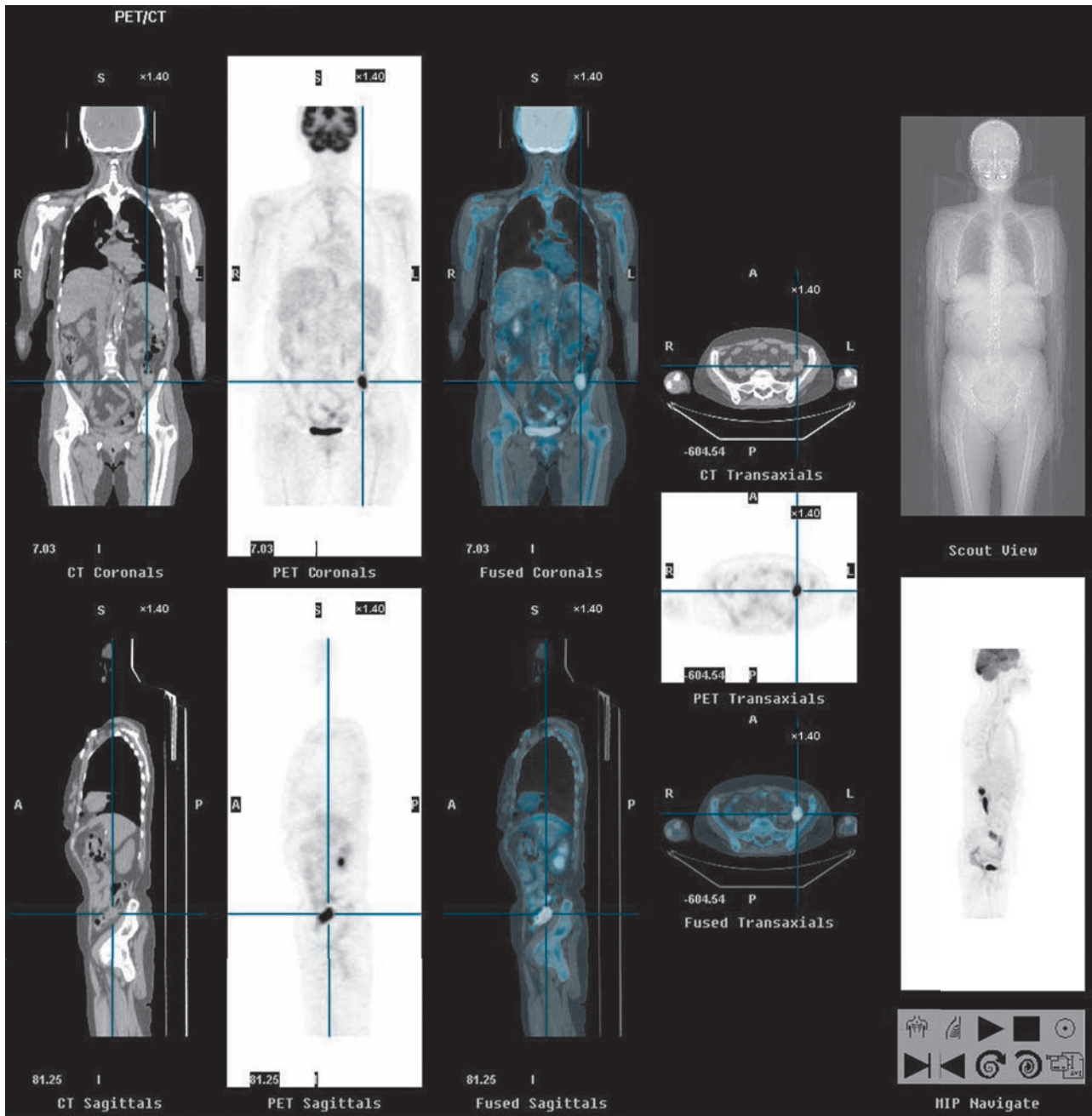


Figure 4-73

This positron emission tomography (PET)/CT case is a 59-year-old white woman previously diagnosed with stomach carcinoma with resection 13 months before this examination. Before the procedure, the patient received a single IV dose of 15.78 mCi of F-18 FDG. The PET/CT study was conducted to more accurately stage the stomach carcinoma.

At the time of this study, a large area of abnormal uptake was found in the proximal sigmoid colon near the junction with the descending colon. Although this may have been metastatic disease from the stomach carcinoma, biopsy results determined that the mass was a second primary site determined to be colon carcinoma.

## Questions

1. Describe the shape and location of the sigmoid colon.
2. Would the top of the sigmoid colon be on the right or left side of the patient?
3. Describe the relationship between the sigmoid colon and the pelvic diaphragm. What part of the alimentary tract extends through the pelvic diaphragm?
4. Describe the contents and location of the ischiorectal fossae.
5. Compare the peritoneal location of the adnexal areas with the sigmoid colon.



## Case Study 4-6

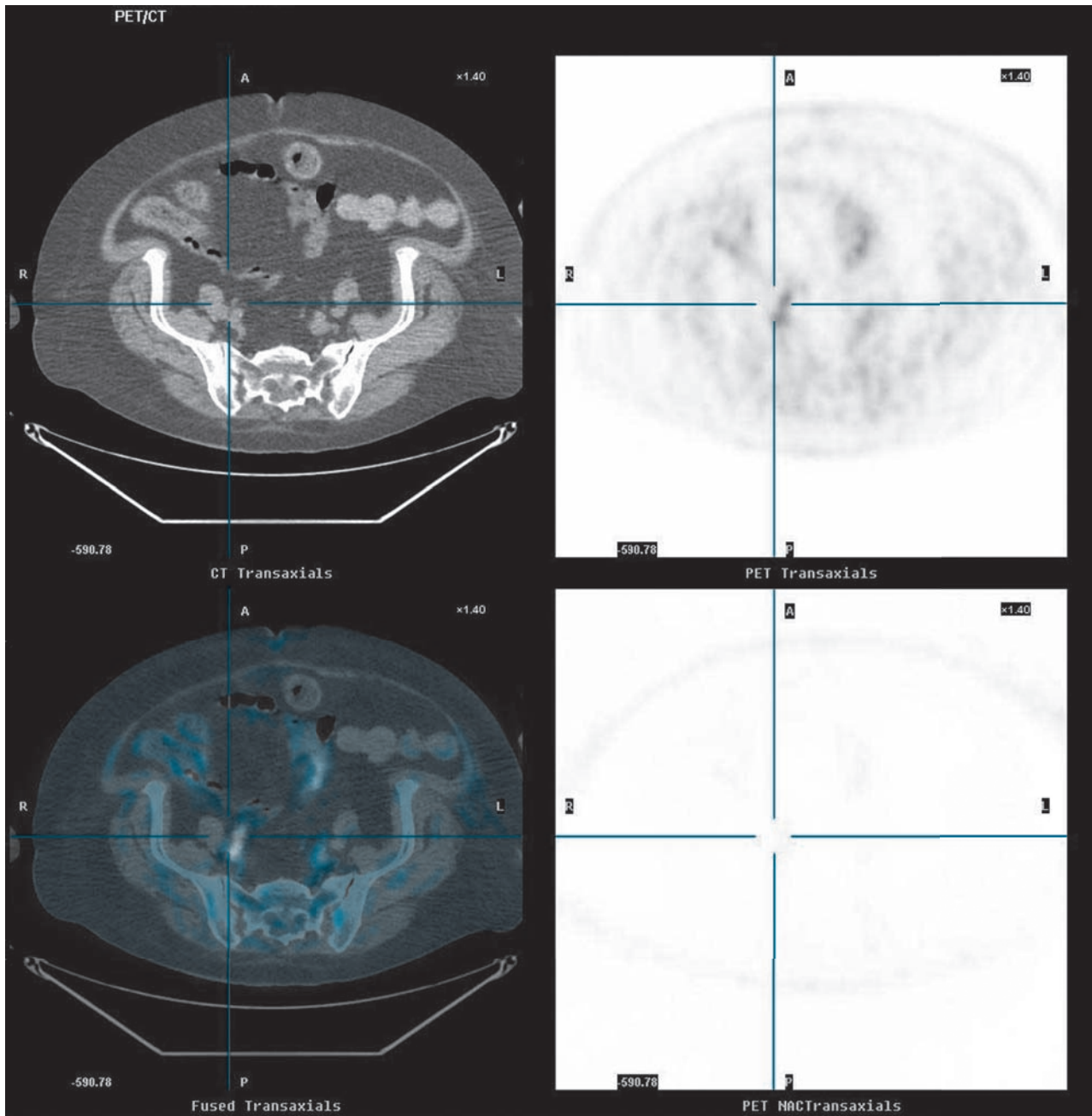


Figure 4-74

This positron emission tomography (PET)/CT case is a 75-year-old white woman previously diagnosed with breast carcinoma. Before the procedure, the patient received a single IV dose of 17.77 mCi of F-18 FDG. The PET/CT study was conducted to more accurately stage the breast carcinoma. As indicated by the marker lines, an elevated

metabolic activity is evident in the right iliac region. By comparison with subsequent sections, the signal was determined to originate in the right iliac chain of lymph nodes. Although not shown in the images above, this patient was also found to have areas of elevated activity in the left femur and right gluteal region.

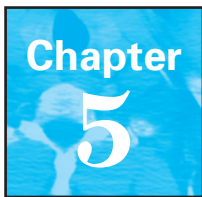
## Questions

1. Describe the iliacus muscle.
2. What part of the urinary system would be closest to the marked signal indicated above?
3. Which part of the large bowel is found in the right greater pelvis?
4. Which part of the large bowel is found just above the left greater pelvis?
5. In the greater pelvis, what would the loops of bowel found centrally most likely be?



## CLINICAL APPLICATIONS

1. The \_\_\_\_\_ supplies most of the structures within the lesser pelvic cavity with arterial blood.
2. The acetabulum is formed by the following bones: \_\_\_\_\_ forms the upper part, \_\_\_\_\_ forms the lower anterior part, and \_\_\_\_\_ forms the lower posterior part.
3. True or false: The femoral vein is located lateral to the femoral artery.
4. Which sacral segment corresponds with the origin of the rectum from the sigmoid colon?
  - A. S1
  - B. S2
  - C. S3
  - D. S4
5. Which of the following would not be considered part of the adnexal area?
  - A. Uterus
  - B. Ovaries
  - C. Broad ligament
  - D. Oviduct
6. To enter the abdominal cavity, the spermatic cord passes (above, below) \_\_\_\_\_ the pubic bones.
7. The ovaries are located on which side of the broad ligament? (Anterior or posterior)
8. Which of the following spaces forms the lowest part of the abdominal cavity?
  - A. Ischiorectal fossa
  - B. Adnexal area
  - C. Area above bladder
  - D. Rectouterine pouch
9. Describe the parts of the uterus.
10. If you were asked to perform a computed tomography (CT) examination of the pelvis, what bony structures would need to be included within the first and last axial images to ensure that all the pelvic structures would be visualized?



# Head

## OBJECTIVES

Upon completion of this chapter, the student should be able to:

1. Describe the inferior boundary of the head.
2. Identify and describe the bones making up the skull.
3. Identify and describe the location of the central nervous system structures within the head.
4. Describe the structures separating the skull cavity.
5. Describe the dural venous system and the major arteries in the head.
6. List the general functions of the cerebrum, cerebellum, basal ganglia, and brainstem and each structure's locations on sagittal, coronal, and axial images.
7. Follow the course of the cerebrospinal fluid (CSF) as it passes through the central nervous system.
8. Describe the cranial nerves.
9. Explain the relationships among structures located within the skull.
10. Correctly identify anatomic structures on patient computed tomography (CT) and magnetic resonance (MR) images of the head.

## ANATOMIC OVERVIEW

Most students consider the head to be one of the more difficult regions of the body to study, owing to the large number of structures in a relatively small area. The major bony structure, the skull, houses the brain and the organs of the special senses. When imaging the head, the base of the skull is the inferior boundary of the head. The bones making up the skull will be reviewed first to provide a framework for learning the soft tissue structures.

### ■ Skeleton

**Ethmoid** (*ETH-moyd*). The bone between the orbits (Fig. 5-1); generally described as spongy, because it has thin layers of bone separated by air pockets and numerous channels.

**Cribriform** (*KRIB-rifōrm*) *plate*. The section of the ethmoid that forms part of the floor midline in the anterior cranial cavity (the term means “like a sieve”). It is filled with perforations that transmit the olfactory nerves origi-

nating from the mucous membrane within the nasal cavity to the first pair of cranial nerves.

**Crista galli** (*KRIS-tă GAL-li*). A triangular process projecting upward from the cribriform plate that provides attachment for the falx cerebri.

**Perpendicular plate**. Also called the vertical plate. Part of the ethmoid that is found below the cribriform plate that joins with the vomer and septal cartilage to separate the nasal cavity into right and left parts.

**Sinuses**. Also called *air cells*. Their number and arrangement within the ethmoid are highly variable; there are generally 3 to 18 cells. Collectively, they form the two ethmoidal sinuses on the right and left sides of the nasal cavity. The mucous membrane-lined cells drain into the nasal cavity in the superior and middle meatus and have interconnections with the sphenoid sinus.

**Nasal conchae** (*KON-kă*). Two thin, seashell-shaped bones on either side of the ethmoid that project into the nasal cavity, forming the superior and middle conchae. Their unique scroll shape provides efficient circulation and filtration of inhaled air before it passes on to the trachea and lungs.

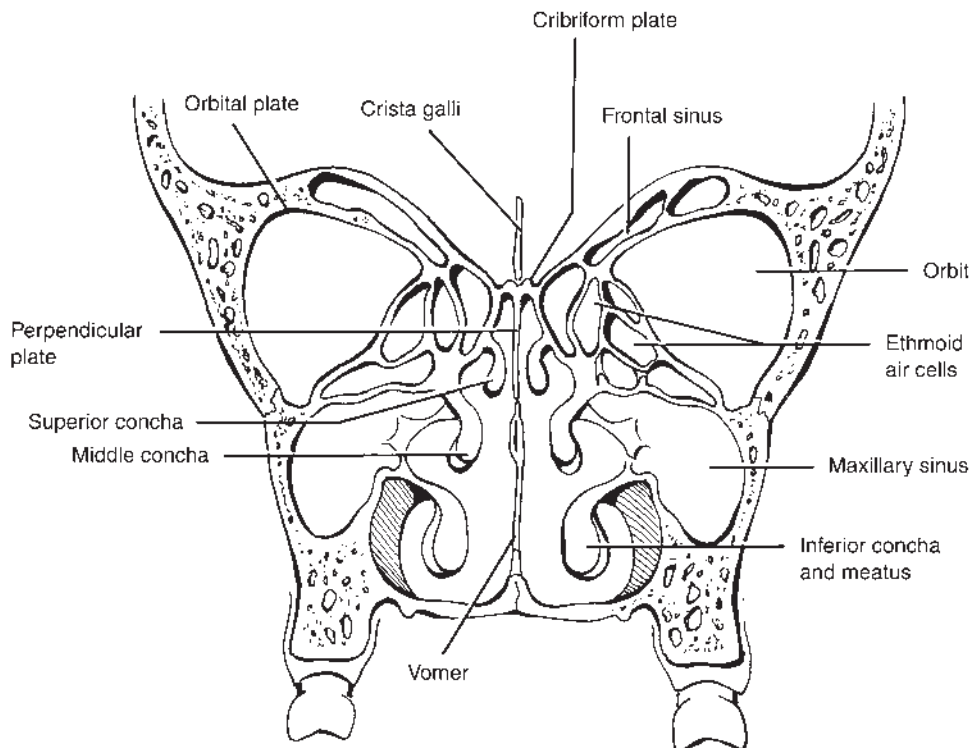


**Figure 5-1** Drawing demonstrating a posterior coronal view of the nasal cavity.

**Frontal.** The bone forming the forehead, the anterior part of the skull, and the roofs of the orbital cavities (Figs. 5-1 and 5-2).

**Sinuses.** Compartments of air centrally located within the frontal bone that are usually separated by a septum and drain into the nasal cavity in the middle meatus (opening below middle concha).

**Orbital plate.** The part of the frontal bone that forms the roof of the orbital cavities. The frontal sinuses extend over the orbits in some individuals (Fig. 5-1).

**Lacrimal** (*LAK-ri-mäl*). The small bone forming the floor of the nasolacrimal duct on the anteromedial wall of the orbit (Fig. 5-2).

**Maxilla** (*mak-SIL-ä*). Made up of the two maxillary (*MAK-si-lär-ē*) bones, which unite to form the upper part of the mouth and the anterior three-quarters of the hard palate. Every bone in the face articulates with the maxilla except the mandible.

**Sinuses.** Each maxillary bone contains a pocket of air that empties into the nasal cavity through the middle meatus (Fig. 5-1).

**Nasals.** Two fused bones that form the upper bridge of the nose. Cartilage and skin extend inferiorly, forming the lower nose (Fig. 5-2).

**Zygomatics** (*ZĪ-gō-MAT-iks*). Commonly called the cheek bones, because they form a prominence on either side of

the face. The bones form much of the inferior and lateral walls of the orbit and have a process that articulates with the temporal bone to form the zygomatic arch.

**Mandible.** Commonly called the jaw bone. The only movable bone in the skull and the largest and strongest facial bone. It is frequently divided into two major parts: The ramus (*RĀ-mūs*), the vertical projection of bone on either side, and the body, the horizontal projection containing the teeth.

**Condyles** (*KON-dīlz*). The rounded processes above the mandibular rami (*RĀ-mi*) that articulate with the temporal bones to form the temporomandibular (*TEM-pō-rō-man-DIB-yū-lär*) joints.

**Vomer** (*VŌ-mer*). Forms the posterior part of the nasal septum. A thin, flat bone extending from the hard palate and articulating with the perpendicular plate of the ethmoid (Figs. 5-1 and 5-3).

**Palatines** (*PAL-ä-tīnz*). Pair of bones forming the posterior part of the hard palate (Fig. 5-3). Because they are L-shaped, they also form part of the lateral walls and floor of the nasal cavity.

**Parietals** (*pä-RĪ-ē-tälz*). Pair of flat bones that form much of the lateral walls and roof of the cranial cavity (Fig. 5-2).

**Sphenoid** (*SFĒ-noyd*). Found within the floor of the cranial cavity. Called the keystone of the cranium, because it articulates with all the other cranial bones (Figs. 5-2 to 5-4).



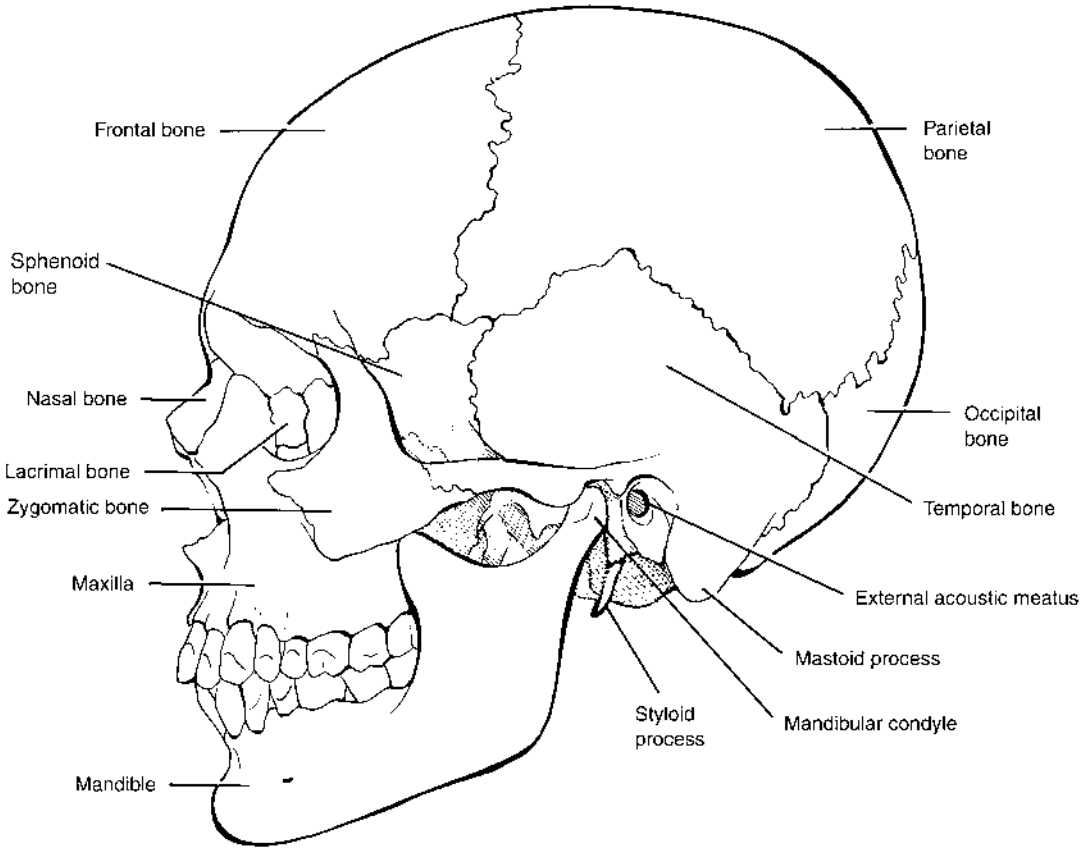


Figure 5-2 Lateral view of the bony skull.

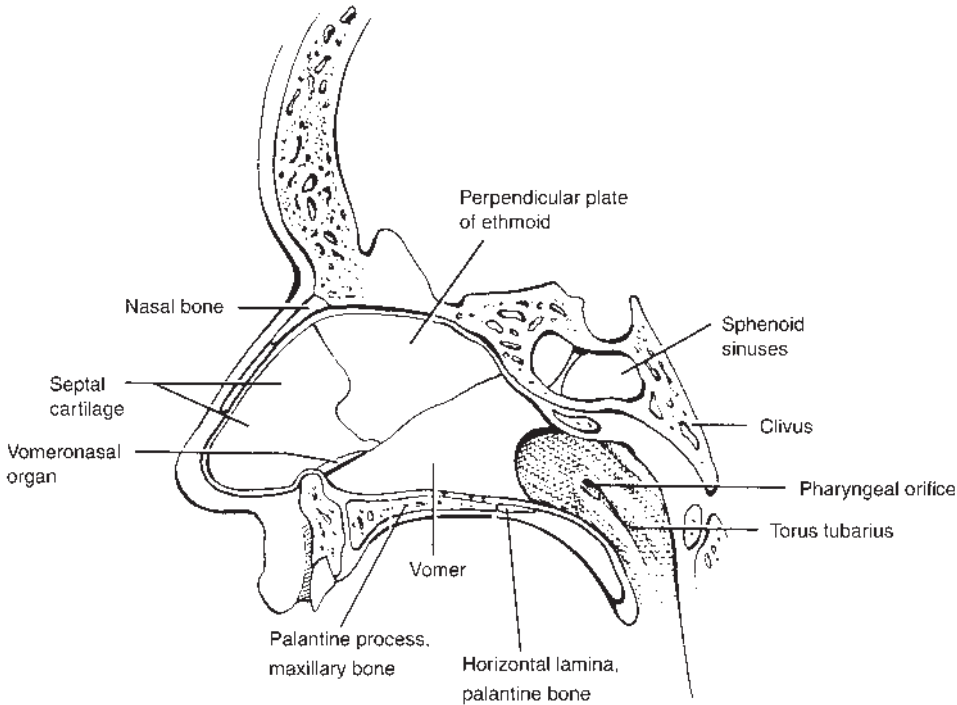
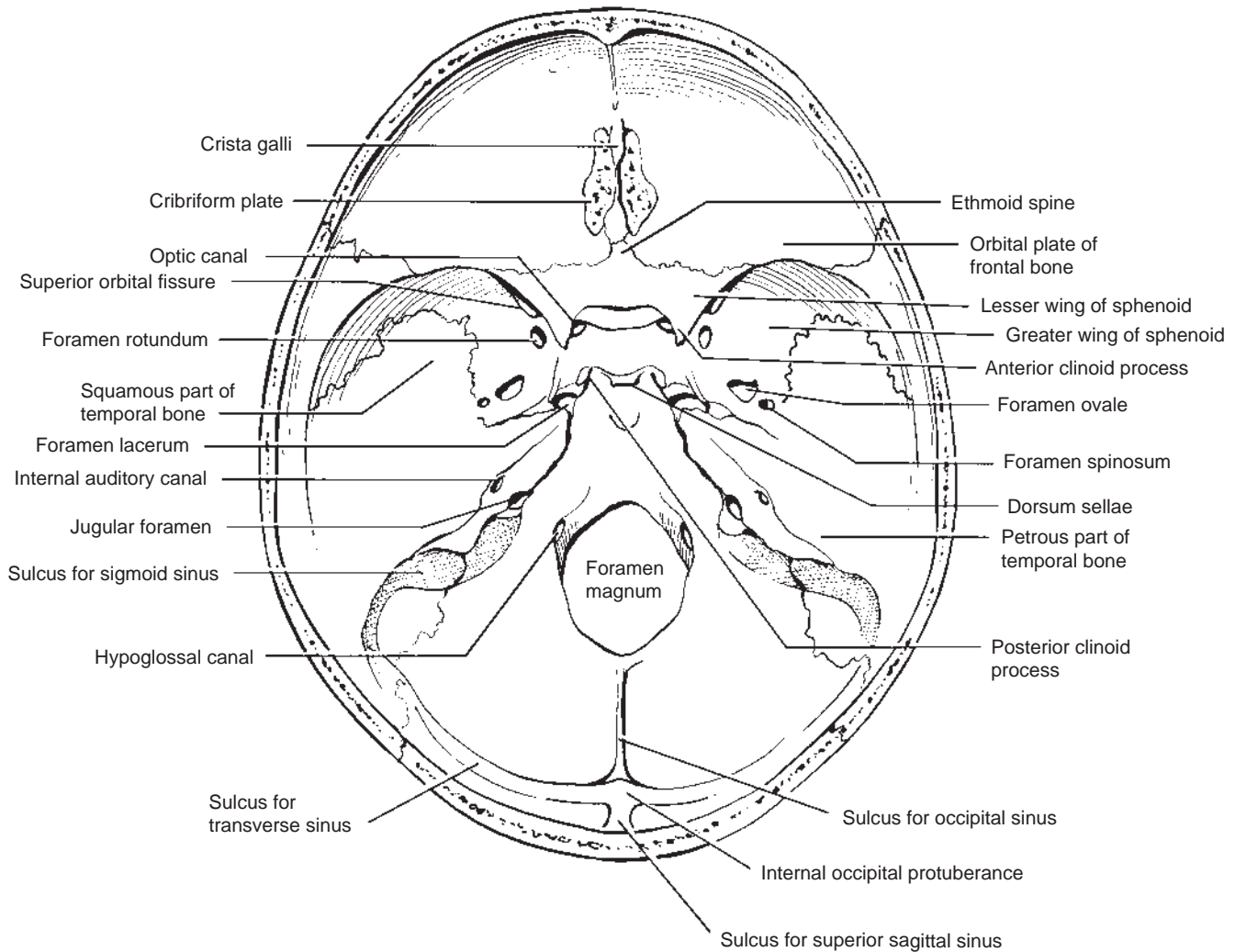


Figure 5-3 Median sagittal view of the bony skull.





**Figure 5-4** Superior axial view of the base of the skull.

**Clivus** (*KLĪ-vūs*). The bony structure within the posterior cranial fossa (*FOS-ā*) between the dorsum sellae and the foramen magnum (Fig. 5-3). The upper part lies just posterior to the dorsum sellae and is formed by the body of the sphenoid bone. On the other end, the lower part extends to the foramen magnum and is formed by the basilar part of the occipital bone.

**Sinuses**. The central portion of the sphenoid bone, located inferior to the sella turcica (*SEL-ā TUR-sī-kā*), usually contains two air cells asymmetrically divided by a septum and continuous with the posterior nasal cavity.

**Greater and lesser wings**. Within the cranial floor, the wings of the sphenoid bone are lateral to the sella turcica (Fig. 5-4). The lesser wings are anterior and superior to the sella turcica and form part of the posterior part of the bony orbit. The greater wings are larger and more inferior; they form part of the floor of the cranial cavity and part of the lateral cranial walls (Fig. 5-2).

**Anterior and posterior clinoid (*KLĪ-noyld*) processes**. They surround the sella turcica and provide a site of attachment for the dura mater, anchoring the pituitary gland within the sella turcica (Fig. 5-4).

**Dorsum sellae** (*DŌR-sūm SEL-ē*). The posterior boundary of the sella turcica, containing the posterior clinoid processes and forming the upper part of the clivus.

**Temporals** (*TEM-pŏ-rālz*). Pair of irregularly shaped bones that form the inferior part of the lateral wall of the cranial cavity and much of the middle cranial floor (Figs. 5-2 and 5-4). Its petrous (*PET-rūs*) portion, within the floor of the cranial cavity, contains the internal ear.

**External auditory meatus** (*mē-Ā-tūs*). Found on the lateral side of the skull (Fig. 5-2). The opening within the temporal bone that forms a canal to reach the middle ear.

**Mastoid** (*MAS-toyld*) **sinuses**. Found within the mastoid processes of the temporal bones (posterior and inferior to

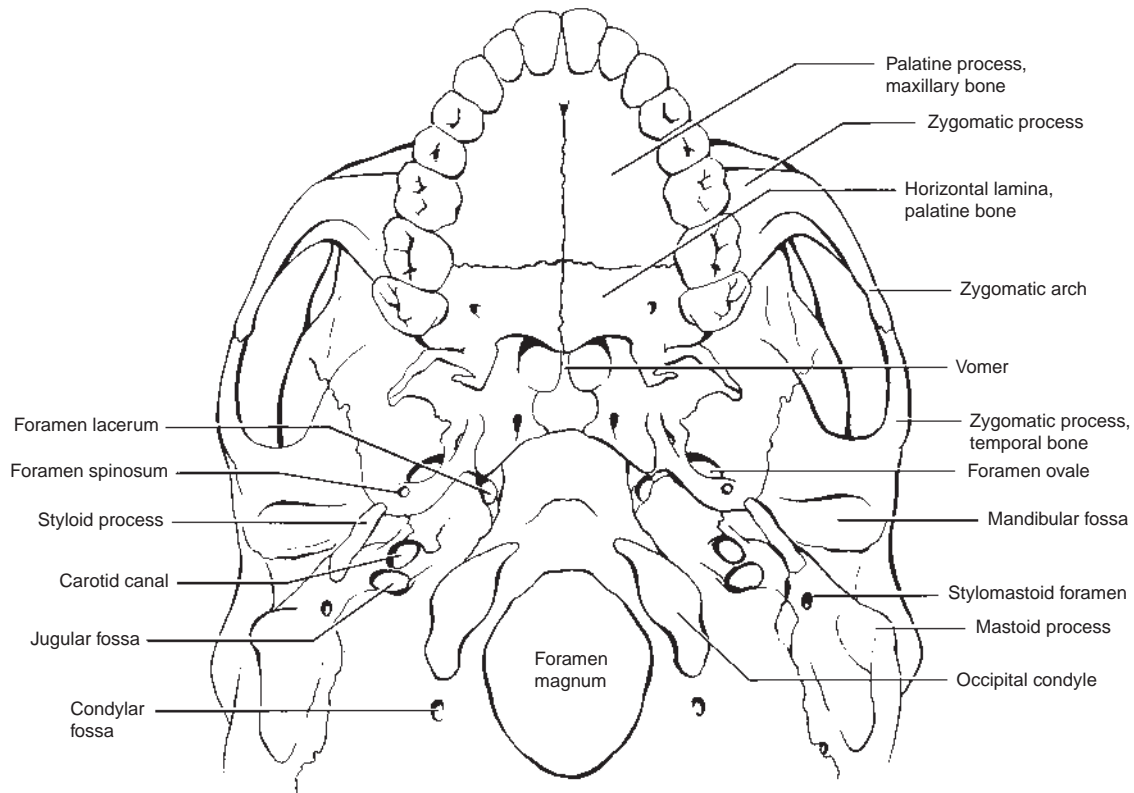


**Figure 5-5** Inferior view of the base of the skull.

the external auditory meatus). They are continuous with the inner ear.

**Occipital** (*ok-SIP-i-tāl*). Forms the posterior part of the cranium and contains the largest opening of the skull, the foramen magnum (Fig. 5-4).

### ■ Foramina (*fō-RAM-i-nā*)

All are bilateral, except the foramen (*fō-RĀ-men*) magnum.

**Carotid** (*ka-ROT-id*). Located within the petrous portion of the temporal bone. Transmits the internal carotid artery into the cranial cavity.

**Cribriform** (*KRIB-ri-fōrm*). Found in the ethmoid bone (Fig. 5-4). Transmits bundles of nerve fibers originating from mucous membranes lining the nasal cavity to the olfactory nerves.

**Hypoglossal** (*hī-pō-GLOS-āl*) **canal**. Transmits the hypoglossal nerve out of the skull through the occipital bone just above the occipital condyles.

**Internal auditory canal**. Also called the internal acoustic meatus. Located within the petrous part of the temporal bone, it transmits the facial and the acoustic nerves.

**Jugular** (*JŪG-yū-lar*). Located just posterior to the carotid foramen between the petrous part of the temporal bone and the occipital bone. Contains the internal jugular vein and the glossopharyngeal, vagus, and spinal accessory nerves.

**Lacerum** (*LAS-er-ūm*). Found between the occipital, temporal, and sphenoid bones. Transmits small vessels, nerves, and lymphatics.

**Magnum** (*MAG-nūm*). Found at the base of the occipital bone. Transmits the spinal cord.

**Optic**. Located within the lesser wing of the sphenoid bone. Transmits the optic nerve and the ophthalmic (*of-THAL-mik*) artery into the orbital cavity (Fig. 5-4).

**Ovale** (*Ō-vā-lē*). The opening through the greater wing of the sphenoid bone. Transmits the mandibular branch of the trigeminal nerve to the lower face (Figs. 5-4 and 5-5).

**Superior orbital fissure**. Found between the lesser and greater wings of the sphenoid bone. Transmits the oculomotor, trochlear, and abducens nerves and the ophthalmic branch of the trigeminal nerve.

### ■ Cranial Nerves

All are paired. The mnemonic for remembering the cranial nerves is “On old Olympus towering tops a Finn and Greek viewed some hops.”

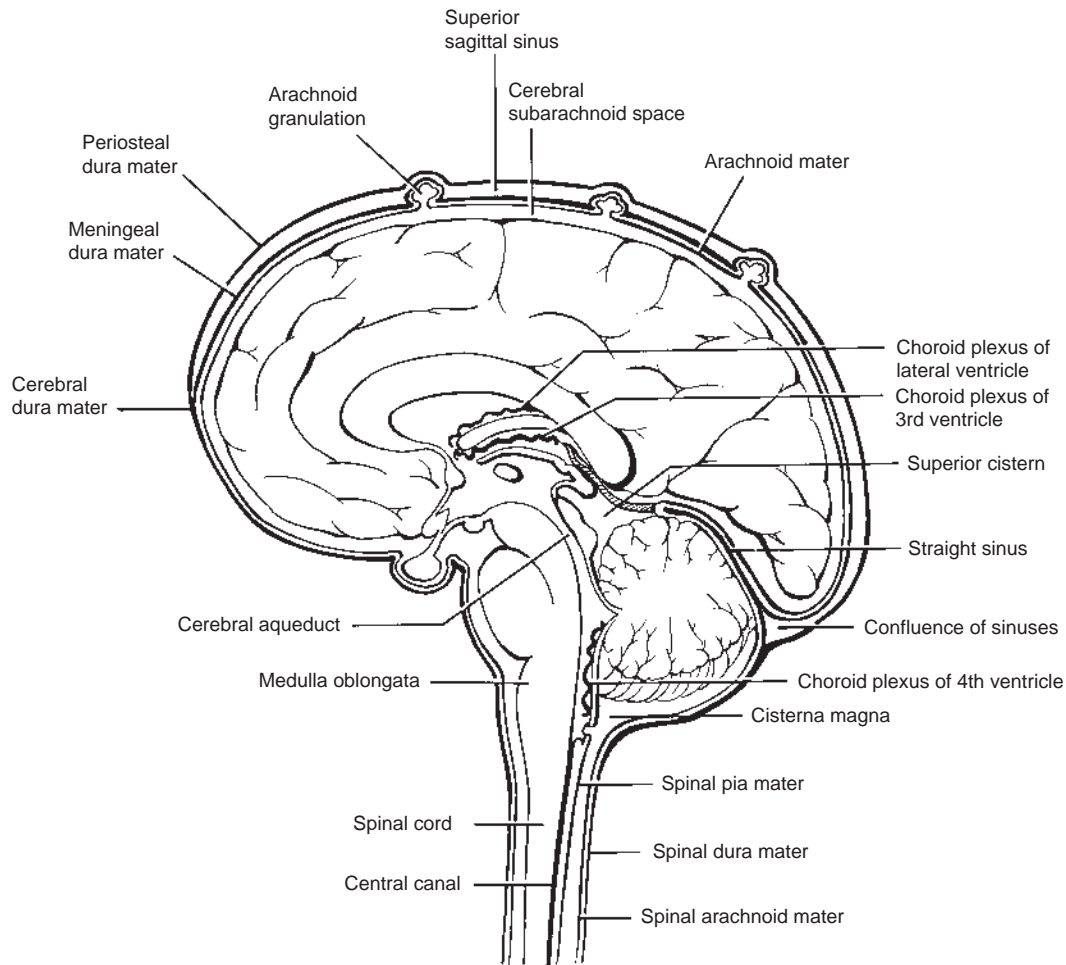


**Figure 5-6** Median sagittal drawing of the central nervous system.

**I: olfactory** (*ol-FAK-tō-rē*). Originate from the olfactory bulb and terminate within the nasal cavity in the mucous membranes. Transmit the sense of smell.

**II: optic**. Originates from the retina. Transmits the sense of sight.

**III: oculomotor** (*OK-yū-lō-MŌ-tōr*). Originate from the interpeduncular fossa. Innervate the external muscles of the eyes, except the superior oblique and lateral rectus muscles.

**IV: trochlear** (*TROK-lē-ar*). Originate lateral to the cerebral peduncles. Innervate the superior oblique muscles of the eyes.

**V: trigeminal** (*trī-JEM-i-nāl*). Emerge from the lateral side of the pons and have both sensory and motor functions. The three branches provide sensory fibers to most of the head and the motor fibers innervate the muscles of mastication.

**VI: abducens** (*ab-DŪ-senz*). Emerge from the groove between the pons and medulla. Innervate the lateral rectus muscles of the eyes.

**VII: facial**. Attach to the brainstem at the cerebellopontine (*ser-e-BEL-ō-PON-tēn*) angle and have both sensory and motor functions. The sensory fibers carry the sense of taste from the anterior two-thirds of the tongue, and the motor fibers innervate the muscles of facial expression.

**VIII: acoustic**. Extend from the brainstem beside the facial nerve. Transmit the senses of equilibrium and hearing.

**IX: glossopharyngeal** (*GLOS-ō-fā-RIN-jē-āl*). Emerge from the medulla and have both sensory and motor functions. The sensory fibers transmit the sense of taste from the posterior third of the tongue, and the motor fibers innervate the muscles of the pharynx.

**X: vagus** (*VĀ-gūs*). Emerge from the medulla. Carry both sensory and motor fibers from the pharynx, larynx, thorax, and abdomen.

**XI: spinal accessory**. Emerge from the medulla. Innervate the trapezius (*tra-Pē-zē-ūs*) and sternocleidomastoid (*STER-nō-KLĪ-dō-MAS-toyd*) muscles.

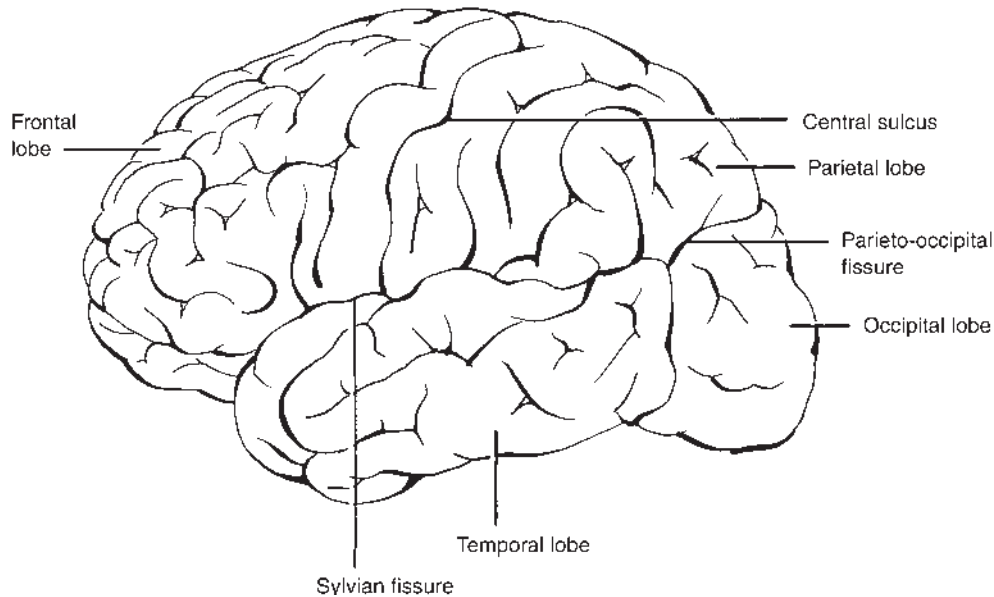


**Figure 5-7** Lateral view of the cerebrum.

**XII: hypoglossal** (*hi-pō-GLOS-āl*). Emerge from the medulla. Innervate the muscles of the tongue.

## ■ Brain

**Cerebellum** (*ser-e-BEL-ŭm*). The second largest part of the brain. Located behind the face and brainstem in the posterior cranial fossa (Fig. 5-6). Its outer layer, containing a concentration of cell bodies, is called gray matter; its deeper layers, containing mostly cell processes and supportive cells, is called white matter. Coordinates movements and maintains posture and balance.

**Vermis** (*VER-mis*). The constricted region joining the two cerebellar hemispheres.

**Pedunculi** (*pe-DŪNG-kyū-lī*). Bundles of nerves traveling between the cerebellum and the brainstem. The superior joins the midbrain, the middle connects with the pons, and the inferior extends to the medulla and spinal cord.

**Cerebellar tonsils**. Located on the lower and medial part of the cerebellar hemispheres, next to the foramen magnum.

**Cerebrum** (*SER-ĉ-brŭm*). The largest part of the brain, it consists of two hemispheres. The cortex contains mostly nerve cell bodies and appears as gray matter in unstained specimens. Below the cortex, nerve fibers traveling toward and away from the cortex form the white matter. Most regions function as association areas related to memory, reasoning, judgment, intelligence, and personality.

**Sylvian** (*SIL-vē-an*) **fissure**. Also called the lateral cerebral sulcus (*SŪL-kŭs*). Located on the lateral side of the cerebrum (Fig. 5-7), where many grooves or sulci are found between rounded protrusions or gyri (*JĪ-rī*). It is deeper than the sulci and divides the lateral cerebrum into the temporal and frontal lobes.

**Central sulcus**. A centrally located sulcus found on the top of the cerebrum, extending around the upper hemispheres dividing the frontal and parietal lobes.

**Frontal lobe**. Part of the cerebral hemispheres, located anterior to the central sulcus and above the Sylvian fissure. The motor, or muscle, control areas are found just in front of the central sulcus; and the association areas are found in the anterior frontal lobe.

**Parietal** (*pā-RĪ-ĉ-tāl*) **lobe**. Located between the central sulcus and the parieto-occipital fissure and found above the Sylvian fissure. The general sensory, or somesthetic, areas that represent specific parts of the body are found directly posterior to the central sulcus. The remaining section functions as part of the association areas.

**Temporal lobe**. Located inferior to the Sylvian fissure and anterior to an extension of the parieto-occipital fissure. The upper part contains the primary auditory area, and the rest is thought to be part of the association areas.

**Hippocampal** (*hip-ō-KAM-pāl*) **formation**. Deep within the temporal lobe, this curved sheet of gray matter extends upward into the floor of the lateral ventricle (*VEN-tri-kl*). It is considered part of the limbic system and is involved in the emotional aspects of behavior.

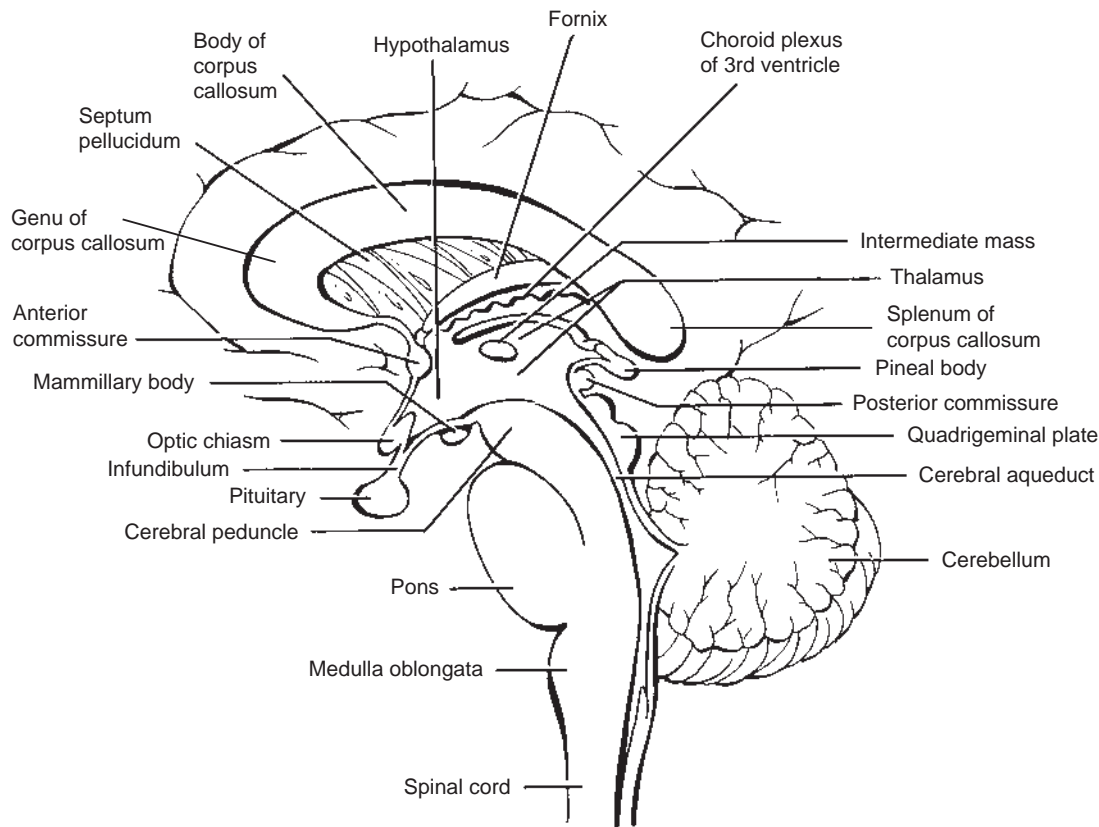


**Figure 5-8** Median sagittal view of the brain stem and adjoining structures.

**Occipital lobe.** The posterior part of the cerebral hemisphere, located behind the parieto-occipital fissure. Considered the primary visual area of the brain.

**Corpus callosum** (*KÖR-pūs ka-LŌ-süm*). Large bundles of transverse or commissural fibers of white matter connecting the right and left cerebral hemispheres. The commissural fibers transmit impulses from a gyrus on one cerebral hemisphere to the corresponding gyrus on the opposite side (Fig. 5-8).

**Genu** (*JĒ-nū*). Describes the anterior part of the corpus callosum, which transmits commissural fibers between the frontal lobes (Latin for “bend” or “kneel”).

**Body.** The middle part of the corpus callosum, formed by commissural fibers from the parietal and temporal lobes extending to the opposite hemisphere.

**Splenium** (*SPLĒ-nē-üm*). The posterior and thicker part of the corpus callosum formed by fibers extending from the posterior parietal and occipital lobes to the corresponding lobe on the opposite side.

**Fornix** (*FÖR-niks*). On either side, the arched columns formed by tracts of fibers joining together posteriorly

under the splenium of the corpus callosum. Together, they form the roof of the third ventricle.

**Septum pellucidum** (*SEP-tüm pe-LŪ-sid-üm*). A thin, double-layered membrane between the columns of the fornix and the corpus callosum that separates the anterior horns of the lateral ventricles.

**Anterior commissure.** An oval-shaped bundle of fibers traveling between the temporal and frontal lobes of the right and left cerebral hemispheres. Found below the inferior end of the fornix, it forms part of the anterior wall of the third ventricle.

**Posterior commissure.** A complex bundle of fibers traveling between hemispheres from a variety of nuclei. Forms part of the posterior wall of the third ventricle.

**Pineal** (*PIN-ē-äl*) **body.** Pinecone-shaped endocrine gland attached to the roof of the third ventricle; found below the splenium of the corpus callosum. At about the time of puberty, it starts to calcify or collect what is commonly called brain sand.

**Intermediate mass.** Also called the interthalamic adhesion. A bundle of gray matter that serves as a bridge



through the third ventricle, joining the right and left thalamic nuclei.

**Thalamus** (*THAL-ă-mŭs*). Oval-shaped nucleus that forms the lateral walls of the third ventricle; usually about 2.5 cm (1 in) long. Although the nucleus is mostly gray matter, it does contain small areas of white matter, subdividing the structure into smaller groups. Primarily serves as the “switching center” for directing sensory impulses to the appropriate region of the cerebral cortex.

**Hypothalamus** (*HĪ-pō-THAL-ă-mŭs*). Forms the floor and part of the lateral walls of the third ventricle. The nucleus includes the mammillary body and is protected by the upper part of the sphenoid bone. Although relatively small, it controls many bodily functions related to maintaining homeostasis, or stability, within the body.

**Pituitary** (*pi-TŪ-i-tār-ē*). Also called the hypophysis (*hĪ-POF-i-sis*). Located within the sella turcica of the sphenoid bone. An endocrine gland that regulates so many of the body’s activities it is often called the “master gland”; the hormones are absorbed by a capillary plexus surrounding the gland.

**Infundibulum** (*in-fŭn-DIB-yŭ-lŭm*). The stalk connecting the pituitary to the hypothalamus.

**Midbrain.** The bundle of nervous tissue connecting the cerebrum with the cerebellum and spinal cord. Although the majority of the area consists of nerve fibers, a variety of nuclei are found embedded within the white matter.

**Cerebral peduncles** (*pe-DŪNG-klz*). Found on the anterior portion of the midbrain. A pair of large fiber bundles that carry motor impulses from the cerebral cortex to the pons and spinal cord.

**Red nucleus.** Found below the thalamus in the superior part of the cerebral peduncles. An oval-shaped region of gray matter considered to be a motor nucleus. Fibers from the cerebral cortex and cerebellum terminate here and give rise to fibers traveling downward in the spinal cord.

**Substantia nigra** (*sŭb-STAN-shē-ă NĪ-gră*). The layer of deeply pigmented gray matter lining much of the posterior surface of the cerebral peduncles. Fibers from the cell bodies within the nucleus project to the cerebral cortex, basal nuclei, thalamus, hypothalamus, and other regions of the brain.

**Quadrigeminal** (*KWAH-dri-JEM-i-năl*) *plate*. Also called the corpora quadrigemina. The posterior portion of the midbrain, behind the cerebral aqueduct. Consists of four rounded eminences containing small nuclei. Responsible for reflex movements in response to auditory and visual stimuli.

**Pons** (*ponz*). Located anterior to the cerebellum. The enlarged portion of the brainstem where fibers from the cerebellum join those from the cerebrum and spinal cord. Like the midbrain, it consists of mostly white matter but also contains a number of nuclei.

**Medulla oblongata** (*me-DŪL-ă ob-long-GAH-tă*). Forms the lower brainstem directly below the pons and contains all the ascending and descending tracts that communicate between the spinal cord and the brain. Despite having a large amount of white matter formed by the nerve fibers, it contains a variety of nuclei. Many motor nerve fibers decussate (*DĒ-kŭ-săt*), or cross over, to the opposite side, causing one side of the brain to control motor function on the opposite side of the body.

**Spinal cord.** Found within the spinal foramina. It connects the brain with the body. Like the cerebrum and cerebellum, it consists of both gray and white matter; however, unlike the cerebrum and cerebellum, its outer layer is white matter.

**Caudate** (*KAW-dăt*) **nucleus.** C-shaped area of gray matter found following the curve of the lateral ventricle. Involved in muscle control (Fig. 5-9).

**Head.** The enlarged part of the caudate nucleus bulges into the floor of the anterior horn of the lateral ventricle.

**Body.** The central portion of the caudate nucleus anterior to the collateral trigone (*TRĪ-gōn*) of the lateral ventricle.

**Tail.** The tapered part of the caudate nucleus in the roof of the inferior horn of the lateral ventricle.

**Internal capsule.** The group of sensory and motor nerves connecting the cerebral cortex with the brainstem and spinal cord (Fig. 5-10). Because the tracts separate the thalamus from the basal ganglia (globus pallidus, putamen, and caudate), they form what appears as a “capsule” for the thalamus.

**Lenticular** (*len-TIK-YŪ-lăr*) **nuclei.** Found lateral to the internal capsule and the thalamus. Shaped like an acorn, with the pointed end surrounded by internal capsule. Consist of the globus pallidus and the putamen.

**Globus pallidus** (*GLŌ-bŭs PAL-i-dŭs*). The medial lenticular nucleus located next to the internal capsule. Laterally, it is separated from the putamen by a small lamina of fibers. Considered primarily a motor nucleus. Cellular extensions from the structure connect with most of the nuclei within the brain and the cerebral cortex.

**Putamen** (*pyŭ-TĀ-men*). The lateral lenticular nucleus found next to the globus pallidus and medial to the external capsule. Has numerous connections and is generally considered a motor nucleus thought to inhibit function of cortical induced motor activity.

**External capsule.** A thin layer of white matter between the putamen and the claustrum. Its fibers are derived from the insula; the subthalamic connections are unknown.

**Clastrum** (*KLAWS-trŭm*). A sheet of gray matter bounded by laminae of white matter on either side, the

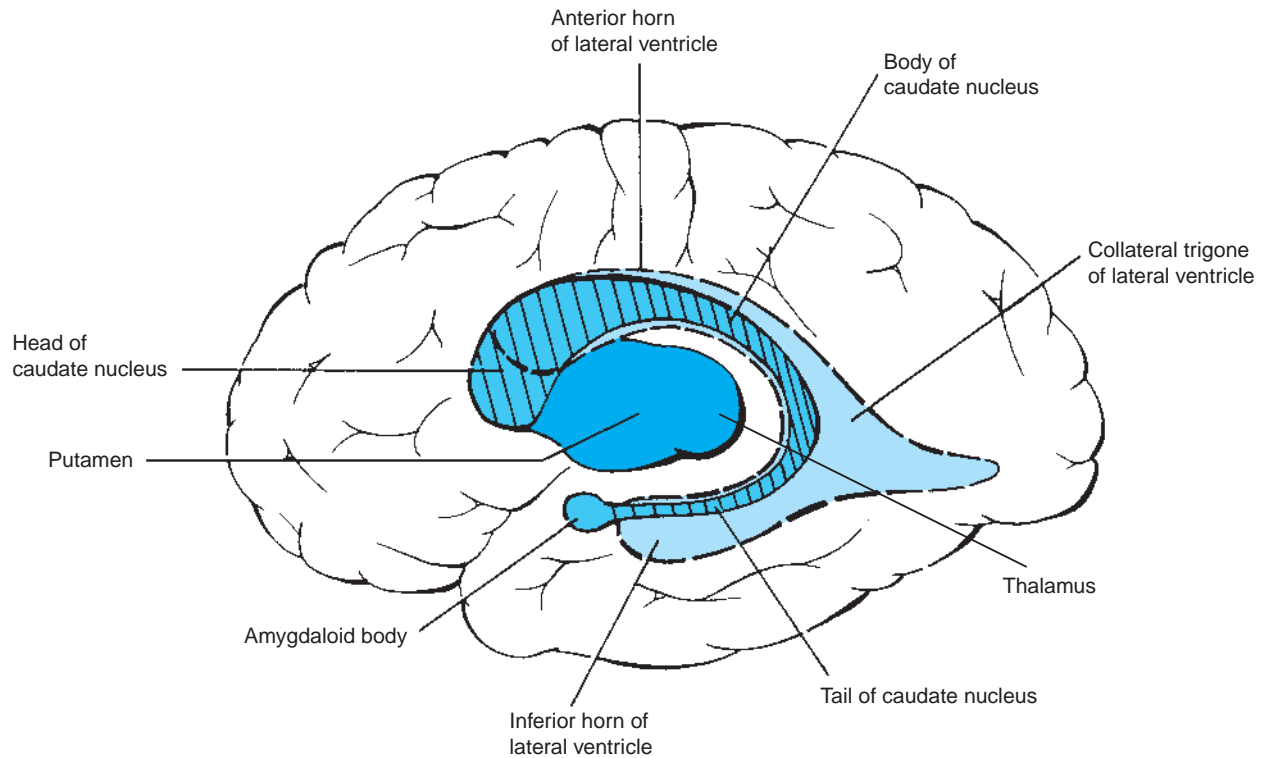


**Figure 5-9** Drawing from the lateral view of the brain demonstrating the location of the basal ganglia and thalamus.

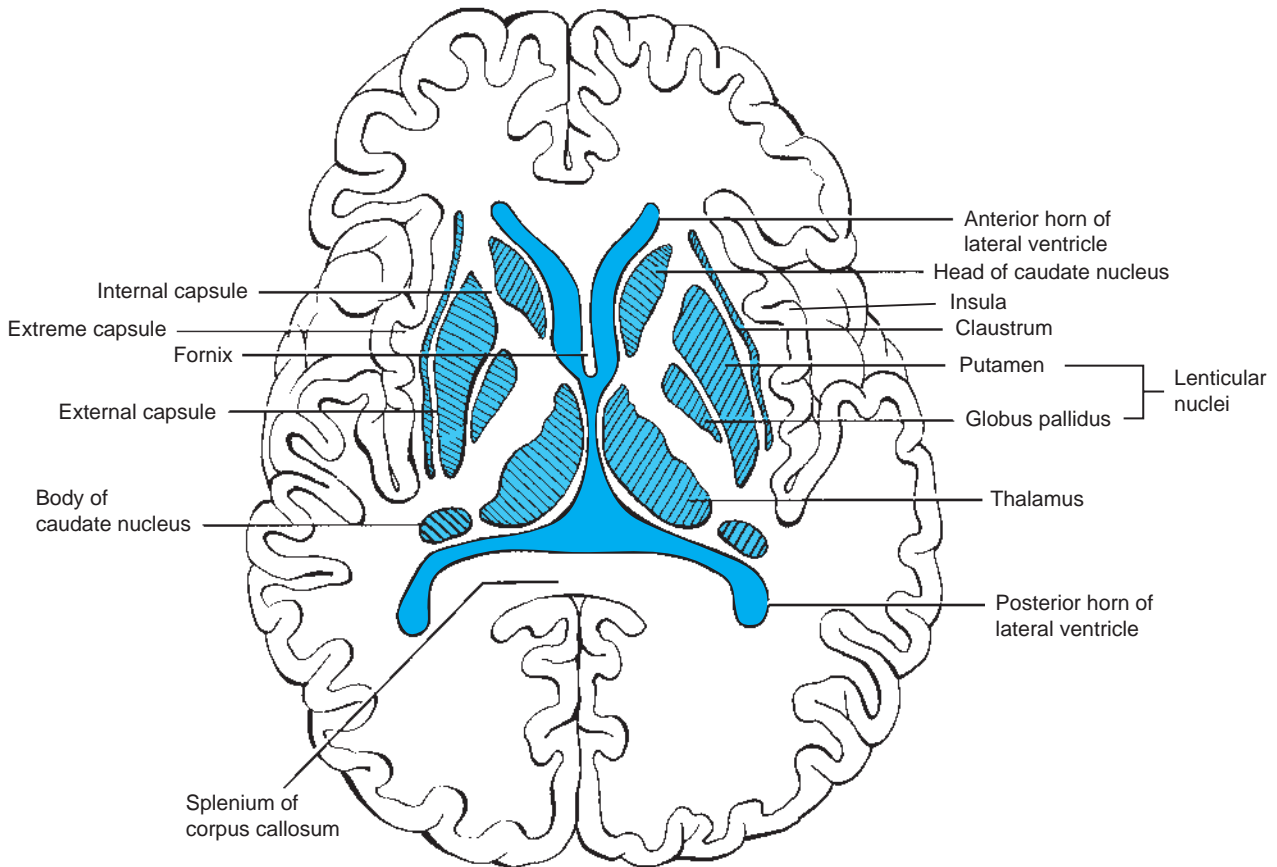


**Figure 5-10** Axial section through the head demonstrating the basal ganglia and thalamic nuclei.

external capsule medially, and the extreme capsule laterally. The connections and function of the nucleus are not yet clearly understood.

**Extreme capsule.** The thin layer of white matter between the claustrum and insula. Contains fibers from both areas.

**Insula** (*IN-sū-lă*). Commonly called the inner lobe. The region of the cerebral cortex located deep within the Sylvian or lateral cerebral fissure. Medially, it is separated from the claustrum by the extreme capsule, which carries its fibers to other parts of the brain and spinal cord. Although the function is not clearly understood, stimulation results in visceral sensations and autonomic responses.

**Corona radiata** (*kō-RŌ-nă RĀ-dē-ă-tă*). Found above the thalamus and basal ganglia. Fibers radiating between the internal capsule and the cerebral cortex form sheets, creating a crown of white matter above the nuclei (Fig. 5-11).

## ■ Enclosing Structures

**Dura mater** (*DŪ-ră MA-ter*). The outermost and toughest of the three membranes covering the brain and spinal cord (Latin for “hard mother”). The meningeal layer located closest to the bone surrounding the central nervous system (Fig. 5-12). Although not shown in Figure 5-12, meningeal arteries are frequently found between the dura mater and calvarial bone in the epidural space. The arachnoid mater is deep to the dura mater, and the two membranes can be separated, creating a subdural space.

**Arachnoid** (*ă-RAK-noyd*) **mater.** The middle, delicate meningeal membrane covering the brain and spinal cord. Connected to the underlying pia mater by trabeculae (*tră-BEK-yū-lă*), or thin fibrous threads, much like spider webs. Between the trabeculae, the subarachnoid space is filled with CSF and contains most of the major arteries supplying blood to the brain.

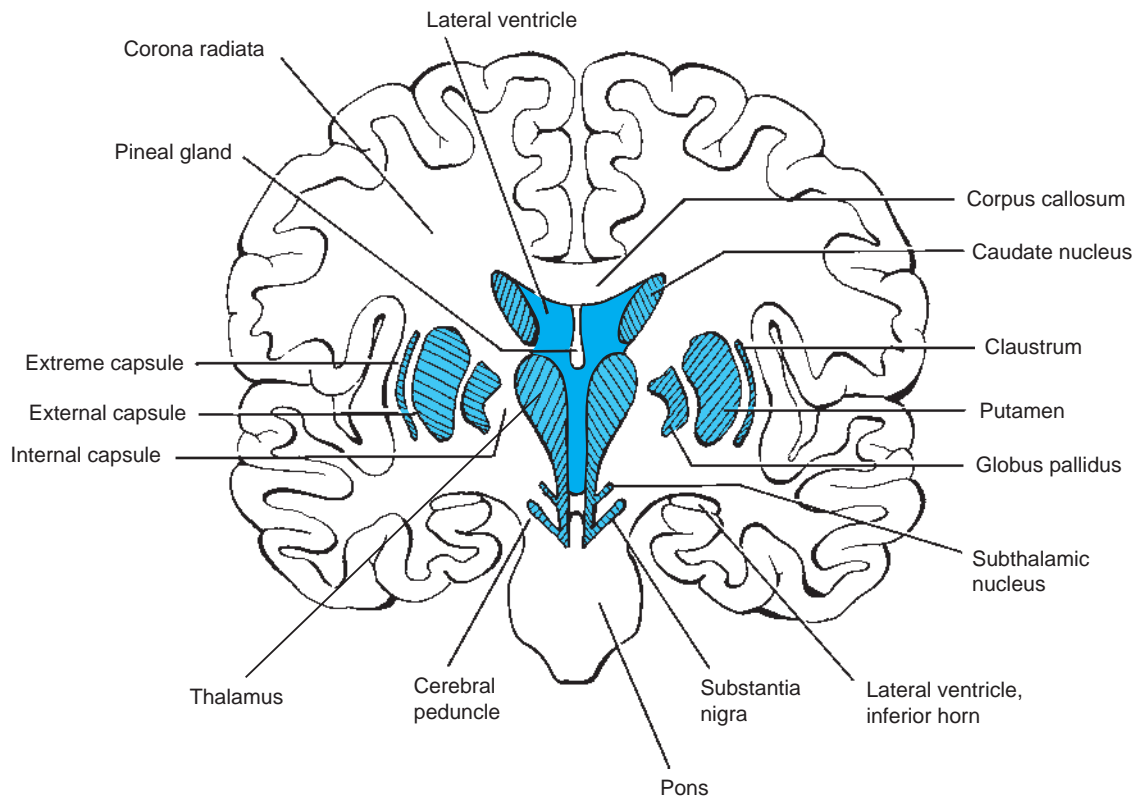


**Figure 5-11** Coronal section through the brain demonstrating relationships between the basal ganglia and thalamic nuclei.



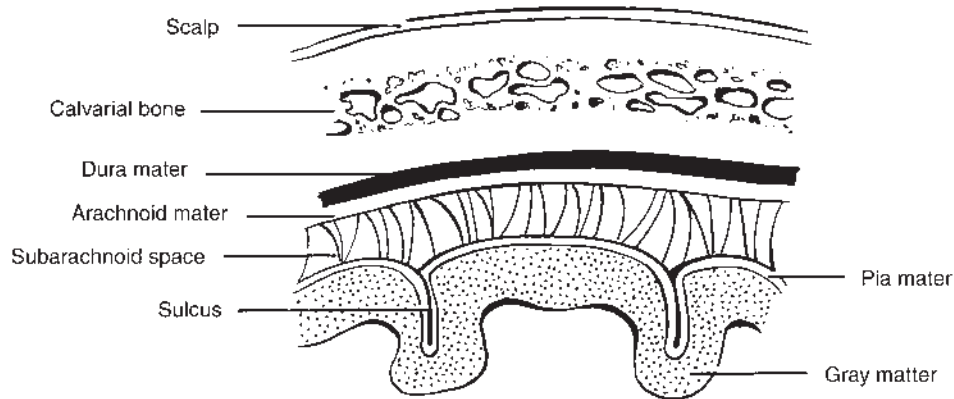


**Figure 5-12** Drawing of the outer coverings of the brain.

**Pia (PĪ-ă) mater.** The innermost membrane surrounding the brain and spinal cord. In a cadaver specimen, it is difficult to separate from the nervous system structures, because it is tightly adhered and intimately related to the surface of the brain and spinal cord.

**Falx cerebri (falks se-RĒ-bri).** Separates the cerebral hemispheres. A reflection of dura mater that extends cau-

dally from the upper calvarium and ends just above the corpus callosum (Fig. 5-13). Its anterior end attaches to the crista galli of the ethmoid bone, and the posterior end joins other dural reflections in the posterior cranial fossa.

**Falx cerebelli (ser-Ĕ-BEL-i).** The reflection of dura mater separating the cerebellar hemispheres in the posterior cranial cavity.

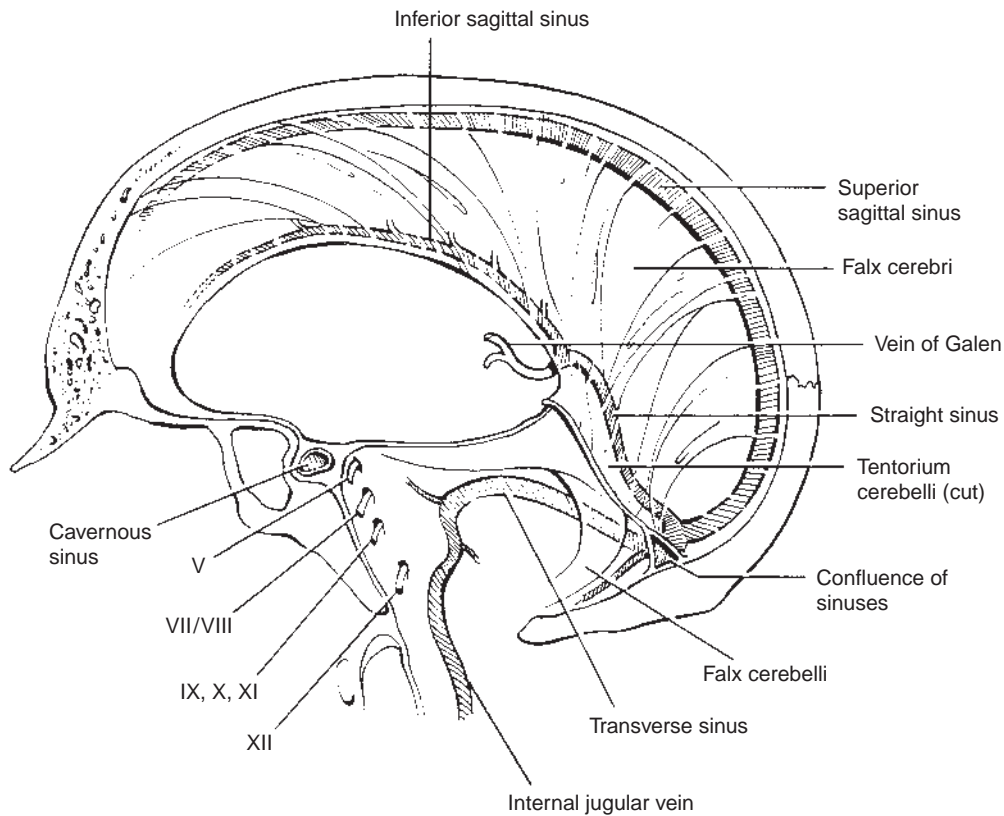


**Figure 5-13** Dural reflections and associated venous sinuses within the head.

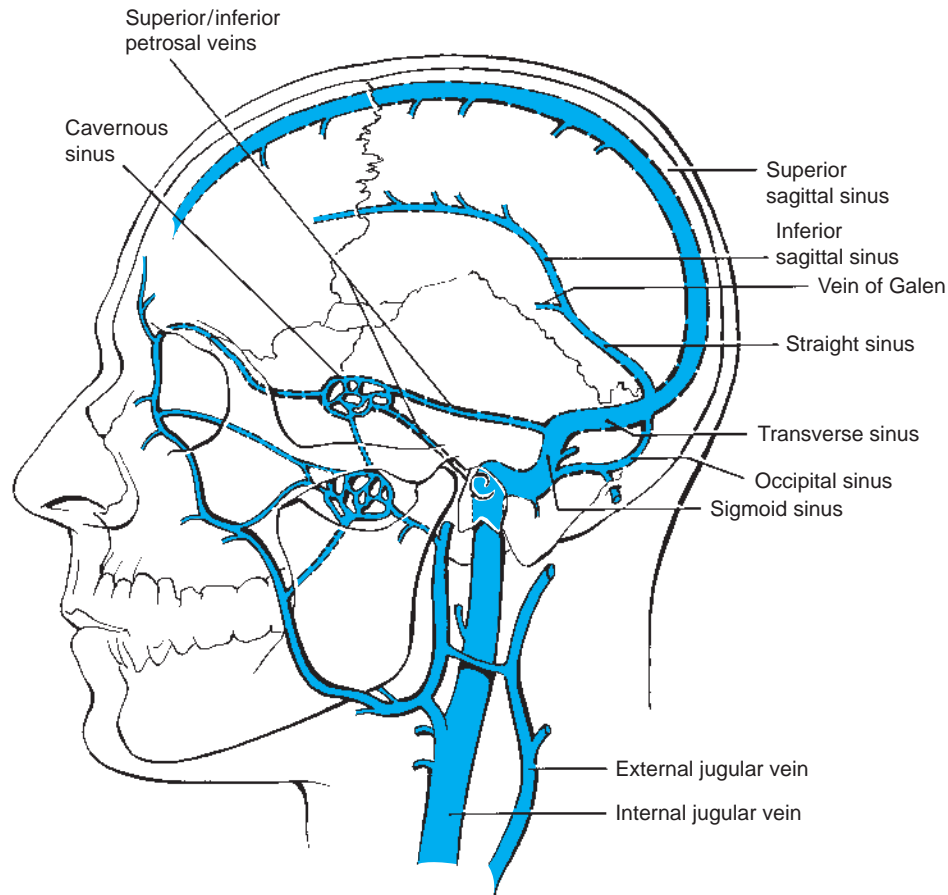


**Figure 5-14** Major venous structures within the head.

**Tentorium (*ten-TŌ-rē-ŭm*) cerebelli.** The dural reflection extending horizontally between the cerebrum and cerebellum. Laterally, it is attached to the petrous ridge on either side; it extends posteriorly to the juncture of the falx cerebri and falx cerebelli.

## ■ Dural Sinuses and Veins

**Superior sagittal (*SAJ-i-tāl*) sinus.** Within the upper margin of the falx cerebri, the layers of dura form a sinus for venous blood draining from the upper cerebral hemispheres. Following the superior margin of the falx cerebri, it lies near the inner surface of the calvarium.

**Inferior sagittal sinus.** Within the lower margin of the falx cerebri, venous blood from the medial part of the cerebral hemispheres is collected in a space between the layers of dura. In a coronal section, it is demonstrated between the cerebral hemispheres just above the corpus callosum.

**Vein of Galen.** Located below the splenium of the corpus callosum, it drains the internal cerebral hemispheres into the straight sinus.

**Straight sinus.** The space for venous blood between the layers of the dura mater at the juncture of the falx cerebri, falx cerebelli, and tentorium cerebelli. Receiving blood from the inferior sagittal sinus and the vein of Galen, it extends posteriorly to empty into the confluence of sinuses.

**Confluence of sinuses.** The opening formed between the layers of dura mater where the superior sagittal, straight, occipital, and transverse sinuses meet.

**Transverse sinuses.** Within the posterior margin of the tentorium cerebelli, they extend laterally on either side (Fig. 5-14). Within the layers of dura, each one drains venous blood from the confluence of sinuses to the petrous part of the temporal bone where it bends caudally to join the sigmoid sinus.

**Sigmoid (*SIG-moyd*) sinuses.** Drain venous blood from the transverse and petrosal sinuses into the internal jugular veins. They curve through the petrous parts of the temporal bones.

**Internal jugular veins.** Originating from the sigmoid sinuses, they are the major route for drainage of venous blood from the head. Each one exits the base of the skull

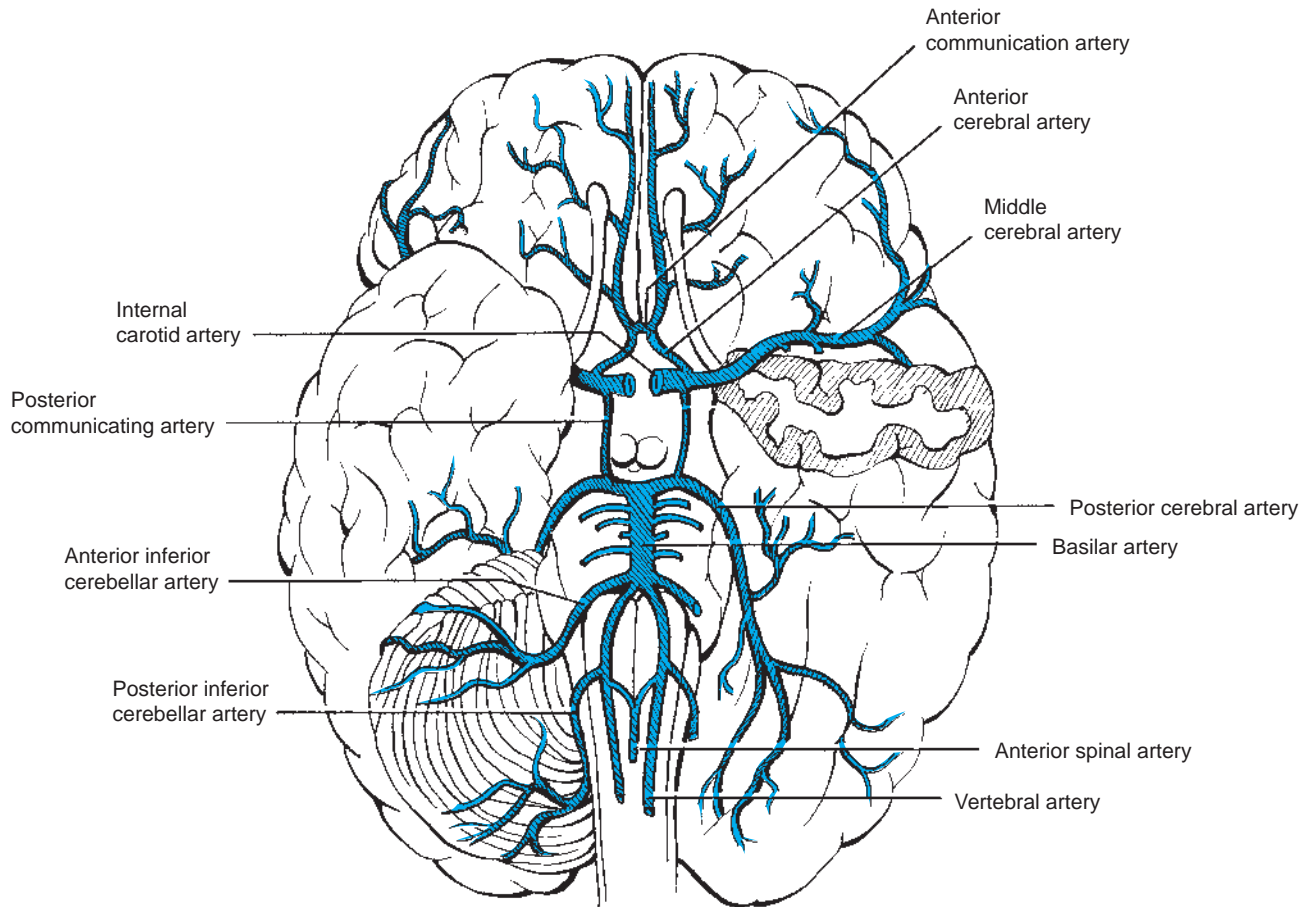


**Figure 5-15** Inferior view of the major arteries of the brain.

through the jugular foramen on the inferior surface of the petrous part of the temporal bone and extends through the neck to join the brachiocephalic vein in the chest.

## ■ Arteries

To help you learn the location of the major arteries, think of a stick man named Willis. Willis's legs are formed by the vertebral arteries, his trunk is formed by the basilar artery, his arms are the posterior cerebral arteries, and his head is formed by the circle of Willis (Fig. 5-15).

**Vertebral** (*VER-tě-bräl*). Originating from the subclavian arteries in the thorax, these bilateral arteries ascend through the transverse foramina of C6 through C1. Superior to C1, they pass through the foramen magnum and the dura mater to enter the subarachnoid space. Found on either side of the medulla oblongata, the right and left arteries merge to give rise to the basilar artery at the level of the lower pons.

**Basilar** (*BAS-i-lär*). Found near the midline on the anterior surface of the pons, this artery is within the subarachnoid space and originates from the juncture of the right and left vertebral arteries. Extending to the upper border of the pons, it divides and gives rise to the right and left posterior cerebral arteries.

**Circle of Willis.** A ring of vessels located within the subarachnoid space below the hypothalamus and midbrain that supplies arterial blood to the cerebrum.

**Posterior cerebral.** Located along the upper border of the pons, these bilateral arteries originate from the basilar artery and extend above the tentorium cerebelli to supply the occipital lobes with arterial blood. The right and left arteries are separated by the falx cerebri and appear to wrap around the splenium of the corpus callosum joining the right and left cerebral hemispheres.

**Posterior communicating.** Shortly after the posterior cerebral artery originates from the basilar artery, a small branch connects with the internal carotid artery. Although

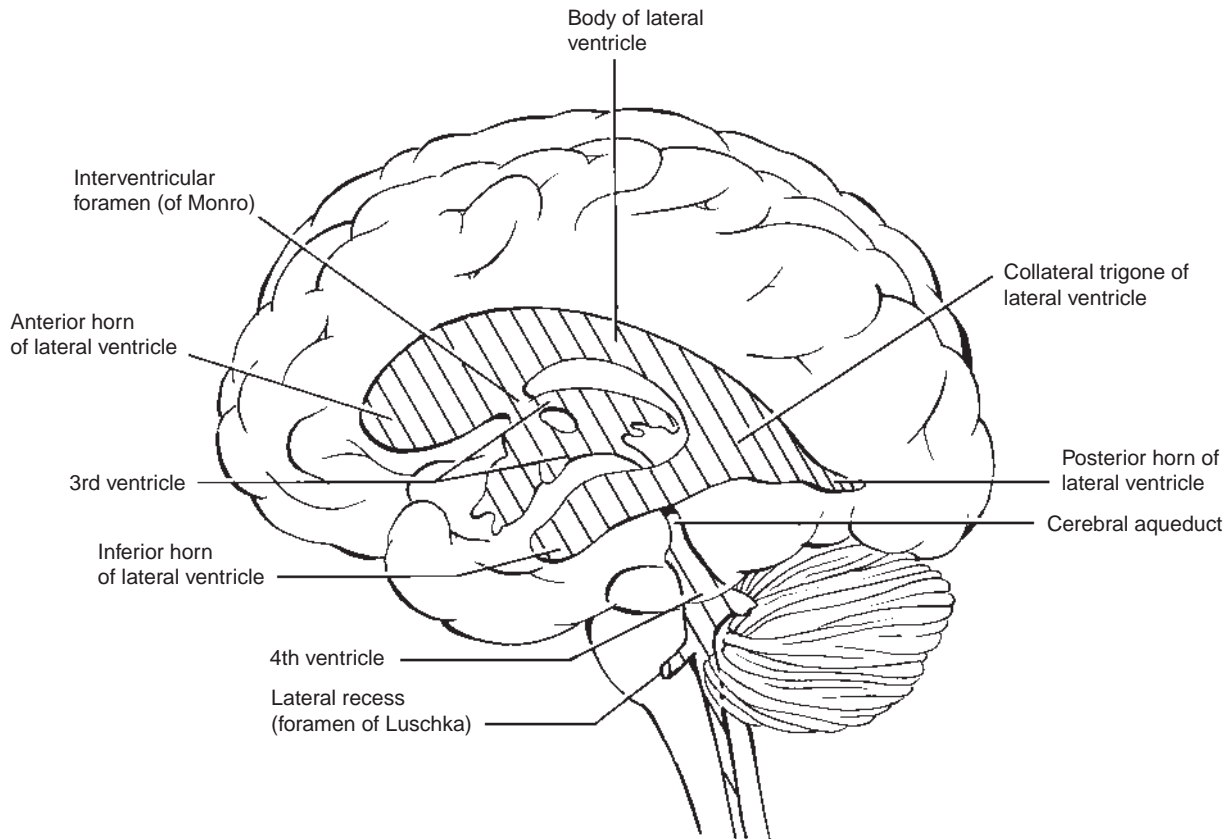


**Figure 5-16** Lateral view of the brain demonstrating the ventricular structures within the brain.

small, these arteries provide a collateral route for blood flow between the major arteries (vertebral and internal carotid) that supply arterial blood to the brain.

**Internal carotid.** Beginning at the bifurcation of the common carotids in the neck, these arteries ascend next to the internal jugular veins to enter the skull through the carotid canals. As they pass along the S-shaped groove on the lateral surface of the sella turcica, they extend through the dural layers of the cavernous sinus to enter the subarachnoid space. Within the subarachnoid space, they branch to form the posterior communicating, middle cerebral, and anterior cerebral arteries.

**Middle cerebral.** The major branches from the internal carotid arteries, these arteries extend laterally through the Sylvian fissures to supply blood to the temporal and parietal lobes.

**Anterior cerebral.** Slightly smaller than the middle cerebral artery, these branches of the internal carotid arteries travel anteriorly in the interhemispheric fissure. The right and left arteries are found on either side of the falx cerebri and appear to wrap around the genu of the corpus callosum to supply blood to the frontal and medial part of the parietal lobes.

**Anterior communicating.** The anterior cerebral arteries are joined by a small vessel that provides a collateral route for blood flow between the right and left sides.

## ■ Ventricles and Cisterns

**Lateral ventricles.** Within each cerebral hemisphere, there is a C-shaped cavity with a horn radiating from the posterior part of the curve (Fig. 5-16). The cavities are lined by ependyma (*ep-EN-di-mă*), which in certain regions is highly vascularized, forming the choroid plexus (*KO-royd PLEK-sūs*). The choroid plexus produces CSF from the blood to fill the ventricles.

**Anterior horn.** The part of the lateral ventricles found within the frontal lobe. The roof is formed by the corpus callosum, the floor and lateral wall are formed by the head of the caudate nucleus, and the medial wall is formed by the septum pellucidum.

**Body.** The anterior horn continues posteriorly to join with the body of the lateral ventricle within the parietal lobe. Like the anterior horn, the roof is formed by the corpus callosum and the medial wall is formed by the septum

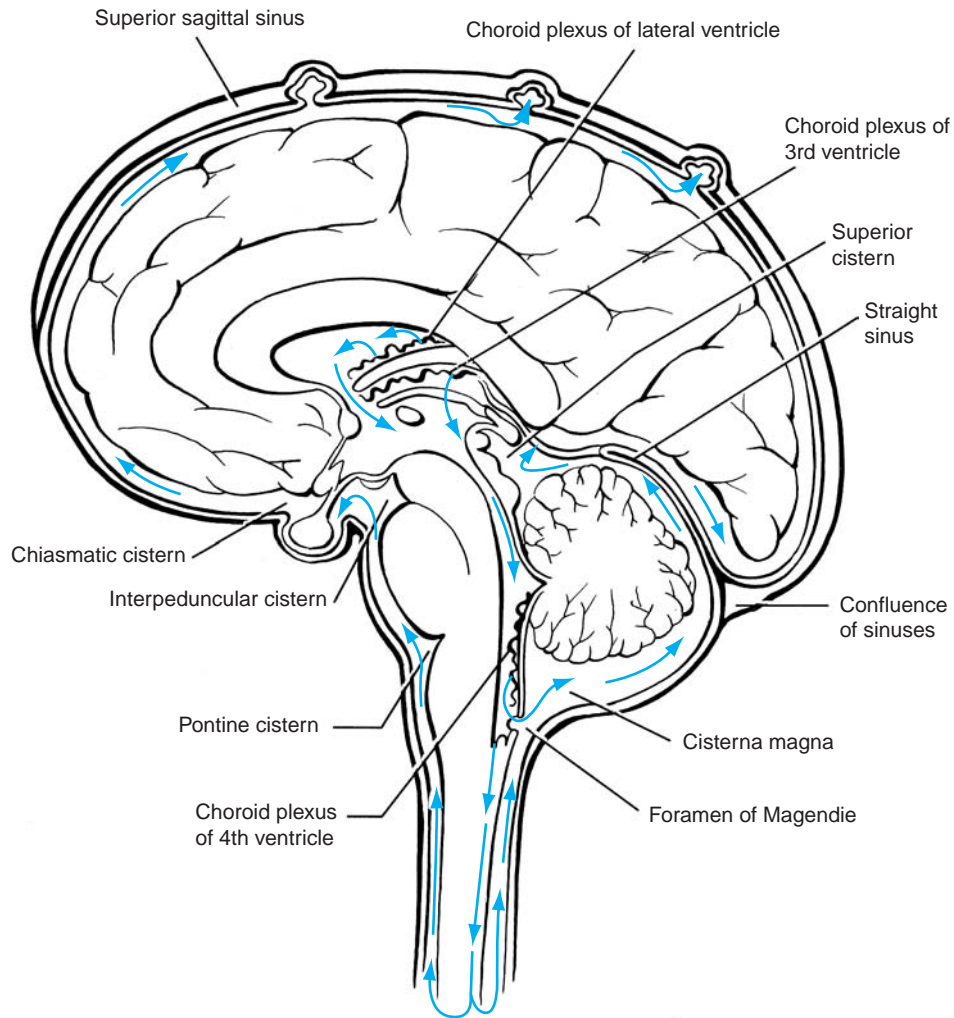


**Figure 5-17** Drawing of the cerebrospinal circulation throughout the central nervous system.

pellucidum. In this region, however, the floor is formed by the body of the caudate and the thalamus.

**Collateral trigone.** The triangle-shaped regions of the lateral ventricles that join the body, posterior horn, and inferior horn.

**Posterior horn.** The posterior part of the lateral ventricle. Found within the occipital lobe of the cerebrum. The roof and lateral walls are formed by groups of myelinated fibers extending to the splenium of the corpus callosum. In coronal section, it is found near the center of the cerebral hemisphere and is roughly triangular in shape. In all other planes of section, it is continuous with the collateral trigones.

**Inferior or lateral horn.** Located within the temporal lobe. Part of the lateral ventricle that extends forward and inferiorly from the collateral trigone. It is near the center of the temporal lobe and is lateral to all the other ventricular structures.

**Interventricular foramen.** Also called the foramen of Monro. Small openings that join the lateral ventricles with the third ventricle.

**Third ventricle.** A small, narrow opening found near the median sagittal plane between the thalamic and hypothalamic nuclei. CSF, produced by the choroid plexuses of the lateral ventricles, travels through the interventricular foramina to drain into this structure (Fig 5-17).

**Cerebral aqueduct.** The opening transmitting CSF from the lateral and third ventricles to the fourth ventricle. Located within the posterior part of the midbrain, this small opening is found in the midline between the cerebral peduncles and the quadrigeminal plate.

**Fourth ventricle.** The base of this pyramid-shaped structure rests on the pons and medulla oblongata; the apex extends toward the cerebellum. This opening receives CSF

through the cerebral aqueduct. Like the other ventricles, its choroid plexus produces CSF that travels either down through the spinal cord or empties out into the subarachnoid space.

*Lateral recess.* Although a large section of the fourth ventricle can be found at the midline, it has an opening extending laterally on each side. CSF in the lateral recess drains through the lateral aperture, the foramen of Luschka, and into the subarachnoid space (Fig. 5-16).

**Superior cistern.** Also called the superior cerebellar cistern. An enlarged region of subarachnoid space above the cerebellum below the tentorium cerebelli (Fig. 5-17). Located posterior to the midbrain, the opening is near the cerebral aqueduct. In axial sections, they are frequently demonstrated together.

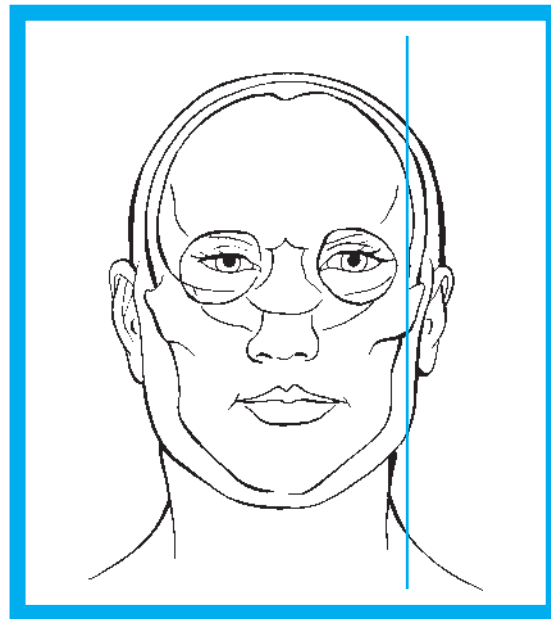
**Cisterna magna.** Also called the cerebellomedullaris cistern. An enlarged region of subarachnoid space located posterior to the medulla oblongata between the cerebellum and the occipital bone.



## Sagittal MR Images

The following eight sagittal MR images of the head are described at 8.0-mm intervals from the left side to the mid-sagittal plane. The right side will not be described, because the structures are generally the same as those on the left

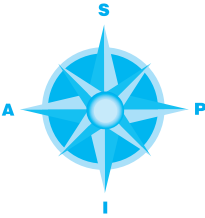
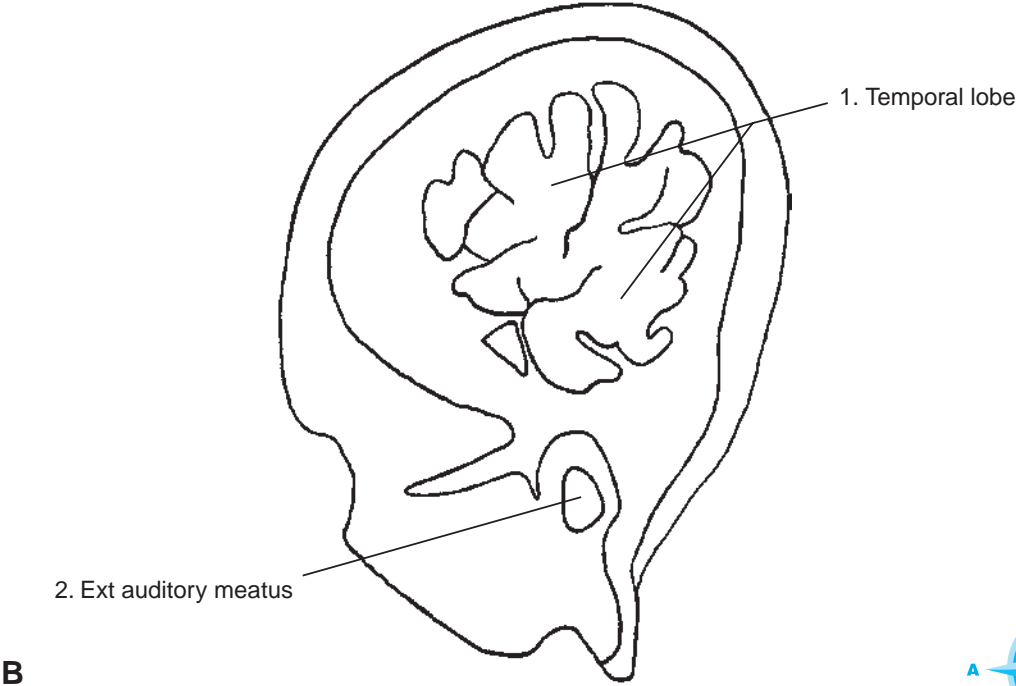
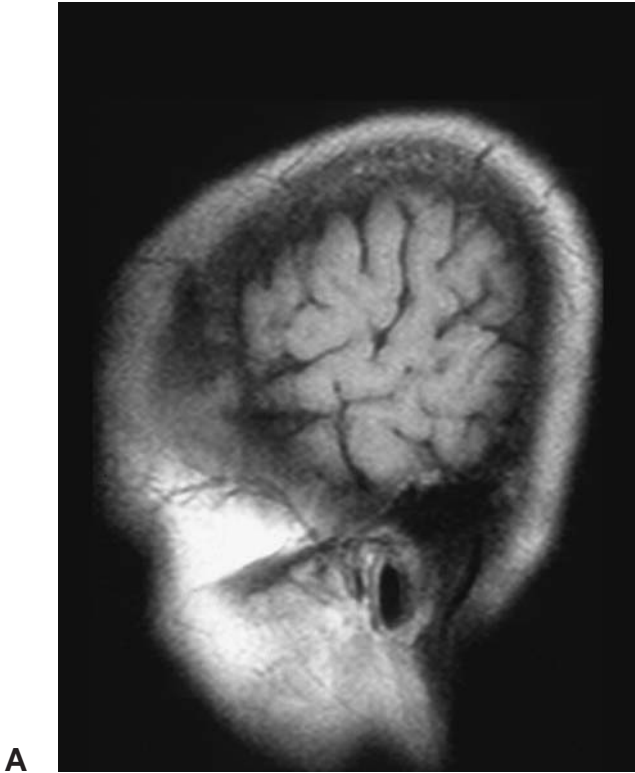
side. The images were generated at the following technical factors: repetition time (TR) = 650 ms; echo time (TE) = 20 ms; radiofrequency (RF) = 90°; field of view (FOV) = 25 cm; slice thickness (TH) = 7.5 mm.



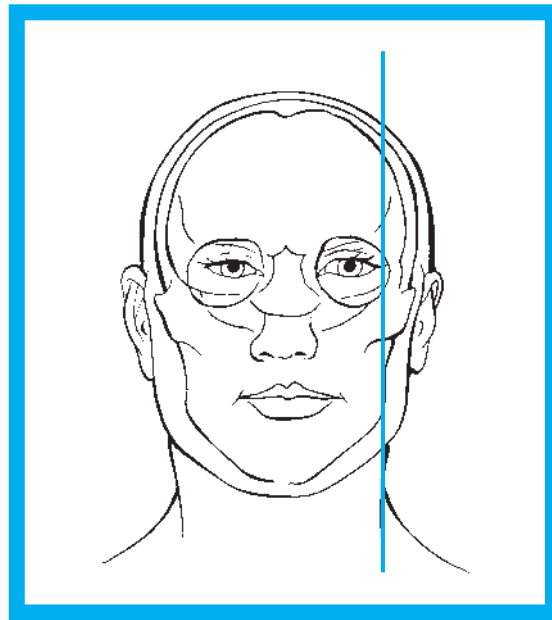
**Figure 5-18 (A,B)** Sagittal MR image 1.

The image generated on the left side of the head is the first sagittal section demonstrating brain anatomy and would be the first in a series of sagittal images throughout the brain (Fig. 5-18). At first glance, the sulci can be seen separating the gyri of the temporal lobe. The darkened area surrounding the temporal lobe represents the bones of the skull. Inferior to the temporal lobe within the region of the bones of the skull, the oblong structure represents the external auditory meatus. To the left of the meatus, the lateral edge of the face is demonstrated as a bright area, owing to the amount of fat and glandular material found just anterior to the ear.



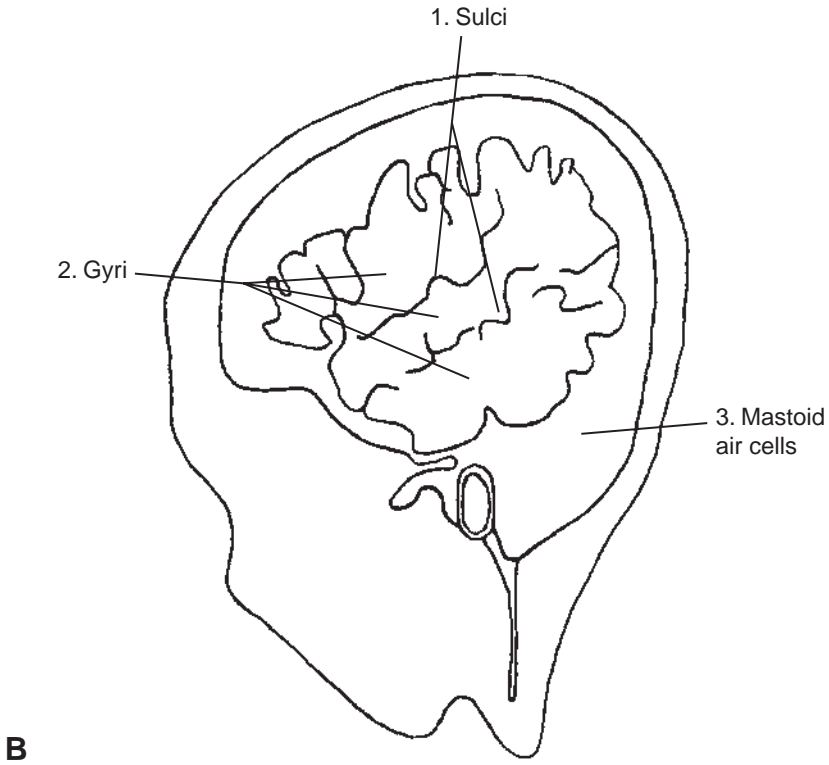
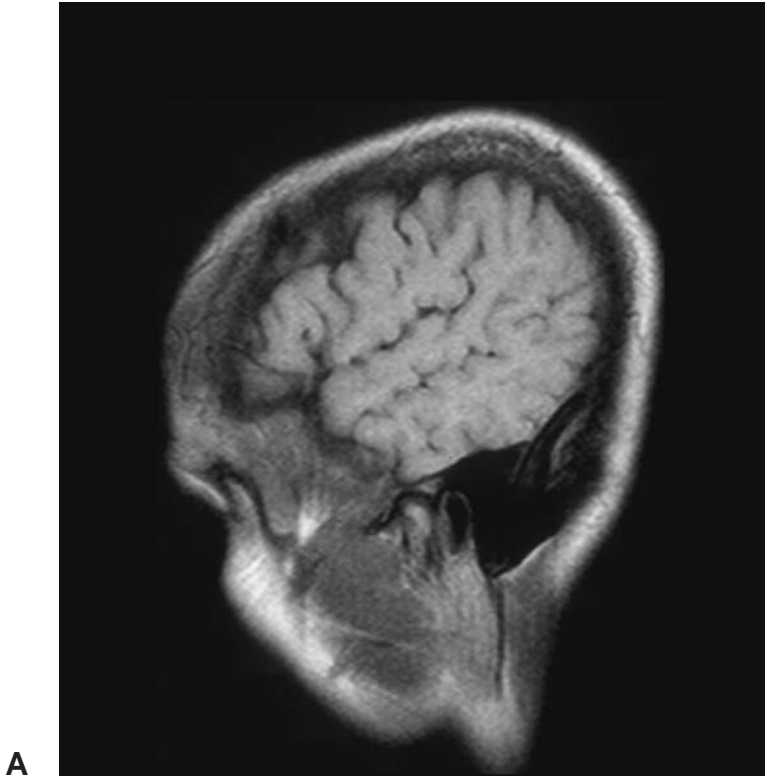


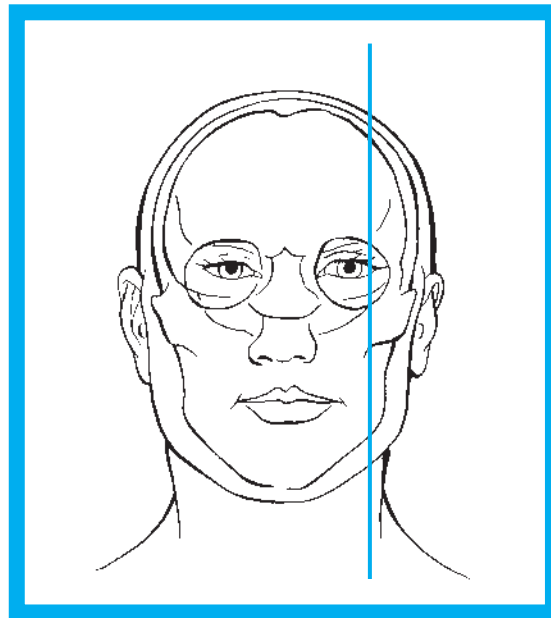




**Figure 5–19 (A,B)** Sagittal MR image 2.

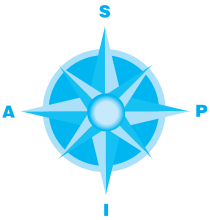
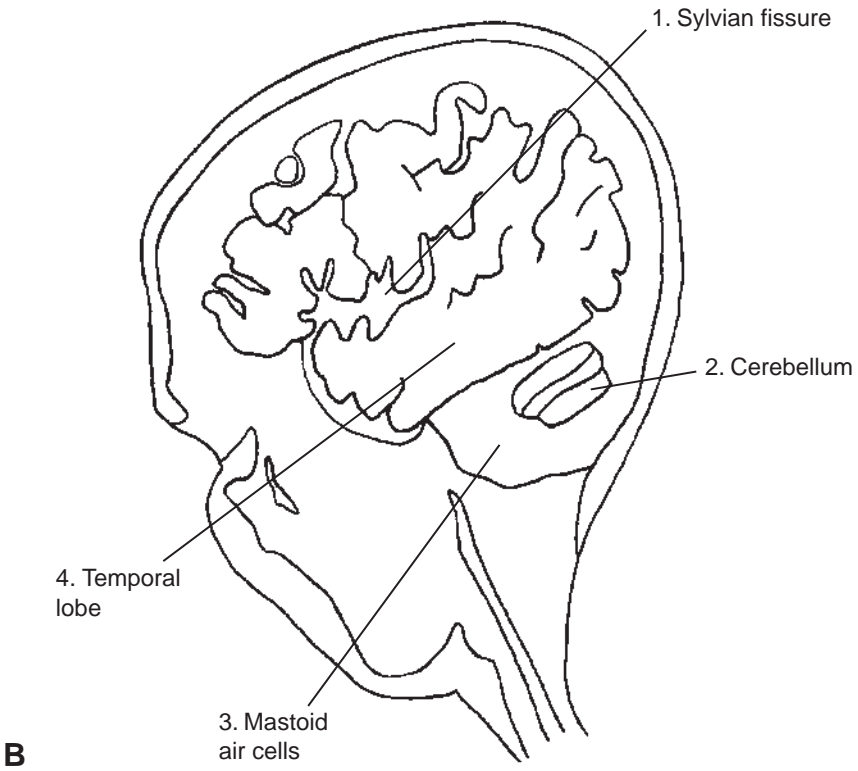
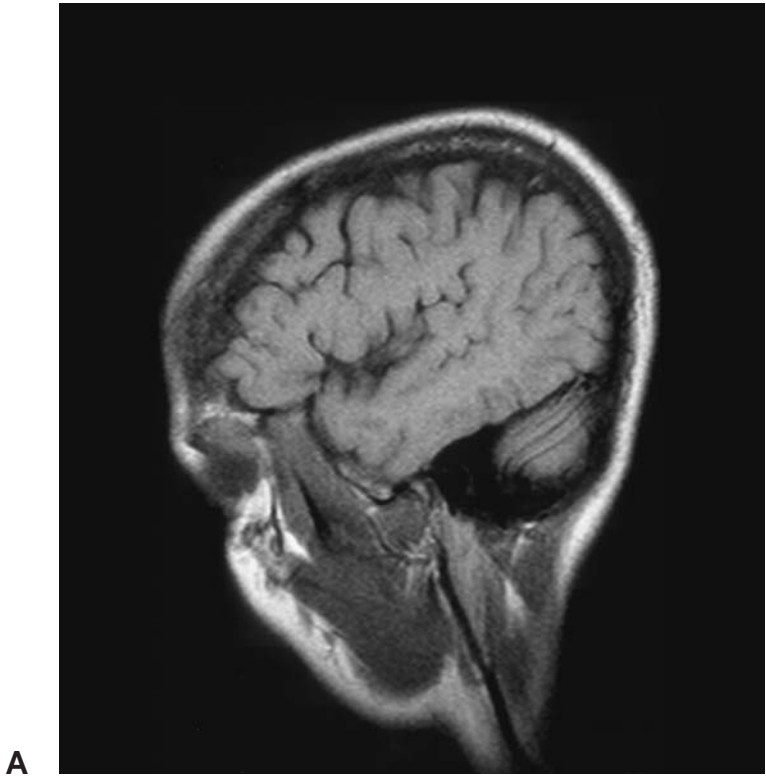
Compared to the previous image, more of the cerebral hemisphere is shown in this sagittal section, which also demonstrates the sulci dividing the gyri of the temporal lobe. Surrounding the temporal lobe, the darkened area representing the bones of the skull contains the opening of the external auditory meatus below the cerebrum. Within this darkened region, an enlarged, low-density area is found immediately posterior to the external auditory meatus and represents the mastoid air cells. Anterior to the meatus, the muscles of the cheek are now sectioned below the fat and glandular material, as described in the previous section.





**Figure 5–20 (A,B)** Sagittal MR image 3.

This section is distinctly different from the two previous images because the brain can now be distinguished as having three identifiable parts. The temporal lobe is separated from the parietal lobe by the darkened region of the Sylvian fissure. Below the temporal lobe, the mastoid air cells are again found as an enlarged region of the skull, shown as a darkened area. In contrast to previous images, part of the brain can now be seen adjacent to the mastoid air cells with a more linear pattern than the convoluted pattern of the cerebrum. Located within the posterior cranial fossa, the posterior part of the brain is the cerebellum.



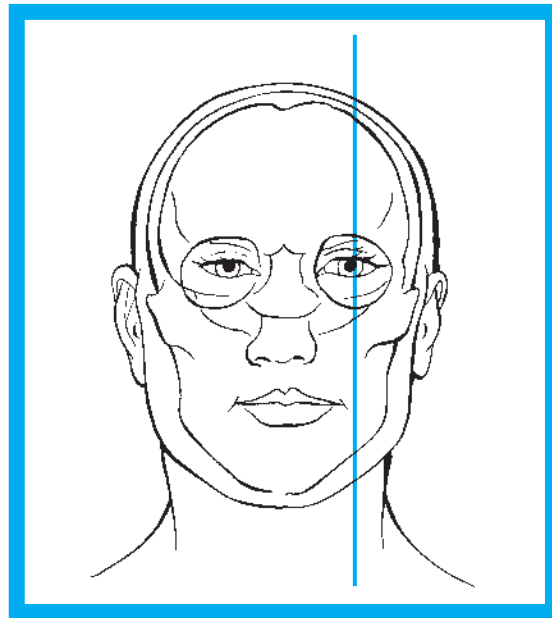
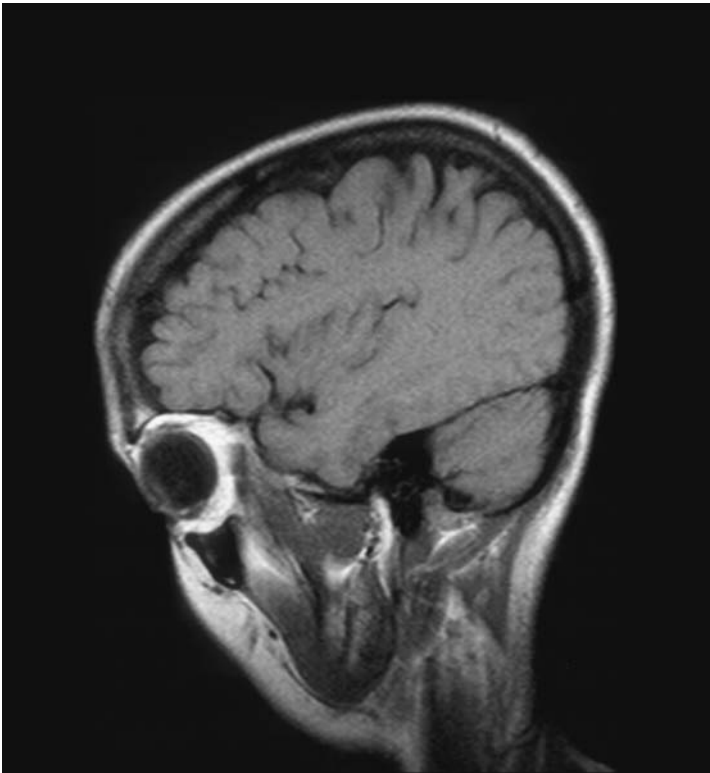
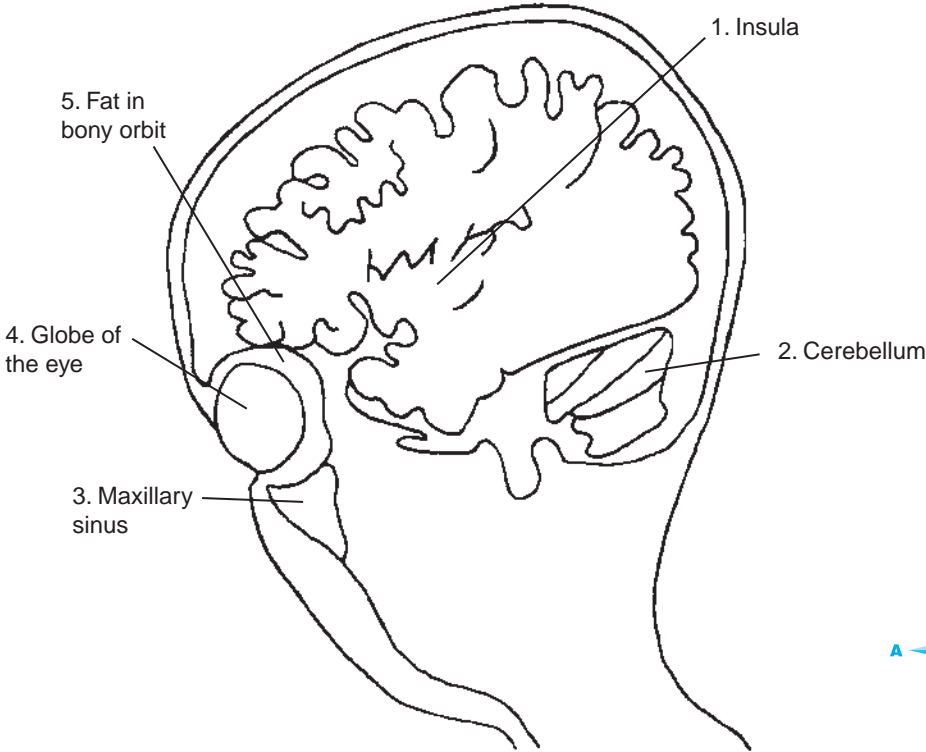


**Figure 5–21 (A,B)** Sagittal MR image 4.

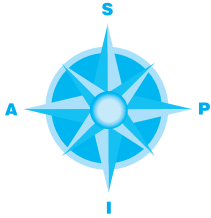
At first glance, the most readily identifiable structure on this image is the globe of the eye, which is surrounded by a layer of fat within the bony orbital cavity. The area of high signal intensity represents the fat between the dark area of the globe of the eye and the more inferiorly located maxillary sinus. Posterior to the eye, the medial border of the Sylvian fissure is now seen extending toward the insula, or the inner lobe of the cerebrum. Similar to the previous image, the parietal lobe is found above the insula and the temporal lobe is below the insula. These lobes are not labeled here, because the borders cannot clearly be seen at this level. Below the temporal lobe, a larger portion of the cerebellum is shown. Because most of the section is below the surface of the cerebellum, the linear striations are less evident than in the previous image.

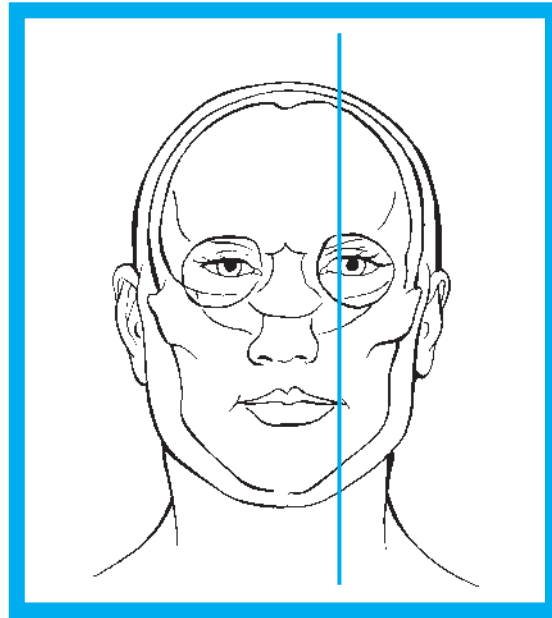


A



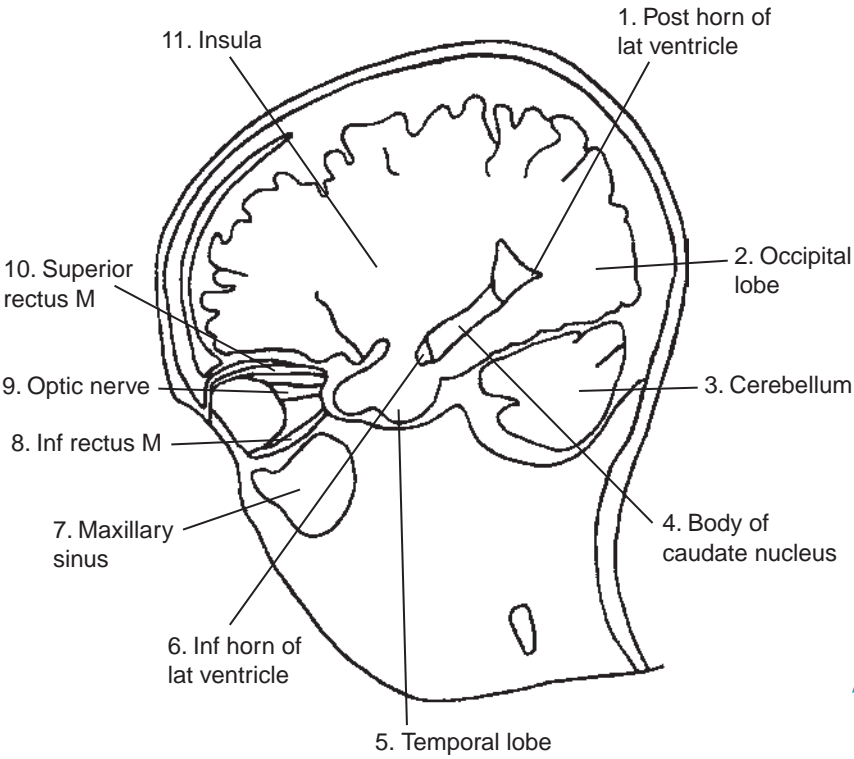
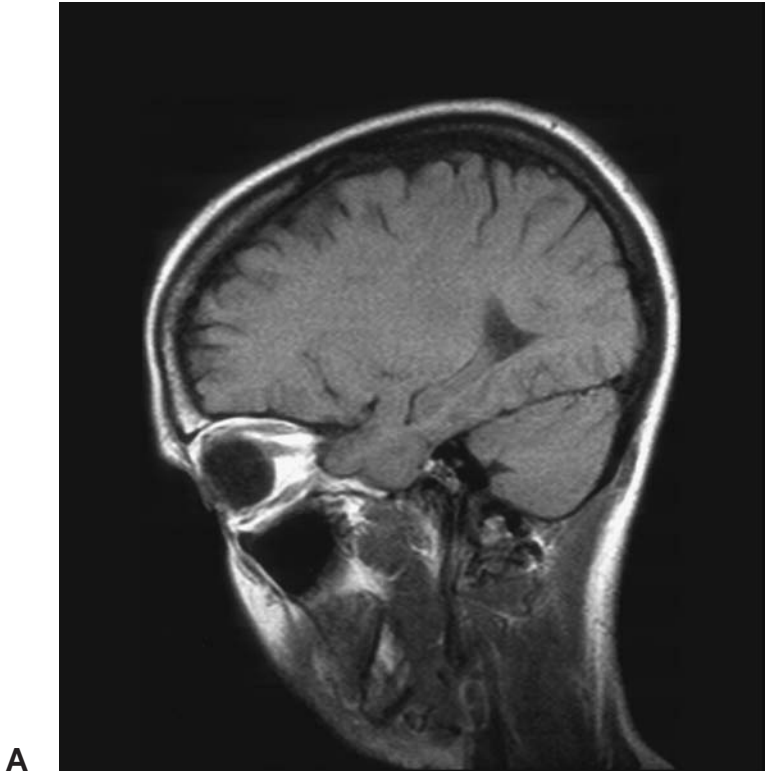
B



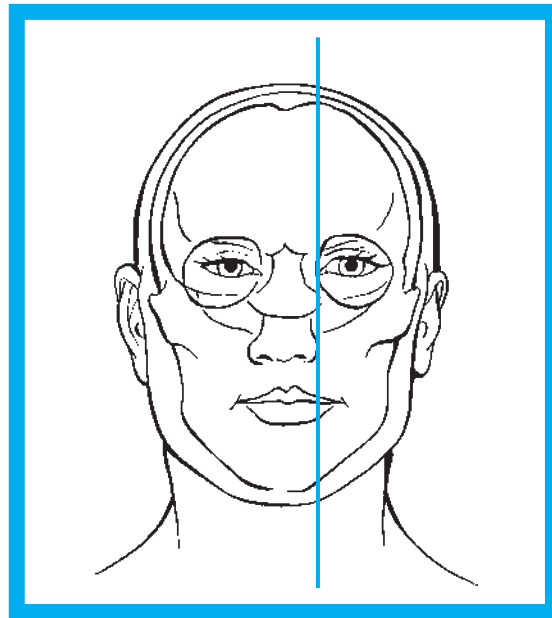


**Figure 5–22 (A,B)** Sagittal MR image 5.

The anatomy within this section lies near the midline of the left eye. Similar to the previous image, the globe of the eye can be readily identified. In addition, the optic nerve is longitudinally sectioned, extending off the posterior aspect of the eye through the layer of orbital fat. Attached to the upper pole of the globe of the eye, the superior rectus muscle is extending back through the orbital fat to attach to the skull. On the inferior pole of the eye, the inferior rectus muscle can also be seen extending back through the orbital fat to attach to the skull. As in the previous image, the maxillary sinus appears as a dark area immediately below the region of the eye. Inside the cranial cavity, the central lobe of the brain, the insula, is found above the temporal lobe. In the deep temporal lobe, the inferior horn of the lateral ventricle is shown along with the body of the caudate nucleus. In this section, the inferior horn appears separate from the triangle-shaped area of the posterior horn located deep within the occipital lobe. Inferior to the occipital lobe, the cerebellum is shown in the posterior cranial fossa.

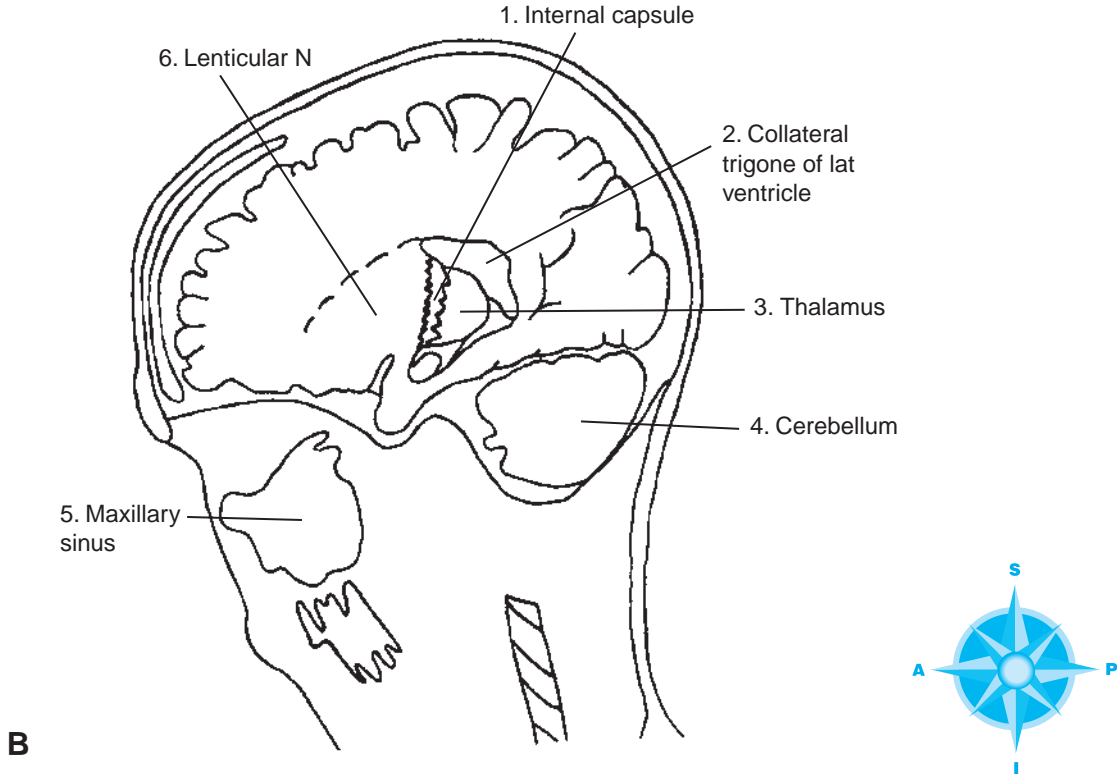
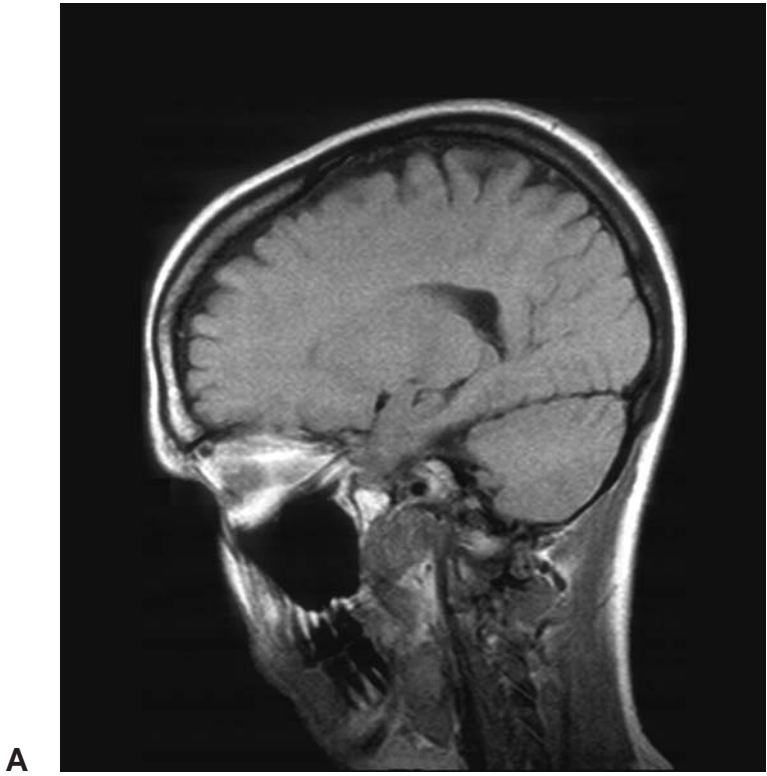


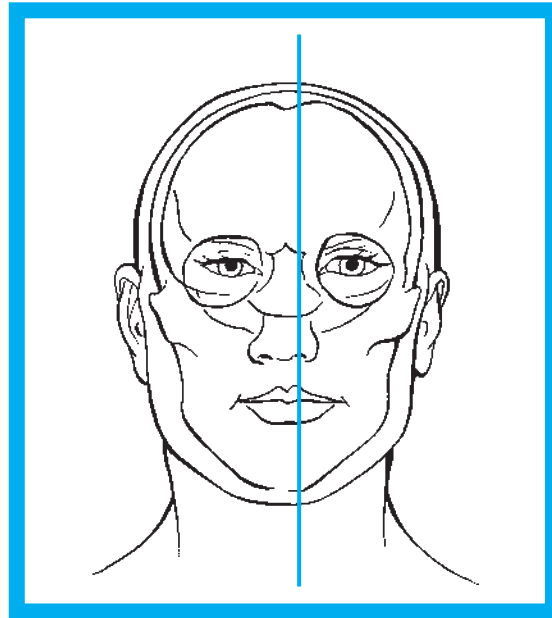




**Figure 5–23 (A,B)** Sagittal MR image 6.

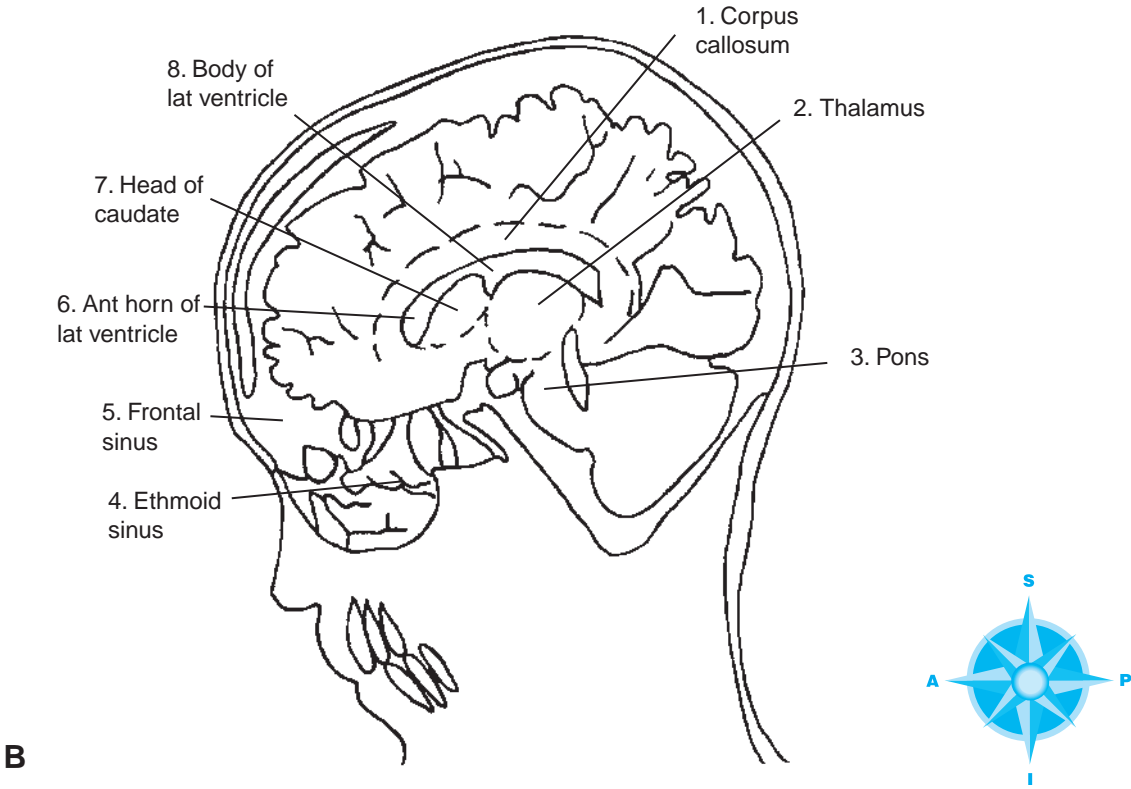
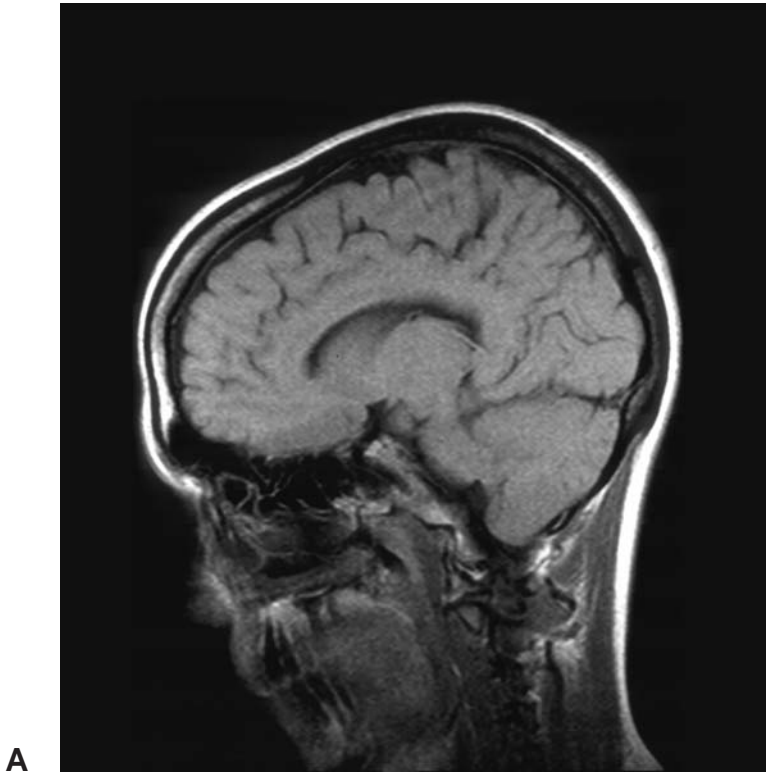
This image shows the largest part of the maxillary sinus. Within the cranial cavity, the nuclei sectioned deep to the insula are the lenticular nuclei, the putamen, and the globus pallidus. The lenticular nuclei are separated from the thalamus by a collection of nerve processes collectively referred to as the internal capsule. Because the previous section included the inferior and posterior horns of the lateral ventricles, the enlarged region of the lateral ventricle now sectioned is labeled as the collateral trigone. As in previous images, the cerebellum is shown below the occipital lobes of the cerebrum.





**Figure 5–24 (A,B)** Sagittal MR image 7.

This image is nearing the midline, as evidenced by the surface outline, which demonstrates a small part of the lateral aspect of the nose. The maxillary sinus is no longer seen, and has been replaced by the ethmoid air cells. Above the ethmoid air cells, an enlarged region of the skull represents the frontal sinus in the position formerly occupied by the upper bony orbit. Within the cranial cavity, the body of the lateral ventricle is longitudinally sectioned continuous with the anterior horn in the frontal lobe of the cerebrum. Forming the roof of the lateral ventricle, the corpus callosum is a band of white matter formed by commissural fibers projecting between the right and left cerebral hemispheres. Below the lateral ventricles, the head of the caudate nucleus is protruding into the anterior horn of the lateral ventricle, and the thalamus is protruding into the body of the lateral ventricle. Below the thalamus, the pons can be seen as an enlarged region of the brainstem anterior to the cerebellum.



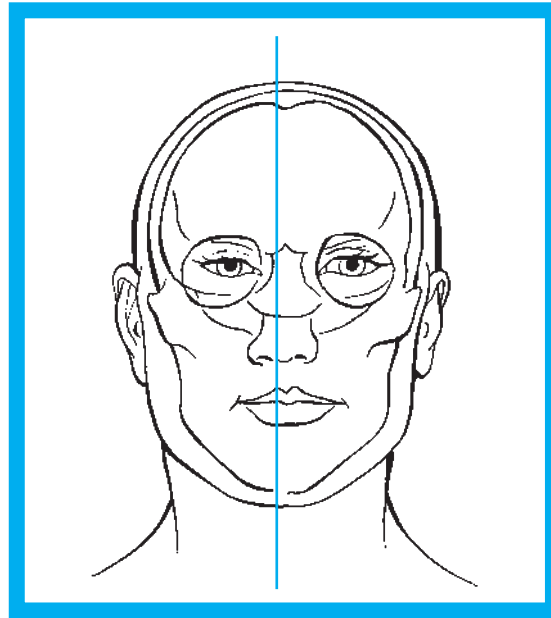
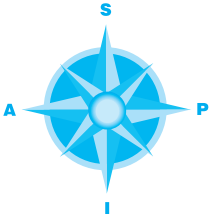
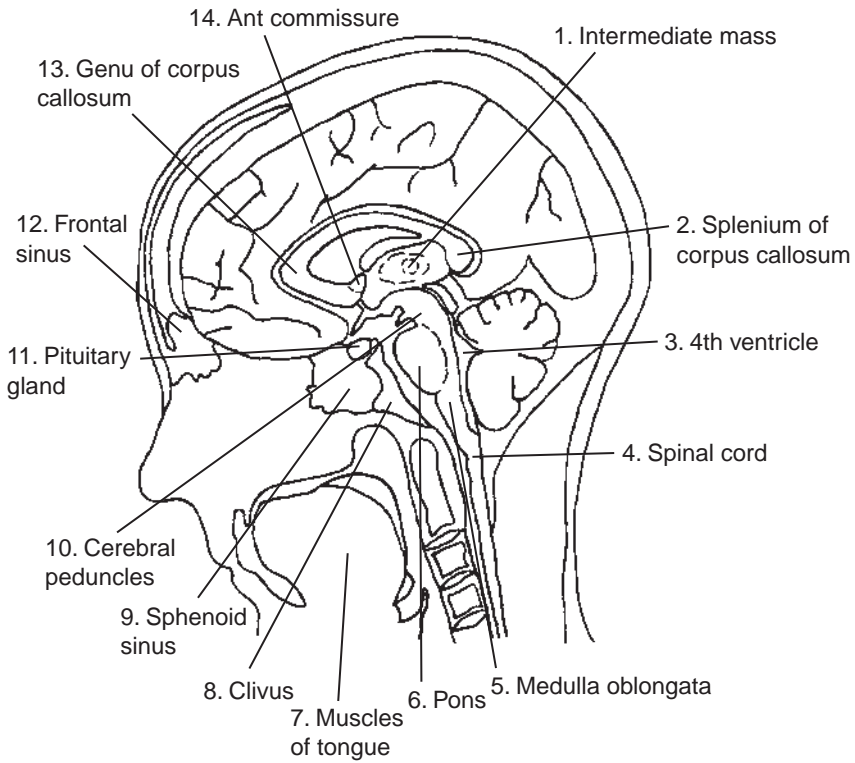
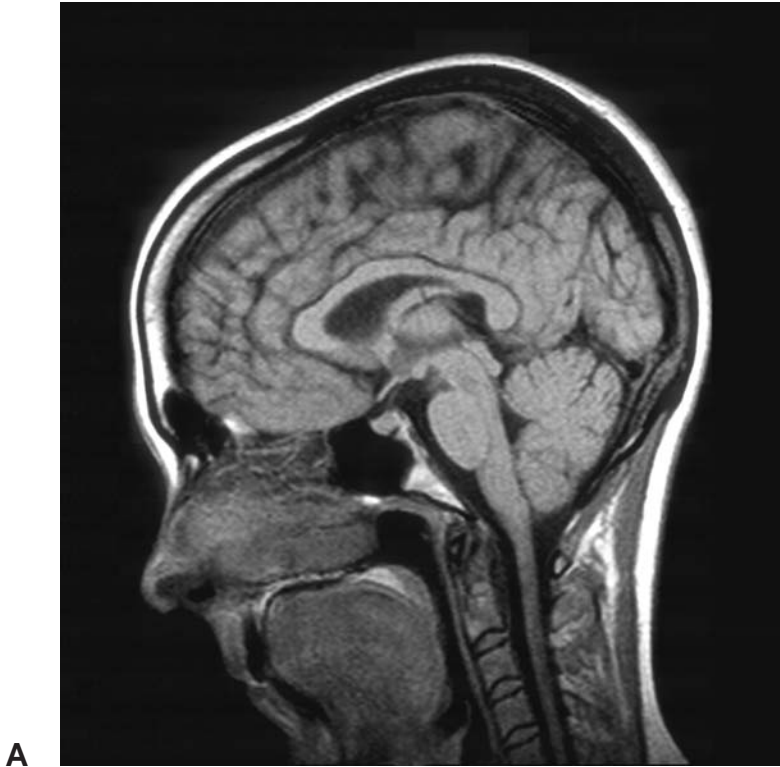


**Figure 5–25 (A,B)** Sagittal MR image 8.

On the surface outline of this image, the nose is shown in full profile, indicating that this section is near the midsagittal plane. Below the nasal cavity, the muscles of the tongue are shown in front of the vertebral column. Similar to the previous image, the frontal sinus appears as an enlarged area of the skull just above the nasal cavity. Because this image is near the midline, the ethmoid air cells are no longer visible, and an enlarged region of the skull (the sphenoid sinus) is forming the posterior border of the nasal cavity. Immediately posterior to the sphenoid sinus, a dense area formed by the sphenoid bone and basilar part of the occipital bone is labeled the clivus. In the upper part of the sphenoid sinus, the pituitary gland is demonstrated on the base of the brain centrally situated between the cerebral hemispheres. The commissural fibers of the corpus callosum are now found anteriorly forming a bend, or genu, that gives rise to the anterior commissure at its most inferior point. Posteriorly, the enlarged part of the corpus callosum forms the splenium. In the region previously occupied by the thalamus, a round commissural bundle called the intermediate mass is shown in cross-section as it extends through the third ventricle between the right and left thalamic nuclei. In this section, the fibers connecting with the cerebrum are shown forming the most superior part of the brainstem, the cerebral peduncles. Below the cerebral peduncles, the fibers from the cerebellum join those from the cerebrum, forming an enlarged region (the pons) that makes up the anterior border of the fourth ventricle. The lower part of the brainstem, the medulla oblongata, gradually narrows as it travels toward the foramen magnum, where it continues as the spinal cord as it exits the cranial cavity.

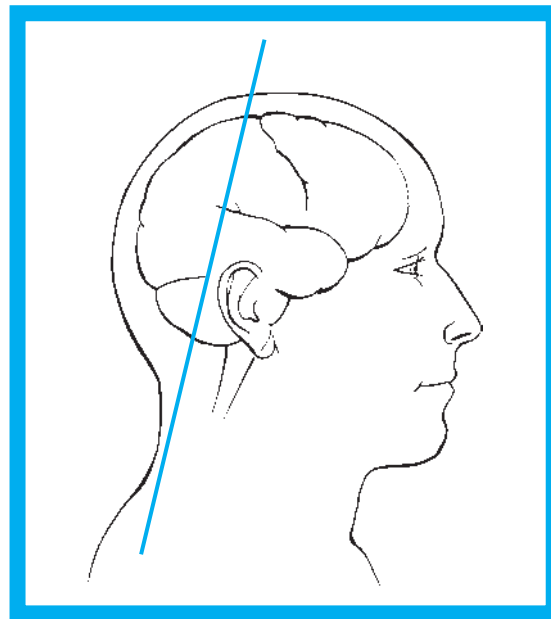




## Coronal MR Images

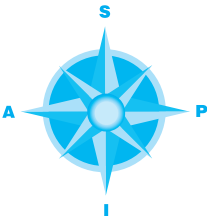
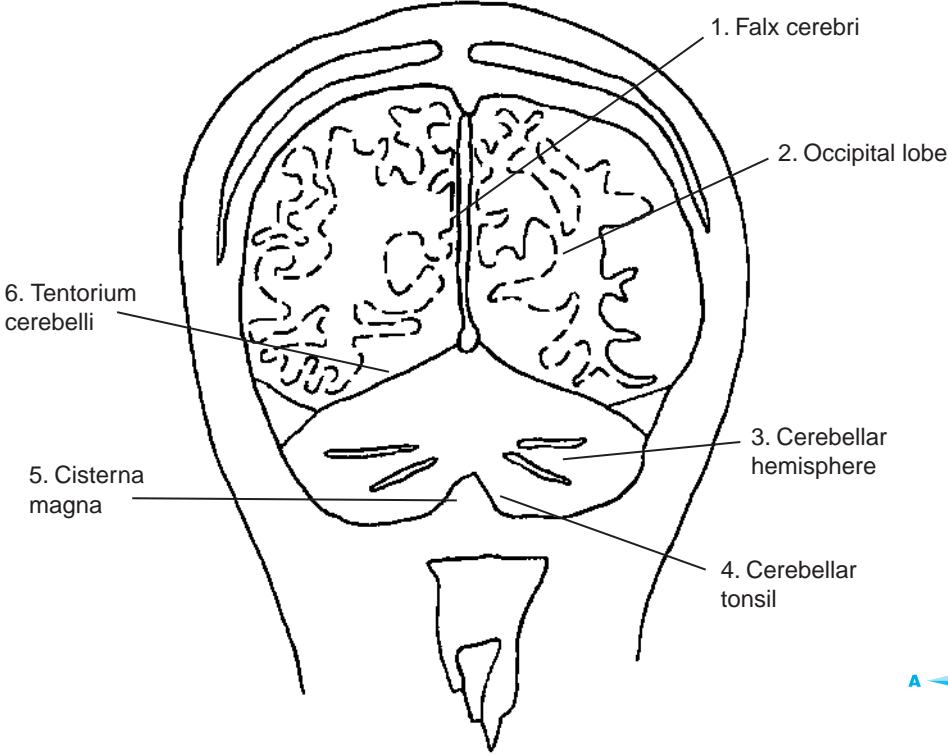
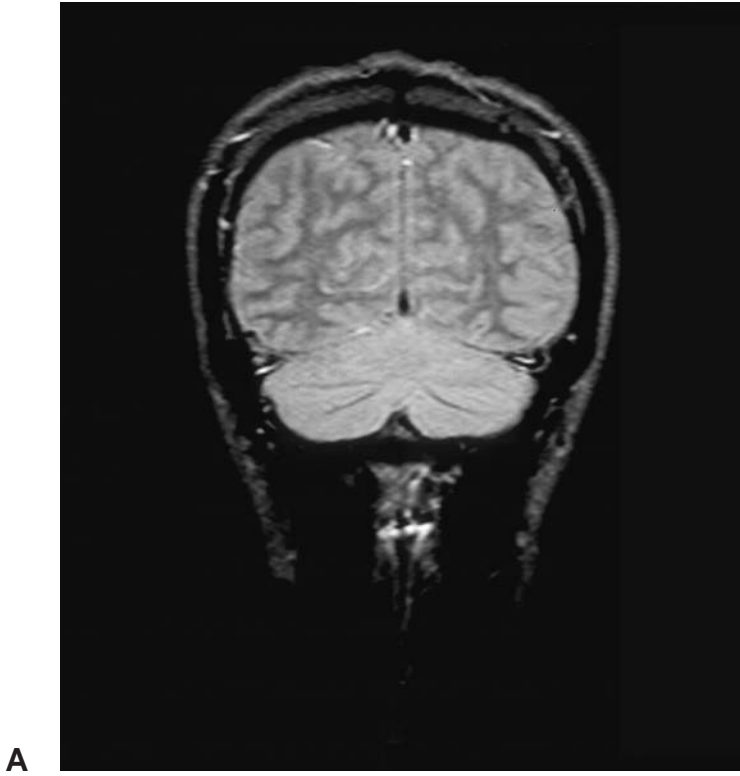
The following 16 images of the head are described at 5.5-mm intervals from posterior to anterior. The images were generated at the following technical factors: repetition

time (TR) = 2,000 ms; echo time (TE) = 80 ms; radiofrequency (RF) = 90°; field of view (FOV) = 25 cm; slice thickness (TH) = 5.0 mm.

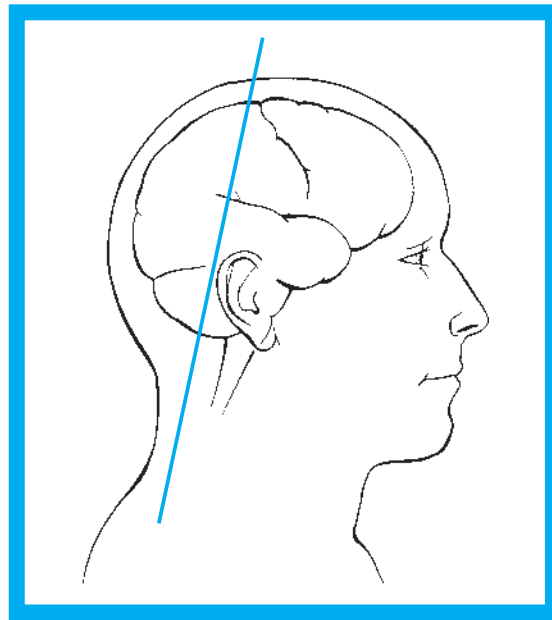


**Figure 5–26 (A,B)** Coronal MR image 1.

Generated through the posterior brain, this view demonstrates the occipital lobes and the underlying cerebellum in the posterior cranial fossa. The right and left cerebral hemispheres are separated by the falx cerebri, and the cerebrum is separated from the underlying cerebellum by the tentorium cerebelli. Unlike the cerebral hemispheres, the cerebellar hemispheres are not clearly separable, except on the lower border where the indentation creates the enlarged subarachnoid space just above the foramen magnum known as the cisterna magna. On either side of the cisterna magna, the cerebellar tonsils are labeled as the lower and medial segments of the cerebellar hemispheres.

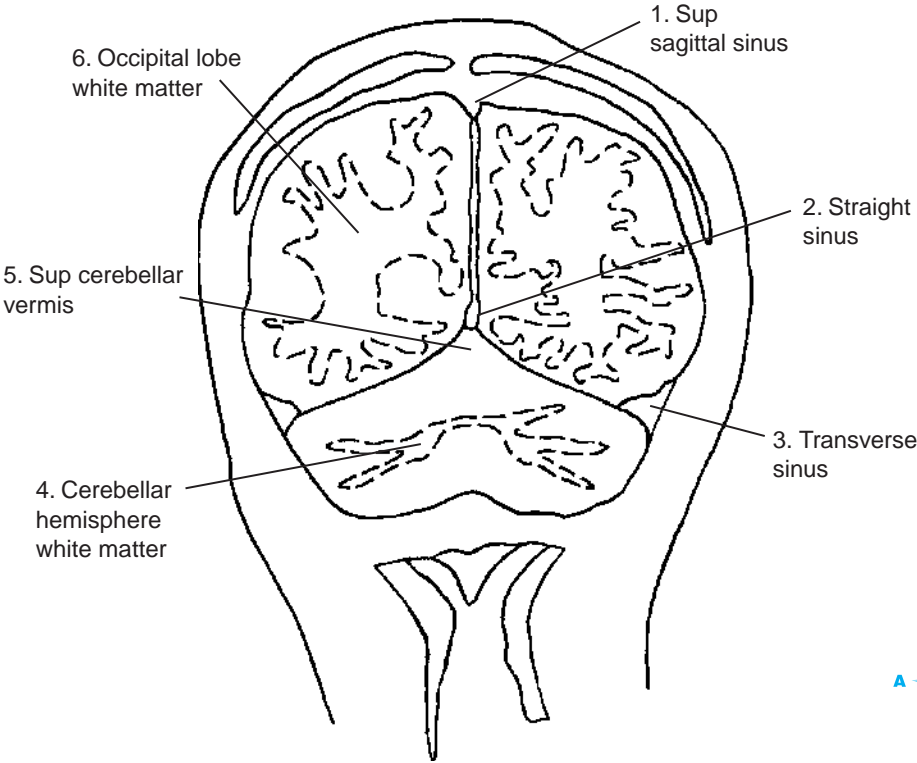
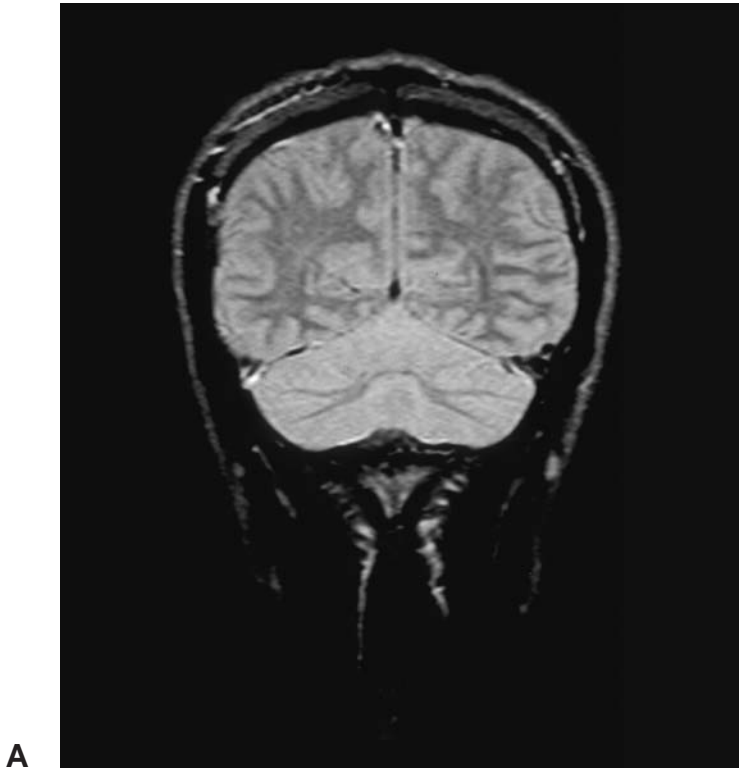


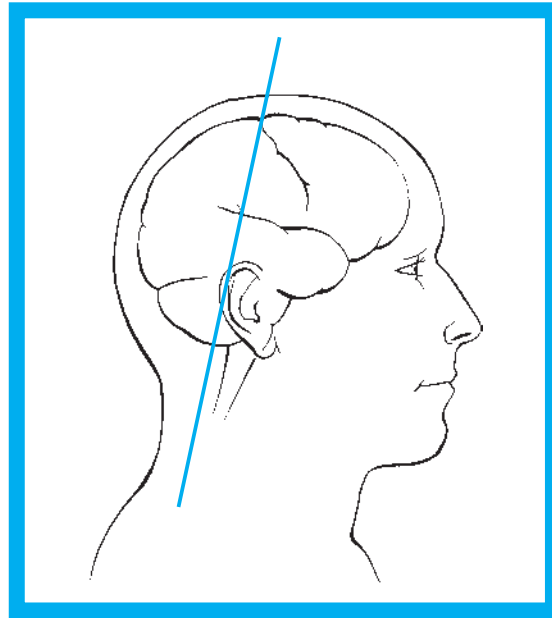




**Figure 5–27 (A,B)** Coronal MR image 2.

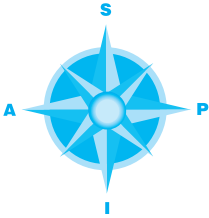
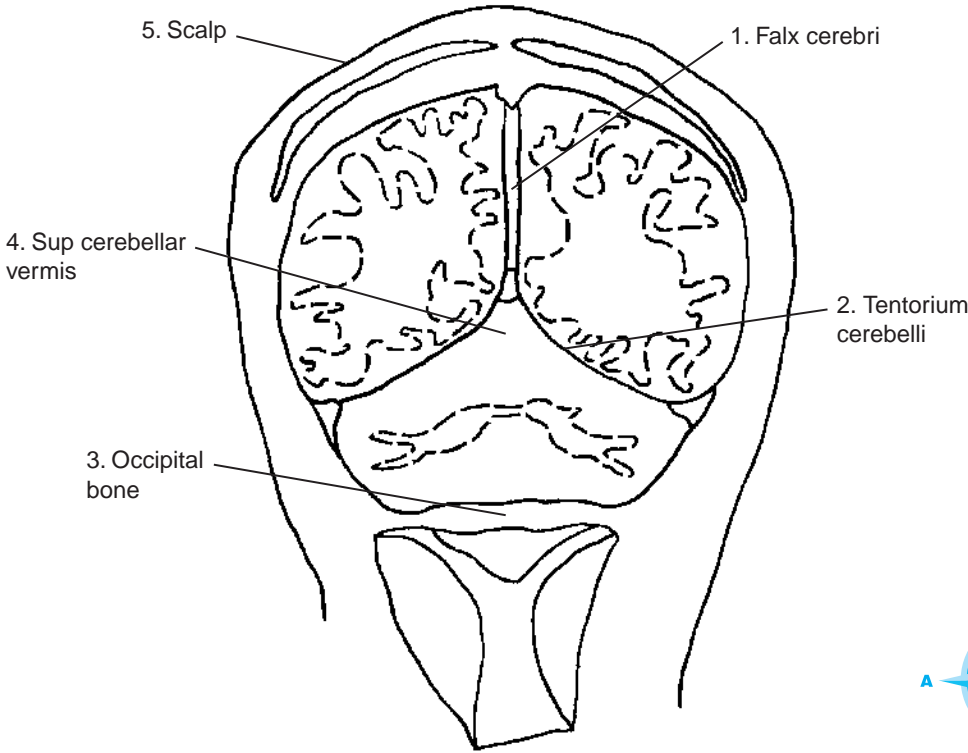
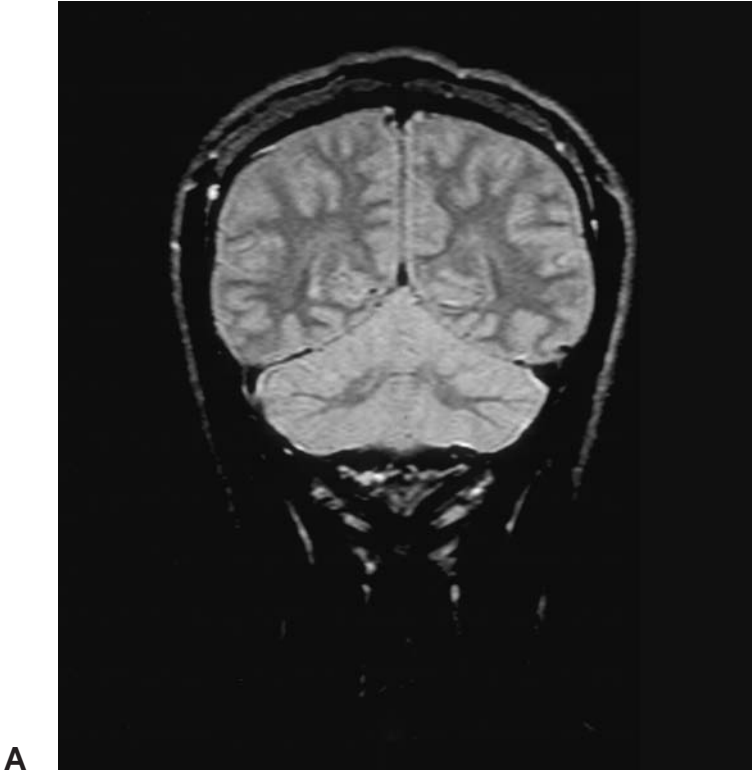
Compared to the previous image, the more anterior location of this section better demonstrates the white matter within the occipital lobe surrounded by the gray matter of the cortex. The falx cerebri separates the right and left cerebral lobes. Along the borders, folds of dura mater create the straight sinus and superior sagittal sinus. Similar to that within the cerebral hemispheres, the white matter within the cerebellar hemispheres is now better visualized within the central part of the cerebellum. Although the cerebellar tonsils are no longer seen on the lower cerebellum, the superior cerebellar vermis is sectioned as it joins the two cerebellar hemispheres. As described in the previous image, the tentorium cerebelli separates the cerebrum and cerebellum. The lateral borders of the tentorium cerebelli and the endosteal dura lining the inside of the skull form the transverse sinuses. In the midline, the tentorium cerebelli and the falx cerebri join together to form the straight sinus.

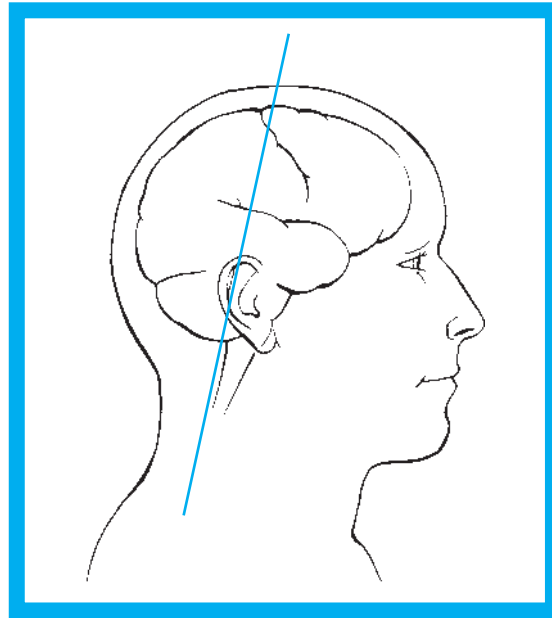




**Figure 5–28 (A,B)** Coronal MR image 3.

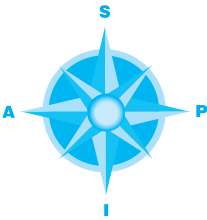
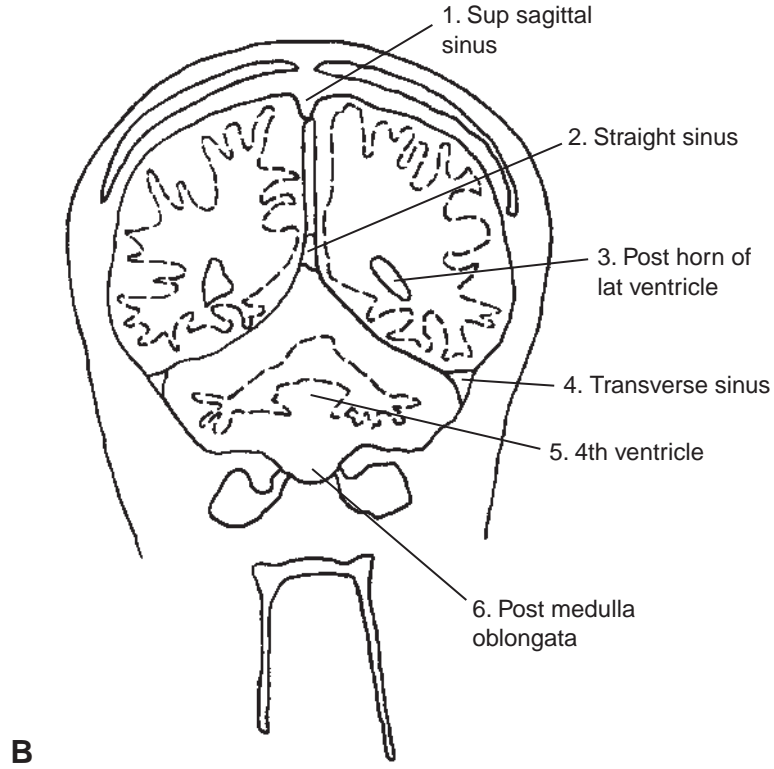
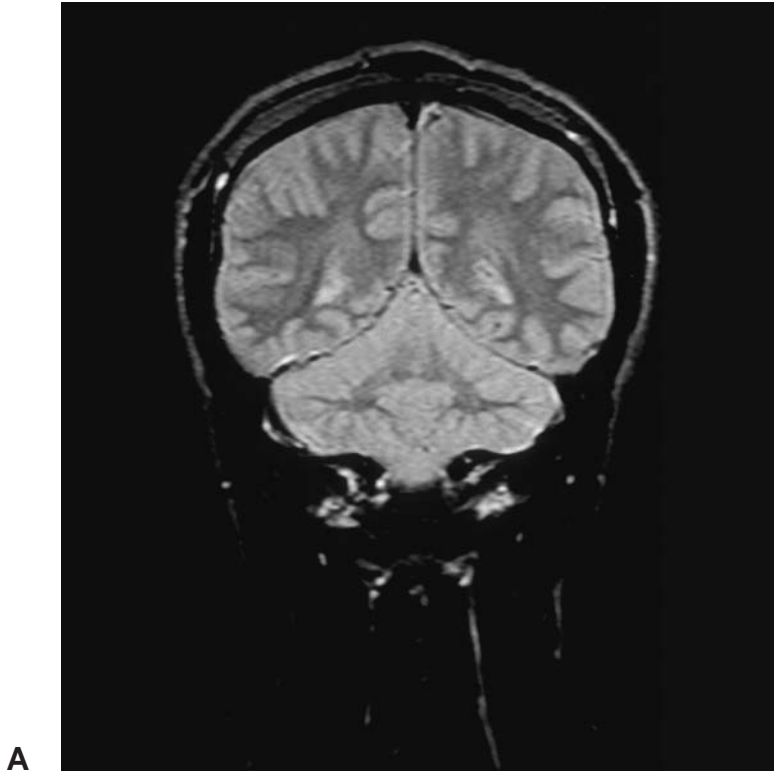
As in the previous images, the falx cerebri separates the right and left cerebral hemispheres. Below the cerebrum, the cerebellum appears more triangular in shape and the superior cerebellar vermis lies directly below the tentorium cerebelli. The cerebellar vermis is a median strip joining the right and left cerebellar hemispheres. Below the cerebellum, the occipital bone is seen as a dark area extending around the neural structures just described. Outside of the occipital bone, several layers of the scalp can be delineated on the top of the skull.





**Figure 5–29 (A,B)** Coronal MR image 4.

The unique shape of the cerebellum in this image demonstrates that the plane of section is near the anterior part of the cerebellum. Compared to the previous image, an inferior projection now appears continuous with the cerebellum, representing the posterior medulla oblongata. Although it cannot clearly be delineated here, the fourth ventricle is above the posterior medulla oblongata in the central region of the cerebellum. On either side of the cerebellar hemispheres, the transverse sinuses are within the lateral margin of the tentorium cerebelli. Above the cerebellum, the straight sinus is near the midline in the tentorium cerebelli and is connected via the falx cerebri to the superior sagittal sinus. Within the cerebral hemispheres, fluid-filled regions within the white matter are now discernible, representing the posterior horns of the lateral ventricles.



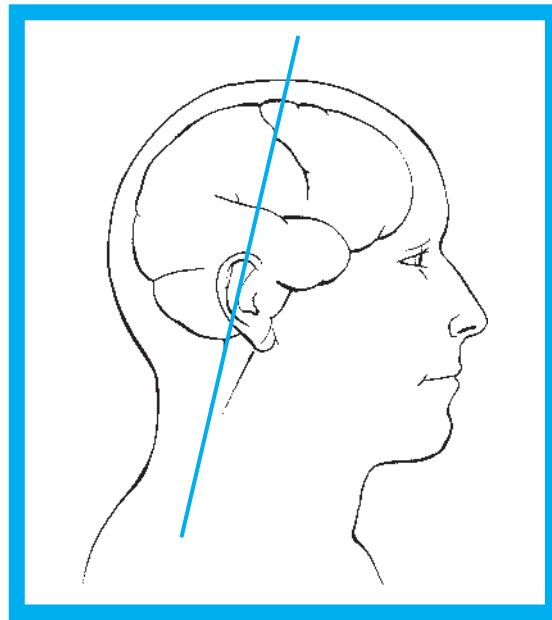
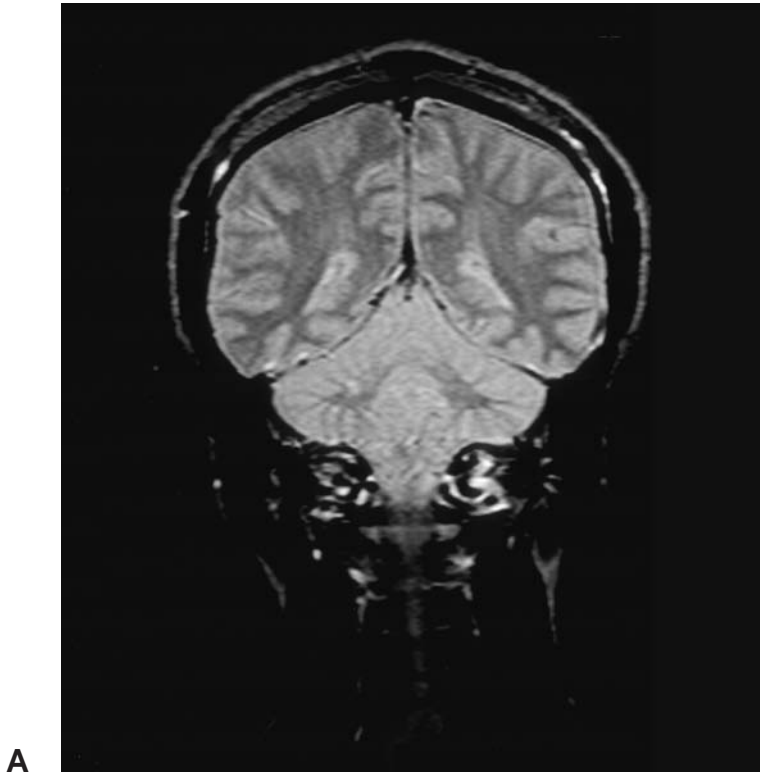
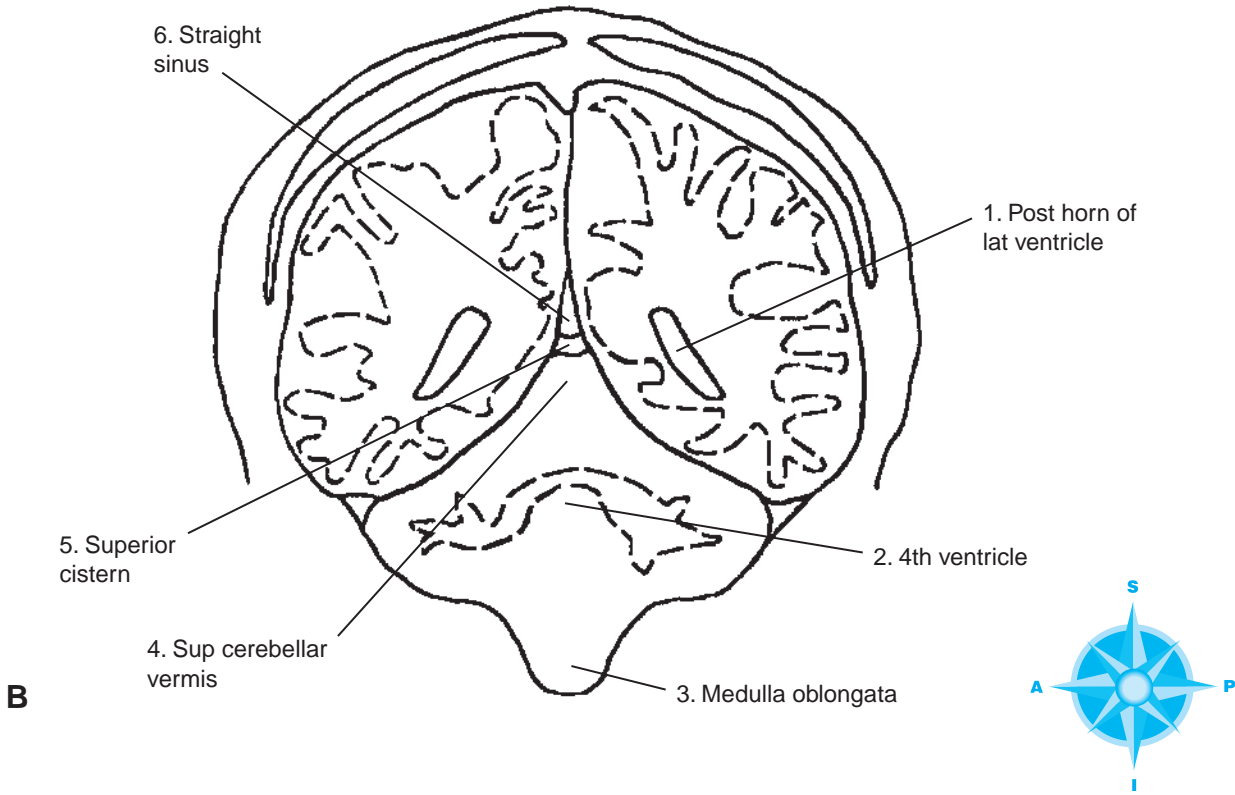


**Figure 5–30 (A,B)** Coronal MR image 5.

The diamond shape of the cerebellar region in this image indicates that this section includes the anterior cerebellum and the lower part of the brainstem, the medulla oblongata. Although not clearly discernible, the fourth ventricle is within the central cerebellum and the superior cerebellar vermis is just below the superior cistern. Together, these structures lie just below the tentorium cerebelli that joins with the falx cerebri to form the straight sinus. Within the cerebral hemispheres, the enlarged hyperdense regions within the white matter are labeled the posterior horns of the lateral ventricles within the occipital lobes.



A



B



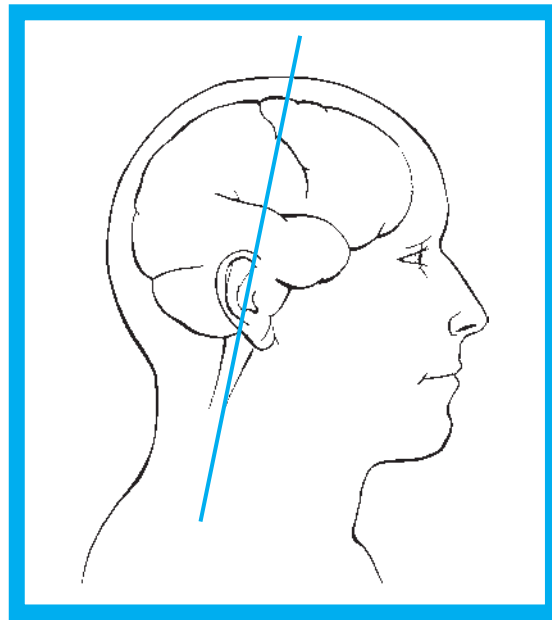
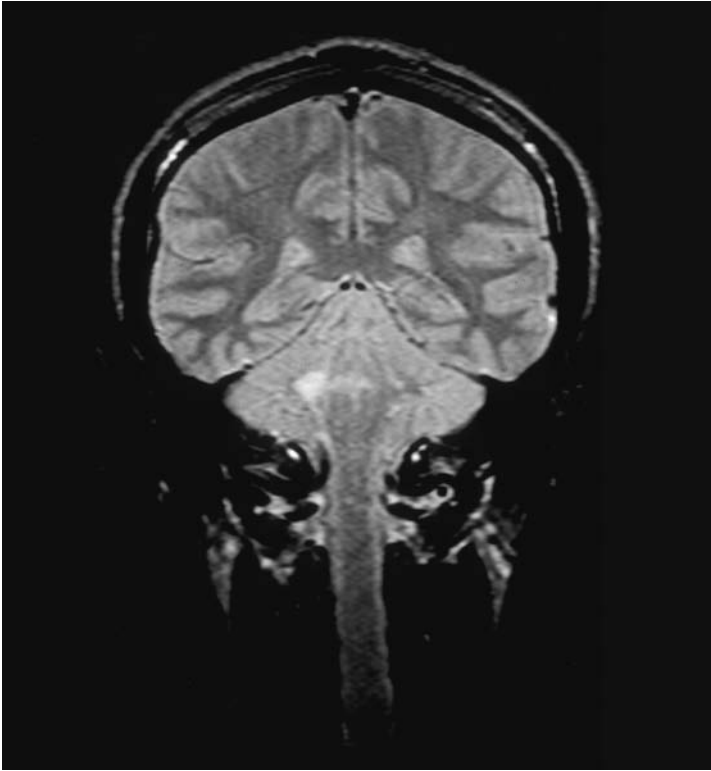
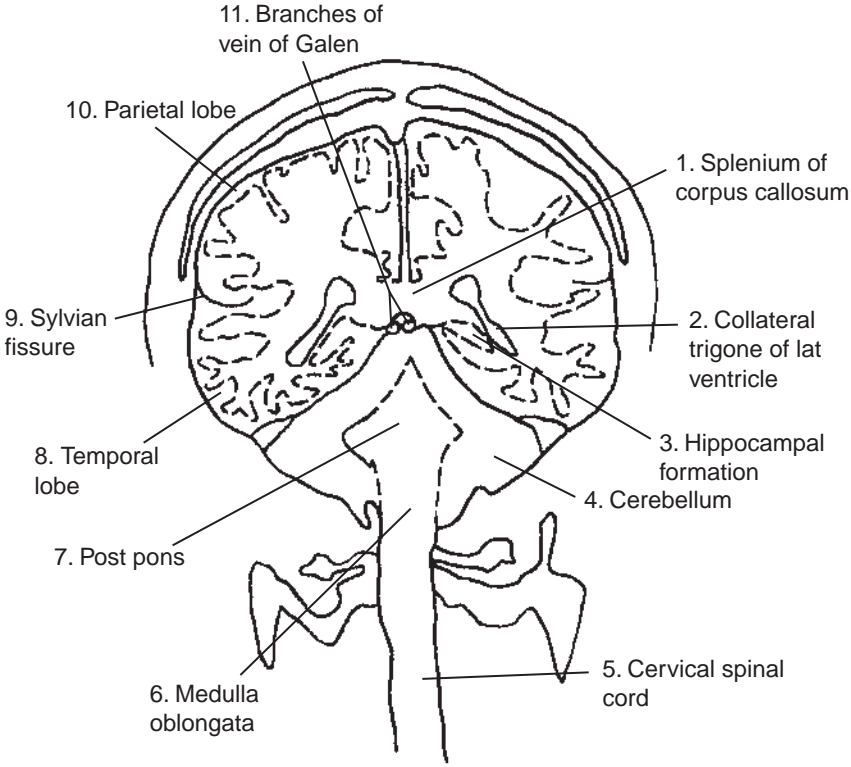


**Figure 5–31 (A,B)** Coronal MR image 6.

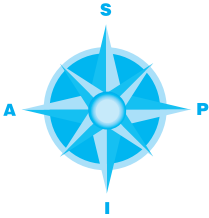
The cervical spinal cord on the lower part of this image indicates that the plane of this section includes the contents of the foramen magnum. Forming the lower brainstem, the medulla oblongata and the posterior pons are surrounded on either side by the margins of the right and left cerebellar hemispheres. Although the lateral margins and transverse sinuses are still found between the cerebrum and cerebellum, the tentorium cerebelli and straight sinus are no longer seen centrally. Instead, a pair of internal cerebral veins is directly below the splenium of the corpus callosum. This pair of internal cerebral veins drains into the vein of Galen that extends only a short distance before emptying into the straight sinus. As described earlier, the splenium of the corpus callosum is continuous with the white matter of the cerebral hemispheres and acts as a commissural route for fibers to extend between the right and left cerebral hemispheres. Lateral to the splenium of the corpus callosum, the deep groove of the Sylvian fissure divides the parietal and temporal lobes of the cerebrum. Within the white matter of these lobes, the cerebrospinal fluid (CSF)-filled lateral ventricle appears enlarged, representing the region of the collateral trigone. Immediately below the collateral trigone of the lateral ventricle, a convoluted region of gray matter deep within the temporal lobe represents the hippocampal formation. As described previously, the hippocampal formation is considered part of the limbic system and serves a vital role in emotional behavior.

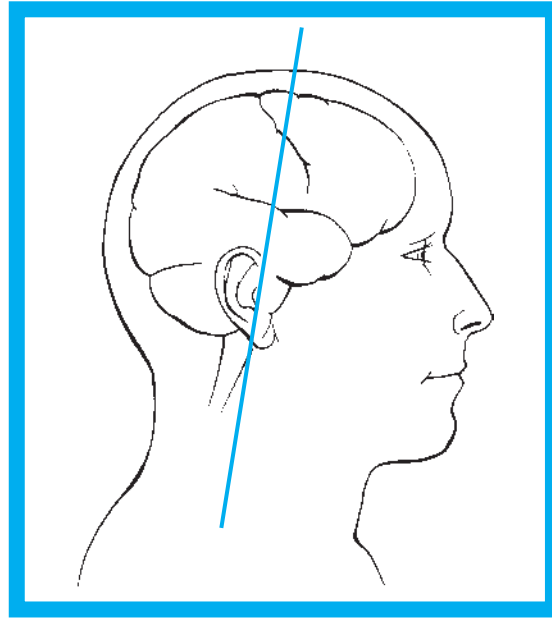


A



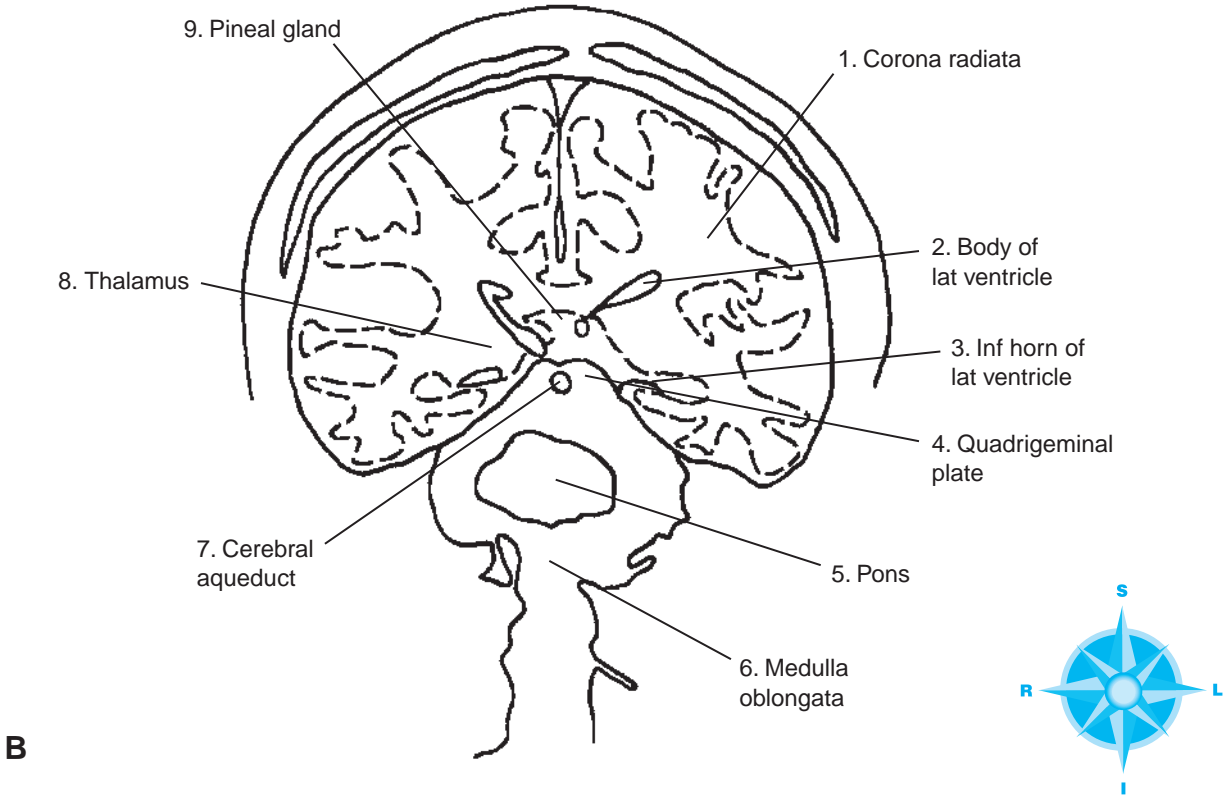
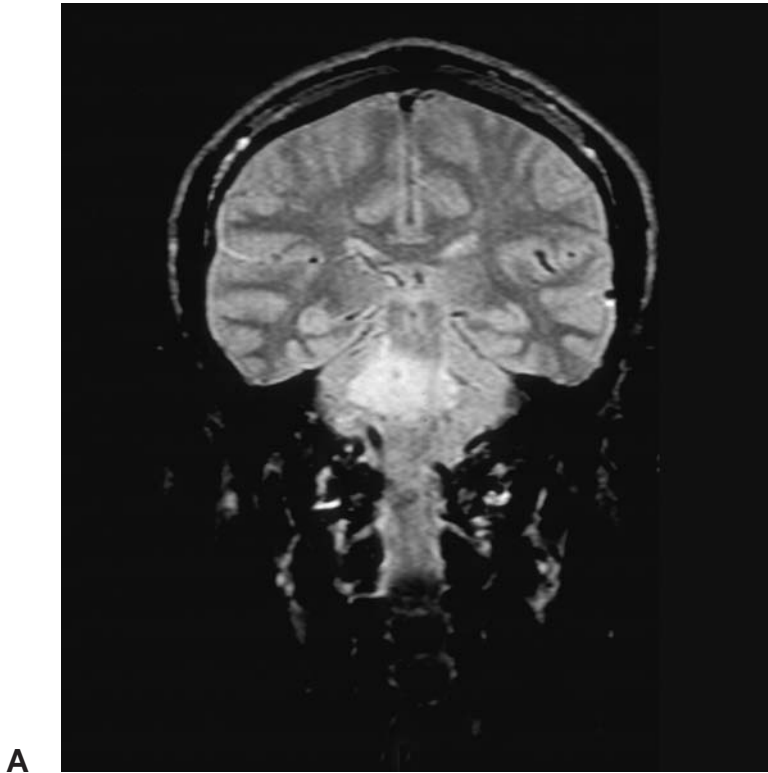
B





**Figure 5–32 (A,B)** Coronal MR image 7.

The absence of much of the cerebellar hemispheres in this image indicates that the plane of the section is near the midline of the head. The enlarged region of the brainstem (the pons) is centrally located in the region previously occupied by the cerebellum. Immediately below the pons, the medulla oblongata appears as the enlarged part of the brainstem that continues as the spinal cord below the occipital bone. Unlike previous images, this section demonstrates all three parts of the brainstem: The medulla oblongata, the pons, and the midbrain. Although not labeled the midbrain, the quadrigeminal plate and the cerebral aqueduct are within the midbrain region of the brainstem. The quadrigeminal plate is found in the region previously occupied by the cerebellar vermis. Below the quadrigeminal plate, the opening of the cerebral aqueduct is cross-sectioned, extending between the third and fourth ventricles. The pineal gland is found medially between the bodies of the lateral ventricles. In this more anterior section, the collateral trigone of the lateral ventricle has given rise to the body and inferior horns of the lateral ventricles separated by a region of gray matter, the thalamus. As in previous images, the white matter extending between the cerebral cortex and the basal ganglia are collectively called the corona radiata.



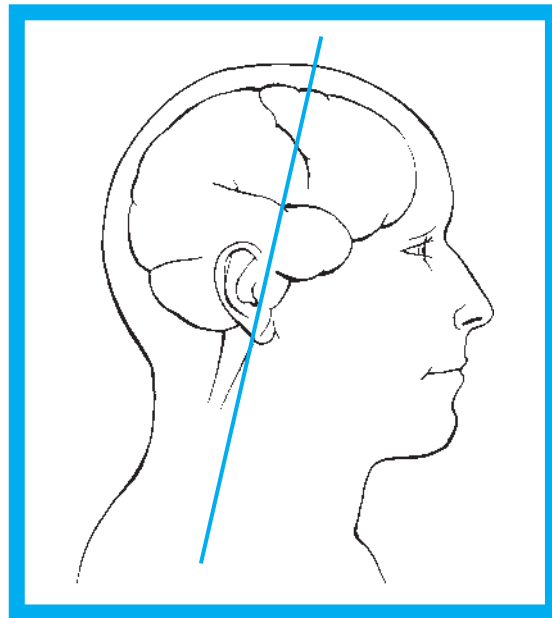
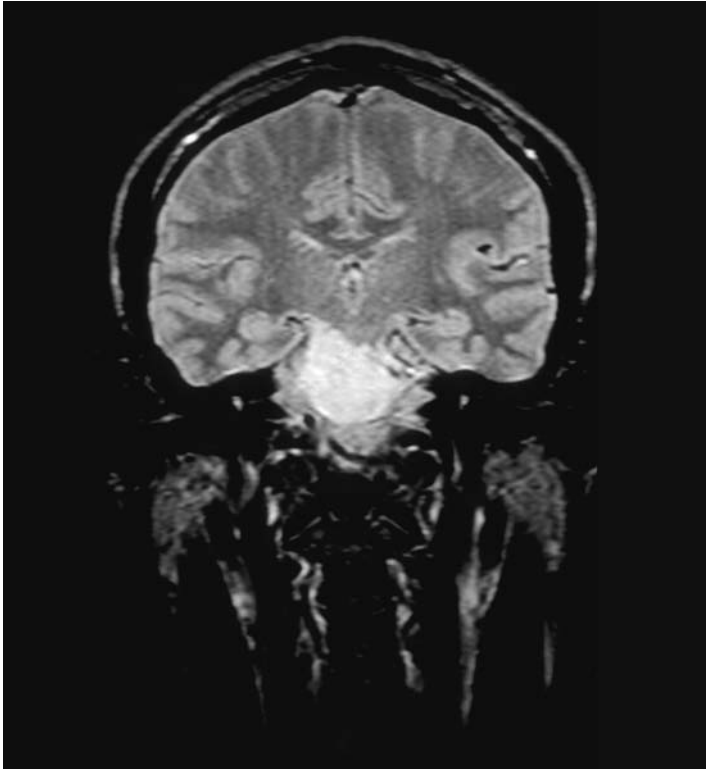
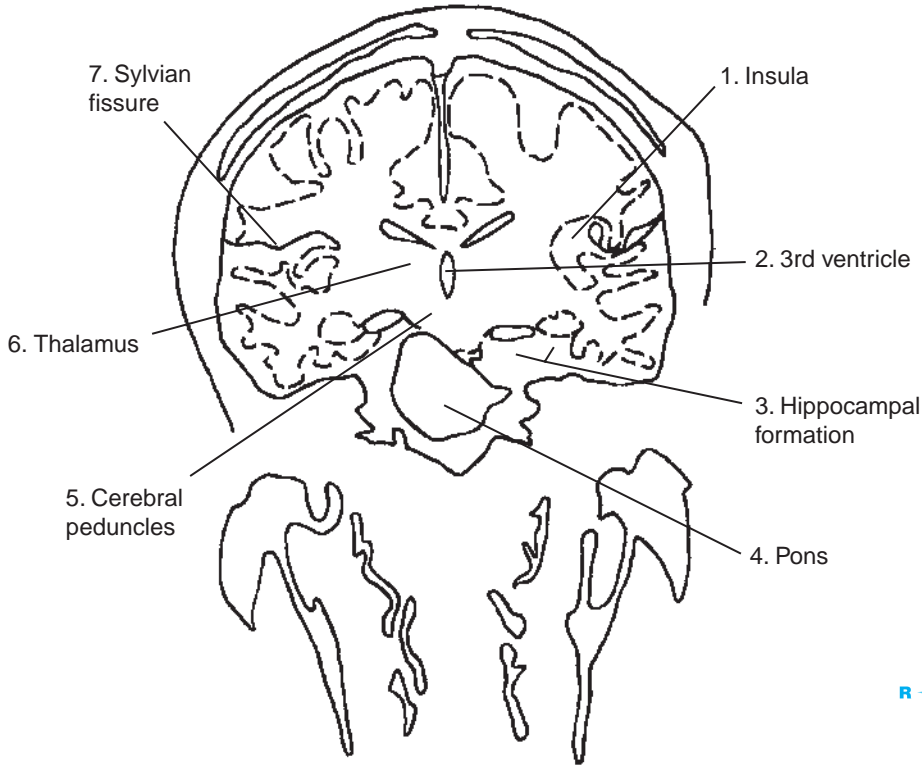


**Figure 5–33 (A,B)** Coronal MR image 8.

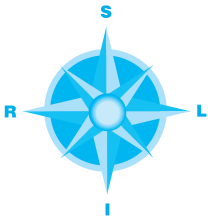
The pons is a hyperdense region near the center of this image, below the cerebral hemispheres. Directly above the pons, the cerebral peduncles are found below the opening of the third ventricle. On either side of the third ventricle, the thalamic nuclei are found between the body and inferior horns of the lateral ventricles. Directly below the inferior horn of the lateral ventricle, the convoluted regions of gray matter represent the hippocampal formations. Lateral to the thalamic nuclei, the deep groove or Sylvian fissure is found dividing the cerebral hemispheres. Surrounding the medial part of the Sylvian fissure, the insula is the region of gray matter forming what is also referred to as the inner lobe of the brain.

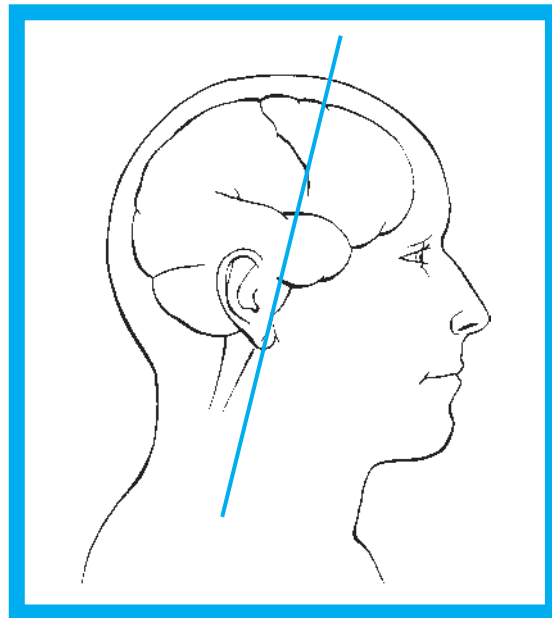


A



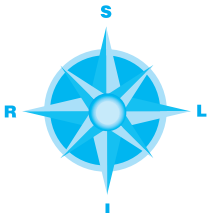
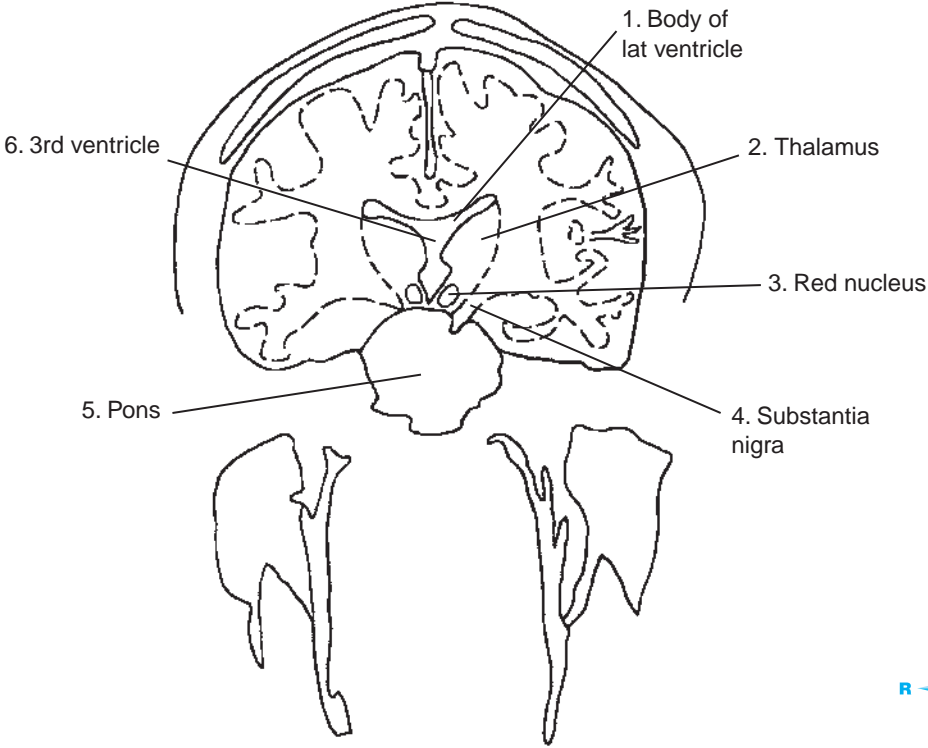
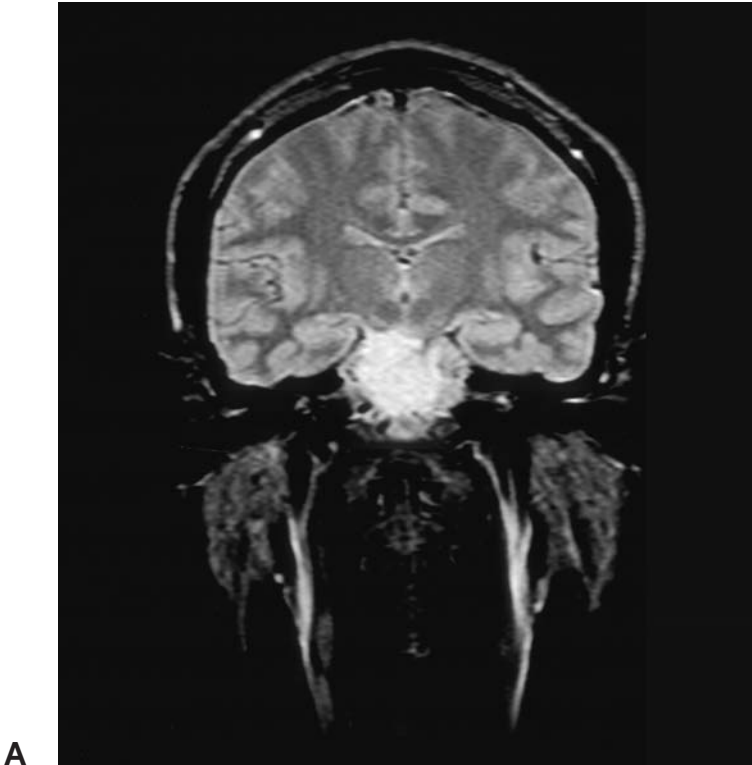
B



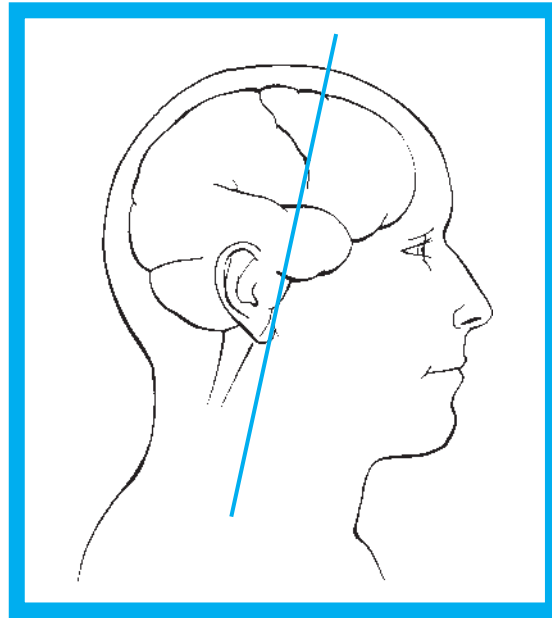


**Figure 5–34 (A,B)** Coronal MR image 9.

Similar to the previous image, the pons can be readily identified as a hyperdense region immediately below the cerebral hemispheres. Directly above the pons, the third ventricle is demonstrated in the midline and appears continuous with the lateral ventricles. On either side of the third ventricle, the oval-shaped thalamic nuclei occupy a medial location in the cerebral hemispheres. Below the thalamic nuclei, a small pair of round nuclei, the red nuclei, is demonstrated within the upper midbrain. Below the red nuclei, the substantia nigrae appear as thin striations of gray matter within the cerebral peduncles of the midbrain.

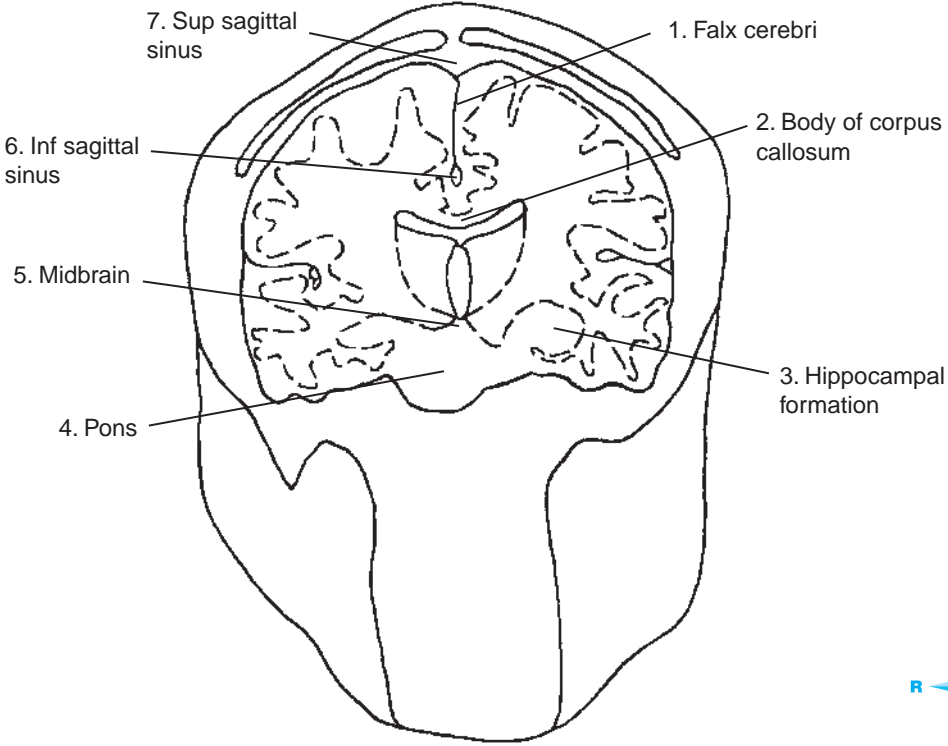
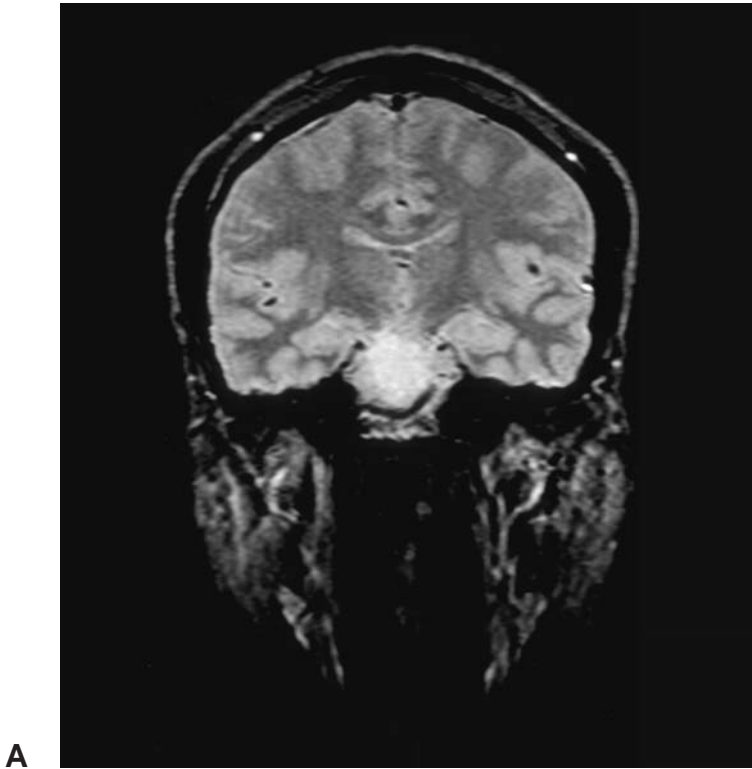


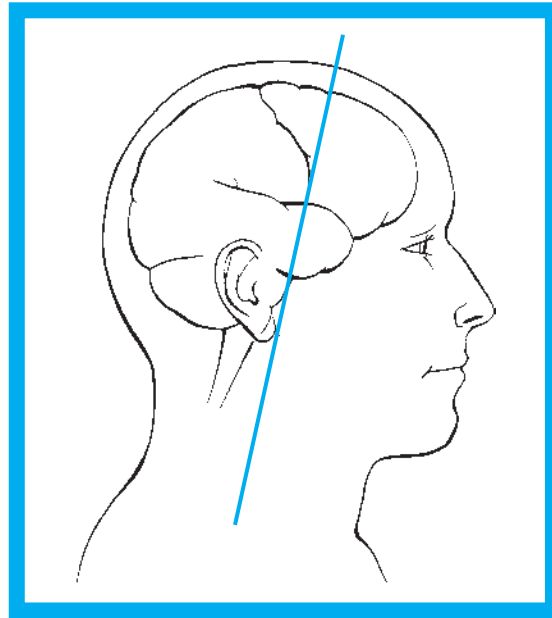




**Figure 5-35 (A,B)** Coronal MR image 10.

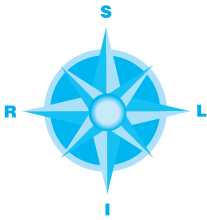
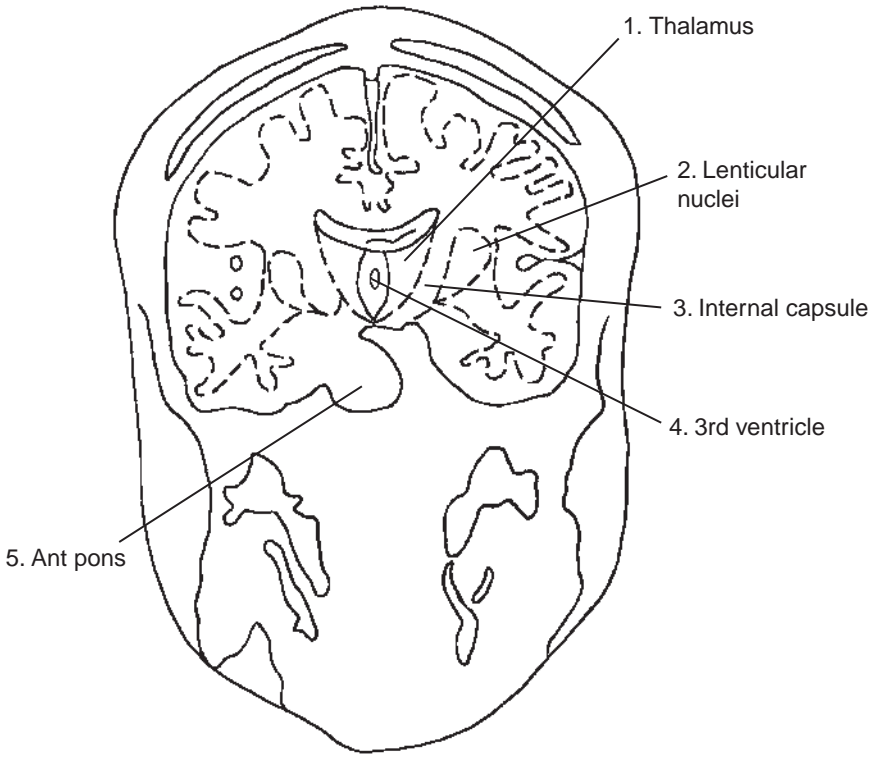
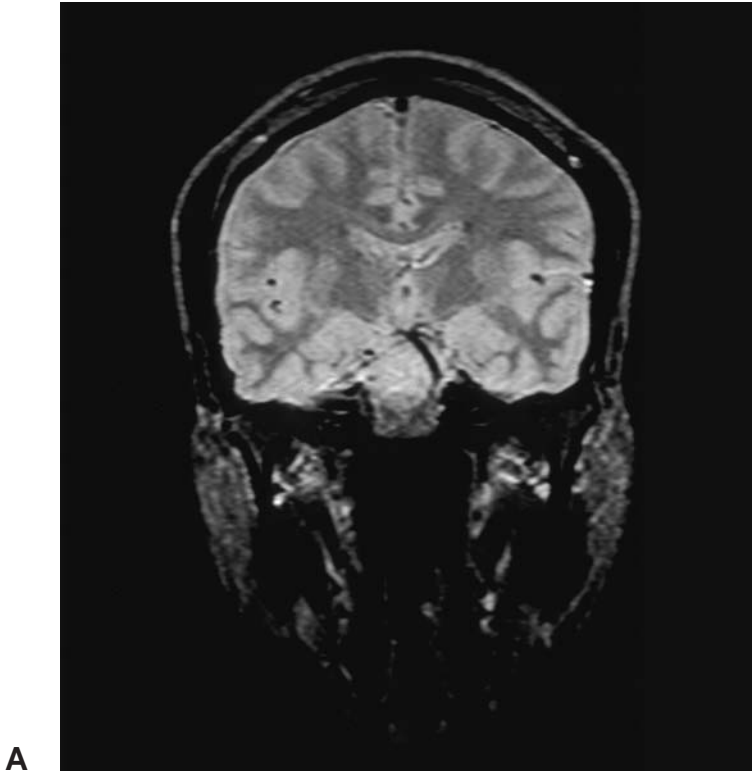
Although slightly smaller than in previous images, the pons appears as a hyperdense region just below the cerebral hemispheres. The midbrain connects the pons with the cerebral hemispheres and is found just below the third ventricle. Within the lower part of the cerebral hemispheres, in the region previously occupied by the inferior horn of the lateral ventricle, the gray matter of the hippocampal formation lies deep within the temporal lobe. Above the lateral ventricles, the body of the corpus callosum extends between the right and left cerebral hemispheres. Immediately above the corpus callosum, the lower margin of the falx cerebri forms a dural venous sinus known as the inferior sagittal sinus. On the superior margin of the falx cerebri and directly below the parietal bones, the superior sagittal sinus, which reabsorbs the majority of the cerebrospinal fluid (CSF) into the venous bloodstream, is formed.

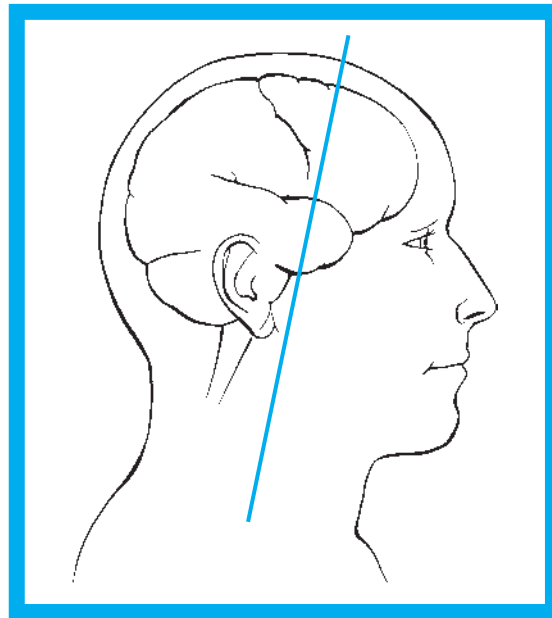




**Figure 5–36 (A,B)** Coronal MR image 11.

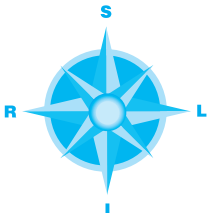
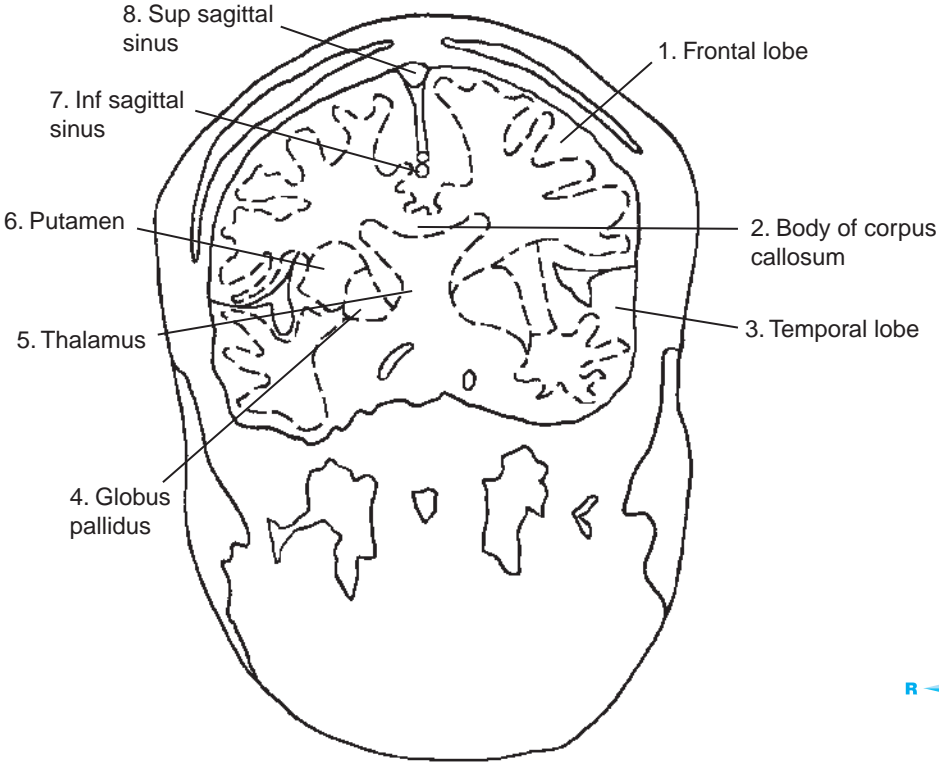
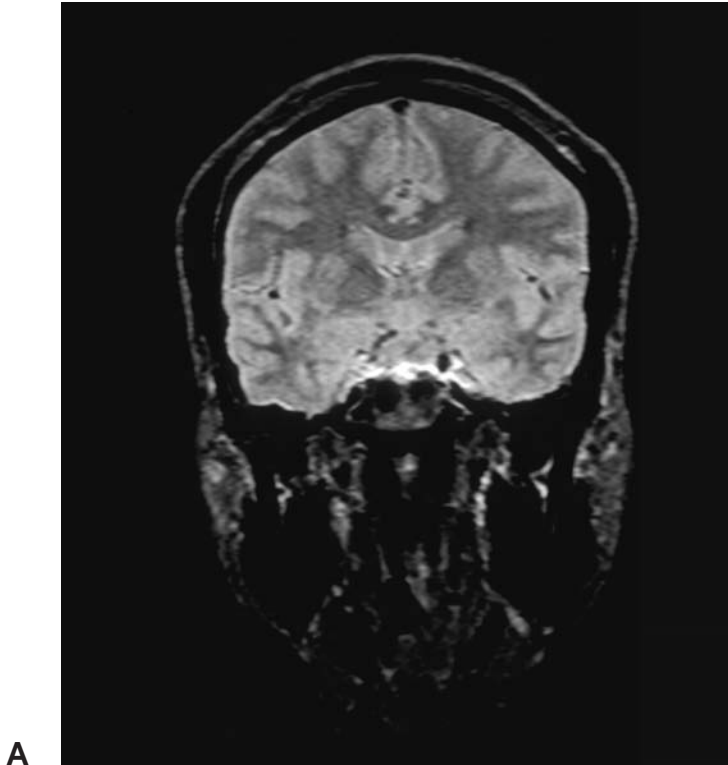
At this level, only the most anterior part of the pons is seen below the cerebral hemispheres. Similar to the previous images, the third ventricle is found medially located between the thalamic nuclei. A band of white matter forms what appears as a capsule surrounding the thalamus. The internal capsule separates the thalamus from the lenticular nuclei, the globus pallidus, and the putamen.

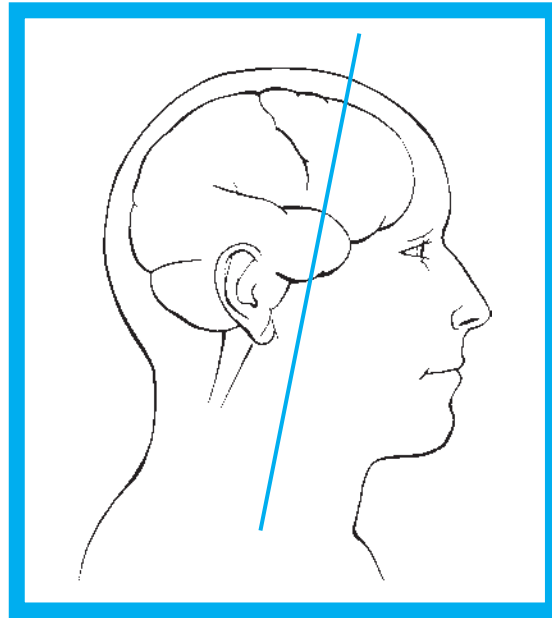




**Figure 5–37 (A,B)** Coronal MR image 12.

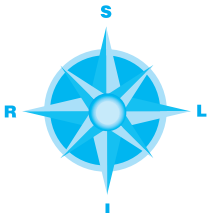
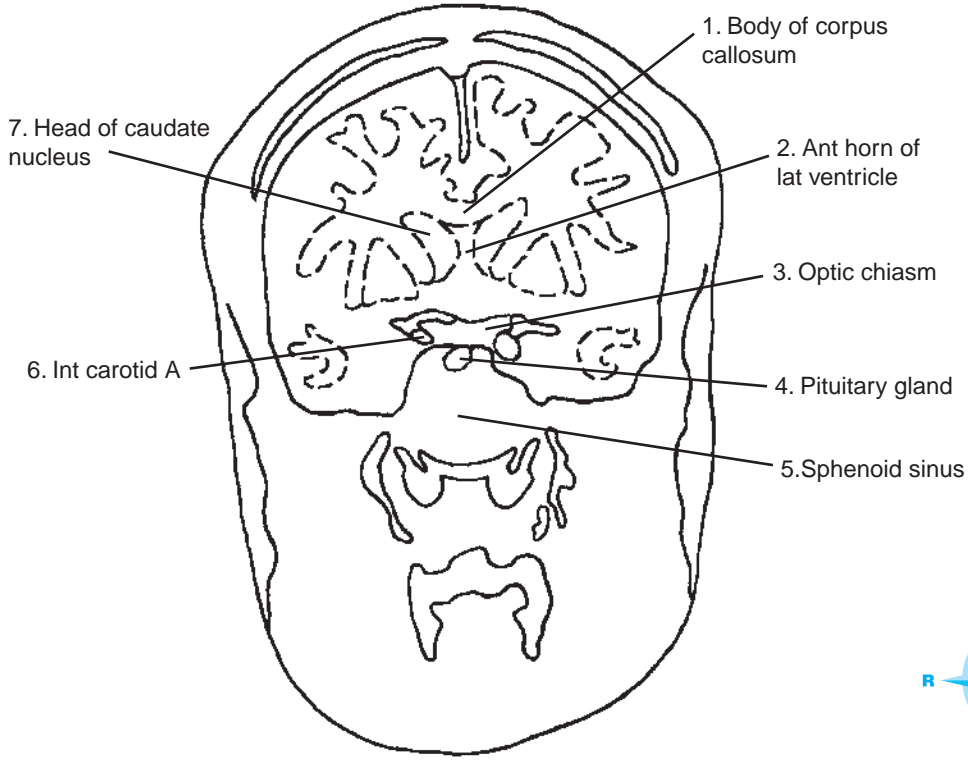
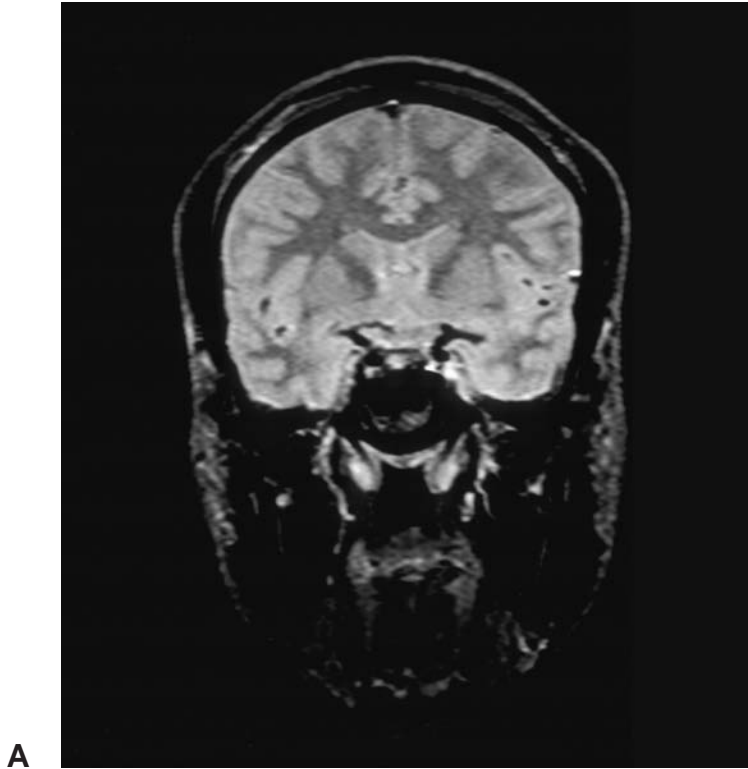
The right and left cerebral hemispheres are separated by the falx cerebri, which contains the superior sagittal sinus and inferior sagittal sinus. Directly below the falx cerebri, the body of the corpus callosum is found joining the right and left cerebral hemispheres. The Sylvian fissure divides each cerebral hemisphere into parietal and temporal lobes. Although not clearly seen here, the third ventricle would again occupy a medial position below the body of the corpus callosum separating the anterior part of the thalamic nuclei. Lateral to the thalamic nuclei, the lenticular nuclei are now separable into the globus pallidus and the putamen.



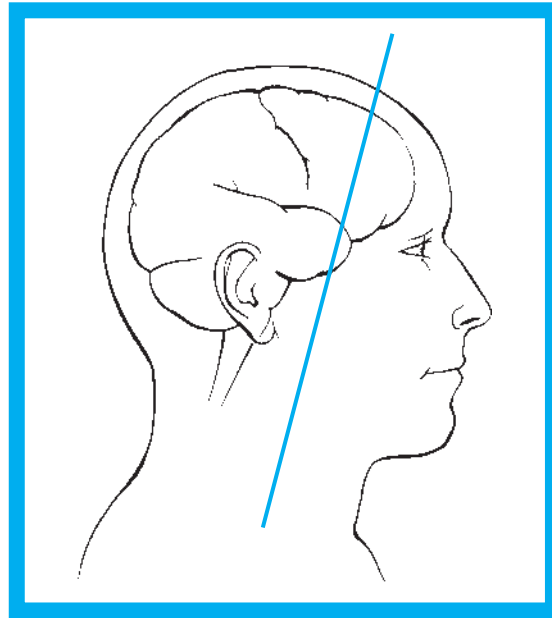


**Figure 5–38 (A,B)** Coronal MR image 13.

Directly below the cerebral hemispheres in the region previously occupied by the pons, an enlarged region of the skull can be seen representing the sphenoid sinus. Just above the sphenoid sinus in the region of the sella turcica, the oval-shaped pituitary gland can be identified below the cerebrum. Directly above the pituitary gland, the nerve fibers within the optic chiasma are sectioned as they extend from the cerebral hemispheres toward the globes of the eyes. On either side of the optic chiasma, the internal carotid arteries are sectioned as they ascend to bifurcate into the anterior and middle cerebral arteries. Although the lumina are not readily apparent, the anterior horns of the lateral ventricles are found directly below the body of the corpus callosum. Within the anterior horns of the lateral ventricles, the heads of the caudate nuclei are shown protruding into the opening on either side.

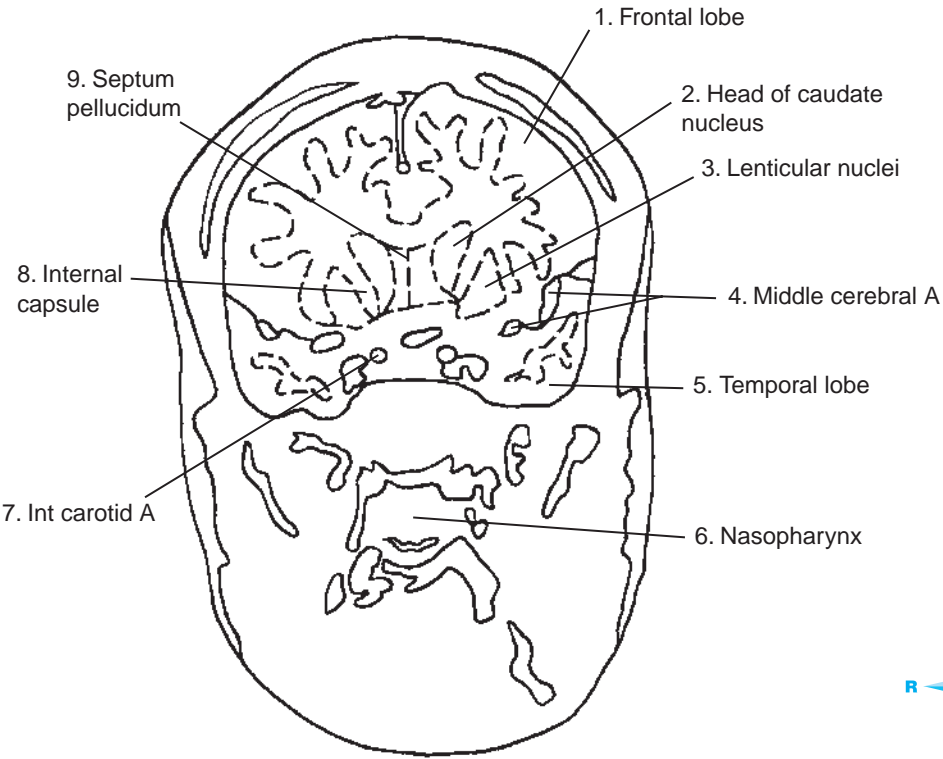
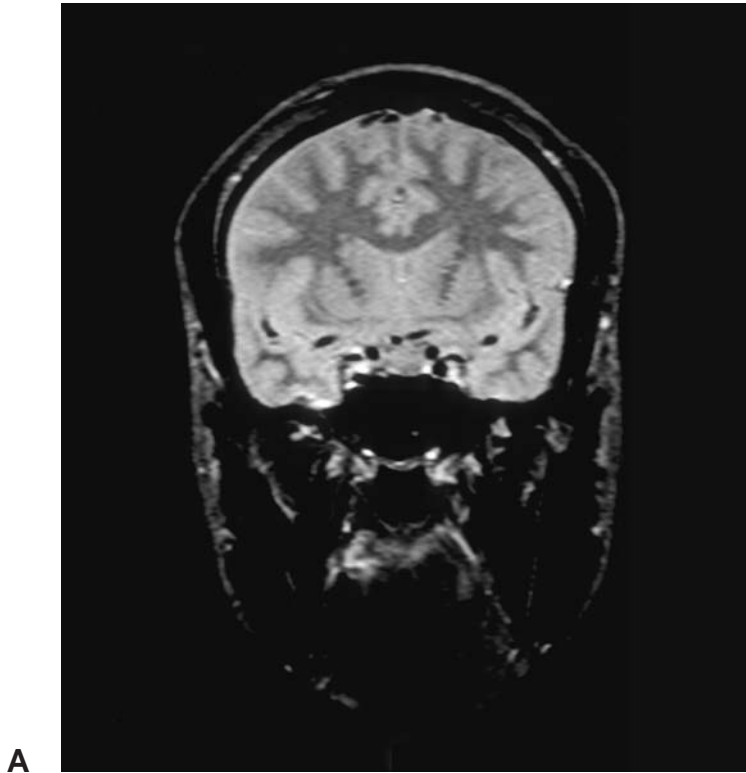


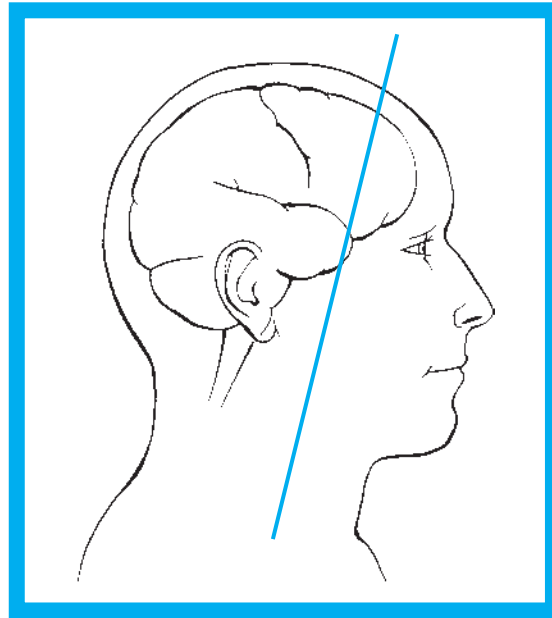




**Figure 5–39 (A,B)** Coronal MR image 14.

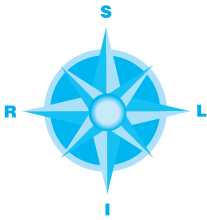
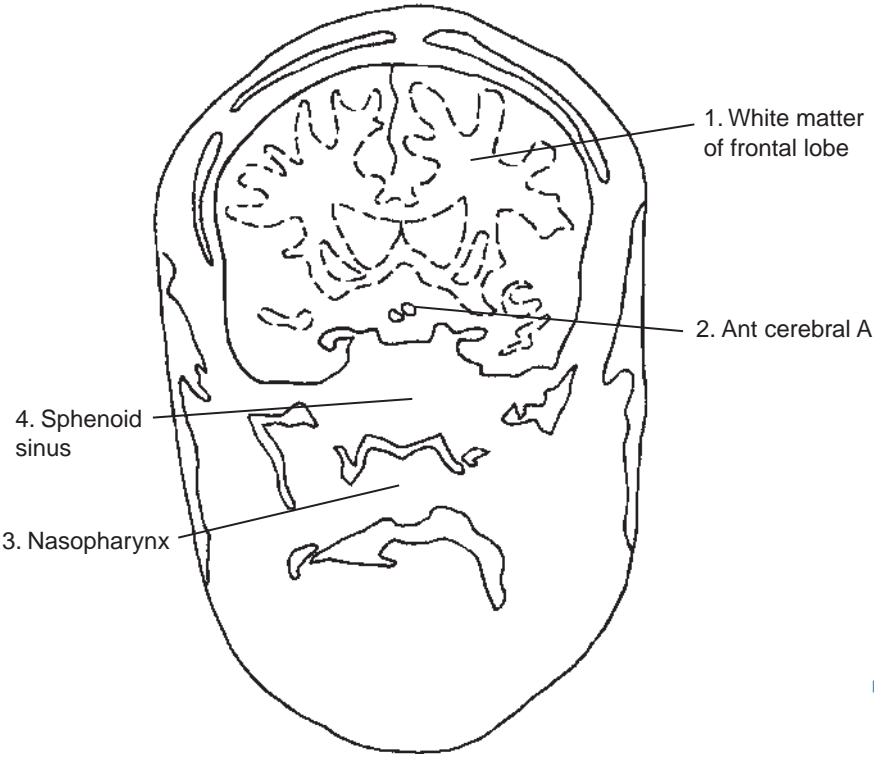
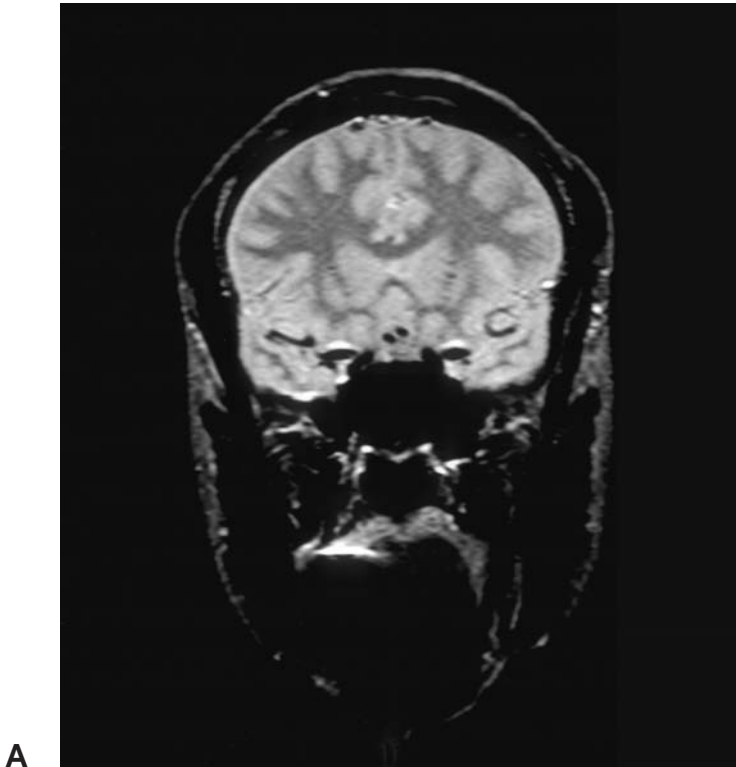
Sectioned through the anterior cerebrum, the frontal lobe is separated from the anterior part of the temporal lobe by the Sylvian fissure, which contains branches of the middle cerebral artery. As described earlier, the middle cerebral artery originates from the internal carotid artery just above the sphenoid sinus. Similar to the previous image, the anterior horns of the lateral ventricles are barely visible between the septum pellucidum and the heads of the caudate nuclei. The internal capsule is the band of white matter separating the gray matter of the caudate nucleus from that of the lenticular nuclei. On the lower part of the image, a distinct hypodense region can be identified below the sphenoid sinus as the region of the nasopharynx.





**Figure 5–40 (A,B)** Coronal MR image 15.

This image of the anterior head clearly demonstrates the relationship between the nasopharynx and the more superiorly located sphenoid sinus. Directly above the sphenoid sinus, the anterior cerebral arteries are cut in cross-section as they extend from their origin, the internal carotid arteries, to their destination in the anterior cerebrum. Within the cerebral hemispheres, the white matter is formed by a collection of nerve fibers, and the gray matter of the cerebral cortex is formed by a collection of nerve cell bodies.



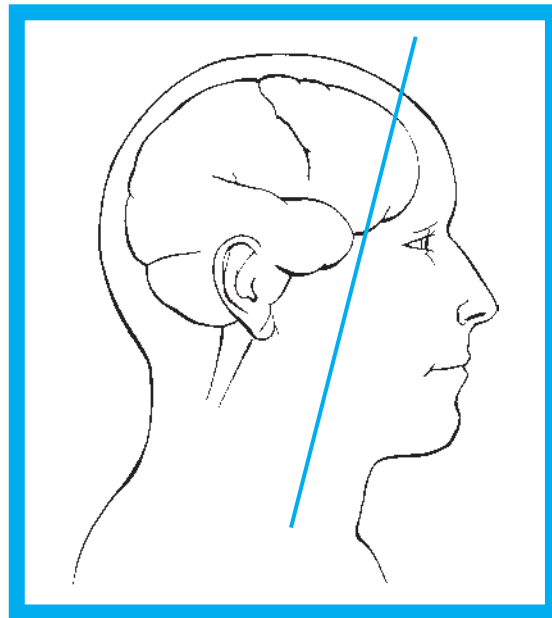
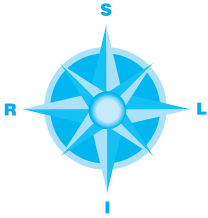
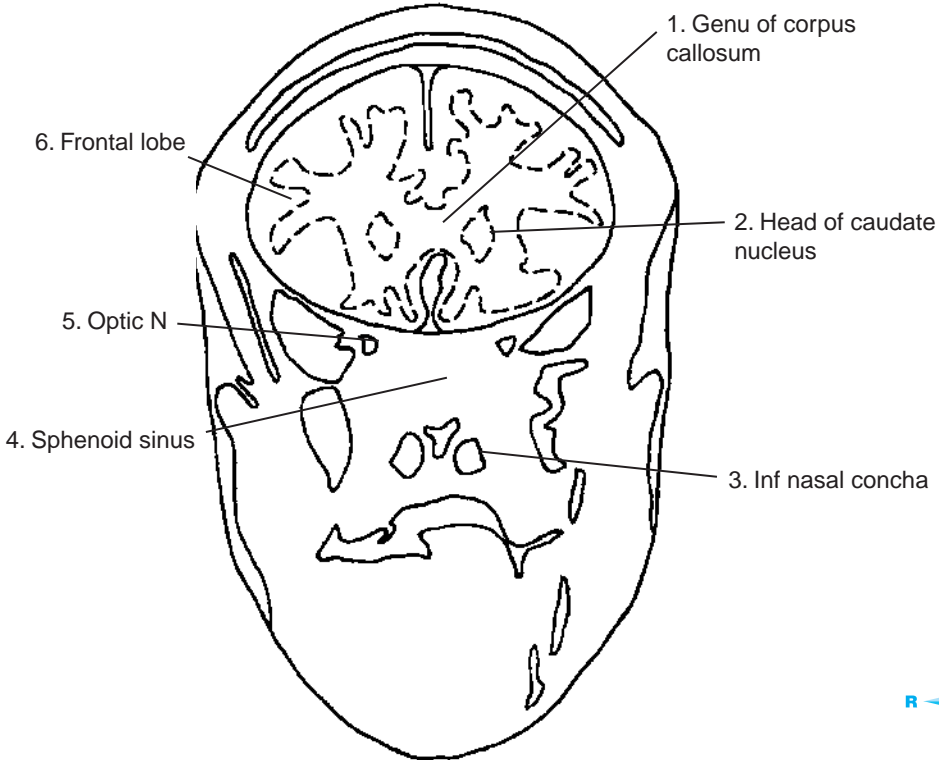
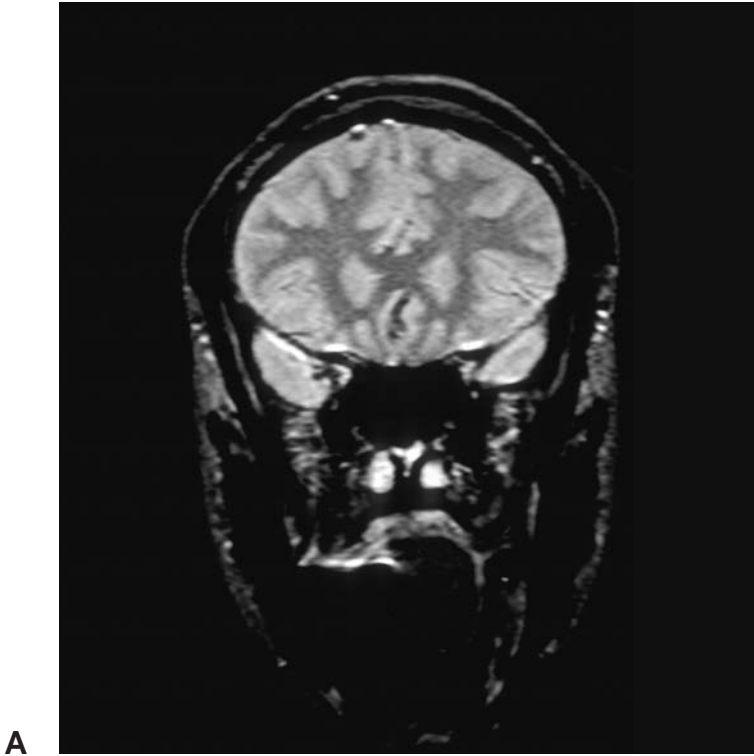


**Figure 5–41 (A,B)** Coronal MR image 16.

This image shows the anterior-most section through the cerebral hemispheres. The right and left frontal lobes are connected through the commissural fibers forming the genu of the corpus callosum located between the hemispheres. In the region previously occupied by the anterior horn of the lateral ventricle, the head of the caudate nucleus appears as an island of gray matter surrounded by white matter. Below the cerebrum, the right and left optic nerves are found in cross-section as they extend toward the globe of the eye. In the midline, the hypodense region of the sphenoid sinus is labeled between the optic nerves. Below the sphenoid sinus, in the location previously occupied by the nasopharynx, the inferior nasal conchae are sectioned on either side within the nasal cavity.

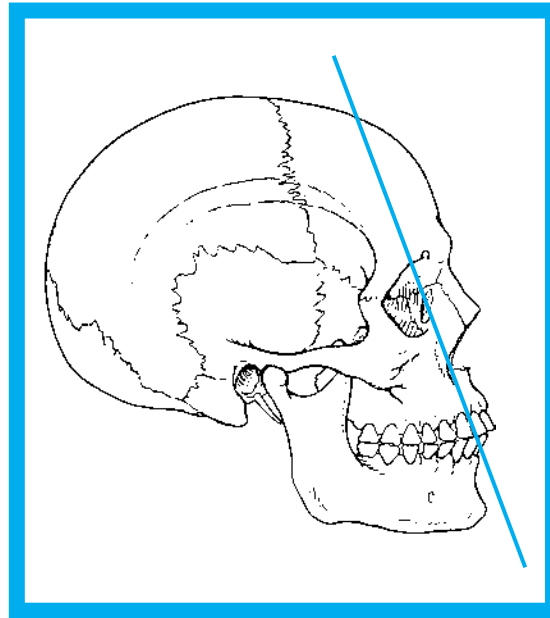




## Coronal CT Images

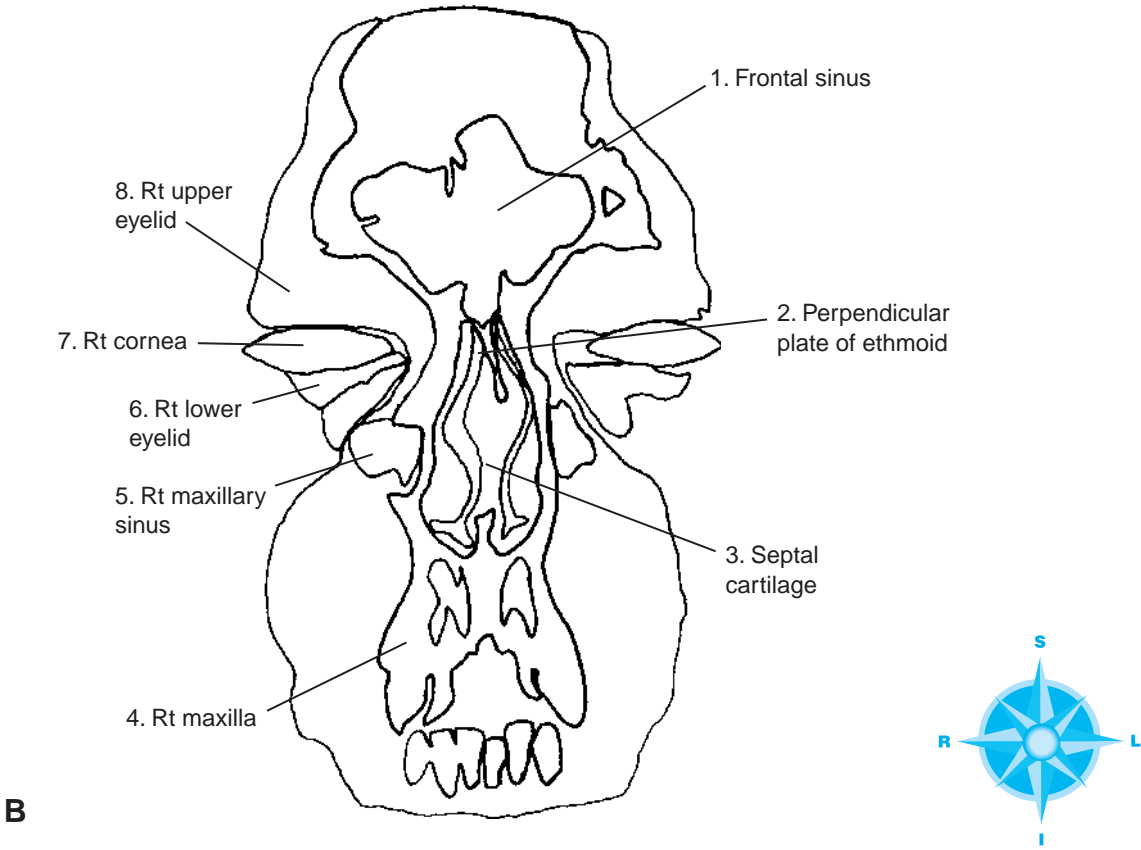
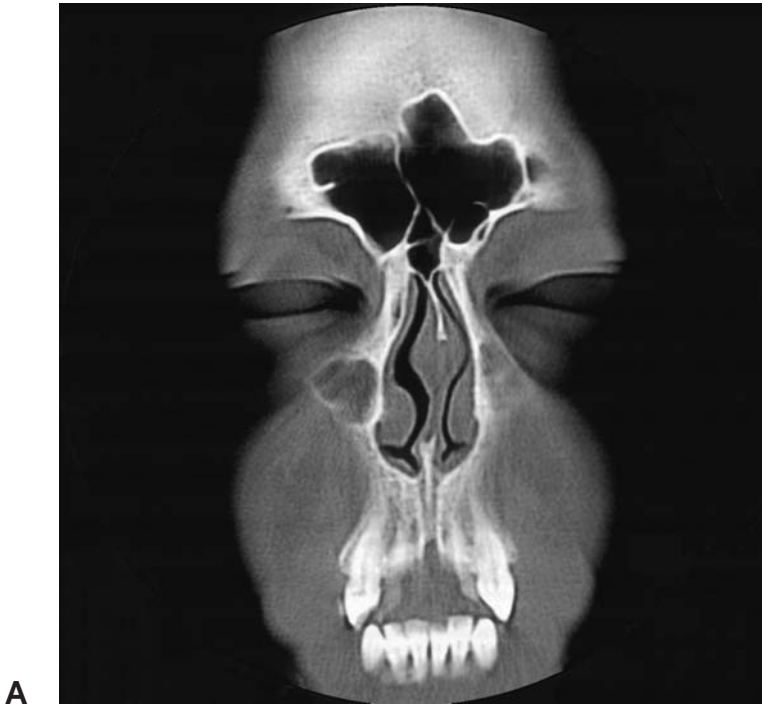
The following five images of the face are described at 4.0-mm intervals from anterior to posterior. The images were gener-

ated at the following technical factors: 120 kilovolt peak (kVp) and 180 milliamperes-second (mA-s).

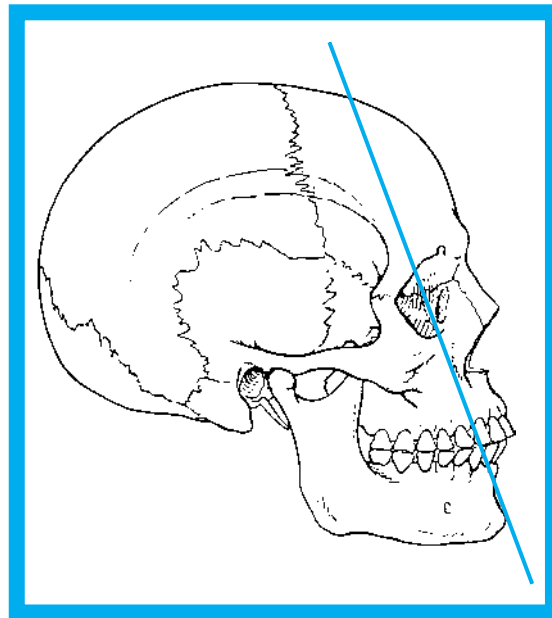


**Figure 5–42 (A,B)** Coronal CT image 1.

The frontal sinus is readily identified encased within the frontal bone (**top**), and is found above the nasal cavity. Within the nasal cavity, the perpendicular plate of the ethmoid bone and septal cartilage divide the area into right and left parts. Below the nasal cavity, the maxillary bones extend to the upper teeth bordering the anterior oral cavity. On the right side, the anteriormost part of the right maxillary sinus is found between the nasal cavity and the region of the right eye. Because this plane of section runs through the anteriormost part of the eye, the right cornea is shown between the upper and lower eyelids.

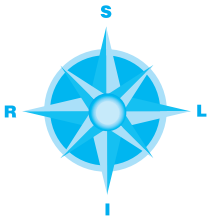
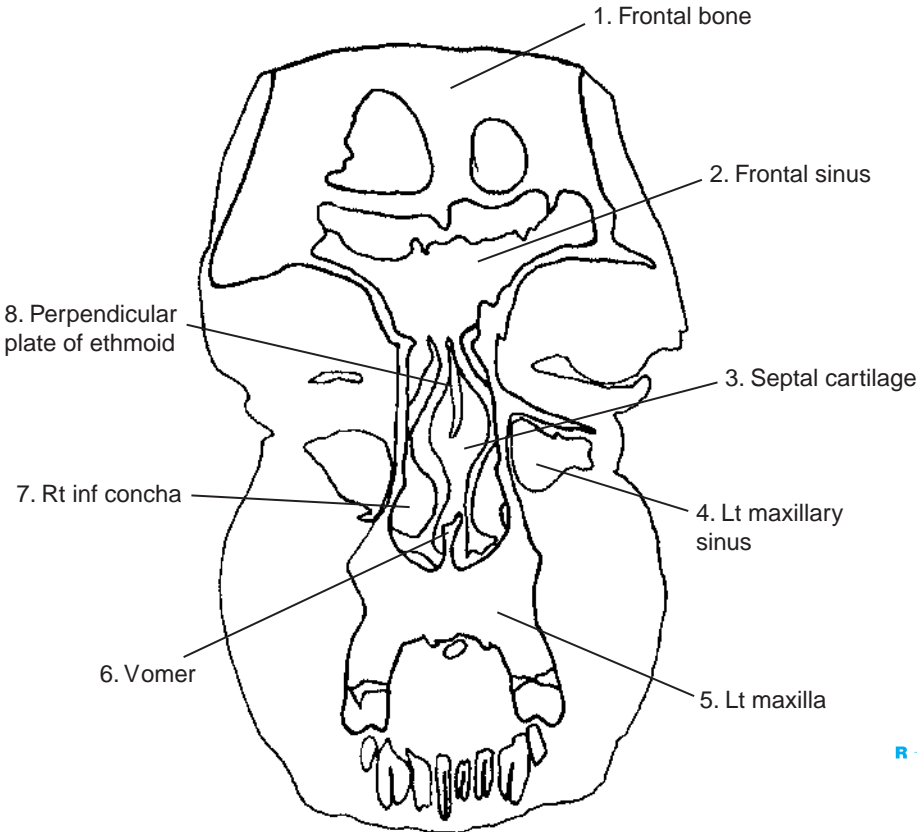
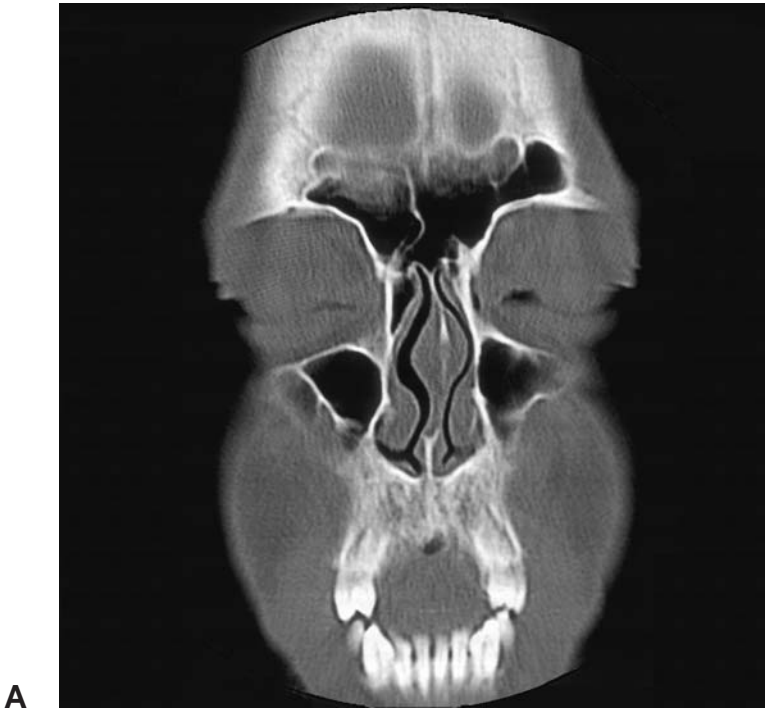


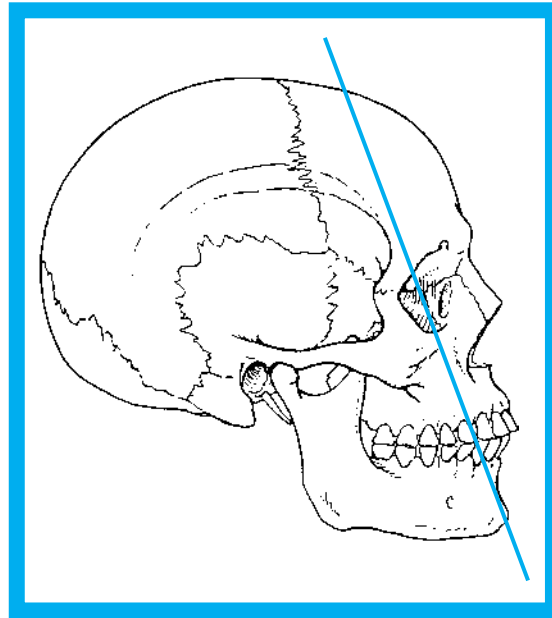




**Figure 5–43 (A,B)** Coronal CT image 2.

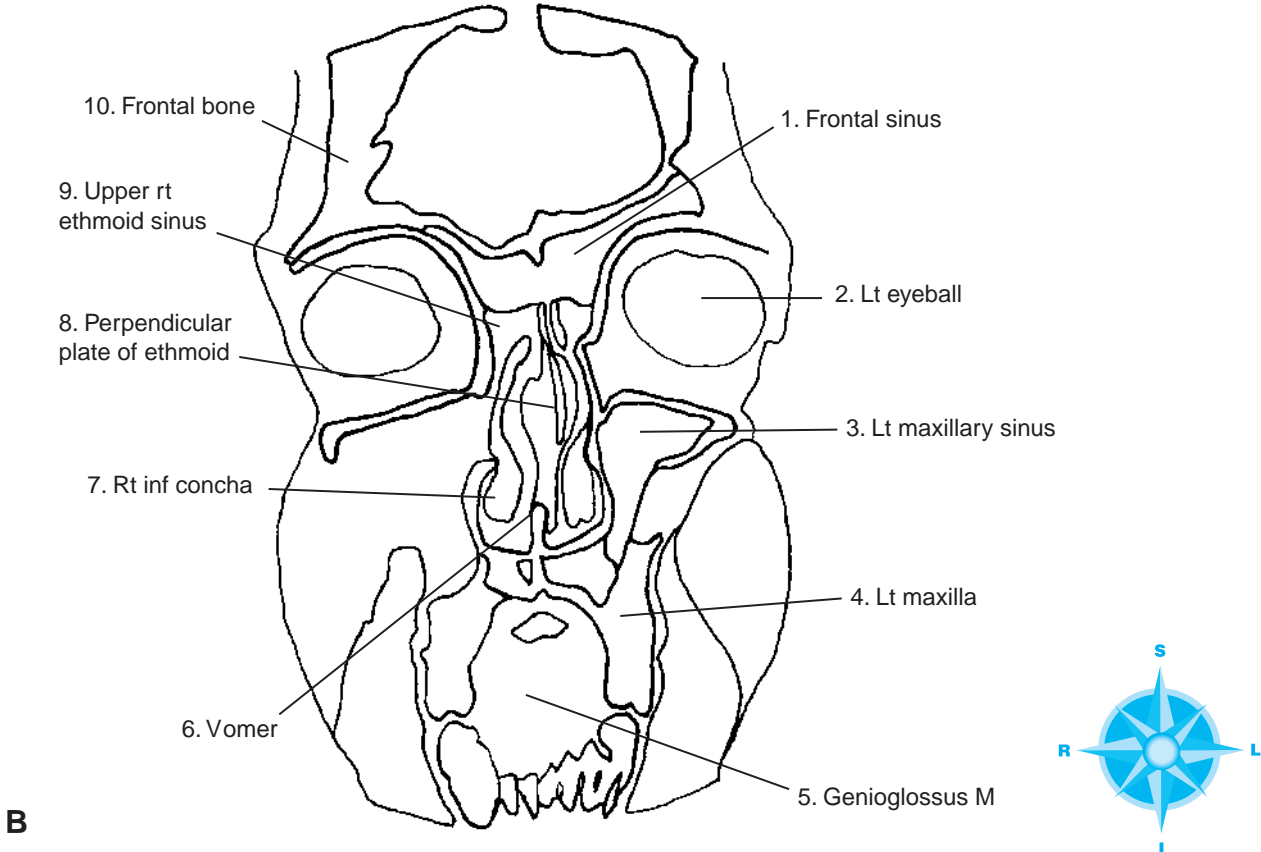
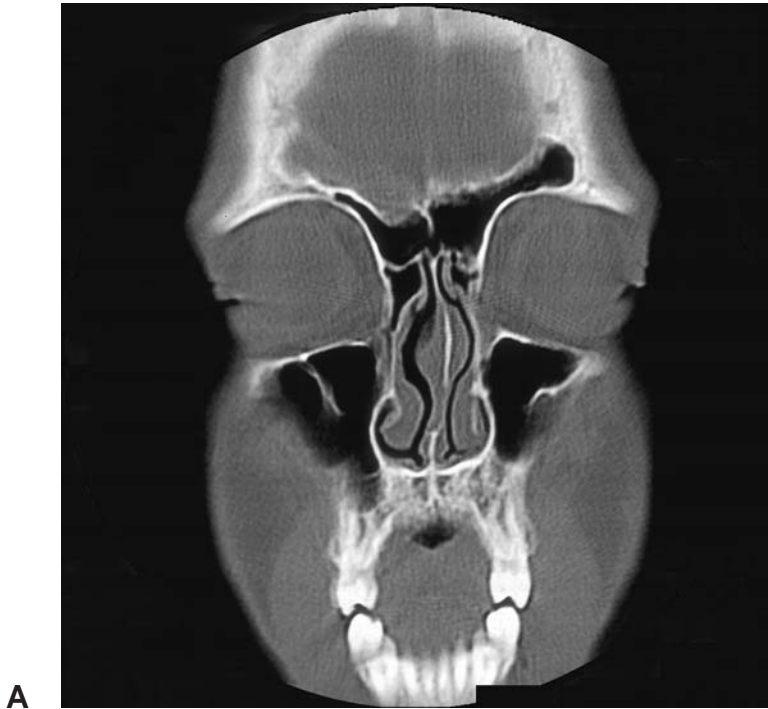
The frontal bone is again shown to contain the frontal sinus, which is located above the contents of the nasal cavity. Within the nasal cavity, the nasal septum is formed by two bony projections on either end that are separated by septal cartilage. As described earlier and shown in Figure 5-3, the perpendicular plate of the ethmoid bone forms the upper part of the nasal septum, whereas the vomer forms the lower part. On either side of the nasal septum, the inferior conchae are found adjacent to the wall of the maxillary sinus. Below the nasal cavity, the maxillary bones are shown projecting downward to the teeth on either side, and form the roof of the oral cavity.

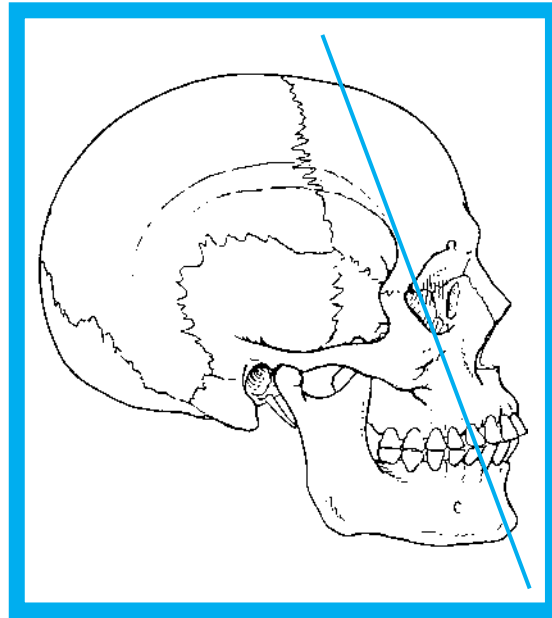




**Figure 5–44 (A,B)** Coronal CT image 3.

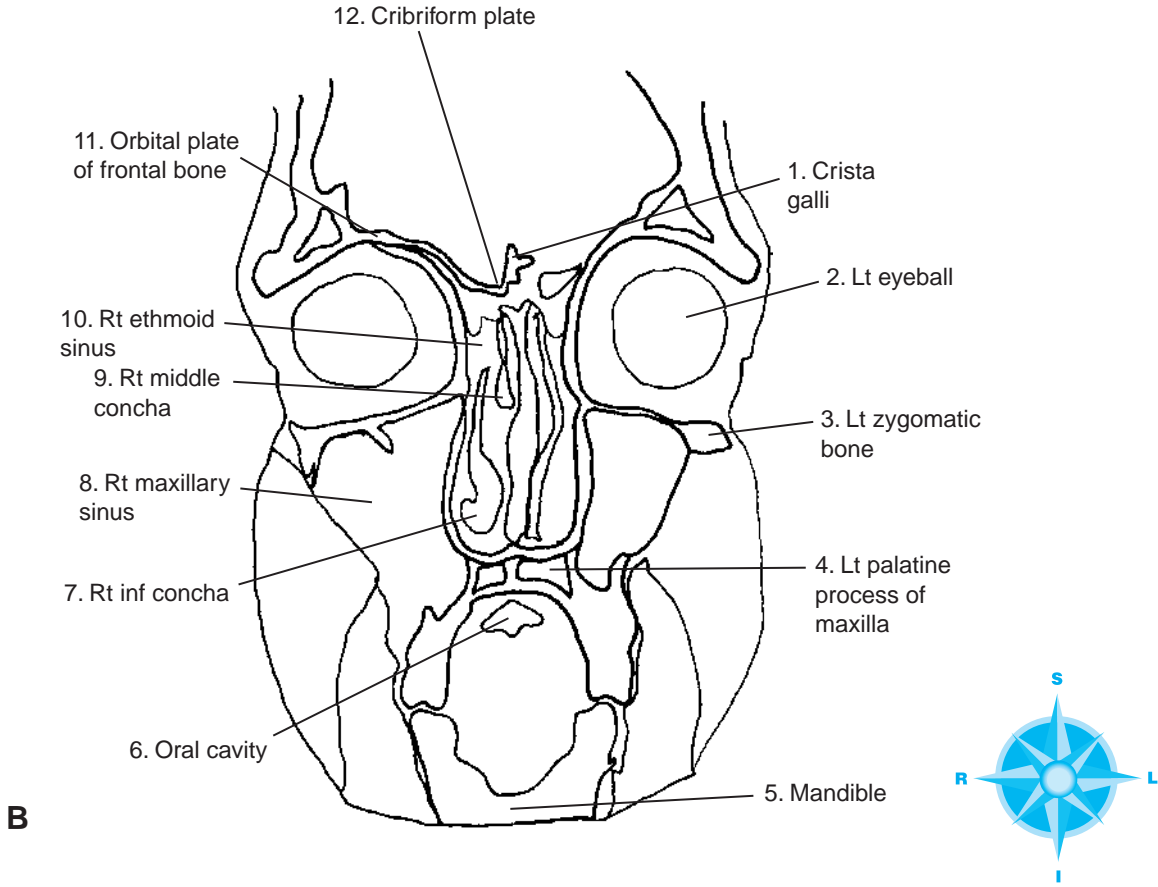
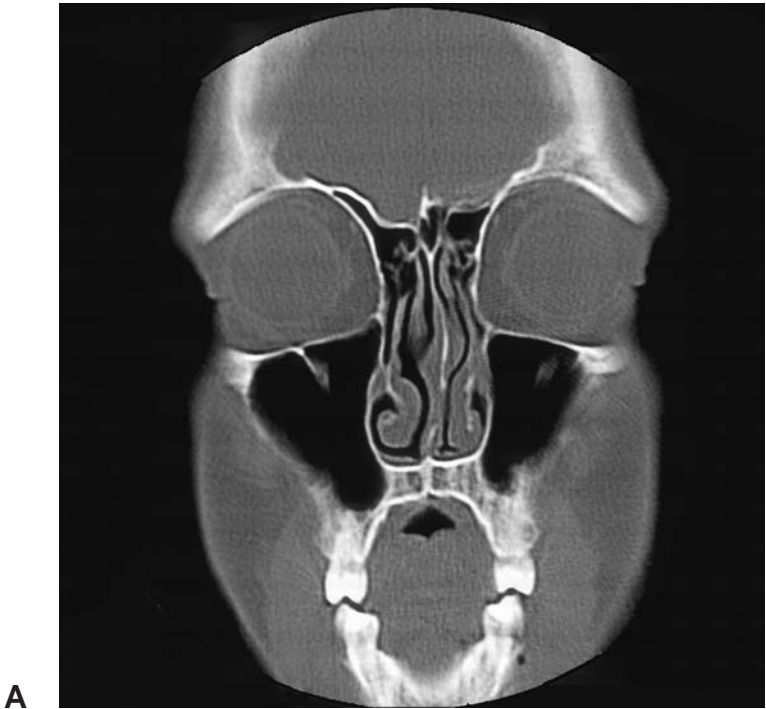
Similar to the previous images, the frontal sinus is shown encased by the frontal bone, but it appears smaller in this image. Although the frontal sinus is still located above the nasal cavity, several air cells found directly between the eyes separate the frontal sinus from the lower nasal cavity. Similar to the previous image, the septum dividing the nasal cavity is formed by the perpendicular plate of the ethmoid, septal cartilage, and vomer. Although one would expect this nasal septum to divide the nasal cavity into equal and symmetrical parts, the deviation of the septum to the left side seen in this patient is not an uncommon finding. On either side of the nasal septum, the inferior conchae span from superior to inferior through most of the nasal cavity. On either side of the nasal cavity, the maxillary sinuses are shown within the maxillary bones and are larger than in previous images. The maxillary bones extend downward on either side, forming the roof of the oral cavity, which is filled with the musculature of the upper tongue, the genioglossus muscle.





**Figure 5–45 (A,B)** Coronal CT image 4.

At this level through the anterior face, the orbital plate of the frontal bone is shown forming the upper margin of the bony orbit. Between the right and left orbital cavities, several specific structures can now be identified within the ethmoid bone. Near the midline, a small projection of bone can be seen extending upward, representing the crista galli, which is surrounded on either side by the cribriform plate. As described earlier, perforations in the cribriform plate transmit the first pair of cranial nerves, the olfactory nerves, from the mucous membranes lining the nasal cavity. Below the cribriform plate, the air cells forming the ethmoid sinus are again shown between the orbits. In this more posterior plane, the inferior and middle conchae are shown in either side of the nasal cavity. By comparison, the middle conchae are shorter and more superior than the inferior conchae. On either side of the nasal cavity, air is found within the large, triangle-shaped maxillary sinuses. On the lateral side of the face, the zygomatic bones are now shown, in section, forming the lower lateral boundary of the bony orbit. Below the nasal cavity, the palatine process of the maxilla is shown forming the roof of the oral cavity. Below the oral cavity, the tongue, or genioglossus muscle, is again shown and is bounded inferiorly by the mandible.



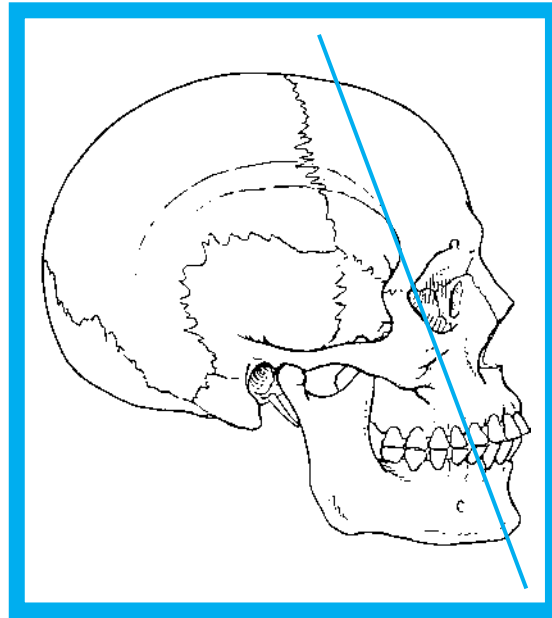
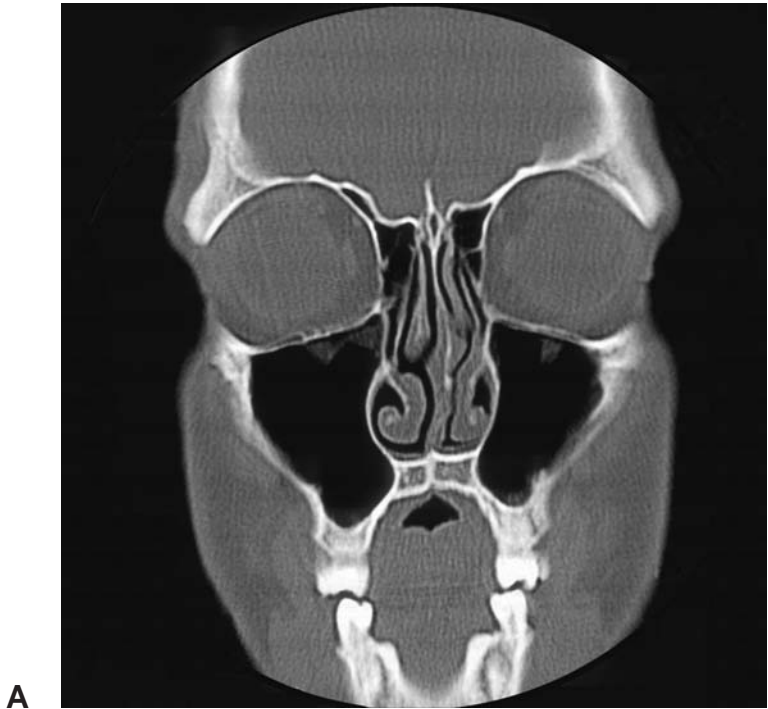
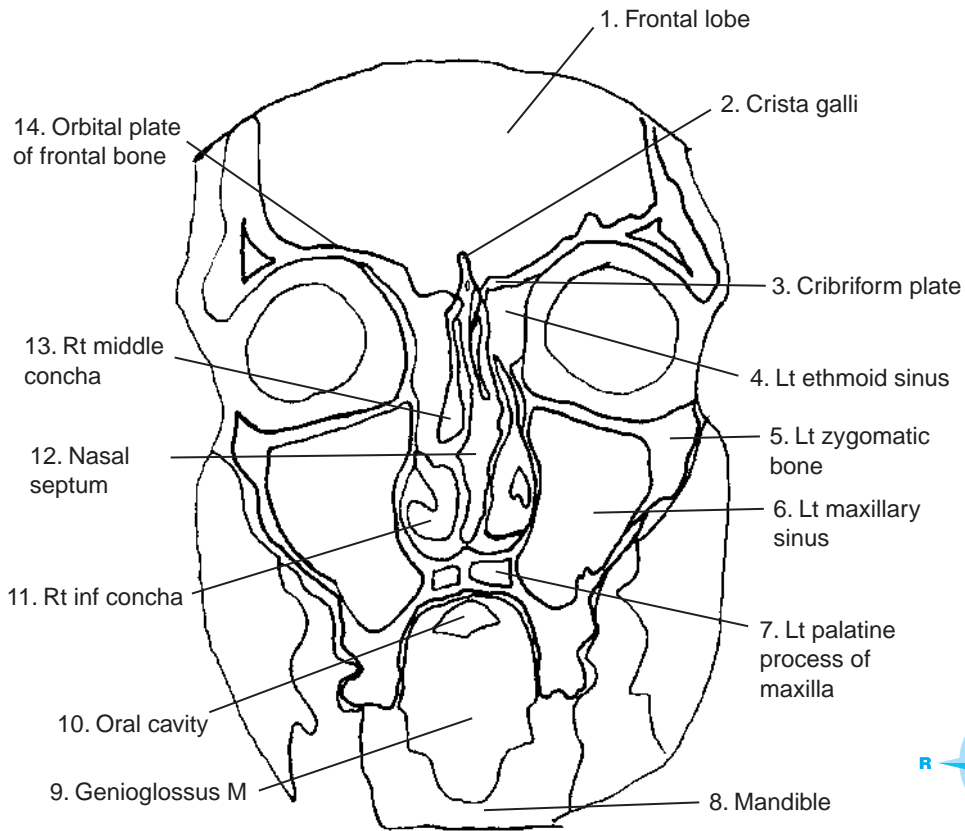


**Figure 5–46 (A,B)** Coronal CT image 5.

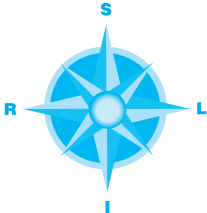
The orbital plate of the frontal bone separates the contents of the orbital cavity from the frontal lobe of the cerebrum. Near the midline, the bony extension of the ethmoid bone projecting upward into the cranial cavity can again be labeled the crista galli, which is bounded on either side by the cribriform plate. Also within the ethmoid bone, the air cells forming the ethmoid sinuses are shown sectioned between the orbits; the middle and inferior conchae are shown on either side of the nasal septum. Similar to the previous image, the large triangle-shaped maxillary sinuses can be seen on either side of the nasal cavity. On the lateral aspect of the maxillary sinuses, the zygomatic bones form the lower outer margin of the bony orbits. Forming the lower margin of the maxillary sinuses, the palatine processes of the maxillae form the roof of the oral cavity, which is labeled above the musculature of the tongue (the genioglossus muscle) and the mandible.



A



B







## Axial CT Images

The following 16 axial CT images of the head are described at 8.0-mm intervals from the base to the top of the skull. The sections were taken in a plane 15°–20° caudal to the line extending from the infraorbital ridge to the external auditory

meatus and the middle of the occipital bone. The images were generated immediately after the administration of venous contrast at the following technical factors: 120 kilovolt peak (kVp) and 250 milliamperere-second (mA-s).

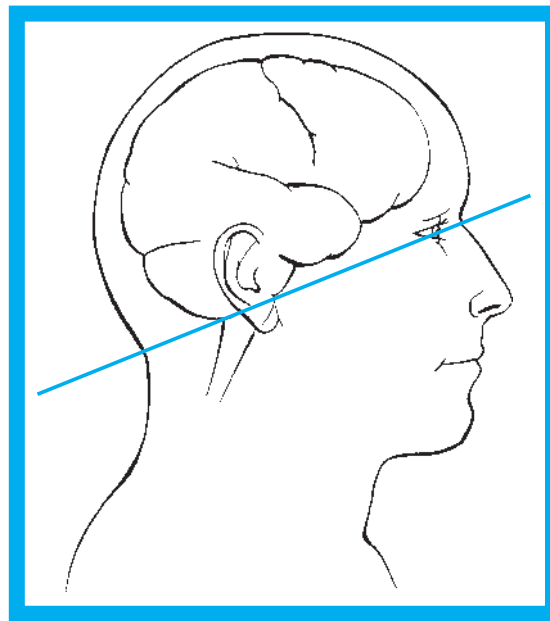
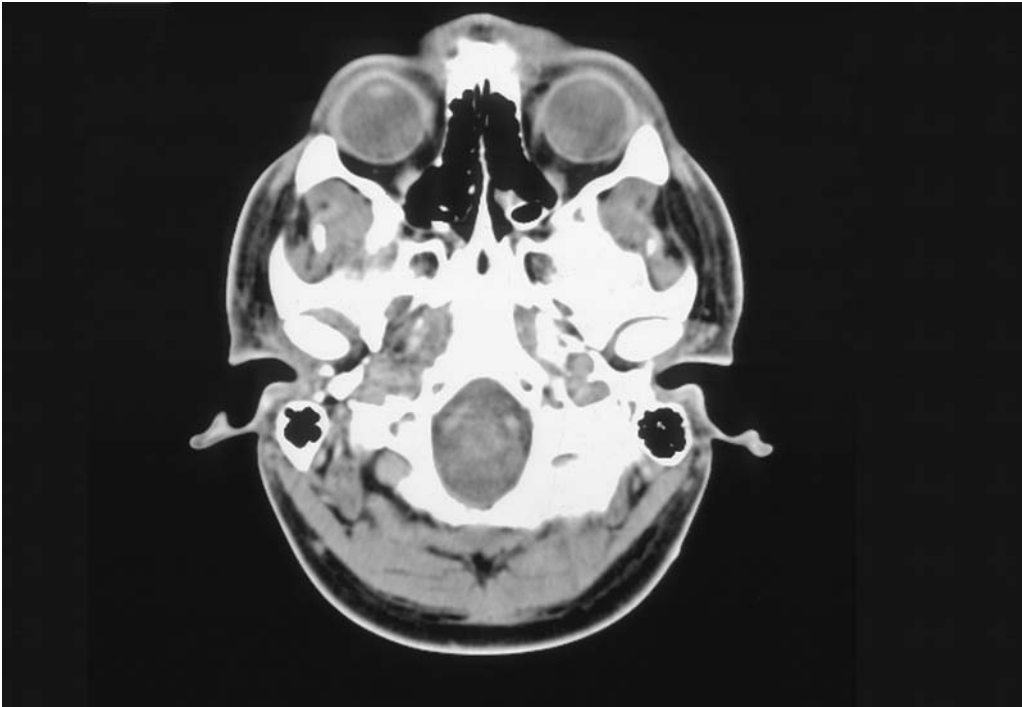
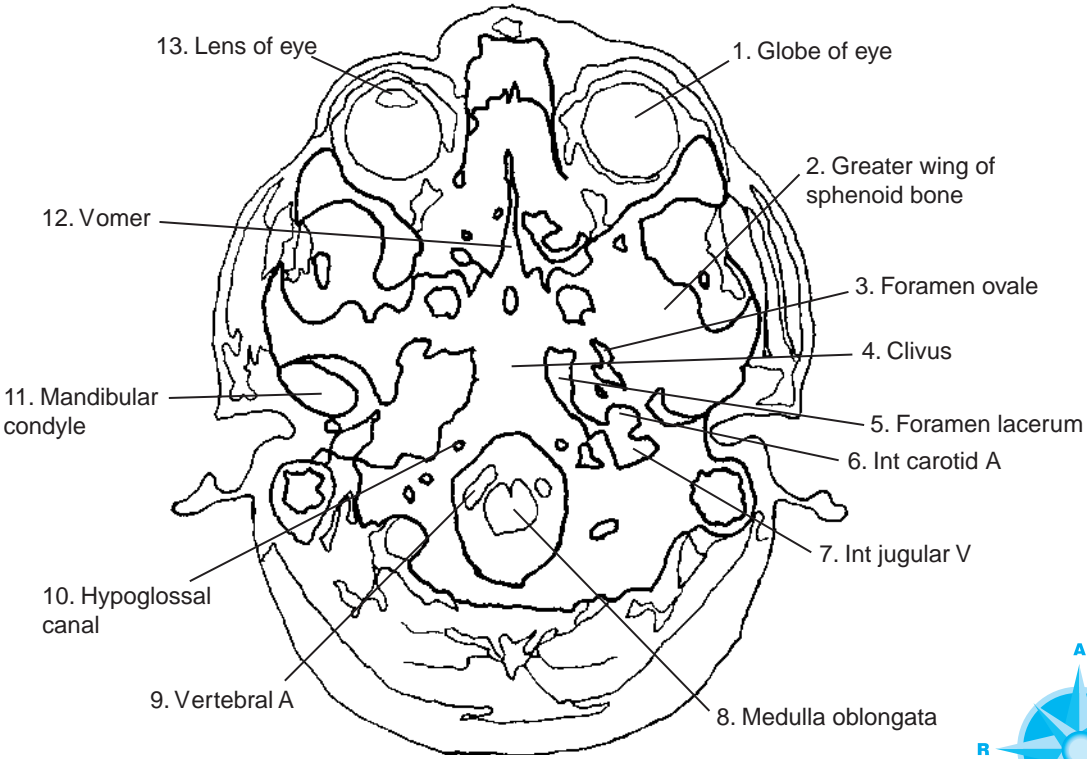


**Figure 5–47 (A,B)** Axial CT image 1.

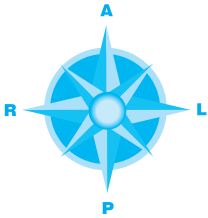
Demonstrating the anatomy at the base of the skull, this image would be the first in a series of scans through the region of the head. Most noticeably, the eyes are shown on either side and the lens is apparent on the patient's right side. Between the eyes, the nasal cavity is found, including the medially located vomer bone, which acts to separate much of the right and left nasal cavity. Forming the posterior wall of the bony orbital cavity, the greater wing of the sphenoid is demonstrated. On the left side, the foramen ovale is shown which transmits the mandibular branch of the trigeminal nerve. The clivus, formed by the body of the sphenoid bone and the basilar part of the occipital bone, is shown centrally located within the base of the skull. On either side of the clivus, the foramina lacerum are shown at the juncture of the occipital, temporal, and sphenoid bones. Within the petrous portion of the temporal bone, the openings of the internal carotid artery and internal jugular vein can also be seen on the left side of the patient. Lateral to the foramina, the mandibular condyle can be identified within the temporomandibular joint. Within the occipital bone, the hypoglossal canal is demonstrated on either side anterolateral to the foramen magnum. Because this section demonstrates the contents within the base of the skull, the major structures found within the foramen magnum are the medulla oblongata and the vertebral arteries. In this patient, the left vertebral artery is difficult to discern, because it does not appear to be enhanced by contrast.



A



B



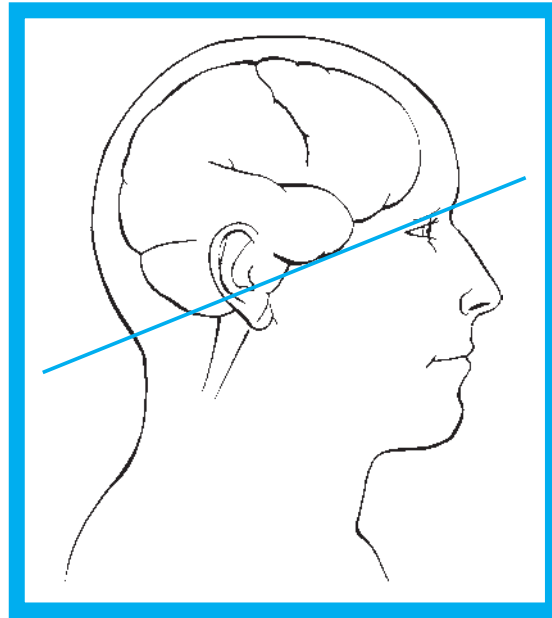
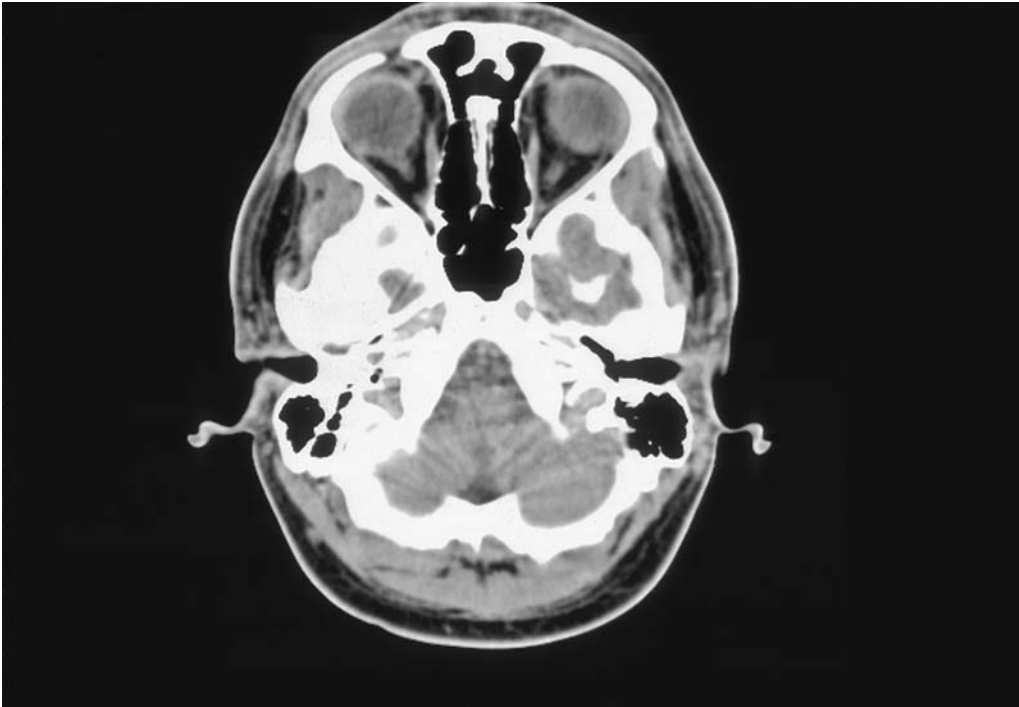
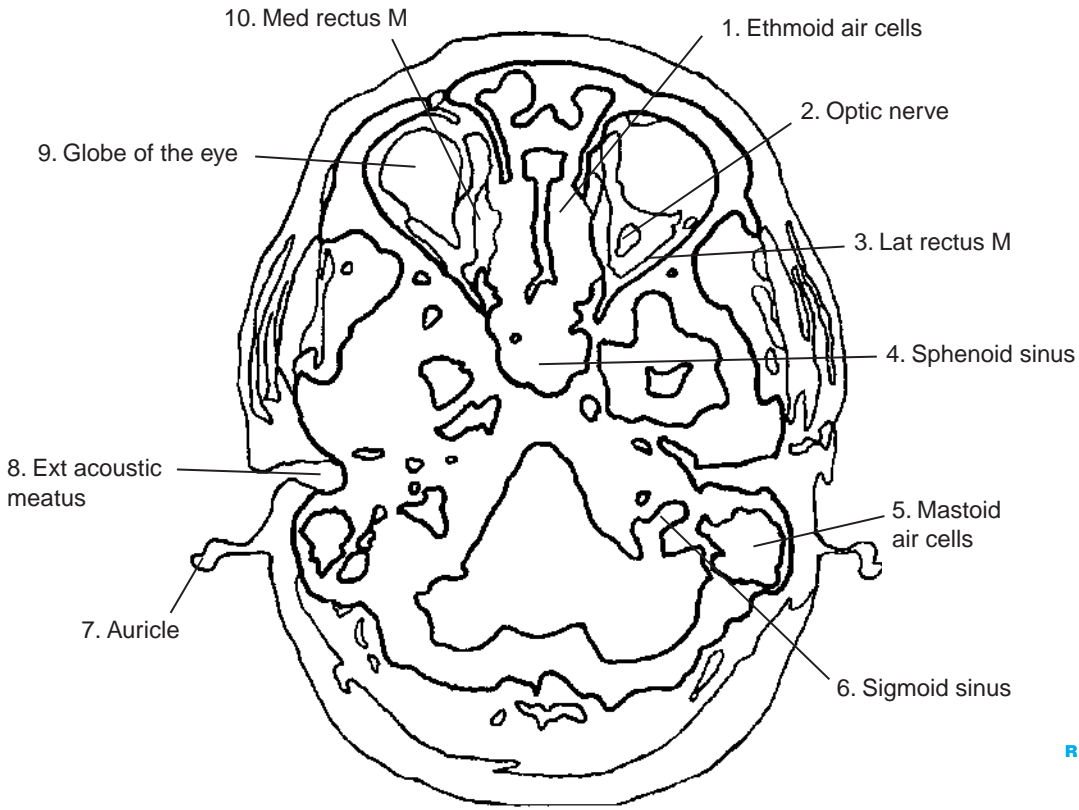


**Figure 5–48 (A,B)** Axial CT image 2.

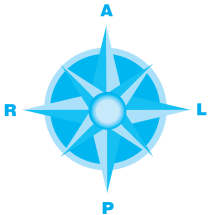
The absence of the foramen magnum and the large petrous part of the temporal bone indicates that the level of this image is just above the base of the skull. Within the petrous part of the temporal bones, the mastoid air cells are hypodense areas just posterior to the external acoustic meatus and deep to the auricle of the ear. Also within the petrous part of the temporal bone, the opening of the sigmoid sinus can be clearly identified on the left side as it extends from the transverse sinus down to the opening on the inferior surface of the skull where it drains into the internal jugular vein. Anterior to the temporal bones, the sphenoid bone is sectioned at the level of the sphenoid sinus directly behind the ethmoid air cells within the nasal cavity. Together, the ethmoid and sphenoid bones make up much of the bony orbital margin, which at this level contains the optic nerve, the medial rectus muscle, and the lateral rectus muscle.



A



B



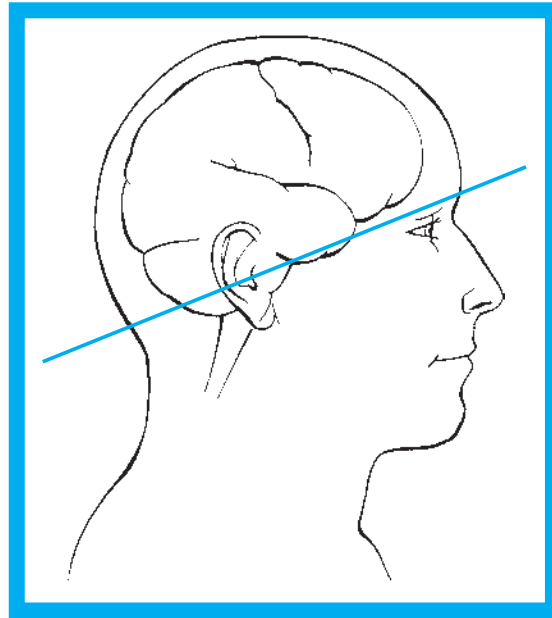
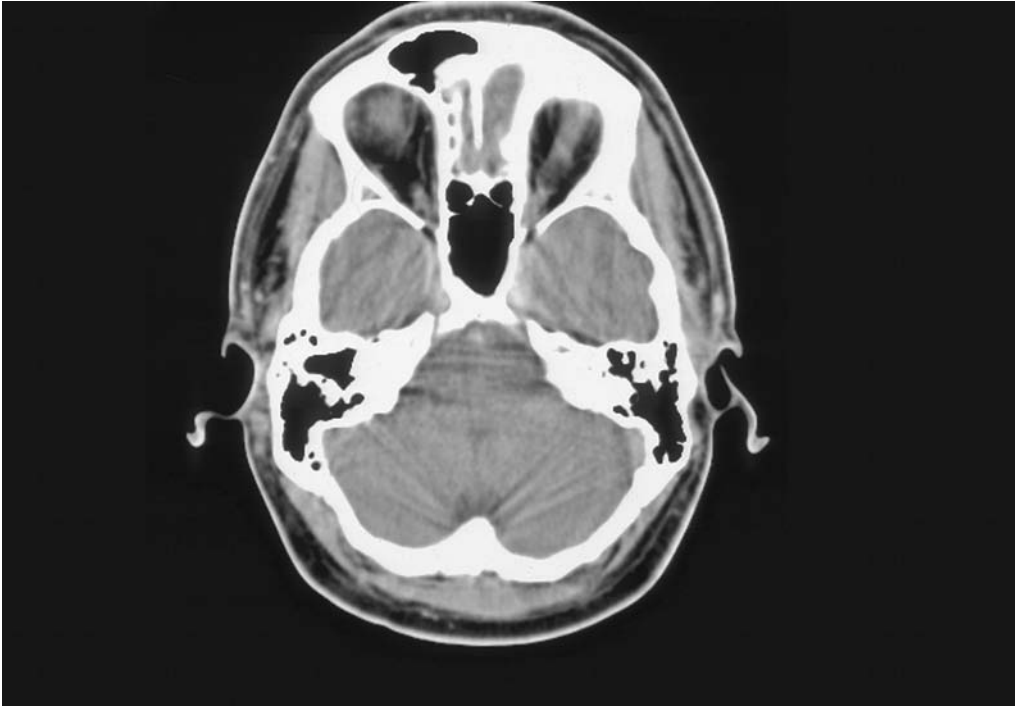
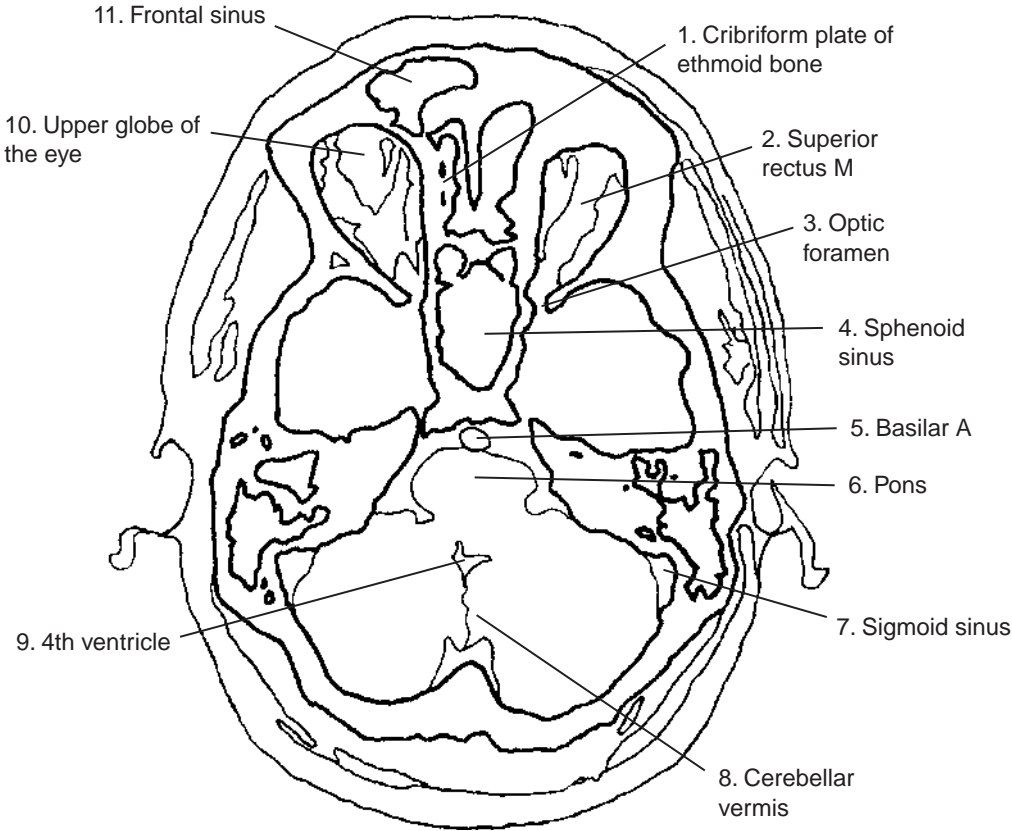


**Figure 5–49 (A,B)** Axial CT image 3.

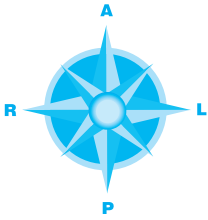
The presence of the frontal and sphenoid sinuses indicate the level of this section to be in a region of the skull near the top of the orbits. Within the nasal cavity, the ethmoid bone is shown on the right side sectioned through the region of the cribriform plate. The foramina within the cribriform plate transmit the olfactory, or the first cranial, nerves from the mucous membranes within the nasal cavity. Within the orbital cavities, the upper part of the globe can be seen on the right side, and the left side is slightly higher, demonstrating the superior rectus muscle. In the posteromedial aspect of the bony orbital margin, the optic foramina are shown on either side between the lesser wings and body of the sphenoid bone. Within the soft tissue structures found within the posterior cranial cavity, a contrast-enhanced vessel, the basilar artery, is found directly posterior to the sphenoid sinus. Although most of the posterior cranial fossa is occupied by the lobes of the cerebellum, much of the region between the petrous parts of the temporal bones is occupied by the pons, which is just anterior to the fourth ventricle. Directly behind the fourth ventricle, the cerebellar vermis is shown to be the constricted region joining the right and left cerebellar hemispheres. On the lateral aspect of the cerebellar hemisphere, the sigmoid sinus is shown sectioned within the petrous part of the temporal bone as it extends downward from the transverse sinus to drain into the internal jugular vein.

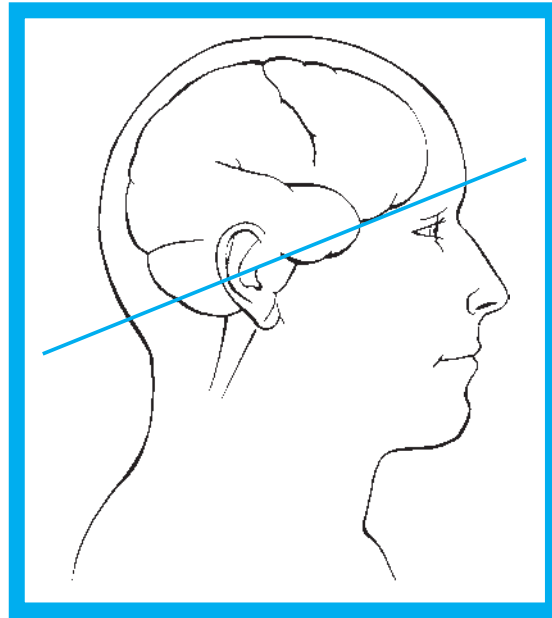


A



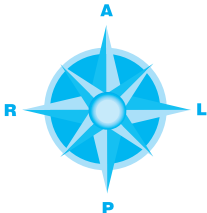
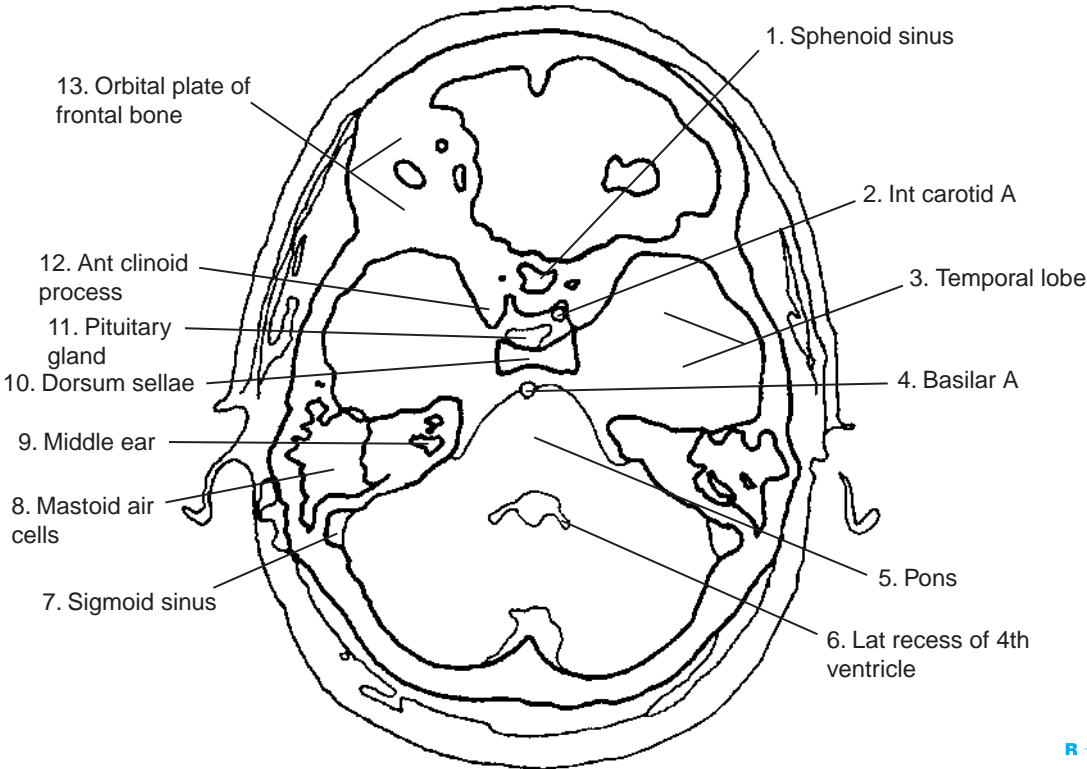
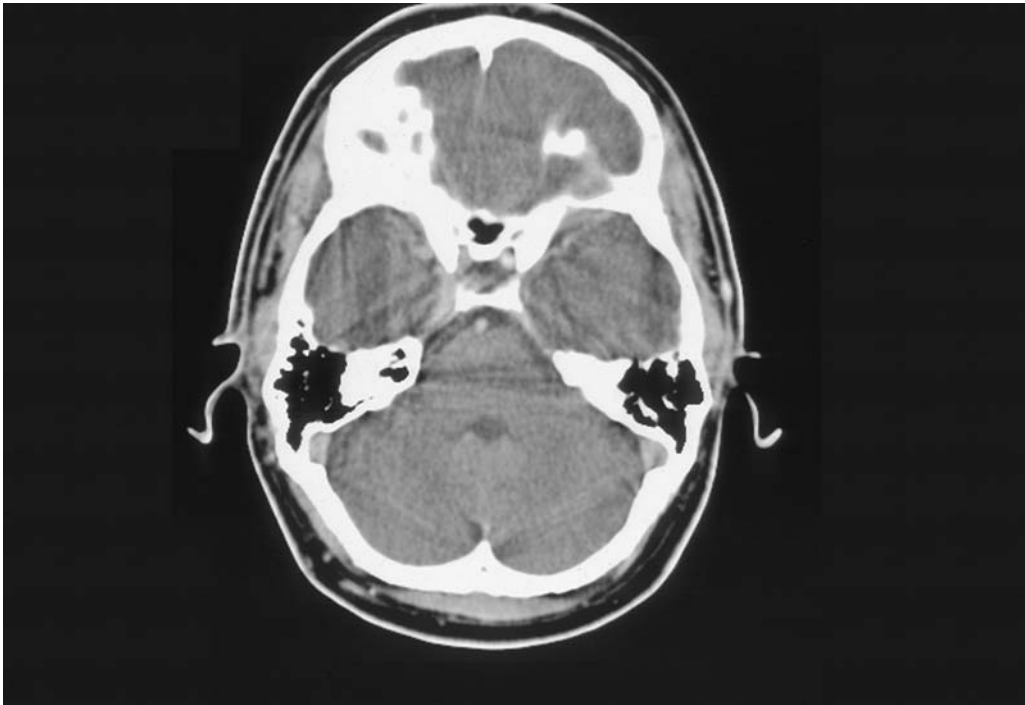
B





**Figure 5–50 (A,B)** Axial CT image 4.

As seen on the right side of this patient, the orbital plate of the frontal bone forms the roof of the bony orbital cavity. Centrally, the anterior clinoid processes are extending toward the dorsum sellae to form the sella turcica. As in the previous images, a small part of the sphenoid sinus can still be seen within the body of the sphenoid bone, and the mastoid air cells can be found within the petrous parts of the temporal bones. Within the sella turcica, the pituitary gland lies behind the internal carotid artery, which is readily identified on the left side owing to contrast enhancement. In this image, the contrast-enhanced vessel is labeled the internal carotid artery, because it has not yet joined the circle of Willis to give rise to the middle cerebral and anterior cerebral arteries. On either side of the sella turcica, the neural tissue in the middle cranial fossa represents the lower parts of the temporal lobes of the cerebrum. Similar to the previous image, the contrast-enhanced basilar artery is shown sectioned directly in front of the region of the pons. At this level, the fourth ventricle is again demonstrated between the pons and the cerebellum; however, this image shows the lateral recesses of the fourth ventricle, which extend laterally to join the subarachnoid space on either side through the foramina of Luschka. Between the cerebellum and the petrous part of the temporal bones, the sigmoid sinuses appear as indentations. On the right side of this patient, the dark area within the petrous part of the temporal bone represents the middle ear cavity.





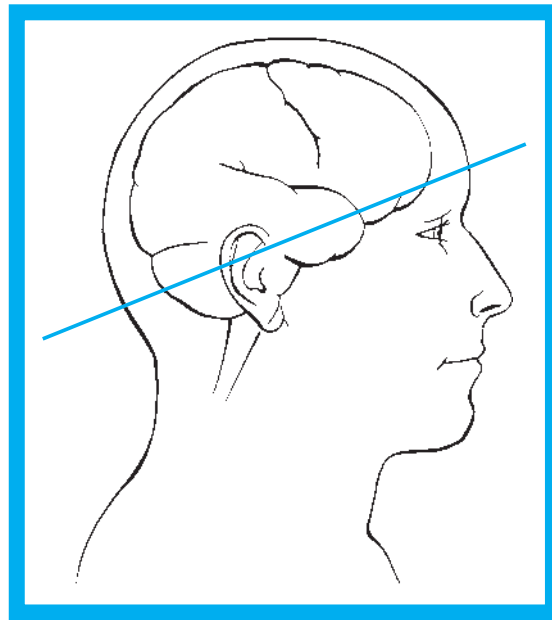
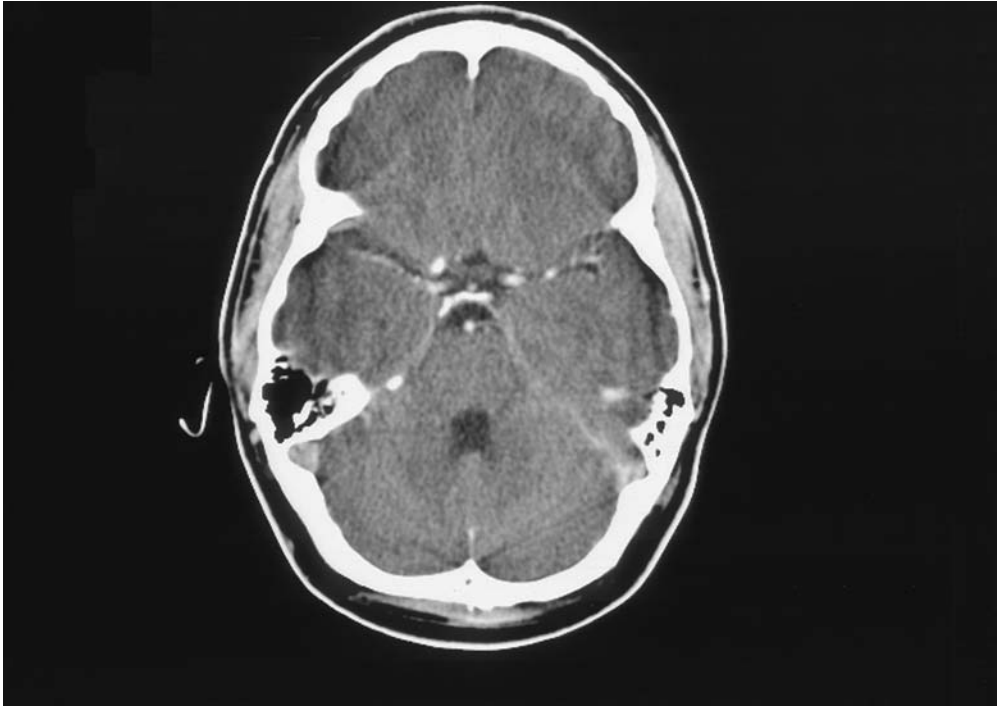
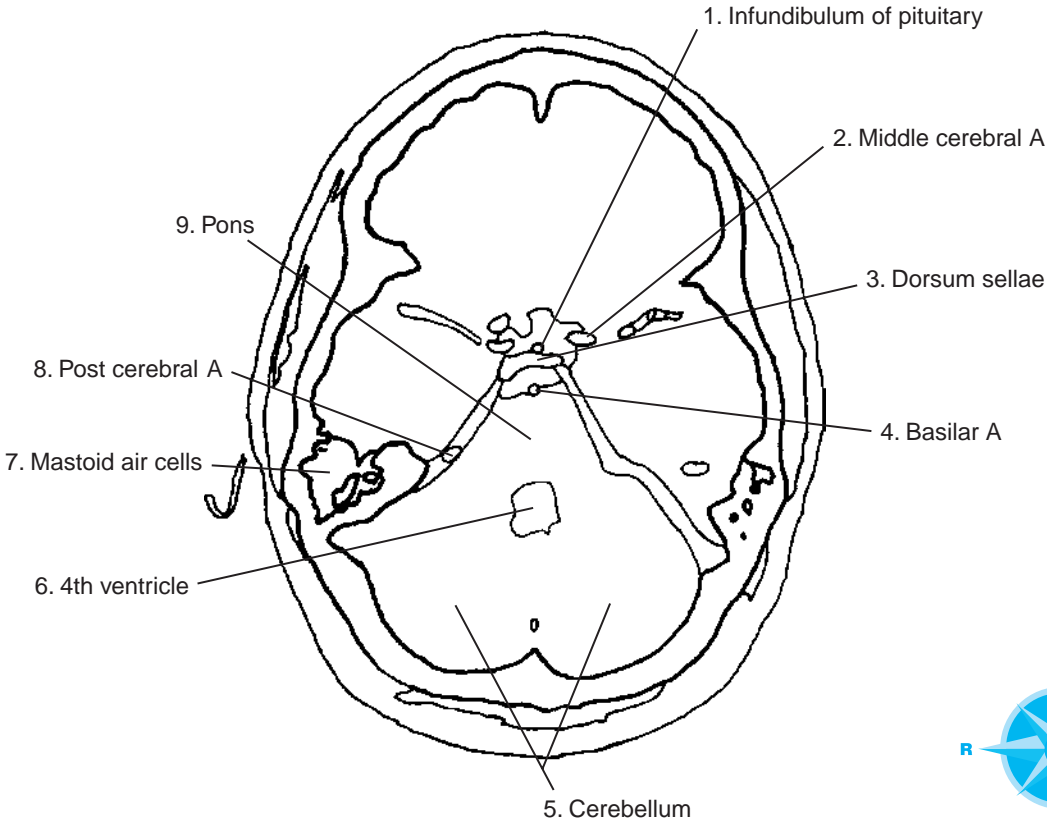


**Figure 5–51 (A,B)** Axial CT image 5.

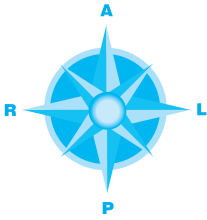
Most of the cranial cavity is occupied by neural tissue, and the only bony parts labeled are the dorsum sellae and the mastoid air cells. Unlike the previous image, in which the pituitary gland was found directly anterior to the dorsum sellae, the stalk or infundibulum of the pituitary gland is now shown in cross-section at a higher level. In the area previously occupied by the internal carotid artery, the middle cerebral artery is now shown obliquely sectioned as it extends laterally through the Sylvian fissure. Directly posterior to the dorsum sellae, the contrast-enhanced basilar artery is shown in cross-section as it lies anterior to the pons. On the right side of the pons, the contrast-enhanced posterior cerebral artery is sectioned as it extends from the circle of Willis located just above the sella turcica to supply blood to the posterior cerebral hemisphere. As in previous images, the fourth ventricle is between the pons and the cerebellum within the posterior cranial fossa.



A



B



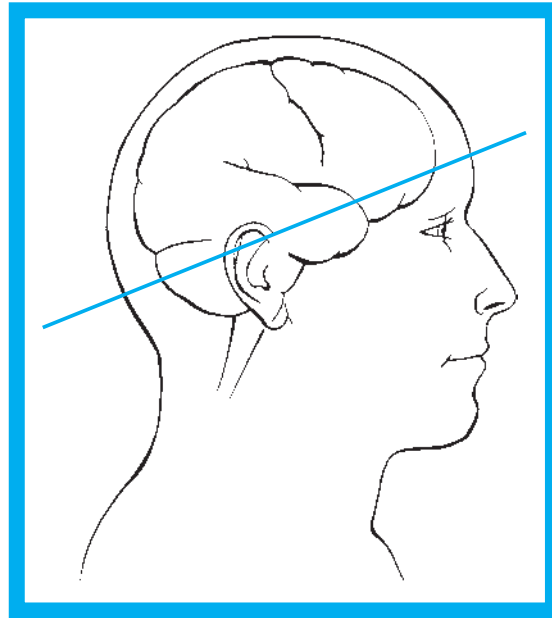
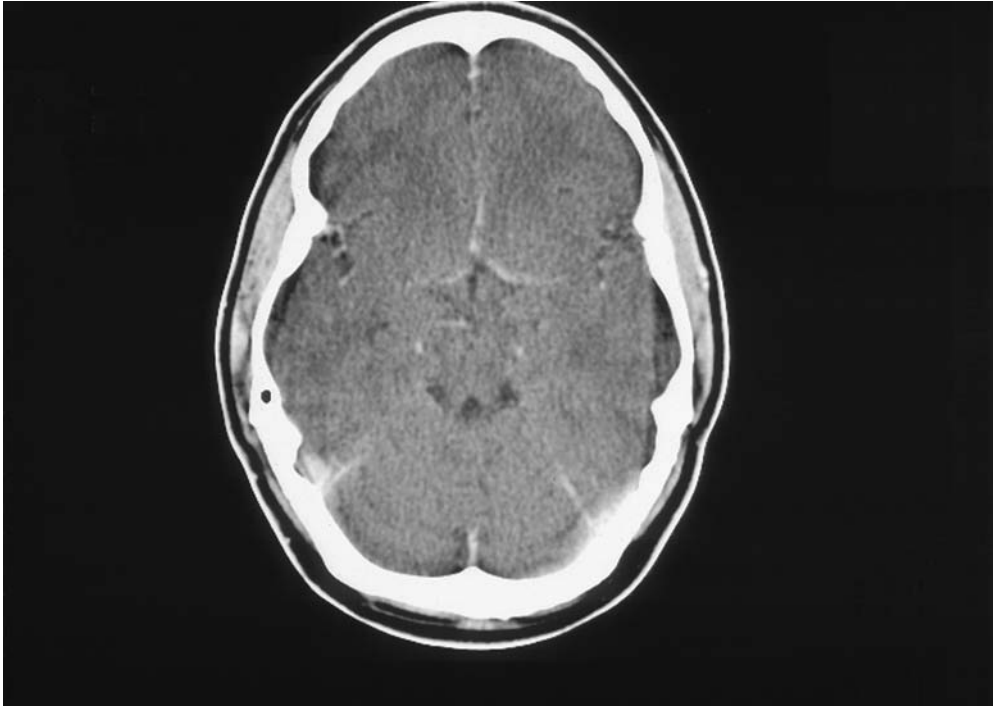
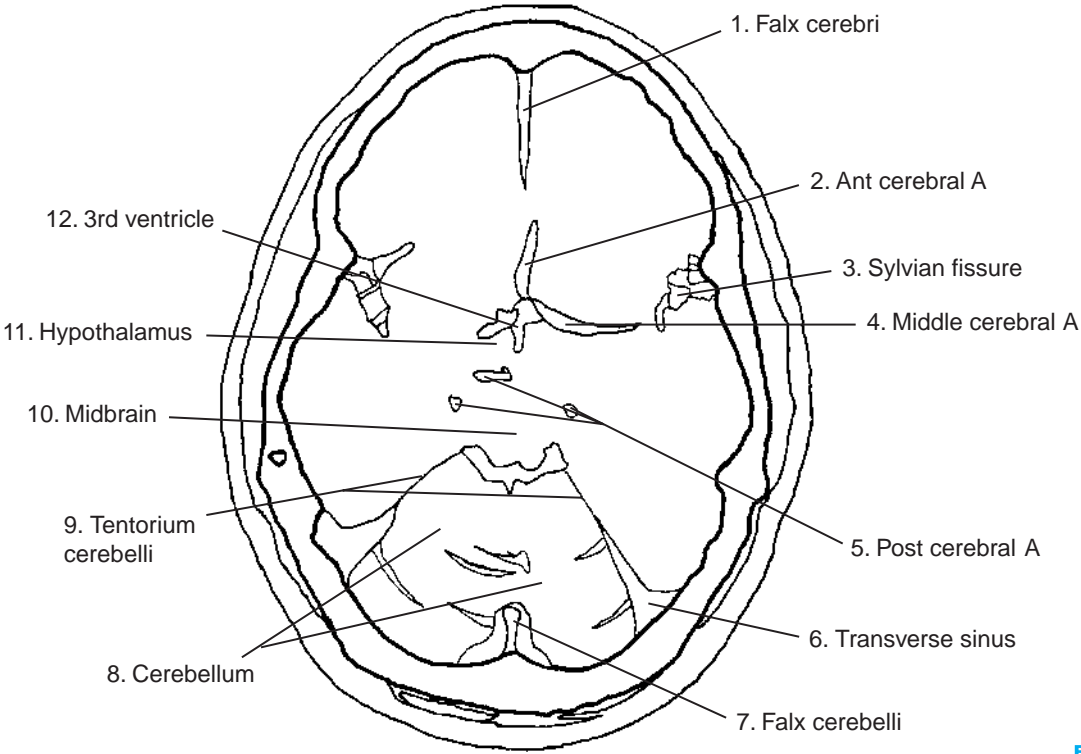


**Figure 5–52 (A,B)** Axial CT image 6.

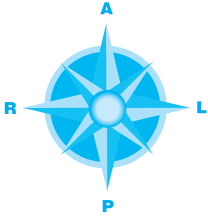
The bony structures making up the base of the skull are no longer seen, and the indentations of the inner skull indicate the margins between the neural structures. Anteriorly, the structure found medially extending between the right and left cerebral hemispheres can be identified as the falx cerebri. On the anterolateral aspects of the skull, the Sylvian fissures can be identified near the indentations of the skull as they divide the temporal and frontal lobes of the cerebrum. Posterolaterally, the transverse sinus is demonstrated forming the margin of the tentorium cerebelli that separates the cerebellum from the cerebrum. On the posterior aspect of the skull, the projection between the right and left lobes of the cerebellum can be identified as the falx cerebelli. At this level, the midbrain is found between the cerebrum and cerebellum. In the region of the posterior cerebrum, the contrast-enhanced posterior cerebral arteries are shown sectioned in several places as they extend from the region of the sella turcica to the posterior cerebrum. By comparison, the left middle cerebral artery is longitudinally sectioned, extending from the region previously occupied by the internal carotid artery to the region of the middle cerebrum. Anteriorly, the contrast-enhanced right anterior cerebral artery is also shown projecting from the region of the sella turcica toward the falx cerebri to supply the region of the anterior cerebrum with arterial blood. Although quite small at this level, the midline opening within the cerebrum represents the third ventricle between the right and left hypothalamus.



A



B



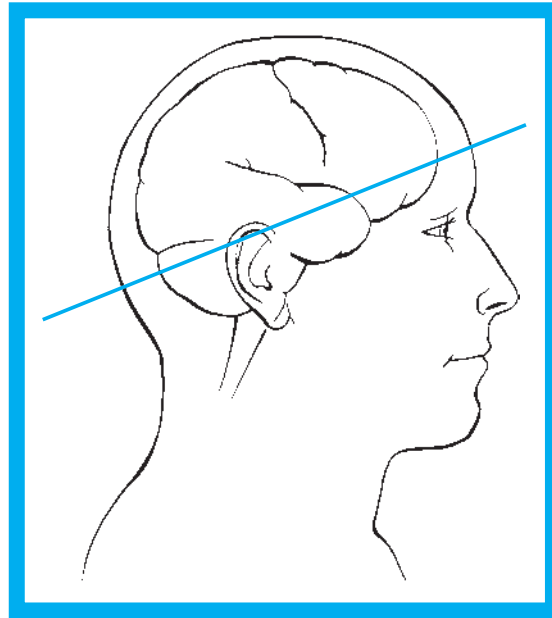
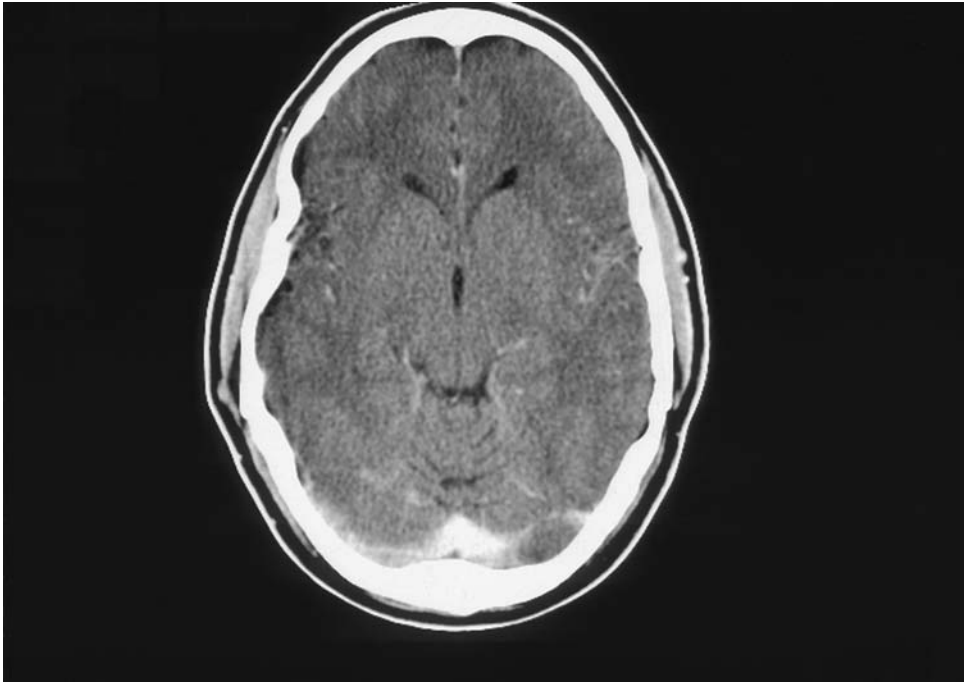
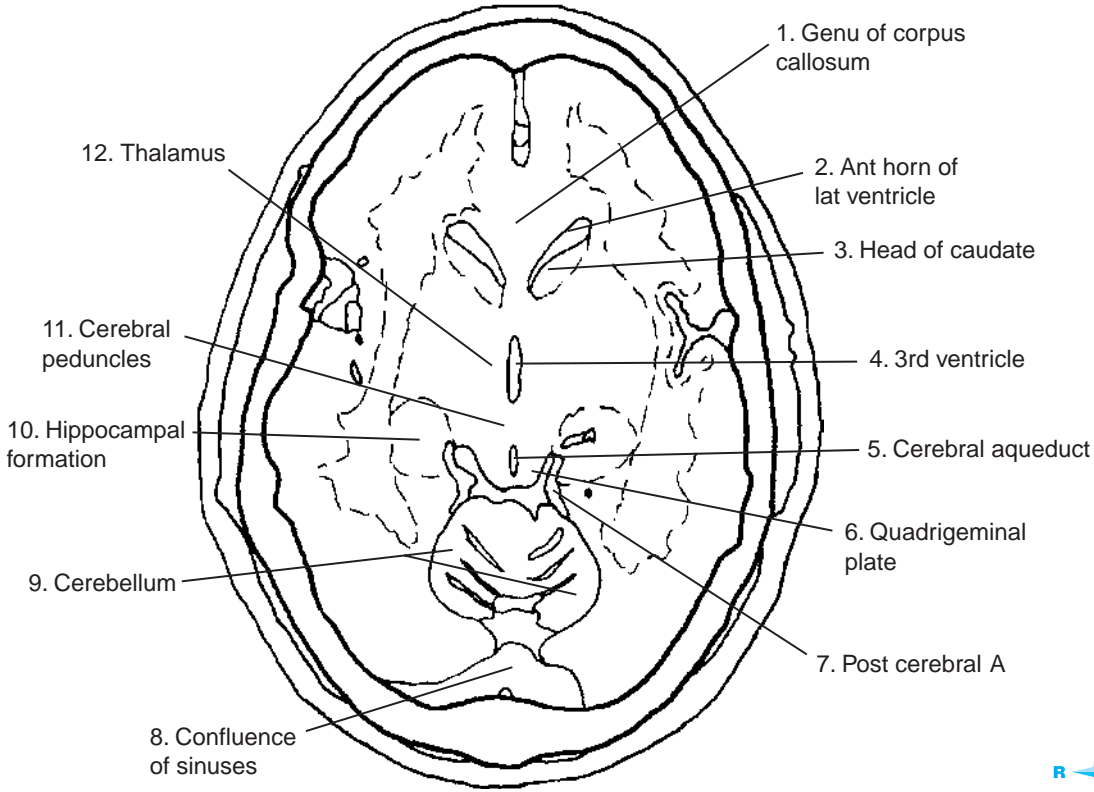


**Figure 5–53 (A,B)** Axial CT image 7.

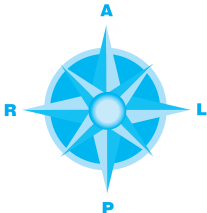
Although a small part of the upper cerebellum can still be seen within the posterior part of this image, the majority of the brain cavity is occupied by the cerebral hemispheres. In the posterior part of the skull cavity, the contrast-enhanced confluence of sinuses marks the boundary between the cerebellar and cerebral hemispheres. Between the hemispheres, the midbrain is sectioned, demonstrating the cerebral peduncles, the cerebral aqueduct, and the posteriorly situated quadrigeminal plate. Within the cerebrum, the most easily identified landmarks are the radiolucent areas of the ventricles. In the midline, the third ventricle is a narrow opening between the thalamic nuclei. Within the cerebral hemispheres, the anterior horns of the lateral ventricles are bounded by the genu of the corpus callosum and the heads of the caudate nuclei. At this level, the inferior horns of the lateral ventricles are not yet sectioned but will appear in the region of the hippocampal formation in the following images. Medial to the hippocampal formation, the contrast-enhanced posterior cerebral artery is obliquely sectioned as it extends from the circle of Willis to the posterior cerebrum.



A



B



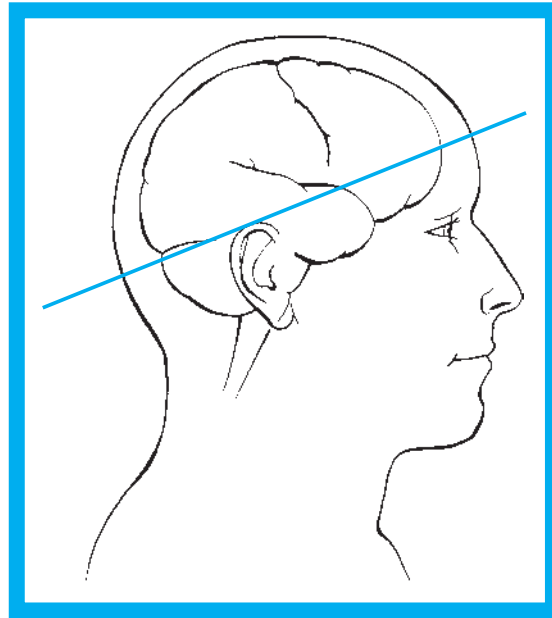
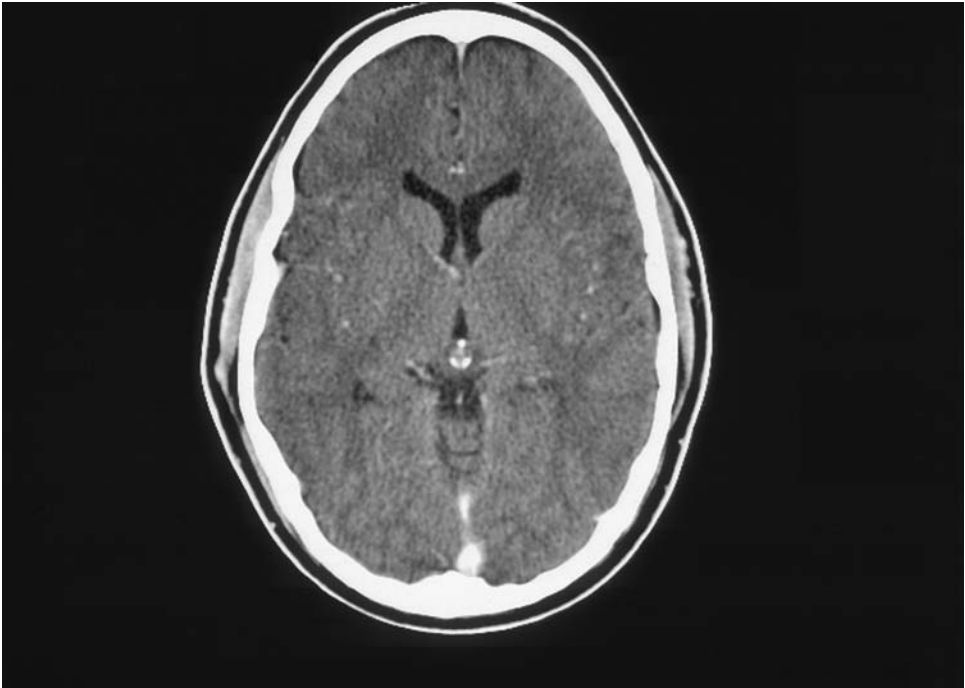
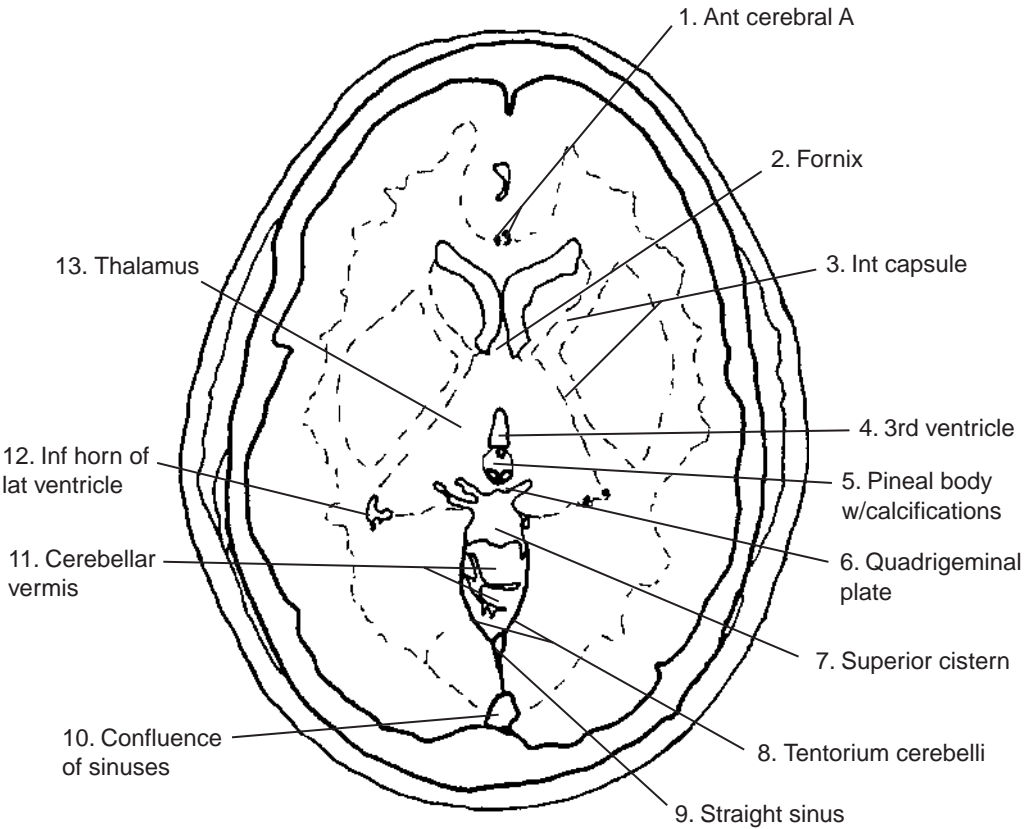


**Figure 5-54 (A,B)** Axial CT image 8.

At this level, the radiolucent areas of the anterior horns of the lateral ventricles are divided by the fornix, and the inferior horn of the lateral ventricle can now be labeled on the right side of this patient. Between the cerebral hemispheres, the anterior cerebral arteries are cut in cross-section as they ascend from the circle of Willis in the region of the sella turcica to the anterior cerebrum. Near the center of the image, the third ventricle appears as a clearly distinct radiolucent area between the thalamic nuclei, which are surrounded by the internal capsules. Although spots of high density appear to be within the third ventricle, they are calcifications within the pineal gland found outside the third ventricle between the quadrigeminal plate and the splenium of the corpus callosum. Although the radiolucent area between the pineal body and the cerebellar vermis appears to be the same density as the ventricle previously described, this area is formed by an enlarged part of the subarachnoid space outside of the brain, the superior cistern. Forming the border between the occipital lobes of the cerebrum and the upper part of the cerebellum, the tentorium cerebelli is sectioned, demonstrating the straight sinus and the confluence of sinuses that are formed in part by an extension of dura mater from the tentorium cerebelli.



A



B



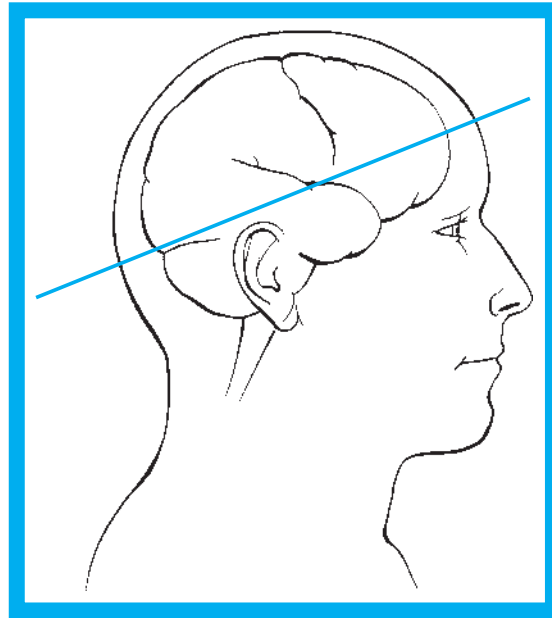
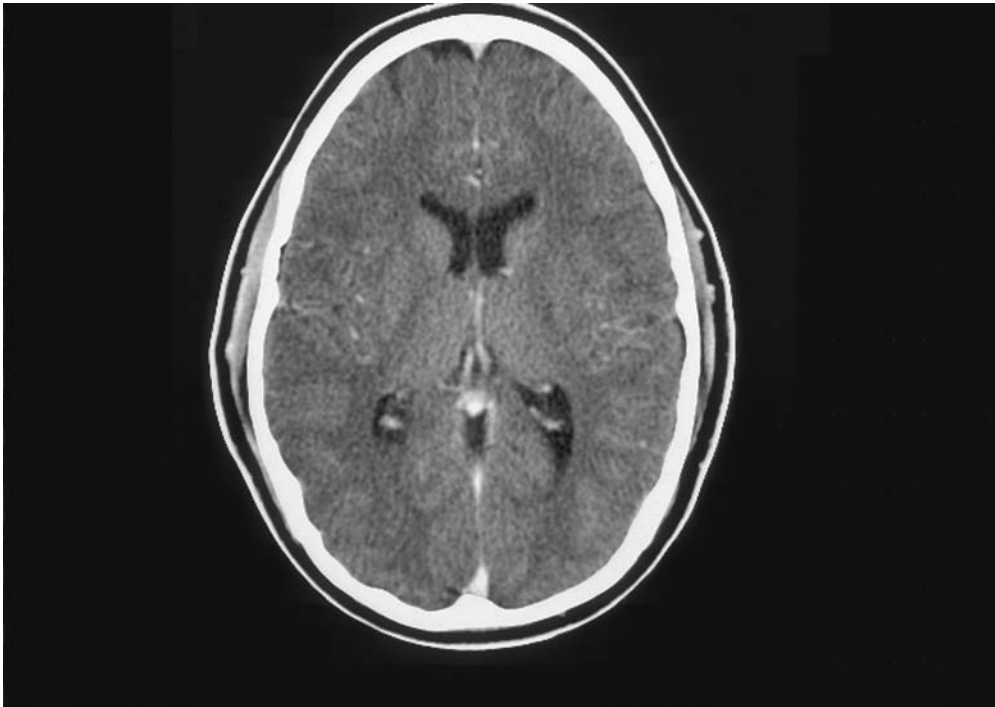
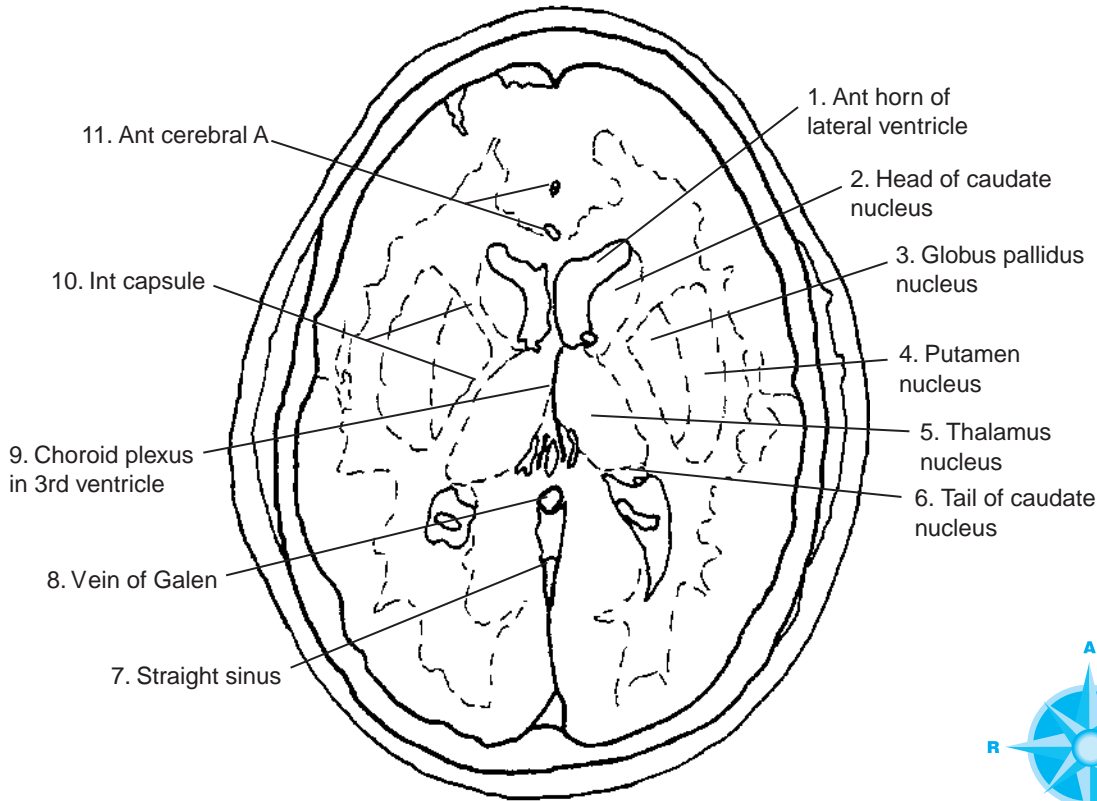


**Figure 5–55 (A,B)** Axial CT image 9.

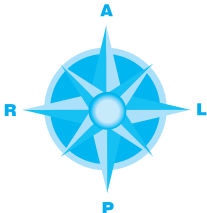
The darkened areas representing parts of the lateral ventricles can be readily identified on either side. Anteriorly, the heads of the caudate nuclei are shown protruding into the anterior horns of the lateral ventricles. Between the cerebral hemispheres, the contrast-enhanced anterior cerebral arteries are shown in cross-section as they extend from the base of the brain where they originate from the circle of Willis to extend upward to supply blood to the anterior cerebral hemispheres. At this level, the midline ventricle previously identified as the third ventricle is sectioned near the top of the opening. Within the ventricles, the choroid plexuses are enhanced by contrast, because they are highly vascular and are responsible for the production of cerebrospinal fluid (CSF). As described previously, the lateral walls of the third ventricle are formed by the thalamic nuclei. On the opposite side of the thalamic nuclei, the internal capsules act to separate the thalamic nuclei from the basal ganglia: Caudate nucleus, globus pallidus, and putamen. Posterior to the thalamic nuclei, the tails of the caudate nuclei are shown in cross-section as they extend toward the inferior horns of the lateral ventricles. In the midline between the cerebral hemispheres, the vein of Galen is shown in cross-section as a large contrast-enhanced vessel directly behind the third ventricle. The vein of Galen drains venous blood into the straight sinus obliquely sectioned between the posterior cerebral hemispheres.



A



B



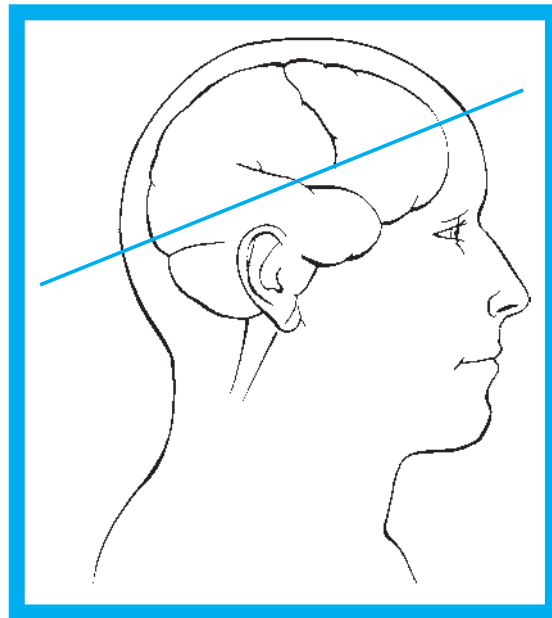
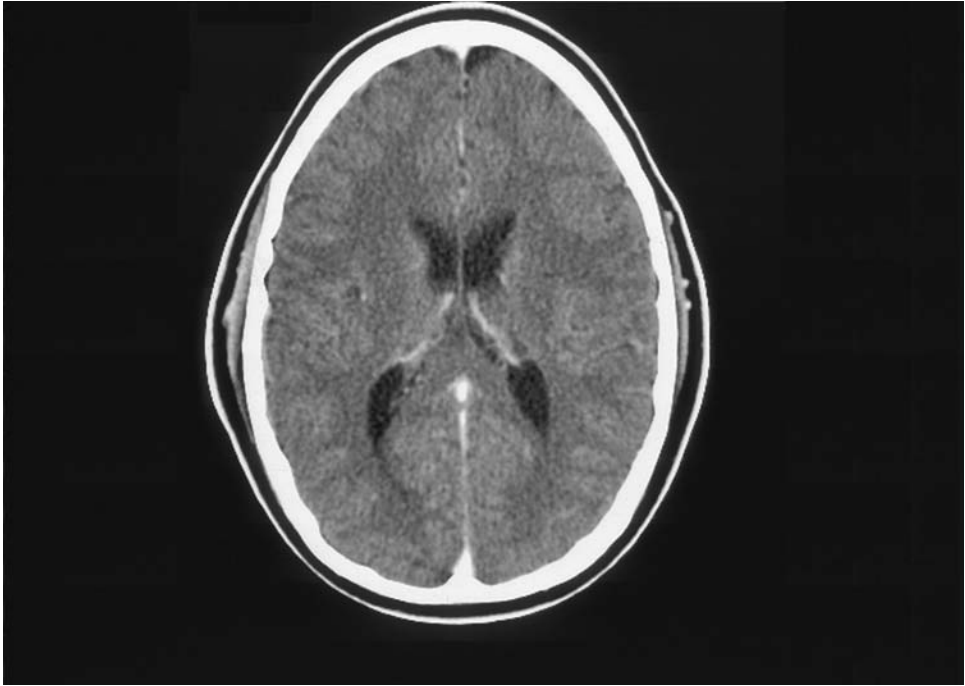
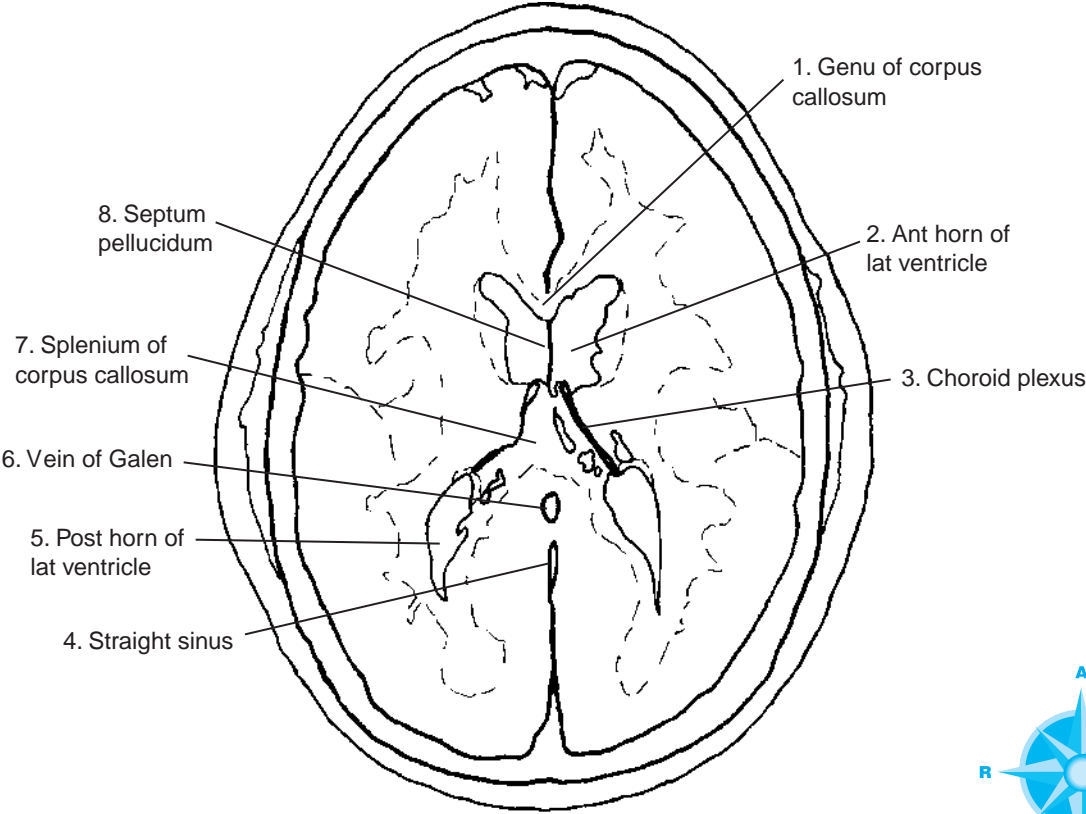


**Figure 5–56 (A,B)** Axial CT image 10.

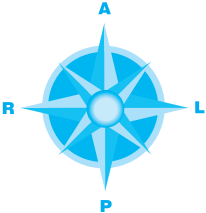
At this level, the third ventricle is no longer seen and has been replaced by the structure forming the roof of the third ventricle, the splenium of the corpus callosum. Similar to previous images, the anterior horns of the lateral ventricles are readily identified as radiolucent areas within the anterior cerebral hemispheres. The anterior horns of the lateral ventricles are separated by the septum pellucidum, which extends between the splenium and genu of the corpus callosum. Between the anterior and posterior horns of the lateral ventricles, the contrast-enhanced choroid plexus lies within the bodies of the lateral ventricles. Similar to the previous image, the contrast-enhanced vein of Galen and straight sinus are sectioned between the posterior cerebral hemispheres.



A



B



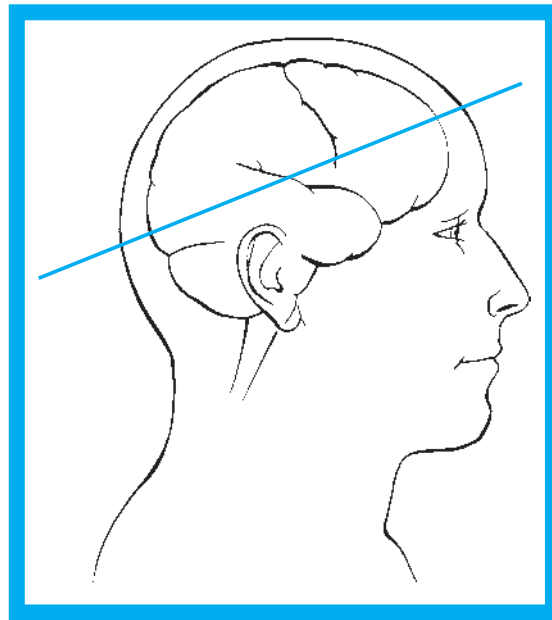
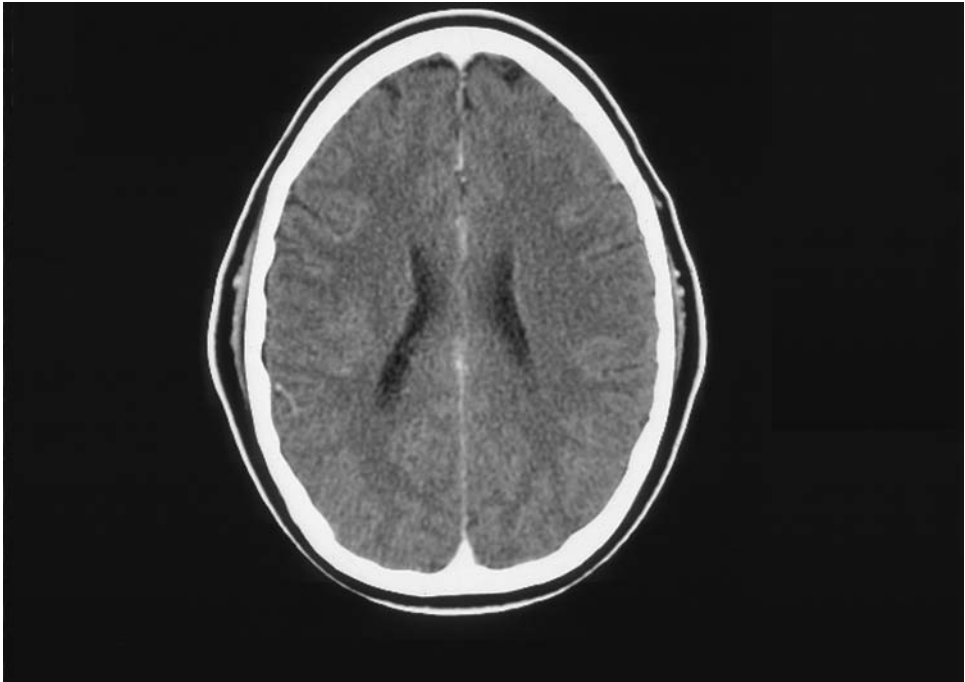
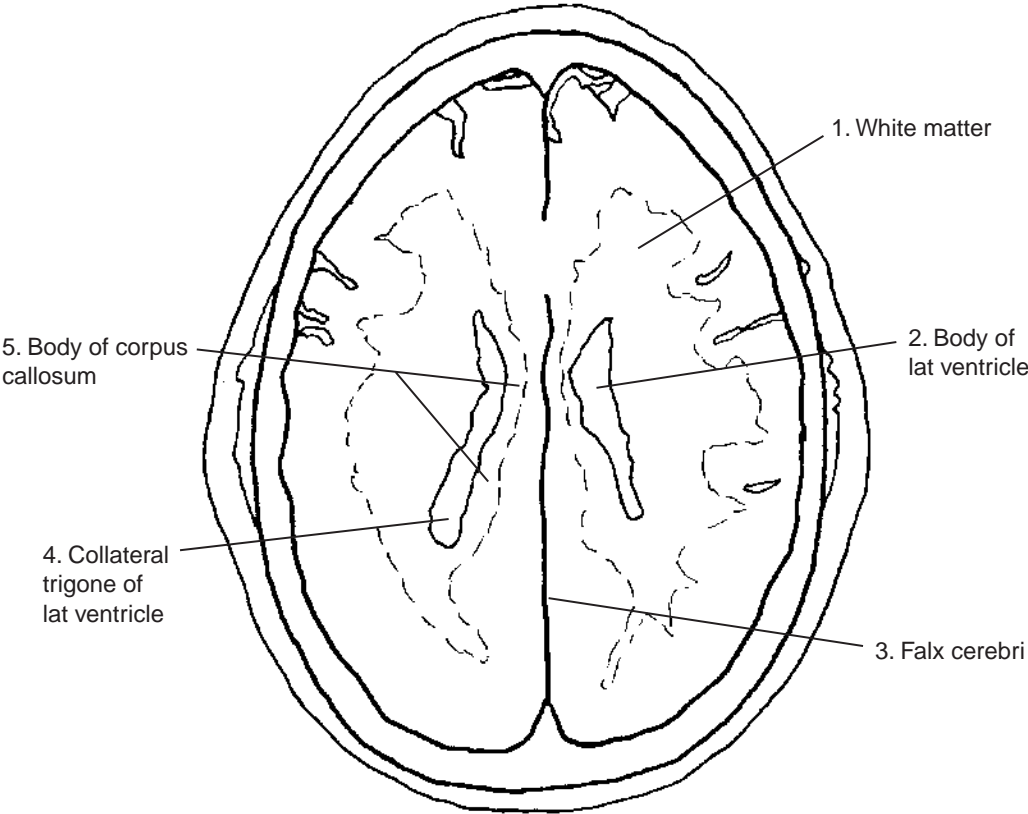


**Figure 5–57 (A,B)** Axial CT image 11.

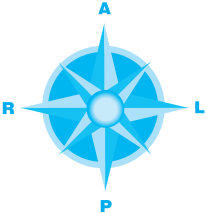
In this image, the bodies of the lateral ventricles are the most readily identifiable landmarks. On the patient's right side, the posterior part of the lateral ventricle is labeled the collateral trigone, which is where the inferior and posterior horns join the body of the lateral ventricle. On either side, the ventricles are surrounded by an area of white matter formed primarily of neural fibers extending to and from the gray matter of the cerebral cortex. Just medial to the lateral ventricles, the region of white matter represents the body of the corpus callosum and consists of a group of nerve fibers extending between the right and left cerebral hemispheres. In the midline, the falx cerebri is formed by a reflection of dura mater separating the right and left cerebral hemispheres.



A



B



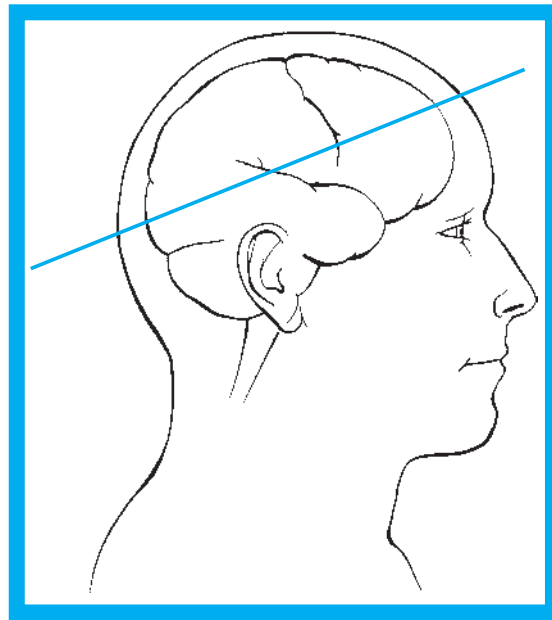
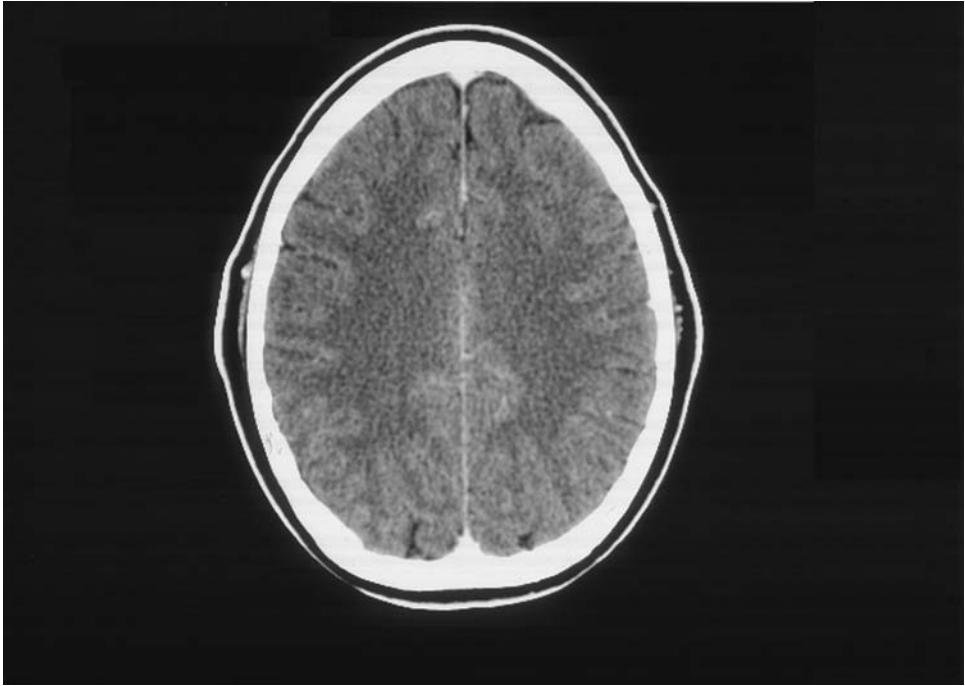
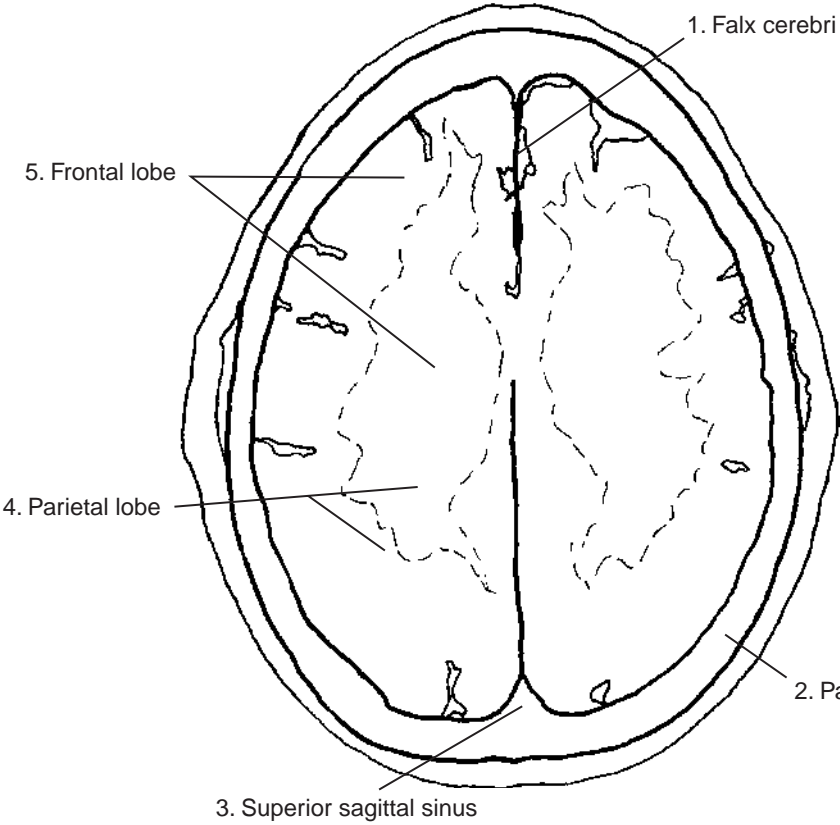


**Figure 5–58 (A,B)** Axial CT image 12.

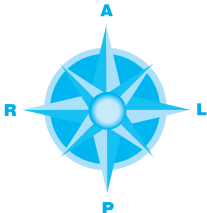
Owing to the absence of ventricular structures, this axial section is through the upper part of the brain. Similar to the previous image, the falx cerebri is shown separating the right and left cerebral hemispheres. Along its margin, the falx cerebri forms the superior sagittal sinus, and is labeled on the posterior part of the image adjacent to the parietal bone. Within the cerebral hemispheres, the regions of the frontal and parietal lobes are labeled and contain both white and gray matter.



A



B





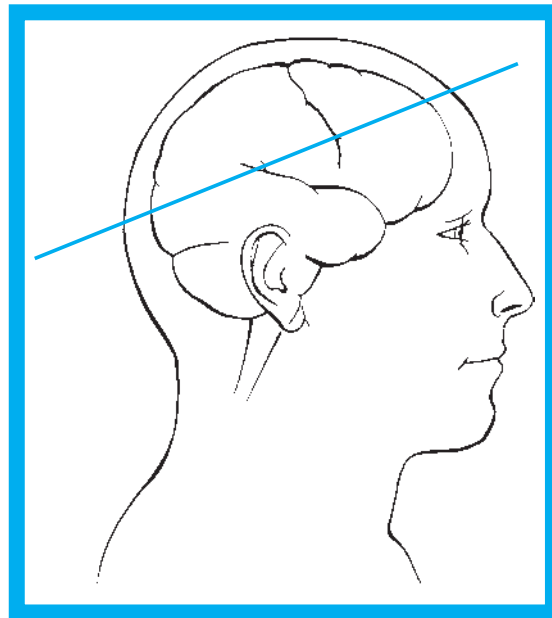
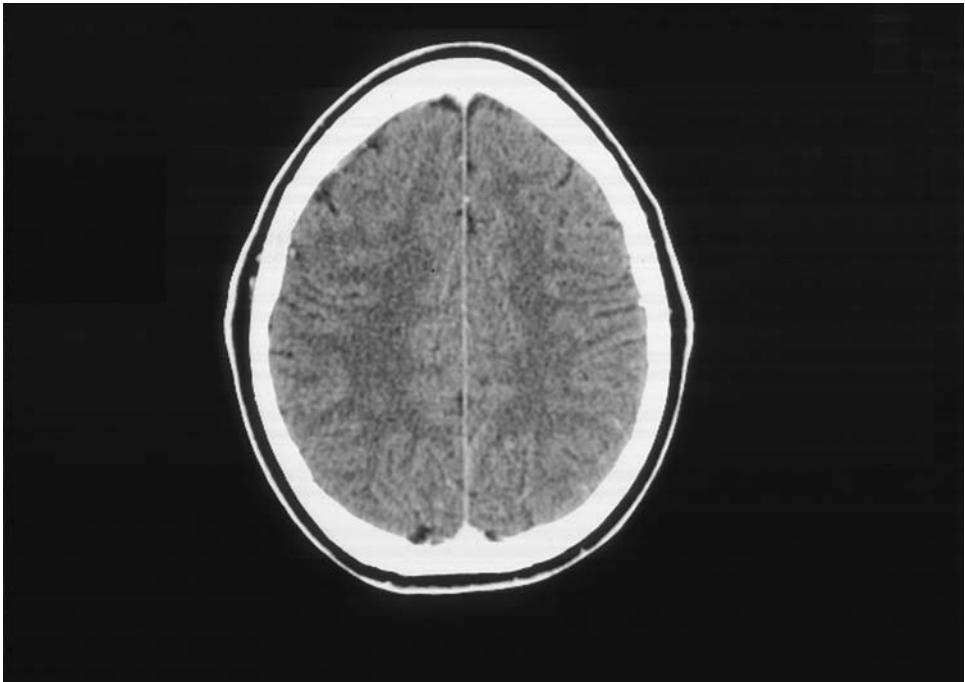
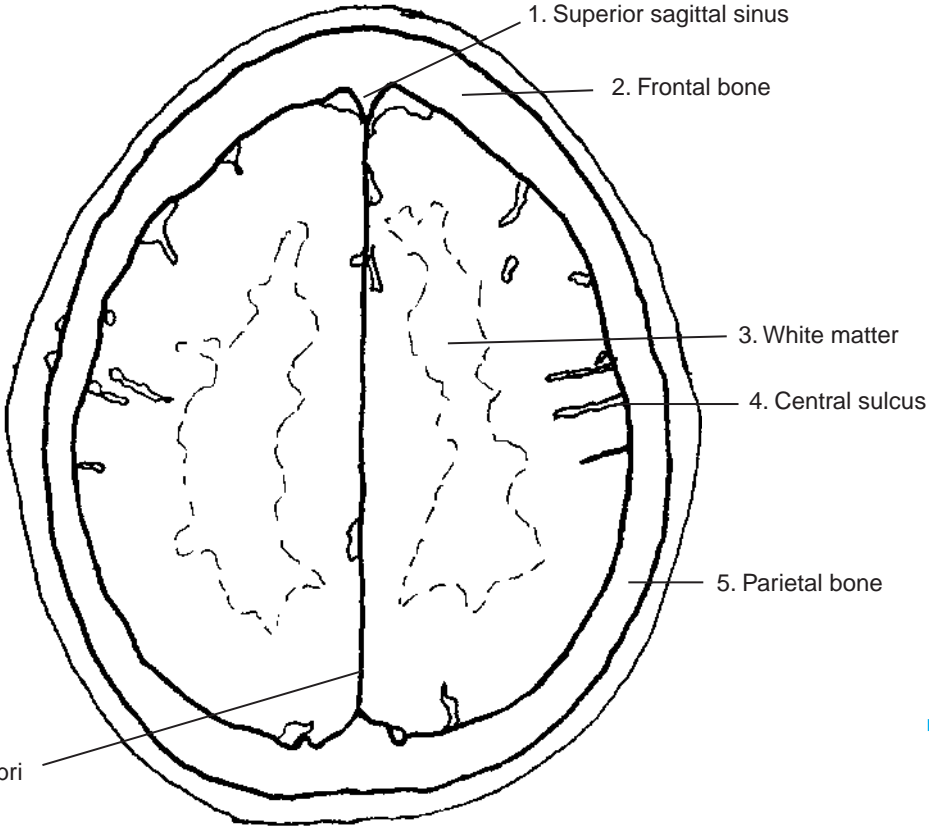


**Figure 5–59 (A,B)** Axial CT image 13.

Nearing the top of the head, the falx cerebri is again shown separating the right and left cerebral hemispheres. The superior sagittal sinus is labeled anteriorly, bounded by the dural reflections from the falx cerebri and the frontal bone. Although it is not labeled, the superior sagittal sinus is also within the posterior margin of the falx cerebri adjacent to the parietal bone. Within the cerebral hemispheres, white matter is shown surrounded by the gray matter following the convoluted appearance of the external cerebral hemispheres. Within this section, the enlarged central sulcus can be identified separating the frontal and parietal lobes of the cerebrum.



A



B

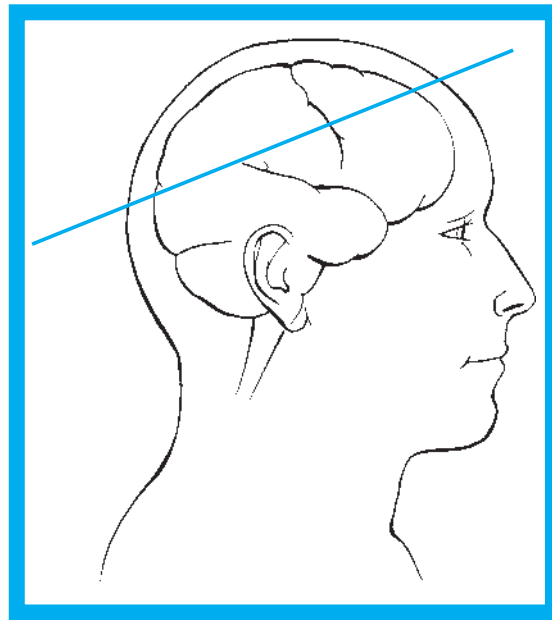
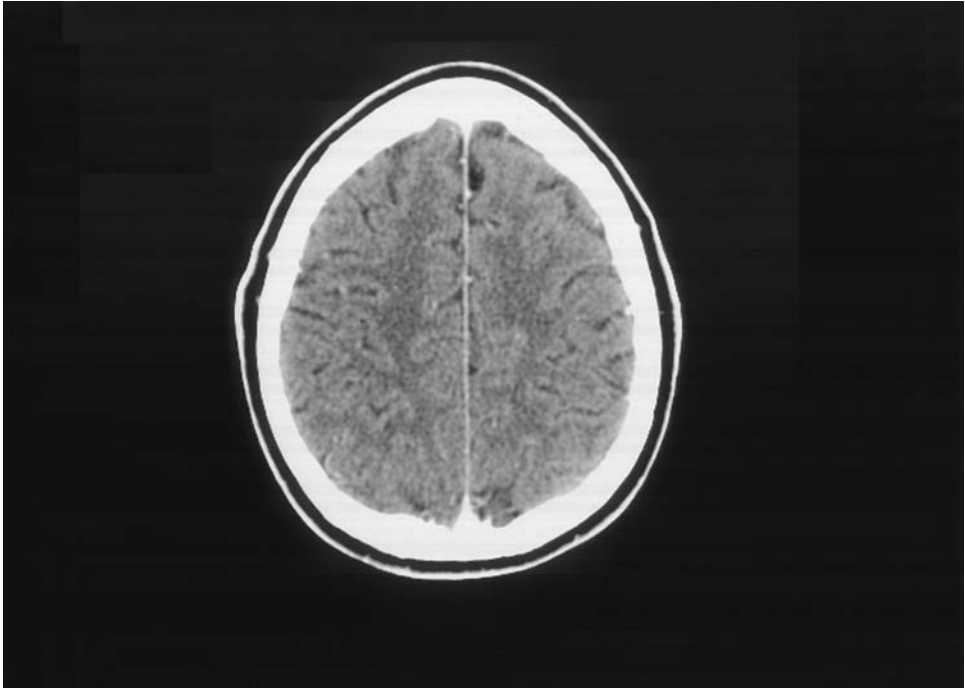
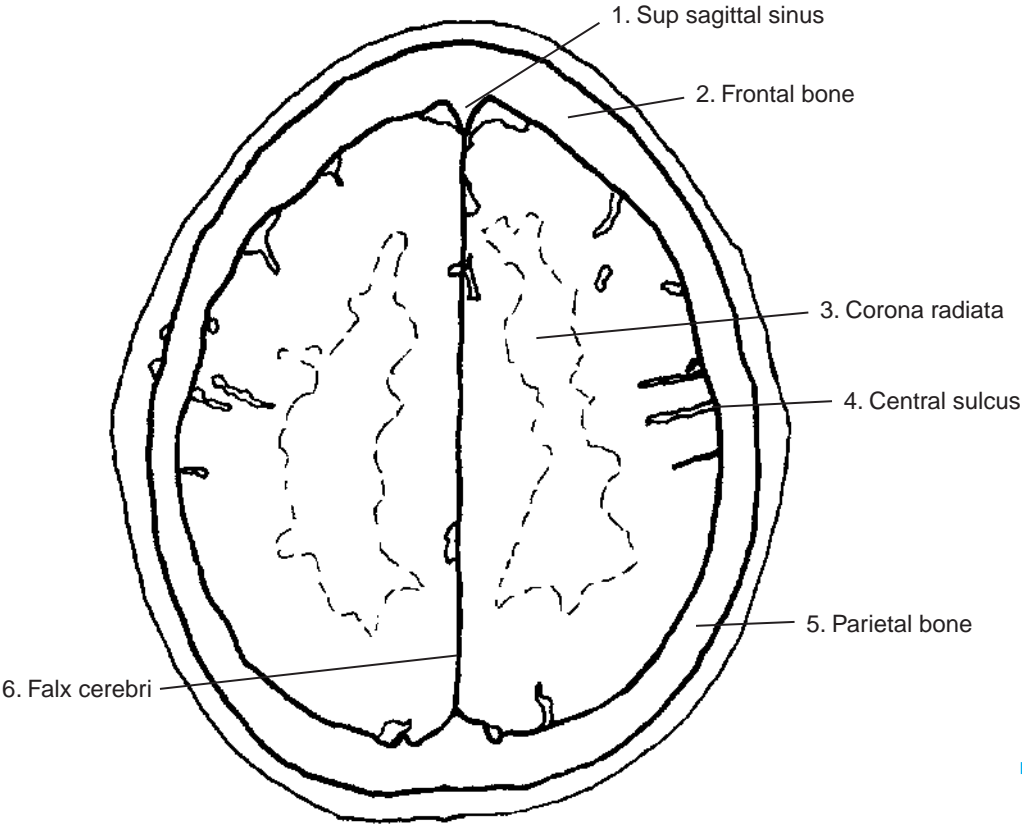


**Figure 5–60 (A,B)** Axial CT image 14.

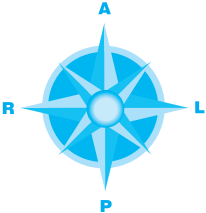
The convoluted appearance of the neural structures indicates that the section lies near the top of the cerebral hemispheres. Because this section represents the anatomy of the upper head, the frontal bone is labeled anteriorly and the parietal bone is labeled posteriorly, even though the coronal suture cannot be identified. Internally, the central sulcus can be identified and marks the boundary between the frontal and parietal lobes of the cerebrum. In the midline, the superior sagittal sinus is labeled along the margin of the falx cerebri extending between the right and left cerebral hemispheres. Within the cerebral hemispheres, the corona radiata appear as regions of white matter on either side surrounded by the gray matter of the cerebral cortex.



A



B



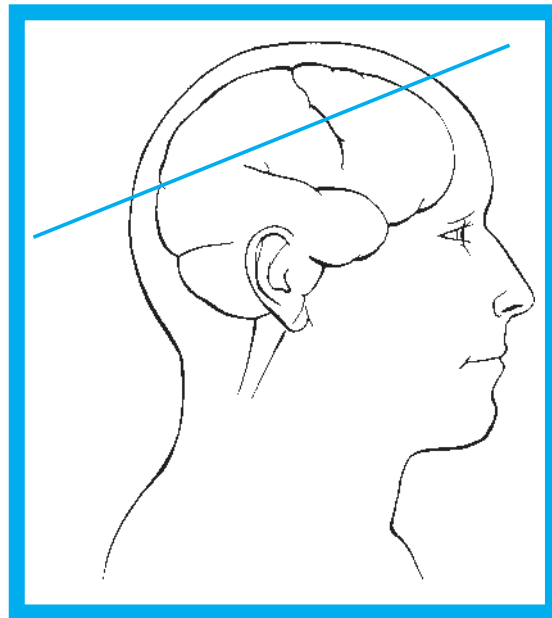
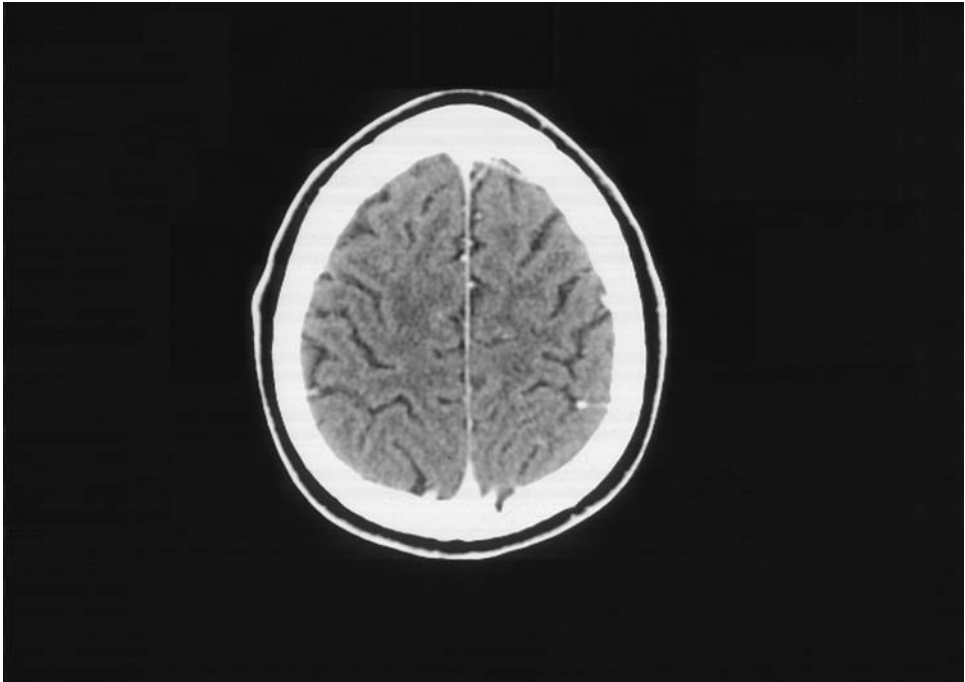
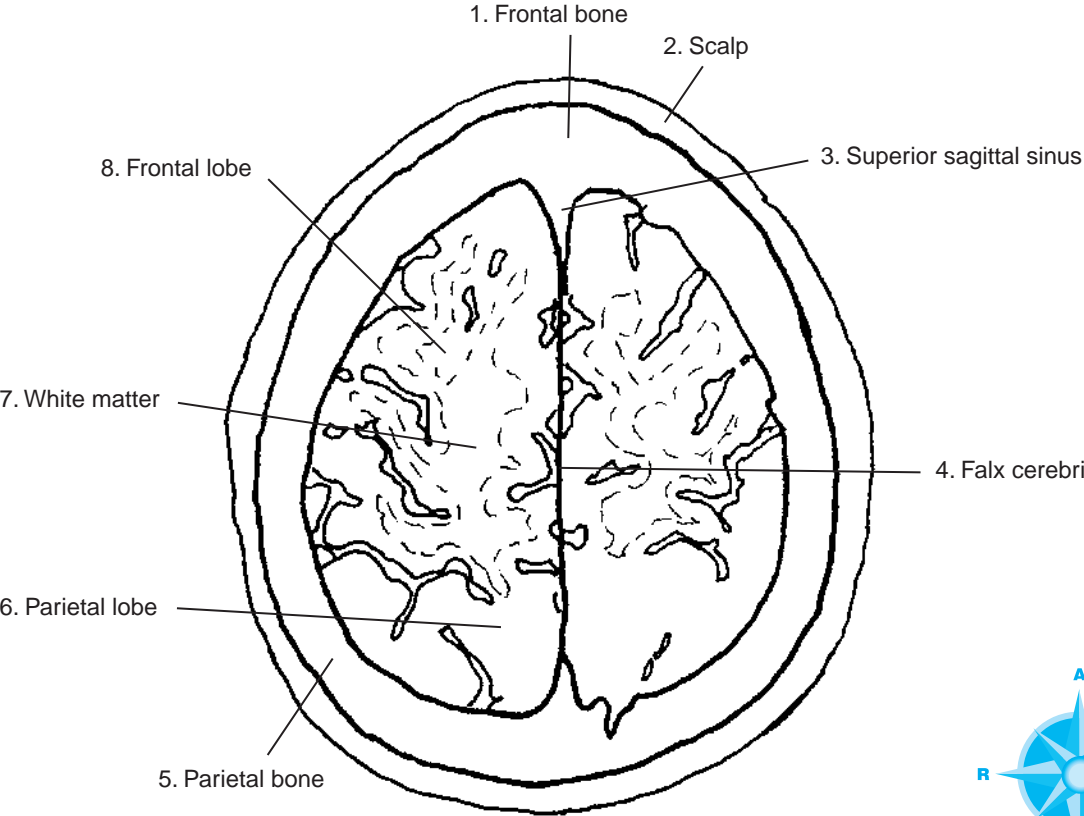


**Figure 5–61 (A,B)** Axial CT image 15.

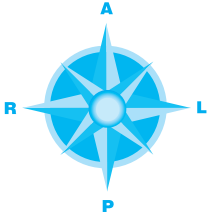
The appearance of sulci and gyri within the majority of the neural tissue indicates that the image is nearing the top of the brain. Despite the predominance of surface anatomy, a small amount of white matter can be identified on either side within the frontal and parietal lobes of the cerebrum. Similar to previous images, the falx cerebri extends between the parietal and frontal bones, and contains the superior sagittal sinus along its bony margin. Surrounding the skull, the scalp appears as two distinct layers: The outer layer of skin is dense and consists primarily of dense connective tissue and skin; and the inner layer consists primarily of loose connective tissue, fat, and blood vessels.



A



B



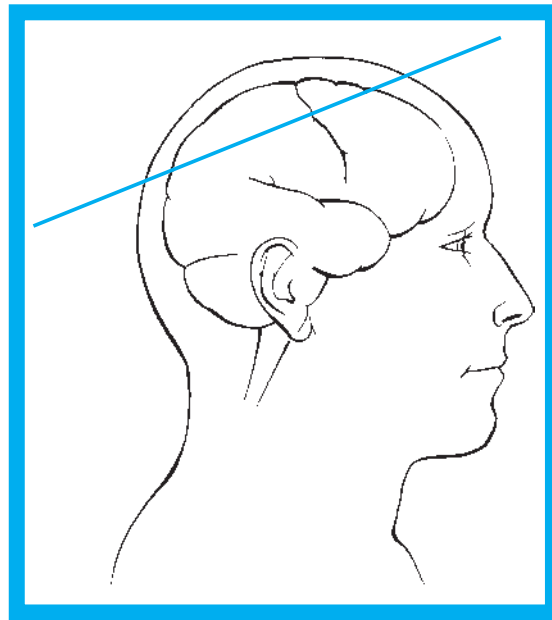
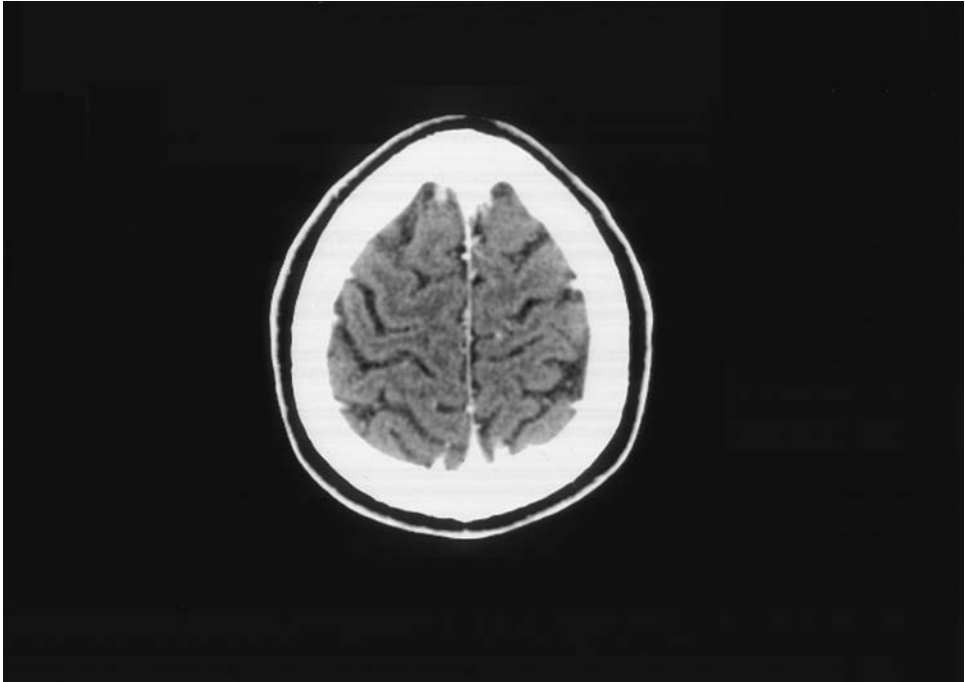
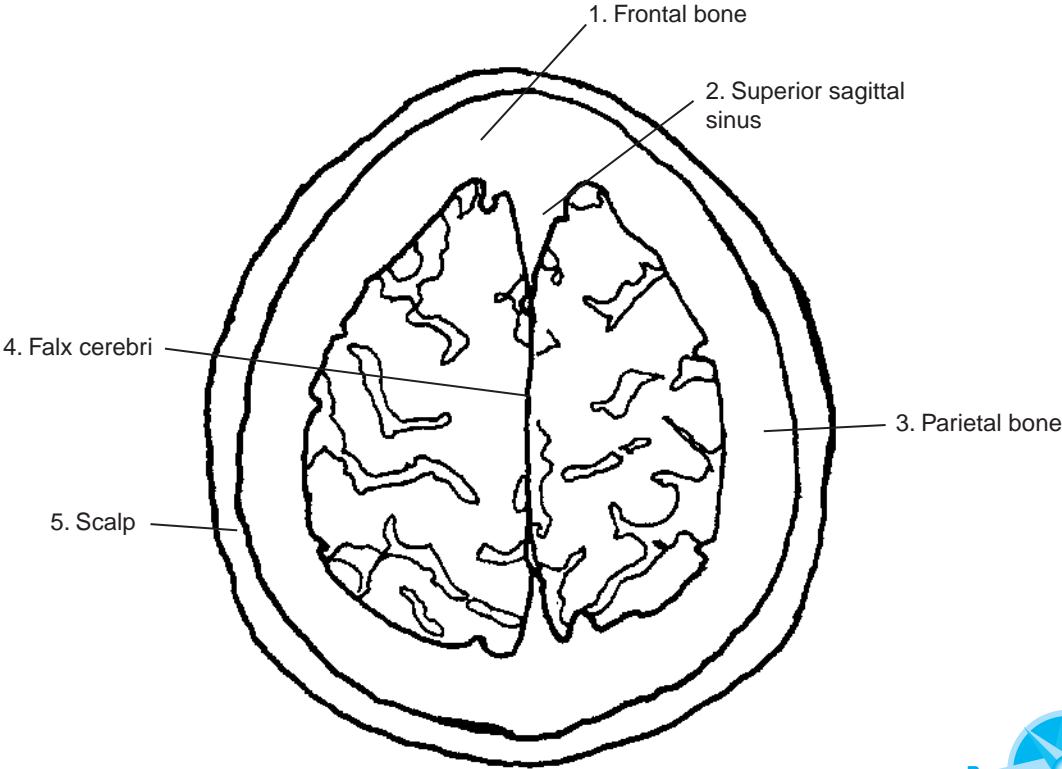


**Figure 5–62 (A,B)** Axial CT image 16.

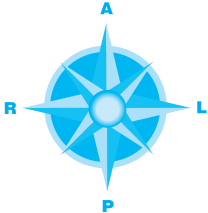
This section demonstrates the anatomy typically seen in the most superior scan of the head. Within the image, the falx cerebri is again shown containing the superior sagittal sinus within its bony margin, which attaches to the frontal and parietal bones. Outside of the bones of the skull, the scalp appears as two distinct layers; the inner is radiolucent and the outer is radiodense.



A



B







## Case Study 5-1

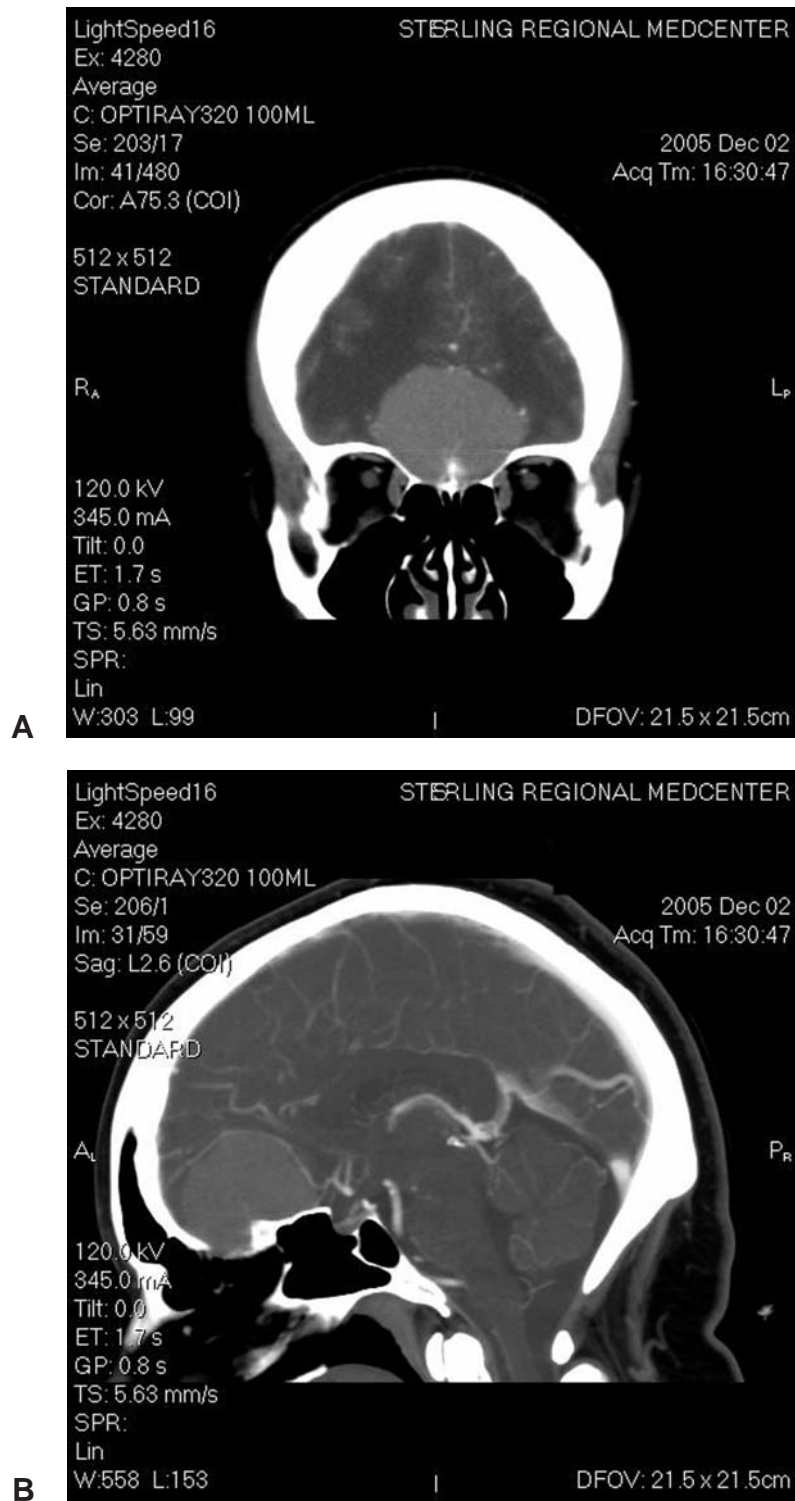


Figure 5-63

## Clinical Correlations

This 38-year-old woman was referred for a computed tomography angiography (CTA) examination by her ophthalmologist, who suspected an aneurysm might be causing her acute diplopia (double vision) and headaches. Following spiral axial imaging with thin collimation, reconstructed images in the coronal and sagittal planes were generated; select examples are provided above. There is a round, strongly enhancing mass in the anterior cranial fossa measuring  $4.3 \times 4.1$  cm. The mass is midline and lies above the

lesser wing of the sphenoid and the cribriform plate of the frontal bone. The mass appears to be extra-axial (does not arise from the brain itself), and there is no detectable bone sclerosis (thickening or hyperplasia due to injury). The anterior cerebral arteries are draped over the top of the mass, and no aneurysm was identified. Following surgical resection, pathology examination results determined that the mass was a meningioma, a slow growing tumor originating from the arachnoid mater.

## Questions

1. Describe where the circle of Willis is located as compared to the brain and the skull.
2. Where is the circle of Willis located as compared to the meningeal layers?
3. Where is most of the venous blood found within the skull as compared to the meningeal layers?
4. Where is the CSF found on both the inside and outside of the brain?
5. In the sagittal image, which vessel is shown filled with contrast providing arterial blood to the occipital lobe of the cerebrum?



## Case Study 5-2

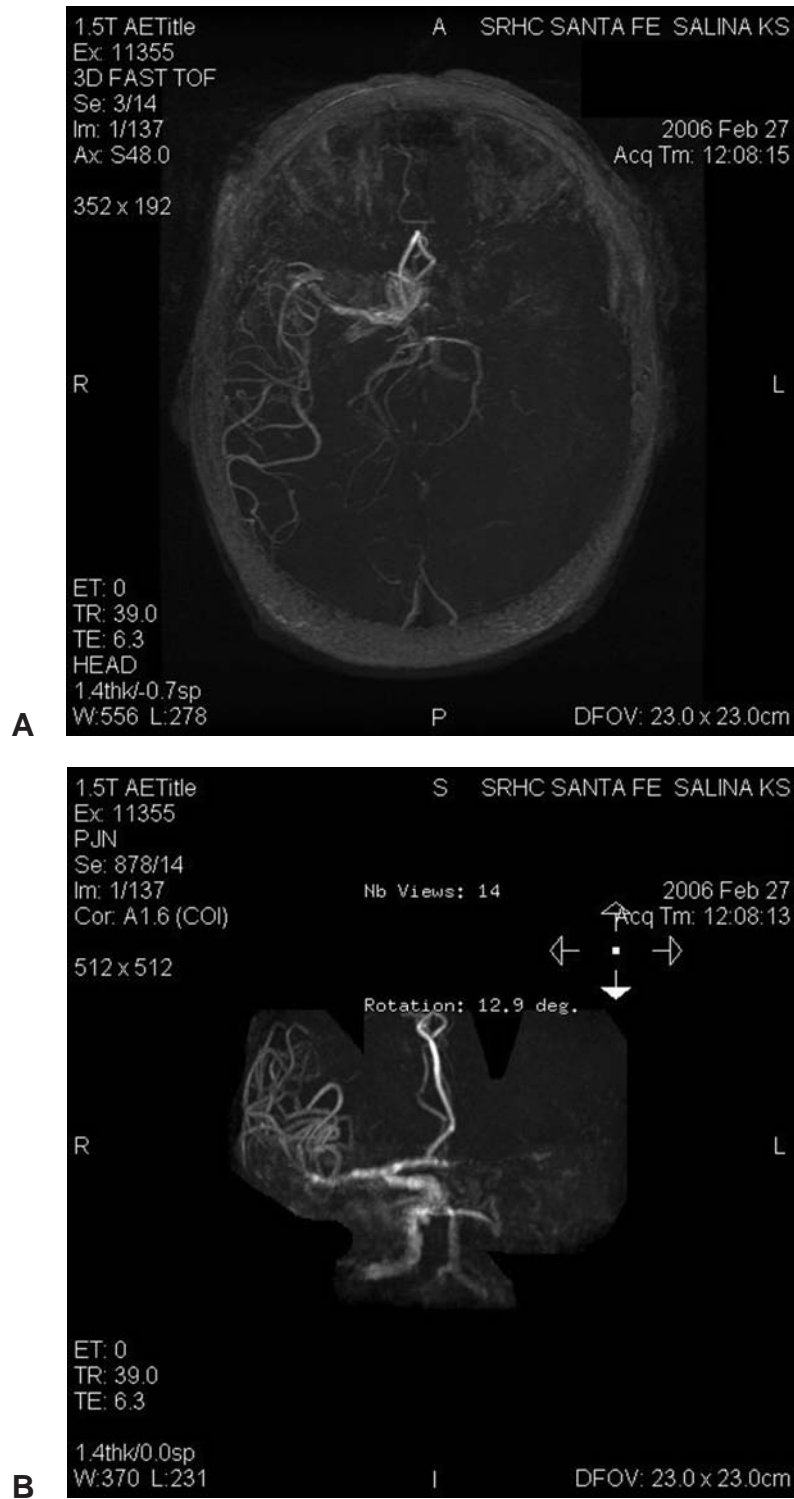


Figure 5-64

This 84-year-old woman was referred for a magnetic resonance angiography (MRA) examination by an emergency room physician to evaluate a suspected stroke. Multisequence MR imaging of the brain was performed, and selected images are shown above. The MRA of the brain demonstrates lack of flow within the left internal carotid artery. As compared to the normal flow shown on the right side, the left cerebral vasculature is not seen and

significant cross-flow is not apparent. Typically, cerebrovascular disease is found to result from atherosclerosis which builds up over a lifetime and most often affects older patients. Unfortunately, this is a common disease and is the third most common cause of death in the United States. If the patient survives, the cerebrovascular disease often results in permanent disabilities making it the most common crippling disease.

## Questions

1. Describe the origin of the internal carotid artery.
2. Explain how the internal carotid artery travels through the base of the skull.
3. Where does the internal carotid artery join the circle of Willis?
4. If the arterial flow is restricted or diminished on the left side, how will this affect the cerebral structures supplied by this vessel?
5. In the axial image, which vessel is shown filled with contrast providing arterial blood to the frontal lobe of the cerebrum?



## Case Study 5-3

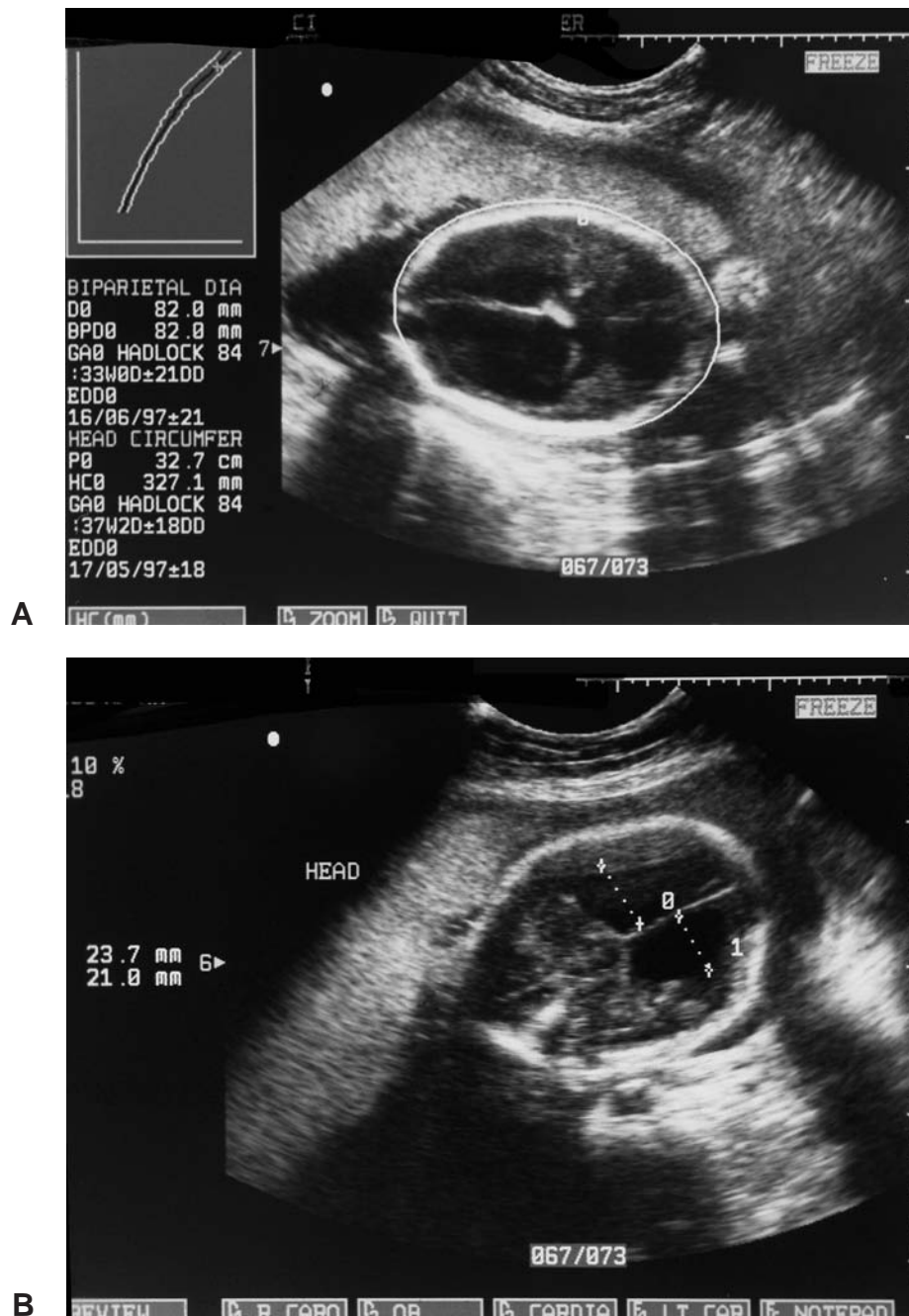


Figure 5-65

This 37-year-old woman was referred for a real-time ultrasound examination. A single fetus was identified in breech presentation. Fetal movement and fetal heart motion were identified, and averaging various fetal parameters indicated a gestational age of 31 to 32 weeks. As marked in the figure, the circumference of the head was measured at 32.7 cm and a biparietal diameter measured at 82 mm. The prominent dilation of the lateral ventricles within the

fetal calvarium is clearly evident (Fig. 5-65B), and measurements are marked at 23.7 mm and 21 mm. Comparing the head circumference to the abdominal circumference gave a ratio of 1.23, which is above the normal limit and would be further evidence of hydrocephalus. This condition results from an excessive accumulation of CSF resulting in dilation of the cerebral ventricles and raised intracranial pressure.

## Questions

1. Where is the CSF produced?
2. Where is the CSF reabsorbed?
3. Describe the CSF circulation.
4. What happens when part of the CSF system becomes blocked?
5. What are the enlarged regions of the subarachnoid space called?



## Case Study 5-4

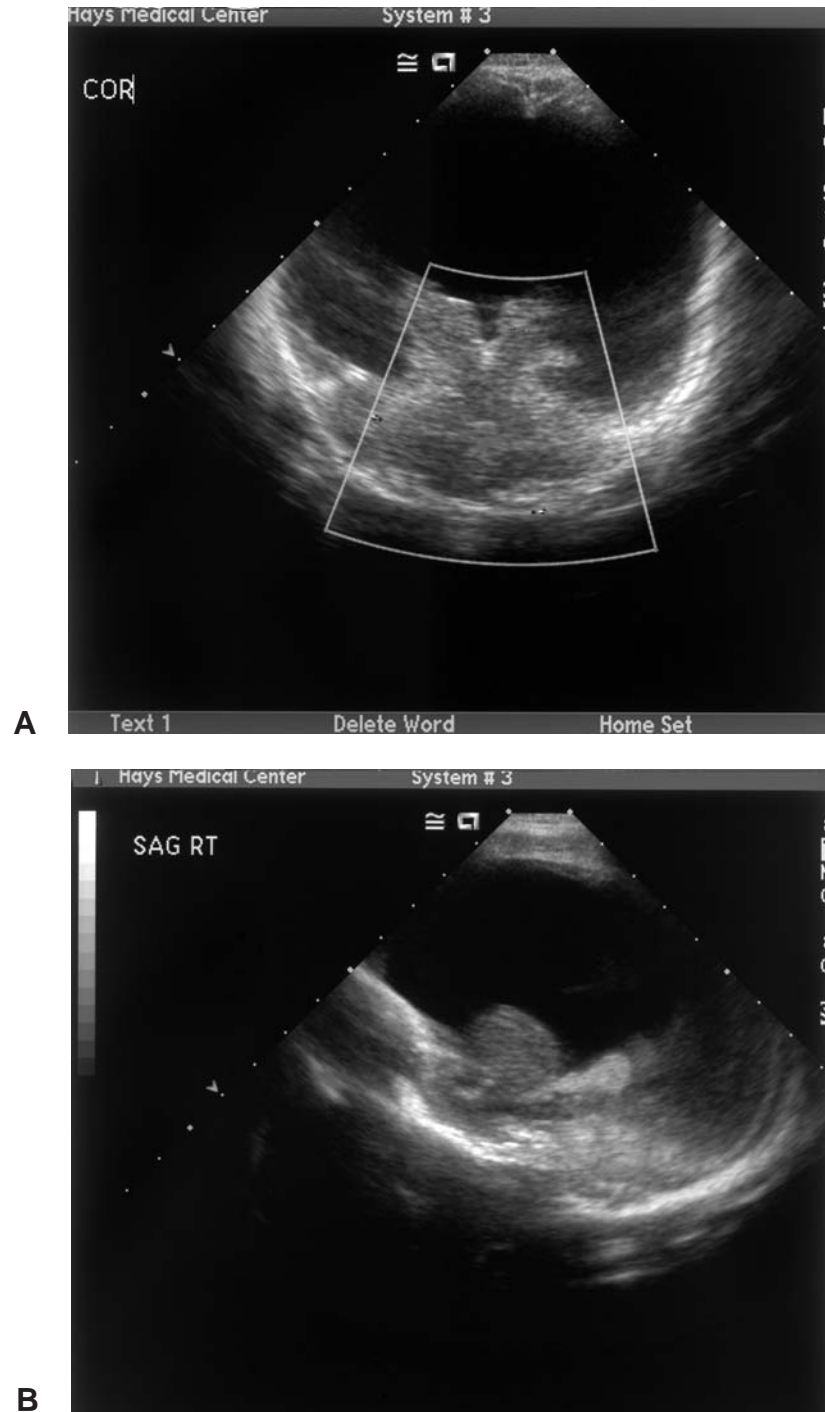


Figure 5-66

This 4-day-old girl was referred for an ultrasound examination of the head to initially evaluate for suspected hydranencephaly. This is a rare condition in which the brain's cerebral hemispheres are absent and replaced by sacs filled with CSF. In the coronal section shown in Figure 5-66A, most of the skull was found to be hypoechoic due to the large accumulation of CSF outside the brain. In the lower part of the cranial cavity, most of the neural tissue is contained within

the marker lines. In the sagittal section shown as Figure 5-66B, the cerebral structures are shown in the lower cranial cavity, and most of the cavity appears to be filled with CSF. Infants with hydranencephaly may appear normal at birth. The infant's head size and spontaneous reflexes such as sucking, swallowing, crying, and moving the arms and legs may all seem normal. This patient was referred for CT examination of the head as described in Case Study 5-5.

## Questions

1. How does your body make CSF?
2. In a coronal section through the head, which ventricle will be found deep within the temporal lobe?
3. Describe the meningeal layers starting with the layer closest to the brain and ending with the layer closest to the skull.
4. Which of the ventricles is located between the thalamic and hypothalamic nuclei?
5. What is the ventricle found between the cerebellum and the brainstem?





## Case Study 5-5

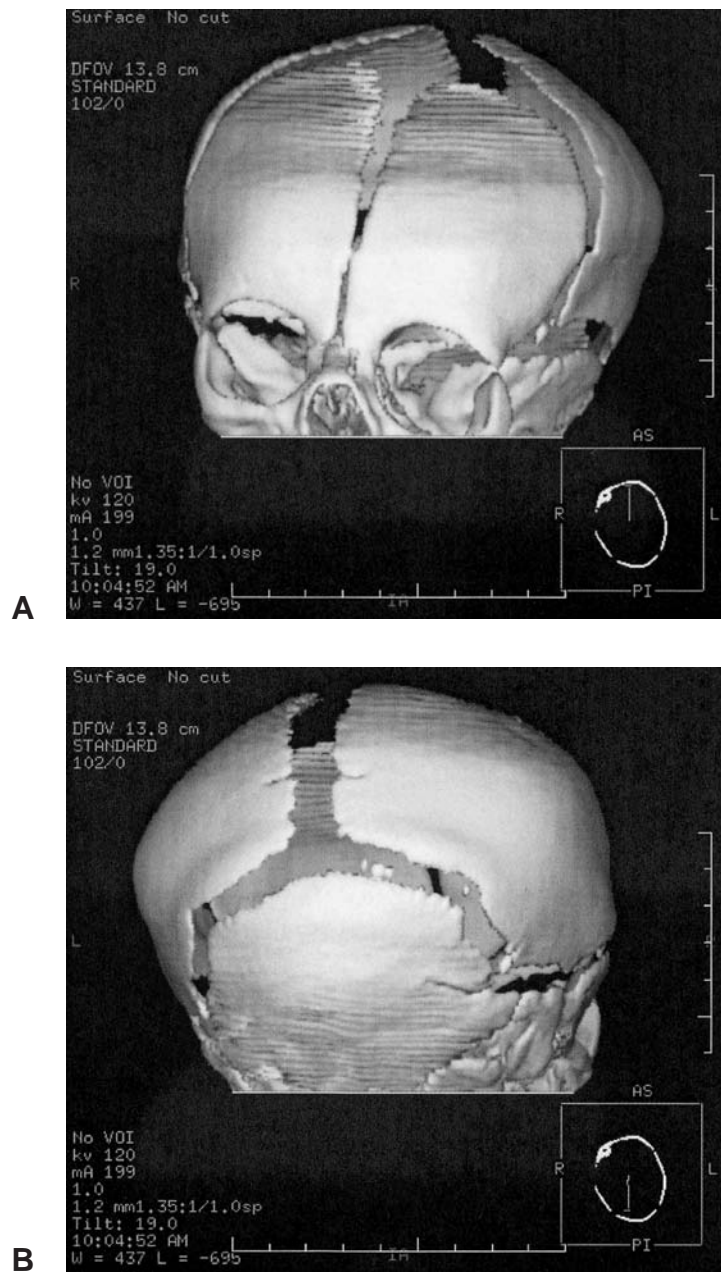


Figure 5-67

This CT examination was performed as a follow-up examination to the ultrasound examination of a 4-day-old girl diagnosed with hydranencephaly as described in Case Study 5-4. The three-dimensional reconstructed images show that the joints on the infant skull (sutures) have not joined, so the separate bones can be clearly outlined. Although the sutures may appear like fractures, they are normal and may be seen at up to 18 months of age. Regrettably, CT sectional images confirmed the hydranencephaly found in the prior ultrasound examination. Although the infant initially appeared normal, after a few days the infant became irritable and had increased muscle tone. Over time, seizures and hydrocephalus (excessive accumulation of CSF in the brain) may develop. Other

symptoms may include visual impairment, lack of growth, deafness, blindness, spastic quadriplegia (paralysis), and intellectual deficits. Hydranencephaly is considered to be an extreme form of porencephaly (a rare disorder characterized by a cyst or cavity in the cerebral hemispheres) and may be caused by vascular infections or traumatic disorders after the 12th week of pregnancy. In some cases, diagnosis may be delayed for several months because early behavior appears to be relatively normal. Some infants may have additional abnormalities at birth including seizures, myoclonus (spasm or twitching of a muscle or group of muscles), and respiratory problems. Treatment is palliative, and the outlook for children with hydranencephaly is poor. Hydranencephaly generally results in death before age 1.

## Questions

1. Describe the structure and shape of the corona radiata.
2. Explain the shape of the caudate nucleus and describe the relationship with the lateral ventricle.
3. Describe the shape and fibers forming the pons.
4. In a median sagittal section through the head, is the cerebellum or cerebrum normally found occupying much of the lower cranial cavity?
5. In a median sagittal section through the head, is the cerebellum or cerebrum normally found occupying much of the upper cranial cavity?



## Case Study 5-6

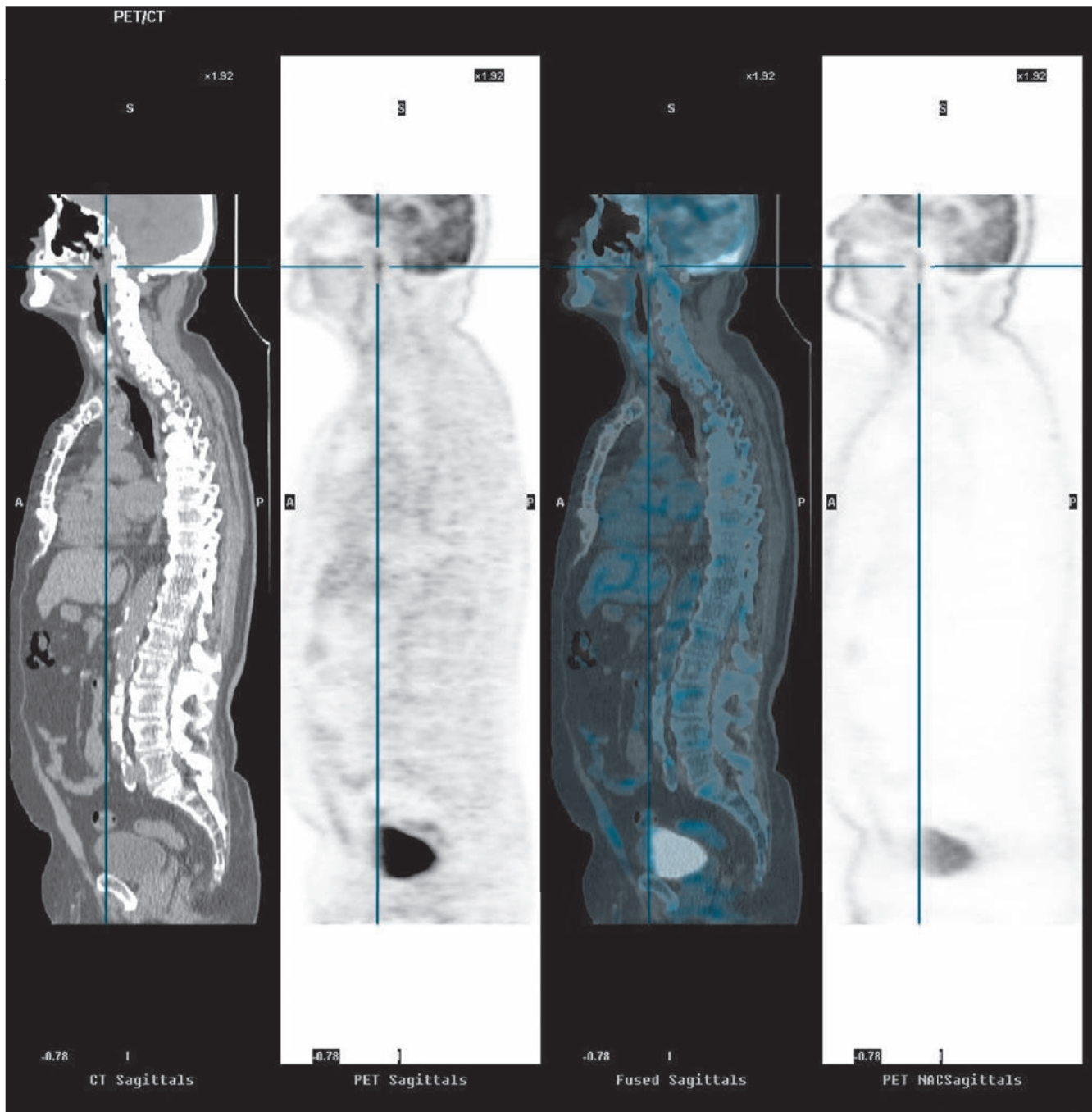


Figure 5-68

This positron emission tomography (PET)/CT case is a 68-year-old white man previously diagnosed with recurrent squamous cell carcinoma of the lung. Before the procedure, the patient received a single IV dose of 12.47 mCi of F-18 FDG for this examination. As indicated by the marker lines, a large area of abnormal uptake was found in the retropharyngeal region. CT does not show any oste-

olytic changes within adjacent vertebrae, and the hypermetabolic region corresponds with the prevertebral soft tissue structures. Because multiple lesions were also found within other regions of the body, the increased metabolic activity was determined to most likely represent squamous cell metastasis.

## Questions

1. How would squamous cell carcinoma originating within the lung travel to the head? Please list in order the anatomic structures involved in the transmission of the malignant cells.
2. Would the mass marked above best be described as superior or inferior to the circle of Willis? Please explain your answer.
3. Which part of the brain would be located posterior to the marked mass?
4. Which part of the brain is located most anteriorly?
5. What would a collection of air-filled sinuses found just above and anterior to the mass be called?



## CLINICAL APPLICATIONS

1. When imaging the head, the \_\_\_\_\_ is considered the inferior boundary of the region.
2. The \_\_\_\_\_ foramen within the greater wing of the sphenoid bone transmits the mandibular branch of the trigeminal nerve.
3. Describe the palatine bones.
4. The meningeal layers surrounding the central nervous system are the \_\_\_\_\_, closest to the skull; the \_\_\_\_\_, the intermediate layer; and the \_\_\_\_\_, closest to the brain.
5. Which of the following is not considered part of the midbrain?
  - A. Pineal body
  - B. Quadrigeminal plate
  - C. Red nucleus
  - D. Substantia nigra
6. Describe the location and function of the hippocampal formation.
7. The \_\_\_\_\_ is an enlarged region of the subarachnoid space between the cerebellum and the tentorium cerebelli.
8. Describe the location of the middle cerebral artery.
9. The optic nerve passes through the \_\_\_\_\_ bone to enter the orbital cavity.

# Chapter 6

# Neck

## OBJECTIVES

Upon completion of this chapter, the student should be able to:

1. State the superior and inferior boundaries of the neck.
2. Explain the distinguishing characteristics of the third through sixth cervical vertebrae.
3. Describe the atlas and axis.
4. Describe the glandular structures located within the neck.
5. Identify and describe the cartilaginous structures forming the larynx.
6. Describe the openings within the larynx and pharynx.
7. Identify and describe the folds of skin found within either the larynx or the pharynx.
8. Identify and describe the major vessels within the neck.
9. Describe the position of major vessels within the neck in relation to other structures.
10. Correctly identify anatomical structures on patient computed tomography (CT) and magnetic resonance (MR) images of the neck.

## ANATOMICAL OVERVIEW

The anatomy within the neck is generally symmetrical and is described as the region between the base of the skull and the bony thoracic cage.

### ■ Skeleton

**Cervical** (*SER-vĭ-kal*) **vertebrae**. The uppermost seven vertebrae located between the base of the skull and the thoracic vertebrae (Fig. 6-1). Easily distinguished from other vertebrae by their small size and the foramina (*fō-RAM-i-nă*) in their transverse processes, the transverse foramina (Figs. 6-2 to 6-4).

**Atlas**. The first cervical vertebra, which supports the head. Named for Atlas, the mythical Greek Titan who was thought to have supported the world on his shoulders. The most atypical vertebra, because it lacks a body and a true spinous process and is roughly circular in shape (Fig. 6-2). The front and back of the vertebra are formed by the anterior and posterior arches; the lateral masses form the sides.

**Anterior arch**. Marked feature of the atlas. An arch of bone with a central expanded area, the anterior tubercle

(*TŪ-ber-kl*). In the vertebral (*VER-tĕ-brăĭl*) column, the centrum that would have given rise to the body of the atlas is fused to the second cervical vertebral body and is directly posterior to the anterior arch.

**Posterior arch**. Does not have a true spinous process, which would be expected; instead, has a much smaller posterior tubercle.

**Lateral mass**. The bulky bony structures lateral to the vertebral foramen (*fō-RĀ-men*) with articular facets. The superior articular facets correspond to the occipital condyles (*ok-SIP-i-tăĭl KON-dĭlz*) and are large oval-shaped structures facing medially and upward. They are usually constricted in the middle and may be divided in some individuals. The inferior articular facets are also large but are roughly round in shape.

**Axis**. The second cervical vertebra, or epistropheus (*ep-i-STRŌ-fĕ-ŭs*), forms the pivot for rotation of the atlas and head. It is easily distinguished by the body, which is long and extends cranially, forming the dens, or odontoid process (Fig. 6-3).

**Dens**. A bony structure, roughly 1.5-cm long, that projects from the vertebral body of the axis and acts as the body for the atlas. Highly involved in the rotational and nodding

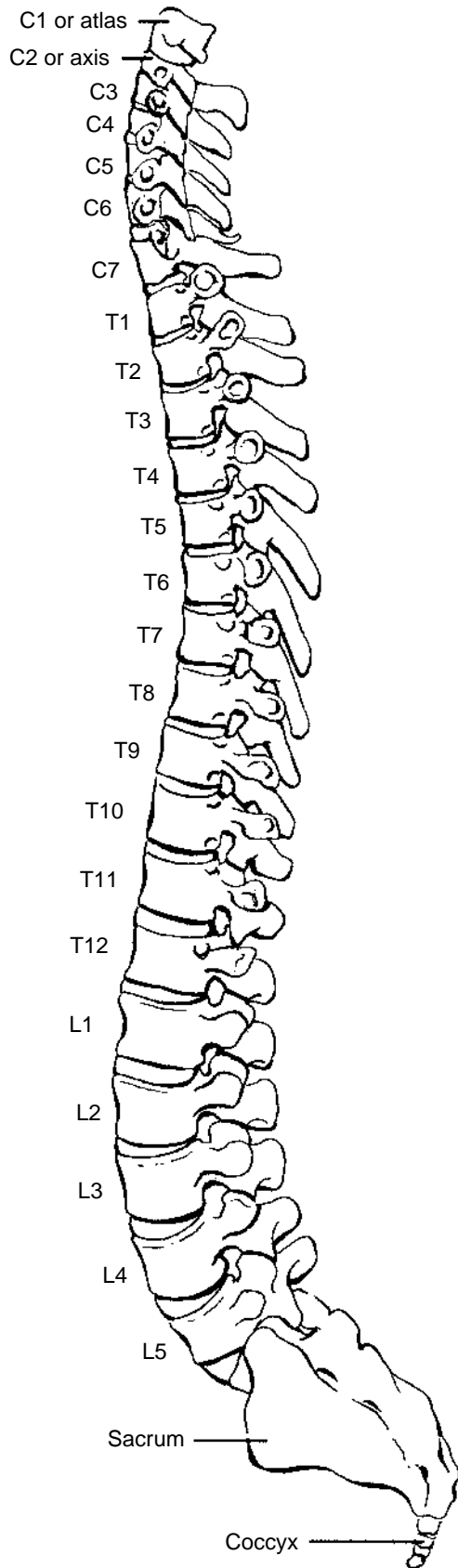


**Figure 6-1** Lateral view of entire vertebral column.

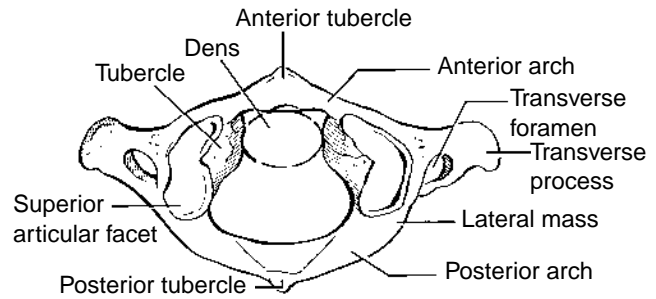


**Figure 6-2** Superior view of the atlas.

movements of the head and is often the sight of trauma. When the head is forced into hyperflexion or hyperextension, as in whiplash injuries, it may become fractured. Because it forms the anterior wall of the spinal foramen, a fracture may be life-threatening if the spinal cord is involved. Hence, immobilization is critical when neck injury is suspected.

**C3 through C6.** The typical cervical vertebrae can be divided into two main parts: A body and a vertebral arch, which surround and house the spinal cord (Fig. 6-4).

*Vertebral foramina.* Large and triangular openings within the cervical vertebrae between the body and the vertebral arch. Although thoracic and lumbar vertebrae are larger than cervical vertebrae, their vertebral foramina are smaller and rounder.

*Spinous processes.* The terminal processes of cervical vertebrae are usually bifid, resulting in tubercles of unequal size. Except for C6 and C7, cervical vertebrae have shorter spinous processes than other vertebrae. The spinous processes of C6 and C7 are longer than those of other vertebrae and extend caudally in the median plane.

*Transverse processes.* The most distinctive feature of cervical vertebrae are the transverse foramina, which are located centrally in the processes and encase the vertebral arteries and veins.

*Articular (ar-TIK-yū-lār) processes.* The bony structures directly lateral to the vertebral foramen. They extend upward and downward from the points where the pedicles

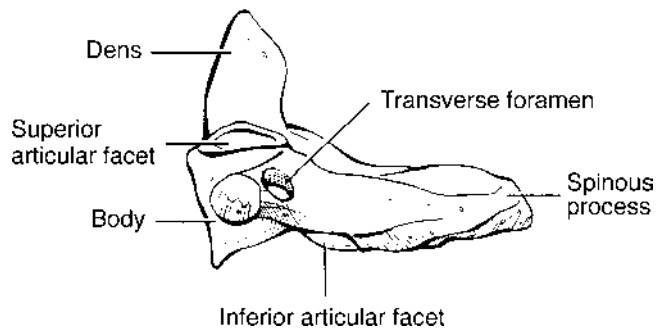


**Figure 6-3** Lateral view of the axis.



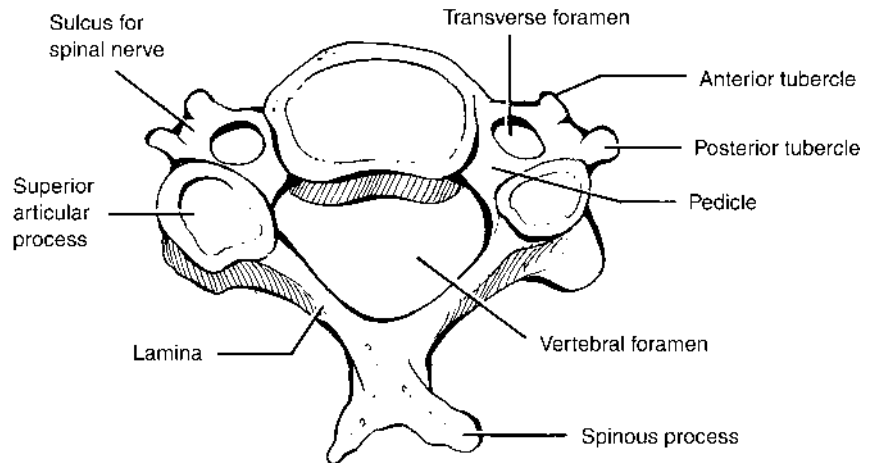


**Figure 6-4** Superior view of a cervical vertebra.

(*PED-ĭ-klz*) and laminae (*LAM-i-nē*) join. The upward projection, the superior articular process, has the articular surface facing posteriorly. The adjacent surface, the inferior articular process, is the downward projection of bone that faces anteriorly. Together, the processes form the zygapophyseal (*ZĪ-gă-pō-FIZ-ē-ăl*) joints between adjacent vertebrae.

**Vertebra prominens** (*PROM-i-nens*). C7 is the most distinctive of the lower cervical vertebrae, owing primarily to its large spinous process. The process is a thick bony projection that extends in a horizontal fashion posteriorly and can be easily palpated on the posterior base of the neck. In contrast to the typical vertebrae, the spinous process is not bifid, but ends in a single tubercle. Because this structure is easily distinguished on a lateral radiograph and can be easily palpated, it is often used as a landmark for the separation between the cervical and thoracic vertebrae.

**Hyoid** (*HĪ-oyd*). A U-shaped bone located just below the mandible at the level of C3 (Fig. 6-5). It can be located by placing the thumb under the chin and moving it backward until it stops at the angle of the neck. This angle is formed by a series of flat muscles that originate at the mandible and thoracic cage and insert on the hyoid bone. The bone also has ligamentous attachments with the larynx, or the voice box (Fig. 6-6).

## ■ Cartilage and Other Structures

**Larynx** (*LAR-ingks*). Commonly called the voice box. Part of the air passageway in the anterior neck. Averages approximately 4.5 cm in length, but is typically shorter in women and children, and extends from the level of C3 to C6 (Fig. 6-5). The laryngeal (*lă-RIN-jē-ăl*) cartilages are uniquely arranged and are interconnected by a series of ligaments and muscles capable of voice production (Fig. 6-6).

**Thyroid** (*THĪ-royd*) **cartilage**. Found just below the hyoid bone. The largest of the cartilaginous structures within the larynx. Similar to the hyoid, it is roughly U shaped, is open posteriorly, and has an irregular surface. Anteriorly, its superior margin forms the laryngeal prominence (commonly called the Adam's apple) at the approximate level of C4 (Fig. 6-5).

**Epiglottis** (*ep-i-GLOT-is*). Single spoon-shaped cartilage that closes the opening of the larynx when food or drink is moved down the pharynx (Fig. 6-6). As seen posteriorly, its inferior part is narrow and anchors to the thyroid cartilage. Superiorly, it is larger, extending upward adjacent to the hyoid bone to a position posterior to the tongue. As food or drink is swallowed, the tongue moves posteriorly, bending the epiglottis over the opening of the larynx.

**Cricoid** (*KRĪ-koyd*) **cartilage**. Single cartilage found in the larynx just below the thyroid cartilage. It encircles the airway. Seen from above, it is circular; when viewed from the lateral aspect, the ring is much wider posteriorly. Consequently, the posterior cricoid cartilage may be visualized without the anterior portion in axial sections.

**Arytenoid** (*ar-i-TĒ-noyd*) **cartilages**. From a posterior view of the larynx, the two pyramid-shaped cartilages are found resting on the posterior cricoid cartilage. Owing to the wide posterior arch of the cricoid cartilage, these cartilages are just below the laryngeal prominence of the thyroid cartilage.

**Aryepiglottic** (*AR-ē-ep-i-GLOT-ik*) **folds**. As seen in median section, a fold of skin on each side extends between the arytenoid cartilage and the margin of the epiglottis. Besides covering the ligaments connecting the cartilaginous structures, they mark the lateral boundaries between the larynx and the pharynx.

**Vocal cords** (or folds). The ligaments extending between the arytenoid cartilages and the thyroid cartilage covered with a mucous membrane. Muscles acting on the cartilages move them with respect to one another, changing the tension



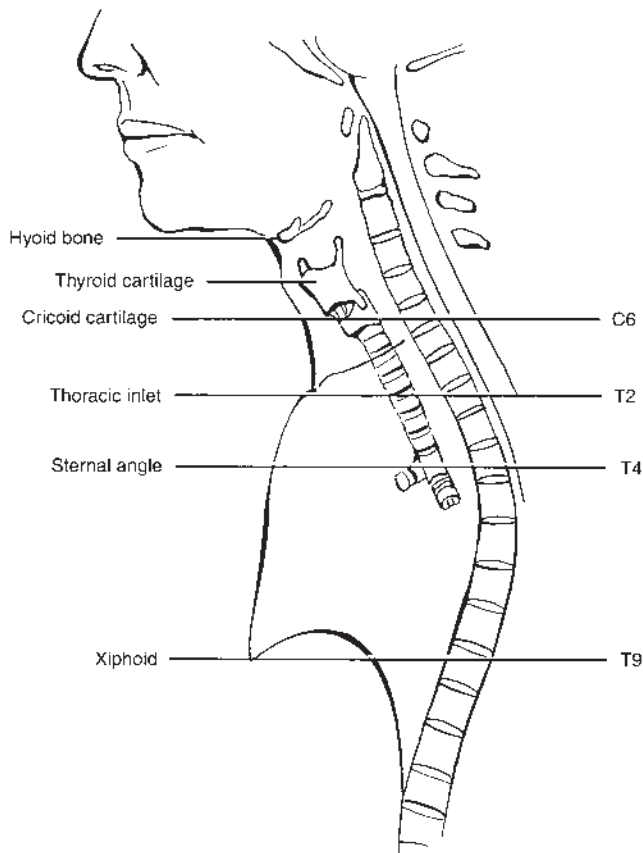


**Figure 6-5** Relationships of cervical and thoracic vertebrae to the major airway structures.

of the ligaments and modulating the sound emitted when air moves through the larynx.

**Vestibular** (*ves-TIB-yū-lār*)  **folds**. Often called the false vocal cords. The mucous membrane structures situated just above the glottic space. Unlike the vocal folds, they do not have an underlying ligament and have little to no role in voice production.

**Laryngeal vestibule**. A space within the upper larynx bounded by the aryepiglottic folds, epiglottis, arytenoid cartilages, and vestibular folds. In sectional images, it is seen immediately behind the epiglottis.

**Glottic** (*GLOT-ik*)  **space**. Also called the ventricle (*VEN-tri-kl*). The space within the larynx bounded by the vestibular folds and the vocal folds.

**Infraglottic space**. The opening within the larynx below the vocal folds that is continuous inferiorly with the opening of the trachea.

**Trachea** (*TRĀ-kē-ă*). The major airway, extending from the larynx and terminating in the main bronchi (*BRONG-kī*), from approximately the level of C6 to T4. Centrally located in the neck and immediately anterior to the esophagus and the vertebral bodies.

**Pharynx** (*FAR-ingks*). A muscular tube extending from the base of the skull to the level of approximately C6, where it is continuous with the esophagus (Fig. 6-7). Lies adjacent to the vertebral bodies and is divided into several parts: Nasopharynx, oropharynx, and laryngeal pharynx.

**Nasopharynx** (*NĀ-zō-FAR-ingks*). The first division of the pharynx. Located posterior to the nasal cavity and extending from the base of the skull to the soft palate.

**Oropharynx** (*ŌR-ō-FAR-ingks*). The second division of the pharynx. Located posterior to the oral cavity and extending from the soft palate to the tip of the epiglottis.

**Median glossoepiglottic** (*GLOS-ō-ep-i-GLOT-ik*)  **fold**. The fold of skin that extends between the posterior tongue and the tip of the epiglottis (Fig. 6-8).

**Valleculae** (*vă-LEK-yū-lē*). Spaces on either side of the median glossoepiglottic fold, between the posterior tongue and the epiglottis. During swallowing, the tongue moves backward folding the valleculae and bending the epiglottis to close the opening to the larynx.

**Laryngeal pharynx**. The third division of the pharynx. Located posterior to the larynx (Fig. 6-7). In a coronal section through the posterior pharynx, the aryepiglottic folds are bilaterally situated around the inlet of the larynx, marking the boundary between the pharynx and larynx.

**Piriform** (*PIR-i-fōrm*)  **sinuses**. Within the laryngeal pharynx, a sinus can be found on either side of the larynx.

**Esophagus** (*ē-SOF-ă-gŭs*). Originates at the level of C6, at the end of the pharynx. Situated medially, just anterior to the vertebral bodies, and descends inferiorly to terminate at the stomach. In sectional images, it is between the trachea and the vertebral bodies near the median plane of the body.

## ■ Other Viscera (*VIS-er-ă*)

**Submandibular** (*sŭb-man-DIB-yū-lār*)  **glands**. A pair of glands just below the mandible (*MAN-di-bl*), on either side, that are easily palpable as a spongy area just below the posterior half of the mandible (Fig. 6-9). They are the second largest salivary glands, about the size of a walnut. Secretions from the glands are drained by the submandibular duct (Wharton's duct) to an opening in the anterior floor of the mouth.

**Thyroid gland**. U-shaped single gland, just inferior to the larynx in the anterior neck, that surrounds the upper region of the trachea. Its two lobes are situated on either side of the trachea, connected by a narrowed region, called the isthmus, on the anterior trachea.

## ■ Arteries

**Common carotids** (*ka-ROT-idz*). On the right side, the carotid originates from the brachiocephalic artery; on the

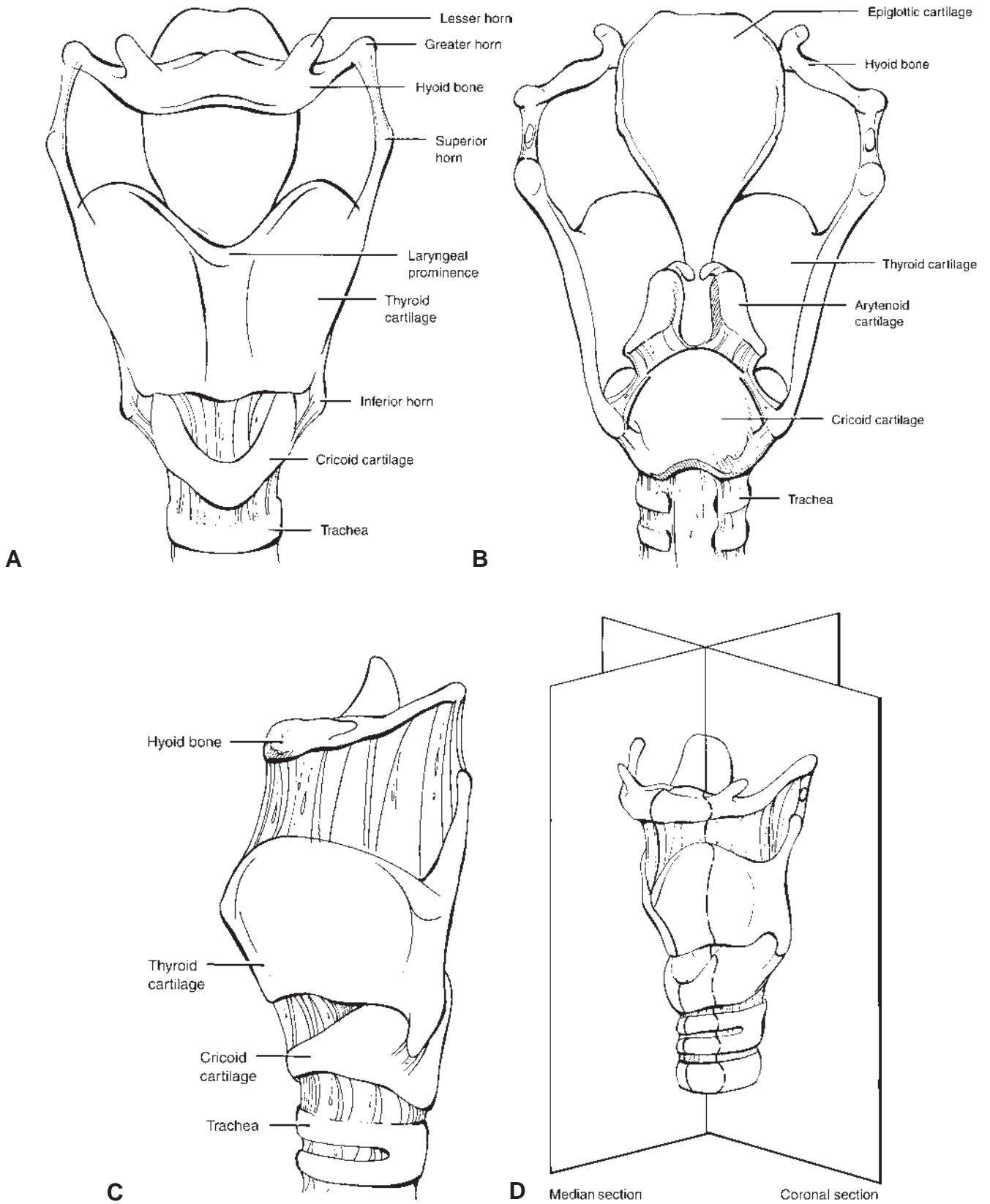


**Figure 6-6** The larynx. **A:** Anterior; **B:** Posterior; **C:** Left lateral aspect; **D:** Left anterolateral aspect demonstrating planes of section. (continued)

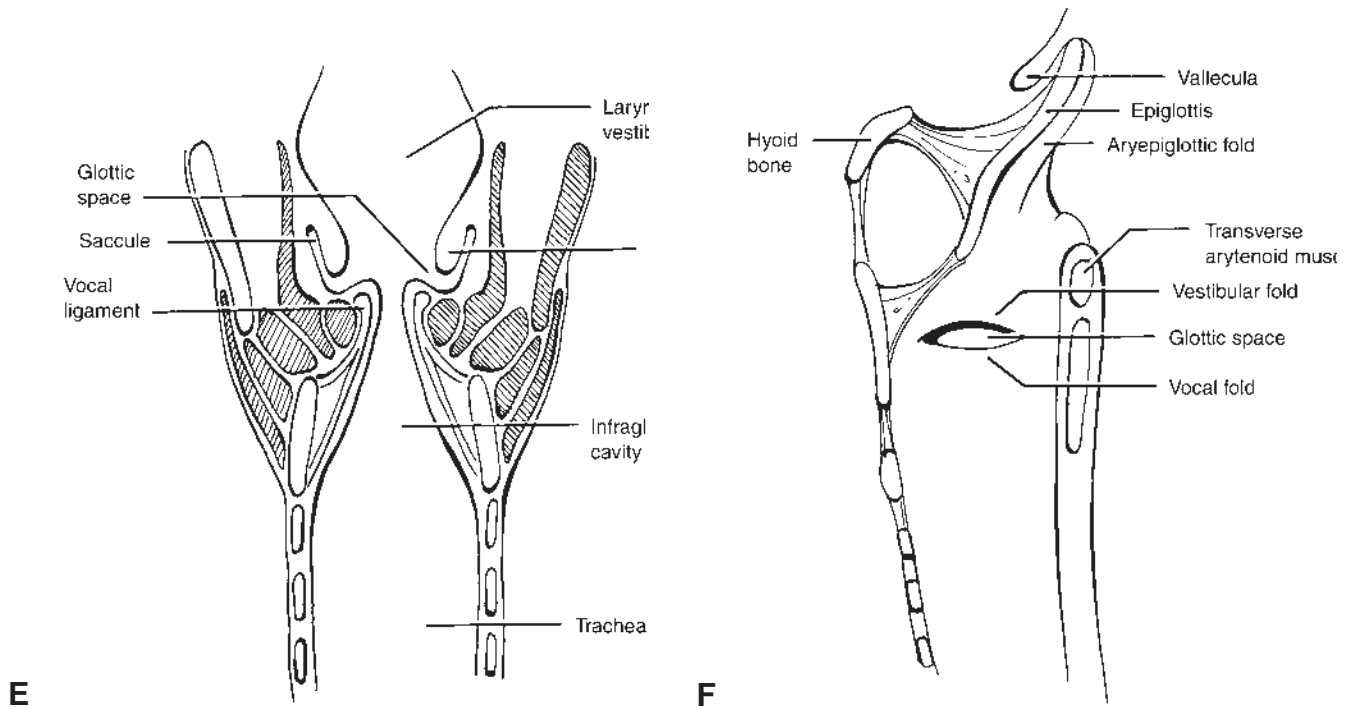


**Figure 6-6** The larynx. (*continued*) **E:** Coronal section; **F:** Median section.

left side, it is the second major branch off the aortic arch. On both sides, they ascend through the neck, with the internal jugular veins, beside the trachea. Above the thyroid cartilage, or at approximately the level of the intervertebral disk between C3 and C4, they bifurcate into the internal and external carotid arteries.

**Internal carotids.** Originating from the common carotid arteries, they ascend through the neck next to the internal jugular veins. At the base of the skull, they exit the upper neck through the carotid foramen to supply blood to the middle and anterior cerebrum (*SER-ě-brĭm*) (Fig. 6-10).

**External carotids.** Arising from the common carotid arteries, they ascend through the upper neck to supply blood to the external head. They are more superficially located in the anterior neck than are the internal carotids.

**Vertebals.** As the name implies, they are closely associated with the vertebral column and ascend through the transverse foramina of the cervical vertebrae. On both sides, they originate from the subclavian (*sŭb-KLĀ-vē-an*) arteries and enter the skull through the foramen magnum (*MAG-nŭm*) to supply blood to the posterior brain.

## ■ Veins

**Internal jugulars** (*JŮG-yŭ-larz*). Two major veins located on either side of the neck next to the common carotid arteries. They are more superficial and usually larger than the adjacent arteries (Figs. 6-9 and 6-11).

**External jugulars.** Originating from the superficial head, they descend superficially through the neck and terminate in the subclavian vein. Their slow gentle pulse can usually be felt near the middle of the sternocleidomastoid muscle. Besides providing a reference for palpating the vein, the sternocleidomastoid muscle is also a useful landmark for identifying the external jugular vein in sectional images.

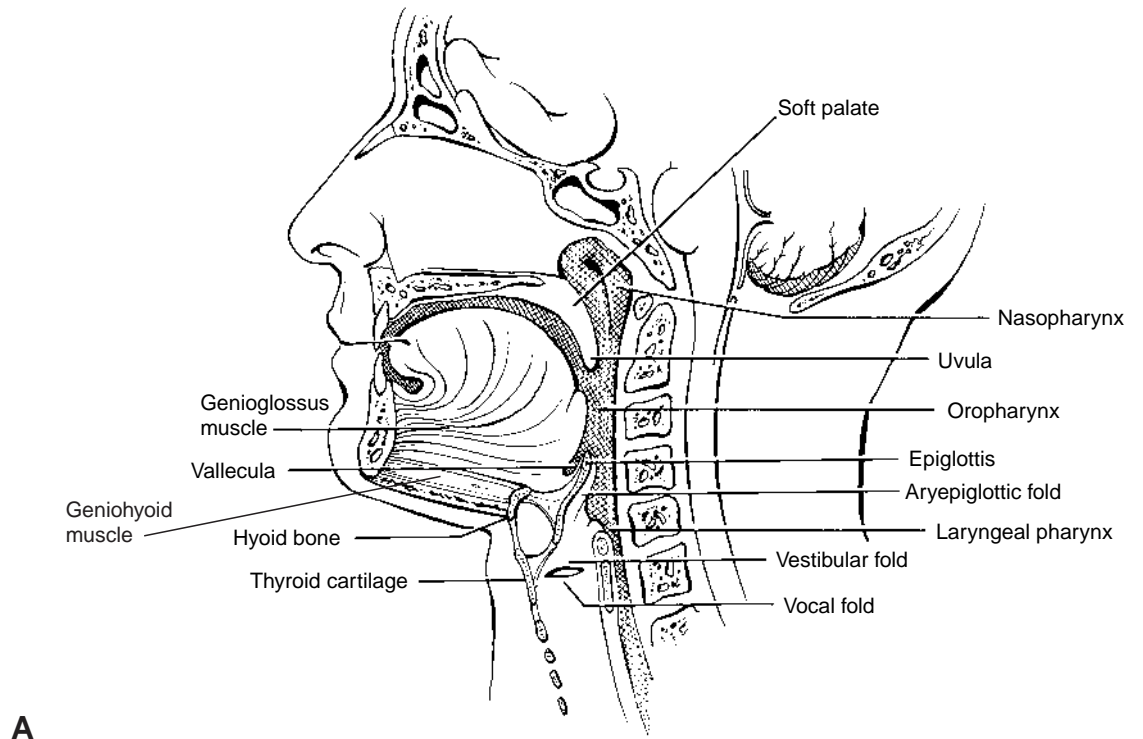
**Retromandibular** (*RE-trō-man-DIB-yŭ-lār*). Two smaller veins on either side of the head just posterior to the mandible. They originate from smaller veins in the temporal (*TEM-pō-rĕl*) and maxillary (*MAK-si-lār-ē*) regions and descend to terminate in the external jugular veins. During their course, they pass within the parotid (*pĀ-ROT-id*) glands and are superficial to the external carotid arteries.

**Vertebals.** The venous plexuses (*PLEK-sŭs-ez*) within the transverse foramina surrounding the vertebral arteries on either side of the neck. They drain blood from the spine and descend into the chest, emptying into the subclavian veins.

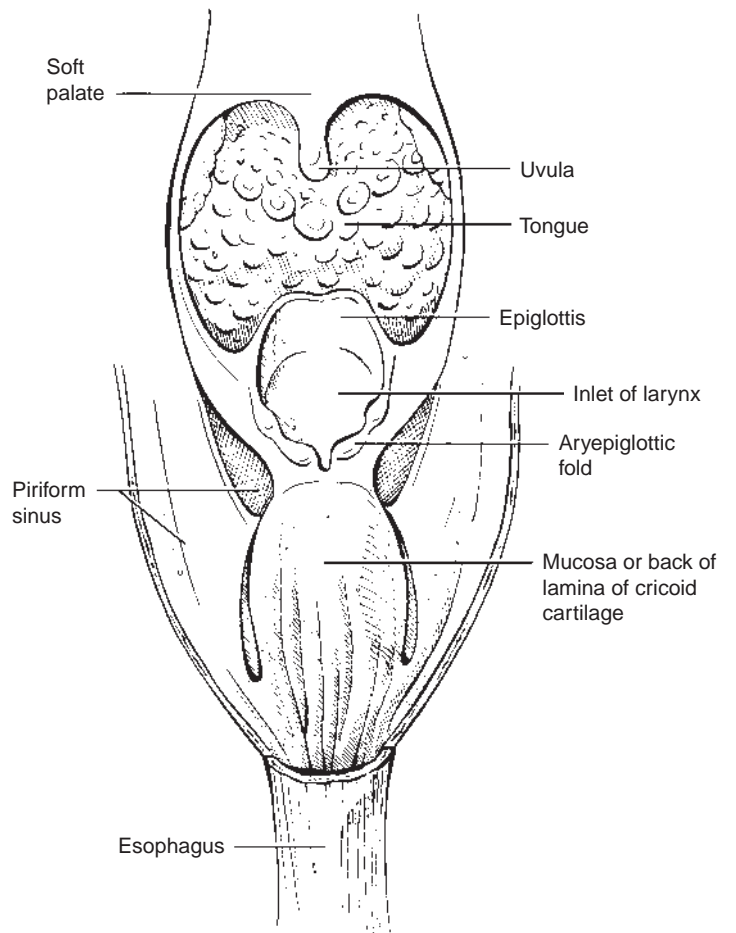
## ■ Muscles

All are bilateral.

**Genioglossus** (*JĚ-nē-ō-GLOS-ŭs*). Originate from the superior mental spine on the posterior aspect of the mandible and insert on the hyoid bone. These are large,



A



B

**Figure 6-7** The pharynx. **A:** Median section; **B:** Posterior view of a coronal section.

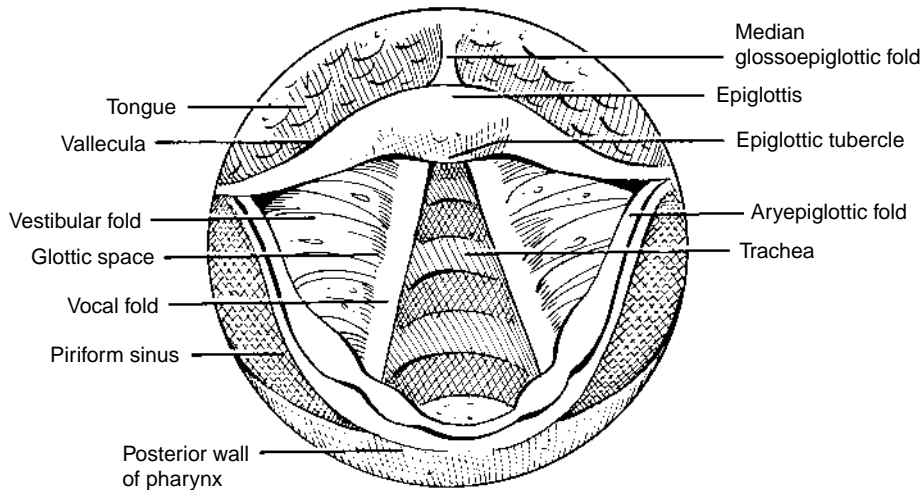


**Figure 6–8** Superior aspect of the larynx during inspiration.

thick muscles that form the majority of the musculature of the tongue.

**Geniohyoid** (*jě-NĪ-ōw-HĪ-oyd*). Originate from the inferior mental spine and insert on the hyoid bone just below the genioglossus muscle. These thin strap muscles act to raise the hyoid and depress the mandible.

**Sternocleidomastoid** (*STER-nō-KLĪ-dō-MAST-toyd*). Originate from the sternum and clavicle and insert on the mastoid process of the temporal bone. Their action is generally described as bending and rotating the head. Owing to their superficial location, they provide landmarks for identifying superficial structures within the neck.

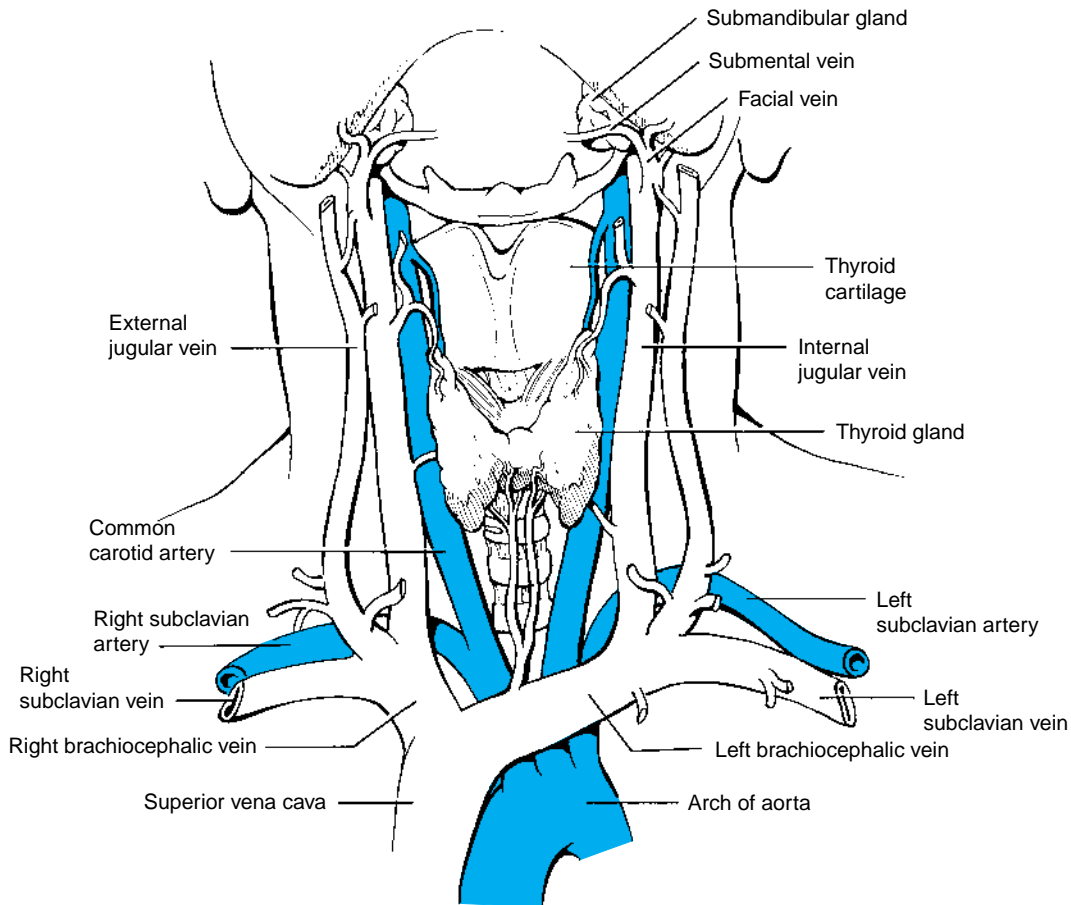


**Figure 6–9** Major vessels in the neck.

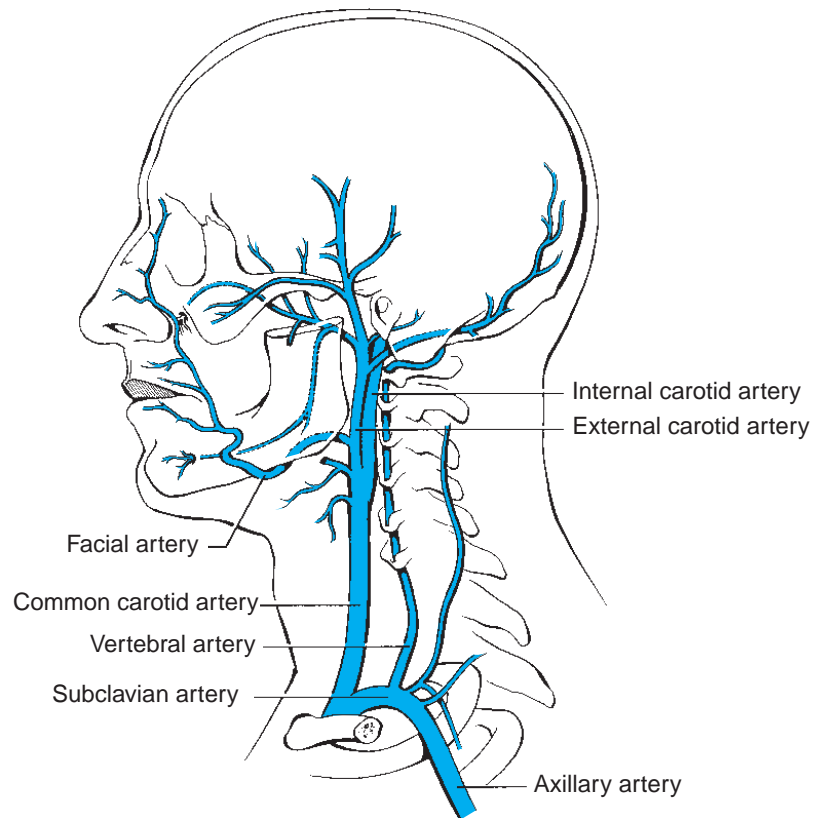


**Figure 6–10** Major arteries of the head and neck from the left lateral aspect.

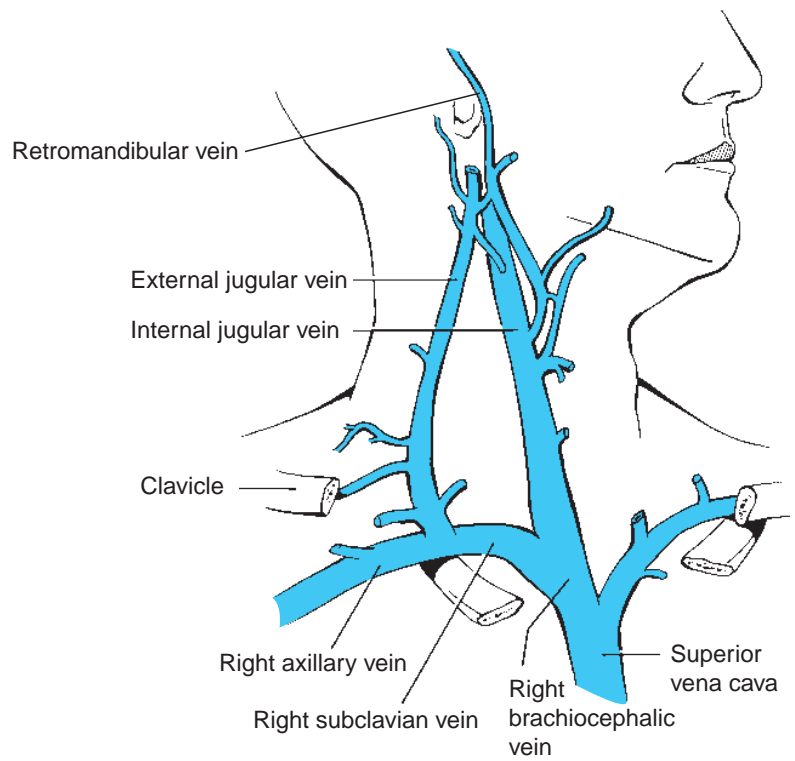


**Figure 6–11** Major veins of the head and neck from the right anterolateral aspect.



## Sagittal MR Images

The following two sagittal MR images of the neck are described at 5.0 mm intervals from the midsagittal plane to the left side. The right side is not described, because the structures are similar to those described on the left side.

The images were generated at the following technical factors: repetition time (TR) = 500 ms; echo time (TE) = 20 ms; radiofrequency (RF) = 90°; field of view (FOV) = 30 cm.

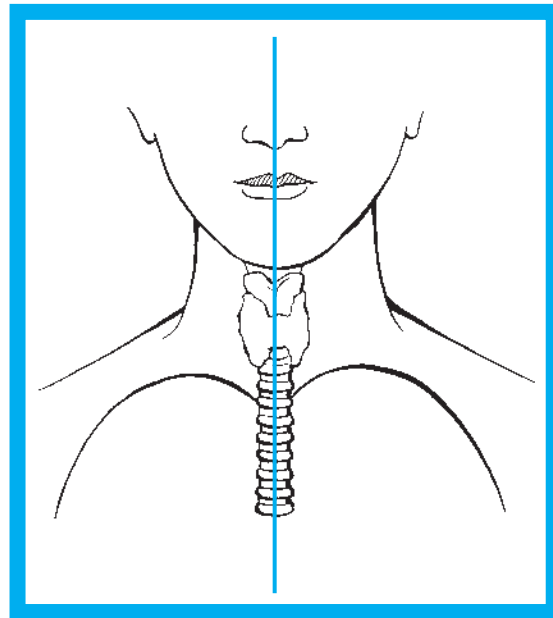


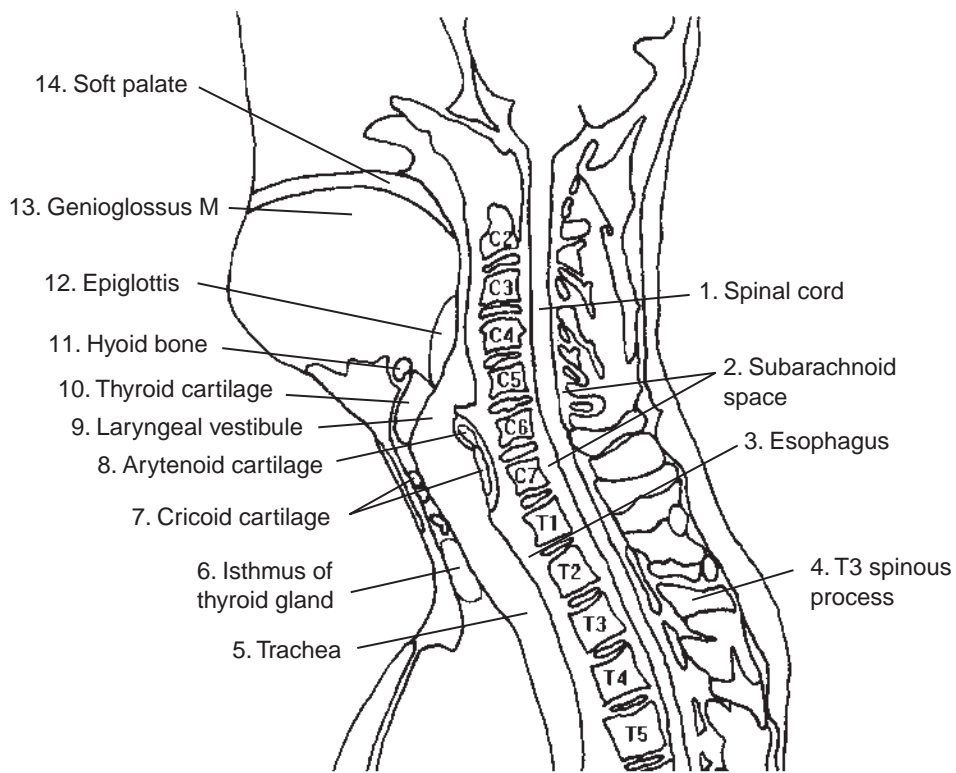
**Figure 6–12 (A,B)** Sagittal MR image 1.

Near the center of the image, the bodies of the cervical and thoracic vertebrae are shown in cross-section to form a highly organized pattern. Just behind the vertebral bodies, the subarachnoid space is shown on either side of the spinal cord. Based on the thickness of the spinal cord and its presence through most of the image, this anatomy lies near the midsagittal plane. Posterior to the spinal canal, the spinous processes of the cervical and thoracic vertebrae are seen projecting posteriorly and are covered by a layer of superficial fat. Anterior to the vertebral column, the openings of the pharynx, larynx, and surrounding soft tissue structures are cross-sectioned. In the region of the nasopharynx, the soft palate projects posteriorly from the hard (or bony) palate to separate the nasopharynx from the oropharynx. Directly below the soft palate, the genioglossus muscle is shown to be the largest muscle found within the tongue. On the lower aspect of the genioglossus muscle, the cartilage of the epiglottis can be identified, forming part of the anterior wall of the oropharynx. As described earlier, the epiglottis attaches inferiorly to the thyroid cartilage, which is located just below the hyoid bone. Although both of these structures are U shaped, the thickness of the image demonstrates only their most anterior parts, causing them to appear irregular, or oval. The thyroid cartilage forms part of the upper larynx and contains the laryngeal vestibule. Because this section is taken through the midsagittal plane, the vestibular and vocal folds are not seen. The arytenoid and the cricoid cartilages, however, are cross-sectioned adjacent to the lower laryngeal space. Below the larynx, the isthmus of the thyroid gland is cross-sectioned as it extends between the lobes located on either side of the trachea. Between the trachea and the vertebral column, the esophagus is labeled as it extends from the region of the laryngeal pharynx down to the stomach.





A



B



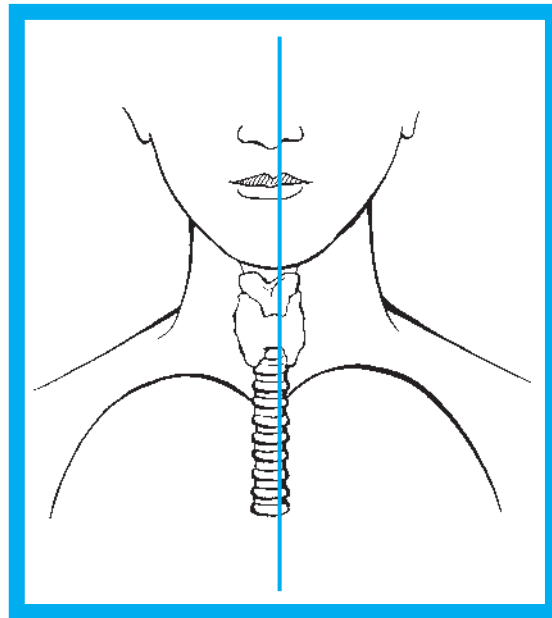
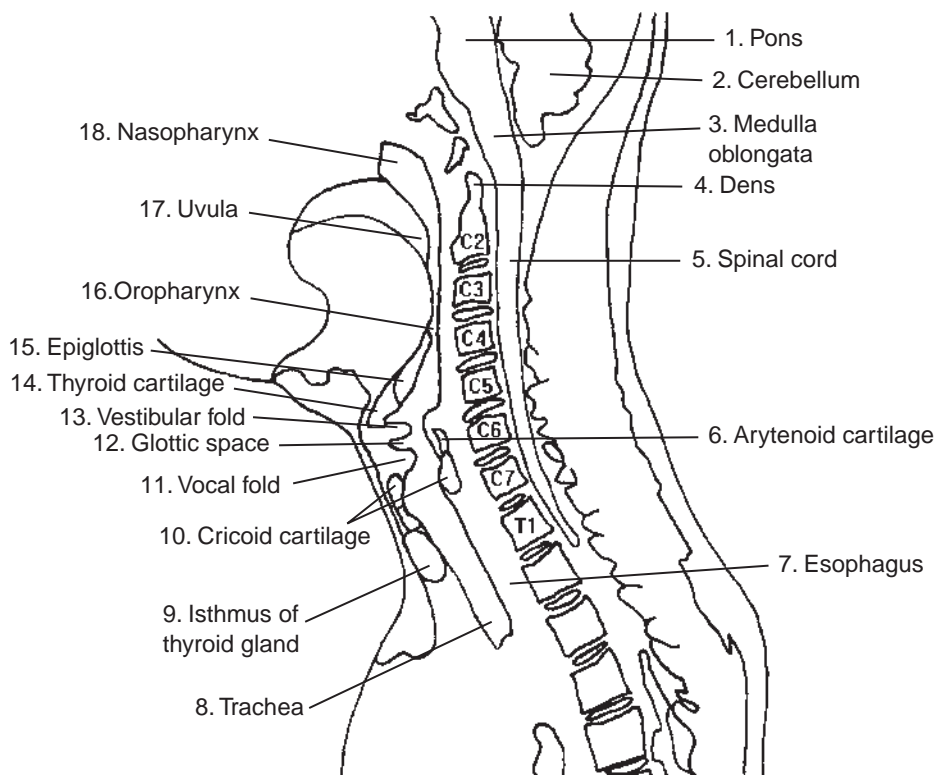


**Figure 6–13 (A,B)** Sagittal MR image 2.

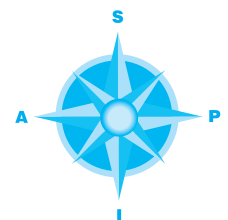
As in the previous image, this image shows the regular pattern of the cervical and thoracic vertebrae; however, here the spinal cord is slightly thicker superiorly where it joins the brainstem, located within the skull cavity. In this image, the medulla oblongata and the pons are shown just anterior to the cerebellum. Lying just below the skull, a projection of bone (the dens) is sectioned, extending upward from the body of C2 to form the body of C1, the atlas. The dark area behind the nasal cavity, representing the nasopharynx, lies above the soft palate and is shown with its most caudal extension, the uvula (*YŪ-vyū-lā*). Below the nasopharynx, the oropharynx is the space posterior to the tongue between the uvula and the epiglottis. Below the level of C4, the spinal cord begins to narrow and is absent through much of the thoracic region, indicating that the lower half of the image demonstrates structures on the patient's left side. Because this image is slightly to the left of the midsagittal plane, we can now identify the vestibular fold above the vocal fold, or true vocal cord. Both of these folds extend between the thyroid and the arytenoid cartilages. As described earlier, the arytenoid cartilage is found resting on the posterior part of the ring-shaped cricoid cartilage. Between the folds of skin, the middle laryngeal space can now be labeled the glottic space. As in the previous image, the trachea can be seen as it extends downward from the larynx between the isthmus of the thyroid gland and the esophagus.



A



B





## Axial CT Images

The following 18 axial CT images of the neck are described at 5.0 mm intervals from superior to inferior. The images were generated immediately after the administration of

100 mL venous contrast at the following scanning factors: 120 kVp (kilovolt peak) and 150 mA-s (milliamperere-second).

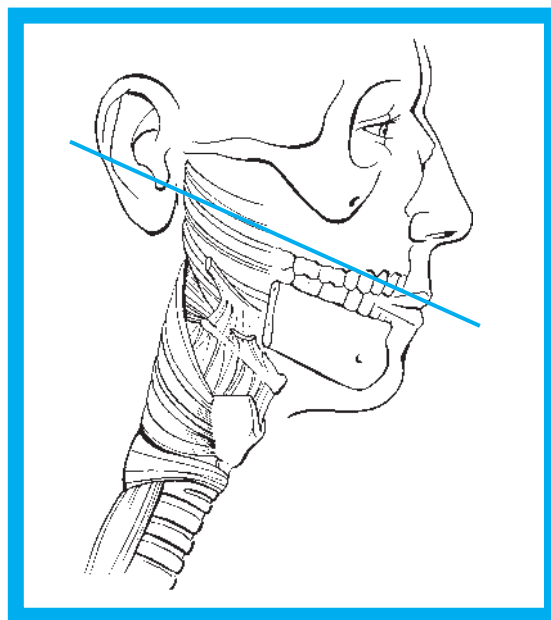
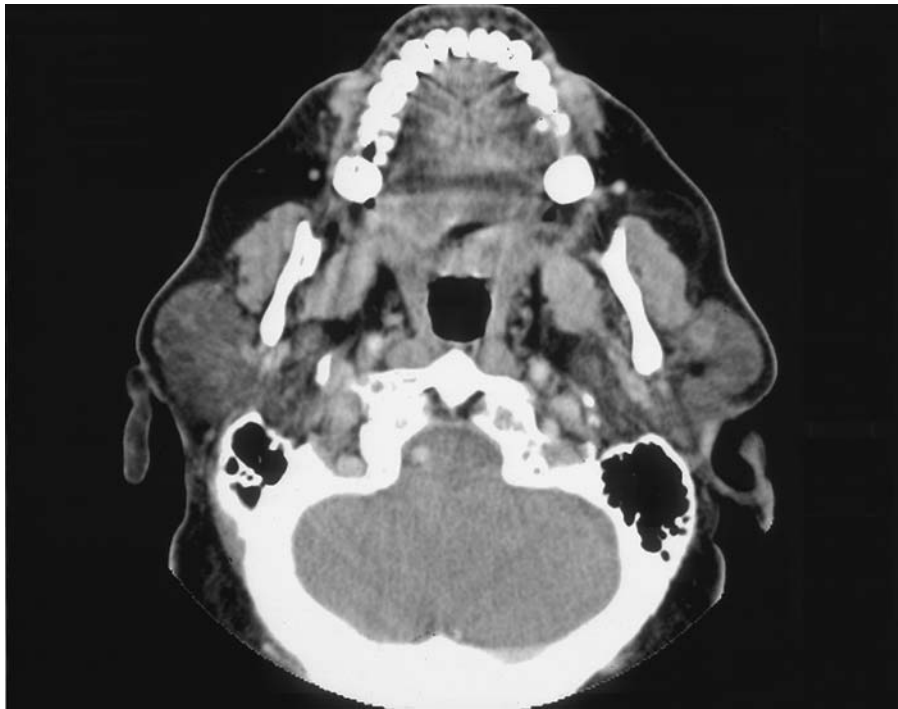
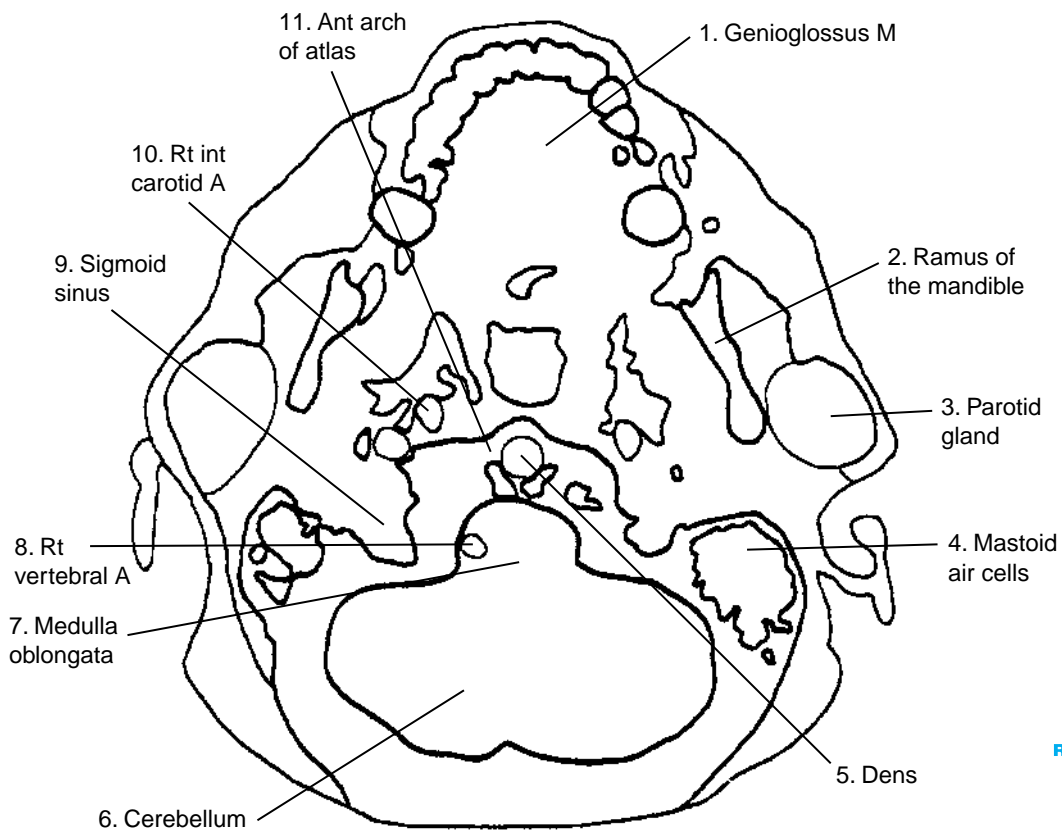


**Figure 6–14 (A,B)** Axial CT image 1.

When looking at the bony anatomy in this image, one can readily identify the lower teeth in front of the rami of the mandible. Within the temporal bone, the mastoid air cells can be easily identified on either side. Medially, projections from the occipital bone appear continuous with the anterior arch of the atlas, which surrounds the dens that projects upward from the vertebral body of C2. Surrounded by the occipital bone, the contents of the lower posterior cranial fossa are labeled the cerebellum and the medulla oblongata. On either side of the medulla oblongata, the vertebral arteries should be found; however, only the contrast-enhanced right vertebral artery can be identified in this patient. The sigmoid sinus is found on either side in what appears as a notch in the lower petrous part of the temporal bone; it will be shown at lower levels to drain into the internal jugular vein. Anteriorly, the internal carotid arteries are the contrast-enhanced structures near the atlas, or C1. Superficial to these vessels, the parotid gland can be identified by its characteristic consistency on either side posterolateral to the rami of the mandible. Similar to the sagittal sections, the soft tissue structure within the mouth is labeled the genioglossus muscle.



A



B

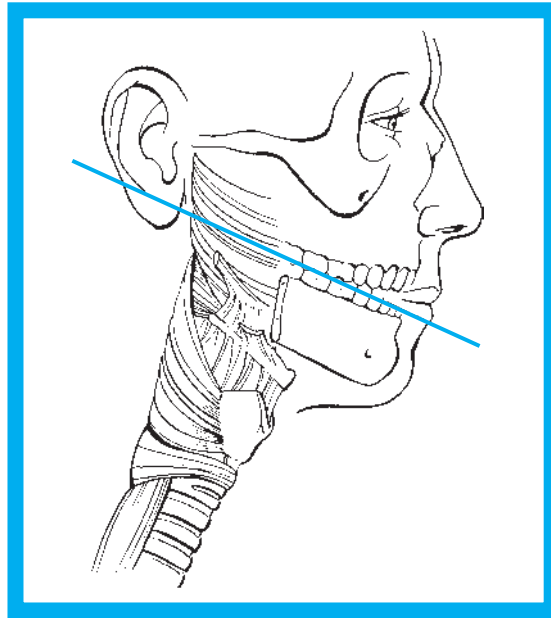
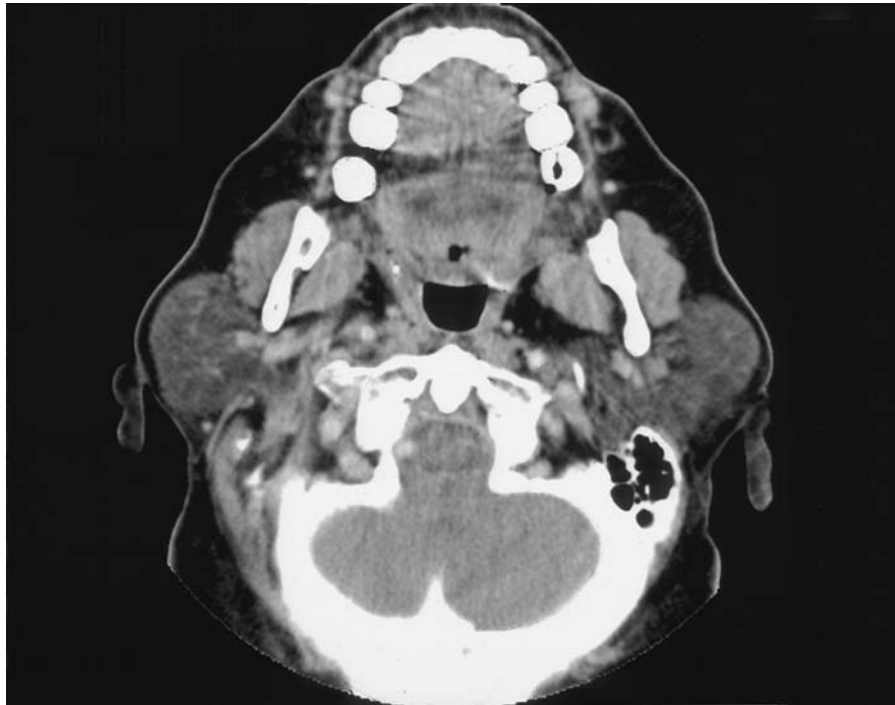
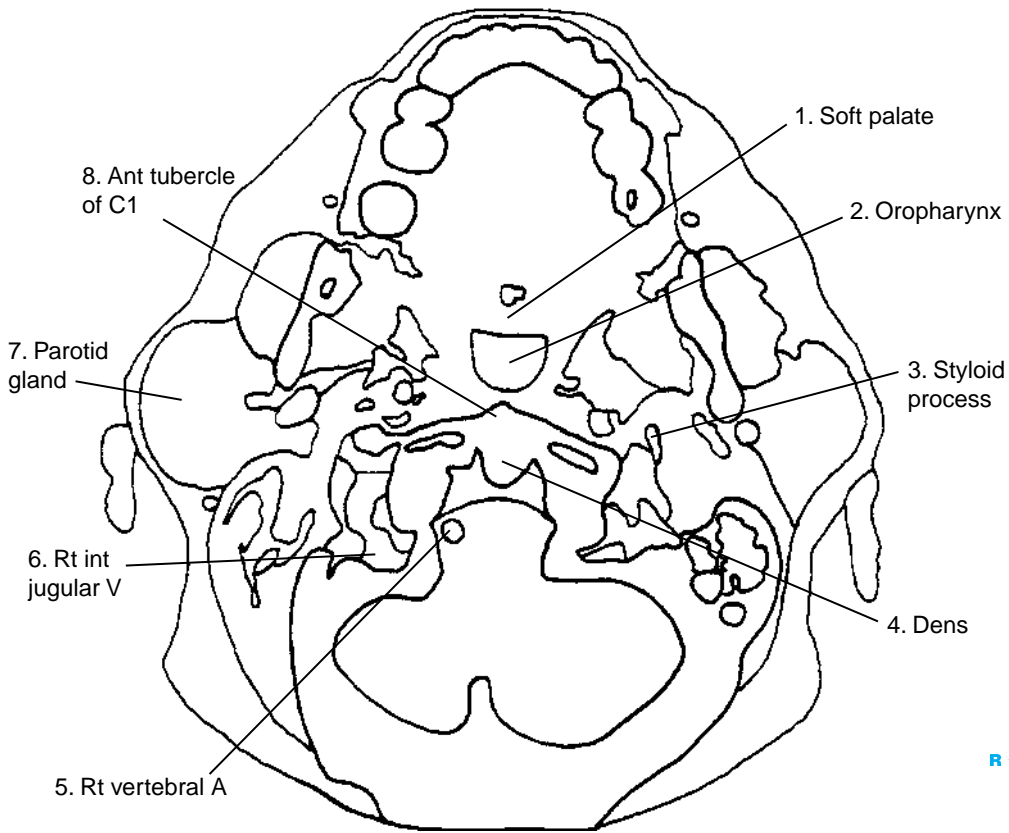


**Figure 6–15 (A,B)** Axial CT image 2.

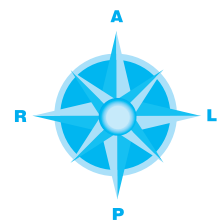
The lower teeth and the mandibular rami can be readily identified on the anterior part of this image. Posteriorly, the lower parts of the occipital and temporal bones are shown with the anterior part of C 1, the atlas; the dens is seen projecting from the body of C2, the axis. The vertebral artery can be seen on the right side of the patient; the left does not appear enhanced by contrast. Within what appears as a notch in the lower petrous part of the temporal bone, the sigmoid sinus is now labeled the internal jugular vein, because it is exiting the skull. On the left side of the patient, a small section of the styloid process of the temporal bone is sectioned between the atlas and the superficially situated parotid gland. Medially, the oropharynx appears as a radiolucent area directly behind the soft palate.



A



B



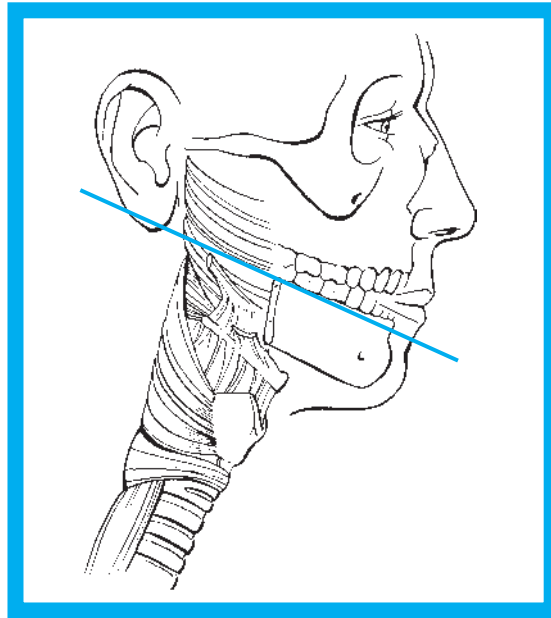
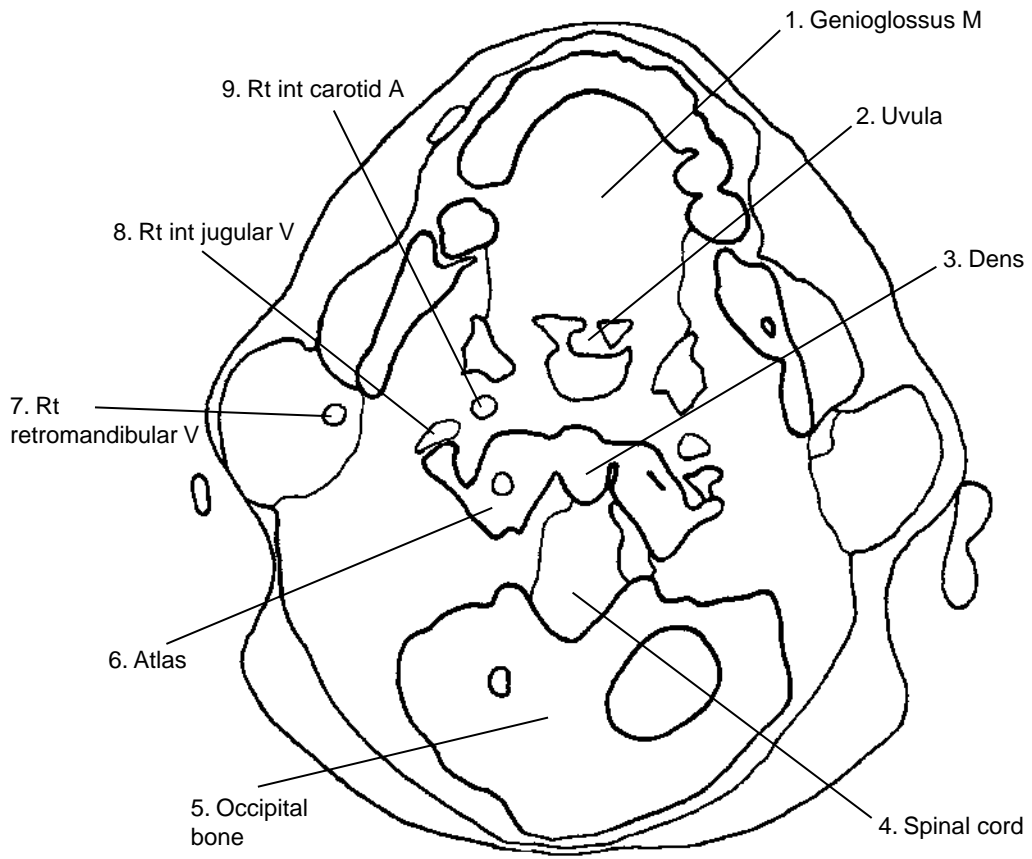


**Figure 6–16 (A,B)** Axial CT image 3.

Similar to previous images, the dens can readily be identified centrally along with the adjacent atlas, C1. At this level, the spinal cord is found between the cervical spine structures and the lower part of the occipital bone, because it lies below the level of the foramen magnum. Anterior to the cervical spine, the contrast-enhanced internal carotid artery and internal jugular vein can be identified on the right. In general, the carotid artery will lie deep to the internal jugular vein as the vessels extend through the region of the neck. Within the parotid gland, the retromandibular vein is shown in cross-section below its origin from the smaller veins in the temporal and maxillary regions. In lower images, the retromandibular vein will be shown to drain into the external jugular vein. Between the cervical spine structures and the genioglossus muscle, the extension of the soft palate known as the uvula is labeled within the opening of the oropharynx.



A



B



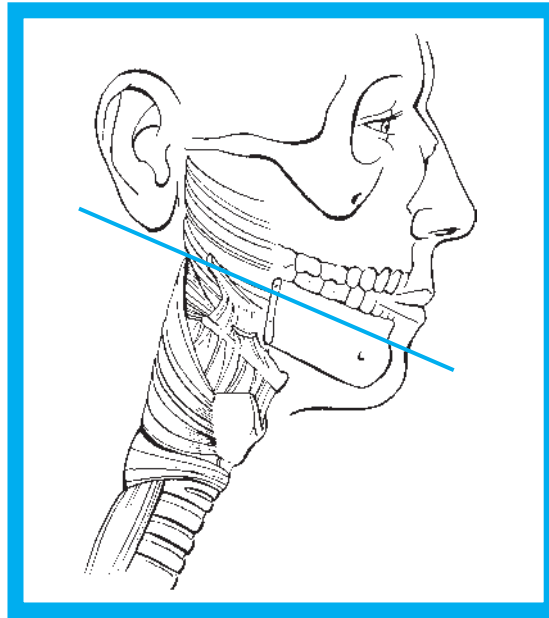
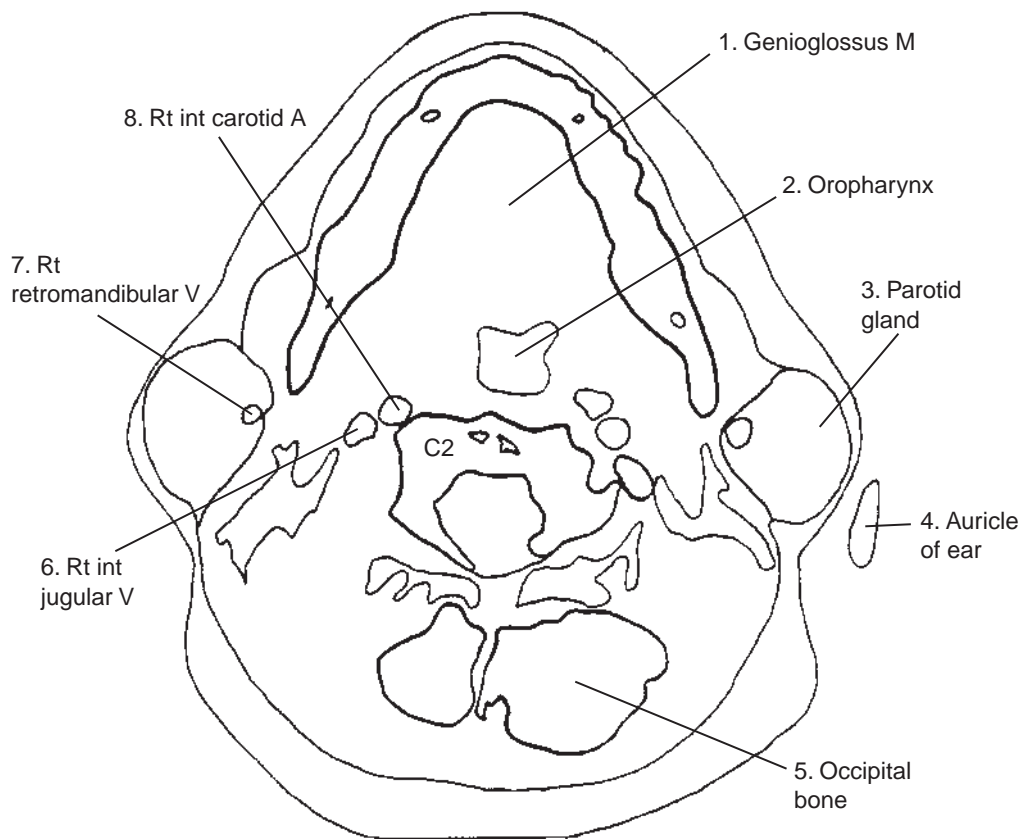


**Figure 6–17 (A,B)** Axial CT image 4.

At this level, the lower teeth are joining the body of the mandible and the rami can no longer be clearly identified as separate structures. Between the mandible and the cervical spine, the genioglossus and oropharynx can again be seen. On either side of C2, the contrast-enhanced internal carotid arteries are found deep to the internal jugular veins. Superficially, the characteristic consistency of the parotid gland is again shown to include the contrast-enhanced retromandibular veins. Posterior to the left parotid gland, a small part of the auricle of the ear is shown, sectioned separate from the other structures within this image. The occipital bone is again found posterior to the cervical spine but here has an irregular appearance, because the image demonstrates the lowermost part of the bone.



A



B

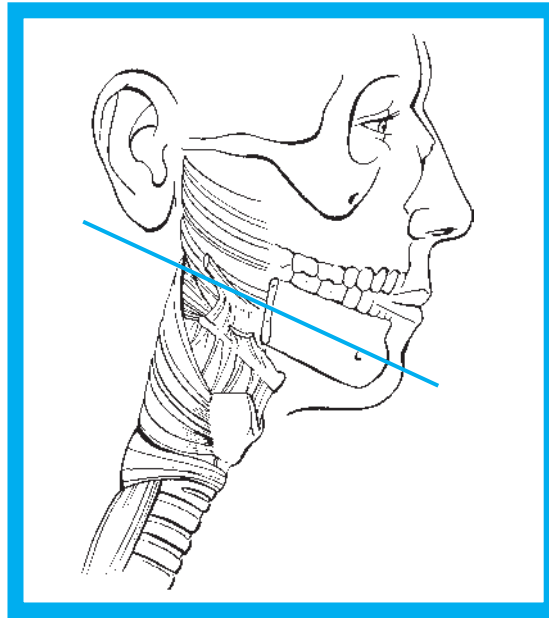
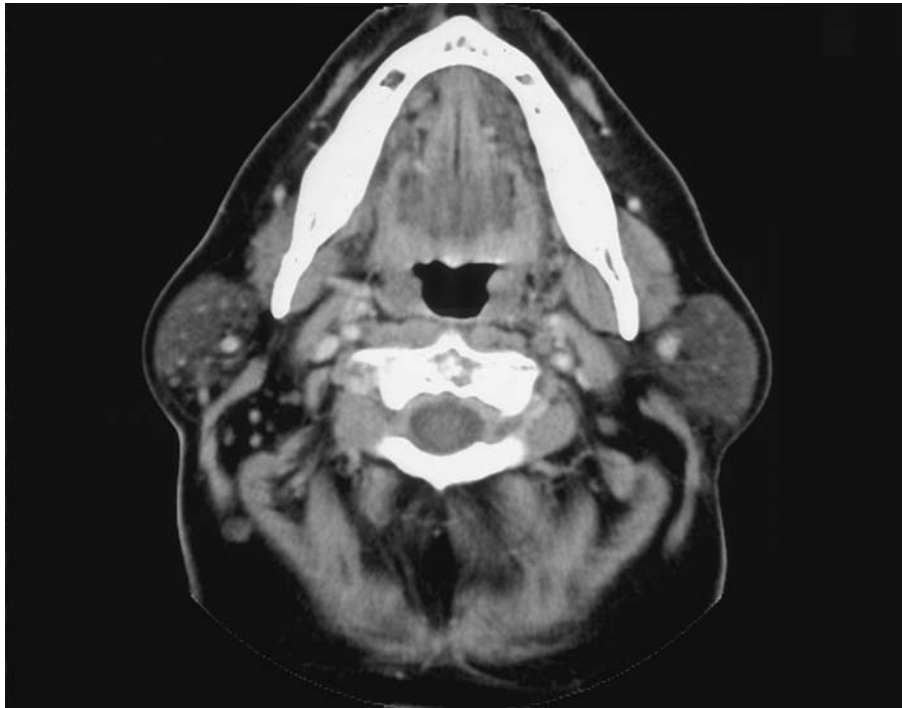
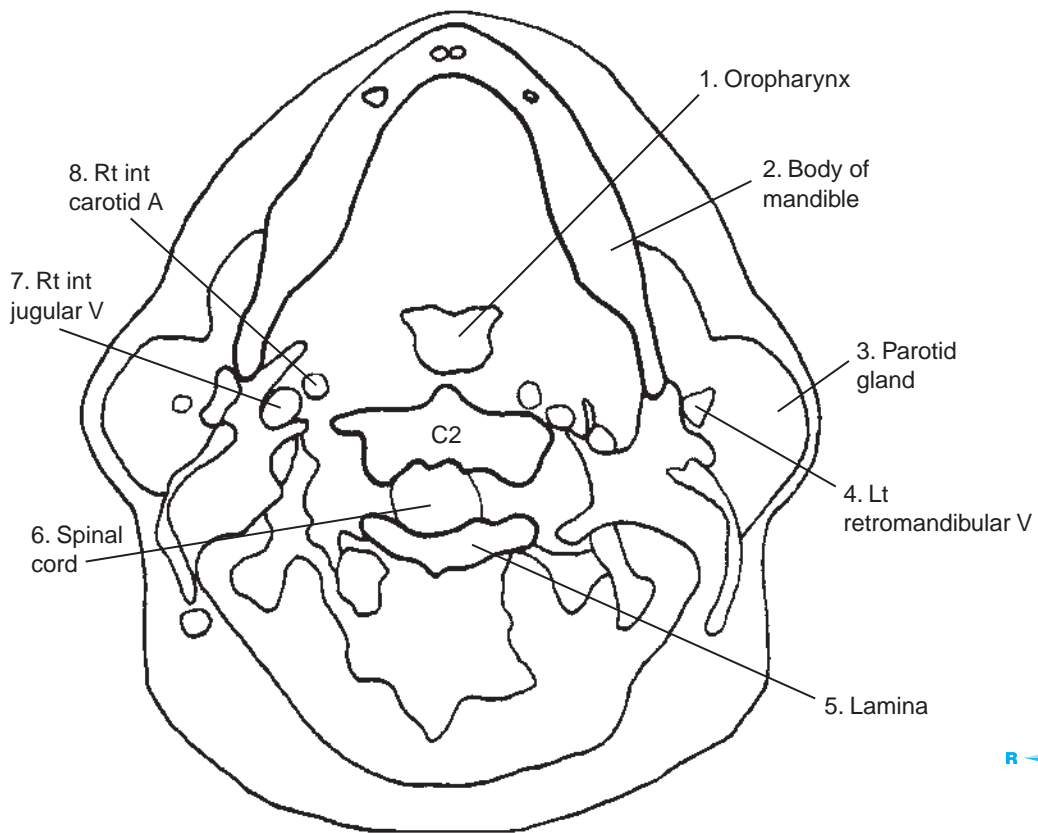


**Figure 6–18 (A,B)** Axial CT image 5.

The occipital bone is no longer seen, and the teeth have been replaced by the body of the mandible. Centrally, the spinal cord is separating the body and laminae of C2. Similar to previous images, the oropharynx is located anterior to the cervical spine. Anterolateral to the body of C2, the internal carotid arteries and internal jugular veins are readily distinguished from surrounding structures by contrast enhancement. Superficially, the characteristic consistency of the parotid gland can be found on either side encompassing the retromandibular veins.



A



B

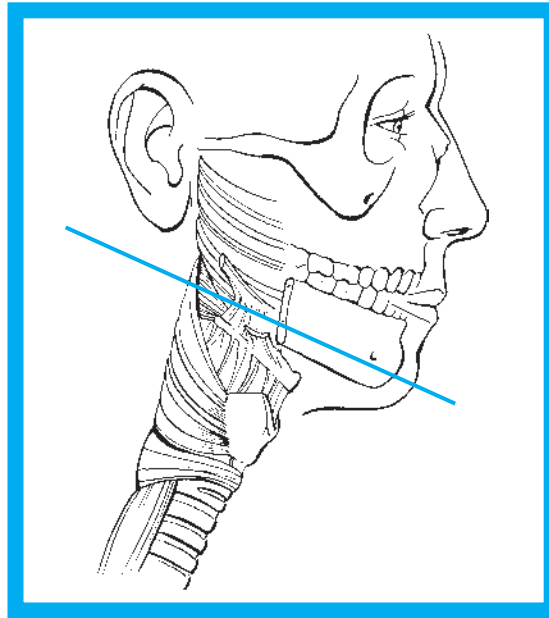
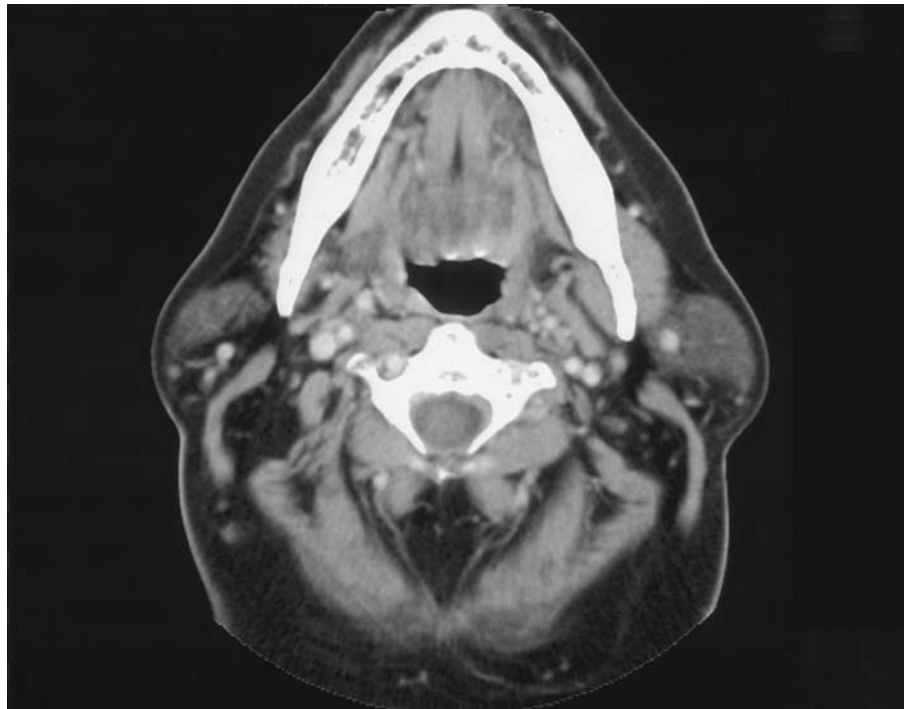
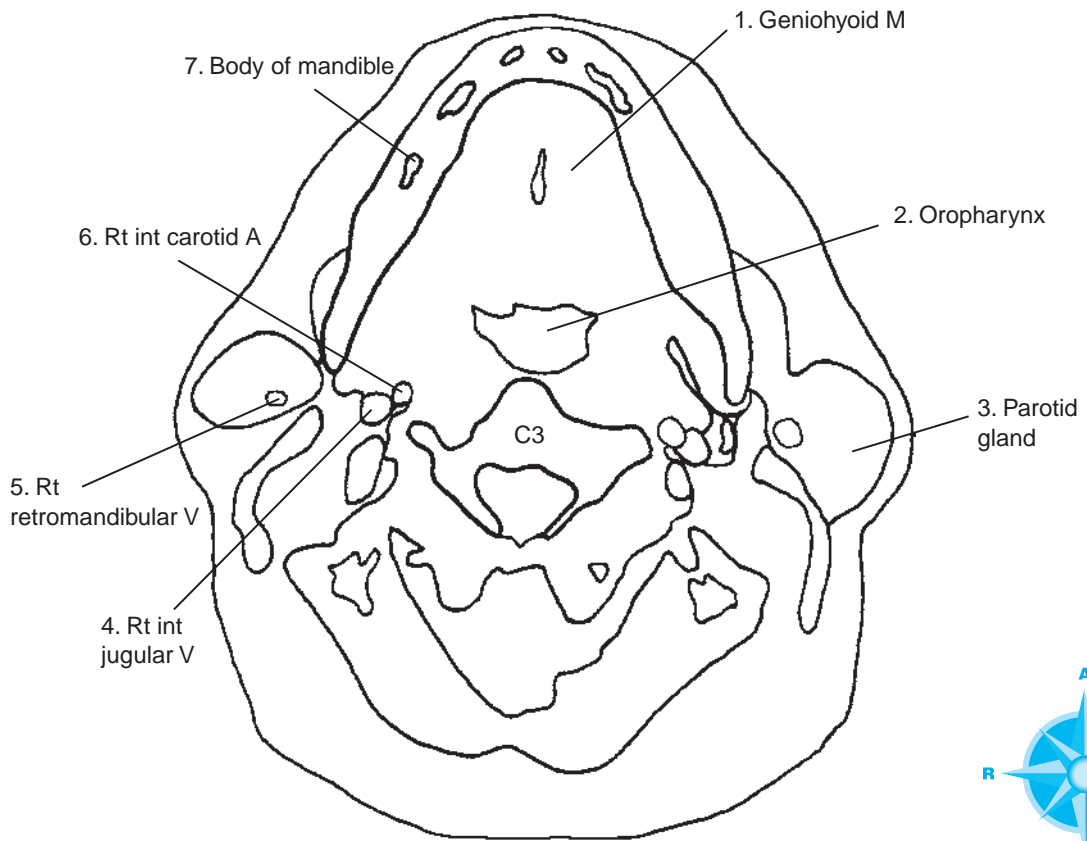


**Figure 6–19 (A,B)** Axial CT image 6.

The bony structures in this image can be labeled the body of the mandible and the third cervical vertebra. Although the oropharynx is again found just anterior to the body of C3, the genioglossus muscle seen in higher images has been replaced by the thinner geniohyoid muscles that extend between the inferior mental spine on the mandible to the hyoid bone, forming the floor of the mouth. On the right side of C3, the internal carotid artery is labeled deep to the internal jugular vein, and the right retromandibular vein is labeled within the parotid gland.



A



B

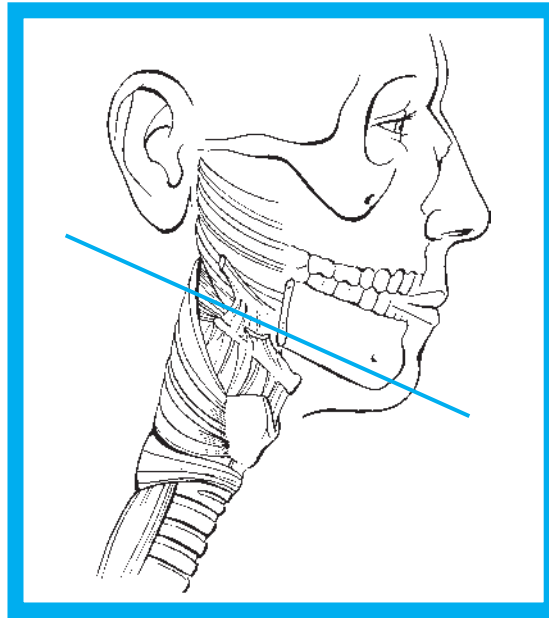
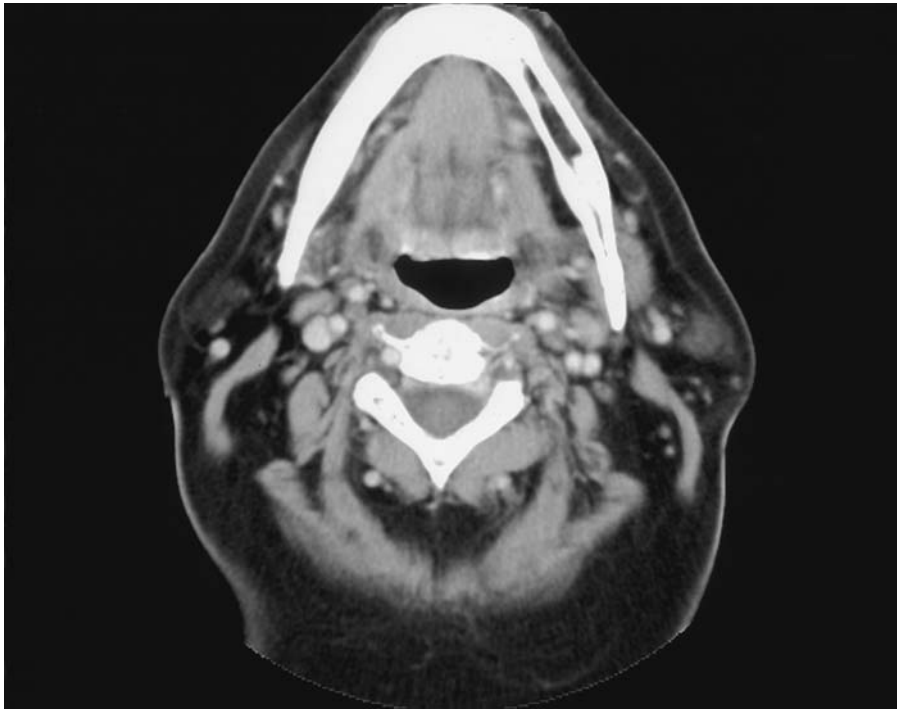
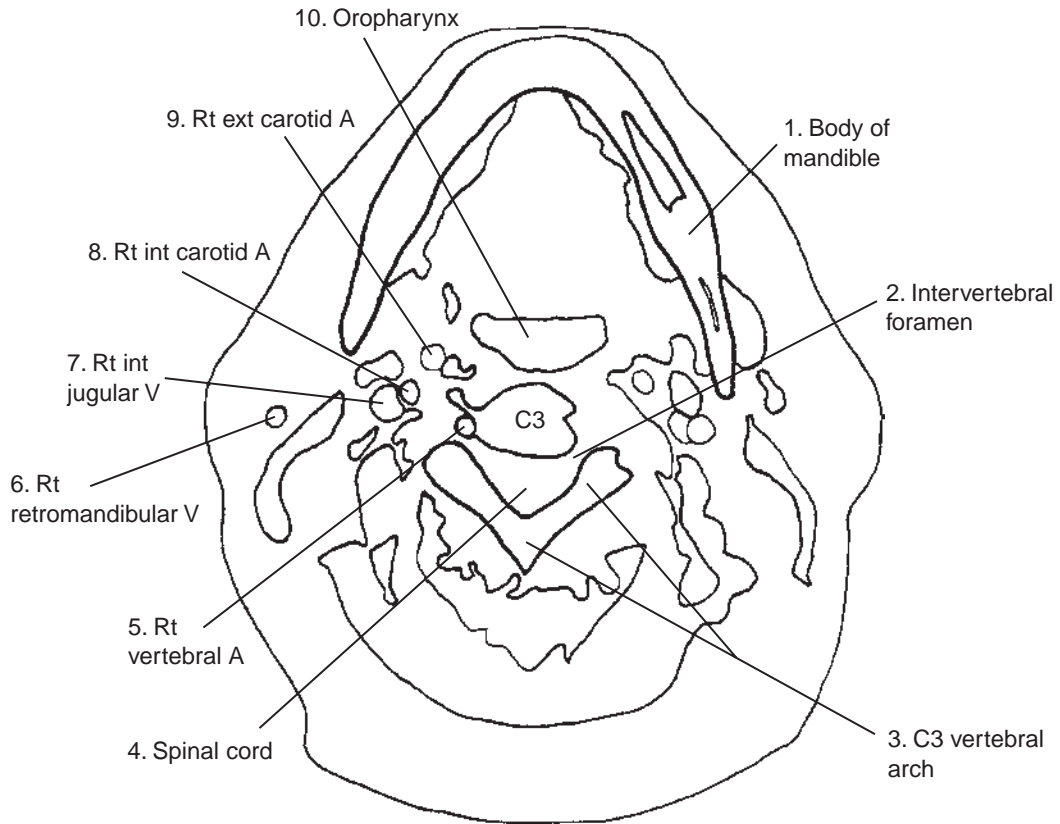


**Figure 6–20 (A,B)** Axial CT image 7.

With regard to bony anatomy structures, the body of the mandible is shown in its entirety anterior to C3. In this image, the body of C3 is found directly behind the oropharynx and is separated from the vertebral arch by the intervertebral foramina. On the right side of the patient, the right vertebral artery can be seen as a contrast-enhanced vessel sectioned near the transverse foramen. Lateral to the vertebral body, the internal carotid artery is again demonstrated deep to the internal jugular vein. However, the external carotid artery can now be seen as a contrast-enhanced vessel anterior to the internal carotid artery. Superficially, the retromandibular vein is now found outside of the parotid gland and will be seen in subsequent sections to drain into the external jugular vein.



A



B



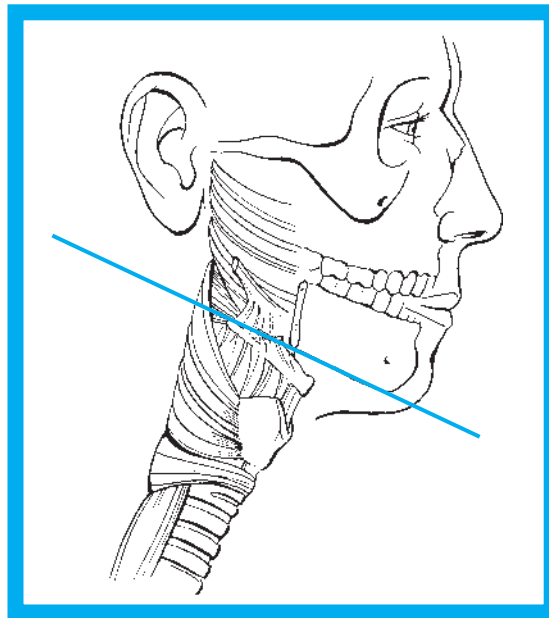
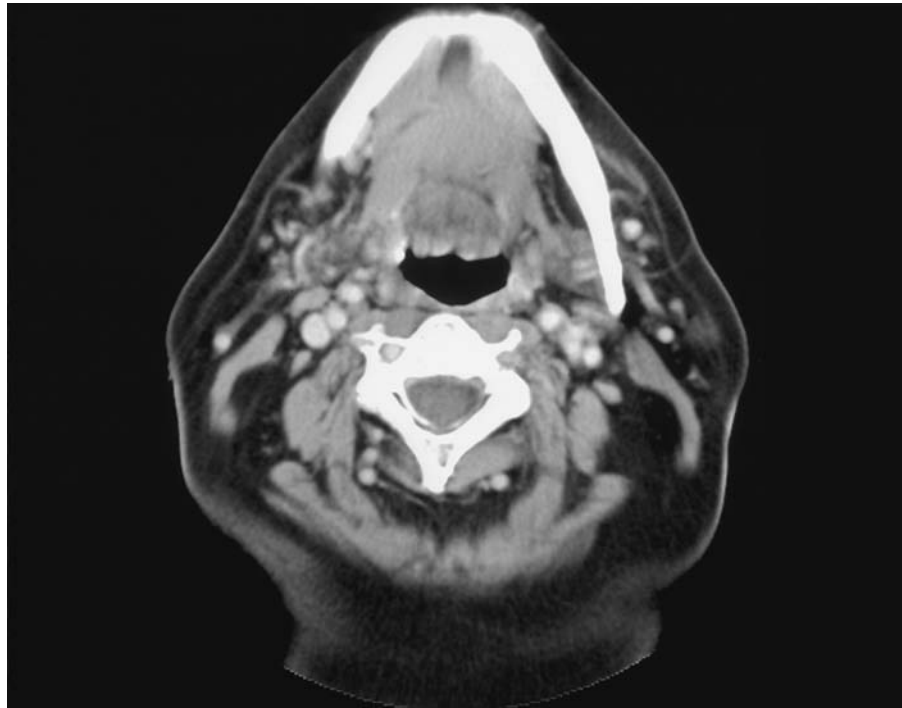
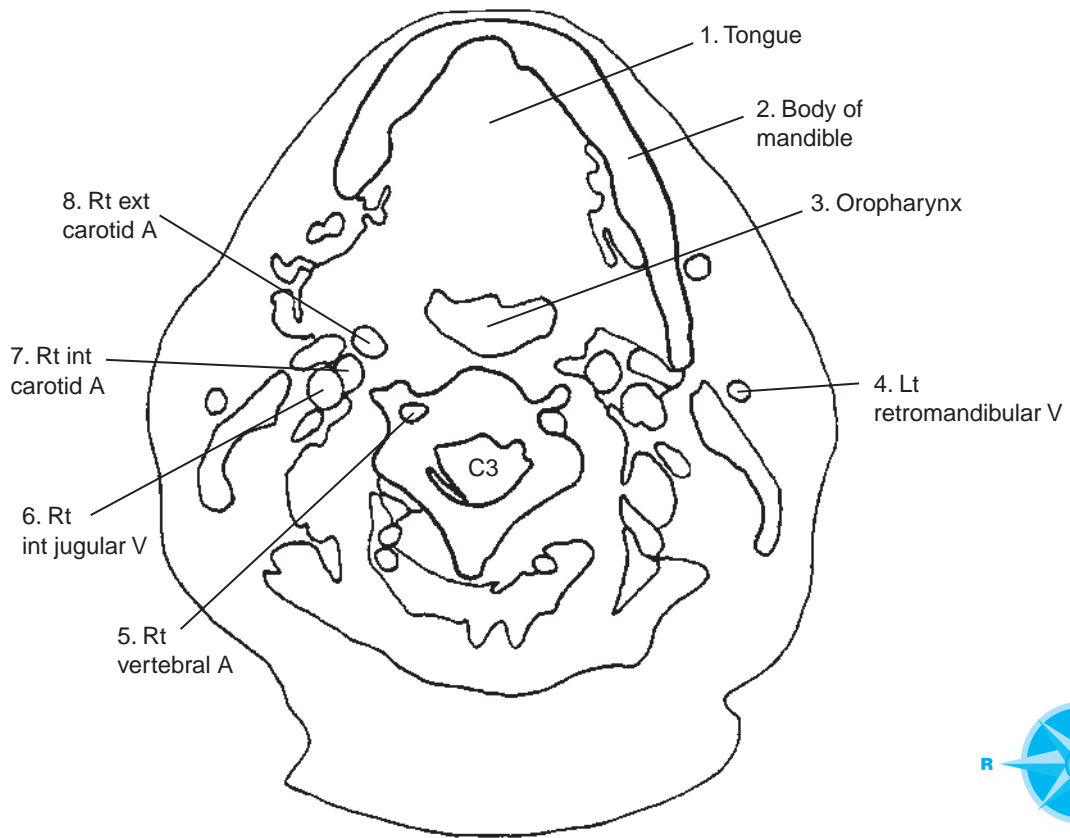


**Figure 6–21 (A,B)** Axial CT image 8.

The muscles of the tongue and the oropharynx are found between the body of the mandible and C3. On the right side of the patient, the right vertebral artery is the contrast-enhanced vessel within the transverse foramen. Lateral to the cervical vertebra, the internal carotid artery can be distinguished from the adjacent internal jugular vein, because the vein is larger and more superficially located. Compared with the previous image, the external carotid artery and the internal carotid artery are somewhat closer together, but the external carotid artery still occupies a more anterior position. Separated from these vessels by the sternocleidomastoid muscle, the retromandibular vein is found on the side of the neck in a superficial position below the level of the parotid gland.



A



B

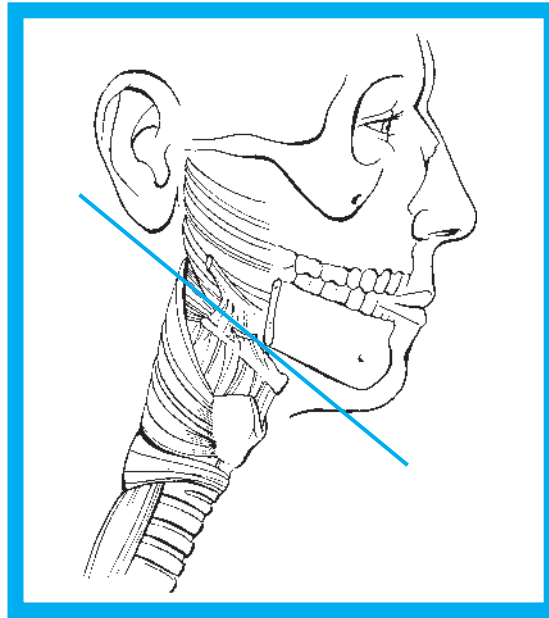
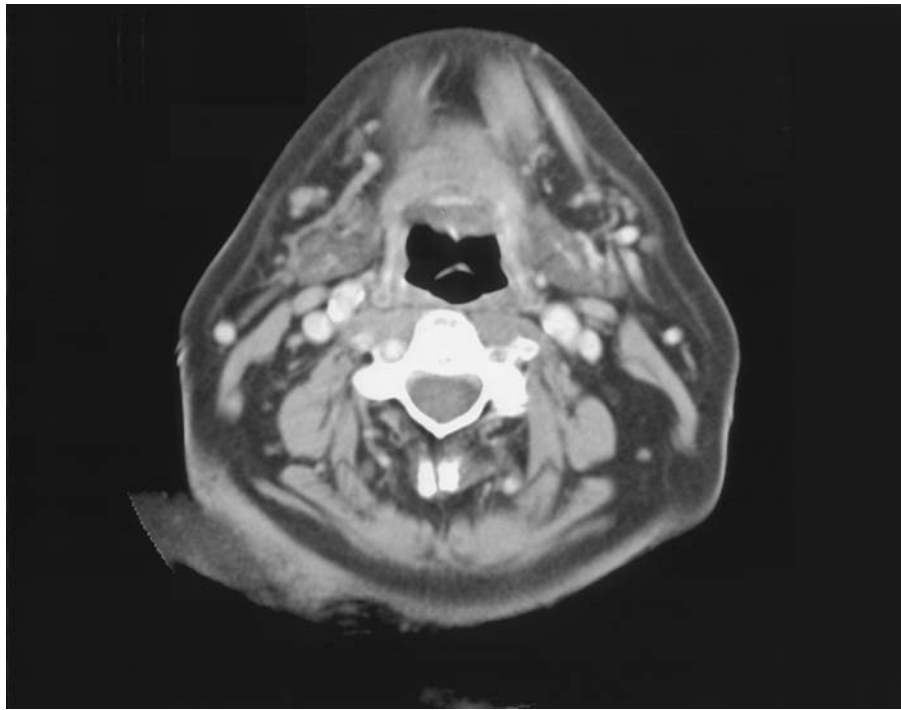
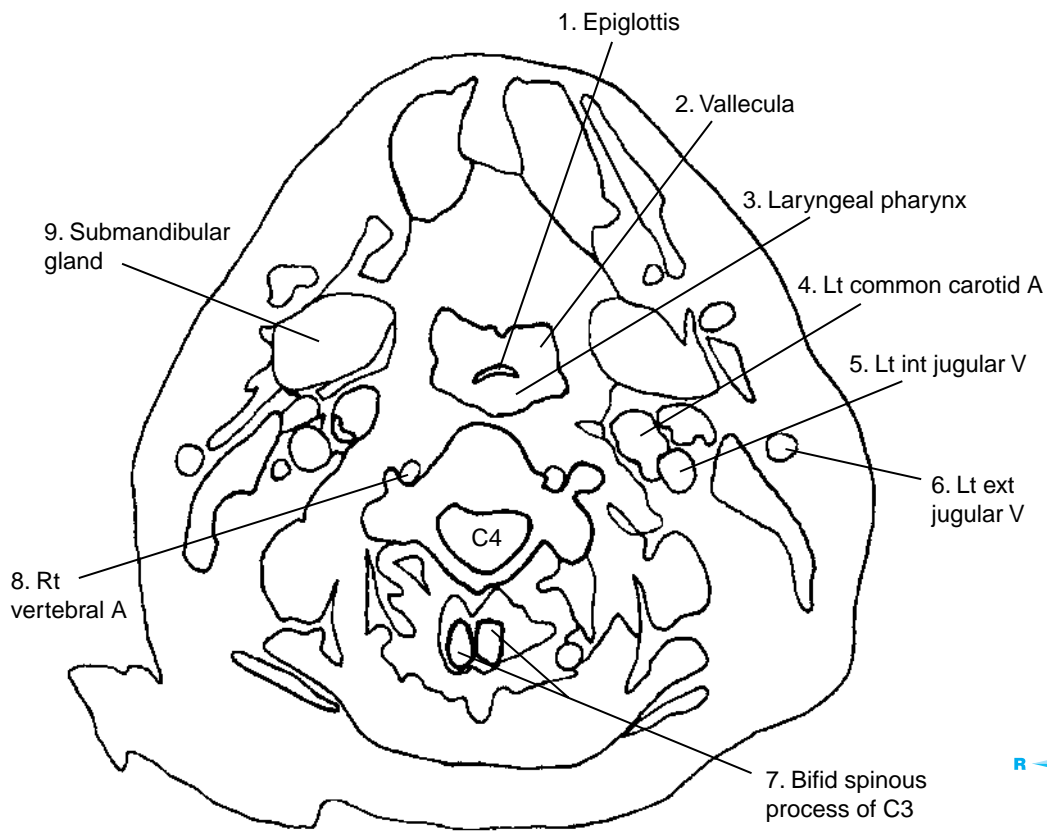


**Figure 6–22 (A,B)** Axial CT image 9.

At this level in the neck, the body of the mandible is no longer seen. Owing to the downward projection of the spinous processes of the cervical vertebrae, the bifid spinous process is demonstrated posterior to C4 extending from C3. On either side of the vertebral body, the vertebral arteries are contrast enhanced and are demonstrated emerging from the transverse foramina. Anterior to the vertebral body, the upper tip of the epiglottis is within the pharynx, indicating that the radiolucent area is the laryngeal pharynx. Between the epiglottis and the muscles of the tongue, the valleculae are spaces on either side and are continuous with the more posteriorly located laryngeal pharynx. The characteristic consistency of the submandibular gland can be identified on either side of the pharynx, just anterior to the major vessels of the neck. At this level, the external and internal carotid arteries have joined to form the contrast-enhanced common carotid artery deep to the internal jugular veins. Because we are now below the level of the mandible, the retromandibular vein has given rise to the external jugular vein, which continues in a superficial location in the anterolateral neck.



A



B

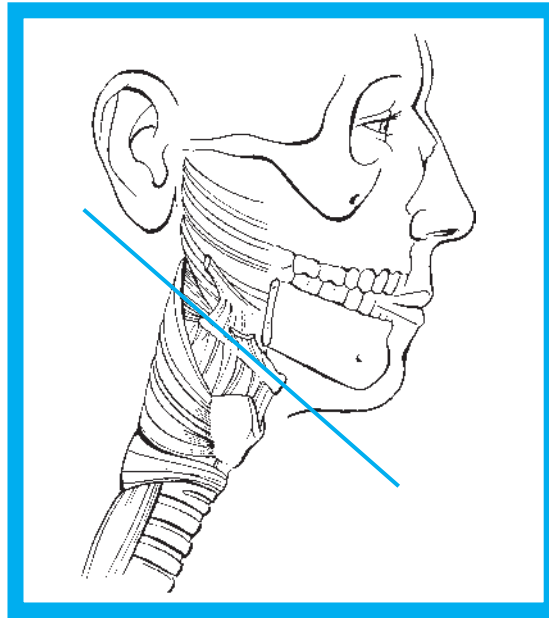
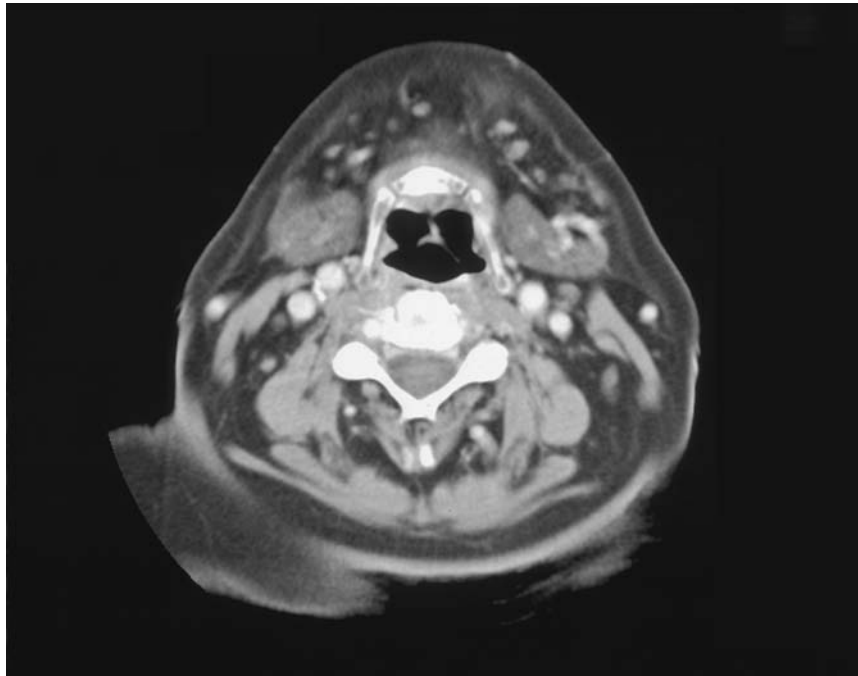
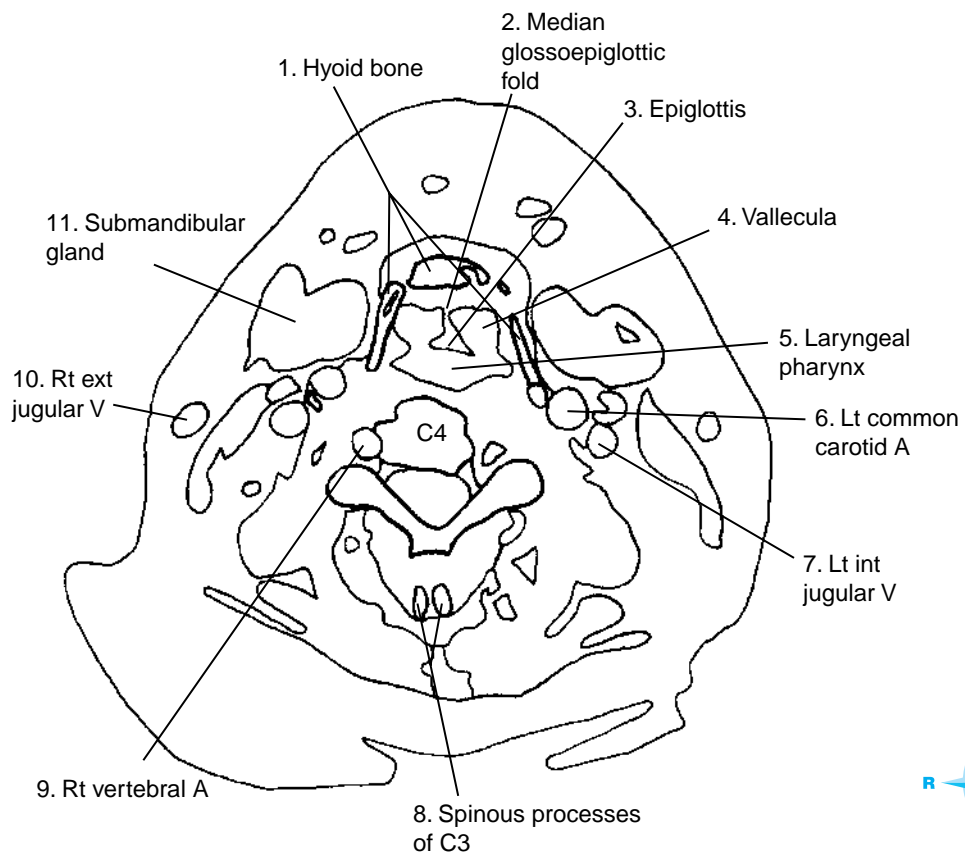


**Figure 6–23 (A,B)** Axial CT image 10.

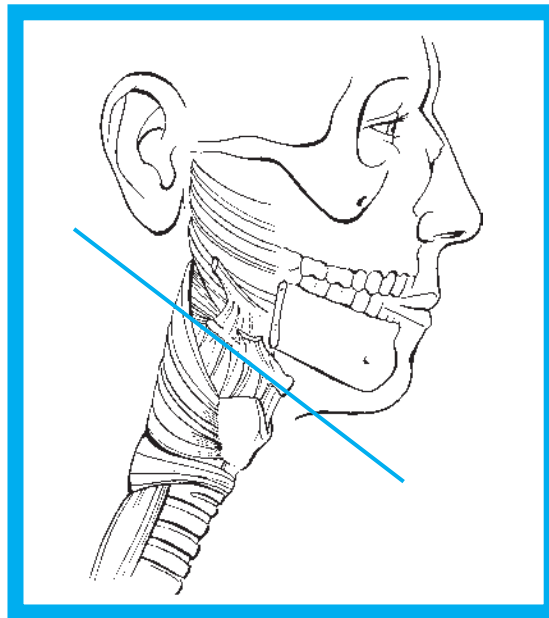
Centrally, C4 is shown anterior to the spinous process of C3, which projects inferiorly into this section. On the right side of the body of C4, the contrast-enhanced vertebral artery is labeled in the location previously described as the transverse foramen. Anterior to the cervical vertebra, the small U-shaped hyoid bone is seen surrounding the pharynx and, because of its smaller size and deeper location within the neck, should not be confused with the mandible. Similar to the previous image, the upper epiglottis is sectioned and divides the laryngeal pharynx from the valleculae. At this lower level, the valleculae are on either side of the median glossoepiglottic fold and extend from the posterior tongue to the epiglottis. Outside of the hyoid bone, the characteristic consistency of the submandibular gland is seen anterior to the contrast-enhanced external jugular veins. Deep to the external jugular veins, the internal jugular veins are cross-sectioned posterolateral to the common carotid arteries.



A

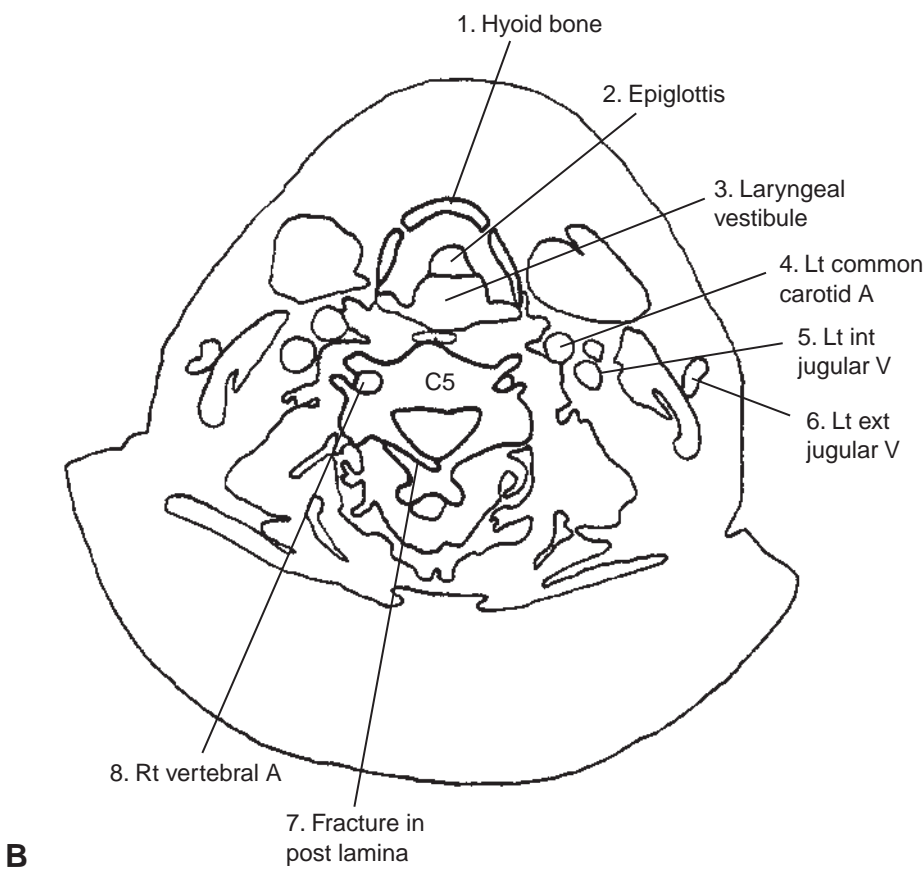
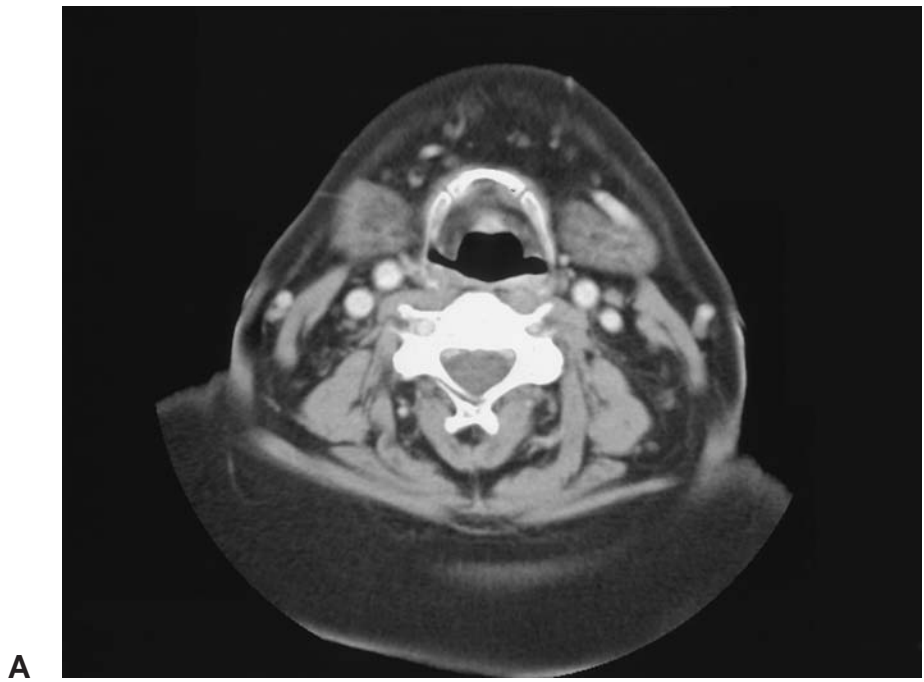


B

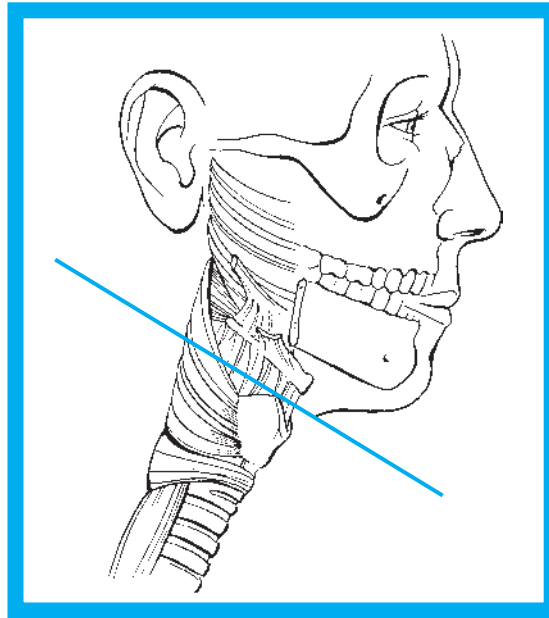


**Figure 6–24 (A,B)** Axial CT image 11.

This image clearly demonstrates the bony anatomy of C5, which contains a fracture in the posterior lamina on the right side. On either side of the vertebral body, the vertebral arteries are contrast-enhanced structures within the transverse foramina. As indicated in previous images, the size and contrast enhancement of the right vertebral artery is normal. On the left side, the vertebral artery is smaller than normal, indicating reduced blood flow. Anteriorly, the U-shaped hyoid bone arches around the epiglottis and laryngeal vestibule. On the lateral side of the neck, the deep contrast-enhanced vessels can be labeled as the common carotid artery and the more superficially located internal jugular vein. On the other side of the sternocleidomastoid muscle, the vessel just below the skin is the external jugular vein.

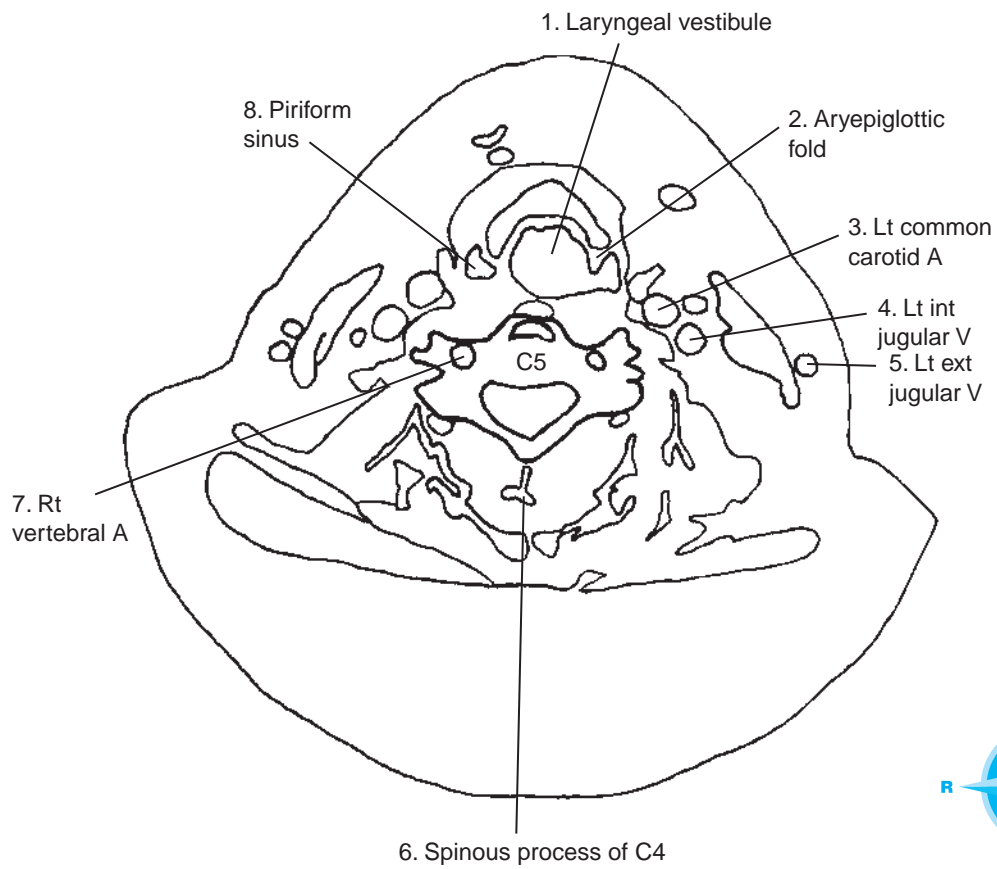
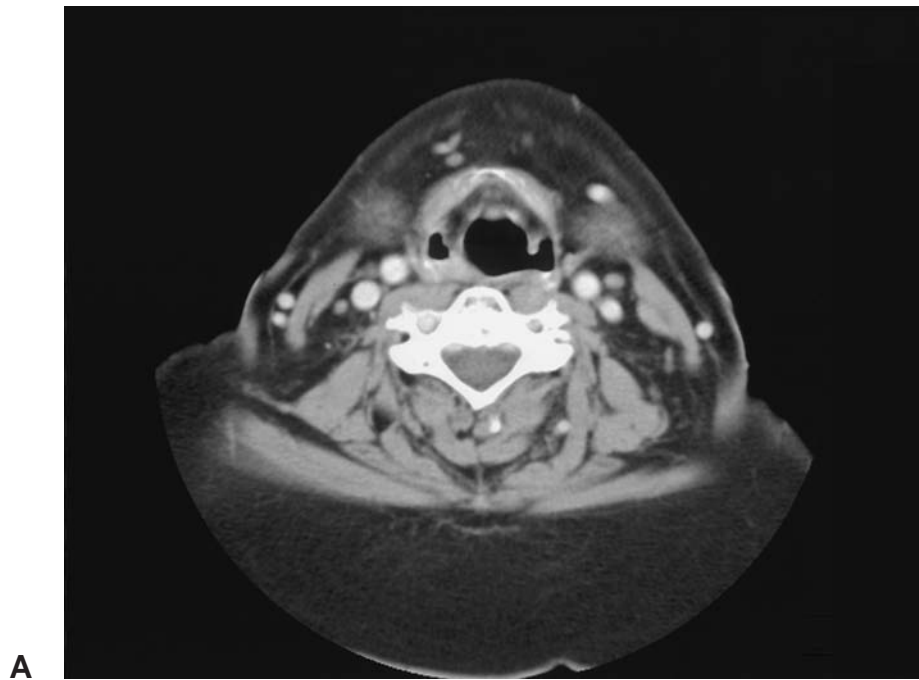


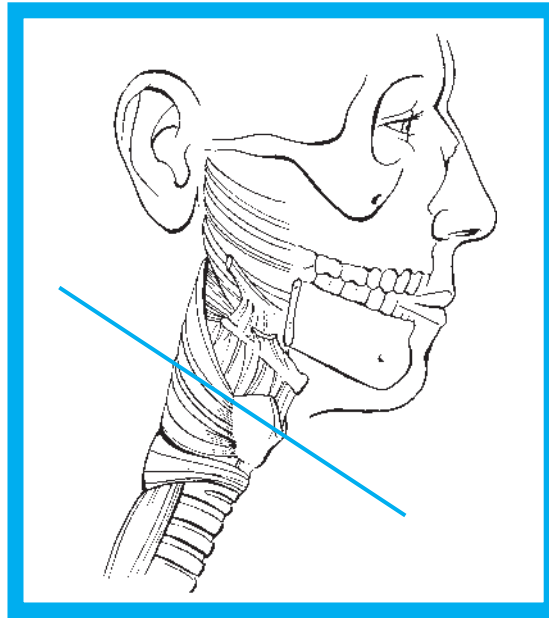




**Figure 6–25 (A,B)** Axial CT image 12.

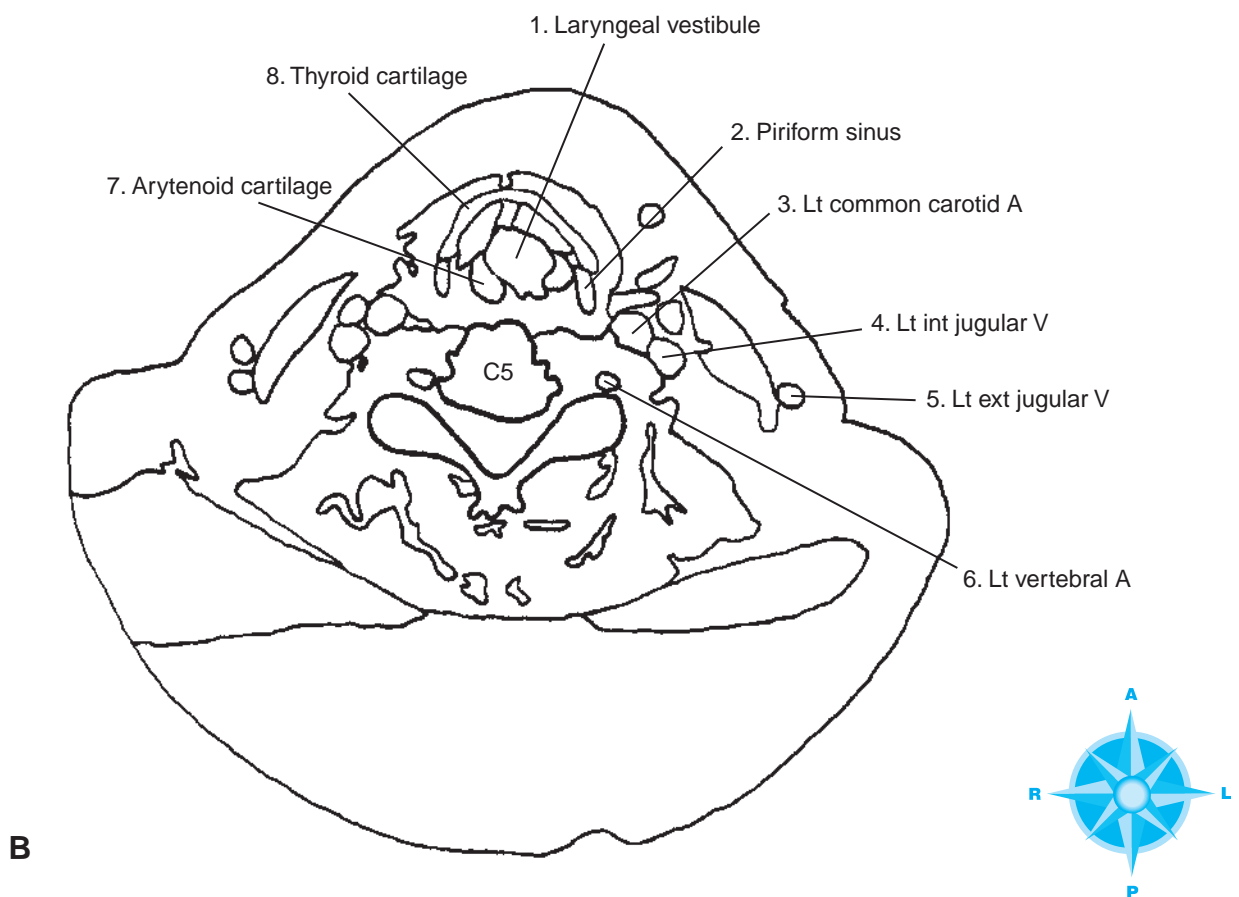
The fifth cervical vertebra occupies a central position in this image. As for other cervical vertebrae, the vertebral arteries are located within the transverse foramina on either side of the vertebral body. Owing to the downward projection of the spinous processes in the cervical vertebrae, the spinous process of C4 is labeled posterior to C5. Anteriorly, the laryngeal openings are now divided into three separate spaces by the aryepiglottic folds. As described earlier, the aryepiglottic folds of skin extend from the margins of the epiglottis to the posteriorly located arytenoid cartilages. Within the aryepiglottic folds, the laryngeal vestibule is the larger opening, which will be seen (in subsequent sections) to lead to the vocal cords. Lateral to the aryepiglottic folds, the piriform sinuses are formed on either side outside of the larynx. When food is swallowed, the tongue moves posteriorly pushing the epiglottis down over the laryngeal vestibule so that the food continues down outside the larynx into the esophageal opening. On the lateral part of the neck, the external jugular vein is again seen more superficially located than the common carotid arteries and internal jugular veins.





**Figure 6–26 (A,B)** Axial CT image 13.

The lower part of C5 is centrally located in this image, and the contrast-enhanced vertebral arteries are on either side of the vertebral body. The right vertebral artery, which is normal in size, appears considerably larger than the diminished left vertebral artery in this patient. Anterior to the cervical vertebra, the U-shaped thyroid cartilage surrounds the contents of the larynx. The main opening leading into the larynx, the laryngeal vestibule, is centrally located between the piriform sinuses on either side. On the right side of the patient, the arytenoid cartilage is found on the posterolateral aspect of the laryngeal vestibule and will be shown in subsequent sections as the posterior attachment for the vocal cords. On the lateral side of the neck, the common carotid artery is found anteromedial to the internal jugular vein, both of which are deeper than the superficially located external jugular vein.



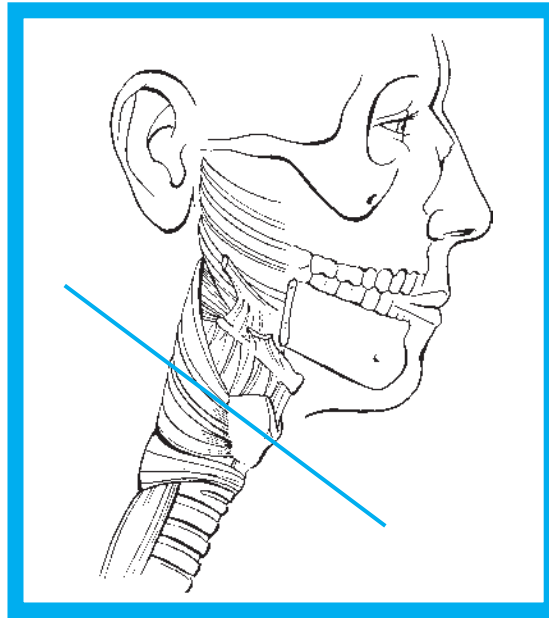
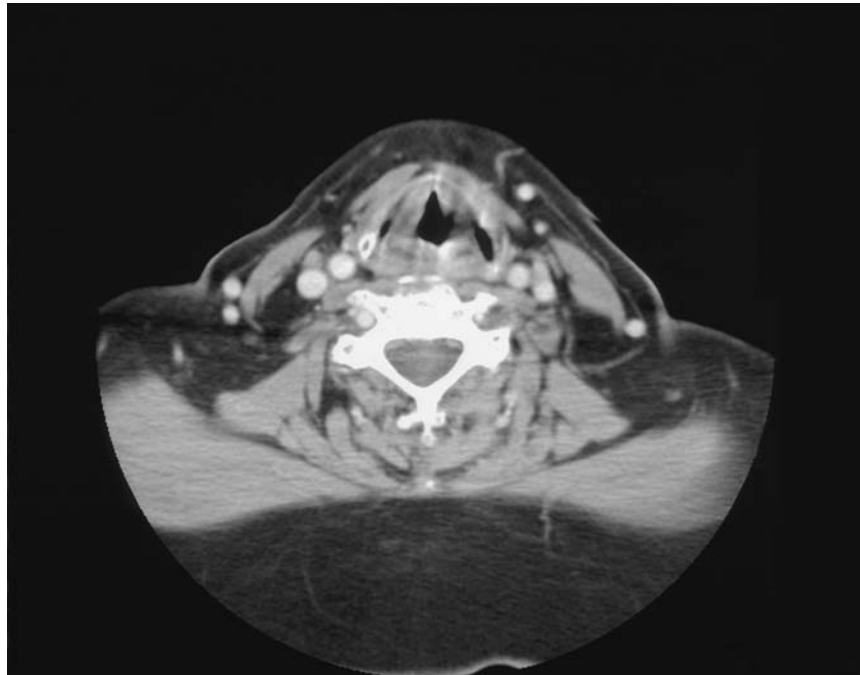
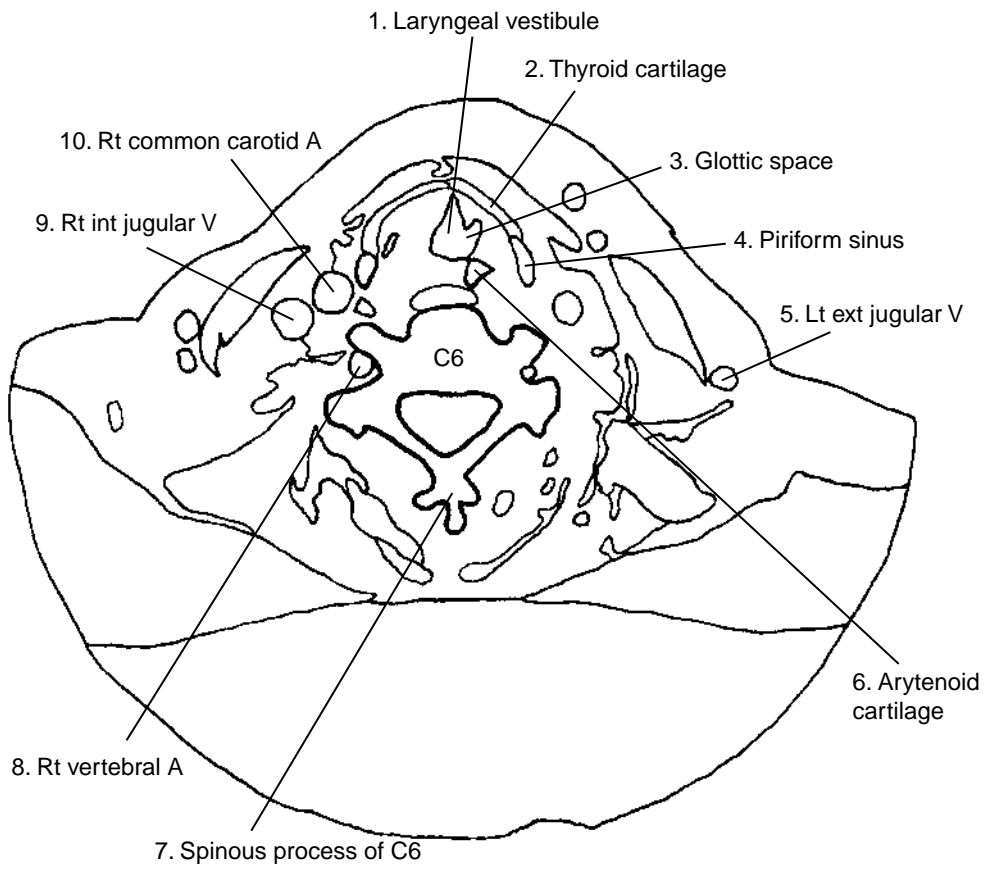


**Figure 6–27 (A,B)** Axial CT image 14.

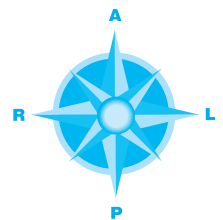
C6 is in the center of this image and is demonstrated forming a complete enclosure around the vertebral foramen. Owing to the cervical curvature, the lower cervical vertebrae occupy a more horizontal position, as demonstrated in this image, because the spinous process of C6 is demonstrated along with the vertebral body. Similar to other cervical vertebrae, the vertebral arteries are found on either side within the transverse processes. In this patient, the left vertebral artery is significantly smaller than the normal right vertebral artery. In the anterior neck, the thyroid cartilage arches over the contents of the larynx. The main opening extending into the larynx, the laryngeal vestibule, is found between the thyroid and arytenoid cartilages. Located between the vestibular and vocal folds, the glottic space is shown on the left side continuous with the laryngeal vestibule. The spaces on either side of the laryngeal vestibule outside of the larynx represent the piriform sinuses. Located outside the larynx, the piriform sinuses are continuous with the esophageal opening posterior to the arytenoid cartilages. On the lateral aspect of the neck, the external jugular vein again occupies a superficial location and the internal jugular vein and common carotid artery are more deeply situated under the superficial musculature of the neck.

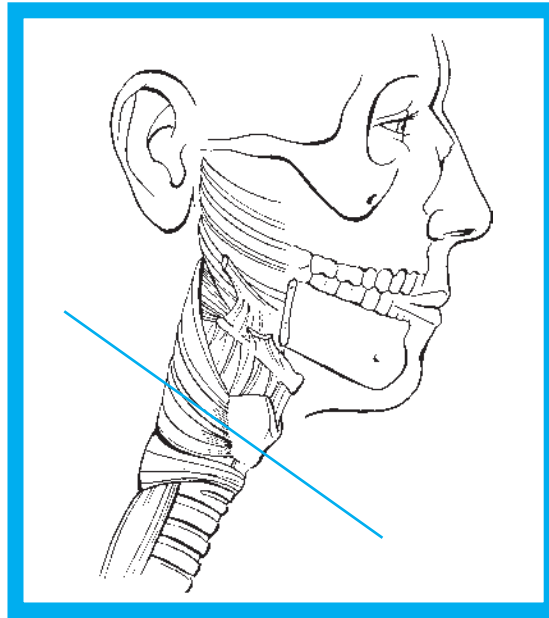


A



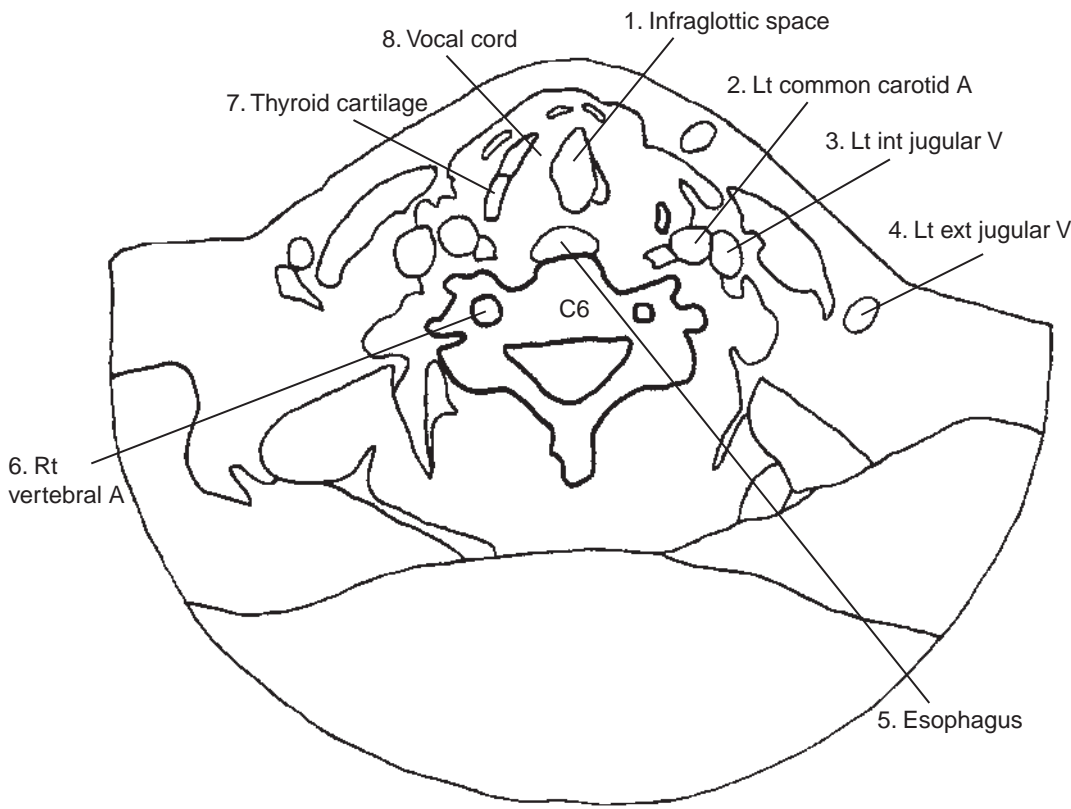
B



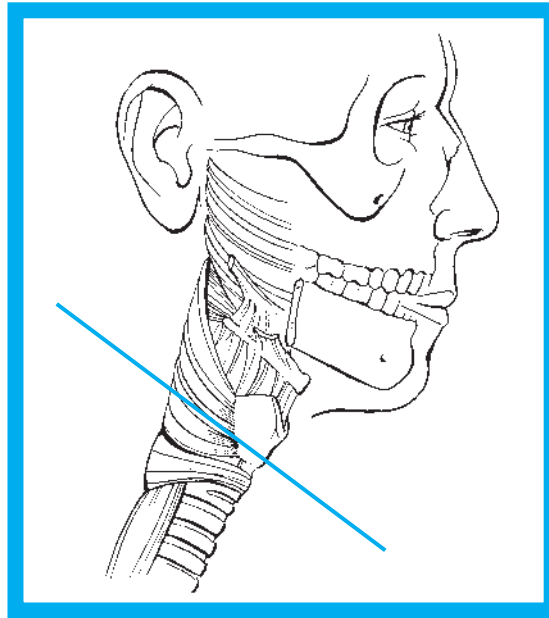


**Figure 6–28 (A,B)** Axial CT image 15.

Owing to the larger size of the lower cervical vertebrae, C6 is again seen centrally located in this image, and the vertebral arteries are located in the transverse processes on either side. At this level, the thyroid cartilage is found anterior to the radiolucent area representing the openings within the larynx. Within the larynx, the space is now labeled the infraglottic space, because we are at a level below the vocal cords, which are labeled on the right side. Between the body of the cervical vertebra and the infraglottic space, the oval-shaped region of musculature is formed by the walls of the esophagus, which are collapsed (thus the esophageal opening is not shown in this image). On the lateral aspect of the neck, the common carotid artery is found deep to the adjacent internal jugular vein, and both vessels lie deeper within the neck than the superficially located external jugular vein.

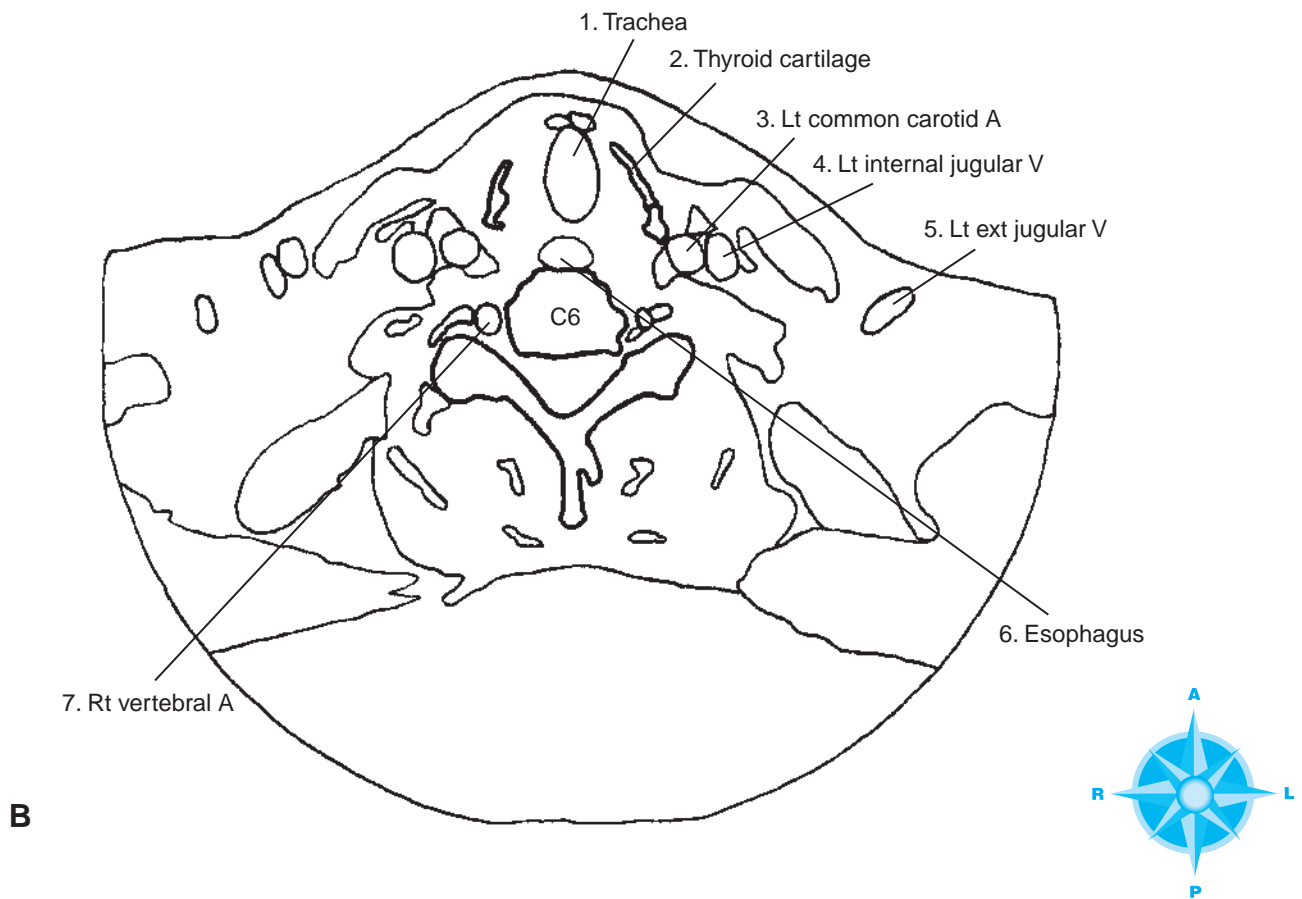
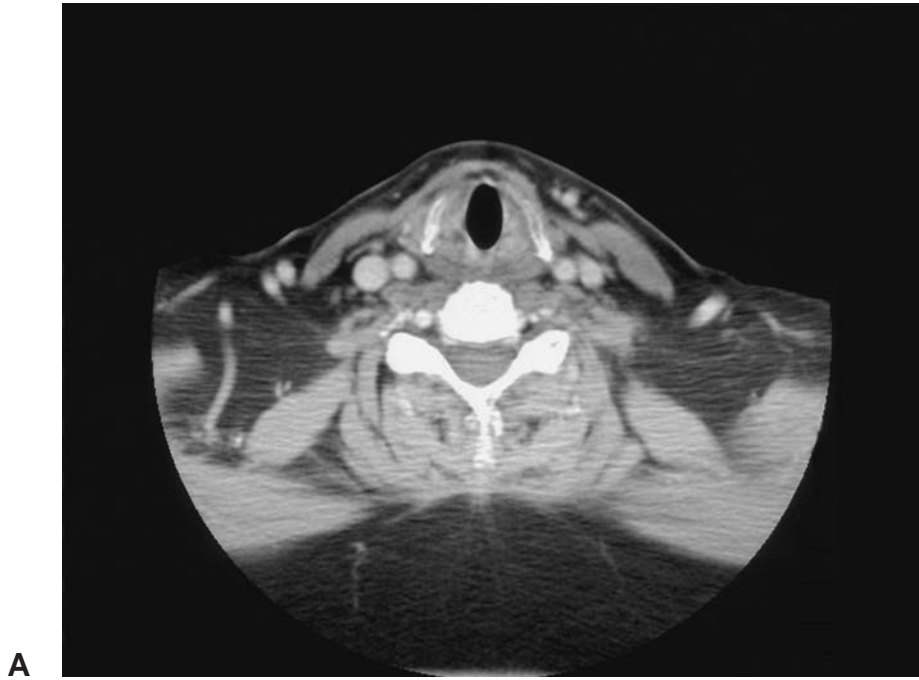






**Figure 6–29 (A,B)** Axial CT image 16.

The bony anatomy in this image again demonstrates the lower part of C6. Similar to the previous images, the right vertebral artery appears as a normal-sized contrast-enhanced vessel, whereas the left vertebral artery is difficult to distinguish because it is so small. Directly in front of the vertebral body, the esophagus and trachea are cross-sectioned within the deep neck. In the anterior neck, the thyroid cartilage is sectioned on either side of the opening of the trachea. On the lateral aspect of the neck, the common carotid artery is again found deep to the internal jugular vein, and together they are covered by the musculature of the superficial neck. Compared to previous images, the superficially located external jugular vein now occupies a more lateral location as it extends downward to the subclavian vein of the chest.



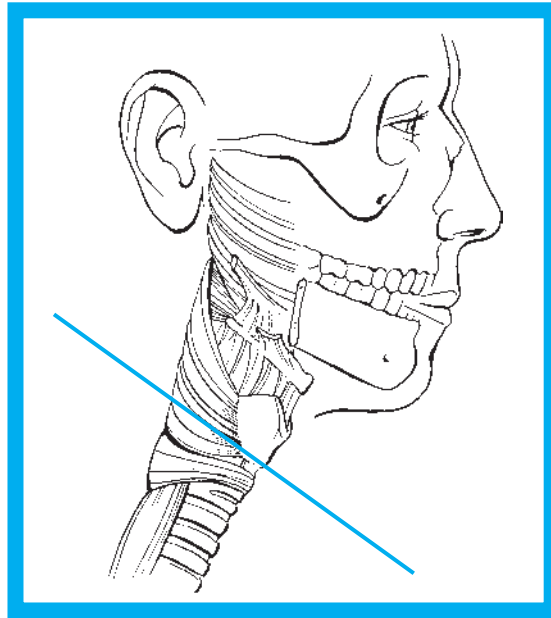
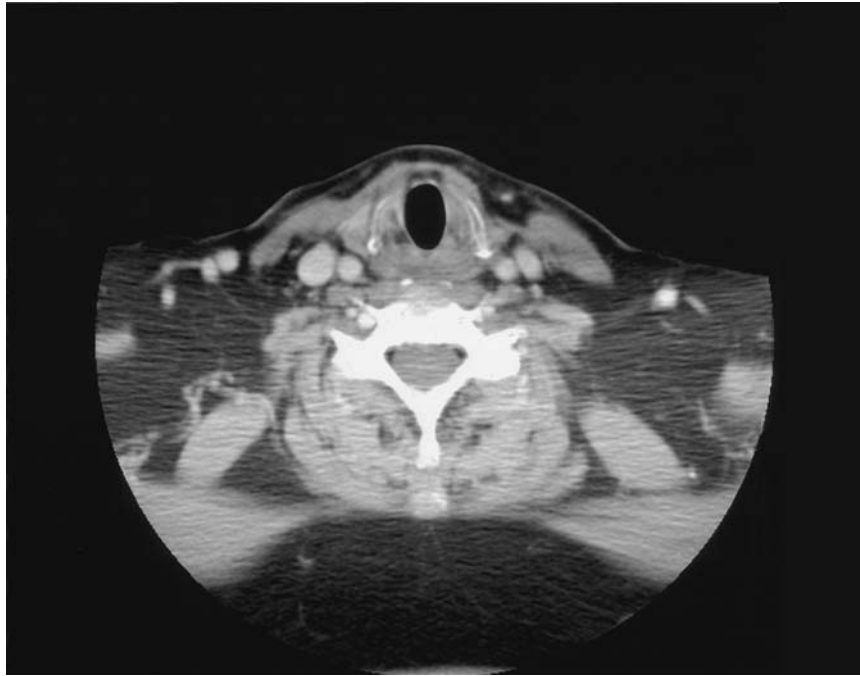
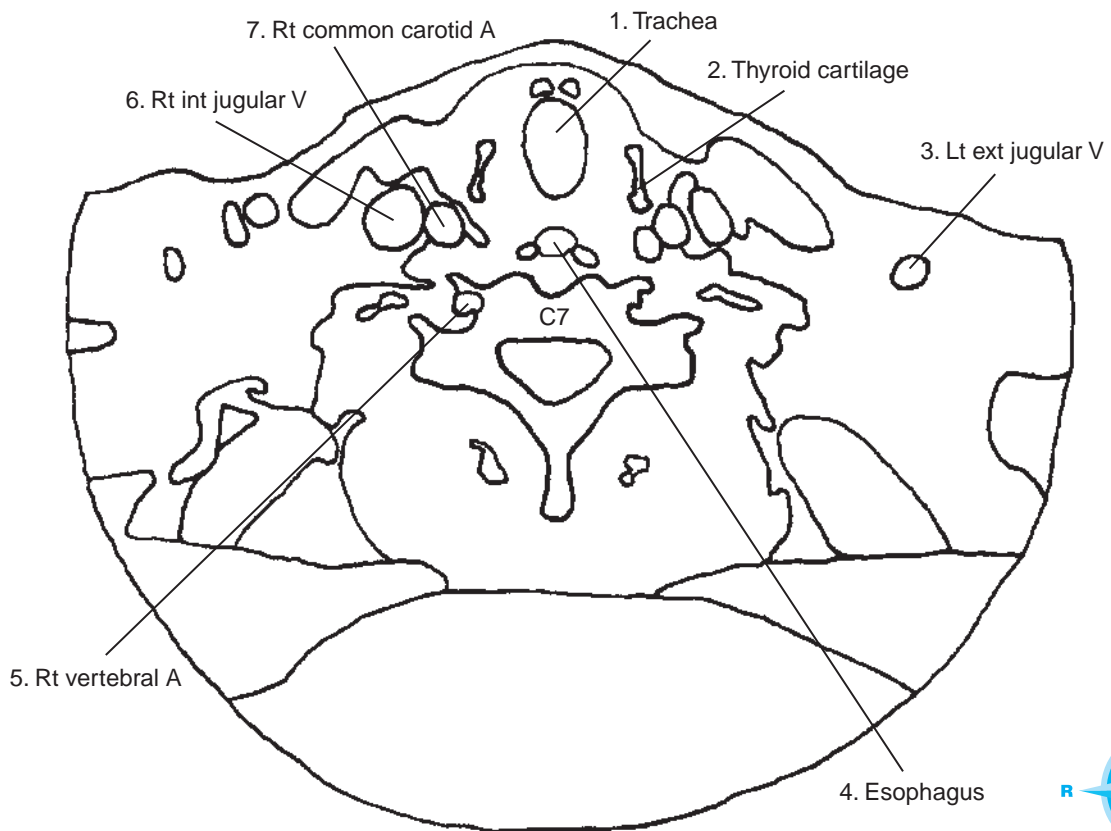


**Figure 6–30 (A,B)** Axial CT image 17.

The upper part of C7 can be seen centrally in this image. Although this section shows only the upper part of C7, the spinous process appears quite large compared to the other cervical vertebrae. Similar to previous images, the vertebral arteries are located in the transverse processes on either side, and the left vertebral artery is significantly diminished in size. Anterior to the vertebral body, the oval-shaped musculature of the esophagus lies directly behind the opening of the trachea. On either side of the trachea, the lower parts of the thyroid cartilage are sectioned anterior to the common carotid arteries and internal jugular veins. Similar to the previous image, the external jugular veins are found laterally as they extend toward the subclavian veins in the chest.



A



B

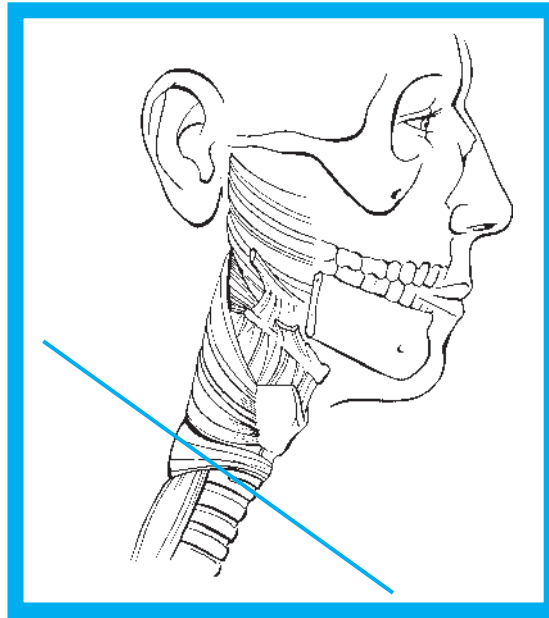
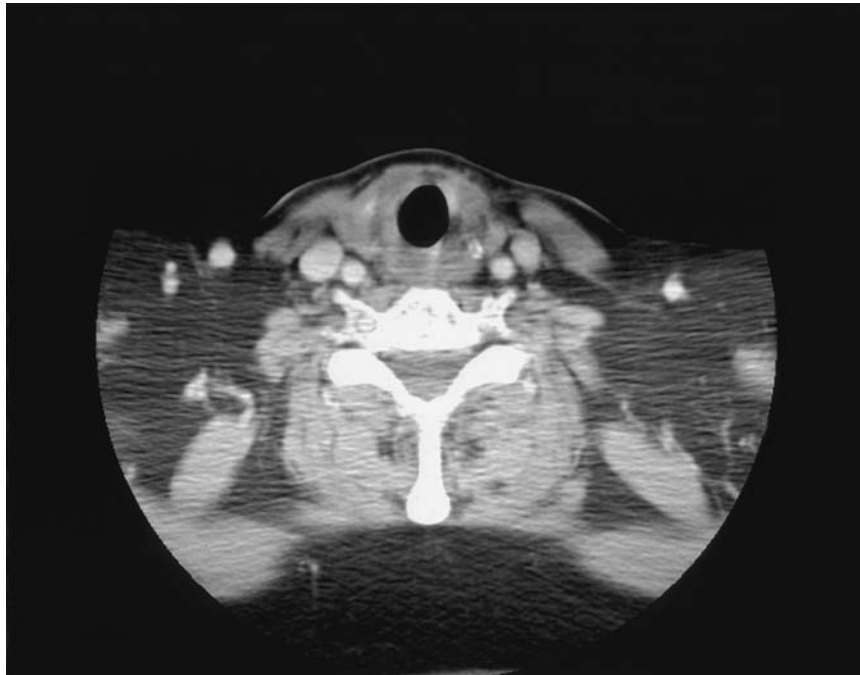
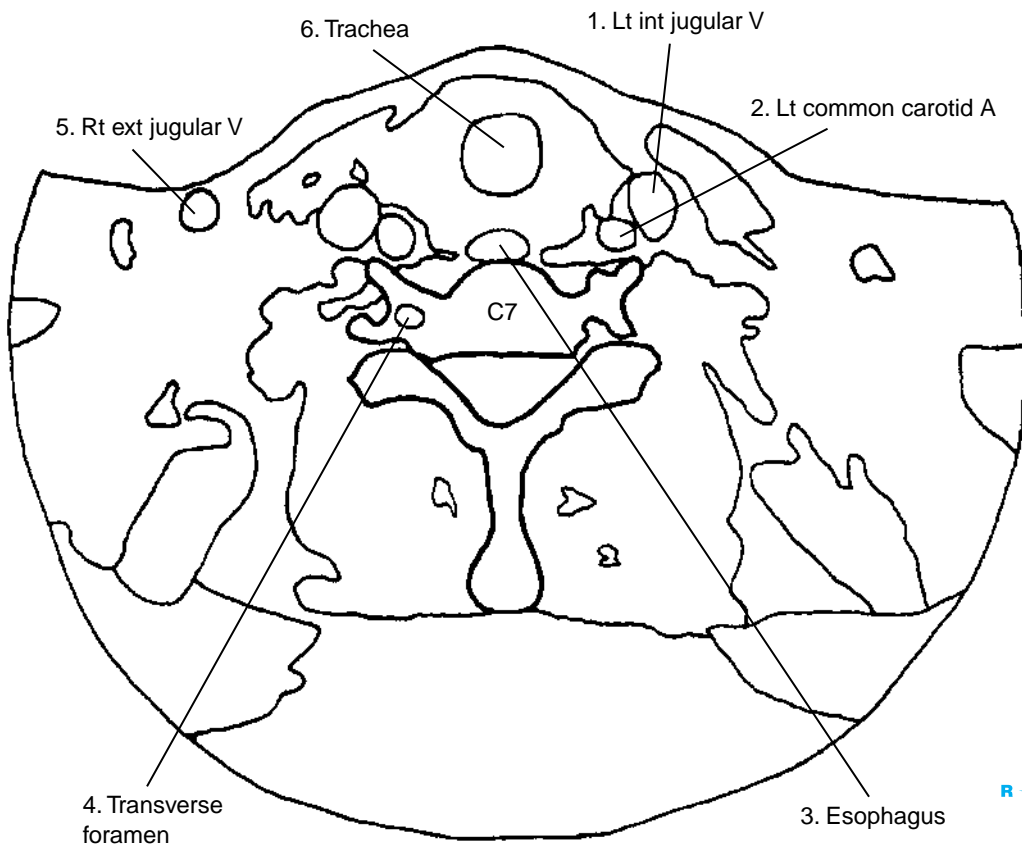


**Figure 6–31 (A,B)** Axial CT image 18.

This image clearly demonstrates the enlarged spinous process of C7, known as the vertebra prominens. The inferior location of C7 makes it difficult to image, because it is at the juncture of the neck and the torso. Aliasing or beam-hardening artifacts are frequently seen in CT images as a result of the thickness of the shoulders compared to the neck. Like all cervical vertebrae, the transverse processes of C7 contain transverse foramina. However, the vertebral arteries are not found within the foramina, because they pass in front of the transverse processes of C7. Between the opening of the trachea and the vertebral body, the esophagus appears as an oval-shaped muscular tube and is difficult to discern from the surrounding soft tissue structures. Lateral to the esophagus, the common carotid artery is found deep to the internal jugular vein below the superficial musculature of the neck. In the superficial neck, the external jugular veins occupy a lateral position at this level, because they are nearing the subclavian veins in the chest.



A



B



## Case Study 6-1

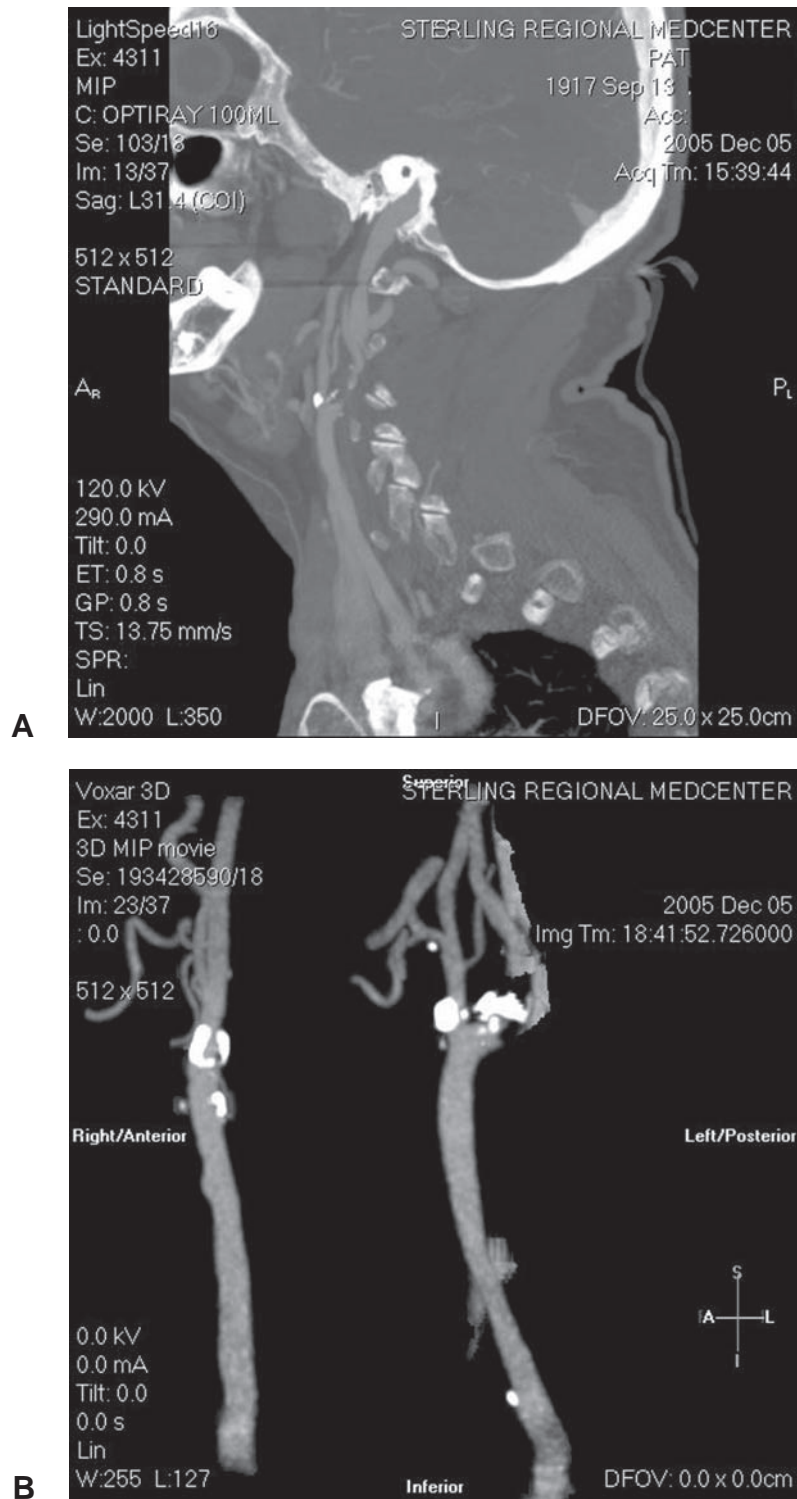


Figure 6-32

### Clinical Correlations

This 88-year-old man underwent a helical dynamic contrast-enhanced arterial phase CT scan during the injection of 100 mL of Optiray 320 to evaluate his carotid arteries. CT angiogram included coronal reformations as shown in Fig. 6-32A. The carotid artery is ascending through the neck and the point of bifurcation is marked by the presence of atherosclerotic disease. Although the perfusion of the external carotid artery seems to be good,

there is high-grade stenosis at the origin of the left internal carotid artery which is at least 99% with a string sign flow around the obstruction. In the reconstructed three-dimensional image shown in Fig. 6-32B, the plaque and resulting stenosis is apparent even though limited flow is above the stricture. Similar to the left artery, the atherosclerotic plaques are also shown at the origin of the right internal carotid artery resulting in an estimated 60 to 70% stenosis.

### Questions

1. What regions of the head are supplied with arterial blood via the internal carotid arteries?
2. Describe the vessel that supplies arterial blood to the superficial chin and nose.
3. Which vessel in the neck is found superficial to the sternocleidomastoid muscle?
4. Which vein lies next to the internal carotid artery?
5. What is the name of the vein found deep within the parotid gland?





## Case Study 6-2

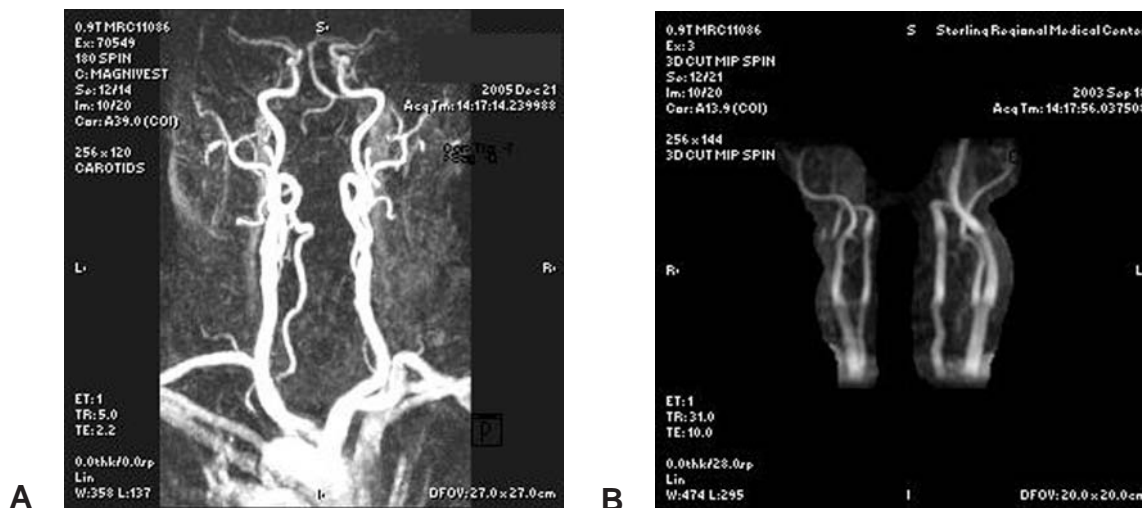


Figure 6-33

(A) This 70-year-old man was referred for an MRA (magnetic resonance angiography) examination to evaluate arterial blood flow through the region of the neck. As shown on the selected image above, the MRA demonstrates strong arterial blood flow in both internal carotid arteries found extending toward the top of the image. As compared to the 74-year-old woman shown (B), although strong flow is evident in the internal carotid artery on the right side, the left internal carotid artery is not readily apparent due to a lack

of blood flow. Unlike the normal flow seen on the left side, the right common carotid artery appears to terminate at the origin of the external carotid artery. Although not shown in this flow sequence, the blockage results from atherosclerotic plaques that build up over a lifetime, and in some cases (as shown in A), can significantly reduce arterial blood flow to the brain. This lack of blood flow can result in neurological changes and deficits, and is generally described as cerebrovascular disease.

### Questions

1. Explain the relationship of the common carotid artery with adjacent structures.
2. What regions of the head are supplied with arterial blood via the external carotid artery?
3. Describe the origin and course of the vertebral arteries including their location in the images above.
4. The right common carotid artery originates from which vessel?
5. The left common carotid artery originates from which vessel?



## Case Study 6-3

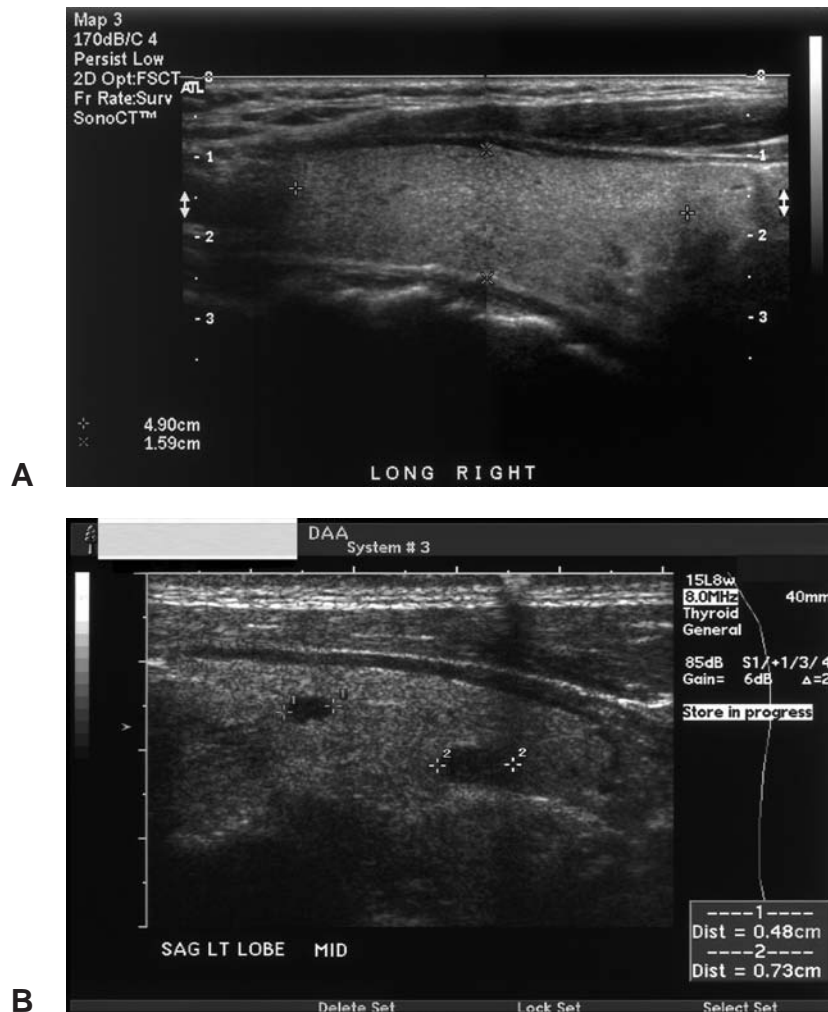


**Figure 6-34** **B**

This 39-year-old woman was referred for an ultrasound examination of her thyroid gland because she was suspected to suffer from hyperthyroidism (Fig. 6-34A). The right lobe measured is enlarged and in this longitudinal section measures  $4.9 \times 1.6$  cm. Between the marked points, the thyroid gland appears to be homogenous, demonstrating a uniform consistency throughout the gland. By comparison, the

lower image was generated on a 61-year-old male patient reporting similar symptoms (Fig. 6-34B). As shown by the marked measurements, there are two large nodules evident in this longitudinal section through the thyroid gland measuring 0.5 cm and 0.7 cm in diameter. The small nodules appear to be simple cysts that are hypoechoic and were also shown scattered throughout the left thyroid lobe.

## Questions

1. Describe the relationship of the thyroid gland to adjacent airway structures.
2. What are the large vessels found just posterior to the lateral margins of the thyroid gland?
3. Describe the shape of the thyroid gland.
4. In an axial section, would the thyroid gland be anterior or posterior to the arytenoid cartilage?
5. In a median sagittal section, would the thyroid cartilage or the thyroid gland be more superior?



## Case Study 6-4

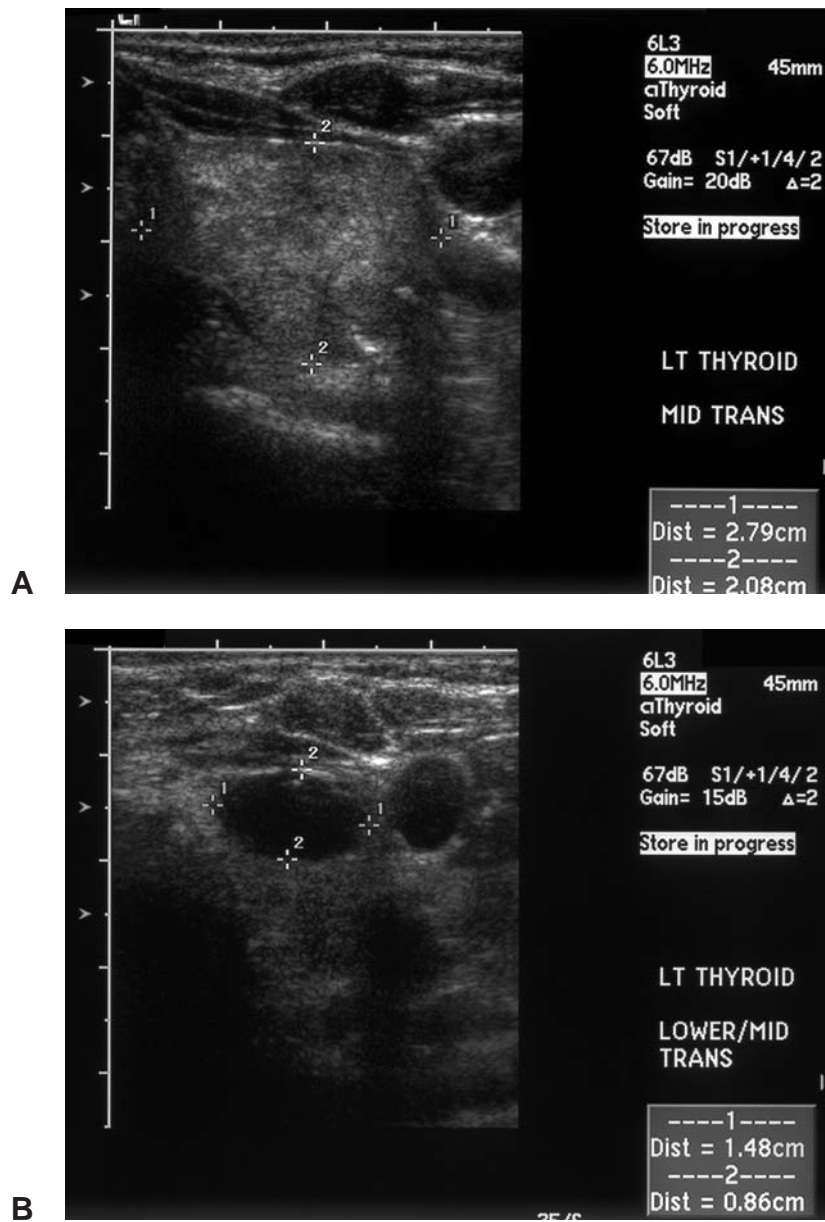


Figure 6–35

This 66-year-old man was referred for an ultrasound examination of the thyroid because he was reporting hypothyroid symptoms including restlessness, weight loss, diarrhea, sweating, and tachycardia (rapid heart beat over 100 beats per minute). Within the left lobe (Fig. 6-35A), the midtransverse section demonstrates a homogenous consistency to the thyroid gland measuring  $2.8 \times 2.1$  cm. By comparison, a lower transverse section (Fig. 6-35B)

includes a hypoechoic region that appears as a simple cyst and is measured to be  $1.5 \times 0.9$  cm. Similarly, multiple nodules were also shown in other sections and the patient's condition was described as multinodular goiter, which results from a collection of nodules that deform the thyroid gland. Most goiters are euthyroid; that is, they do not cause either hyperthyroidism or hypothyroidism.

## Questions

1. Is the thyroid gland located superior or inferior to the hyoid bone?
2. Describe the anatomic relationship between the thyroid gland and the esophagus.
3. In a median sagittal section, which part of the thyroid would be shown?
4. Is the thyroid cartilage found superior or inferior to the thyroid gland?
5. Is the internal or external jugular vein located closest to the thyroid gland?



## Case Study 6-5

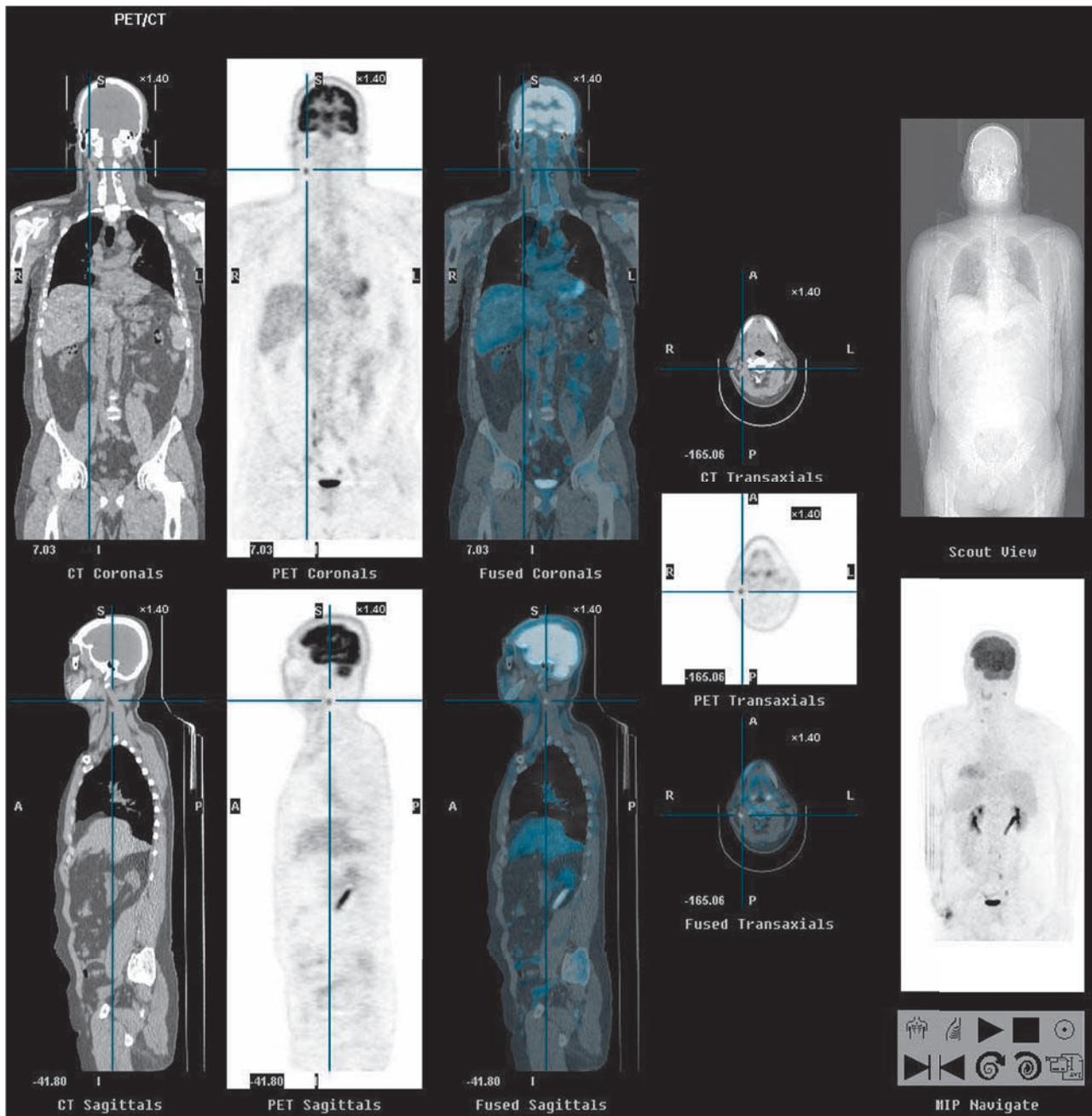


Figure 6-36

This PET/CT case is a 49-year-old white man previously diagnosed with melanoma. Before the procedure, the patient received a single IV dose of 15.7 mCi of F-18 FDG for this examination. As indicated by the marker lines, a large area of abnormal uptake was found in a solitary lymph node immediately posterior to the external jugular vein. On the right side of the neck, there is a 1-cm lymph node lying deep to the anterior edge of the sterno-

cleidomastoid muscle. Originating from the melanocytes in the skin, malignant melanoma is a very fast growing neoplasm and distant metastases are frequently found when the primary site is diagnosed. Although the most common treatment for suspected lesions is surgical resection, metastatic sites must be treated with radiation therapy and chemotherapy. The overall 5-year survival for all forms of melanoma is 60%.

## Questions

1. Describe the relationship of the external jugular vein to the sternocleidomastoid muscle.
2. What is the purpose of the external jugular vein?
3. Describe the origin, insertion, and action of the sternocleidomastoid muscle.
4. The external jugular vein drains blood into which vessel?
5. What are the thin strap muscles called that originate from the mandible and insert on the hyoid bone that act to raise the hyoid and depress the mandible?





# Case Study 6-6

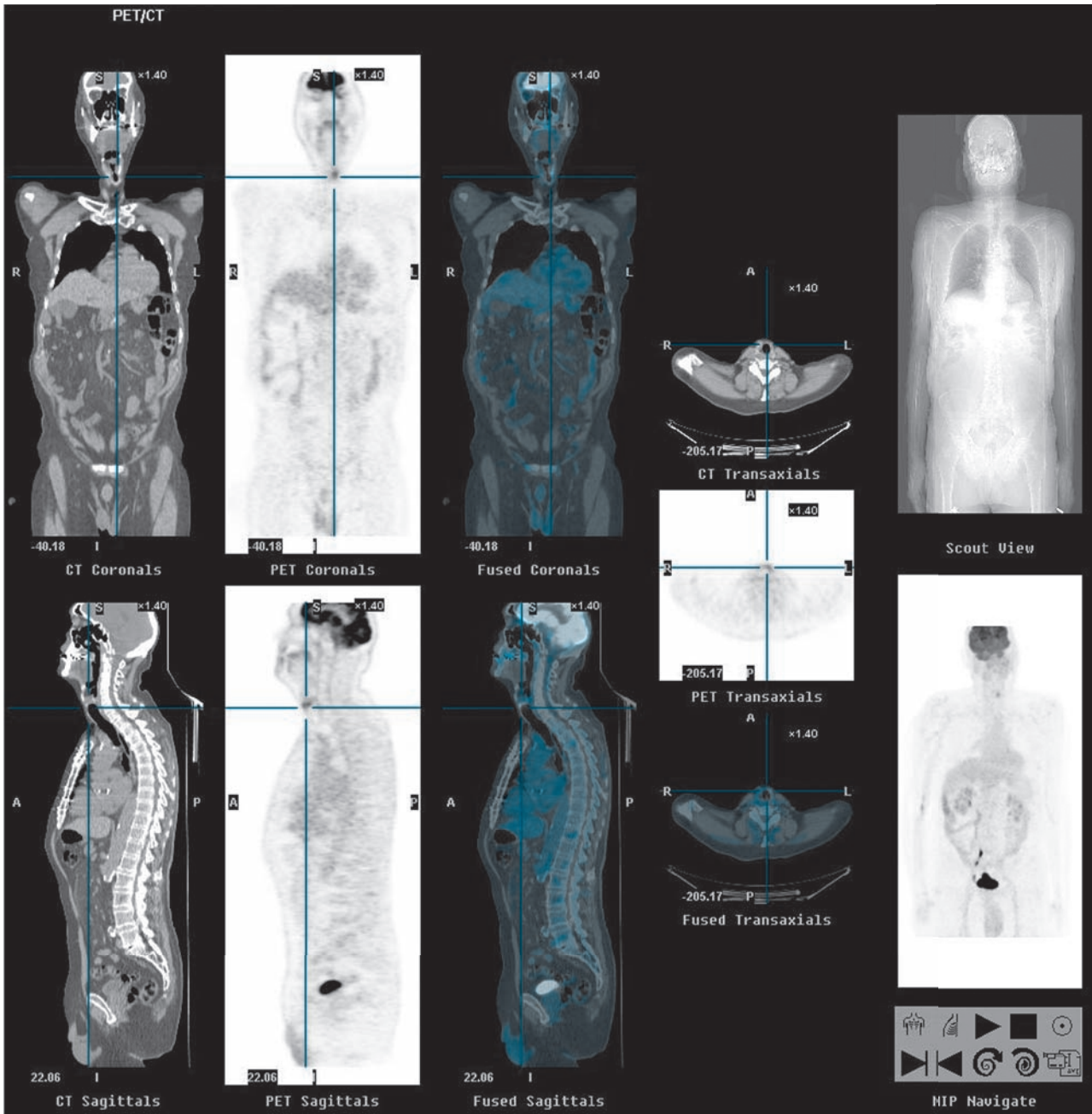


Figure 6-37

This PET/CT case is a 78-year-old white man previously diagnosed with a laryngeal tumor. Before the procedure, the patient received a single IV dose of 12.2 mCi of F-18 FDG for this examination. At the time of this study, abnormal uptake was clearly shown within the neck in the region of the left vocal cord. Because this was the site where previous biopsy samples had been obtained, the increased activity may correspond to a healing response. Within the neck,

thorax, and abdomen, no abnormal metabolic activity could be identified. Although biopsy results indicated this patient had a laryngeal neoplasm, no evidence of metastatic disease was detected in this PET/CT examination. Carcinoma of the larynx accounts for about one of every 50 diagnosed cancer patients and has been linked to smoking and chronic alcohol intake. The disease is seven times more likely in men, and the rate of incidence increases with advancing age.

## Questions

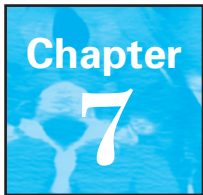
1. Looking down into the larynx, what is the first fold of skin called?
2. After passing down over the upper fold, what is the next fold of skin within the larynx called?
3. In a coronal section, describe the openings from superior to inferior found within the larynx.
4. Describe the location and shape of the epiglottis.
5. Where are the piriform sinuses located?





## CLINICAL APPLICATIONS

1. The neck is the region of the body between the \_\_\_\_\_ and the \_\_\_\_\_.
2. The hyoid bone is found at a level corresponding to the \_\_\_\_\_ cervical vertebra.
3. List the three spaces within the larynx: \_\_\_\_\_ is superior, \_\_\_\_\_ is in the middle, and \_\_\_\_\_ is inferior.
4. Briefly describe the location of the valleculae.
5. The common carotid arteries bifurcate into the internal and external branches at the level of the intervertebral disk between \_\_\_\_\_ and \_\_\_\_\_.
6. Which of the following best describes the location of the piriform sinuses?
  - A. Between the epiglottis and tongue
  - B. Below the vocal fold
  - C. On either side of the larynx
  - D. Between the vestibular and vocal folds
7. The epiglottis attaches inferiorly to the \_\_\_\_\_ and forms part of the (anterior / posterior) wall of the opening within the larynx.
8. The \_\_\_\_\_ are the spaces on either side of the median glossoepiglottic fold.
9. The \_\_\_\_\_ cartilages are pyramid-shaped and rest on the posterior arch of the \_\_\_\_\_ cartilage.
10. List the three parts of the pharynx: \_\_\_\_\_ is superior, \_\_\_\_\_ is in the middle, and \_\_\_\_\_ is inferior.



# Spine

## OBJECTIVES

Upon completion of this chapter, the student should be able to:

1. State the number of vertebrae in each region of the spine.
2. Explain the distinguishing characteristics of the vertebrae in each region.
3. Identify and describe the relationships between vertebrae.
4. Describe the components of the intervertebral disk.
5. Describe the ligaments of the spine.
6. Identify and describe the openings within the spine.
7. Describe the parts of the spinal cord.
8. Identify and describe the meningeal coverings of the spinal cord and nerve roots.
9. Describe the position of nerve roots within the spine in relation to other structures.
10. Correctly identify anatomic structures on patient computed tomography (CT) and magnetic resonance (MR) images of the spine.

## ANATOMIC OVERVIEW

The anatomy of the spine is symmetric and is described as the assemblage of vertebrae below the cranium and including the coccyx.

### ■ Skeleton

**Cervical vertebrae** (*SER-vī-kal VER-tě-brē*). The uppermost seven vertebrae, located between the cranium and the thoracic vertebrae (Fig. 7-1). They are easily distinguished from other vertebrae by their small size and the foramina in the transverse processes. See Chapter 6 for more details.

**Thoracic** (*thō-RAS-ik*) **vertebrae**. The 12 vertebrae of the chest, found in the spine forming the posterior border of the thoracic cage. They are of average size and are distinguishable by the presence of costal facets for articulation with the ribs. See Chapter 2 for more details.

**Lumbar** (*LŮM-bar*) **vertebrae**. The vertebrae that form the posterior border of the abdominal cavity. Five are usually found; however, four and six are common anomalies, which may confuse the viewer when determining image

location. They can be distinguished by their large size and the absence of costal facets and transverse foramina.

**Vertebral** (*VER-tě-brāl*) **structures**. With the exception of the atlas (C1), all vertebrae contain a body, two pedicles, two laminae, and seven processes (two transverse, four articular, and one spinous).

**Vertebral body**. The largest and heaviest portion of the vertebra. Located anterior to the vertebral arch, forming the anterior margin of the vertebral foramen (*fō-RĀ-men*). Their size increases as one moves down the vertebral column (Fig. 7-1). The bodies of thoracic vertebrae have superior and inferior costal facets for articulating with the ribs.

**Pedicles** (*PED-ī-klz*). Bony projections that form the lateral walls of the vertebral foramen and connect the vertebral body to the transverse processes.

**Laminae** (*LAM-i-nē*). The remainder of the vertebral arch. They form the posterolateral walls of vertebral foramen, connecting the transverse processes with the spinous process.

**Transverse processes**. Bony structures originating from the juncture of the laminae and pedicles that project laterally and  
(text continues on page 496)

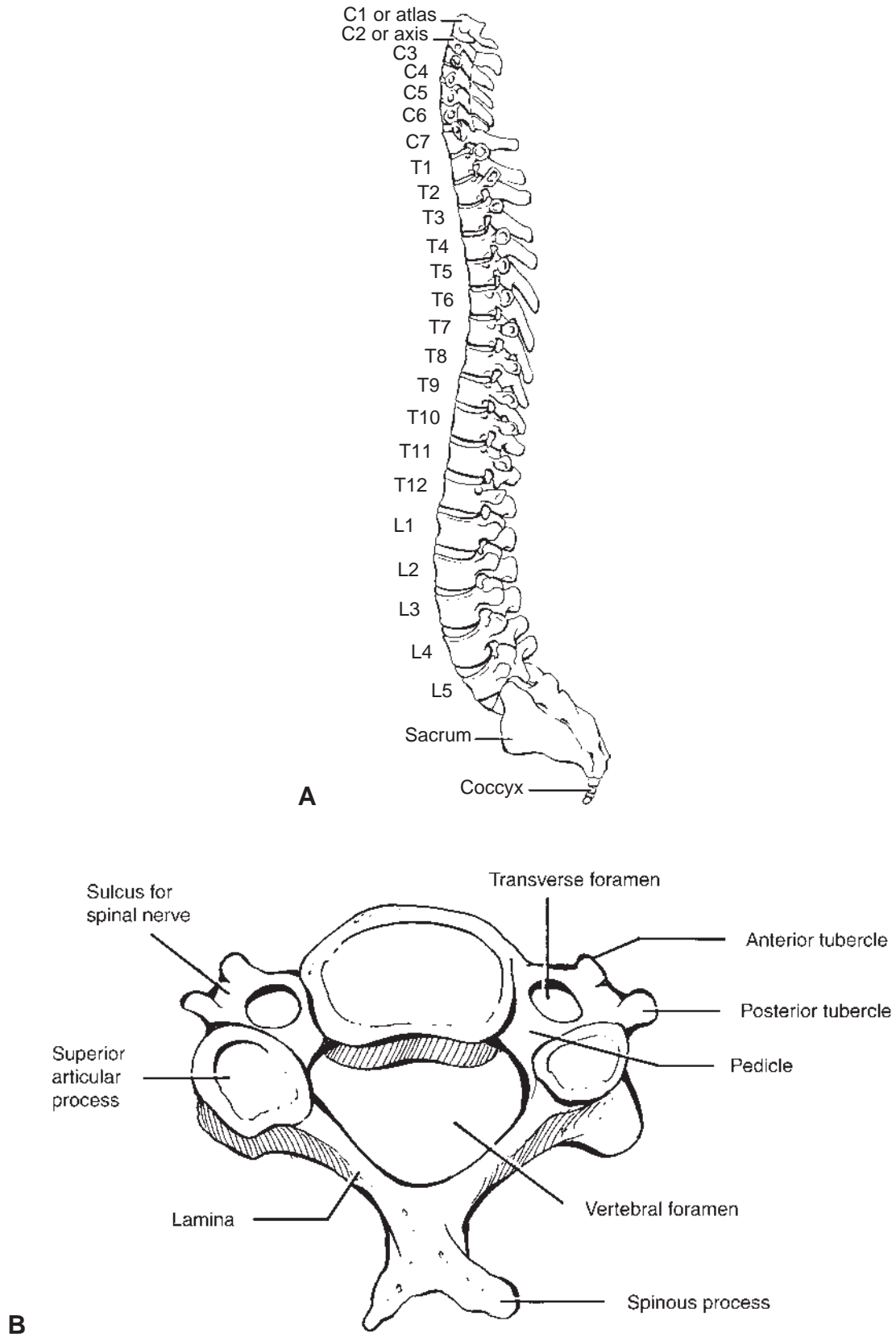


**Figure 7-1** A: Lateral view of entire vertebral column with assorted views of individual vertebrae. B: Superior view of a cervical vertebra. (*continued*)

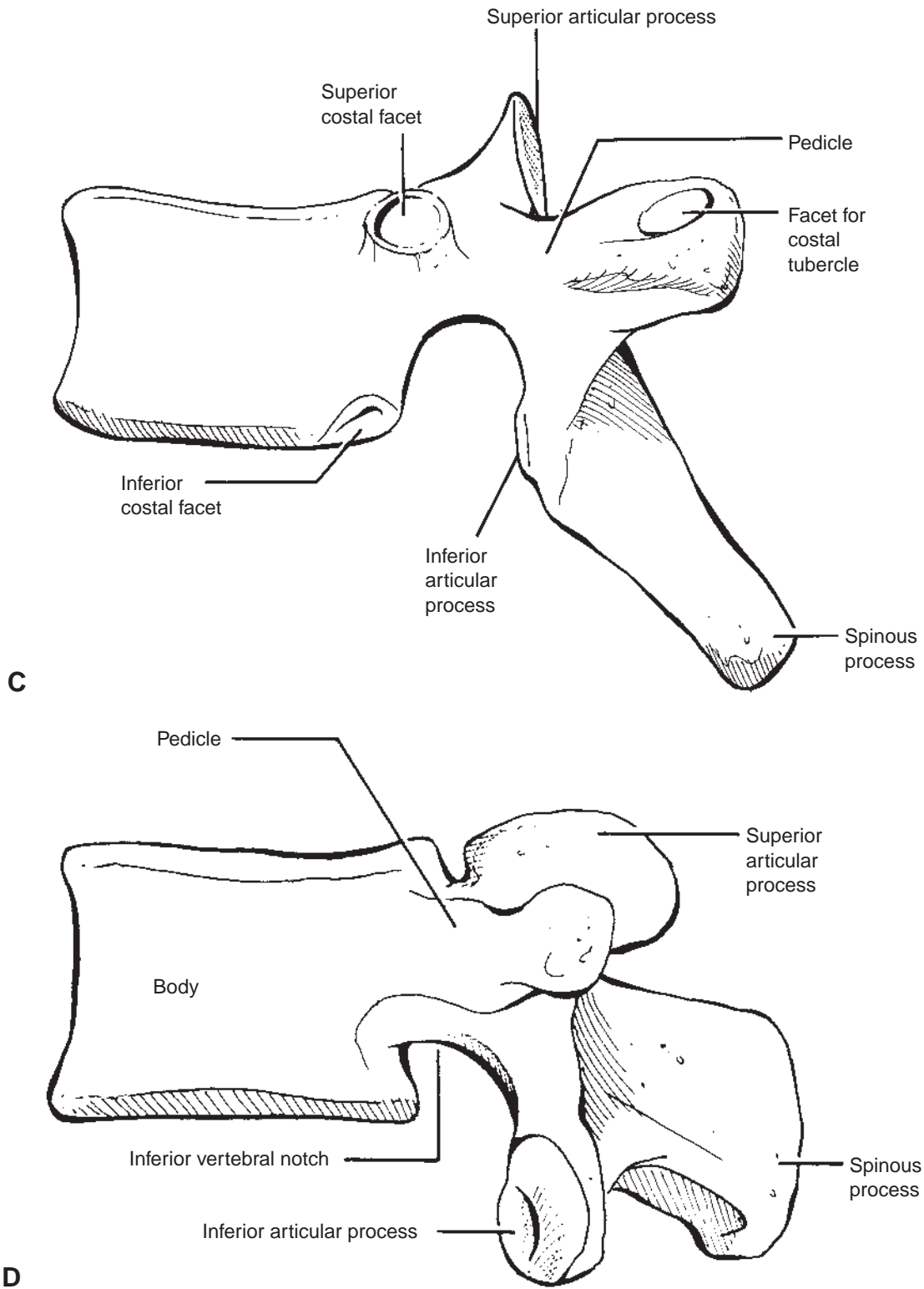


**Figure 7-1** (continued) **C:** Lateral view of a thoracic vertebra. **D:** Lateral view of a lumbar vertebra.

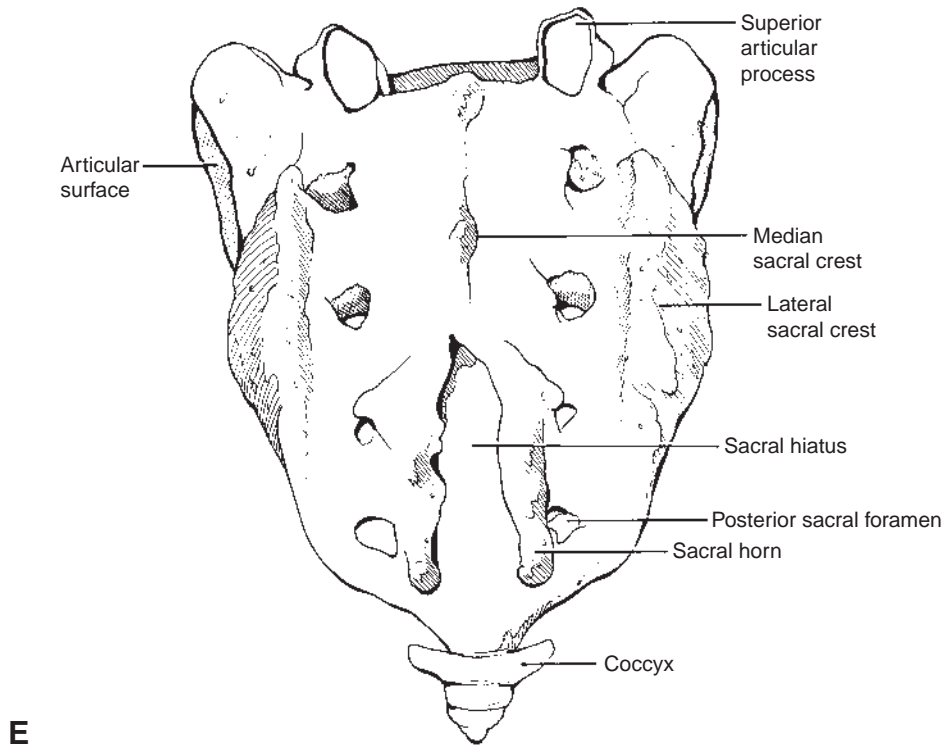


**Figure 7-1** (continued) **E:** Posterior view of the sacrum.

provide a site of attachment for the deep muscles of the back. Cervical vertebrae have transverse foramina, and thoracic vertebrae have articular facets for the tubercles of the ribs.

**Articular processes.** Bony structures that are directly lateral to the vertebral foramen and extend upward and downward from the points at which the pedicles and laminae join. On the superior articular process, the upward projection, the articular surface faces posteriorly. The inferior articular process, the downward projection of bone, faces anteriorly. Together, they form the zygapophyseal (*ZĪ-gǎ-pō-FIZ-ē-ǎl*) joints between adjacent vertebrae.

**Spinous processes.** Originate from the posterior union of the laminae. Bony processes that extend posteriorly and provide a site of attachment for the muscles of the back. Those on cervical vertebrae are shorter than those on thoracic and lumbar vertebrae, with the exception of the vertebra prominens on C7. The terminal processes of cervical vertebrae are usually bifid, unlike the single processes of other vertebrae.

**Sacrum** (*SĀ-krĭm*). Composed of five fused vertebral segments. The triangular bone that forms the posterior portion of the pelvis. Because the sacrum articulates with the fused ilia on either side, the foramina for the sacral spinal nerves open both anteriorly and posteriorly.

**Coccyx** (*KOK-siks*). Usually composed of four small rudimentary vertebral segments that form the caudal end of the spinal column. Common anomalies include three and five vertebral segments.

## ■ Foramina (*fō-RAM-i-nǎ*) of the Spine

**Vertebral foramina.** The large triangular openings within the vertebrae between the body and the vertebral arch. Together, they create the opening for the spinal cord. Because the opening narrows as it extends downward, the foramina in the thoracic and lumbar vertebrae are smaller and rounder than those in the cervical vertebrae.

**Intervertebral foramina.** Between the vertebrae, the opening formed on either side of the vertebral foramen that allows nerve roots to enter and exit the spinal column. Their size and shape depend on the alignment of the two adjoining vertebrae (Fig. 7-2).

## ■ Intervertebral Joints

**Zygapophysis** (*ZĪ-gǎ-POF-i-sis*). The joint between the superior and inferior articular processes of adjacent

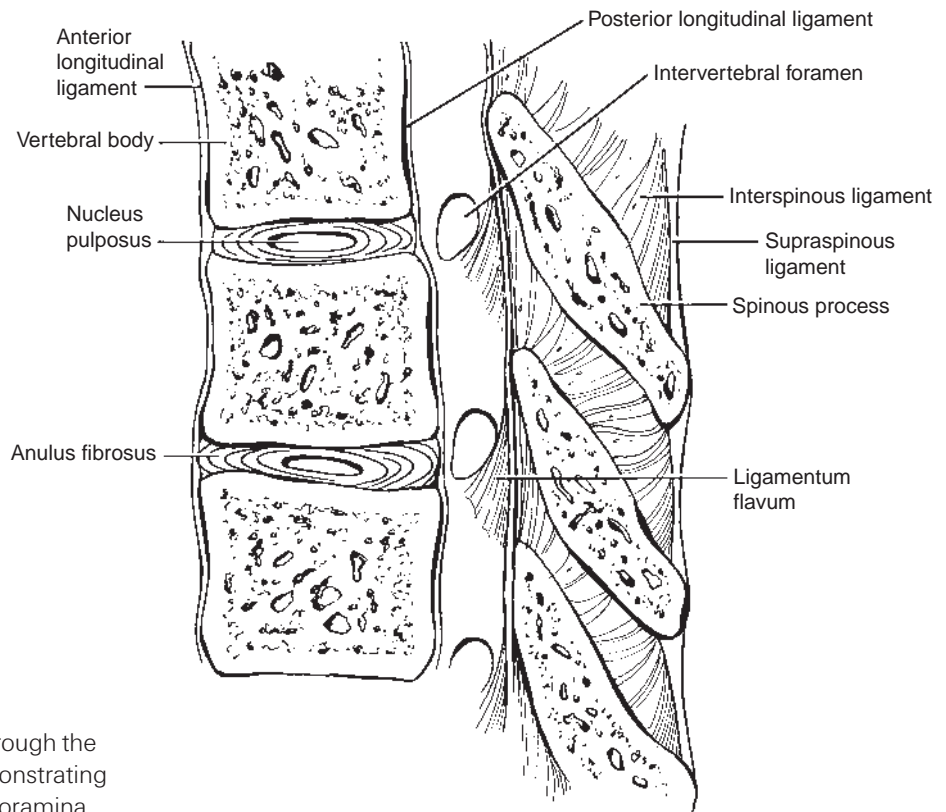


**Figure 7-2** Midsagittal section through the vertebral column demonstrating bone, ligaments, and foramina.

vertebrae. In axial or sagittal section, the superior articular process is found anterior and lateral to the inferior articular process.

**Anterior longitudinal ligament.** The layer of dense connective tissue tightly attached to the anterior surfaces of vertebrae and intervertebral disks extending from C2 to the sacrum.

**Posterior longitudinal ligament.** The layer of dense connective tissue tightly attached to the posterior surfaces of vertebrae and intervertebral disks extending from C2 to the sacrum.

**Intervertebral disks.** Connective tissue found between the vertebral bodies from C2 to the sacrum. They are of different sizes and help form the curvatures of the spine. They make up approximately one-quarter of the length of the vertebral column. Although their primary function is to form part of the amphiarthrodial (*AM-fi-ar-THRŌ-dē-ăl*) joints within the spine, they are also important in absorbing shock to the spine.

**Anulus fibrosus** (*AN-yū-lūs fi-brō-sūs*). A concentric ring of fibrous tissue and fibrocartilage that forms the periphery of the disk.

**Nucleus pulposus** (*NŪ-klē-ūs pŭl-PŌ-sūs*). The soft, pulpy, elastic material found within the center of the disk.

## ■ Spinal Cord and Coverings

**Conus medullaris** (*KŌ-nūs MED-ŭ-LĀ-ris*). The caudal tip of the spinal cord found between L1 and L3 (Fig. 7-3).

**Cauda equina** (*KAW-dā Ē-kwīn-ă*). Within the dural sheath, the bundle of lumbar and sacral nerves descending below the termination of the spinal cord. Resembles the caudal end of a horse (a horse's tail).

**Nerve roots.** At each vertebral level, a pair of nerve roots exits the spine through the intervertebral foramina on either side to form the right and left spinal nerves (Fig. 7-4). They originate from the spinal cord and are separated into anterior and posterior roots. Surrounded by a sleeve of meninges (*mĕ-NIN-jēz*), they join together outside the intervertebral foramen to form a spinal nerve. With the exception of the cervical vertebrae, the spinal nerves exit below the corresponding vertebrae (Fig. 7-3). In the cervical region, there are eight spinal nerves, because the C1 spinal nerves are found between the skull and C1. Consequently, cervical spinal nerves are above the corresponding vertebrae and spinal nerve 8 is found between C7 and T1.

**Posterior (dorsal) nerve root.** Nerve fibers originating from the posterior spinal cord. Responsible for carrying motor stimuli to muscles within the body (Fig. 7-4).

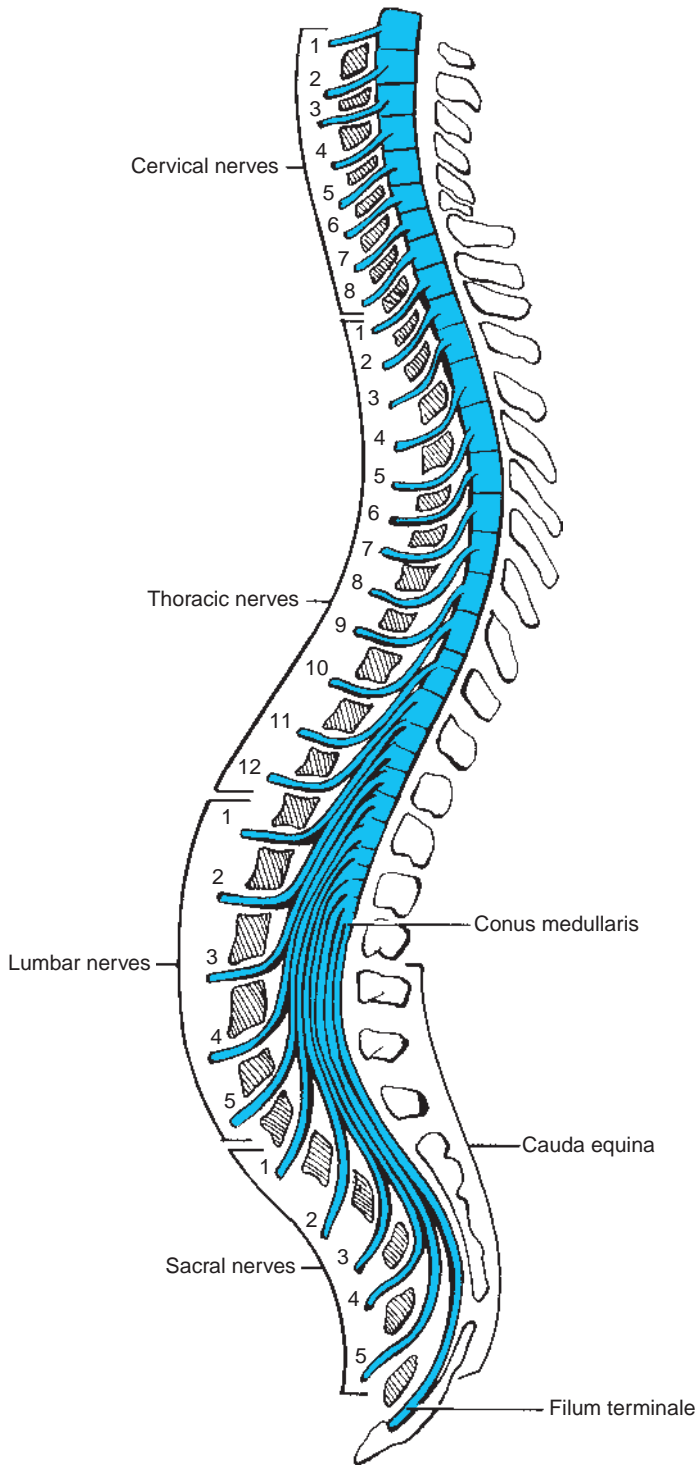


**Figure 7-3** Drawing of the spinal cord and nerve roots.

*Posterior (dorsal) root ganglion (GANG-glē-on).* Formed by the collection of motor nerve cell bodies as the nerves pass through the intervertebral foramen.

*Anterior (ventral) nerve root.* Nerve fibers carrying sensory signals and terminating in the anterior spinal cord.

**Spinal meninges.** A continuation of the meningeal layers described within the head that surround and protect the spinal cord. As nerve roots exit through the intervertebral foramina, they are protected by a sleeve of meningeal layers that terminates as the spinal nerves are formed outside the spine.

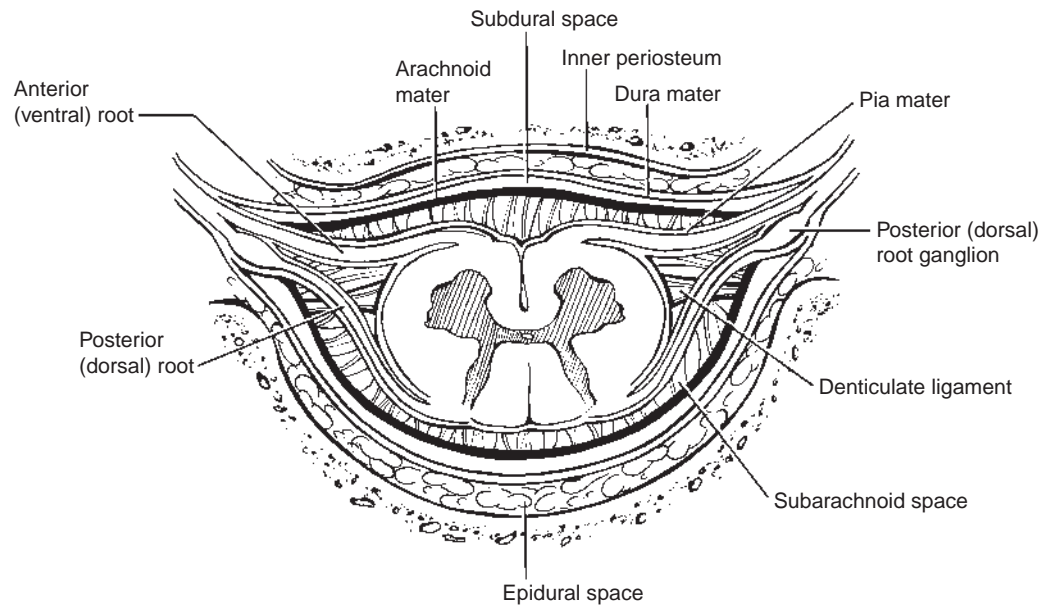


**Figure 7-4** Axial drawing of the vertebral foramen demonstrating the spinal cord, nerve roots, and the surrounding meninges.

*Pia mater* (PĪ-ă MA-ter). The innermost layer. Continuous with the surface of the spinal cord and nerve roots.

*Arachnoid* (ă-RAK-noyd) *mater*. The middle covering. Composed of thin, delicate fibers known as arachnoid trabeculae (tră-BEK-yū-lē).

*Subarachnoid space*. Between the arachnoid mater and the pia mater. Continuous with the space

of the cranium and filled with cerebrospinal fluid (CSF).

*Dura* (Dū-ră) *mater*. The tough outer layer; surrounded by fat in the epidural space within the vertebral foramen. Like the other meningeal layers, it forms a sheath around the nerve roots within the intervertebral foramen.

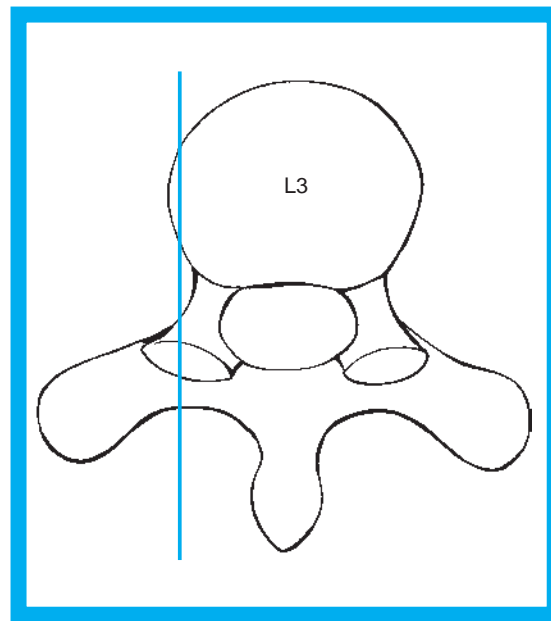




## Sagittal Magnetic Resonance (MR) Images

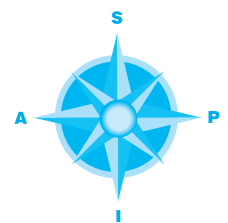
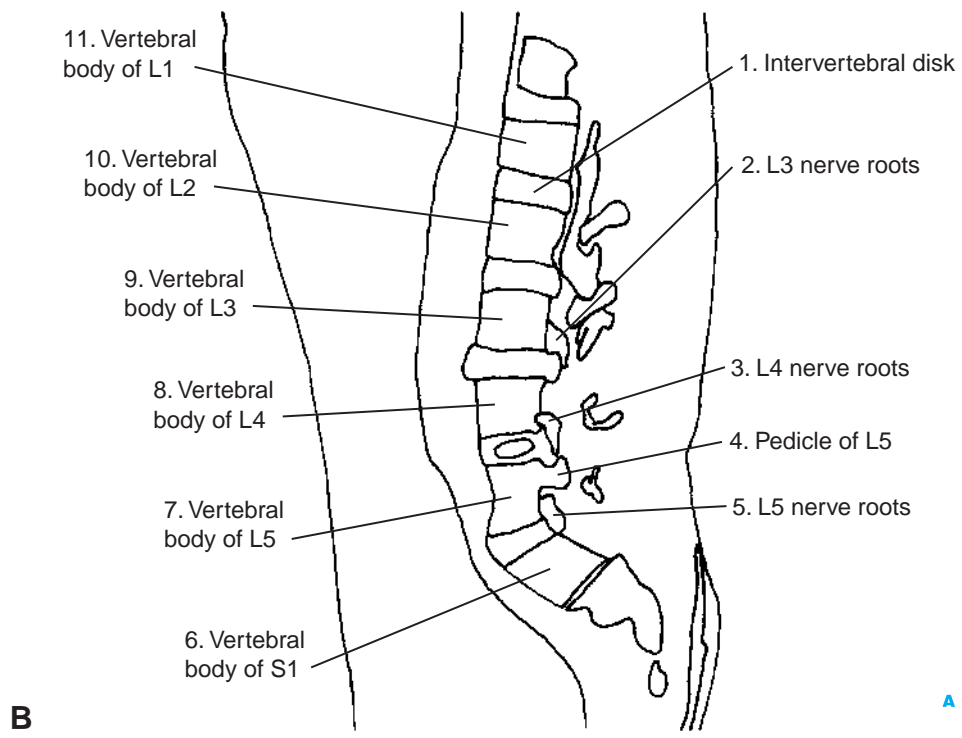
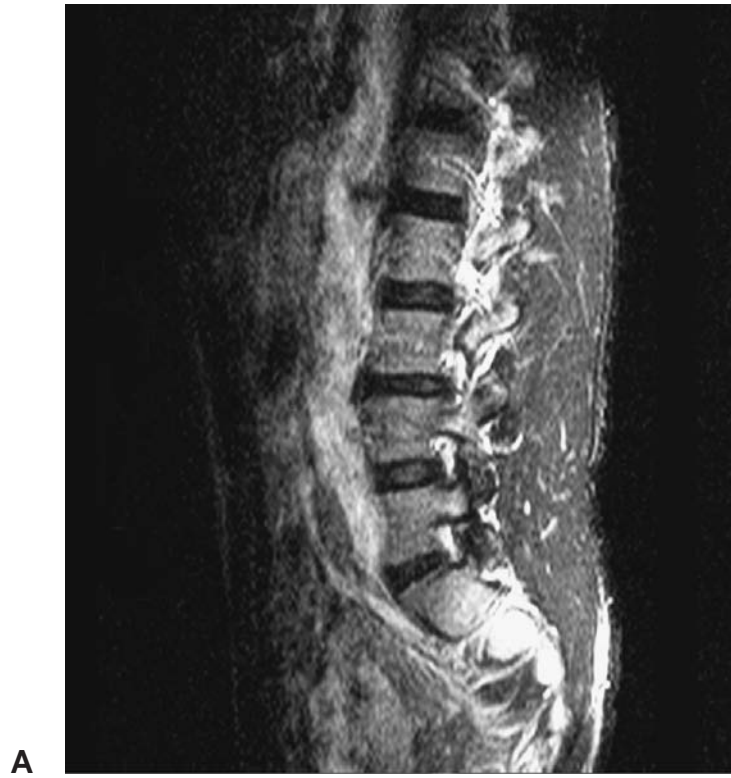
Although a typical scan of the spine would generate a series of images throughout the entire region, the following are eight selected sagittal MR images of the lumbar spine. The images are generated at 5.0-mm

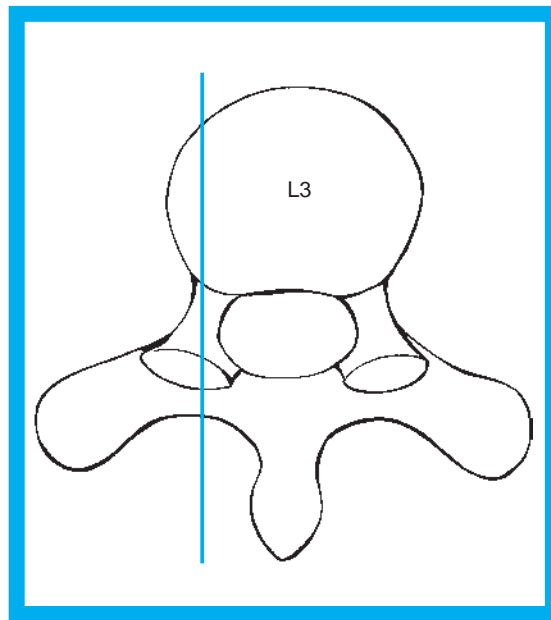
intervals from right to left at the following technical factors: repetition time (TR) = 500; echo time (TE) = 20; radiofrequency (RF) = 90°; field of view (FOV) = 30 cm.



**Figure 7-5 (A,B)** Sagittal MR image 1.

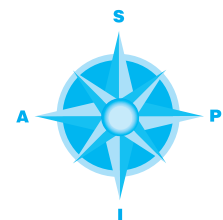
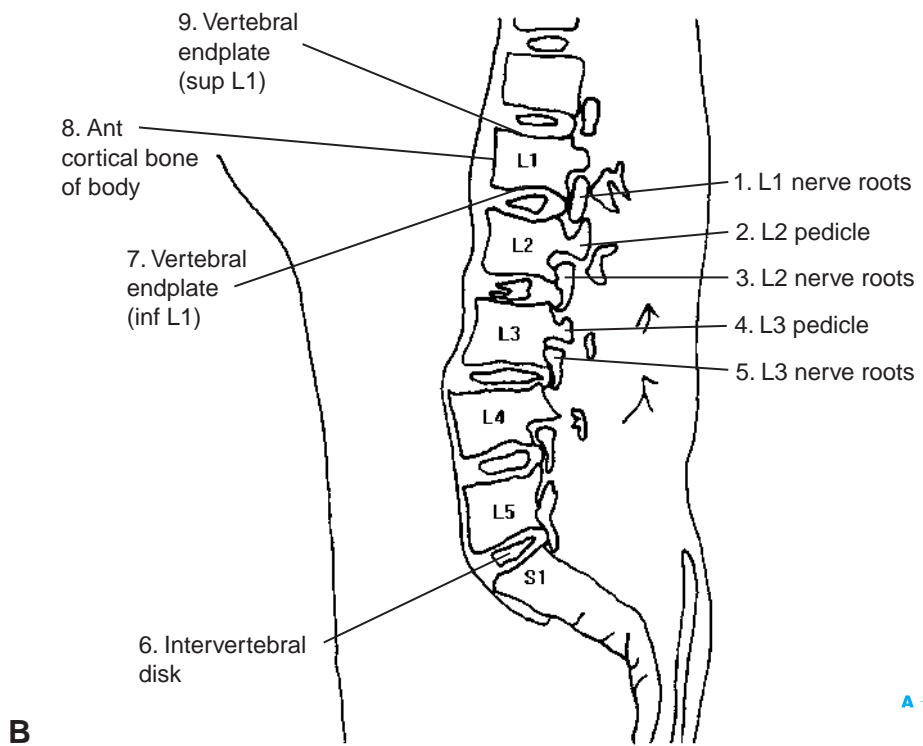
Because of the absence of the spinal cord within the vertebral foramina, this image demonstrates structures found on the right side of the vertebral column. The noticeable angle between the lower vertebral bodies demarcates the L5-S1 intervertebral joint. Below this joint, the tilted orientation of the vertebral body of S1 is characteristic of the upper sacral segments within the pelvis. Above the level of the sacrum, the vertebral bodies of L1 through L5 are separated by the intervertebral disks. At the level of L5, a bony process can be seen projecting posteriorly from the vertebral body as the pedicle of L5. As described earlier, the intervertebral foramina are located between the pedicles of adjacent vertebrae. Several areas of intense signal found within the intervertebral foramina are labeled the nerve roots of L3 through L5. As described earlier, the nerve roots are found just below the corresponding pedicle. For example, the L5 nerve roots are found just below the pedicle of L5.

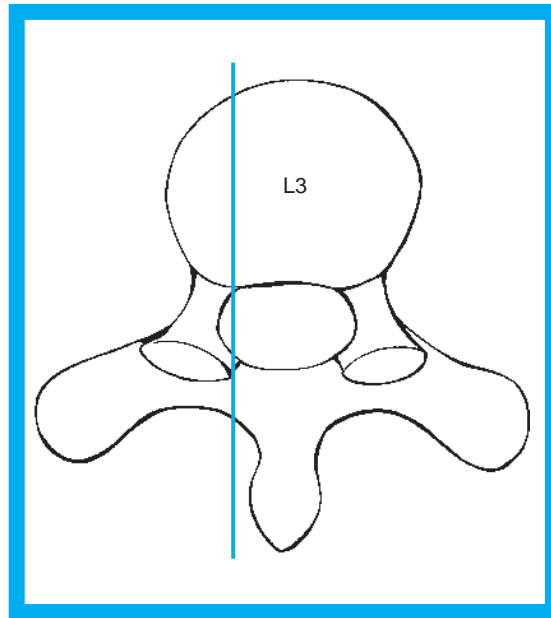




**Figure 7-6 (A,B)** Sagittal MR image 2.

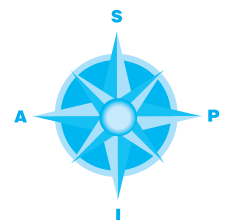
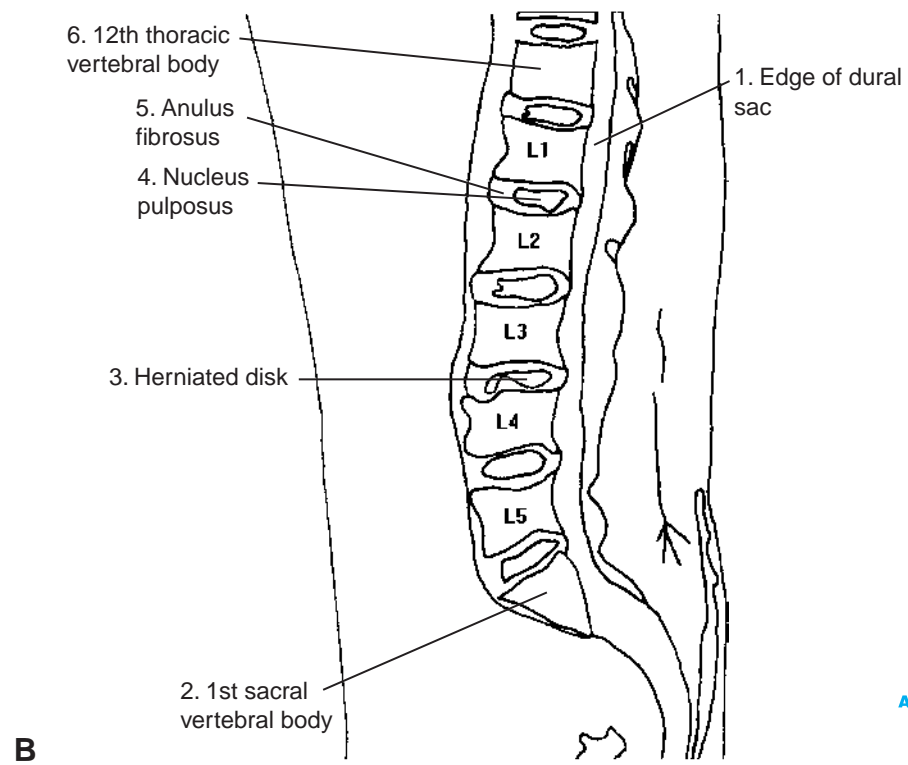
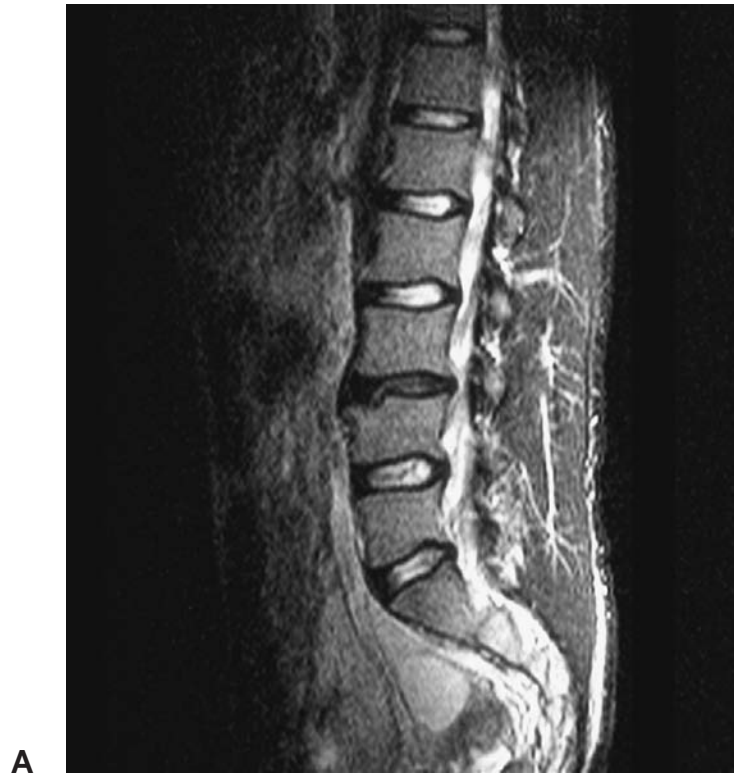
Compared to the previous image, the visualization of the lumbar pedicles along with the intervertebral foramina indicate that this image is nearing the contents of the spinal canal. Similar to the previous image, nerve roots are labeled as the intense signal areas within the intervertebral foramina corresponding to the vertebral body located just above. Because this image is closer to the midline, the margins of the vertebral bodies are more clearly demonstrated adjacent to the intervertebral disks. As demonstrated in L1, each of the vertebral bodies has a region of cortical bone surrounding the periphery of the body. The superior and inferior regions of cortical bone form the vertebral endplates that are located adjacent to the intervertebral disks.

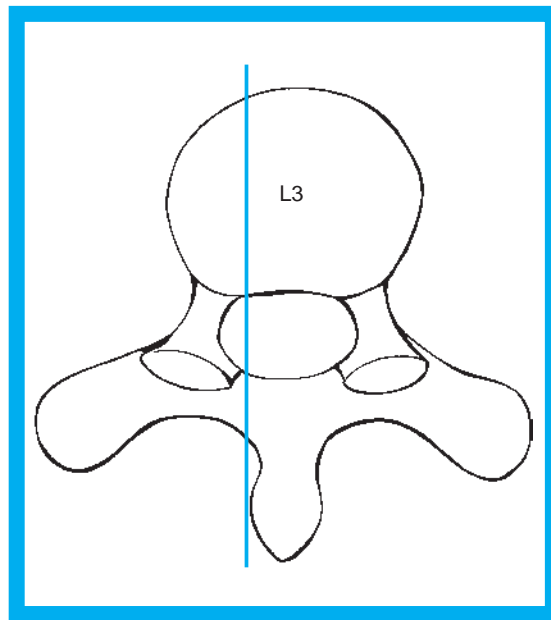




**Figure 7-7 (A,B)** Sagittal MR image 3.

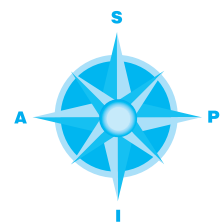
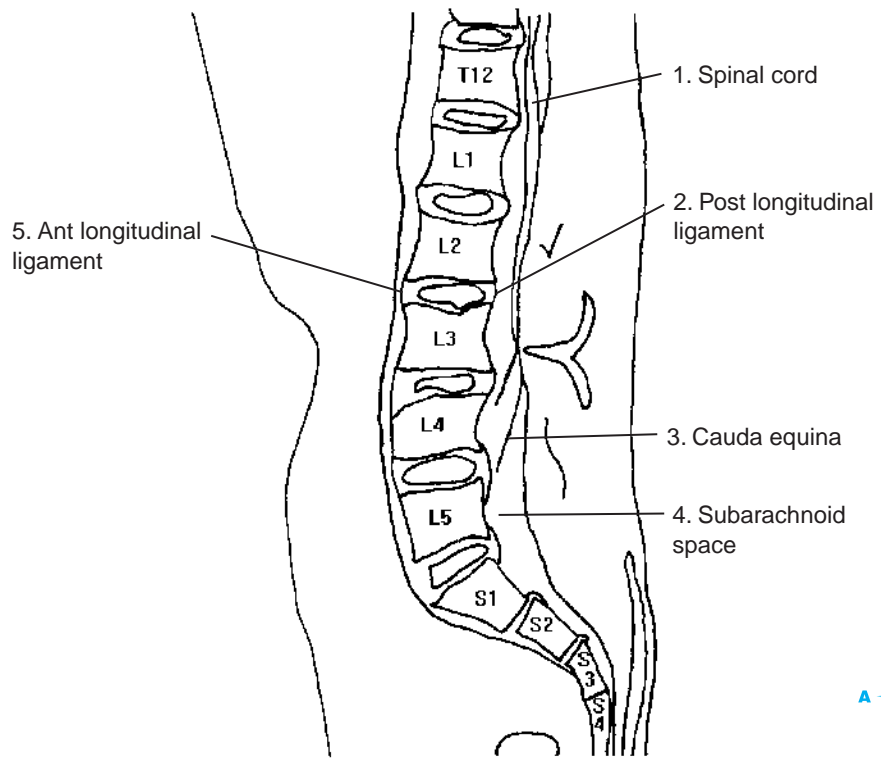
Although the vertebral bodies of L1 through S1 are again shown separated by the intervertebral disks, the pedicles are no longer seen (indicating that the plane of section is through the spinal canal). In the area previously occupied by the pedicles, a low-signal area can be identified directly posterior to the vertebral bodies, representing the edge of the dural sac. Within the vertebral column, the superior endplate of L4 has an irregular appearance owing to the adjoining herniated disk. Within a normal intervertebral disk, demonstrated in this image between L1 and L2, the boundary between the nucleus pulposus and the annulus fibrosus is not clearly discernible. However, the nucleus pulposus has slightly less signal intensity than the surrounding annulus fibrosus.



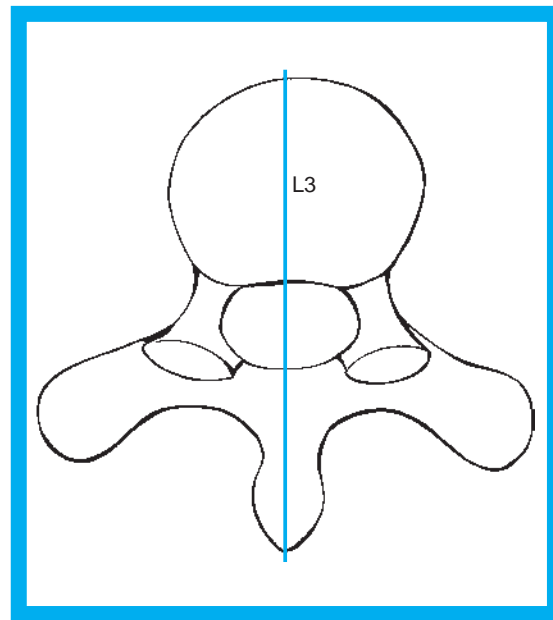


**Figure 7-8 (A,B)** Sagittal MR image 4.

Within the spinal canal, the spinal cord can be seen within the dural sac on the superior part of this image. As the spinal cord descends below the upper lumbar vertebrae, the spinal cord terminates and gives rise to bundles of nerve roots extending to the lower lumbar and sacral regions, collectively known as the cauda equina. Surrounding the cauda equina, the cerebrospinal fluid-filled subarachnoid space has a low signal activity. Between the dural sac and the vertebral column, the posterior longitudinal ligament is labeled as it covers the posterior surface of the vertebral column. Anterior to the vertebral column, the anterior longitudinal ligament is not clearly separable from the intervertebral disks and the anterior cortical margins of the vertebral bodies.

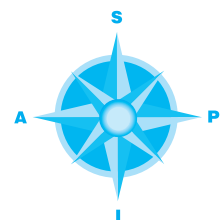
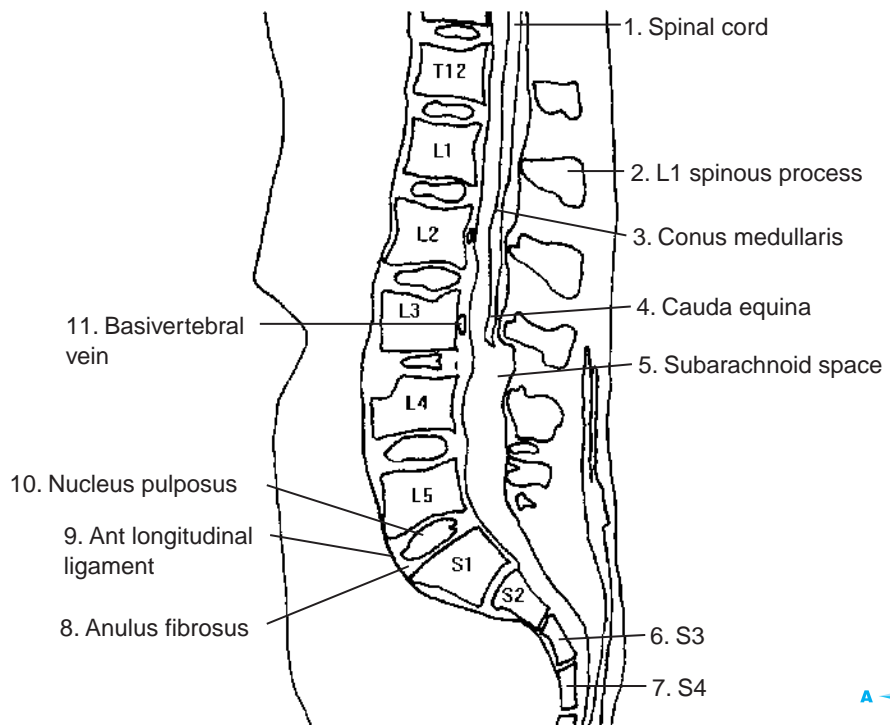






**Figure 7–9 (A,B)** Sagittal MR image 5.

In this image, most of the lower spinal cord is demonstrated in cross-section, including its termination at the conus medullaris at the L1-L2 vertebral level. Below the termination of the spinal cord, the lower lumbar and sacral spinal nerve roots continue as the cauda equina. All of the spinal nerve structures just described are surrounded by the low-signal subarachnoid space that lies within the dural sac between the pia mater and arachnoid mater, which is closely associated with the dura mater. In this near midsagittal image, the small basivertebral veins can be seen extending into the posterior cortical margin of the vertebral bodies of L2 and L3. Although this appearance could be misinterpreted as a fracture within the vertebral body, the presence of the basivertebral veins is a normal finding and should not be confused with any sort of pathologic condition. The characteristic angulation of the intervertebral joint between L5 and S1 demonstrates a normal intervertebral disk. Owing to the angulation of this joint, the L5-S1 intervertebral disk is often wedge-shaped and thicker adjacent to the anterior longitudinal ligament. Similar to other intervertebral disks, the less intense nucleus pulposus is surrounded by the anulus fibrosus.



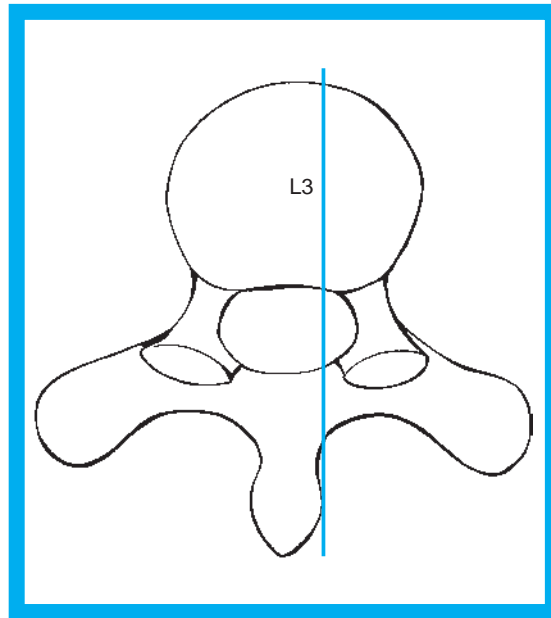
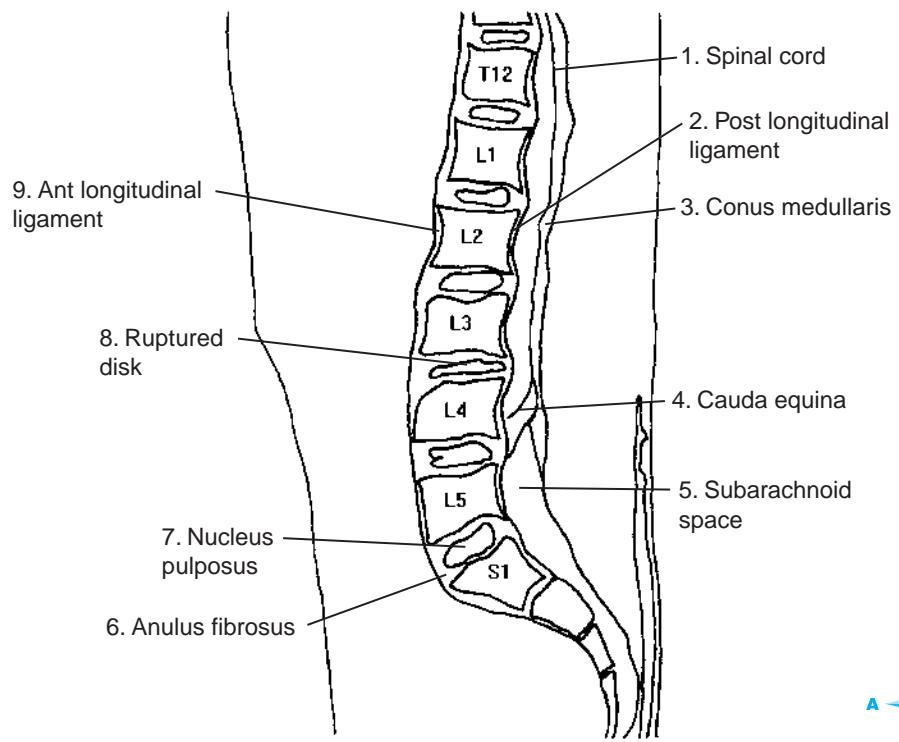


**Figure 7–10 (A,B)** Sagittal MR image 6.

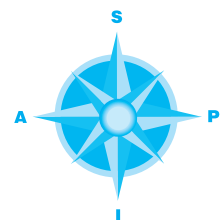
This image shows the spinal cord in cross-section terminating at the conus medullaris posterior to L1-L2. The nerve roots exiting the spine at the lower lumbar and sacral levels originate above the conus medullaris (L1-L2), forming the cauda equina. Considered part of the central nervous system, all of the structures just described are surrounded by cerebrospinal fluid within the subarachnoid space. The vertebral column appears much like it did in previous images, bound by the anterior and posterior longitudinal ligaments. A ruptured disk is again demonstrated between L3 and L4. The normal, wedge-shaped intervertebral disk found between L5 and S1 consists of a nucleus pulposus surrounded by an annulus fibrosus.

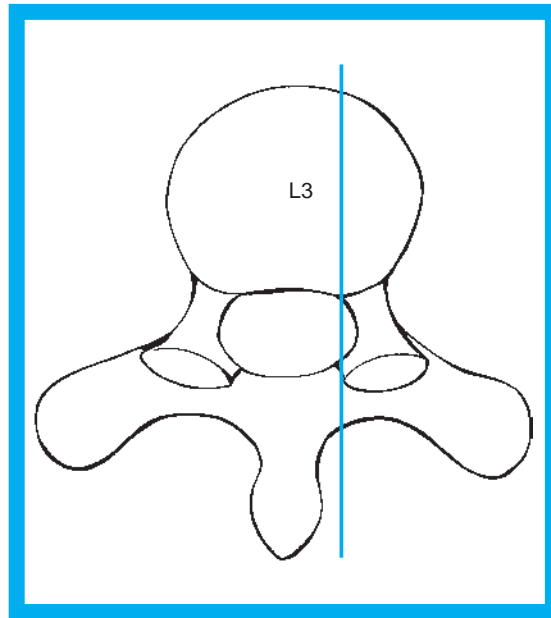


A



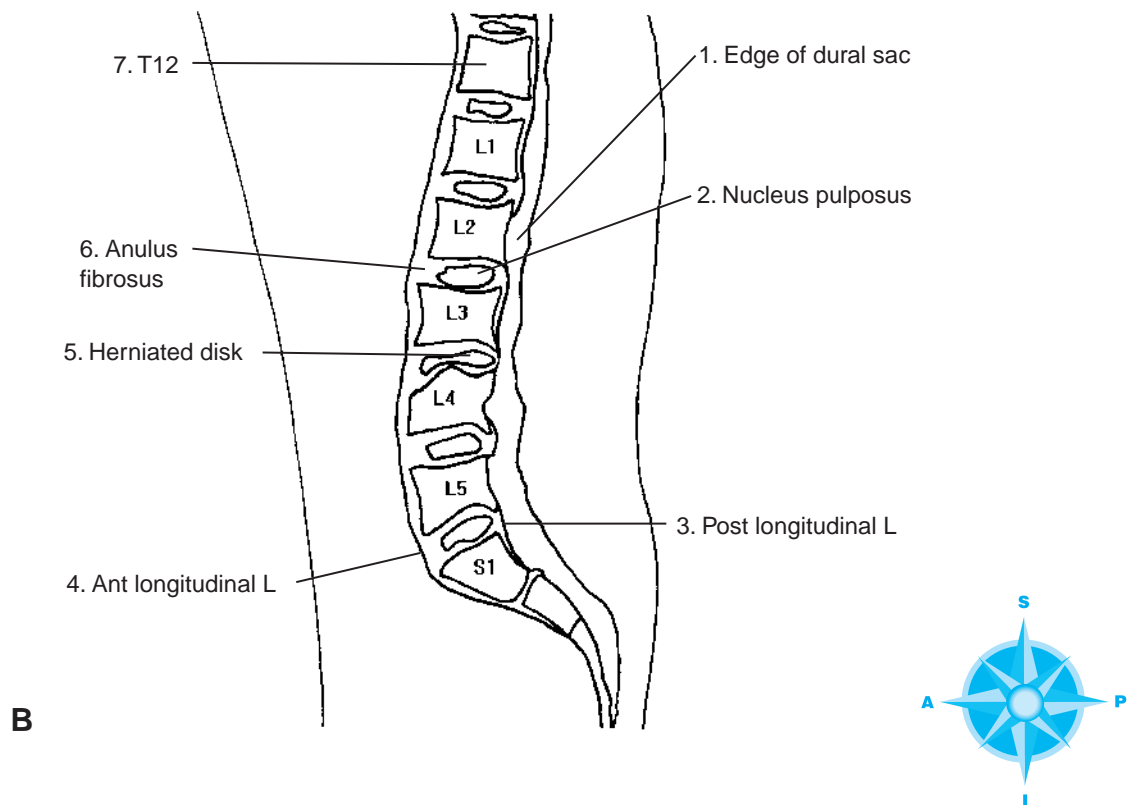
B





**Figure 7-11 (A,B)** Sagittal MR image 7.

Because only the edge of the dural sac is seen in this image, the anatomy demonstrated is found along the left side of the spinal canal. Similar to previous images, the vertebral column is bound on either side by the anterior and posterior longitudinal ligaments. The intervertebral disks, consisting of the nucleus pulposus and the anulus fibrosus, are normal at all levels except L3-L4, where a herniated disk can be identified.



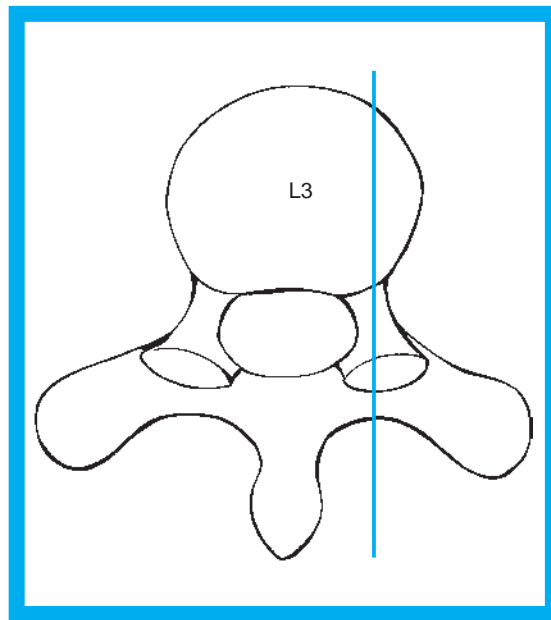
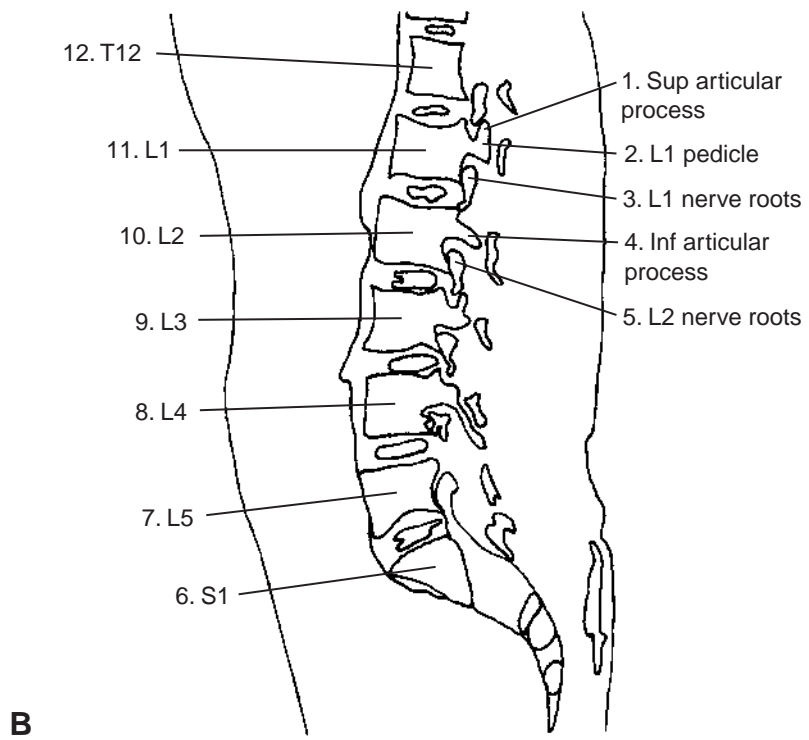


**Figure 7-12 (A,B)** Sagittal MR image 8.

Owing to the presence of pedicles extending posteriorly from the vertebral bodies in this image, the anatomy demonstrated lies outside of the spinal canal. Between the pedicles, high-intensity signal areas represent the nerve roots within the intervertebral foramina. At the termination of the pedicle, the superior articular process articulates with the inferior articular process of the adjoining vertebra. Each nerve root lies just below the corresponding vertebra and consists of an anterior and posterior root as described earlier. Surrounded by a sheath of dura mater, the nerve roots terminate outside the intervertebral foramina at the origin of the spinal nerve.







## Axial Computed Tomography (CT) Images

The following nine selected CT images of the lumbar and sacral regions of the spine will be described at 8-mm intervals from superior to inferior. In a typical scan of the spine using a disk protocol, the images are generated at 4-mm intervals through the intervertebral disk and the cortical margins of the adjacent vertebrae. To reduce density-averaging artifacts caused by slice thickness, the plane of section is set parallel to the cortical margin of the vertebrae

for each intervertebral disk. To enhance visualization of the dural sac, the following images were generated immediately after the administration of 5 mL of 180 iohexol into the subarachnoid space. The patient was rolled and then taken to CT where the scans were obtained via a disk protocol at the following technical factors: 130 kilovolt peaks (kVp); 300 milliamperere-seconds (mA-s); and slice thickness (TH) = 4.0 mm.

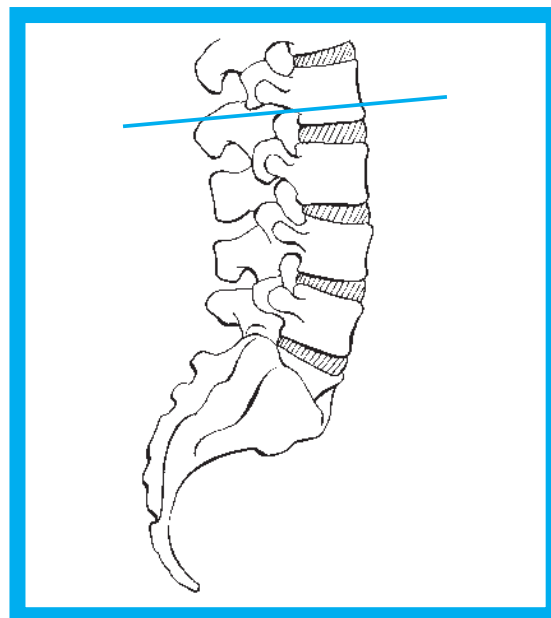
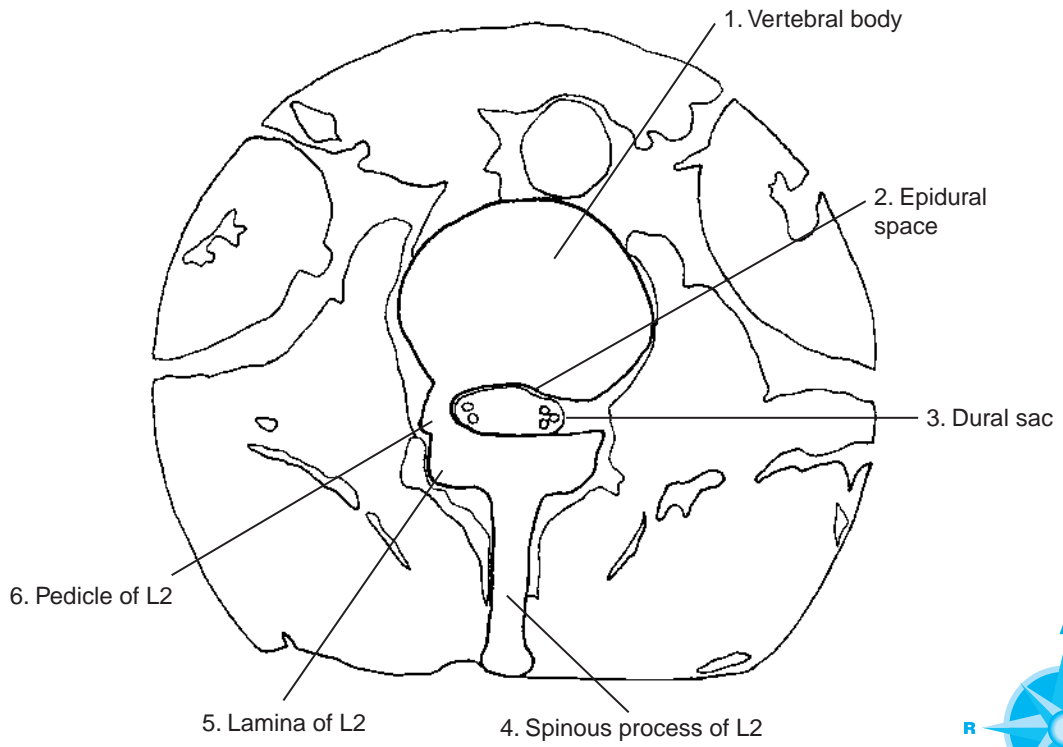


**Figure 7–13 (A,B)** Axial CT image 1.

Between the vertebral body and the laminae, the pedicle is seen on only the left side of the vertebral foramen, indicating the level of section is through the middle of L2. Within the vertebral foramen, the epidural space is visualized just outside of the dural sac. Extending posteriorly from the vertebral foramen, the large singular spinous process of L2 is demonstrated between the muscles of the back.



A



B

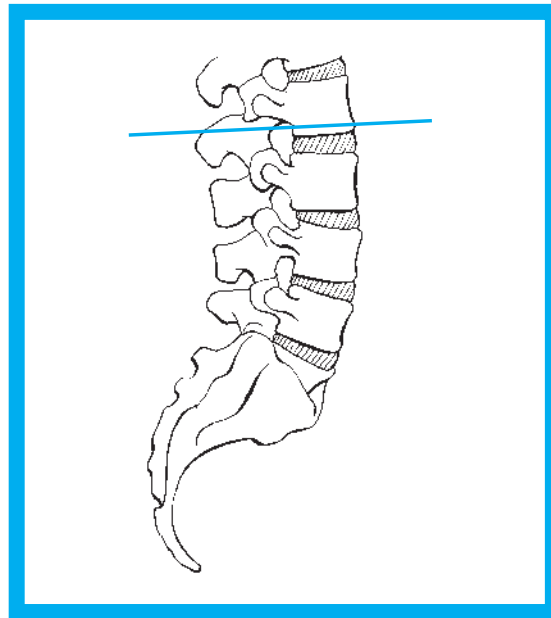
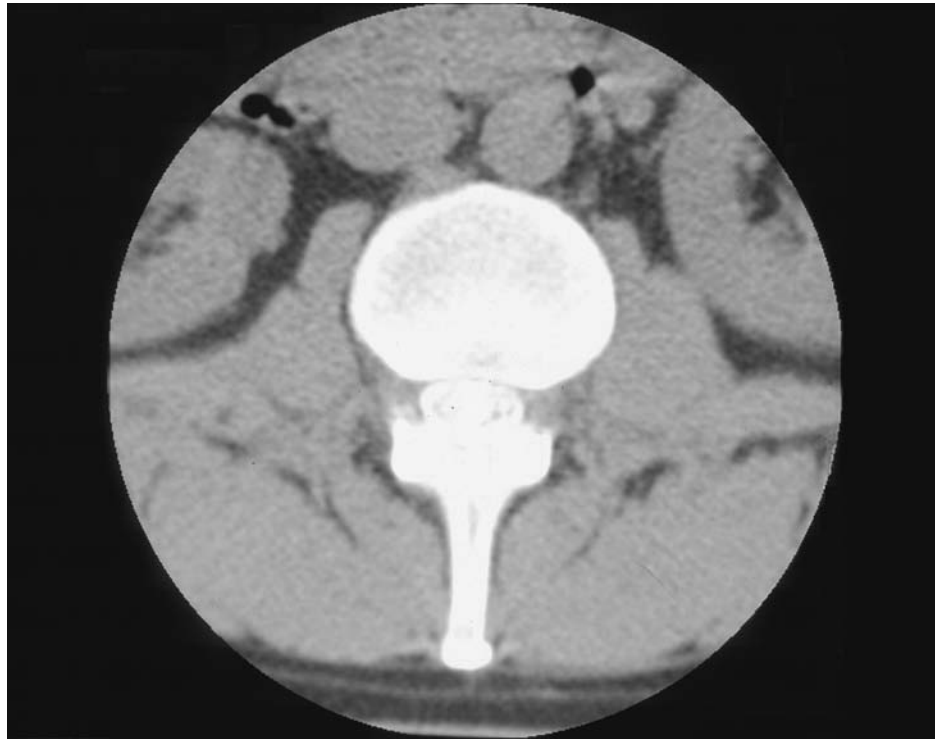
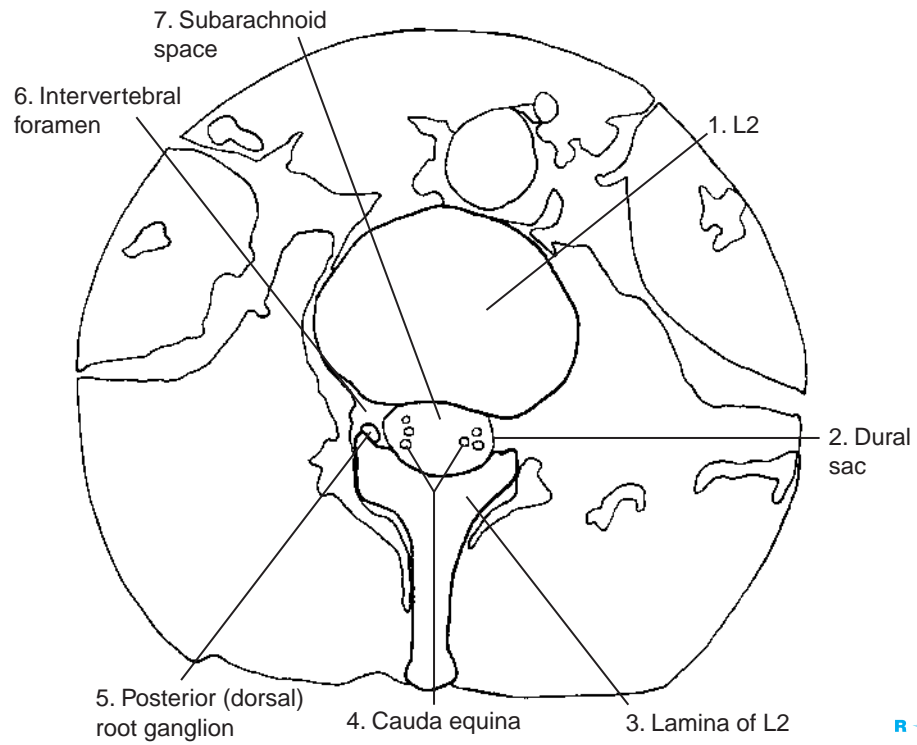


**Figure 7-14 (A,B)** Axial CT image 2.

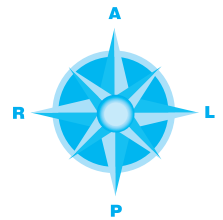
At this level, no pedicles are seen connecting the laminae with the vertebral body, indicating that the level of this section is in the lower part of the L2 vertebral body. In the areas previously occupied by the pedicles, the intervertebral foramina now form openings through which spinal nerves can enter or exit the vertebral foramen. Similar to the previous image, the dural sac is within the vertebral foramen and is clearly demonstrated, because contrast has been injected into the subarachnoid space. Although it is difficult to clearly discern each nerve bundle, nerve roots can be seen within the dural sac and are collectively referred to as the cauda equina. On the right side, an oval-shaped region is enhanced by contrast and represents the area of the posterior (dorsal) root ganglia, which is a collection of motor nerve cell bodies.



A



B



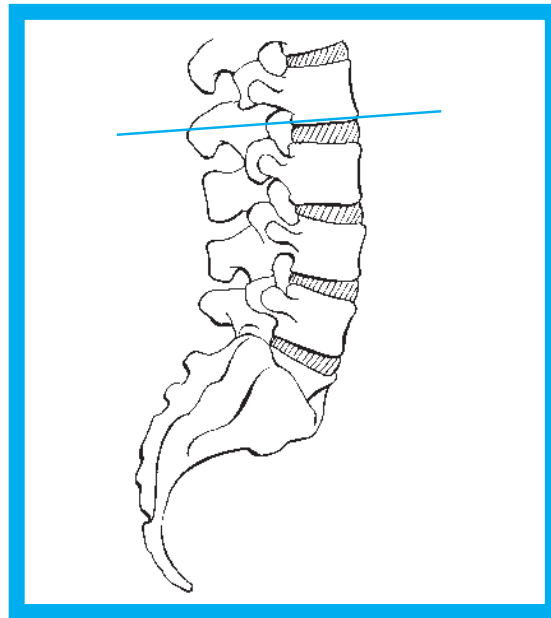
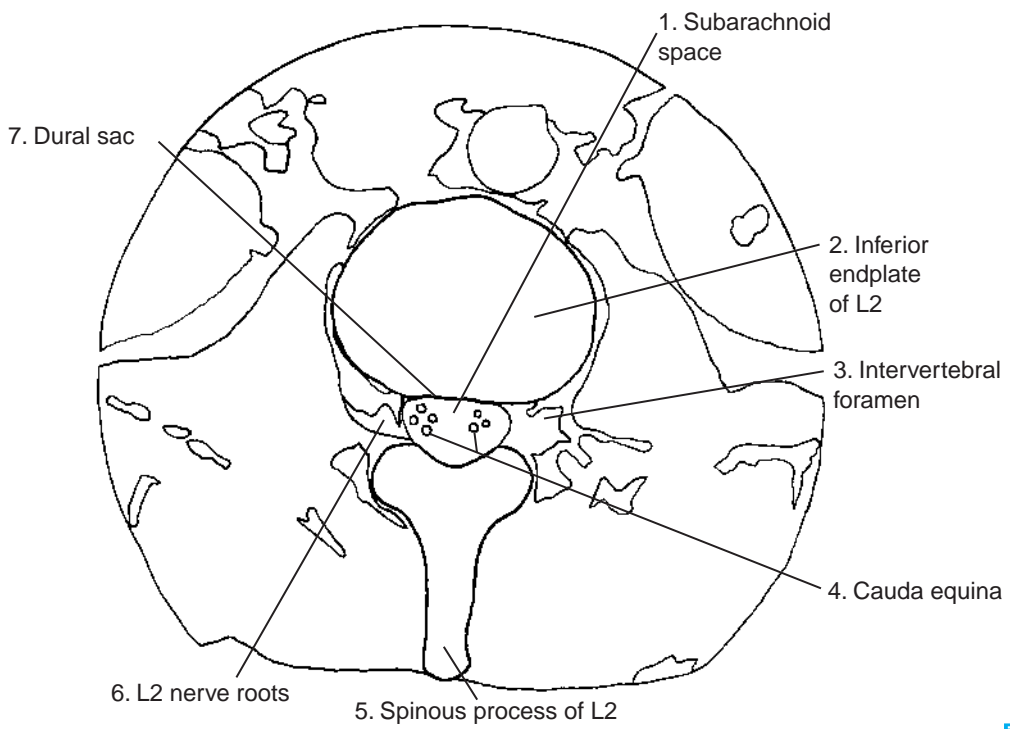


**Figure 7–15 (A,B)** Axial CT image 3.

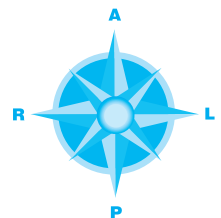
As in the previous image, the intervertebral foramina in this image are between the vertebral body and the posterior vertebral arch, which includes the spinous process. Because the level of this section is through the lowest part of L2, the vertebral body is referred to as the inferior endplate, which is adjacent to the underlying intervertebral disk. Within the vertebral foramen, the dural sac is enhanced by contrast within the subarachnoid space. Within the dural sac, the radiolucent areas formed by nerve root bundles are collectively known as the cauda equina. Emerging from the right side of the dural sac, the L2 nerve roots are also enhanced by the contrast within the subarachnoid space.



A



B



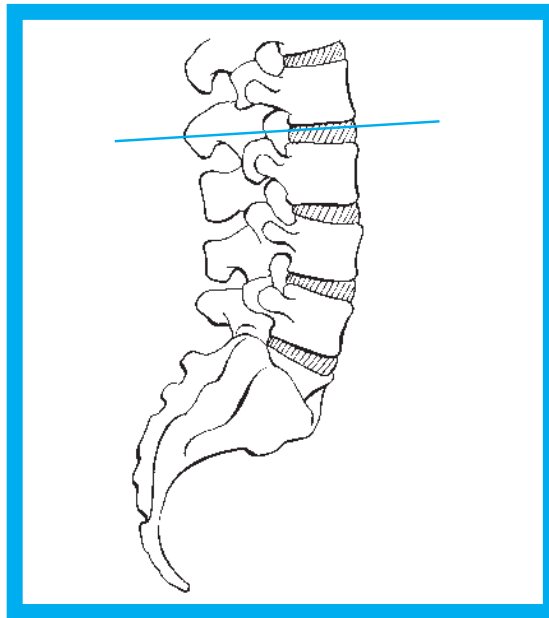
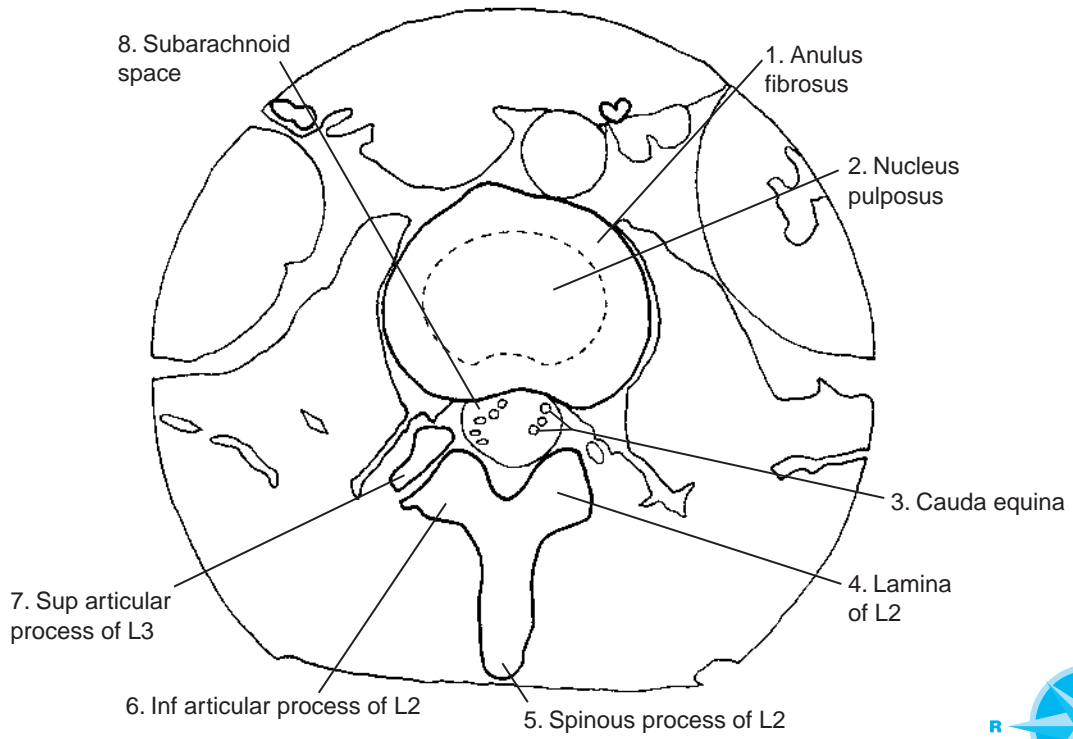


**Figure 7-16 (A,B)** Axial CT image 4.

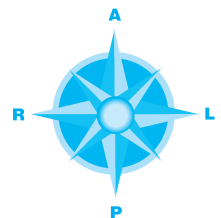
Although the laminae and spinous process can still be identified on the posterior part of this image, the inferior endplate of L2 as described in the previous image has now been replaced by an intervertebral disk. Although it is difficult to find a specific boundary between the nucleus pulposus and the anulus fibrosus, the region in the center of the disk is more radiolucent than the periphery. Posterior to the intervertebral disk, the contrast-enhanced subarachnoid space is again seen within the dural sac, outlining the nerve roots representing the cauda equina. At this level, the superior articular process of L3 is found articulating with the inferior articular process of L2. To help identify the articular processes, remember that the inferior articular processes are always located “inside” compared to the superior articular processes.



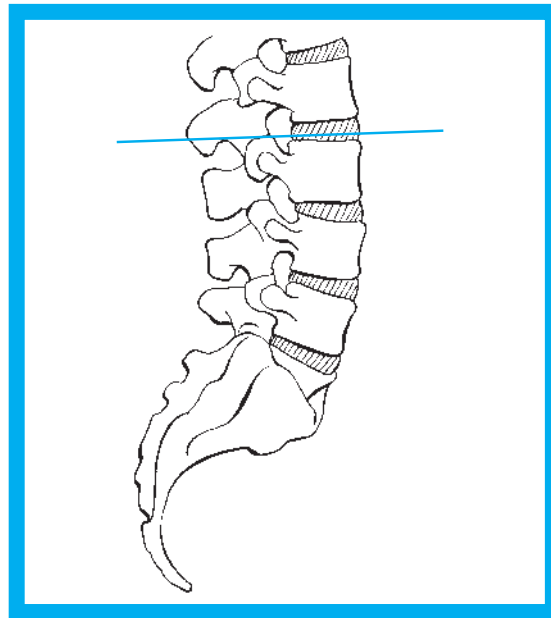
A



B

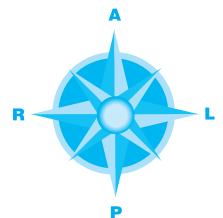
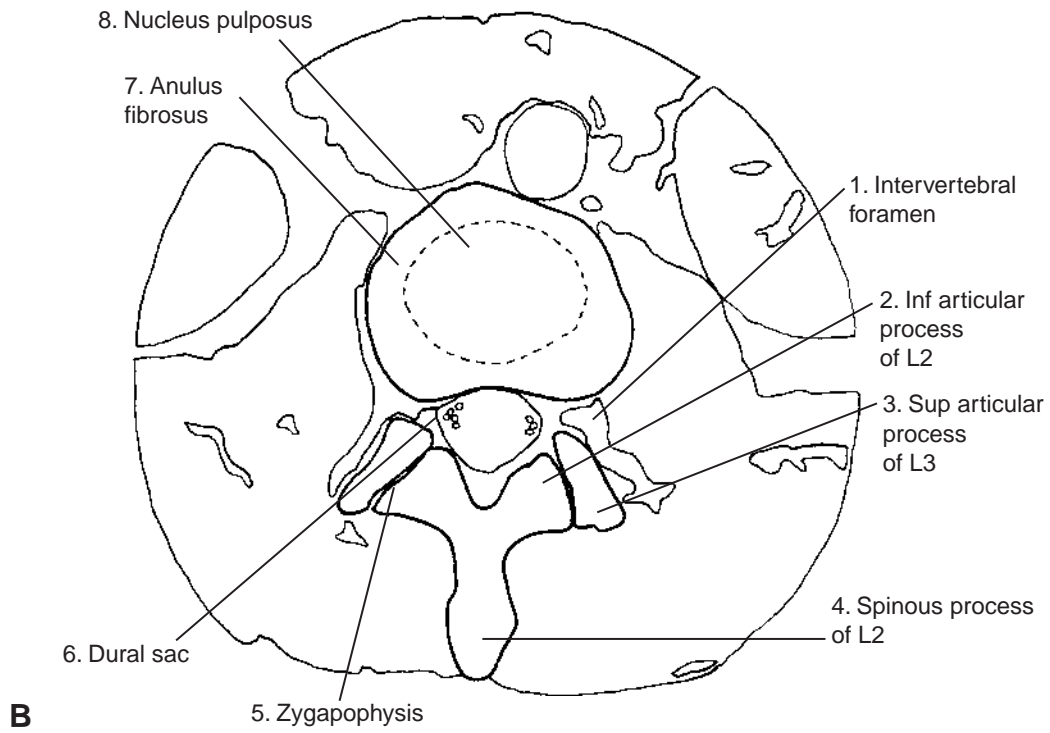






**Figure 7-17 (A,B)** Axial CT image 5.

At this level, the zygapophyseal joints are shown in cross-section on either side formed by the superior and inferior articular processes. Similar to the previous image, the spinous process of L2 can be seen separating the musculature of the back, and the intervertebral disk is demonstrated in the area previously occupied by the vertebral body. Although it is again difficult to discern a clear boundary between the regions within the intervertebral disk, the nucleus pulposus occupies the central region and is slightly more radiolucent than the surrounding annulus fibrosus. Between the intervertebral disk and the bony structures forming the posterior vertebral arch, the dural sac is enhanced by contrast within the subarachnoid space. On either side of the vertebral foramen, the intervertebral foramina are found between the posterolateral margin of the intervertebral disk and the superior articular processes of L3. Although the anatomy demonstrated within this image is normal, it clearly demonstrates how a posterolateral projection of a herniated disk could cause stenosis of the intervertebral foramen.



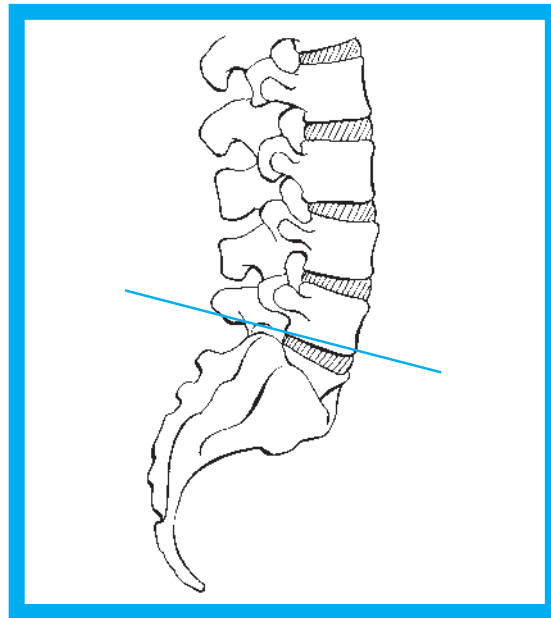
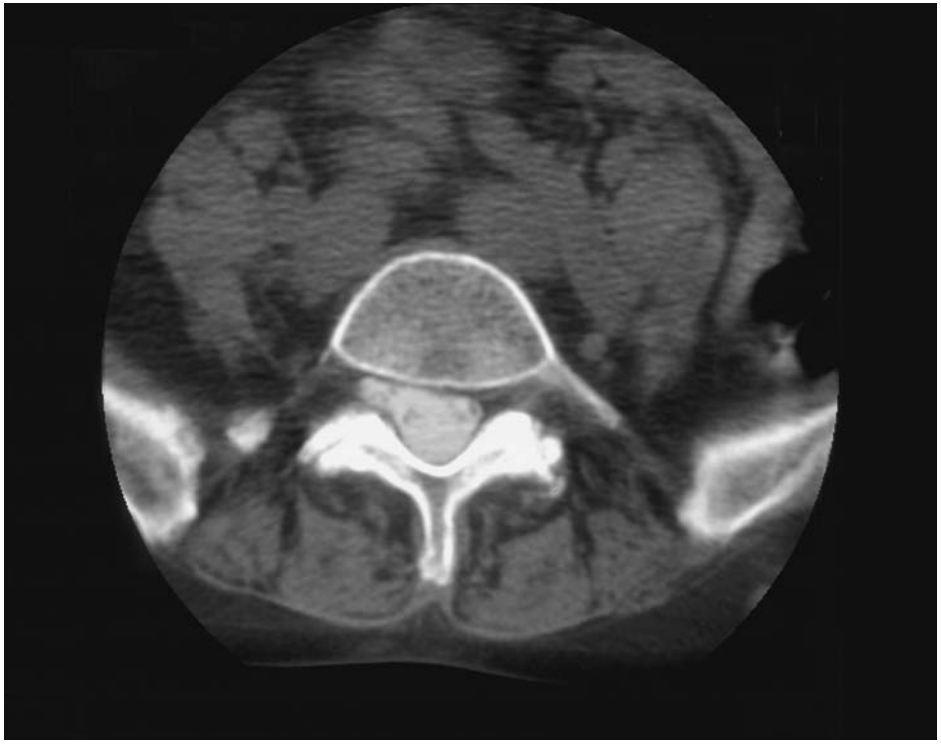
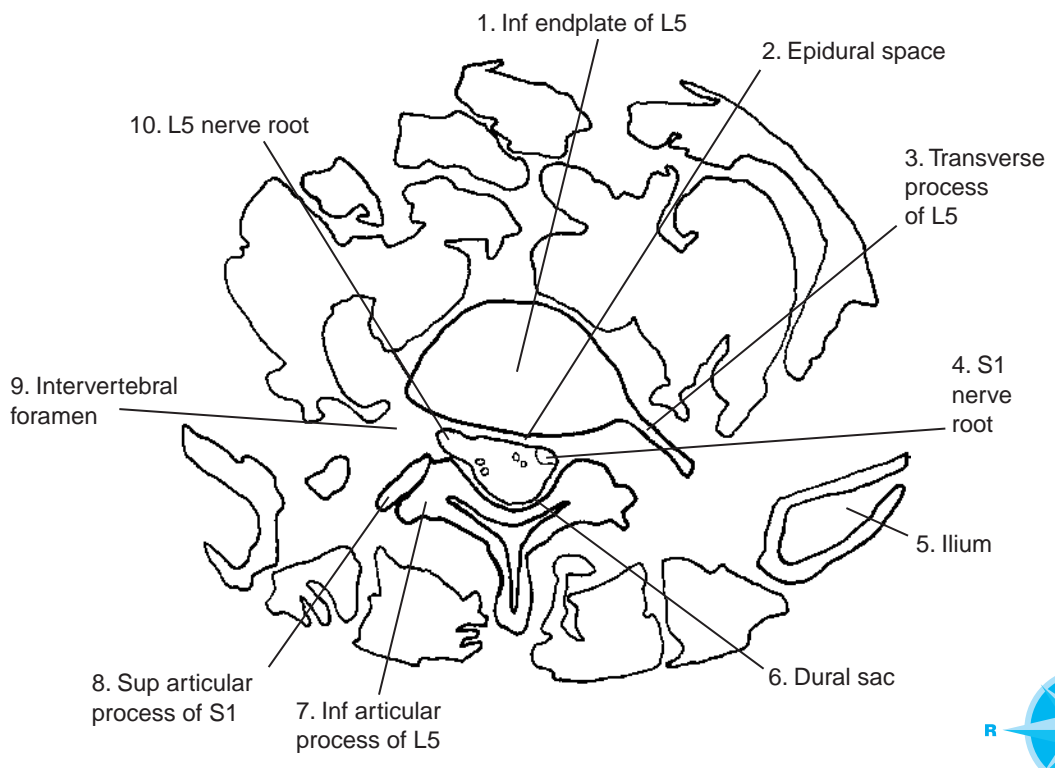


**Figure 7-18 (A,B)** Axial CT image 6.

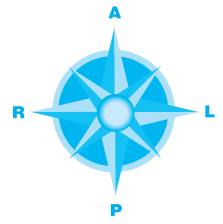
The inferior endplate of L5 is centrally located in this image, and the transverse process is shown on the left side extending toward the ilium. Posterior to the vertebral body of L5, the contents of the dural sac are enhanced by contrast within the subarachnoid space. On the right side, the sheath of dura mater is found within the intervertebral foramen surrounding the L5 nerve root. On the left side, the nerve root of S1 is beginning to separate from the contents of the dural sac. Between the vertebral body and the dural sac, a thin line of epidural space is shown that contains fat and blood vessels. Forming part of the posterior vertebral arch, the zygapophyseal joint is formed by the inferior articular process of L5 and the superior articular process of S1.



**A**



**B**



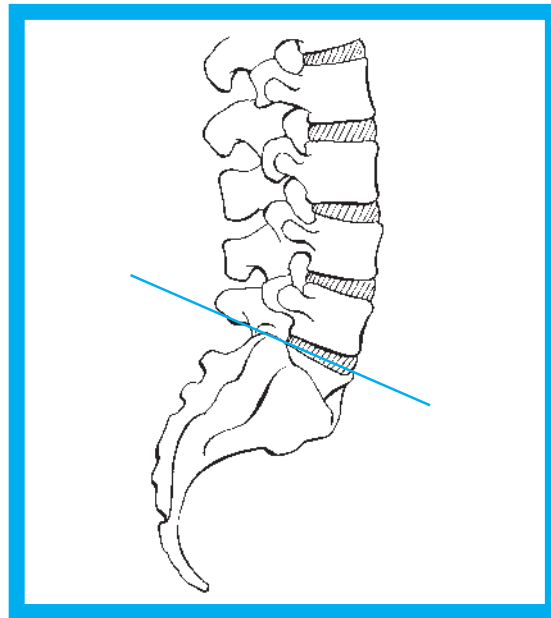
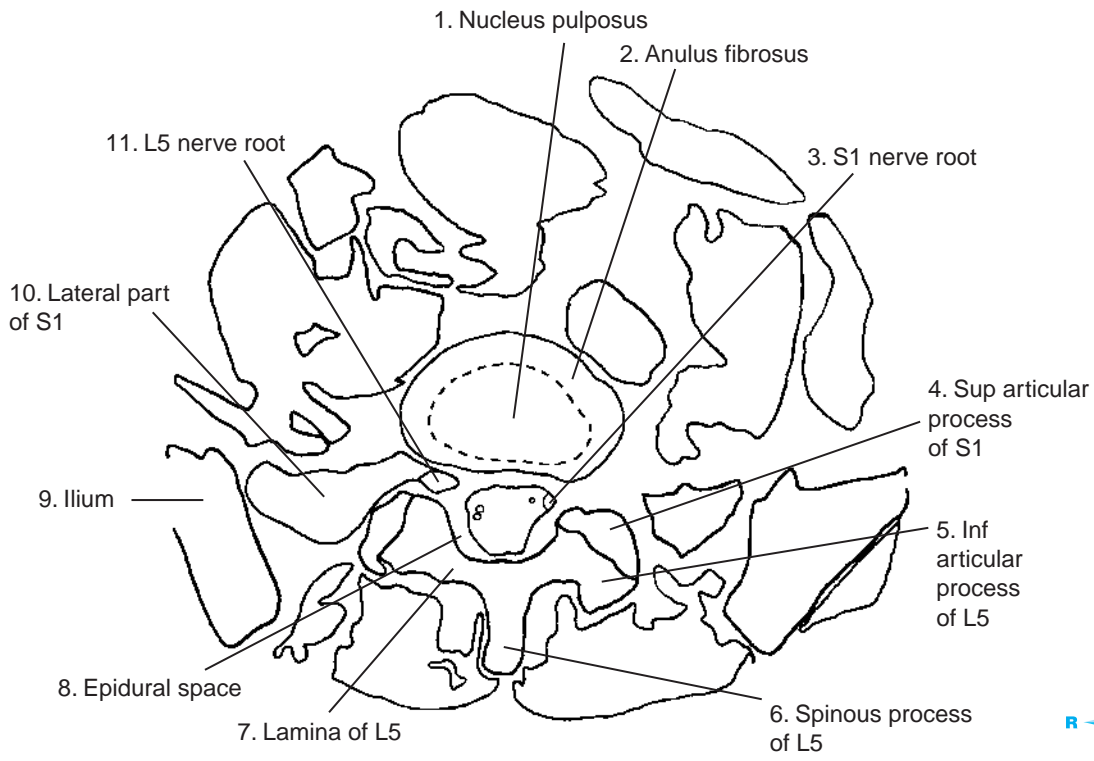


**Figure 7–19 (A,B)** Axial CT image 7.

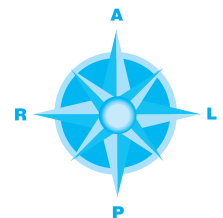
In the central location previously occupied by the inferior endplate of L5, the intervertebral disk is shown in cross-section. The central, more radiolucent area of the disk represents the pulpy fluid known as the nucleus pulposus, which is surrounded by a concentric ring of fibrous tissue known as the anulus fibrosus. In this patient, the intervertebral disk located at L5-S1 is normal and does not cause any stenosis of the neural foramina. In the position previously occupied by the transverse process of L5, the lateral part of S1 is now shown as a triangle-shaped bone between the intervertebral disk and the iliac bones. Within the vertebral foramen, the contrast-enhanced subarachnoid space demonstrates the extent of the dura in this region. Although the nerve roots are usually more symmetric, the S1 nerve root seen on the left side of this patient indicates that the spinal nerves are coming off at a higher level on the left side. For example, the S1 nerve root is emerging from the dural sac on the left side, whereas on the right side, the S1 nerve root is not yet discernible. Forming the posterior vertebral arch, the spinous process and laminae of L5 are shown in this section to be continuous with the inferior articular processes. As described earlier, the inferior articular processes are found “inside” compared to the superior articular processes.



A



B



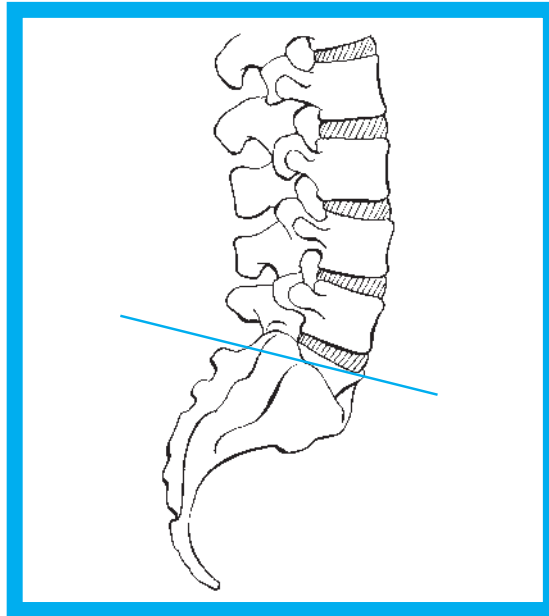
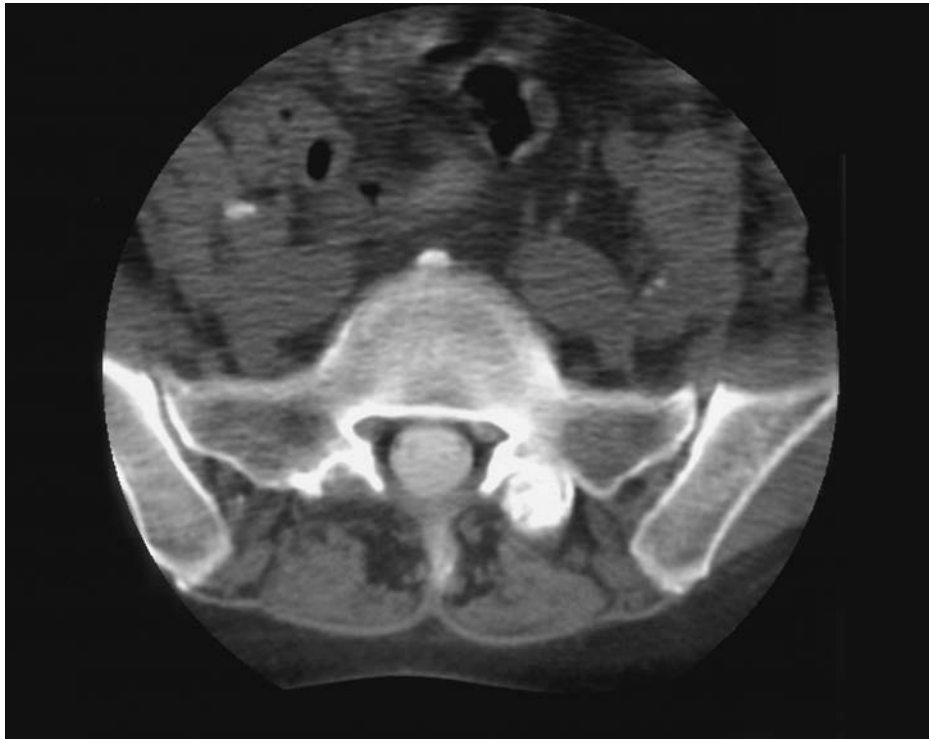
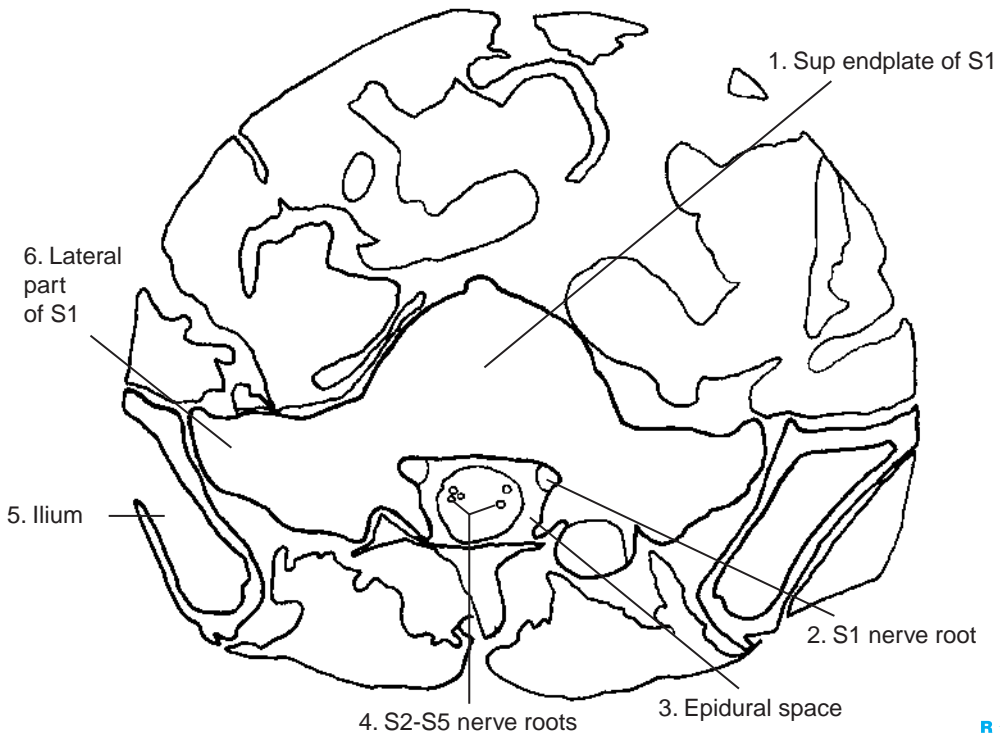


**Figure 7–20 (A,B)** Axial CT image 8.

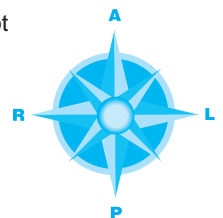
The unique structure of the superior endplate of S1 gives the bony structure—centrally located in this image—the characteristic batlike appearance of the sacrum. The lateral parts of the sacrum extending from the vertebral body on either side appear like wings as they extend toward the iliac bones. Posterior to the S1 segment, the oval-shaped dural sac is enhanced by contrast within the subarachnoid space and occupies a central location within the vertebral foramen. Within the dural sac, the areas of radiolucency represent the S2 through S5 nerve roots, or the lower cauda equina. Outside of the dural sac, the epidural space can be found within the vertebral foramen. Within the lateral recesses of the vertebral foramen, the S1 nerve roots can be identified on either side as they extend from the spinal cord to the sacral foramina.



A



B





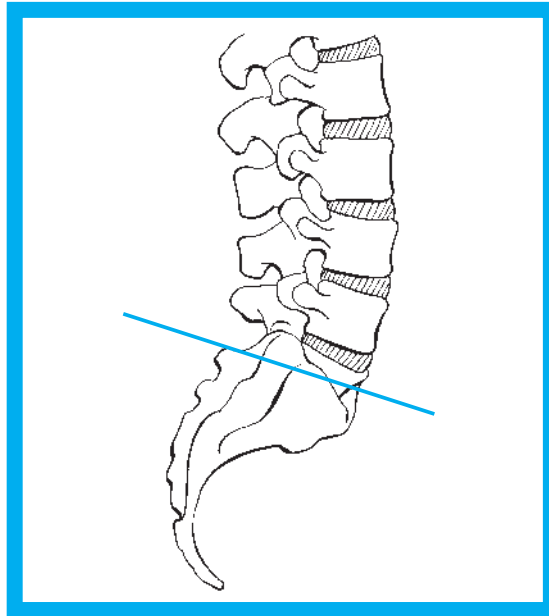
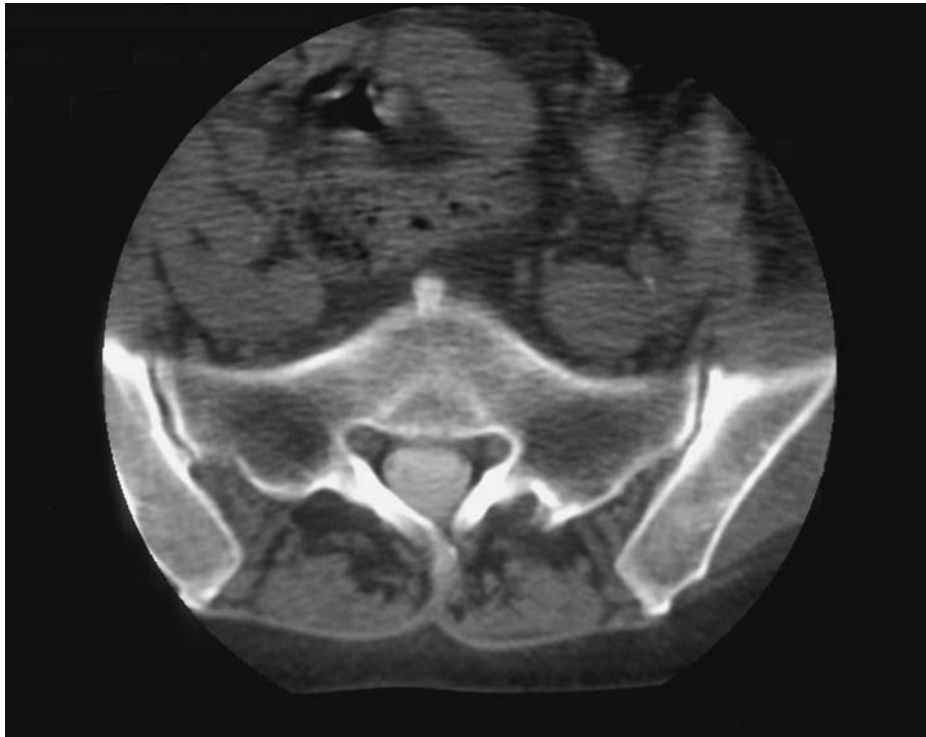
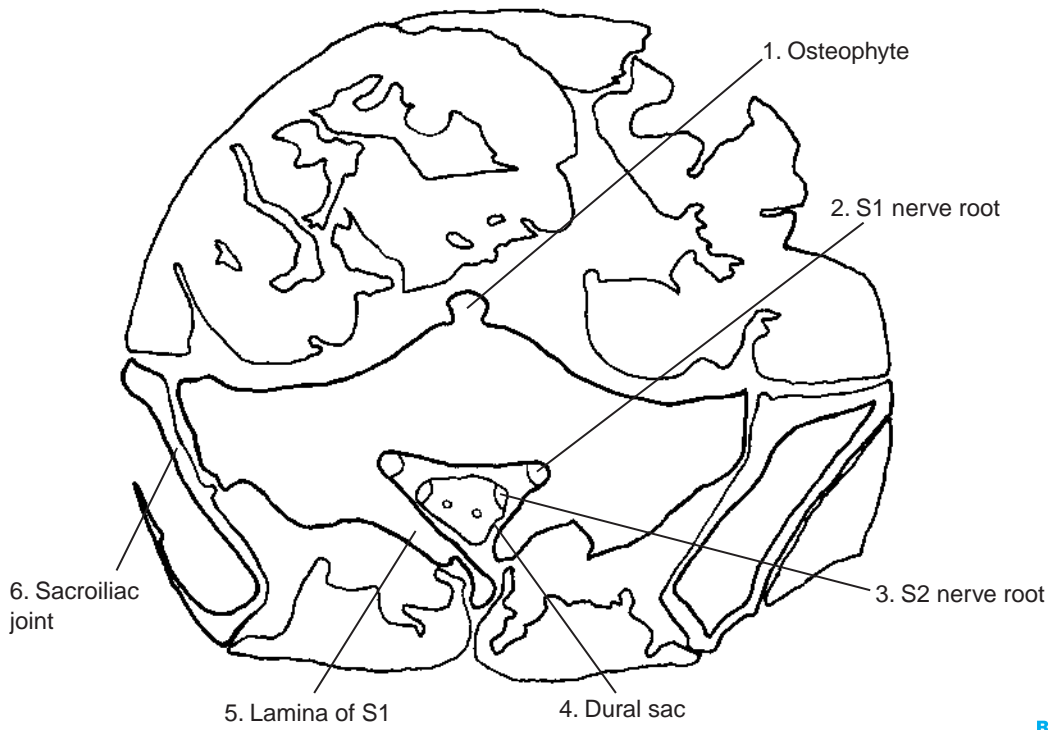


**Figure 7-21 (A,B)** Axial CT image 9.

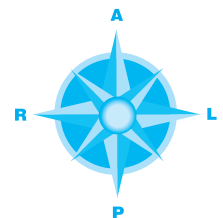
As in the previous figure, the batlike appearance of the sacrum in this image indicates the plane of section to be within the region of the pelvis. On either side, the lateral part of the sacrum is demonstrated articulating with the iliac bones, creating the sacroiliac joints. Although the vertebral segment of S1 typically has a round appearance, a small bony outgrowth, known as an osteophyte, is demonstrated on the anterior cortical margin. At this level, the laminae of S1 can be found on either side, forming the posterior arch around the vertebral foramen. As described in previous images, the contrast-enhanced dural sac is centrally located within the vertebral foramen and contains radiolucent areas representing the S2 through S5 nerve roots. At this level, the S2 nerve roots are within the anterolateral portion of the dural sac, and the S1 nerve roots are within the lateral recesses of the vertebral foramen.



A



B





## Case Study 7-1

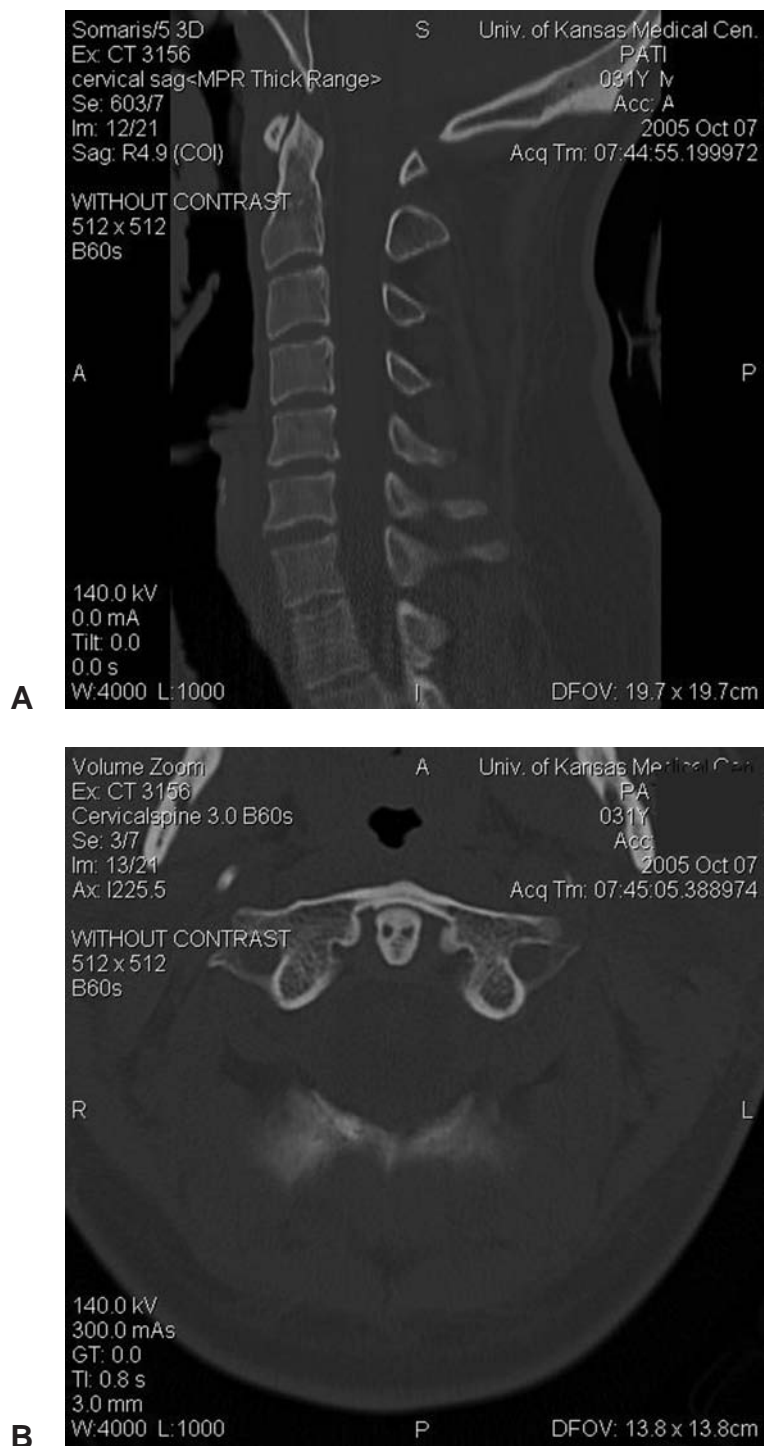


Figure 7-22

## Clinical Correlations

This 31-year-old man involved in a motor vehicle accident underwent a helical computed tomography (CT) scan to evaluate his cervical spine for trauma injury. As shown in the sagittal image (Figure 7-22A), the cervical vertebral bodies appear to be arranged in an orderly stack and there is no major displacement of vertebrae. Notably different as compared to other vertebral bodies, the body of the axis (C2) has an upward projection called the dens that acts as the body of the atlas (C1). In the

axial section (Figure 7-22B), the dens lies just posterior to the anterior arch of the atlas. Together, the first two cervical vertebrae allow much of the rotation and nodding movements of the head, and consequently, the dens may be fractured in extreme hyperextension and hyperflexion. Because it forms the anterior margin of the spinal foramen, a fracture may be life-threatening if the spinal cord is involved. In this case, no injury was found and the complete immobilization restrictions were discontinued.

## Questions

1. Describe the shape of the atlas.
2. Does the cervical spine normally have a curvature?
3. What is located within the transverse foramina?
4. Describe the shape of the axis.
5. Does the atlas have transverse foramina?



## Case Study 7-2

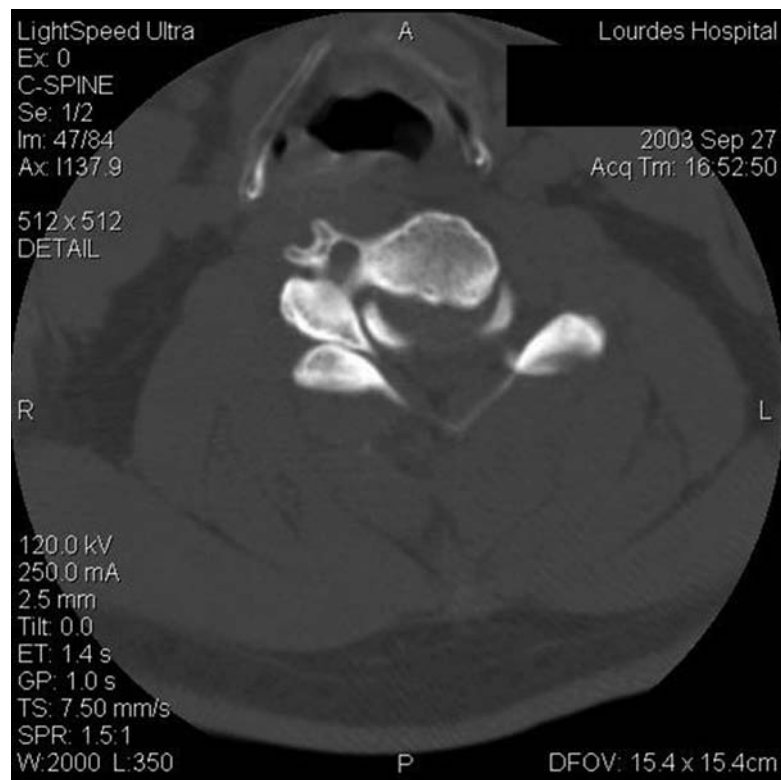


**Figure 7-23**

This patient is a 54-year-old man who was brought to the emergency room by ambulance following an all-terrain vehicle accident. The helical computed tomography (CT) scan was completed to evaluate his cervical spine for suspected whiplash injury. The nature of the accident involved the patient's body being jerked backward due to a sudden impact. In the axial image, there is a subluxation of the cervical spine located at the C4/C5 level with an anterior displace-

ment of C4. There is disruption of the zygapophyseal joints that is most apparent on the right where the C4 inferior facet has not only slipped, but also locked in front of the superior articular facet of C5. In the soft tissue of the neck, there is also a great deal of swelling noted surrounding the cervical spine injury. Due to the extent of the subluxation, this injury was surgically repaired and the patient was able to recover fully except for minor limitations in neck movements.

### Questions

1. In an axial section through a normal spine, is the superior or inferior articular process located most anteriorly?
2. On the right side of this patient, is the superior or inferior articular process located most anteriorly?
3. On the right side of this patient, the intervertebral foramen would be constricted by which part of the vertebra?
4. What nervous tissue would be found within the intervertebral foramen?
5. Is dura mater found within the intervertebral foramen?



## Case Study 7-3



**Figure 7-24**

This patient is a 19-year-old man who arrived in the emergency room with a gunshot wound in the left supraclavicular neck. In the selected sagittal computed tomography (CT) image, the shrapnel from the bullet and bone fragments are in the C6 and C7 spinal canal. Found just above the shrapnel, a bone fragment is shown that originated

from the surrounding vertebra and was carried into the spinal canal by the bullet fragment. In adjoining slices, other bone fragments were also found surrounding the shrapnel lodged within the spinal canal. In this case, the bullet and bone fragments transected part of the spinal cord and this patient was unable to recover from the injury.

### Questions

1. Describe the dura mater in the spinal cord.
2. Are the nerves within the central nervous system able to heal like most other tissues in the body?
3. Describe the cerebrospinal fluid (CSF) flow in the spinal cord.
4. Describe the arachnoid mater in the spinal cord.
5. Describe the pia mater of the spinal cord.



## Case Study 7-4



**Figure 7-25**

This 30-year-old female patient was in a motor vehicle accident and was brought by ambulance to the emergency room. In the selected sagittal magnetic resonance (MR) image, the spinal cord is shown to be completely transected near the level of T11. Although the thoracic vertebral bodies appear in an orderly arrangement, the intervertebral segment at the junction of T11 and T12 appears narrowed indicating injury to the disk. Within the spinal canal, there is a strong signal from the cerebrospinal fluid clearly demarcating the central nervous system structures. The spinal cord is

shown to be continuous above the level of T10 and below the level of T12. Corresponding with the intervertebral segment at T11 and T12, the spinal cord appears to be cut or transected, and is surrounded by an enlarged subarachnoid space. As a result of major trauma, the upper thoracic spine was forced forward resulting in a tearing of the spinal cord at the T11 and T12 intervertebral segment. Unlike most other tissues within the body, the nervous tissues could not be repaired and this patient was unable to recover spinal cord function below the level of T11.

### Questions

1. Was the anterior longitudinal ligament torn in this injury?
2. Was the posterior longitudinal ligament torn in this injury?
3. Was the T11 and T12 intervertebral disk damaged?
4. What caused the enlarged subarachnoid space described above?
5. Will all of the sensory nerves within the spinal cord above the site of injury continue to function?



## Case Study 7-5



Figure 7-26

This 76-year-old woman was having a magnetic resonance imaging (MRI) of the lumbar spine due to reported chronic low back pain. There was no known trauma, but her age was consistent with degenerative disc disease. The high signal within the cerebrospinal fluid clearly demonstrates intervertebral disks bulging into the spinal canal. At the level corresponding to bulging disks, several of the intervertebral joint spaces

also appear to be narrowed. With advancing age and a lifetime of wear and tear, some of the rings of the annulus fibrosus break down allowing the liquid center (nucleus pulposus) to expand the outer rings causing the disks to bulge. In these cases, the patient suffers from chronic low back pain and other symptoms including muscle spasms, numbness, and tingling sensation traveling down the legs and into the feet.

### Questions

1. Would the bulging disks compress the cauda equina?
2. Describe the conus medullaris.
3. Would bulging disks affect the spinal nerve roots exiting at that level?
4. Which ligament in the spinal canal would be most affected by degenerative disk disease?
5. How can you distinguish a lumbar vertebra from those found in the thoracic and cervical parts of the spine?





## Case Study 7-6

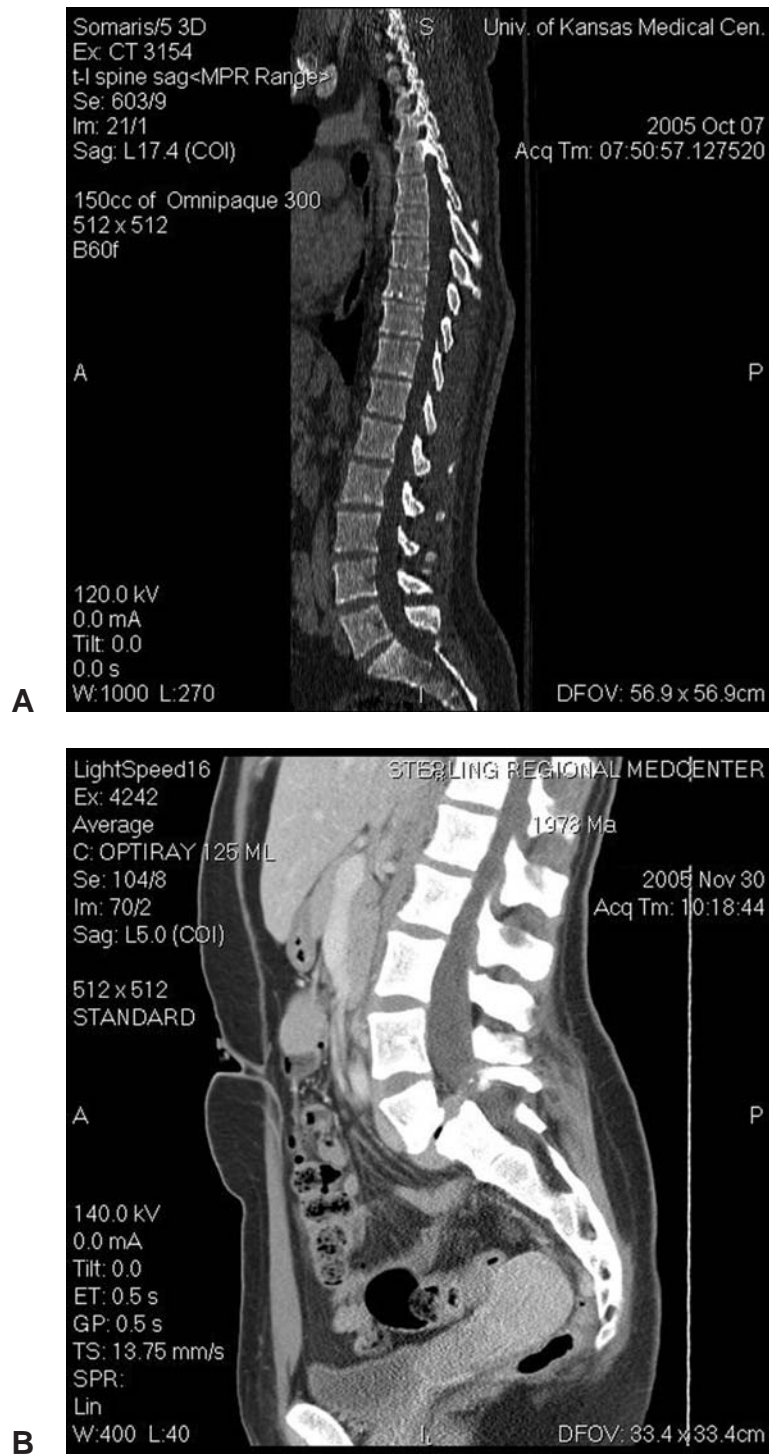


Figure 7-27

In the sagittal image (Fig. 7-27A), the vertebral bodies forming the spine are shown arranged in an orderly stack. In this normal study, there is curvature within the spine and the vertebral bodies are aligned with adjacent vertebrae. The patient shown below (Fig. 7-27B) has spondylolisthesis at the level of L5-S1 whereby the vertebral body of L5 appears to have slipped forward as compared to S1. As compared to a normal intervertebral space and

disk, the intervertebral space at L5-S1 is narrowed and the disk is damaged. Spondylolisthesis is most often found at L5-S1 because it acts as the joint between the upper and lower body. Through other vertebrae, the weight of the upper body is transmitted via L5 to the sacrum. As part of the pelvis, the sacrum acts to connect the lower half of the body with the upper half via the L5-S1 intervertebral joint.

### Questions

1. When a patient has spondylolisthesis, will the spinal nerve roots exiting at that level be affected?
2. What ligaments normally keep the vertebrae in an orderly stacked arrangement?
3. Can spondylolisthesis also be found at other levels in the spine?
4. When a patient has spondylolisthesis, will the spinal canal be affected at that level?
5. Will spondylolisthesis most likely cause an increase or a decrease in the intervertebral disk space?



## CLINICAL APPLICATIONS

1. The \_\_\_\_\_ spinal nerve is found between C1 and C2, and the \_\_\_\_\_ spinal nerve is found between L5 and S1.
2. The unique feature that can be used to identify thoracic vertebrae is the \_\_\_\_\_.
3. The \_\_\_\_\_ is a concentric ring of fibrous tissue forming the periphery of the intervertebral disk.
4. True or false: The intervertebral disks are responsible for approximately one-quarter of the length of the vertebral column.
5. The \_\_\_\_\_ and \_\_\_\_\_ form the posterior boundary of an intervertebral foramen.
6. The posterior (dorsal) nerve root carries (sensory / motor) signals.
7. In an axial section through the vertebrae, which articular process is found inside, or most medially?
8. Where does the extension of dura mater known as a dural sheath terminate?
9. True or false: The CSF within the subarachnoid space in the spine is continuous with that found within the cranium.
10. The \_\_\_\_\_ is a loose collection of nerve roots below the level of L1.

# Chapter 8

# Joints

## OBJECTIVES

Upon completion of this chapter, the student should be able to:

1. Define the general regions that include one or more joints.
2. List the bones forming each joint and indicate the classification and range of movements.
3. Identify and describe the unique bone structures associated with each joint.
4. Identify and describe the cartilages associated with each joint.
5. Describe the relationships of the articular surfaces within each joint.
6. Describe the major ligaments involved in stabilizing each joint.
7. Identify and describe the muscles and tendons passing around each joint.
8. Describe the origin, insertion, and action of muscles passing around each joint.
9. Describe the relationships among the structures forming each joint.
10. Correctly identify anatomic structures on patient computed tomography (CT) and magnetic resonance (MR) images of the joints.

## Part A Shoulder

### ANATOMIC OVERVIEW

The anatomy of the shoulder girdle is generally described as the junction of the upper extremity with the trunk. The shoulder girdle consists of two bones, the clavicle and the scapula, which attach to the axial skeleton via the sternoclavicular joint. On the opposite end of the shoulder girdle, the shoulder joint is formed by the glenoid fossa of the scapula, which articulates with the head of the humerus, forming an enarthrodial, or ball-and-socket, joint.

#### ■ Skeleton

**Humerus** (*HYU-mer-ŭs*). Located in the upper arm. The largest and longest bone of the upper extremity (Fig. 8-1).

**Head**. The most proximal part of the humerus. It is round, forming a smooth articular (*ar-TIK-yu-lār*) surface.

**Surgical neck**. A constricted part of the humerus just below the tubercles. A frequent site for fractures in the proximal end of the humerus.

**Greater tubercle** (*TU-ber-kl*). The small protrusion, or bump, on the lateral humerus between the head and surgical neck (Fig. 8-2). Together, the more medial lesser tubercle and the greater tubercle form a groove for the tendon of the long head of the biceps muscle.

**Scapula** (*SKAP-yu-lā*). Forms the posterior part of the bony shoulder. Generally described as flat and triangular (Fig. 8-1).

**Acromion** (*ă-KRŌ-mĒ-on*) **process**. Originates from the spine on the posterior surface of the scapula. A flattened process that extends anteriorly to articulate with the distal clavicle (*KLAV-i-kl*), forming the acromioclavicular (*ă-KRŌ-mĒ-ŏ-klav-ĪK-yū-lār*) joint. Together, the acromion process and clavicle are often described as forming the roof of the shoulder joint.

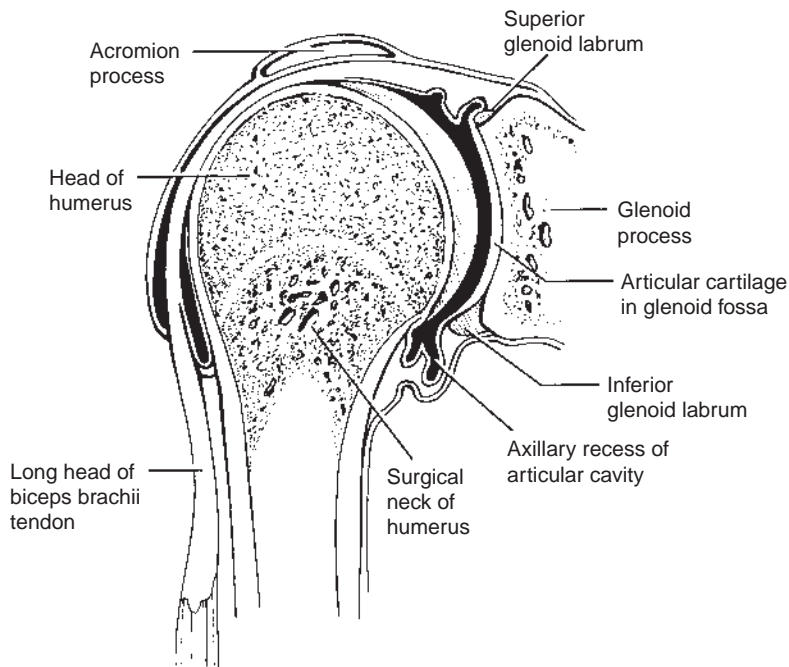


Figure 8-1 Coronal view of the shoulder.

*Glenoid (GLE-noyd) process.* The lateral part of the scapula. Articulates with the head of the humerus.

*Glenoid fossa (FOS-ă).* Also called the glenoid cavity. A cup-shaped depression located inside the outer edge of the glenoid process.

### Joint

**Articular cartilage.** Provides a smooth surface for the shoulder joint and covers both the glenoid cavity and the head of the humerus. Consists mostly of hyaline (HI-ă-lin)

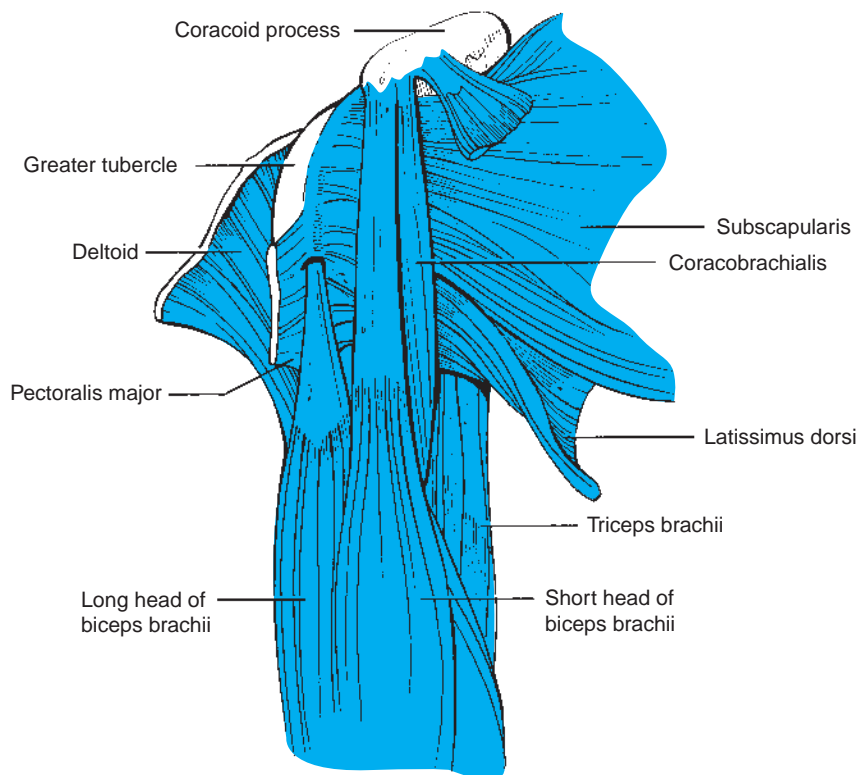


Figure 8-2 Anterior view of the brachial muscles.

cartilage. Within the joint space, synovial (*sin-NŌ-vē-āl*) fluid acts like oil, allowing the surfaces to slide easily on one another during movement.

**Glenoid labrum** (*LA-brŭm*). Surrounds the glenoid fossa. A ridge of fibrocartilage that acts to deepen the fossa and protect the bone. Because the tendon of the long head of the biceps muscle inserts on the superior glenoid process, the terminal part of the tendon is continuous with superior glenoid labrum.

**Axillary** (*AK-sil-ar-e*) **recess of the articular cavity**. The joint space below the inferior glenoid labrum lined with synovial membrane and surrounded by the connective tissue of the articular capsule. Because the shoulder joint is strengthened by muscles that run behind, above, and in front of the joint, dislocation most commonly occurs when the arm is abducted through the axillary articular capsule.

## Musculature

**Trapezius** (*tra-PĒ-ze-ŭs*). Origin: ligament covering spinous processes of cervical vertebrae (*SER-vŭ-kal VER-tě-bre*) and thoracic vertebrae. Insertion: clavicle, medial acromion, and spine of scapula. Action: adducts and rotates scapula. NB: not shown in Figure 8-1.

**Deltoid** (*DEL-toyd*). Origin: upper surface of clavicle, upper surface of acromion, and spine of scapula. Insertion:

deltoid tubercle of humerus. Action: abducts and rotates arm medially and laterally (Fig. 8-2).

**Long head of biceps brachii** (*BI-seps BRA-kē-i*). Origin: supraglenoid tuberosity (*TU-bēr-OS-i-tē*). Insertion: radial tuberosity. Action: flexes arm and forearm.

**Short head of biceps brachii**. Origin: coracoid (*KŌR-ă-koyd*) process of scapula. Insertion: radial tuberosity. Action: supinates the hand.

**Coracobrachialis** (*KŌR-ă-kō-brā-kē-Ā-lis*). Origin: coracoid process of scapula. Insertion: middle shaft of humerus. Action: flexes and adducts the arm.

**Subscapularis** (*sŭb-skap-yŭ-LA-ris*). Origin: subscapular fossa. Insertion: lesser tubercle of humerus and shoulder joint articular capsule. Action: rotates arm medially.

**Supraspinatus** (*su-pră-spi-NA-tŭs*). Origin: supraspinous fossa. Insertion: greater tubercle of humerus. Action: abducts arm (Fig. 8-3).

**Infraspinatus** (*in-fră-spi-NA-tŭs*). Origin: infraspinous fossa. Insertion: greater tubercle of humerus. Action: rotates arm laterally.

**Teres** (*TER-ez*) **major**. Origin: inferior angle of scapula. Insertion: lesser tubercle of humerus. Action: adducts, extends, and rotates arm medially.

**Teres minor**. Origin: axillary border of scapula. Insertion: greater tubercle of humerus. Action: rotates laterally and adducts arm.

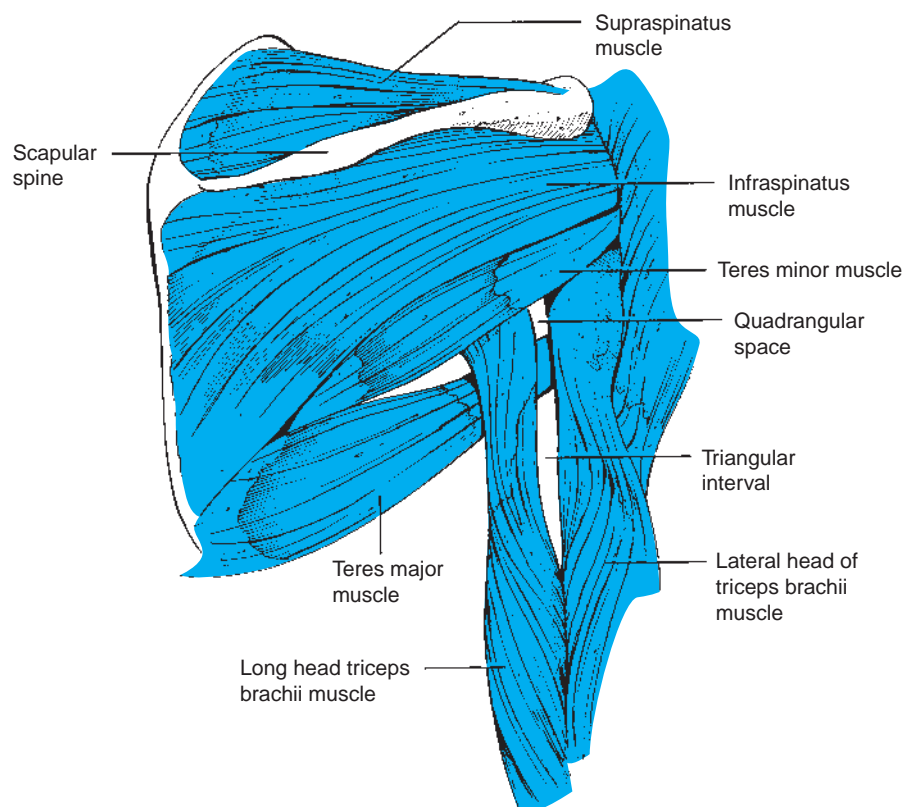


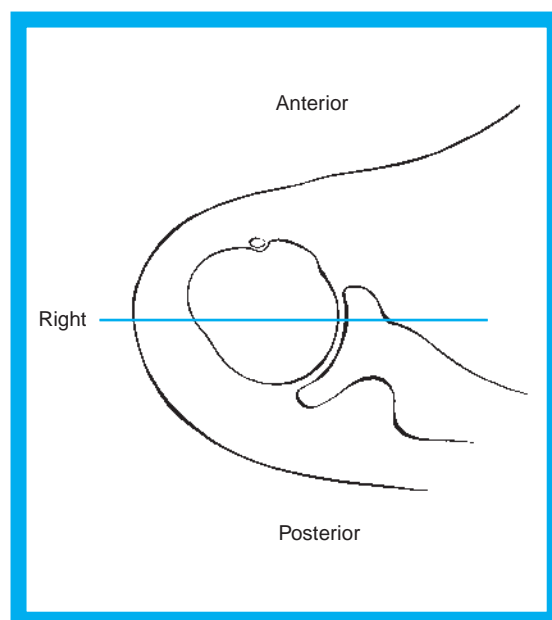
**Figure 8-3** Posterior view of the scapular and brachial muscles.



## Coronal Magnetic Resonance (MR) Images

In a typical scan of the shoulder, images are generated throughout the entire region. Here, the descriptions are limited to the following four selected images described at 3.5-mm intervals from posterior to anterior through the

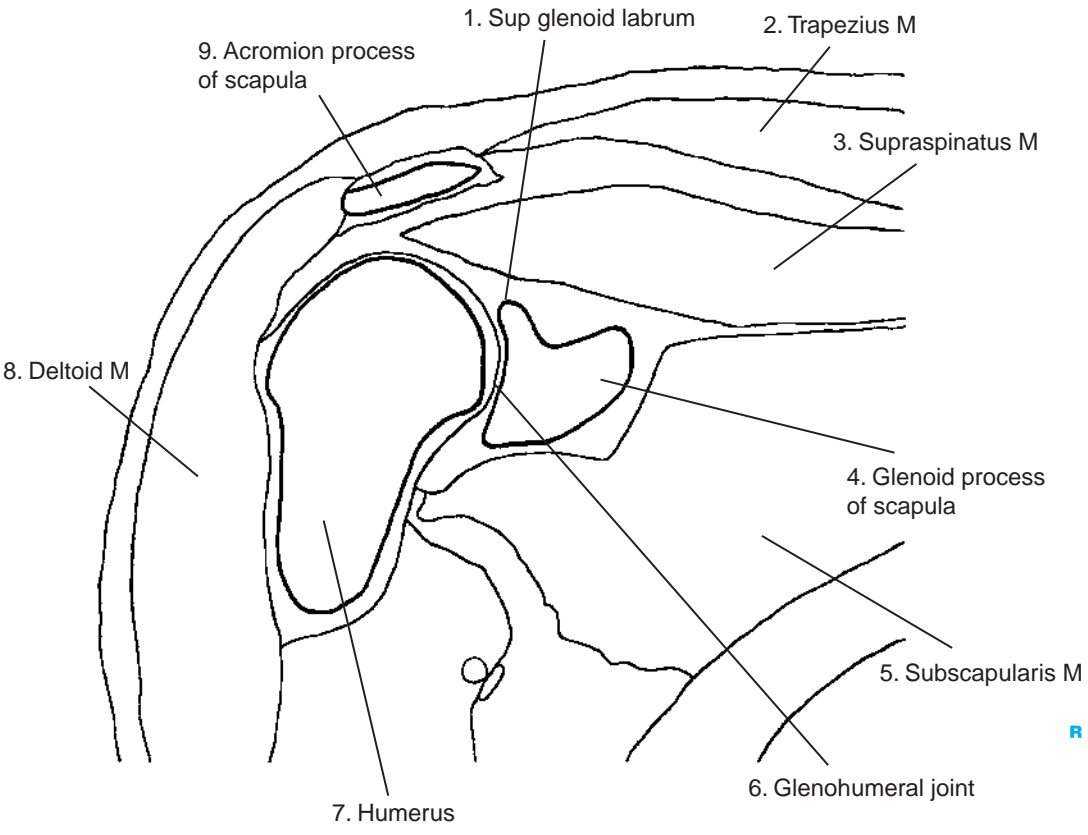
right shoulder joint. The images were generated at the following technical factors: repetition time (TR) = 900 ms; echo time (TE) = 20 ms; radiofrequency (RF) = 90°; field of view (FOV) = 16 cm.



**Figure 8–4 (A,B)** Coronal MR image 1.

Because this image demonstrates the posterior glenohumeral joint, the bony anatomy can be used to locate the position of the section. Owing to its characteristic appearance, the humerus is shown obliquely, sectioned near the glenoid process of the scapula with the intervening glenohumeral joint. On the upper aspect of the glenoid process of the scapula, the superior glenoid labrum is labeled and represents an area of dense fibrous tissue that acts to deepen and stabilize the glenohumeral joint. Above the joint, the acromion process of the scapula is shown and is often described as forming the roof over the glenohumeral joint. Besides the bones previously described, most of the strength of the shoulder joint is provided by the surrounding musculature. Originating primarily from the spinous processes of the cervical and thoracic vertebrae, the thin flat muscle of the trapezius can be seen as it extends toward its insertion on the medial margin of the acromion process of the scapula. Below the trapezius muscle, the supraspinatus muscle is also demonstrated extending from its origin in the supraspinous fossa on the posterior aspect of the scapula to insert on the greater tubercle of the humerus. Separated by a thin line of low signal intensity, the subscapularis muscle can be identified extending from its origin on the anterior surface of the scapula to insert on the lesser tubercle of the humerus. Both the supraspinatus and subscapularis muscles form part of the rotator cuff along with the infraspinatus and teres minor, which surround the posterior articular capsule. Originating from the acromion process of the scapula and the upper surface of the clavicle, the deltoid muscle is lateral to the humerus as it extends toward its insertion on the deltoid tubercle found approximately midshaft on the humerus.







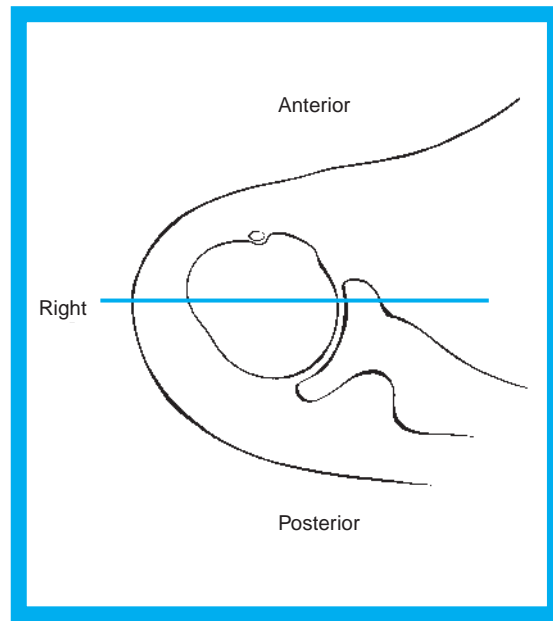
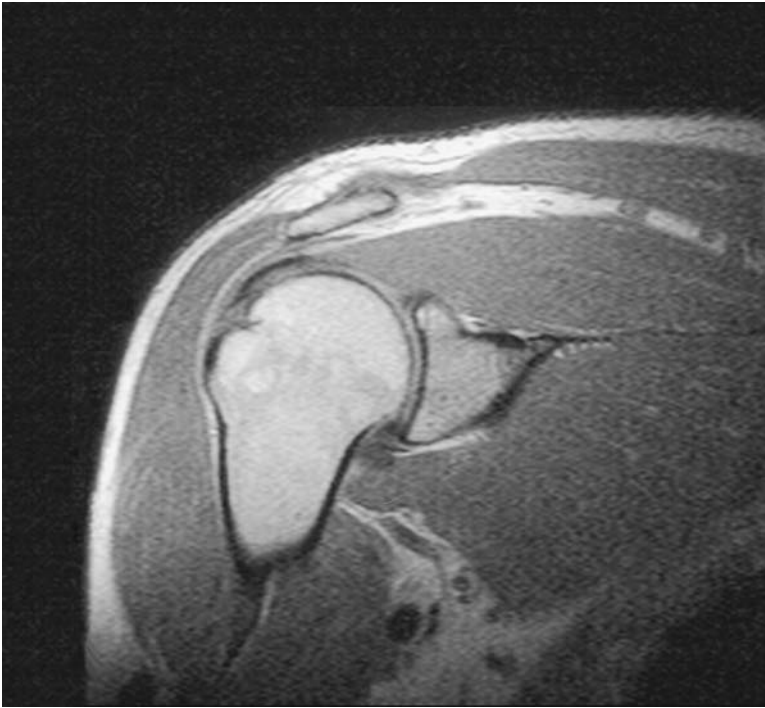
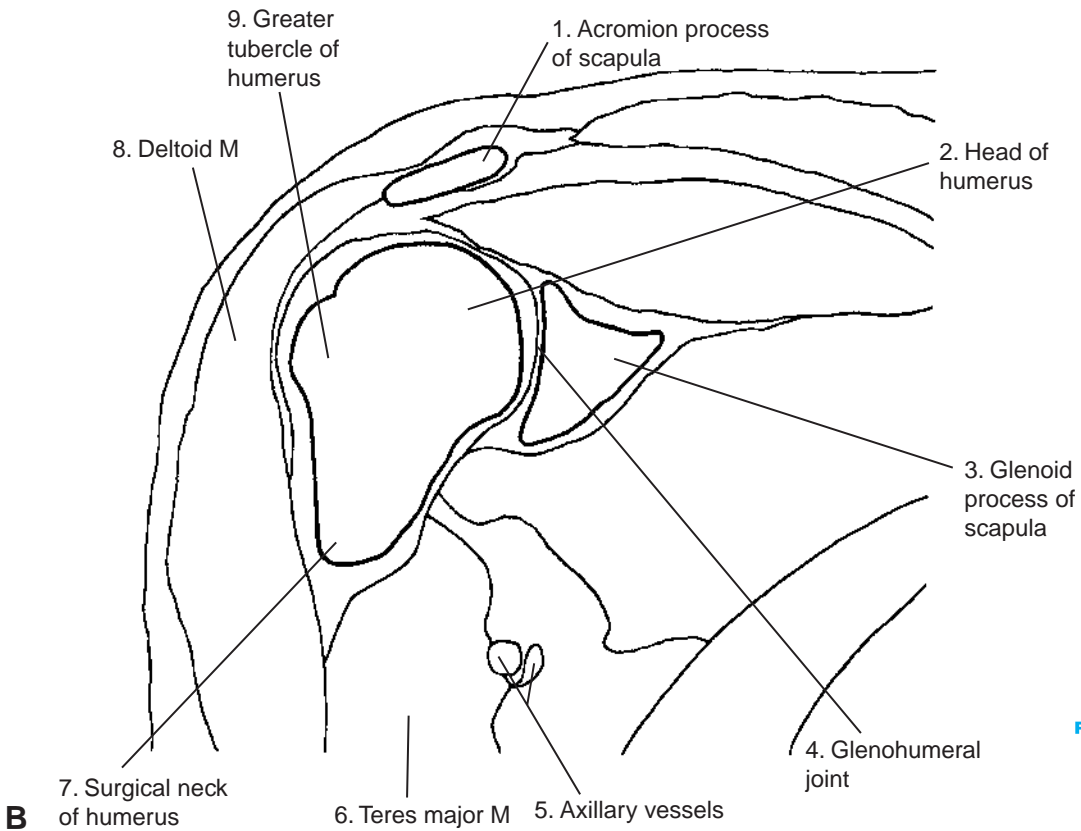


**Figure 8-5 (A,B)** Coronal MR image 2.

The acromion and glenoid processes of the scapula in this image appear much like they do in the previous image; however, the greater tuberosity is clearly identified on the lateral aspect between the head and the surgical neck of the humerus. Similar to the previous image, the deltoid muscle is shown originating from the acromion process of the scapula and covers the proximal end of the humerus as it extends downward to insert on the deltoid tuberosity. Medial to the deltoid muscle, the teres major muscle is shown in cross-section extending from its origin on the inferior angle of the scapula to insert on the lesser tuberosity of the humerus. Next to the teres major muscle, several axillary vessels are shown in cross-section as they extend between the thoracic cage and the arm.



A



B

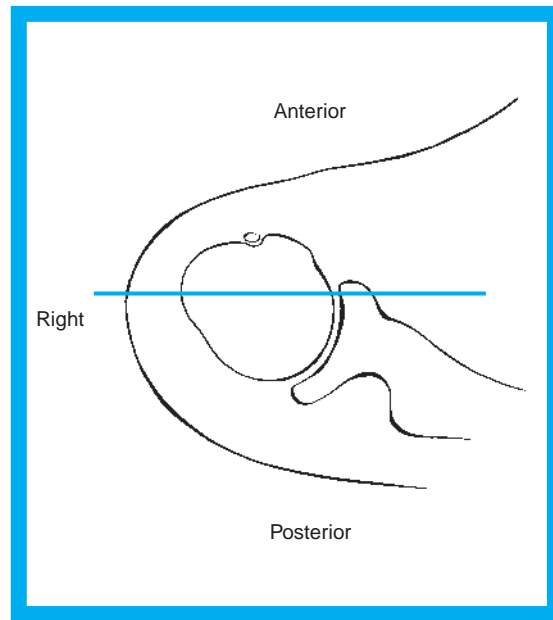
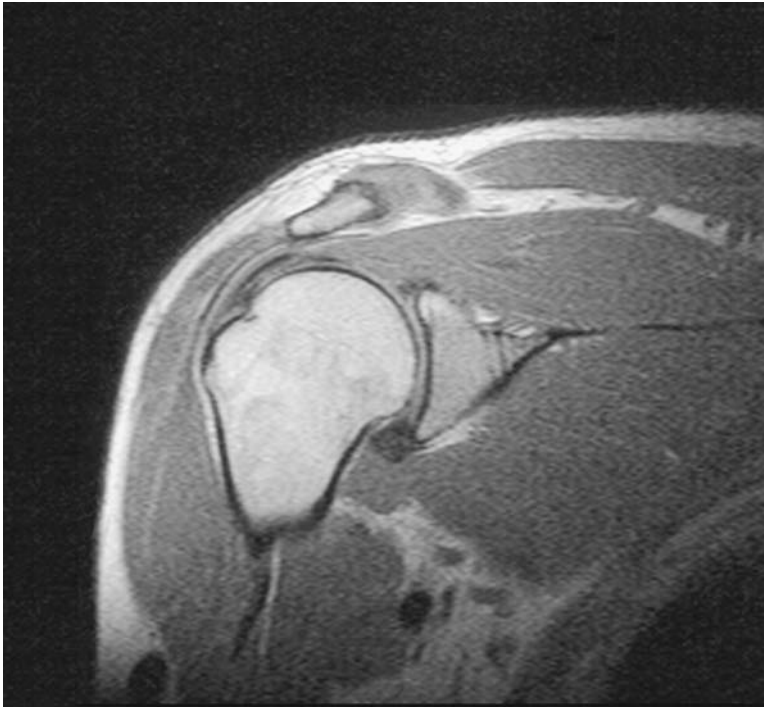
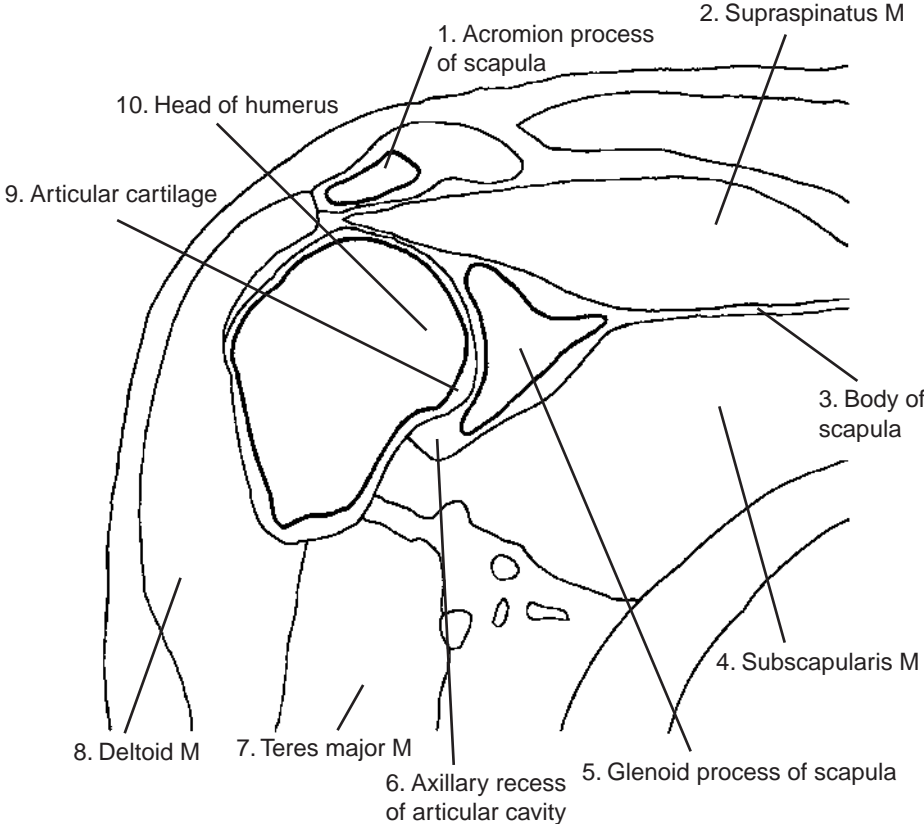


**Figure 8–6 (A,B)** Coronal MR image 3.

As in the previous images, the acromion and glenoid processes of the scapula are sectioned near the head of the humerus. Although it appears as a region of low signal intensity, the articular cartilage of the head of the humerus is labeled within the glenohumeral joint. Continuous with the glenohumeral joint, another region of low signal intensity is identified inferiorly representing the axillary recess of the articular cavity. The recess is continuous with the glenohumeral joint and decreases in size as the arm is abducted, causing an increased tension on the inferior articular capsule. Similar to the previous image, the teres major and deltoid muscles are labeled on either side of the neck of the humerus. Medially, the supraspinatus and subscapularis muscles are separated by a thin line of low signal intensity representing the body of the scapula.



A



B

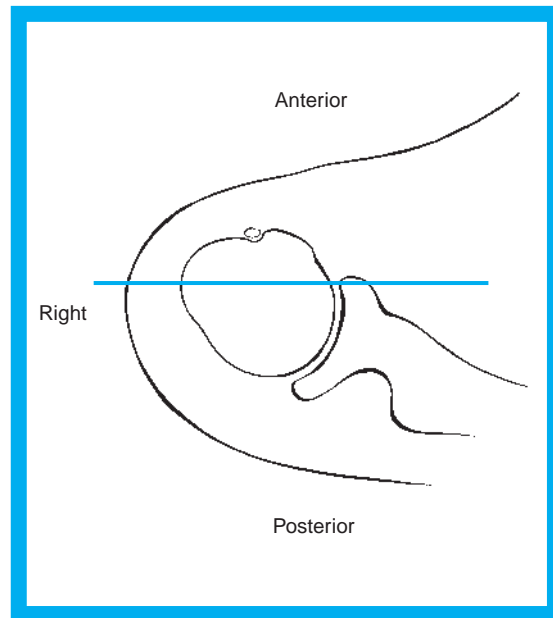
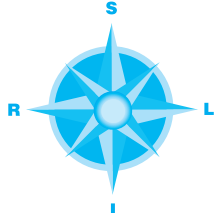
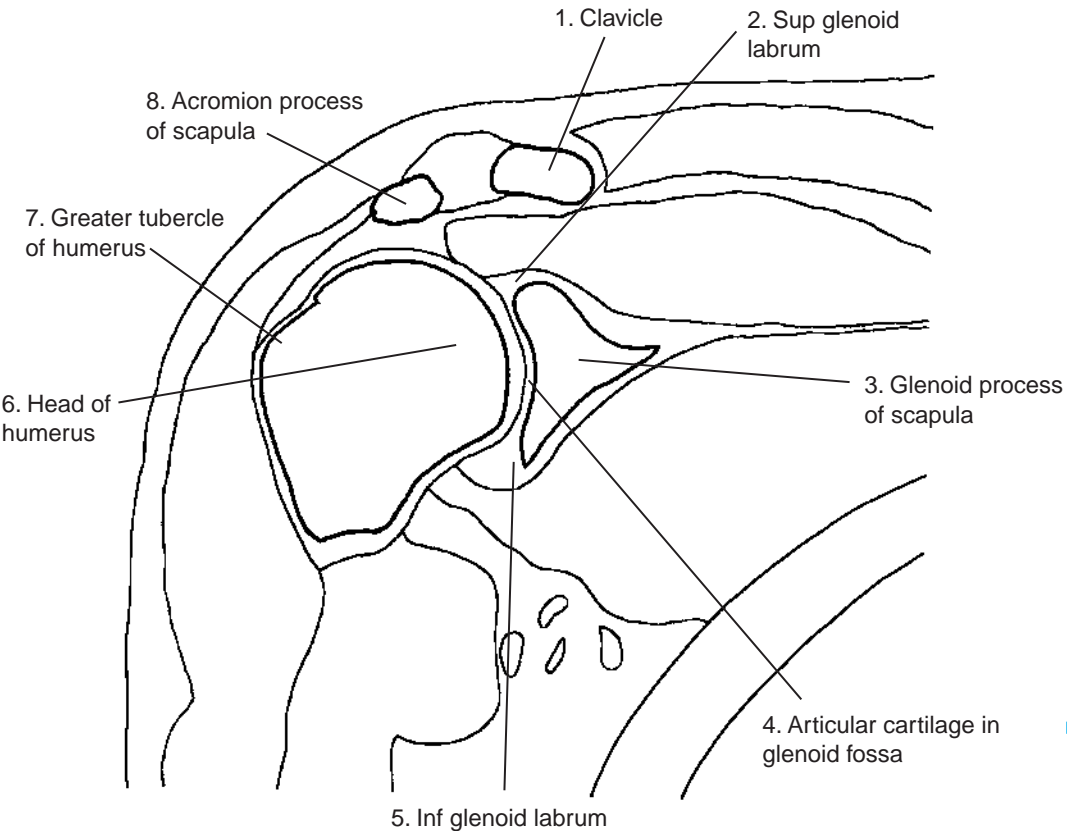
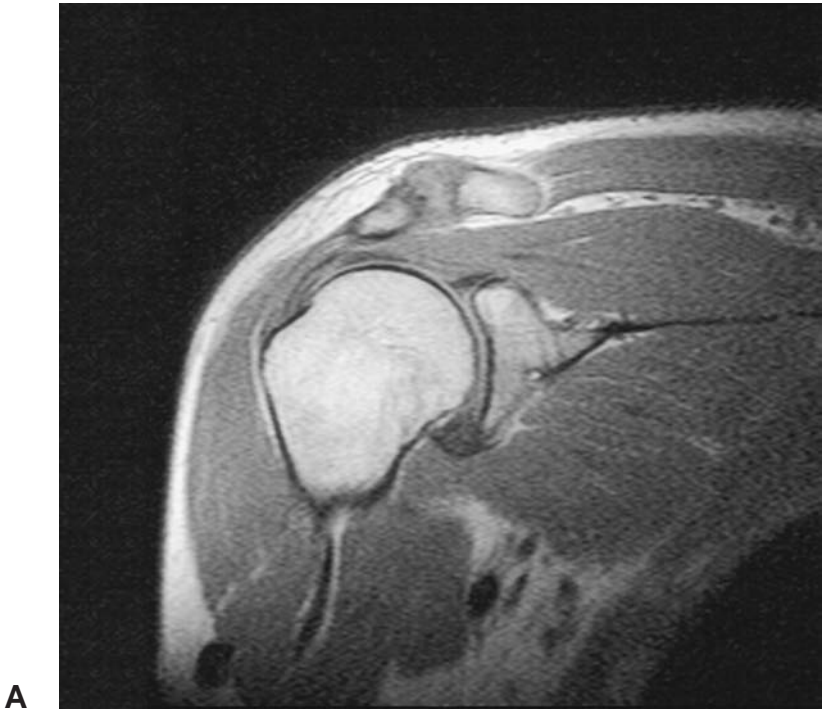


**Figure 8–7 (A,B)** Coronal MR image 4.

Because this image is anterior to the previous images, the distal end of the clavicle is now sectioned in close proximity to the acromion process of the scapula. As described earlier, the clavicle and the scapula are the bones making up the shoulder girdle and are responsible for attaching the upper extremity with the trunk of the body. The glenohumeral joint is shown between the glenoid process of the scapula and the head of the humerus. Articular cartilage not only covers the head of the humerus but is also found lining the glenoid fossa. Continuous with the articular cartilage, the glenoid labrum surrounding the edge of the glenoid fossa is sectioned, forming the upper and lower margins of the glenohumeral joint.



## Part B Elbow

### ANATOMIC OVERVIEW

The joint connecting the arm to the forearm is considered a ginglymus, or hinge-type, joint capable of flexion and extension. To form the joint, the distal humerus articulates with the proximal ends of the radius and ulna.

#### ■ Skeleton

**Humerus.** The largest and longest bone of the upper extremity (Fig. 8-8).

**Medial and lateral epicondyles** (*ep-i-KON-dilz*). Found on the distal humerus. The medial is longer and thinner than the lateral.

**Trochlea** (*TROK-le-e*). The articulating surface on the distal humerus below the medial epicondyle. Articulates with the trochlear notch of the ulna.

**Capitulum** (*kă-PIT-yu-lŭm*). The little head or small eminence of bone on the distal humerus below the lateral epicondyle. Articulates with the fovea on the head of the radius.

**Olecranon** (*ō-LEK-ră-non*) *fossa*. The depression on the posterior surface of the distal humerus between the medial and lateral epicondyles.

**Coronoid** (*KŌR-ō-noyd*) *fossa*. The depression on the anterior surface of the distal humerus between the medial and lateral epicondyles.

**Radius.** The shorter and more lateral bone of the forearm (Fig. 8-9).

**Head.** The enlarged, proximal part of the radius. Appears flattened on the end that articulates with the capitulum of the humerus.

**Fovea** (*FŌ-ve-ă*). The small pit or depression on the head of the radius.

**Neck.** Located directly below the head. The narrow region above the radial tuberosity.

**Radial tuberosity.** The projection of bone on the shaft of the proximal radius. Provides attachment for the biceps muscle.

**Ulna** (*ŪL-nă*). The longer and more medial bone of the forearm that articulates with the distal humerus.

**Olecranon process.** The most proximal part of the ulna. Projects behind the distal humerus.

**Coronoid process.** Projection found on the proximal end of the ulna that is anterior to the distal humerus.

**Trochlear notch.** The surfaces on the olecranon and coronoid processes that articulate with the trochlea of the humerus.

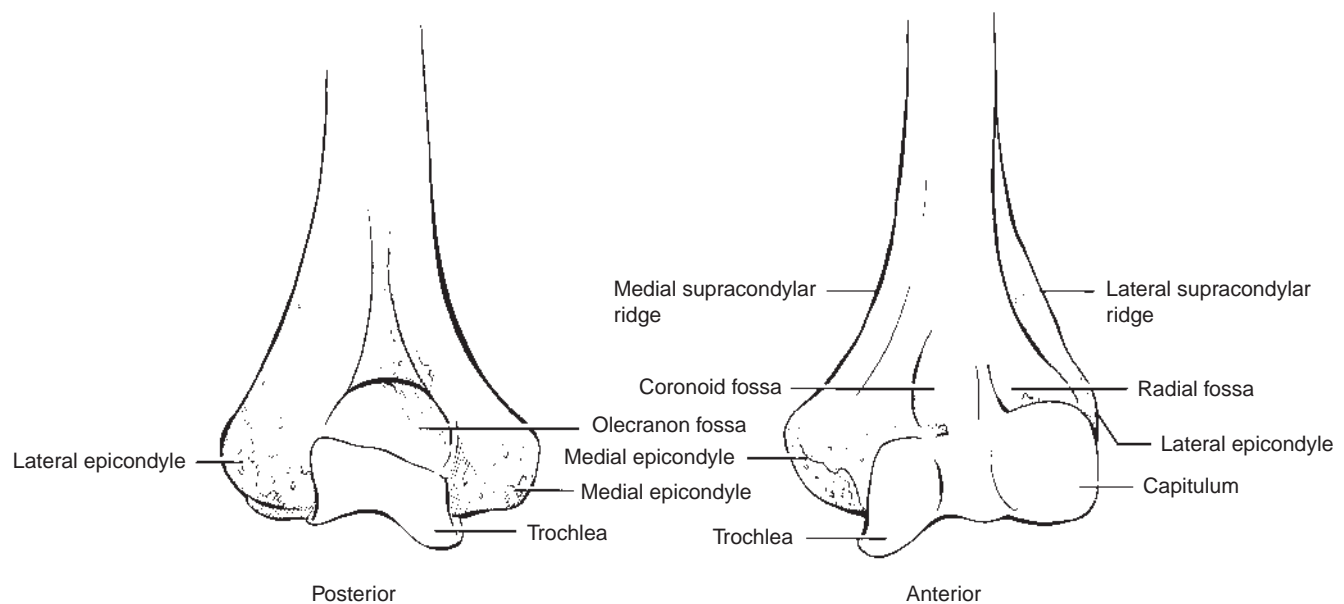


**Figure 8-8** Distal extremity of the left humerus.

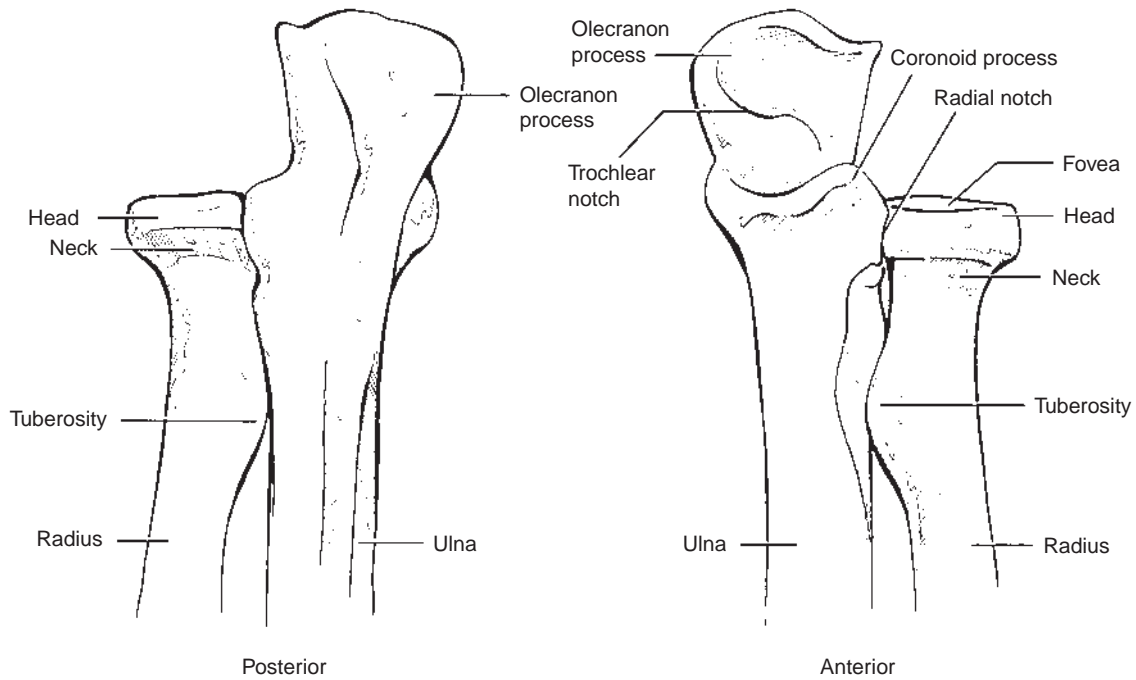


**Figure 8-9** Proximal posterior extremity of the left ulna and radius.

**Musculature**

**Triceps** (*TRI-seps*). Origin: upper humerus and infraglenoid (*IN-fră-GLĒ-noyd*) tuberosity of scapula. Insertion: posterior olecranon and fascia of forearm. Action: extends forearm (Fig. 8-10).

**Brachialis** (*bră-ke-A-lis*). Origin: lower half anterior humerus. Insertion: coronoid process and tuberosity of ulna. Action: flexes forearm.

**Brachioradialis** (*BRA-ke-ō-ra-dē-A-lis*). Origin: lateral supracondylar ridge of humerus. Insertion: styloid process of radius. Action: flexes forearm.

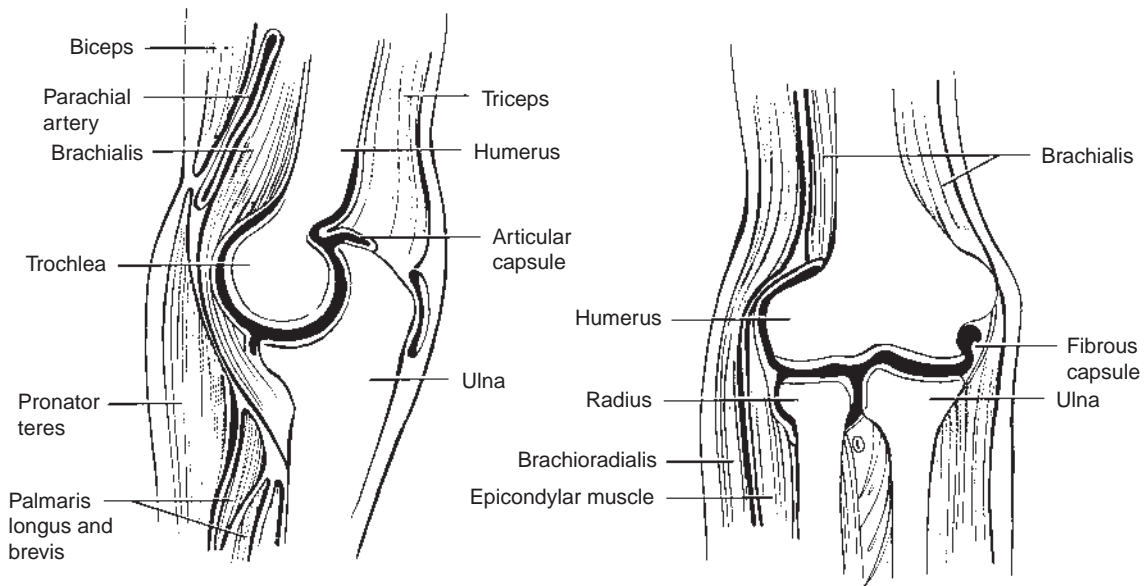


**Figure 8-10** Right: Sagittal section of the elbow. Left: Coronal section of the elbow.





## Axial Magnetic Resonance (MR) Image

The following is a selected axial MR image of the left elbow joint generated at the following technical factors: repetition time (TR) = 400 ms; echo time (TE) = 20 ms;

radiofrequency (RF) = 90°; field of view (FOV) = 16 cm; slice thickness (TH) = 3.5 mm.

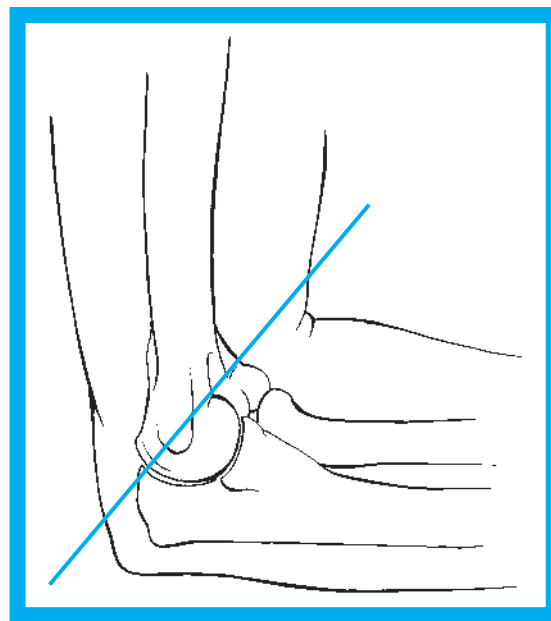
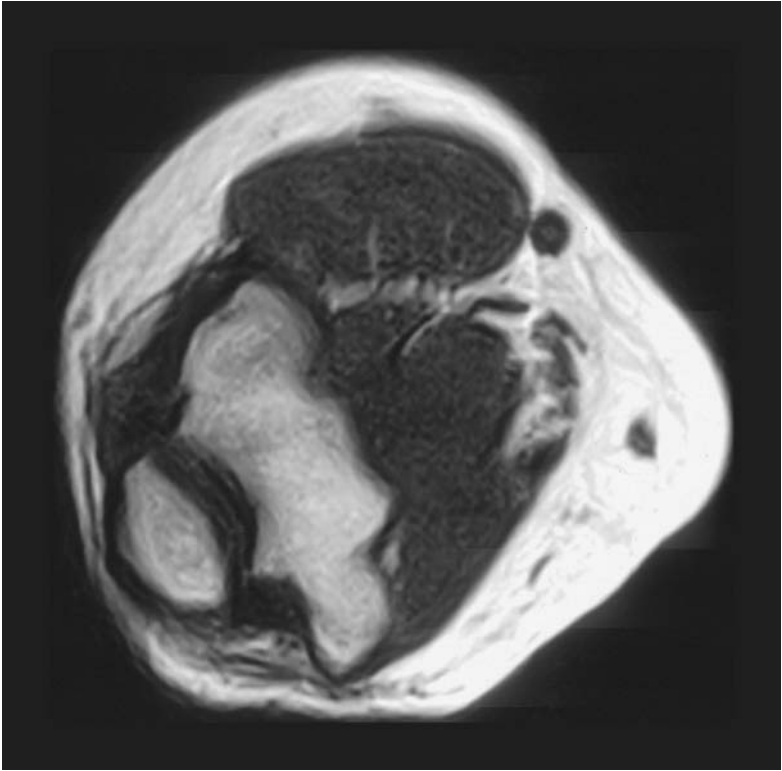
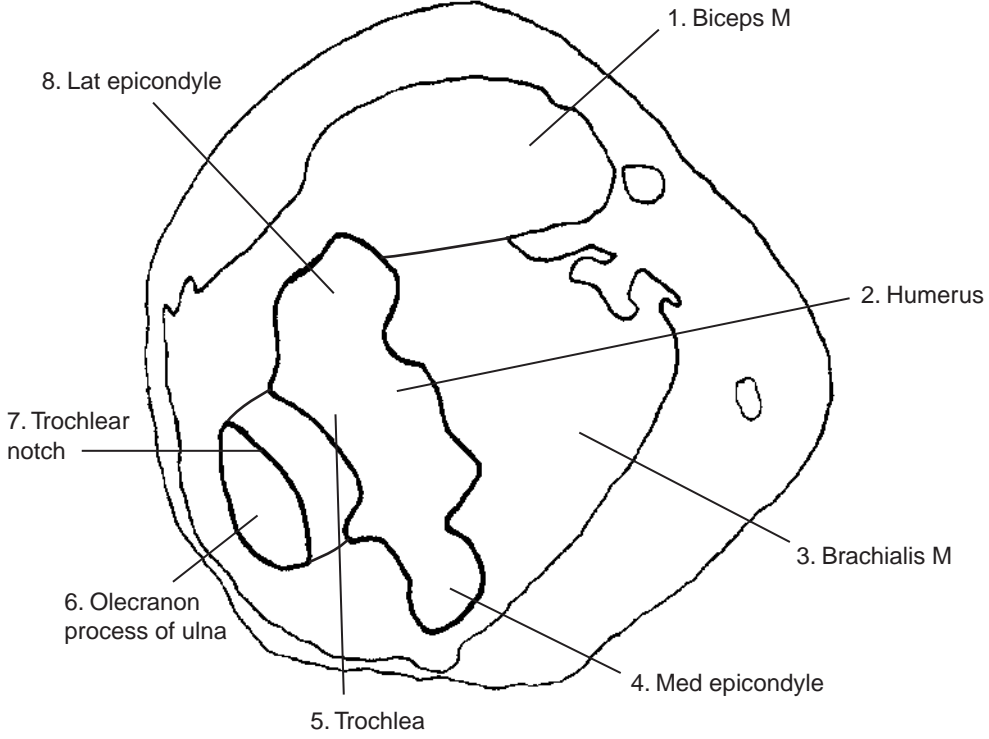


**Figure 8–11 (A,B)** Axial MR image 1.

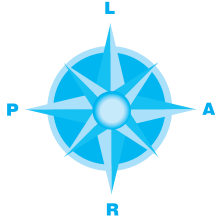
This image demonstrates the upper elbow joint formed between the ulna and the humerus. As described earlier, the trochlear notch of the ulna is the part of the olecranon process that articulates with the trochlea of the humerus and forms the upper part of the elbow joint. On either side of the trochlea, the epicondyles of the humerus are shown in cross-section; the medial epicondyle is somewhat thinner and longer than the lateral epicondyle. On the anterior surface of the humerus, two large muscle groups can be identified as the biceps and the brachialis.



A



B





## Coronal Magnetic Resonance (MR) Image

The following is a selected coronal MR image of the left elbow generated at the following technical factors: repetition time (TR) = 400 ms; echo time (TE) = 20 ms;

radiofrequency (RF) = 90°; field of view (FOV) = 16 cm; slice thickness (TH) = 3.5 mm.

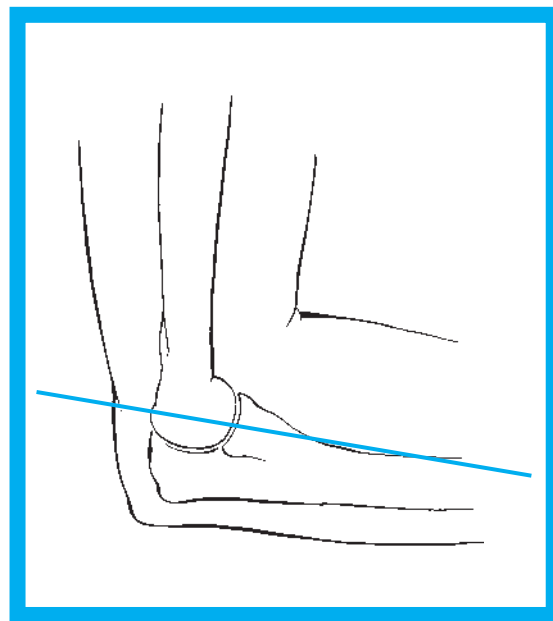
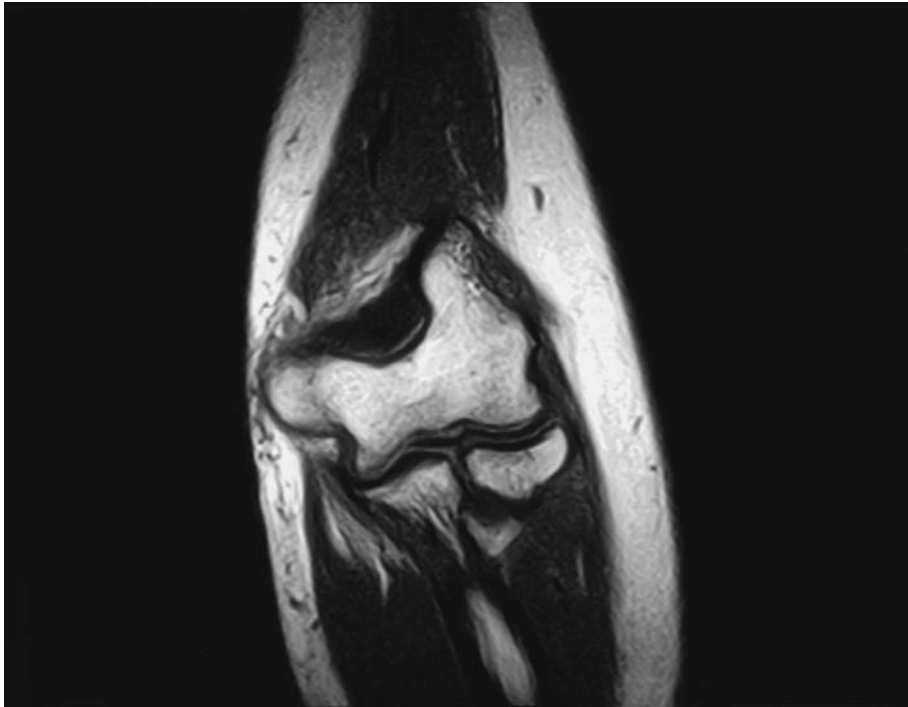
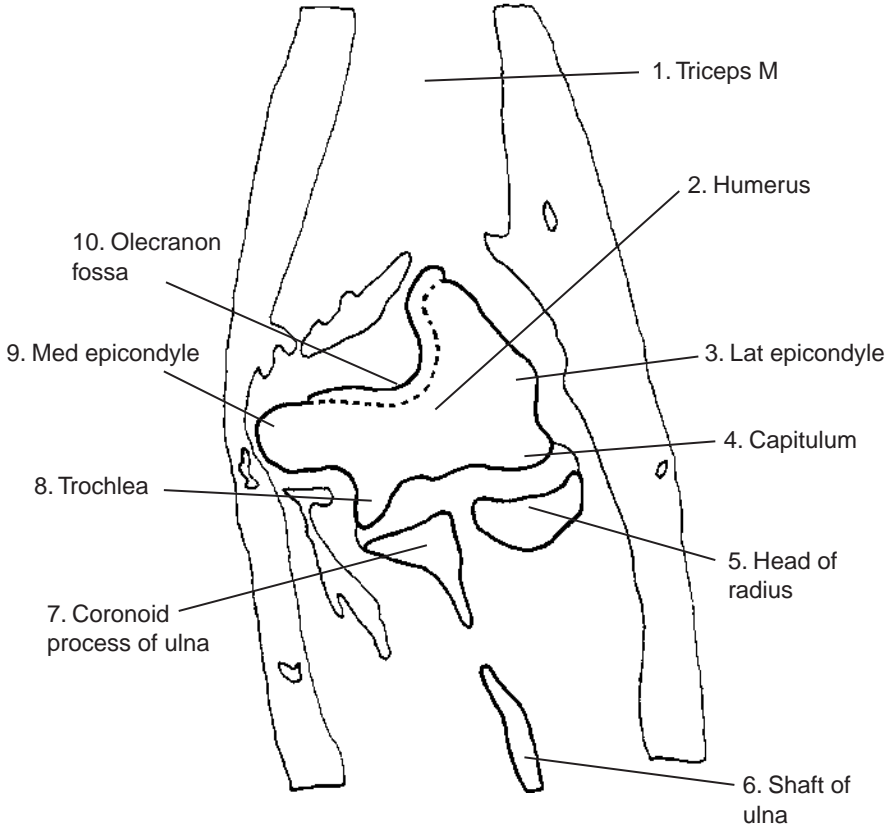


**Figure 8–12 (A,B)** Coronal MR image 1.

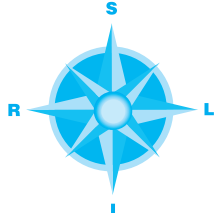
This image demonstrates the articulation of the distal end of the humerus with both the radius and the ulna. A small part of the head of the radius is identified on the lateral side articulating with the capitulum of the humerus, found just below the lateral epicondyle. Medially, the shaft and the coronoid process of the ulna are shown aligning with the trochlea of the humerus below the medial epicondyle. On the posterior surface of the distal humerus, the olecranon fossa appears as a deep depression of low signal intensity. Above the humerus, this section shows a part of the triceps muscle on the posterior aspect of the arm. Extending downward from the upper arm, this muscle inserts on the olecranon process of the ulna and the fascia of the forearm, and acts to extend the forearm.



A



B





## Sagittal Magnetic Resonance (MR) Images

The following two selected sagittal MR images of the left elbow joint were generated at 15-mm intervals from medial to lateral at the following technical factors: repetition

time (TR) = 1,100 ms; echo time (TE) = 20 ms; radiofrequency (RF) = 90°; field of view (FOV) = 16 cm; slice thickness (TH) = 3.5 mm.

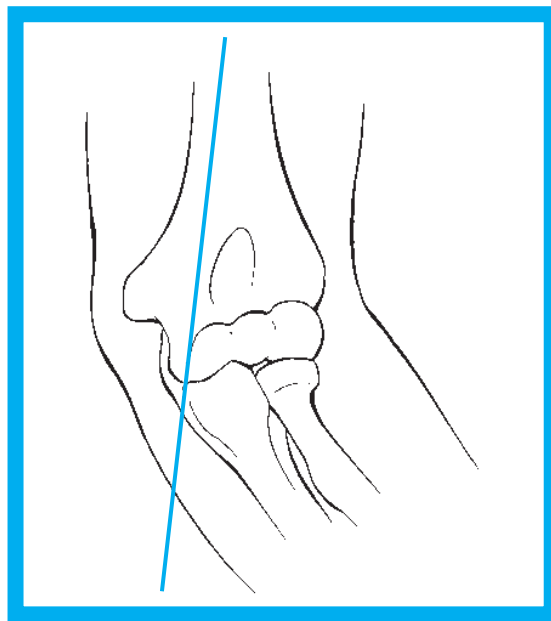
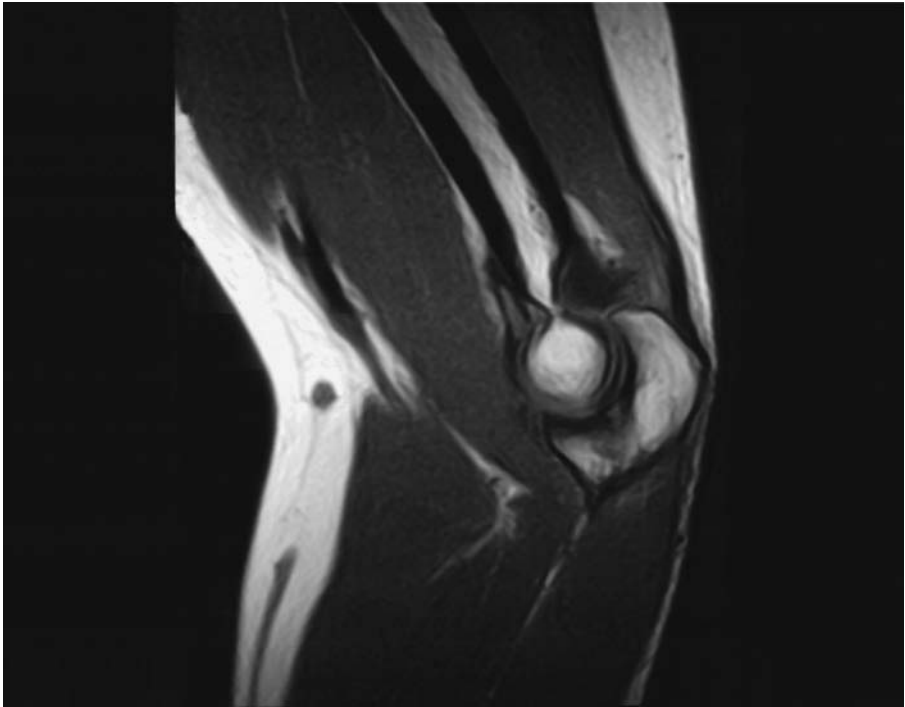
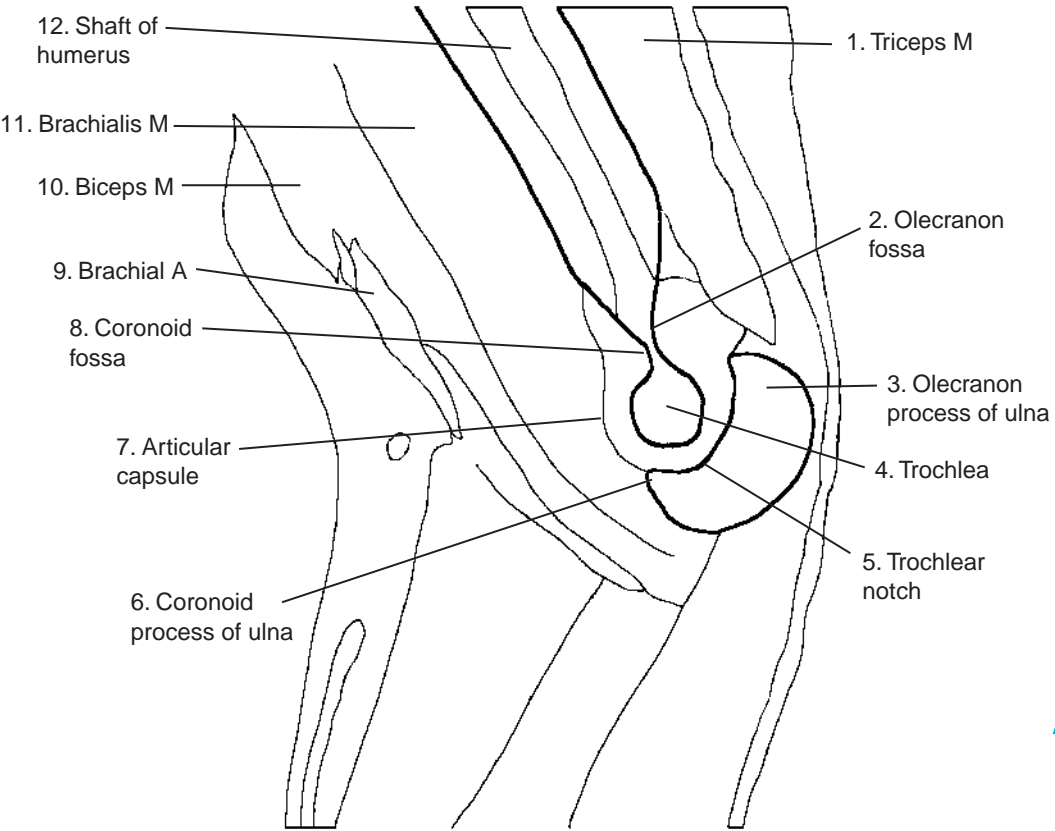


**Figure 8–13 (A,B)** Sagittal MR image 1.

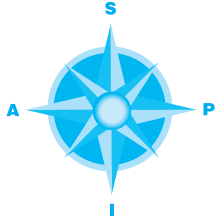
This image shows the unique appearance of the distal end of the humerus. The shaft extends downward, narrowing as a result of the coronoid and olecranon fossae, which together cause a further narrowing of the humerus to a point at which the intervening region is nearly paper thin. Below the fossae, the humerus enlarges in a spherical manner to form the trochlea, which articulates with the proximal ulna of the forearm. Appearing as a crescent-shaped region of bone, the proximal ulna demonstrates both the coronoid and olecranon processes, which form the trochlear notch. Between the humerus and the ulna, the elbow joint space is separated from the surrounding musculature by the articular capsule. In this section, the articular capsule extends from the coronoid and olecranon processes of the ulna to attach to the shaft of the humerus. The humerus separates the posterior triceps muscle from the brachialis and the biceps muscles on the anterior surface of the upper arm. The brachialis muscle, which originates from the lower half of the humerus, inserts on the coronoid process of the ulna. This position allows the brachialis muscle to flex the forearm and makes it a deeper muscle than the biceps. Shown obliquely sectioned on the anterior brachialis muscle, the brachial artery is sectioned as it extends downward along the medial border of the biceps muscle to give rise to the radial artery in the forearm.



A



B



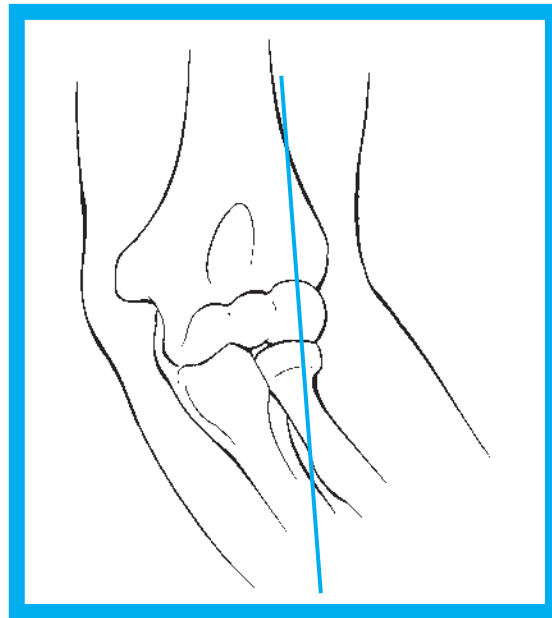
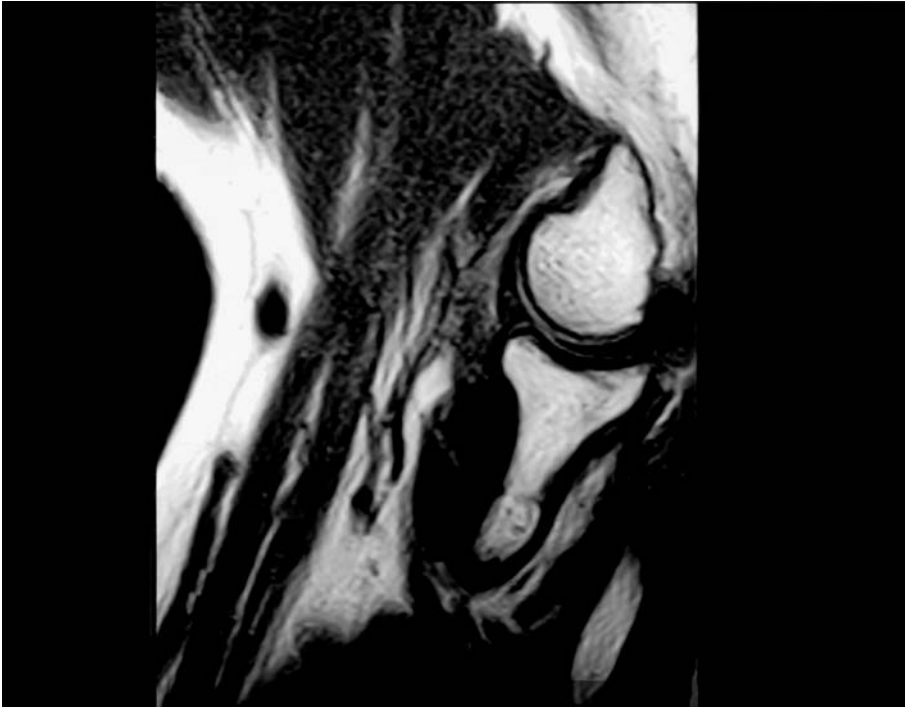
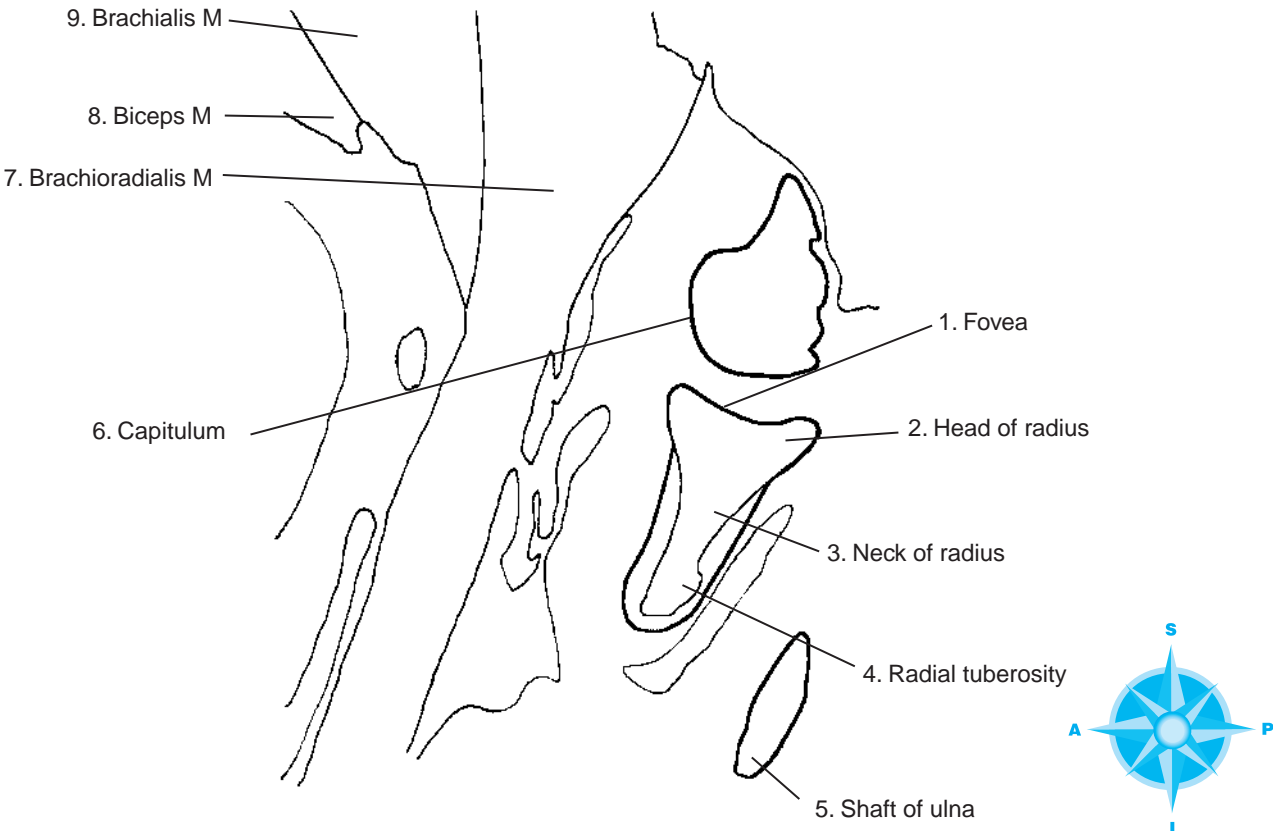


**Figure 8–14 (A,B)** Sagittal MR image 2.

This section through the lateral region of the elbow shows the head of the radius articulating with the capitulum of the humerus. The capitulum is an enlarged region of the distal humerus that articulates with the fovea, or the depressed region on the head of the radius, to form the lateral elbow joint. On the lower part of the radius, the radial tuberosity is separated from the head by the narrowed region representing the neck of the radius. Compared to the ulna, the shaft of the radius is more anterior within the proximal forearm. Similar to the previous figure, the brachialis and biceps muscles can be identified in the upper part of the image, but the lateral location of this section also includes part of the brachioradialis muscle.



A



B



## Part C Wrist

### ANATOMIC OVERVIEW

The wrist is generally described as the part of the upper limb between the forearm and hand. Together, the carpal bones articulate to provide a wide range of movements of the hand with respect to the forearm. The wrist contains eight bones that are arranged in groups of four into proximal and distal rows (Fig. 8-15).

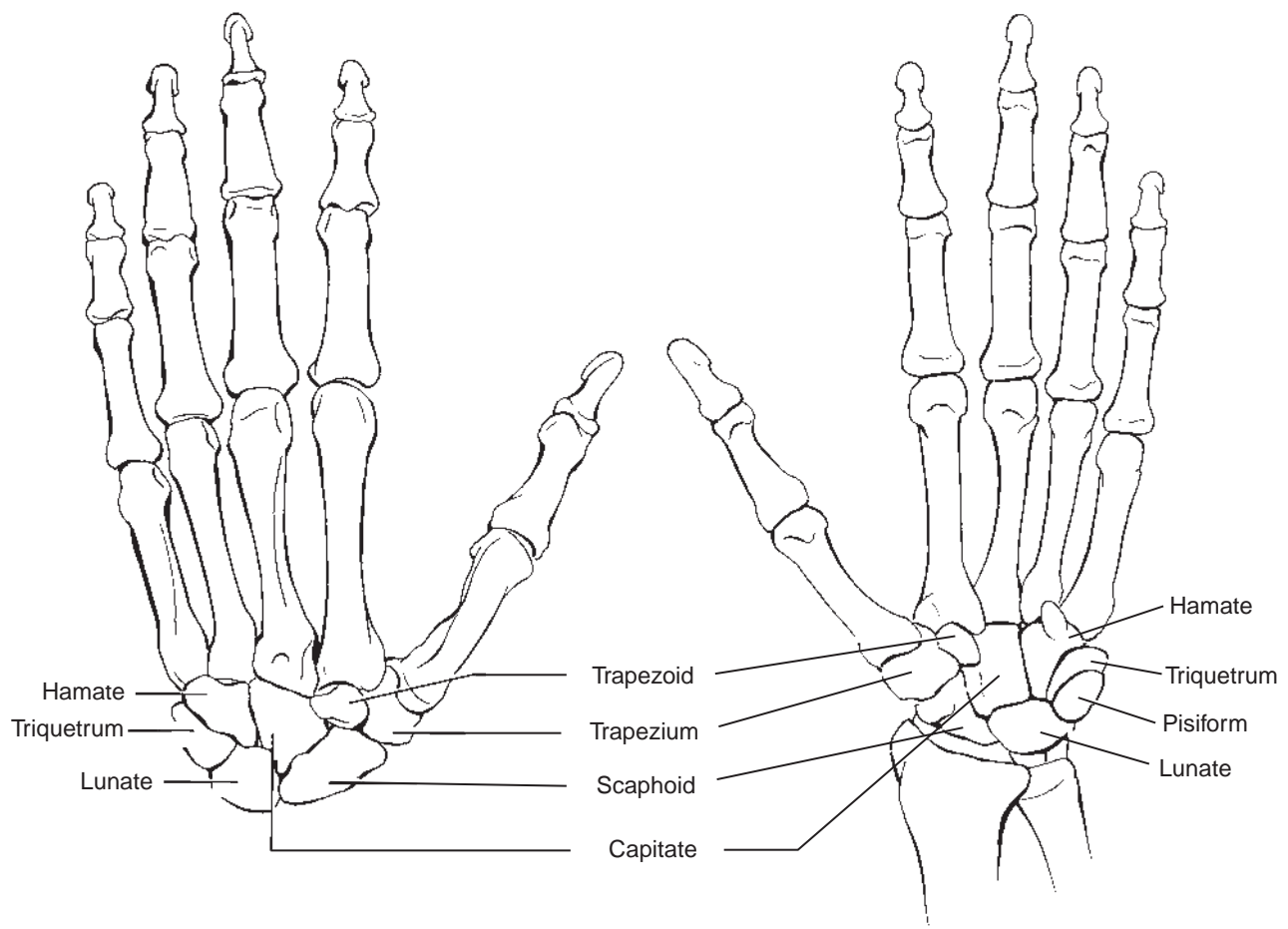
#### ■ Skeleton

Hint: The mnemonic for remembering the order of the carpal bones, starting from the lateral side in the proximal row, is “Send letter to Peter to tell’m (to) come home.”

mal row, is “Send letter to Peter to tell’m (to) come home.”

**Scaphoid** (*SKAF-oyd*). Also called the navicular (*nă-VIK-yŭ-lăr*) bone. The largest and most lateral bone of the proximal row. Articulates with the radius. Because the radius is the only bone of the forearm that articulates with the carpal bones, the force of falls frequently results in fractures of the scaphoid bone. Approximately 75% of carpal fractures are found within this bone.

**Lunate** (*LU-nat*). Also called the semilunar bone. Crescent-shaped bone within the proximal row. Articulates with the radius.



A

**Figure 8-15** A: Dorsal and palmar view of wrist and hand bones. (*continued*)

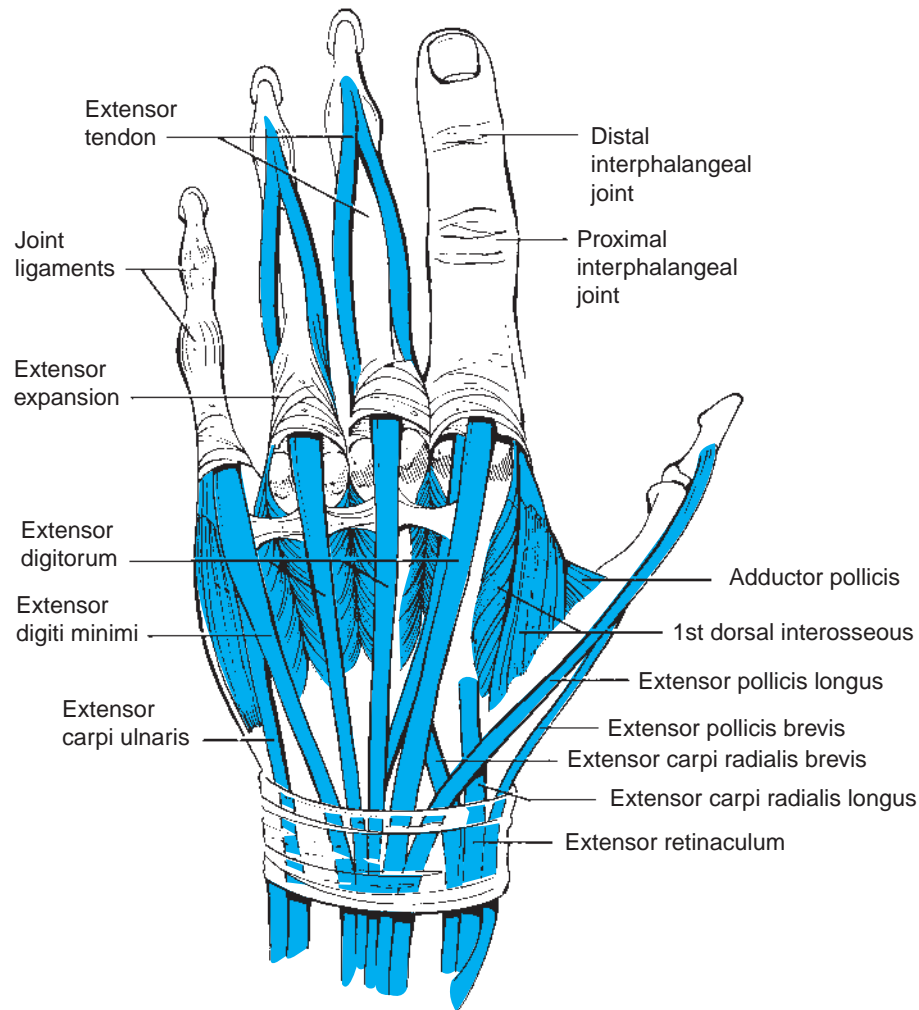


**Figure 8-15** (continued) **B:** Dorsal view of muscles and tendons of the wrist and hand.

**Triquetrum** (*tri-KWĒ-trūm*). Also called the triangular or cuneiform bone. Pyramid-shaped bone with an articular facet on its palmar surface for the pisiform.

**Pisiform** (*PIS-i-fōrm*). The most medial bone of the proximal row. Small, oval-shaped bone situated on the palmar surface of the triquetrum. Unlike the other proximal carpal bones, a muscle of the forearm, the flexor carpi ulnaris, inserts on this bone.

**Trapezium** (*tra-PĒ-ze-ŭm*). Also called the greater multangular bone. The most lateral carpal of the distal row. Articulates with the first metacarpal (*MET-ă-KAR-păł*), and is mostly on the palmar surface of the wrist.

**Trapezoid** (*TRAP-ĕ-zoyd*). Also called the lesser multangular bone. Wedge-shaped bone and the smallest of

the distal row of carpal bones. Articulates with the second metacarpal. On the palmar surface, it has an oblique deep groove, giving it a unique appearance in sectional images.

**Capitate** (*KAP-i-tat*). Also called the os magnum bone. The largest of the carpal bones and located in the center of the wrist. Articulates with the third metacarpal. Owing to its shape and location, it forms the keystone of the carpal tunnel, found on the anterior wrist.

**Hamate** (*HAM-at*). Also called the unciform (*ŪN-si-fōrm*) bone. The most medial carpus in the distal row. Articulates with the fourth and fifth metacarpals. Has a unique shape owing to its hooklike process on the palmar surface, the hamulus (*HAM-yu-lŭs*).

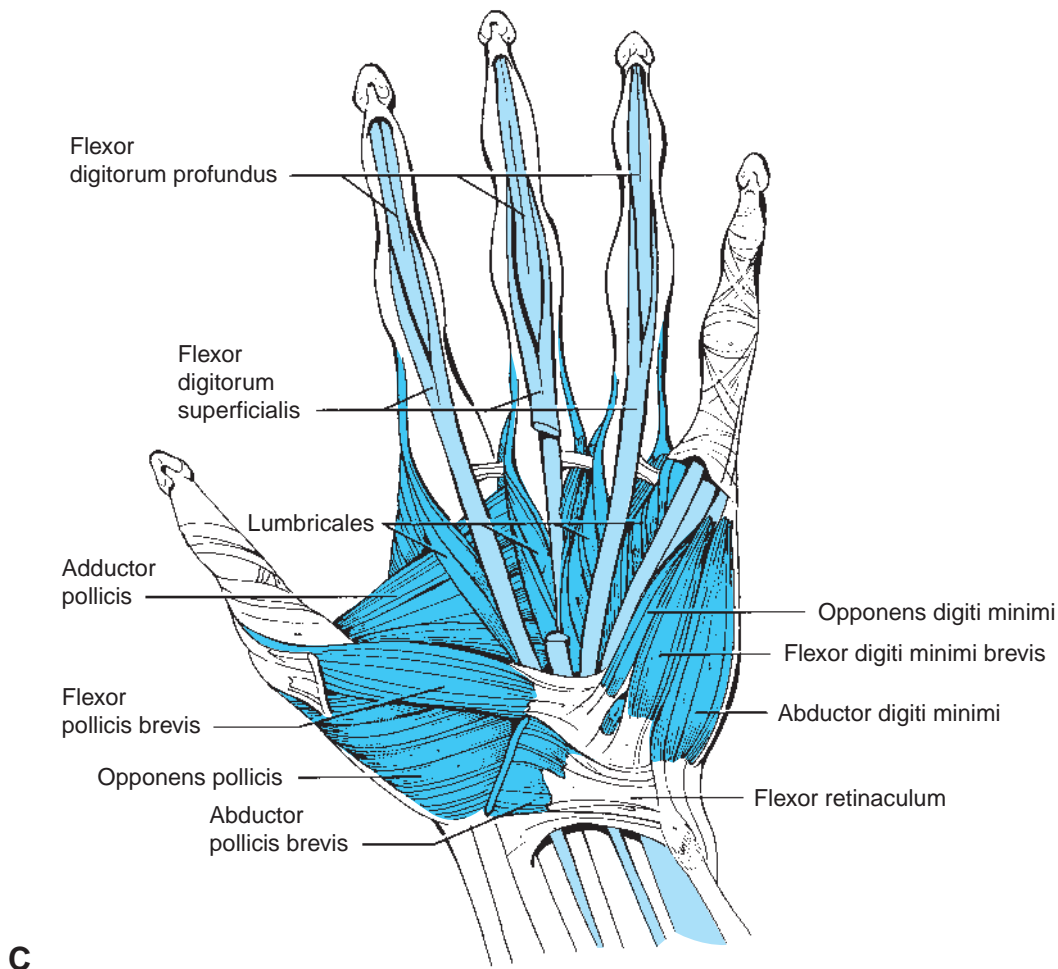


**Figure 8–15** (continued) **C:** Palmar view of muscles and tendons of the wrist and hand.

## ■ Musculature

**Abductor digiti minimi** (*DIJ-i-ti MIN-i-mi*). Origin: pisiform and tendon of flexor carpi ulnaris. Insertion: first phalanx (*FA-langks*) of fifth digit. Action: abducts fifth digit and flexes first phalanx.

**Abductor pollicis brevis** (*POL-i-sis BREV-is*). Origin: flexor retinaculum (*ret-i-NAK-yu-lim*), scaphoid, and trapezium. Insertion: first phalanx of the first digit. Action: abducts first digit.

**Opponens** (*ō-PŌ-nens*) **pollicis**. Origin: flexor retinaculum and trapezium. Insertion: first metacarpal. Action: abducts, flexes, and rotates the first metacarpal.

**Flexor digitorum superficialis** (*dij-i-TŌ-rim SU-per-fish-e-A-lis*). Origin: medial epicondyle of humerus, corono-

noid process of ulna, and midradius. Insertion: second phalanx of digits two through five. Action: flexes second phalanges (*fa-LAN-jez*), hand, and forearm.

**Flexor digitorum profundus** (*prō-FÜN-dūs*). Origin: midulna and interosseous membrane. Insertion: distal phalanx of digits two through five. Action: flexes digits and flexes hand.

**Extensor carpi ulnaris** (*KAR-piül-NA-ris*). Origin: lateral epicondyle of humerus and proximal ulna. Insertion: base of the fifth metacarpal. Action: extends and abducts the hand.

**Extensor digiti minimi**. Origin: common extensor tendon. Insertion: first phalanx of the fifth digit. Action: extends fifth digit.

**Extensor digitorum.** Origin: lateral epicondyle of humerus. Insertion: bases of second and third phalanges of digits two through five. Action: extends the digits and extends the hand.

**Extensor indicis** (*IN-di-sez*). Origin: posterior shaft of the ulna and the interosseous membrane. Insertion: extensor digitorum tendon of the second digit. Action: extends and adducts the second digit. NB: not shown in Figure 8-15.

**Extensor pollicis longus.** Origin: posterior surface of ulna. Insertion: base of the last phalanx of the first digit. Action: extends first phalanx of the first digit and abducts the hand.

**Extensor carpi radialis** (*ra-de-A-lis*) **longus.** Origin: lateral supracondylar ridge of humerus. Insertion: base of the second metacarpal. Action: extends and abducts the hand.



## Axial Computed Tomography (CT) Images

The following two selected CT images of both wrists are described at 3-mm intervals from proximal to distal. The images were generated at the following technical

factors: 120 kilovolt peaks (kVp); 150 milliampereseconds (mA-s); field of view (FOV) = 25 cm; slice thickness (TH) = 3 mm.

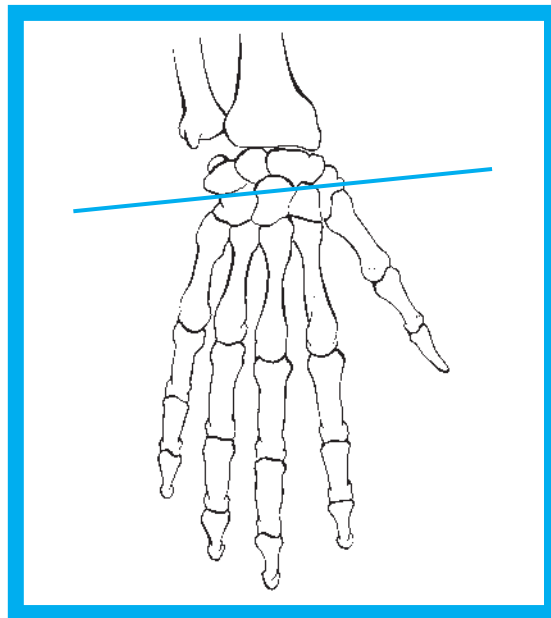
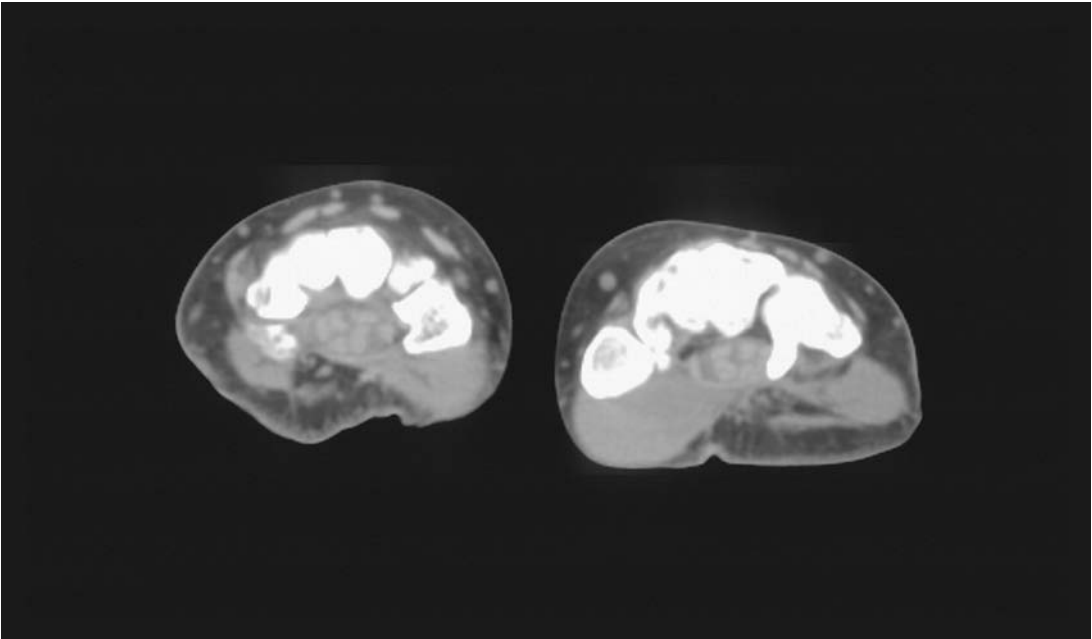
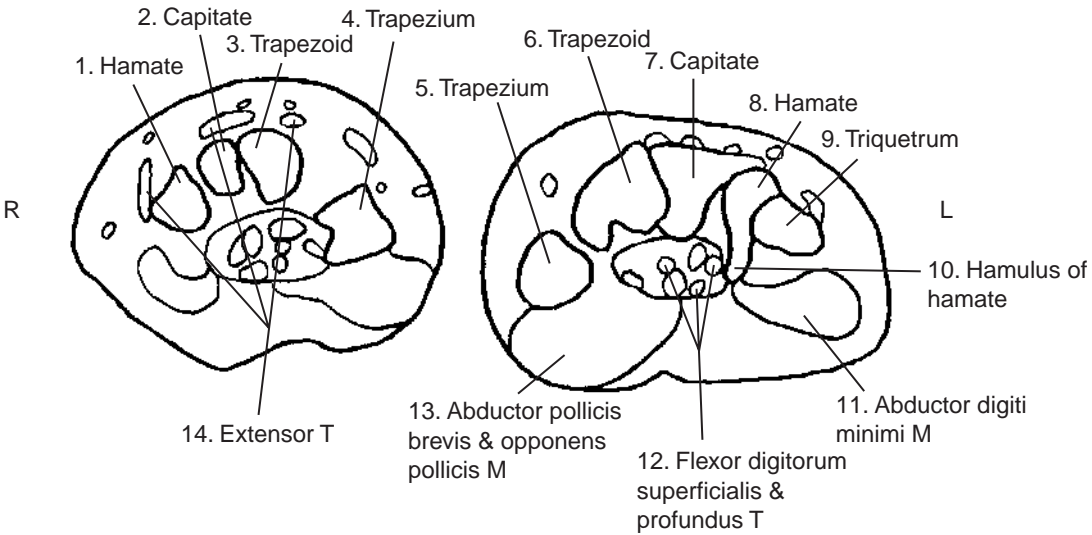


**Figure 8–16 (A,B)** Axial CT image 1.

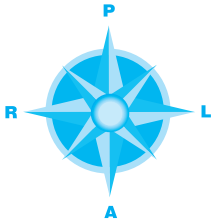
For comparison, this image includes both of the patient's wrists, which were placed side by side within the gantry. The patient's left wrist is on the right side of the image, as though the patient were facing us. In this position, the lateral parts of both wrists are located toward the middle of the image. When looking at the left wrist, one can see that the unique appearance of the hamate bone is readily distinguished owing to the presence of the hook, or hamulus, on the palmar surface. Because the plane of section is slightly higher on the left wrist, an additional carpus is shown lateral to the hamate bone. Owing to its location, the bone is the triquetrum, or the third bone of the proximal row between the hamate and the pisiform bones. Articulating with the lateral side of the hamate bone, the capitate is identified and is often described as the bone within the center of the wrist. Moving medially, we note the next carpus of the distal row is the trapezoid, shown with its characteristic groove on the palmar surface. The first bone of the distal row, the trapezium, is found near the palmar surface. Together, the bones form part of a bony arch over what is known as the carpal tunnel, which contains the flexor digitorum superficialis and profundus tendons passing from the forearm into the palmar surface of the hand. In addition, the abductor digiti minimi muscle is sectioned as it extends from its origin on the pisiform bone and tendon of flexor carpi ulnaris to insert on the first phalanx of the fifth digit. On the lateral side of the wrist, the abductor pollicis brevis and opponens pollicis muscles are cross-sectioned as they originate from the flexor retinaculum and trapezium. Although reversed from the sequence described for the left wrist, all four bones of the distal row can be identified—in a slightly different plane of section—within the right wrist. Like the bones, the muscles of the right wrist are reversed in position compared to the left side. On the dorsal surface of the wrist, the tendons sectioned are collectively called the extensor tendons and include the extensor pollicis longus, extensor carpi radialis longus, extensor indices, extensor digitorum, extensor digiti minimi, and extensor carpi ulnaris.



A



B



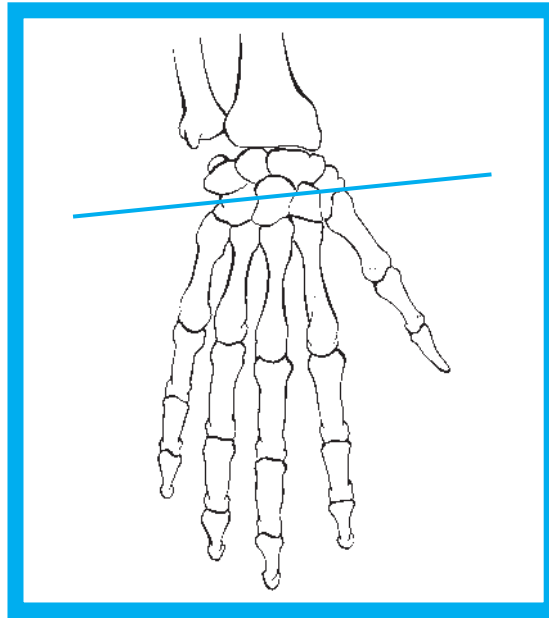
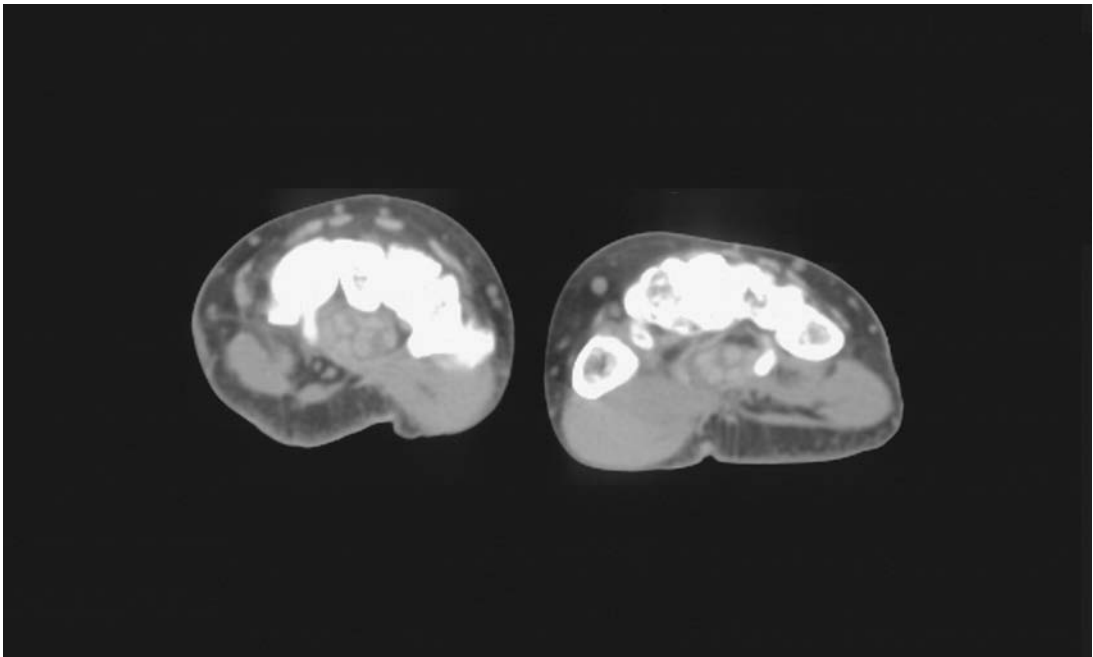
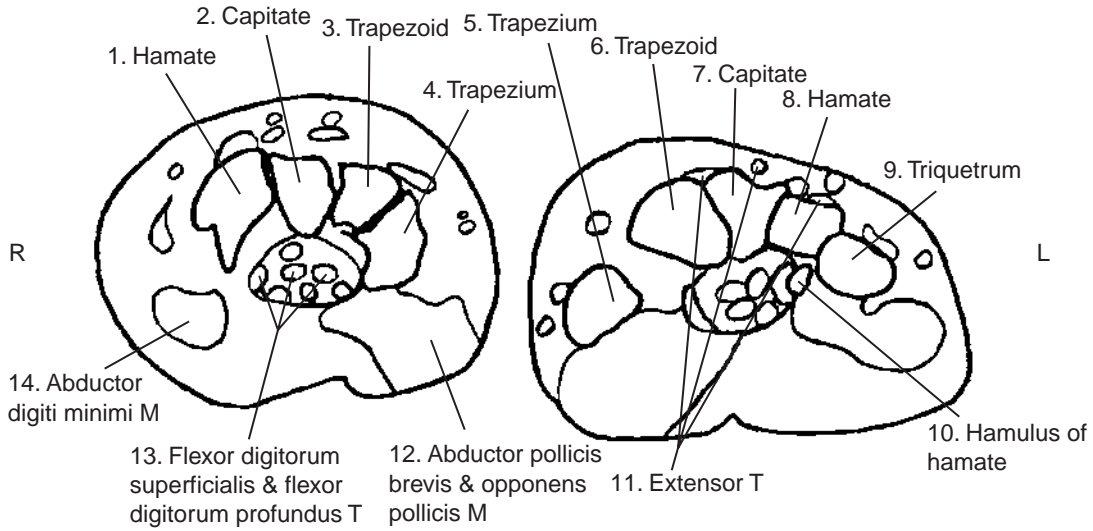


**Figure 8–17 (A,B)** Axial CT image 2.

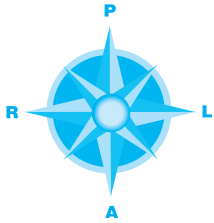
Because this image is 3 mm distal to the previous image, the anatomy demonstrated lies closer to the metacarpals. As before, this image demonstrates both the right and left wrists. The four bones of the distal row can be identified within the right wrist. The capitate bone is in the center of the wrist separating the hamate from the trapezoid. In this position, the trapezium or most lateral bone of the distal row is demonstrated in its characteristic location toward the palmar surface. Together, these four bones form part of the bony arch over the carpal tunnel. Within the left wrist, the four bones of the distal row can also be identified in reverse sequence; the most lateral is the hamate. Although somewhat light owing to slice thickness averaging, the hamulus of the hamate bone is demonstrated on the palmar surface. Because the plane of section is slightly higher on the left wrist than on the right, the triquetrum of the proximal row is sectioned. The triquetrum separates the hamate from the small, oval-shaped pisiform bone. Much like the previous image, the flexor digitorum superficialis and profundus tendons are within the carpal tunnel and are labeled in the right wrist. The flexor tendons are separated from the abductor digiti minimi, abductor pollicis brevis, and opponens pollicis muscles by the flexor retinaculum. On the dorsal surface of the carpal bones, extensor tendons are sectioned but are not individually labeled in this image.



A



B





## Part D Hip

### ANATOMIC OVERVIEW

Generally described as the juncture of the lower limb with the pelvic girdle, or hip bone, which is made up of the ilium, ischium, and pubis. Formed between the head of the femur and the acetabulum, the joint is considered a ball-and-socket type (enarthrosis); it is capable of a wide range of movements, including internal and external rotation.

#### ■ Skeleton

**Femur** (*Fe-mūr*). The longest and strongest bone in the body. Found within the thigh (Fig. 8-18).

**Head.** The round, proximal end of the femur that forms the ball part of the hip joint.

**Greater trochanter.** Projection of bone found on the lateral aspect of the proximal femur. Site of attachment for many muscles within the gluteal (*GLU-te-äl*) region.

**Fovea capitis femoris** (*FŌ-ve-ä KAP-i-tis FEM-ö-ris*). A depression in the head of the femur where the ligamentum capitis femoris is attached. Unlike most ligaments, the ligamentum capitis femoris has little function in maintaining the

structure of the joint. Instead, it acts to guide an artery through the fovea capitis to provide the major arterial blood supply to the head of the femur.

**Neck.** The narrowed region between the trochanters and the head of the femur that forms an angle of 120° to 125° with the shaft.

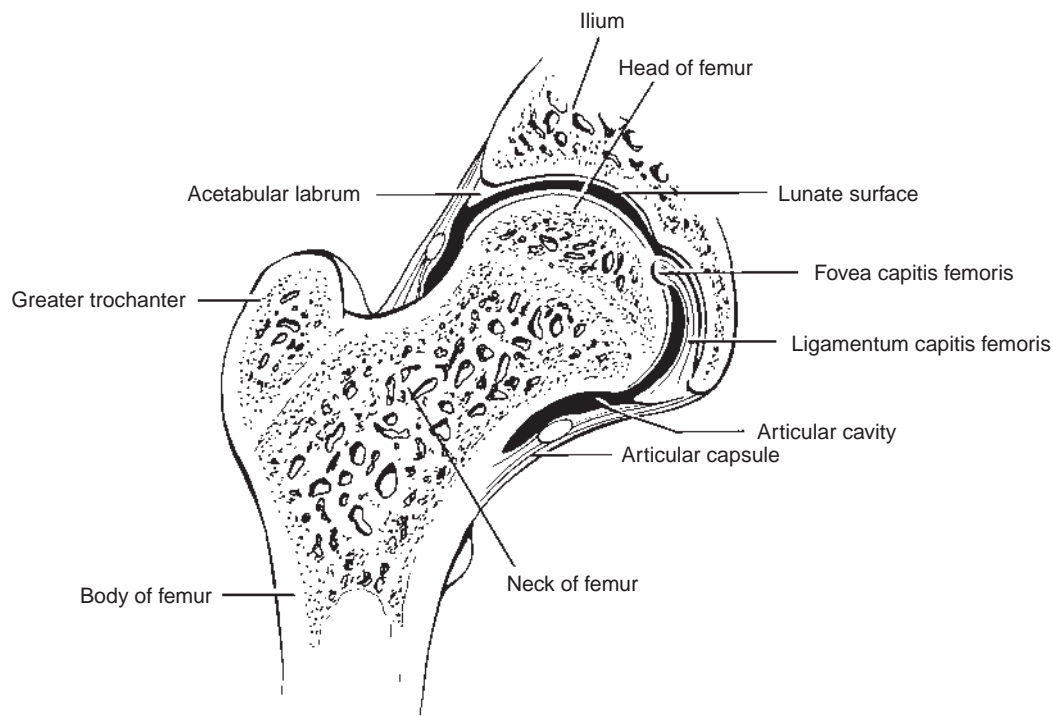
**Acetabulum** (*as-ě-TAB-yu-lüm*). A depression on the lateral aspect of the pelvic girdle formed by the juncture of the ilium (*IL-e-üm*), ischium (*IS-ke-üm*), and pubic bones. Forms the socket of the hip joint.

**Lunate surface.** The crescent-shaped articular surface within the acetabulum (Latin for “moon”). Surrounds the fossa containing the ligamentum capitis femoris.

#### ■ Musculature

**Iliopsoas** (*IL-e-Ō-SŌ-as*). Origin: transverse processes of L1 through L5 and the upper iliac fossa. Insertion: lesser trochanter of the femur. Action: flexes the thigh and rotates the thigh laterally.

**Gluteus maximus** (*glu-TE-üs MAK-si-müs*). Origin: upper ilium and sacrotuberous ligament. Insertion: gluteal



A

**Figure 8-18** A. Coronal section of the hip. (*continued*)

tuberosity of the femur. Action: Extends and laterally rotates the thigh.

**Obturator internus** (*OB-tu-rā-tōr in-TER-nūs*). Origin: inner obturator membrane. Insertion: greater trochanter. Action: abducts and rotates the thigh laterally.

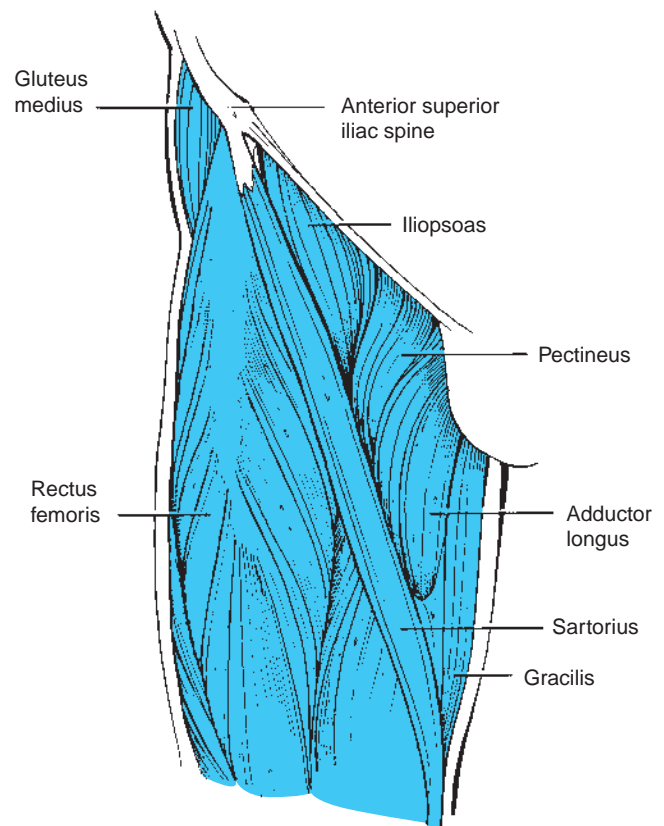
**Superior gemellus** (*jě-MEL-ūs*). Origin: outer ischial spine. Insertion: tendon of the obturator internus muscle. Action: abducts and laterally rotates the thigh.

**Tensor fascia latae** (*FASH-e-ă LA-te*). Origin: anterior iliac crest. Insertion: iliotibial tract, Action: abducts, flexes, and rotates the thigh medially. NB: not shown in Figure 8-18.

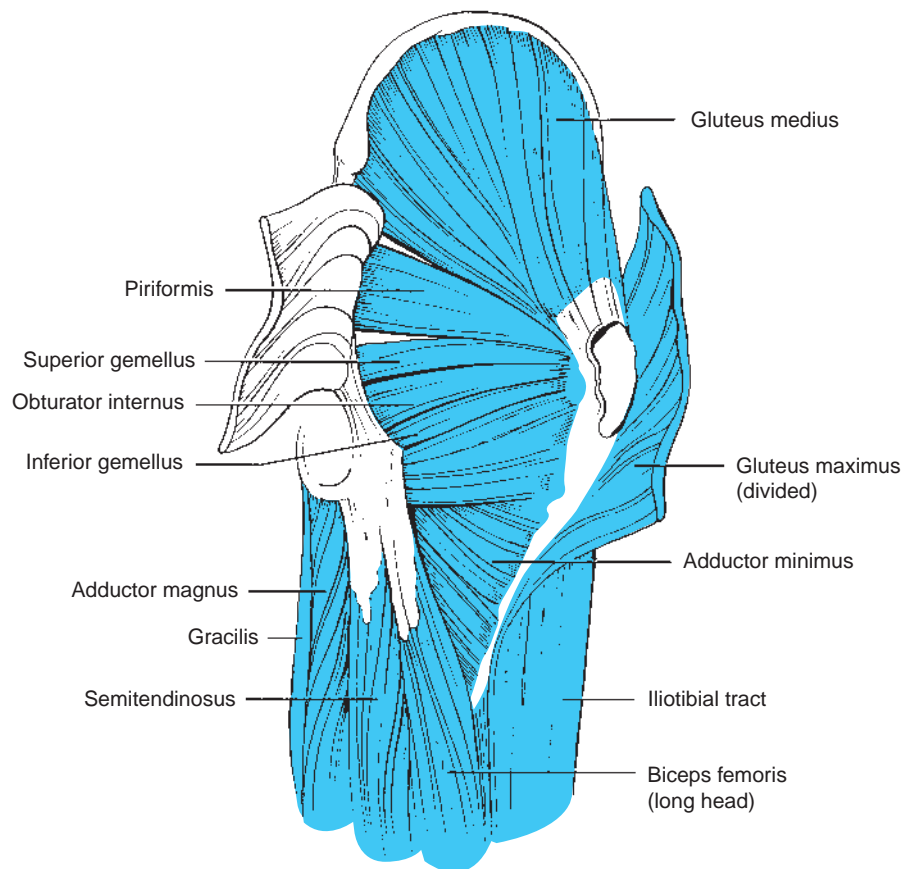
**Rectus femoris** (*REK-tūs*). Origin: anterior inferior iliac spine. Insertion: base of the patella. Action: flexes the thigh and extends the leg.

**Sartorius** (*sar-TŌR-e-ūs*). Origin: anterior superior iliac spine. Insertion: upper medial tibia. Action: flexes and rotates the thigh laterally.

**Pectineus** (*PEK-ti-NĒ-ūs*). Origin: pectineal line of the pubis. Insertion: pectineal line of the femur. Action: flexes, adducts, and laterally rotates the thigh.



**B**



**C**

**Figure 8-18** (continued) **B.** Anterior view of muscles covering the hip joint. **C.** Posterior view of muscles covering the hip joint.



## Axial Computed Tomography (CT) Images

The following two selected CT images of the hip joint are described at 5-mm intervals from superior to inferior. They were generated at the following technical

factors: 120 kilovolt peak (kVp); 280 milliamperesecond (mA-s); field of view (FOV) = 30 cm; slice thickness (TH) = 5 mm.

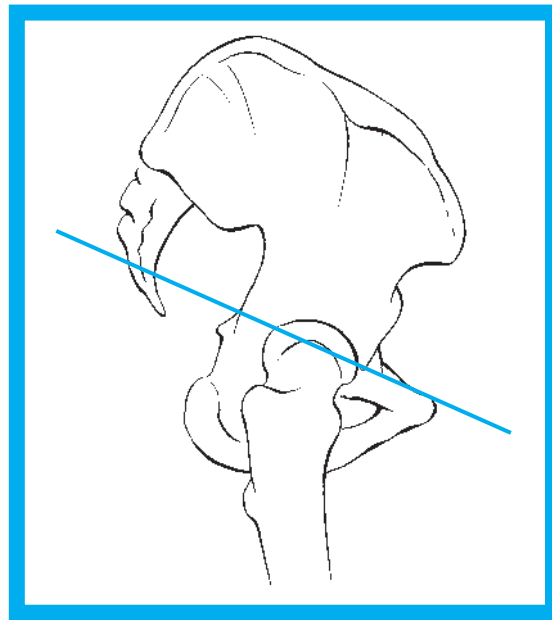
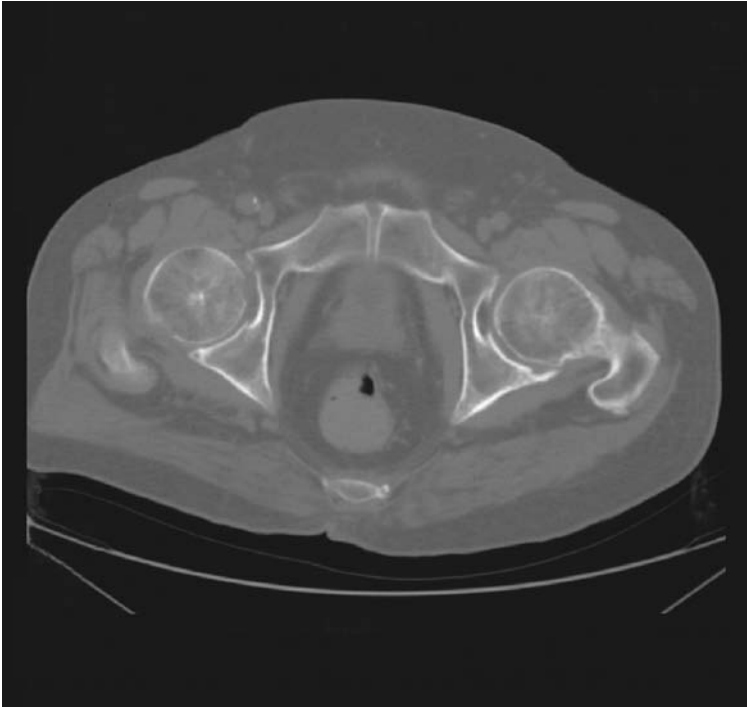
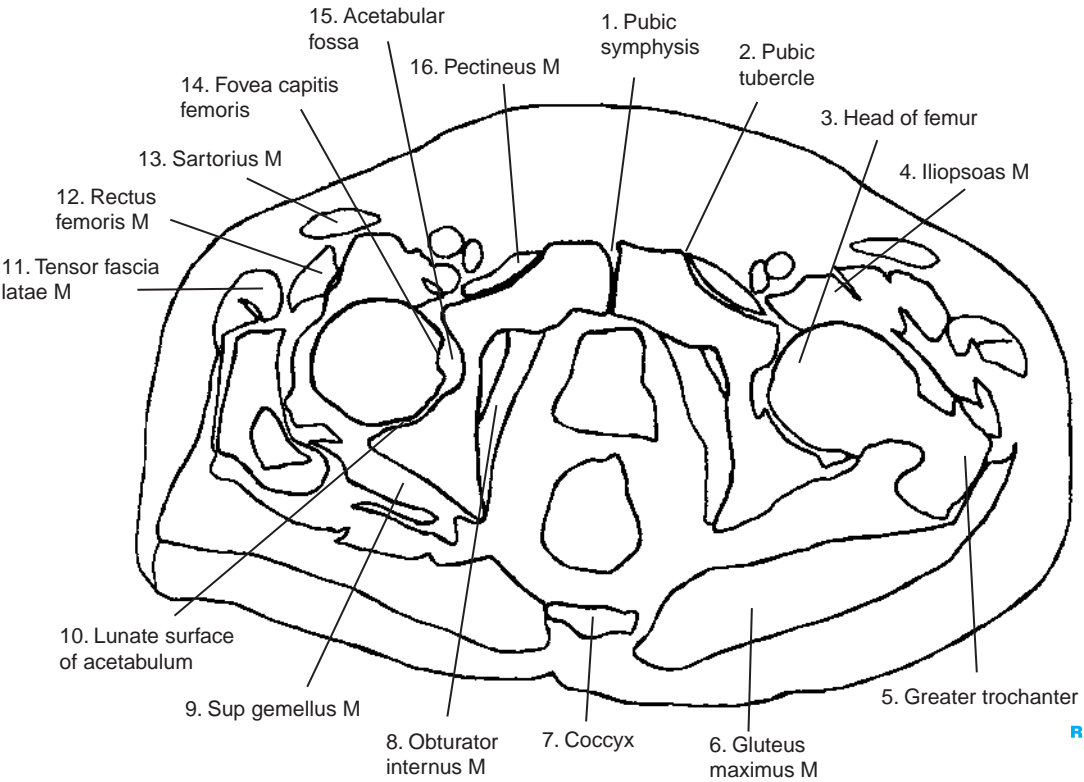


**Figure 8–19 (A,B)** Axial CT image 1.

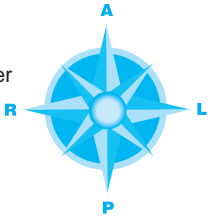
At this level, the coccyx is found posterior and separate from the other parts of the bony pelvis. Anteriorly, the pubic symphysis separates the two pubic bones, and the pubic tubercles are shown in profile. On either side, the heads of the femurs are found within the acetabula that are formed by the bones of the pelvic girdle: pubic, ischium, and ilium. Even though the greater trochanters are shown on both sides, the left side is more inferior than the right. Within the right hip joint, the articular surface of the acetabulum, or the lunate surface, is labeled beside the acetabular fossa. Although not clearly delineated, the ligamentum capitis femoris would extend within the acetabular fossa to the fovea capitis femoris. As described earlier, the ligamentum capitis femoris has little function other than protecting and transmitting the major arterial supply to the femoral head. Covering the anterior surface of the articular capsule, the iliopsoas muscles are sectioned as they extend down to insert on the lesser trochanters. Medial to the iliopsoas muscles, the pectineus muscles are sectioned near their origin on the pubic bones and would be seen in lower sections to insert on the proximal femur. Anterolateral to the hip joints, the sartorius, rectus femoris, and tensor fascia latae muscles are sectioned as they extend downward to insert on the leg. The sartorius is more superficial than the underlying rectus femoris, and the tensor fascia latae is the most lateral of the three. On the posterior surface of the hip joint, the gluteus maximus is a large flat muscle covered with a layer of superficial fat. Deep to the gluteus maximus, the superior gemellus is sectioned, extending from its origin on the ischial spine to insert on the tendon of the obturator internus. Although the obturator internus is labeled near its origin on the inner obturator membrane, the muscle travels below the superior gemellus to insert on the greater trochanter of the femur.



A



B



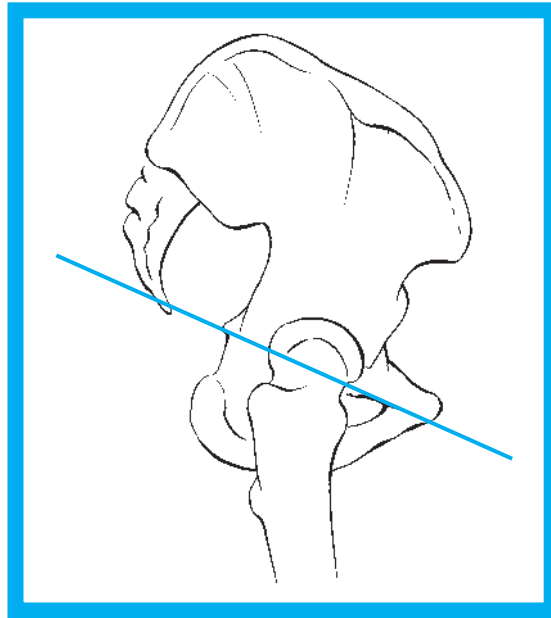
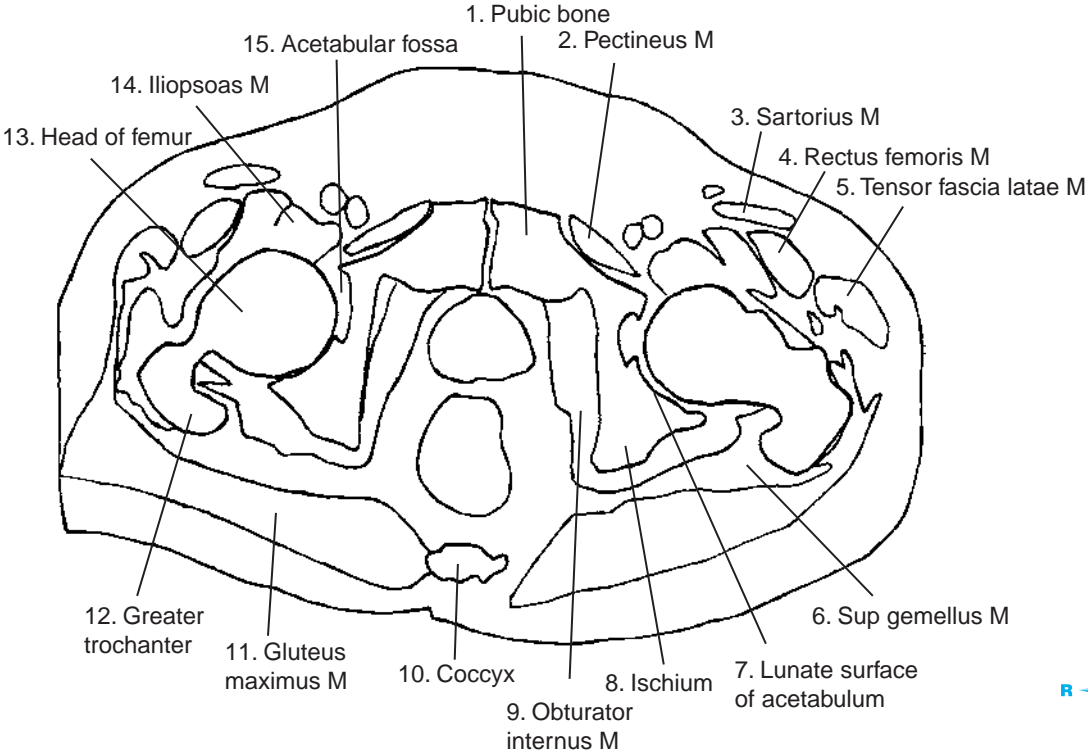


**Figure 8–20 (A,B)** Axial CT image 2.

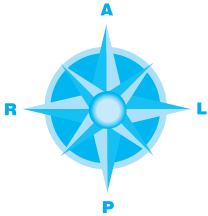
Similar to the previous image, the coccyx is shown forming the posterior boundary of the pelvis and appearing separate from the pelvic girdle. At this lower level, the ischial and pubic bones are nearing the opening of the obturator foramen, which separates the two bones on the anterolateral aspect of the pelvis. On either side, the acetabular fossae can be identified next to the lunate surfaces of the acetabula. The heads and greater trochanters of the femurs can be identified on either side, but their appearance is slightly different, indicating that the anatomy represented is slightly higher on the patient's right side. In this section, the muscles surrounding the hip joint are much the same as described in the previous section. The iliopsoas muscles are covering the anterior articular capsule, and the pectineus muscles are sectioned near their origin on the pubic bones. On the anterolateral hip, the sartorius, the rectus femoris, and tensor fascia latae are sectioned as they extend down to insert on the leg. On the posterior hip joint, the gluteus maximus is covering the superior gemellus and the obturator internus. Although the obturator internus muscle is labeled near its origin on the inner obturator membrane, the muscle extends behind the ischium and inserts on the greater trochanter of the femur. Originating from the ischial spine, the superior gemellus muscle is labeled near its insertion on the tendon of the obturator internus.



A



B



## Part E *Knee*

### ANATOMIC OVERVIEW

The knee is the largest joint in the body and is defined as the region between the thigh and the lower leg. Formed by the distal femur articulating with the tibia and the patella, the knee contains two separate joints. The joint between the femur and the tibia is considered a ginglymus, or hinge-type, joint; and the joint between the femur and the patella is arthrodiar, or gliding, joint. Although the fibula does not articulate with the distal femur, ligaments between the two bones are important in stabilizing the knee joint. Much like the shoulder, ligaments are important in limiting the movements of the joint but the majority of the joint strength is provided by the surrounding musculature.

#### ■ Skeleton

**Femur.** Its most distal part is formed by the medial and lateral condyles that are located on either side of the knee joint (Fig. 8-21). Because these rounded surfaces articulate with the tibia, they are covered with a layer of articular cartilage that helps create a smooth surface and protect the underlying bone.

**Tibia** (*TIB-e-ă*). Commonly called the shin bone. The second longest bone of the body. Within the lower leg, the larger and more medial bone. Its proximal end has medial and lateral condyles that articulate with those of the distal femur. Ligaments are located in the intercondyloid area (between the condylar processes). Although not shown, the central intercondyloid area has intercondylar eminences where ligaments attach to the tibia.

**Fibula** (*FIB-yu-lă*). In the lower leg, the more slender bone found on the lateral side. Proximally, its head articulates with the lateral condyle of the tibia, forming the proximal tibiofibular joints. Distally, it articulates with the talus, forming part of the ankle joint.

**Patella** (*pa-TEL-ă*). Commonly called the knee cap. The largest of the sesamoid (*SES-ă-moyd*) bones. Irregularly shaped bone located in front of the knee joint (Fig. 8-22). Its rough anterior surface provides attachment for the quadriceps femoris tendon. Medial and lateral articular facets on the posterior surface join with the femur to form the femoropatellar joint.

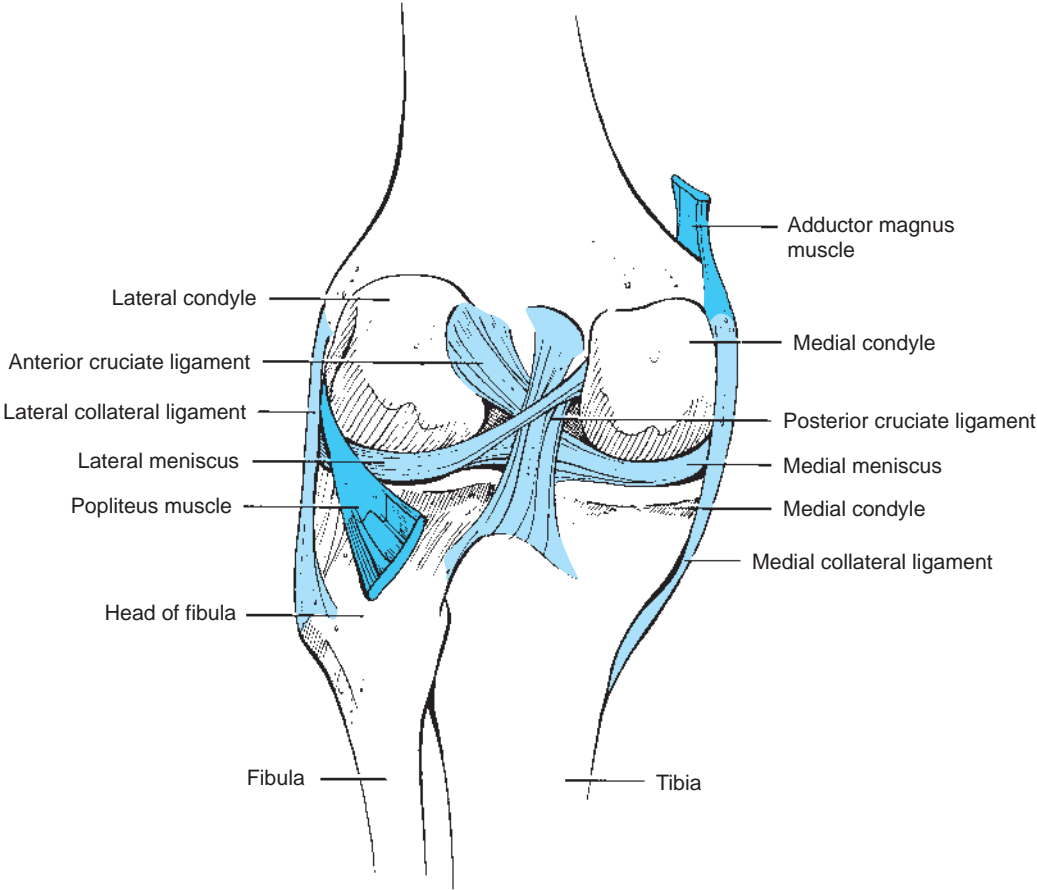


**Figure 8-21** Posterior view of the bones and ligaments of the left knee.



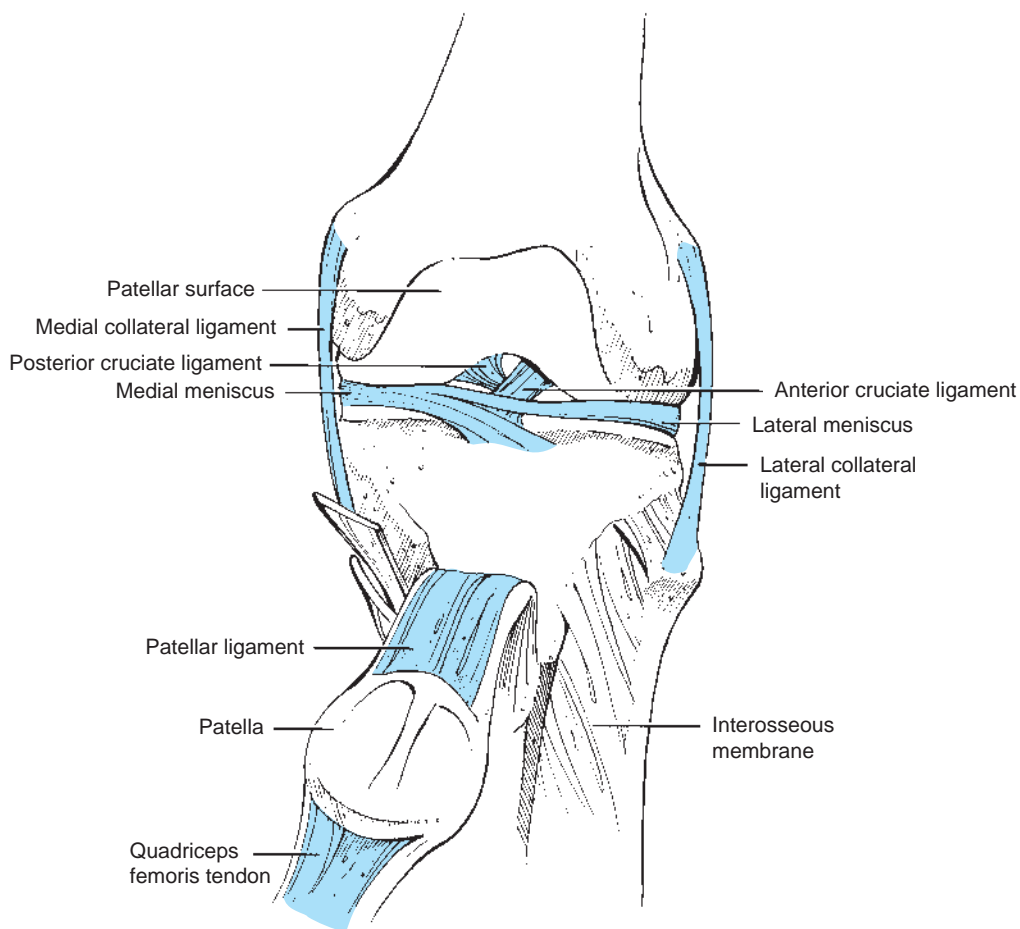


**Figure 8-22** Anterior view of the bones and ligaments of the left knee.

## ■ Ligaments

**Anterior cruciate** (*KRŪ-shē-āt*). Round ligament extending from the anterior intercondylar fossa to the back of the lateral femoral condyle (Figs. 8-21 to 8-23). Checks extension, lateral rotation, and anterior slipping of the tibia on the femur.

**Posterior cruciate**. Round ligament extending from the posterior intercondylar fossa to the front of the medial femoral condyle. Checks flexion, lateral rotation, and posterior slipping of tibia on the femur.

**Medial collateral**. Flat ligament extending from the medial femoral condyle to the medial condyle and body of the tibia. Prevents lateral bending and checks extension, hyperflexion, and lateral rotation.

**Lateral collateral**. Flat ligament extending from the lateral femoral condyle to the head and styloid process of the fibula. Checks hyperextension.

**Patellar**. Largest ligament of the knee. Extends between the patella and the tibial tuberosity, and is a continuation of the quadriceps femoris tendon below the level of the patella (Fig. 8-22). Acts to extend the lower leg.

**Medial meniscus** (*mĕ-NIS-kŭs*). Crescent-shaped ligament that attaches to the tibia in front of the anterior cruciate ligament and in the posterior intercondylar fossa (Fig. 8-23). Functions to deepen the medial tibial condyle.

**Lateral meniscus**. Nearly circular ligament that attaches to the tibia in front of the anterior cruciate ligament and behind the intercondylar eminence. Functions to deepen the lateral tibial condyle.

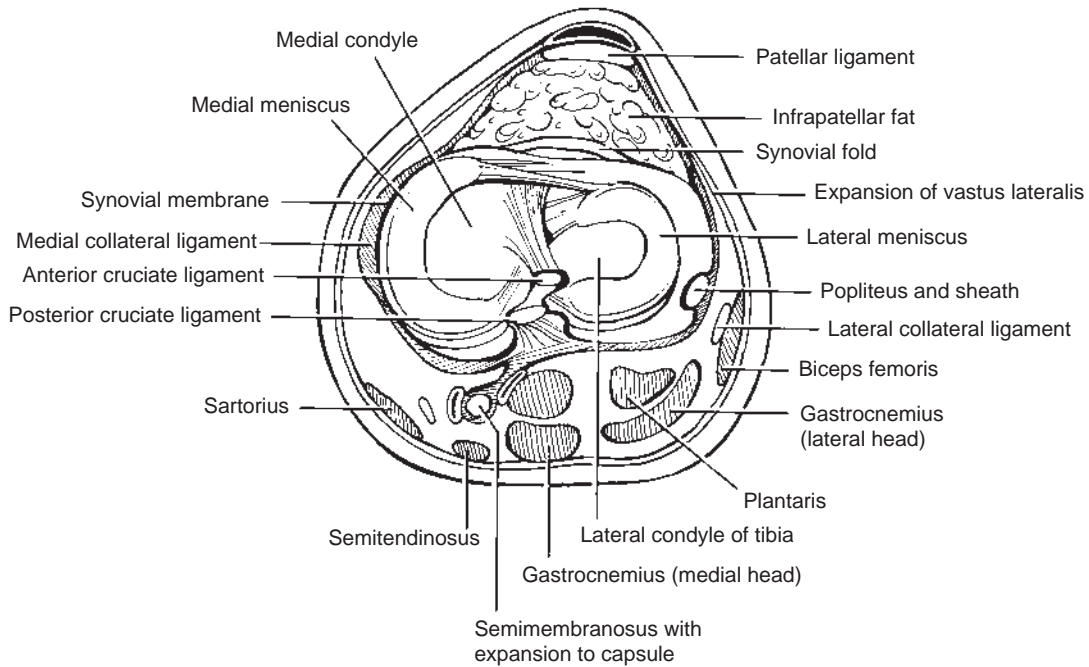


**Figure 8–23** Axial image of the lower knee joint.

## ■ Musculature and Other Structures

**Quadriceps (*KWAH-dri-seps*) femoris.** Origin: inferior iliac spine and rim of acetabulum. Insertion: base of patella. Action: flexes thigh and extends lower leg.

**Popliteus (*pop-li-TEÛs*).** Origin: lateral condyle of femur. Insertion: posterior tibia above soleal line. Action: flexes and rotates lower leg medially.

**Gastrocnemius (*gas-trok-NEÛ-mē-Ûs*).** Origin: medial and lateral femoral condyles. Insertion: through tendo calcaneus to posterior calcaneus. Action: flexes lower leg, plantar flexes and inverts foot.

**Infrapatellar fat pad.** A collection of fatty tissue posterior to the patella that protects the underlying femur and tibia.



## Sagittal Magnetic Resonance (MR) Images

The following three selected sagittal MR images of the left knee joint were generated at 8-mm intervals from medial to lateral at the following technical factors: repetition time

(TR) = 1,100 ms; echo time (TE) = 20 ms; radiofrequency (RF) = 90°; field of view (FOV) = 16 cm; slice thickness (TH) = 3.5 mm.

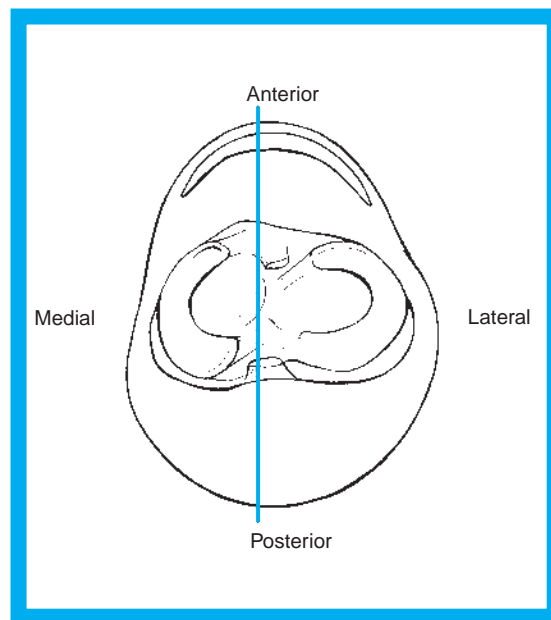
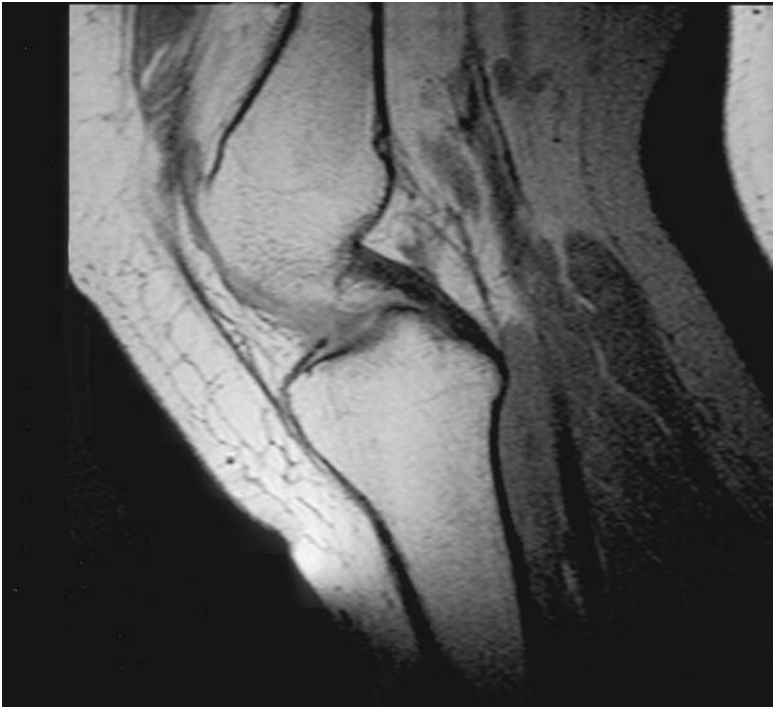
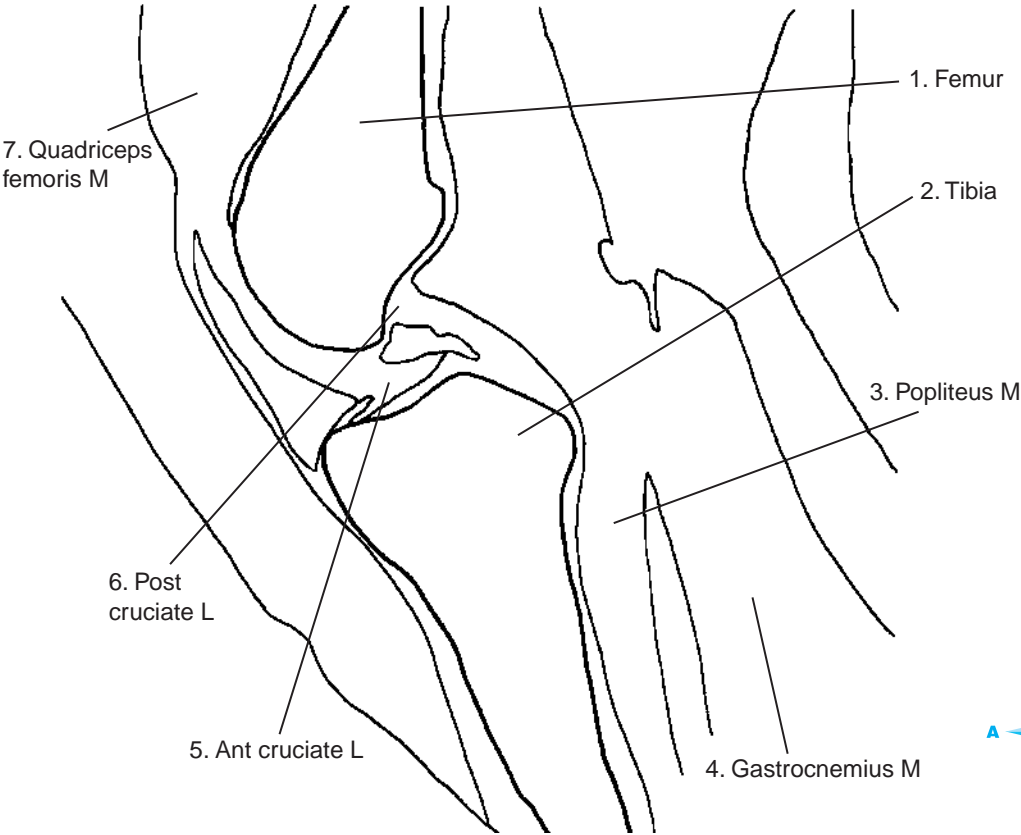


**Figure 8-24 (A,B)** Sagittal MR image 1.

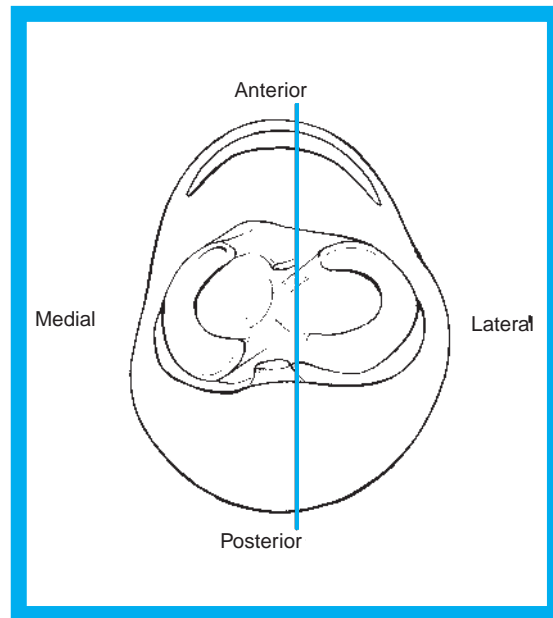
This sagittal image demonstrates a near midsagittal section of the femur and the tibia. Because the plane of this section lies near the midline, the anterior cruciate ligament appears as a low-signal area, extending from the anterior intercondylar fossa. As the anterior cruciate ligament ascends to attach to the back of the lateral femoral condyle, it crosses the posterior cruciate ligament. As described earlier, the posterior cruciate ligament originates from the posterior intercondylar fossa and ascends to insert on the medial femoral condyle. The relationship between these two ligaments is described by the term cruciate, which means shaped like a cross. Outside the knee joint, the popliteus and gastrocnemius muscles are found posterior to the tibia, and the quadriceps femoris muscle is found on the anterior surface of the femur.



A

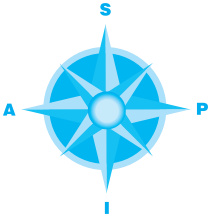
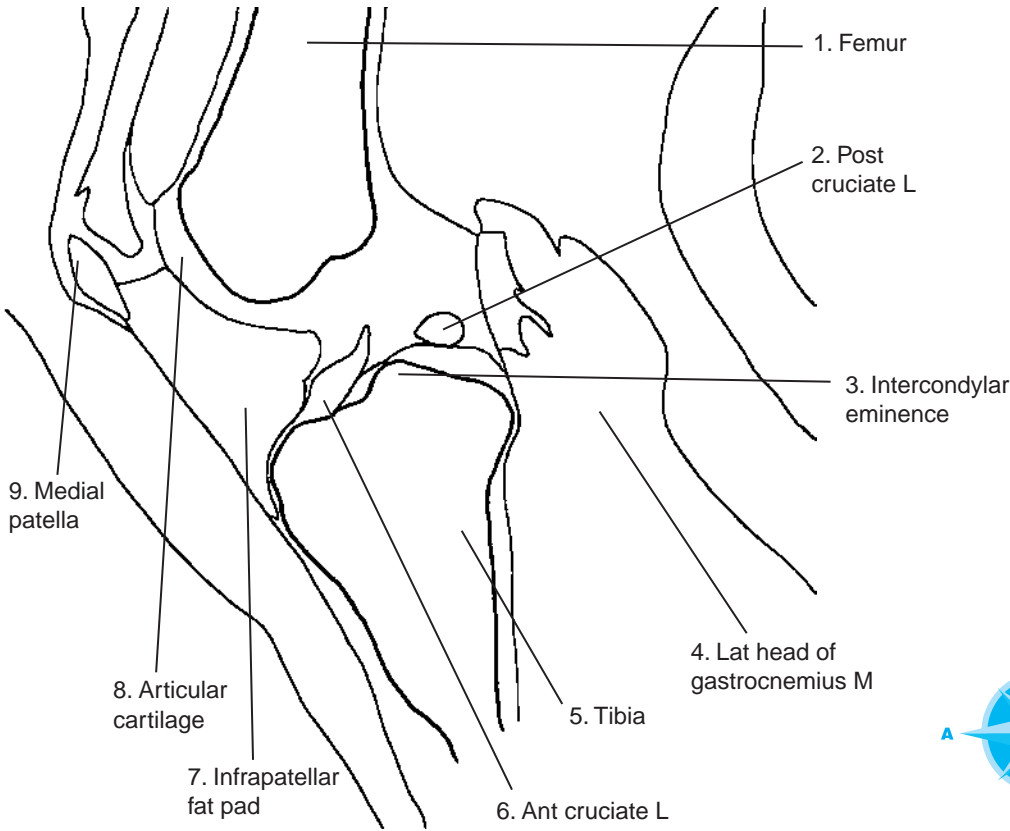
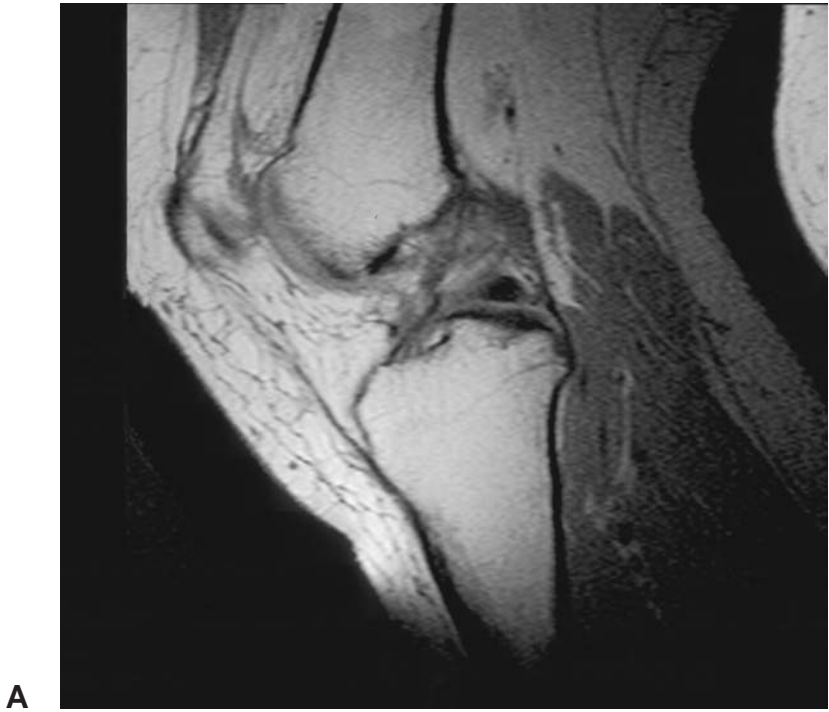


B



**Figure 8–25 (A,B)** Sagittal MR image 2.

Although the femur appears much like it did in the previous image, its lower anterior part is covered with articular cartilage, indicating the beginning of the lateral femoral condyle. Anterior to the distal femur, a small section of the medial patella is demonstrated just below the space previously occupied by the quadriceps femoris muscle. The tibia looks smaller than it did in the previous figure. On the superior surface of the tibia, an intercondylar eminence is labeled between the anterior and posterior cruciate ligaments. In this image, only the distal parts of the anterior and posterior cruciate ligaments are demonstrated near their attachments within the intercondylar fossae. Between the knee joint and the medial patella, an area of high signal intensity represents the area of the infrapatellar fat pad, which protects the underlying bones and joint from blows to the patella. On the posterior surface of the joint, the lateral head of the gastrocnemius muscle is found extending from its origin on the lateral femoral condyle to insert on the posterior calcaneus.



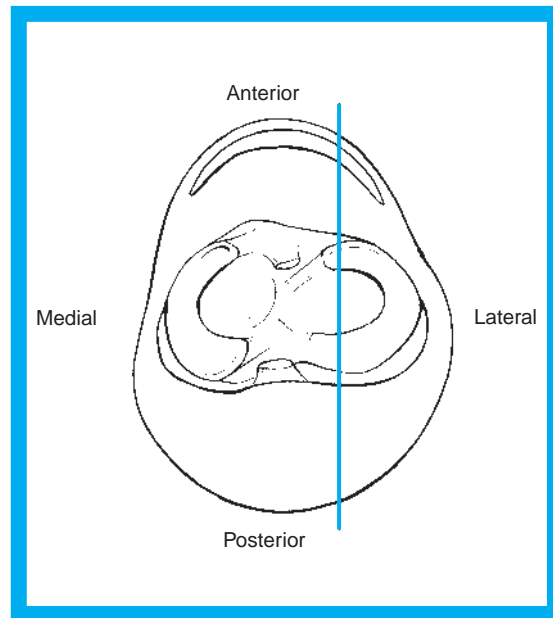
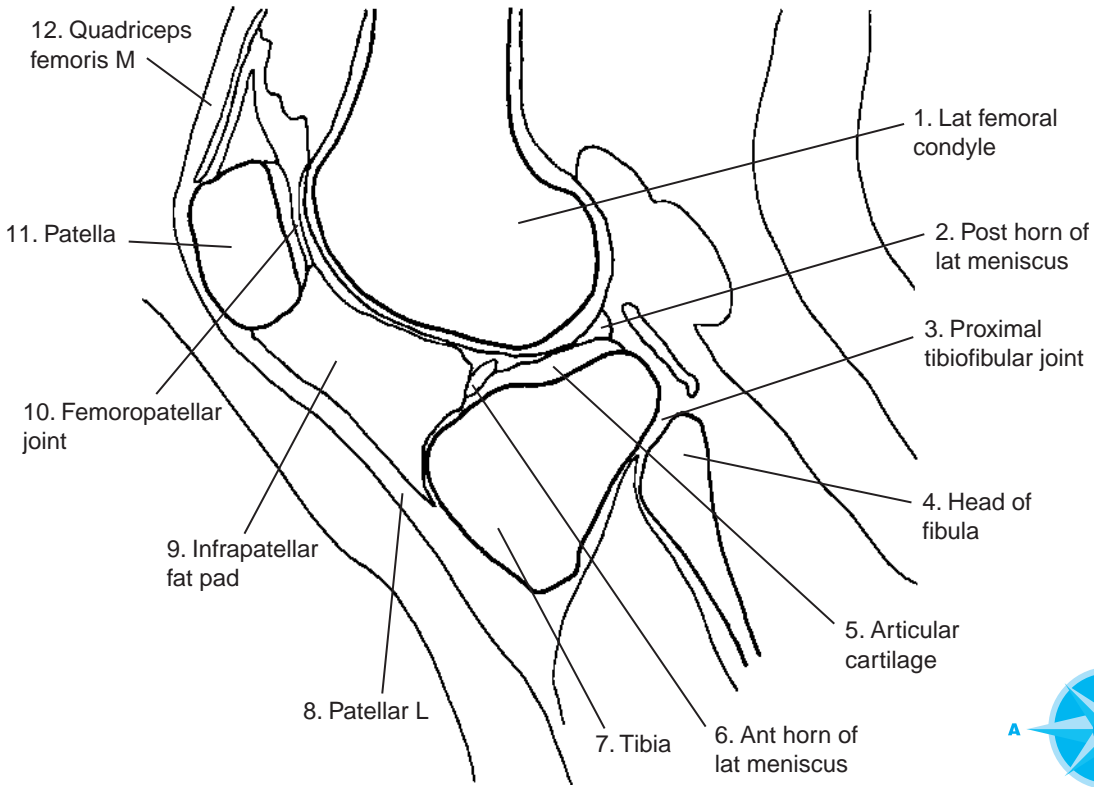


**Figure 8–26 (A,B)** Sagittal MR image 3.

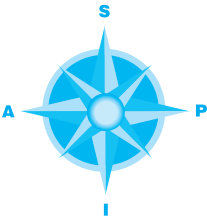
This image demonstrates the lateral femoral condyle, in full view directly behind the patella, creating the femoropatellar joint. As described earlier, the patella is embedded in the back of the quadriceps femoris tendon and is attached to the tibia via the patellar ligament. Compared to previous views, only a small part of the lateral tibia is demonstrated in this image. The proximal tibia articulates with the head of the fibula, forming the proximal tibiofibular joint. Within the knee joint, articular cartilage is shown along the periphery of the femoral condyle and the superior surface of the tibia, which are shown adjacent to one another. The anterior and posterior horns of the lateral meniscus, deepening the knee joint, are demonstrated in cross-section in regions of low signal intensity adjacent to the site of articulation between the femur and the tibia.



A



B



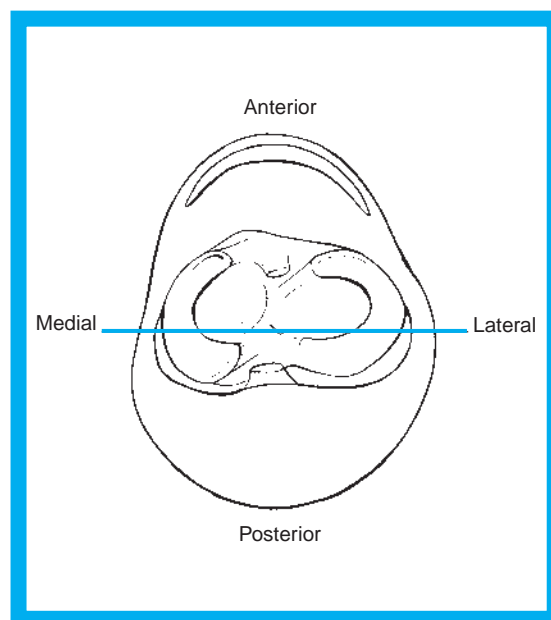




## Coronal Magnetic Resonance (MR) Images

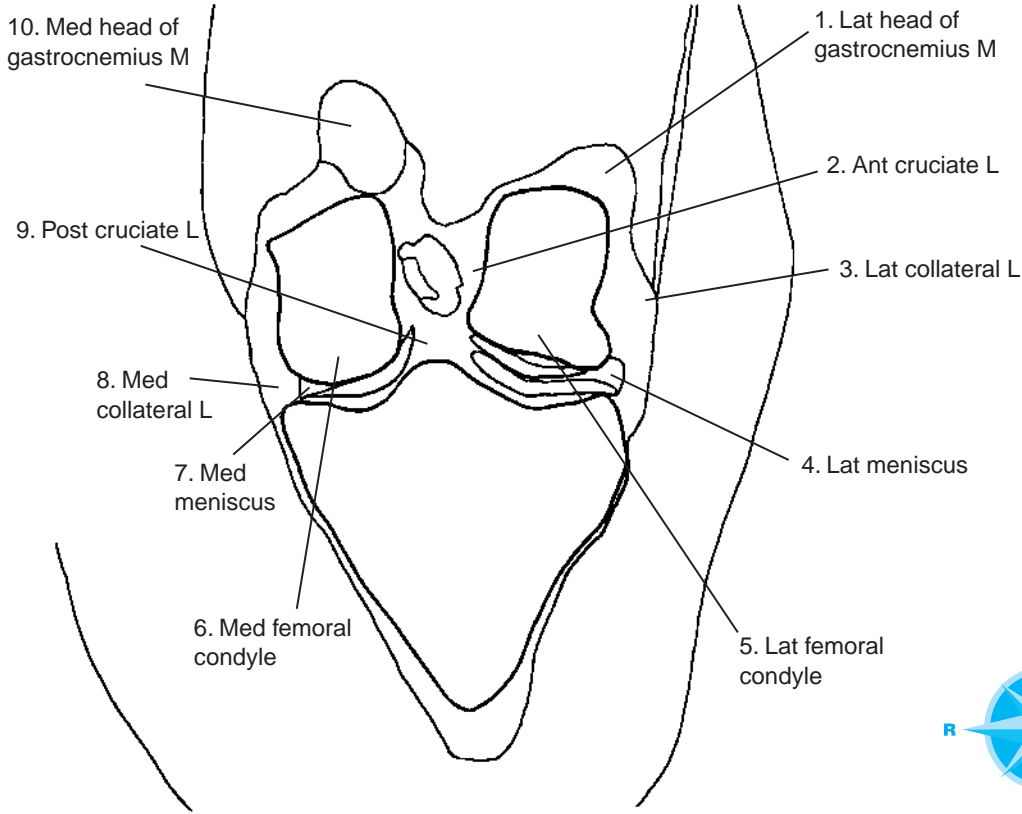
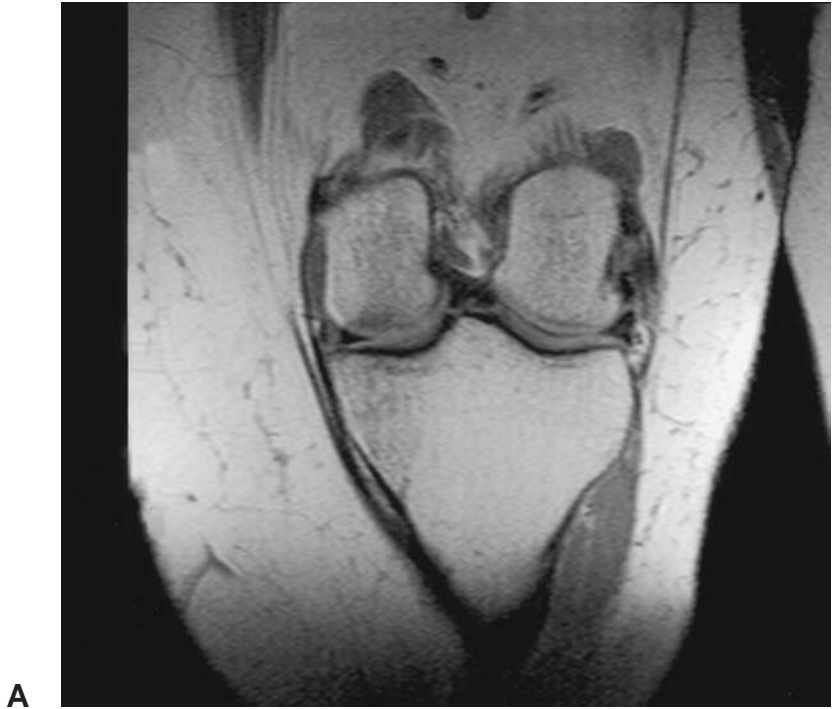
The following four selected coronal MR images of the left knee joint were generated at 4-mm intervals from posterior to anterior. The images were taken at the following techni-

cal factors: repetition time (TR) = 1,100 ms; echo time (TE) = 20 ms; radiofrequency (RF) = 90°; field of view (FOV) = 16 cm; slice thickness (TH) = 3.5 mm.



**Figure 8–27 (A,B)** Coronal MR image 1.

This image demonstrates the anatomy within the posterior knee joint, including the medial and lateral femoral condyles and the proximal tibia. Between the femoral condyles and the proximal tibia, the medial and lateral menisci are in their respective locations within the posterior knee joint. Forming the medial boundary of the knee joint, the medial collateral ligament is extending from the medial femoral condyle to the proximal tibia. On the lateral side of the knee joint, the lateral collateral ligament is shown near its attachment on the lateral condyle of the femur; in more posterior sections it would be seen to extend downward to attach to the head and styloid process of the fibula. Between the medial and lateral femoral condyles, the cruciate ligaments appear obliquely sectioned as regions of low signal intensity. The posterior cruciate ligament is shown near its distal end, or attachment in the posterior intercondylar fossa. In contrast, the proximal end of the anterior cruciate ligament is shown near the back of the lateral femoral condyle. Above the femoral condyles, the medial and lateral heads of the gastrocnemius muscles are shown originating on the distal femur.



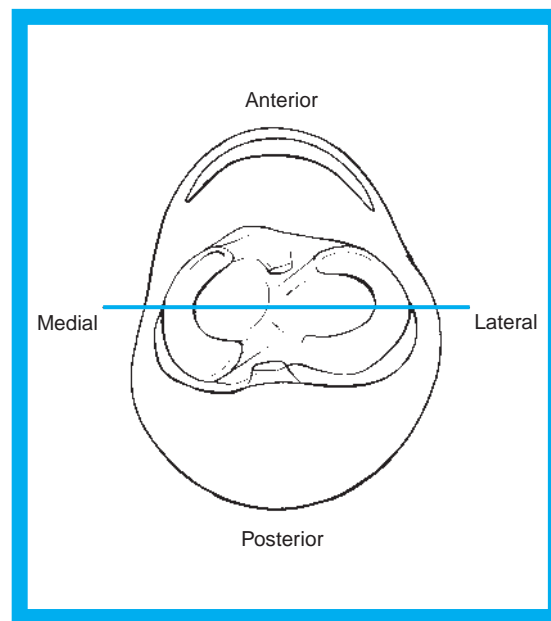
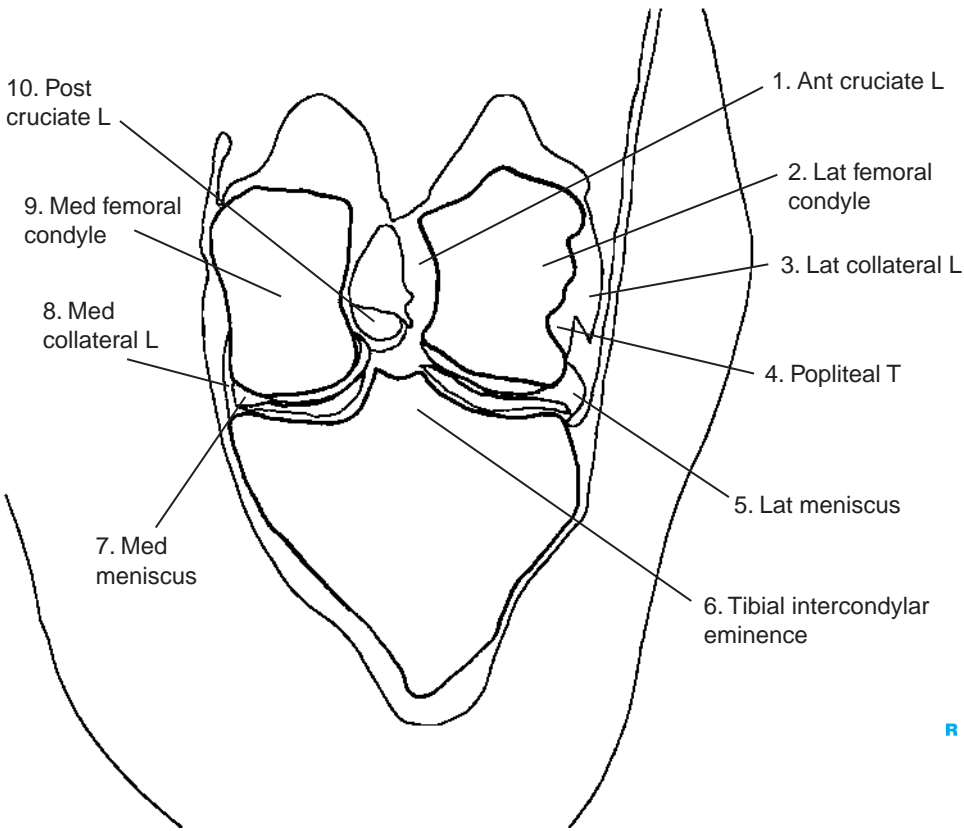


**Figure 8–28 (A,B)** Coronal MR image 2.

Compared to the previous figure, the medial and lateral femoral condyles are larger, indicating that we are nearing the body of the femur. Lower in the image, the proximal tibia is sectioned and clearly demonstrates the intercondylar eminence projecting upward between the femoral condyles. The medial and lateral menisci are cross-sectioned and appear as regions of low signal intensity below the femoral condyles. Extending between the medial femoral condyle and the tibia, the medial collateral ligament is shown forming the medial boundary of the knee joint. Laterally, the lateral collateral ligament is shown above the knee joint near its proximal attachment on the lateral femoral condyle. Because the lateral collateral ligament extends downward to attach to the head and styloid process of the fibula, in more posterior sections it would be shown closer to the knee joint. Found medial to the lateral collateral ligament, the popliteal tendon is originating from the lateral condyle of the femur. Between the medial and the lateral femoral condyles, the anterior and posterior cruciate ligaments appear as irregularly shaped regions of low signal intensity. The anterior cruciate ligament is sectioned near its proximal attachment on the lateral femoral condyle, and the posterior cruciate ligament is moving away from its distal attachment on the posterior intercondylar fossa.



A



B

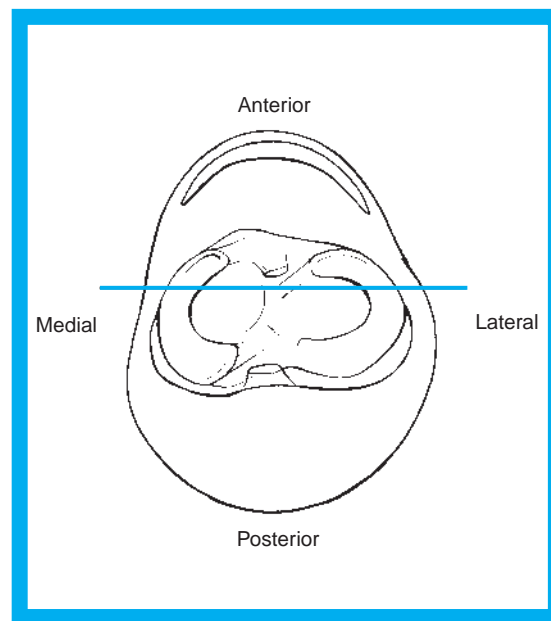
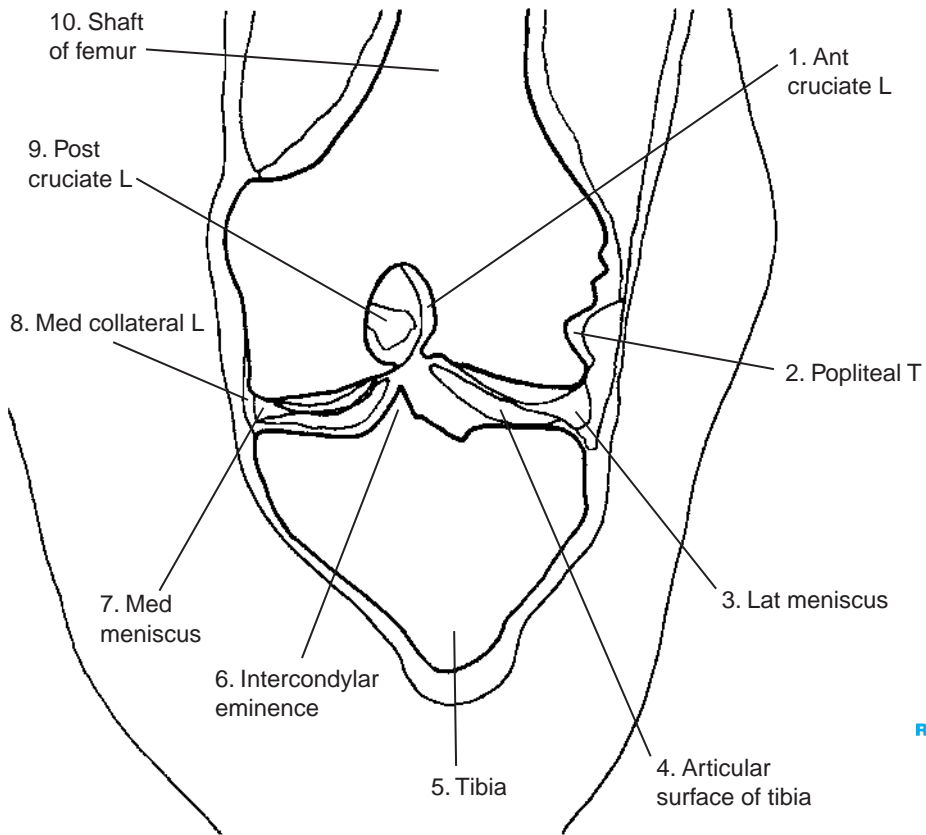


**Figure 8–29 (A,B)** Coronal MR image 3.

In this image, the femoral condyles have joined with the body of the femur, and the shaft is shown extending upward. On the lower part of the image, the posterior tibia is again sectioned, demonstrating an intercondylar eminence that appears as a sharp projection upward between the medial and lateral condyles of the femur. Superior to the intercondylar eminence, the posterior cruciate ligament is sectioned medial to the anterior cruciate ligament as it extends upward to attach to the medial femoral condyle. On either side of the intercondylar eminence, the articular surfaces of the femur and the tibia are shown adjacent to each other except in regions of low signal intensity representing either the medial or lateral menisci. Forming the medial boundary of the knee joint, the medial collateral ligament is again longitudinally sectioned as it extends between the medial femoral condyle to the tibia. On the lateral surface of the knee joint, the popliteal tendon can be identified near its point of origin on the lateral femoral condyle. In this image, however, the lateral collateral ligament is indistinguishable because it separates from the articular capsule as it extends downward to attach to the head and styloid process of the fibula.



A



B

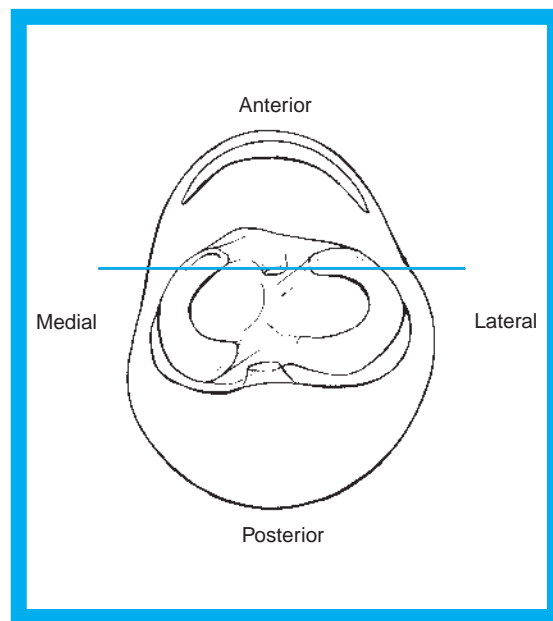
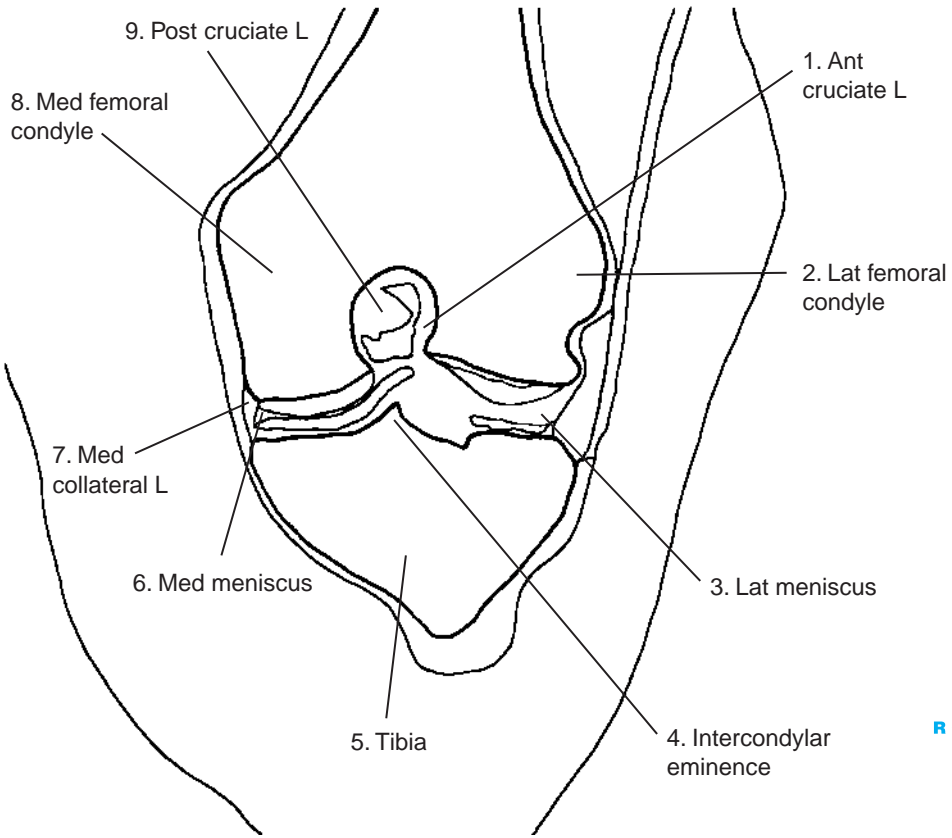


**Figure 8–30 (A,B)** Coronal MR image 4.

The medial and lateral femoral condyles are shown articulating with the proximal end of the tibia. Similar to previous images, the superior surface of the tibia is irregularly shaped owing to the intercondylar eminence projecting upward between the medial and lateral femoral condyles. Above the intercondylar eminence, the proximal end of the posterior cruciate ligament is shown near its site of attachment on the medial femoral condyle. By comparison, the distal end of the anterior cruciate ligament is shown near its origin, the anterior intercondylar fossa. On the medial side of the knee joint, a triangular region of low signal intensity represents the medial meniscus that lies adjacent to the medial collateral ligament. On the lateral side of the joint, the articular surfaces are separated by a thick lateral meniscus, indicating that this plane of section traverses through the anterior part of the circular ligament.





## Part F Ankle

### ANATOMIC OVERVIEW

The ankle describes the region of articulation between the lower leg and the foot. Within this region, the ankle joint is formed by the distal tibia and fibula articulating with the talus. The ankle joint is considered a ginglymus, or hinge-type, joint that allows dorsiflexion and plantar flexion. The other movements of the foot are the result of articulations between the tarsal bones—calcaneus, talus, cuboid, navicular, and cuneiforms—which are considered arthrodial joints, because they are capable of gliding movements and have limited rotation.

#### ■ Skeleton

Hint: The mnemonic for remembering the order of the tarsals is “Come to Colorado Next 3 Christmases.”

**Calcaneus** (*kal-KA-ne-ŭs*). Commonly called the heel bone; also called the os calcis. The upper part of this roughly quadrangular bone articulates with the talus and the cuboid bones (Fig. 8-31). Carries approximately 25% of the body’s weight in the standing position.

*Sustentaculum tali* (*SŪS-ten-TAK-yŭ-lŭm TĀ-lī*). The process on the upper medial calcaneus that acts as a shelf to support the head of the talus. On the lower surface, the process acts much like a pulley for the tendon of the flexor

hallucis longus muscle as it passes through the medial side of the ankle.

**Talus** (*TĀ-lŭ*). Also called the astragalus (*as-TRAG-ă-lŭs*). The most proximal tarsal bone. Articulates with the tibia and fibula to form the ankle joint. On the distal end, it transmits approximately 50% of the body’s weight to the calcaneus and navicular bones.

**Cuboid** (*KYŪ-boyd*). Resembles a cube and is found on the lateral side of the foot between the calcaneus and the bases of the fourth and fifth metatarsals.

**Navicular** (*nă-VIK-yŭ-lăr*). Also called the scaphoid (*SKAF-oyd*). Boat-shaped bone found between the talus and the three cuneiform bones on the medial side of the foot.

**Cuneiforms** (*KYŪ-nē-i-fōrmz*). Three tarsal bones located between the navicular and the bases of the first three metatarsals (Latin for “wedge shaped”). They are either numbered one to three from medial to lateral or are referred to as medial, intermediate, and lateral.

**Metatarsals** (*MET-ă-TAR-sălz*). The five bones are numbered one to five from medial to lateral. On the proximal ends, their bases form arthrodial (gliding) joints with the cuboid and cuneiform bones. On the distal ends, their heads form ellipsoidal or condyloid joints with the proximal phalanges. In the standing position, the heads of the metatarsals of each foot bear 25% of the body’s weight (10% on the first metatarsal and 3.75% each on the other metatarsals).

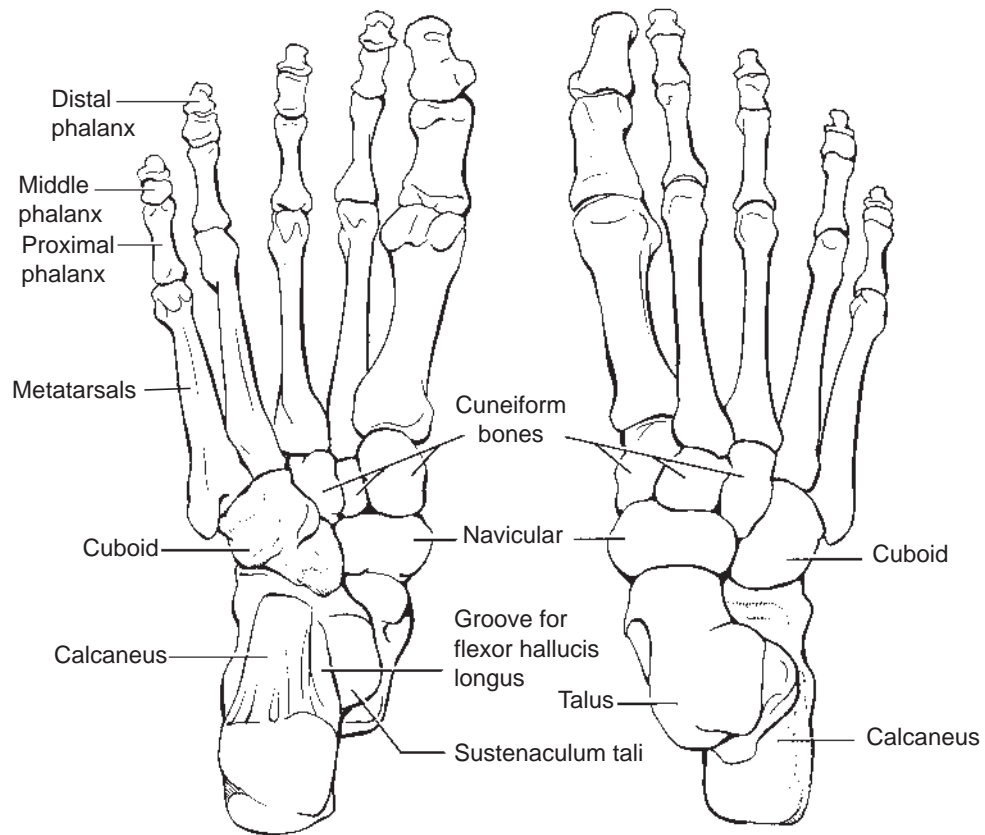


**Figure 8–31** **Left:** Plantar view of the bones of the ankle and foot. **Right:** Dorsal view of the bones of the ankle and foot.

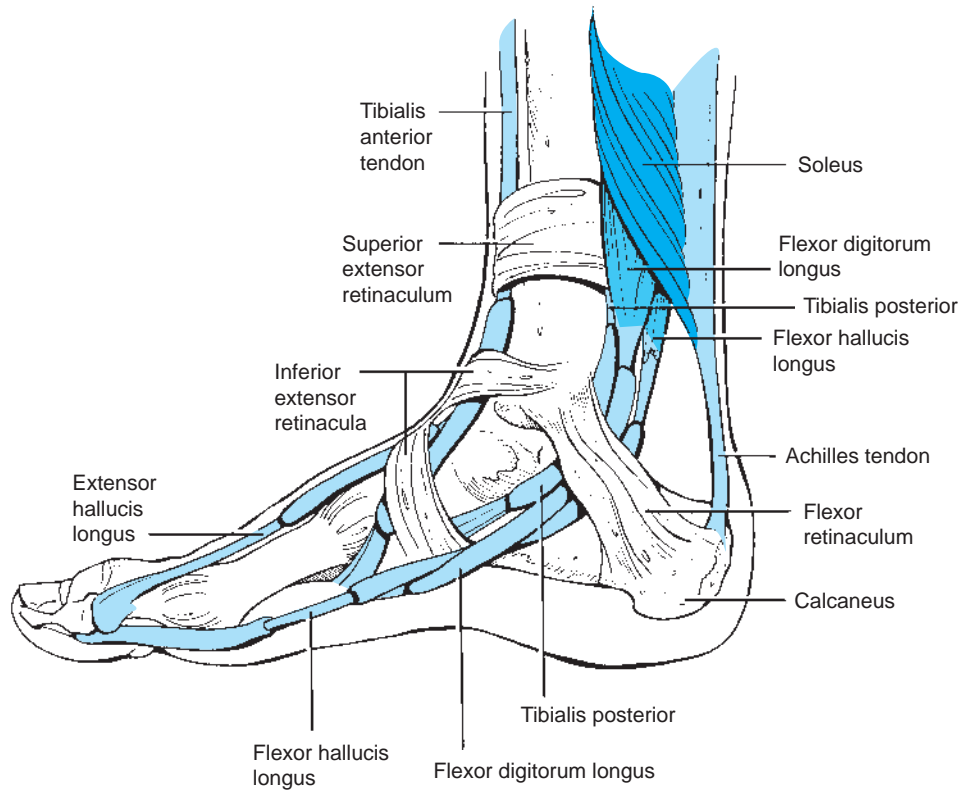


**Figure 8–32** Medial view of the muscles and tendons of the ankle and foot.

## ■ Musculature

**Tibialis (*tib-ē-Ā-lis*) anterior.** Origin: lateral tibial condyle and lateral tibia. Insertion: first cuneiform and base of first metatarsal. Action: dorsiflexes and inverts foot (Figs. 8-32 and 8-33).

**Extensor hallucis (*HAL-lū-sis*) longus.** Origin: middle anterior fibula. Insertion: distal phalanx of first digit. Action: extends first digit and everts foot.

**Tibialis posterior.** Origin: posterior shaft of tibia and upper shaft of fibula. Insertion: navicular, cuneiforms one, two, and three, cuboid, bases of second to fourth metatarsals. Action: adducts, plantar flexes, and inverts foot.

**Flexor digitorum longus.** Origin: posterior tibia below soleal line. Insertion: distal phalanges of digits two to five. Action: plantar flexes and inverts foot.

**Flexor hallucis longus.** Origin: lower two thirds of posterior fibula. Insertion: distal phalanx of first digit. Action: flexes distal phalanx and inverts foot.

**Extensor digitorum longus.** Origin: lateral tibial condyle and anterior crest of fibula. Insertion: distal phalanges of digits two to five. Action: extends toes, dorsiflexes and everts foot.

**Peroneus (*per-ō-NĒ-ŭs*) longus and brevis.** Origin: head and shaft of fibula and lateral tibial condyle. Insertion: first cuneiform and fifth metatarsal. Action: plantar flexes and everts foot.

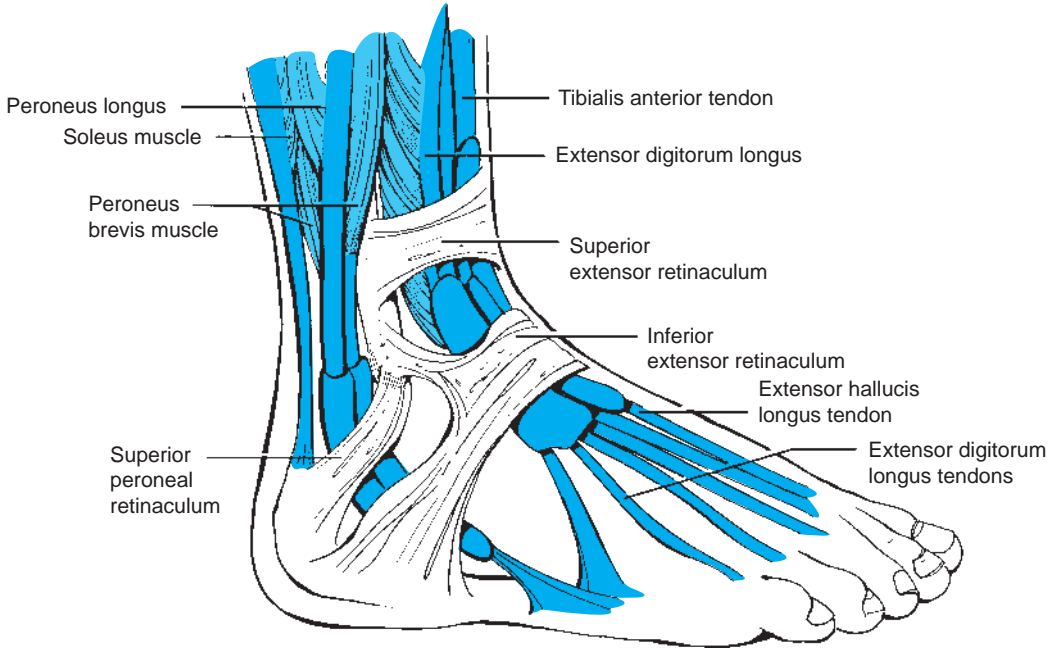


**Figure 8-33** Lateral view of the muscles and tendons of the ankle and foot.



## Sagittal Magnetic Resonance (MR) Images

The following are two selected sagittal MR images of the right ankle generated from medial to lateral at 100-mm intervals at the following technical factors: repetition time

(TR) = 1,100 ms; echo time (TE) = 20 ms; radiofrequency (RF) = 90°; field of view (FOV) = 16 cm; slice thickness (TH) = 3.5 mm.

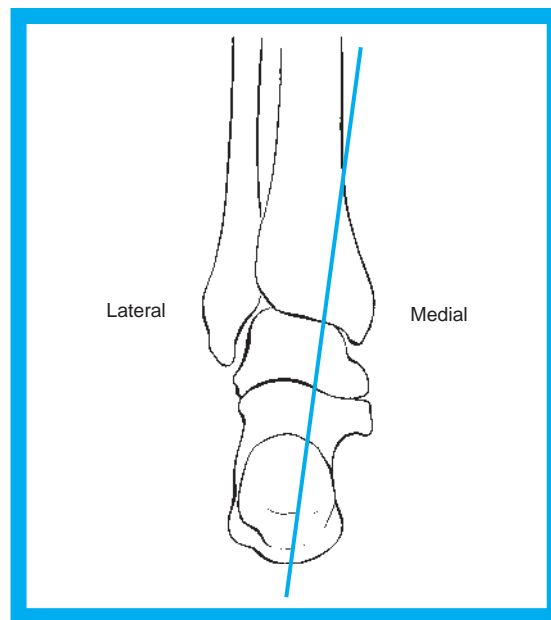
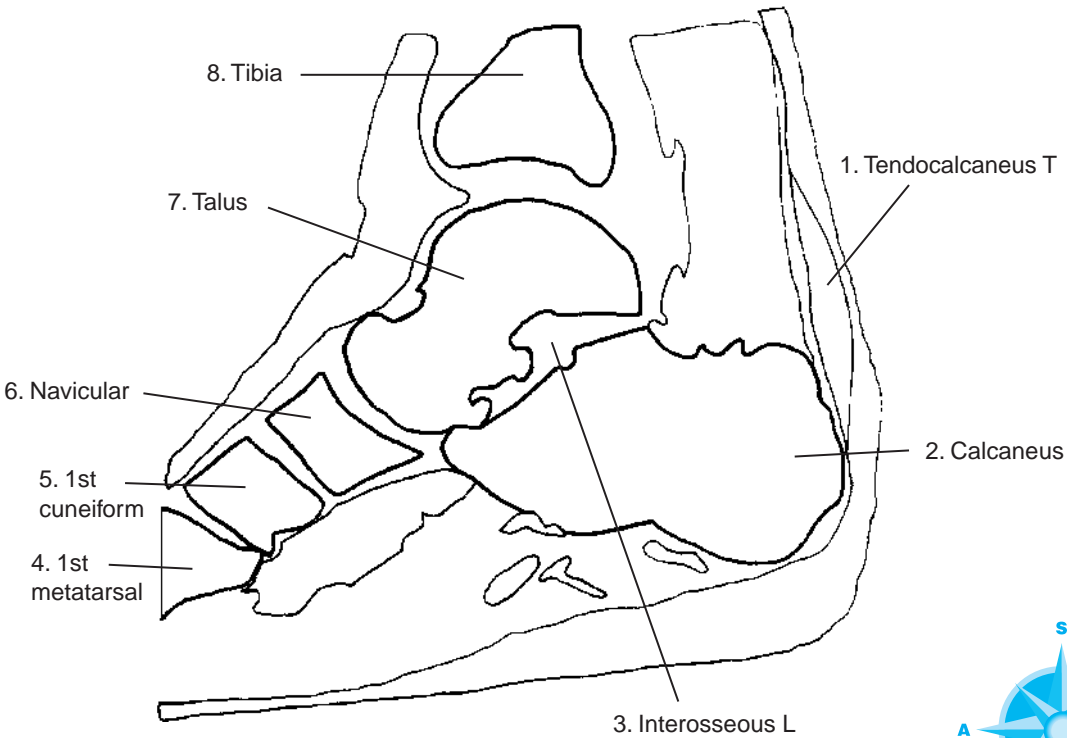


**Figure 8–34 (A,B)** Sagittal MR image 1.

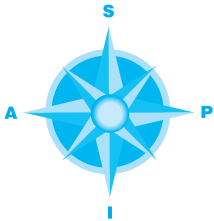
This image demonstrates the medial side of the right ankle. With the exception of the distal tibia, all of the bones identified within this image are part of the medial arch of the foot. On the upper part of the image, the distal tibia is shown articulating with the talus, forming the ankle joint. Below the talus, interosseous ligaments extend through the subtalar joint between the talus and the calcaneus. Anterior to the talus, the boat-shaped navicular bone is cross-sectioned above the first cuneiform and the first metatarsal. On the plantar surface of the foot, it is difficult to discern the individual muscles and tendons, but on the posterior lower leg, an oblique section of the tendo calcaneus tendon is shown near its insertion on the posterior calcaneus. As described earlier for the knee, the medial and lateral heads of the gastrocnemius muscle insert through the tendo calcaneus tendon onto the posterior calcaneus and act to flex the lower leg, plantar flex, and invert the foot.



A



B



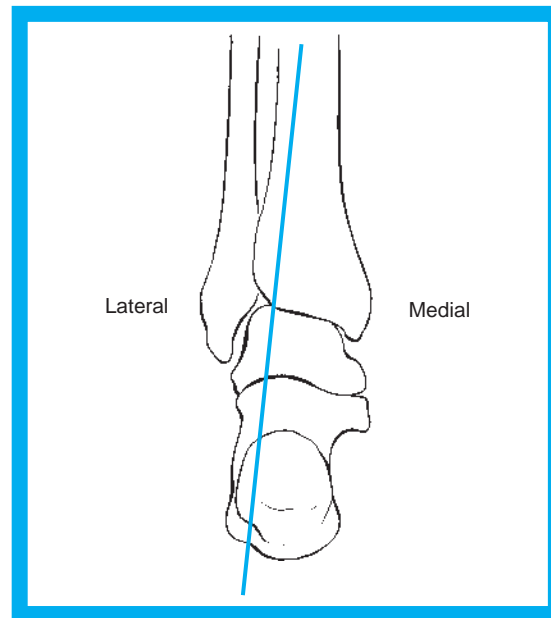
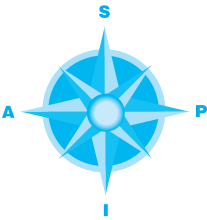
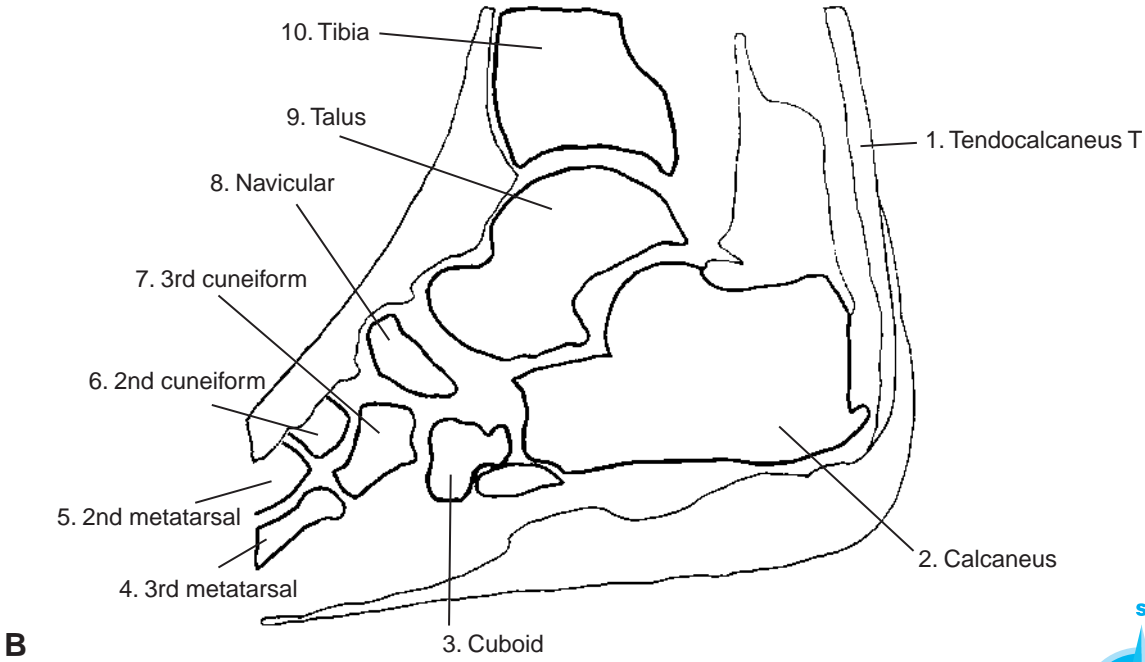
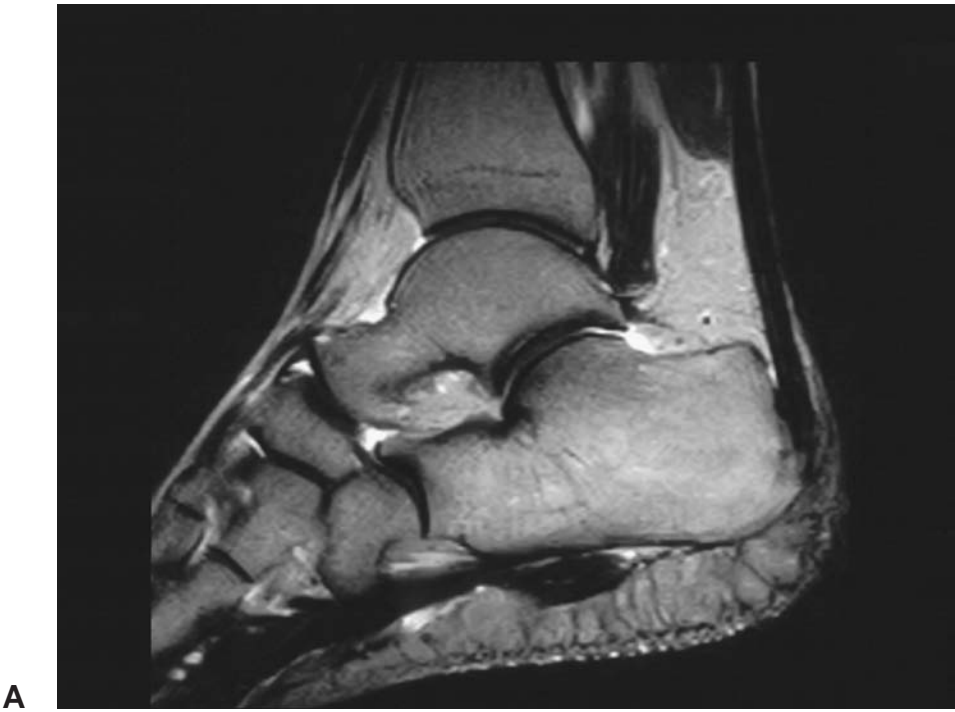


**Figure 8–35 (A,B)** Sagittal MR image 2.

In contrast to the previous image, this section demonstrates much of the anatomy found within the lateral ankle. Similar to the previous image, the articulation between the distal tibia and talus form the ankle joint. Below the talus, the subtalar joint is formed between the calcaneus and the underside of the talus. Anteriorly, the talus articulates with the lateral part of the navicular and the calcaneus articulates with the cuboid, forming the calcaneocuboid joint. Because the cuneiforms are found anterior to the navicular bone, the second and third cuneiform can be identified within this image above the second and third metatarsals, respectively. As described earlier, the distal cuboid articulates with the bases of the fourth and fifth metatarsals, which are not in this section. Similar to the previous image, the tendo calcaneus tendon is found inserting on the posterior calcaneus, even though many ligaments and muscles on the plantar surface of the foot are difficult to discern.



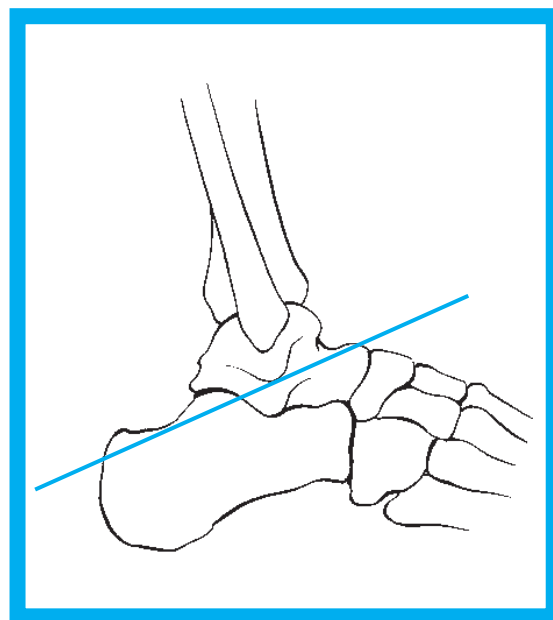




## Axial Magnetic Resonance (MR) Images

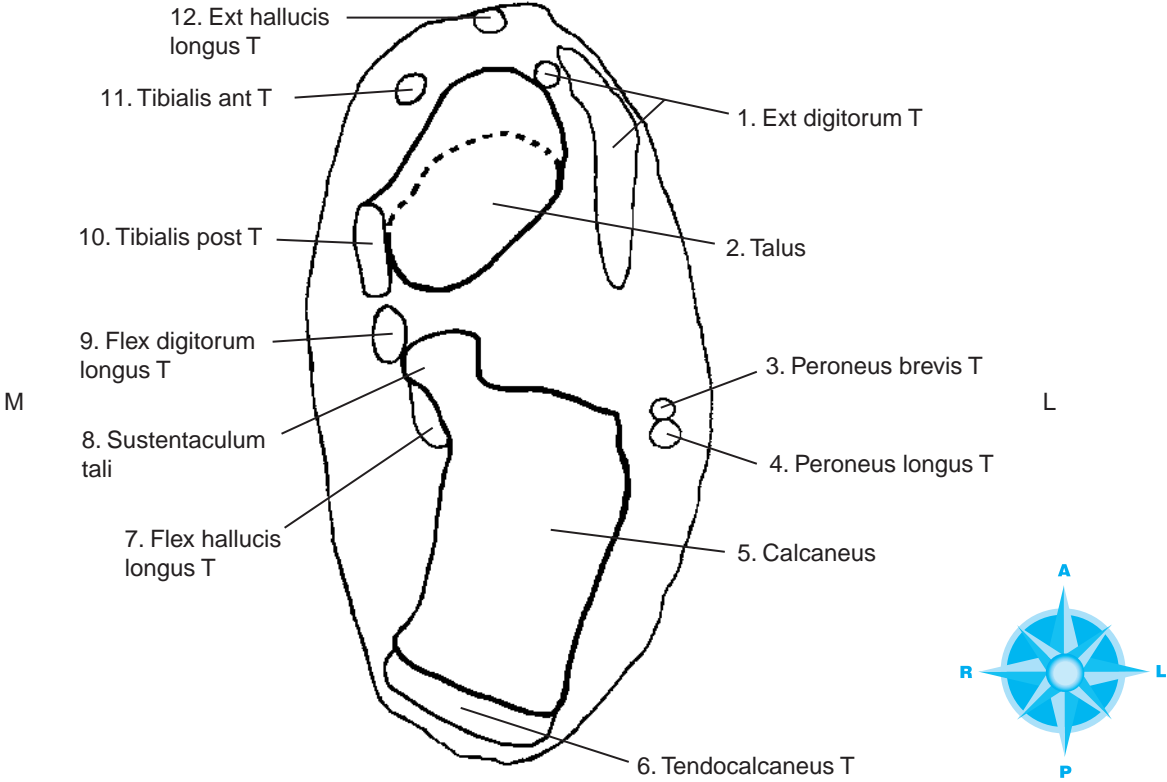
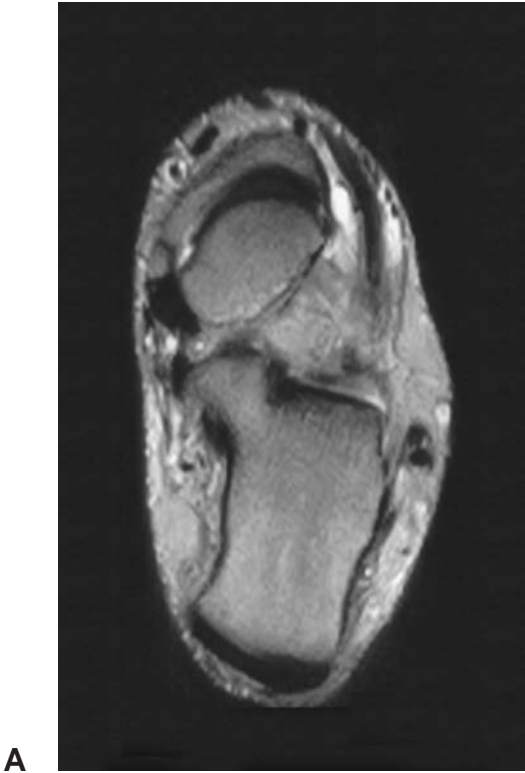
The following are three selected axial MR images of the right ankle from superior to inferior generated at the following technical factors: Repetition time (TR) = 1,100

ms; echo time (TE) = 20 ms; radiofrequency (RF) = 90°; field of view (FOV) = 16 cm; slice thickness (TH) = 3.5 mm.



**Figure 8–36 (A,B)** Axial MR image 1.

This image demonstrates the anatomy just below the ankle joint, because the two parts of the talus can be identified. The upper part of the talus, posterior to the hatched line, represents the surface that articulates with the distal tibia and fibula, forming the ankle joint. The distal part of the talus, anterior to the hatched line, articulates with the underlying tarsals. Posteriorly, the upper calcaneus appears irregularly shaped, because the sustentaculum tali is projecting medially. Appearing as low signal areas, a variety of tendons can be found surrounding these bones. Similar to the sagittal sections, the broad, flat region of low signal intensity posterior to the calcaneus represents the tendo calcaneus tendon. Medial to the sustentaculum tali, the tendon of the flexor hallucis longus muscle is shown as it extends through the medial side of the ankle from its origin on the posterior fibula to insert on the distal phalanx of the first digit. Near the anterior margin of the sustentaculum tali, the flexor digitorum longus tendon is shown as it passes along the medial side of the ankle extending from its origin on the posterior tibia to insert on the distal phalanges of the second to fifth digits. Lying near the posteromedial border of the talus, the tibialis posterior tendon is obliquely sectioned extending through the medial ankle from the muscle, which originates on the tibia and fibula, to insert on the tarsals anterior to the talus and the bases of the second to fourth metatarsals. On the anterior part of the ankle, the tibialis anterior, the extensor hallucis longus, and the extensor digitorum tendons are also sectioned as they extend downward from muscles in the lower leg to insert on the foot. On the lateral side of the ankle, the peroneus brevis and longus tendons are cross-sectioned near the anterior calcaneus.



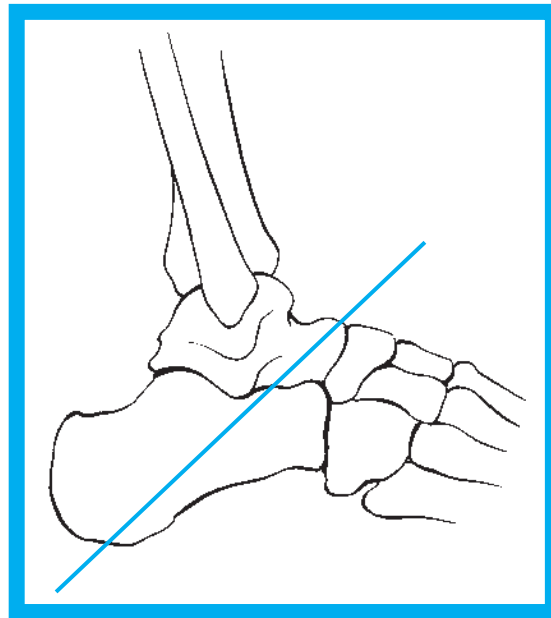
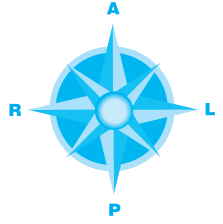
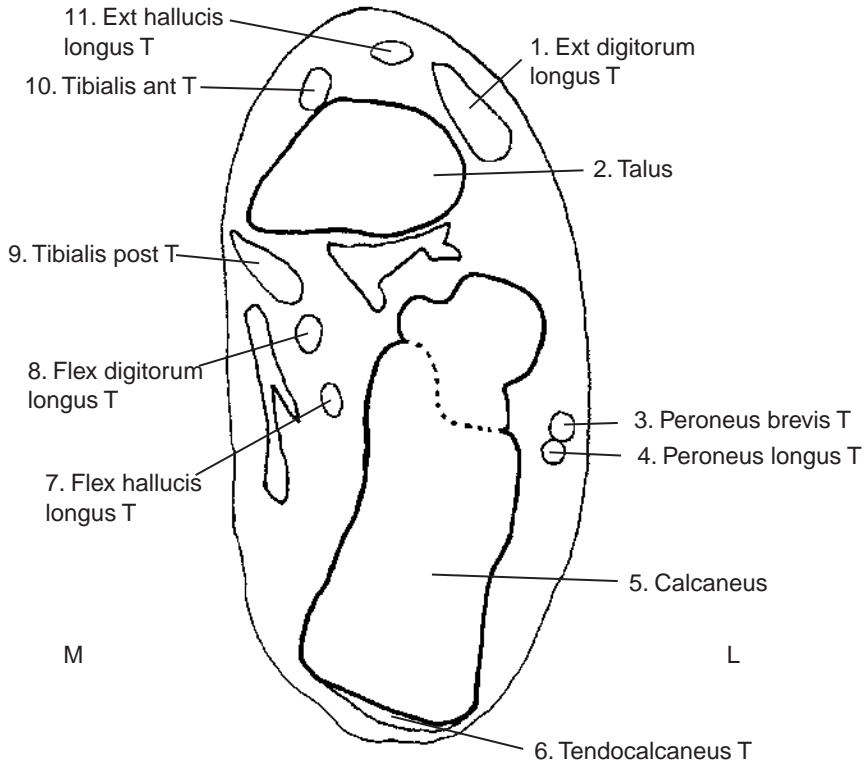
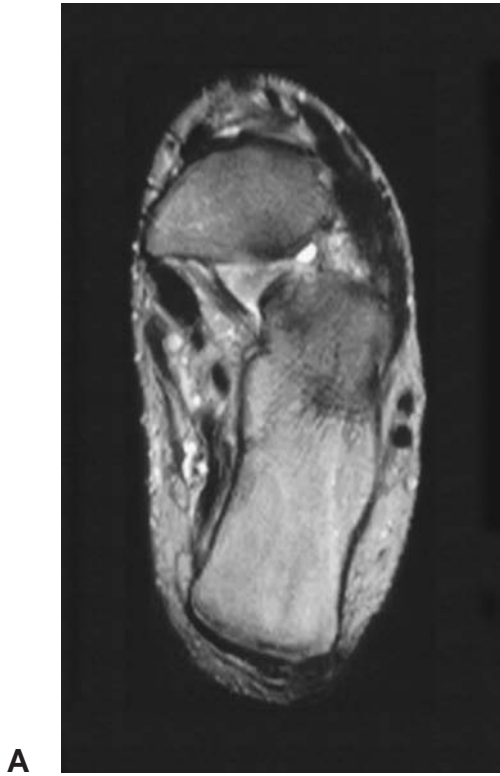


**Figure 8-37 (A,B)** Axial MR image 2.

Owing to the absence of either upper or lower articular surfaces on the talus, this image demonstrates the middle of the talus with the more posteriorly situated upper calcaneus. Similar to the previous image, the flexor hallucis longus, the flexor digitorum longus, and the tibialis posterior tendons are found on the medial side of the ankle. Anterior to the talus, the tibialis anterior tendon is sectioned extending downward to insert on the first cuneiform and the base of the first metatarsal. The most anterior tendon demonstrated is the extensor hallucis longus muscle, which originates from the anterior fibula and inserts on the distal phalanx of the first digit. Lateral to the talus, the extensor digitorum muscle tendon is sectioned as it extends downward to insert on the distal phalanges of the second to fifth digits. On the lateral side of the calcaneus, the tendons of the peroneus brevis and longus muscles are again shown in cross-section; the peroneus brevis is the more anterior. On the posterior aspect of the calcaneus, the tendo calcaneus appears as a broad, flat tendon.



B

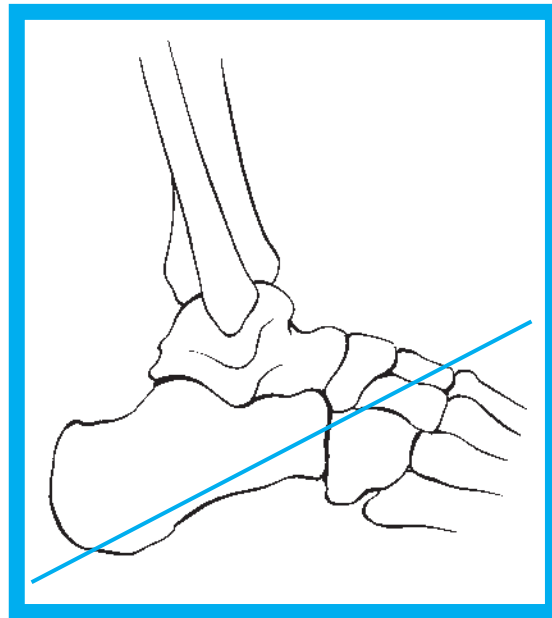
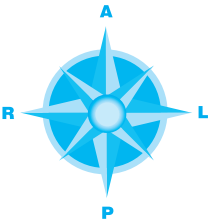
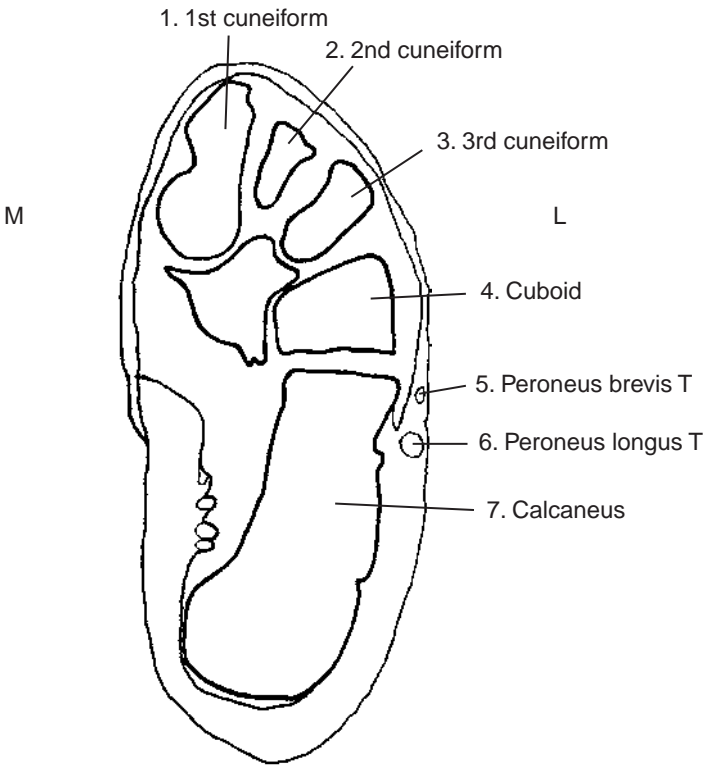
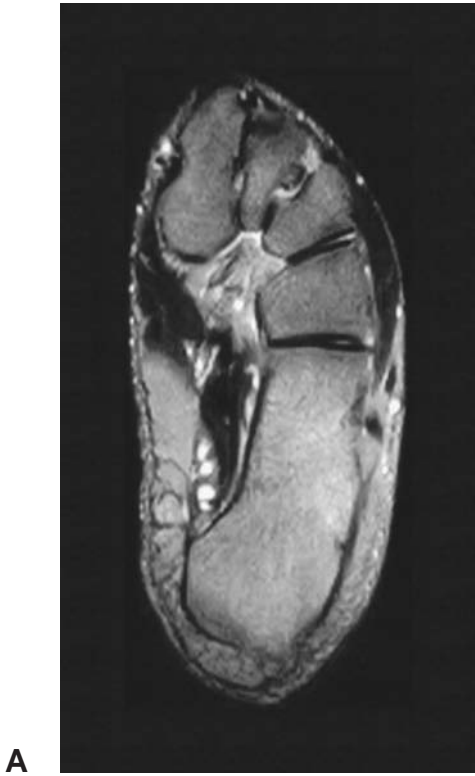


**Figure 8–38 (A,B)** Axial MR image 3.

This image is below the level of the talus and navicular and demonstrates most of the bones associated with forming the transverse arch of the foot. Posteriorly, the calcaneus is shown projecting toward the cuboid, forming the calcaneocuboid joint. Anterior and medial to the cuboid, the three wedge-shaped cuneiform bones can be identified and are labeled first, second, and third, based on their location. Similar to the sagittal images, the muscles and tendons on the plantar surface of the foot are difficult to discern; however, the peroneus brevis and longus tendons can be identified on the lateral surface of the calcaneus. As described earlier, the peroneus longus and brevis muscles originate from the upper part of the fibula and tibia and extend down around the lateral surface of the ankle to insert on the first cuneiform and fifth metatarsal.





## Case Study 8-1



**Figure 8–39**

This 25-year-old man underwent a helical computed tomography (CT) scan followed by three-dimensional reconstruction with shadowing to evaluate a torsion fracture at the right elbow. This fracture resulted from a twisting action on the arm causing fractures near the elbow joint. In a normal elbow joint, the trochlea of the distal humerus will articulate with the trochlear notch of the ulna. In this patient, the round shaped trochlea is still in the elbow joint

even though it has separated from the rest of the humerus. The fracture appears as a jagged edge on the upper trochlea. From the twisting force, the distal humerus rotated backward fracturing the olecranon process of the ulna. The olecranon process is a bone fragment on the right side of the image corresponding with the posterior surface of the elbow. Because of the displaced fragments, this fracture was surgically reduced and repaired.

### Questions

1. Describe the classification and movement of the elbow joint.
2. Describe the bony structures forming the medial articulation within the elbow joint.
3. Describe the bony structures forming the lateral articulation within the elbow joint.
4. The head of the radius articulates with what part of the humerus?
5. The olecranon process articulates with what part of the humerus?



## Case Study 8-2

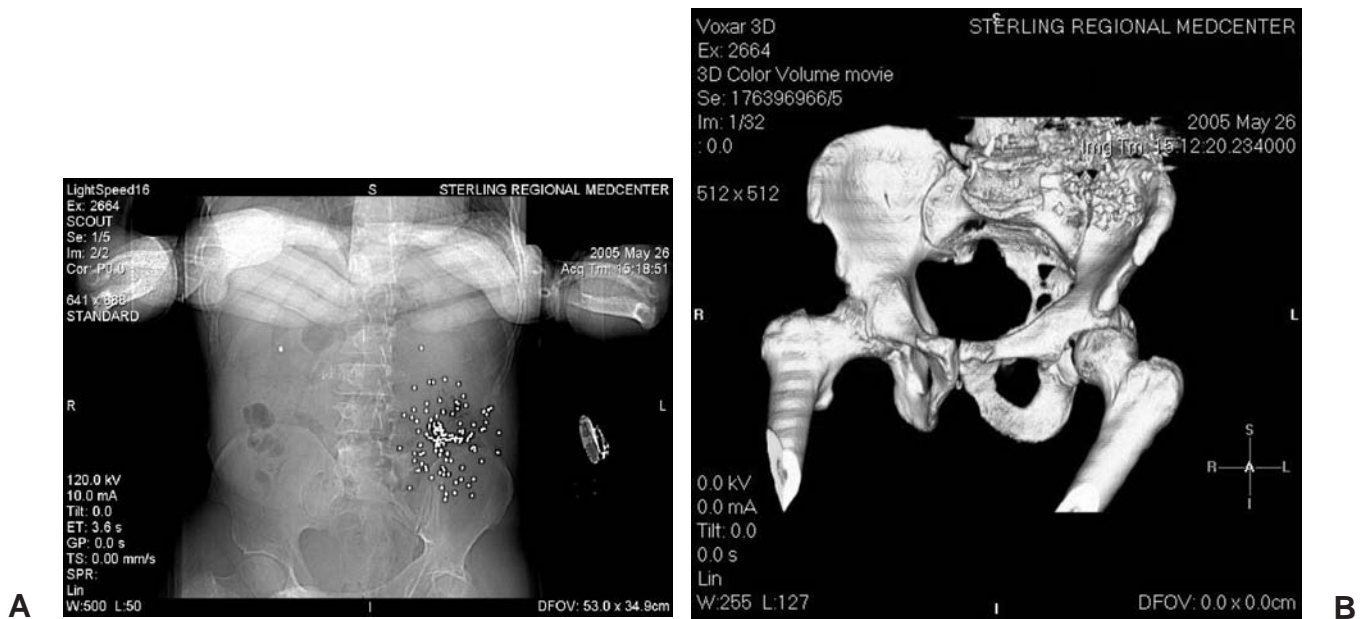


Figure 8-40

This 59-year-old man underwent a helical dynamic computed tomography (CT) scan with three-dimensional (3D) reconstruction to evaluate a shotgun wound to the pelvis. As shown on the scout film, the pellets form a tight pattern indicating that the shotgun was in close proximity to the patient during the accident. The pellets are found concentrated in the lower left abdominal cavity and the iliac

region of the pelvis. For comparison, the 3D reconstructed image also shows the pellets that appear like snowflakes in the left upper pelvis. Due to the impact of the blast, the acetabulum on the left was fractured exposing the head of the femur. Despite the fractured acetabulum, there are no fractures evident in the femur, and the head and neck appear to be intact.

## Questions

1. Describe the bones forming the hip joint.
2. What bones form the acetabulum?
3. Is the greater trochanter found on the medial or lateral aspect of the femur?
4. What is the classification and movement of the hip joint?
5. Describe the origin, insertion, and action of the pectineus muscle?





## Case Study 8-3

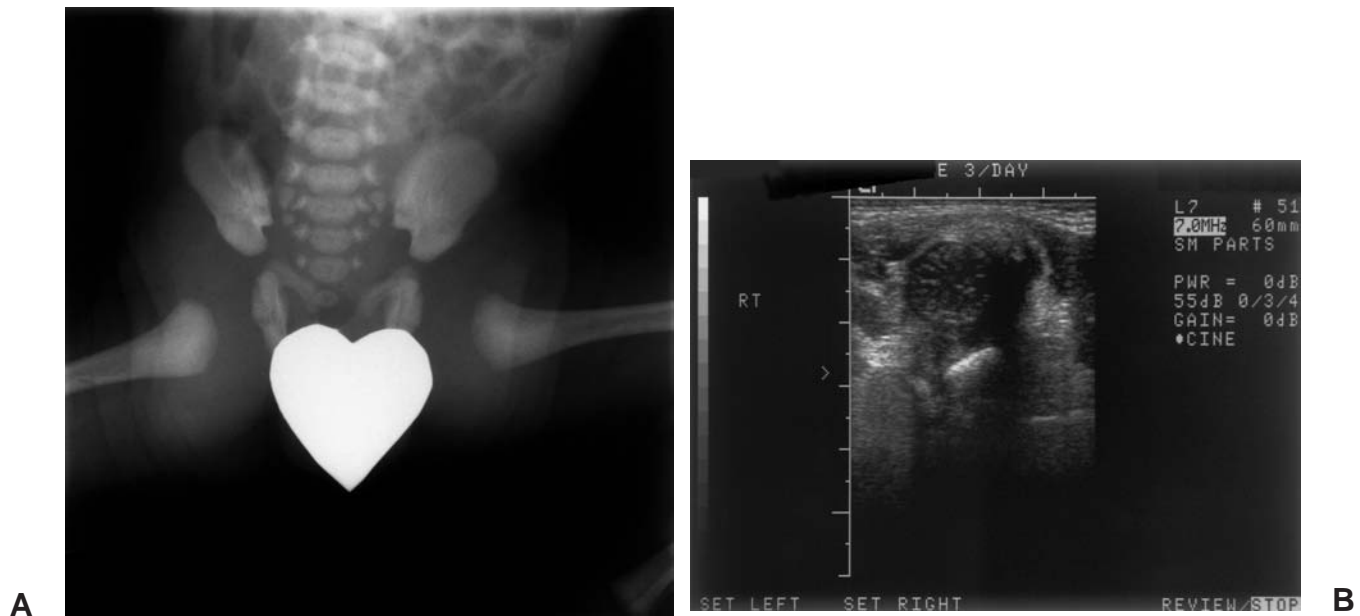


Figure 8-41

This 2-day-old boy was referred for a radiographic examination of the hip for suspected Legg-Calve-Perthes disease or osteochondritis deformans. This condition is ischemic necrosis leading to the flattening of the head of the femur caused by vascular interruption, resulting in osteochondritis of the epiphysis. In the plain film shown in Figure 8-41A, the bones in this baby's pelvis are still growing, and the sutures can clearly be seen separating the bones forming the pelvic girdle. Similarly, bone is found surrounding the primary ossification centers found within the shafts of the

femurs (diaphyses), but has not yet formed in the secondary centers within the femoral heads (epiphyses). The next day, the baby was further evaluated with ultrasound as shown in Figure 8-41B. With ultrasound, the cartilage forming the right femoral head can be seen as an oval-shaped structure near the top of the image. Unfortunately, the right femoral head does appear to be somewhat flattened which would be consistent with the suspected disease. Because of continued degenerative changes, surgical correction was implemented to minimize permanent damage.

### Questions

1. In a patient with Legg-Calve-Perthes disease or osteochondritis deformans, which ligament has been damaged and is most likely causing the ischemic necrosis leading to the flattening of the head of the femur?
2. Describe the structure and function of the fovea capitis femoris.
3. Is the superior gemellus muscle found anterior or posterior to the hip joint?
4. Is the obturator internus muscle found anterior or posterior to the hip joint?
5. Which part of the pelvic girdle supports most of the upper body's weight in the sitting position?



## Case Study 8-4



Figure 8-42

This 92-year-old man was referred for a computed tomography (CT) examination to evaluate a suspected fracture of the right ankle or foot. Even though no fractures were shown, there was substantial decreased calcification within all the bones of the foot and ankle. The bones have a radiolucent appearance due to the low bone density, and the osteopenia appears most severe in the calcaneus.

Although men do not lose bone at the accelerated rate that postmenopausal women do, they still lose 0.4% a year starting at age 50. Osteoporosis due to advanced age is termed senile osteoporosis and may affect both women and men. Symptoms may not be evident for years until fractures (which may be frequent) start to occur, and will most often affect the weight-bearing bones of the body.

### Questions

1. Describe the classification and movement of the ankle joint.
2. Describe the classification and movement of tarsal bone joints within the foot.
3. In the standing position, how much of the body's weight rests on the calcaneus?
4. Which tarsal bone articulates with the tibia and fibula to form the ankle joint?
5. Is the cuboid tarsal bone found on the medial or lateral side of the foot?



## Case Study 8-5

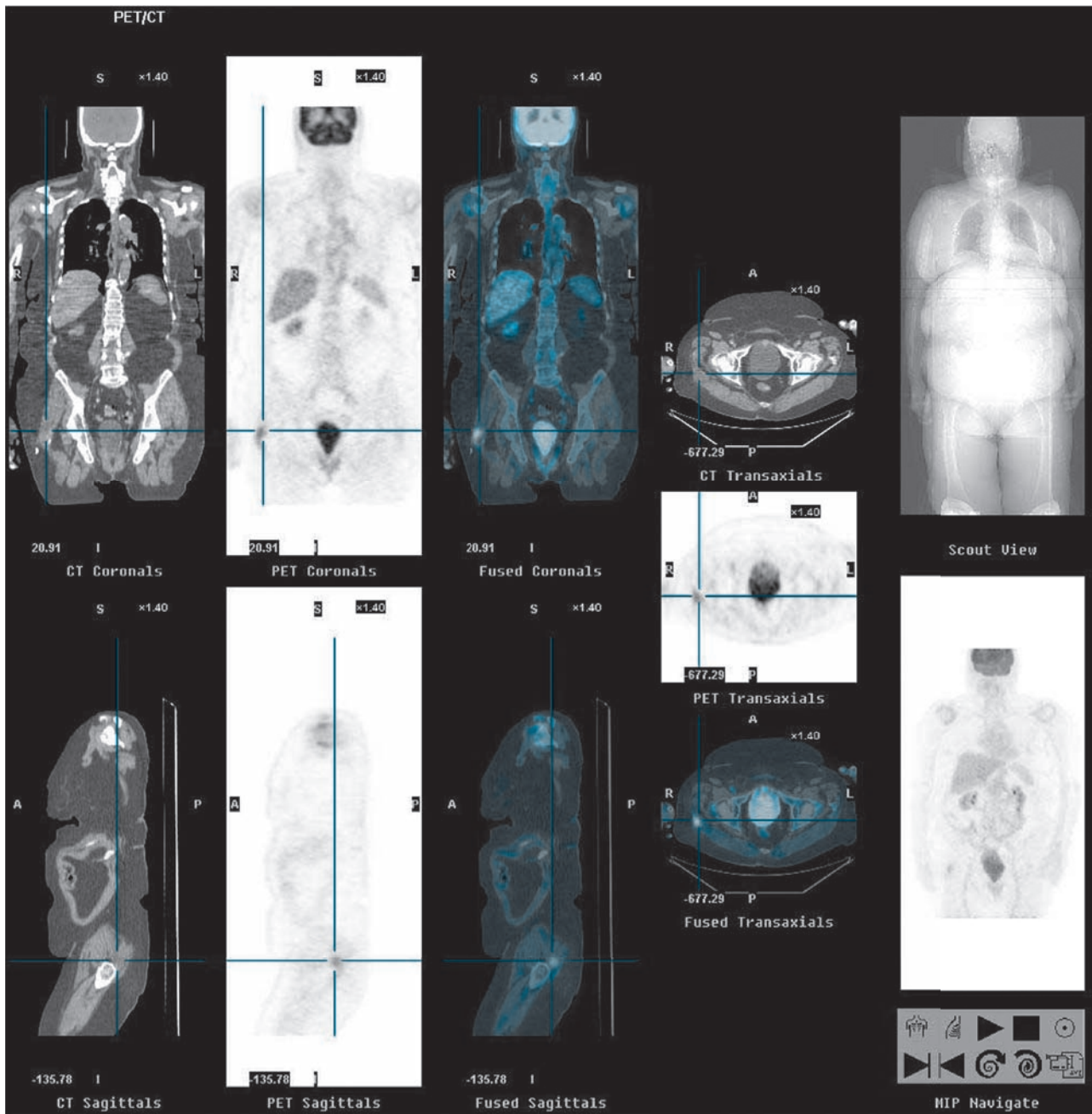


Figure 8-43

This positron emission tomography/computed tomography (PET/CT) case is a 75-year-old Caucasian woman previously diagnosed with breast carcinoma. Before the procedure, the patient received a single IV dose of 17.77 mCi of F-18 FDG for this examination. The PET/CT study was conducted to more accurately stage the breast carcinoma. At the time of this study, a large area of abnor-

mal uptake was found in the pelvis deep to the gluteus muscle. Upon further investigation, this patient reported that she had recently had an injection into the right gluteus muscle. Based on this history, the increased metabolic rate deep to the gluteus muscle was considered to be part of a healing response and not considered evidence of metastases.

## Questions

1. How would a malignant disease originating in the breast travel to the gluteus muscle?
2. Can the cells of the breast grow through bony structures within the body like the ilium of the pelvis?
3. Is the pectineus muscle on the anterior or posterior surface of the hip joint?
4. Describe the sartorius muscle.
5. Compared to the other muscles covering the posterior hip joint, how would you describe the size of the gluteus muscle: Larger or smaller?



# Case Study 8-6

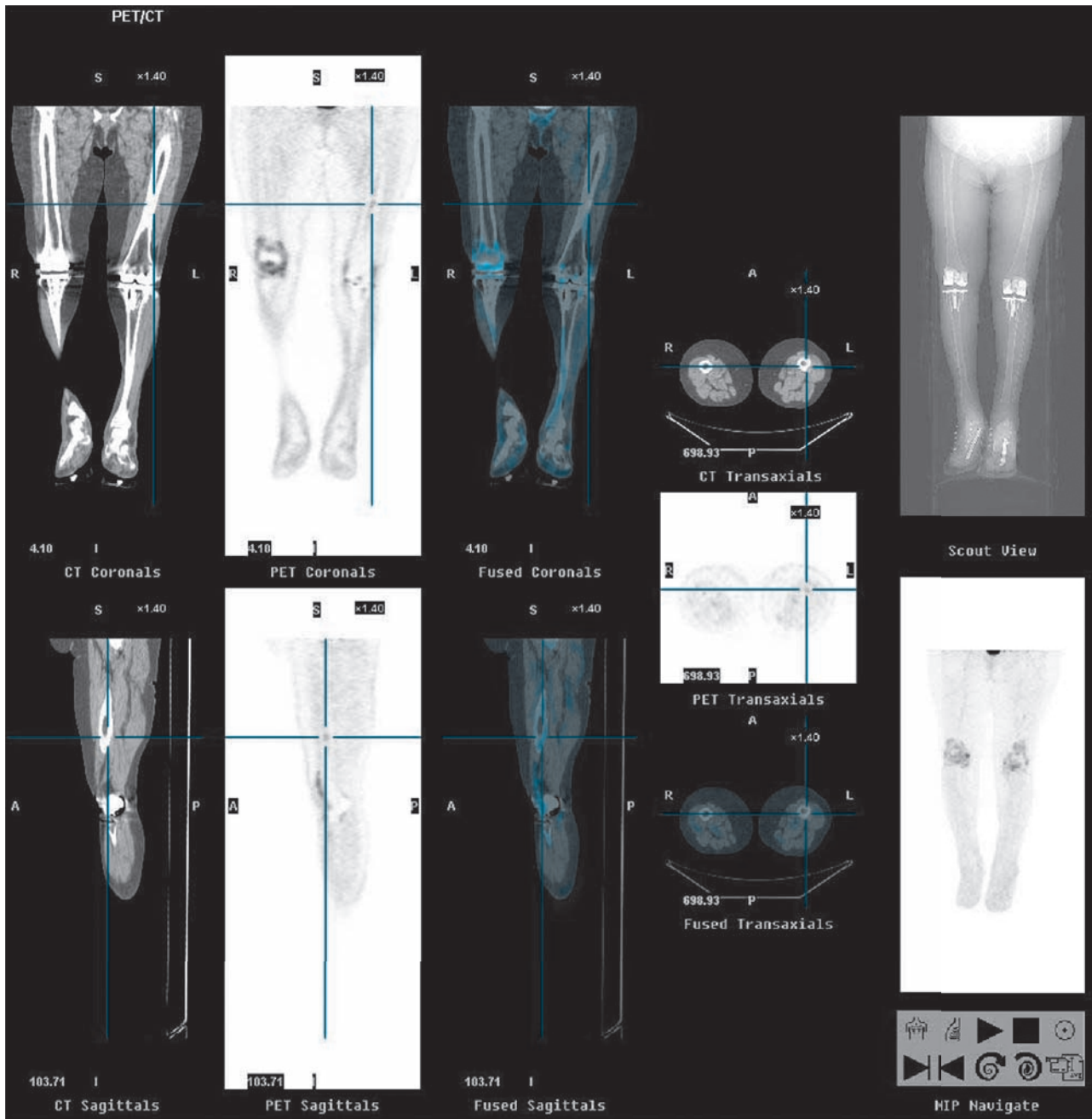


Figure 8-44

This positron emission tomography/computed tomography (PET/CT) case is a 75-year-old Caucasian woman previously diagnosed with breast carcinoma and shown in Case Study 8-4. As indicated by the marker lines, elevated metabolic activity is evident in the left femur as a small focus of signal abnormality within the bone marrow. Because the increased activity was considered

marginal (below 2.5 standard uptake value [SUV]), a follow-up examination was repeated three months following this study. In the subsequent examination, the region in question was found to have an increased signal and, consistent with metastatic disease, a high metabolic rate was detected in the right iliac chain of lymph nodes.

## Questions

1. If the metabolic activity within the left femur was attributed to metastases, would you also expect to find malignant cells in a similar location within the right femur?
2. Can you identify other areas of increased metabolic activity aside from the region identified with the marker lines?
3. If there are other regions of increased metabolic activity within the legs, what condition would most likely be responsible for the increased level?
4. Staging of tumors is done to assess the extent of tumor spread. In this case, would you describe this patient to have a low or high degree of metastases?
5. In a patient in whom multiple sites of metastases are apparent, how would you describe the prognosis for the patient: Good or poor?



## CLINICAL APPLICATIONS

1. Describe the shoulder girdle.
2. List the bones forming the knee joint: \_\_\_\_\_, \_\_\_\_\_, and \_\_\_\_\_.
3. The \_\_\_\_\_ meniscus is described as a nearly circular ligament within the knee joint.
4. Describe the function of the glenoid labrum.
5. The capitulum is the articular surface that articulates with the ulna: True or false?
6. List the muscles making up the rotator cuff found within the shoulder.
7. The coronoid fossa is located on the (anterior / posterior) side of the humerus.
8. The cuboid is found on the (medial / lateral) side of the ankle.
9. List in order from lateral to medial the proximal row of carpal bones.
10. The anterior cruciate extends from the \_\_\_\_\_ intercondylar fossa to the back of the \_\_\_\_\_ femoral condyle.





# Appendix A

## Answers to Clinical Application Questions

### CHAPTER 1

1. A sectional image represents a slice of anatomy found within the patient in a given plane of section. Although the thickness may vary, the image will represent a specific section of anatomy which is used to generate the image.
2. Left
3. Coronal or frontal
4. Arthrodi
5. Diarthrosis
6. Enarthrosis
7. Air is  $-1,000$ , water is  $0$ , and bone is  $+1,000$
8. T1
9. Glucose or FDG
10. By generating high-frequency sound waves through the patient, and collecting the reflected sound wave, echoes are recorded and displayed as a real-time visual image.

### CHAPTER 2

1. The azygos vein is located inside the right posterior thoracic cage adjacent to the right side of the vertebral bodies. It drains the posterior thorax and upper abdomen into the superior vena cava.
2. Lamina
3. C
4. A
5. Left
6. Left
7. Parietal pleura / visceral pleura
8. B
9. A
10. Hilum

#### CASE STUDIES

##### Case Study 2-1

1. left ventricle
2. right ventricle
3. right atrium
4. left
5. right

##### Case Study 2-2

1. right
2. tricuspid valve

3. left ventricle
4. mitral or bicuspid valve
5. left atrium

##### Case Study 2-3

1. superficial
2. subclavian vein
3. azygos vein
4. accessory hemiazygos vein
5. superior vena cava

##### Case Study 2-4

1. parietal pleura
2. upper and lower lobes
3. upper and lower lobes
4. clavicle
5. axillary artery

##### Case Study 2-5

1. The aorta descends in the posterior mediastinum on the left side of the vertebral column.
2. The esophagus descends in the posterior mediastinum and travels between the heart and the vertebral column.
3. superior vena cava
4. pulmonary trunk and left main bronchus
5. the carina

##### Case Study 2-6

1. left pulmonary artery
2. pulmonary veins
3. brachiocephalic, left common carotid, and left subclavian vein
4. common carotid artery and the slightly larger, more superficial
5. internal jugular vein

### CHAPTER 3

1. Right renal vein
2. The spleen lies against the diaphragm on the upper left side of the abdomen within the thoracic cage. Its size and shape vary considerably, partially depending on the adjacent structures. The anterior surface is next to the stomach, the posterior surface is next to the left kidney, the superior surface is next to the diaphragm, and the inferior surface is next to the left splenic flexure of the colon.



3. Hepatic duct, portal vein, and proper hepatic artery
4. Caudate
5. Celiac trunk, superior mesenteric, renal, inferior mesenteric, and common iliac
6. D
7. Gallbladder
8. Visceral peritoneum / parietal peritoneum
9. Right
10. Inferior mesenteric / splenic

### CASE STUDIES

#### Case Study 3-1

1. The kidneys are found on either side of the vertebral column and typically are centered at the level of the first lumbar segment. They are located posterior to the peritoneum lining the abdominal cavity and are described as retroperitoneal.
2. The right renal artery is usually longer since it passes posterior to the inferior vena cava.
3. The splenic artery is very tortuous and originates from the celiac trunk.
4. right
5. adrenal glands

#### Case Study 3-2

1. liver
2. Originating at the diaphragm, the aorta extends through the abdomen along the left side of the vertebral column to terminate as the common iliac arteries.
3. The vein passes in front of the aorta and the right renal artery.
4. The kidney acts to filter fluid and waste products from the blood.
5. spleen

#### Case Study 3-3

1. The gland lies just below the anterior liver and creates an impression on the lower or visceral surface.
2. The gland acts as a reservoir for the bile produced by the liver.
3. hepatic and cystic
4. posterior
5. quadrate

#### Case Study 3-4

1. pancreatic duct
2. hepatic ducts, portal vein, and proper hepatic artery
3. The right side of the H is formed by the gallbladder and the inferior vena cava; the horizontal bar is formed by the porta hepatis; and the left side of the H is formed by the ligamentum teres and the ligamentum venosum.
4. pancreas
5. The celiac trunk is the short (1-2 cm), first branch of the abdominal aorta originating just below the diaphragm between the lesser curvature of the stomach and the liver.

#### Case Study 3-5

1. The stomach is found within the upper left abdominal cavity just below the diaphragm. The liver is found on the right side and the spleen is found on the left side. Near the center of the abdomen, the pancreas lies between the stomach and the vertebral column.
2. fundus, body, and pyloric part
3. right
4. The duodenum drains the contents of the stomach and is found on the right side below the liver. The duodenum joins with the jejunum which is the small bowel generally located in the upper anterior abdominal cavity. The ileum is the last part of the small bowel and is generally located in the lower anterior abdominal cavity.
5. splenic flexure of colon

#### Case Study 3-6

1. superior mesenteric and splenic
2. The portal system is a network of venous structures that drain nutrient rich blood from the gastrointestinal tract into the liver.
3. neck of the pancreas
4. head of the pancreas
5. inferior mesenteric

## CHAPTER 4

1. Internal iliac artery
2. Ilium / pubis / ischium
3. False
4. C
5. A
6. Above
7. Posterior
8. D
9. Fundus: the dome-shaped roof of the uterus found above the oviduct. Body: the largest part of the uterus; centrally located and tapered in shape. Cervix: the most inferior constricted region of the uterus opening into the vagina.
10. The first image must be above the iliac crest, and the last image must be below the ischium.

### CASE STUDIES

#### Case Study 4-1

1. When used to describe a vessel, patient is open or unrestricted blood flow.
2. Device used to maintain a vessel wall that will fuse with adjacent structures and maintain blood flow or perfusion of affected tissues.
3. Right
4. External
5. Artery

**Case Study 4-2**

1. The abdominal aorta descends into the greater pelvis where it divides into the right and left common iliac arteries.
2. The inferior vena cava is found on the right side the abdominal aorta, and much like the corresponding arteries, bifurcates into the common iliac veins in the greater pelvis.
3. Atherosclerotic
4. Unlike vessels seen in other regions of the body, the external iliac artery is more superficial as compared to the corresponding vein which lies deeper within the pelvis. In regard to appearance, the vein is usually slightly larger and less round in shape due to lower venous blood pressure.
5. The abdominal aorta divides into the common iliac arteries, and each of these arteries extend deeper into the pelvis before dividing into the external and internal iliac arteries. The internal iliac artery extends through the posterior bony pelvis to give rise to the gluteal arteries in the region of the buttocks.

**Case Study 4-3**

1. The prostate is found between the bladder and the pelvic diaphragm, and surrounds the upper urethra.
2. The prostate is one of the most dense glands owing to the high concentrations of connective tissue and smooth muscle.
3. The seminal vesicles are above the prostate and found between the bladder and the rectum on either side of the ductus (vas) deferens. Within the prostate, the seminal vesicle ducts join with the ductus (vas) deferens to join the prostatic urethra.
4. During ejaculation, the seminal vesicles secrete an alkaline fluid rich in sugar that contributes to sperm viability.
5. Corpus spongiosum

**Case Study 4-4**

1. The testicles are surrounded by the scrotal sack, and are located outside and below the bony pelvis.
2. The ductus (vas) deferens extends from the testicle, and passes over the pubis and bladder to join within the prostate gland to the urethra.
3. During embryonic development, the testis are formed inside the abdominal cavity. As they descend during fetal development, they move through the anterior abdominal wall so the spermatic cord will attach to the anterior abdominal wall to enter the greater pelvic cavity, above the symphysis pubis.
4. Originating below the bladder, the urethra is about 20 cm in length and travels through the prostate, pelvic diaphragm, and penis.
5. The urethra is found behind the pubis and traverses through the pelvic diaphragm to exit the lower pelvis.

**Case Study 4-5**

1. An S-shaped alimentary structure that begins at the pelvic brim and extends down through the pelvis to terminate near the front of S3.
2. Left
3. The sigmoid colon is found contained within the pelvis and is located well above the pelvic diaphragm. The sigmoid joins with the rectum which extends through the pelvic diaphragm to the anal canal found on the lower part of the pelvis.
4. The wedge-shaped, fat-filled spaces containing rectal vessels and nerves between the rectum and ischium.
5. The ovaries, oviducts, ligaments, etc. forming the adnexal area are located on either side of the uterus and are found below the peritoneum lining the abdominal cavity. By comparison, the sigmoid colon is found posterior and superior to the adnexal areas and is fixed to the posterior wall by mesentery.

**Case Study 4-6**

1. A flat muscle originating from the inner surfaces of the iliac crest that joins with the psoas muscle to insert on the lesser trochanter of the femur and acts to flex the thigh.
2. Right ureter
3. Cecum
4. Descending colon
5. Ileum

**CHAPTER 5**

1. Base of the skull
2. Ovale
3. This pair of bones forms the posterior part of the hard palate. Because the bones are L-shaped, they also form part of the lateral walls and floor of the nasal cavity.
4. Dura mater / arachnoid mater / pia mater
5. A
6. Deep within the temporal lobe, this curved sheet of gray matter extends upward into the floor of the lateral ventricle. Considered part of the limbic system, the hippocampal formation is involved in the emotional aspects of behavior.
7. Superior cistern
8. Arising from the internal carotid artery near the hypothalamus, the artery extends laterally as it travels upward through the Sylvian fissure.
9. Sphenoid

**CASE STUDIES****Case Study 5-1**

1. The arteries forming the circle of Willis are found on the inferior surface of the brain between the midbrain and the upper part of the sphenoid bone found in the base of the skull.

2. The arteries forming the circle of Willis are found within the subarachnoid space.
3. The venous sinuses are formed by folds of the dura mater and many like the transverse sinus create grooves on the inside of the skull. Although most of the venous blood within the skull is drained into the internal jugular veins, small amounts of venous blood also drain through the face to empty into the external jugular veins.
4. On the inside, the CSF is found within the ventricles embedded deep within the brain. On the outside, the brain is covered with pia mater while the dura mater lines the inside of the skull. Between these two layers, the arachnoid mater contains spaces filled with CSF.
5. posterior cerebral artery

### Case Study 5-2

1. Begins at the bifurcation of the common carotid artery into the internal and external carotid arteries in the neck near the level of C4.
2. The artery passes through the carotid foramen within the petrous part of the temporal bone.
3. Each internal carotid artery has branches that form the anterior cerebral and posterior communicating arteries. The continuation of the internal carotid artery after the branches originate is called the middle cerebral artery.
4. The cerebral tissue supplied by the vessel will undergo ischemic necrosis or infarction.
5. anterior cerebral artery

### Case Study 5-3

1. The CSF is produced by the highly vascularized choroid plexuses located within the ventricles found deep within the brain.
2. The CSF is reabsorbed on the top of the brain by the arachnoid villi acting as one-way valves allowing the CSF to drain into the superior sagittal sinus. In addition, CSF is also absorbed by some of the vessels and the cells lining the central nervous system.
3. The CSF produced within the ventricles of the brain circulates through a series of ventricles and aqueducts to exit via foramina to the outside of the central nervous system. The CSF eventually flows to the top of the brain to be absorbed into the venous blood of the superior sagittal sinus.
4. If the CSF circulation becomes obstructed, continued production of CSF will result in an increased hydrostatic pressure. Clinically, this condition is called hydrocephalus and will appear as a progressive dilation of the ventricular system.
5. Cisterns are enclosed spaces serving as a reservoir for cerebrospinal fluid.

### Case Study 5-4

1. Inside the brain, the choroid plexus found in the ventricles produces CSF from the blood.
2. Inferior horn of lateral ventricle
3. The pia mater surrounds the outer surface of the brain. The middle layer is called arachnoid mater since the web like projections extends through the subarachnoid space that is filled with cerebrospinal fluid. The dura mater is a tough dense layer found lining the inside of the bony skull.
4. Third ventricle
5. Fourth ventricle

### Case Study 5-5

1. Nerve fibers radiating between the nuclei and the cerebral cortex. Altogether, the sheets of nerve fibers form a crown extending upward to the cerebral cortex.
2. The C-shaped collection of gray matter forming the caudate nucleus and can be described as lining the inner curvature of the lateral ventricle.
3. The enlarged region of the brainstem sometimes called the belly is formed by nerve fibers from the cerebellum joining those from the cerebrum and spinal cord.
4. cerebellum
5. cerebrum

### Case Study 5-6

1. Malignant cells lose their ability to adhere so some of the cells would be taken via the venous blood stream into the pulmonary veins. The cells would be carried to the heart and would pass through the left atrium and left ventricle. The malignant cells would leave the heart through the aorta and would ascend into the neck via the common carotid artery. At about the level of C4, the cells would continue upward in the internal jugular artery and continue out in smaller branches until they became lodged within the deep neck.
2. The mass is inferior to the circle of Willis. The mass above appears to be located in the prevertebral area within the deep face. By comparison, the circle of Willis is just inferior to the midbrain and above the sphenoid bone in the base of the skull.
3. The cerebellum is the lowermost part of the brain and is often described as being behind the face. If you follow the horizontal marker line posteriorly, it passes through the most inferior part of the brain, the cerebellum.
4. The frontal lobe is the most anterior part of the cerebrum and is found next to the frontal bone of the skull forming part of the patient's forehead.
5. ethmoid sinuses

**CHAPTER 6**

1. Base of the skull / bony thoracic cage
2. Third
3. Laryngeal vestibule / glottic space / infraglottic space
4. It is located between the posterior tongue and the epiglottis, on either side of the median glossoepiglottic fold.
5. C3 / C4
6. C
7. Thyroid cartilage / anterior
8. Valleculae
9. Arytenoid / cricoid
10. Nasopharynx / oropharynx / laryngeal pharynx

**CASE STUDIES****Case Study 6-1**

1. They ascend in the deep neck and travel through the base of the skull to supply blood to the middle and anterior cerebrum.
2. The facial artery is a branch of the external carotid that extends over the lower edge of the mandible to supply blood to the external face.
3. External jugular vein
4. Internal jugular vein
5. Retromandibular vein

**Case Study 6-2**

1. The common carotid artery ascends through the neck beside the posterior trachea and is found deep to the internal jugular vein.
2. The external carotid artery ascends through the superficial upper neck to supply arterial blood to the external head including the face and scalp.
3. The vertebral arteries originate from the subclavian arteries and ascend through the transverse foramina of C6 through C1 to enter the skull through the foramen magnum. In the images above, the vertebral arteries are found medial and posterior to the common carotid arteries.
4. brachiocephalic artery
5. aortic arch

**Case Study 6-3**

1. Located inferior to the larynx, the thyroid gland surrounds the upper region of the trachea.
2. Common carotid artery and internal jugular vein
3. The U-shaped gland wraps around the upper trachea. There are two lobes located on either side of the trachea, connected by a narrowed region called the isthmus.
4. anterior
5. thyroid cartilage

**Case Study 6-4**

1. Inferior
2. The thyroid gland and esophagus are separated by the trachea. The thyroid gland wraps around the anterior surface of the trachea while the esophagus lies near the midline posteriorly.
3. Isthmus of the thyroid gland
4. Superior
5. Internal

**Case Study 6-5**

1. The external jugular vein descends superficial to the sternocleidomastoid muscle. The slow gentle pulse can often be found near the middle of the muscle.
2. The external jugular vein drains venous blood from the superficial structures of the head.
3. A flat muscle band that originates from the sternum and clavicle and inserts on the mastoid process of the temporal bone. The muscle acts to bend the neck and rotate the head.
4. Subclavian vein
5. Geniohyoid

**Case Study 6-6**

1. The vestibular fold or false vocal cords
2. The vocal fold covering the vocal cords
3. Laryngeal vestibule, glottic space, and infraglottic cavity
4. Located in the upper part of the larynx, the spoon-shaped cartilage is folded over the opening of the larynx moving food or drink into the laryngeal pharynx.
5. The sinuses found within the pharynx on either side of the larynx.

**CHAPTER 7**

1. C2 / L5
2. Costal facets on the vertebral body and transverse processes
3. Annulus fibrosus
4. True
5. Inferior articular process / superior articular process
6. Motor
7. Inferior articular process
8. Within the intervertebral foramen at the origin of the spinal nerve
9. True
10. Cauda equina

**CASE STUDIES****Case Study 7-1**

1. The first and most atypical vertebra, because it lacks a body and a true spinous process and is roughly circular in shape. The front and back of the vertebra are

formed by the anterior and posterior arches; the lateral masses form the sides.

2. Yes, normally the cervical curvature causes C3 & C4 to be more anterior as compared to the surrounding vertebrae.
3. The vertebral arteries and veins
4. The second cervical vertebra forms the pivot for rotation of the atlas and head. It is easily distinguished by the body, which is long and extends cranially, forming the dens.
5. Yes, all cervical vertebrae have transverse foramina.

### Case Study 7-2

1. The superior articular process is found anterior and lateral to the inferior articular process.
2. The inferior articular process is locked in front of the superior articular facet.
3. The inferior articular process is within the intervertebral foramen.
4. The facet is compressing the right nerve root containing both sensory and motor nerve fibers passing through the intervertebral foramen.
5. Like the other meningeal layers, the dura mater forms a sheath around the nerve roots within the intervertebral foramen.

### Case Study 7-3

1. The tough outer layer; surrounded by fat in the epidural space within the vertebral foramen.
2. No, nerve cells are fully differentiated and are unable to revert to an undifferentiated or dividing state to replace cells that are lost as a result of injury.
3. The CSF originating in the ventricles in the brain flows down through the central canal inside the spinal cord and exits at the conus medullaris. Outside the spinal cord, the fluid travels upward in the subarachnoid space to return to the top of the brain where it is reabsorbed into the venous blood stream.
4. The middle covering composed of thin, delicate fibers known as arachnoid trabeculae which are bathed in CSF.
5. The innermost meningeal layer continuous with the surface of the spinal cord and nerve roots.

### Case Study 7-4

1. No, the layer of dense connective tissue tightly attached to the anterior surfaces of vertebrae and intervertebral disks was probably intact since the vertebral column maintained its orderly stacked arrangement.
2. Yes, the layer of dense connective tissue tightly attached to the posterior surfaces of vertebrae and intervertebral disks was torn.
3. Yes, the tearing of the posterior longitudinal ligament also resulted in damage to the intervertebral disk.

4. The meningeal layers surrounding the spinal cord are encased by the ligaments and bony structures forming the vertebral foramen. Due to injury to these connective tissues, the subarachnoid space enlarged due to an outward bulging of the meningeal layers beyond the normal limits of the spinal foramen.
5. Since the sensory nerves below the injury will be unable to provide signal, select sensory nerve cells above the injury site will no longer be functional. Phantom pains often occur due to a crossing over of nerve signals within the central nervous system.

### Case Study 7-5

1. Yes, when the vertebral body slides forward, the articular facets will also move forward resulting in a pinching of spinal nerve roots passing through the intervertebral foramina.
2. All of the spinal ligaments including the anterior longitudinal ligament, posterior longitudinal ligament, ligamentum flavum, interspinous ligament, etc.
3. Yes, spondylolisthesis can occur between any two vertebrae but occurs most often at L5-S1.
4. Yes, when the vertebral body slides forward, the pedicles and laminae will also move forward resulting in a narrowing of the spinal canal.
5. Decrease

### Case Study 7-6

1. Yes, the bundle of lumbar and sacral nerves descending below the termination of the spinal cord would be compressed by the bulging disks.
2. The caudal tip of the spinal cord found between L1 and L3.
3. Yes, a bulging disk will often narrow the intervertebral foramina and pinch spinal nerve roots resulting in numbness and a tingling sensation traveling down the legs and into feet.
4. The posterior longitudinal ligament attached to the posterior surfaces of vertebrae and intervertebral disks.
5. Lumbar vertebrae can be distinguished by their large size and the absence of costal facets (thoracic vertebrae) and transverse foramina (cervical vertebrae).

## CHAPTER 8

1. The shoulder girdle consists of two bones—the clavicle and the scapula—that attach to the axial skeleton via the sternoclavicular joint. On the opposite end of the shoulder girdle, the shoulder joint is formed by the glenoid fossa of the scapula, which articulates with the head of the humerus to form an enarthrodial, or ball-and-socket, joint.
2. Femur / tibia / patella



3. Lateral
4. This ridge of fibrocartilage acts to deepen the glenoid fossa and protect the bone.
5. False
6. Supraspinatus, subscapularis, infraspinatus, and teres minor
7. Anterior
8. Lateral
9. Scaphoid, lunate, triquetral, and pisiform
10. Anterior / lateral

## CASE STUDIES

### Case Study 8-1

1. The joint connecting the arm to the forearm is considered a ginglymus, or hinge-type, joint capable of flexion and extension.
2. The medial articulating surface on the distal humerus called the trochlea articulates with the trochlear notch of the ulna.
3. The little head or small eminence of bone on the distal humerus called the capitulum articulates with the fovea on the head of the radius.
4. capitulum
5. trochlea

### Case Study 8-2

1. Generally described as the juncture of the femur with the pelvic girdle which is made up of the ilium, ischium, and pubis.
2. The ilium, ischium, and pubic bones form the socket of the hip joint.
3. lateral
4. The joint is considered a ball-and-socket type (enarthrosis); it is capable of a wide range of movements, including internal and external rotation.
5. Origin: pectineal line of the pubis. Insertion: pectineal line of the femur. Action: flexes, adducts, and laterally rotates the thigh.

### Case Study 8-3

1. ligamentum capitis femoris
2. A depression in the head of the femur where the ligamentum capitis femoris is attached. Unlike most ligaments, the ligamentum capitis femoris has little function in maintaining the structure of the joint. Instead, it acts to guide an artery through the fovea capitis to provide the major arterial blood supply to the head of the femur.
3. posterior

4. posterior
5. The ischium is the lowermost part of the pelvic girdle and supports most of the upper body weight in the sitting position.

### Case Study 8-4

1. Malignant cells lose their ability to adhere to adjoining cells so they are often carried via the blood stream or lymphatic circulation. When they settle in the new sites, they continue to divide and reproduce other malignant cells forming metastases.
2. Yes, even though the malignant cells are categorized as a soft tissue, they have osteolytic capabilities enabling the neoplastic cells to grow through bony structures within the body.
3. Anterior
4. Originating on the anterior superior iliac spine, the sartorius muscle inserts on the upper medial tibia, and acts to flex and rotates the thigh laterally.
5. Larger since the gluteus maximus covers all of the smaller muscles posterior to the hip joint.

### Case Study 8-5

1. No, although the malignant cells can move to any part of the body, it would be highly unlikely that they would form a symmetrical arrangement within the femurs.
2. Yes, high activity can be seen in both knees and is most evident on the upper right knee.
3. The increase metabolism in the region of the knees was attributed to a healing process related to a history of osteoarthritis affecting both knees.
4. High, since the primary site was in the breast and multiple metastatic sites were found in the body including the lymphatic system.
5. Poor, since the disease has already spread to other parts of the body.

### Case Study 8-6

1. The ankle joint is considered a ginglymus, or hinge-type, joint that allows dorsiflexion and plantar flexion.
2. The other movements of the foot are the result of articulations between the tarsal bones—calcaneus, talus, cuboid, navicular, and cuneiforms—which are considered arthrodial joints, because they are capable of gliding movements and have limited rotation.
3. Each calcaneus or heel bone carries approximately 25% of the body's weight in the standing position
4. Talus
5. Lateral



# Appendix B

## Glossary

### A

- Abduct.** To move away from midline; opposite of adduct.  
**Adduct.** To move toward the midline of the body; opposite of abduct.  
**Afferent.** Carrying toward a center.  
**Alveolus.** A small, hollow area or cavity; bony socket of a tooth; pouch in lung air sac.  
**Ampulla.** A saclike dilation of a duct or tube.  
**Annulus.** A ring-shaped opening or structure.  
**Antrum.** A nearly closed cavity or chamber; often within a bone.  
**Artery.** A blood vessel that carries blood away from the heart.  
**Articular.** Refers to an articulation or a joint.  
**Articulation.** A joint or connection between bones.  
**Atrophy.** A wasting away of tissue; results in a decrease in tissue size.  
**Axial plane.** A section perpendicular to the median.  
**Axillary.** Pertaining to the armpit.  
**Axon.** The process of a neuron that carries the impulse away from the cell body.  
**Azygos.** Certain vessels or nerves not in pairs.

### B

- Benign neoplasm.** An abnormal slow growth of tissue that remains discrete in an area.  
**Bifurcate.** To divide or separate into two parts.  
**Body.** The broadest or longest mass of a structure.  
**Brachial.** Pertaining to the arm.  
**Bursa.** A sac or pouch of synovial fluid located between friction points, especially in the region of the joints.

### C

- Cancer.** A malignant, invasive growth of abnormal tissue that has the capability to spread throughout the body.  
**Cardiac.** Pertaining to the heart.  
**Cartilage.** A tough fibrous connective tissue.  
**Central nervous system.** The brain and the spinal cord.  
**Chronic.** Persisting for a long time.  
**Concave.** Having a curved, depressed surface.  
**Condyle.** A rounded projection at the end of a bone that articulates with another bone.  
**Convex.** Having a curved protruding surface.

- Coronal plane.** A longitudinal section that runs at right angles to sagittal planes dividing the body into anterior and posterior parts.  
**Cortex.** The outer surface layer of an organ.  
**Costal.** Pertaining to the ribs.  
**Cranial.** Pertaining to the skull.  
**Crest.** A bony ridge or border.  
**Cruciate ligaments.** Overlapping or cross-shaped structures.  
**Cyst.** A sac with a distinct wall containing fluid or other material.

### D

- Dendrite.** The process of a neuron that conducts the impulse toward the cell body.  
**Diaphragm.** Any partition that separates one area from another.  
**Diarthrosis.** A freely movable joint.  
**Dislocation.** Displacement of a bone from a joint space.  
**Distal.** Farthest from the center or the midpoint.  
**Dorsal.** Pertaining to the back or posterior.  
**Duct.** A canal or passageway.

### E

- Edema.** An abnormal accumulation of fluid within the body causing swelling.  
**Efferent.** Carrying away from an area or an organ.  
**Epicondyle.** An elevation near a condyle.  
**Extremity.** A limb, such as the arm or the leg.

### F

- Fascia.** A connective tissue wrapping around muscular structures and other tissues.  
**Fissure.** A groove or cleft.  
**Flexor.** A muscle that decreases the angle between bones.  
**Foramen.** A hole or opening in a bone or between body cavities.  
**Fossa.** A shallow depression often forming an articular surface.  
**Fovea.** A small pit or depression for attachment rather than articulation.  
**Fundus.** The base of an organ.

## G

**Ganglion.** A group of nerve cell bodies usually located outside the central nervous system.

**Genu.** Any structure that resembles a flexed knee.

**Gland.** An organ specialized to secrete or excrete substances within the body.

**Glenoid.** Having the form of a shallow cavity or articular depression or socket of a joint.

**Gyrus.** A convolution on the outer cerebral cortex.

## H

**Hematoma.** A blood clot located outside a blood vessel.

**Hypertrophy.** An increase in the size of a tissue or organ beyond normal growth.

## I

**Inguinal.** Pertaining to the groin region near the thigh.

**Innervation.** The supply or distribution of nerve stimuli to a part.

**Insertion.** The place of attachment for a muscle on the movable end.

**Invert.** To turn inward.

## J

**Joint.** The junction of two or more bones forming an articulation.

**Jugular.** Belonging to the neck.

## L

**Labia.** A lip-like structure.

**Lacrimal.** Pertaining to tears.

**Lamina.** A plate or thin layer.

**Ligament.** A concentration of fibrous tissue connecting bones or parts.

**Lobe.** A curved or rounded structure or projection.

**Lumen.** The space inside a tube.

**Lymph.** The watery fluid in lymph vessels.

## M

**Malignant.** Pertains to diseases that are likely to spread.

**Meatus.** The external opening of a canal.

**Medial.** Toward the midline of the body.

**Mesentery.** The double layer of peritoneum that attaches the intestine to the posterior abdominal wall.

**Mucous membranes.** The membranes that line the digestive, respiratory, reproductive, and urinary tracts.

**Muscle.** Organ capable of contraction and producing movement.

**Myelin.** The white substance forming a sheath around the axon of some nerve cells.

## N

**Nasal.** Relating to the nose.

**Neoplasm.** Any new and abnormal growth of tissue.

**Nerve.** A group of nerve cell fibers found outside the central nervous system.

**Neuron.** The basic unit of the nervous system made up of the nerve cell body plus its processes.

**Nucleus.** A collection or concentration of nerve cell bodies within the central nervous system.

## O

**Omentum.** Folds of peritoneum connecting the abdominal viscera with the stomach.

**Optic.** Pertaining to the eye.

**Organ.** A part of the body composed of two or more tissues to perform a specialized function.

**Origin.** The end of attachment of a muscle that remains fixed during contraction.

## P

**Palate.** The roof of the mouth.

**Palmar.** The anterior surface of the hands.

**Palpation.** Examination by touch.

**Parenchyma.** The functional or glandular components of an organ.

**Peripheral nervous system.** A system of nerves connecting the outer parts of the body with the central nervous system.

**Plexus.** A network of nerves, blood vessels, or lymphatics.

**Proximal.** Toward the attached end of a limb or the center.

**Pulmonary.** Pertaining to the lungs.

## R

**Ramus.** A branch of a bone, vessel, or nerve.

**Renal.** Pertaining to the kidney.

## S

**Spine.** A short, pointed projection of bone.

**Stroma.** The supportive elements of an organ including connective tissue, nerves, and vessels.

**Sulcus.** A furrow or linear groove that is not as deep as a fissure.



## 628 Introduction to Sectional Anatomy

**Supine.** The body lying horizontally with the face upward.

**Suture.** Immovable joints that bind bones together.

**Symphysis.** A slightly movable joint between the right and left sides of the pelvis, which join in the midline.

**Systemic.** Pertaining to the whole body.

### T

**Tendon.** A dense band of fibrous tissue that joins a muscle to a bone.

**Tissue.** A group of similar cells that form a distinct structure.

**Trauma.** An injury or wound usually produced by external forces acting on the body.

**Trochanter.** A large blunt process.

**Trochlea.** A spool-shaped or pulleylike articular surface.

**Tubercle.** A small rounded process or bump.

**Tuberosity.** A large conspicuous bump, larger than a tubercle.

**Tumor.** An abnormal growth of cells.

### V

**Vas.** A duct or vessel that conveys a liquid.

**Vein.** A vessel carrying blood away from the tissue toward the heart.

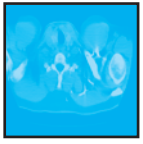
**Ventral.** Toward the anterior or the front.

**Ventricle.** A small cavity or pouch; found in the heart and brain.

**Vesicle.** A liquid filled pouch or sac.

**Vestibule.** A chamber or space resembling an entrance to some other body cavity or space.

**Viscera.** The internal organs.



# Appendix C

## Bibliography

### A

- Afifi AK, Bergman RA. *Basic Neuroanatomy*. 2nd ed. Baltimore: McGraw-Hill Medical; 2005.
- Agur AMR, Dalley AF. *Grant's Atlas of Anatomy*. 11th ed. Philadelphia: Lippincott Williams & Wilkins; 2004.
- Akesson EJ, Loeb JA, Wilson-Pauwels L. *Thomson's Core Textbook of Anatomy*. 2nd ed. Philadelphia: Lippincott; 1990.
- Anderson D, Keith J, Novak P, et al. *Dorland's Illustrated Medical Dictionary*. 28th ed. Philadelphia: Saunders; 1994.
- Anderson JE. *Grant's Atlas of Anatomy*. 8th ed. Baltimore: Williams & Wilkins; 1983.

### B

- Ballinger PW, Frank ED. *Merill's Atlas of Radiographic Positions and Radiologic Procedures*. 10th ed. St. Louis: Mosby; 2003.
- Barrett CP, Anderson, LD, Holder LE, et al. *Primer of Sectional Anatomy with MRI and CT Correlation*. 2nd ed. Baltimore: Williams & Wilkins; 1994.
- Basmajian JV, Slonecker CE. *Grant's Method of Anatomy*. 11th ed. Baltimore: Williams & Wilkins; 1989.
- Bates B. *A Guide to Physical Examination*. 3rd ed. Philadelphia: Lippincott; 1983.
- Berquist TH. *Pocket Atlas of MRI Body Anatomy*. 2nd ed. Philadelphia: Lippincott & Raven; 1995.
- Bo W, Wolfman N, Krueger W, et al. *Basic Atlas of Sectional Anatomy with Correlated Imaging*. 2nd ed. Philadelphia: Saunders; 1990.
- Bontrager KL, Lampignano J. *Textbook of Radiographic Positioning and Related Anatomy*. 4th ed. St. Louis: Elsevier Mosby; 2005.

### C

- Cahill DR, Orland MJ. *Atlas of Human Cross-sectional Anatomy*. Philadelphia: Lea & Febiger; 1984.
- Christoforidis JA. *Atlas of Axial, Sagittal, and Coronal Anatomy with CT and MRI*. Philadelphia: Saunders; 1988.
- Clemente CD, ed. *Gray's Anatomy of the Human Body*. 30th ed. Philadelphia: Lea & Febiger; 1985.

- Clemente CD. *Clemente's Dissector*. Philadelphia: Lippincott Williams & Wilkins; 2002.
- Crafts RC. *A Textbook of Human Anatomy*. 3rd ed. New York: Churchill Livingstone; 1985.
- Crowley LV. *An Introduction to Human Disease*. Sudbury: Jones and Bartlett; 2007.

### D

- Damjanov I. *Pathology for the Health Professions*. St. Louis: Elsevier Saunders; 2006.

### E

- Eisenberg RL. *Clinical Imaging: An Atlas of Differential Diagnosis*. 2nd ed. Gaithersburg, MD: Aspen; 1992.
- Eisenberg RL, Johnson NM. *Comprehensive Radiographic Pathology*. St. Louis: Mosby; 2003.
- Ellis H, Logan BM, Dixon A. *Human Cross-sectional Anatomy Atlas of Body Sections and CT Images*. Oxford, UK: Butterworth-Heinemann; 1991.

### F

- Frick H, Kummer B, Putz R. *Wolf-Heidegger's Atlas of Human Anatomy*. 4th ed. Farmington, CT: Karger, 1990.

### G

- Gardner E, Gray DJ, O'Rahilly R. *Anatomy: A Regional Study of Human Structure*. 4th ed. Philadelphia: Saunders; 1975.
- Greathouse JS. *Radiographic Positioning and Procedures: A Comprehensive Approach*. Albany: Delmar; 2006.
- Grossman CG, Gonzalez CF, Palacio E. *Computed Brain and Orbital Tomography: Technique and Interpretation*. New York: Wiley; 1976.

### H

- Hamilton WJ, ed. *Textbook of Human Anatomy*. 2nd ed. St. Louis: Mosby; 1976.
- Hollinshead WH, Rosse C. *Textbook of Anatomy*. 4th ed. New York: Harper & Row; 1985.

## 630 Introduction to Sectional Anatomy

House EL, Rosse C. *A Systemic Approach to Neuroanatomy*. 3rd ed. New York: McGraw-Hill; 1979.

### I

International Anatomical Nomenclature Committee. *Nomina Anatomica*. 6th ed. Baltimore: Waverly; 1989.

### L

Lane A, Sharfaei H. *Modern Sectional Anatomy*. Philadelphia: Saunders; 1992.

Langman J, Woerdeman MW. *Atlas of Medical Anatomy*. Philadelphia: Saunders; 1982.

Laudicina PF. *Applied Pathology for Radiographers*. Philadelphia: Saunders; 1989.

Lee JKT, Sagel SS, Stanley RJ. *Computed Body Tomography with MRI Correlation*. 2nd ed. New York: Raven; 1989.

### M

Mace DM, Kowalczyk N. *Radiographic Pathology for Technologists*. 4th ed. St. Louis: Mosby Year Book; 2004.

Martini FH, Timmons MJ, Tallitsch RB. *Human Anatomy*. 5th ed. San Francisco: Pearson Benjamin Cummings; 2006.

McGrath P, Mills P. *Atlas of Sectional Anatomy*. Farmington, CT: Karger; 1985.

McMinn RMH, Hutchings RT. *Color Atlas of Human Anatomy*. 2nd ed. Chicago: Year Book Medical; 1988.

Meschan I. *An Atlas of Anatomy Basic to Radiology*. Philadelphia: Lea & Febiger; 1975.

Moore KL, Dalley AF. *Clinically Oriented Anatomy*. 5th ed. Baltimore: Williams & Wilkins; 2005.

Moore KL, Agur AMR. *Essential Clinical Anatomy*. Philadelphia: Lippincott Williams & Wilkins; 2006.

### N

Nolte J. *The Human Brain*. 3rd ed. St. Louis: Mosby; 1992.

Norkin C, LeVange P. *Joint Structure and Function: A Comprehensive Analysis*. Philadelphia: FA Davis; 1983.

Novellin RA, Squire LF. *Living Anatomy, a Working Atlas Using Computed Tomography, Magnetic Resonance and Angiography Images*. Philadelphia: Hanley & Belfus; 1987.

### P

Pansky B. *Review of Gross Anatomy*. 6th ed. New York: Macmillan; 1996.

### R

Robbins SL, Kumar V. *Basic Pathology*. 4th ed. Philadelphia: Saunders; 1987.

Rodgers AW. *Textbook of Anatomy*. New York: Churchill Livingstone; 1992.

Romanes GJ, ed. *Cunningham's Manuals of Practical Anatomy*. 15th ed. London: Oxford University Press; 1986.

### S

Seeram ERT. *Computed Tomography Technology*. Philadelphia: Saunders; 1982.

Slaby FJ, McCune SK, Summers RW. *Gross Anatomy in the Practice of Medicine*. Philadelphia: Lea & Febiger; 1994.

Smith JW, Murphy TR, Blair JSG, et al. *Regional Anatomy Illustrated*. New York: Churchill Livingstone; 1983.

Snell RS. *Clinical Anatomy for Medical Students*. 4th ed. Boston: Little, Brown; 1992.

Soderberg GL. *Kinesiology, Application to Pathological Motion*. Baltimore: Williams & Wilkins; 1986.

*Stedman's Medical Dictionary for the Health Professions and Nursing*. 5th ed. Philadelphia: Lippincott Williams & Wilkins; 2005.

### T

Tortora GR, Anagnostakos NP. *Principles of Anatomy and Physiology*. 4th ed. New York: Harper & Row; 1984.

Twietmeyer A, McCracken T. *Regional Guide to Human Anatomy*. Philadelphia: Lea & Febiger; 1988.

### W

Wagner M, Lawson TL. *Segmental Anatomy*. New York: Macmillan; 1982.

Wegener OH. *Whole Body Computed Tomography*. 2nd ed. Boston: Blackwell Scientific; 1992.

Weir J, Abrahams PH, eds. *An Imaging Atlas of Human Anatomy*. St. Louis: Mosby Year Book; 1992.

Wicke L. *Atlas of Radiologic Anatomy*. 5th ed. Philadelphia: Lea & Febiger; 1994.

Williams PL, Warwick R, eds. *Gray's Anatomy*. 36th ed. Philadelphia: Saunders; 1980.

Woodburne RT. *Essentials of Human Anatomy*. 9th ed. New York: Oxford University Press; 1994.

# Index

NOTE: Page numbers followed by *f* indicate figure.

## A

- Abdomen, 101–174  
anatomical overview of, 101–115  
arteries in, 108–110  
cavity/contents (anterior view) in, 104*f*, 105*f*  
enclosing structures in, 101–102, 102*f*  
median sagittal view in, 103*f*  
muscles in, 115  
skeletal parts in, 101  
veins in, 110, 113*f*, 114–115  
viscera in, 102–108, 103*f*–108*f*  
wall (posterior) in, 114*f*  
case studies  
colorectal carcinoma and PET/CT scan in, 172*f*, 173  
gallbladder and ultrasound image in, 166, 166*f*  
gallbladder carcinoma and ultrasound image in, 168, 168*f*  
renal arterial blood flow and MRA and, 164, 164*f*  
renal transplant and MRA in, 165, 165*f*  
stomach carcinoma and PET/CT scan in, 170*f*, 171, 308*f*, 309  
CT images (axial) of, 116, 116*f*–163*f*  
Abdominis muscle, transverse, 114*f*  
Abducens nerves, 318, 324*f*  
Abductor digiti minimi muscle, 566, 566*f*, 569*f*, 571*f*  
Abductor pollicis brevis muscle, 566, 566*f*, 569*f*, 571*f*  
Absorption values, 3, 4*f*  
Acetabular fossa, 575*f*, 577*f*  
Acetabular labrum, 572*f*  
Acetabulum, 176*f*, 177*f*, 572  
Achilles tendon, 598*f*  
Acoustic nerves, 318, 324*f*  
Acromion process, 10*f*, 11, 39*f*, 543, 544*f*, 547*f*, 549*f*, 551*f*, 553*f*  
Adductor longus, 573*f*  
Adductor magnus, 573*f*, 579*f*  
Adductor minimus, 573*f*  
Adductor pollicis, 565*f*  
Adnexal area(s), 185  
left, 261*f*, 263*f*, 295*f*  
right, 293*f*  
Adrenal gland(s), 108, 109*f*, 114*f*  
left, 129*f*, 131*f*, 133*f*  
right, 127*f*, 129*f*  
Air cells, 313  
ethmoid, 391*f*  
mastoid, 333*f*, 335*f*, 391*f*, 395*f*, 397*f*, 447*f*  
Amphiarthrosis joints, 3  
Amygdaloid body, 322*f*  
Anal sphincter, 297*f*, 299*f*, 301*f*  
Ankle, 596–609  
anatomical overview of, 596–599  
musculature in, 598, 598*f*, 599*f*  
skeletal parts in, 596, 597*f*  
bones of  
dorsal view of, 597*f*  
plantar view of, 597*f*  
MR images of  
axial, 604, 604*f*–609*f*  
sagittal, 600, 600*f*–603*f*  
muscles/tendons  
lateral view of, 599*f*  
medial view of, 598*f*  
Anterior arch, 433, 434*f*  
Anulus fibrosus, 497, 497*f*, 505*f*, 509*f*, 511*f*, 513*f*, 523*f*, 525*f*, 529*f*  
Aorta, 12*f*, 17, 105*f*, 111*f*, 112*f*, 179*f*  
abdominal, 105*f*, 108, 145*f*, 147*f*, 149*f*, 151*f*, 153*f*, 287*f*  
bifurcation of, 155*f*  
lower, 112*f*  
ascending, 17, 18*f*, 35*f*, 59*f*, 61*f*, 63*f*, 65*f*, 67*f*  
descending, 17, 20*f*, 35*f*, 37*f*, 59*f*, 61*f*, 63*f*, 71*f*, 73*f*, 75*f*, 77*f*, 81*f*, 87*f*, 89*f*, 104*f*, 117*f*, 119*f*, 121*f*, 123*f*, 125*f*, 131*f*, 135*f*, 139*f*, 143*f*  
Aortic arch, 17, 17*f*, 18*f*, 27*f*, 29*f*, 31*f*, 33*f*, 35*f*, 37*f*, 55*f*, 57*f*, 440*f*  
axial sections of, 3, 3*f*  
bottom of, 59*f*  
wall of, 25*f*  
Aortic hiatus, 102*f*  
Appendix, 105*f*  
Arachnoid granulation, 318*f*  
Arachnoid mater, 318*f*, 323, 324*f*, 499, 499*f*  
spinal, 318*f*  
Arcuate ligament  
lateral, 102*f*  
medial, 102*f*  
Arteries. *See specific arteries*  
Arthrodia joints, 3  
Articular capsule, 555*f*, 561*f*, 572*f*  
Articular cartilage, 544–545, 544*f*, 551*f*, 585*f*, 587*f*  
glenoid fossa, 553*f*  
Articular cavity, 572*f*  
Articular facet  
inferior, 434*f*  
superior, 434*f*  
Articular process, 434–435, 496  
inferior, 495*f*, 515*f*  
L2, 523*f*, 525*f*  
L5, 527*f*, 529*f*  
superior, 435*f*, 494*f*, 495*f*, 496*f*, 515*f*  
L3, 523*f*, 525*f*  
S1, 527*f*, 529*f*  
Articular surface, 496*f*, 593*f*  
Aryepiglottic folds, 435, 438*f*, 439*f*, 440*f*, 469*f*  
Arytenoid cartilages, 435, 437*f*, 443*f*, 445*f*, 471*f*, 473*f*  
Arytenoid muscle, transverse, 438*f*  
Atherosclerotic disease, 483  
neck CTA and, 482*f*, 483  
Atlas, 433, 434*f*, 451*f*, 494*f*  
anterior arch of, 447*f*  
superior view of, 434*f*  
Atrium, 73*f*  
left, 16, 16*f*, 17*f*, 27*f*, 29*f*, 31*f*, 33*f*, 35*f*, 37*f*, 65*f*, 67*f*, 69*f*, 71*f*, 73*f*  
right, 16, 16*f*, 17*f*, 25*f*, 27*f*, 29*f*, 67*f*, 69*f*, 71*f*, 75*f*, 77*f*, 79*f*  
Auditory canal, internal, 316*f*, 317  
Auditory meatus, external, 314*f*, 315*f*, 316, 331*f*, 391*f*  
Auricle, 391*f*, 453*f*

- Axial plane, 3, 4*f*  
Axillary arteries, 16*f*, 17*f*, 18, 18*f*, 19*f*, 441*f*  
left, 45*f*  
Axillary recess, 544*f*, 545, 551*f*  
Axillary veins, 19, 20*f*  
left, 41*f*  
right, 441*f*  
Axillary vessels, 549*f*  
Axis, 433, 434*f*, 494*f*  
body of, 434*f*  
lateral view of, 434*f*  
Azygos arch, 57*f*  
Azygos vein, 12*f*, 19, 21, 21*f*, 75*f*, 79*f*, 83*f*, 87*f*, 89*f*, 117*f*, 119*f*, 121*f*, 123*f*, 125*f*
- ## B
- Basal ganglia, 322*f*, 323*f*  
Basilar arteries, 326, 326*f*, 393*f*, 395*f*, 397*f*  
Basivertebral vein, 509*f*  
Biceps brachii muscle  
long head of, 544*f*, 545  
short head of, 544*f*, 545  
Biceps femoris (long head), 573*f*, 581*f*  
Biceps muscle, 555*f*, 557*f*, 561*f*, 563*f*  
Bifid spinous process, C3, 463*f*  
Bile duct  
anterior view of, 107*f*  
common, 106*f*, 107, 107*f*, 108*f*, 133*f*  
Bladder, 103*f*, 205*f*, 207*f*, 209*f*, 211*f*, 213*f*, 215*f*, 217*f*, 219*f*, 255*f*, 257*f*, 259*f*, 261*f*, 263*f*, 265*f*, 281*f*, 283*f*, 287*f*, 289*f*, 291*f*  
bottom of, 267*f*  
female, 182, 183*f*  
male, 180, 182, 182*f*  
posterior, 293*f*, 295*f*, 297*f*  
posterior wall of, 291*f*  
top of, 203*f*  
Bony orbit, fat in, 337*f*  
Brachial artery, 561*f*  
Brachial muscles  
anterior view of, 544*f*  
posterior view of, 545*f*  
Brachialis muscle, 555, 555*f*, 557*f*, 561*f*, 563*f*  
Brachiocephalic artery, 16*f*, 17, 18*f*, 27*f*, 29*f*, 49*f*, 51*f*, 53*f*  
Brachiocephalic vein(s), 19, 21*f*  
left, 17*f*, 18*f*, 27*f*, 29*f*, 31*f*, 33*f*, 47*f*, 49*f*, 51*f*, 53*f*, 55*f*, 440*f*  
bifurcation of, 45*f*  
right, 17*f*, 18*f*, 20*f*, 47*f*, 49*f*, 51*f*, 53*f*, 55*f*, 440*f*, 441*f*  
Brachioradialis muscle, 555, 555*f*, 563*f*  
Brain, 319–323  
arteries of, 326–327  
inferior view of, 326*f*  
basal ganglia *v.* thalamic nuclei in  
axial section and, 322*f*  
coronal section and, 323*f*  
lateral view and, 322*f*  
outer coverings of, 324*f*  
stem (median sagittal view), 320*f*  
ventricular structures within, 327–329  
lateral view of, 327*f*

- Breast(s)  
 benign cysts in, 94, 94f  
 ultrasound and, 94, 94f  
 carcinoma in, 92f, 93  
 PET/CT scans and, 96–97, 96f, 310f, 311, 614f, 615, 616f, 617  
 ultrasound and, 92f, 93
- Broad ligaments, 183, 184f, 185  
 anterior layer of, 184f  
 anterior view of, 184f  
 ovary and sagittal section through, 184f  
 posterior layer of, 184f
- Bronchi, 14  
 left, 20f, 33f, 35f, 37f  
 lingular, 15f  
 lower lobe, 15f, 16  
 left, 15f, 67f  
 right, 15f, 69f  
 main, 14, 15f  
 left, 15f, 61f, 65f  
 right, 15f, 61f  
 middle lobe, 15f, 16  
 right, 15f, 69f  
 upper lobe, 14, 15f  
 left, 15f, 65f, 67f  
 right, 15f, 61f
- Bronchus intermedius, 14, 15f, 65f
- C**
- Calcaneus, 596, 597f, 598f, 601f, 603f, 605f, 607f, 609f
- Calvarial bone, 324f
- Capitate, 564f, 565, 569f, 571f
- Capitulum, 554, 554f, 559f, 563f
- Car accidents, spine CT scans and, 534f, 535, 536, 536f
- Carcinoma  
 breast  
 PET/CT scans and, 96–97, 96f, 310f, 311, 614f, 615, 616f, 617  
 ultrasound imaging of, 92f, 93  
 colorectal, 172f, 173  
 PET/CT scan and, 172f, 173  
 gallbladder, 168  
 ultrasound imaging of, 168, 168f  
 head and squamous cell, PET/CT scans in, 430f, 431  
 lung, PET/CT scans and, 98–99, 98f  
 PET/CT scan and laryngeal, 490f, 491  
 stomach, 170f, 171  
 PET/CT scans of, 170f, 171, 308f, 309  
 testicular, 306f, 307  
 ultrasound imaging and, 306, 307f
- Carina, 14, 15f, 61f
- Carotid artery(ies)  
 common, 16f, 17–18, 17f, 18f, 19f, 436, 438, 440f, 441f  
 left, 16f, 17f, 18f, 43f, 45f, 47f, 49f, 51f, 53f, 463f, 465f, 467f, 469f, 471f, 475f, 477f, 481f  
 right, 18f, 39f, 41f, 45f, 47f, 473f, 479f  
 external, 19f, 438, 441f  
 right, 459f, 461f  
 internal, 19f, 326f, 327, 371f, 373f, 389f, 395f, 438, 441f  
 right, 447f, 451f, 453f, 455f, 457f, 459f, 461f
- Carotid canal, 317f
- Carotid foramen, 317
- Case studies  
 abdomen  
 colorectal carcinoma and PET/CT scan in, 172f, 173  
 gallbladder and ultrasound image in, 166, 166f  
 gallbladder carcinoma and ultrasound image in, 168, 168f  
 renal arterial blood flow and MRA and, 164, 164f  
 renal transplant and MRA in, 165, 165f  
 stomach carcinoma and PET/CT scan in, 170f, 171, 308f, 309  
 chest, heart and CTAs in, 90–91, 90f, 91f  
 elbow, torsion fracture and CT scan in, 610, 610f  
 head  
 cerebrovascular disease and MRA in, 422f, 423  
 hydranencephaly and CT exam in, 428f, 429  
 hydranencephaly and ultrasound exam in, 426f, 427  
 hydrocephalus and ultrasound exam in, 424f, 425  
 meningioma and CTA in, 420f, 421  
 squamous cell carcinoma and PET/CT scans in, 430f, 431  
 neck  
 atherosclerotic disease and CTA in, 482f, 483  
 cerebrovascular disease and MRA in, 484, 484f  
 cyst and ultrasound in, 485, 485f  
 goiter and ultrasound in, 486f, 487  
 larynx carcinoma and PET/CT scan in, 490f, 491  
 melanoma and PET/CT scan in, 488f, 489  
 pelvis  
 abdominal aortic aneurysm and CT scan in, 304, 304f  
 aortobilateral iliac endografting and CT scan in, 302f, 303  
 prostate and ultrasound image in, 305, 305f  
 shotgun wound and CT scan in, 611, 611f  
 testicles and ultrasound image in, 306f, 307  
 spine  
 back pain and MR image in, 539, 539f  
 car accident and MR scan in, 538, 538f  
 car accidents and CT scans in, 534f, 535, 536, 536f  
 gunshot wound and CT scan in, 537, 537f  
 spondylolisthesis in, 540f, 541
- Cauda equina, 497, 498f, 507f, 509f, 511f, 519f, 521f, 523f
- Caudate lobe, 106f, 107, 125f, 127f
- Caudate nucleus, 321, 323f  
 body of, 321, 322f, 339f  
 head of, 321, 322f, 343f, 371f, 373f, 377f, 401f, 405f  
 tail of, 321, 322f, 405f
- Caval foramen, 102f
- Cecum, 104, 105f, 111f, 155f, 157f, 159f, 161f, 163f, 187f, 189f, 193f, 197f, 201f, 229f, 231f, 233f, 235f, 237f, 281f, 283f, 285f
- Celiac artery, 114f
- Celiac trunk, 109, 110f, 133f  
 branches of, 110f
- Central canal, 318f
- Central nervous system. *See also* Head  
 cerebrospinal circulation throughout, 328f  
 median sagittal drawing of, 318f
- Central sulcus, 319, 319f, 413f, 415f
- Cerebellar hemisphere, 347f  
 white matter, 349f
- Cerebellar tonsils, 319, 347f
- Cerebellar vermis, 393f, 403f  
 superior, 349f, 351f, 355f
- Cerebellum, 319, 320f, 335f, 337f, 339f, 341f, 357f, 397f, 399f, 401f, 445f, 447f
- Cerebral aqueduct, 318f, 320f, 327f, 328, 359f, 401f
- Cerebral artery(ies)  
 anterior, 326f, 327, 375f, 399f, 403f, 405f  
 inferior, 326f  
 middle, 326f, 327, 373f, 397f, 399f  
 posterior, 326, 326f, 397f, 399f, 401f  
 inferior, 326f
- Cerebral peduncles, 320f, 321, 323f, 345f, 361f, 401f
- Cerebral subarachnoid space, 318f
- Cerebrospinal circulation, central nervous system and, 328f
- Cerebrospinal fluid (CSF), 425
- Cerebrovascular disease, 423, 484  
 head MRA and, 422f, 423  
 neck MRA and, 484, 484f
- Cerebrum, 319  
 lateral view of, 319f
- Cervical nerves, 498f
- Cervical vertebrae, 433, 493, 494f  
 C1, 434f, 494f  
 anterior tubercle of, 449f  
 C2, 434f, 453f, 455f, 494f  
 C3, 434f, 457f, 459f, 461f, 494f  
 bifid spinous process of, 463f  
 spinous processes of, 465f  
 C4, 434f, 463f, 465f, 494f  
 spinous process of, 469f  
 C5, 434f, 467f, 469f, 471f, 494f  
 C6, 434f, 473f, 475f, 477f, 494f  
 spinous process of, 473f  
 C7, 434f, 435, 479f, 481f, 494f  
 superior view of, 435f, 494f  
 thoracic vertebra v., 436f
- Cervix, 183, 183f, 184f, 267f, 269f, 271f, 293f, 295f
- Cheek bones. *See* Zygomatic bone
- Chest, 9–100  
 anatomical overview of, 9–21  
 airway structures in, 13–16, 13f, 14f, 15f  
 apex in, 13f, 14f, 15f  
 arteries in, 17–18, 18f, 19f, 20f  
 enclosing structures in, 12–13, 12f  
 skeletal parts in, 9–12, 10f, 11f  
 veins in, 18–21, 20f, 21f  
 viscera in, 16–17, 16f, 17f  
 case studies, heart and CTAs in, 90–91, 90f, 91f  
 CT images (axial) of, 38, 38f–89f  
 MR images (sagittal) of, 22, 22f–37f
- Chiasmatic cistern, 328f
- Cholecystectomy, 168
- Cholelithiasis (gallstones), 166, 168
- Choroid plexus, 407f  
 of fourth ventricle, 318f, 328f  
 of lateral ventricle, 318f, 328f  
 of third ventricle, 318f, 320f, 328f, 405f
- Circle of Willis, 326
- Cisterna magna, 318f, 328f, 329, 347f
- Clastrum, 321, 322f, 323, 323f
- Clavicles, 9, 10f, 11f, 39f, 441f, 553f  
 left, 47f, 49f, 51f
- Clinoid process  
 anterior, 316, 316f, 395f  
 posterior, 316, 316f
- Clivus, 315f, 316, 345f, 389f
- Coccygeus muscle, 179f, 180, 181f
- Coccyx, 176f, 177, 181f, 215f, 259f, 261f, 434f, 494f, 496, 496f, 575f, 577f  
 tip of, 263f, 265f
- Colic artery  
 left, 112f  
 middle, 111f, 112f  
 right, 111f



- Colic vein  
left, 113f  
middle, 113f  
right, 113f
- Collateral ligament  
lateral, 579f, 580, 580f, 581f, 589f, 591f  
medial, 579f, 580, 580f, 581f, 589f, 591f, 593f, 595f
- Colon  
ascending, 104, 105f, 111f, 145f, 147f, 149f, 151f, 153f  
carcinoma of rectum and, 172f, 173  
descending, 105f, 106, 111f, 112f, 129f, 131f, 133f, 135f, 137f, 139f, 141f, 143f, 145f, 149f, 151f, 153f, 155f, 157f, 159f, 161f, 163f, 189f, 193f, 195f, 197f, 201f, 203f, 229f, 231f, 235f, 237f, 239f, 243f, 245f, 247f, 281f, 283f, 285f  
hepatic flexure of, 105f, 106, 137f, 141f, 143f  
meso-, 103f  
sigmoid, 103f, 105f, 112f, 178, 179f, 180f, 205f, 239f, 241f, 243f, 245f, 247f, 249f, 251f, 253f, 255f, 281f, 283f, 287f, 289f, 291f, 293f, 295f, 297f, 299f, 301f  
fecal matter in, 257f  
top of, 201f, 203f  
splenic flexure of, 85f, 87f, 89f, 105f, 106, 125f, 127f  
transverse, 103f, 105f, 106, 111f, 112f, 129f, 131f, 133f, 135f, 137f, 139f, 141f, 143f, 145f  
superior reflection of, 111f
- Commissure  
anterior, 320, 320f, 345f  
posterior, 320, 320f
- Communicating arteries  
anterior, 326f, 327  
posterior, 326–327, 326f
- Computed tomography angiographs (CTAs), 90  
atherosclerotic disease and neck, 482f, 483  
case studies and heart, 90–91, 90f, 91f  
meningioma and head, 420f, 421
- Computed tomography (CT) images, 3  
abdomen and axial computed, 116, 116f–163f  
case studies  
abdominal aortic aneurysm and, 304, 304f  
aortobilateral iliac endografting and, 302f, 303  
car accidents and spine in, 534f, 535, 536, 536f  
gunshot wound and spine in, 537, 537f  
shotgun wound and pelvis in, 611, 611f  
torsion fracture of elbow in, 610, 610f  
chest and axial computed, 38, 38f–89f  
description of, 1–2, 3  
head  
axial computed, 388, 388f–419f  
coronal computed, 378, 378f–387f  
hydranencephaly in, 428f, 429  
hip and axial computed, 574, 574f–577f  
neck and axial computed, 446, 446f–481f  
pelvis and axial computed  
female, 228, 228f–279f  
male, 186, 186f–227f  
PET scan combined with, 5, 7f  
breast carcinoma and, 96–97, 96f, 310f, 311, 614f, 615, 616f, 617  
colorectal carcinoma and, 172f, 173  
larynx carcinoma in, 490f, 491  
lung carcinoma and, 98–99, 98f  
neck melanoma in, 488f, 489  
squamous cell carcinoma of head in, 430f, 431  
stomach carcinoma and, 170f, 171, 308f, 309  
sectional images, 1–3  
spine and axial computed, 516, 516f–533f  
wrist and axial computed, 568, 568f–571f
- Concha  
inferior, 314f  
right, 381f, 383f, 387f  
middle, 314f  
right, 385f, 387f  
superior, 314f
- Condylar fossa, 317f
- Condyle(s), 314  
femoral  
lateral, 587f, 589f, 591f, 595f  
medial, 589f, 591f, 595f  
lateral, 579f, 581f  
mandibular, 315f, 389f  
medial, 579f, 581f  
occipital, 317f
- Conus medullaris, 497, 498f, 509f, 511f
- Coracobrachialis muscle, 544f, 545
- Coracoid process, 10f, 11, 43f, 544f
- Cornea, right, 379f
- Corona radiata, 323, 323f, 359f, 415f
- Coronal plane, 3, 4f
- Coronoid fossa, 554, 554f, 561f
- Coronoid process, 554, 555f, 559f, 561f
- Corpus callosum, 320, 323f, 343f  
body of, 320f, 365f, 369f, 371f, 409f  
genu of, 320, 320f, 345f, 377f, 401f, 407f  
splenium of, 320, 320f, 322f, 345f, 357f, 407f
- Corpus cavernosum, 182, 225f, 227f
- Corpus spongiosum, 182, 182f, 225f, 227f
- Cortical bone, anterior, 503f
- Costal facet  
inferior, 495f  
superior, 495f
- Costal pleura, 12f
- Costodiaphragmatic recesses, 12f, 13
- Costophrenic angle, 89f
- Cowper's gland, 182f
- Cranial nerves, 317–319
- Cribriform foramen, 317
- Cribriform plate, 313, 314f, 316f, 385f, 387f, 393f
- Cricoid cartilage, 435, 436f, 437f, 443f, 445f  
mucosa of, 439f
- Crista galli, 313, 314f, 316f, 385f, 387f
- Cruciate ligament  
anterior, 579f, 580, 580f, 581f, 583f, 585f, 589f, 591f, 593f, 595f  
posterior, 579f, 580, 580f, 581f, 583f, 585f, 589f, 591f, 593f, 595f
- CSF. *See* Cerebrospinal fluid (CSF)
- CT images. *See* Computed tomography images
- CTAs. *See* Computed tomography angiographs
- Cuboid, 596, 597f, 603f, 609f
- Cuneiform(s), 596, 597f  
first, 601f, 609f  
second, 603f, 609f  
third, 603f, 609f
- Cystic duct, 106f, 107f
- Cystic vein, 113f
- Cysts  
ultrasound and breast, 94, 94f  
ultrasound and thyroid gland, 485, 485f
- D**
- Deltoid muscle, 544f, 545, 547f, 549f, 551f
- Dens, 433–434, 434f, 445f, 447f, 449f, 451f
- Denticulate ligament, 499f
- Diaphragm, 12f, 13, 17f, 101. *See also* Pelvic diaphragm  
crura (crus) of, 101–102, 102f  
left, 125f  
right, 123f, 125f, 131f  
interior surface of, 102f
- Diaphragmatic pleura, 12f
- Diarthrosis joints, 3
- Dorsal interosseus, first, 565f
- Dorsum sellae, 316, 316f, 395f, 397f
- Ductus deferens, 182f
- Duodenum, 103, 103f, 104f, 108f, 135f, 137f, 147f  
ascending, 104f  
descending, 104f  
inferior, 104f  
superior, 104f
- Dura mater, 323, 324f, 499, 499f  
cerebral, 318f  
meningeal, 318f  
periosteal, 318f  
spinal, 318f
- Dural sacs, 517f, 519f, 521f, 525f, 527f, 533f  
edge of, 505f, 513f
- Dural veins, 325–326
- E**
- Ear  
auricle of, 391f, 453f  
middle, 395f
- Elbow, 554–563  
anatomical overview of, 554–555  
musculature in, 555, 555f  
skeletal parts in, 554, 555f  
case study, torsion fracture and CT scan in, 610, 610f  
coronal section of, 555f  
MR images  
axial computed, 556, 556f, 557f  
coronal, 558, 558f, 559f  
sagittal, 560, 560f–563f  
sagittal section of, 555f
- Ellipsoid joints, 3
- Emergency Medical Information (EMI)  
scale, 4f
- EMI scale. *See* Emergency Medical Information scale
- Enarthrosis joints, 3
- Endograft, 303  
CT scan and aortobilateral iliac, 302f, 303
- Epicondyle(s), 555f  
lateral, 554, 554f, 557f, 559f  
medial, 554, 554f, 557f, 559f
- Epidural space, 499f, 517f, 527f, 529f, 531f
- Epiglottic cartilage, 437f
- Epiglottis, 435, 438f, 439f, 440f, 443f, 445f, 463f, 465f, 467f
- Epiplioic branches, 110f
- Esophageal hiatus, 102f
- Esophageal plexus, 113f
- Esophageal veins, 113f
- Esophagus, 16–17, 20f, 27f, 39f, 45f, 49f, 51f, 53f, 55f, 57f, 63f, 67f, 71f, 73f, 75f, 77f, 79f, 83f, 85f, 104f, 117f, 119f, 121f, 436, 439f, 443f, 445f, 475f, 477f, 479f, 481f
- Ethmoid bone, 313, 314f
- Ethmoid sinuses, 313, 314f
- Ethmoid spine, 316f
- Extensor carpi radialis brevis, 565f
- Extensor carpi radialis longus, 565f, 566f, 567
- Extensor carpi ulnaris, 565f, 566, 566f
- Extensor digiti minimi, 565f, 566, 566f
- Extensor digitorum tendon, 565f, 566f, 567, 605f  
longus, 598, 599f, 607f

Extensor expansion, 565f  
 Extensor hallucis longus tendon, 598, 598f, 599f, 605f, 607f  
 Extensor indicis, 566f, 567  
 Extensor pollicis brevis, 565f  
 Extensor pollicis longus, 565f, 566f, 567  
 Extensor retinaculum, 565f  
   inferior, 598f, 599f  
   superior, 598f, 599f  
 Extensor tendon, 565f, 569f, 571f  
 External capsule, 321, 322f, 323f  
 Extreme capsule, 322f, 323, 323f  
 Eye  
   globe of, 337f, 389f, 391f  
     upper, 393f  
   left, 383f, 385f  
   lens of, 389f  
 Eyelid, right upper, 379f

## F

Facial artery, 19f, 441f  
 Facial nerves, 318, 324f  
 Facial vein, 440f  
 Falciform ligament, 106f  
 False ribs, 11, 12  
 Falx cerebelli, 324, 324f, 399f  
 Falx cerebri, 324, 324f, 347f, 351f, 365f, 399f, 409f, 411f, 413f, 415f, 417f, 419f  
 FDG (fluorodeoxyglucose), 5, 96, 97, 173, 308, 311, 489, 491  
 Femora. *See* Femur(s)  
 Femoral artery(ies), 178–179  
   left, 213f, 215f, 217f, 221f, 225f, 263f, 265f  
   right, 219f, 223f, 261f, 267f  
 Femoral sheath, contents of, 273f  
 Femoral vein(s), 179  
   left, 213f, 215f, 217f, 221f, 225f, 263f, 265f  
   right, 219f, 223f, 261f, 267f  
 Femoral vessels  
   left, 227f, 277f, 279f  
   right, 269f, 271f, 275f  
 Femoropatellar joint, 587f  
 Femur(s), 177–178, 178f, 572, 578, 583f, 585f. *See also* Trochanter  
   anterior/posterior surface of, 178f  
   body of, 572f  
   head of, 572, 572f, 575f, 577f  
   left, 225f  
     head of, 211f, 213f, 215f, 287f  
     neck of, 221f, 267f  
     posterior head of, 295f, 297f  
     shaft of, 227f, 289f  
   neck of, 223f, 291f, 572, 572f  
   right, 271f  
     head of, 217f, 259f, 261f, 263f, 265f, 285f, 291f  
     neck of, 269f  
     shaft of, 273f, 275f, 277f, 279f  
     shaft of, 593f  
 Fibrous capsule, 109f, 555f  
 Fibula, 578, 579f  
   head of, 579f, 587f  
 Filum terminale, 498f  
 Fissure  
   horizontal, 13f, 14, 14f  
   oblique, 13f, 14, 14f  
 Flexor digitorum longus tendon, 598, 598f, 605f, 607f  
 Flexor digitorum profundus tendon, 566, 566f, 569f, 571f  
 Flexor digitorum superficialis tendon, 566, 566f, 569f, 571f

Flexor hallucis longus tendon, 598, 598f, 605f, 607f  
   groove for, 597f  
 Flexor retinaculum, 598f  
 Floating ribs, 11, 11f  
 Fluorodeoxyglucose. *See* FDG  
 Foot  
   bones of  
     dorsal view of, 597f  
     plantar view of, 597f  
   muscles/tendons of  
     lateral view of, 599f  
     medial view of, 598f  
 Foramen lacerum, 316f, 317, 317f, 389f  
 Foramen magnum, 316f, 317, 317f  
 Foramen of Luschka, 327f, 329  
 Foramen of Magendie, 328f  
 Foramen of Monro, 327f, 328  
 Foramen ovale, 316f, 317, 317f, 389f  
 Foramen rotundum, 316f  
 Foramen spinosum, 316f, 317f  
 Fornix  
   of brain, 320, 320f, 322f, 403f  
   vaginal, 183, 183f  
     posterior, 183f, 271f  
 Fovea, 178f, 554, 555f, 563f  
 Fovea capitis femoris, 572, 572f, 575f  
   left, 291f  
   right, 289f  
 Frontal bone, 314, 314f, 315f, 381f, 383f, 413f, 415f, 417f, 419f  
 Frontal lobe, 319, 319f, 369f, 373f, 377f, 387f, 411f, 417f  
   white matter of, 375f  
 Frontal plane, 3, 4f  
 Fundus  
   of stomach, 83f, 85f, 104f, 117f, 119f, 121f  
   of uterus, 183, 183f, 259f, 293f, 295f

## G

Gadolinium, 164  
 Gallbladder, 105f, 106f, 107, 107f, 127f, 129f  
   carcinoma of, 168, 168f  
     ultrasound imaging of, 168, 168f  
     ultrasound imaging of, 166–169, 166f, 168f  
 Gallstones. *See* Cholelithiasis  
 Gastric artery(ies)  
   left, 110f  
   short, 110f  
 Gastric vein, 113f  
 Gastrocnemius muscle, 581, 581f, 583f  
   lateral head of, 585f, 589f  
   medial head of, 589f  
 Gastroduodenal artery, 110f  
 Gastroepiploic artery, right, 110f  
 Gastroepiploic vein, 113f  
 Gastroesophageal junction, 87f, 123f  
 Gemellus muscle  
   inferior, 573f  
   superior, 573, 573f, 575f, 577f  
 Genioglossus muscle, 383f, 387f, 438, 439, 439f, 443f, 447f, 451f, 453f  
 Geniohyoid muscle, 439f, 440, 457f  
 Genitourinary system. *See* Urogenital system  
 Genu, 320, 320f, 345f, 377f, 407f  
 Ginglymus joints, 3  
 Glenohumeral joint, 547f, 549f  
 Glenoid fossa, 544, 544f  
   articular cartilage in, 553f  
 Glenoid labrum, 545  
   inferior, 544f, 553f  
   superior, 544f, 547f, 553f

Glenoid process, 11, 11f, 41f, 544, 544f, 547f, 549f, 551f, 553f  
 Globus pallidus, 321, 322f, 323f, 369f  
   nucleus, 405f  
 Glossoepiglottic fold, median, 436, 440f, 465f  
 Glossopharyngeal nerves, 318, 324f  
 Glottic space, 436, 438f, 440f, 445f, 473f  
 Gluteal arteries, 178  
 Gluteal line, posterior, 177f  
 Gluteal veins, 179  
 Gluteus maximus muscle, 572–573, 575f, 577f  
   divided, 573f  
 Gluteus medius, 573f  
 Goiters, 487  
   ultrasound and thyroid, 486f, 487  
 Gracilis, 573f  
 Gray matter, 324f  
 Greater horn, 437f  
 Greater omentum, 103f, 110f  
 Greater trochanter. *See* Trochanter, greater  
 Gunshot wound, spinal CT scan and, 537, 537f  
 Gyri, 333f

## H

Hamate, 564f, 565, 569f, 571f  
   hamulus of, 569f, 571f  
 Hand  
   bones of, dorsal and palmar view, 564f  
   muscles/tendons of  
     dorsal view of, 565f  
     palmar view of, 566f  
 Head, 313–432  
   anatomical overview of, 313–329  
   arteries in, 326–327, 441f  
   brain in, 319–323  
   cranial nerves in, 317–319  
   dural sinuses and veins in, 325–326, 325f  
   enclosing structures in, 323–325  
   foramina in, 317, 317f  
   skeletal parts in, 313–317  
   ventricles and cisterns in, 327–359  
   axial slices through, 2f  
   case studies  
     cerebrovascular disease and MRA in, 422f, 423  
     hydranencephaly and CT exam in, 428f, 429  
     hydranencephaly and ultrasound exam in, 426f, 427  
     hydrocephalus and ultrasound exam in, 424f, 425  
     meningioma and CTA in, 420f, 421  
     squamous cell carcinoma and PET/CT scans in, 430f, 431  
   CT images of  
     axial, 388, 388f–419f  
     coronal, 378, 378f–387f  
   MR images of  
     coronal, 346, 346f–377f  
     sagittal, 2f, 330, 330f–345f  
 Heart, 16, 16f, 17f. *See also* Atrium; Ventricle(s), heart  
   case studies, CTAs in, 90–91, 90f, 91f  
 Hemiazzygos veins, 21, 21f, 79f, 83f, 87f, 89f, 121f, 123f, 125f, 143f  
   accessory, 21, 21f  
 Hepatic artery(ies), 106f, 107f, 131f  
   common, 109, 110f  
   proper, 110f, 127f  
 Hepatic duct, 107f  
 Hepatic flexure, 105f, 106, 137f, 141f, 143f  
 Hepatic vein(s), 114  
   left, 113f  
   right, 113f

- Herniated disk, 505f, 513f  
Hilar region, 23f  
Hilum, 14  
Hip, 572–577  
  anatomical overview of, 572–573  
  musculature in, 572–573, 573f  
  skeletal parts in, 572, 572f  
  anterior view of muscles in, 573f  
  coronal section of, 572f  
  CT images (axial computed) of, 574, 574f–577f  
  Legg-Calve Perthes disease and, 612, 612f  
  posterior view of muscles in, 573f  
Hippocampal formation, 319, 357f, 361f, 365f, 401f  
Hook. *See* Coracoid process  
Hounsfield scale, 3, 4f  
Humerus, 11, 11f, 543, 547f, 554, 555f, 557f, 559f  
  head of, 41f, 543, 544f, 549f, 551f, 553f  
  left, distal extremity of, 554f  
  shaft of, 561f  
  surgical neck of, 543, 544f, 549f  
Hydranencephaly, 427, 429  
  CT exam of head and, 428f, 429  
  ultrasound exam of head and, 426f, 427  
Hydrocephalus, 425, 429  
  ultrasound exam of head and, 424f, 425  
Hyoid bone, 435, 436f, 437f, 438f, 439f, 443f, 465f  
Hyperthyroidism, 485  
Hypoglossal canal, 316f, 317, 389f  
Hypoglossal nerves, 319, 324f  
Hypophysis, 321  
Hypothalamus, 320f, 321, 399f
- I**
- Ileal veins, 113f  
Ileocolic artery, 111f  
Ileocolic vein, 113f  
Ileum, 103, 105f, 111f, 155f, 157f, 159f, 231f, 235f, 249f  
  loops of, 251f, 253f  
  terminal, 105f  
Iliac artery(ies)  
  common, 105f, 110, 112f, 179f  
  branches of, 112f  
  left, 157f, 159f, 161f, 163f, 187f, 189f, 191f, 193f, 229f, 231f, 233f, 235f, 237f  
  right, 157f, 159f, 161f, 163f, 187f, 189f, 191f, 193f, 229f, 231f, 233f, 287f  
  external, 178, 195f, 243f  
  left, 197f, 199f, 203f, 205f, 207f, 209f, 211f, 239f, 241f, 245f, 247f, 249f, 251f, 253f, 255f, 257f, 283f, 287f  
  right, 114f, 201f, 237f, 239f, 241f, 243f, 285f  
  internal, 178, 179f, 195f  
  left, 199f, 203f, 205f, 239f, 241f, 243f, 245f, 247f, 249f, 251f, 253f, 255f, 293f, 297f  
  right, 201f, 237f, 239f, 241f, 243f, 291f, 295f  
Iliac bone, left, 207f  
Iliac crest, 159f, 177f  
  left, 189f, 229f  
  right, 231f  
Iliac spine, anterior superior, 573f  
Iliac vein(s)  
  common, 113f, 115, 180f  
  bifurcation of left, 245f  
  left, 161f, 163f, 191f, 193f, 195f, 197f, 199f, 229f, 231f, 233f, 235f, 237f, 239f, 241f, 243f  
  right, 161f, 163f, 191f, 193f, 229f, 231f, 233f  
  external, 113f, 179  
  left, 203f, 205f, 207f, 209f, 211f, 247f, 249f, 251f, 253f, 255f, 257f, 283f, 287f  
  right, 201f, 237f, 239f, 241f, 243f, 285f  
  internal, 113f, 179, 180f  
  left, 203f, 205f, 247f, 249f, 251f, 253f, 255f, 293f, 297f  
  right, 201f, 237f, 239f, 241f, 243f, 291f, 295f  
Iliac vessels, left internal, 207f  
Iliacus muscle, 114f, 181f  
  left, 201f, 243f, 289f  
  right, 195f, 197f, 235f, 247f, 283f, 287f  
Iliopsoas muscle, 181f, 572, 573f, 575f, 577f  
  right, 251f  
Iliotibial tract, 573f  
Ilium, 175, 289f, 527f, 529f, 531f, 572f  
  left, 193f, 281f, 285f, 287f  
  ala of, 233f  
  right, 197f, 203f, 211f, 245f, 249f, 251f, 253f, 255f, 257f, 259f, 283f, 299f, 301f  
  ala of, 237f, 243f  
Infraglottic cavity, 438f  
Infraglottic space, 436, 475f  
Infrapatellar fat pad, 581, 581f, 585f, 587f  
Infraspinatus muscle, 545, 545f  
Infundibulum, 320f, 321, 397f  
Inner periosteum, 499f  
Innominate, 175  
Insula, 322f, 323, 337f, 339f, 361f  
Intercondylar eminence, 585f, 591f, 593f, 595f  
Intercostal vein, 21f  
Interlobar artery, 109f  
Intermediate mass, 320–321, 320f, 345f  
Internal capsule, 321, 322f, 323f, 341f, 367f, 373f, 403f, 405f  
Interosseous ligament, 601f  
Interosseous membrane, 580f  
Interpeduncular cistern, 328f  
Interphalangeal joint  
  distal, 565f  
  proximal, 565f  
Interspinous ligament, 497f  
Intertransverse muscle, 181f  
Intertrochanteric crest, 178f  
Interventricular foramen, 327f, 328  
Interventricular septum, 73f, 75f, 77f, 79f, 81f  
Intervertebral disks, 153f, 159f, 187f, 193f, 497, 501f, 503f  
Intervertebral foramen, 459f, 496, 519f, 521f, 525f, 527f  
Intervertebral joints, 496–497  
Intestinal arteries, 111f  
Ischial ramus, 177f  
  left, 271f  
  right, 225f, 273f, 275f  
Ischial spine, 176f  
Ischial tuberosity, 177f  
  left, 221f  
  right, 223f, 269f, 271f, 273f, 275f, 299f, 301f  
Ischiorectal fossae, 178  
  left, 267f, 269f, 271f, 273f, 275f, 297f, 301f  
  right, 217f, 219f, 223f, 299f  
Ischium, 177, 577f  
  right, 217f, 219f, 265f, 267f, 277f
- J**
- Jaw bone. *See* Mandible  
Jejunal veins, 113f  
Jejunum, 103, 105f, 111f  
Joint ligaments, 565f  
Joints, 3, 543–618. *See also specific joints*  
  ankle, 596–609  
  classification of, 3  
  elbow, 554–563  
  hip, 572–577  
  knee, 578–595  
  shoulder, 543–553  
  wrist, 564–571  
Jugular foramen, 316f, 317  
Jugular fossa, 317f  
Jugular vein(s), 19  
  external, 20f, 325f, 438, 440f, 441f  
  left, 463f, 467f, 469f, 471f, 473f, 475f, 477f, 479f  
  right, 465f, 481f  
  internal, 17f, 20f, 324f, 325–326, 325f, 389f, 438, 440f, 441f  
  left, 18f, 43f, 463f, 465f, 467f, 469f, 471f, 475f, 477f, 481f  
  right, 18f, 39f, 41f, 43f, 449f, 451f, 453f, 455f, 457f, 459f, 461f, 473f, 479f
- K**
- Kidney(s), 104f, 105f, 108  
  contents of, 109f  
  left, 131f  
  lower pole of, 147f  
  upper pole of, 127f, 129f  
  right, 141f  
  upper pole of, 127f, 129f  
Knee, 578–595  
  anatomical overview of, 578–581  
  ligaments in, 580, 580f, 581f  
  musculature/other structures in, 581  
  skeletal parts in, 578, 579f–580f  
  axial image of lower, 581f  
  bones/ligaments of, 579  
  anterior view of, 580f  
  posterior view of, 579f  
  MR images of  
  coronal, 588, 588f–595f  
  sagittal, 582, 582f–587f
- L**
- Labia majora, 183, 183f, 277f, 279f  
  left, 285f, 287f, 291f, 295f  
  right, 293f  
Labia, opening between, 279f  
Lacrimal bone, 314, 315f  
Laminae, 9, 10f, 71f, 435f, 455f, 493, 494f  
  L2, 517f, 519f, 523f  
  L5, 529f  
  left, 191f, 229f  
  posterior, fracture in, 467f  
  S1, 533f  
  T1, 39f  
Large intestine, 103–104, 105f, 106  
Laryngeal pharynx, 436, 439f, 463f, 465f  
Laryngeal prominence, 437f  
Laryngeal vestibule, 436, 438f, 443f, 467f, 469f, 471f, 473f  
Larynx, 435  
  anterior, 437f  
  coronal section of, 438f  
  inlet of, 439f  
  left anterolateral aspect of, 437f  
  left lateral aspect of, 437f  
  median section of, 438f  
  PET/CT scan and carcinoma of, 490f, 491  
  posterior, 437f  
  superior aspect of, 440f  
Lateral mass, 433  
Lateral recess, 327f, 329  
  of fourth ventricle, 395f



Lateral ventricles. *See* Ventricle(s), brain, lateral

Latissimus dorsi, 544f

Legg-Calve Perthes disease, 612, 612f

Lenticular nuclei, 321, 322f, 341f, 367f, 373f

Lesser horn, 437f

Lesser trochanter. *See* Trochanter, lesser

Levator ani muscle, 179f, 180, 180f, 181f

Ligamentum capitis femoris, 572f

Ligamentum flavum, 497f

Ligamentum teres, 106f, 125f

Ligamentum venosum, 106f

Linea aspera, 178f

Liver, 23f, 25f, 27f, 37f, 81f, 83f, 85f, 87f, 89f, 103f, 105f, 106–107, 117f, 119f, 121f, 135f, 139f, 143f

lobe of

caudate, 106f, 107, 125f, 127f

left, 106f, 107, 123f, 125f

quadrate, 106f, 107, 127f

right, 106f, 107, 123f

sinusoids of, 113f

visceral surface of, 106f

Longitudinal ligament

anterior, 497, 497f, 507f, 509f, 511f, 513f

posterior, 497, 497f, 507f, 511f, 513f

Lumbar nerves, 498f

Lumbar vertebrae, 101, 493, 494f

L1, 102f, 434f, 494f, 515f

nerve roots, 503f, 515f

pedicle, 515f

spinous process, 509f

vertebral body, 501f

L2, 102f, 434f, 494f, 515f, 519f

inferior articular process, 523f, 525f

inferior endplate, 521f

lamina, 517f, 519f, 523f

nerve roots, 503f, 515f, 521f

pedicle, 503f, 517f

spinous process, 517f, 521f, 523f, 525f

vertebral body, 501f

L3, 102f, 434f, 494f, 515f

body of, 151f

nerve roots, 501f, 503f

pedicle, 503f

superior articular process, 525f

vertebral body, 501f

L4, 289f, 291f, 293f, 295f, 434f, 494f, 515f

nerve roots, 501f

vertebral body, 501f

L5, 189f, 193f, 289f, 291f, 293f, 295f, 297f, 434f, 494f, 515f

inferior articular process, 527f, 529f

inferior endplate, 527f

lamina, 529f

left lamina of, 229f

nerve roots, 501f, 527f, 529f

pedicle, 501f

right pedicle, 229f

spinous process, 229f, 529f

transverse process, 527f

vertebral body, 501f

lateral view of, 495f

Lumborum muscle, quadratus, 114f, 181f

Lunate, 564, 564f

Lunate surface, 572, 572f, 575f, 577f

Lung(s)

carcinoma of, 98–99, 98f

PET/CT scans and, 98–99, 99f

left, 12f, 13f, 14, 14f, 15, 81f, 85f, 117f, 119f, 121f

lower lobe, 13f, 14, 15f

upper lobe, 13f, 14, 15f, 43f

lobes of, 13, 13f

right, 12f, 13–14, 13f, 14f, 77f, 87f, 117f, 119f

lower lobe, 13, 13f, 14f, 23f, 25f

middle lobe, 13, 13f, 14f

upper lobe, 13, 13f, 14f, 23f, 25f, 27f, 37f, 43f

## M

Magnetic resonance angiographs (MRAs), 164

abdomen, 164–165, 164f, 165f

cerebrovascular disease and head, 422f, 423

cerebrovascular disease and neck, 484, 484f

Magnetic resonance (MR) images, 3, 6f

ankle

axial, 604, 604f–609f

sagittal, 600, 600f–603f

case studies

car accident and spine in, 538, 538f

spine and back pain in, 539, 539f

chest and sagittal, 22, 22f–37f

description of, 1, 3, 5

elbow

axial, 556, 556f, 557f

coronal, 558, 558f, 559f

sagittal, 560, 560f–563f

head

coronal, 346, 346f–377f

sagittal, 2f, 330, 330f–345f

knee

coronal, 588, 588f–595f

sagittal, 582, 582f–587f

neck and sagittal, 442, 442f–445f

pelvis (female) and coronal, 280, 280f–301f

shoulder and coronal, 546, 546f–553f

spine and sagittal, 500, 500f–515f

Mamillary body, 320f

Mandible, 314, 315f, 385f, 387f

body of, 455f, 457f, 459f, 461f

ramus of, 447f

Mandibular fossa, 317f

Manubrium, 10f, 11, 51f, 53f, 55f, 57f

Mastoid process, 315f, 317f

Maxilla, 314, 315f

left, 381f, 383f

right, 379f

Maxillary bone, 317f

Median plane, 3, 4f

Mediastinal pleura, 12, 12f, 59f

Medulla oblongata, 318f, 320f, 321, 345f, 355f, 357f, 359f, 389f, 445f, 447f

posterior, 353f

Melanoma, PET/CT scan and neck, 488f, 489

Meningioma, 421

CTA of head and, 420f, 421

Meniscus

lateral, 579f, 580, 580f, 581f, 589f, 591f, 593f, 595f

anterior horn of, 587f

posterior horn of, 587f

medial, 579f, 580, 580f, 581f, 589f, 591f, 593f, 595f

Mesenteric artery

inferior, 110, 112f, 151f, 153f

branches of, 112f

superior, 107f, 109–110, 111f, 114f, 137f, 139f, 141f

branches of, 111f

Mesenteric vein

inferior, 108f, 113f, 114

superior, 107f, 113f, 114, 139f, 141f

Mesenteric vessels, 143f, 147f, 151f

superior, 145f

Mesentery, 102, 103f

loops of, 281f, 283f, 285f

Mesometrium, 183. *See also* Broad ligaments

Metatarsal(s), 596, 597f

first, 601f

second, 603f

third, 603f

Midbrain, 321, 365f, 399f

Midsagittal plane, 3, 4f

MR images. *See* Magnetic resonance images

MRAs. *See* Magnetic resonance angiographs

Muscles. *See specific muscles*

## N

Nasal bone, 314, 315f

Nasal cavity, coronal view of, 314f

Nasal conchae, 313

inferior, 377f

Nasal septum, 387f

Nasopharynx, 373f, 375f, 436, 439f, 445f

Navicular, 596, 597f, 601f, 603f

Neck, 433–492

anatomical overview of, 433–441

arteries in, 436–438, 441f

cartilage/other structures in, 435–436

muscles in, 438–441

skeletal parts in, 433–435

veins in, 438, 441f

vessels in, 440f

viscera in, 436

case studies

atherosclerotic disease and CTA in, 482f, 483

cerebrovascular disease and MRA in, 484, 484f

cyst and ultrasound in, 485, 485f

goiter and ultrasound in, 486f, 487

larynx carcinoma and PET/CT scan in, 490f, 491

melanoma and PET/CT scan in, 488f, 489

CT images (axial) of, 446, 446f–481f

MR images (sagittal) of, 442, 442f–445f

Nerve root(s), 497

anterior (ventral), 498, 499f

drawing of spinal cord and, 498f

L1, 503f, 515f

L2, 503f, 515f, 521f

L3, 501f, 503f

L4, 501f

L5, 501f, 527f, 529f

posterior (dorsal), 497, 499f

S1, 527f, 529f, 531f, 533f

S2, 531f

S3, 531f

S4, 531f

S5, 531f

Nerves. *See specific nerves*

Nucleus pulposus, 497, 497f, 505f, 509f, 511f, 513f, 523f, 525f, 529f

## O

Obturator canal, 181f

Obturator crest, 177f

Obturator foramen, 176f, 177, 177f

left, 221f, 269f

right, 223f, 271f

Obturator internus muscle, 573, 573f, 575f, 577f

Occipital bone, 315f, 317, 319f, 351f, 451f, 453f

Occipital lobe, 320, 339f, 347f

white matter, 349f

Occipital protuberance, internal, 316f  
 Oculomotor nerves, 318, 324f  
 Olecranon fossa, 554, 554f, 559f, 561f  
 Olecranon process, 554, 555f, 557f, 561f  
 Olfactory nerves, 318, 324f  
 Omental bursa, 103f  
 Opponens pollicis muscle, 566, 566f, 569f, 571f  
 Optic canal, 316f  
 Optic chiasm, 320f, 371f  
 Optic foramen, 317, 393f  
 Optic nerves, 318, 324f, 339f, 377f, 391f  
 Oral cavity, 385f, 387f  
 Orbital fissure, superior, 316f, 317  
 Orbital plate, 314, 314f, 316f, 385f, 387f, 395f  
 Orbits, 314, 314f  
 Oropharynx, 436, 439f, 445f, 449f, 453f, 455f, 457f, 459f, 461f  
 Osteochondritis, 612, 612f  
 Osteophyte, 533f  
 Osteoporosis, 613, 613f  
 Ovarian ligament, 184f  
 Ovaries, 184f, 185  
   sagittal section through broad ligament at level of, 184f  
 Oviducts, 184f, 185

## P

Palatine bone, 314, 315f  
   horizontal lamina of, 317f  
 Palatine process, 315f, 317f  
   left, 385f, 387f  
 Palmaris  
   brevis, 555f  
   longus, 555f  
 Pancreas, 103f, 107  
   body of, 104f, 108, 108f, 129f, 131f, 135f  
   head of, 104f, 107, 107f, 108f, 133f  
   neck of, 104f  
   posterior view of, 108f  
   tail of, 104f, 108, 108f, 131f  
   uncinate process of, 108f  
 Pancreatic duct, 107f  
 Parachial artery, 555f  
 Paraumbilical vein, 113f  
 Parietal bone, 314, 315f, 411f, 413f, 415f, 417f, 419f  
 Parietal lobe, 319, 319f, 357f, 411f, 417f  
 Parietal pericardium, 12f, 13  
 Parietal pleura, 12f, 20f  
 Parieto-occipital fissure, 319f  
 Parotid gland, 447f, 449f, 453f, 455f, 457f  
 Patella, 578, 580f, 587f  
   medial, 585f  
 Patellar ligament, 580, 580f, 581f, 587f  
 Patellar surface, 580f  
 Pecten, 177f  
 Pectineus muscle, 573, 573f, 575f, 577f  
 Pectoralis major, 544f  
 Pedicle(s), 9, 10f, 71f, 435f, 493, 494f, 495f  
   L1, 515f  
   L2, 503f, 517f  
   L3, 503f  
   L5, 501f  
   right, 229f  
   T1, 39f  
 Pedunculi, 319  
 Pelvic diaphragm, 180, 263f, 265f, 267f, 269f, 271f, 273f, 275f, 297f, 299f, 301f  
   left, 215f, 217f, 219f, 221f, 289f  
   muscles (inferior view) in, 181f  
   right, 223f  
 Pelvic girdle, 175  
   lateral view of, 177f  
 Pelvis, 175–312  
   anatomical overview of, 175–183  
   arteries in, 178–179  
   bony (anterior/posterior view), 176f  
   female urogenital system in, 182–183, 183f, 184f, 185  
   male urogenital system in, 180, 182, 182f  
   muscles in, 180, 181f  
   skeletal parts in, 175–178, 176f–178f  
   veins in, 179, 180f  
   viscera in, 178, 179f  
   case studies  
     abdominal aortic aneurysm and CT scan in, 304, 304f  
     aortobilateral iliac endografting and CT scan in, 302f, 303  
     prostate and ultrasound image in, 305, 305f  
     shotgun wound and CT scan in, 611, 611f  
     testicles and ultrasound image in, 306f, 307  
     CT images (axial computed) of  
       female and, 228, 228f–279f  
       male and, 186, 186f–227f  
     MR images (coronal) of female, 280, 280f–301f  
 Pericardial cavity, 20f  
 Pericardium, 12f, 13  
 Peritoneum, 102  
 Peroneal retinaculum, superior, 599f  
 Peroneus tendon  
   brevis, 598, 599f, 605f, 607f, 609f  
   longus, 598, 599f, 605f, 607f, 609f  
 Perpendicular plate, 313, 314f, 315f, 379f, 381f, 383f  
 PET scan. *See* Positron emission tomography scan  
 Petrosal veins  
   inferior, 325f  
   superior, 325f  
 Phalanx  
   distal, 597f  
   middle, 597f  
   proximal, 597f  
 Pharyngeal orifice, 315f  
 Pharynx, 436  
   posterior wall of, 440f  
 Phrenic nerve, 20f  
 Pia mater, 324, 324f, 499f  
   spinal, 318f  
 Pineal body, 320, 320f  
   with calcifications, 403f  
 Pineal gland, 323f, 359f  
 Piriformis, 573f  
 Pisiform, 564f, 565  
 Pituitary gland, 320f, 321, 345f, 371f, 395f  
 Planes, of body, 3, 4f  
 Plantaris, 581f  
 Pleurae. *See specific pleura*  
 Pleural cavity, 12f, 13, 20f, 33f  
 Pleural membranes, 13  
 Pleural reflection, 13f, 14f, 15f  
 Pons, 320f, 321, 323f, 343f, 345f, 359f, 361f, 363f, 365f, 393f, 395f, 397f, 445f  
   anterior, 367f  
   posterior, 357f  
 Pontine cistern, 328f  
 Popliteal tendon, 591f, 593f  
 Popliteus muscle, 579f, 581, 581f, 583f  
 Portal vein, 106f, 108f, 113f, 114, 125f, 127f, 129f, 131f, 133f, 135f, 137f  
 Positron emission tomography (PET) scan, 5  
   CT combined with, 5, 7f  
   breast carcinoma and, 96–97, 96f, 310f, 311, 614f, 615, 616f, 617

  colorectal carcinoma and, 172f, 173  
   larynx carcinoma in, 490f, 491  
   lung carcinoma and, 98–99, 98f  
   neck melanoma and, 488f, 489  
   squamous cell carcinoma of head in, 430f, 431  
   stomach carcinoma and, 170f, 171, 308f, 309  
 Posterior arch, 433, 434f  
 Pronator teres, 555f  
 Prostate, 103f, 182, 182f, 221f, 223f  
   ultrasound image of, 305, 305f  
 Prostate specific antigen (PSA), 305  
 PSA. *See* Prostate specific antigen  
 Psoas muscle, 115  
   left, 151f, 155f, 159f, 163f, 187f, 193f, 201f, 235f, 243f, 249f, 289f  
   major, 114f, 181f  
   right, 195f, 197f, 233f, 247f, 283f, 287f  
 Pubic bone, 577f  
 Pubic ramus  
   left inferior, 223f  
   right, 271f, 273f  
 Pubis, 103f, 177, 177f, 182f  
   left, 221f, 285f, 287f  
   right, 217f, 219f, 265f, 267f, 269f, 281f, 283f  
 Pudendal artery, inferior, 179f  
 Pudendal vein, 180f  
 Pulmonary artery(ies), 16f, 17f, 18, 18f, 20f  
   left, 16f, 18f, 61f  
   descending branch of, 65f  
   right, 16f, 25f, 27f, 29f, 31f, 33f, 35f, 63f  
 Pulmonary trunk, 18, 18f, 37f, 63f  
   origin of, 65f  
 Pulmonary vein(s)  
   left, 16f  
   inferior, 71f  
   superior, 63f, 65f  
   right, 16f, 25f  
   superior, 65f, 67f  
 Putamen, 321, 322f, 323f, 369f  
   nucleus, 405f  
 Pyloric antrum, 133f, 135f  
 Pyloric part, 104f

## Q

Quadrangular space, 545f  
 Quadrate lobe, 106f, 107  
 Quadriceps femoris muscle, 583f, 587f  
 Quadriceps femoris tendon, 580f, 581  
 Quadrigeminal plate, 320f, 321, 359f, 401f, 403f

## R

Radial fossa, 554f  
 Radial notch, 555f  
 Radial tuberosity, 554, 563f  
 Radiographs, conventional, 1, 2f  
 Radius, 554, 555f  
   head of, 554, 555f, 559f, 563f  
   neck of, 554, 555f, 563f  
   proximal posterior extremity of radius and, 555f  
 Rectal artery  
   inferior, 112f, 179f  
   middle, 112f, 179f  
   superior, 112f  
 Rectal plexus, 113f  
 Rectal vein  
   inferior, 180f  
   right, 113f  
   middle, 180f  
   right, 113f  
   superior, 113f

Rectal venous plexus, 180f  
 Rectouterine pouch, 183, 183f  
 Rectum, 103f, 112f, 178, 181f, 182f, 209f, 211f, 213f, 215f, 217f, 219f, 221f, 223f, 249f, 251f, 253f, 255f, 257f, 259f, 263f, 265f, 267f, 269f, 271f, 273f, 297f, 299f, 301f  
   carcinoma of colon and, 172f, 173  
   feces in, 261f  
   top of, 207f  
 Rectus femoris muscle, 573, 573f, 575f, 577f  
 Rectus muscle  
   inferior, 339f  
   lateral, 391f  
   medial, 391f  
   superior, 339f, 393f  
 Red nucleus, 321, 363f  
 Renal artery(ies), 109f, 110, 111f  
   left, 141f  
   right, 141f  
 Renal column, 109f  
 Renal cortex, 109f  
 Renal hilum, 109f  
 Renal pelvis, 109f  
   right, 143f  
 Renal pyramid, 109f  
 Renal vein(s), 111f, 114  
   left, 111f, 139f, 141f  
   right, 111f, 114f  
 Retromandibular vein(s), 438, 441f  
   left, 455f, 461f  
   right, 451f, 453f, 457f, 459f  
 Retroperitoneum, 102  
 Rib(s), 10f, 11–12, 11f, 43f  
   eleventh, 102f  
   false, 11, 12  
   first, 39f, 41f  
   floating, 11, 11f  
   second, 41f  
   twelfth, 102f, 181f  
 Root ganglion, posterior (dorsal), 498, 499f, 519f  
 Round ligament, 184f  
 Ruptured disk, 511f

## S

Sacculae, 438f  
 Sacral canal, 195f, 197f, 199f, 237f, 245f  
 Sacral crest  
   lateral, 496f  
   median, 496f  
 Sacral foramen, 245f  
   left, 197f  
   posterior, 496f  
 Sacral foramina, left, 199f  
 Sacral hiatus, 496f  
 Sacral horn, 496f  
 Sacral nerves, 498f  
 Sacral vertebrae  
   S1, 193f, 195f, 233f, 235f, 299f, 515f  
     lamina, 533f  
     lateral part of, 529f, 531f  
     nerve root, 527f, 529f, 531f, 533f  
     superior articular process, 527f, 529f  
     superior endplate, 531f  
     upper, 297f  
     vertebral body of, 501f  
   S2, 193f  
     nerve root, 533f  
   S3, 509f  
   S4, 509f  
   S5, 255f, 257f  
 Sacroiliac joint(s), 176f, 177, 533f  
   left, 245f  
     lower, 249f  
     right, 199f, 237f, 301f  
 Sacrum, 176f, 177, 203f, 251f, 301f, 434f, 494f, 496  
   lateral part of, 247f  
   posterior view of, 496f  
   tip of, 211f  
 Saddle joints, 3  
 Sagittal plane, 3, 4f  
 Sartorius muscle, 573, 573f, 575f, 577f, 581f  
 Scalp, 324f, 351f, 417f, 419f  
 Scaphoid, 564, 564f  
 Scapulae, 10f, 11f, 45f, 543  
   body of, 551f  
 Scapular muscles, posterior view of, 545f  
 Scapular spine, 545f  
 Sciatic foramen, greater, 179f  
 Sciatic notch  
   greater, 177f  
   lesser, 177f  
 Sectional anatomy, 1  
 Sectional images, 1–3  
 Semimembranosus, 581f  
 Seminal vesicle(s), 182, 182f  
   left, 217f  
   right, 219f  
 Semitendinosus, 573f, 581f  
 Septal cartilage, 315f, 379f, 381f  
 Septum pellucidum, 320, 320f, 373f, 407f  
 Shotgun wound, pelvis CT scan and, 611, 611f  
 Shoulder, 543–553  
   anatomical overview of, 543–545  
   joints in, 544–545  
   musculature in, 545  
   skeletal parts in, 543–544  
   coronal view of, 544f  
   MR images (coronal) of, 546, 546f–553f  
 Sigmoid artery, 112f  
 Signal intensities, 5, 5f  
 Sinus(es)  
   cavernous, 324f, 325f  
   confluence of, 318f, 324f, 325, 328f, 401f, 403f  
   dural, 325–326, 325f  
   ethmoid, 313, 314f, 343f  
     left, 387f  
     right, 385f  
     upper right, 383f  
   frontal, 314, 314f, 343f, 345f, 379f, 381f, 383f, 393f  
   inferior sagittal, 324f, 325, 325f, 365f, 369f  
   mastoid, 316–317  
   maxillary, 314, 314f, 337f, 339f, 341f  
     left, 381f, 383f, 387f  
     right, 379f, 385f  
   occipital, 325f  
     sulcus for, 316f  
   piriform, 436, 439f, 440f, 469f, 471f, 473f  
   sigmoid, 325, 325f, 391f, 393f, 395f, 447f  
     sulcus for, 316f  
   sphenoid, 315f, 316, 345f, 371f, 375f, 377f, 391f, 393f, 395f  
   straight, 318f, 324f, 325, 325f, 328f, 349f, 353f, 355f, 403f, 405f, 407f  
   superior sagittal, 318f, 324f, 325, 325f, 328f, 349f, 353f, 365f, 369f, 411f, 413f, 415f, 417f, 419f  
     sulcus for, 316f  
   transverse, 324f, 325, 325f, 349f, 353f, 399f  
     sulcus for, 316f

Skull. *See also* Head  
   base of  
     inferior view, 317f  
     superior axial view, 316f  
   bones of, 313–317  
   foramina of, 317, 317f  
   lateral image of, 1, 2f  
   lateral view of bony, 315f  
   median sagittal view of bony, 315f  
 Slice, of body, 1, 2f  
 Small bowel, 151f, 155f, 157f, 159f, 161f, 163f, 205f, 231f, 233f, 235f, 295f, 297f  
   air in, 201f  
   loops of, 137f, 139f, 141f, 143f, 145f, 147f, 149f, 153f, 163f, 195f, 199f, 281f, 283f, 285f, 287f, 289f, 291f, 293f  
 Small intestine, 102–103, 103f. *See also* Small bowel  
 Soft palate, 439f, 443f, 449f  
 Soleus, 598f, 599f  
 Spermatic cord(s), 182  
   left, 223f, 225f, 227f  
   right, 221f  
 Sphenoid bone, 314, 315f, 316f  
   greater wing of, 316, 316f, 389f  
   lesser wing of, 316, 316f  
   sinuses in, 315f, 316  
 Spinal accessory nerves, 318, 324f  
 Spinal artery, anterior, 326f  
 Spinal cord, 318f, 320f, 321, 345f, 443f, 445f, 451f, 455f, 459f, 497–499, 507f, 509f, 511f  
   cervical, 357f  
   coverings of, 497–499  
   drawing of nerve roots and, 498f  
 Spinal meninges, 498–499  
 Spinal nerve, sulcus for, 435f, 494f  
 Spine, 493–542  
   anatomical overview of, 493–499  
   foramina in, 496  
   intervertebral joints in, 496–497  
   skeletal parts in, 493–496  
   spinal cord and coverings in, 497–499  
   anterior inferior, 177f  
   anterior superior, 176f, 177f  
   case studies  
     back pain and MR in, 539, 539f  
     car accident and MR scan in, 538, 538f  
     car accidents and CT scans in, 534f, 535, 536, 536f  
     gunshot wound and CT scan in, 537, 537f  
     spondylolisthesis in, 540f, 541  
   CT images (axial computed) of, 516, 516f–533f  
   ischial, 176f, 177f, 181f  
   MR images (sagittal) of, 500, 500f–515f  
   posterior superior, 177f  
 Spinous process, 10f, 11f, 57f, 229f, 247f, 434, 434f, 435f, 494f, 495f, 496, 497f  
   C3, 465f  
   C4, 469f  
   C6, 473f  
   L1, 509f  
   L2, 517f, 521f, 523f, 525f  
   L5, 229f, 529f  
   T1, 39f  
   T3, 443f  
 Spleen, 85f, 89f, 104f, 105f, 108, 110f, 117f, 119f, 121f, 123f, 125f, 127f, 133f, 135f, 137f, 139f  
 Splenic artery, 108f, 109, 110f, 131f  
 Splenic flexure, 85f, 87f, 89f, 105f, 106, 125f, 127f  
 Splenic vein, 108f, 113f, 114, 129f, 131f, 133f, 135f  
 Splenium, 320, 320f, 322f, 345f, 357f, 407f  
 Spondylolisthesis, 540f, 541

- Sternal angle, 436f  
 Sternocleidomastoid muscle, 440, 489  
 Sternum, 10f, 11  
 Stomach, 102, 103f, 105f, 107f  
   air in, 125f  
   body of, 87f, 89f, 104f, 123f, 127f, 129f, 131f  
   carcinoma of, 170f, 171, 308f, 309  
     PET/CT scans and, 170f, 171, 308f, 309  
   fundus of, 83f, 85f, 104f, 117f, 119f, 121f  
   greater curvature of, 104f  
   lesser curvature of, 104f  
   parts of, 104f  
   pyloric antrum of, 133f, 135f  
 Styloid process, 315f, 317f, 449f  
 Stylomastoid foramen, 317f  
 Subarachnoid space, 324f, 443f, 499, 499f, 507f, 509f, 511f, 519f, 521f, 523f  
 Subclavian artery(ies), 16f, 17f, 18, 18f, 19f, 441f  
   left, 16f, 17f, 18f, 45f, 47f, 49f, 51f, 53f, 440f  
   right, 17f, 18f, 45f, 440f  
     origin of, 47f  
 Subclavian vein(s), 19, 20f, 21f  
   left, 17f, 18f, 41f, 43f, 440f  
   right, 17f, 18f, 20f, 440f, 441f  
 Subdural space, 499f  
 Submandibular glands, 436, 440f, 463f, 465f  
 Submental vein, 440f  
 Subscapularis muscle, 544f, 545, 547f, 551f  
 Substantia nigra, 321, 323f, 363f  
 Subthalamic nucleus, 323f  
 Sulci, brain, 333f  
 Superior cistern, 318f, 328f, 329, 355f, 403f  
 Superior horn, 437f  
 Supracondylar ridge  
   lateral, 554f  
   medial, 554f  
 Suprarenal gland, 104f, 105f  
 Supraspinatus muscle, 545, 545f, 547f, 551f  
 Supraspinous ligament, 497f  
 Sustentaculum tali, 596, 597f, 605f  
 Sylvian fissure, 319, 319f, 335f, 357f, 361f, 399f  
 Symphysis joints, 3  
 Symphysis pubis, 176f, 177, 221f, 267f, 269f, 271f, 281f, 283f, 285f, 575f  
 Synarthrosis joints, 3  
 Syndesmosis joints, 3  
 Synovial fold, 581f  
 Synovial membrane, 581f
- T**
- T1-weighted images, 5, 5f, 6f  
 T2-weighted images, 5, 5f, 6f  
 Talus, 596, 597f, 601f, 603f, 605f, 607f  
 Temporal bone, 315f, 316, 317f  
   petrous part of, 316f  
   squamous part of, 316f  
 Temporal lobe, 319, 319f, 331f, 335f, 339f, 357f, 369f, 373f, 395f  
 Tendocalcaneus tendon, 601f, 603f, 605f, 607f  
 Tensor fascia latae muscle, 573, 575f, 577f  
 Tentorium cerebelli, 324f, 325, 347f, 351f, 399f, 403f  
 Teres major muscle, 545, 545f, 549f, 551f  
 Teres minor muscle, 545, 545f  
 Testicular artery, 114f  
 Testicular carcinoma, 306f, 307  
 Testicular vein, 114f  
 Thalamal nuclei, 322f, 323f  
 Thalamus, 320f, 321, 322f, 323f, 341f, 343f, 359f, 361f, 363f, 367f, 369f, 401f, 403f  
   nucleus, 405f  
 Thoracic inlet, 436f  
 Thoracic nerves, 498f  
 Thoracic vertebrae, 9, 10f, 493, 494f  
   cervical vertebrae *v.*, 436f  
   lateral view of, 495f  
   T1, 434f, 494f  
     laminae, 39f  
     pedicles, 39f  
     spinous process, 39f  
   T2, 434f, 494f  
   T3, 434f, 494f  
   T4, 434f, 494f  
   T5, 434f, 494f  
   T6, 434f, 494f  
   T7, 434f, 494f  
   T8, 434f, 494f  
   T9, 434f, 494f  
   T10, 434f, 494f  
   T11, 434f, 494f  
   T12, 434f, 494f, 513f, 515f  
 Thyroid cartilage, 435, 436f, 437f, 439f, 440f, 443f, 445f, 471f, 473f, 475f, 477f, 479f  
 Thyroid gland, 41f, 436, 440f  
   isthmus of, 443f, 445f  
   ultrasound and cyst in, 485, 485f  
   ultrasound and goiter in, 486f, 487  
 Tibia, 578, 579f, 583f, 585f, 587f, 593f, 595f, 601f, 603f  
 Tibialis anterior tendon, 598, 598f, 599f, 605f, 607f  
 Tibialis posterior tendon, 598, 598f, 605f, 607f  
 Tibiofibular joint, proximal, 587f  
 Tongue, 439f, 440f, 461f  
   muscles of, 345f  
 Torus tubarius, 315f  
 Trachea, 14, 15f, 27f, 29f, 31f, 39f, 43f, 45f, 49f, 51f, 53f, 55f, 57f, 436, 437f, 440f, 443f, 445f, 477f, 479f, 481f  
   bifurcation of, 59f  
 Transverse foramen, 434f, 435f, 481f, 494f  
 Transverse plane, 3, 4f  
 Transverse process, 57f, 434, 434f, 493, 496  
   L5, 527f  
 Trapezium, 564f, 565, 569f, 571f  
 Trapezius muscle, 545, 547f  
 Trapezoid, 564f, 565, 569f, 571f  
 Triangular interval, 545f  
 Triceps brachii muscle, 544f  
   lateral head of, 545f  
   long head of, 545f  
 Triceps muscle, 555, 555f, 559f, 561f  
 Trigeminal nerves, 318, 324f  
 Triquetrum, 564f, 565, 569f, 571f  
 Trochanter  
   greater, 178f, 181f, 219f, 267f, 291f, 572, 572f, 575f, 577f  
   left, 217f, 289f  
   right, 267f, 269f  
   lesser, 178f, 297f  
 Trochlea, 554, 554f, 555f, 557f, 559f, 561f  
 Trochlear nerves, 318, 324f  
 Trochlear notch, 554, 555f, 557f, 561f  
 Trochoid joints, 3  
 Tubercle, 434f  
   anterior, 434f, 435f, 494f  
   costal, 495f  
     facet for, 495f  
   epiglottic, 440f  
   greater, 543, 544f, 549f, 553f  
   posterior, 434f, 435f, 494f  
   pubic, 177f, 575f  
 Tuberosity, 555f  
 Tubo-ovarian ligament, 184f
- U**
- Ulna, 554, 555f  
   proximal posterior extremity of radius and, 555f  
   shaft of, 559f, 563f  
 Ultrasound imaging, 5, 6f  
   abdomen, 166–169, 166f, 168f  
   breast  
   benign cysts in, 94, 94f  
   carcinoma in, 92f, 93  
   cyst in thyroid gland and, 485, 485f  
   gallbladder, 166–169, 166f, 168f  
   carcinoma in, 168, 168f  
   goiter in thyroid and, 486f, 487  
   head  
   hydranencephaly in, 426f, 427  
   hydrocephalus in, 424f, 425  
   prostate and, 305, 305f  
   uncinate process, 108f  
 Ureter(s), 105f, 108, 109f, 114f, 182f  
   left, 104f, 147f, 155f, 163f, 187f, 191f, 193f, 195f, 197f, 199f, 203f, 205f, 209f, 229f, 231f, 233f, 235f, 237f, 239f, 241f, 245f, 249f, 251f, 253f, 255f, 257f, 261f  
   entering bladder, 261f  
   right, 145f, 149f, 151f, 157f, 159f, 161f, 189f, 191f, 201f, 231f, 239f  
 Urethra, 225f, 271f, 273f, 291f  
   female, 183, 183f  
   male, 182, 182f  
 Urogenital system  
   female, 182–183, 183f, 184f, 185  
   male, 180, 182, 182f  
 Uterine tubes. *See* Oviducts  
 Uterine vessels, 184f  
 Uterus, 183, 183f  
   body of, 183, 183f, 261f, 263f, 265f, 293f  
   cervix of, 183, 183f, 184f  
   fundus of, 183, 183f, 259f, 293f, 295f  
 Uvula, 439f, 445f, 451f
- V**
- Vagina, 183, 183f, 184f, 273f, 275f, 293f, 295f  
 Vagus nerves, 318, 324f  
 Valleculae, 436, 438f, 439f, 440f, 463f, 465f  
 Vastus lateralis, expansion of, 581f  
 Vein of Galen, 324f, 325, 325f, 405f, 407f  
   branches of, 357f  
 Veins. *See* specific veins  
 Vena cava  
   inferior, 16f, 21, 25f, 79f, 81f, 83f, 85f, 87f, 89f, 104f, 105f, 106f, 110, 111f, 113f, 114, 114f, 117f, 119f, 121f, 123f, 125f, 127f, 129f, 131f, 133f, 135f, 137f, 139f, 141f, 143f, 145f, 147f, 149f, 151f, 153f, 155f, 157f, 180f, 187f  
   bifurcation of, 159f, 189f  
   superior, 16f, 17f, 18–19, 18f, 20f, 21f, 23f, 25f, 57f, 59f, 61f, 63f, 65f, 440f, 441f  
 Ventricle(s), brain, 327  
   fourth, 327f, 328–329, 345f, 353f, 355f, 393f, 397f  
   choroid plexus of, 318f, 328f  
   lateral recess of, 395f  
   lateral, 323f, 327–328  
   anterior horn of, 322f, 327, 327f, 343f, 371f, 401f, 405f, 407f  
   body of, 327–328, 327f, 343f, 359f, 363f, 409f  
   choroid plexus of, 318f, 328f  
   collateral trigone of, 322f, 327f, 328, 341f, 357f, 409f

## 640 Index

- Ventricle(s), brain (*continued*)  
inferior/lateral horn of, 322f, 323f, 327f, 328, 339f, 359f, 403f  
posterior horn of, 322f, 327f, 328, 339f, 353f, 355f, 407f  
third, 327f, 328, 361f, 363f, 367f, 399f, 401f, 403f  
choroid plexus of, 318f, 320f, 328f, 405f
- Ventricle(s), heart  
left, 16, 16f, 17f, 35f, 37f, 69f, 71f, 73f, 75f, 77f, 79f, 81f, 83f, 117f, 119f  
right, 16, 16f, 17f, 31f, 33f, 35f, 37f, 67f, 69f, 71f, 73f, 75f, 77f, 81f, 83f, 117f, 119f  
wall of, 73f
- Vermis, 319
- Vertebra prominens, 435
- Vertebral arch, 9  
C3, 459f  
left, 471f  
right, 461f, 465f, 467f, 469f, 473f, 475f, 477f, 479f
- Vertebral artery(ies), 16f, 17f, 18, 18f, 19f, 326f, 389f, 438, 441f  
cranial, 326  
left, 39f, 41f, 43f, 45f  
right, 447f, 449f, 459f, 463f
- Vertebral body, 9, 57f, 191f, 247f, 493, 497f, 517f  
first sacral, 505f  
L1, 501f  
L2, 501f  
L3, 501f  
L4, 501f  
L5, 501f  
S1, 501f  
twelfth thoracic, 505f
- Vertebral column, 434f  
lateral view of, 434f, 494f  
midsagittal section through, 497f
- Vertebral endplate, 503f  
inferior L1, 503f  
superior L1, 503f
- Vertebral foramen, 187f, 299f, 301f, 434, 435f, 494f, 496  
axial drawing of, 499f  
left, 195f, 237f
- Vertebral notch(es), inferior, 191f, 495f
- Vertebral structures, 493, 496
- Vertebral veins, 438
- Vestibular folds, 436, 438f, 439f, 440f, 445f
- Vestibule, 183, 277f
- Visceral pericardium, 12f, 13
- Visceral pleura, 12f, 20f
- Vocal cords. *See* Vocal fold
- Vocal fold, 435–436, 438f, 439f, 440f, 445f, 475f
- Vocal ligament, 438f
- Vomer, 314, 314f, 315f, 317f, 381f, 383f, 389f
- Vomeronasal organ, 315f
- W**
- Weighted images, 5, 5f  
T1, 5, 5f, 6f  
T2, 5, 5f, 6f
- White matter, 409f, 413f, 417f  
of cerebellar hemisphere, 349f  
of frontal lobe, 375f  
of occipital lobe, 349f
- Wrist, 564–571  
anatomical overview of, 564–567  
musculature in, 566–567  
skeletal parts in, 564–565, 565f–566f  
bones in, dorsal and palmar view of, 564f  
CT images (axially computed) of, 568, 568f–571f  
muscles/tendons in  
dorsal view of, 565f  
palmar view of, 566f
- X**
- Xiphoid process, 10f, 11, 436f
- Z**
- Zygapophysis joint, 496–497, 525f
- Zygomatic arch, 317f
- Zygomatic bone, 314, 315f  
left, 385f, 387f
- Zygomatic process, 317f